Musculoskeletal Research and Basic Science

Feza Korkusuz
Editor

Springer

Musculoskeletal Research and Basic Science


Türk Ortopedi ve Travmatoloji
Birliği Derneği


Türk Ortopedi ve Travmatoloji Eğitim Konseyi
2001
TOTEK


TURKISH ORTHOPEDIC RESEARCH COUNCIL
TOAK
2013

Feza Korkusuz
Editor

Musculoskeletal Research and Basic Science

Springer

Editor
Feza Korkusuz
Department of Sports Medicine
Hacettepe University Medical Faculty
Ankara
Turkey

ISBN 978-3-319-20776-6 ISBN 978-3-319-20777-3 (eBook)
DOI 10.1007/978-3-319-20777-3

Library of Congress Control Number: 2015954078

Springer Cham Heidelberg New York Dordrecht London

Printed on acid-free paper

Springer International Publishing AG Switzerland is part of Springer Science+Business Media (www.springer.com)

Dedicated to
Professor Edip Zeki Korkusuz, MD
who always advised to his students to study the micro- and nano-world of the musculoskeletal system.

Preface

Musculoskeletal Research and Basic Science aims to relate basic science with clinical practice. Basic science and research are integral to the understanding and improvement of orthopedic surgery and hence to educating good clinical practitioners.

Examples of conditions for which treatment is influenced by basic science include osteoarthritis and osteoporosis, both of which often disable the elderly; high impact trauma due to road traffic accidents and war injuries frequently disable the young. Implants are used to replace joints or fix fractures. More recently regenerative and reconstructive approaches using cells, scaffolds, and signaling molecules are improved to treat joint cartilage injuries, skeletal muscle, and peripheral nerves. Updating background information on musculoskeletal tissues, biomaterials, and biomechanics was the incentive of editing this book.

We organized this book into seven sections. Imaging and anatomy sections were provided at the request of orthopedic residents. The five other sections include biomaterials and biomechanics, musculoskeletal tissues and their functions, basic pathology, oncogenesis and tumors, and basic pharmacology. While the practices of residents in training and fully trained orthopedists may all benefit from this volume, we assume basic and clinical scientists studying and working on musculoskeletal tissues will benefit the most by providing perspective.

We depended on the section editors and authors while preparing this book. All are well respected in their research areas. We cordially thank them for their generous contributions, for without their efforts, this book would not be possible.

The Turkish Orthopedic and Trauma Association (TOTBID) and its Education (TOTEK) and Research (TORC) Councils supported the publication of this book. We thank their long-term encouragement. *Musculoskeletal Research and Basic Science* is the main source of Basic Science and Research School of TOTEK held for more than 10 years with more than 1250 graduates.

I personally thank my Springer family including Dr. William F. Curtis, Sadie Forester, Irmela Bohn, Gabriele Schroeder, Claus-Dieter Bachem, Magesh Rajagopalan, and Saanthi Shankhararaman. The smooth transition from a collection of lecture notes to a book would be not possible without their kind support.

We hope this book will provide a strong reference work for today's musculoskeletal scientists, provide a strong basis for orthopedic practice, and suggest new horizons for future research.

Ankara, Turkey — Feza Korkusuz, MD

Motivation and Acknowledgments

Roots of this book go to the Mediterranean Coast of Summer 2007 where Professor Ahmet Turan Aydın, Professor İzge Günal, and I were drafting the means of musculoskeletal research and basic science education in Turkey. Our first step was to organize the Basic Science and Research School that has been running smoothly for more than 10 years. Feedback of more than 1250 orthopedic surgeons of this school shaped the context of this book.

Most of the authors and section editors of this book are members of the Turkish Orthopedic and Trauma Association (TOTBID), its Education (TOTEK) and Research (TORC) Councils. They regularly teach at the Basic Science and Research School of TOTEK. The transition from lecture notes to a Turkish book and to this updated English book was smoothly accepted by all of them. Chapters were prepared on time with precision.

My personal story of musculoskeletal research and basic science however goes back to the 1960s. My first exposure to musculoskeletal science must have been physically cutting presentation slides for my father Professor Edip Zeki Korkusuz, MD, when I was six. Repeated conversations with colleagues of my father at home must have influenced me to some extent. My turn to medicine from engineering was a hard decision. My mother told me, "*I want to see you in white coats!*" and the decision was made. However, I retained an interest in mathematics and physics and the concepts of biomechanics, motion analysis, and biomaterials were never too far away.

Professors Keiro Ono, Atsumasa Uchida, Kazuo Yonenobu, Takahiro Ochi, Kunio Takaoka, and Hideki Yoshikawa of Osaka University Graduate School of Medicine, Department of Orthopaedic Surgery, were role models in my academic carrier. During my two-year study in Japan, I remember once taking the train with Professor Ono and I asked him the future of musculoskeletal research and basic science. He answered, "*I do not know, but it is your responsibility and that of the younger generations to shape the future.*" I remain in touch with my Japanese Professors and colleagues who keep inspiring me.

Working at Middle East Technical University for 20 years closed my research gaps between orthopedic surgery, biomechanics, bioceramics, medical polymers, and all other interphase areas of biomedical engineering. There were four special scientists who contributed to my interdisciplinary studies significantly. Professors Nuri Akkaş, Muharrem Timuçin, Turgut Tümer, and Erdal Bayramlı with their students worked with me for hours and days. Professor Timuçin in one of his lectures stated that he produced new bioc-

eramic compositions each year for me and finally one was used in patients after many hours in the laboratory.

Dr. Richard Brand influenced me in the writing of science, and various social and cultural issues related to orthopedics. He joined us at a turning point for our Scientific Writing Workshop organization. He was a role model to me for traveling half way around the world to nourish knowledge eager young scientists.

Hacettepe University Medical Faculty is my new home and individuals from several departments provided considerable contribution to this book.

All these scientists lit their candle of knowledge that converted into a book of flame. I bow in front of all of them and wish they accepted my sincere thanks.

Sincerely
Feza Korkusuz
Editor

Contents

Part I

Biomaterials and Biomechanics

Nusret Köse

Biological Response to Orthopedic Implants and Biomaterials

1

Nusret Köse

Abstract

The rate of orthopedic implant use is increasing, and this trend is expected to continue in the next decades due to aging population and improving medical care. Biomaterials can be grouped under the four headings metallic, ceramic, polymeric, and composite materials. In addition to the competency of the surgeon, the success of these synthetic or natural biomaterials is dependent on the properties of the biomaterial, biocompatibility of the implant, and the condition of the recipient tissue. Despite major advances in orthopedic biomaterials and allergic and foreign body response, biomaterials-related complications such as implant loosening and infection are still restricting the use of biomaterials in daily practice. Surface modification of biomaterials has been developed for tailoring of surface properties of the orthopedic implants. These altered surface properties mostly improve tissue-biomaterial interactions and also mechanical characteristics of the implants.

Learning Outcomes

After reading this chapter, you will understand the following:

1. Rationale for use of the different biomaterials in clinical applications
2. Structure and properties of different metals commonly used for making orthopedic implants
3. The general definition, classifications, and common properties of different bioceramics
4. Principles underlying surface modification techniques
5. Biological response to orthopedic implants

N. Köse, MD
Department of Orthopedics and Traumatology,
Eskisehir Osmangazi University, Eskisehir, Turkey
e-mail: drnkose@gmail.com; nkose@ogu.edu.tr

F. Korkusuz (ed.), *Musculoskeletal Research and Basic Science*,
DOI 10.1007/978-3-319-20777-3_1

Terminology

Biocompatibility Acceptance of an artificial implant by the surrounding tissues and by the body as a whole.

Biodegradation Materials that could be broken down by nature either through hydrolytic mechanisms without the help of enzymes or enzymatic mechanism.

Biomaterial A synthetic material used to make devices to replace part of a living system or to function in intimate contact with living tissue.

Bone cement Mixture of polymethylmethacrylate powder and methylmethacrylate monomer liquid to be used as a grouting material for the fixation of orthopedic joint implants.

Calcium phosphate A family of calcium phosphate ceramics including calcium phosphate, hydroxyapatite, and tricalcium phosphate (TCP) are used to substitute or augment bony structures and deliver drugs.

Corrosion Unwanted reaction of metal with environment.

Fibrous membrane Thin layer of soft tissue which covers an implant to isolate from the body.

Graft Set of living cells, living tissue, or living organ surgically inserted into a body to replace a damaged part or a defect of an organ. This is an *autograft* if the donor and recipient is the same individual; this is an *allograft* when the donor and recipient belong to the same species but are genetically distinct; this is a *xenograft* when the donor and recipient are of different species.

Hydroxyapatite A calcium phosphate ceramic with a calcium-to-phosphorus ratio of 5/3 and a nominal composition Ca1O(PO4)6(OH)2. Hydroxyapatite is the mineral constituent of bone.

Implant An implant is a medical device (apparatus, prosthesis, etc.) made of one or several biomaterials, which is introduced into the human body in the long term to replace an organ or to supply a function or to treat a disease.

Osseointegration Direct contact of bone tissues to an implant surface without fibrous membrane.

Osteolysis Dissolution of bone mineral from the bone matrix.

Passivation Production of corrosion resistance by a surface layer of reaction products.

Prosthesis A device implanted in the body to supply a missing organ (limb, tissue) or to restore a deficient function.

Stress shielding Bone is protected from stress by the stiff implant.

Clinical Relevance

1. Refer to Fig. 1.1 and consider a 66-year-old patient with a total knee arthroplasty. This modular knee arthroplasty implant is composed of a cobalt-chrome femoral component, titanium alloy tibial component, and a polyethylene insert. Would you be concern of crevice and galvanic forms of corrosion in this patient?

   When you have a total knee replacement, the surgeon removes damaged cartilage and bone from the surface of the knee joint and replaces them with a metal and plastic. Because of the modularity of the cobalt-chromium femoral and titanium tibial components, crevice corrosion will be relevant. Because there is a polyethylene insert separating the cobalt-chromium component and the titanium plate, galvanic corrosion will be limited. Though wear through of the liner would present other concerns as well [31].

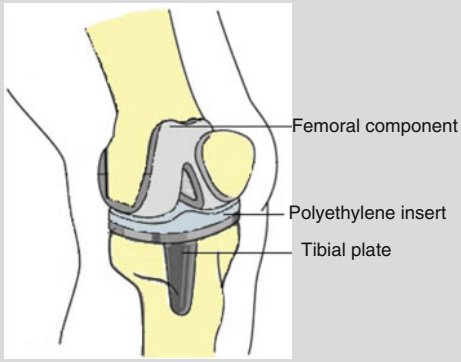

Fig. 1.1 Total knee artroplasty

In engineering any substance that is used for manufacturing is called material. Biomaterials are natural or synthetic materials that treat, augment, or replace tissues and organs. Biomaterials are utilized to fulfill or support the task of living tissue in the human body which continuously or periodically comes into contact with body fluids. Biomaterials are different from other materials in the sense that they must have the ability to remain in contact with tissues from the human body without creating too much adverse or a hostile response. If a material is used in a human body, it has to be able to resist mechanical forces and chemical effects. Also this material is expected to exhibit osseointegration properties [1–4].

Men have used various materials to replace organs or parts of organs since the beginning of history. Glass for eyes, wood for teeth, gold in dentistry, and linen, horsehair, and cotton for suture were some examples of the uses of materials for various replacements. These materials were those used in everyday life. The evidence of their use as implants or prostheses were mainly discovered on human skeletons during the excavations of sites from different ancient civilizations: Egyptian, Roman, and Greek. Gold, as a metal, appears to be one of the earliest and main materials used by old civilizations, and, incredibly, it is still used today [5].

Musculoskeletal disorders are the principal cause of disability in all over the world and are responsible for chronic conditions. For a very long time, the use of materials mainly was more cosmetic than functional. Then surgeons and scientists were interested in the subject, and they developed functional materials for orthopedic and other surgeries. Because of their mechanical properties and resistance to corrosion, simple metals were chosen in the beginning, but incredible development of the plastics and ceramic sciences make possible the use of new materials, with diverse physicochemical and mechanical properties. The rate of orthopedic implant use is increasing, and this trend is expected to continue in the next decades due to aging population and improving medical care. Nowadays, the development of new biomaterials and their use in medicine has been an important domain. Despite major advances in orthopedic biomaterials and allergic and foreign body response, biomaterials-related complications such as implant loosening and infection are still restricting the use of biomaterials in daily practice [1–6].

The response of a material to deforming forces is characterized by its mechanical properties. Mechanical properties of biomaterials determine the deformation, failure behavior, and fracture of materials under the action of tensile, compressive, torsional, or combinations of these forces. As an example, mechanical properties would be very important for a joint replacement implant because it would be expected to withstand heavy loads generated during walking, and such loads can be very high. To determine the mechanical properties of a material, force versus deformation tests are conducted. In these tests, samples of a material are loaded at a constant rate, and both the deformation and the force required to cause that deformation are measured at various time points.

Biomaterials can be grouped under the four headings metallic, ceramic, polymeric, and composite materials. The biomaterials most commonly used in orthopedic surgery are metallic implants such as steel, cobalt-chrome, or titanium alloys, as they provide satisfactory mechanical performance. Screws, plates, and nails used for the treatment of fractures, hip and knee prostheses used in joint diseases, and spine implants are typical examples of metallic biomaterials used in orthopedic surgery.

Most commonly used implantation devices in orthopedic surgery are made of metallic, ceramic, and polymeric biomaterials [1–4].

Metals

All materials are constituted of atoms that are bonded together by interactions. In metals, metallic atoms are closely packed in a crystal structure, and atoms are held together through a nondirectional strong metallic bond. Metals are group of materials with high corrosion resistance, biocompatibility, high wear resistance, and excellent mechanical properties such as good ductility and strength. Due to their crystal structure and strong metallic bonds with superior mechanical properties, they are used frequently as implant material. Metals have been preferred practically completely for load-bearing applications, such as joint arthroplasties and fracture fixation wires, pins, screws, and plates. Although pure metals can be used, metal alloys are preferable. Some characteristics, such as strength and corrosion resistance of metal implants, can be improved when used as a metal alloy by varying the composition or by using different manufacturing processes [7, 8].

Convenient mechanical properties, corrosion resistance, biocompatibility, and reasonable cost are the main considerations in preferring metal alloys for implant use. It is important to know the physical and chemical properties of the different metal alloys used in a surgery as well as their interaction with the host tissue of the human body, to be able to make knowledgeable decisions. Elastic modulus, yield stress, ultimate tensile stress, and fatigue stress are the most important characteristics of a metal implant defining its strength and stiffness. These properties of a metal can be seen from stress-strain curves. The strength characteristics of a metal can be influenced by the grain size, inclusion content, and surface porosity. A metal with a smaller grain size has a higher tensile and fatigue strength compared to the larger grain size. High surface porosity and too much inclusion content will weaken the metals [7, 8].

Extracellular fluid of human body contains various ions such as dissolved oxygen, chloride, and hydroxide. Therefore, the human body with a different ion concentration and pH changes in fluids is a highly corrosive environment for metals when used as implants. Corrosion is degradation of materials' properties due to interactions with their environments, and corrosion of most metals is inevitable. While primarily associated with metallic materials, all material types are susceptible to degradation. Corrosion weakens the material; also corrosion products that enter into tissues can cause damage to cells. Three types of corrosion are common in implant materials: fatigue, galvanic, and crevice corrosion. Fatigue is the weakening of a material caused by repeatedly applied loads. It is the progressive and localized structural damage that occurs when a material is subjected to cyclic loading. If the loads are above a certain threshold, microscopic cracks will begin to form at the stress concentrators such as the surface and grain interfaces. Eventually a crack will reach a critical size, and the structure will fracture. Galvanic corrosion occurs when two different metals have physical or electrical contact with each other. An electric current is established between two metals that cause degradation. To avoid tragic galvanic corrosion, stainless steels should never be used with cobalt or titanium alloys. Crevice corrosion is a localized form of corrosion occurring in confined spaces, to which the fluid in contact with a metal becomes stagnant, resulting in a local oxygen depletion and decrease in pH. Stainless steel corrodes more readily than other alloys. Approaches available for controlling corrosion include the application of protective coatings to metal surfaces to act as a barrier or alteration of an alloy chemistry to make it more resistant to corrosion and the treatment of the surface of a metal to increase its resistance to corrosion. The chromium and molybdenum content of alloys produces a corrosion-resistant surface layer. Titanium alloys have an oxide passive film layer that provides their corrosion resistance. Nitric acid, by forming an oxide surface layer, is used to make the surface of the implant passive to corrosion [1–4].

The mechanical properties of the metal are important and should satisfy the requirements of

the specific application in the body. For instance, when a metal is used to augment a bone, the elastic modulus of the metal should be ideally equivalent to that of the bone. If the elastic modulus of the metal is greater than that of bone, then the load experienced by the bone is reduced due to a phenomenon known as stress shielding. This can cause the bone to remodel to adjust to the lower load and eventually result in the loss of bone quality. Metals are passed through a series of processes to provide materials desired properties such as harder, softer, or durable.

Three material groups dominate biomedical metal implants: stainless steel, cobalt-chromium alloy, and titanium alloys. Other metals used in the biomedical industry include nitinol, tantalum, and magnesium. Nitinol, a nickel-titanium alloy, belongs to the class of shape memory alloys. At low temperature, these alloys can be plastically deformed but return back to their original predeformed shape when exposed to a high temperature. Tantalum (Ta) has been used for making biomedical implants and devices, either in its commercially pure (99.9 %) state or as an alloying element in titanium alloys. Tantalum is well known for its excellent corrosion resistance and biocompatibility because of a stable surface oxide layer. It has also been used as coatings on other metallic devices, such as 316 L stainless steel, to improve the substrate's corrosion resistance and to enhance biocompatibility. The use of magnesium (Mg) for orthopedic applications dates back nearly half a century. Mg is well known for its light weight and biodegradability. The density, elastic modulus, yield strength, and fracture toughness of Mg are close to that of bone [1–9].

Stainless Steel

Stainless steel was successfully used as the first material in surgery. Stainless steel is essentially iron and carbon alloy which contain at least 10, 5 % chromium. Molybdenum and a small amount of manganese and silicon are added. The corrosion resistance of stainless steel is due to the formation of chromium oxide (Cr2O3) on its surface. The corrosion-resistant properties of stainless steel can be further improved by increasing the chromium content. These properties and other physical and mechanical properties can also be improved by the addition of several other alloying elements. For instance, addition of molybdenum increases pitting corrosion resistance, while the addition of nitrogen increases mechanical strength and pitting corrosion resistance.

Stainless steel is the common name for a number of different steels. Stainless steels with a smaller percentage of carbon, which are labeled 316 L, are used for orthopedic implants. The letter "L" represents low carbon content (<0.030 %). The low carbon content is highly preferred for excellent corrosion resistance. 316 L stainless steel consists of primarily iron (60–65 %), chromium (17–20 %), nickel (12–14 %), and smaller amounts of molybdenum, manganese, copper, carbon, nitrogen, phosphorous, silicon, and sulfur.

Stainless steel has been used for wide range of application due to easy availability, lower cost, excellent fabrication properties, accepted biocompatibility, and great strength. Despite composition modification, stainless steels are susceptible to corrosion; therefore, they are most appropriate for temporary implants such as plates, screws, hip nails, and intramedullary nails. The most common reason for corrosion of stainless steels is incorrect metal composition, which increases the chance that galvanic corrosion will occur. Molybdenum that is added in 316 L stainless steels hardens the passive layer and increases corrosion resistance. Another reason for corrosion is mismatch of implant components, especially when plates and screws are used. It is important to use implants manufactured by the same company with similar lots to avoid compositional differences of implant components [1–8].

Cobalt-Chrome Alloys

The cobalt-based alloys are characterized by high fatigue and wear resistance and high tensile strength levels. These properties make them desirable for load-bearing and articulating surface applications, appropriate for applications

requiring long time use and ability to resist fracture. Cobalt-chromium alloys can be separated into two types: first one which has been used for making artificial joints consists of Cr (27–30 %), Mo (5–7 %), and Ni (2.5 %) and the second one which has been used for making the stems of prostheses contains Cr (19–21 %), Ni (33–37 %), and Mo (9–11 %). Cobalt-based alloys are highly resistant to corrosion due to spontaneous formation of passive oxide layer within the human body. Molybdenum is added to produce finer grains which result in higher strength. Elastic modulus of the alloy containing cobalt is greater than that of stainless steel. The corrosion products of Co-Cr-Mo are more toxic than those of stainless steel [1–4].

Titanium Alloys

Titanium alloys due to its outstanding characteristics such as lightweight, high strength, good resistance to corrosion, improved biocompatibility, and better elastic modulus are a suitable choice of metal for implantation. Although it is a lightweight material, titanium provides excellent mechanical and chemical properties comparable to stainless steel and cobalt-chromium alloy. Long-term use of titanium alloys has raised some concerns because of releasing aluminum and vanadium ions which might be related to Alzheimer disease and neuropathy.

The mechanical properties of materials are very important when using load-bearing orthopedic implants. Some mechanical properties of metallic biomaterials are listed in Table 1.1. The mechanical properties of an implant depend not only on the type of metal used but also on the processes used to manufacture the material and implant. The elastic moduli of the most metals listed in Table 1.2 are many times greater than that of natural bone. Titanium alloys have a surface passive oxide layer which is mainly responsible for its extremely good corrosion resistance and biocompatibility. Titanium alloy plates are gaining popularity because of these material characteristics [1–5].

Table 1.1 Mechanical properties of tissues [4]

	Modulus (GPa)	Tensile strength (MPa)
Cortical bone (longitudinal direction)	17.7	133
Cortical bone (transverse direction)	12.8	52
Cancellous bone	0.4	7.4
Articular cartilage	0.010	27.5
Fibrocartilage	0.159	10.4
Ligament	0.303	29.5
Tendon	0.401	46.5

Polymers

Polymers are organic materials that form large chains made up of many repeating units. Compared to metallic implants, polymeric materials are used on a variety of applications in surgery. Flexibility, resistance to biochemical attack, good biocompatibility, to be lightweight, and to be available in diverse compositions are their unique properties. Polymethyl methacrylate (PMMA) and ultrahigh-molecular-weight polyethylene (UHMWPE) are two main classes of polymer used in orthopedic surgery.

Polymers have the advantage that they can be easily formed into desired shapes using a variety

Table 1.2 Mechanical properties of metallic biomaterials [4]

Material	Young's modulus (GPa)	Yield strength (MPa)	Tensile strength (MPa)	Fatigue limit (MPa)
Stainless steel	190	221–1,213	586–1,351	241–820
Co-Cr alloys	210–253	448–1,606	655–1,896	207–950
Titanium (Ti)	110	485	760	300
Ti-6Al-4V	116	896–1,034	965–1,103	620
Magnesium	41–45	65–100		
Cortical bone	15–30	30–70	70–150	

of techniques. Polymers can also be made reactive so that different chemical molecules can be attached to the surface of implants in order to make them more compatible with the surrounding environment in the body. Some polymers are biodegradable in the body. If used to make implants for temporary needs, these polymers offer the advantage that the implant can gradually biodegrade within the body after it has served its function, thus mitigating the potential for any long-term complications. If a biodegradable polymer is used as an implant, it can potentially also be designed to release therapeutic drugs or growth factors during the degradation process. Composition and structure of the macromolecular chains and their molecular weight affect the mechanical properties of polymers. Polymers are usually not as robust or rigid as metals or ceramics and therefore may not be the right choice when an implant is required to carry large loads in its function.

Polymethyl Methacrylate (PMMA)

PMMA is used as bone cement in orthopedics to stabilize joint prostheses as well as a bone substitute in pathologic vertebral and other fractures. The success of any joint prostheses used with bone cement is dependent on the performance of the PMMA cement. Bone cement does not adhere well to either metal or adjacent bone. It is not an adhesive and functions mostly as a space-filler or grout. Increased surface roughness of the metal and higher porosity of adjacent bone both result in better infiltration of the polymer and better interlocking. On the other hand, the presence of air bubbles at the metal interface leads to decreased adhesion and possible failure.

The bone cement used clinically is available as a kit that contains a dry component and a liquid component. The dry powder component consists of prepolymerized PMMA beads, barium sulfate (opacifier), and dibenzoyl peroxide (initiator). The initiator is the source of free radicals that starts the reaction. The liquid component contains the MMA monomer and N,N-dimethyl-p-toluidine, which is an accelerator. Once the solid and liquid components are mixed, the initiator, aided by the accelerator, produces free radicals which drive the polymerization of the monomer. The polymerization reaction can cause tissue damage due to an increase in temperature. The polymerization reaction is characterized by different time periods. The dough time typically lasts for 2–4 min and is the time elapsed from the point of the initial mixing of the solid-liquid components to the time when the mixture has reached enough viscosity that it can be handled as a mass. The time period between the end of the dough time and the point where the polymer is too hard to mold is known as the working time.

The inclusion of antibiotics with bone cement has led to a decrease in infections. However, the inclusion of antibiotics also leads to a lower strength for the PMMA. Other potential problems with the use of PMMA in medical applications include the release of monomer into the blood stream, leading to toxic effects such as a drop in blood pressure and death in extreme cases [1–11].

Ultrahigh-Molecular-Weight Polyethylene (UHMWPE)

With 90 % success rates at 15 years of metal on polyethylene articulation, UHMWPE is commonly used as a bearing surface in total hip, knee, and shoulder joint arthroplasty. UHMWPE has better wear properties compared to other polymers. Although UHMWPE has good wear characteristics in terms of degree of wear, it produces submicron and nano-sized wear debris in large quantities which can exceed the body's ability to remove the debris material. This problem was encountered more by the oxidation of UHMWPE if it is sterilized in air using gamma radiation.

Osteolysis or bone loss in the surroundings of total joint prostheses was first thought to be due to bone cement (PMMA). Therefore, it was called cement disease. Later it was discovered that this osteolysis, which often results in the loosening of implants, is caused by the wear particles shed by the UHMWPE components of the prostheses. It was estimated that billions of such particles were

released into the surrounding tissue every year. In recent years, cross-linking of the UHMWPE in a non-oxygen environment has led to significantly reduced wear and osteolysis.

Polylactic Acid (PLA) and Polyglycolic Acid (PGA)

Polylactic acid (PLA) and polyglycolic acid (PGA) and their family of materials are biodegradable polymers. These polymers and their copolymers are used commonly in the field of orthopedics as fixation devices for bone and soft tissue in the form of biodegradable plates, screws, and anchors. They are also very popular as the scaffolding material for tissue engineering applications. Additionally, they are used for a variety of controlled drug-delivery applications.

Ceramics

Ceramics are another materials used in orthopedics. Ceramics are polycrystalline materials which are usually known as inorganic, nonmetallic materials. Depending on the atomic arrangements, ceramics can either exist as amorphous or crystalline structures. An example of an amorphous ceramic is glass, whereas an example of a crystalline ceramic is porcelain. The atomic bonds in a ceramic crystal have both covalent and ionic characteristics. These strong bonds are responsible for the great stability of ceramics and impart very useful properties such as hardness, high modulus of elasticity, and resistance to heat and chemical attack. Ceramics are also strong in compression but weak in tension.

Ceramics can be grouped as inert, degradable or resorbable, and bioactive ceramics according to their reactivity. Inert ceramics, such as alumina and zirconia, are chemically stable, that is, they do not corrode, wear, or react to the host environment. Inert ceramics do not induce any immunologic host reactions and little or no chemical change occurs during the long-term exposure to the host environment. Resorbable and surface reactive ceramics react to the host resulting in surface chemical changes. Bioglass and glass ceramics are bioactive. Bioactive glass is an example of surface reactive ceramics. Calcium phosphate ceramics such as hydroxyapatite and tricalcium phosphate are examples of bioresorbable ceramics, and these ceramics are capable of degrading in the presence of a biological environment. The main purpose of the use of biodegradable porous ceramics implantation in bone tissue is to provide replacement for defective region.

The first-generation bioceramics are inert ceramics used in medicine, whereas the second-generation bioceramics include degradable and surface reactive ceramics. The main applications of inert ceramics in orthopedics are related to total hip and knee replacement. The use of bioceramic components has reduced the wear rate and the amount of ion release to a negligible level. The bioactivity of the porous ceramic material is limited mostly to osteoconductivity. Ceramic composites may be used alone or in conjunction with other materials with osteogenic, osteoinductive, or osteoconductive properties to enhance bone healing. Ceramics used as temporary structures or scaffolds in regenerative medicine are known as the third-generation bioceramics. Ceramics can also be used as carriers for cells, growth factors, antibiotics, and anticancer drugs [12, 13].

Alumina

The harmful effects of implant loosening due to polyethylene wear debris caused interest in using other materials at the articulating surface. Aluminum oxide, also known as alumina (Al2O3), has been used since 1960s as an implant biomaterial. High-density and high-purity alumina hip replacement was the first ceramic application widely used as femoral head because it shows excellent corrosion resistance, good biocompatibility, and high wear resistance and high strength. Then, ceramic material is used as the acetabular cup. The reason for the excellent wear behavior of alumina related to the frictionless surface of this ceramic. Alumina is very responsive to microstructural defect which could result in wear and breakage. Alumina-on-alumina joint

articulations produce almost 5,000 times less wear than metal-on-polyethylene articulations. The elastic modulus of aluminum oxide is 20 times greater than that of cortical bone.

Zirconia

Zirconia also known as zirconium oxide (ZrO2) is one of the ceramic used in orthopedic with the highest power. High mechanical strength and fracture toughness are main characteristics of zirconia. The mechanical and wear properties of zirconium oxide are superior to those of aluminum oxide. The main application of zirconia ceramics is to replace the femoral head used in hip arthroplasties. There are some concerns that zirconia may contain very small traces of radioelements. The cytotoxicity of zirconia was also speculated in some experimental studies.

Bioglass Ceramics

Bioactive glasses are silicate-based material containing calcium and phosphate. As an implantable material, the porosity of bioglass is advantageous for resorption and bioactivity. Bioactive glasses have been widely used for filling of bone defects and modification of the implant surface characteristic (coating material).

Calcium Phosphate Ceramics

Several different forms of calcium phosphate (CaP) ceramics including hydroxyapatite (HA) and tricalcium phosphate (TCP) can be found in a human bone. In addition to the naturally occurring forms of CaP ceramics, these ceramics can be synthetically produced in the laboratory. The synthetically produced CaP ceramics are similar in composition, biodegradation, bioactivity, and osteoconductivity to the biological apatites. Calcium phosphate ceramics form a bone-like apatite layer on their surface which offers property of bioactivity and bond to living bone. Porosity is one of the main characteristics of calcium phosphate ceramics. The optimum pore size for bioceramic is identical to that of spongy bone. In general, the degradation rate of CaP ceramics is dependent on porosity, grain or crystal size, crystal perfection, inclusion of chemical impurities, and chemical composition.

HA, TCP, and biphasic CaP (combination of HA and TCP) are commonly used CaP phases in biomedical applications. The most commonly known crystalline CaP biomaterial is hydroxyapatite (HA) also known as calcium hydroxide phosphate. HA is an osteoconductive material and used as coatings on metallic implant surfaces to enhance bone healing rather than as solid ceramic implants for orthopedic applications. Another popular crystalline CaP ceramic used in the fabrication of medical devices is tricalcium phosphate (TCP). Having the chemical formula, Ca3(PO4)2, TCP can exist in two forms, namely, α-TCP and β-TCP. The rate of solubility for α-TCP is more rapid compared to β-TCP. Therefore, α-TCP degrades and resorbs more quickly in the body. To take advantage of the benefits of both HA and TCP, biphasic CaP ceramics have also been introduced as biomaterials. These composites benefit from the osteoconductivity of HA and the absorbability of the TCP [1–13].

Biological Response to Orthopedic Implants

In today's healthcare environment, a large number of devices and implants are being inserted into the human body at an increasing rate. The success of these synthetic or natural biomaterials and implants is highly dependent on three major factors: the properties of the biomaterial (mechanical, chemical, and tribological), the biocompatibility of the implant, and the condition of the recipient tissue/the competency of the surgeon. The design of implants and prostheses is a challenging process since the intended materials must respond to specific requirements and must be biocompatible. The most important prerequisite for a biomaterial is its acceptability by the human body. Many orthopedic implants come into contact with body fluid, whether permanently or temporarily. Any foreign material inserted into the body will cause a host response. The word of

biocompatibility is used to indicate the biological performance of materials. It implies the ability of a material to cause an appropriate host response. Biocompatibility is the capacity to exist in contact with tissues of the human body without causing an unacceptable degree of injury to the body. It is not only associated to toxicity, but it must be noncarcinogenic, nonpyrogenic, nontoxic, nonantigenic, blood compatible, nonthrombogenic, and noninflammatory [14, 15].

In contrast to living organ transplants, biomaterials when used in a human body are not generally "rejected," because biomaterials typically do not generate a specific immune response like living organ transplants. All materials implanted into human body as medical implants cause tissue responses. The host responses to these materials are varied. Under certain conditions, some materials are well tolerated by the body, whereas the some materials are not well tolerated. Materials are classified into several categories such as biotolerant, bioinert, bioactive, and biodegradable. Biotolerant materials induce the worst tissue response. These tissue reactions include injury of implantation, inflammatory state and wound healing, foreign body reactions, and fibrous encapsulation of the implants. When biotolerant materials such as PMMA, polyethylene, and stainless steel are used for implantation, the body produces fibrous tissue layer between the bone and the implant in order to confine the material. The fibrous tissue accommodates plenty of macrophages and foreign body giant cells. The implants made of biotolerant materials release undesirable particles and metal ions which are nonbiocompatible. These wear particles may pile up in tissues, surrounding the implant or they may be moved to other parts of the body. When the wear debris from articulating joint surfaces are not controlled well, the inability of inflammatory cells to phagocytose particles larger than a critical size can lead to the release of enzymes and chemical mediators, such as prostaglandin, tumor necrosis factor-alpha, and interleukin-1, and cause injury to the host tissues. Thus, inflammatory cell products have the capability to damage tissue adjacent to implants. Debris generation has to be minimized [16–18].

Host Tissue Response to Implantation

Implantation of a biomaterial to the human body results in injury to tissues. This injury leads to a series of cellular activity which will cause wound healing that is the part of homeostatic mechanisms. The response of body to this initial injury is variable. The extent of injury, the status of basement membrane, blood-material interactions, the extent of cellular necrosis, and the degree of the inflammatory response all play a role. Host tissue reactions continue with inflammatory and wound healing responses, foreign body reactions, and finally fibrous encapsulation of the medical implants. All these may affect the extent of granulation tissue formation, foreign body reaction, and fibrosis. Blood-implant exposure and beginning of the inflammatory response are closely associated. The aforementioned events can lead to the production of chemical factors that mediate cellular responses of inflammation. In general, neutrophils are main cells during the first couple of days following injury, and then they are replaced by monocytes as the predominant cell type. Depending on the extent of injury, acute inflammation may last minutes to days. Exudation of fluid and plasma proteins also occurs. Neutrophils move to perivascular tissues and the injury/implantation site. Chronic inflammation is variable histologically compared to acute inflammation. Macrophages, monocytes, and lymphocytes, with the proliferation of blood vessels and connective tissue, are main cellular elements of chronic inflammation. This is a foreign body reaction, a special form of nonspecific inflammation. At the implant site, monocytes and macrophages launch healing events, followed by proliferation of fibroblasts and vascular endothelial cells, leading to the formation of granulation tissue. Depending on the extent of injury, granulation tissue may be seen as early as 3–5 days following implantation of a biomaterial. The most important cells in the foreign body reaction are macrophages. Macrophages attempt to phagocytose the material with a varying success. The macrophages, activated in the process of dealing with a biomaterial, may develop cytokines which stimulate inflammation or fibrosis. In general, fibrosis surrounds the implant with foreign body reaction

and keeps apart the implant from the local tissue environment. Fibrosis or fibrous encapsulation is the end stage of healing response to biomaterials with exceptions of porous materials implanted into the bone [19–26].

In the wide sense, bioinert materials cause minimal tissue response. Titanium and cobalt-chromium alloys are typical of bioinert materials which usually cause minimal tissue response. Bioactive materials such as calcium phosphate ceramics cause the best tissue response. The body usually responds without local or systemic toxicity without any inflammatory or foreign body reaction. Degradable or resorbable materials such as certain polymers are incorporated into the surrounding tissue or may even dissolve completely over a period of time.

Metal Allergy

"Metal allergy" is a well-recognized incident. It is commonly related to the use of nickel alloy jewelry and can also occur in association with metallic implants. By themselves, metal ions lack the structural complexity required to challenge the immune system. However, when combined with proteins, such as those available in the skin and connective tissues, a wide variety of metals induce immune responses, and this can have clinical effects. Implant degradation products have been shown to be associated with dermatitis, urticaria, and vasculitis. If cutaneous signs of an allergic response appear after implantation of a metal device, metal sensitivity should be considered. Cobalt, chromium, and nickel are included in this category, with nickel perhaps the most potent; at least 10 % of a normal population will be sensitive by skin test to one or more of these metals [27–29].

Surface Modification

The characteristics of biomaterials can be generally divided into two categories: bulk and surface. Material's bulk controls the mechanical and physical behavior of medical devices. The material's surface properties are important because the surface properties of a material describe the interactions that occur at the interface with its environment. These usually occur within a narrow depth of less than 1 nm on the surface. The biological response to implants is controlled largely by their surface chemistry and structure. Surface properties can be important because these characteristics influence whether cells would attach to the implant or determine how proteins will interact with the surface.

Surface modification of biomaterials allows the tailoring of surface properties without affecting bulk material properties. Materials can be surface modified by using biological, mechanical, or physicochemical methods. Surface modifications fall into three categories: (1) chemically or physically altering the atoms, compounds, or molecules in the existing surface (chemical modification, etching, and mechanical roughening); (2) overcoating the existing surface with a material having a different composition (coating with thin film); and (3) creating surface textures or patterns. Nanotechnology involves the tailoring of materials at atomic level to obtain unique properties for the desired applications. Nanotechnology has impacted the field of biomaterials in several areas, including the manipulation of surface characteristics. These altered surface properties mostly improve tissue-biomaterial interactions. Modification of biomaterial surfaces may also be performed for the purpose of improving surface mechanical properties such as wear resistance, and these ultimately determine the success or failure of a device placed in the human body [30].

References

1. Agrawal CM et al (2014) Introduction to biomaterials: basic theory with engineering applications. Cambridge University Press, Cambridge, UK
2. Ong KL et al (2014) Orthopaedic biomaterials in research and practice, 2nd edn. CRC Press, Taylor & Francis Group, LLC, Boca Raton
3. Gupta R, Caiozzo V, Cook SD, Barrack RL, Skinner HB (2003) Basic science in orthopedic surgery. In: Skinner HB (ed) Current diagnosis and treatment in orthopedics, 3rd edn. Mc Graw Hill, New York
4. Patel NR, Gohil PP (2012) A review on biomaterials: scope, applications & human anatomy significance.

Int J Emerg Technol Adv Eng 2(4):91–101, Website: www.ijetae.com (ISSN 2250-2459)
5. Migonney V (2014) History of biomaterials. In: Migonney V (ed) Biomaterials. Wiley, Hoboken. doi:10.1002/9781119043553.ch1
6. ASM International (2009) Biomaterials in orthopaedic surgery. In: Introduction to biomaterials in orthopaedic surgery, Chapter 1. ASM International, Ohio
7. Nasab MB, Hassan MR, Sahari BB (2010) Metallic biomaterials of knee and hip – a review trends biomater. Artif Organs 24(Metallic Biomaterials of 2): 69–82
8. Iorio R, Robb WJ, Healy WL et al (2008) Orthopaedic surgeon workforce and volume assessment for total hip and knee replacement in the United States: preparing for an epidemic. J Bone Joint Surg Am 90:1598–1605
9. Staiger MP, Pietak AM, Huadmani J, Dias G (2006) Magnesium and its alloys as orthopedic biomaterials: a review. Biomaterials 27(9):1728–1734
10. Charnley J (1960) Anchorage of the femoral head prosthesis of the shaft of the femur. J Bone Joint Surg [Br] 42:28–30
11. Bahraminasab M, Sahari BB, Edwards KL, Farahmand F, Arumugam M, Hong TS (2012) Aseptic loosening of femoral components – a review of current and future trends in materials used. Mater Des 42:459–470
12. Dorozhkin SV (2010) Calcium orthophosphates as bioceramics: state of the art. J Funct Biomater 1(1): 22–107
13. Dalton JE, Cook SD, Thomas KA, Kay JF (1995) The effect of operative fit and hydroxyapatite coating on the mechanical and biological response to porous implants. J Bone Joint Surg 77A:97–110
14. Williams DF (2008) On the mechanisms of biocompatibility. Biomaterials 29(20):2941–2953. doi:10.1016/j.biomaterials.2008
15. Dorr LD, Bloebaum R, Emmanual J, Meldrum R (1990) Histologic, biochemical and ion analysis of tissue and fluids retrieved during total hip arthroplasty. Clin Orthop 261:82–95
16. Treves C, Martinesi M, Stio M, Gutiérrez A, Jiménez JA, López MF (2010) In vitro biocompatibility evaluation of surface-modified titanium alloys. J Biomed Mater Res 92A:1623–1634. doi:10.1002/jbm.a.32507
17. Goodman SB (1994) The effects of micromotion and particulate materials on tissue differentiation: bone chamber studies in rabbits. Acta Orthop Scand Suppl 258:1–43
18. Hicks DG, Judkins AR, Sickel JZ, Rosier RN, Puzas JE, O'Keefe RJ (1996) Granular histiocytosis of pelvic lymph nodes following total hip arthroplasty: the presence of wear debris, cytokine production and immunologically activated macrophages. J Bone Joint Surg 78A:482–496
19. Anderson JM (2001) Biological responses to materials. Annu Rev Mater Res 31:81–110
20. Schoen FJ (2013) Introduction: biological responses to biomaterials. In: An introduction to materials. Medicine in biomaterials science, 3rd edn. Academic Press; Oxford, pp 499–503
21. Jacobs JJ, Goodman SB, Sumner DR, Hallab NJ (2000) Biologic response to orthopaedic implants. In: Buckwalter JA, Einhorn TA, Simon SR (eds) Orthopaedic basic sciences, 2nd edn. American Academy of Orthopaedic Surgeons, Rosemont, p 401
22. Korkusuz P, Korkusuz F Hard tissue-biomaterial interactions. In: Yaszemski MJ, Trantolo DJ, Lewandrowski KU, Hasırcı V, Altobelli DE, Wise DL (eds) (2003) Biomaterials in orthopedics. Marcel Dekker, New York, pp 1–210
23. Dee KC, Puleo DA, Bizios R (2002) Biomaterials. In: An introduction to tissue-biomaterial interactions. Wiley, New York. doi: 10.1002/0471270598.ch1
24. Murray DW, Rushton N (1990) Macrophages stimulates bone resorption when they phagocytose particles. J Bone Joint Surg (Br) 72:988
25. Goodman SB, Huie P, Song Y et al (1997) Loosening and osteolysis of cemented joint arthroplasties: a biologic spectrum. Clin Orthop 337:149–163
26. Urban RM, Jacobs JJ, Gilbert JL, Galante JO (1994) Migration of corrosion products from modular hip prostheses: particle microanalysis and histopathological findings. J Bone Joint Surg 76A:1345–1359
27. Jacobs JJ, Skipor AK, Patterson LM, Hallab NJ, Paprosky WG, Black J, Galante JO (1998) Metal release in patients who have had a primary total hip arthroplasty. J Bone Joint Surg 80-A:1447–1458
28. Case CP, Langkamer VG, James C et al (1994) Widespread dissemination of metal debris from implants. J Bone Joint Surg 76(B):701–712
29. Deutman R, Mulder TJ, Brian R, Nater JP (1977) Metal sensitivity before and after total hip arthroplasty. J Bone Joint Surg 59(A):862–865
30. Ratner BD, Hoffman AS (2013) Physicochemical surface modification of materials used in medicine. In: An introduction to materials. Medicine in biomaterials science, 3rd edn. Academic Press; Oxford, pp 259–276
31. Kretzer JP, Reinders J, Sonntag R, Hagmann S, Streit M, Jeager S, Moradi B (2014) Wear in total knee arthroplasty – just a question of polyethylene? Metal ion release in total knee arthroplasty. Int Orthop 38(2):335–340

Fundamentals of Musculoskeletal Biomechanics

2

Mustafa Ünal, Ozan Akkuş, and Randall E. Marcus

Abstract

Biomechanics is the field of study which applies fundamental principles of mechanics to biological problems. Mass, time, and length are the basic variables of the biomechanics, and they are scalar quantities which can be described by a magnitude. Force and moment are vector quantities that take direction (or line) of action into account in addition to the magnitude. Time rate of change of position is velocity, and time rate of change of velocity is acceleration. Force and moment (torque) are the two important concepts at the basis of biomechanics which give forth to linear and rotational motion, respectively. The magnitude of the forces is equal to mass times acceleration. The magnitude of the moment is equal to the force times its moment arm.

The analyses in biomechanics are based on two broad branches of the mechanics: rigid body mechanics and deformable body mechanics. Statics and dynamics are two sub-branches of rigid body mechanics. When the sum of all the forces and moments acting on a body is zero, the body is said to be in static equilibrium. The equations of static equilibrium are often

M. Ünal (✉)
Department of Mechanical and Aerospace Engineering, Case Western Reserve University, Cleveland, OH 44106, USA
e-mail: mxu30@case.edu

O. Akkuş
Department of Mechanical and Aerospace Engineering, Case Western Reserve University, Cleveland, OH 44106, USA

Department of Biomedical Engineering, Case Western Reserve University, Cleveland, OH 44106, USA

Department of Orthopaedics, Case Western Reserve University, Cleveland, OH 44106, USA
e-mail: oxa@case.edu

R.E. Marcus
Department of Orthopaedics, Case Western Reserve University, Cleveland, OH 44106, USA
e-mail: randall.marcus@uhhospitals.org

F. Korkusuz (ed.), *Musculoskeletal Research and Basic Science*,
DOI 10.1007/978-3-319-20777-3_2

used to calculate unknown forces and moments acting on a rigid body. Dynamics is divided into two subfields: kinematics and kinetics where kinematics explains the motion in linear (meters) or angular (radians, degrees) units. Kinetics is the analysis of forces and moments which give forth to the motion. Newton's laws, the work–energy relationship, and the principle of energy conservation can be used to document the relationship between force and motion. Motion in the concept of deformable body mechanics is considered as local changes of the shape within a body (internal movement of the body), called deformations. The focus of deformable body mechanics is to analyze experimentally determined relationships between forces and deformations. Forces and deformations apply to structures such as whole bones or implants. At the material level, load and deformation are required to be normalized by cross-sectional area and length, respectively, to obtain stress and strain. Stress–strain relations reveal material properties such as elastic modulus, resilience, ultimate strength, and toughness. Stress–strain curves provide information about the resistance of the material to fracture at a single loading episode, such as trauma. On the other hand, repeated low level of stress results in failure by fatigue. Material properties of materials are dependent on several factors: their composition, environmental and test conditions, and loading schemes. Biological tissues are viscoelastic materials meaning that their deformation depends on the rate and time of loading. Musculoskeletal tissues are also considered as composite materials meaning that they are composed of at least two different materials. The bone is an example where mineral crystals reinforce a ductile collagen matrix. These tissues are also anisotropic materials meaning that their material properties depend on loading direction. For instance, tendon is the strongest when pulled along its longer axis. Finally, it is essential to determine a safe stress level for a structure in order to account for possible uncertainties in its environment.

Learning Outcomes

This chapter will introduce basic concepts, terms, laws, and principles of mechanics which are required to analyze the complex biomechanical problems in the musculoskeletal system. Next, the concepts related to rigid body mechanics will be described, and their utilization in the static and dynamic analyses of a body will be shown. The last section will introduce the mechanics of deformable bodies and determination of material properties. Throughout this chapter, examples relevant to the musculoskeletal system will be provided.

Terminology

Velocity The rate of change of an object's position over time

Acceleration The rate of change of velocity over time

Force A load quantity causing an object to move or change its shape/volume

Moment A load quantity causing an object to rotate

Statics The field of the mechanics which is concerned with effects of force and moment on a body in equilibrium

Dynamics The field of the mechanics which is concerned with the effects of force and moment on the motion of a body

Energy The ability of an object to do work

Power The time rate of change in work or an amount of the energy consumed per unit time

Stress Force that is normalized by the area of the object

Strain Amount of deformation that is normalized by the original length of an object

Deformation Local changes in the shape of a body

Elastic deformation The amount of deformation of a material that is recoverable upon unloading

Plastic deformation The amount of deformation of a material that is not recoverable upon unloading

Ductility The ability of the material to undergo plastic deformation

Brittleness Material behavior which is described as a sudden failure with little or no plastic deformation

Isotropy Uniformity of material properties in all orientations

Viscosity The ability of resistance to flow

Fatigue Degradation of material properties under cyclic loading

Clinical Relevance

Why do some patients who undergo internal fixation for femoral neck fractures experience iatrogenic subtrochanteric fractures?

A 67-year-old female patient experienced an osteoporotic fracture of the femoral neck. The fracture was fixed by a lateral placement of internal fixation screws (Fig. 2.1). Approximately, 1-month postoperatively, the patient experienced an iatrogenic subtrochanteric femur fracture, requiring a revision surgery during which a cephalomedullary nail was placed to stabilize the subtrochanteric fracture.

Occurrence of the iatrogenic subtrochanteric fracture is a highly biomechanical point in nature. It involves the concepts of load, tensile stress generation on the lateral aspect of proximal femur, amplification of stress at holes, and initiation and growth of microcracks under cyclic load as the patient ambulates.

The proximal femoral cortex is one of the most highly stressed regions in the human body. A free body diagram of the proximal femur would show that joint reaction forces at the hip

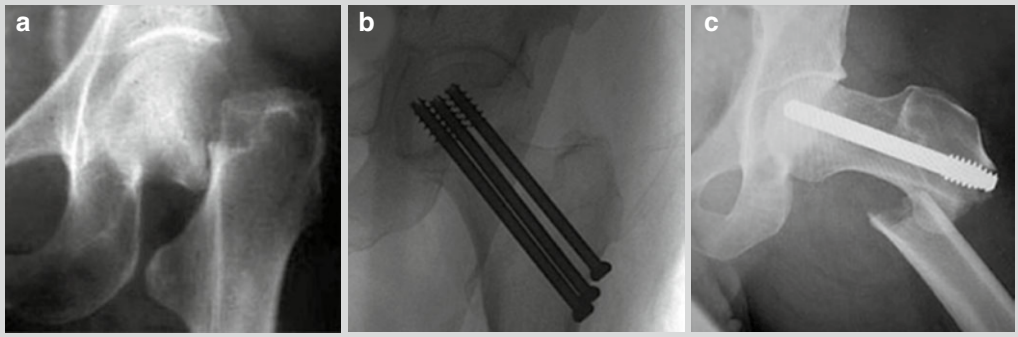

Fig. 2.1 (**a**) Radiograph of preoperative fractured hip, (**b**) radiograph of postoperative *left* hip repaired by internal fixation screws, and (**c**) radiograph of an iatrogenic subtrochanteric fracture in association with the screw hole location at the lateral cortex for treatment of avascular necrosis of the femoral head

and the abductor muscle force at the greater trochanter act collectively to induce tensile stresses at the screw hole sites. The tension is created indirectly through the moment arms via which the joint forces and muscle forces act. As it will be discussed in this chapter, stress concentration occurs at this region due to the abrupt changes in the shape of the structure and causes increase in local stresses at this area. Since there is an abrupt shape change in the screw hole region compared to the whole femoral shape, the stress concentration emerges from this region which in turn to increases the possibility of iatrogenic subtrochanteric fracture risk.

Amplified stresses, when applied repeatedly, may produce microcracks and other forms of plastic damage in the bone, locally around the screw holes. Normally, these microcracks are repaired by the bone itself in a healthy person and do not cause a sudden bone failure. However, in the situation of reduction in bone quality, these microcracks may gradually accumulate under the cyclic loading which results in progressive damage that may result in a fatigue fracture.

Introduction

Biomechanics is a multidisciplinary field integrating biology and fundamental principles of mechanics for studying various biological systems. In biomechanics, the biological system is idealized as a mechanism or a machine, and a broad range of concepts and laws of mechanics including statics, dynamics, deformable body mechanics, and fluid mechanics are used to analyze various biological concepts. These include native and disease states in biological tissues, mechanism of blood circulation, mechanism of air flow in the lung, and gait. Biomechanics is also an essential aspect of improving medical diagnosis and treatment, as well as designing artificial tissues and implants, as well as medical equipment and devices.

Biomechanics is divided into several applied subfields such as kinesiology, cardiovascular biomechanics, sports biomechanics, computational biomechanics, animal biomechanics, plant biomechanics, and musculoskeletal and orthopedic biomechanics. In general, musculoskeletal/orthopedic biomechanics is concerned with the behavior of musculoskeletal systems and implants under external and internal forces. Musculoskeletal/orthopedic biomechanics is also

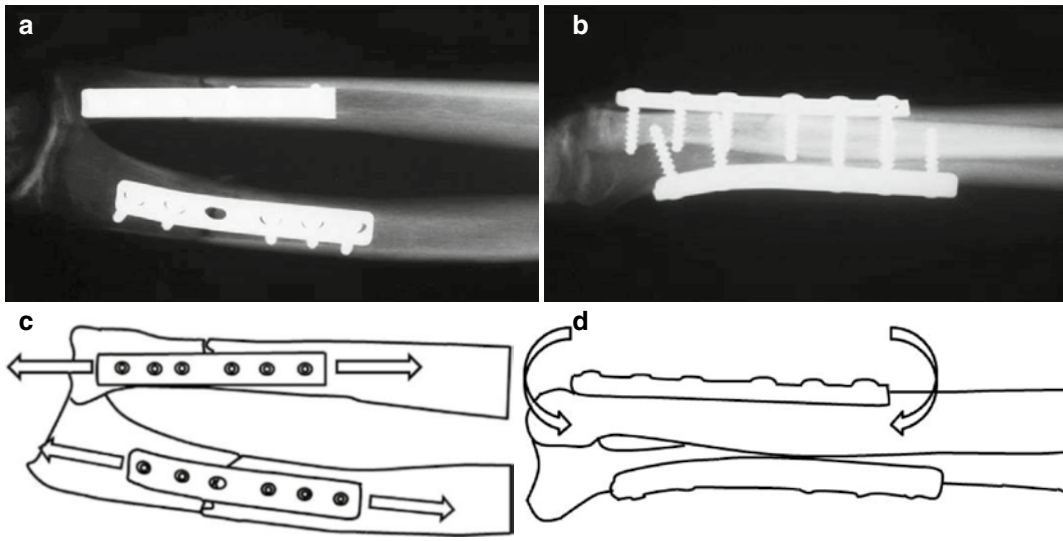

Fig. 2.2 (**a**–**b**) Radiography of internal fixation plates on forearm fractures of the radius and ulna. The plates are load-bearing constructs and must withstand (**c**) tension and (**d**) bending forces until fracture healing is complete

highly relevant to post-surgery rehabilitation. For example, the applied load is shared between the fracture fixation plate and the healing bone (Fig. 2.2). Material and dimensions of the implant will determine whether stresses in implants and native bone tissue will be well within yield stress of each phase. An overly stiff fracture fixation plate may shield the forces from the healing bone, resulting in reduced bone formation and increased bone resorption around the implant. Therefore, it is essential to predict physiological ranges of forces acting on musculoskeletal tissues during daily activities, and it is also critical to predict the mechanical behavior of musculoskeletal tissues and implants under the forces.

Basic Concepts, Principles, and Terms

The term of mechanics in biomechanics refers to classical (Newtonian) mechanics. *Mass*, *time*, and *length* are the basic concepts of classical mechanics and are independent of each other. *Mass* is the amount of matter in an object, and in the International System of Units (SI), its base unit is kilogram (kg). *Time* is the measure of durations of an event and its base unit is second (sec) in SI. *Length* is the measure of dimension of an object and its base unit is meter (m) in SI. All other concepts of mechanics, including *velocity*, *acceleration*, *force*, *moment (torque)*, *work*, *energy*, *stress*, *strain*, etc., are basically derived from these three basic concepts. For example, by definition, *velocity* is the rate of change of an object's position over time, and the change in position is measured by length. Therefore, *velocity* is equal to *length* divided by *time* (m/sec in SI). *Acceleration* is the rate of change of *velocity* over time. Thus, *acceleration* is equal to change in *velocity* divided by *time* over which the change occurred (m/sec^2 in SI).

Before describing the terms and concepts of biomechanics in detail, it is necessary to introduce the meanings of *scalar*, *vector*, and *tensor* concepts. *Scalar* is a quantity that can be represented by a single number representing magnitude. For example, *mass*, *length*, and *time* are scalar quantities: 10 kg, 5 m, and 15 s. On the other hand, *vector* is a quantity that requires the knowledge of direction of action besides the magnitude. It is represented by a line segment with an arrow in which the length of the line represents its magnitude, the location of the arrowhead represents its direction, and the angular position of the line represents its orientation. *Force* and *moment* are examples of *vector* quantities. *Tensor* is an entity that requires magnitude, direction of action, and definition of the area on which the entity is acting. Stress and strain, which will be described in later sections, are *tensor* quantities.

Force and Moment

A force is defined as a load quantity causing an object to move and change the direction and/or amplitude of its motion or the shape/volume of the object. A *force* is a *vector*. The magnitude of *force* is equal to the *mass* of an object multiplied by its *acceleration*:

$$\text{Force} = \text{Mass} * \text{Acceleration} \quad (\mathbf{F} = \text{ma}) \qquad (2.1)$$

Therefore, the unit of *force* in SI is kg.m/sec^2 which is also denoted as a Newton (N). Forces can be categorized in various ways based on their orientation to surface, their direction, or their effects on the object. For example, based on their orientation to the surface of an object, forces can be classified as *normal* or *tangential. Normal force* acts on a direction which is perpendicular to the area on which the force is acting. Joint contact forces, due to lack of friction, are always normal forces. A *tangential force* acts within the plane on which it acts. *Frictional force* is a good example of *tangential force* since it occurs between two contact surfaces in a direction that is parallel to the surfaces when one surface slides over the other.

Normal forces can be classified as *tensile* or *compressive forces*. A *tensile force* tends to elongate the object along the direction of action of the force, whereas a *compressive force* tends to shrink the object along the direction of the force (Fig. 2.3b). For example, tendons experience tensile forces predominantly, whereas some bones such as vertebral bodies undergo compressive forces. *Weight* (*or gravitational force*) is a form of force that is exerted on the object by the gravitation of the Earth to induce a constant accelera-

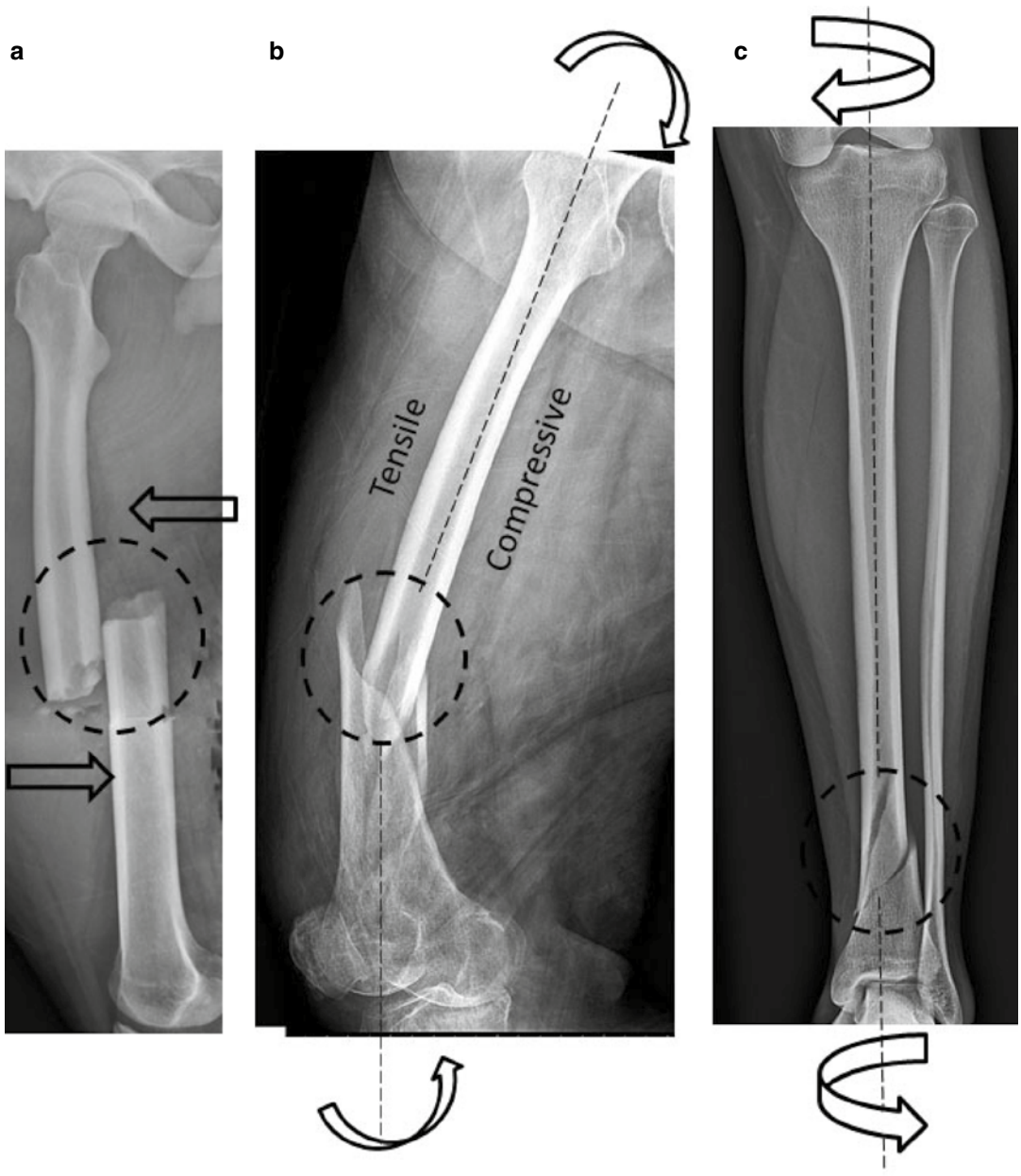

Fig. 2.3 Different loading modes induce different fracture patterns: (**a**) shear, (**b**) butterfly fracture resulting from bending, and (**c**) spiral fracture pattern resulting from torsion. *Arrows* indicate direction of applied forces or moments

tion of 9.8 m/s. Considering a musculoskeletal system, gravitational force is considered as an *external force*, whereas active tension of muscles, passive tension of a tendon, or joint contact forces are considered as *internal forces*.

A *moment* is described as a quantity which causes an object to rotate or distort. One form of moment is the *bending moment* which imparts tensile and compressive forces on the opposing faces of a long bone (or a fracture fixation plate) (Figs. 2.2b–d and 2.3b). *Torque* is another form of moment where the moment is applied about the longer axis of a long object in a twisting action (Fig. 2.3c). The magnitude of the *moment*

of a force about a point is equal to the *applied force* multiplied by the length of the shortest distance between the point and line of action of the applied force, also knowing as *lever or the moment arm*:

$$\text{Moment} = \text{Force} * \text{Moment arm} \quad (\mathbf{M} = \mathbf{F}\mathrm{d}) \tag{2.2}$$

The unit of moment in SI is $kg.m^2/sec^2$ which is also called a Newton meter (N-m). A *moment or torque* is a *vector* entity and is symbolized by a bold *M* or *T*, respectively. The direction of *moment (torque)* vector can be discerned by the right-hand rule. In this rule, the fingers of the right hand that are curled with the segment of the finger from the knuckles to the tips of the fingers are pointed along the applied force. In this state, the right-hand thumb will point in the direction of the moment (torque) vector.

Rigid Body Mechanics

Musculoskeletal system can be considered as a mechanism or a machine involving an actuator, rigid links, and constraint elements. Therefore, the analyses in the biomechanics are based on two broad branches of the mechanics: *rigid body mechanics* and *deformable body mechanics*. Rigid body mechanics itself is divided into two broad categories, *statics* and *dynamics*. The basic assumption in both *statics* and *dynamics* is that a body is not deformed under applied forces. This kind of body is defined as a rigid body. Actually, this assumption is essential to analyze forces and moments acting on a body so as to calculate unknown forces or moments.

Statics is the field of the mechanics which is concerned with effects of force and moment on a body in equilibrium. *Dynamics*, on the other hand, is the field of the mechanics which is concerned with effects of force and moment on a change in the motion of a body. *Dynamics* itself is divided into two subcategories, *kinetics* and *kinematics*, which will be described later in this section.

Musculoskeletal biomechanics, and in fact, entire rigid body mechanics, is concerned with forces and motions and is based on three basic laws (Newton's laws) that govern the relationship between force and motion: (i) *if the net force acting upon a body is zero, the body is either at rest or moves in a straight direction with constant velocity*; (ii) *if the net force acting upon a body is not zero, the body accelerates in the direction of the net force, and the acceleration magnitude is directly proportional to the net force magnitude*; and (iii) *if a body exerts a force upon a second body, the second body simultaneously exerts a force equal in magnitude, but opposite in direction on the first body* [1, 2]. Any type of motion in biomechanics can be explained using the relationship between force and motion.

Newton's laws rest on two assumptions: physical equilibrium and the conservation of energy. Equilibrium is positioned in the first and second laws, whereas the conservation of energy is positioned in the third law [1, 2]. The equilibrium can be *static* or *dynamic*.

Using the description of the first law, if a body is at rest, it is clear that there cannot be any unbalanced applied forces on the body. In this definition, a body that is not moving or a body that is moving at constant velocity is considered to be at rest. Therefore, static equilibrium is a lack of acceleration, not necessarily the lack of motion. This situation is termed as *static equilibrium*. In static equilibrium, the sum of the forces acting on the body must be zero. The extension of this law is that the sum of the external moments must also be zero for the body to be at rest. This law for static equilibrium can be expressed as

$$\sum \text{Forces} = 0 \tag{2.3}$$

$$\sum \text{Moment} = 0 \tag{2.4}$$

where the symbol Σ is the sum of all forces/moments or net force/moment. These two equations can be applied to all body parts assumed in static equilibrium and used to calculate forces/moments acting on the musculoskeletal systems. Using these equations, the unknown forces/moments in a static equilibrium can be also calculated. For instance, known ground reaction forces and limb weight can be used to predict the joint forces and moments at the knee.

The general approach in static analysis to determine the magnitude and directions of the unknown forces/moments is as follows:

1. Sketch a *free body diagram*. Construction of the diagram involves a "virtual dissection" process which isolates the part of the body whose free body diagram is to be constructed.
   (a) When ligaments, tendons, and muscles are "dissected," they are replaced with tensile forces.
   (b) When the dissection is along a joint articulation surface, a joint reaction force is introduced. The joint reaction force is generally oriented perpendicularly to the joint surface with its line of action directed toward the center of rotation of the joint (e.g., the center of the femoral head, with the femoral head idealized as a hemisphere).
   (c) The gravitational forces due to the weights of limbs are applied to the diagram at the center of the mass of the limb. Anthropometric data on limb weights as a fraction of whole body weight and locations of limb centers of masses are available in the literature ([3] or see appendix 2 in [4]).
   (d) If the dissection is performed away from the limb and away from the articulation surfaces, then tensile forces for dissecting muscles and internal reaction forces and moments for dissecting the bone are to be added (see the example of free body diagram in the example below).
2. Sum of the forces and moments in the x-, y-, and z-axes is equal to zero. In three-dimensional space, these provide six equations using which up to six unknown forces and/or moments can be solved for per diagram. In two-dimensional problems, three equations can be derived: two for force balance in the x- and y-axes and one for moment along the z-axis.
3. Solve for the unknown forces/moments using linear algebraic equations.

A *free body diagram* is a simplified drawing of an object including the approximate location, direction, and magnitude of all the forces and moments acting on the object, excluding any flexible joints. For example, the free body diagram of a raised arm holding a dumbbell (Fig. 2.4a) that is detached at the shoulder joint includes gravitational forces due to the mass of the arm and the dumbbell, a joint reaction force on the humerus from the glenoid, and the force of the deltoid muscle contraction (Fig. 2.4b). The anatomical knowledge on the muscle line of actions, muscle attachment points, and bone morphology is useful and needed in constructing the diagram.

When a body is not in *static equilibrium*, the net force on the body cannot be zero, and the body is accelerating along the direction of the net force. A motion herein can be classified as linear (translational), angular (rotational), or general (both linear and angular) motion [2]. *Linear motion or translation* is the simultaneous movement of all parts of the body by the same distance and in the same direction, such as pushing a block on a horizontal surface. *Angular motion* is the simultaneous circular movement of all parts of a body by the same angle and in the same direction, such as the example of the thigh during walking that rotates about the hip. In angular motion, the force acts eccentrically to the center of mass (center of rotation) that causes rotation. *General motion* is the occurrence of both linear and angular motions simultaneously. For example, the lower extremities have both linear and angular motion during walking. The concepts of statics are not valid anymore if a body is accelerating under one or more of these three motions, and the concepts of dynamics begin to apply. In fact, the fundamental concepts of dynamics are space (displacement), time, mass, and force. Velocity, acceleration, torque, moment, work, energy, power, impulse, and momentum are the derived concepts from the fundamental concepts of dynamics.

Dynamics is divided into two subcategories, *kinematics* and *kinetics. Kinematics* is concerned with description of the motion of a point, an

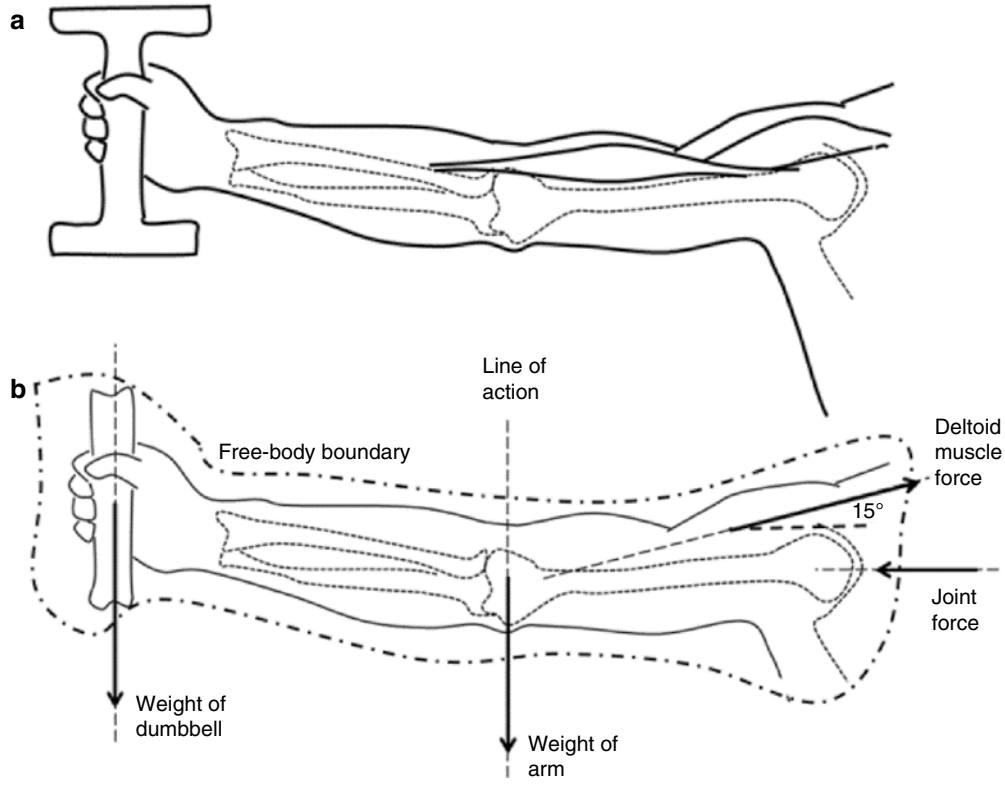

Fig. 2.4 (**a**) Anatomical view and (**b**) the free body diagram of a raised arm holding a dumbbell that is dissected at the shoulder joint

object, or a system without dealing with forces and torques causing the motion. Kinematic analyses involve the understanding of the relationship between displacement, velocity, and acceleration vectors. *Kinetics*, on the other hand, is concerned with the analysis of forces and torques that cause the motion. Both kinematics and kinetics are bound by Newton's second law which is also known as the law of acceleration [2]. The law states that if the net force acting upon a body is not zero, a body accelerates in the direction of the net force, and the acceleration magnitude is directly proportional to the net force magnitude. Using this description in the second law, if a body is not in static equilibrium, it is clear that there is at least one unbalanced applied force on the body that causes the motion. The extension of this law is that the sum of the external moments is not zero if the body has a motion. This situation is described by *dynamic equilibrium*. The law for dynamic equilibrium then can be expressed in the following equations:

$$\sum \text{Forces} = ma \tag{2.5}$$

$$\sum \text{Moment} = I\alpha \tag{2.6}$$

where m is the mass of a body, a is the acceleration of the center of mass, I is the moment of inertia that is the distribution of mass about the center of rotation and is dependent on the shape of the body, and α is the angular acceleration (radian/sec^2 in SI unit). These two equations can be applied to all body parts assumed in dynamic equilibrium and used to calculate forces/moments acting on the musculoskeletal systems. Using these equations, the unknown forces/moments in a dynamic equilibrium can also be

calculated. The general approach in dynamic analysis is to determine the magnitude and directions of unknown variables in the following:

1. Sketch a *free body diagram*, and indicate correct directions of all known forces, moments, or accelerations. If the direction of them is not known, it can be then assumed as positive direction.
2. Choose convenient coordinate systems such as the Cartesian or polar coordinates.
3. Apply the equations of motion, and solve for the unknown variables.
4. If the result appears with a negative value, it means that the originally chosen directions are to be reversed.

Using the equation of motion (Newton's second law) for kinetic characteristic of a body is convenient if the applied forces or moments are constant. However, the solution of the equations sometimes may be difficult and complex in terms of having no constant force and moment. In such a situation, the concepts of *work* and *energy* can be applied to solve this kind of complex problem.

Work is defined as a quantity of force required to move an object through a distance or is the product of a force that is corresponding to displacement. W*ork* is a scalar quantity, and the *work* done by a constant force is equal to the magnitude of the *force* multiplied by the *displacement* moved in the direction of the force:

$$\text{Work} = \text{Force} * \text{Displacement} \quad (W = \text{Fx}) \tag{2.7}$$

The work done by a force that is changing with time, on the other hand, can be calculated as the integral of the force over the distance applied:

$$\text{Work} = \int_{x1}^{x2} \text{Force}_x \, dx \quad \left(W = \int_{x1}^{x2} F_x \, dx \right) \tag{2.8}$$

Therefore, the standard unit of *work* in SI is kg.m^2/sec^2 which is also called a Newton meter (N-m) or joule (J). For a force to do *work*, a body must have a displacement. Moreover, *work* done by force can be positive or negative. For example, if a force applied on a body has the same direction of displacement, the work done by the force is positive. However, if the force and displacement have opposite directions as in the example of a frictional force, the work done by the frictional force is negative.

Energy can be simply defined as the ability to do work. Actually, *work* is the result of releasing of the energy from an object. The *energy* can be in various forms including mechanical, chemical, or thermal. In mechanics, the energy can be categorized as *potential* or *kinetic energy*.

Potential energy refers to stored energy associated with position and elevation of an object. *Energy* is a scalar quantity, and *potential energy* is equal to the magnitude of the *weight (mass x gravitational acceleration)* multiplied by the *height* of the object measured relative to a reference point:

$$\text{Potential energy} = \text{Weight} * \text{Height} \quad (E_P = \text{mgh}) \tag{2.9}$$

Kinetic energy, on the other hand, refers to the energy of motion, and every moving object, in fact, has kinetic energy. *Kinetic energy* is associated with velocity and is equal to the magnitude of one-half of the *mass* multiplied by the square of *velocity* of the object:

$$\text{Kinetic energy} = \frac{1}{2} * \text{Mass} * \text{Velocity}^2 \quad \left(E_K = \frac{1}{2} \text{m} v^2 \right) \tag{2.10}$$

Therefore, the standard unit of *energy* is the same with *work*, in SI kg.m^2/sec^2 which is also called a Newton meter (N-meter) or joule (J). The concept of *energy* is closely associated with the concept of *work* such that the net work done on an object to move from one position to another is actually equal to the change in its kinetic energy. This relationship between *kinetic energy* and *work* is known as the *work–energy theorem*:

$$\text{Net Work} = \text{Kinetic energy}_2 - \text{Kinetic energy}_1 \quad (W_{\text{net}} = E_{K2} - E_{K1}) \tag{2.11}$$

Another important principle in the *energy* concept is the *conservation of energy* defined as the concept that the total energy of a system (sum of both kinetic and potential energy) remains constant during motion. It means that *energy* can be converted to another type of energy throughout a motion; however, the sum does not change. This principle can be stated between any two points for mechanical energy as follows:

$$\text{Kinetic energy}_1 + \text{Potential energy}_1 = \text{Kinetic energy}_2 + \text{Potential energy}_2 \quad (2.12)$$

Power, as a part of work and energy concepts, can be defined as the rate time of doing *work* or an amount of the *energy* consumed per unit time. Power is also a scalar quantity and is equal to the *work* divided by *time*:

$$\text{Power} = \text{Work} / \text{Time} \quad \left(P = \text{W} / \text{t}\right) \quad (2.13)$$

Therefore, the standard unit of *power* is in SI $kg.m^2/sec^3$ which is also called as watt (W).

Describing the terms of *work* and *energy*, using the equation of motion (the second law) for the kinetic characteristic of a body is not convenient if the applied forces or moments are not constant. *The work–energy theorem* and the *principle of conservation of energy* provide an alternative solution approach for this kind of problem in dynamics. Especially, the problem involving nonconservative forces can be solved using *the work–energy theorem*, whereas the problem involving only conservative forces can be solved using the *principle of conversation of energy.* Comparing this to the equation of motion, both of these methods are easier to apply especially when the problem or solution involves information about velocity rather than acceleration. Definitions of important concepts introduced through this section and various methods of analyses in biomechanics are summarized in Table 2.1.

In general terms, the focus of the concepts of rigid body mechanics in the field of biomechanics is to predict and analyze the internal forces or moments of the musculoskeletal system when supporting the external forces and moments during motion of the skeleton as well as joint stability in various activities. For example, in order to move, lift, or carry on an object, musculoskeletal system must generate different types of internal forces: muscle forces, joint contact forces, as well as passive soft tissue forces throughout the upper limbs and lower limbs. Another example for the application of rigid body mechanics to musculoskeletal biomechanics is joint stability. The primary function of joints is to provide mobility to the skeletal system with a degree of stability which is maintained through the muscle forces around the joints as well as joint contact forces. The problem of interest in biomechanics using the concepts of rigid body mechanics is to analyze these internal forces generated by the musculoskeletal system in order to understand the various activities performed by the musculoskeletal system.

Table 2.1 Summary of basic equations and formulas in biomechanics

Static equilibrium	$\sum F = 0, \sum M = 0$
Dynamic equilibrium (equation of motion)	$\sum F = \text{ma}, \sum M = \text{I}\alpha$
Work done by a constant force	$W = \text{Fx}$
Work done by a varying force	$W = \int_{x1}^{x2} F_x \, dx$
Potential energy	$E_P = \text{mgh}$
Kinetic energy	$E_K = \frac{1}{2}\text{mv}^2$
Work–energy theorem	$W_{net} = E_{K2} - E_{K1}$
Conservation of energy principle	$E_{K1} + E_{P1} = E_{K2} + E_{P2}$

Mechanical Behavior of Materials

The previous section defined the concepts of force and moment and examined their effects on a rigid body in which the body is in equilibrium and does not deform under applied forces (i.e., musculoskeletal system). This examination is performed by isolating a portion of a structure as a free body diagram and applying the basic principles of rigid body mechanics in order to find the forces and moments acting on the body. In this section, an overview of the ability of musculoskeletal materi-

als (e.g., tissues, implants' material, and so on) to withstand external or internal forces will be provided. This involves the basic principles of deformable body mechanics in order to analyze these forces. In deformable body mechanics, a body is not considered as a rigid body anymore, and the deformability and material behaviors of the body are also incorporated into the analyses. Upon the action of forces, the size and/or shape of an object changes. Deformable body mechanics will be covered as *elastic*, *plastic*, and *viscoelastic materials*. The focus of deformable body mechanics is to analyze experimentally determined relationships between applied forces and deformations for musculoskeletal systems and implants. In addition to applied forces, changes in shape and/or size are associated with material properties of the body as well as other factors which will be discussed in detail later in the following sections. Before describing more advanced concepts and principles of deformable body mechanics, it is essential to understand the basic concepts of *stress* and *strain*.

Stress and Strain

It is important to make the distinction between the "structure" and "material" at this point. Material is the basic building block which makes up the structure. For instance, all tendons are made up of collagen-rich material. At the material level, all tendons have comparable *material properties*. On the other hand, tendons may differ substantially in terms of their *structural mechanical properties*, such as the weak and nimble flexor tendons vs. the bulky Achilles tendon. Force acting on structures causes a deformation. The magnitude of required force for such deformation depends on geometry of the structures. Force-displacement concept characterizes structural level (i.e., geometry-dependent) mechanical properties. On the other hand, force-displacement concept does not reveal material level properties which are geometry-indepedent. For example, if we consider two femurs with different cross-sectional areas (thickness of mid-shaft), the required forces to deform the smaller femur are less than that of the femur having larger cross-sectional area (Fig. 2.5). Therefore, the forces acting on the body must be normalized to the cross-sectional area so as to reveal material level reincarnation of force. Force that is normalized by area is called *stress*. Stress is a tensor quality and symbolized by σ. The magnitude of *stress* is equal to *force* divided by the *cross-sectional area (per unit area)*:

$$\text{Stress} = \text{Force} / \text{Area} \quad \left(\boldsymbol{\sigma} = \mathbf{F} / A\right) \tag{2.14}$$

Therefore, the standard unit of *stress* in SI is kg/m.sec^2 which is also called a Newton/meter^2 (N/m^2) or pascal (Pa). *Stress* can be categorized in various ways based on its orientation to the

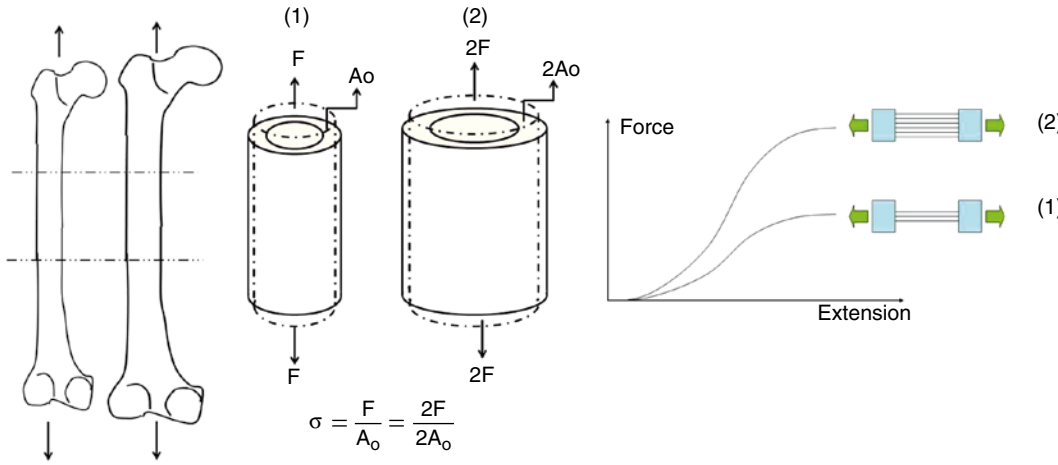

Fig. 2.5 Stress concept: forces acting on the body must be normalized to the cross-sectional area so as to reveal material level reincarnation of force

object surface or loading direction. For example, it is called *normal stress* if the stress is acting perpendicular (normal) to the object surface or it is called *shear stress* (Fig. 2.3a) (symbolized by τ) if the stress is acting parallel or tangential to the surface. Moreover, if stress is emerging from an applied force that is in tensile mode, then the stress is called a *tensile stress*, and vice versa applies for *compressive stress* (Fig. 2.3b).

Strain is another important concept in deformable body mechanics to properly measure the amount/intensity of deformation in a body. If we again consider two femurs with same cross-sectional area but with different lengths, the longer body will deform proportionally more under the same amount of tensile force. Therefore, in order to eliminate this size dependence of deformation, the amount of the elongation is normalized by the original length of the body, resulting in *strain (unit deformation).* Strain also is a tensor quality and symbolized by ε (Fig. 2.6). For tensile loading, the magnitude of *strain* is equal to *amount of the elongation* divided by *original length* of the body:

$$\text{Strain} = \text{Amount of elongation} / \text{original length} \quad \left(\varepsilon = \Delta L / L_o\right) \tag{2.15}$$

In more general terms, strain is calculated by dividing a length quantity by the original length quantity. Since length is normalized to length, the unit of *strain* is dimensionless meaning that there is no standard unit for it. However, strain is generally used with the term of millimeter/millimeter (mm/mm). Furthermore, strain can be also reported as a percent elongation, such that the value of strain is multiplied by 100 % (e.g., 0.3 strain equals 30 % strain, where the body which was 1 unit in length was elongated to 1.3 units in length). Another form of depiction of strain is μstrain. As an example, 5000 μstrain is 5000/1,000,000 = 0.005 strain that is also equivalent to 0.5 % strain.

Strain can be basically categorized as *normal* and *shear strain. Normal strain* is emerged due to the axial forces (tensile or compressive) and associated with a change (increase or decrease, respectively) in length. It could be a positive or a negative quantity depending on tension or compressive forces, respectively. Another form of strain is called *shear strain* (symbolized by γ) which is strain due to shear forces. In shear strain, the deformation is associated with the change in the angle of a surface of a body, calculated as the tangent of the angle (Fig. 2.7). Therefore, shear strain distorts the body and changes its shape. Like normal strain, shear strain is dimensionless.

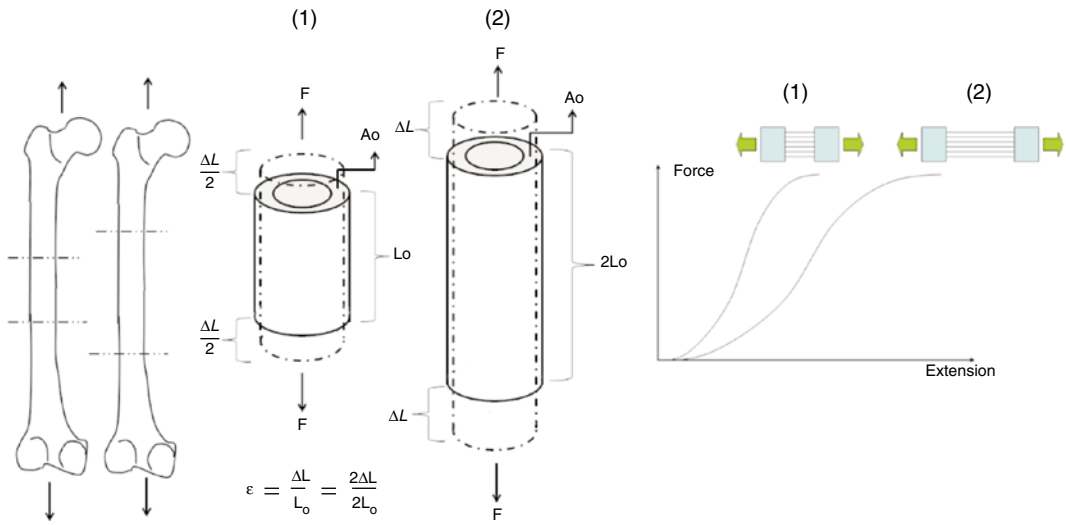

Fig. 2.6 Strain concept: the amount of the elongation is normalized by the original length of the body

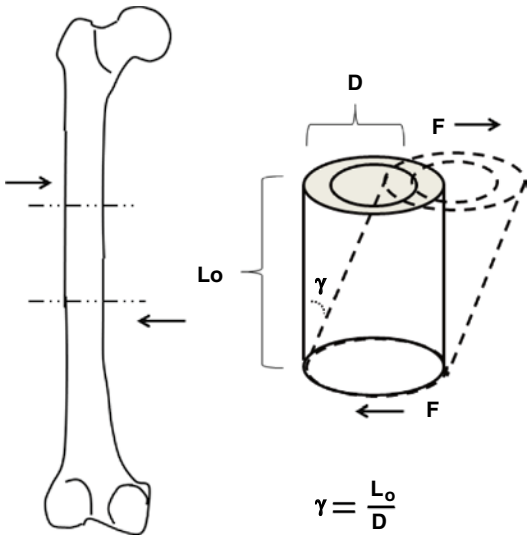

Fig. 2.7 Shear strain concept: the deformation is associated with the change in the angle of a surface of the body, calculated as tangent of the angle

It is important to state that stress and strain described herein is called *engineering stress* and *engineering strain* where stress and strain calculated based on the original dimensions (i.e., cross-sectional area and gauge length) of the sample and not the instantaneous values of the dimensions during mechanical strength test. If the latter are employed, resulting values are termed as *true stress* and *true strain*.

Stress–Strain Curves

In order to analyze the material behavior and properties, the most common approach is to conduct mechanical strength tests during which force and displacement of the material are measured under various loading schemes: tension, compression, shear, or bending. Loading rates can be varied to emulate habitual physiological loading rates or high rates encountered during trauma. Force–displacement data obtained from the mechanical strength tests provide information on the structural properties and do not provide any direct information about material properties. On the other hand, stress-strain curves converted from force-deformation curves using Eqs. 2.14 and 2.15 can be used to determine the material properties.

The relationship between stress and strain is demonstrated with a graph where stress (σ) is along the *y*-axis and strain (ε) along the *x*-axis. This graph is called *stress–strain curve (diagram)* which has several variables and regions of interest. Different materials exhibit different stress–strain curves such that the magnitude and shape of the curves depend on compositional and structural properties of the materials. Therefore, comparison of any two stress–strain curves allows determining which material is relatively more ductile, more brittle, stiffer, or tougher. These concepts are described in detail later in this section.

In general, the stress–strain curve includes different characteristic points depending on the material itself and/or the mechanical test type (i.e., tension, compression, or bending). These characteristic points on the curve may include *origin* (O), *elastic (E)*, *yield* (Y), *ultimate strength* (US), and *failure* (*fracture)* (F) points (Fig. 2.8a). While some materials exhibit all these characteristic points on the curve, others may not exhibit all clearly. If we look at a stress–strain curve in Fig. 2.8a, the point O is the origin of the stress–strain curve, and there is no load and deformation at this point. Point E on the curve is the elastic limit of the material. Between points O and E, the stress and strain are linearly proportional, and the deformation is *elastic* (i.e., recoverable) such that the material returns to its original size and shape upon unloading. Point Y represents the *yield point* which marks the transition from the elastic regime to the *plastic* (permanent) regime during which the material will not return to its original size and shape upon unloading. The corresponding material strength at point Y is called as *yield strength* (σ_y), and the strain at this level is called as *yield strain*. Another hallmark of yield point is that the slope of the stress–strain curve reduces; in other words, it takes less stress to induce more deformation. Point U at the curve represents the maximum stress of the material and is called its *ultimate strength* (σ_u), and the strain at this point is called its *ultimate strain*. After point U, depending on the material or test type, the stress can be decreased (this phenomenon is called necking) or continued at the same level until

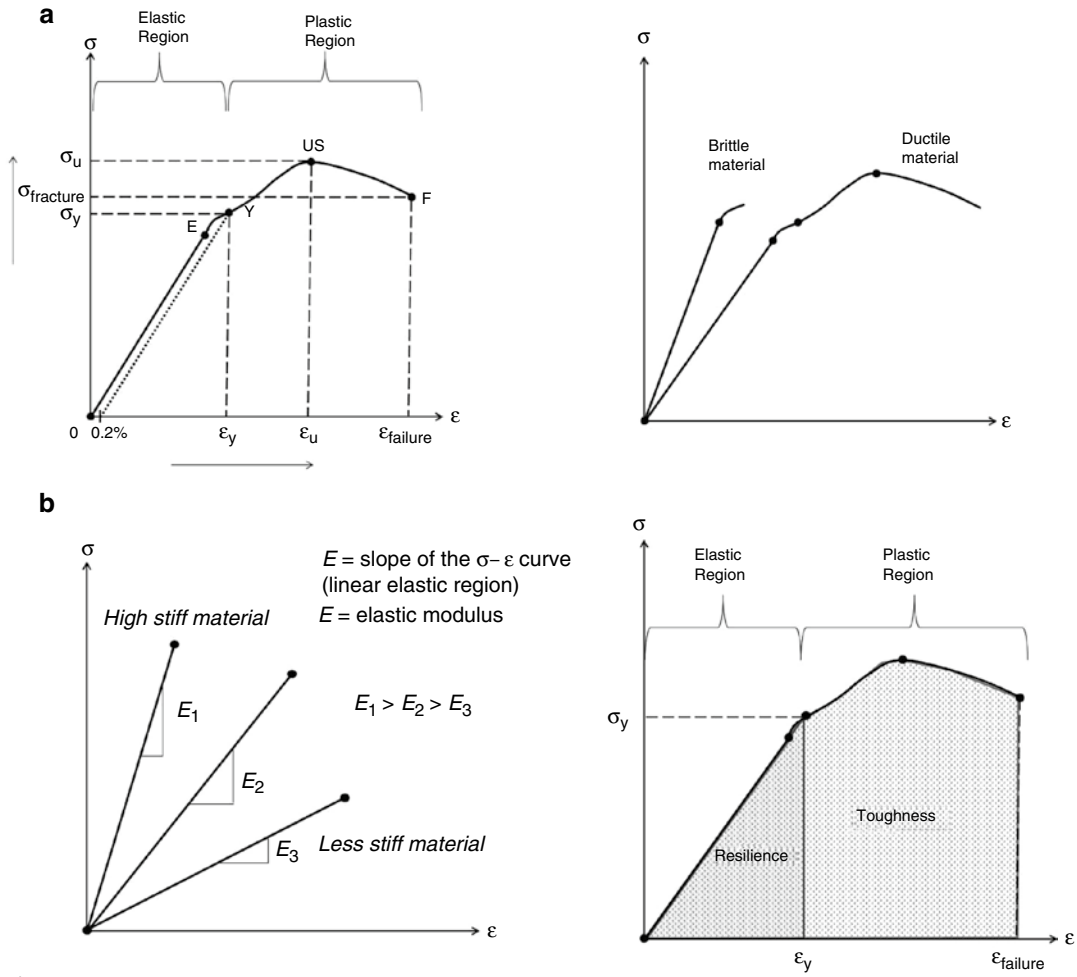

Fig. 2.8 (**a**) Stress–strain curve with its characteristic points and stress–strain curve of brittle and ductile material, respectively. (**b**) The elastic modulus (*E*) is closely associated with stiffness such that the higher the elastic modulus, the stiffer material and the internal work in the elastic and entire region are equal to the areas under the corresponding regions which are called as resilience (area under the elastic region) and toughness (area under the entire region).

point F which is the last point on the curve and represents the *failure (fracture)* or *rupture* point of the material.

In some materials, it is not easy to distinguish specific yield point of the material. The yield point, in this situation, is determined by using the *offset method* which entails drawing a line parallel to the linear part of the stress–strain curve but offset by a strain level at about 0.2 % or 0.002. The intersection point of the line with the stress–strain curve is considered the yield point (Fig. 2.8a).

Depending on the stress–strain curve, material behaviors can be divided into two broad categories: *ductile* or *brittle.* Ductile behavior (ductility) is characterized by the ability of the material to undergo post-yield deformation. Brittle behavior, on the other hand, is characterized by failure soon after passing the elastic point. In this perspective, it can be said that a *ductile material* exhibits a larger plastic deformation prior the failure, whereas a *brittle material* exhibits sudden failure without revealing much plastic deformation (Fig. 2.8a). However, this does not necessarily mean that the brittle material is weak compared to the ductile material. Another categorization is quasi-brittle behavior which is a crossover between ductile and brittle.

Bone is considered quasi-brittle, at least relative to tissues such as ligaments. Ceramics and glass are fine examples of brittle materials. They may have high strength and high stiffness, but at the same time they fail without a significant amount of plastic deformation. Failure of brittle materials is often catastrophic and occurs without any signs. Conversely, ductile materials deform notably prior to frank fracture which helps to determine the onset of the failure.

Table 2.2 Elastic modulus of bone and selective materials in orthopedic applications

Alumina	380 GPa
316 steel	190 GPa
Co–Cr–Mo	210 GPa
Ti-6AL-4 V	110 GPa
Cortical bone	17 GPa
Bone cement	2 GPa
UHMWPE	1 GPa
Cancellous bone	10 MPa- 1 GPa

Mechanical Behavior of Materials

As mentioned earlier in this section, the stress–strain curve of a material reveals many material properties of a body. If we consider the region of the stress–strain curve between origin (O) and yield point (Y) (Fig. 2.8a), the stress is linearly proportional to strain as shown by a straight line with the constant proportionality which is the slope of the straight line. The deformation in this region is called elastic which is totally recoverable upon unloading (this ability of a material is known as elasticity). This behavior of a material is actually similar to that of a spring, such that the material is also able to store potential energy under applied forces, and the energy is then released upon removing the forces to return its original shape. This linear relationship in the elastic region is known as Hooke's law and described as

$$\sigma = E\varepsilon \tag{2.16}$$

where E is the slope, and its value is not related to size or shape of the material, only to the material itself. The value of E is a material property that is referred to as the *modulus of elasticity*, and it is also often called the *elastic modulus* or *Young's modulus*. Young's modulus represents the resistance of the material to deformation under axial loading (tension or compression) which is called the *stiffness (rigidity)* of the material. The elastic modulus is closely associated with stiffness such that the higher the elastic modulus, the stiffer the material and the higher its resistance to deformation (Fig. 2.8b). Since the unit of stress is pascal (Pa) and strain is dimensionless, the unit of elastic modulus then becomes pascal (Pa) as well. Generally the modulus of materials is represented as a megapascal (MPa) or gigapascal (GPa). Elastic modulus of selective materials used in orthopedic applications is summarized in Table 2.2.

On the other hand, shear stress–strain curve also exhibits the same linear relationship in the elastic region and is described with

$$\tau = G\gamma \tag{2.17}$$

where G is termed as *modulus of rigidity* and is often called as *shear modulus*. Like the elastic modulus, the shear modulus is also a material property which is a measure of resistance of the material under shear or torsional loading.

The third type of elastic material concept is called the *Poisson's effect* which is quantified by comparing the strain magnitude in the direction perpendicular to loading with the strain magnitude in the direction of loading. In more specific terms, when a body is longitudinally stretched (positive strain), it transversely contracts (negative strain) simultaneously, and within the elastic region of a stress–strain curve, the ratio of transverse (lateral) strain to longitudinal (axial) strain is constant which is called *Poisson's ratio* denoted by the symbol ν:

$$\nu = \frac{-\varepsilon_{\text{trans}}}{\varepsilon_{\text{long}}} \tag{2.18}$$

The negative sign ensures a positive ratio for most materials because the transverse and longitudinal strains have opposite signs. *Poisson's ratio* is less than 0.5 (in general the range from 0 to 0.5). Most materials have Poisson's ratio values in the 0.2–0.3 range. Materials with ratio values closer to zero are those materials which contract minimally in the transverse direction. A cork is a good example of this type of material.

The theoretical upper limit of 0.5 implies incompressibility meaning that under tension or compression load, the material's volume does not change. Every material has three elastic material properties which are the *elastic modulus*, *shear modulus*, and *Poisson's ratio*. These three properties are interrelated and each can be calculated by using the other two:

$$G = \frac{E}{2\times(1+\nu)} \tag{2.19}$$

In previous sections, we discussed the concept of work as force multiplied by the displacement in the direction of the force and the concept of energy as the potential to do work. Since stress and strain are associated with force and displacement, respectively, the concepts of work and energy are applicable in deformable body mechanics such that stress multiplied by strain is equal to the work done on a body per unit of volume by the applied forces. This is referred to as *internal work*, and this work is stored as *internal strain energy* in the material. Therefore, if we consider the stress–strain curve, the internal work in the elastic region (until yield point) is equal to the area under the corresponding region which is the area of the triangle (Fig. 2.8b). This quantity reveals another important material property, that is, the ability of the material to absorb energy without plastic deformation, called the *resilience* of the material and measured by *modulus of resilience* as $\sigma_y\varepsilon_y/2$. Its unit is the same as stress or modulus of elasticity since the unit of strain energy per unit volume is N/m^2 or a pascal (Pa).

Up until this point, the elastic region of the stress–strain curve has been examined in detail. However, many material properties can also be obtained from the stress–strain curve beyond the elastic region which is called as plastic region where permanent deformation occurs. As discussed above, applying the concepts of work and energy to the entire region (both elastic and plastic) of the stress–strain curve reveals the material property that is the ability of the material to absorb energy before failure. This material property is called *toughness*, and the larger the area under the curve, the tougher the material (Fig. 2.8b). The mechanical strength of a material can be expressed in terms of maximum stress or toughness of the material. It is important to note that two materials can be equally tough although their other material properties (i.e., elastic modulus, ultimate strength, or stiffness) are different.

As discussed earlier in this section, the corresponding material strength at the yield point is called its *yield strength* which represents the upper limit of the load that can be applied without plastic deformation. Especially, in orthopedic applications, it is critical to avoid reaching the yield point of biological tissues or implants (Fig. 2.9a) in order to ensure that they continue to sustain their proper structure and functions. The maximum stress of the material called *ultimate strength* is another material property representing the highest stress level that can be reached without failure. In orthopedic applications, when the forces exceed the implant's ultimate strength, the implant fractures (Fig. 2.9b). The *ductility* of material, on the other hand, is another material property obtained from the curve which represents the amount of plastic strain that it can store before failure.

It is important to note that many factors affect stress–strain curve of a material such as environmental conditions (e.g., temperature, humidity), test protocol (i.e., loading time and strain rate), and different load modes (i.e., static or cyclic loading) which will be discussed in the following sections. When possible, biomechanical tests should be conducted under loading rates, temperature, and fluid conditions (serum, synovium) which approximate those encountered physiologically.

Even though they are not directly associated with the stress–strain curve, there are other important material behaviors affecting material properties. To this point, it is considered that the composition and microstructure of the materials are uniformly distributed in all regions of a body. Therefore, the obtained material properties have also been considered uniform (homogeneously distributed) throughout the volume of a body meaning that the material properties are independent of the direction or orientation (longitudinal or transverse) of the loading. This

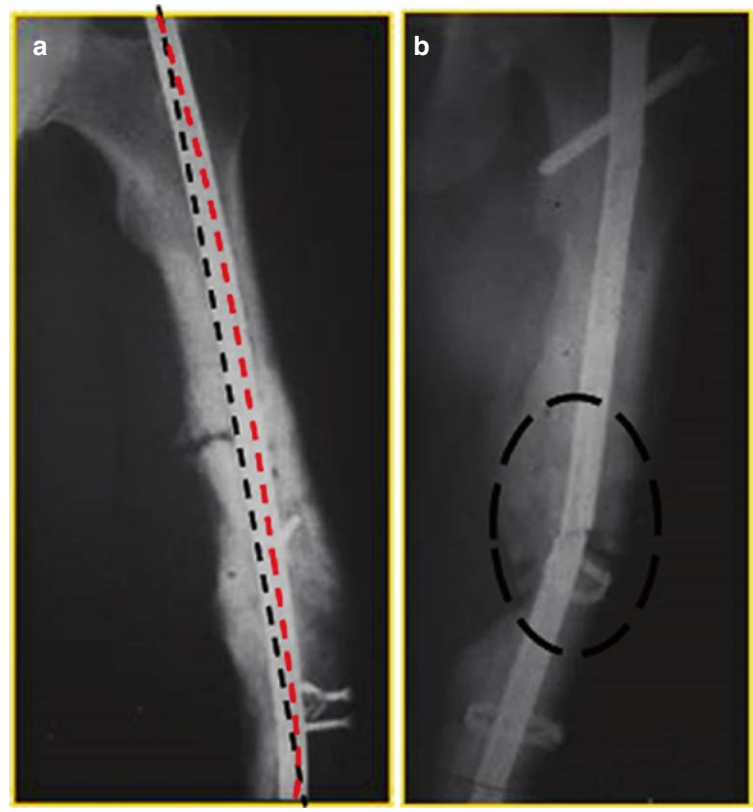

Fig. 2.9 (**a**) Intramedullary nail with plastic deformation. The stress forces have exceeded the implant's elastic (*E*) limit. *Black dashed line* is the natural axis of the implant. *Red dashed line* indicates plastic deformation due to the bending force. (**b**) Intramedullary nail that has fractured. The stress forces have exceeded the implant's ultimate strength (*US*)

phenomenon is called *isotropy*. Therefore, if the material properties are independent of the loading direction, the material is termed as *isotropic material* such as metals, ceramics, and plastics. However, the composition and microstructure of most biological tissues (e.g., bone, cartilage, tendon, and so on) are inhomogeneous throughout their volume. Therefore, the material properties also display variety depending on loading direction [5, 6]. This kind of material is referred an *anisotropic material*. For instance, the bone is a good example of an anisotropic material since the strength of the bone is dependent on its density and microstructure as well as the direction which the strength is measured, such that the typical material properties (elastic modulus, toughness, stiffness, and so on) measured from healthy (or young) bone are much higher than that of osteoporotic (or aged) bone [7–9]. Furthermore, even within the same healthy bone samples, the material properties measured in the loading direction corresponding to the long axis (longitudinal) of the bone are quite different than those in the loading direction parallel to transverse direction in the bone [10, 11] (Fig. 2.10a).

Beyond homogeneity of the biological tissues, the environmental conditions (e.g., temperature and humidity) can also affect the material properties of biological tissues [5, 12]. For example, it is well known that increasing temperature causes dehydration of bone which in turn changes its material properties [11, 13].

So far, the relationship between stress and strain has been considered as independent of loading time and strain rate, and materials are considered elastic materials when they can return to their original shapes upon removing the applied loads or plastic materials when they are permanently deformed upon loading. In both cases, the material behaviors are not dependent on loading time and rate. However, a different group of materials including polymers and almost all biological tissues displays time-dependent behavior involving

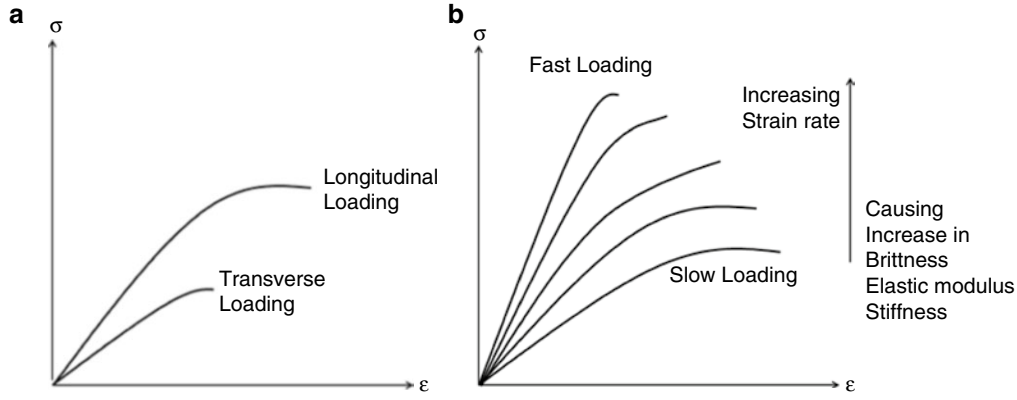

Fig. 2.10 (**a**) The direction-dependent stress–strain *curves* for bone. (**b**) The strain rate-dependent stress–strain curves for cortical bone

gradual deformation and recovery upon loading and unloading. This time-dependent material behavior is called *viscoelasticity.*

Before discussing viscoelasticity in detail, it is important to distinguish between deformations in solid and fluid material which are quite different from each other. The deformation in a solid material takes the form of size and/or shape changes and continues to a certain point, whereas the deformation in fluid materials takes the form of flow and continuously proceeds. Viscosity, in this perspective, is a fluid property which is the ability of resistance to flow deformation. In nature, there are a group of materials which carry both solid-like and fluid-like characteristics. Such materials are termed as *viscoelastic materials*. The material properties of viscoelastic materials are dependent on how quickly the material is loaded and unloaded at a prescribed strain rate (amount of deformation per unit time). The bone is a good example of a viscoelastic material since it exhibits time-dependent behavior such that an increasing rate of stress loading in a mechanical test causes an increase in its elastic modulus, strength, and brittleness of the bone [11, 14, 15] (Fig. 2.10b). That is why traumatic fracture of the bone is generally comminuted with multiple fracture fragments.

The responses of viscoelastic materials to changes in stress and strain are examined through two experiments involving the application of a constant force and deformation. When a viscoelastic material is subjected to a constant force (Fig. 2.11a), the response of the material is a time-dependent increase in deformation, referred to as *creep.* Upon unloading, the response of the material is called *recovery* (Fig. 2.11b). On the other hand, when a viscoelastic material is subjected to a constant deformation (elongation) (Fig. 2.11c), the response of the material is a time-dependent decrease in stress, called *stress relaxation* (Fig. 2.11d). In order to explain the viscoelastic behavior of a material, the common approach is to fit the data into one of the three empirical models involving the combination of springs (elastic solids) and dashpots (viscous fluid): Maxwell, Voigt–Kelvin, or standard linear solid models [16]. Sometimes, for more complex deformation processes of biological tissues, models of greater complexity may be required to describe the response of the viscoelastic material. Such empirical models can reproduce creep and stress relaxation behaviors under different loading modes.

Another important factor affecting material behavior and properties is the loading mode: *static* or *cyclic loading*. The deformation and material properties obtained from the stress–strain curve are due to the static load when the force is applied at greater amplitudes until a certain deformation or failure is reached. This testing mode is essential to predict the limits of performance of the materials such as the maximum load that can be safely carried or the rigid-

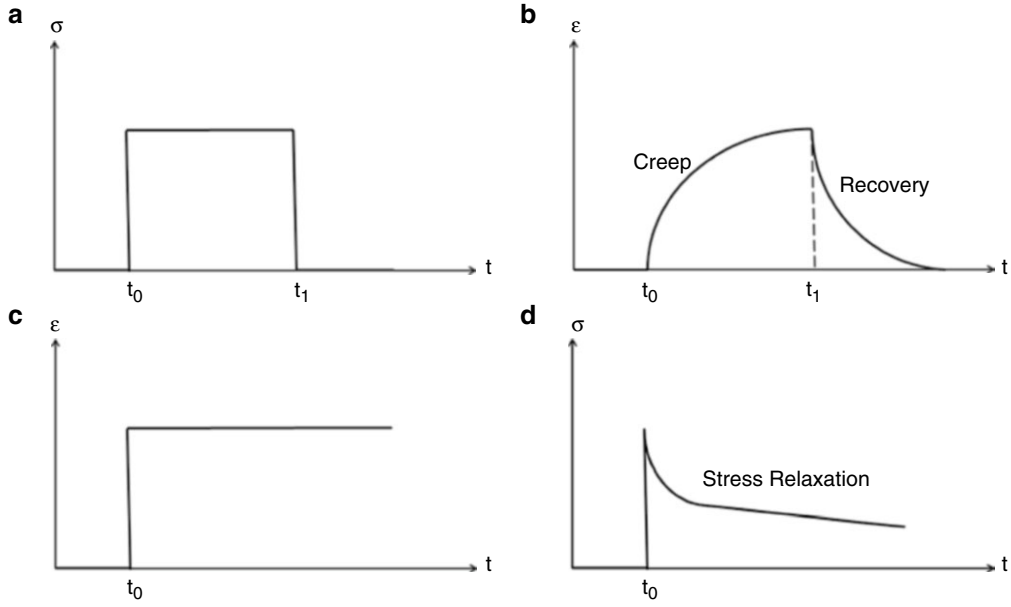

Fig. 2.11 The responses of viscoelastic material to changes in stress and strain are examined through two experiments: (**a**) Viscoelastic material is subjected to a constant force. (**b**) The response of the material is called as creep and recovery. (**c**) Viscoelastic material is subjected to a constant strain. (**d**) The response of the material is called as stress relaxation

ity of the body. Static loading is relevant to trauma conditions. However, musculoskeletal tissues and most biological tissues are subjected to cyclic loading (repeated loading and unloading) during daily activities. The load levels are generally significantly below the yield limit. For instance, *in vivo* strains in the bone are less than 0.1 %, whereas the yield strain of the bone is about 0.8 % strain. Despite the low amplitude, when that stress is applied for a prolonged number of cycles, failure may occur at levels below the yield stress point. This occurs mostly because intrinsic flaws (such as accumulation of osteoclast resorption cavities in a particular region of the bone) combined with cyclic loading can produce microstructural damages which accumulate and propagate under sustained cyclic loading, resulting in failure in a process referred to as *fatigue*. In other words, fatigue is a progressive deformation which causes a decrease in yield and ultimate strength of the material as a function of cyclic loading. Fatigue may occur after a few cycles of loading or tens of million cycles of loading depending on several factors: the intensity of the applied load, the size and physical properties of a body, the environmental conditions, and the surface quality which will be discussed briefly in the following section.

The analysis of material behavior due to the cyclic loading is quite complicated compared with that of static loading. Unlike the stress–strain curve due to static loading, the result of a cyclic loading (fatigue) test is reported as a single curve on a graph with the cyclic stress amplitude (σ) along the y-axis and the number of cycles to failure (N) along the x-axis (log scale) (Fig. 2.12). This curve displays an increasing fatigue life with decreasing stress amplitude. As the stress is lowered further, the stress limit can be reached below which the fatigue life is assumed infinite for practical purposes. This limit is termed the *endurance stress or limit* (σ_e) of the material. The fatigue behavior of the materials is closely associated with several factors. The higher the temperature, the lower the fatigue strength, and the higher the stress amplitude, the lower the fatigue life [11, 16]. In an orthopedic implant testing

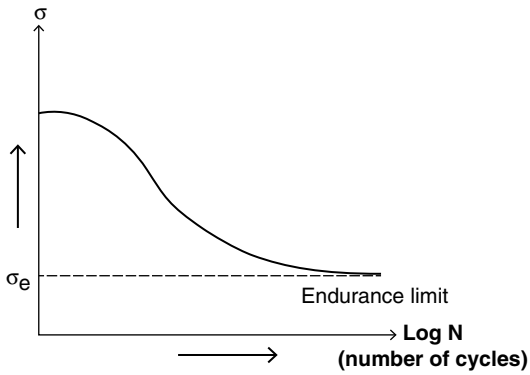

Fig. 2.12 Fatigue test is reported as a single *curve* on a graph where cyclic stress amplitude along the *y*-axis and the number of cycles to failure along the *x*-axis (log scale)

concept, corrosive effects of bodily fluids may affect the longevity in fatigue. Fatigue tests can be carried out in tension, compression, shear, or their combinations.

Additionally, another important concept related to failure is *stress concentration* which is the geometric effect on a material causing an increase in local stresses sometimes beyond the endurance limit which in turn can dramatically reduce the fatigue life of the material due to the initiation of microcrack/damage emerging from this region. Stress concentration mostly arises from the abrupt changes in shape of the body due to the holes, cracks, scratches, or notches. Therefore, by avoiding sudden shape changes as well as increasing surface quality, the effects of stress concentration can be minimized. Such considerations of stress concentration are particularly critical in implant design. Ductile materials tolerate stress concentrations more effectively than brittle materials.

On occasion, the designed structure (e.g., implants) may have unexpectedly high loads or experience other environmental effects which cause alteration the physical properties of the material. Therefore, it is essential to determine a safe stress level in order to account for these uncertainties. This safe stress level is called *allowable stress* which is always considerably lower than the ultimate strength of a material. The *safety factor*, which is the ratio of the ultimate strength of the material to the allowable stress, can dramatically reduce the effects of the uncertainties. Also, this safety factor can be calculated using the endurance strength or yield strength of the material instead of the ultimate strength depending on the applications and needs. This factor is always greater than 1, and choosing a larger safety factor is essential to maintain that the stress induced on a structure properly sustains its functions.

In summary, the concepts of deformable body mechanics in biomechanics allow for the determination of the mechanical properties of biological tissues. This in turn can describe their behaviors under various loading conditions. The tissues of the musculoskeletal system (e.g., bone, tendon, ligament, muscle, and cartilage) and all biological tissues can be considered as a composite engineering material (composed of at least two different materials with different material properties) with nonhomogeneous and anisotropic properties. The concepts and principles of deformable body mechanics can then be utilized to analyze their biomechanical properties. However, it is important to note that biological tissues have different characteristics than other engineering materials in that they are *self-adapting* and *self-repairing*. Since biological tissues are composite, anisotropic, and viscoelastic materials, most of the material properties reported are actually approximations and dependent on several factors as discussed throughout this chapter. Therefore, it is important that the test conditions for these tissues must be also provided when reporting the material properties of biological tissues.

In the perspective of joint replacements and surgical implants, the concepts of deformable body mechanics are essential in order to determine the safest and most efficacious operative treatment based on a clear understanding of the material properties of biological tissues. The concepts of deformable body mechanics are also important for the successful design, material selection, and manufacturing that can sustain the combined effects of the internal forces in the biological environment.

References

1. Meriam J, Kraige L (2011) Engineering mechanics: statics, 7/e. Wiley, New York
2. Meriam JL, Kraige LG (2012) Engineering mechanics: dynamics (vol 2), 7/e. Wiley, New York
3. Drillis R, Contini R (1966) Body segment parameters. New York University, School of Engineering and Science, Research Division, New york
4. Tözeren A (2000) Human body dynamics: classical mechanics and human movement. Springer, New York
5. Fung Y, Cowin S (1994) Biomechanics: mechanical properties of living tissues. J Appl Mech 61:1007
6. Bartel DL, Davy DT, Keaveny TM (2006) Orthopaedic biomechanics: mechanics and design in musculoskeletal systems. Prentice Hall, New Jersey
7. Seeman E, Delmas PD (2006) Bone quality—the material and structural basis of bone strength and fragility. New Engl J Med 354(21):2250–2261
8. Ammann P, Rizzoli R (2003) Bone strength and its determinants. Osteoporos Int J Established Result Cooperation Between Eur Found Osteoporos Nat Osteoporos Found USA 14(Suppl 3):S13–S18. doi:10.1007/s00198-002-1345-4
9. Zioupos P, Currey J (1998) Changes in the stiffness, strength, and toughness of human cortical bone with age. Bone 22(1):57–66
10. Rho J-Y, Kuhn-Spearing L, Zioupos P (1998) Mechanical properties and the hierarchical structure of bone. Med Eng Phys 20(2):92–102
11. Wang X, Nyman J, Dong X, Leng H, Reyes M (2010) Fundamental biomechanics in bone tissue engineering. Synth Lect Tissue Eng 2(1):1–225
12. Sedlin ED, Hirsch C (1966) Factors affecting the determination of the physical properties of femoral cortical bone. Acta Orthop 37(1):29–48
13. Nyman JS, Roy A, Shen X, Acuna RL, Tyler JH, Wang X (2006) The influence of water removal on the strength and toughness of cortical bone. J Biomech 39(5):931–938. doi:10.1016/j.jbiomech.2005.01.012
14. Lucas GL, Cooke FW, Friis E (1999) A primer of biomechanics. Springer, New York
15. Burstein AH, Wright TM (1994) Fundamentals of orthopaedic biomechanics. Williams & Wilkins, Baltimore
16. Özkaya N, Nordin M, Goldsheyder D, Leger D (2012) Fundamentals of biomechanics: equilibrium, motion, and deformation. Springer, New york

Applying Biomechanics in Orthopedics

3

A. Esat Kiter and Abdullah Milcan

Abstract

Biological response of tissues constituting the skeletal system against load and trauma will be discussed in this chapter. Real-life situations due to individual differences such as genetics, age, gender and anatomy are sometimes difficult to simulate. Mathematical formulation of the relationship between joints and movement can be theorized easily with some assumptions. Basic methodology of orthopedic diseases treatment, however, is closely associated with this biological response.

Learning Objectives

After you have studied this chapter, you will have an understanding of (1) biomechanical properties of musculoskeletal tissues, (2) response of musculoskeletal tissues to load and gravity, (3) injury mechanisms musculoskeletal tissues, and (4) Young's modulus. This chapter furthermore includes basic notions involved in the biocompatibility of metal implants used in orthopedics.

Terminology

Anisotropia Changing of material behavior depending on the direction of the load. For instance, the bone is strong to support loads in the longitudinal direction since it is used to receive loads in this direction.

Avulsion fracture It is a bone fracture at the insertion points of tendon or ligaments, which occurs when a fragment of bone tears away

A.E. Kiter (✉)
Orthopaedics, Pamukkale University School of Medicine Depth, Denizli, Turkey
e-mail: esatkiter@gmail.com

A. Milcan
Orthopaedics, Mersin University School of Medicine Depth, Mersin, Turkey
e-mail: amilcan@mersin.edu.tr

F. Korkusuz (ed.), *Musculoskeletal Research and Basic Science*,
DOI 10.1007/978-3-319-20777-3_3

from the main mass of bone as a result of physical trauma.

Collagen Collagen is a protein that is a major constituent of the extracellular matrix of connective tissue.

Distraction forces A force applied to a body part to separate bony fragments or joint surfaces.

Elastin Like collagen, is a protein, which is a major constituent of the extracellular matrix. It provides elasticity to connective tissue.

Elongation of fibrous tissues Plastic deformation of fibrous tissues that may lead to instability.

Instability Extramobility of joints due to insufficiency of stabilizing tissues that exceed the physiological motion limits.

Gravity The force of attraction by which terrestrial bodies tend to fall toward the center of the earth.

Isotropia Keeping of material uniformity in all orientations of load. Glass and metals are examples of isotropic materials.

Ligament A band of oriented fibrous tissue connecting bones of a joint.

Shear loadings Is defined as the component of stress coplanar with a material cross-section.

Stiffness See elasticity modulus or Young's modulus.

Strength An ability to withstand an applied load without plastic deformation or failure.

Tendon The fibrous tissue by which muscle attaches to bone.

Viscoelasticity Time-dependent property of materials that exhibit both viscous and elastic characteristics when undergoing deformation.

Young's modulus The ratio of stress (force per unit area) to corresponding strain in a material under tension or compression. It is related with tissue property that describes its elasticity or stiffness.

Clinical Relevance

With the absence of the major trauma, what is the differential diagnosis? Plateau fracture, osteonecrosis, or tumor?

Patient was admitted to our clinic with symptoms of knee pain. Pain was located at the medial side of the right knee during weight bearing. There was no history of major trauma but running each day average 5 km for last 10 years. Physical examination revealed tenderness with palpation at the medial proximal tibial metaphyses. With the diagnosis of medial tibial plateau stress fracture, physician prescribed immobilization in long leg cast at 15° flexion for 4 weeks. Weight bearing was allowed partially with crutches after removal of the cast and fully at the end of the 8 weeks (Fig. 3.1).

Although precise pathology is unknown, stress fracture refers to an overuse injury resulting in structural damage to the bone from repetitive weight bearing or increasing stressful muscular activity. Normal physiological loading provokes a range of deformation reactions in bone. The bone exhibits an intrinsic ability to adapt to alterations in chronic loading to withstand future loads of the same nature, a phenomenon referred to as Wolff's law. The bone normally responds to strain by increasing the rate of remodeling. In this process, the lamellar bone is resorbed by osteoclasts, creating resorption cavities, which are subsequently replaced with denser bone by osteoblasts. Because there is a lag between increased activity of the osteoclasts and osteoblasts, the bone is weakened during this time.

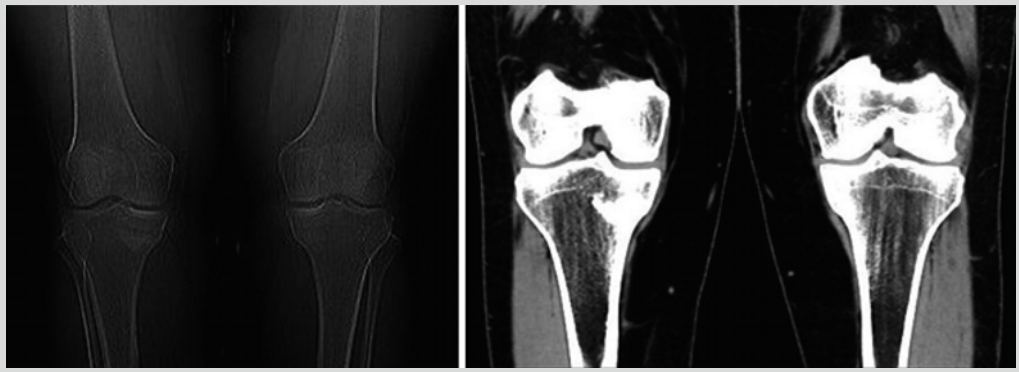

Fig. 3.1 Bilateral standing X-ray of a 48-year-old male patient. After the history and physical exam findings, stress fracture of the medial tibial plateau was diagnosed

With cyclic loading, remodeling is given insufficient time to repair damage and additional loading cycles enabling damage to accumulate. Therefore, the bone fails to adapt adequately to the repetitive mechanical load experienced during physical activity [20]. In such cases, cessation of the load provides sufficient time period to remodeling phase.

Biomechanical factors may predispose to stress fractures by creating areas of stress concentration in the bone or promoting muscle fatigue. High arches, pes planus, leg length inequality, and medial deviation of the knee mechanical axes may predispose to various lower extremity stress fractures [21].

Stress fractures should be differentiated from insufficiency fractures which are bone injury in weakened bone (osteoporotic bone) from normal activity [22].

Introduction

Human musculoskeletal system works on principles based on a complicated cascade of movement and loads generated by gravity. The human body resists against applied loads and moves accordingly. The main components of the musculoskeletal system are bones, cartilages, tendons, and ligaments. Before proceeding with the biomechanical characteristics of these tissues, it may be appropriate to explain the term "load."

Loads Generated on Musculoskeletal Tissues

Gravity is the most fundamental and consistent force on musculoskeletal tissues. Human movement is performed primarily against gravity. Resistance to gravity generated by skeletal muscles establishes the basis of the internal forces. Trauma however is associated with external forces affecting the skeletal system. Basically, the loads having an influence on the skeletal system and particularly on the bones are listed below (Fig. 3.2).

Load Types

Compressive Load

Forces inducing a compression leading to volume reduction by affecting the edges of an object. As will be discussed later, these forces have significance with regard to bone formation. However, a compressive load exceeding the compressive strength of the bones results in fractures. The most effective resistance to compressive load is manifested by the trabecular bone. Therefore, the loss of trabecular bone mass seen in osteoporosis is the leading reason behind spine and hip fractures.

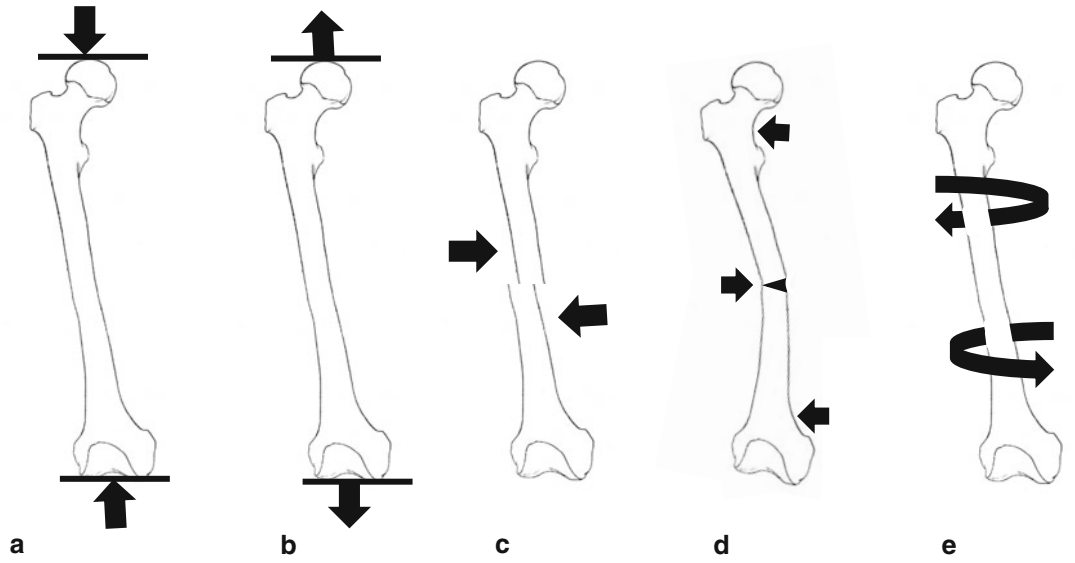

Fig. 3.2 Schematic drawing of loads on femur. (**a**) Compression, (**b**) distraction, (**c**) shear, (**d**) bending, (**e**) torsion

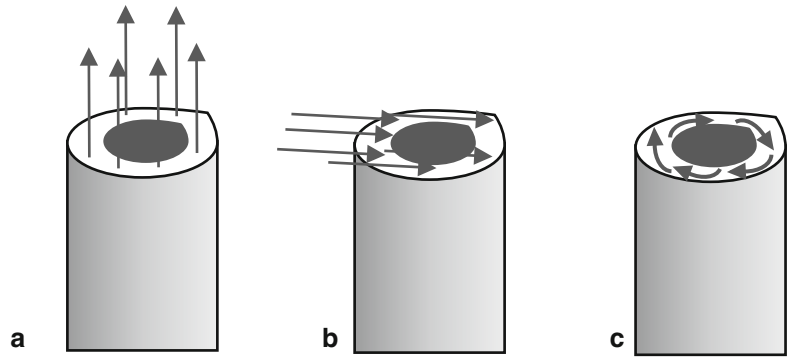

Fig. 3.3 Force vectors of loads. (**a**) Distraction, (**b**) shear, (**c**) torsion

Tensile Load

Forces aiming to stretch the length of a bone in the applied direction. As a result of the stretching effect, the width will decrease. Generally, this force is applied by the muscles of the body and transmitted by tendons to the bones. Primary resistance against the tensile forces is generated by the collagen fibers. Therefore, collagen fibers exhibit a longitudinal orientation at the bone-tendon attachment. Tensile force is the principal cause of the presence of apophysis. These growth centers located at the points of attachment between tendons and bones undergo ossification with age and remain as tubercles on the bones. In this regard, the tibial tubercle, to which patellar tendon is attached, is a good example. When the bone fails to exert adequate resistance to the tensile load transferred via tendon, avulsion fracture occurs. These fractures are often encountered in children. In some cases, injuries are observed in the apophysis prior to fracture. Such injuries are commonly observed in children making sports involving jumping. Apophysitis is seen at the tibial tubercle in Osgood-Schlatter disease and at the base of the fifth metatarsal bone in Iselin disease. The basic mechanism of injury in distention and sprain cases is also associated with tensile strength.

Shear Load

Shear stress arises from the force vector component parallel to the cross-section (Fig. 3.3). The main components of shear strength are compressive and

Table 3.1 Estimated long bone fractures by applied loads

Fracture pattern	Mechanism of injury	Location of soft tissue hinge	Energy
Transverse	Bending	Concavity	Low
Spiral	Torsion	Vertical segment	Low
Oblique-transverse	Compression-bending	Concavity or side of butterfly	Moderate
Oblique	Compression -bending	Concavity (often destroyed)	Moderate
Comminuted	Torsion variable	Destroyed	High
Metaphyseal compression	Compression	Variable	Variable

Redrawn from Wood [2]

tensile loads. The resistance potential of bone to shear forces is considerably low. Distal femoral and proximal tibial fractures occur because of shear strain associated with varus and valgus during knee hyperextension.

Bending Load

Bending is a combination of compression and tension: tensile stresses and strains on one side of the neutral axis and compressive stresses and strains on the other side. Because the bone is asymmetrical, the compressive and tensile stresses may not be equal. Bending strength may occur with a three- or four-point load. The application of strength at three points usually involves strengths applied perpendicularly to the bone at the ends of the bone, with a strength applied in the opposite direction in the middle of the bone. Fracture begins on the tension side in adult bone as bone is weaker in tension than compression (Fig. 3.2d). A bending load is applied at four points with the application of two equal and opposite pairs of strength in each end of the bone [1]. In the case of four-point bending, the bone will break at the weakest point. An axial force applied on a nonunion of femoral fracture leads to the fracture to sustain a four-point bending load.

Torsion Strength

The shear stress induced by the rotational forces (Fig. 3.2e). As the distance of the point receiving the rotational forces increases, the torsion strength of the injury site rises as well. Such injuries are observed particularly in spiral oblique fractures [2] (Table 3.1). Nonetheless, torsional loads also play a role in intervertebral disk injuries.

Action Forms of Loads

Three components of loading bear importance in understanding the subsequent injury: magnitude of load, duration of loading, and number of repeats. The magnitude of the applied load shows positive correlation with the magnitude of the response and the severity of the injury. This has a direct relationship with the first law of thermodynamics: "Energy cannot be created or destroyed, but it can change in form or be absorbed." The resultant damage depends on the magnitude of the absorbed energy. At this point, it would be helpful to remember the third law of movement by Newton in predicting the injury to be induced: "When one object exerts a force on a second object, the second object simultaneously exerts a force equal in magnitude and opposite in direction on the first object." If the object sustaining the load exerts a responsive force lower than that of the load, the exceeding portion of the load is absorbed by the object leading to its deformation. The body cannot respond adequately to the high energy released in traffic accidents; therefore, the exceeding energy is absorbed by the body and the resultant hardness leads to various damages in various tissues.

Duration of loading is also a factor in the resultant damage. In every speed of load placement, the bone can bear higher loads before fail. The bone that receives load slowly breaks with a load that is approximately half of that it could support if the load is more quickly applied. As we will see in the following pages, the duration of loading on biologic tissues plays a critical role in the severity of the damage as well as in the treatment.

Repeated loading induces a deformation depending on the magnitude and frequency of the

loading. When applied with a repeated pattern, even the lowest loads can induce injuries on biological tissues. Stress fracture can be given as an example of such injuries [3].

Reading to Stress-Strain Curve

The main characteristic of tissues in the skeletal system is to manifest resistance to the applied forces. As happens in each object, the absorption of the applied force results in deformation in the biological tissues. The attributes of deformation shown by the material under load are evaluated with stress-strain curve. This evaluation gives us information about the stiffness and strength of the object. The area below the curve up to the failure of the biological tissue represents the toughness of the object which is one way to assess strength of the object, indicating the energy absorbed before the failure. Stiffness is about the inclination of the curve at elastic deformation stage which is expressed by Young's modulus (stress/strain). As Young's modulus value increases, the curve becomes steeper and the object becomes stiffer (Fig. 3.4). Depending on the variety of the terms of stiffness and strength, some objects may be described as stiff and strong (steel, iron), while some are described as stiff and weak (glass, copper). Fiberglass and silk are defined as flexible and strong, while spider web and lead are defined as flexible and weak materials. The bone is a flexible and weak material as well (Fig. 3.5).

Biomechanical Features of Noncontractile Skeletal Tissues

Bone

Bone differs from other tissues of the skeletal system with its strength. It is composed of organic and inorganic materials. The collagen fibers render bones both strong and elastic. Since it is the body component that bears various loads, it sustains both and internal and external forces. In the human body, the presence of these forces becomes an advantage for the bone, and the applied load shapes the bone metabolic turnover. Therefore, there can be no healthy bone tissue if there is no loading (movement). This notion can be defined by the term *Wolf's Law*. Julius Wolf, a German anatomist-surgeon has noted that the bone tissue becomes denser under compressive stress, while scattering under tensile stress. This adaptation, manifesting itself as alteration of the bone porosity, is caused by the osteoblastic activity in the first instance and by the osteoclastic activity in the second instance. The bones in a human body are not of uniform character (*not*

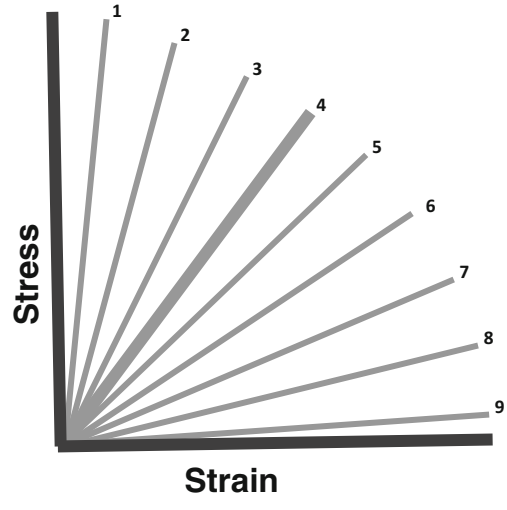

Fig. 3.4 Young's modulus of the various materials, steepness of elastic deformation address to hardness (relative values of Young's modulus)

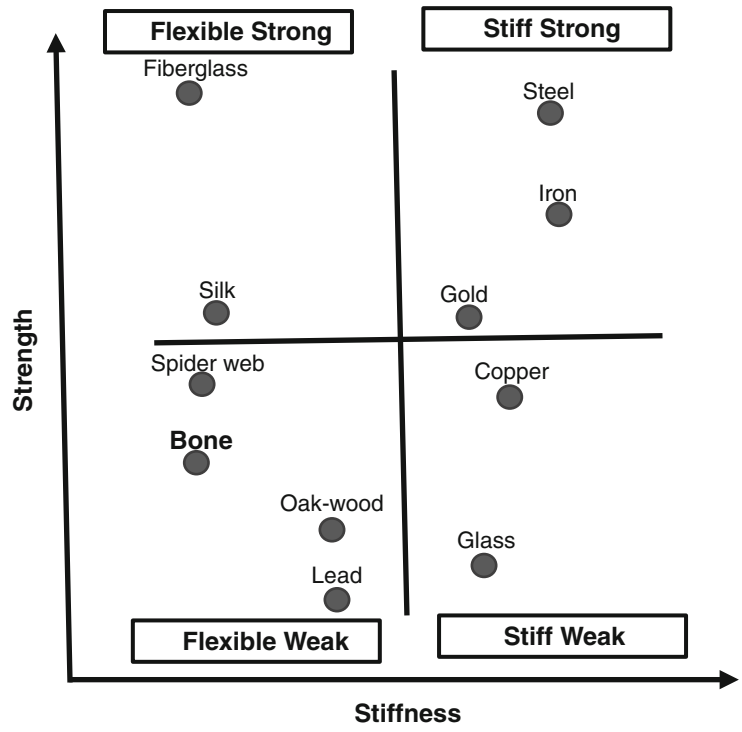

Fig. 3.5 Definitions of some materials in terms of stiffness and strength

like a series of pipes) and always sustain different loads with various angles during movement. Therefore, the skeletal system in motion continuously updates itself by internal reactions [4]. This adaptive process is of everlasting character, with personal differences relative to varying factors involved in a person's life. For instance, professional tennis players demonstrate 5–10 % increase in the ulnar and radial bone masses [5] which is a good example of the bone's adaptive capability against the applied stresses.

About 70 % of the bone tissue is composed of calcium and phosphate minerals as well as collagen. The remaining 30 % is composed of water. The primary resistance against tensile forces is exerted by collagen fibers, while the primary resistance against compressive forces is exerted by mineral density and water. As one ages, decreasing mineral density renders the bone more susceptible to compressive forces. The responses of the bone to the mechanical forces depend on the structural characteristics. Bone tissue is viscoelastic and anisotropic. Cortical bone is much denser than cancellous bone while being more brittle as well. A strain of only 2 % suffices to cause fracture in the cortical bone in vitro; however, cancellous bone requires a strain of >75 % to fracture at same conditions. Basically, bone porosity is held responsible for this difference because it increases the energy absorption potential.

The components of the skeletal system are anisotropic materials, which makes it more difficult to perform any calculation. The anisotropic attribute of the bone manifests itself with different stress-strain curves in loads with different directions. In other words, the strength and stiffness of the bone tissue varies depending on the spatial position of the bone or the load (Fig. 3.6).

Tendon and Ligaments

Tendons and ligaments closely resemble each other in structure, however, differ in function. Tendons are responsible of movement at points where muscles are connected to the bones. On the other hand, ligaments mainly contribute to the sta-

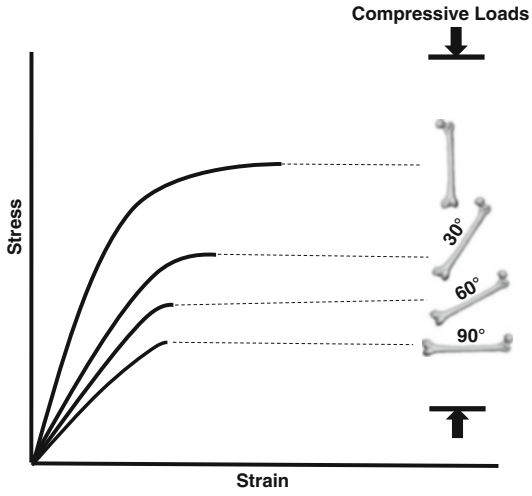

Fig. 3.6 Anisotropy, bone *responds with different* stress-strain curves, if forces are applied in different directions. Femur is the feeblest if forces are exposed with right angle to shaft

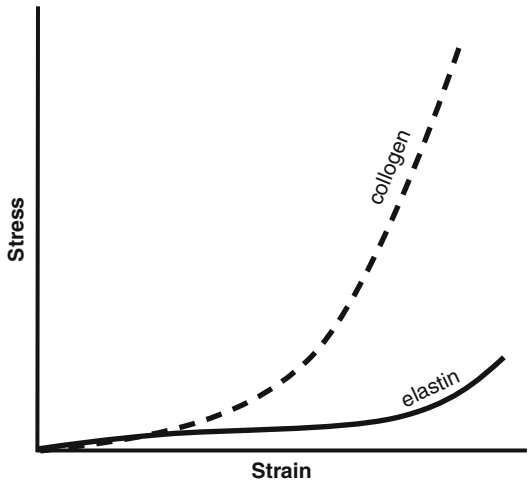

Fig. 3.7 Difference of collagen and elastin fibers under tensile load (relative values)

bility of the skeletal system, thereby extending from bone to bone. These tissues are actually composed of three types of fibers: collagen, elastin, and reticulin, combined with nonfibrous ground substance. They are responsible for the strength and stiffness of the collagen tendons or ligaments. Primarily, collagen fibers resist to tensile loads. Therefore, particularly in tendons, collagen fibers display an orientation parallel to the tendon [6]. There is a similar situation at the ligaments as well; however, the collagen fibers are less parallel in ligaments resisting to forces other than tensile load (*if it is not subjected to large forces from a particular direction*). On the other hand, elastin fibers are responsible of extensibility and are considerably different from collagen fibers with regard to biomechanics. Collagens rapidly elongate under light forces and preserve their stiffness until failure. However, elastin fibers under light forces manifest elongation more slowly and fail without deformation (Fig. 3.7). The principal differences between tendons and ligaments are associated with function. These differences have been shown. Accordingly, tendons that almost always sustain tensile forces contain higher amount of collagen fibers, whereas ligaments contain more elastin fibers (Table 3.2). Moreover, reticulin fibers contribute to the bulk of the tissue.

Just like the bone, tendons and ligaments adapt to the load in time, depending on the magnitude and type. When we consider a joint model, ligaments manifest a more stable reaction to slowly applied loads; therefore, if the loading continues, the risk of tendon failure at the bone junction increases (*avulsion fracture*). However, ligament is affected most if the load is of high amplitude and applied rapidly [7]. If the load is of very high magnitude but applied briefly, the ligaments may transform from elastic deformation to plastic

Table 3.2 Mechanical and associated biomechanical values of some skeletal connective tissues

Material	Ultimate tensile strength (Mpa)	Ultimate tensile strain (%)	Collagen (% dry weight)	Elastin (% dry weight)
Tendon	50–100	10–15	75–85	<3
Ligament	50–100	10–15	70–80	10–15
Articular cartilage	9–40	60–120	40–70	–

Adapted from Holzapfel

deformation stage. If the loading is stopped before any ligament failure, elongation after plastic deformation and resultant instability may occur.

We know that the collagen fibers in tendons and ligaments increase with exercise and decrease with immobilization [8, 9]. This finding indicates that tendons and ligaments are more susceptible to injury after immobilization. In conclusion, ligaments, just like bones, depend on movement and movement-related loads in order to stay healthy.

Articular Cartilage

Articular cartilage consists of 70–85 % water in the weigth of the whole mass. The remainder of the tissue is composed primarily of proteoglycans (30 %) and collagen (%70). Near the articular surface, proteoglycan concentration is relatively low, and the water content is the highest [10]. Structural organization of collagen is responsible for the mechanical properties of cartilage.

Under tension, cartilage responds by realigning the collagen fibers that carry the tensile load. In stress-strain curve, initially, low slope of the curve is thought to be the result of the alignment of the collagen fibers, but the final, more linear, and steep portion represents the tensile stiffness of the collagen itself. Under loads, articular cartilage acts as a sponge and its permeability change with deformation rate. With deformation, fluid flows through the cartilage and across the articular surface. With loss of water, the solid matrix of cartilage carries the majority of the load and the response is stiffer than in the initial phase.

Viscoelastic Response

Viscosity is particularly important in biological tissues such as ligaments and tendons and in their in vivo reaction. Viscosity is time dependent. The amount of deformation that occurs depends not only on the amount of force but on the rate at which the force is applied [7]. Against the forces biological tissues give three specific responses: creep, stress relaxation, and hysteresis.

Creep

Creep is time-dependent elongation of a tissue when subjected to a constant stress (Fig. 3.8). For example, in an isometric contraction, the tendon will lengthen slightly, and more muscle fibers will be recruited in order to maintain the position of the limb. In the aspect of the ligaments, joint will loosen with time under constant stress. This loosening provides more flexibility to joints and decreases the possibility of injury. Some recent

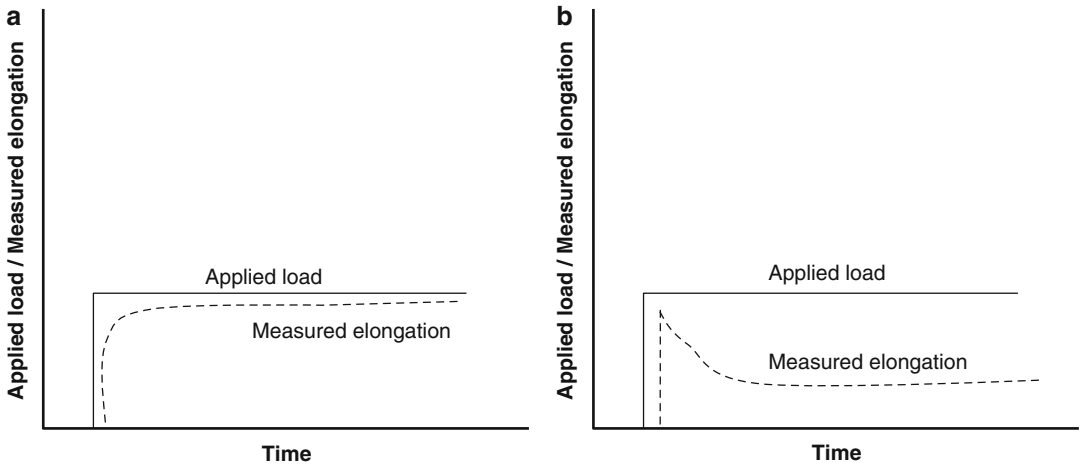

Fig. 3.8 Creep and stress relaxation of viscoelastic tissues. (**a**) Creep is an increase in strain under constant stress. (**b**) Stress relaxation is a decrease in stress under constant strain

studies show that the rate of recovery is faster than the rate of creep. This difference would appear to be of physiologic benefit, biased toward maintaining ligaments in their "normal" resting length [11].

Stress Relaxation

Like creep, time-dependent elongation occurs, but applied stress required to maintain a constant elongation is decrease (Fig. 3.8). In an isotonic contraction of muscle, transferred stress to tendons will decrease with time. If initial loads constantly continue over time, the tendency for the material to return to its original shape is decreased. In the skeletal system, creep and relaxation may occur simultaneously under combined loading.

Hysteresis

Hysteresis is energy lost within the tissue between loading and unloading. The unloading curve does not follow the loading curve [12]. The area between two curves represents the amount of energy that is dissipated or during loading. Subsequent use of same force results in greater deformation (Fig. 3.9).

Focus on Spine Biomechanics

The spine is a complex skeletal part, serves to protect the spinal cord and nerve roots, and provides an incredible amount of flexibility to the trunk. Particularly in erect posture, it bears various gravity forces during different movements. Its elaborate mechanical behavior makes it the most interesting combined unit of the skeletal system. The vertebral column is constituted by vertebrae which have different anatomical properties due to location in spine. These anatomical features are tightly related with the function of each segmental part. The volume of the vertebral body, orientation of the facet joints, and presence of costovertebral joints in thoracic region are the most evident specifications of the different segments.

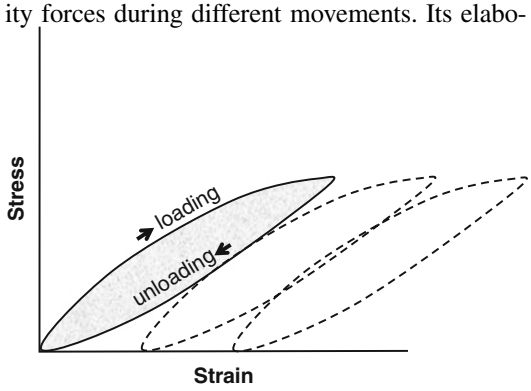

Fig. 3.9 *Shaded area* represents the energy lost during reversion; subsequent loads create more strain (*dotted lines*)

Orientation of Facet Joints

Facet joints are typical diarthrodial joints with cartilage surfaces that provide a low-friction interface to facilitate motion during normal conditions in a healthy spine. Orientation of the joint surfaces represents marked distinction from cervical to lumbar. In cervical and thoracic region, joint surfaces are in coronal plane. With the lower thoracic levels, inclination begins to change toward the sagittal plane (Fig. 3.10). Therefore, lumbar vertebrae move in large range in sagittal plane (flexion-extension) [13]. Changing orientation of facet joints also explains the coupling movements which is the presence of associated rotation with the vertebral colon lateral bending movement.

Functional Spinal Unit and Instantaneous Axis of Rotation

Functional spinal unit (FSU) is an artificial hypothetic model to explain biomechanical features of the spine under loads. It has been used in research and tested for mobility and strength under various conditions of fatigue and weight. It is considered the smallest possible representation of the spine, made up of one intervertebral disk, two vertebrae, two intact facet joints, and interconnecting ligaments (Fig. 3.11). Ligamentous structures help to keep the uniformity of the spine in the case of excessive movement and loads. Anterior longitudinal ligament is the most powerful ligament. Posterior ligamentous complex (PLC) consists of ligamentum flavum, interspinous ligament, supraspinous ligament, and

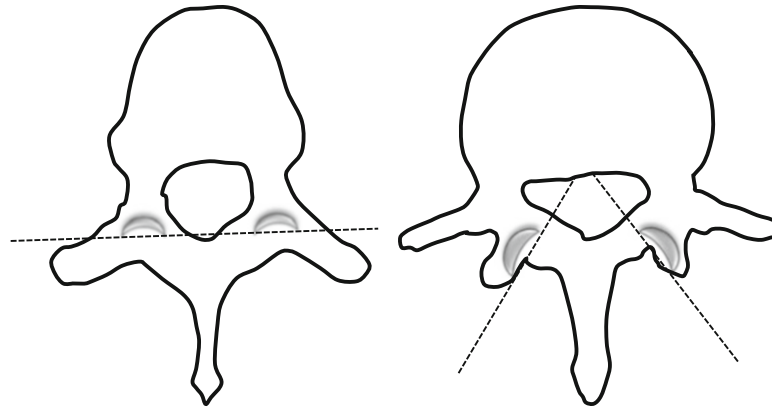

Fig. 3.10 Facet orientation of thoracic and lumbar vertebra

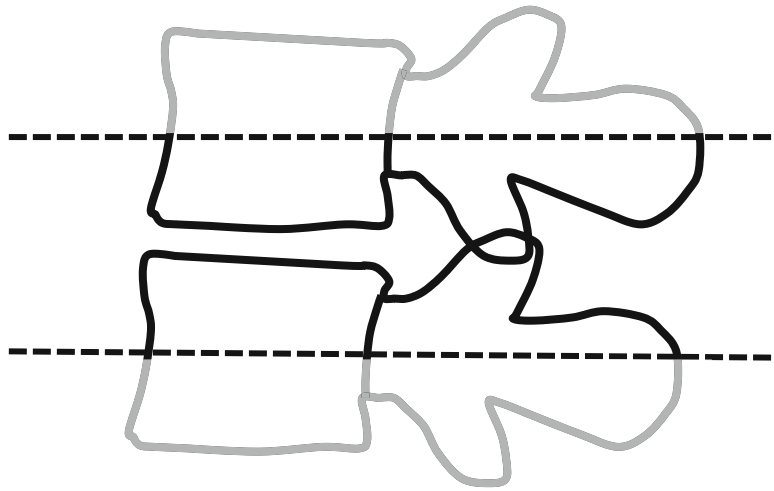

Fig. 3.11 Functional spinal unit: one intervertebral disk, two vertebra, two intact facet joints, and interconnecting ligaments

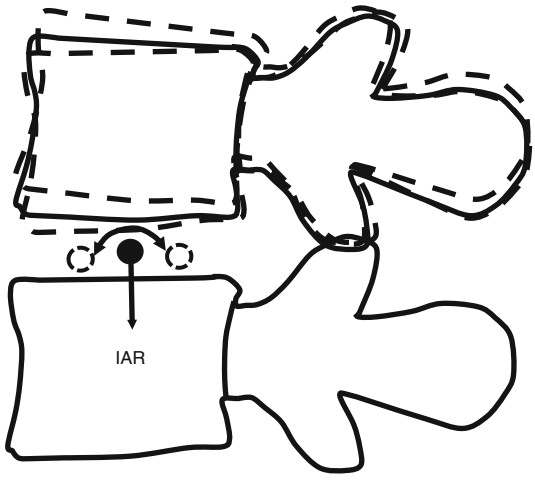

Fig. 3.12 Rotation center of the functional spinal unit is tentative during movements

facet capsules. After trauma, disruption of PLC is the major determiner of spinal unit instability.

For any arc of movement defined by a given starting position and a given end position of the moving vertebra, the center of movement is known as the instantaneous axis of rotation (IAR) [14]. IAR is a dynamic description and is not constant but varies in location depending on the position of the joint (Fig. 3.12).

Load Distribution Principles of the Spine

During daily life, spine bears, transmits, and absorbs remarkable intensity loads. Intervertebral disk is the most important structure to maintain such

spinal functions. In the normal disk, water-binding proteoglycans with intact annulus fibrosus act like a car tire and helps in uniform distribution of load across and plate. With degeneration, the nucleus becomes depressurized, and an increasingly larger load is transmitted through the annulus [15]. This condition leads to annular splitting which is the actuator of many degenerative spinal diseases. In the presence of disrupted disk, large amount of transferred load shifts posteriorly, and posterior structures of vertebral colon became prone to further degenerative changes [19] (Fig. 3.13).

In the classical works of Nachemson et al. and Wilke et al. [16, 17, 18], interdiscal pressure has been measured in different positions which are faced in normal daily life. Lying down puts considerably less pressure on disk compared to standing position. Leaning forward while sitting or standing substantially increases disk pressure. Holding a load remarkably increases pressure on the disks while leaning forward (Fig. 3.14).

Understanding the biomechanical behaviors of human spine is a puzzler. Complexity of intimately structured anatomical tissues, alteration due to aging, and unique bipedal walking make more difficult the prediction of natural biomechanics of vertebral column.

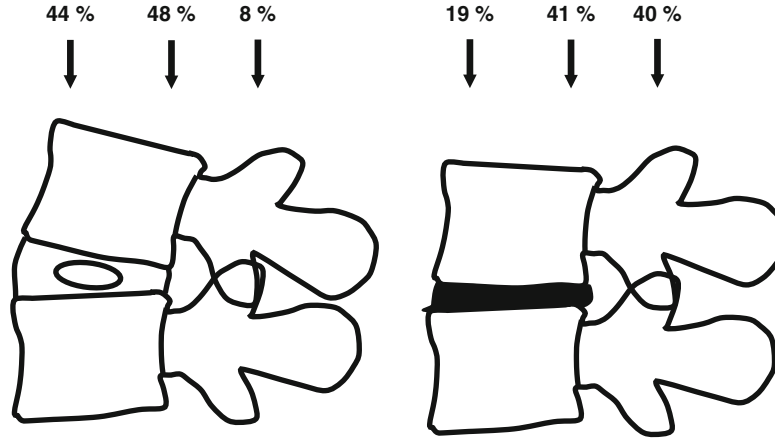

Fig. 3.13 Load distribution in erect posture. In case of the disk degeneration, main load transfer shifts to posterior (Redrawn from Pollintine [19])

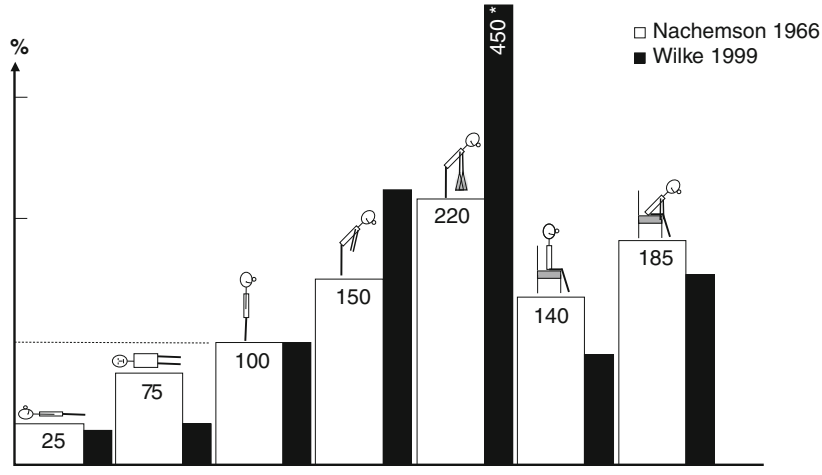

Fig. 3.14 Intradiscal pressure in common postures, normalized to standing. * Lifting waits are 20 kg (Wilke) and 10 kg (Nachemson)

References

1. Lopez MJ, Markel MD (2000) Bending test of bone. In: An YH, Draughn RA (eds) Mechanical testing of bone and the bone- implant interface. CRC Press, Florida, pp 207–219
2. Wood GV II (2013) General principles of fracture treatment. In: Canale ST, Beaty CH (eds) Campbell's operative orthopaedics. Elsevier/Mosby, Philadelphia, p 2591
3. Ermanno B (2000) Basic composition and structure of bone. In: An YH, Draughn RA (eds) Mechanical testing of bone and the bone- implant interface. CRC Press, Florida, pp 3–21
4. Rubin C, Rubin J (2006) Biomechanics and mechanobiology of bone. In: Favus MJ (ed) Primer on the metabolic bone disease and disorders of mineral metabolism, 6th edn. American Society for Bone and Mineral research, Washington, DC, pp 36–42
5. Ducher G, Prouteau S, Courteix D et al (2004) Cortical and trabecular bone at the forearm show different adaptation patterns in response to tennis playing. J Clin Densitom 7:399–405
6. Holzapfel GA (2001) Biomechanics of soft tissue. In: Lemaitre J (ed) The handbook of materials behavior models. Academic, Boston, pp 1049–1063
7. Cornwall MW (1984) Biomechanics of noncontractile tissue. A review. Phys Ther 12:1869–1873
8. Miller BF, Olesen JL, Hansen M et al (2005) Coordinated collagen and muscle protein synthesis in human patella tendon and quadriceps muscle after exercise. J Physiol 567:1021–1033
9. Woo SL, Gomez MA, Sites TJ et al (1987) The biomechanical and morphological changes in the medial collateral ligament of the rabbit after immobilization and remobilization. J Bone Joint Surg Am 69:1200–1211
10. Mansour JM (2003) Biomechanics of cartilage. In: Oatis CA (ed) Kinesiology: the mechanics and pathomechanics of human movement. Lippincott Williams and Wilkins, Philadelphia, pp 66–79
11. Jensen KT, Dwyer KW, Lakes R et al (2004) The rate of viscoelastic recovery is faster than the rate of creep, 50th ORS, San Francisco, 7–10 Mar 2004
12. Jung HJ, Fisher MB, Woo SL (2009) Role of biomechanics in the understanding of normal, injured, and healing ligaments and tendons. Sports Med Arthrosc Rehabil Ther Technol 20:9
13. Jaumard NV, Welch WC, Winkelstein BA (2011) Spinal facet joint biomechanics and mechanotransduction in normal, injury and degenerative conditions. J Biomech Eng 133:071010
14. Bogduk N (1997) Clinical anatomy of the lumbar spine and sacrum, 3rd edn. Churchill Livingstone, Edinburgh, p 91
15. Sengupta DK et al (2004) Dynamic stabilization – the non-fusion techniques in the surgical treatment of low back pain. In: Wiesel SW, Herkowitz H (eds) The lumbar spine, 2nd edn. ISSLS, LWW, Philadelphia, pp 373–383
16. Nachemson A, Morrıs IM (1964) In vivo measurements of intradiscal pressure. Discometry, a method for the determination of pressure in the lower lumbar discs. J Bone Joint Surg Am 46:1077–1092
17. Nachemson A (1966) The load on lumbar disks in different positions of the body. Clin Orthop Relat Res 45:107–122
18. Wilke HJ, Neef P, Caimi M et al (1999) New in vivo measurements of pressures in the intervertebral disc in daily life. Spine 24:755–762
19. Pollintine P, Dolan P, Tobias JH et al (2004) Intervertebral disc degeneration can lead to "stress-shielding" of the anterior vertebral body: a cause of osteoporotic vertebral fracture? Spine 2004(297): 774–782
20. Warden SJ, Burr DB, Brukner PD (2006) Stress fractures: pathophysiology, epidemiology, and risk factors. Curr Osteoporos Rep 4:103–109
21. Wilder RP, Sethi S (2004) Overuse injuries: tendinopathies, stress fractures, compartment syndrome, and shin splints. Clin Sports Med 23:55–81
22. Prasad N, Murray JM, Kumar D, Davies SG (2006) Insufficiency fracture of the tibial plateau: an often missed diagnosis. Acta Orthop Belg 72: 587–591

Finite Element Analysis

4

Mehmet Yetmez

Abstract

In this chapter, essentials of finite element analysis on musculoskeletal biomechanics are studied. For this reason, some fundamental types of finite elements, methodology, and difficulties of finite element analysis are considered. Also, some information on well-known general purpose finite element codes preferred in biomechanics and biomaterials world is given. Before discussing orthopedic researches for clinical relevance, an example of two-dimensional finite element analysis is examined.

Learning Outcomes

1. Be able to find fundamental knowledge about the finite element analysis with most frequently cited references.
2. Be familiar with the popular general purpose finite element codes used in biomechanical studies.
3. Be capable of interpreting the current understanding of finite element analysis with some simplifications and difficulties on biomaterials and biomechanical studies.
4. Be able to find a discussion on clinical relevance and some references of contemporary technical articles.

Terminology

E_{mean} Mean elastic modulus
FEA Finite element analysis
GML Geometry-material-load
HV Vickers hardness
J-integral Energy per unit fracture surface area
SR Singularity ratio

Introduction

As a structural material, the bone plays an important role in musculoskeletal biomechanics. Although focus on the compact bone, i.e., central part of the long bones, seems to be critical, the trabecular bone is the main character for the structural (skeletal) analysis/optimization [1].

Among the structural analyses, FEA is a very popular tool. Basically, FEA is a numerical analysis with low-degree polynomials. It is obvious that the smaller the element, the better

M. Yetmez
Department of Mechanical Engineering,
Bulent Ecevit University, Zonguldak 67100, Turkey
e-mail: yetmez@beun.edu.tr

F. Korkusuz (ed.), *Musculoskeletal Research and Basic Science*,
DOI 10.1007/978-3-319-20777-3_4

the approximation. Based on the polynomials, FEA is clearly addressed to solve biomechanical problems involving complex GML conditions. In addition to the approximate solution, FEA may help for suitable GML conditions with respect to specified optimization rule and computer properties. More information on this issue can be found in Brown's work [2]. It is also possible that inappropriate local mechanical stress related to both material and loading conditions can be computed in musculoskeletal researches. For this case, it is generally recommended that computational models used are to be reorganized by using trial-error procedure derived from experiments/clinical experiences. In other words, in order to prevent the failure and to predict the repair results, rational two-dimensional or three-dimensional finite element modeling with linear or nonlinear material properties is to be sought by understanding the biological structure as a function of time [3–7].

In this chapter, essentials of FEA on musculoskeletal biomechanics are studied. For this reason, only three types of finite elements, namely, triangular element, quadrilateral element, and brick element, are introduced. Before discussing orthopedic researches for clinical relevance, an example of two-dimensional FEA is also examined.

Node-Element-Mesh: Fundamental Concept

Orthogonal polynomials are helpful for the area of numerical integration. For this purpose, the Gaussian quadrature rule is still preferred and gives very acceptable result with respect to the positive weight (coefficient) function. More information on this issue is given in [8–10].

Using this type of numerical techniques, a skeletal problem is solved by dividing its structural parts into small but finite elements. And, these elements are handled with a specified coordinate system (namely, *grid*) where numerically definable points of the elements (namely, *nodes*) are introduced. Then, some of the GML conditions for the element are considered, and master stiffness matrix of all the elements is formed by using a matrix assembly procedure. Therefore, once the inverse matrix is calculated again by GML conditions, stress and strain fields of the problem are able to be computed with respect to the strain-displacement relationship.

Two-dimensional triangular element is defined as a 3- or 6-noded element with quadratic interpolation functions (Fig. 4.1: A1, A2). While basic

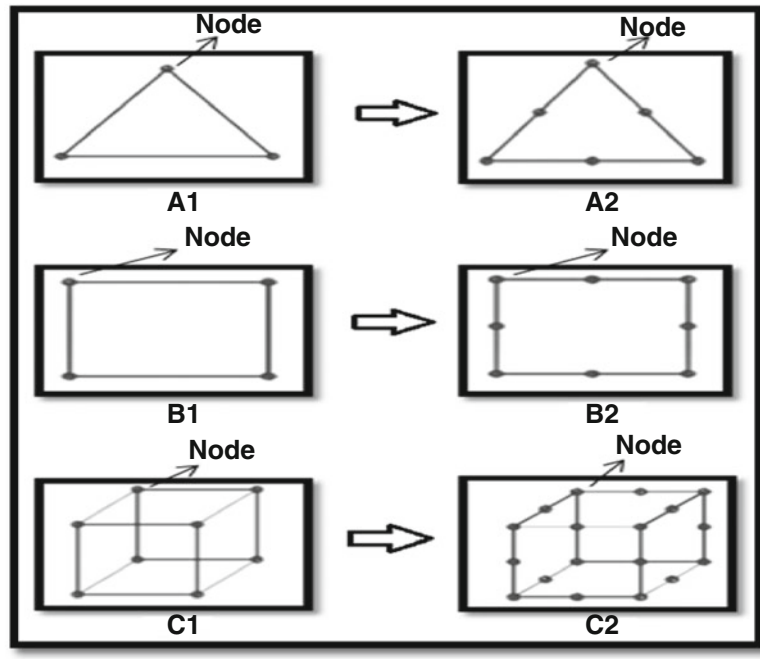

Fig. 4.1 *A1*, *A2* 3- and 6-noded triangular elements; *B1*, *B2* 4- and 8-noded isoparametric elements; *C1*, *C2* 8- and 20-noded isoparametric three-dimensional brick elements

Table 4.1 General purpose finite element codes for biomaterial or biomechanical applications

Code	Reference(s)	Major remarks
Abaqus™	[16–20]	Dynamic problems
		Poroelastic element
Ansys®	[21–24]	Joint contact problems
		Crack element
MSC. Nastran®	[25]	Linear problems
		Element for large deflection
MSC. Marc®	[26, 27]	Nonlinear problems
		Element with full or reduced integration

two-dimensional isoparametric quadrilateral element is designed as a 4-noded bilinear element, the advanced isoparametric quadrilateral elements are 8- or 9-noded distorted elements with biquadratic interpolation (Fig. 4.1: B1, B2). Three-dimensional brick element is defined as an 8- or a 20-noded element with trilinear/triquadratic interpolation (Fig. 4.1: C1, C2).

On one hand, computations for two-dimensional problems are ended up with reduced integration approach (4-point Gaussian integration) or full integration approach (9-point Gaussian integration). On the other hand, computations for three-dimensional problems are analyzed by reduced integration approach (8-point Gaussian integration) or full integration approach (27-point Gaussian integration). Reference [11] is strongly recommended reading for details on finite element library.

For biomaterial or biomechanical applications, one may agree that Abaqus™ [12], Ansys® [13], MSC.Nastran® [14] and MSC.Marc® [15], are considered as a general purpose finite element code with most powerful element library. Major remarks for each of the four codes are given in Table 4.1.

About Difficulties of an FEA for Biomaterials/Biomechanics

Actually, achievement of an FEA for biomaterials and biomechanics depends on its exact flow chart of modeling. In other words, it is to be introduced special terms depending on the simulation concepts [28], mesh quality [29], and patient-specific parameters [30]. Making a decision to obtain accurate prediction follows a highly acceptable flow chart of modeling including sometimes two-dimensional FEA [18, 19, 23] and sometimes three-dimensional FEA [20, 24, 31–33].

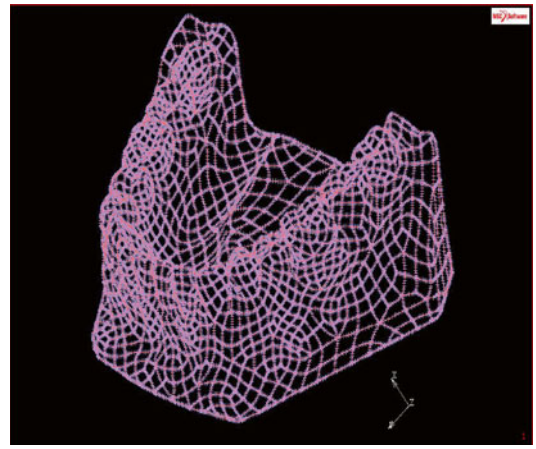

Fig. 4.2 Representation of a human lower jaw pre-model

Moreover, there is a possibility to simplify the three-dimensional FEA using realistic interface boundary conditions. For example, a human lower jaw, one of the complex geometries in orthodontic mechanics, may be reduced to be a cube with respect to "an inclusion problem," i.e., mini implant (see Figs. 4.2 and 4.3).

As given below, one can list general difficulties for an FEA for biomaterial or biomechanical applications:

- In biomechanical studies, sometimes, auto-meshing techniques give unacceptable results. To avoid the creation of undesired elements, suitable surface is to be created in the model.
- It may be recollected that bias factor is a very good tool for using as the basis to generate a much finer mesh surrounding the critical area (inclusion, defect, crack, etc.). Singularity at the critical area can be easily reproduced by choosing the second-order isoparametric elements.
- For the contact problems in biomedical engineering applications, FEA is to be covered by three steps: initial conditions, contact pair

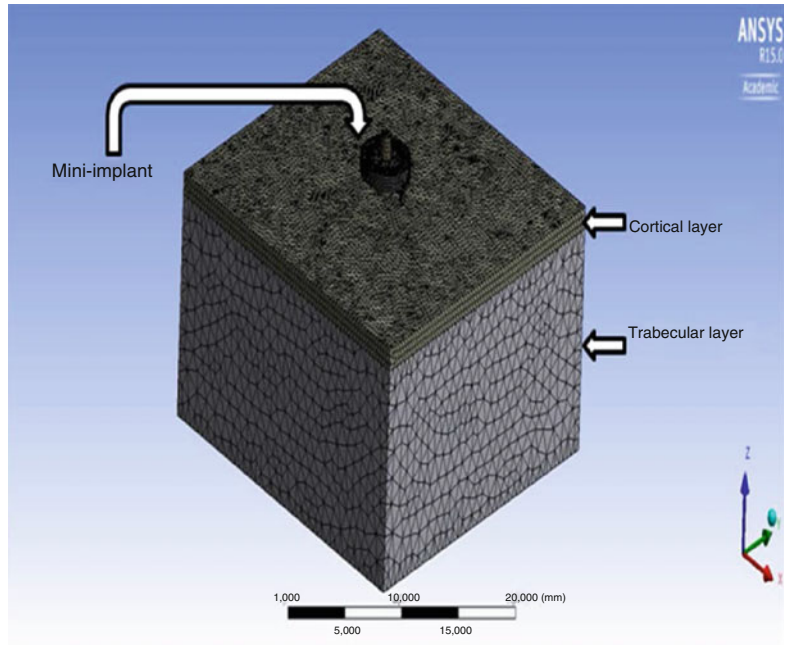

Fig. 4.3 A simplified three-dimensional finite element model

(edge in two-dimensional FEA, surface in three-dimensional FEA), and surface interaction.

- According to Galerkin formulation, dynamically adaptive finite element grid method with dependent variables is to be considered. Details are given in [9].
- Generally, numerical difficulty appeared while searching for a suitable refined mesh to give accurate result. For the sake of the geometry with its biomechanical nature, a number of elements are highly skewed or have large aspect ratios. Consequently, (1) the meshes are not considered suitable for accurate evaluation of stresses up to failure, and (2) due to the fact that force-displacement results are much less sensitive to mesh quality, computation of elastic behavior is considered suitable.

A Simple Example of FEA for Biomaterials

MSC.Marc® [34] is taken into consideration for the crack length prediction based on the work [35] of HV measurement with 200 g indentation load. For this purpose, a finite element model is introduced to predict J-integral field statically. It is

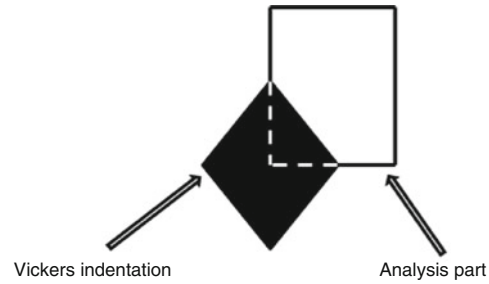

Fig. 4.4 Quarter part of the HV indentation region for the model

claimed that the model proposed is very suitable for the prediction of fracture toughness of bioceramics with early indentation load. The model includes a quarter part of the indentation region as shown in Fig. 4.4. Acceptable fine mesh is defined to represent the critical part (i.e., crack) properly and to calculate reasonably correct J-integral values. Figure 4.5 indicates the fine-meshed model with 4-noded quadrilateral plane elements.

The fine-meshed model with 4-noded quadrilateral plane stress elements is analyzed by 10,000 elements without any bias factor. In this analysis of crack length prediction, full integration technique is preferred.

Under linear elastic [35, 36] plane stress and Palmqvist cracking-mode conditions [37],

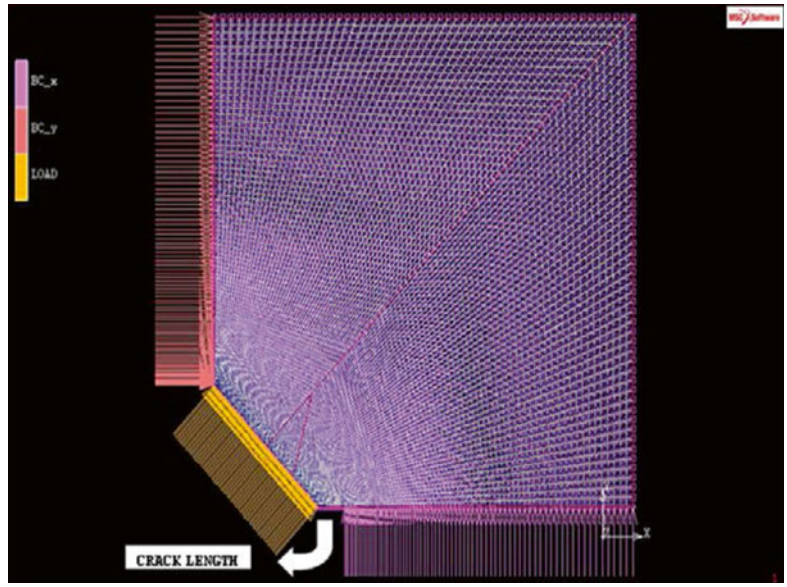

Fig. 4.5 Finite element model for the HV indentation region with general GML conditions

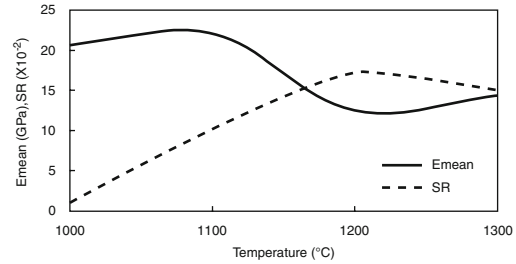

Fig. 4.6 Comparison of SR with E_{mean} at different sintering temperatures

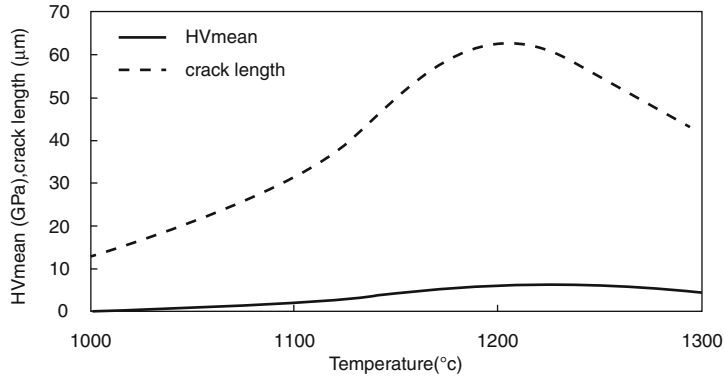

Fig. 4.7 Comparison of crack length with mean values of HV at different sintering temperatures

variations of E_{mean} and SR of the finite element model proposed with respect to sintering temperature are given in Fig. 4.6.

In the temperature range of 1100–1300 °C, it is noted from Fig. 4.6 that asymptotic curve of E_{mean} decreases and then increases while increasing and falling curve of SR increases and then decreases respectively. Therefore, one can conclude that geometrical effect of the crack length prediction in the range of 1100–1300 °C is more clear than that of 1000 °C. In other words, crack length at 1000 °C is expected to be lower value than the others.

Finally, Fig. 4.7 shows that the variation of crack length prediction is similar to that of the HV. As expected, crack length at 1000 °C is lower than that of the other sintering temperatures.

FEA with Clinical Significance

Based on appropriate physical examinations and complex GML conditions, biomechanical simulation and its FEA of an anatomic structure help the medical applications. As an example, in order to analyze a hip joint which is a very complex anatomic structure with different anatomic variations [38], a standard finite element-modeling methodology is to be developed to reach a clinically relevant knowledge (i.e., proper boundary condition and acceptable prediction) [39, 40]. When a model of the methodology is created for solving the difficult parts (such as the trabecular part [41]) of the hip, FEA will provide well-defended results for each subpart of the hip. Once the finite element model is validated and improved by using patient-specific data [42, 43], one can easily compare the differences between the model and the real hip to redesign the artificial hip (clinical trials) [44]. Moreover, the improvement limit of the finite element model is directly related to an anatomical subject-specific data [45].

For further clinical studies, this loop mentioned above is very important to estimate the risk range of the patient (from allowable to critical/fracture) in a correct manner. In other words, for the clinical applications with surgical techniques, FEA is a very useful tool to simulate stress distribution and to predict lifetime; in case of suitable model geometry, related material properties are considered [46–48].

Shortly, one may assume that a human being is a function of sex, age, and living condition. Once this function is considered to create a finite element model, the model may be uncertain to provide clinically useful information. This type of model is called general model. When adding a parameter such as nutritional condition, the model may become certain and is called patient-specific model. That is, it is clearly advised that the analyst who creates the models is to consider the assumptions carefully. For another instance, prosthesis and cement relationship for a patient-specific study can be taken into consideration by defining the major loading conditions as shown in Fig. 4.8. It is obvious that Fig. 4.8 provides a flow diagram to understand whether (1) the FEA coincides with clinical experiences and (2) finite element model is improved for the patient-specific studies (reverse engineering).

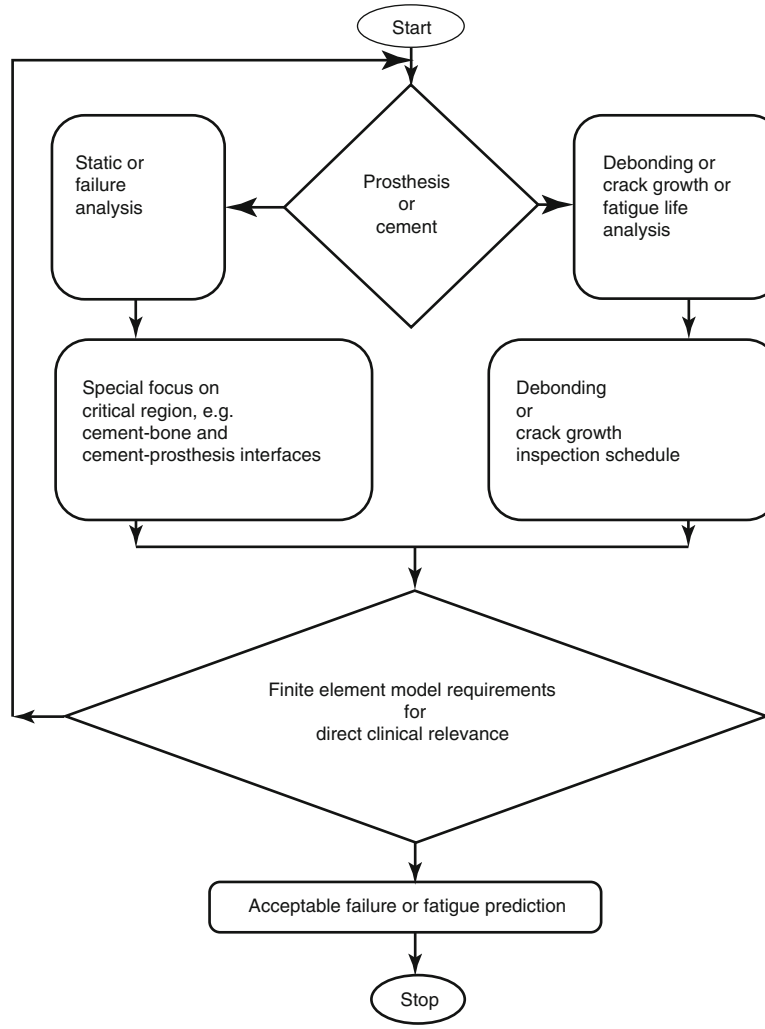

Fig. 4.8 A flowchart example for identification of clinical study versus finite element prediction

References

1. Huiskes R (2000) If bone is the answer, then what is the question? J Anat 197:145–156
2. Brown TD (2004) Finite element modeling in musculoskeletal biomechanics. J Appl Biomech 20:336–366
3. van der Meulen MCH, Huiskes R (2002) Why mechanobiology?: a survey article. J Biomech 35(4):401–414. doi:10.1016/S0021-9290(01)00184-1
4. Doblare M, Garcia JM, Gomez MJ (2004) Modelling bone tissue fracture and healing: a review. Eng Fract Mech 71:1809–1840. doi:10.1016/j.engfracmech.2003.08.003
5. Rapoff AJ (2006) Orthotropic index for bone. J Mater Sci-Mater Med 17:803–805. doi:10.1007/s10856-006-9838-x
6. Harris MD, Anderson AE, Henak CR et al (2012) Finite element prediction of cartilage contact stresses in normal human hips. J Orthop Res 30:1133–1139. doi:10.1002/jor.22040
7. Freutel M, Schmidt H, Dürselen L et al (2014) Finite element modeling of soft tissues: material models, tissue interaction and challenges. Clin Biomech 29:363–372. doi:10.1016/j.clinbiomech.2014.01.006
8. Kythe PK, Puri P (2002) Computational methods for linear integral equations. Birkhauser, Boston
9. Thompson JF, Warsi ZUA, Mastin CW (1985) Numerical grid generation: foundations and applications. North-Holland Publication, Amsterdam
10. Stancu DD, Stroud AH (1963) Quadrature formulas with simple Gaussian nodes and multiple fixed nodes. Math Comput 17(84):384–394

11. Zienkiewicz OC, Taylor RL (2000) The finite element method, vol 1, 5th edn. Butterworth-Heinemann, Oxford
12. http://imechanica.org/files/l2-elements.pdf. Accessed 02 Dec 2014
13. http://www.ansys.stuba.sk/html/elem_55/EBooktoc.htm. Accessed 02 Dec 2014
14. http://www.aero.polimi.it/~lanz/bacheca/downloads/cost/aa10_11/MD_Nastran_Elements_1.pdf. Accessed 02 Dec 2014
15. http://www.mate.tue.nl/~piet/inf/mrc/pdf/volb.pdf. Accessed 02 Dec 2014
16. Wu JZ, Herzog W, Epstein M (1998) Evaluation of the finite element software ABAQUS for biomechanical modelling of biphasic tissue. J Biomech 31:165–169
17. Giner E, Sukumar N, Tarancon JE et al (2009) An abaqus implementation of the extended finite element method. Eng Fract Mech 76:347–368. doi:10.1016/j.engfracmech.2008.10.015
18. Sarkalkan N, Waarsing JH, Bos PK et al (2014) Statistical shape and appearance models for fast and automated estimation of proximal femur fracture load using 2D finite element models. J Biomech 47:3107–3114. doi:10.1016/j.jbiomech.2014.06.027
19. D'Amore A, Amoroso N, Gottardi R et al (2014) From single fiber to macro-level mechanics: a structural finite-element model for elastomeric fibrous biomaterials. J Mech Behav Biomed Mater 39:146–161. doi:10.1016/j.jmbbm.2014.07.016
20. Yu T, Liu X, Ye J et al (2014) Investigation of mechanical behavior of CPC/bone specimens by finite element analysis. Ceram Int 40:2933–2942. doi:10.1016/j.ceramint.2013.10.018
21. Nareliya R, Kumar V (2011) Biomechanical analysis of human femur bone. Int J Eng Sci Technol 3(4):3090–3094
22. Payan Y (ed) (2012) Soft tissue biomechanical modeling for computer assisted surgery. Springer, Berlin
23. Adewusi S, Thomas M, Vu HV (2014) Natural frequencies of the human hand-arm system using finite element method and experimental modal analysis. Trans Control Mech Syst 3(2):11–18
24. Schmidt H, Bashkuev M, Galbusera F et al (2014) Finite element study of human lumbar disc nucleus replacements. Comput Methods Biomech 17(16):1762–1776. doi:10.1080/10255842.2013.766722
25. Ghotge RS (2010) Effect of fixation using locked compression plate versus lag screws on biomechanics of talonavicular joint: a human cadaveric foot model. MSc. Thesis, The University of Tennessee and The University of Memphis
26. Middleton J, Jones ML, Pande GN (eds) (1998) Computer methods in biomechanics and biomedical engineering-2. Gordon and Breach Science Publishers, Amsterdam
27. Bonnet AS, Postaire M, Lipinski P (2009) Biomechanical study of mandible bone supporting a four-implant retained bridge: finite element analysis of the influence of bone anisotropy and food stuff position. Med Eng Phys 31:806–815. doi:10.1016/j.medengphy.2009.03.004
28. Erdemir A, Guess TM, Halloran J et al (2012) Considerations for reporting finite element analysis studies in biomechanics. J Biomech 45:625–633. doi:10.1016/j.jbiomech.2011.11.038
29. Burkhart TA, Andrews DM, Dunning CE (2013) Finite element modeling mesh quality, energy balance and validation methods: a review with recommendations associated with the modeling of bone tissue. J Biomech 46:1477–1488. doi:10.1016/j.jbiomech.2013.03.022
30. van den Munckhof S, Zadpoor AA (2014) How accurately can we predict the fracture load of the proximal femur using finite element models? Clin Biomech 29:373–380. doi:10.1016/j.clinbiomech.2013.12.018
31. Halonen KS, Mononen ME, Jurvelin JS et al (2014) Deformation of articular cartilage during static loading of a knee joint – experimental and finite element analysis. J Biomech 47:2467–2474. doi:10.1016/j.jbiomech.2014.04.013
32. Webb JD, Blemker SS, Delp SL (2014) 3D finite element models of shoulder muscles for computing lines of actions and moment arms. Comput Methods Biomech 17(8):829–837. doi:10.1080/10255842.2012.719605
33. Matsuura Y, Giambini H, Ogawa Y et al (2014) Specimen-specific nonlinear finite element modeling to predict vertebrae fracture loads after vertebroplasty. Spine 39(22):E1291–E1296. doi:10.1097/BRS.0000000000000540
34. MSC.Marc (2013) Mac Neal - Schwendler Corporation (MSC), USA
35. Yetmez M (2014) Sintering behavior and mechanical properties of biphasic calcium phosphate ceramics. Adv Mater Sci Eng 871749:1–5. doi:10.1155/2014/871749
36. Bronzino J (ed) (2000) Biomedical engineering handbook. CRC Press, Boca Raton
37. Houdkova S, Kasparova M (2013) Experimental study of indentation fracture toughness in HVOF sprayed hardmetal coatings. Eng Fract Mech 110:468–476. doi:10.1016/j.engfracmech.2013.05.001
38. Bowman KL Jr, Fox J, Sekiya JK (2010) A clinically relevant review of hip biomechanics. Arthroscopy 26(8):1118–1129. doi:10.1016/j.arthro.2010.01.027
39. Zachariah SG, Sanders JE (1996) Interface mechanics in lower-limb external prosthetics: a review of finite element method. IEEE Trans Rehabil Eng 4(4):288–302
40. Prendergast PJ (1997) Finite element models in tissue mechanics and orthopaedic implant design. Clin Biomech 12(6):343–366
41. Keaveny TM, Morgan EF, Niebur GL et al (2001) Biomechanics of trabecular bone. Annu Rev Biomed Eng 3:307–333
42. Crawford RP, Cann CE, Keaveny TM (2003) Finite element models predict in vitro vertebral body compressive strength better than quantitative computed

tomography. Bone 33:744–750. doi:10.1016/S8756-3282(03)00210-2
43. Fernandez JW, Hunter PJ (2005) An anatomically based patient-specific finite element model of patella articulation: towards a diagnostic tool. Biomech Model Mech 4:20–38. doi:10.1016/S8756-3282(03)00210-2
44. Jiang HB (2007) Static and dynamic mechanics analysis on artificial hip joints with different interface designs by the finite element method. J Bionic Eng 4:123–131. doi:10.1016/S1672-6529(07)60024-9
45. Duchemin L, Mitton D, Jolivet E et al (2008) An anatomical subject-specific FE-model for hip fracture load prediction. Comput Methods Biomech 11(2):105–111. doi:10.1080/10255840701535965
46. Anderson AE, Ellis BJ, Maas SA et al (2010) Effects of idealized joint geometry on finite element predictions of cartilage contact stresses in the hip. J Biomech 43:1351–1357. doi:10.1016/j.jbiomech.2010.01.010
47. Birnbaum K, Pandorf T (2011) Finite element model of the proximal femur under consideration of the hip centralizing forces of the iliotibial tract. Clin Biomech 26:58–64. doi:10.1016/j.clinbiomech.2010.09.005
48. van de Groes S, de Waal-Melefijt M, Verdonschot N (2014) Probability of mechanical loosening of the femoral component in high flexion total knee arthroplasty can be reduced by rather simple surgical techniques. Knee 21:209–215. doi:10.1016/j.knee.2013.05.003

Mechanical Testing Standards of Orthopedic Implants

5

Teyfik Demir and Mustafa Özkaya

Abstract

The orthopedic implants are widely used in spinal, trauma, and arthroplasty surgeries. The mechanical tests for orthopedic implants are performed in accordance with ASTM and ISO standards to determine the lifetime of an implant and the load-bearing capacities. An implant which will be used in the orthopedic surgeries must provide some critical requirements specified by these standards. The mechanical tests for the implants are performed under two main loading conditions which are the static and dynamic loading. The load-bearing capacities of the implant are obtained using the static loading procedure. Furthermore, the lifetime of the implants is evaluated by using the dynamic loading procedure. This chapter aims to evaluate the mechanical testing procedures of the orthopedic implants. The orthopedic implants are categorized with regard to for what purpose they are used. For each orthopedic implant, the test procedures and the test setups are introduced. The critical requirements and interpretation of the results are determined.

Learning Outcomes

After you have studied this chapter, you will have an understanding of (1) orthopedic implants, which are spinal, trauma, and arthroplasty; (2) mechanical test procedures; (3) test setups; (4) critical requirements; and (5) interpretation of results for spinal, trauma, and arthroplasty implants.

Terminology

0.2 % offset displacement, q (mm) permanent deformation which is equivalent to 0.2 % of the center span distance (point A in Fig. 5.3).

Center span, a (mm) the distance between the loading rollers (see Fig. 5.2).

Loading span, h (mm) the distance between a loading roller and the nearest support of the test setup (see Fig. 5.2).

Assoc. Prof. Dr. T. Demir (✉) • M. Özkaya
TOBB University of Economics and Technology,
Department of Mechanical Engineering,
Sogutozu cad. No: 43, Ankara, Turkey
e-mail: tdemir@etu.edu.tr; m.ozkaya@etu.edu.tr

F. Korkusuz (ed.), *Musculoskeletal Research and Basic Science*,
DOI 10.1007/978-3-319-20777-3_5

Bending strength (Nm) of a bone plate the bending moment which induces a 0.2 % offset displacement in the bone plate. The bending strength of the bone plate is determined by Eq. 5.1.

$$\text{bending strength} = \frac{Ph}{2} \quad (5.1)$$

If the bone plate fractures before the proof point (yield point), the bending strength is defined as the bending moment at fracture. In this case, fracture load, F_{max}, takes the place of P in the above bending strength equation.

Bending stiffness, K (N/mm) of a bone plate the slope of the linear elastic portion of load versus displacement curve (slope of the straight line, Om; see Fig. 5.3).

Bending structural stiffness, El_e (Nm^2) of a specimen normalized effective bending stiffness of specimen that takes account of the effects of test configuration. The bending structural stiffness of the specimen is determined by Eq. 5.2.

$$El_e = \frac{(2h+3a)Kh^2}{12} \quad (5.2)$$

Proof Load, P (N) applied load at the intersection point of offset line with load versus displacement curve. It can be referred as yield load also.

M-N diagram a diagram of maximum moment versus number of cycles. A semi-log M-N diagram characterizes the general fatigue behavior of the (specimen) under a range of bending loadings.

Maximum and minimum moments the applied bending moments which have the highest and lowest algebraic values, respectively.

Median fatigue strength at N cycles at a given R ratio, an estimation of the maximum moment at the situation that 50 % of the test specimens would be expected to survive until N cycles.

R ratio the ratio of minimum moment to maximum moment.

Run-out number of cycles at which the testing of the specimen completed without failure. The run-out is specified before the test. If the purpose is to determine fatigue strength at N cycles, the run-out is generally determined as N cycles.

Lever arm of an angled device, L (mm) the distance between the line of load application and sideplate surface that contact with rigid support mimicking the bone.

Compression-bending stiffness, K (N/m), of an angled device calculated like bending stiffness of a bone plate in ASTM F382 (slope of the straight line, Om; see Fig. 5.3).

Compression-bending strength, (Nm), of an angled device the bending moment which induces a 0.2 % offset displacement in the angled device. The bending strength of the angled device is determined by Eq. 5.3.

$$\text{Compression bending strength} = P \times L \quad (5.3)$$

If the angled device failed before the proof point (yield point), the compression-bending strength is defined as the bending moment at fracture. In this case, F_{max} takes the place of P in the bending strength equation above.

Torsional yield strength, N specified by 2° offset method in the linear elastic portion of the torque versus angle of rotation curve. Point Y (see Fig. 5.8) is the torsional yield strength of the bone screw.

Maximum torque, Nm the largest value obtained from the torque versus angle of rotation curve.

The breaking angle, degrees the angle value that occurs when the negative slope (most rapid descent) in the torque versus angle of rotation curve is observed (B.A. point in Fig. 5.8).

Insertion and removal torques, Nm the insertion torque is the maximum torque which occurs in initial four revolutions of the specimen. The removal torque is the maximum

torque required to remove the screw from the test block in initial four revolutions of the specimen. Both torques must be less than torsional yield strength of the screw.

Axial pullout strength, N the maximum load obtained from the load versus displacement curve. It is critical for pullout test of the bone screws.

Self-tapping force, N the axial compression force which is necessary to engage self-tapping feature.

Total span, L sum of the center span and two loading spans ($a+2h$).

Bending moment of an IMFD, M **(Nm)** moment produced by bending load. Calculated from Eq. 5.4.

$$M = Fh/2 \tag{5.4}$$

Torsional stiffness the slope of the straight line which is observed in linear elastic portion of the torque versus rotation curve.

Bending yield load specified by 2° offset method in the linear elastic portion of the load versus displacement curve.

Maximum applied load, F **(N)** the maximum applied load to each loading span is determined by Eq. 5.5.

$$F = \frac{2M_{max}}{h} \tag{5.5}$$

In-plane compressive stiffness the maximum slope of the initial portion of the load versus displacement curve.

In-plane compressive yield strength specified by 2° offset method in the linear elastic portion of the load versus displacement curve.

In-plane maximum compressive strength the maximum load value obtained from the load versus displacement curve.

Block moment arm for spinal implant subassemblies the distance between the insertion point of a screw and axis of the hinge point, perpendicular to the applied load. The moment arms of thoracolumbar, lumbar, and lumbosacral subassemblies are 40 mm. For cervical subassemblies, the distance is 30 mm.

Active length of the longitudinal elements for spinal implant subassemblies the longitudinal distance between insertion points of the superior and inferior screws. It is recommended as 76 mm for thoracolumbar, lumbar, and lumbosacral subassemblies and 35 mm for cervical subassemblies.

Ultimate bending strength the maximum load value obtained from the load versus displacement curve.

S-N diagram a diagram of maximum strength versus number of cycles. A semi-log S-N diagram characterizes the general fatigue behavior of spinal implant constructs under a range of bending loads.

Maximum run-out load the maximum load which can be applied to a test sample in the situation that all of the tested samples survive N cycles without a failure.

R **ratio** the ratio of minimum load to maximum load.

Active length of longitudinal element for interconnection mechanism the distance between the rigid supports (clamps).

Axial gripping capacity the maximum load that occurs on the interconnection mechanism within the first 1.5 mm of permanent displacement between connected components.

Torsional gripping capacity the maximum moment that occurs on the interconnection mechanism within the first 5° of permanent rotation between connected components.

Loosening torque the torque required to disconnect the connected components of interconnection mechanism.

Maximum run-out load/moment the maximum load or moment which can be applied to subassembly in the situation that all the tested constructs survive until N cycles.

Loosening torque the torque required to disconnect the connected components of interconnection mechanism.

Bending stiffness, K (N/mm) of a rod the slope of the linear elastic portion of load versus displacement curve (slope of the straight Om line; see Fig. 5.3).

Bending yield moment, (Nm) the bending moment which induces a 0.2 % offset displacement in the rod.

Bending ultimate moment, (Nm) maximum bending moment value which is applied to a test specimen.

Bending fatigue run-out moment, (N*mm) the maximum moment which can be applied to a test specimen in the situation that all tested specimens survive until N cycles at a specified R ratio.

Ultimate displacement (mm or degree) the displacement occurring when the ultimate load or moment is observed.

Yield displacement (mm or degree) the displacement occurring when the yield load or moment is observed.

Functional failure permanent deformation of the devices which can cause ineffectiveness in load carrying.

Mechanical failure fatigue crack or surface wear of the intervertebral body fusion devices.

Locking mechanism a design feature which restricts the movement between the acetabular liner and shell.

CT distance distance from the most distal point of the stem to the center of the femoral head.

Endurance limit, F_D maximum load that is applied for N_D cycles without failure of specimen.

Endurance cycles, N_D described number of cycles.

Wear material loss from the joint of the components due to movement and loading.

Moment arm for tibial tray, d_{ap} determined as perpendicular distance between the mediolateral centerline of the tibial tray and the axis of load application.

Moment arm for tibial tray, d_{ml} determined as perpendicular distance between the anteroposterior centerline of the tibial tray and the axis of load application.

Introduction

The orthopedic implants are mechanically tested to determine the lifetime of an implant under physiologic loading conditions and load-bearing capacities. Mechanical tests for the inactive medical devices can be evaluated under two main categories with regard to loading conditions. These are static and dynamic loading procedures. Static tests are conducted under quasi-static loading conditions until the fracture or yielding occurrence. The term quasi-static means very small loading speeds that allowed the material to recover to some extent. Moreover, dynamic tests are generally time dependent and the application of higher numbers of cycles takes place. By this type of tests, fatigue or wear performance of the implants can be evaluated. It is important to note that an implant cannot be evaluated with static tests only. In addition, to test an implant on dynamic loading conditions, static tests are prerequisites.

In this chapter, implants will be categorized under three main subcategories to give the message as a whole picture. These are the implants that are used in spinal, trauma, and arthroplasty surgeries and will be named as spinal implants, trauma implants, and arthroplasty implants, respectively. The trauma implants are metallic bone plates, metallic angled orthopedic fracture fixation devices, metallic medical bone screws, intramedullary fixation devices, and external skeletal fixation devices. The spinal implants are pedicle screws, hooks, rods, intervertebral body fusion devices, and spinal artificial disks. The arthroplasty implants are hip joint prosthesis and knee joint prosthesis. The implants can also be categorized under two subcategories in a different approach. These are fusion implants and motion-preserving implants. The motion-preserving implants are the spinal artificial disks, hip joint prosthesis, and knee joint prosthesis. The other implants are the fusion implants.

Trauma Implants

Metallic Bone Plates

Metallic bone plates used in the treatment of trauma fractures are tested according to ASTM F382 [1]. Static testing and dynamic testing were performed to determine bending properties of the plates. The materials which show linear-elastic behavior are tested with this method, so the method is not valid for materials showing nonlinear elastic behavior. A sample of the metallic bone plate is shown in Fig. 5.1.

Static Testing

Four-point bending test is used as static testing to measure the relevant bending properties of bone plates, which are bending stiffness, bending structural stiffness, and bending strength.

Apparatus and Procedure

The test setup can be seen in Fig. 5.2. The vertical load must be applied to bone plates through loading rollers which directly contact to bone plates. The load acts increasingly to the bone plates. The load versus displacement diagram obtained during the test can be seen in Fig. 5.3. The diagram is used to calculate the bending strength.

An alternative test configuration (see Fig. 5.4) can be performed to determine the bending properties of bone plates if the bone plates do not have sufficiently long section or do not have a section of symmetry. In this configuration, the bone plates are attached with rigid extension segments for the purpose of lengthening. The loading rollers directly contact the rigid extension segments during the test unlike the configuration seen in Fig. 5.2.

Interpretation of Results

If the bone plate fractures before the proof point (yield point), the bending strength is defined as the bending moment at fracture. In this case, fracture load, F_{max}, takes the place of P in the above bending strength equation.

Dynamic Testing

The fatigue test is used as dynamic testing for such bone plates. The test method is used to determine the fatigue life of the bone implant under a specific or over a range of maximum bending moment levels. Moreover, fatigue strength (endurance limit) for a specified number of fatigue cycles of bone plates can be determined.

Fig. 5.1 A sample of the metallic bone plate

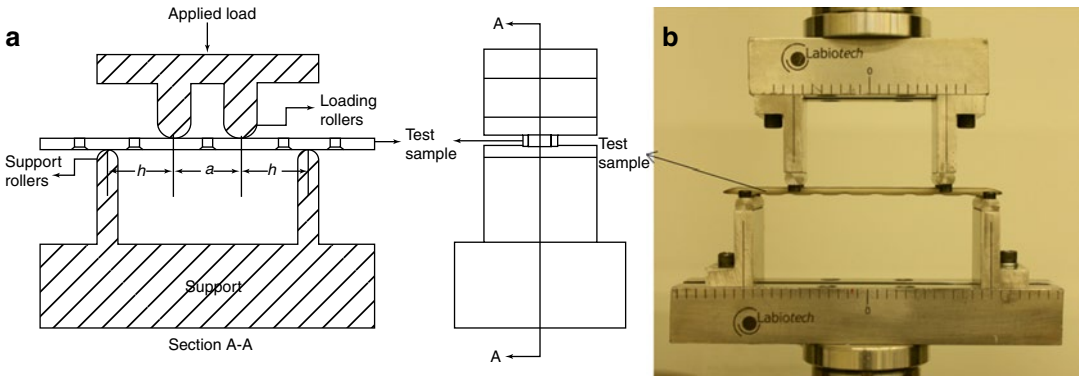

Fig. 5.2 Four-point bending test setup for the metallic bone plates. (**a**) Schematic view, (**b**) view obtained from test

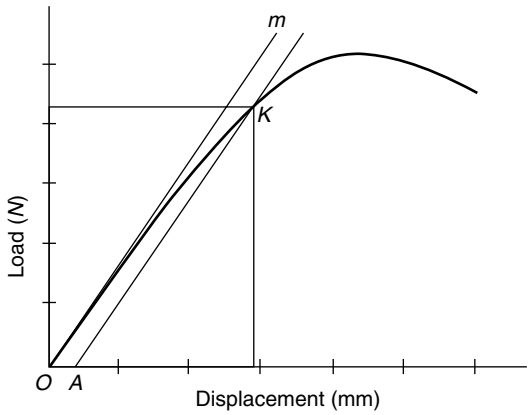

Fig. 5.3 Load versus displacement diagram for the metallic bone plates

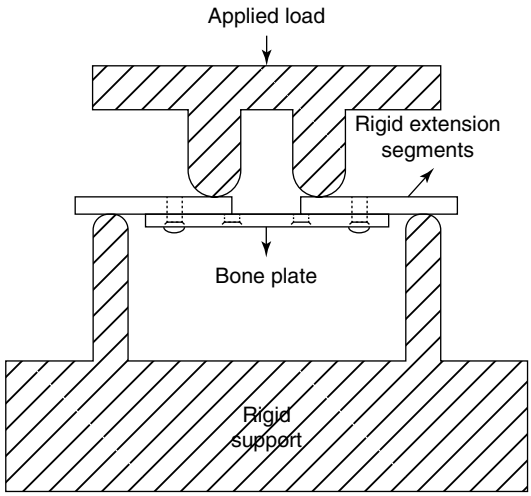

Fig. 5.4 Alternative test setup of the four-point bending test for metallic bone plates

Apparatus and Procedure

The test setup of fatigue testing is the same as static test setup (see Fig. 5.2). A constant frequency, sinusoidal waveform cyclic load is implemented to the bone plate. To complete the test timely, the frequency is generally set to 5 Hz but it is not limited with 5 Hz. The fatigue loading proceeds until the failure of the specimen, a limit which is an indication of failure, or the run-out cycle count which is determined before to stop the test.

Interpretation of Results

The recommended fatigue strength is described as the strength occurring at 1,000,000 cycles without failure. In the estimation of median fatigue strength, N is accepted as 1,000,000 cycles. The recommended *R* ratio is 0.1. The run out is specified before the test. If the purpose is to determine fatigue strength at *N* cycles, the run-out is generally determined as *N* cycles.

If a specimen fails before the 1,000,000 cycles, the next specimen is tested after decreasing the load. The test is repeated until a specimen does not fail before the 1,000,000 cycles. Then, it is tried to reach that three consecutive specimens run out to 1,000,000 cycles when load is increased or decreased. This method is used to determine fatigue curve of the tested implant.

Metallic Angled Orthopedic Fracture Fixation Devices

Metallic angled devices are used in internal fixation of the skeletal system and tested in accordance with ASTM F384 [2]. Static testing and dynamic testing are performed.

Static Testing

Compression-bending test is performed as static testing. The test method is used to measure the compression-bending stiffness and compression-bending strength of the angled devices.

Apparatus and Procedure

The test apparatus of static testing is shown in Fig. 5.5. The angled device attaches to rigid support by the sideplate of the device. The load is parallel to the sideplate's long axis. The load must be applied to lever arm length. The lever arm length is equivalent to 80 % of either blade length or the longest screw. The load must be applied increasingly with the constant crosshead speed of 10 mm/min. The load versus displacement diagram is the same as ASTM F382.

Interpretation of Results

The specifications of ASTM F382 are used during determining the bending stiffness, bending structural stiffness, and bending strength of sideplate.

If the angled device failed before the proof point (yield point), the compression-bending strength is defined as the bending moment at

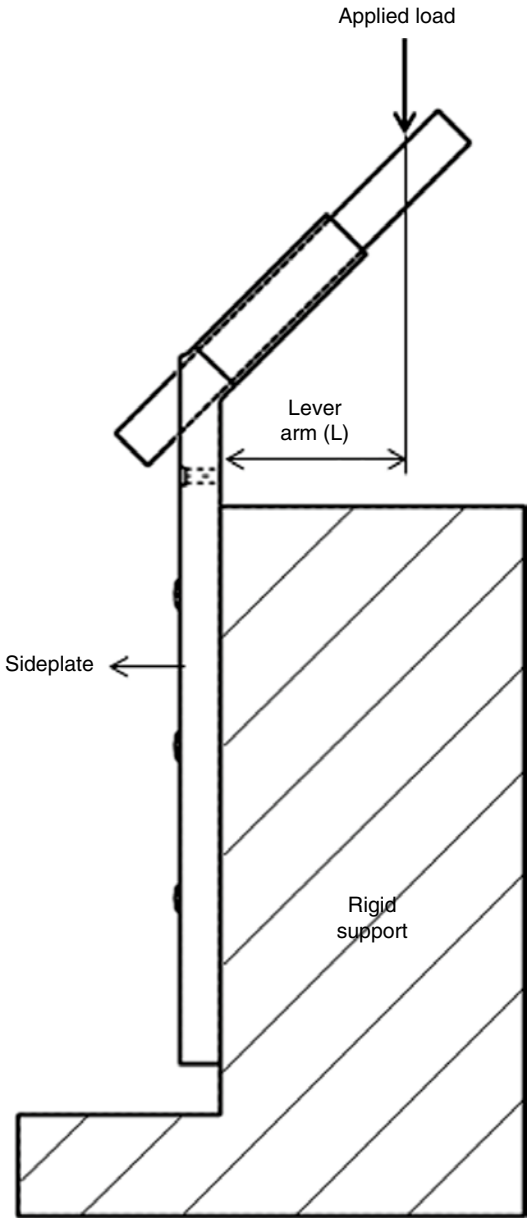

Fig. 5.5 Compression-bending test setup for the metallic angled orthopedic fracture fixation devices

fracture. In this case, F_{max} takes the place of P in the bending strength equation above.

Dynamic Testing

The test method specifies the bending fatigue life of the angled device under a specific or over a range of maximum bending moment levels. Additionally, fatigue strength for a specified number of fatigue cycles of bone plates can be determined.

Fig. 5.6 A sample of the metallic medical bone screws

Apparatus and Procedure

Fatigue test is used in this method as dynamic testing. The test setup of dynamic testing is the same as static testing (see Fig. 5.5). The testing procedure is identical with those specified in ASTM F382.

Interpretation of Results

The M-N diagram, maximum and minimum moments, median fatigue strength at N cycles, and R ratio are defined before in ASTM F382.

If the purpose of the study is to test termination data, the semilog graph of M-N diagram must be plotted. If the purpose of the study is to specify the fatigue strength at 1,000,000 cycles, the fatigue strength is specified as the median fatigue limit (50 % survival).

Metallic Medical Bone Screws

Metallic medical bone screws are tested according to ASTM F543 [3]. The static test systems are used in the method, which are torsion testing, driving torque testing, axial pullout testing, and self-tapping performance testing, to determine the structural properties of metallic bone screw. A sample of the metallic medical bone screws is shown in Fig. 5.6.

Static Testing

Apparatus and Procedure

Torsional yield strength, maximum torque (ultimate), and breaking angle of the bone screw are determined by using torsion test setup under standard conditions. The test setup for torsion test can be seen in Fig. 5.7. The threaded end of the bone screw is held by a clamp which prevents its rotation. The clamp must not hold the screw so tight because this can damage its mechanical structure. The head side of the screw is held by a screwdriver, and the screwdriver rotates the screw

during the test. The speed of the screwdriver can be 1–5 r/min. Torque versus angle of rotation curve (see Fig. 5.8) is gained from the test. The torsional yield strength, maximum torque, and breaking angle are determined by using the torque versus angle of rotation curve.

The torque which is required to drive the bone screw into the standard materials is gained from the driving torque testing. The test setup for driving torque testing is shown in Fig. 5.9. The bone screw is inserted in the test block which has a pilot hole. The test block holder holds the test block rigid but not too tight, because this can deform the test block during the clamping and change the performance of the test. A replaceable bushing is placed between the screw and the test block for the purpose of suitable insertion of a screw to the test block. The screwdriver applied torsional force with the speed of 1–5 r/min.

The axial tensile force required to fail or remove the bone screw from the standard material is measured by using this method. The suitable test configuration for pullout testing is shown in Fig. 5.10. The bone screw is inserted into the test block which is fixated by the base jaw and test block holder. The axial tensile load acts on the bone screw with a rate of 5 mm/min and should be aligned with the screw's long axis. The load is transferred through the head of the screw. The load fixture must not be in contact with the shaft of the screw and must only capture the head of the screw. The screw is inserted with a depth of 20 mm. The insertion depth is determined as 60 % of the threaded length of the screw

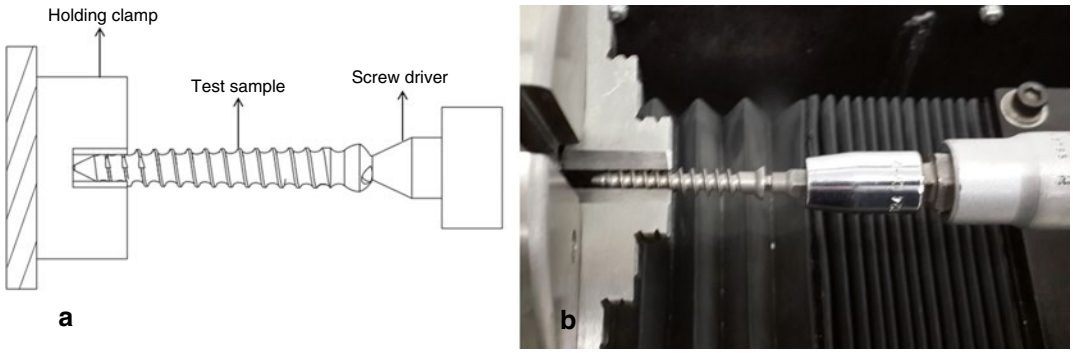

Fig. 5.7 Torsion test setup for the bone screws. (**a**) Schematic view, (**b**) view obtained from the test

Fig. 5.8 Torque versus angle of rotation curve for the bone screws

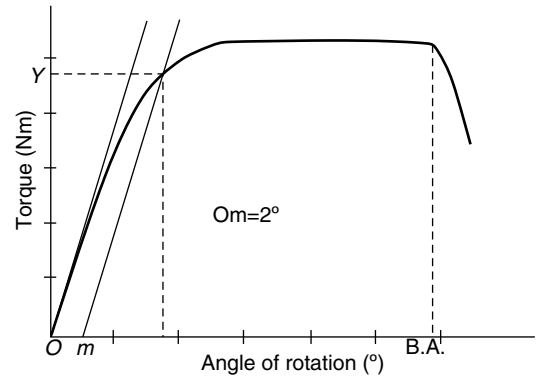

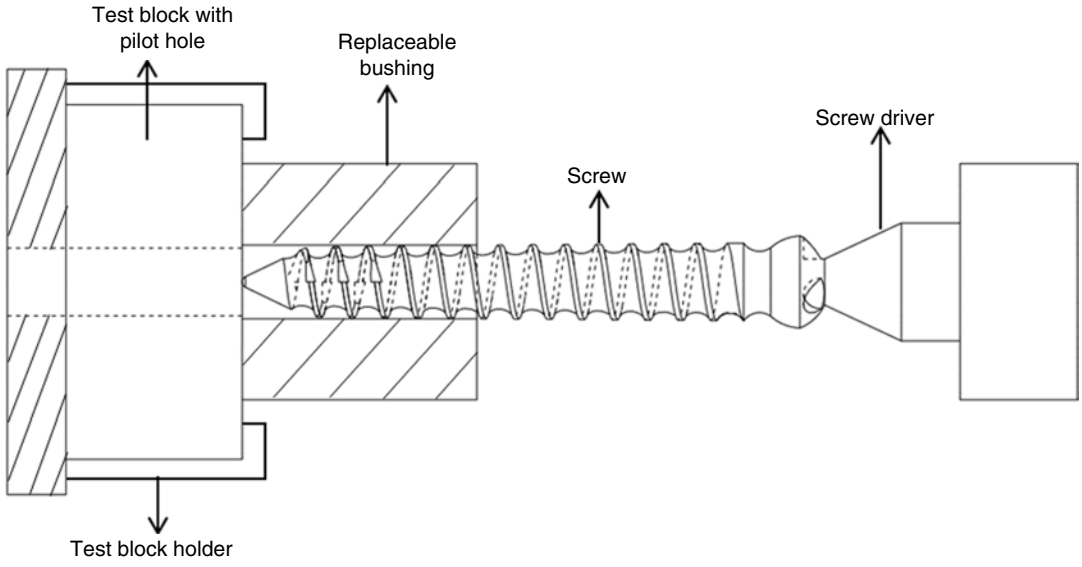

Fig. 5.9 Driving torque test setup for the bone screws

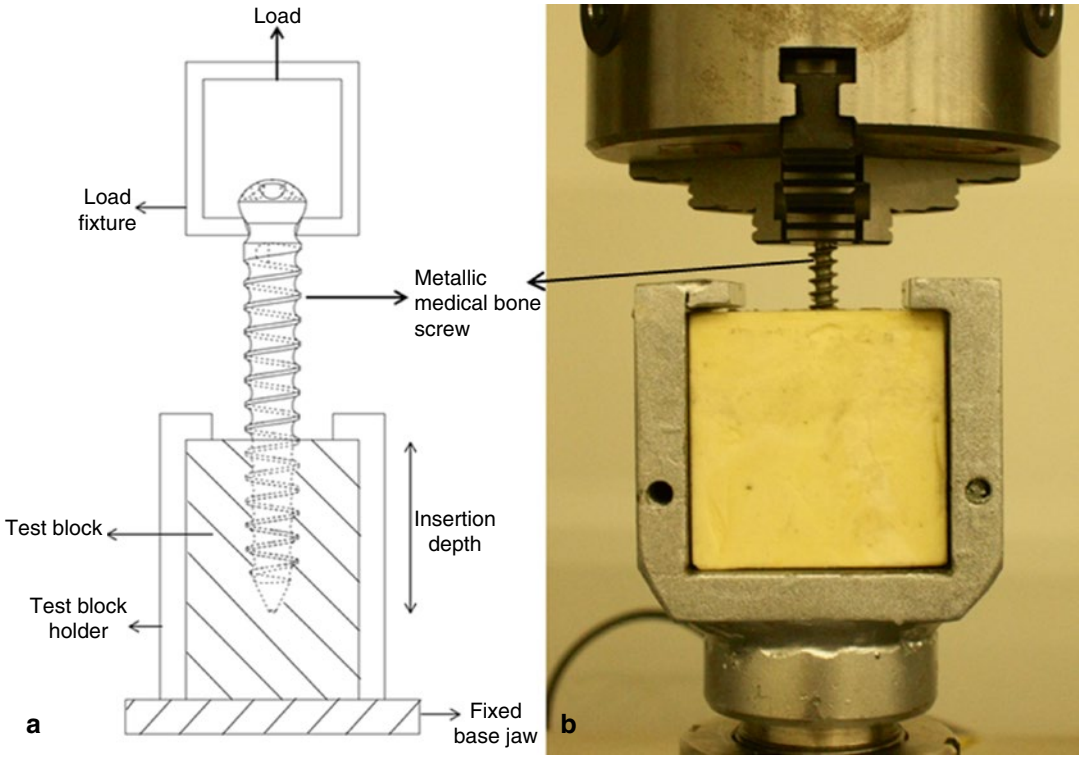

Fig. 5.10 Pullout test setup for the bone screws. (**a**) Schematic view, (**b**) view obtained from test

for fully threaded screws, while the threaded depth is less than 20 mm. All threads should be inserted for partially threaded screws. The screw either can be released from the test block or can fail during the test.

The self-tapping performance testing of the self-tapping medical bone screws is used to measure axial compression load that is required to engage self-tapping feature. The test apparatus indicated in Fig. 5.9 can be used for the test apparatus of self-tapping performance testing. There is no need for the replaceable bushing for this testing method. A pilot hole is needed to be drilled before the testing. The axial load cell measures the axial compression load during the testing. A rotational force should be applied with a constant speed of 30 r/min, and the axial compression force should be applied with a constant rate of 2 N/s.

Interpretation of Results

The removal torque is the maximum torque required to remove the screw from the test block in the initial four revolutions of the specimen. Both torques must be less than the torsional yield strength of the screw.

HA and HB types of metallic medical bone screws are currently used. Torsional strength and breaking angle requirements for the HA and HB types screws are shown in Table 5.1.

Table 5.1 Torsional strength and breaking angle requirements

Type and size	Minimum required values for acceptance	
	Torque, Nm	Breaking angle, °
HA 1.5	0.2	150
HA 2.0	0.35	150
HA 2.7	1.0	180
HA 3.5	2.3	180
HA 4.0	4.0	180
HA 4.5	4.4	180
HA 5.0	5.5	180
HB 4.0	1.3	90
HB 6.5	6.2	90

Intramedullary Fixation Devices (IMFDs)

Clinical Relevance

In Gaebler's study [4], the case reports of the fractures of the intramedullary fixation devices are investigated. Eight hundred thirty-nine patients who had unstable peritrochanteric and subtrochanteric fractures were treated with intramedullary fixation devices (gamma nail) from 1992 to 1996. In two patients (0.2 %), implant failure had occurred. The gamma nails failed at the hole of the locking screw in both cases. Metallurgic and scanning electron microscopic (SEM) examinations were done on the failed implants.

In May 1996, a peritrochanteric fracture was treated with gamma interlocking nail (12 mm in diameter) in an 81-year-old woman. The patient was discharged from the hospital 10 days after the injury. The patient complained about pain at the site of the locking screws at follow-up. No changes in the implant or femur were seen on X-ray. The patient fell again and was brought to the hospital in September 1996. A fracture at the gamma nail located at the level of the hole of the locking screw and a fracture of the femur at the same level were seen on X-ray (Fig. 5.11).

The metallurgic and SEM examinations of gamma nail showed that gamma nail has a main weak point at the grooves of the clover-leaf diameter. The cross-section reduces at the grooves, and this causes increased stress concentration at the site. A photograph of the fracture surface can be seen in Fig. 5.12. Beach-mark shapes can be seen in the figure. These beach marks start from the right corner and spread to the

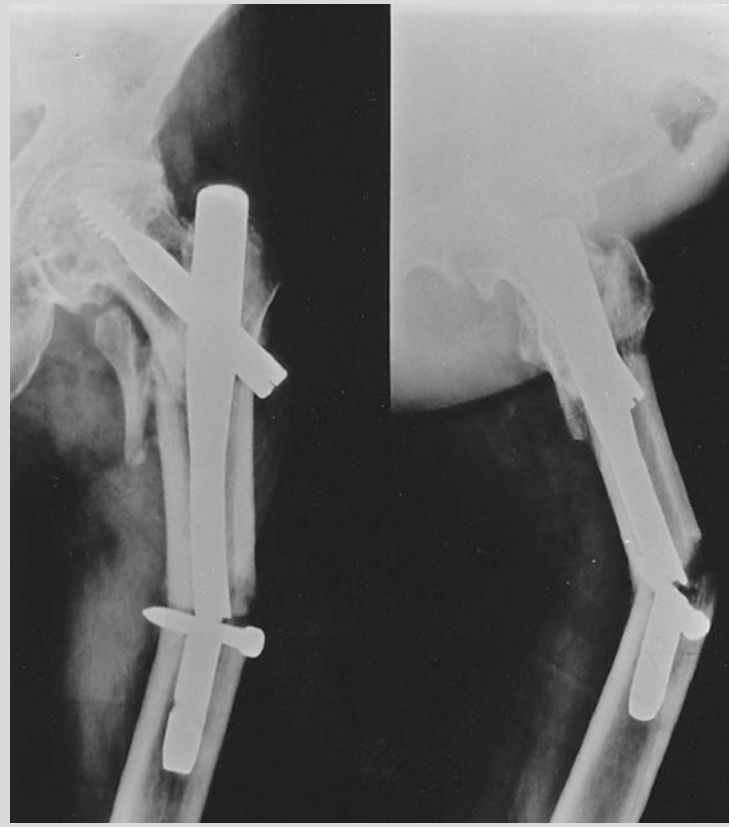

Fig. 5.11 The fracture at the femur and gamma nail (Reproduced from Gaebler et al. [4])

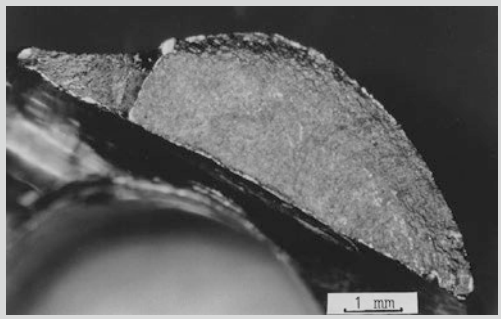

Fig. 5.12 The photograph of the fracture surface which shows the fatigue failure (Reproduced from Gaebler et al. [4])

left corner and finally leave the bowed marks on the fracture surface. This shape on the fracture surface indicates the fatigue failure of the gamma nail.

To prevent the fatigue failures mentioned above in the clinical relevance, the static and dynamic tests of the IMFDs are performed.

IMFDs are used generally in the femur, tibia, ulna, and humerus as surgical fixation devices. IMFDs are tested in accordance with ASTM F1264 [5]. The specifications have the static and dynamic testing of IMFDs and the dynamic testing of IMFD locking screws. A sample of the IMFDs can be seen in Fig. 5.13.

Static Testing

Static test method for IMFDs is the four-point bending test and torsion test.

Apparatus and Procedure

On the determination of the bending strength and bending stiffness of the IMFD, four-point bending test is performed. For the four-point bending test for IMFD, the test apparatus shown in Fig. 5.2 can be used. The bending load is implemented through the loading spans equally with a constant speed. The constant cross-head speed must not exceed 1 mm/s. Load versus displacement curve which is obtained during the test is used when determining the bending stiffness, yield load, and bending moment.

Torsion tests are conducted to measure the torsional stiffness of the IMFDs. The test setup can be seen in Fig. 5.14. The fixed grip holds one end of the test specimen, and load is applied to the other end by load frame. The test specimen must have a central portion with uniform cross-section, and a gauge length of 23 cm must be placed into this uniform section. Torque versus rotation curve is recorded during the test. The torque is applied until the rotation of the specimen reaches 5° or until a straight line of the torque versus rotation curve is obtained.

Fig. 5.13 A sample of the IMFDs

Dynamic Testing

Fatigue test is performed for IMFDs and IMFD locking screws.

Apparatus and Procedure

Fatigue test of IMFD measures the fatigue life of the IMFD under a specific or over a range of maximum bending moment levels. Moreover, fatigue strength for a specified number of fatigue cycles can be determined. The test setup which is used in the static bending test of IMFD is the same setup for fatigue tests with the differences on loading conditions. The sinusoidal cyclic load at a specified frequency is applied to the test specimen. The frequency of load should not be greater than 5 Hz, and the advised R ratio is 0.1.

The bending test is used as the fatigue test of IMFD locking screws also. The bending tests can be four-point bending or three-point bending, depending on the screw length. When four-point bending fatigue test is performed, the four-point bending test setup which is shown in Fig. 5.2 is used. The screws, which have no sufficient length to fit the four-point bending test setup, are tested on the three-point bending test setup as can be seen in Fig. 5.15. There is only one loading roller in the test setup of the three-point bending test, and loading roller is placed at equal distance from each support roller. The frequency of load should not be greater than 5 Hz.

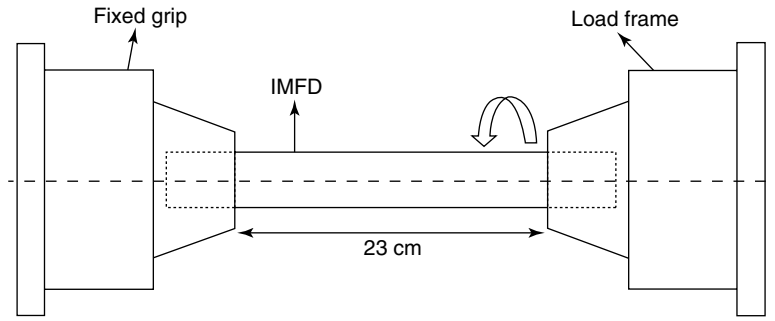

Fig. 5.14 Torsion test setup for the IMFD

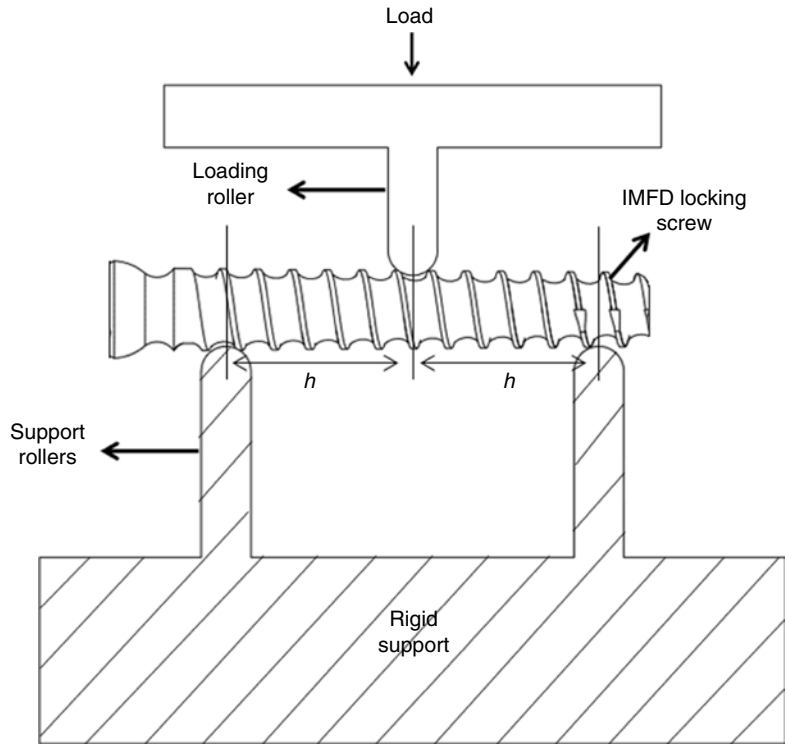

Fig. 5.15 Three-point bending test setup for the IMFD locking screws

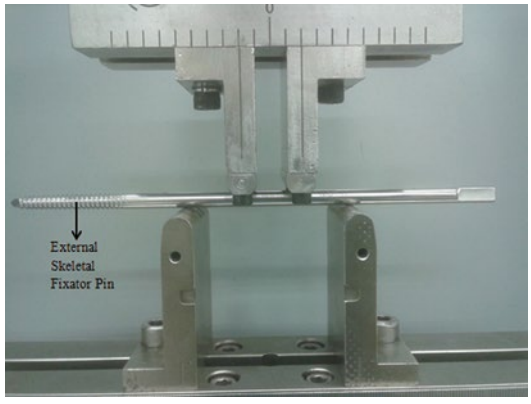

Fig. 5.16 Four-point bending test setup for the external skeletal fixation pins and a sample

Interpretation of Results

The recommended fatigue strength is described as the strength occurring at 1,000,000 cycles without failure. In the estimation of median fatigue strength, N is accepted as 1,000,000 cycles. The recommended *R* ratio is 0.1. The run-out is specified before the test.

External Skeletal Fixation Devices

External skeletal fixation devices are tested according to ASTM F1541 [6]. The method covers the testing of circular ring or ring segment bridge elements and testing of external skeletal fixator pins and subassemblies. A sample of external skeletal fixator pins is shown in Fig. 5.16. The subassembly contains pins, base and mobile segments, and a longitudinal element.

Static Testing

Circular ring or ring segment bridge elements are tested statically to determine their in-plane compressive strength and stiffness.

Static bending tests and torsion tests are performed to determine the bending and torsional strength of the external skeletal fixator pins.

Static bending tests are performed to determine the stiffness and strength of the external skeletal fixator subassemblies.

Apparatus and Procedure

When determining the static bending strength of the external skeletal fixator pins, the four-point test is performed. The testing apparatus can be seen in Fig. 5.16, and the testing procedure of ASTM F382 can be used in this method for external skeletal fixator pins. When determining the torsional strength of the external skeletal fixator pins, the test apparatus and procedure of the ASTM F543 can be used similarly.

The testing apparatus, used for determining in-plane compressive properties of circular ring or ring segment bridge elements, is shown in Fig. 5.17. A circular ring bridge element is not a complete circle. To form a single circular ring, arcs or segments are joined together with connection bolts. Moreover a ring segment's span is less than 180°. A ring segment bridge element's span is more than 180° and less than 360°. The circular ring bridge elements or ring segment bridge elements are attached to the test frame with pins and U-shaped metal jaw fixture. Compressive load is applied increasingly to the test component until any failure occurs. Load versus displacement curve is recorded to determine in-plane compressive properties.

The static test apparatus of external skeletal fixator subassemblies are shown in Fig. 5.18. Load is applied through input loading platen quasistatically. Load versus deformation curves are gained for each specimen after tests. Stiffness and strength values are calculated from these curves.

Interpretation of Results

Interpretation of results of the four-point bending testing for the external skeletal fixator pins is similar with ASTM F382. Additionally, interpretation of results of the torsion testing is similar with ASTM F543.

The stiffness and strength values of external skeletal fixator subassemblies are calculated by load versus displacement curves using the same procedures mentioned before in other methods.

Dynamic Testing

Dynamic tests of external skeletal fixator subassemblies are performed to determine fatigue life of the specimens.

Apparatus and Procedure

The dynamic test apparatus of the external skeletal fixator subassemblies is the same as the testing apparatus of the static test (see Fig. 5.18). The frequency of input loading should not be more than 5 Hz. The input loading should be in a cyclic waveform.

Interpretation of Results

Fatigue life and strength of the external skeletal fixator subassemblies are determined.

Spinal Implants

Pedicle Screw, Hook, and Rod Systems

Pedicle screws and rods used in spinal surgeries are tested according to test protocols of ASTM F543, F1717 [7], F1798 [8], and F2193 [9]. The static torsion and static pullout tests of pedicle screws are tested according to ASTM F543 and will not be discussed again in this section. The static and dynamic tests of spinal implant constructs (vertebrectomy models) of the pedicle screws and rods are performed in accordance to ASTM F1717. Static and dynamic tests of the interconnection mechanism and subassemblies of the pedicle screw and rod constructs are also performed according to ASTM F1798. Moreover, the rods are tested according to ASTM F2193. Samples of the pedicle screws and rods are shown in Fig. 5.19.

Spinal Implant Constructs in Vertebrectomy Model

Static and dynamic test methods are performed to measure the stiffness and strength of the spinal implant subassemblies according to ASTM F1717 [7]. Test methods of cervical, thoracolumbar, lumbar, and lumbosacral spinal implant subassemblies are similar. The pedicle screw constructs are shown in the figures which are related to this method. The test method also covers hook and transverse element constructs. The test apparatus for hook and transverse element constructs was not indicated in figures because

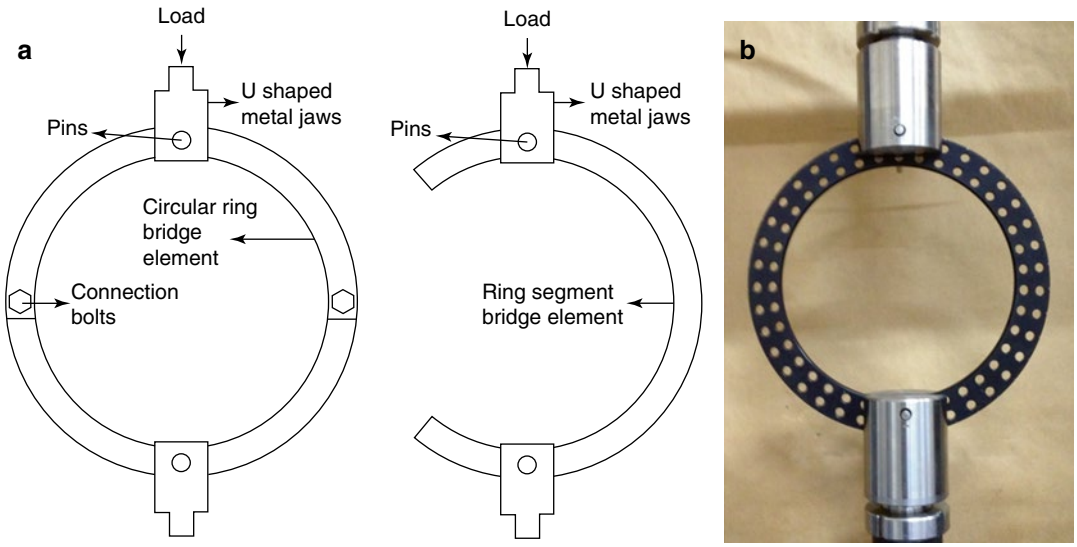

Fig. 5.17 In-plane compressive test setup for the circular ring or ring segment bridge elements. (**a**) Schematic view, (**b**) view obtained from test

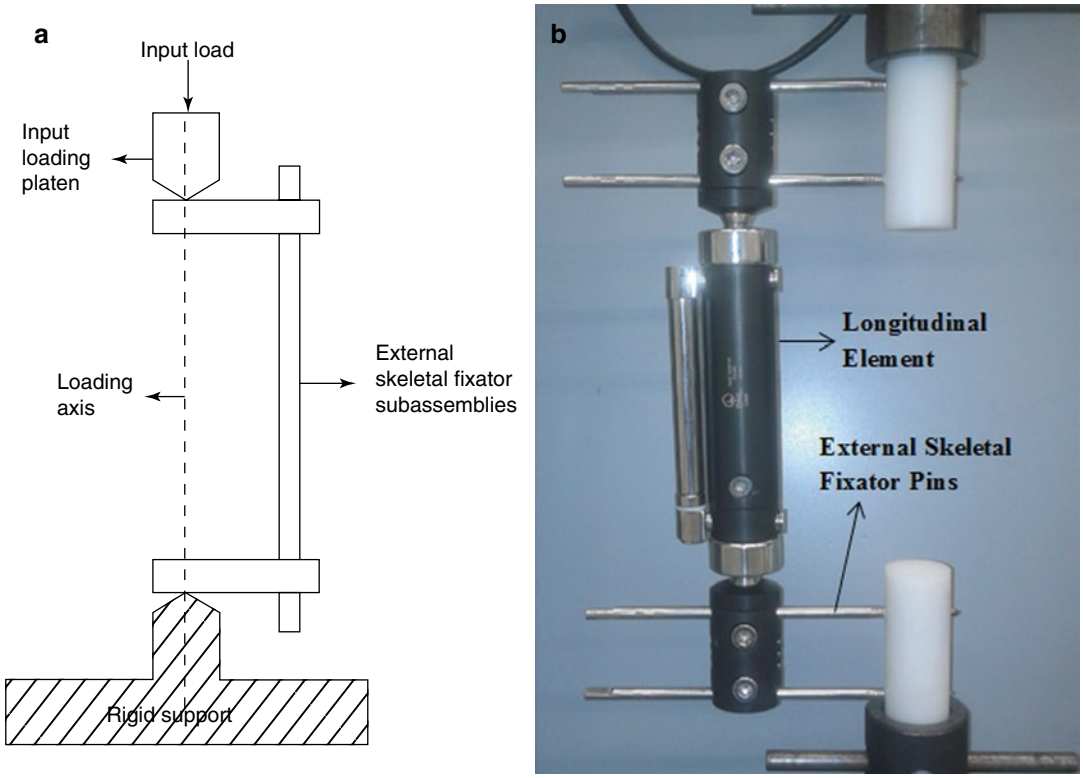

Fig. 5.18 Test setup for the external skeletal fixator subassemblies. (**a**) Schematic view, (**b**) view obtained from test

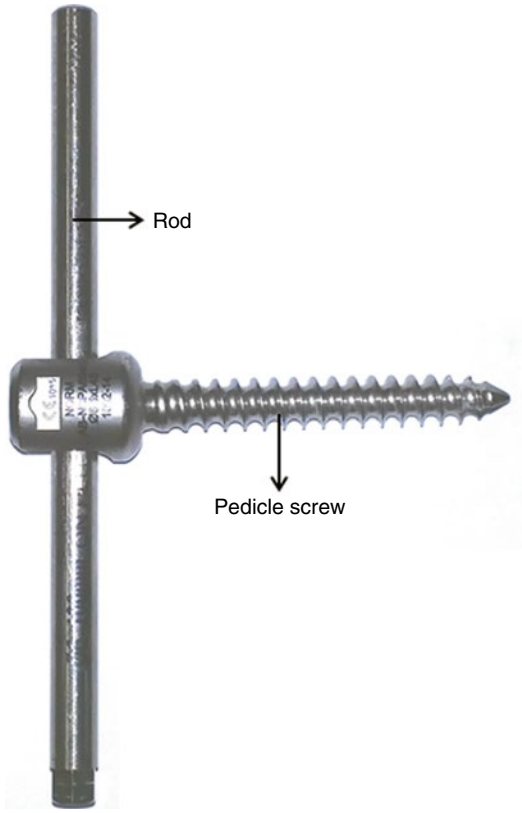

Fig. 5.19 Samples of the pedicle screws and rods

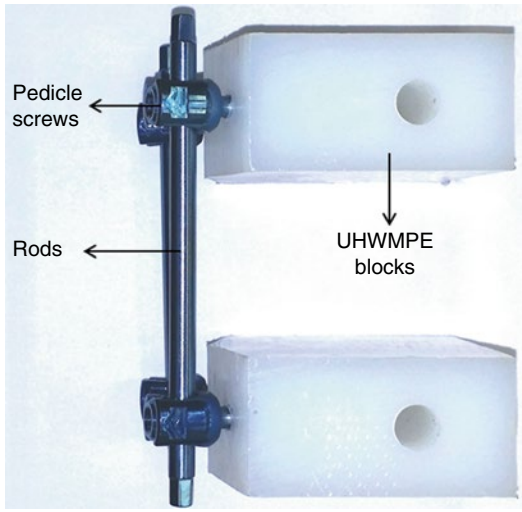

Fig. 5.20 A sample of the spinal implant subassemblies

they are similar with the test apparatus of pedicle screw constructs. A sample of the spinal implant subassemblies is shown in Fig. 5.20. Spinal implant subassemblies contain longitudinal elements, pedicle screws, and ultrahigh-molecular-weight polyethylene (UHMWPE) blocks.

Static Testing

The static tests of the spinal implant subassemblies are compression-bending, tensile-bending, and torsion tests.

Apparatus and Procedure

The test setups for compression-bending and torsion tests are shown in Fig. 5.21. The figures also shows the critical dimensions of the subassemblies required for the test method. Ultrahigh-molecular-weight polyethylene blocks are used as the standard material which the screws are inserted in. Two UHMWPE blocks are used; one block is connected with a fixed frame and the other one is connected with a loading frame via hinge pins. The load is applied to the axis of the hinge pin for bending test through the direction of the Z axis. The maximum rate must be up to 25 mm/min when applying the load for bending test.

For the torsion tests, torque is applied about the Z axis. The maximum loading rate must be up to 60°/min on the torque application during the test. Load versus displacement and torque versus angle of rotation curves are used to determine the stiffness and strength.

Interpretation of Results

The moment arms of thoracolumbar, lumbar, and lumbosacral subassemblies are 40 mm. For cervical subassemblies, the distance is 30 mm.

Active length of the longitudinal elements is recommended as 76 mm for thoracolumbar, lumbar, and lumbosacral subassemblies and 35 mm for cervical subassemblies.

The compressive bending yield strength, compressive bending stiffness, torsional yield strength, and torsional stiffness of spinal implant constructs can be determined using the load versus displacement curve and torque and angle at rotation curves as mentioned before in ASTM F382 and ASTM F543 sections.

Dynamic Testing

Compression-bending fatigue test is used as dynamic testing. The fatigue test measures the fatigue strength or life of the spinal implant constructs.

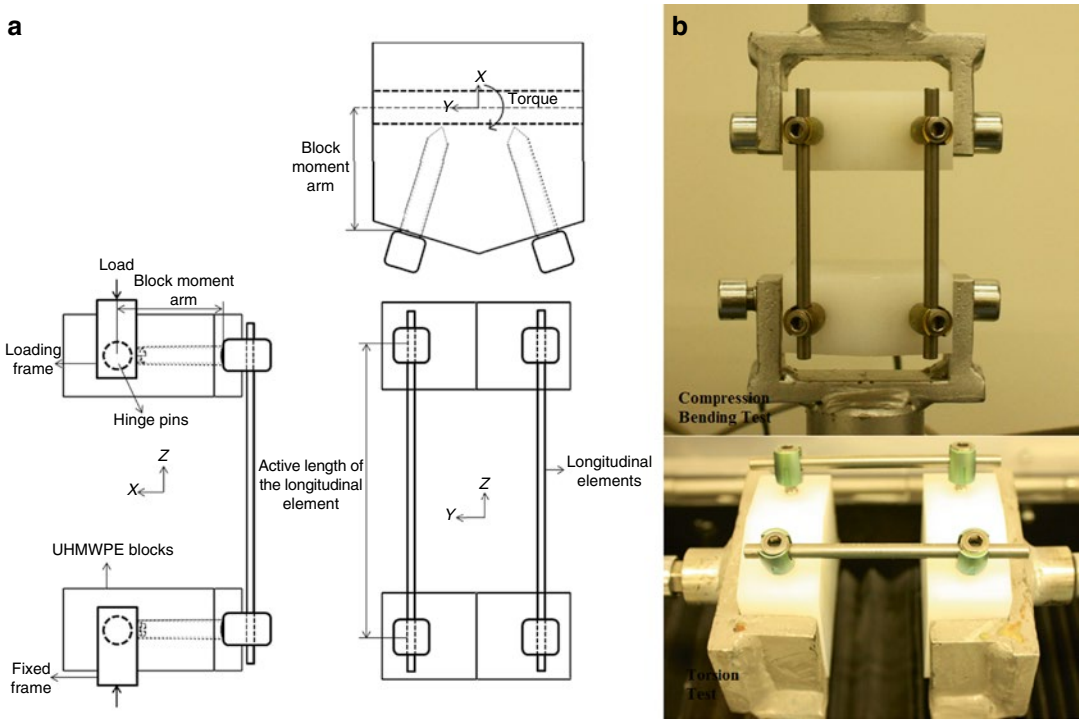

Fig. 5.21 The test setups of the compression-bending and torsion tests for spinal implant subassemblies. (**a**) Schematic view, (**b**) view obtained from test

Apparatus and Procedure

The test setup is the same as the compression-bending test setup of static testing. A cyclic load is applied to test specimens. The recommended frequency of the test is 5 Hz. Compression-bending load versus the number of cycles to failure curve is obtained after the fatigue testing. Run-out cycle is considered as 5,000,000.

Interpretation of Results

The recommended fatigue strength is described as the strength occurring at 5,000,000 cycles. When estimating the maximum run-out load, N is accepted as 5,000,000 cycles. The *R* ratio must be equal to or higher than 10.

For the fatigue tests, suggested initial fatigue loads can be selected as 75, 50, and 25 % of the ultimate compression-bending load values of static testing. One of these fatigue levels must survive until 5,000,000 cycles without failure. The difference between the maximum run-out load and a load which caused failure in a spinal construct must be less than 10 % of the compression-bending ultimate load values.

Interconnection Mechanisms and Subassemblies Used in Spinal Arthrodesis Implants

Interconnection mechanisms and subassemblies are tested in accordance with ASTM F1798 [8]. The static and dynamic tests are performed. The method is used for interconnection mechanisms which include screws, hooks, and transverse elements connected with rods.

Static Testing

Flexion/extension moment test, axial gripping capacity test, and torsional gripping capacity test are performed as static test. The aim of the test method is to measure the flexion/extension moment, axial gripping capacity, and axial torque gripping capacity. Loosening torque can be also measured.

Apparatus and Procedure

Flexion/extension moment test setup with critical dimensions is shown in Fig. 5.22. In the figure, a subassembly of a pedicle screw and a rod is shown, but a hook or a transverse element can also be replaced with the pedicle screw. The

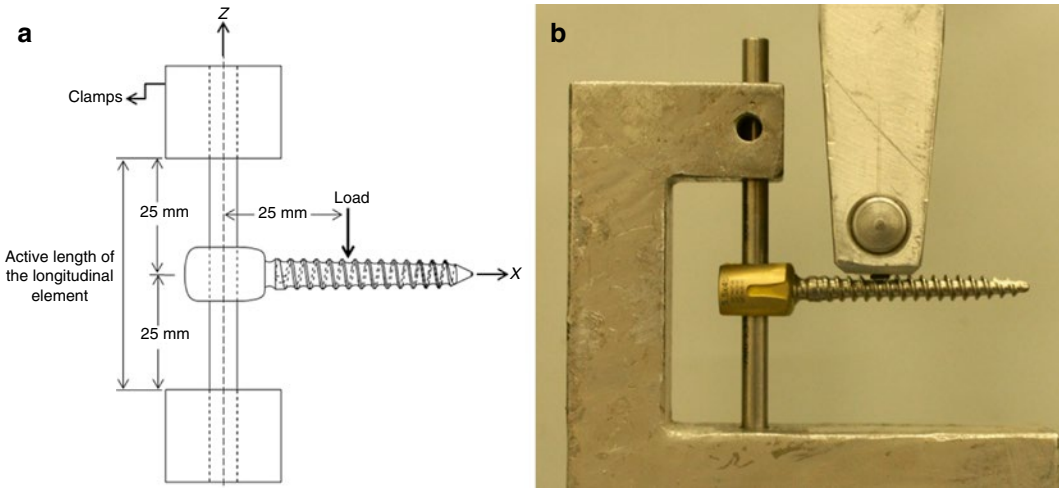

Fig. 5.22 Flexion/extension moment test setup with critical dimensions for the subassemblies. (**a**) Schematic view, (**b**) view obtained from test

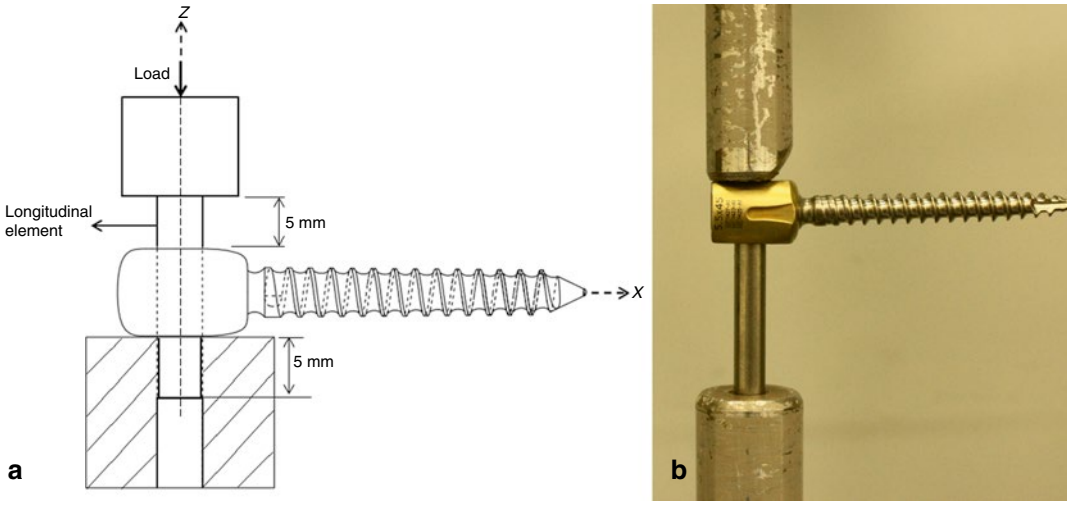

Fig. 5.23 The axial gripping capacity test setup with critical dimensions for interconnection mechanism. (**a**) Schematic view, (**b**) view obtained from test

clamps rigidly hold the rod. A load perpendicular to the axis of screw shaft (*X* axis) is applied to a 25 mm distance from the rod (longitudinal element) axis. The applied load is in the direction of the *Z* axis with the maximum rate of 25 mm/min. Interconnection mechanism is centered on a 50 mm section of the rod.

In Fig. 5.23, the test apparatus for axial gripping capacity testing can be shown with the critical dimensions. The axial load is applied to the longitudinal element in the direction of the *Z* axis with the maximum rate of 25 mm/min.

Test apparatus for torsional gripping capacity tests with the required dimensions can be seen in Fig. 5.24. A torsional load is applied to the longitudinal element with a maximum rate of 25°/min through a collet. A block with a component-shaped cavity captures the component as can be seen in Fig. 5.24.

Interpretation of Results

Active length of longitudinal element is defined as 50 mm (see Fig. 5.22).

The failure of a subassembly is described as permanent deformation which is caused by frac-

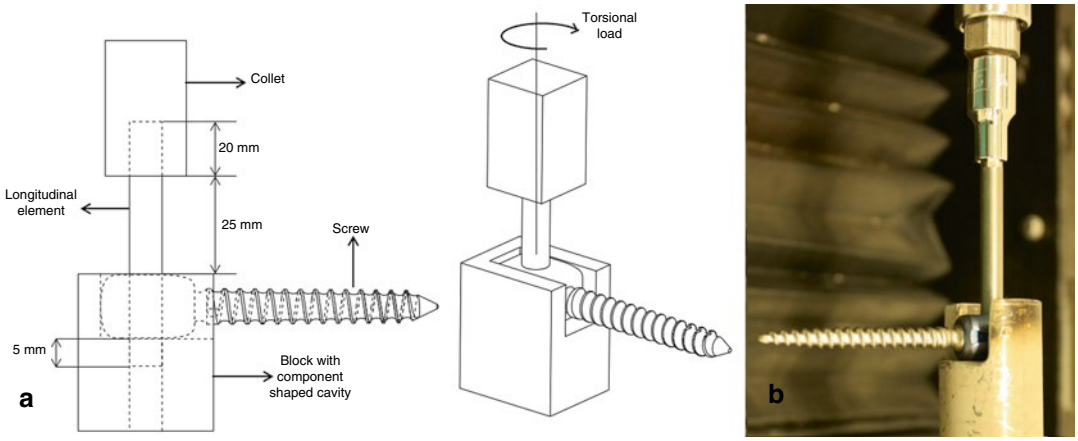

Fig. 5.24 The torsional gripping capacity test setup with the required dimensions for interconnection mechanism. (**a**) Schematic view, (**b**) view obtained from test

ture, loosening, or slippage. The permanent deformation can result in decreasing or lack of the load-bearing capacity of the subassembly.

Dynamic Testing

Flexion/extension moment fatigue run-out, axial fatigue run-out, and axial torsional fatigue run-out loads are measured for the interconnection test sample subassemblies.

Apparatus and Procedure

The test setups for dynamic tests are the same as static test setups (see Figs. 5.22, 5.23, and 5.24). The continuous amplitude cyclical load is applied to the interconnection test sample subassemblies. There is no specified maximum frequency of cyclic loading.

Interpretation of Results

When maximum run-out load/moment is described, survival limit is accepted as 2,500,000.

For the fatigue tests, maximum loads for initial dynamic test can be selected as 75, 50, and 25 % of the ultimate moment values of static testing. One of these fatigue levels must survive until 2,500,000 cycles without failure.

If a specimen fails before the 2,500,000 cycles, the next specimen is tested with decreased load. The test is repeated until a specimen does not fail before the 2,500,000 cycles. Then, it is tried to reach that three consecutive specimens run out to 2,500,000 cycles when load is increased or decreased. This method is used to determine the fatigue curve of the tested samples.

The differences between the maximum run-out load and a load occurring at the failure of the construct must be less than 10 % of the compression-bending ultimate load.

Rods

The rods that are used as longitudinal element in spinal arthrodesis implants for surgical fixations are tested in accordance with ASTM F2193 [9]. Static and dynamic tests are performed within this test method.

Static Testing

The four-point bending test is implemented as static test method. The static test method is used to measure the bending stiffness, bending yield moment, and bending ultimate moment of the rods.

Apparatus and Procedure

For spinal rods, the four-point bending test apparatus shown in Fig. 5.2 can be used. When applying the load, the displacement rate must not exceed 10 mm/min. Load versus displacement curve is recorded during the test (similar with Fig. 5.3). The bending test procedure is very similar with the four-point bending test procedures mentioned before.

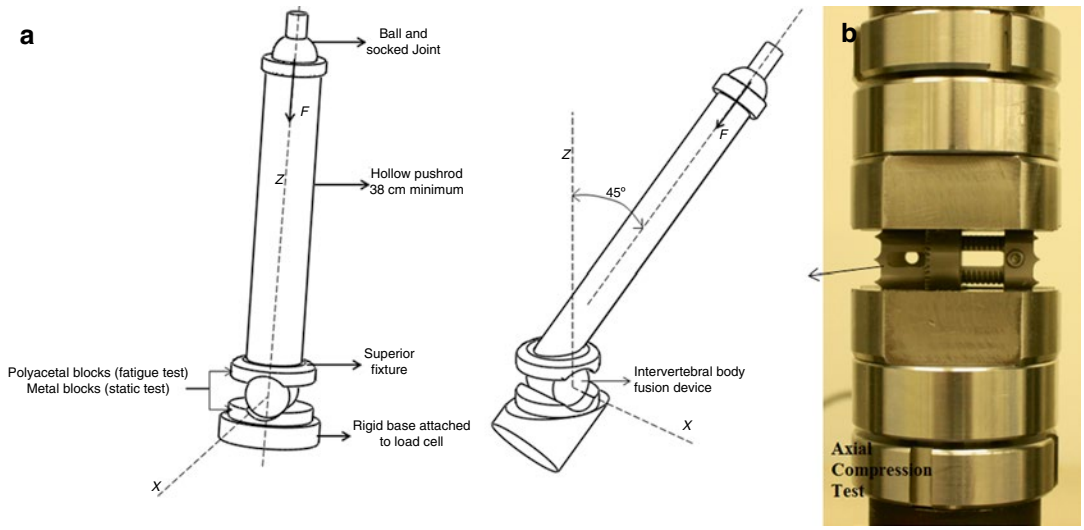

Fig. 5.25 Axial compression and compression-shear test setups for the intervertebral body fusion devices. (**a**) Schematic view, (**b**) view obtained from test

Dynamic Testing

Fatigue test is used in the method as a dynamic method. The bending fatigue run-out moment is determined by the method.

Apparatus and Procedure

The four-point bending test apparatus which can be seen in Fig. 5.2 is also used as dynamic test setup. The frequency of the cyclic loading must be maximum 30 Hz. *R* ratio can be used as 0.10.

Interpretation of Results

Survival limit for bending fatigue run-out moment is 2,500,000 cycles.

For fatigue test, maximum loads for initial dynamic test can be selected as 75, 50, and 25 % of the ultimate moment values of static testing. The specimens of one of these fatigue levels must survive until 2,500,000 cycles without failure.

The differences between the maximum run-out load and a load occurring at the failure of the construct must be less than 10 % of the compression-bending ultimate load.

Intervertebral Body Fusion Devices

Intervertebral body fusion devices are used to achieve arthrodesis at a given spinal motion segment. Static and dynamic testing of the intervertebral body fusion devices are performed in accordance with ASTM F2077 [10].

Static Testing

Axial compression testing, compression-shear testing, and torsion testing are applied to a test specimen to determine yield displacement (axial or torsional), stiffness (axial or torsional), ultimate load or moment, yield load or moment, and ultimate displacement (axial or torsional).

Apparatus and Procedure

The test apparatus for axial compression test can be seen in Fig. 5.25. Actuator of the test machine applies to axial load to a hollow pushrod by a ball and socket joint. The length of the pushrod is 38 cm. A sphere-shaped superior fixture connects with the pushrod. Two metal blocks hold the intervertebral body fusion devices. The metal blocks have appropriate surfaces to mate geo-

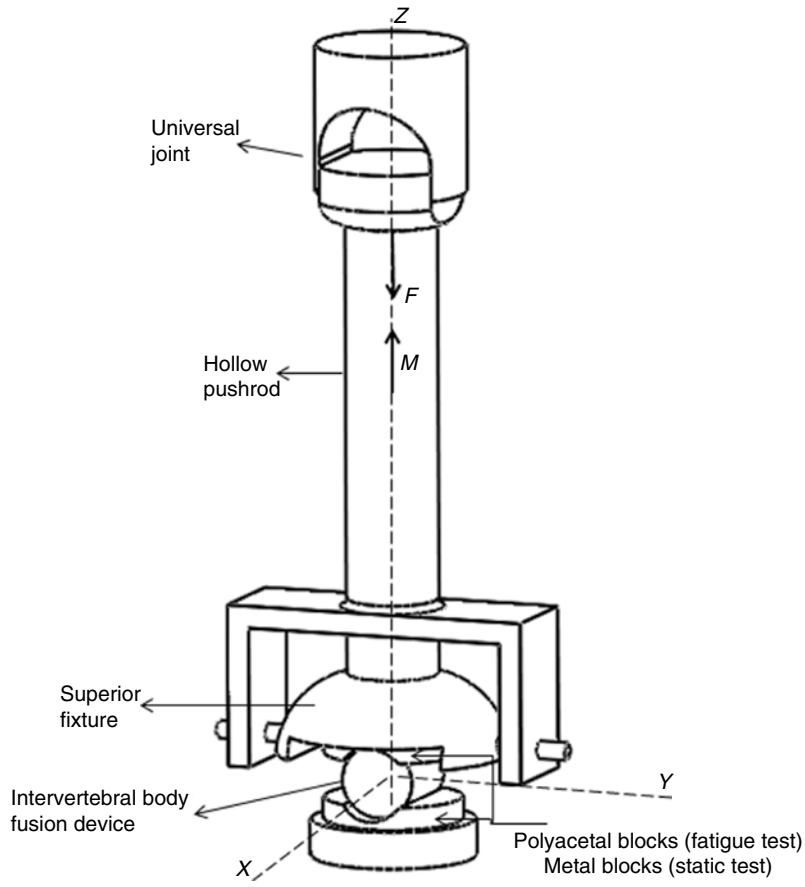

Fig. 5.26 Torsion test setup for the intervertebral body fusion devices

metrically with the intervertebral body fusion device's geometry. One of the metal block contacts to superior fixture and the other to a rigid base which is attached to a load cell. Axial force is applied in the direction of the pushrod axis. The pushrod axis must be coincident with the Z axis of the device and also collinear with axial load. The load passes through the center of sphere of the superior fixture. The load is applied with a rate of maximum 25 mm/min. The load and displacement curve is recorded during the test.

The compression-shear testing apparatus is shown in Fig. 5.25. There is an angle of 45° between the pushrod axis and the *Z* axis of the devices in the direction of flexion. This is necessary to constitute a shear load on the device. The applied load is coincident with the axis of the hollow pushrod and passes through the center of the sphere of the superior fixture.

The test apparatus for the torsion testing (see Fig. 5.26) is similar with axial compression testing. A torsional load with a rate of maximum 60°/min is applied in addition to an axial load. Torque versus angle at rotation curve is recorded.

The intradiscal height is recommended as 10 mm for the lumbar spine, 6 mm for the thoracic spine, and 4 mm for the cervical spine.

Interpretation of Results

Yield load or moment, ultimate load or moment, and stiffness are determined as mentioned before in the previous methods. The load versus displacement and torque versus angle at rotation curves are used on the determination.

Dynamic Testing

Fatigue test is employed as dynamic test.

Apparatus and Procedure

The test apparatus for dynamic testing are the same apparatus used in static tests (see Figs. 5.25 and 5.26). Polyacetal blocks are used in dynamic tests instead of metal blocks in static tests. For axial compression and compression-shear testing, the *R* ratio should be selected as 10. The *R* ratio should be selected as -1 for torsional testing. The frequency of cyclic load can be determined by test professionals.

Interpretation of Results

The 25, 50, and 75 % of ultimate load in static testing are selected as suggested initial fatigue loads for dynamic testing. The test ends when a sample survives until 5,000,000 cycles or functional failure of the sample occurs.

Functional failure is described as permanent deformation of the devices which can cause ineffectiveness in load carrying.

Mechanical failure is described as the fatigue crack or surface wear of the intervertebral body fusion devices.

When estimating the maximum run-out load or moment, survival limit is accepted as 5,000,000 cycles.

The differences between the maximum run-out load and a load occurring at the failure of the construct must be less than 10 % of the compression-bending ultimate load.

Spinal Artificial Disks

Spinal artificial disks are tested according to ASTM F2346 [11]. The static and dynamic test methods are used. Axial compression testing, compression-shear testing, and torsion testing are performed to spinal artificial disks as static and dynamic test methods.

The testing apparatus and procedures of the static and dynamic test methods are the same as ASTM F2077 (see Figs. 5.25 and 5.26). The only difference is geometric considerations of the test samples. The spinal artificial disks and intervertebral body fusion devices have different geometries. Because of this reason, the polyacetal and metal blocks used in this method are different from F2077 with regard to the geometry. There are no other differences in testing apparatus or the used procedure.

Interpretation of results is also identical with ASTM F2077 except maximum run-out load or moment. The maximum run-out load or moment of the spinal artificial disks is determined as that the maximum load or moment which can be applied to a test specimen in the situation that all tested specimens survive until 10,000,000 cycles without mechanical failure. There are no other differences in the static and dynamic tests between spinal artificial disks and intervertebral body fusion devices.

The intervertebral height, H, is recommended as 4 mm for the cervical spine, 6 mm for the thoracic spine, and 10 mm for the lumbar spine.

Arthroplasty Implants

Hip Joint Prosthesis

Clinical Relevance

In Ishaque's study [12], a 57-year-old woman who had osteoarthritis in her hip was treated with total hip joint prosthesis in April 2011. A bone-preserving femoral neck prosthesis was used. 6 months after operation, the patient complained about her femoral leg pain. In 2005, she was unable to walk without using crutches because of her severe pain. The reason of the pain was not trauma because she never fell. Surgeons suspected stem fracture of the femoral component after the radiographic examination.

SEM analysis was performed on the fractured stem following the extraction of the femoral component. The fractured stem and fracture surface can be seen in

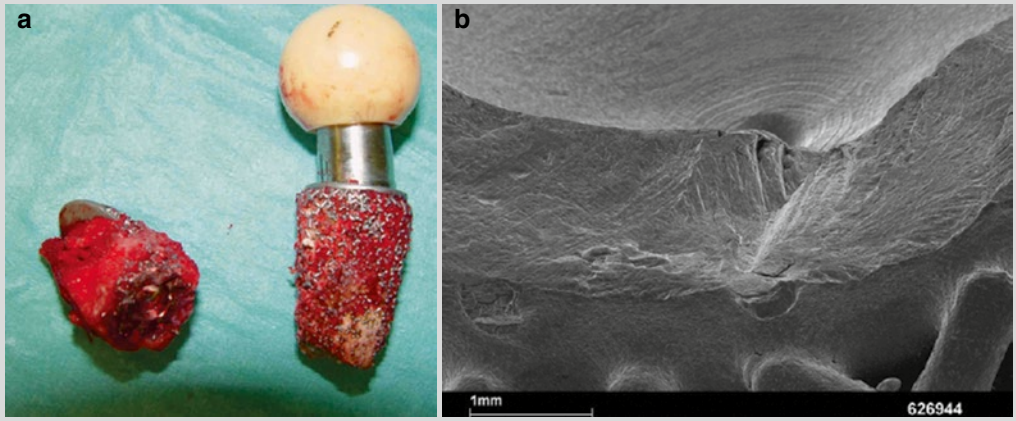

Fig. 5.27 (**a**) The fractured stem, (**b**) the photograph of the fracture surface which shows the fatigue failure (Reproduced from Ishaque et al. [12])

Fig. 5.27. The SEM analysis clearly showed that the fracture surface had indications of fatigue crack. The fatigue crack propagation and beach marks are shown in the figure. The spongy metal structures of the femoral component are the sites where stress concentration increases, and the fatigue crack probably began at those sites.

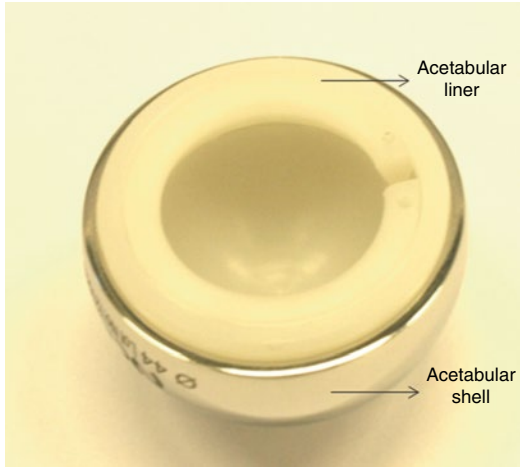

Fig. 5.28 The samples of acetabular shells and liners

Static and dynamic tests are performed to hip joint prosthesis to prevent the failures mentioned above in the clinical relevance. Axial disassembly of an acetabular device testing (push off testing) is used as static testing. On the dynamic side, fatigue and wear testing of total or partial hip joint prosthesis are performed. A sample of acetabular shell and liner are shown in Fig. 5.28.

Static Testing

Axial disassembly of an acetabular device testing is performed according to ASTM F1820 [13]. The test method is used to measure the attachment strength (axial locking strength) between the modular acetabular shell and the liner.

Apparatus and Procedure

The test setup for push-off testing can be seen in Fig. 5.29. The apparatus only supports acetabular shell as can be seen. The direction of the axial load must be perpendicular to the face center of the acetabular shell. Axial load is applied with a rate of 5.1 cm/min over drill blank on the shell to disassemble the acetabular liner freely. The maximum load required for disassembling the liner from the shell is recorded. The shell can be used

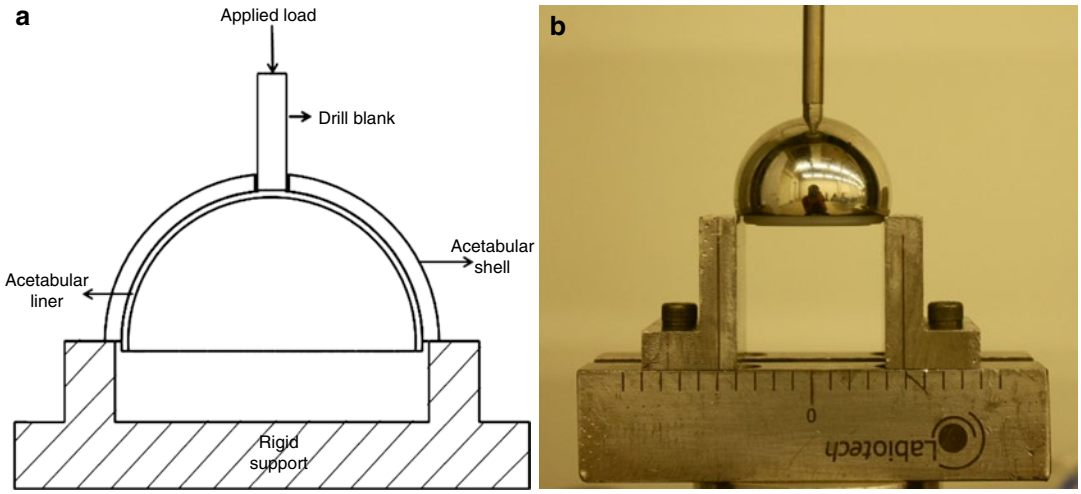

Fig. 5.29 The test setup for push-off testing. (**a**) Schematic view, (**b**) view obtained from test

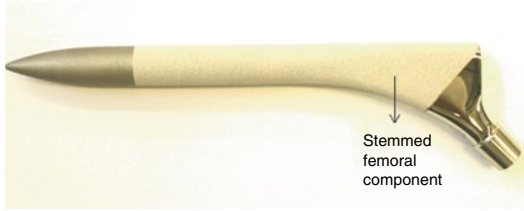

Fig. 5.30 A sample of stemmed femoral components of total hip joint prosthesis

more than once if it has no damage after the test, but the liner cannot.

Dynamic Testing

The fatigue testing of stemmed femoral components of total hip joint prosthesis is performed in accordance with ISO 7206-4 [14]. The endurance limit and endurance cycles are specified with the method. A sample of stemmed femoral components of total hip joint prosthesis is shown in Fig. 5.30.

The wear testing of the total hip joint prosthesis is performed according to ISO 14242. The method determines relative angular movement between articulating components and the pattern of the applied force.

Apparatus and Procedure

The test setup for fatigue testing of stemmed femoral components of total hip joint prosthesis is shown in Fig. 5.31. The inferior part of the test specimen is embedded in a solid material as can be seen in the figure. The loading mechanism applies a cyclic load. The cyclic load, which produces axial compression, two-plane bending, and torsion, is applied to the head of the test specimen through metal loading plate. The frequency is 5 Hz or less.

The wear testing of total hip joint prosthesis is performed by testing machines which are capable of 3-axis motion. Normal configuration of the femoral and acetabular components of a test specimen is provided before the test. A specified time-varying force together with specified relative angular displacements is transmitted to the components by the test setup. When performing the wear testing of total hip joint prosthesis, the specified time-varying force (see Fig. 5.32) is applied to the specimen along the loading axis according to ISO 14242-1 [15]. Additionally, specified relative angular movement applied to the femoral test specimen can be seen in Fig. 5.33. The applied angular movement is in three directions for wear testing: flexion-extension direction, adduction-abduction direction, and inward-outward direction. When considering the orbital bearing wear simulator of total hip joint prosthesis, ISO 14242-3 [16] must be taken into account. For orbital bearing wear simulator, specified time-varying force is the same as Fig. 5.32; however specified relative

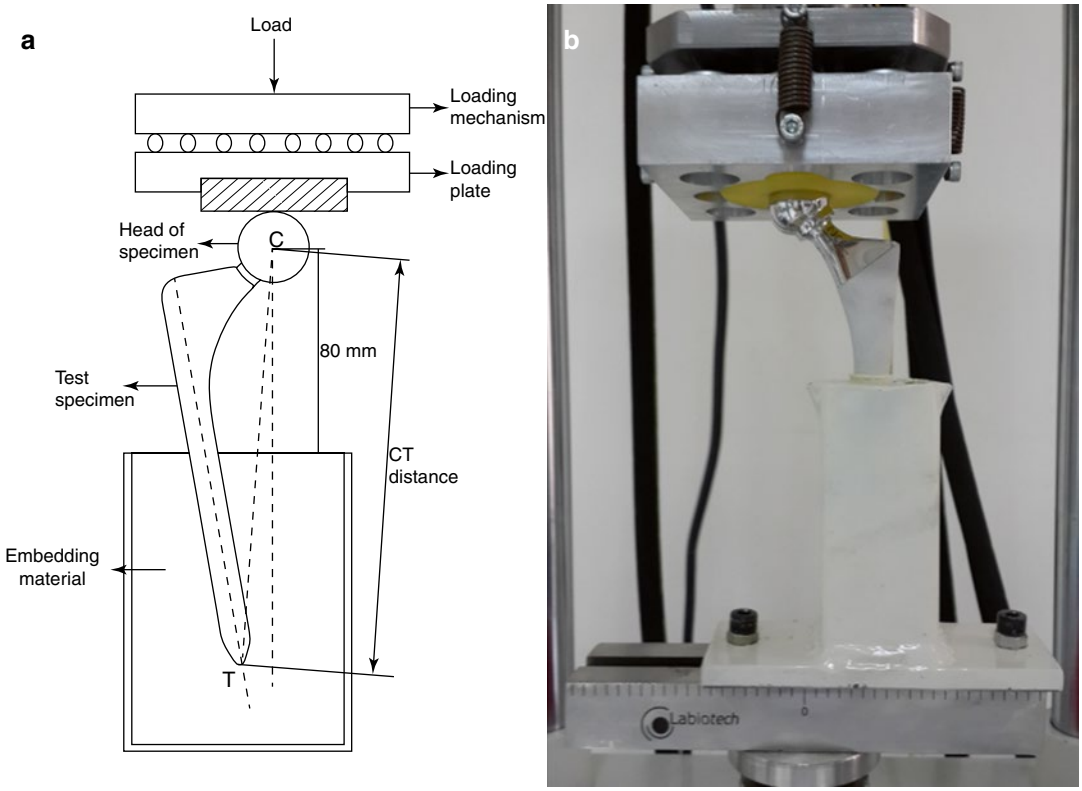

Fig. 5.31 Fatigue test setup for the stemmed femoral components of the total hip joint prosthesis. (**a**) Schematic view, (**b**) view obtained from test

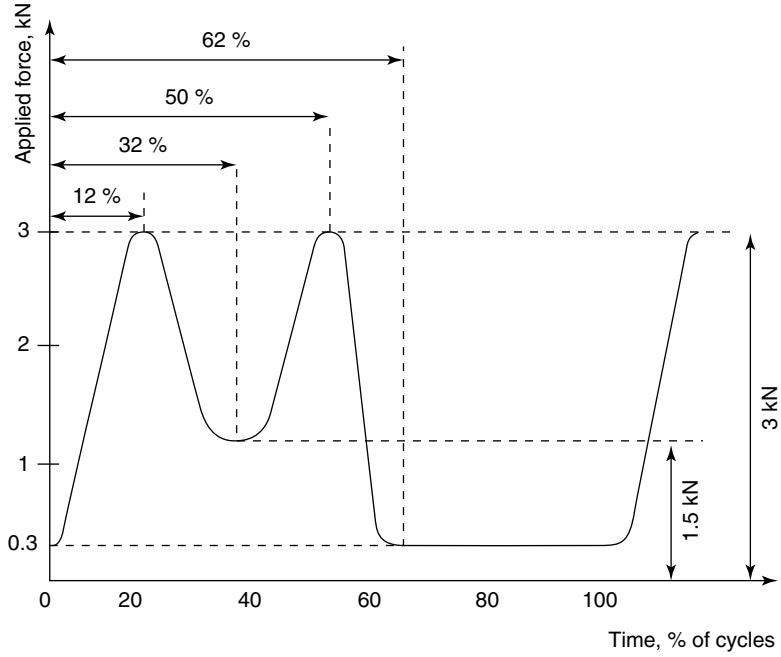

Fig. 5.32 The specified time-varying force of the wear test for the total hip joint prosthesis

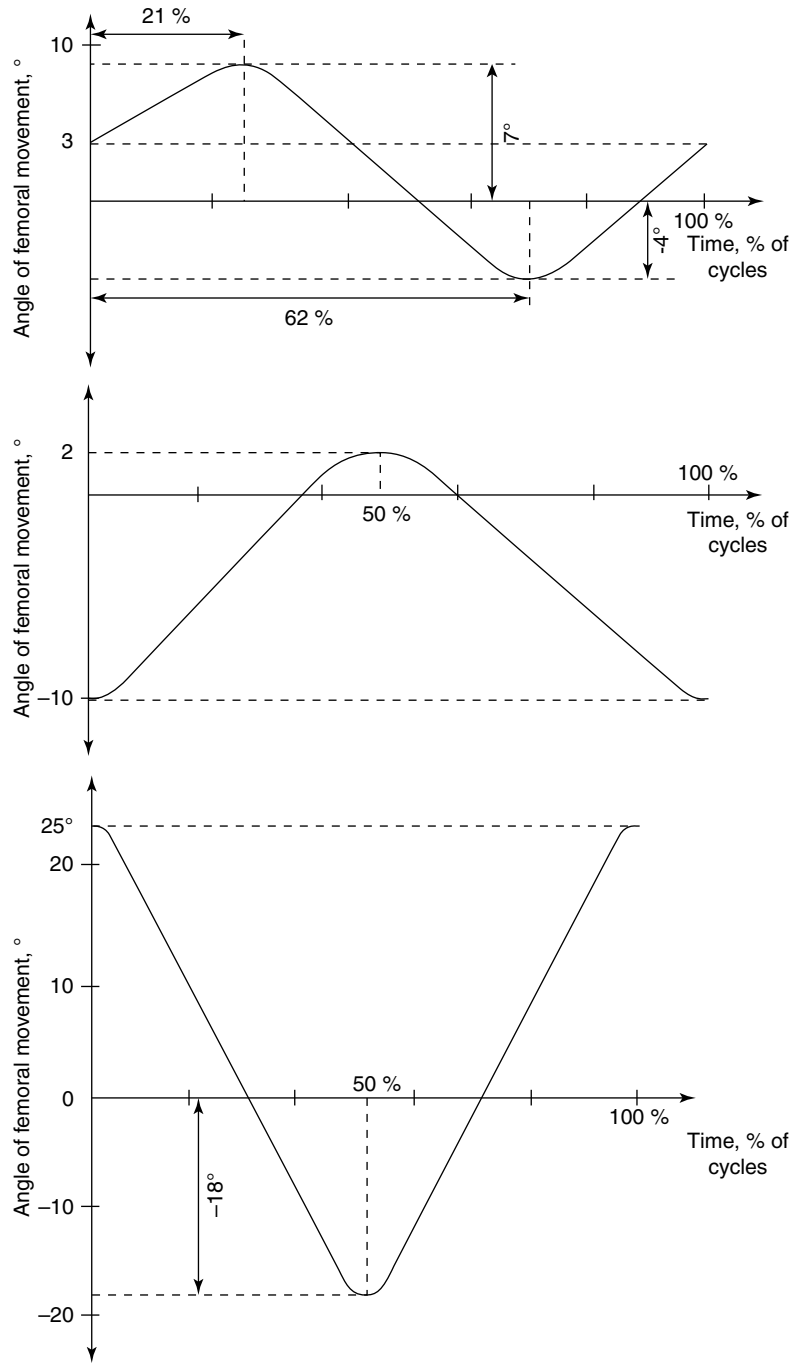

Fig. 5.33 The specified relative angular movement of the wear test for the total hip joint prosthesis according to ISO 14242-1

angular movement is applied as can be seen in Fig. 5.34. The applied angular movement is in two directions for the orbital bearing wear simulator: flexion-extension direction and adduction-abduction direction. Angular movement of femoral component is shown in Fig. 5.35. Although the motion of the orbital bearing wear simulator is simpler and less anatomic than the motion described in ISO 14242-1, the orbital bearing wear simulator has been used

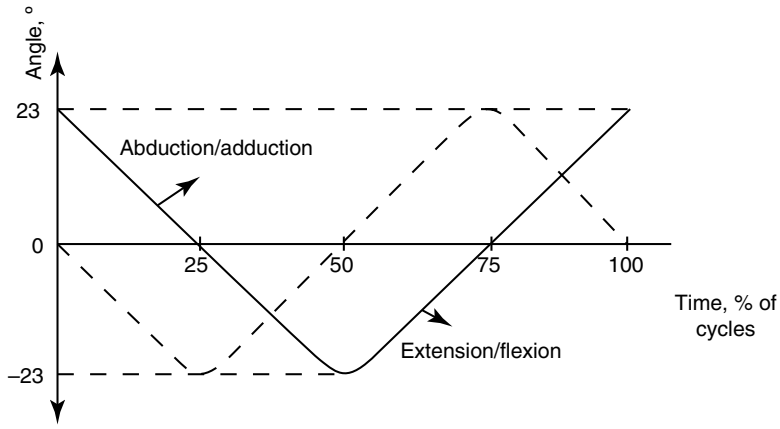

Fig. 5.34 The specified relative angular movement of the wear test for the total hip joint prosthesis according to ISO 14242-3

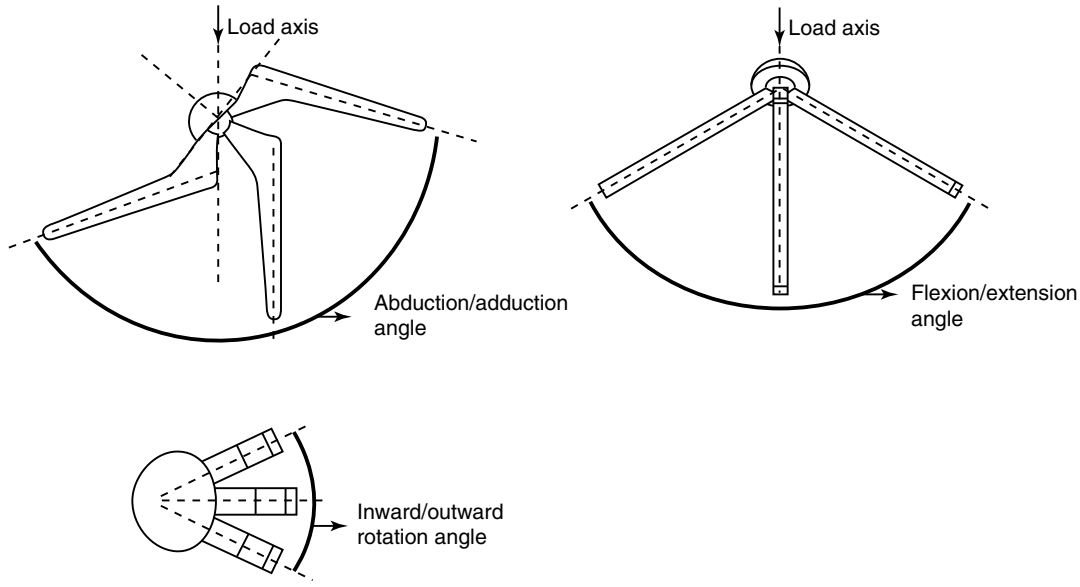

Fig. 5.35 Angular movement of femoral component

for hip joint prosthesis for many years. The testing machine operates at a frequency of 1 Hz. During the testing, the test is stopped every 500,000 cycles to take wear measurements according to the ISO 14242-2 [17]. The test sample is removed from the lubricant, cleaned, dried, weighed, and measured and then reinstalled to the test apparatus. The wear of the test sample is evaluated by testing for the loss in the mass of a hip joint (gravimetric method) or change in the volume (dimensional method).

Interpretation of Results

The method considers the test conditions for CT distance ≤120 mm, 120 mm<CT≤250 mm, and CT distance >250 mm. The required endurance limit is determined where the six specimens survive 5,000,000 cycles.

The test of a specimen proceeds until 5,000,000 cycles or failure of the specimen in the fatigue tests.

For wear testing, the test proceeds until 5,000,000 cycles or a breakup or delamination of the articulating surfaces.

Knee Joint Prosthesis

The dynamic tests are performed to knee joint prosthesis. Cyclic fatigue testing of metallic tibial tray component and wear testing of total knee joint prosthesis are used as dynamic testing. A sample of the metallic tibial tray can be seen in Fig. 5.36.

Dynamic Testing

Fatigue testing of the metallic tibial tray component is performed according to ASTM F1800 [18]. The method measures the fatigue performance of the metallic tibial tray component of the knee joint prosthesis.

The wear testing of the total knee joint prosthesis is performed according to ISO 14243. The method determines relative angular movement between articulating components and the pattern of the applied force.

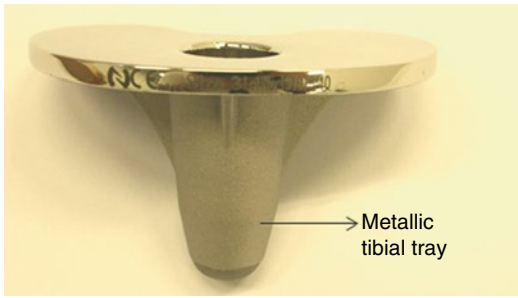

Fig. 5.36 A sample of the metallic tibial trays

Apparatus and Procedure

The test apparatus for the fatigue test of the metallic tibial tray components are shown in Fig. 5.37. The metallic tibial tray is fixated as a cantilever beam construct. When positioning the tibial tray, the anteroposterior centerline of the tray and fixture centerline must be aligned. A plastic spacer is placed between the load applicator metal intender and loading point of the tibial tray which is placed on the unsupported condyle of the tibial tray. The spacer is used to distribute load to the tibial tray for preventing fretting fatigue on contact point between the metal intender and the tibial tray. The applied load must be perpendicular to the superior surface of the tibial tray. The frequency of the test can be 30 Hz or less.

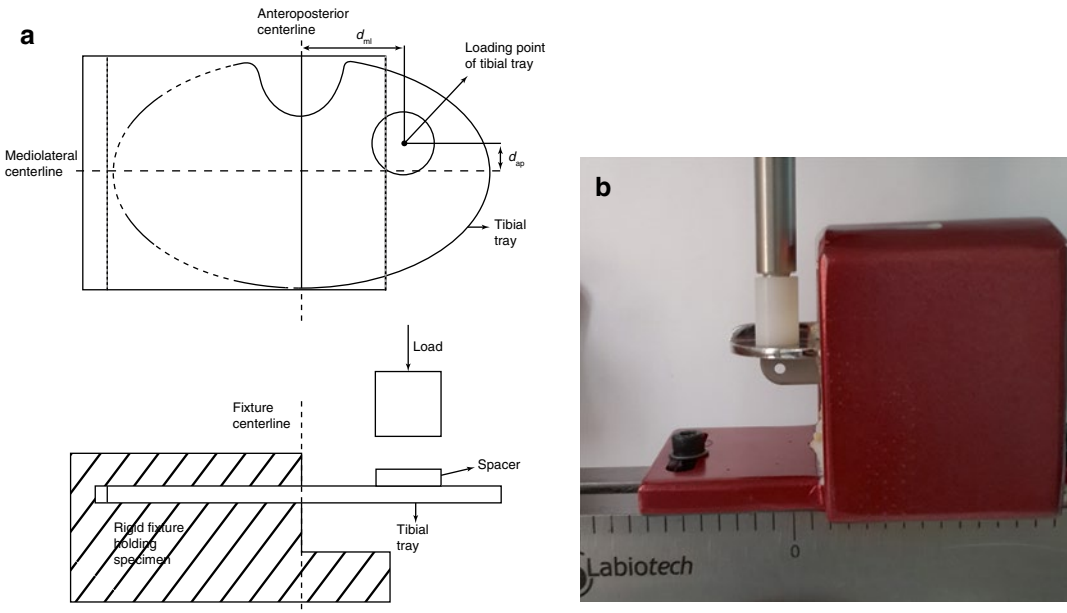

Fig. 5.37 The fatigue test setup for the metallic tibial tray components. (**a**) Schematic view, (**b**) view obtained from test

In the wear testing of knee joint prosthesis, testing was performed in accordance with ISO 14243-1 [19] and ISO 14243-3 [20]. The total knee joint prosthesis is mounted to a test apparatus which allows controlling the displacement and force. Under the applied forces and displacements, the tibial component is free to move relatively to the femoral component. The test apparatus applies cyclic variations of flexion/extension angle, axial forces, anterior-posterior (AP) force, and tibial rotation torque to the interface between the tibial and femoral components for the ISO 14243-1. Figure 5.38 indicates the applied forces and displacements. The test apparatus applies cyclic variations of flexion/extension angle, tibial rotation angle, and AP displacement and axial force to the interface between the tibial and femoral components for the ISO 14243-3. Figure 5.39 indicates the applied forces and displacements. These applied forces and displacements simulate the physiological loading conditions. Forces, torques, and motions of a total knee joint prosthesis are shown in Fig. 5.40 with illustration. A fluid test medium is used for simulating the human synovial fluid. The contacting surfaces of the tibial and femoral components are immersed in the fluid. The wear testing is performed with the frequency of 1 Hz. During the tests, every 500,000 cycles, the test is stopped to take wear measurements according to the ISO 142243-2 [21]. The test sample is removed from the lubricant, cleaned, dried, weighed, and measured and then reinstalled to the test apparatus. The wear of the test sample is evaluated by testing for the loss in the mass of a knee joint (gravimetric method).

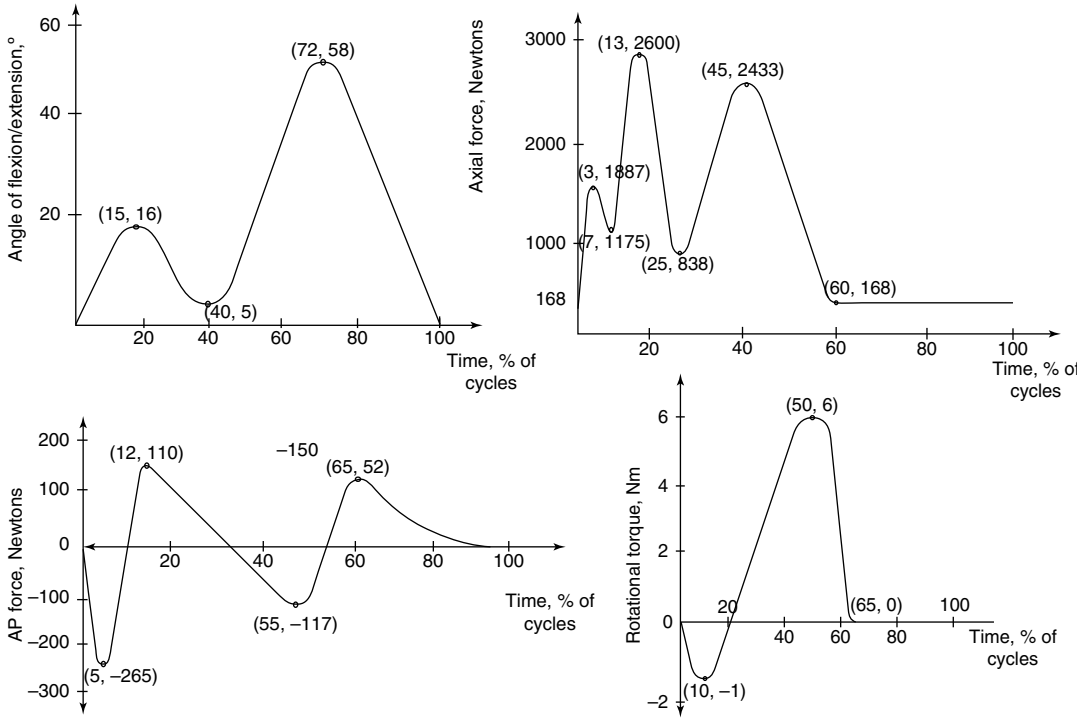

Fig. 5.38 Applied forces and displacements to the interface between the tibial and femoral components according to ISO 14243-1

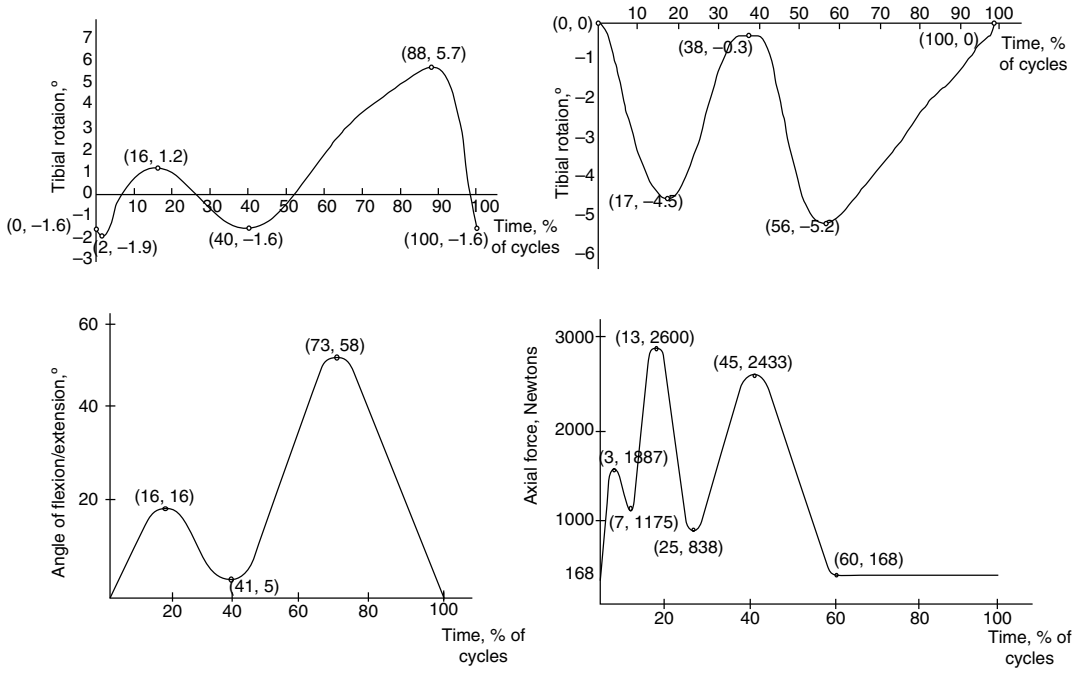

Fig. 5.39 Applied forces and displacements to the interface between the tibial and femoral components according to ISO 14243-3

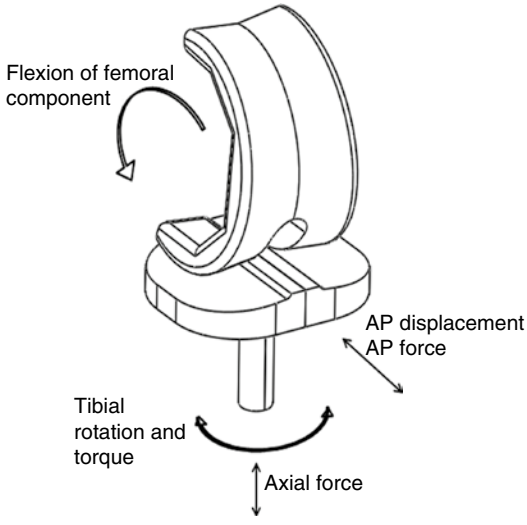

Fig. 5.40 Forces, torques, and motions of a total knee joint prosthesis

Interpretation of Results

The recommended *R* ratio is 10.0 for the method of fatigue test.

The test proceeds until the tibial tray fails or a specified number of cycles is reached. For the fatigue testing of tibial tray, the recommended number of cycles is 10,000,000 cycles.

For wear testing, the test proceeds until 5,000,000 cycles or a breakup or delamination of the articulating surfaces.

References

1. ASTM F382-99(2008)e1 (2008) Standard specification and test method for metallic bone plates. ASTM International, West Conshohocken
2. ASTM F384-12 (2012) Standard specifications and test methods for metallic angled orthopedic fracture fixation devices. ASTM International, West Conshohocken

3. ASTM F543-13e1 (2013) Standard specification and test methods for metallic medical bone screws. ASTM International, West Conshohocken
4. Gaebler C, Stanzl-Tschegg S, Tschegg EK et al (1999) Implant failure of the gamma nail. Inj Int J Care Inj 30:91–99
5. ASTM F1264-03(2012) (2012) Standard specification and test methods for intramedullary fixation devices. ASTM International, West Conshohocken
6. ASTM F1541-02(2011)e1 (2011) Standard specification and test methods for external skeletal fixation devices. ASTM International, West Conshohocken
7. ASTM F1717-14 (2014) Standard test methods for spinal implant constructs in a vertebrectomy model. ASTM International, West Conshohocken
8. ASTM F1798-13 (2013) Standard test method for evaluating the static and fatigue properties of interconnection mechanisms and subassemblies used in spinal arthrodesis implants. ASTM International, West Conshohocken
9. ASTM F2193-02(2007) (2007) Standard specifications and test methods for components used in the surgical fixation of the spinal skeletal system. ASTM International, West Conshohocken
10. ASTM F2077-11 (2011) Test methods for intervertebral body fusion devices. ASTM International, West Conshohocken
11. ASTM F2346-05(2011) (2011) Standard test methods for static and dynamic characterization of spinal artificial discs. ASTM International, West Conshohocken
12. Ishaque BA, Stürz H, Basad E (2011) Fatigue fracture of a short stem hip replacement: a failure analysis with electron microscopy and review of the literature. J Arthroplasty 26:17–20
13. ASTM F1820-13 (2013) Standard test method for determining the forces for disassembly of modular acetabular devices. ASTM International, West Conshohocken
14. ISO 7206-4 (2010) Implants for surgery – partial and total hip joint prostheses – part 4: determination of endurance properties and performance of stemmed femoral components. International Organization for Standardization, Geneva
15. ISO 14242-1 (2014) Implants for surgery – wear of total hip-joint prostheses – part 1: loading and displacement parameters for wear-testing machines and corresponding environmental conditions for test. International Organization for Standardization, Geneva
16. ISO 14242-3 (2009) Implants for surgery – wear of total hip-joint prostheses – part 3: loading and displacement parameters for orbital bearing type wear testing machines and corresponding environmental conditions for test. International Organization for Standardization, Geneva
17. ISO 14242-2 (2000) Implants for surgery – wear of total hip-joint prostheses – part 2: methods of measurement. International Organization for Standardization, Geneva
18. ASTM F1800-12 (2012) Standard practice for cyclic fatigue testing of metal tibial tray components of total knee joint replacements. ASTM International, West Conshohocken
19. ISO 14243-1 (2009) Implants for surgery – wear of total knee-joint prostheses – part 1: loading and displacement parameters for wear-testing machines with load control and corresponding environmental conditions for test. International Organization for Standardization, Geneva
20. ISO 14243-3 (2014) Implants for surgery – wear of total knee-joint prostheses – part 3: loading and displacement parameters for wear-testing machines with displacement control and corresponding environmental conditions for test. International Organization for Standardization, Geneva
21. ISO 14243-2 (2009) Implants for surgery – wear of total knee-joint prostheses – part 2: methods of measurement. International Organization for Standardization, Geneva

Fundamentals of Quantitative Gait Analysis

6

Bayram Kaymak and Abdullah Ruhi Soylu

Abstract

Gait assessment is an important part of neurologic and orthopaedic examination. Visual gait analysis provides significant contribution to diagnosis of neuromuscular disorders, treatment planning and follow-up. However, three-dimensional motion of the segments during walking cannot be detected simultaneously in all planes. In addition to this, the physician does not have any information about the moment and power which are the causes of motion. 3D motion analysis systems have been used to overcome these limitations of visual gait assessment. These systems present motion, moment, power and electromyographic data of a gait cycle in the form of graphs for the use of clinicians. Physicians should have sufficient knowledge about functional anatomy, neural control of locomotion, muscle and motion mechanics and kinesiological electromyography to interpret these data.

Learning Outcomes

After studying this chapter, you will have brief information about (1) neural control of locomotion, (2) muscle mechanics, (3) kinematics and kinetics of gait and (4) kinesiological electromyography in gait analysis.

Terminology

Cross talk Receiving motor unit action potential of an adjacent muscle by the electromyography electrodes on a target muscle

External forces Forces originating outside the body

Internal forces Forces generated by muscle contraction or passive anatomical structures

Moment Product of force and lever arm

Motor unit An alpha motor neuron in the anterior horn of the spinal cord and the muscle fibers innervated by the axon of this neuron

B. Kaymak, MD (✉)
Department of Physical Medicine and Rehabilitation, Hacettepe University, Medical School, Ankara, Turkey
e-mail: bayramkaymak@yahoo.com

A.R. Soylu, MD
Department of Biophysics, Hacettepe University, Medical School, Ankara, Turkey
e-mail: a.ruhi.soylu@gmail.com

F. Korkusuz (ed.), *Musculoskeletal Research and Basic Science*,
DOI 10.1007/978-3-319-20777-3_6

Kinematics Division of dynamics dealing with the geometry and time-dependent aspect of motion without considering the forces causing the motion

Kinetics Division of dynamics dealing with the forces causing motion without considering motion itself

Kinetic energy Energy possessing due to the motion of an object

Lever arm Perpendicular distance from the joint centre of rotation to the force vector line

Momentum Product of the mass and velocity of an object

Motor unit action potential (MUAP) Sum of electrical signals arising from muscle fibers forming a motor unit

Parallel elastic component Connective tissue that surrounds the contractile elements in a muscle

Physiological cross-sectional area Cross-sectional area of a muscle perpendicular to muscle fibers

Potential energy Energy possessing due to position of an object in a force field

Power The amount of work done in a per unit time

Series elastic component All connective tissues in series with the contractile elements in a muscle

Work Measure of the energy flow from one body to another

Introduction

Gait analysis has an important place in the diagnosis, treatment planning and follow-up of neurologic and orthopaedic disorders. 3D computerised gait analysis systems have been used to measure kinematic, kinetic and muscle contraction variables of walking. Rapid developments seen in camera systems, force plate and kinesiological electromyography (EMG) technologies provide accurate and reliable quantification of the motion, force and muscle contractions that occur during walking. Obtained motion, moment, power and EMG data are presented in the form of graphs for the use of clinicians [9].

Motion, force and muscle potentials are recorded by special transducers and then converted into digital signals using gait analysis systems. All these signals must be free of noises and artefacts, because artefacts and noises cause misinterpretation of walking [13].

To assess the gait pathologies in a correct manner, clinicians must have sufficient knowledge about functional anatomy, neural control of locomotion, muscle and motion mechanics and kinesiological EMG. Gait disorders may be due to the primary pathology, or it may also occur to compensate the mechanical failure caused by the primary pathology. Making the distinction between primary and secondary gait disturbances is also essential in the diagnosis and treatment planning of the patients with neuromuscular disorders. Anamnesis and interpretation of the gait data along with a detailed physical examination helps the clinician in making this distinction [4].

Gait pathologies are beyond the scope of this chapter; only fundamentals of quantitative analysis of normal gait will be discussed here.

Neural Control of Locomotion

Human walking is a form of locomotion. As other forms of locomotion (swimming, flying, crawling, etc.), walking is achieved by alternating and rhythmic movements of body segments. Locomotion is controlled automatically by relatively low levels of the central nervous system (CNS) without intervention by higher centres. However, in unfamiliar environments or involving unpredictable situations, locomotor movements must continuously be modified. Modifications in locomotion are provided at relatively higher cortical centres [7].

CNS parts that are responsible for locomotor control are the cortical motor centres, basal ganglia, cerebellum, brain stem motor nuclei and spinal cord. Stimulus initiating the movement is the “thought” that can arise in certain areas of the

brain. This stimulus generated by the thought stimulates the neurons in cortical motor centres. Axons of the neurons located in the cortical motor centres extend to the brain stem and the spinal cord, forming the corticobulb and corticospinal tract, respectively. They make synapses with the second motor neuron in the brain stem nuclei and anterior horn of the spinal cord and provide a voluntary muscle contraction.

The basal ganglia play an important role in the properly planning and initiation of voluntary movement. The cerebellum is responsible for truncal balance and smooth execution and completion of movements. The brain stem nuclei provide the necessary tone and posture during performance of voluntary movement. The spinal cord with its own reflex arcs (stretch reflex, etc.) involves in controlling of the movement and tuning of muscle tone.

Fine control of the movement by CNS depends on healthy proprioceptive stimuli from the periphery. Proprioceptive stimuli are detected by specific receptors in muscles (muscle spindles), tendons (Golgi tendon organs), skin, ligaments and joints. Some of these receptors are static sensors and can detect relative position of the body portion in space. Others are dynamic sensors and determine the direction, velocity and acceleration of the motion and tension in the musculotendinous junction. These specific receptors send information to higher CNS centres. Proprioceptive information may lead to reflex responses (such as stretch reflex) in medulla spinalis and also evaluated in the higher centres of the CNS to provide a smooth excursion of the movement.

During walking, lower extremity, pelvis and trunk muscles contract to control segmental motion and provide stability around the joints. Type (eccentric, concentric and isometric), timing and strength of the muscle contraction are under the control of the above-mentioned centres of the CNS receiving proprioceptive information from the periphery [4].

Muscle Mechanics

Muscles are the sole power source in the body. Active contractile structures (fibers) of the muscle are enclosed by the fascia which is a connective tissue. *Fascia* surrounding the muscles separates muscle fibers as groups (fascicle) and attaches them to both ends of the tendon. Some of the connective tissue of a muscle is parallel to the contractile element; the others are in series with them. Length of the muscle fibers, pennation angle and muscle physiological cross-sectional area (PCSA) of the muscle are important architectural features that affect the muscle mechanics [8] (Fig. 6.1).

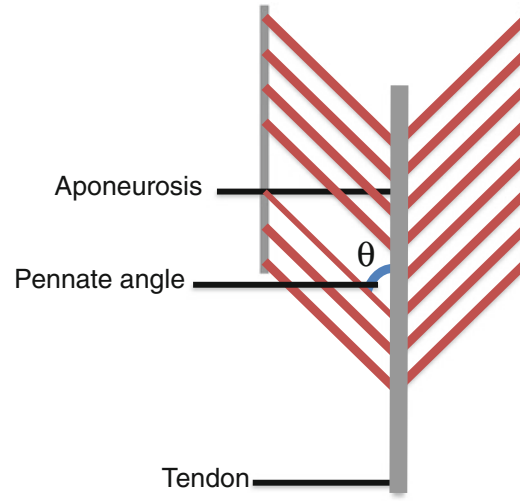

Fig. 6.1 Muscle architecture

PCSA of a muscle is calculated using the formula

$$\text{PCSA} = \frac{\text{Muscle volume}.\cos\theta}{\text{Fiber length}}$$

Muscles with small pennation angle and long muscle fiber size (e.g. hamstrings and tibialis anterior) provide large excursion and higher contractile velocity. However muscles with greater pennation angle, small muscle fiber length and large muscle physiological cross-sectional area (e.g. soleus) produce higher force at the expense of excursion and contractile velocity [13].

An alpha motor neuron in the anterior horn of the spinal cord and the muscle fibers innervated by the axon of this neuron form a *motor unit*. The motor unit is the smallest subunit that is under neural control in a muscle. The number of the muscle fibers in a motor unit is related with the function of that muscle. Muscles contributing fine motor movement have less muscle fibers in a motor unit than the muscles exerting crude

movement. The alpha motor neuron axon gives branches to synapses with the muscle fibers of a motor unit. When an alpha motor neuron is evoked, the electrical signals pass to the muscle fibers via neuromuscular junctions. These electrical signals may generate an action potential in the membrane of the muscle fibers. The sum of the action potentials of the muscle fibers forms a motor unit action potential (MUAP). The result is a mechanical twitch of tension. Tension increase in a muscle occurs via consecutive mechanisms. First, stimulation rate increases in the related motor unite, and then the other motor units are activated (recruitment). Reverse sequences cause decreases of tension in the muscle. While performing movements the human body tries to spend little energy as possible to conserve energy expended. Entire motor units in a muscle are not necessarily activated during performing a movement. Needed tension force for a movement determines the amount of motor unit recruitment via neuromotor control mechanism. When tension force requirement increases, a greater number of motor units will be activated. First, the smallest motor units are recruited, and then large motor unites are recruited. This is called as "size principle" [2].

Motor units are divided into two main types. The alpha motor neuron innervating the muscle fibers determines the type of motor unit. Smaller slow-twitch motor units (type 1) are called tonic units. They produce twitches with lower peak tension in a long time. The large fast-twitch motor units (type 2) are called phasic units. They have larger peak stress with a short time to peak. Muscles performing strong and phasic contractions have type 1 and type 2 muscle fibers equally. The gastrocnemius is an example to this type of muscles. During the terminal stance phase of the gait, gastrocnemius muscle contracts strongly in a phasic manner. Type 1 fibers especially exist in the tonic postural muscles. An example of such muscles is soleus. It creates tonic contraction during the second rocker of the gait [13].

As noted above, muscles contain contractile active cells (muscle fibers) and passive elements of connective tissue. The force-length curve of a muscle consists of a combination of the force-length characteristics of both active and passive

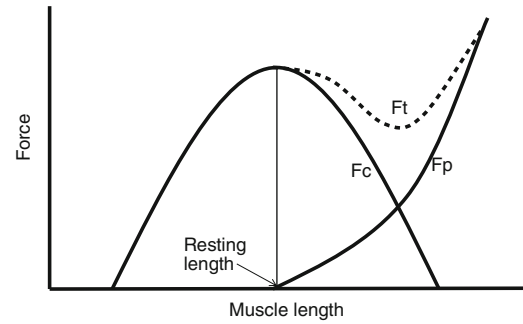

Fig. 6.2 Force-length characteristics of a muscle

structures in the muscle (Fig. 6.2). Interactions between myofibrillar structures at sarcomere level determine the shape of the force-length curve. Resting sarcomere length is 2.5 μm. At this situation, maximum number of cross-bridges occurs between the filaments; hence, maximum tension is generated by the active elements. As the muscle undergoes lengthening or shortening, cross-bridges between the filaments are reduced, and the tension produced by muscle fibers decreases. Connective tissue of the muscle whether in parallel or series has significant effects on the tension generated. Connective tissue that surrounds the contractile elements is called as *parallel elastic component* and behaves like an elastic band. It is in a slack state when the muscles are at rest or in a shorter position. In this situation parallel elastic component does not constitute to total tension. As the muscle length increases, elastic component causes increases in the tension. This increase occurs first slowly then quickly. All connective tissues, including tendon, in series with the contractile elements, are called the *series elastic component*. During the isometric contraction the series elastic component is under tension and undergoes limited stretching. Total length of the muscle and tendinous structure does not change as the muscle shortens during this kind of contraction. Shortening of the muscle fibers stretches the serial elastic component of the muscle. This is called *internal shortening*. When the muscle isometrically contracts, stretched series elastic component stores large amounts of energy. As an example of this, the gastrocnemius muscle contracts and stores energy in the terminal stance phase of the gait to generate propulsion power during push off. Series elastic component stores

large amounts of energy at the terminal stance phase during contraction of the gastrocnemius muscle. This contraction causes only little plantar flexion movement at the ankle, because the body weight is still supported by the ipsilateral lower extremity and there is considerable amount of dorsiflexor moment generated by ground reaction force. In the preswing phase of the gait, considerable part of the body weight is transmitted to the contralateral limb. Hence, the dorsiflexor moment of ground reaction forces around the ankle is reduced significantly. Then, energy stored in the series elastic component causes rapid plantar flexion at the ankle joint and propulsion is provided. Muscle length is shortened during concentric contraction. Besides, intramuscular tension also decreases. There is an inverse relationship between muscle shortening velocity and tension [13].

Gait Cycle

Lower extremities move in a specific order during gait. A gait cycle (stride) begins with the ground contact of the foot and ends when the same foot touches the ground. According to the foot contact with the ground, a gait cycle is divided into periods and phases. There are two periods (stance and swing) in a gait cycle (Fig. 6.3).

Stance period constitutes about 60 % of a gait cycle. In this period the foot is in contact with ground. In the first and last 10 % percentage of stance period, the feet are in contact with the ground. These phases are called as *double-limb stance*. During these phases body weight is transferred between two lower extremities. During the middle of the stance period (40 % percentage of gait cycle), one foot has a contact with the ground. This phase is defined as *single-limb support*. Meanwhile contralateral foot is in the swing period. Ratio between double-limb stance and single-limb support depends on the walking speed. Ratio decreases proportionally with the

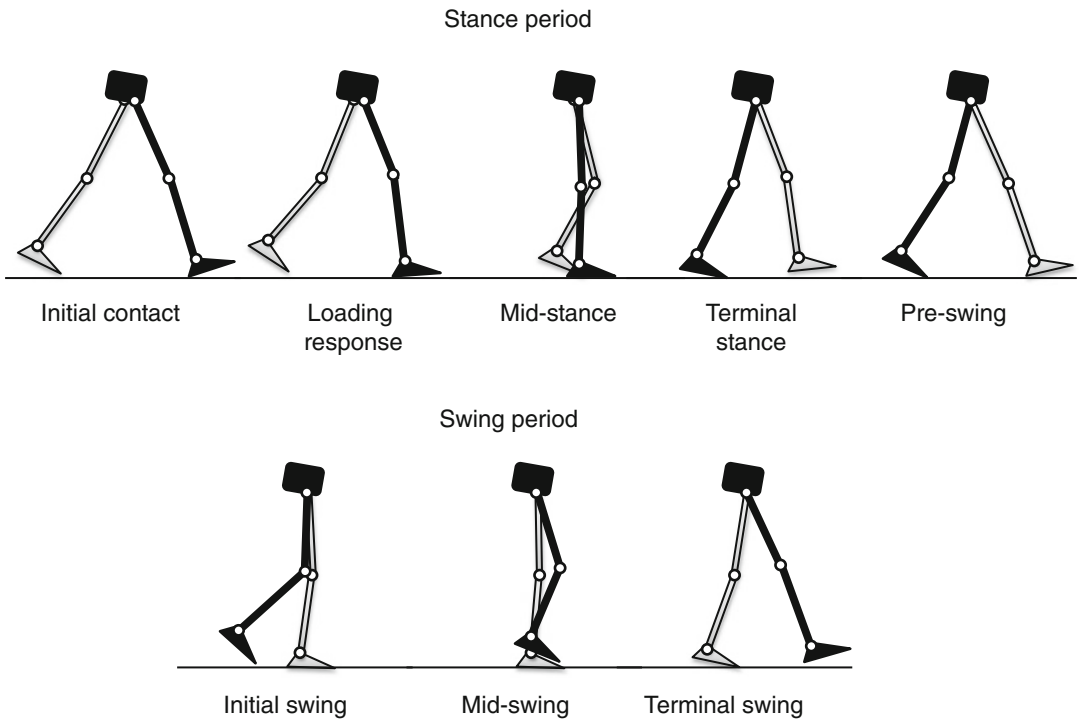

Fig. 6.3 Gait cycle

increase of walking speed. The last 40 % percentage of a gait cycle is called as swing period. In this phase the foot does not make any contact with the ground and exerts a pendular movement. Contralateral foot is in single-limb support phase. Furthermore the stance and swing period is also divided into several phases (Fig. 6.3). In order the phases of stance period are initial contact, loading response, mid-stance, terminal stance and preswing. The phases of swing period are initial swing, mid-swing and terminal swing. In a normal walking, stance period begins with heel strike and ends with toe off. The swing period begins with the toe off ends with the heel strike. However in neuromuscular pathology initial ground contact of the foot may be with forefoot rather than the heel. For that reason, "heel strike" terminology has not been using to define the first contact of the foot with the ground.

A gait cycle can also be evaluated in three different tasks. These are weight acceptance, single-limb support and limb advancement. Weight acceptance includes the first two phases of stance period – initial contact and loading response. Single-limb support includes the mid-stance and terminal stance phases. Advancement includes the last phase of stance (preswing) and whole phases of swing period [10].

Centre of gravity (COG) of the body moving horizontally during walking also changes its position in vertical (approximately 3.2 ± 0.8 cm) and lateral (3.5 ± 0.9 cm) directions. COG reaches its maximum height in the mid-stance phase. Then it falls through the initial contact phase. Meanwhile, the potential energy of the body endowed by the height from the ground transforms into kinetic energy. Impact at the initial contact must be absorbed to protect musculoskeletal structure from injury. Heel fat pad and tibialis anterior and quadriceps eccentric contractions absorb this impact during initial contact and loading response, respectively. This is defined as *weight acceptance*. After initial contact COG again begins to rise to its peak height at the mid-stance phase. Meanwhile, kinetic energy is stored as potential energy. Energy required for horizontal and vertical movement of COG is produced by strong contraction of ankle plantarflexor muscles in the terminal stance phase. During single-limb support, hip abductors of the lower limb contract to protect the pelvis from falling to the other side. In limb advancement, the lower extremity acts as a compound pendulum and moves forward due to the repulsive effect of the gastrocnemius muscle contraction. The inertial force has an important role in this progress [5, 11].

Four rockers occurring during the stance period of the gait yield the body's forward progress. During rockers movements are performed around the points called fulcrum [11]. The first rocker appears during initial contact and loading response. In this rocker the foot moves to the ground, and the tibia goes forward. The fulcrum is the heel. Ground reaction force (GRF) acts through the heel and passes behind the ankle. It generates a plantar flexion moment at the ankle. If the movement was made only under the effect of this force, the forefoot would hit the ground strongly. To prevent this, the ankle dorsiflexor muscles contract to yield smooth and controlled dropping of the foot. While the foot moves to the ground, the contracting tibialis anterior muscle pulls the tibia forward. As mentioned earlier, during terminal swing the foot falls to contact with the ground in the beginning of the stance phase. The body has momentum due to its mass and velocity. Some part of the force generated during the collision is absorbed by the fat pad of the heel. The other part is absorbed by foot dorsiflexors contracting eccentrically. The purpose of the first rocker is shock absorption. The second rocker occurs in mid-stance phase. The fulcrum is the ankle. The foot has a full contact with the ground, and the tibia moves forward around the ankle joint. Motion of the tibia causes dorsiflexion of the ankle. GRF vector passes in front of the ankle joint resulting in external dorsiflexor moment. Meanwhile, the soleus muscle contracts eccentrically to control forward falling of the body. Thus excessive forward movement of the tibia is prevented, and the GRF vector is held in front of the knee. In the second half of the mid-stance, the GRF vector passes behind the hip joint and contributes the stability of the hip. The third rocker occurs in the terminal stance phase. At the end of the mid-stance, plantarflexors contract concentri-

cally and stop the forward movement of the tibia and foot dorsiflexion. Metatarsal heads are the fulcrum in this rocker. The foot goes to plantar flexion, and the heel moves upward from the ground. In the first two rockers, muscles contract eccentrically to cause deceleration, but in the third rocker strong concentric contraction of the plantarflexors is seen to accelerate the lower limb. Power required for forward progression of the body is provided by this strong concentric contraction of the ankle plantarflexors in the terminal stance. The fourth rocker is formed in preswing phase. The fulcrum is the most anterior margin of the medial forefoot and great toe.

The purpose of the swing period is to advance the lower extremities, provide foot clearance, allow the cadence change and ensure energy conservation. The lower extremity moves as a compound pendulum during the swing period. At the first part of pendular movement, muscles contract for acceleration, but at the second part the muscle contracts for deceleration [5].

Quantitative Gait Analysis

When visual gait analysis is performed by a skilled physician in a systematic way, it provides significant contribution to diagnosis of neuromuscular disorders, treatment planning and follow-up. Particularly, gait analysis with slow-motion video provides better assessment of the fast motion which may not be captured by the naked eye. However, with visual analysis of the gait, three-dimensional motion cannot be detected simultaneously in all planes. In addition to this, physician does not have any information about the moment and power which are the causes of motion. 3D motion analysis systems have been used to overcome these limitations and performed quantitative analysis of the gait.

All variables measured during gait analysis are signals which are changing over time. Some of these variables are measured directly. These are acceleration, force signals from transducers or MUAPs from muscles. However, moments and powers are indirectly calculated using mathematical procedures. The obtained signals are processed, cleaned from artefacts and averaged. All these data – kinematic, kinetic and kinesiology EMG – are presented as graphs for the use of clinicians.

Kinematics

Kinematics deals with the geometry and time-dependent aspect of motion without considering the forces causing the motion [6].

Quantitative analysis of the body segment motion during walking is performed using various motion analysis systems. Television-based 3D motion imaging systems which are used for this purpose are the newest and high technology system. Multiple cameras emitting and sensing infrared light are often used in these systems. Markers placed on the body segments reflect the infrared light. Then infrared light reflected from markers is detected by these cameras. Hence 3D (x, y, z) coordinates of the markers are detected. Determining the coordinates of a point means to quantify its position in space. In order to detect three-dimensional coordinates of a marker, infrared light reflecting from that marker must be captured by at least two cameras. Coordinates of the markers are detected according to the absolute coordinate system that is placed around the force plate on the ground of gait laboratory. Apart from the absolute coordinate system, two relative coordinate systems are also used in kinematics analysis. One of them is marker coordinate system generated with the markers placed on the body segments. The other is the anatomical coordinate system whose origin locates in the centre of mass of each segment. In gait analysis the pelvis, thighs, legs and feet are usually examined as separate segments and the head, arms and body, as a single segment [13].

To calculate the joint angles, coordinate data of the markers determined according to absolute reference system are transferred to the anatomical axis of the body segment. Joint angles calculated using anatomical coordinate systems of two segments are relative. It means that joint angle data do not provide information about the position of the segment according to the reference coordinate system, but information about the position of the two segments with each other.

Clinical Relevance

A 9-year-old patient with the diagnosis of diplegic cerebral palsy was admitted to the outpatient clinic suffering from walking difficulty. It was stated that her feet make initial contact with forefoot rather than heel during walking. Her ankle dorsiflexions were in normal range, even a little bit increased due to the midfoot break. However, she has significant knee flexion contracture.

During normal gait the heel strikes the ground at initial contact. At that time there is a relative angle about 90° between the foot and leg segment (Fig. 6.4a). It should be kept in mind that the foot contact side with the ground is not determined by the relative angle between the leg and foot segment, but by the orientation of the foot with the ground. As seen in this patient even though there is a 90° relative angle between the foot and the leg segments, the heel would not contact with the ground. Because knee flexion contracture changes the orientation of the foot according to ground, the forefoot contacts with the ground at initial contact (Fig. 6.4b).

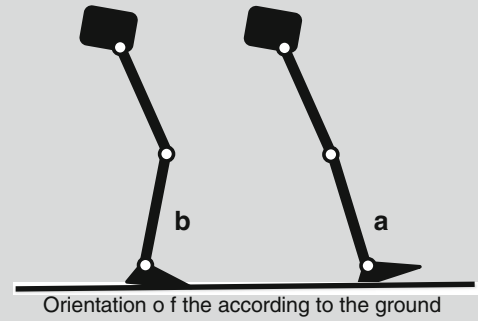

Fig. 6.4 Orientation of the foot according to the ground

The angle between the anatomical reference system of a segment and absolute reference system is defined as absolute angle. This angle gives information about the segment position according to the ground of the gait laboratory. The movements of the pelvis and foot progression angle are calculated according to the absolute reference system [12].

Position of the markers placed on segments changes with time during a gait cycle. Changing marker positions (coordinates) and time data are used to calculate the linear and angular velocity and acceleration. Kinematic data obtained using the 3D gait analysis system are presented with the graphs. Three-dimensional angular motions around the joints include flexion and extension on sagittal plane, abduction and adduction on coronal plane and internal and external rotation on axial plane. Changes of the angular motion around the joint during a gait cycle are assessed by the clinician using these kinematic graphs. In the gait analysis systems, foot rotation in the coronal plan cannot be calculated, because the model used in ankle kinematics analysis is one-dimensional.

Besides of the amount of excursion, kinematic graphs also give information about the velocity and acceleration of angular movement around the joints. In the kinematic graphs, the X and Y axes represent a gait cycle (as percentages) and angular displacement (as degrees), respectively. The greater the amount of displacement in a gait cycle unit, the higher the angular velocity. The slope of the tangent at any point on the displacement curve gives instantaneous velocity. Increase and decrease in the slope of the tangent lines with time are defined as acceleration and deceleration, respectively. Figure 6.5 shows knee flexion-extension kinematic graph. According to the Y axis, upward displacement is flexion, and downward displacement is extension. Tangent lines are drawn roughly on the flexion/extension curve on the graph. At the point which the first and sixth tangent lines contact with the curve, direction of the knee motion changes extension to flexion and flexion to extension, respectively. It can easily be seen that the slope of these lines is zero. It means that instantaneous velocity is zero at this point. Slope of the tangent lines (from the first through third) increases showing *acceleration*, and slope of the tangent lines (from fourth through sixth) decreases showing *deceleration*. During acceleration, moment has the same direction with the motion. However the direction of the moment is opposite to the motion during deceleration.

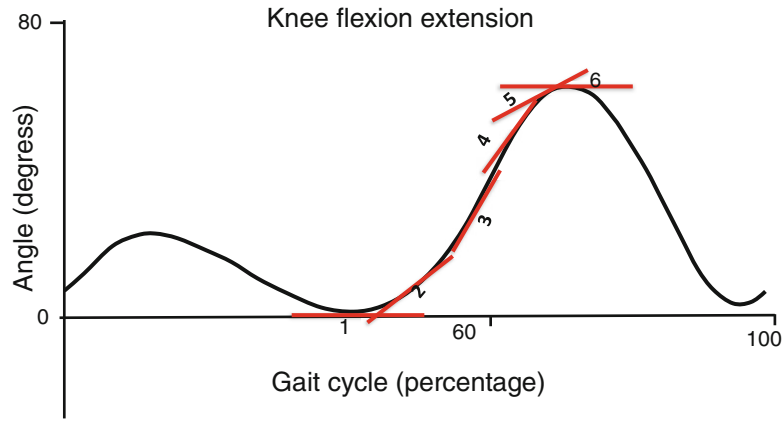

Fig. 6.5 Knee flexion/extension motion graph

Kinetics

Kinetics does not deal with the motion itself, but the forces that cause motion. Kinematic data, force plate data and anthropometric measurements (mass, height, distance between anterior superior iliac spines, leg length and knee and ankle width) are used to calculate kinetic variables as moment and power formed around the joints. As stated previously moment and power around the joints cannot be measured directly, but calculated using mathematical formulas. This process is called as inverse solution. Unlike kinematic data, kinetic data provides information about the neural control mechanisms of the motion and compensation strategies.

The forces acting on the body segments result from internal and/or external sources. *Internal forces* (tension and friction forces) are generated by muscle contraction or passive anatomical structures. Passive structures are the muscle itself, ligaments, tendons and fascia. Viscoelastic property of the passive structures has an important effect on producing internal forces. During gait the important part of the internal forces is used to control the movement generated by external forces. *External forces* originate outside the body. GRF is the external force applied to the body during gait. The body applies forces to the ground proportional to its mass. The ground also applies forces to the body in the opposite direction as a reaction force. Reaction forces distribute on the contact surface of the foot with the ground. The compound vector of all these reaction forces is called as GRF vector assumed to act at a point on the contact surface of the sole. This point is defined as the centre of pressure (COP). During normal gait, COP shifts from the rare foot to the forefoot. Force plate is a force transducer detecting COP. The forces exerted on the force transducer create strain in mechanical sensors. Electrical signals generated by the sensors are proportional to the magnitude of force and strain acting on force plate. GRF formed by one vertical and two shear forces (medio-lateral and anterior-posterior) are three-dimensional (3D). In the gait analysis laboratories, two force plates are used to measure the ground reaction forces acting on both feet independently and simultaneously [13].

Moments around a joint are generated by external and internal forces. To result in a moment, the force vector must be in an orientation which yields a perpendicular distance from the joint centre of rotation to the force vector line. This distance is defined as *lever arm*. Multiplication of the force and its lever arm gives moment around the joint. When the lever arm increases, mechanical advantage of the muscle increases. The cost of this increase is the decrease in angular motion around the joints. When the lever arm decreases, moment decreases and angular motion around the joint increases. This is particularly important for the multijoint muscles. A multijoint muscle may produce different excursion and moment around the joints they cross because of a different lever arm. Biarticular major muscles of the lower limb are the hamstrings, rectus femoris and gastrocnemius. Lever arm of the gastrocnemius muscle at the ankle joint is around 5 cm and larger than its lever arm at the

knee (3.5 cm). Similarly, the lever arm of the hamstring muscles at the hip (6–7 cm) is larger than the lever arm at the knee (3.5 cm). Because the lever arm of the hamstring and gastrocnemius muscles are greater in the hip and ankle than the knee, during stance phase these muscles act as a hip and ankle extensor rather than knee flexor. Their effect on the thigh and calf prevents the body from collapsing.

Motion of the segments during gait is generated by the moment of force around the joints and the segments' internal force of the momentum (inertial effects). *Momentum* is calculated by multiplying the velocity with the mass of the body segment. Because contribution of the momentum to the total moment around the joint is less than the effect of the force and lever arm, it can be omitted in calculating kinetic data. However, omitting inertial effects causes some calculation error increasing towards the distal to proximal. Calculation error is 1 % in the ankle, 5 % in the knee, 8 % in the hip and 14 % in the trunk [3].

Essentially the cause of the motion is mechanical energy flow. There are two types of *mechanical energy*: potential energy and kinetic energy. The body has potential energy due to the gravitational force. Potential energy increases with the height of the body segment from the reference location. The ground is the reference location during gait. Energy produced by translational or rotational motion is called as *kinetic energy*. If there is no motion, the body is at rest and kinetic energy is zero. Total energy of the body is approximately constant, which would change between the three kinds of energy (potential, kinetic translational and rotational kinetic). Most of the body segments have various combinations of these three types of energy in any time during motion.

Work is defined as the measure of the energy flow from one body to another. Energy flow results in segmental energy exchanges either inside the segment or between adjacent segments. Upper body potential energy change during gait is an example for segmental energy changes. Potential energy of the upper part of the body is maximum, and forward velocity is minimum in mid-stance phases of the gait. While the body falls through the double support, it loses height, and velocity increases. At double-limb support potential energy is minimum and forward velocity is maximum. In a body segment while potential energy increases, kinetic energy decreases during gait. As mentioned above energy is also transferred between segments. The energy transferred between segments does not cause an increase or decrease in total body energy. Muscles perform energy transfer function between two segments. However the muscle can apply this function when two segments are moving in the same direction.

Tension force produced by the muscle contraction moves the body segment. Meanwhile, energy generated by the muscle flows into the moving body segment. Regardless of the flow of energy, this energy can cause translational and rotational motion or be stored as potential energy in that segment. The lower extremities are multisegmental structures, and energy flow between segments is seen during walking. Connected segment applies forces with each other during gait. Mechanical energy flows continuously from one segment to the other segment. Mechanical energy transfer can occur only when there is segmental motion around the joint. This means that one segment can do work on another segment. Mechanical energy transfer between adjacent segments is important to conserve the energy of motion [13].

Muscles are the sole source of mechanical energy in the human body. When a muscle contracts concentrically, it causes moment of force in the same direction with rotational motion of the body segment. Hence muscles make positive work on the body segments (*generation*). Moment generated by the muscle and angular velocity has the same sign (negative or positive). When a muscle contracts eccentrically, it causes moment of force in the opposite direction with rotational motion of the body segment. Hence the muscle makes negative work on the body segments. Moment generated by the muscle and angular velocity has opposite sign. Eccentric contraction of the muscles during gait is seen to control the movement caused by the moment of

GRF. Meanwhile energy flows through the body segment to the muscle (*absorption*). Simultaneous eccentric and concentric contractions, however, occur for the formation of the desired movement during gait. This is somewhat inefficient and leads to energy loss.

Power is the amount of work done per unit of time. Unit of the power is watt (joules/s). Power can be positive or negative, such as the work. Sign of the power can change several times during normal joint motion. Power graphs provide information about energy exchange. Gait assessment without power data can result in significant mistakes in making diagnosis and treatment planning of the neuromuscular pathologies.

Gait analysis systems present internal moment and power data in graphical form. As mentioned above, internal moment is calculated with inverse dynamic solution. Sign of the internal moment does not determine the direction of motion. If the angular velocity and moment has the same sign, positive work is done (generation). If the angular velocity and moment has an opposite sign, negative work is done (absorption). Therefore moment graphs and kinematic graphs (angular displacement) must be evaluated together. Figure 6.6a illustrates knee flexor/extensor moment graph. Part of the curve above the X-axis shows internal extensor moment. Part of the curve below the X-axis shows internal flexor moment. Knee extensor moment is seen in 8–25 % of the gait cycle. External moment initially slows the knee flexion motion (deceleration). Meanwhile, knee extensors contract eccentrically and absorb the energy generated during knee flexion. Then they contract concentrically and extent knee (acceler-

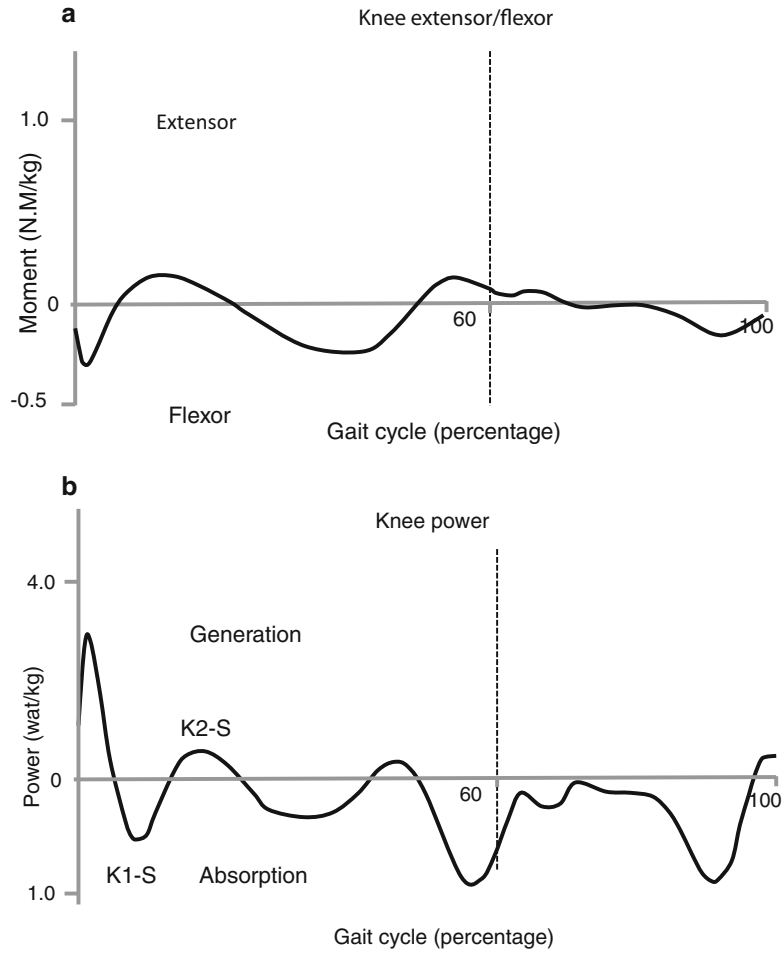

Fig. 6.6 (**a**) Knee extension/flexion moment graph. (**b**) Knee extension/flexion power graph

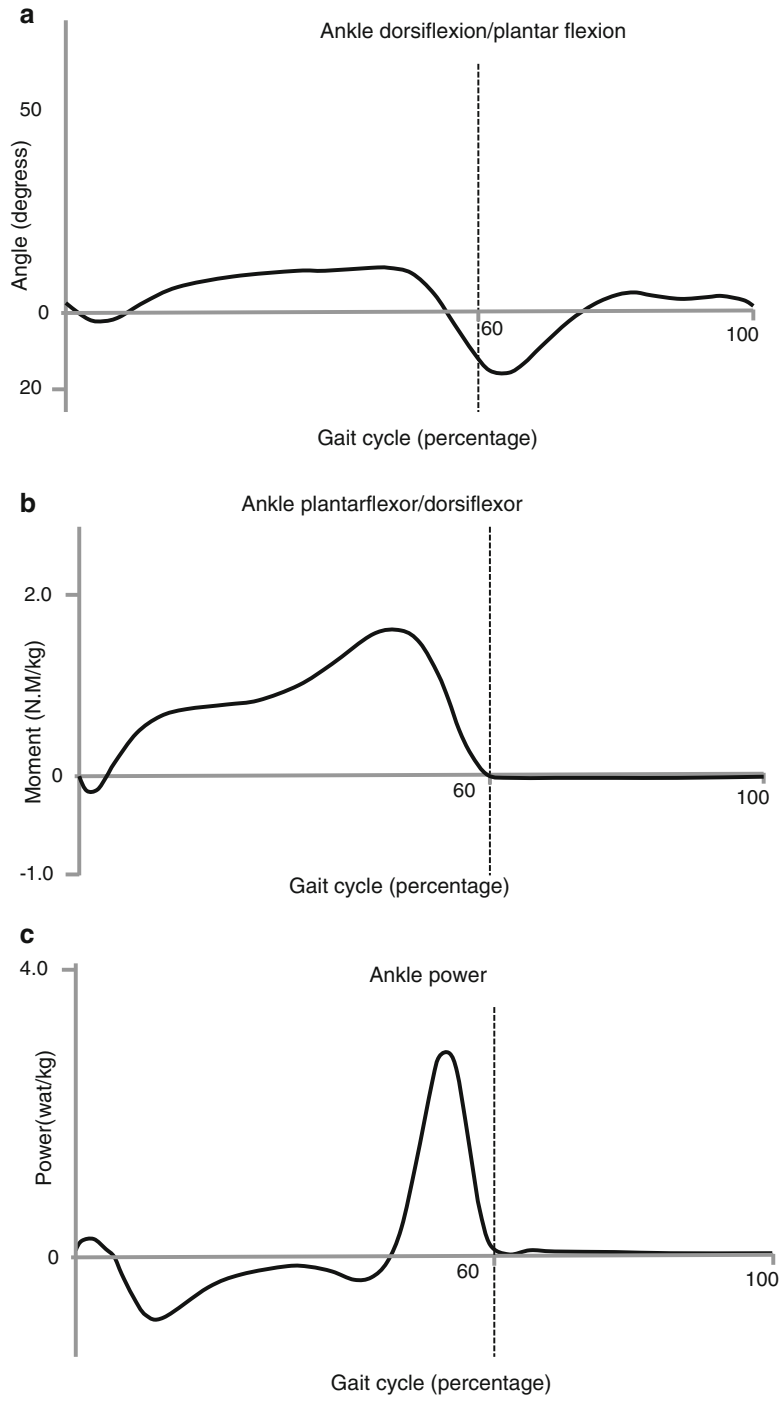

Fig. 6.7 (**a**) Ankle dorsiflexion/In a normal walking stance graph. (**b**) Ankle flexion/extension moment graph. (**c**) Ankle flexion/extension power graph

ation). Power graph (Fig. 6.6b) shows deceleration and acceleration as absorption (K1-S) and generation (K2-S), respectively.

Power is calculated by multiplying the angular velocity and force. Power increases when the angular velocity increases. Even though moment is great, little angular displacement causes low power. When there is no segmental motion, power will be zero. Figure 6.7 shows ankle sagittal plane kinematic and kinetic graphs. Kinematic

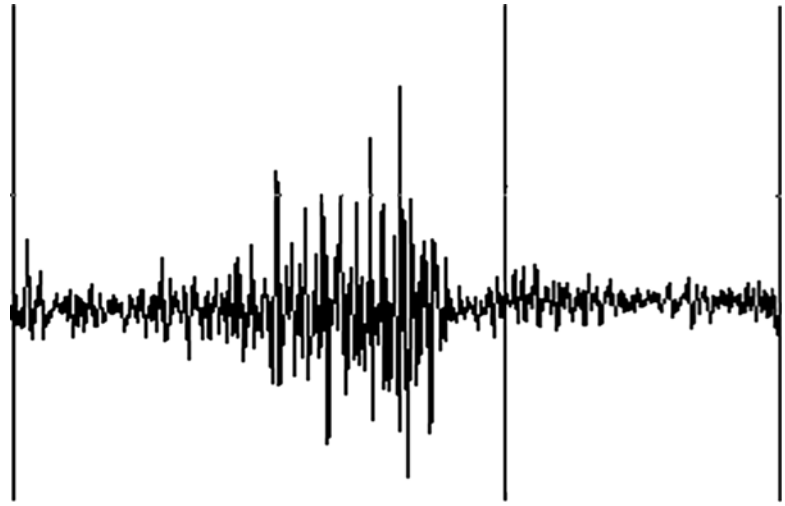

Fig. 6.8 Gastrocnemius muscle contraction during a gait cycle

graph shows that the ankle undergoes 10–15° dorsiflexion during mid-stance and first part of the terminal stance (Fig. 6.7a). Velocity of ankle dorsiflexion is too small. Although significant moment exists during this period (Fig. 6.7b), there is only little absorption power because of low velocity (Fig. 6.7c). During the second part of terminal stance and the first part of preswing, there is significant power generation (Fig. 6.7a), because plantar flexion velocity is higher in this period (Fig. 6.7a).

Trunk segment has large mass; therefore, even slight deviations of trunk cause changing the direction of the GRF resulting in significant moment around the lower extremity joints. Changing the trunk position can be used as a compensatory mechanism by the patients having weakness in the lower extremities due to neuromuscular diseases.

Kinesiological Electromyography

As previously mentioned movement takes place under the neural control of central nervous system. Muscle contraction is the last motor output of neural control. Determination of the membrane action potential of muscle fibers provides information about the neural control of movement. Motor unit action potentials are obtained using surface or indwelling electrodes. EMG signal amplitude density increases with the increase the number of motor units activated. During gait analysis kinematic data are synchronised with kinesiological EMG data. Hence the clinician has information about muscle contraction times, duration and intensity during movement.

A motor unit action potential (MUAP) is formed by the electrical signals arising from muscle fibers forming a motor unit. Surface or indwelling electrodes placed on the muscle detect the algebraic sum of the MUAPs receiving to the electrode at that time. Motor units which are far from electrode form small MUAPs, but closer motor units form large MUAPs.

Detectible pick-up distances for small motor units are approximately 0.5 cm; however, for large motor units this distance is 1.5 cm [13]. Correct placement of the electrode on the muscle is important to ideally collect the MUAPs of the muscle evaluated. Superficial anatomy knowledge is essential to do electrode placement easily.

EMG electrodes may receive MUAPs originating from adjacent muscle motor units. This is called as *cross-talk*. Cross-talk may cause significant problem in interpretation of the EMG data of a muscle. Therefore recommendations for surface electromyography recording and electrode placement procedures must be followed [1].

Obtaining clean EMG signal is a problematic process. EMG signals must be undistorted and free of noise and artefacts. Filtered and cleaned EMG signals from noise and artefacts can display in dif-

ferent ways. EMG signals, which did not undergo any process, can be presented as peak to peak oscilloscopic display. This display is called as raw EMG data. It includes all the EMG signals and is used to determine the temporal characteristics of muscle contraction (when it started and how long it lasts) during gait. Figure 6.8 shows gastrocnemius muscle contraction during a gait cycle.

In summary, gait assessment is an important part of neurologic and orthopaedic examination. Visual gait assessment has some limitations, although it is useful in the diagnosis of neuromuscular disorders, treatment planning and follow-up. 3D motion analysis systems have been used to overcome these limitations of visual assessment. Furthermore, clinicians should have sufficient knowledge about functional anatomy, neural control of locomotion, muscle and motion mechanics and kinesiological EMG to interpret the gait data.

References

1. Criswell E (2011) Cram's introduction to surface electromyography, 2nd edn. Jones and Bartlett Publishers, Boston
2. Enoka RM, Pearson KG (2013) The motor unite and muscle action. In: Kandel ER, Schwartz JH, Jessell TM, Siegelbaum SA, Hudspeth AJ (eds) Principles of neural science, 5th edn. The Mc Graw-Hill Companies, New York, pp 768–789
3. Esquenazi A, Talaty M (2011) In: Braddom RL (ed) Physical medicine and rehabilitation, 4th edn. Elsevier Saunders, Philadelphia, p 116
4. Gage JR, Schwartz M (2004) Pathological gait and lever-arm dysfunction. In: Gage JR (ed) The treatment of gait problems in cerebral palsy. Mac Keith Press, London, pp 180–204
5. Gage JR (2004) A qualitative description of normal gait. In: Gage JR (ed) The treatment of gait problems in cerebral palsy. Mac Keith Press, London, pp 42–70
6. Hibbeler RC (2007) Engineering mechanics dynamics, 11th edn. Prencite Hall, Singapore
7. Kandel ER, Schwartz JH, Jessell TM, Siegelbaum SA, Hudspeth AJ (2013) Principles of neural science, 5th edn. The Mc Graw-Hill Companies, New York, pp 812–834
8. Lieber RL (2010) Skeletal muscle structure, function, and plasticity: the physiological basis of rehabilitation, 3rd edn. Lippincott Williams & Wilkins, Baltimore, pp 93–140
9. Perry J, Burnfield JM (2010) Gait analysis: normal and pathological function, 2nd edn. SLACK Incorporated, New Jersey, pp 403–469
10. Perry J, Burnfield JM (2010) Gait analysis: normal and pathological function, 2nd edn. SLACK Incorporated, New Jersey, pp 9–16
11. Perry J, Burnfield JM (2010) Gait analysis: normal and pathological function, 2nd edn. SLACK Incorporated, New Jersey, pp 19–47
12. Schwartz M (2004) Kinematics of normal gait. In: Gage JR (ed) The treatment of gait problems in cerebral palsy. Mac Keith Press, London, pp 42–70
13. Winter DA (2009) Biomechanics and motor control of human movement, 4th edn. Wiley, Hoboken

Part II

Imaging

Cemil Yıldız

The Radiographic Evaluation of the Musculoskeletal System and Spine

7

Kenan Koca and Samet Verim

Abstract

Bone and calcified tissues are less permeable to x-rays. They absorb much more of the beam and appear radiopaque (white) on radiographs. Tissues like lung and fat are more permeable, so they absorb less x-ray resulting in a radiolucent (black) view on radiographs. Soft tissues generally appear as gray. Bones are very dense and attenuate a great deal of the x-ray beams. The cortex, which consists of compact bone, appears more opaque; however, the medulla, which consists of trabecular bone, appears less opaque. Dose of radiographs depends on anatomic region, thickness of subcutaneous tissue, and age. Information of age, sex, occupation, and clinical findings of the patient helps us during making a diagnosis. While evaluating the patients, we should obtain at least two plane views. At a trauma case, proximal and distal joints of injured bone should be visualized. Anatomic location and extension of the fracture line and soft tissue swelling should be evaluated. Fracture line should be made differential diagnosis from trace of nutrition artery. At pediatric population, bilateral radiographies should be obtained because of the open growth plates. Localization of the lesion should be evaluated, that is, focal or diffuse, solitary or multiple. Periosteal reaction or bony destruction should be noted. Also morphologic anomalies of bone should be carefully evaluated. While history and physical findings of patient are correlated with radiographic lesions, exact diagnosis is tried to achieve.

K. Koca (✉)
Department of Orthopedics and Traumatology,
Gulhane Military Medical Faculty,
Etlik 06018, Ankara, Turkey

Ortopedi ve Travmatoloji Anabilim Dalı, Gülhane
Askeri Tıp Akademisi ve Askeri Tıp Fakültesi,
Etlik, Ankara 06018, Turkey
e-mail: drkenankoca@gmail.com;
drkenankoca@yahoo.com

S. Verim
Department of Radiology, Ankara Military Hospital,
Etlik, Ankara 06018, Turkey
e-mail: drsametverim@yahoo.com

F. Korkusuz (ed.), *Musculoskeletal Research and Basic Science*,
DOI 10.1007/978-3-319-20777-3_7

Learning Targets

- After meticulous evaluation of the patient, making a correct radiographic order
- Assessment of radiographies whether it is in the appropriate position and dose
- Evaluation of the lower and upper joints of the regions that were thought pathological
- Taking of the double-sided radiographies in children than true evaluation of the epiphyseal regions
- Learning of special radiography methods and to evaluate these radiographies which are needed in some situations
- Drawing attention to common mistakes made on radiographic evaluation

Terminology

Angulation Disruption in the alignment of long bones that have been affected by injury or disease in both anteroposterior and lateral planes.

Bony Destruction Some areas of bone are destroyed and appeared as radiolucent lesions especially in benign aggressive or malignant lesions of bones.

Clear Space Area that is seen vivid.

Displacement Out of the normal location or position.

Epiphyseal Region A part of a long bone developed from a secondary center of ossification and covered with articular cartilage.

Growth Plate (Epiphyseal Plate) The disk of hyaline cartilage between the metaphysis and the epiphysis of an immature long bone that permits the bone to grow longer.

Inclination A deviation from the true vertical or horizontal.

Integrity Unity or completeness of structure; a sound or unimpaired condition.

Osteophyte (Exositozis) Bone spurs or parrot beak that form along joint margins.

Overlap Superposition of two different tissues.

Periosteal Reaction Radiographically detectable new subperiosteal bone formed as a reaction to soft tissue or osseous disease.

Permeable Permitting the passage of substances (x-ray beams, liquids, gases, heat), as through a bone or other structure.

Radiodense (Radiopaque) Exhibiting more opacity by x-rays or any other form of radiation.

Separation The act or process of moving apart or forcing something apart.

Subluxation An incomplete luxation or dislocation; although a relationship is altered, contact between joint surfaces remains.

Tilt An inclination or slope.

Introduction

X-ray beams were firstly discovered by German physics Professor Wilhelm Roentgen in 1895. Six years later, Wilhelm Roentgen was awarded the Nobel Prize in physics. French physicist Henry Becquerel discovered radioactivity afterward. Then, the x-rays and radioactivity have a very important place in the diagnosis and treatment of the diseases. X-ray beams can pass through the tissues. Due to this characteristic features, they do not accumulate in the body.

Radiological images are named as a radiogram and the formation process of the image is

named as radiography. Radiological images are composed of shades of gray from white to black. Dark tones indicate tissues that hold least beam (very permeable) such as lung and adipose tissues; open tones indicate tissues that hold much beam (less permeable) such as the bone and the areas of calcification. Soft tissues are seen in gray tones. Bones attenuate x-ray energy more than the other tissues. Cortex, which is composed of compact bone, is most opaque structure. The medulla that is composed of trabecular bone is less opaque structure.

After a detailed history and physical examination, patients should be evaluated with the most appropriate radiographs. Information of the patient's age, gender, occupation, and other clinical findings during radiographic evaluation helps to make a diagnosis. Traumatized bone and adjacent two joints should be evaluated by at least two plain radiographies. Anatomic location and elongation of fracture and shadow of soft tissue edema that occurred in the fracture line should be evaluated. Because of the epiphysis lines in children, radiographies of joint should be compared with the opposite side in children. The characters of the lesion, that is, focal or diffuse, solitary or multiple, presence or absence of the periosteal reaction or destruction, is important when assessing radiographies. Bone deformity should be evaluated carefully. Because of the forming natural contrast with the environment, radiography is the first and most important diagnostic method for evaluation of the skeletal system. The majority of bone lesions can be diagnosed by x-ray. When the lesion cannot be diagnosed by x-ray, firstly, computerized tomography (CT), magnetic resonance imaging (MRI), ultrasound (USG), scintigraphy, and positron emission tomography (PET) can be used.

Radiographic evaluation of the long bones is not very specific. Appropriate doses of two plain x-rays are usually sufficient in the evaluation of the long bones. Adjustment of dose should be done according to the extremity, age, and weight. Joint and periarticular structures show characteristics on the radiographic assessment. Radiographic evaluation of the joint area will be discussed in the order of subtitles.

Radiographic Evaluation of the Shoulder

Shoulder consists of bones, joints, muscles, and ligaments that work together to provide stabilization and motion of the upper extremity. Primarily, the clavicle, glenoid, acromion, coracoid, and body of the scapula appeared on shoulder radiography. In addition, the tuberculum majus, tuberculum minus, and head and proximal metaphyseal region of the humerus can be seen on shoulder view.

Although there are several imaging methods for the evaluation of the shoulder area, radiography must be the first choice method. Series of radiographic images of the shoulder are used for injury, arthritis, instability, and impingement syndrome. Anteroposterior (AP), Grashey, axillary, or scapular Y radiographs should be preferred for shoulder trauma. Radiographs of Grashey, outlet, and axillary should be preferred in the case of arthritis. Radiographs of internal rotation AP, axillary, Stryker notch, Grashey, and West Point should be preferred for instability of the shoulder. Radiographs of axillary, outlet, Rockwood, and Grashey should be preferred for impingement syndrome (Table 7.1). In the presence of tenderness or a deformity in the sternoclavicular joint, stability of the joint should be evaluated. The proximal end of the clavicle may be subluxated or dislocated anteriorly or posteriorly to the sternum. Stabilization of joints is evaluated by serendipity radiography. Posterior dislocations may compress the trachea and mediastinal structures that reduction must be made.

Serendipity view: The patient is placed in a supine position. While x-ray beams are giving with 40° cephalic and caudal slope, anteroposterior radiographs of the sternoclavicular joint are taken. The presence of subluxation or dislocation can be detected by evaluating the relative position of the clavicle to the sternum. In cases that a definitive diagnosis cannot be found, computed tomography is utilized.

AP view of the shoulder: It is the first-line and most useful imaging study in the evaluation of shoulder pathologies that may be taken in stand-

Table 7.1 Shoulder pathologies are classified as causing malalignment, changing the density, causing chondral lesions, and damaging soft tissue

Special series of the shoulder	Shooting technique	Findings
Anteroposterior (AP)	Patient in the standing or supine position Cassette is parallel to the coronal plane of the body Beam is directed in a true AP direction to center of the coracoid	First choice radiography for pathologies in shoulder Provides initial assessment of the glenohumeral joint, acromioclavicular joint, and distal clavicle pathologies
Grashey view (TRUE AP)	Patient is rotated posteriorly approximately 35–45° in the standing position Beam is directed perpendicular to the cassette	Allows for better evaluation of the glenohumeral joint cartilage, joint space, joint congruity, and humeral head subluxation
Axillary view	Patient is placed in supine position and the shoulder is abducted at 90° Beam is centered on the mid-glenohumeral joint and directed 15–30° toward the spine	Used for evaluating dislocations, subluxations of the humeral head, cartilage thickness, or bone Bankart lesions
West Point view	The patient is placed in the prone position with the arm abducted 90° and the patient's forearm is pronated Beam is centered at the glenohumeral joint tilted 15–25° superior and tilted 25° toward the spine	Anteroinferior glenoid rim and bone Bankart lesions are clearly seen with this view
Scapular Y view	Patient in standing or supine position Shoulder is rotated 45° anteriorly, arm is dropped near the body, and comes over the scapula Beam is directed from posterior to anterior	Used for assessment of anterior and posterior shoulder dislocations, Hill–Sachs lesions, acromion, and subacromial osteophytes
Rockwood view	Patient in standing or supine position Cassette is parallel to the coronal plane of the body X-ray beams come tilted 30° caudally to the shoulder	Provides preferable visualization of Acromion and subacromial space Preferred at impingement syndrome to evaluate the acromion and subacromial space
Supraspinatus outlet view	Patient in standing or supine position; the shoulder is rotated 45° anteriorly; the arm is dropped near the body and comes over the scapula X-ray is perpendicular to scapular body and parallel to joint surface of glenoid. Beams are tilted 10–15° caudally	Provides preferable visualization of the acromion and subacromial space Used for exhibiting the acromial and subacromial pathologies
Stryker notch view	Patient is placed in supine position Arm is externally rotated and abducted. The patient's hand is located under his head; the elbow looks to plafond X-ray is directed to the coracoid and angled 10° cephalic	Used for assessment of posterolateral aspect of the humeral head, Hill–Sachs deformity, or flattening of the posterolateral humeral head The most sensitive radiography detecting the Hill–Sachs lesion on the humeral head

ing or supine position. AP radiography is important for evaluating fractures or dislocations in trauma cases and evaluating calcific tendonitis or bursitis and AC joint arthritis in the cases of chronic shoulder pain and provides complete visualization of glenohumeral joint, acromioclavicular joint, distal clavicle, acromion, and the proximal part of the humerus. While film cassette is placed parallel to the broad surface of the scapula, x-ray beams should point to the centers of the coracoid. Because of the glenoid articular surface has 35–40° anteversion, the glenoid and humeral head overlap on the AP radiograph [1]. Three different AP projections can be obtained, with the arm in external rotation, internal rotation, or neutral position. Tuberculum minus and tuberculum

majus are seen on the lateral side; humeral head that has resemblance to an Indian ax is seen on the medial side on AP radiography that is taken with the arm in external rotation. Anatomic neck is seen between the tubercula (majus and minus) and the humeral head. The average interval between the humeral head and the acromion is 7 mm. The humeral head is seen as a rounded shape similar to the ice cream cone on AP radiographs, which is taken with the arm in internal rotation. Shoulder pain may be reflected from lung pathology, so the evaluation of the lungs in the same radiography will be beneficial.

Rockwood view: It is a modified AP radiography that is preferred at impingement syndrome to evaluate the acromion and subacromial space. While film cassette is placed parallel to the broad surface of the scapula, x-ray beams come tilted 30° caudally to the shoulder. The acromion and subacromial space can be clearly visualized with this view. Inferior border of the acromion must be over the line of the inferior border of clavicle; otherwise it might be considered as osteophyte or exositozis of the acromion.

Grashey view: The true AP radiography of the shoulder. It provides tangential view of the glenohumeral joint and allows excellent evaluation of the glenohumeral cartilage space and the proximal humerus. Patient is rotated posteriorly or x-ray device is turned lateral to eliminate of glenoid's anterior inclination [2] (Fig. 7.1). In this way, overlapping of the humeral head and glenoid is prevented at AP radiography. The humeral head, cartilage of glenoid, glenohumeral joint space, joint congruence, and joint subluxation can be evaluated more clearly on this radiography [3]. Image quality can be decreased because of the soft tissue thickness.

Axillary view: It is a tangential view of the glenohumeral joint. It is used for assessment of subluxation or dislocation of the humeral head. It is also used for detecting bone Bankart lesion involving the anterior glenoid rim. Patient is placed in supine position and the shoulder is abducted at 90°. X-ray beams are centered on the glenohumeral joint and directed 15–30° toward the spine (Fig. 7.2).

West Point view: It is the modification of axillary radiography that allows excellent evaluation of the anteroinferior border of the glenoid [4]. Bone Bankart lesion of the anterior glenoid rim is detected easily with this view [5]. Patient is in prone position and the shoulder is abducted at 90°; the arm is located on a pillow. The forearm is pronated. X-ray beams are centered and glenohumeral joint tilted 15–25° superiorly and tilted 25° toward the spine (Fig. 7.3). This view can be painful in patients with acute shoulder injury.

Scapular Y view: It is used for assessment of anterior and posterior shoulder dislocations. Position of patient and shooting of x-ray are easier than axillary radiography in acute traumas. There is no difference between scapular Y radiography and axillary radiography for detecting the pathologies [6]. However, scapular Y radiography is also useful in Hill–Sachs lesions. Scapular Y radiography proves scapula, acro-

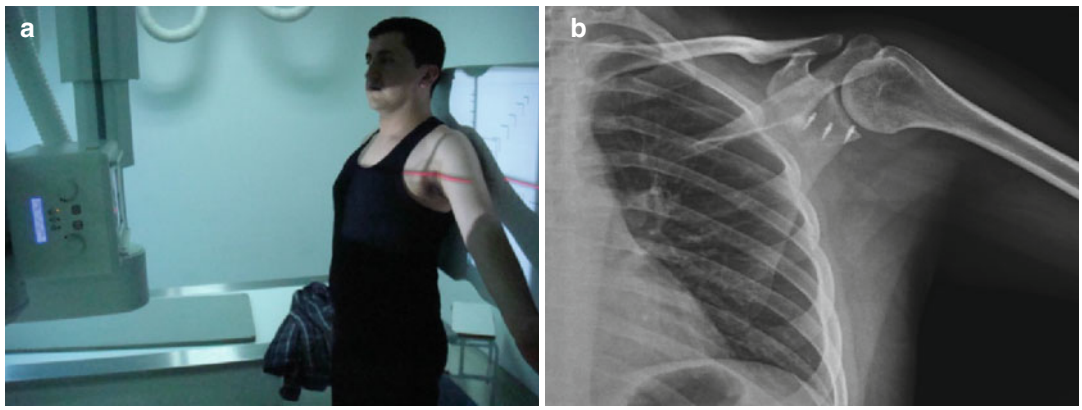

Fig. 7.1 (**a**) Position of the patient and x-ray during the Grashey radiography. (**b**) Image of Grashey radiography

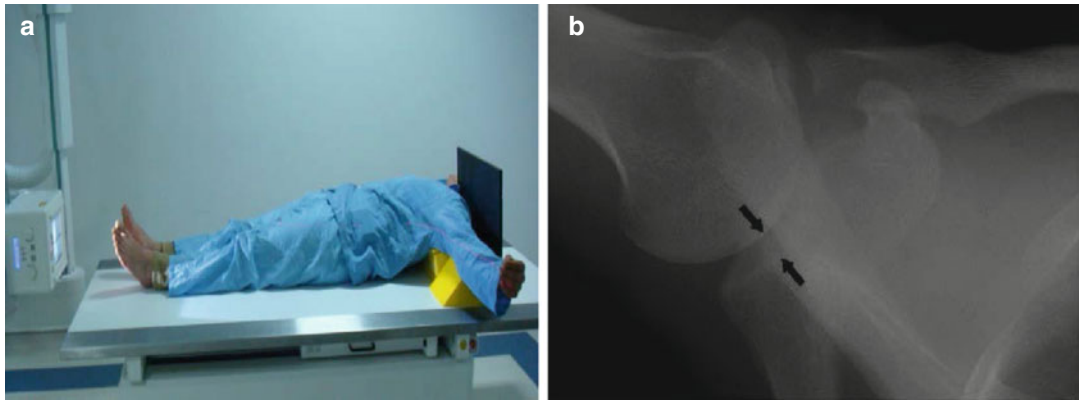

Fig. 7.2 (**a**) Position of the patient and x-ray device during the axillary radiography. (**b**) Image of axillary radiography. *Arrows* show congruousness of glenohumeral joint

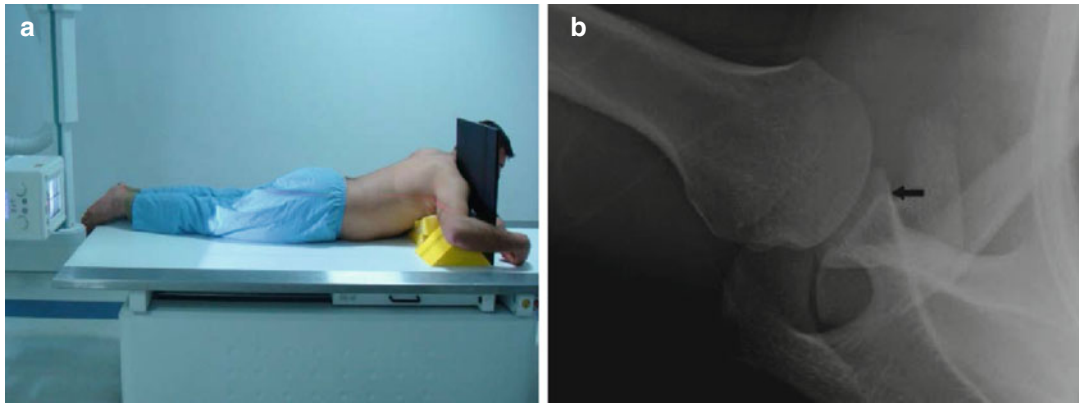

Fig. 7.3 (**a**) Position of the patient and x-ray device during the West Point radiography. (**b**) Image of west point radiography. *Arrows* show location of Bone Bankart Lesion

mion, and coracoid pathologies. Stem of "Y" is made by the scapula's body and legs. Acromion and coracoids composed legs of "Y." It is obtained in supine position or standing position. While the shoulder is rotated 45° anteriorly, x-ray beams are directed from posterior to anterior (Fig. 7.4). The arm is dropped near the body and come over the scapula. The humeral head is centralized on the center of Y. If the humeral head is anteriorly, this condition is called anterior dislocation. If it is posteriorly, this condition is called posterior dislocation. Fractures of the scapula (when shooting arm is positioned anteriorly), acromion, and coracoid process can also be detected with this view.

Supraspinatus outlet view: It is used for exhibiting the acromial and subacromial pathologies. Scapular Y radiography is more useful for detecting the types of acromion, and subacromial osteophytes may cause impingement. Shooting technique is similar to scapular Y radiography, but x-ray beams are tilted 10–15° caudally. X-ray is perpendicular to scapular body and parallel to joint surface of the glenoid.

Stryker notch view: Patient is placed in supine position and the arm is externally rotated and abducted. The patient's hand is located under his head; the elbow looks to plafond. X-ray is directed to the coracoid and angled 10° cephalic. It is used for assessment of posterolateral aspect of the humeral head and Hill–Sachs deformity or flattening of the posterolateral humeral head. It is the most sensitive radiography detecting the Hill–Sachs lesion on the humeral head [4].

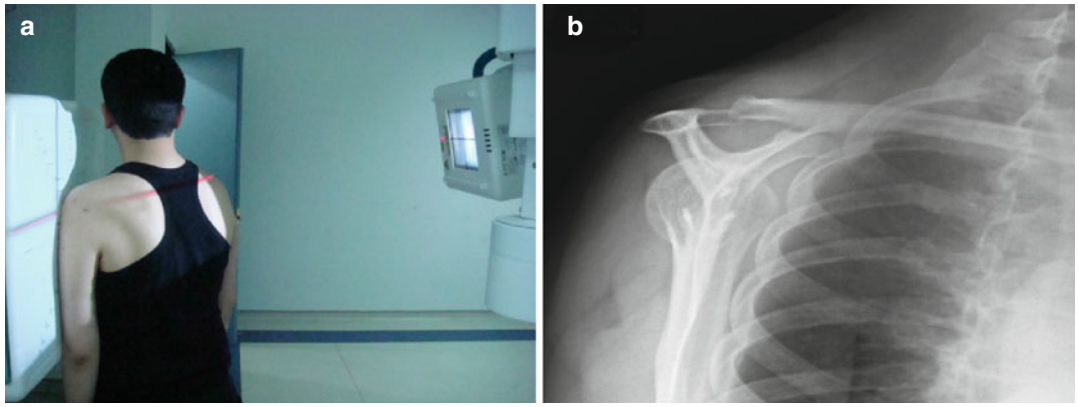

Fig. 7.4 Scapular Y radiography. (**a**) Position of the patient and x-ray device during the scapular Y radiography. (**b**) Image of scapular Y radiography

Malalignments

Fractures

It is important to define the fracture and localize part of fracture in the proximal humerus. In 1970, Neer classified these fractures into four groups. The fracture segments are the humeral head, humeral shaft, tuberculum majus, and tuberculum minus. More than 1 cm separation and more than 45° angulation is defined as displaced. Angulation between the shaft and head has to be evaluated on frontal and lateral plains at surgical neck fractures. Displacement of tubercula could be evaluated on axillary radiography, but patient could have serious pain. Because of this angulation of fractures, the humeral neck on sagittal plain can be evaluated with good dosage transthoracic radiography.

Dislocations

The most of the dislocations of the patients that come to emergency room occurred in shoulders. Anterior (95 %), posterior (5 %), and inferior (subglenoid luxatio erecta 0.5 %) are three types of dislocation. Anterior dislocations usually occurred because of trauma. Humeral head slides anteromedial and below to the glenoid fossa. This can be evaluated with AP radiography, but the axillary view or the scapular Y view is very specific for dislocations. Dislocation may cause recurrence in younger patients. Because of recurrence dislocation, Bankart lesion on anteroinferior rim of the glenoid and Hill–Sachs lesion on the humeral head may occur. It is not important clinically if there is less than 20 % of articular surface of the glenoid. In addition, tuberculum majus fracture may occur during the dislocation. AP radiography is usually enough for diagnosis, but axillary and scapular Y radiography can be taken for confirmation. Hill–Sachs, which occurs during recurrent anterior dislocation, is osteochondral lesion on posterosuperior of the humeral head. Striker notch radiography is the best option to demonstrate Hill–Sachs lesions.

Posterior dislocations are caused by epileptic seizures or electric shock. Most of them are bilateral. Stronger internal rotator muscle contraction causes this situation. The mechanism of posterior shoulder dislocation is thought to be unequal muscle contraction with the internal rotators of the shoulder, causing the humeral head to move superiorly and posteriorly. Osteochondral fracture on anterior part of the humeral head may occur that is called reverse Hill–Sachs lesion, and posterior glenoid rim fracture may occur that is called reverse Bankart lesion. AP radiography is not usually enough and can cause missout. Axillary radiography makes diagnosis at 100 % [7]. If there is pain, scapular Y radiography or computerized tomography can be a choice.

Luxatio erecta is named as inferior or subglenoid dislocations. Arm is hyperabducted and cannot be pulled inferior. It may occur after falling in hyperabduction position. Neurological injury could occur, especially in axillary nerve. AP radiography is enough for diagnosis.

Situations That Change Density

Density changing in the humeral head is caused by chondral lesions and tumors. Most three situations that cause chondral lesions are trauma, steroids, and sickle cell anemia. Sclerosis, collapse, fragmentation, and degenerative changes can be seen in avascular necrosis according to the stage.

Synovial chondromatosis may result from primary or secondary to chondral lesions. In primary, multiple cartilaginous nodules are formed because of synovial membrane proliferation and metaplasia. Tumor lesions can be radiolucent or radiodense.

Situations That Damage the Joint Cartilage and Articular Distance

The most causes are rheumatoid arthritis and osteoarthritis. Diffuse osteopenia, localized erosion, and uniform narrowing on articular space occur in rheumatoid arthritis. Primary osteoarthritis is a rare situation in the shoulder, because it is not a load-bearing joint. Generally, it is secondary to trauma, systemic arthritis, chronic rotator cuff tears, congenital malformations, and acromegaly.

Soft Tissue Lesions

(a) *Calcific tendinitis or calcific bursitis* (hydroxyapatite storage disease) is a typical example. At most, it occurs around the shoulder joint. In more than half of the cases, supraspinatus tendon is involved. Infraspinatus and teres minor tendinitis are seen well on internal rotation because of posterior location. Subscapularis tendinitis is seen anteriorly. It could be symptomatic or asymptomatic.

(b) *Impingement syndrome:* This is impinging of supraspinatus tendon, subacromial–subdeltoid bursae, and biceps tendon between the humeral head and acromion. It is diagnosed generally by clinical and subacromial injection test. For the etiology, radiography must be taken. Acromion could be flat, curved, or hooked. The angle between lower anterior and posterior surfaces of acromion is acromion angle. It helps to determine the shape of the acromion and the amount of resection while performing acromioplasty. Os acromiale, type 3 acromion, acromial osteophyte, and acromioclavicular degeneration must be identified. Supraspinatus outlet radiography is the most beneficial technic. The Rockwood radiography, which is an angled frontal radiography, provides frontal osteophyte view without any overlapping on the acromion. Cortical thickening or subcortical sclerosis on the tuberculum majus has lower specificity at diagnosis of rotator cuff lesions. But the specificity of subchondral cysts is higher.

(c) *Rotator cuff tears:* Direct radiography is usually normal on rotator cuff tears. Glenohumeral distance decreases below 2 mm in hyperabducted radiographies. Loosening of convexity and flattening of supraspinatus muscle at outlet radiography must be thought rotator cuff tears. Lower density layer on normal muscle density must be thought of as fatty degeneration. Acromiohumeral distance decreases below 7 mm because the strength of rotator cuff that detrudes the humeral head is weak according to the strength of the deltoid that elevates the humeral head. At late stages of rotator cuff tears is the rotator cuff arthropathy named as a Milwaukee shoulder syndrome.

Also it is high density because of calcium pyrophosphate dihydrate storage disease, and synovial chondromatosis must not be overlooked.

Radiological Evaluation of the Elbow

The elbow joint is very complex that is formed by the distal humerus and proximal ulna and radius. The types of humeroulnar joint are complex hinge, and other joints of the elbow (radiohumeral and the radioulnar joints) are pivot.

Anatomic structures around the elbow are the distal humerus, olecranon, coronoid, and radial

head. The distal humerus consists of capitellum, trochlea, medial and lateral condyle, and olecranon fossa. There is a 10–12° of valgus angle at anteroposterior plain of the elbow. Distal humerus has 30° anterior tilt at lateral plain. These complex articulations and structures can be evaluated when well-positioned radiographs are obtained.

Appearances of children and adult elbow views are different from each other. In addition, appearance of children elbow view depends on the age of children, because the elbow has many different ossification centers which reveal at different times. So elbow radiographs must be taken bilaterally and compared to noninjured extremity in traumatized patient. Anteroposterior, lateral, and radial head radiographies are routinely used at trauma series. Traction radiographies could be needed at multifragmental and burst fractures [8].

Elbow AP view: AP radiography must be taken at full extension of the elbow and supination of the forearm. X-ray is directed vertical to the joint. The condyles, capitellum, trochlea, radial head, and elbow carry angle that can be assessed on AP radiography [9]. In the proper radiography, radiohumeral and humeroulnar joints and the medial and lateral humeral epicondyles should be clearly shown. The radial head and radial tuberosity should be minimally superimposed on the ulna. If there is flexion contracture, two AP radiographs must be taken. X-ray beams parallel to the forearm in one and humerus in another.

Structures evaluated on elbow AP view:

Radius neck–shaft angle: the angle is between the radial neck and radial diaphysis. The normal value is 15° [10].

Joint surface angle: the angle is between humeral shaft and the line from distal border of the trochlea and capitellum. The normal values are between 82 and 84°.

Elbow carry angle: the elbow is curved laterally when fully extended and supinated. The angle between the center of the arm and forearm is called as a "carry angle." It is used at fractures of the distal humerus and elbow. It is important to evaluate carry angles bilaterally [11]. It is the angle between the line parallel to the humerus and ulna at radiographs. Valgus of trochlear notch and valgus of distal humeral make carry angle [12]. Positive values show valgus angulation. The elbow carry angle increases at adult ages and greater at the dominant hand [13]. Values of carry angles are variable at all ages, in women 11.8° and in men 6.9°. Carry angle is same before puberty in girls and boys, but it increases after puberty in girls, so some authors say it is one of the secondary sex characters [14].

Baumann angle: it is used to evaluate pediatric humeral distal fractures on coronal plain. Baumann angle is used especially in Gartland type 2 fractures which treatment is not clear. This angle best shows alignment of distal humerus on coronal plane [15]. It is the angle between long axis of the humerus and line from lateral condylar physis. Normal value of the angle is 75–80° [16]. There is discussion about the true Baumann angle that has three variants [13].

Trochlear notch angle: The angle is between medial and lateral faces of the trochlea.

Elbow lateral view: It must be taken with abducted shoulder at 90° and flexed elbow at 90° and up-righted thumb, while ulnar face of the forearm is on the table. X-ray must be centered on the radial head. Posterior aspects of supracondylar region must be overlapped for true lateral radiography of the elbow [17]. Olecranon, coronoid, radial head, anterior fat pad, posterior fat pad, anterior humeral line, and radiocapitellar line are evaluated.

Anterior humerocapitellar line: This line that draws along anterior of the distal humerus should pass through middle one third of the capitellum. This measurement is used for treatment of supracondylar fractures in children.

Radiocapitellar line: This line shows the relationship between radial head and capitellum and should pass through the center of the radius neck and middle one third part of capitellum. In dislocation of the radius, this line will not pass through the center of the capitellum.

Anterior angulation of distal humerus joint line: The distal end of the humerus is angled 30° anteriorly.

Olecranon–coronoid angle: This line connects the longitudinal axis of the ulna with the end point of the olecranon and coronoid.

The presence of fat pad: There are anterior and posterior fat pads in the elbow joint. Fat pads consist of tightly packed and fibrous tissue surrounded by lipid cells [18]. Fat pad tissue is intracapsular but extrasynovial. Although the anterior fat pad can be seen in standard lateral radiographs, posterior fat pad could not be seen [19]. Effusions of elbow joint raise both of the anterior and posterior fat pad and make them visible on lateral radiographs. A lifted posterior fat pad demonstrates a hidden intracapsular fracture [20].

Radius head–capitellum view: This radiograph is a modification of lateral elbow radiography. X-ray beams are directed to the radius head tilted 45°. Unlike the lateral radiographs, humeroradial and humeroulnar joints can be displayed better [21]. It is significant for exhibiting posterior half fracture of radial head.

Internal oblique view of the elbow: This radiograph shows the medial epicondyle, trochlear notch, and coronoid tubercle of the ulna. The forearm is pronated at 45°. X-ray beams come perpendicular and centered 2 cm below the medial epicondyle.

External oblique radiography of the elbow: It is used for assessment of the capitellum and radial head. The forearm is supinated at 45°. X-ray beams come perpendicular to the elbow.

Capitellum fractures are best seen in lateral radiographs. There is a double-bubble sign in type 4 capitellum fractures (capitellum fractures with trochlear fractures). Lateral compression can cause Panner disease of the elbow, capitellum OCD, radial head OCD, and angular deformity in the radial head. Fissures, fragmentations, and irregularity occur in early stage, and then reossification and resolution occur in late stage on lateral radiographs [22].

Coronoid bone is very important for elbow stability. It is important to evaluate magnitude of fracture fragment for classification of coronoid fractures. Larger than 50 % of the coronoid fracture fragment leads to instability. Usually, lateral elbow radiography is enough for evaluation. Also coronoid fracture fragment involving the inner or the outer edge is important for determining the direction of instability. Because of the difficulty to detect this situation in lateral elbow radiography, computed tomography can be used.

Usually AP and lateral radiographs of the elbow are enough for diagnosing radial head fractures. However, putting forward the amount of fracture fragmentation and positions of fractured pieces and to view the articular surface clearly, computed tomography would be useful. It should be also known that in children, radial neck fractures occur more likely rather than the radial head fractures.

Elbow dislocations are usually posterior in direction and determined by lateral radiographs. After reduction, to be sure of reduction and to clearly reveal accompanied fractures, AP and lateral radiographs should be taken again. While coronoid and radial head fractures accompany elbow dislocations in adults, medial epicondyle fractures accompany in children (Table 7.2).

Radiological Evaluation of the Hand and Wrist

Standard radiographs included anteroposterior, lateral, and oblique views of the wrist and are sufficient for the determination of most of the pathology occurred with or without trauma. Additional radiographs may include radial or ulnar deviation views, carpal tunnel view, special scaphoid views, and stress views.

AP View of the Wrist

Posteroanterior view is taken with the shoulder abducted 90° and elbow flexed 90° (in the same level with the shoulder). So palmar face of the hand is placed flat on the cassette with the forearm rotated internally.

Distal joint surfaces of the radius and ulna, radial inclination, radial length, and distal radioulnar joint compliance (ulnar variance) are evaluated. In addition to carpal bones, intercarpal joints and radiocarpal joints can be examined.

Joint surfaces of the radius and ulna: Load transfer of the wrist joint occurs with 80 % by radius joint surface and 20 % by ulnar joint

Table 7.2 Common elbow views, technique, and findings

Radiographs	Shooting technique	Findings
Anteroposterior (AP)	Patient in the upright or supine position The elbow should be fully extended with the forearm supinated Cassette is parallel to the coronal plane of the body X-ray beam is directed perpendicular to the cassette	Allowing optimal visualization of the medial and lateral epicondyles, radiocapitellar joint, and estimation of the: Carrying angle Radius neck–shaft angle Joint surface angle Elbow carry angle Baumann angle Trochlear notch angle
Elbow lateral radiography	Patient in the upright or supine position The elbow in 90° of flexion and the forearm in neutral (thumb up) position X-ray must be centered on the radial head	Allows for evaluation of: Olecranon Coronoid Radial head Anterior fat pad Posterior fat pad Anterior humeral line Radiocapitellar line Elbow dislocation
Radius head–capitellum radiograph	Modification of lateral elbow radiograph The x-ray tube directed 45° toward the radius head	Used for better display of: Humeroradial joints Humeroulnar joints Posterior half fractures of radial head
Internal oblique radiography of the elbow	Patient in the upright or supine position The elbow fully extended; shoulder and elbow on the same horizontal plane The hand is pronated and forearm is aligned to long axis of IR The forearm is rotated medially so the distal humerus and the anterior surface of the elbow joint is 45° to IR (palpate epicondyles to determine rotation)	Used for assessment of: Medial epicondyle Coronoid tubercle of the ulna
External oblique radiography of the elbow	Patient in the upright or supine position Arm fully extended; shoulder and elbow on the same horizontal plane The hand is supinated and forearm is aligned to long axis of IR The forearm is rotated laterally so the distal humerus and the anterior surface of elbow joint is 45° to IR (palpate epicondyles to determine rotation)	Gives better information about: Capitellum Radial head

surface. Distal radius fractures usually involve the joint surface. More than 1 mm stepping on the joint surface may be able to lead wrist degeneration. If radiography is insufficient to evaluate stepping on the joint surface, CT could be useful. Distal ulna fractures, mostly styloid, may accompany to distal radial fractures.

Radial inclination: The angle between the transverse line of distal radius joint surface and the line that draws from the ulnar corner of the radius to the radial styloid gives the radial inclination (Fig. 7.5). Normal value of inclination is between 22 and 23°. After distal radius fractures, radial inclination decreases. Seventeen to eighteen degrees can be acceptable for treatment.

Radial length: This is distance between the articular surface and the radial styloid (Fig. 7.5). Normal value of length is between 11 and 12 mm, but it reduces in distal radius fractures. Nine millimeter can be acceptable for treatment.

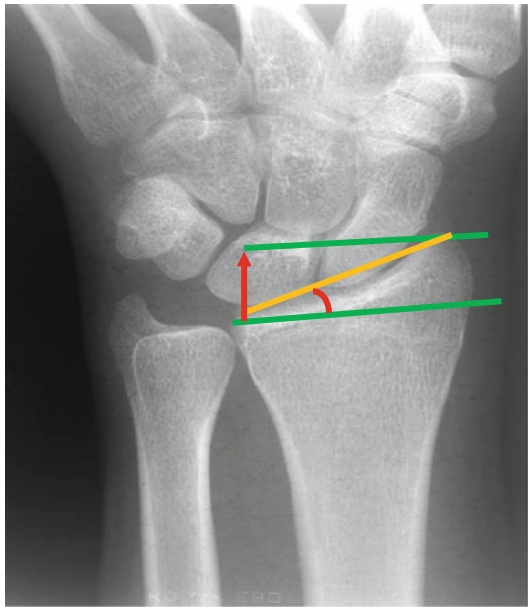

Fig. 7.5 AP view of the wrist

Distal radioulnar joint compliance: Normally, the distal radius joint and the distal ulna joint surfaces are in the same line. If the ulnar surface is above the radial surface (in the same time ulnocarpal distance >0.9 mm), it is named as positive ulnar variance. If the ulnar surface is below the radial surface (in the same time ulna-carpal distance <0.9 mm), it is named as negative ulnar variance.

Carpal bones: The scaphoid, lunatum, triquetrum, and pisiform bones create proximal row, and the trapezium, trapezoideum, capitatum, and hamatum create distal row of the carpal bones. Scaphoid and lunate bones articulate with scaphoid and lunate fossa on the distal radius joint surface. Distal ulna establishes a relationship with carpal bones through triangular fibrocartilaginous complex (TFCC).

Lateral View of the Wrist

Lateral view is taken with the shoulder abducted 90° and elbow flexed 90° in the same level. Then the wrist is placed on cassette with the forearm in neutral position. The long axis of the third metacarpal should be parallel with the long axis of the radius on a true lateral view of a normal wrist. In addition, pisiform should appear directly over the dorsal pole of the scaphoid on a true lateral view.

Volar tilt of distal radius joint, distal radioulnar joint, and radiocarpal joint can be evaluated.

Tilt of the distal radius joint surface: The distal radial tilt accounts for the angle between a line along the distal radial articular surface and the midshaft line of the radius. The distal radius joint surface has a 10° volar tilt on the lateral plane normally. Dorsal angulations occur usually in distal radius fractures. Acceptable volar tilt ranges 2–20° after reduction.

Distal radioulnar joint: Distal radioulnar instability can occur after trauma. Dorsal subluxation of the ulna usually may appear on lateral plane. Especially in the Galeazzi fractures and Essex–Lopresti injuries, care should be taken about distal radioulnar instability.

Carpal Instabilities

The radius, lunatum, capitatum, and long axis of the third metacarpal are at the same line in a normal lateral wrist radiography [23]. This line is broken in the presence of carpal instability and become like a "Z"-shaped line. There is a 30–60° angle between long axis of the scaphoid and the line passes through middle of the lunatum. There is a less than 10–20° angulation between the capitatum and lunatum.

There is less than 3 mm gap between scaphoid, lunatum, and triquetrum bones that create proximal row in the AP view. The gap between scaphoid and lunatum expands in the case of scapholunate ligament injury, and the gap between lunatum and triquetrum expands in the case of lunotriquetral ligament injury.

Ligaments around the lunatum generate little ring that is named as "small arc" on the AP view. A break of this arc demonstrates one or more ligament injury of this ring. The big ring that generated from the bones around the lunatum is named as "big arc." A break of this arc demonstrates one or more fractures of these bones. In addition, three different arcs were

described by Gilula on the AP radiograph [24]. Proximal cortexes of the scaphoid, lunatum, and triquetrum generate "first arc," distal cortexes of same bones generate "second arc," and proximal cortexes of capitate and hamatum generate "third arc." These arcs that have shown normal anatomic structure are broken down in carpal instabilities.

Carpal instabilities, which occurred with proximal row bones separation, are called as dissociative carpal instabilities. These pathologies are caused by ruptures of intrinsic ligaments between proximal row bones. These consist of scapholunate instability, lunotriquetral instability, and perilunate dislocation. Instabilities without separation of proximal row bones are called as non-dissociative carpal instabilities. These pathologies occur with injuries of the extrinsic radiocarpal ligament.

Carpal instabilities are also classified as static and dynamic instabilities. Static instability is carpal malalignment in a fixed position and diagnosed by PA and lateral wrist views in a stable position. Dynamic instability occurs with physical maneuvers and revealed with stress radiographs. While dynamic instabilities are only formed by the dorsal scapholunate ligament injury, static instabilities occurred by complete injury of the scapholunate ligament with palmar radiocarpal ligament injury. Static instabilities can be diagnosed easily in AP and lateral radiographs taken in stable position. While pathologies in dynamic instabilities can't be observed in the radiographs of stable position, they can reveal in dynamic and stress radiographs. These dynamic radiographs are taken in flexion, extension, ulnar, and radial deviation. Stress radiographs are taken in fist-clenched position.

Scapholunate Instability: This instability occurs with scapholunate ligament injury. The scaphoid comes to more vertical position on coronal plane and comes to more flexion position on sagittal plane. The lunatum comes to extension position and tilts dorsally on sagittal plane. This condition is known as dorsal intercalated segment instability (DISI) [25]. Scapholunate gap is more than 3 mm on AP wrist view in this instability. This is called as Terry Thomas or Dave Letterman sign (Fig. 7.6). Superposition occurs in distal edge of the scaphoid with its rotation on own long axis and it seems like shortened. This sign is named as "ring sign." Also the distance between distal end of the scaphoid and proximal end of scaphoid is less than 7 mm. The angle between the scaphoid and lunatum is more than 70°, the angle between lunatum and capitate is more than 10–20°, and the angle between lunatum and long axis of the radius is more than 10° in lateral radiography.

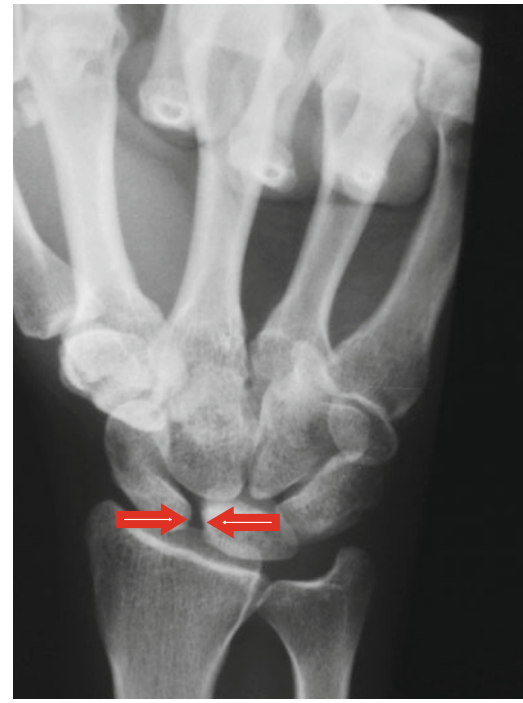

Fig. 7.6 Fist-clenched stress view of the wrist. *Arrows* show increased gap between scaphoid and lunatum

Lunotriquetral Instability: It results from injury or rupture of lunotriquetral ligament. Lunatum angulates volarly, and capitate moves volarly on sagittal plane. This condition is known as VISI (volar intercalated segment instability). In addition, injury of the dorsal radiocarpal ligament might be together with lunotriquetral ligament injury as for development of VISI. The lunatum angulates volar direction and angle of lunocapitate increase on lateral radiography in VISI pattern. Angle of the scapholunate does not change.

Hand AP and Oblique Radiography

Metacarpals, phalanges, metacarpophalangeal joints, and interphalangeal joints are evaluated in hand AP radiography. Boxer fractures that are usually caused by punch at the neck of the fifth metacarpal should not be overlooked. Likewise, there are specific fractures on basis of the first metacarpal described by Bennet and Rolando. Care should be taken for providing normal lengthening of the metacarpals in fractures. It's usually hard to identify rotation deformities of metacarpals and phalanges in radiography. Rotation deformities should be evaluated with physical examination. When all of the fingers are in full flexion position, there must be no overlapping on fingers and fingers must be directed to the scaphoid.

On lateral radiograph, the hand does not give a clear image because of superposition of metacarpals and phalanges. Metacarpals and phalanges are better evaluated on oblique radiography of the hand. However, an exact lateral radiography can be needed in some phalanx fractures.

Radiographic Evaluation of the Pelvis and Hip Joint

The pelvis is a complex bone ring consisted of several anatomic structures. Posterior of this ring consists of the sacrum and iliac bones, lateral consists of iliac bones, and anterior consists of ischium and pubis bones. The pelvis connects the lower extremity with the body. Anatomic structures include sacroiliac and symphysis pubis joints that move not much. There are very strong ligaments contributed to pelvic anatomic integrity.

Pelvis fractures are life-threatening injuries because they are caused by high-energy trauma like traffic accidents and fall from height. To improve the chances of survival, these patients require interventions correctly and without delay. It has been reported that mortality rate in pelvic fractures ranges from 8 % to 17 %. If these fractures are associated with hemorrhagic shock, mortality rate increases up to 40 % [26, 27]. Pelvic fractures are caused by compression forces generated from anteroposterior, lateral, or the combination of both.

Patient with pelvic trauma is first evaluated with a neutral AP pelvis radiography. X-ray device needs to be brought next to the patient in contrast to take the patient near x-ray device to prevent additional injury and intervene faster. If there is a pelvis fractures, oblique pelvis radiographies including inlet AP and outlet AP x-rays should be taken. Pelvic tomography should be taken for final evaluation of pelvic ring injuries after radiography. CT is very useful for evaluation of sacroiliac joints and sacrum.

Symphysis pubis separation occurs with anteroposterior compression force. Sacroiliac separation may be accompanied to symphysis pubis separation. 2.5 cm or more separation of symphysis pubis cause external rotation instability of pelvic ring and comprise surgical indication. L5 vertebra transfers process fracture indicates posterior pelvic ring injuries [28].

Neutral AP views of the pelvis: This image is obtained by perpendicular x-ray beams to the pelvis. It is usually taken as a first radiography that gives general information about the trauma.

Inlet AP views of the pelvis: X-ray beams are directed to the pelvis tilted 40° caudally. Deformities of symphysis pubis and sacroiliac joints on AP plan reveal more clearly.

Outlet AP views of the pelvis: X-ray beams are directed to the pelvis tilted 45° cranially. Sacrum pathologies, vertical displacements of sacroiliac joint, and pathologies of the anterior symphysis pubis are observed more clearly on this radiography.

Acetabular fractures like pelvic fractures usually result from high-energy trauma such as traffic accident or fall from a height. Pelvis neutral AP and 45° oblique (Judet) radiographs should be taken for the evaluation of acetabular fractures. Six standard structures described by Letournel can be evaluated on these radiographs. These structures are iliopectineal line, ilioischial line, anterior wall, posterior wall, acetabular roof, and teardrop. Iliopectineal or iliopubic line starts from sciatic groove, continues to the superior pubic ramus, and extends to the symphysis pubis.

Ilioischial line also starts from sciatic groove, continues to medial edge of ischium, afterward it consists of medial edge of teardrop.

Obturator oblique (internal oblique) view: Radiography is taken while the acetabulum at fracture side is raised and a 45° angulation is provided on the ground (Fig. 7.7). Obturator foramen is viewed as a full ring. Only part of the wing of the iliac bone is seen. Posterior wall and anterior column are seen clearly. Spur sign is observed due to double column fracture of the acetabulum.

Iliac oblique (external oblique) view: These radiographies are taken by rising proportion of the intact acetabulum and providing 45° angle with the ground (Fig. 7.8). Iliac bones can be seen completely. The iliac crest, quadrilateral

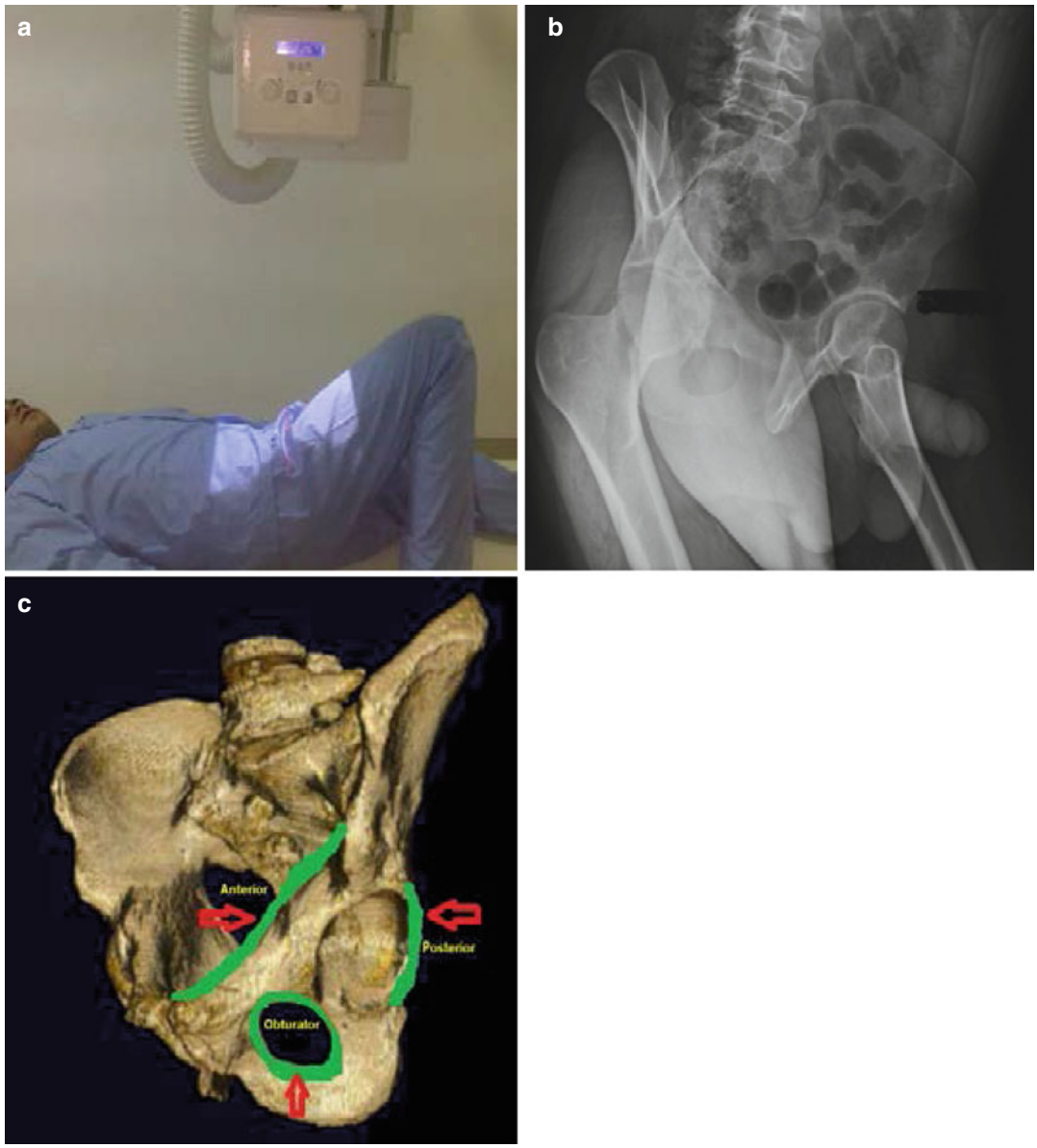

Fig. 7.7 (**a**) The position of the patient and x-ray devices during the obturator oblique–internal oblique radiography. (**b**) The image of internal oblique radiography. (**c**) Three-dimensional CT image

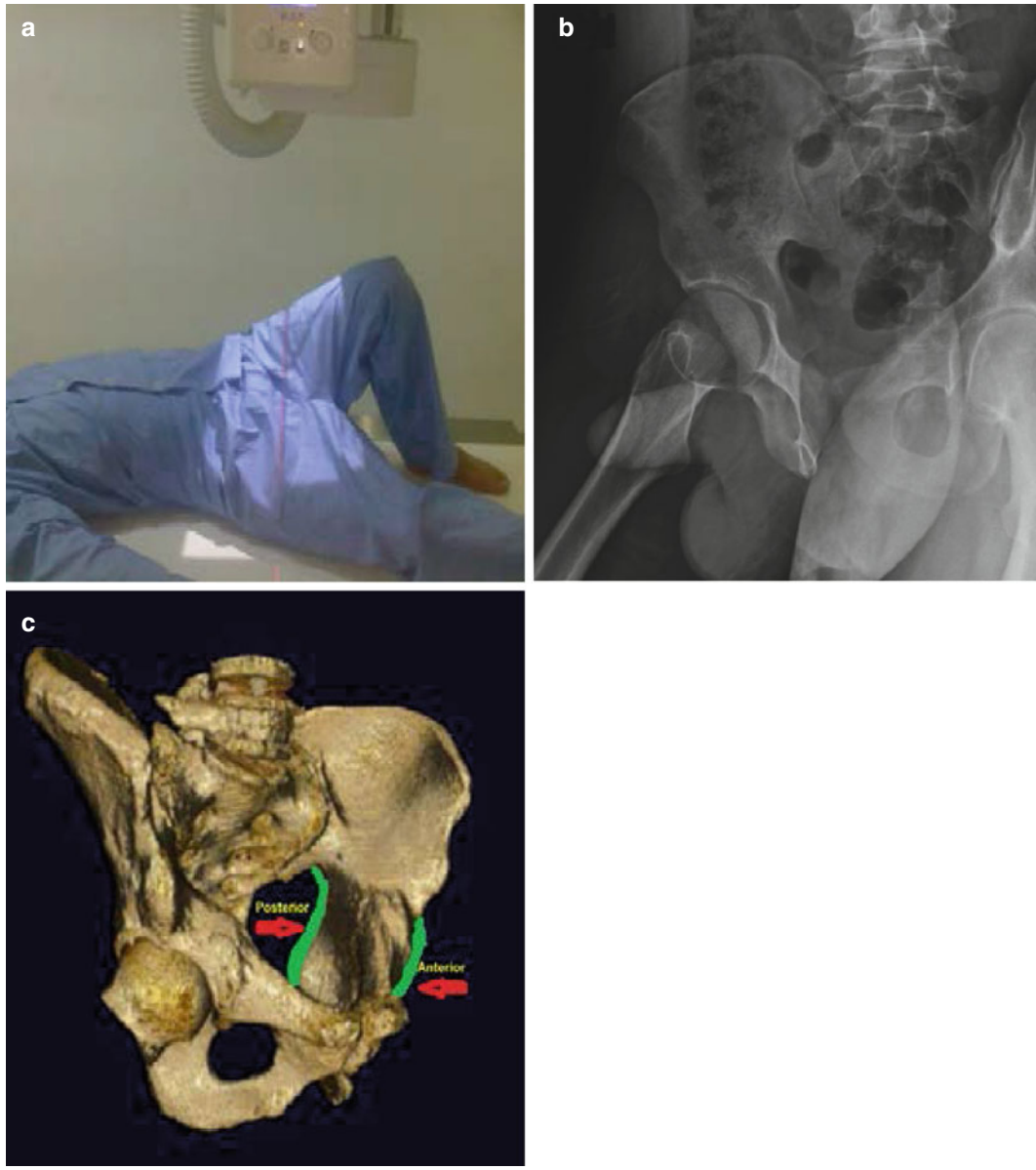

Fig. 7.8 (**a**) The position of the patient and x-ray device during the iliac oblique–external oblique radiography. (**b**) Iliac oblique–external oblique radiography image. (**c**) Three-dimensional CT image

surface, tuber ischium, posterior column, and anterior wall can be seen clearly.

Plain radiographs determine the hip joint pathologies: AP pelvis, cross-table lateral, 45° or 90° Dunn, frog position, and the false-profile radiographs [29].

Anteroposterior pelvis view: Radiography is taken while both of the lower extremities are rotated 15° internally in the supine position. The neck of the femur reveals completely on this radiography. The symphysis pubis and coccyx are at the same level and distance among them is about 1–3 cm. Obturator foramina and iliac wings should be symmetrical. Otherwise, the radiography can't be evaluated correctly. Pelvic tilt and rotation and coxa profunda can be determined on

this radiography. Sacroiliac joint integrity and joint space should be examined. If narrowing is considered in joint space, special sacroiliac joint radiographs, CT and MRI, must be taken.

Acetabular depth: Ilioischial line creates the medial edge of the teardrop. If the base of the acetabulum touches or is medial to ilioischial line, it is defined as a coxa profunda. When the femoral head projects medial to the ilioischial line, acetabular protrusion is present. Conversely, the distance between ilioischial line and femoral head should normally be less than 10 mm. If the distance is more than 10 mm, the acetabular dysplasia and lateralization of femoral head are present. Also the distance between medial border of the femoral head and the deepest point of the acetabulum should be less than 2 mm. If it is more than 2 mm, centralization of the femoral head is not enough.

Acetabular inclination: It can be evaluated by Tönnis angle. A line is drawn to horizontal at the bottom of each two teardrop. Second line is drawn passing through section sclerotic sourcil of the acetabulum as parallel to this line. Finally, the acetabulum inferior and the section of the lateral sclerosis sourcil passing draw a third line. The angle between the second and third line is called Tönnis angle. Normal values are between 10 and 0°. If it is more than10°, structural instability is mentioned. If it is less than 0°, the pincer-type impingement syndrome is mentioned.

The lateral central edge angle: A vertical line is drawn from the femoral head center. Again, a second line is drawn from center of the femoral head to acetabular outer edge. The angle between two lines is called as a central edge angle and it shows superolateral coverage of the femoral head. The normal value is expected to be lower than 20–25°. Above this values shows structural instability.

Direction of the acetabulum (acetabular version): The acetabulum is normally 10° anteverted position. Anterior wall appears on the medial side and posterior wall appears on the lateral side in the pelvic AP radiography. They are not intersected with each other on normal AP radiography. If the image of the anterior wall and posterior wall makes up figure of eight with crossing each other, acetabulum is considered in the retroversion position.

Roundness of the femoral head (sphericity): It is evaluated in AP pelvis radiography, frog-leg lateral radiography, 45–90 Dunn radiography, and cross-table lateral radiography. If the circle is placed on the femoral head, more than 2 mm overflowing is called lost the roundness of the femoral head.

Joint compliance: Convexity of the femoral head and concavity of acetabulum are evaluated for joint congruence. Crescent sign indicated that head surface collapse could be revealed in the femoral head with avascular necrosis. Narrowing of the joint space, subchondral cysts, and distribution of joint surface and osteophytes can be observed in osteoarthritis of the joint.

Angle of the shaft and neck: It is the angle between the line that passes from the center of the femoral neck and line that passes the center of the femoral shaft. Normal values are between 130 and 140°.

Shenton–Menard line: Upper part of the obturator foramen and medial border of the femoral neck show continuity on the curved line. However, AP radiograph of the pelvis must be taken appropriately without tilt and rotation. The line is broken in the case of hip joint dislocation or subluxation.

Perkins quadrants: A vertical line is drawn from the outer edge of the acetabulum. A horizontal line is drawn that passes both triradiate cartilages called the Hilgenreiner line. These two lines divide acetabulum in four equal dials. Femoral head epiphysis should normally be seen in the lower inner quadrant. If the femoral head epiphysis is seen in the upper outer quadrant, dislocation of the hip is mentioned. If the femoral head epiphysis is seen in the lower outer quadrant, it is mentioned as lateralization or subluxation.

Appearance of the femoral head epiphysis: Femoral head epiphysis can appear at 4–5 months old in boys and at 5–6 months old in girls on AP radiography. Appearance of the femoral head epiphysis is delayed or may be smaller than the opposite side in developmental hip dysplasia.

Von Rosen 1: A line is drawn passing from upper edge of the symphysis pubis and parallel to Hilgenreiner line. In the early stages that the femoral head is not ossified, any structure of the femur cannot be seen between Hilgenreiner line and the parallel line. Part of the proximal femoral is below the line that passes from the symphysis pubis. If the femoral metaphysis is seen between the two lines, it is considered the dislocation of the hip.

Cross-table lateral radiography: The patient is laid supine position on table. The hip joint is rotated internal at 15° and the contralateral hip and knee joints are flexed more than 80°. X-ray beams come on the medial with 45° angle to table (Fig. 7.9).

45° and 90° Dunn view: The patient is placed in a supine position. Radiography is taken when the hip joint is brought to 45° or 90° of flexion and 20° abduction. Limbs are in neutral position (no rotation). X-rays are given perpendicular to between the SIAS and symphysis pubis (Fig. 7.10).

Lateral view in the frog-leg position: The patient is placed in a supine position. While the knees are flexed at 30–40° and abducted at 45°, radiography is taken.

Alpha angle: A line is drawn between the femoral head center and the femoral neck center on the lateral radiography. A second line is drawn between center of the femoral head and most prominent point on the head–neck junction. The angle between two lines is called alpha angle. Normally it is smaller than 50°. If it is bigger than 50°, it can be defined as a head–neck offset deformity. This condition may cause a cam type impingement.

Head–neck offset ratio: It is evaluated with lateral radiography. A line is drawn through the center of the femoral neck. Then a second line is drawn parallel to the first line and passes most prominent parts of the anterior femoral neck. Finally, a third line is drawn parallel to the first line and passes the most prominent parts of the anterior femoral head. The ratio between the distance of the second and third line and the diameter of the femoral head gives the head–neck offset ratio. If the values are less than 0.17, it is mentioned as cam type of impingement.

Von Rosen 2: The radiography at 45° hip abduction and at 20–25° internal hip rotation is taken. A line is drawn along the femoral shaft. This line passes under the outer edge of the acetabulum. In the case of hip dislocation, this line passes over the outer edge of the acetabulum.

False-profile view: The involved hip is closer the cassette and patient is 65° angled the cassette on standing position. Radiography is taken while leg is placed parallel to cassette and x-ray beams are targeted center of the femur head.

The anterior center-edge angle: It is also known as the angle of Lequesne. This angle

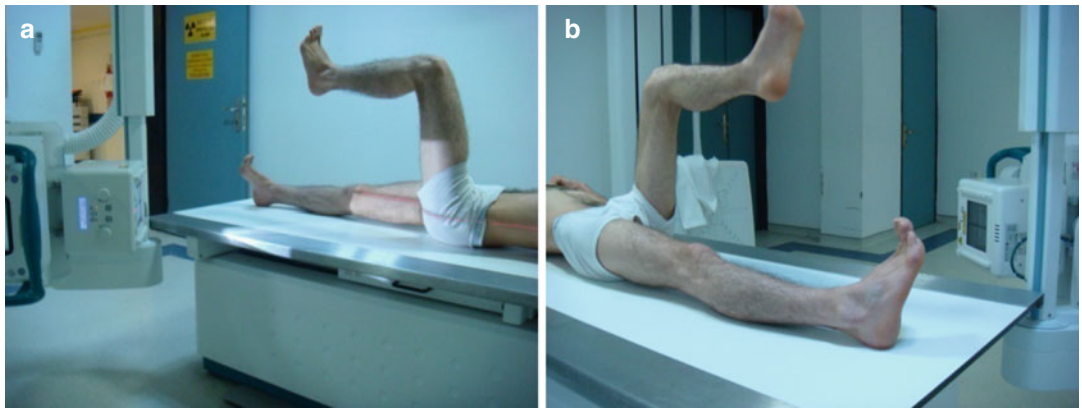

Fig. 7.9 (**a**) The position of the patient and the x-ray device during cross-table lateral radiograph (from the patient's head side). (**b**) The position of the patient and the x-ray device during the cross-table lateral radiograph (the patient's foot end)

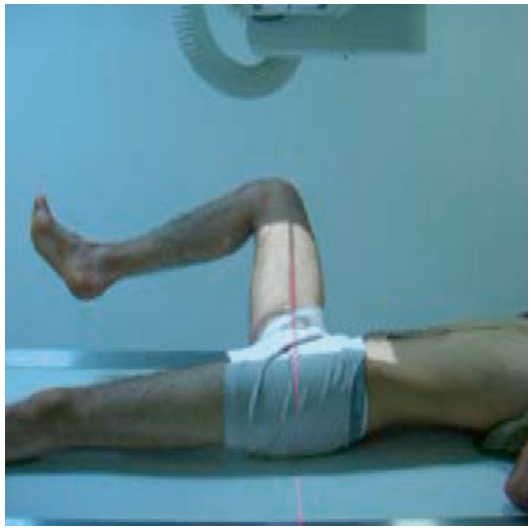

Fig. 7.10 Position of patient and x-ray device for 45 and 90° Dunn view

shows anterior coverage of the femoral head. Vertical line from the center of the femoral head is drawn on the false-profile radiography. Then a second line is drawn from the femoral head center to anterior of the acetabulum. The angle between the two lines is called the anterior center-edge angle that should be below 20°. If it is over 20° that is mentioned as anterior dysplasia. While AP pelvis and false-profile radiographs give very valuable information about the morphology of the acetabulum, Dunn and lateral radiographies provide detailed information about the pathoanatomy of the proximal femur.

Radiographic Evaluation of the Knee

A large majority of knee pathologies reveal as an acute injury or additional symptoms to some conditions. The most common cause of admission to the hospital is anterior knee pain and local or generalized edema [30].

The classical two-side radiographs provide enough information about most of the knee pathologies. Conditions diagnosed by radiography include [31]:

- Soft tissue changes: Soft tissue edema and presence of excess fluid in the knee joint can be easily noticed with plain radiographs.
- Bone quality: It gives information about bone density.
- Alignment: Radiography on standing position provides information about alignment of the lower extremity. Knee is angulated at 5–7° valgus. The surface of proximal tibia has 10° posterior slope.
- Joint space and early arthritic findings: Joint space narrowing, osteophytes, sclerosis, and subchondral cysts can reveal on knee radiographs in standing position more clearly.
- Trauma/fractures: Provide to the diagnosis of distal femur, proximal tibia, and patellar fractures.

Four-side radiographies (AP/lateral/internal oblique/external oblique) can diagnose the fracture in the rate of 85 %. Two-side radiographs (AP /lateral) can diagnose the fracture in the rate of 79 % [32]. In addition, lateral radiographs have a high sensitivity for screening in the diagnosis of fractures after acute knee injury [33].

Ottawa knee rules contain some guidelines for radiography in acute knee injury [34]. Radiographs should be taken in the following conditions:

- 55 years of age or older patients
- Paint with palpation on fibular head
- Isolated patellar tenderness
- Unable to 90° flexion of the knee
- After trauma, difficulty in loading or unable to get four steps

According to the rules of Pittsburgh in 1995, in the case of blunt trauma or fall from height:

- In the patients younger than 12 years of age or older than 50 years
- In the patients that have difficulty in standing or unable to get four steps, presence of knee effusion, or ecchymosis after trauma, fracture risk is high.

With this rules, misdiagnosis of fracture rates has been reduced by 39 % [35].

The x-ray protocols for knee pathologies are shown in Table 7.1.

Knee AP view: Fractures and bone and chondral changes, which are related with degenerative joint diseases, can be seen. Decrease in knee space, osteophytes, sclerosis, and subchondral cysts is observed in gonarthrosis. Traction radiography provides better view of the structure of the distal femoral and proximal tibia in fractures. Segond fracture is an avulsion fracture of the capsule on the tibial lateral plateau. Tibial plateau fractures can be seen in AP radiography, but the amount of depression and separation can be demonstrated more clearly by CT.

Knee lateral view: Fractures around the knee joint can appear on lateral radiography. Especially Hoffa fracture, which is the vertical fracture of the posterior femoral condyle, should not be missed. Patella fractures are seen clearly. Patellar fractures need to be making a differential diagnosis with bipartite patella. Acute knee dislocations can be determined on the knee lateral radiography, but the vast majority of this dislocation reduces automatically before getting to the hospital.

Trochlear depth can be measured with 85 % sensitivity at lateral radiographs.

Dejour et al. reported that when trochlear prominence is greater than 3 mm in trochlear dysplasia, "crosswise sign" is comprised. The most commonly used method for measuring the trochlear notch is "skyline patellar radiography." Sulcus angle can be measured by this radiograph [36].

Patella baja and patella alta, which are height pathologies of the patella, can be evaluated on lateral radiography. Methods of Insall–Salvati, Blackburne–Peel, and Caton–Deschamps can be used for these pathologies.

Evaluation of patellar height:

- *Blumensaat line:* It is seen on radiography taken at 30° of flexion. Roofline of intercondylar notch generates this line. Distal pole of the patella should be above the Blumensaat line, and the proximal pole of the patella should be at the level of the growth plate.
- *Insall–Salvati index:* It is defined as a ratio of the length of the patellar tendon to length of the patellar bone. It can be measured on radiography taken 30° of flexion. Average value is 1.020 ± 0.13. Abnormal values are exceeding 20 % (Fig. 7.11).
- *Blackburne–Peel method (modified Insall–Salvati):* It gives more accurate results compared to Insall–Salvati method. It is the ratio of the patellar tendon to the articular surface of the patella. The length of the patella can be calculated from tibial tubercle to patellar articular surface. The normal value is 1.25. As this ratio ≥2, it is called patella alta.

Knee Merchant view: It is an axial view radiograph of the patella. Patient is placed in the supine position and the knee flexed at 30° (20–45). X-ray beams tilted 30° toward to the femur. It is used to assess patellar tilt and subluxation. Patellofemoral abnormalities decrease in flexion out of this range. It shows dysplasia of the femoral condyles and the intercondylar sulcus. Normal value of sulcus angle is 137–141°.

Knee tangential (skyline, sunrise) view: It is an axial view radiograph of the patella. It provides information about the patella and the patellofemoral joint. The patient is laid on the table in the prone position and the knee joint is flexed at 115°. X-ray beams are directed to center of the patella (Fig. 7.12). It shows dislocation, half dislocations, fractures, or degenerative changes of the patellofemoral joint.

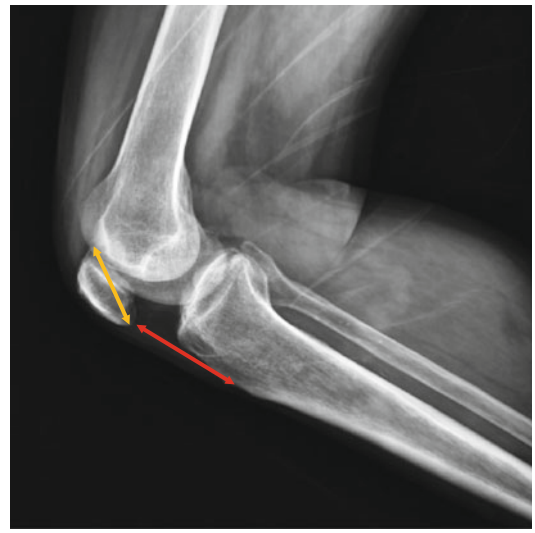

Fig. 7.11 Insall–Salvati index: It is calculated by the ratio of the *yellow line* to *red line*

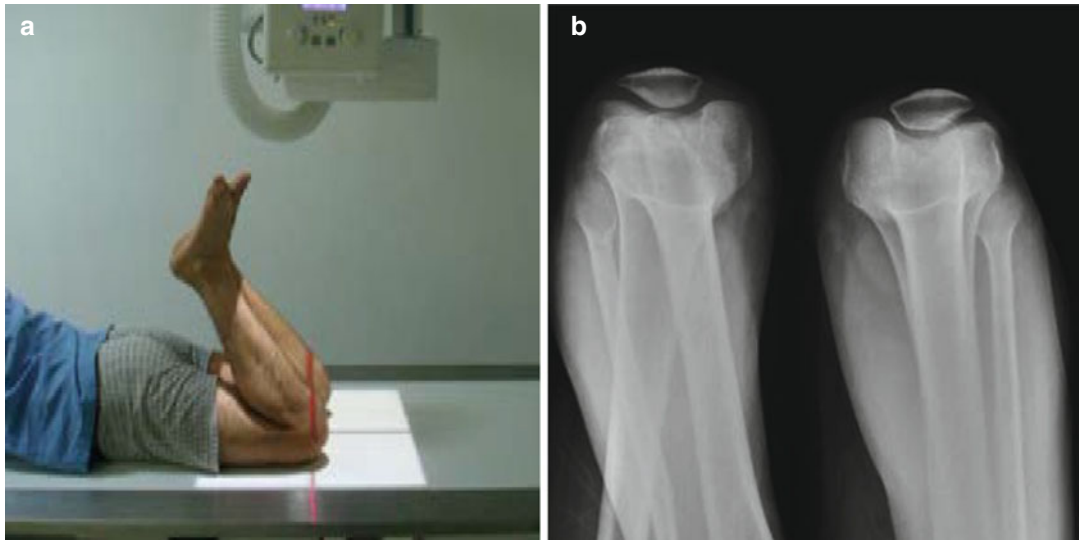

Fig. 7.12 Position of the patient and x-ray during the knee tangential graph

Knee intercondylar notch (tunnel) view: It displays intercondylar notch, femoral condyles, tibial plateau, and tibial eminencies. It provides information about bone or cartilage pathology, osteochondral defects, and joint space narrowing. The patient is placed in a prone position and knee flexed at 40°. X-ray beams are directed to center of the knee joint and tilted 40° vertically.

Standing AP (stress) view: It displays the status of the knee joint during standing or walking. This radiograph reveals the joint space narrowing clearly. The presence of varus or valgus deformities is determined in the knee with osteoarthritis. Mechanical axis passes through 1–2 mm medial from the center of the knee of a healthy person in standing position radiography. The knee joint has 5–7 ° of valgus angulation.

Standing PA view (Rosenberg): It is taken in standing position with 15° of flexion. It gives more clear view than standard radiographs about joint space [37] (Fig. 7.13).

Radiographic Evaluation of the Ankle

Small surface area of the ankle joint has a load of 1.5 times of body weight. Congruence of the ankle mortise is most important factor to continue long-term function [38]. Imaging is very important in the analysis of ankle problems. Plain radiographs are sufficient in many ankle pathologies. In cases of no definitive diagnosis, CT or MRI can be taken [39]. Less than 15 % of patients admitted to the emergency department with ankle trauma have remarkable fractures.

X-ray of the ankle is the third most requested radiological imaging in the emergency department. Ankle and lateral radiography provide 95 % reliability to detect fracture around the ankle [40]. Ottawa ankle rules are used to take unnecessary radiography in patients with ankle injury (Table 7.3). With this Ottawa rules, the number of the radiography has been decreased by 28 % [41].

Standard images used in the assessment of the ankle are AP, mortise, oblique, and lateral radiographs [42]. Proximal tibia and fibula should appear on ankle radiograph in patients with suspected ankle fractures.

This is the best ankle oblique image obtained with 30–35° internal rotation (internal oblique view). This image provides best view of tibiofibular syndesmosis and ankle joint. External oblique image may need for evaluation of anterior tibial tubercle and lateral malleolus.

Mortise radiography is a view similar to AP radiography; however, the ankle is rotated 15°

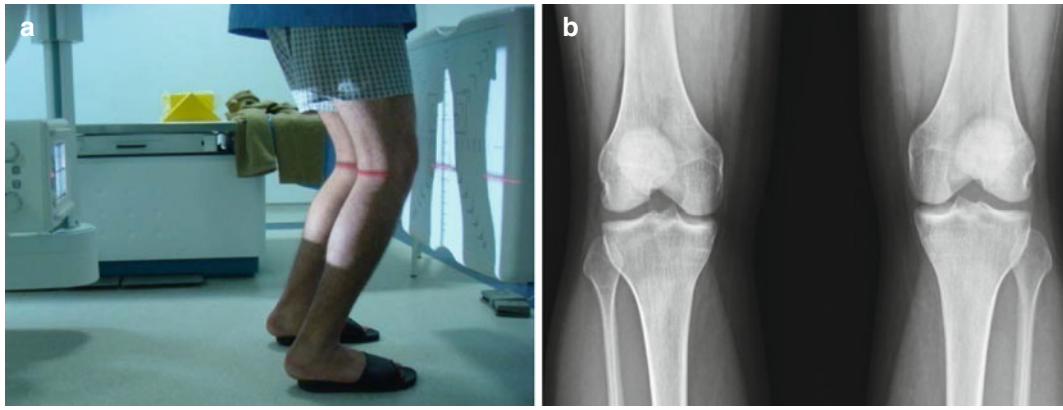

Fig. 7.13 (**a**) Position of the patient with 15° knee flexion in standing and the x-ray device. (**b**) Imaging of Rosenberg radiograph

Table 7.3 Ottawa ankle rules

Ankle view must be taken in the following conditions:
Tenderness in 6 cm of the distal tibia or medial condyle
Tenderness in 6 cm of the distal fibula or lateral condyle
Unable to 4 steps with weight bearing after injury immediately
Foot radiography must be taken in the following conditions:
Tenderness on the base of five metatarsals
Tenderness on the midfoot and navicular bone
Unable to 4 steps with weight bearing after injury immediately

internally. The ankle mortise can be displayed better with this radiography.

Ankle neutral AP and mortise view: These radiographs are most common images in traumatic or nontraumatic ankle problems. Ankle neutral AP radiography is taken with 0° dorsiflexion and neutral rotation. However, ankle mortise radiograph is taken with 0° dorsiflexion and 15–20° internal rotation.

Tibiofibular line: Articular surface of the distal tibia and articular surface of medial fibula show continuity on the same line. Broken part of this line shows shortness and rotation of the fibula or lateral shift [43].

Talocrural angle: It is the angle between the line that parallels the distal tibia articular surface and intermalleolar line. The normal values are between 8 and 15°.

Talar tilt: First line passing through the distal articular surface of the tibia and second line passing through the articular surface of the talus should be parallel to each point. Angles between intermalleolar line and first line and second line are measured separately. Talar tilt is defined as a difference between the measured angles and should be normally 0° (0° ± 1.5 is considered to be normal).

Tibiofibular clear space: It is the distance between medial edge of the fibula and posterolateral edge of the tibia (Fig. 7.14 orange arrow). This measurement is performed 1 cm above the distal tibial joint surface. It should be <6 mm in both AP and mortise radiographs [43]. Increased tibiofibular clear space is the most reliable indicator for syndesmotic injury. A study reported that the tibiofibular clear space was not changed during the mortise radiograph positioning in the spectrum from 5° external rotation to 25° internal rotation [44]. Tibiofibular clear space depends on the tilt of x-ray beams rather than the position ankle.

Tibiofibular overlapping: It is measured by overlapped area on anterior tibial tubercle and lateral malleolus in 1 cm above distal tibia joint surface (Fig. 7.14 green arrow). Overlapping should be >6 mm or more than 42 % of fibula width on the AP radiograph. It must be >1 mm in mortise radiography.

Medial clear space: It is the space between the lateral edge of the medial malleolus and the

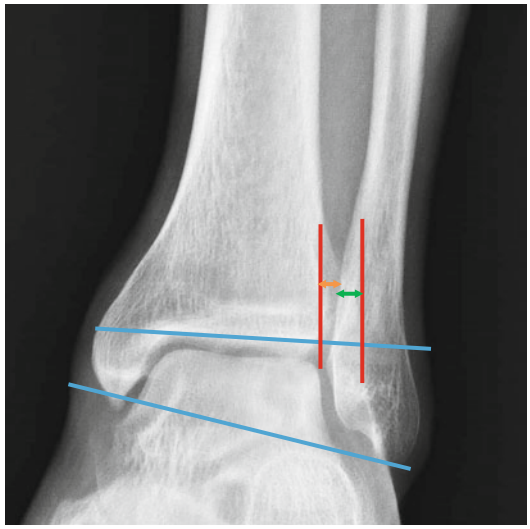

Fig. 7.14 AP view of the ankle

medial edge of the talus. It is measured at the level of the talar dome. Medial clear space must be less or equal than superior clear space measured between talar dome and tibial joint surface in the neutral AP radiograph. If medial clear space increases, injury of deltoid ligament should be considered. Standard radiographs may not be sufficient in the case of ligament injuries and instability. AP, lateral, and mortise radiographs are taken during stress. Stress can be applied manually or with special device (Telos device).

Ankle lateral view: Fractures of the distal tibia, distal fibula, talus, and calcaneus and tibiotalar, talonavicular, and subtalar joint surface can be evaluated. Fractures of cuboid and proximal fifth metatarsal can be detected.

Böhler angle: This angle is between two lines tangent to the calcaneus on the lateral ankle view. These lines are drawn tangent to anterior and posterior processes of the superior calcaneus. The normal values are from 20 to 40°. If the angle decreases, it indicates the collapse of the posterior joint surface.

Gissane angle: This angle is between anterior and posterior joint surfaces of the calcaneus. The normal values are between 130 and 145°. If the angle increases, it indicates the collapse on the posterior side of the joint.

Calcaneal height angle: This angle is between two lines tangent to inferior of the calcaneus. First line is drawn from lowest point of the calcaneus and parallel to the ground on weight-bearing lateral ankle radiography. Second line is drawn between lowest and highest points of the inferior calcaneus on same radiography. The normal values are between 20 and 30°.

Talocalcaneal angle: It is used for diagnosis and follow-up of the pes equinovarus and vertical talus. It is the angle between long axis of the talus and calcaneus. It is between 20 and 40° normally.

Canale view: It gives the best image for the talus dome. While the ankle should be at maximum equine and 15 % pronation, the x-ray beams are tilted 75° with ground to take a good radiography. Hawkins mark is a radiolucent band, which appears 6–8 weeks after fracture of the talus neck. It gives us information about revascularization.

External rotation stress view: It is used for evaluating the deep deltoid ligament and syndesmosis. Medial and lateral space of the joint should be less than 2 mm on AP radiography.

Talar tilt stress view: Talar tilt during varus force to the ankle gives us information about lateral ligament stability. If talar tilt in varus stress is two times bigger than talar tilt in normal ankle or more than 5° of talar tilt, it indicates the tearing of the anterior talofibular and calcaneofibular ligaments.

Inversion stress view: Laterally, collateral ligaments are evaluated. Anterior talofibular ligament can be evaluated on AP radiograph with inversion stress and plantar flexion of the ankle. Both anterior talofibular and calcaneofibular ligaments can be evaluated AP with inversion stress and neutral dorsiflexion of the ankle. Talus is replaced to superior less than 5 mm on inversion stress test normally.

Anterior drawer stress view: X-ray is taken while the tibia is stabilized; ankle is held from calcaneus and pulls forward. If talus is replaced more than 5 mm, injury of anterior talofibular ligament is considered.

Harris view: It shows fractures extending to the subtalar joint in calcaneus, expansion of the

joint surface, and height loss and impingement in peroneal space. Radiography is taken with x-ray tilted 45° axially while ankle in maximal dorsiflexion. It is enough for diagnosis of calcaneal fractures, but it does not give enough information about the fracture geometry.

Broden view: It gives us tangential view of posterior joint surface of the calcaneus. The ankle is rotated 40° internally and dorsiflexed neutral. X-ray beams are directed at the lateral malleolus with tilted 10°-20°-30°-40°angles, respectively [45].

Foot AP, lateral, and oblique views: Tarsal bones, metatarsals, and pathologies of phalanges are detected in the foot radiographs. Fifth metatarsal fracture on diafizo-metafisiyel junction is called Jones fracture. Oblique radiographs may be more useful for metatarsals and phalanges due to overlapping on the lateral graph. There might be a stress fracture on the metatarsals. In addition, findings about Freiberg disease, which is osteochondrosis of the second metatarsal basis, can be observed. Degenerative changes of the first metatarsophalangeal joint should bring to mind diagnosis of hallux rigidus.

Talocalcaneal angle: It is the angle between long axis of the talus and calcaneus on the foot AP radiograph. The normal values are between 30 and 50°. This angle increases in the pes equinovarus deformity.

Lisfranc joint injury: Proximal of the second metatarsal may have shifted to the dorsal on lateral radiography without weight bearing. Malalignment can be seen on the second metatarsal and medial of middle cuneiform in the AP radiography. In addition, distance is increased between first and second metatarsals. Bone fragments at base of the second metatarsal indicate an avulsion of Lisfranc ligament (fleck sign).

Hallux valgus angle: It is an angle between long axis of the first metatarsal and long axis of first proximal phalanges. Normally, it should be under the 15°. This angle increases in hallux valgus.

Intermetatarsal angle: It is an angle between first and second metatarsals. It should be under 9° normally. This angle increases in hallux valgus.

Radiological Assessment of the Spine

Even though various new techniques such as CT and MRI are available for evaluation of the spinal disorders currently, X-ray is the most common and rapid assessment method.

Plain radiographies are the first step of the patient assessment and should be at least two different planes. Various pathologies such as trauma and deformity might affect different spinal regions so radiographs should include the entire spinal column.

Patients affected and symptomatic regions should be evaluated thoroughly. If necessary, oblique and special radiographs should also be obtained.

Imaging of Scoliosis

Ideal imaging modality to assess scoliosis is standing posteroanterior view, which shows the entire spinal column. The patient's head and pelvis should be included at the radiograph. Patients, which can't stand up, such as in severe neuromuscular disorders, could be evaluated with sitting or supine radiographies.

Radiation-sensitive organs such as the breast, thyroid, ovaries, and testes should be protected during radiological studies. Protective aprons could reduce the radiation dose; however, it should be kept in mind that automated dosing systems might use higher radiation beams due to protective apron. Quantity of the radiographs increases the risk for radiation exposure. Studies show that routine radiological examinations could increase the risk of breast cancer up to 70 % compared to general population. X-ray beams directed in posteroanterior plane result in three to seven times less radiation exposure compared to anteroposterior plane [46].

Correct measurement of scoliotic curvature is important not only for making surgical decision but also determining treatment algorithms. Lippman–Cobb method is the common one to measure the severity of scoliosis. End vertebra is defined as the vertebra that is most tilted from the

horizontal apical vertebra. An apical vertebra is the most rotated and the most lateral one from the midsacral line. End plate of the apical vertebra is the most parallel one to the horizontal plane. The angle, which is measured with Lippman–Cobb method, is between tangent line to the end plate of the upper vertebrae and tangent line to the lower vertebrae (Fig. 7.15).

Greenspan et al. described the scoliotic index in 1978. This method is more precise and detailed. A line termed "spinal line" is drawn from just above the upper end vertebra's center to the lower end vertebra's center. Then each vertebra's deviation from spinal line is measured, which contributes to the curvature [47].

There are further factors for the evaluation of scoliotic curvature. Rotation can be evaluated with two different techniques. Position of the spinous process is reference point according to the Cobb technique. If there is no rotation, spinous process is seen at the center of the vertebral body. If rotation increases, location of the spinous process changes. Moe method accepts anteroposterior projection and the symmetry of the pedicles.

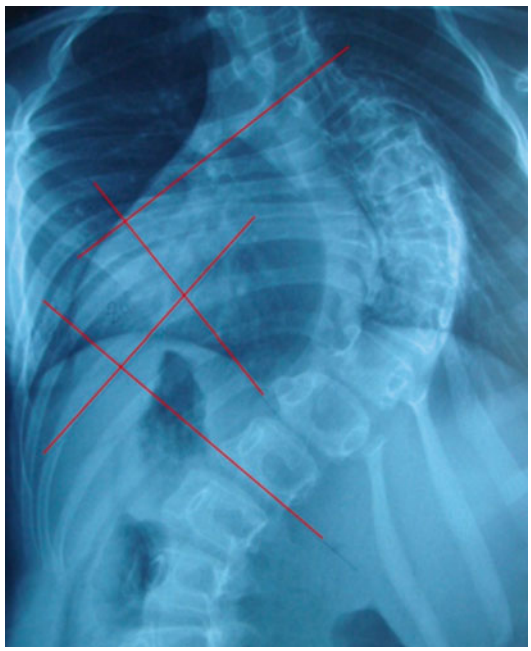

Fig. 7.15 Measurement of Cobb angle on PA spine view

It determines the rotation of the vertebra and the migration of the pedicles to the convexity of the curvature.

There is no rotation in the normal spine and pedicle is equidistant to both spinous processes. At scoliosis, pedicle shadow is skewed as the rotation increases. Both sides of the vertebral body and the lateral edge of the spinal projections are marked with an imaginary line from the midpoint. More lateral than normal vertebral pedicle remains in the line. The pedicle is in the lateral edge on the concave side of the stage 1 rotation. Pedicle shadow is at the level of the outer line on the convex side. Pedicle shadow is between the outer lines to the spinous process on the convex side of the stage 2 rotation. Pedicle is seen in the midline on the convex side of the stage 3 rotation. Pedicle shadow is seen on the opposite side on the convex side of the stage 4 rotation (Fig. 7.16).

Skeletal maturity could be evaluated with x-ray at scoliosis. This is important for both prognosis and treatment especially in adolescent idiopathic scoliosis. At the lack of complete skeletal maturity, scoliosis progression is expected. Ossification of the iliac apophysis is evaluated for skeletal maturity. If iliac apophysis is not ossified, it is defined as stage 0 by Risser (stage 1, 0–25 %; stage 2, 25–50 %; stage 3, 50–75 %; stage 4, 75–100 %). At stage 5, iliac apophysis is completely ossified.

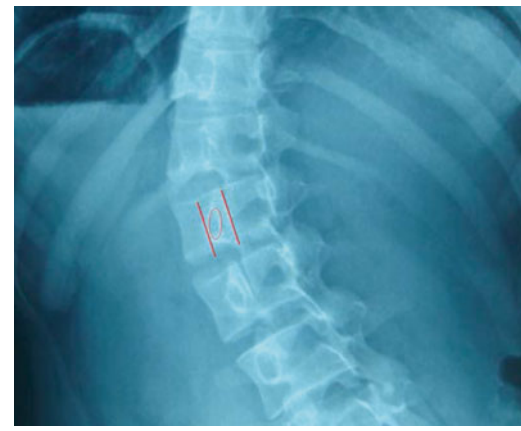

Fig. 7.16 Stage II rotation is seen which is determined by Moe method

Patient's skeletal maturity is also determined by the determination of skeletal age. Radiographs of the patient's hand are the same age as compared with standard hand radiographs.

Lateral bending radiographs are also used for the evaluation of scoliosis curvature. These radiographs assess the reducibility of the curves and determine curves as structural or nonstructural. According to Lenke classification, curves showing more than 25° of correction at bending radiographies are named as "major or structural curves," and curves which have less than 25° of correction are named as minor or compensatory curves. Fulcrum x-rays are similar to bending radiographs and they evaluate the flexibility of the curves. At fulcrum radiographies, fulcrum is positioned at the apex of the curve. All these radiographs help to determine the fusion levels before the surgery.

T1 tilt angle, clavicle angle, and pelvic tilt angle could also be measured at standing PA spine view. These measurements provide information about the patient's overall body balance. These angles are measured according to the line, which is parallel to the ground. The T1 tilt angle is between vertebral end plate of T1 and line that is parallel to the ground.

Clavicle angle is between line that is connecting the highest point of both the clavicle and reference horizontal line. Pelvic tilt angle is between the line connecting the highest point of both iliac wings and reference horizontal line.

Lateral radiographs are used for the assessment of sagittal balance in scoliotic patients. At normal sagittal balance, vertical line drawn from the midpoint of T7 perpendicular to the ground passes through promontorium. If this line passes through anterior of the promontorium, it is called positive sagittal balance. If this line passes through posterior of the promontorium, it is called negative sagittal balance. Maintaining the sagittal balance after surgery is as important as the correction of the scoliosis curvature.

Normal spine anatomy has physiological lordosis of the cervical spine, 21–33° physiological kyphosis of thoracic, and 31–50° physiological lordosis at the lumbar region. As it is mentioned in Lenke classification, an angle of kyphosis and lordosis where structural curve exists reduces. This is particularly evident at the apex of the curvature. In sagittal plane, desired fusion should simulate physiological curvatures.

Radiological evaluation of kyphosis and lordosis patients is done at similar manner as scoliosis. The upper and lower end vertebrae of kyphosis are determined at standing lateral radiographs. These vertebrae are the most upright position to the ground plane. Angle of kyphosis and lordosis can be measured how upper end plate of the upper end vertebra and lower end plate of lower end vertebra are referenced by the Cobb method similar measure of scoliosis. The main objective is similar to the physiological curvature of the sagittal balance with conservative treatment or surgical treatment.

Imaging at Spinal Trauma

Protective precautions of the spine should be continued until spinal injury excluded by physical examination and imaging. The first radiological evaluation should be done after any life-threatening pathology becomes stable. Anteroposterior and lateral radiographs of the entire spine should be evaluated at first. It should be kept in mind that simultaneous injury may occur at more than one region of the spinal column. Sloppy positioning during the radiological examination may worsen patient's current injury [48].

Posterior elements, facet joints, laminae, and vertebral body should be evaluated at anteroposterior radiographs. Vertebral alignment should be checked with anteroposterior radiographs. Asymmetry of the pedicles at any level, abnormality of interpedicular distances compared to adjacent levels, disorders of vertebral body borders, vertebral body height loss, local scoliosis, transverse process fractures, spinous process alignment abnormalities, and abnormal alignment of the facet joints are considered as signs of vertebral fractures.

Distance between the spinous processes, integrity of the vertebral bodies, vertebral body displacement, and vertebral fracture type should

be determined on lateral radiographs. Vertebral body in funneling, irregularity in the lower end plate or the upper end plate, drive off in the distance, height loss of the vertebral body, facet joint absence, irregularity of interspinous distance, pedicle disruption, and sagittal balance corruption are the radiological findings of vertebral fracture. Vertebral body-line which connects the posterior vertebral bodies' irregularity indicates that the compression fracture fragments into the canal.

Soft tissue injury findings of spinal injury can also be identified with plain radiographs. Loss of the psoas line at the lumbar region, thickening of paraspinal shadow at the thoracic regions, and pneumothorax or hemothorax are the signs of spinal injury. Sternal or costal fractures, deviation of the trachea, vacuum phenomenon, and pleural effusion are additional findings of spinal injuries. Sternal fractures, rib fractures, and costovertebral dislocations are signs of instability as well as thoracic vertebral injury. Anterior compression ratio, local kyphosis angle, and sagittal index are assessment methods of lateral radiography in traumatic spine injuries [49]. Anterior compression ratio is the height of vertebral corpus anterior edge to the height of vertebral posterior edge. More than 50 % of the collapse at compression fracture is instability finding. Local kyphosis angle of fractured vertebra is between the upper end plate of the intact vertebra with a lower level in the lower end plate of the intact vertebra. This angle is measured by Cobb method. Local kyphosis angle more than 20° indicates instability. Sagittal index was described by Farey, and it refers to the angle between the upper end plate and the lower end plate of fractured vertebra. Normal sagittal index of L1 vertebra is 0.

At the thoracic vertebrae, anterior side is shorter than posterior and sagittal index calculated, as minus 5°; in lumbar vertebrae, anterior side is longer than the posterior so it is calculated as plus 10°. In lumbar region, 10° is added to calculation and, in thoracic region 5° decreased from calculation. If the sagittal index is above 15°, it is foreseen that posttraumatic kyphosis will proceed. These patients are considered as a candidate for surgery.

One of the most common mistakes made in spinal trauma patients is not evaluating cervicothoracic junction thoroughly. Cervicothoracic junction, especially T1-4 vertebrae, could not be assessed thoroughly at anteroposterior and lateral radiographs because of the superposition of other bones. These patients should be assessed by swimmer's position x-ray. The patient's position is one arm lifted on the head and the other arm of the patient below. The beam is applied to the axillary region. Although cervicothoracic region could be seen with this method, it is not usually preferred due to high-dose application and difficult positioning, and also it cannot be implemented in obese patients or patients with shoulder injuries.

As a result, radiological findings of instability at spine trauma are more than 2 cm of translation showing disruption of main ligaments, expansion of interspinous distance, expansion of facet joints and interpedicular distance, disruption of the posterior vertebral body-line, more than 50 % loss of vertebral body height, and kyphosis more than 20°.

Imaging of Degenerative Spine

Degenerative changes are not visible in plain radiographs unless calcification or ossification occurs within disk. Therefore, early degenerative changes cannot be determined directly in plain radiography, and at degenerative diseases, radiographs provide limited information. Signs of degenerative disk disease, which could be detected at x-ray, are intervertebral space narrowing, irregularity of the end plates with reactive osteosclerosis, osteophytes, calcifications, and intradiskal gas, which is called vacuum phenomenon [50].

X-ray imaging is the first choice of imaging in spinal stenosis. Anteroposterior and lateral radiographs can provide information about possible degenerative pathologies. Additionally, the presence of instability can be identified with flexion and extension radiographies; shift can be detected with dynamic anteroposterior radiographs.

Also, the diameter of the vertebral canal in the cervical spinal stenosis could be measured at

lateral radiographs. Sagittal diameter of the channel is measured as the distance between the midpoint of the wall posterior corpus and spinolaminar line. Torg rate is used for this calculation.

Torg ratio is the ratio of the sagittal diameter of the spinal canal to the height of the vertebral body at the level. Normally, Torg ratio is greater than 1 and less than 0.8 suggests stenosis [51].

Imaging of Spondylolysis and Spondylolisthesis

Lateral radiographs and oblique radiographs are the first choice for spondylolysis and spondylolisthesis. Spondylolysis is a defect at the pars interarticularis without vertebral slipping. Pars interarticularis is defined as the upper and lower articular crotch of the neural arch. Oblique radiographs should be taken to detect spondylolysis because it does not slip [52].

Scottish dog view could be seen at normal lumbar oblique radiographs. The dog's nose is the transverse process, the eyes are the pedicles, the ears are upper articular processes, front feet are lower articular processes, the tail is spinous process, and the neck is pars interarticularis. If the dog has a collar around its neck in the image, it is considered as spondylolysis. If pars interarticularis has defects, the upper vertebra shifts ventrally. The amount of slip should be measured by standing lateral radiographs. The bottom of the upper end plate of the vertebra is taken as reference. The amount of shift is ratio between lengths of the upper vertebra slipping and the end plate of lower vertebra. This ratio is expressed as %. Meyerding staging is carried out according to this measuring process: 25 % grade 1, 26–50 % grade 2, 51–75 % grade 3, 76–100 % grade 4, and spondyloptosis grade 5. There is no shift in normal individuals [53].

Slip angle is another evaluation method at direct radiographies in spondylolisthesis. Slip angle is the angle of the upper end plate of two adjacent vertebrae. It gives information about local kyphosis.

In many cases, the upper end plate of S1 has undergone a number of changes and it is difficult to identify them. Slip angle in between line is the tangent to S1 and S2 body and the upper end plate of L5. Normally, this angle is between −20 and −30°, but the angle increases in the advanced degree shift and is particularly severe dysplastic type.

Inclination of sacral is angle that is between sacrum and perpendicular line. It gives information about the flattening of the sacrum. It is normally between 40 and 60°. The sacrum shows a more upright position at the advanced shifts.

Sagittal Pelvic Tilt Index (SPTI) is a new concept and the prognosis is better evaluated with this. In addition to the relationship between L5 and sacrum, it reveals also the relationship between them and the femoral head. Therefore, L5 vertebral body slipping forwards on the sacrum, the lumbosacral junction kyphosis increases, the sacrum is flattened, and pelvic tilt increases. The center of the femoral head body L5 is greater than the center of the back. This gives valuable information in terms of prognosis. Prognosis is good in cases, which SPTI is more than 0.85 and nonsurgical treatment may use. The cases, which have less than 0.70 of SPTI, have a higher risk of slipping. Surgical treatment is indicated for these conditions.

References

1. Rockwood Jr CA, Matsen F (1998) The shoulder. In: Fractures of the proximal humerus. 2nd edn. WB Saunders, Philadelphia, p 342
2. Merrill V (1986) Shoulder girdle. In: Ballinger PW (ed) Merrill's atlas of radiographic positions and radiographic procedures, vol 1, 6th edn. Mosby, St. Louis, pp 101–150
3. Manaster B et al (2006) Diagnostic and surgical imaging anatomy: musculoskeletal, 1st edn. Amirsys® (Diagnostic and Surgical Imaging Anatomy), Salt Lake, p 11
4. Pavlov H et al (1985) The roentgenographic evaluation of anterior shoulder instability. Clin Orthop Relat Res 194:153–158
5. Rokous JR, Feagin JA, Abbott HG (1972) Modified axillary roentgenogram. A useful adjunct in the diagnosis of recurrent instability of the shoulder. Clin Orthop 82:84–86
6. Silfverskiold JP, Straehley DJ, Jones WW (1990) Roentgenographic evaluation of suspected shoulder dislocation: a prospective study comparing the axil-

lary view and the scapular 'Y' view. Orthopedics 13(1):63–69
7. Hawkins RJ et al (1987) Locked posterior dislocation of the shoulder. J Bone Joint Surg Am Vol 69(1):9–18
8. Galano GJ, Ahmad CS, Levine WN (2010) Current treatment strategies for bicolumnar distal humerus fractures. J Am Acad Orthop Surg 18(1):20–30
9. Rosas HG, Lee KS (2010) Imaging acute trauma of the elbow. Semin Musculoskelet Radiol 14(4): 394–411. doi:10.1055/s-0030-1263255
10. Frick MA (2006) Imaging of the elbow: a review of imaging findings in acute and chronic traumatic disorders of the elbow. J Hand Ther Off J Am Soc Hand Ther 19(2):98–112. doi:10.1197/j.jht.2006.02.007
11. Tukenmez M, Demirel H, Percin S, Tezeren G (2004) Measurement of the carrying angle of the elbow in 2,000 children at ages six and fourteen years. Acta Orthop Traumatol Turc 38(4):274–276
12. Bowyer BL, Gooch JL, Geiringer SR (1993) Sports medicine. 2. Upper extremity injuries. Arch Phys Med Rehabil 74(5-S):S433–S437
13. Paraskevas G, Papadopoulos A, Papaziogas B, Spanidou S, Argiriadou H, Gigis J (2004) Study of the carrying angle of the human elbow joint in full extension: a morphometric analysis. Surg Radiol Anat SRA 26(1):19–23
14. Ruparelia DSP, Zalawadia A, Shah S, Patel SV (2010) Study of carrying angle and its correlation with various parameters. NJIRM 1(3):28–32
15. Pace JL, Wiater B, Schmale G, Jinguji T, Bompadre V, Krengel W 3rd (2012) Baumann angle and radial-ulnar overlap: a radiographic study to control for the angle of the x-ray beam. J Pediatr Orthop 32(5):467–472
16. Acton JD, McNally MA (2001) Baumann's confusing legacy. Injury 32(1):41–43
17. Skibo L, Reed MH A criterion for a true lateral radiograph of the elbow in children. Can Assoc Radiol J. 1994;45(4):287–291.
18. Ramponi DR, Kaufmann JA (2012) Elbow injuries and fractures. Adv Emerg Nurs J 34(2):99–109; quiz 10-1
19. de Beaux AC, Beattie T, Gilbert F (1992) Elbow fat pad sign: implications for clinical management. J R Coll Surg Edinb 37(3):205–206
20. Skaggs DL, Mirzayan R (1999) The posterior fat pad sign in association with occult fracture of the elbow in children. J Bone Joint Surg Am 81(10):1429–1433
21. Greenspan A, Norman A, Rosen H (1984) Radial head-capitellum view in elbow trauma: clinical application and radiographic-anatomic correlation. AJR Am J Roentgenol 143(2):355–359
22. Kobayashi K, Burton KJ, Rodner C, Smith B, Caputo AE (2004) Lateral compression injuries in the pediatric elbow: Panner's disease and osteochondritis dissecans of the capitellum. J Am Acad Orthop Surg 12(4):246–254
23. Gilula LA, Week PM (1978) Post-traumatic ligamentous instabilities of the wrist. Radiology 129(3):641–651
24. Gilula LA (1979) Carpal injuries: analytic approach and case exercises. AJR Am J Roentgenol 133:503–517
25. Schmitt R, Froehner S, Coblenz G, Christopoulos G (2006) Carpal instability. Eur Radiol 16(10): 2161–2178
26. Blackmore CC, Jurkovich GJ, Linnau KF et al (2003) Assessment of volume of hemorrhage and outcome from pelvic fracture. Arch Surg 138:504–509
27. Eastridge BJ, Starr AJ, Minei JP, O'Keefe GE (2002) The importance of fracture pattern in guiding therapeutic decision-making in patients with hemorrhagic shock and pelvic ring disruptions. J Trauma 53:446–451
28. Stambaugh LE 3rd, Blackmore CC (2003) Pelvic ring disruptions in emergency radiology. Eur J Radiol 48(1):71–87, Review
29. Clohisy JC, Carlisle JC, Beaulé PE, Kim YJ, Trousdale RT, Sierra RJ, Leunig M, Schoenecker PL, Millis MB (2008) A systematic approach to the plain radiographic evaluation of the young adult hip. J Bone Joint Surg Am 90(Suppl 4):47–66. doi:10.2106/JBJS.H.00756
30. Ostlere S (2003) Imaging the knee. Br Inst Radiol 15:217–241
31. O'Shea KJ, Murphy KP, Heekin RD, Herzwurm PJ (1996) The diagnostic accuracy of history, physical examination, and radiographs in the evaluation of traumatic knee disorders. Am J Sports Med 24(2):164–167
32. Gray SD, Kaplan PA, Dussault RG et al (1997) Acute knee trauma: how many plain film views are necessary for the initial examination? Skeletal Radiol 26(5):298–302
33. Verma A, Su A, Golin AM, O'Marrah B, Amorosa JK (2001) A screening method for knee trauma. Acad Radiol 8(5):392–397
34. Stiell IG, Wells GA, Hoag RH et al (1997) Implementation of the Ottawa knee rule for the use of radiography in acute knee injuries. JAMA 278(23):2075–2079
35. Bauer SJ, Hollander JE, Fuchs SH, Thode HC Jr (1995) A clinical decision rule in the evaluation of acute knee injuries. J Emerg Med 13(5):611–615
36. Rhee SJ, Pavlou G, Oakley J, Barlow D, Haddad F (2012) Modern management of patellar instability. Int Orthop 36(12):2447–2456. doi:10.1007/s00264-012-1669-4
37. Haklar U (2005) Diz Ekleminde Sinovektomi. TOTBID (Türk Ortopedi ve Travmatoloji Birliği Derneği) Dergisi. 4:(3–4)
38. Clare MP (2008) A rational approach to ankle fractures. Foot Ankle Clin 13(4):593–610
39. Ostlere S (2003) Imaging the ankle and foot. Br Instit Radiol 15:242–269
40. Brage ME, Rockett M, Vraney R, Anderson R, Toledano A (1998) Ankle fracture classification: a comparison of reliability of three X-ray views versus two. Foot Ankle Int Am Orthop Foot Ankle Soc Swiss Foot Ankle Soc 19(8):555–562
41. Stiell I (1996) Ottawa ankle rules. Can Fam Physician 42:478

42. Carr JB, Browner BD, Jupiter JB, Levin MA, Trafton GP (2003) Malleolar fractures and soft tissue injuries of the ankle. Skeletal trauma, vol. 2. 3rd edn. W.B Saunders, Philadelphia, pp 2307–2374
43. Harper MC, Keller TS (1989) A radiographic evaluation of the tibiofibular syndesmosis. Foot Ankle 10(3):156–160
44. Pneumaticos SG, Noble PC, Chatziioannou SN, Trevino SG (2002) The effects of rotation on radiographic evaluation of the tibiofibular syndesmosis. Foot Ankle Int Am Orthop Foot Ankle Soc Swiss Foot Ankle Soc 23(2):107–111
45. Z. Uğur Işıklar (2006) Kalkaneus Kırıkları. TOTBID (Türk Ortopedi ve Travmatoloji Birliği Derneği) Dergisi. Cilt: 5(1–2)
46. Morin Doody M, Lonstein JE, Stovall M et al (2000) Breast cancer mortality after diagnostic radiography: findings from the U.S. Scoliosis Cohort Study. Spine 2000(16):2052–2063
47. Greenspan A (2004) Ch 33. Scoliosis and anomalies with general affect on the skeleton. In: Greenspan A (ed) Orthopedic imaging, 4th edn. Lippincott Williams & Wilkins, Philadelphia, pp 927–939
48. Daffner RH (2000) Cervical radiography for trauma patients: a time effective technique? AJR Am J Roentgenol 75:1309–1311
49. Jiang SD, Wu QZ, Lan SH, Dai LY (2012) Reliability of the measurement of thoracolumbar burst fracture kyphosis with Cobb angle, Gardner angle and sagittal index. Arch Orthop Trauma Surg 132(2):221–225
50. Herzog RJ (1996) The radiologic assessment for a lumbar disc herniation. Spine 21:19S–38S
51. Sesiadek MJ, Bladowska J (2012) Imaging of degenerative spine disease the state of art. Adv Clin Exp Med 21(2):133–142
52. Marchetti PG, Bartolozzi P (1997) Spondylolisthesis classification of spondylolisthesis as a guide for treatment. In: Bridwell K, DeWold RL (eds) The textbook of spinal surgery, 2nd edn. Lipincott-Raven, Philadelphia, pp 1211–1254
53. Li Y, Hresko MT (2012) Radiographic analysis of spondylolisthesis and sagittal spinopelvic deformity. J Am Acad Orthop Surg 20(4):194–205

8 Ultrasonography in Musculoskeletal and Soft Tissue Lesions

Samet Verim

Abstract

In recent years, musculoskeletal ultrasound has been used with increasing frequency particularly in emergency services. In musculoskeletal and soft tissue lesions, plain radiographs are the first-line diagnostic tools. However, in line with technological development, especially in selected cases, ultrasound can be applied in a safe manner in clinical practice. The advantages of ultrasonography are being inexpensive and portable, obtaining images in many planes without radiation. In combination with color Doppler, it may be helpful in management of therapy. By ultrasonography, muscles, joints, tendons, ligaments, nerves, and bone pathologies can be evaluated in detail. Ultrasonography is user dependent and it is the most important limitation of the technique.

Learning Objectives

- To understand the applicability, contribution to the diagnosis, and efficiency of the ultrasonography compared to other imaging methods
- To understand the efficiency of ultrasonography in the light of the latest technological developments
- To understand the easy use of ultrasonography in practice and that it does not have harmful effects
- To understand that ultrasonography is the first-line diagnostic tool in selected cases after direct radiography.
- To understand that ultrasonography is a complementary method in the accuracy of the diagnosis in combination with computed tomography and magnetic resonance

S. Verim, MD
Department of Radiology, Mevki Military Hospital,
Yıldırım Beyazıt Mah, Dışkapı, Ankara, Turkey
e-mail: drsametverim@yahoo.com

F. Korkusuz (ed.), *Musculoskeletal Research and Basic Science*,
DOI 10.1007/978-3-319-20777-3_8

Terminology

Acoustic resistance Opposition to the flow of sound through a surface acoustic resistance is the real component of acoustic impedance and acoustic reactance is the imaginary component.

Arterial resistivity index (RI) An indicator of resistance of an organ to perfusion. In ultrasonography it can be calculated by [peak systolic velocity – end diastolic velocity]/peak systolic velocity.

Color Doppler ultrasonography (CDUS) This technique uses standard ultrasound methods to produce an image of a blood vessel. Also a computer converts the Doppler sounds into colors that are overlaid on the image of the blood vessel and that represent the speed and direction of blood flow through the vessel.

Echogenicity In ultrasonography the extent to which a structure gives rise to reflections of ultrasonic waves. The characteristic ability of a tissue or substance to reflect sound waves and produce echoes.

Elastography This is a newer technique that exploits the fact that a pathological process alters the elastic properties of the involved tissue. This change in elasticity is detected and imaged using elastography.

High-frequency probes/transducers They are single-element contact or immersion transducers designed to produce frequencies of 20 MHz and greater.

Power Doppler ultrasonography This technique is a special type of color Doppler. Power Doppler can get some images that are hard or impossible to get using standard color Doppler. Power Doppler is most commonly used to evaluate blood flow through vessels within solid organs.

Clinical Relevance

1. *Ultrasound is the fastest, easiest, and cheapest imaging method for definitive diagnosis of Achilles tendon partial/full-thickness tears.*

   Ultrasonography (US) is an efficient and accurate way to evaluate the Achilles tendon. The major advantages of sonography include cost, widely available equipment, opportunity of evaluating contralateral tendon, and the ability to perform during joint motion [1]. Additionally, no need of preparation before the procedure is another major advantage. Unlike standard X-rays that provide very limited information regarding soft tissue pathologies, US provides a precise diagnostic examination of soft tissue conditions associated with the Achilles tendon region [2]. A previous study comparing ultrasonographic preoperative evaluation to surgical findings of Achilles tendon disorders showed US to be highly specific and sensitive in the diagnosis of Achilles tendon tears [3]. Compared to magnetic resonance imaging, which is static, US has the capability of demonstrating physiological movement and is simpler and more cost effective [4].

2. *Ultrasound can guide interventional procedures in musculoskeletal pathologies.*

   Ultrasonography is the most appropriate tool for interventional procedures in the musculoskeletal system when the lesion is visible on US. Procedures performed under ultrasonographic guidance include; taking biopsies, draining abscesses, bursitis, or hematomas, repairing muscle tears, treating cystic lesions, diagnostic or therapeutic arthrocentesis, injecting substances into joints or lesions, aspirating calcium deposits, and extracting foreign bodies. Drainage

can be performed with catheters or needles and makes it possible to avoid more aggressive treatments in most cases. Urokinase is useful for draining hematomas or fibrinous collections. Injecting corticoids is useful in the treatment of synovial cysts, Baker's cyst, tendinitis, and noninfective arthritis. Calcifying tendinitis of the shoulder can be treated effectively with percutaneous calcium lavage [5].

3. *Ultrasonography provides a great benefit for the differentiation of soft tissue masses from vascular malformations*.

   Although magnetic resonance imaging (MRI) is the most valuable modality for classification, extension, and their anatomic relationship to adjacent structures of vascular anomalies [6], ultrasonography can also provide great benefit for differentiation of those lesions from cystic/solid mass in the initial evaluation and can specify the lesions that should be needing further evaluation with MRI. On US, prominent vascular channels, phleboliths, and fat can be seen in hemangiomas. Because of their high vascularization on Doppler US, arteriovenous malformations can be differentiated from hemangiomas [7]. Abovementioned features, especially prominent vascular channels and phleboliths, are not characteristic of other musculoskeletal lesions.

4. *In traumatic muscle pathologies*, *the imaging changes occurred in time and after treatment*, *and probable recovery time can be evaluated with follow-up ultrasonographies*.

   The initial extent of injury and degree of separation of the margins of the tear are good predictors of recovery and return to normal function in patients with traumatic muscle tears. Ultrasonography (US) can be helpful in predicting the expected recovery period and is ideal for serial evaluation to monitor muscle healing and recovery [8]. Because of the lack of ionizing radiation, follow-up US examinations can be made without any damage to the patients. US also is a quick and cheap technique that does not require prior preparation compared to the other imaging modalities.

Introduction

Medical imaging methods have an important role in the diagnosis of musculoskeletal system diseases. Based on the location of the disease searched, ultrasonography (US), scintigraphy, computed tomography (CT), magnetic resonance (MR) imaging, and positron emission tomography (PET) could provide concrete data quite helpful to the clinician. In addition to the contributions to the diagnoses, medical imaging methods are significant for planning the treatments and monitoring the treatment results and complications.

Recently, with the introduction of various diagnostic methods in emergency services, musculoskeletal system and soft tissue pathologies are being diagnosed more efficiently and rapidly. In the diagnostic algorithm, anamnesis is the first step and is followed by physical examination, direct radiography, and US.

Two-dimensional images of the three-dimensional structures can be obtained with US. It is possible to examine the target structures completely through some maneuvers with probe.

US has become a widely used tool in musculoskeletal system and soft tissue pathologies in the emergency services since it is not interventional, is easily accessible, does not contain radiation, is reusable, is easily portable, is cheap, and has a wide spectrum of diagnosis. It is possible to visualize the synovitis, intra-articular fluid increase, bone erosions, and cartilage damage that cannot be detected by direct radiography and perform dynamic examination with US. In combination with *power Doppler* (*PD*) imaging, it provides quite useful information for evaluation

of the development of the diseases. The use of high-frequency probe (20 MHz) in musculoskeletal soft tissue lesions is very important. It is possible to obtain high resolution in the near field with high-frequency probes. However, the diagnostic value of the US is directly related to the knowledge and skill of the user of this device.

In recent years, three-dimensional (3D) US devices have been introduced. It is possible to perform automatic echo-volume measurement with a probe placed on the examination area with the help of these devices. In this case, image quality is achieved independent from the operator; however, it is determined according to the capacity of the US device [9]. It was found that PD signal activity and synovial structures and synovial perfusion can be evaluated in a safer manner, and accordingly, more detailed information can be obtained about synovial structures and synovial proliferation pattern in 3D US [10].

Elastography is one of the latest developments in US technology. The basis of the method is that the tissue shows different elastic properties upon application of pressure on the tissue to be examined due to the fact that malign lesions are harder than the adjacent tissues [11]. In the clinical evaluation, the size of the mass is assessed before and after applying force, or different color code spectrum coding is performed in line with the hardness of the tissues. Thus, it is possible to perform evaluation with elastography in the masses in which biopsy is considered and the unnecessary biopsies can be prevented.

Skin and Subcutaneous Tissue Diseases

Skin is the largest organ in the body in respect to weight and volume. Skin weight can be up to 20 kg and its surface area might reach 2 m^2 in an adult. The skin is made up of three layers histologically:

1. Epidermis
2. Dermis (cutis)
3. Hypodermis

Dermis is composed of fibroblasts, sweat glands, sebaceous gland, and hair roots. Below the dermis layer is sebaceous layer. Superficial fascia is found under the skin-subcutaneous sebaceous layer and embodies vascular and nervous structures. Skin-subcutaneous soft tissues are evaluated via high-frequency (7,5–18 MHz) probes.

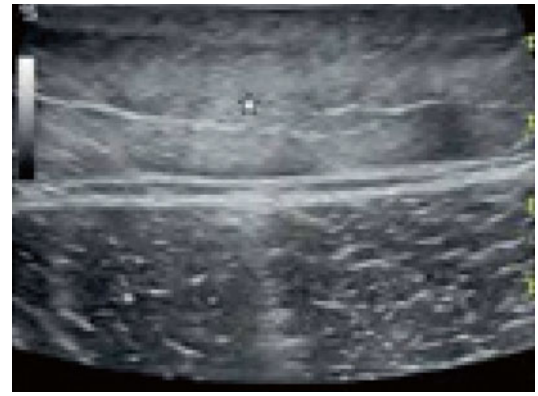

Fig. 8.1 US image of subcutaneous edema on axial plane (*asterisk*, edema)

Edema

Edema refers to the fluid accumulation in interstitial region and body cavities. It can be more visible in regions where generalized or hydrostatic pressure is high. In acute period, firstly, increase is observed between fat lobules (echogenicity increase). Expansion and liquid collection occur in lymph channels (Fig. 8.1). Obstruction and thickness increase in connective tissue emerge in time as a result of the collection. In US, a striated-pattern hypoechoic-anechoic appearance is visualized. It is less evident in some parts while more evident in others. That appearance does not go away with pressure and does not show bleeding pattern in color Doppler US (CDUS) [12].

Cellulitis

It is a kind of infection that diffuses on the skin and in subcutaneous tissues. There might be injury on the skin. It may be characterized with local sensitivity, pain, edema, and erythema. The most

common pathogens are gram (+) aerobic cocci (*S. aureus*, *S. pneumoniae*, *S. pyogenes*) and aerobic and anaerobic gram (−) bacteria. US guides in visualizing the progression of local infection and identifying the necessary interventional procedures [13]. In the US, edematous area (echogenicity increase in heterogeneity) and fibrous connective tissue (increase in hyperechogenicity) become more evident. Increased vascularization pattern helps the diagnosis in CDUS [14].

Cellulitis is treated with antibiotics. In the event that abscess develops, surgical intervention is required. In some cases, an erythematous line, in other words lymphangitis, might extend from cellulitis plaque to the proximal.

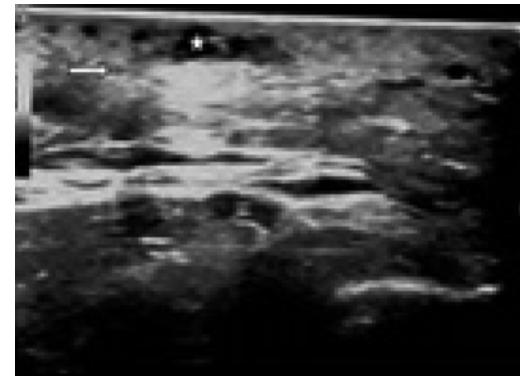

Fig. 8.2 Folliculitis in rectus muscle and edema around it (*asterisk*, folliculitis; *arrow*, edema)

Abscess

It is the collection of pus in the dermis or in deeper layers. Majority of the skin abscesses are polymicrobial, and *S. aureus* is the only factor in 25 % of the cases. Surgical drainage is the most effective treatment in the abscess. Systemic antibiotic treatment is rarely required. US appearance is quite changing (Fig. 8.2). It changes from anechoic fluid collection to irregular hypoechogenicity, to internal echoes, to hyperechoic sediments, to septa, and even to gas formation. Occasionally, only posterior acoustic enhancement is detected. In CDUS, increased vascularization in the abscess wall and adjacent tissues supports the diagnosis. In a PD study, peripheral vascularity increase was observed in 90 % of the cases [15].

Necrotizing Fasciitis

It is a rarely seen progressive soft tissue infection that emerges following minor injuries [16]. Most of the infections are polymicrobial [17]. *S. pyogenes* is the most common pathogen. Chronic diseases (diabetes and immunosuppressive), IV medication administration, and malignity are among the various factors that increase the predisposition to this disease. The diagnostic value of the US is low at the early period, and fascia gets thicker and fluid collects in deep fascia. The fact fluid collected is measured 4 mm at the thickest part is significant in necrotizing fasciitis [18]. In the advanced cases, the possible abscess and gas formation can be indicated [19].

Early diagnosis, wide-spectrum antibiotic treatment, debridement which cleans all necrotic tissues, regulating liquid-electrolyte balance, regulating the oxygenation of the infected area, nutritional support, and analgesia promotion constitute the basis of the treatment [20].

Trauma

The subcutaneous soft tissue changes that emerge following the trauma might range from minor hemorrhage to fat necrosis, hematoma, and abscess. While the hemorrhage is visualized as a hyperechogenic structure at the early period, fat necrosis is visualized as the hypoechoic areas developed secondary to the necrosis within hyperechoic focus. However, in hematoma, US findings change in time [21]. While it appears to be pseudo-solid at the beginning, it becomes anechoic in time. Within almost a month, hematoma is absorbed. If open wound and abscess formation are observed in hematoma emerged following a trauma, the presence of foreign objects should be investigated. Morel-Lavallee syndrome is the intense seroma that collects between deep subcutaneous soft tissue and fascia in traumas that occur in the lateral side of the upper calf. US illustrates a plenty amount of liquid collection on the echogenic fascia [22]. It is

possible to detect the fat necrosis that occurs in this disease and the other affected deep-located structures.

Foreign Body

Foreign bodies might be seen in subcutaneous soft tissue generally following open wounds or perforating traumas. The decision of removing the foreign body is made in line with the size, location, structure, accessibility, and mechanic and inflammatory effects of the object. In case that the pieces that cannot be removed keep staying within the wound and the body cannot figure this foreign object out, a fibrous capsule surrounds it. Inflammation, infection (wound infection, cellulitis, toxicity, tenosynovitis, bursitis, osteomyelitis), and mechanical damage might occur. Foreign object lesions do not have a real neoplasm but are traumatic reactive masses [23]. The sensitivity of the US in foreign bodies is 43–98 % and specificity ranges between 59 and 98 % [24]. It can show wood, bone, sea urchin, and other plant-like objects. A hypoechoic halo like a band occurs around the foreign object in US. It helps it to be differentiated from the neighboring soft tissues. This hypoechoic halo shows increased vascularization pattern in CDUS [25]. Calcification deteriorates the appearance with sesamoid bone and tendon acoustic shadowing. It might be difficult to place probe in places such as interdigital sites, where foreign bodies are found very commonly.

Muscular Diseases

The muscles, which are located around the skeleton, which enable movement, and that we move voluntarily, are skeletal muscles. They make up averagely 40 % of body weight. Skeletal muscle is made up of the combination of hundreds of muscle cells called skeletal muscle fibers with the height ranging between 1 mm and 30 cm. Skeletal muscles have two components, which are muscle fibrils and stromal connective tissue. Fibrils make up fascicles, and fascicles make up muscles. Since the skeletal muscles are structures that can extend from one joint to another, long linear probes are used when they are examined. Two adjacent muscle tissues appear as hyperechoic band formation (Fig. 8.3).

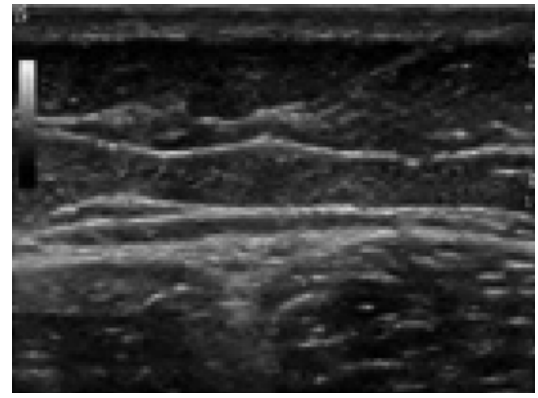

Fig. 8.3 US image of normal muscle tissue on axial plane

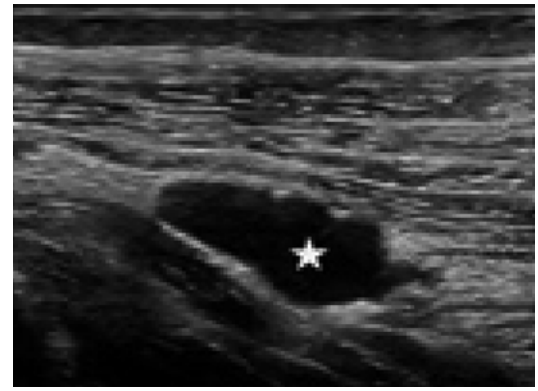

Fig. 8.4 Cyst within the rectus muscle (*star*)

While muscles are visualized as homogenous, multiple, thin parallel echoes on the longitudinal plane, they are more irregular, dispersed thin echoes on the transverse plane. Bright echogenic connective tissue fascia is present around the muscle.

The pathologies of muscles can be assessed with US. These are strain/tear, hematoma, myositis ossificans, myositis, compartment syndrome, rhabdomyolysis, hernia, and tumors [26].

US can detect the presence, the location, and the severity of the anatomic damage. US demonstrates the volume increase, edema, or fluid-pus collection in a detailed manner [27] (Fig. 8.4).

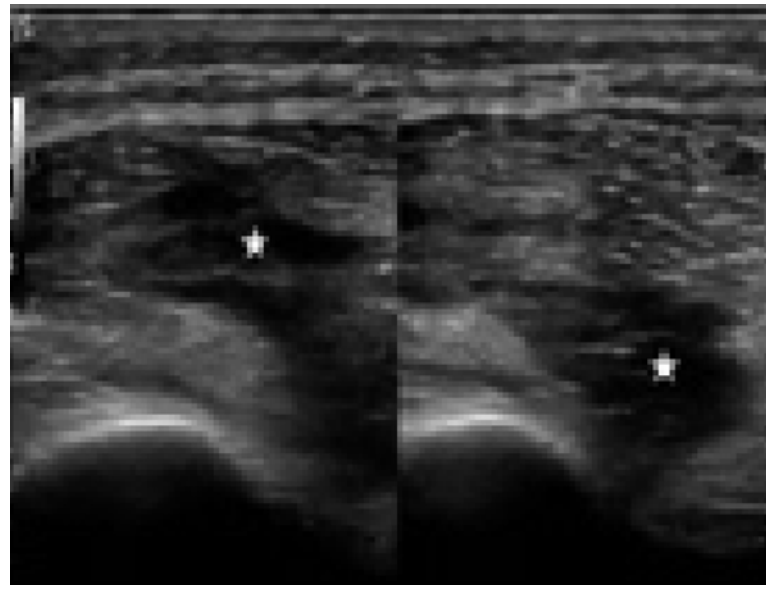

Fig. 8.5 Dispersed hematoma areas secondary to muscle tear (*star*)

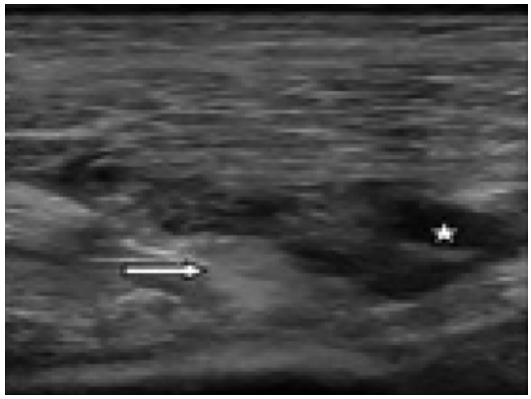

Fig. 8.6 Edema and hematoma areas secondary to muscle tear (*star*, hematoma; *arrow*, edema)

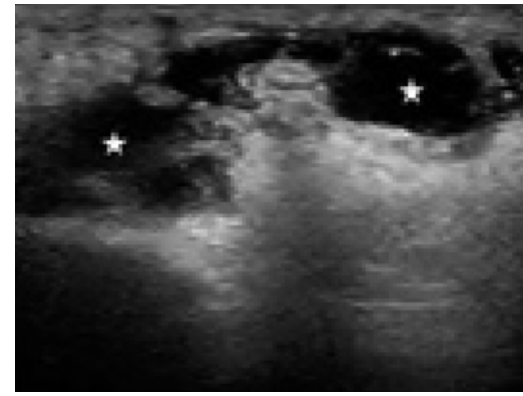

Fig. 8.7 Large hematoma in rectus femoris muscle secondary to rupture (*star*)

Trauma

Trauma constitutes the biggest part of the muscle pathologies. Different situations might emerge according to the cause and location of the lesion. In a minor tear, mild heterogeneity or local hematoma might occur in the muscle tissue, and in the big lesions in myotendinous junction, hematoma might extend to the external fascia (Fig. 8.5).

Muscle damages might have extrinsic or intrinsic causes. Myotendinous junction is the location where partial or complete muscle tears are most commonly seen (Fig. 8.6). Tears might also occur in compartments close to the myotendinous junction.

Type II muscle fibrils located at both sides of the joint and helped with the high energy and rapid movements in the main muscles have higher probability of tearing [28]. Rectus femoris, biceps femoris, and medial head of gastrocnemius muscle are the most commonly affected muscles (Fig. 8.7).

US can assess the separation and retraction of muscle fibrils from tendon or aponeurosis. Four to 6 weeks are needed for complete healing

following the trauma. The fibrous tissue that emerges in the late period appears as hyperechoic areas within the muscle in the US [29]. Residual fibrous tissue scar and recurrent injury risk are directly proportional. One of the rarely seen complications in muscle tear healing is cyst formation within the muscle. Septa formations might be visualized.

Muscle dissection is visible on fascial planes between the muscles. In more severe injuries, intramuscular fluid collection is visible. Big hematomas can cause compartment syndrome with mass effect [30].

Muscle hematoma might be seen in different ways in the US according to the stage. It might contain septa. Intramuscular hematomas are not different from the hematomas in any part of the body. While the active hemorrhage appears hyperechoic, it might be hypoechoic within a couple of hours. Later on, liquid self-leveling might be seen. After a few days, the collection becomes anechoic in a uniform way. These collections are absorbed within several weeks.

Contusion is visualized in fibroadipose septa following direct trauma. This septum is seen as prominently thick in US. Diffuse hemorrhage results in increased echogenicity. Intramuscular hematoma results from the damage to the epimysium vessels.

Muscle contraction and fibrous septa-fascicle relationship can be presented with dynamic US. In case of contraction, while muscle tissue is visualized as thick and hypoechoic, interfibrillar septa can be visualized in different ways.

In children, contusion coexistent with intramuscular bleeding and crush in muscle tissue without damaging the skin integrity directly secondary to the trauma following sports injuries is the most common. Damage occurs to the fibrils and intramuscular hematoma accompanies. In US, pathology is commonly visible in the location where trauma occurs. Thus, it is distinctive from myotendinous tears by appearance.

Primary Pyomyositis

It is a subacute deep bacterial infection of the skeletal muscle mainly seen in tropical regions [31]. Infection is widely visible in quadriceps, gluteal, and iliopsoas muscle and the most common causing factor is *S. aureus* [32, 33].

In addition to the chronic conditions such as immunodeficiency or diabetes mellitus, factors such as malnutrition contribute to its development. Also, secondary pyomyositis might arise in this case [32]. On US, diffuse hyperechogenicity is seen in the involved muscle at the inflammatory phase [13].

While pyomyositis responds to antibiotic treatment at the early phase, drainage is the best treatment option when abscess develops. In CDUS, the finding showing the progress of lesion into abscess is the formation of limited mass with a thick wall at various echogenicity between hypoechoic and hyperechoic, where increased vascularization is visible in the wall or internal septa [15].

Myositis Ossificans

It is a benign lesion described with nonneoplastic heterotopic bone formation in the soft tissue. It results from intramuscular hematoma calcification or ossification. Patients apply to the hospital with a painful hard mass that occurs within the soft tissue and continues to grow. At the beginning, within the first 3 weeks after the trauma, a disorganized, nonhomogenous soft tissue mass is seen on US. At this phase, it is not possible to differentiate the soft tissue tumor with US. Three to 4 weeks after the trauma, calcification becomes visible. These calcifications mainly have peripheral distribution and eventually, ossification occurs. In the course of progression, acoustic shadowing helps the radiologist in making the diagnosis. The absence of abnormal soft tissue distribution enables the distinction from parosteal sarcoma. Normal periosteum adjacent to cortex excludes parosteal sarcoma.

US has an important role in the diagnosis of muscle tumors. The nature (cystic/solid), location (local/diffuse), vascularization pattern, size of the lesion, and its relationship with the adjacent soft tissues can be visualized. In malign tumors, irregular boundary, heterogeneous echo, structural deformities in the adjacent structures secondary to the infiltration are seen. Benign tumors have regular boundary, homogenous echo

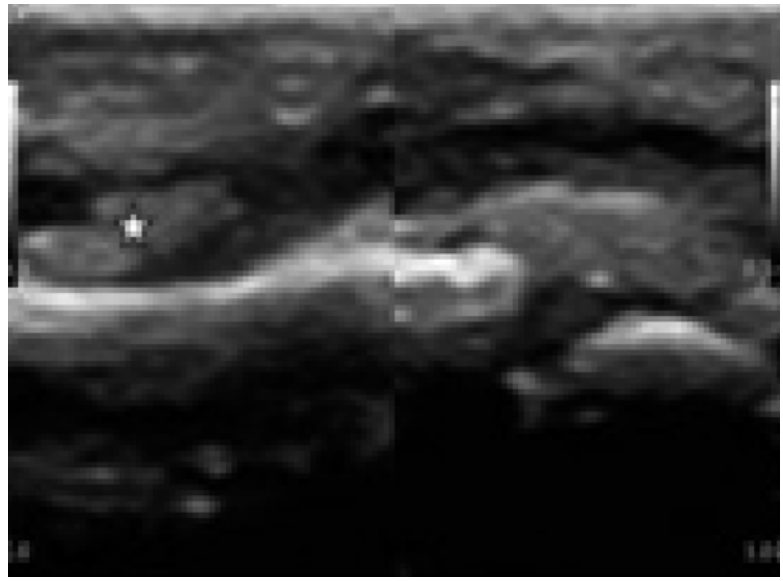

Fig. 8.8 Total tear in the tendon (*asterisk*)

structure. Also, displacement occurs in adjacent tissue.

Tendon Diseases

Tendons connect the muscles to the bones. They help the bones move by transferring the load of the muscle to the bone. Water constitutes 70 % of the wet weight of the tendon. The most visible cells in the tendon are fibroblasts. Tendon is made up of Type I collagen fibrils. Fibrils combine and make up fibers and fibers combine and make up fascicles, which contain blood, vessels, and nerves. This structure helps the tendon to stress and stretch [34].

US is the primary option in tendon pathologies because it allows for dynamic examination. It should be performed along with both longitudinal and axial planes. In longitudinal examination, tendons appear as hyperechoic bands similar to stria, with uniform thickness, and as thin parallel fibril echoes. In transverse examination, round or oval echoic spots with homogenous distribution are visible.

Synovium is visualized as thin hypoechoic frame at the anterior and posterior sides of the tendon. Paratenon (fibrous connective tissue) is visualized as ambiguous hyperechoic tissue that continues with subcutaneous fatty tissue.

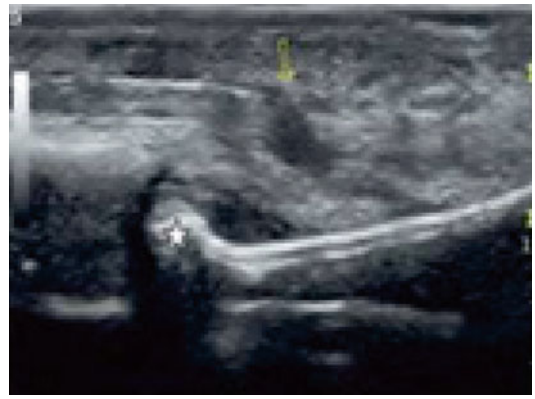

Fig. 8.9 Flexion contracture secondary to the total tendon tear in hand (*arrow*, total tear; *star*, contracture)

Tendon pathologies include tendinosis and partial tear, tendon dislocation, full-thickness tears (Figs. 8.8 and 8.9), inflammatory processes (tenosynovitis and peritendinitis), tendon tumors, and postoperative findings.

Tendonitis

Tendon swelling, irregular fibril appearance, local intratendinous hypoechoic areas, and calcifications are seen. In abnormally thick tendons, increased blood flow pattern, and neovascularization are detected in CDUS. It is assumed that

these changes show aging and tear probability. This is because degeneration, micro tears, and interstitial tears in the tendon can provide similar US findings that complement each other and that can be visualized concurrently [30].

Longitudinal hypoechoic areas are visualized in intratendinous small tears. In case that there is no coexisting hematoma, it is difficult to differentiate from tendonitis. It might be accompanied by degeneration and small fractures. It might be finalized with the healed small tear degeneration. While no volume loss is visible in tendinitis, defect with good boundaries is seen even in the partial tears.

In full-thickness tears, diagnosis is easier with US compared to partial tears. This is because the thickness of the tendon fibers is degenerated totally, the torn edges of the tendon are separated, granulation tissue and hypoechoic hematoma are visible, tendinitis is seen in tendon ends, irregular contours emerge in tendon, and posterior shadowing is visible in the torn edges.

The diagnosis might get difficult in case that the edema that develops in the acute period or tendon that tears in some cases is compensated with another tendon. The absence of tendon retraction and broad defect in the partial tear is an important finding in differentiating it from the full-thickness tear. Dynamic examination is required for making the final diagnosis in tendon tears. It is possible to stress the tendon with mildly passive moves and make it visible [35].

In full-thickness tears accompanied by degenerative diseases in adults and in full-thickness tears secondary to the trauma in children, rupture is observed at the location where tendon attaches the bone [36].

Achilles is the thickest and the strongest tendon in human body. It is made up of the combination of tendinous parts of gastrocnemius and soleus muscles. Achilles tendon rupture is one of the most commonly seen tendon tears. Mostly, it occurs (44–83 %) during exercise and is more widely seen among men than women. Since vascularization is weak, the rupture generally occurs in this 5–7 cm distal of the tendon. On US, normal tendon appearance disappears due to hematoma formation. It is possible to evaluate the tendon thickness with US.

Inflammatory processes of the tendon can be evaluated between a wide range of simple tendinosis and advanced-stage tendon pathologies. On US, thickening in tendon, heterogeneity, and focal hypoechoic areas are seen. On CDUS, increased flow signal is visible in and around the tendon.

An overwhelming majority of the tendons, excluding some tendons like Achilles and plantaris, are covered with a synovial sheath. Therefore, pathologies of the tendon and synovial pathologies are observed.

Tendinitis

Tendinitis refers to tendon inflammation. Etiopathogenesis of the tendinitis is very wide. Trauma, partial rupture, and metabolic and rheumatismal disorders lead to inflammation. Besides, inflammation might arise out of mechanic factors following tendon sheath irritation.

Peritendinitis

It manifests itself in the form of irregular tendon boundaries, peritendinous fluid, peritendinous tissue thickening, fibrosis, and increased vascularity on CDUS.

Tenosynovitis

It might develop following chronic trauma (excessive use, bone fraction, foreign bodies), infection, and arthritis. The most significant finding is the presence of fluid in the sheath. It might be accompanied by synovial thickening. In case of subacute and chronic inflammation, thickening and effusion are seen in synovial sheath [37]. *S. aureus* or *S. pyogenes* is the main factor in acute infective tenosynovitis. Most commonly, digital flexor group muscle tendons are affected. It might emerge following perforating trauma or a foreign body. The fluid in the tendon sheath appears on US in the form of clearly increased effusion. In case of subacute and chronic inflammation, thickening and

effusion are observed in the synovial sheath [38].

Tendon Subluxation

It is the subluxation of the tendons from osteofibrous tunnel with the synovial sheath accompanying itself. In the etiology, injury in osteofibrous channel structure might be the factor. The reason is mostly mechanical trauma. It is possible to detect dislocation and/or tenosynovitis with US, and it is possible to make intermittent subluxation diagnosis and detect spontaneous reduction probability. Subluxation is most frequently seen in biceps tendon head, peroneal tendon, and flexor tendons in the hand. In case the biceps tendon dislocates, bicipital cavity is emptied. Cavity is filled with fluid and tendon displaces to medial. Prominent synovial debris may be the cause of misdiagnosis since it might look like false tendon. Also, in case of internal and external rotation of the shoulder in subluxation, tendon's sliding inside and outside the cavity might lead to misdiagnose.

Tendon Tumors

Fibroma

They are soft tissue masses located within or adjacent to the tendon sheath similar to the giant cell tumors. It is more commonly seen in the upper extremities. It is also more common among men [39].

Typically, this lesion has well-circumscribed boundaries, is less than 3 cm, and is located at the extremity. Some of them are soft and focal cystic tumors. Many lesions manifest themselves in the form of soft tissue masses. It is most frequently seen between the ages of 20 and 50. Excision is the treatment.

Giant Cell Tumor

Unlike the fibromas, it is more commonly seen in older women [40] (Fig. 8.10). It is very difficult to differentiate fibroma through clinical examination, imaging, and pathology. In some cases, demographic features and location might help the diagnosis. Both of the lesions are rather in the upper extremity. However, fibroma is seen less in lower extremities compared to giant cell tumors. Therefore, in the event that a tumor is visible in the lower extremities, it is rather considered a giant cell tumor. On US, it appears as a solid, homogenous, hypoechoic mass [41].

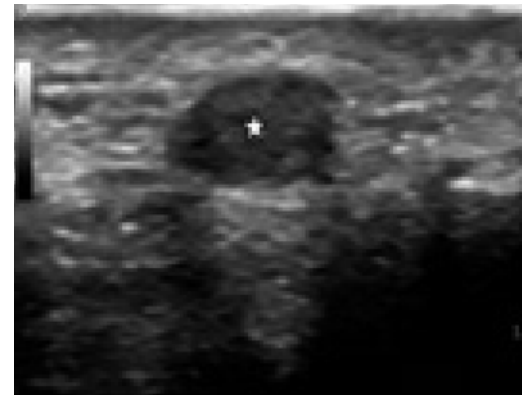

Fig. 8.10 Axial US image of a giant cell tumor (*star*, giant cell tumor)

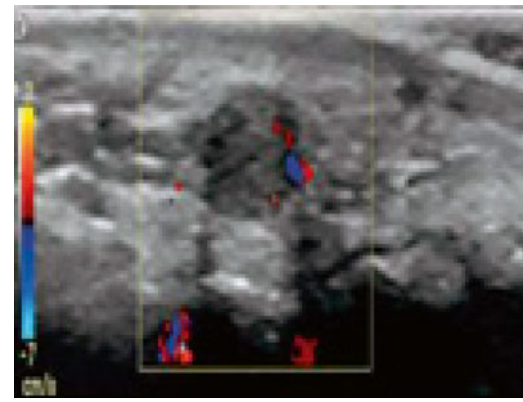

Fig. 8.11 Giant cell tumor. Absence of internal vascularization on axial Doppler examination helps it to be differentiated from localized inflammation

Giant cell tumor is accepted as soft tissue masses secondary to irritation rather than a tumor mass (Fig. 8.11). It is a reactive lesion that develops secondary to irritations such as trauma, infection, metabolic disorders, and inflammation.

Giant cell tumor is a multinodular mass with clear boundaries that have pigmentation of the

dark brown hemosiderin in general. Patients apply to the hospital with slowly progressing, hard, painless mass complaint [42]. However, tendon has normal echo and form. Since this lesion recurs itself frequently, US scans must be performed frequently.

Clear Cell Sarcoma

It is most commonly located relevantly to the tendon and aponeurosis in the lower extremities of the young adults. It is slightly more common in women. Radiological tests are quite helpful in the diagnosis. It is almost always seen as a soft tissue mass that does not show calcification and any change in the adjacent bone [43].

Ganglion Cysts

It is cystic lesion with mucoid content that can arise from tendon sheaths. It shows all the US features of the water. It is common in hand and foot dorsal tendons. Most of them are seen anechoically. Shape and location changes with movement are diagnostic.

Joint Diseases

A normal joint is seen as a hyperechoic line that creates intense shadowing at the backside of the bony structure. A small amount of fluid (1–2 ml) might be visible in synovial cavity. Joint capsule might be seen as a hyperechogenic line. Cartilage is visualized as a structure with homogenous and soft contours parallel to the bone surface. Intra-articular fat tissue is visible as hyperechogenic. Synovial membrane shows itself as an echogenic structure. In some cases, joint capsule might be defined in a better way following the dynamic manipulation of the joint with small active and passive movements [44].

It is possible to detect exudative or proliferative synovitis (hypoechoic thickening in joint capsule), tenosynovitis (anechoic or hypoechoic contour that surrounds the echogenic tendon), synovial cysts, erosive pathologies, soft tissue pathologies, and bursitis with US. Effusion is a significant determinant for the joint diseases. Low amount of intra-articular liquids can be detected with high-resolution US. Joint effusions are anechoic and respond to compression, and no flow is visualized on Doppler examination. If hemorrhage is accompanying, intense echogenic formations are seen.

Synovitis

On CDUS, irregular synovial thickening with increased vascularity is observed. In spectral examination, diastolic flow increase is seen. Pannus involves cartilage, bone, and tendons. It is detected as hypoechoic infiltration. Erosive changes are present.

Fluid collection detected by US might be secondary to the inflammation, infection, or hematoma. In this case, US-guided aspiration is standard method for the diagnosis.

Lipohemarthrosis is the presence of fat content with hemorrhage within synovial cavity. When synovial membrane is ruptured, hemorrhage occurs and fatty yellow bone marrow appears as a result of bone fracture. On US, hyperechogenicity of fatty tissue causes leveling in the joint. Hypoechoic effusion secondary to hemorrhage is seen at the bottom, while hyperechogenicity of fat tissue is observed at the top [45].

Septic Arthritis

It is a condition that one or more than one joint were infected with multiple microorganisms. It destructs the joint in a short time and, left untreated, leads to quite serious complications. In general, it develops hematogenously. The most commonly seen bacterium among adults is *S. aureus* [46].

In the acute phase, where direct radiography results are quite normal, US is highly important due to its sensitivity in revealing the effusion present and since it is guiding for the needle aspiration.

Sacroiliac joint inflammation is the main pathology in the ankylosing spondylitis. Resistivity index (RI) decreases due to the inflammation. It is possible to detect vascularization by PD US.

Ligaments

Ligaments are connective tissues made up of collagen, elastin, and fibrocartilage. US images of the ligaments are similar to tendons. A normal ligament can appear as a bright, hyperechoic, linear line and has different thickness and orders. Ligaments can be visualized in the best way between two bones that they attach to each other through a probe. Ligaments firmly adhere to joint capsule. In case of ligament injuries, thickening, heterogeneity, hypoechoic areas, edema, and hematoma at the adjacent areas can be visualized in the ligament. It is possible to detect the small ruptures, which cannot be shown with direct radiography. Calcifications might be observed in chronic pathologies. In this case, dynamic US is required in order to evaluate the stability of the ligament [47]. When ligaments are torn totally, ligament discontinuity or hypoechoic granulation tissue is seen; however, in partial tears, focal internal hypoechoic areas are present.

Nerve Diseases

It is possible to evaluate neuropathies, nerve luxation, tumors, anatomic variants, developmental anomalies, and traumatic damages with US. Nerves are straight and round cords with uniform characteristics and are made up of one nerve fascicle or are combination of fascicles. On US, hypoechoic areas resembling honeycomb are seen at transverse sections. Also, hyperechoic background of fascicles is seen around them. Besides, hyperechoic epineurium relevant to these hyperechoic areas (connective tissue located around the fascicles) is seen [48]. The longitudinal examination reveals multiple hypoechoic parallel linear areas. These areas are separated from each other with hyperechoic bands. It is possible to show neuropathy, more importantly, the underlying pathology with US [49].

In the event that the nerve tears totally following damage, nerve ends separated from each other are retracted. It might be accompanied by fluid collection. In some cases, partial tears occur and irregular hypoechoic nodules are visualized where nerve integrity is upset (traction neuroma) [50].

US reveals the size of the torn nerve and the scar tissue that might develop postoperatively. Edema can be seen in postoperative period. The most significant postoperative complications are retear and scar formation.

Carpal Tunnel Syndrome

It is the most commonly seen entrapment neuropathy. It results from median nerve compression. It is characterized by nocturnal pain. Median nerve below flexor retinaculum is damaged in connection with predisposing factors (diabetes, hypothyroidism, pregnancy, or mass lesions). Electrophysiological tests are standard. US can help to diagnose the probable cause that leads to neuropathy and can be used with the aim of guiding probable intervention. Since no morphological changes occur at the early period, even if US is normal, carpal tunnel syndrome diagnosis cannot be excluded. The most specific and sensitive US finding is proximal enlargement at scaphoid-pisiform level [51]. In some cases, the bullous enlargement is observed in the nerve and this is called pseudoneuroma.

Bone Diseases

Bone is made up of organic (35 %) and inorganic (65 %) substances. In organic section, Type I collagen is present and in inorganic section mainly calcium hydroxyapatite. All bones consist of cortical bones inside and medullary bones outside. In the medullary area, trabecular bone and bone marrow are present. From outside to inside, periost, cortex, endosteum, and medulla sections are present. Cortex is made up of compact bone, and medulla ends and interior parts of the epiphyses are made up of the spongy bone.

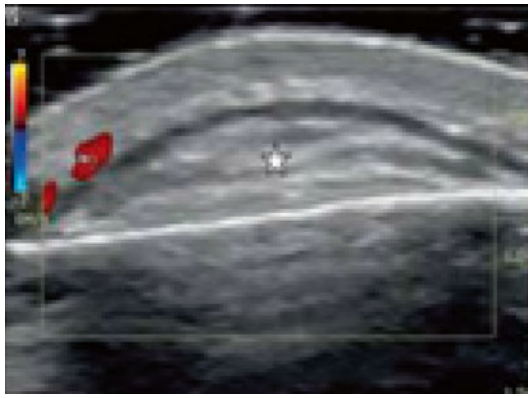

Fig. 8.12 Lipoma in the scalp (*star*)

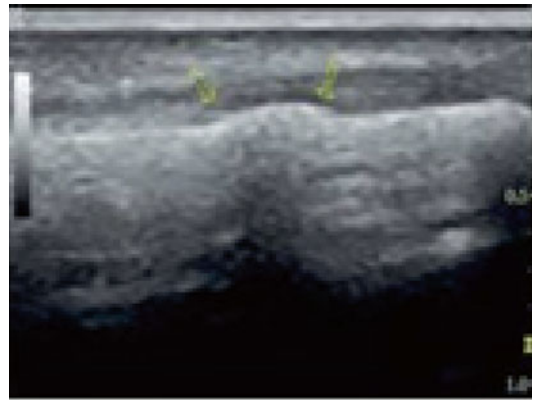

Fig. 8.13 Bone fracture (*arrow*)

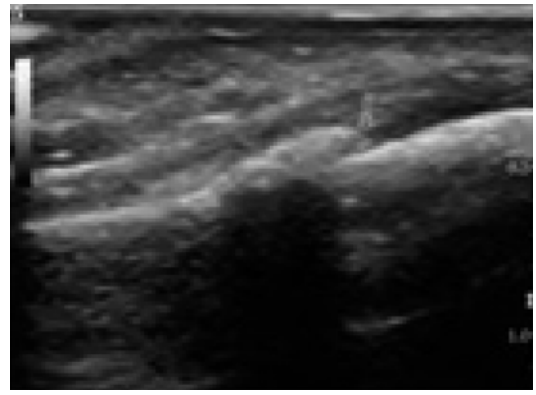

Fig. 8.14 Bone fracture (*arrow*)

On US, 7.5–18 MHz high-frequency probes are used for the examination of the bone and soft tissues. Since the superficial sections close to the transducer are visualized better, linear transducers should be preferred. Because of the acoustic resistance difference, soft tissue-bone interface is seen significantly hyperechoic. This causes limitation in obtaining information. Nevertheless, US provides helpful information in certain cases (Fig. 8.12) [52].

US indications in the bone diseases include:

- Periarticular lesions
- Tumors
- Osteomyelitis (early period)
- Fracture

Periarticular Erosions

Irregular damage is observed in bone cortex. Even the slightest discontinuity in bone cortex is regarded abnormal. It is possible to detect even <1 mm bone erosions with US.

Examination should be performed on longitudinal and transverse planes.

Acute Hematogenous Osteomyelitis

It is common in children and the elderly. The most common pathogen is *S. aureus*. It is followed by *Streptococcus*. It is possible to make differential diagnosis of cellulitis and osteomyelitis with US. Nonspecific soft tissue swelling is an example of early period findings. In adults, fluid collection directly related to the bone might be observed. In children and young adults, subperiosteal fluid collection is seen.

The most important function of US is its guidance for fluid aspiration. US can provide guidance in the percutaneous interventional procedures and evaluate the response to the chemotherapy.

Fracture

Irregularity or damage might be seen in hyperechoic bone cortex (Figs. 8.13 and 8.14). In chondral pathologies, hyaline cartilage gets thinner and loss is present.

In case that there is no subluxation in the ends of the fracture or subluxation is minimal in sternal fractures, radiography might be insufficient. In such a case, it is possible to make a practical diagnosis with US. Other pathologies including associated pleural effusion can be identified with US.

Due to the fact that costal cartilage fractures go unnoticed with direct radiographs, the diagnosis can be made with the discontinuity in the regular anterior contour of the cartilage.

US in Postoperative Orthopedic Patients

Postoperative soft tissue infection, bone effusion, and fracture healing can be diagnosed with US. It is possible to perform space measurement following Ilizarov procedure, evaluate new bone formation, and identify cyst formations in this region. The absence of metal artifact is an advantage of US.

References

1. Dong Q, Fessell DP (2009) Achilles tendon ultrasound technique. AJR Am J Roentgenol 193:W173
2. Blankstein A, Cohen I, Diamant L, Heim M, Dudkiewicz I, Israeli A, Ganel A, Chechick A (2001) Achilles tendon pain and related pathologies: diagnosis by ultrasonography. Israel Med Assoc J 3:575–578
3. Paavola M, Paakkala T, Kannus P, Jarvinen M (1998) Ultrasonography in the differential diagnosis of Achilles tendon injuries and related disorders. A comparison between pre-operative ultrasonography and surgical findings. Acta Radiol 39:612–619
4. Astrom M, Gentz CF, Nilsson P, Pausing A, Sjoberg S, Westlin N (1996) Imaging in chronic achilles tendinopathy: a comparison of ultrasonography, magnetic resonance imaging and surgical findings in 27 histologically verified cases. Skelet Radiol 25:615–620
5. Del Cura JL, Zabala R, Corta I (2010) Ultrasound-guided interventional procedures in the musculoskeletal system. Radiologica 52:525–533
6. Flors L, Leiva-Salinas C, Maged IM, Norton PT, Matsumoto AH, Angle JF, Hugo Bonatti M, Park AW, Ahmad EA, Bozlar U, Housseini AM, Huerta TE, Hagspiel KD (2011) MR imaging of soft-tissue vascular malformations: diagnosis, classification, and therapy follow-up. Radiographics 31:1321–1340
7. Paltiel HJ, Burrows PE, Kozakewich HP, Zurakowski D, Mulliken JB (2000) Soft tissue vascular anomalies: utility of US for diagnosis. Radiology 2014:747–754
8. Tok F, De Muynck M, Kara M, Vanderstraeten G (2012) Musculoskeletal ultrasound for sports injuries. Eur J Phys Rehab Med 48:651–663; quiz 707
9. Downey DB, Fenster A, Williams JC (2000) Clinical utility of three-dimensional US. Radiographics 20(2):559–771
10. Filippuchi E, Lagnocco A, Meenagh G et al (2006) Ultrasound imaging fort the rheumatologist II. Ultrasound of the hand and wrist. Clin Exp Rheumatol 24(2):118–122
11. Cho N, Moon WK, Park JS et al (2008) Nonpalpable breast masses: evaluation by US elastography. Korean J Radiol 9(2):111–118
12. Vincent LM (1988) Ultrasound of soft tissue abnormalities of the extremities. Radiol Clin N Am 26(1):131–144
13. Chau CL, Griffith JF (2005) Musculo skeletal infections; ultrasound appearances. Clin Radiol 60(2):149–159
14. Cardinal E, Bureau NJ, Aubin B et al (2001) Role of ultrasound in musculoskeletal infections. Radiol Clin N Am 39(2):191–201
15. Arslan H, Sakarya ME, Bozkurt M et al (1988) The role of power Doppler sonography in the evaluation of superficial soft tissue abscesses. Eur J Ultrasound 8(2):101–106
16. Singh G, Sinha SK, Adhikary S et al (2002) Necrotizing infections of soft tissues – a clinical profile. Eur J Surg 168(6):366–371
17. Brooks I, Frazier EH (1995) Clinical and microbiological features of necrotizing fasciitis. J Clin Microbiol 33(9):2382–2387
18. Yen ZS, Wang HP, Ma HM et al (2002) Ultrasonographic screening of clinically-suspected necrotizing fasciitis. Acad Emerg Med 9(12):1448–1451
19. Hosek WT, Laeger TC (2009) Early diagnosis of necrotizing fasciitis with soft tissue ultrasound. Acad Emerg Med 16(10):1033
20. Scott SD, Dawes RF, Tate JJ et al (1988) The practical management of Fournier's gangrene. Ann R Coll Surg Engl 70(1):16–20
21. Fernando RA, Somers S, Edmonson RD et al (2003) Subcutaneous fat necrosis hypoechoic appearance on sonography. J Ultrasound Med 22(12):1387–1390
22. Mellado JM, Pérez del Palomar L, Díaz L et al (2004) Long-standing Morel-Lavallée lesions of the trochanteric region and proximal thigh: MRI features in five patients. AJR Am J Roentgenol 182(5):1289–1294
23. Athanasian EA (2005) Bone and soft tissue tumors. In: Green DP, Hotckiss RN, Pederson WC, Wolfe SW (eds) Green's operative hand surgery, 5th edn. Elsevier, Philadelphia, pp 2211–2264
24. Blankenship RB, Baker T (2007) Imaging modalities in wounds and superficial skin infections. Emerg Med Clin North Am 25(1):223–234
25. Davae KC, Sofka CM, DiCarlo E et al (2003) Value of power Doppler imaging and the hypoechoic halo in the sonographic detection of foreign bodies; correlation with histopathologic findings. J Ultrasound Med 22(12):1309–1313

26. Snoecx M, De Munynck M, Van Laere M (1995) Association between muscle trauma and heterotopic ossification in spinal cord injured patients: reflections on their causal relationship and the diagnostic value of ultrasonography. Paraplegia 33(8):464–468
27. Robben SG (2004) Ultrasonography of musculoskeletal infections in children. Eur Radiol 14(Suppl 4):L65–L77
28. Noonan TJ, Garrett WE Jr (1999) Muscle strain injury: diagnosis and treatment. J Am Acad Orthop Surg 7(4):262–269
29. Peetrons P (2002) Ultrasound of muscles. Eur Radiol 12(1):35–43
30. Campbell RS, Graigner AJ (2001) Current concepts in imaging of tendinopathy. Clin Radiol 56(4):253–267
31. Grose C (1998) Bacterial myositis and pyomyositis. In: Feigin RD, Cherry JD (eds) Textbook of pediatric infectious diseases, 4th edn. Saunders, Philadelphia, pp 704–708
32. Chiedozi LC (1979) Pyomyositis. Review of 205 cases in 112 patients. Am J Surg 137(2):255–259
33. Peckett WR, Butler-Manuel A, Apthorp LA (2001) Pyomyositis of the iliacus muscle in a child. J Bone Joint Surg (Br) 83(1):103–105
34. O'Brien M (1992) Functional anatomy and physiology of tendons. Clin J Sport Med 11(3):505–520
35. Schepsis AA, Jon H, Haas AL (2002) Achilles tendon disorders in athletes. Am J Sports Med 30(2):287–305
36. Hall BT, McArthur T (2010) Ultrasound diagnosis of a patellar tendon rupture. Mil Med 175(12):1037–1038
37. Möller M, Kälebo P, Tidebrant G et al (2002) The ultrasonographic appearance of the ruptured Achilles tendon during healing; a longitudinal evaluation of surgical and nonsurgical treatment, with comparisons to MRI appearance. Knee Surg Sports Traumatol Artrosc 10(1):49–56
38. Martinoli C, Bianchi S, Derchi LE (1999) Tendon and nerve sonography. Radiol Clin N Am 37(4): 691–711
39. Fox MG, Kransdorf MJ, Bancroft LW et al (2003) MR imaging of fibroma of the tendon sheath. AJR Am J Roentgenol 180(5):1449–1453
40. Ushijima M, Hashimoto H, Tsuneyoshi M et al (1986) Giant cell tumor of the tendon sheath (nodular tenosynovitis). A study of 207 cases to compare the large joint group with the common digit group. Cancer 57(4):875–884
41. Middleton WD, Patel V, Teefey SA et al (2004) Giant cell tumors of the tendon sheath: analysis of sonographic findings. AJR Am J Roentgenol 183(2): 337–339
42. Beredjiklian B, Donthineni-Rao R (2004) Tumors, review of hand surgery, Part 10. Saunders, Philadelphia. pp 189–206
43. Enzinger FM, Weiss SW (1995) Malignant tumors of the peripheral nerves. In: Enzinger FM, Weiss SW (eds) Soft tissue tumors, 3rd edn. Mosby Year Book, St Louis, pp 913–919
44. van Holsbeeck MT, Introcaso JH (1991) Sonography of large synovial joints. In: van Holsbeeck MT, Introcaso JH (eds) Musculoskeletal ultrasound. Mosby Year Book, Chicago, pp 143–176
45. Adhikari S, Blaivas M (2010) Utility of bedside sonography to distinguish soft tissue abnormalities from joint effusions in the emergency department. J Ultrasound Med 29(4):519–526
46. Kaandorp CJ, Dinant HJ, van de Laar MA et al (1997) Incidence and source of native and prosthetic joint infection: a community based prospective survey. Ann Rheum Dis 56(8):470–475
47. Ahmed R, Nazarian LN (2010) Overview of musculoskeletal sonography. Ultrasound Q 26(1):27–35
48. Stewart JD (2003) Peripheral nerve fascicles: anatomy and clinical relevance. Muscle Nerve 28(5):525–541
49. Hundrfund AN, Boan AJ, Mandrekar JN et al (2011) Sonography in carpal tunnel syndrome. Muscle Nerve 44(4):485–491
50. Graif M, Martinoli C, Rochkind S et al (2004) Sonographic evaluation of brachial plexus pathology. Eur Radiol 14(2):193–200
51. Kaymak B, Özçakar L, Çetin A et al (2008) A comparison of the benefits of sonography and electrophysiologic measurements as predictors of symptom severity and functional status in patients with carpal tunnel syndrome. Arch Phys Med Rehabil 89(4):743–748
52. Cho KH, Lee YH, Lee SM et al (2004) Sonography of bone and bone related diseases of the extremities. J Clin Ultrasound 32(9):511–521

Infant Hip Ultrasound

9

Atil Atilla, İsmail Demirkale, and Cemil Yıldız

Abstract

Developmental dysplasia of the hip (DDH) is one of the most common disorders of the hip and refers to a disease involving both the acetabulum and proximal femur. Early and accurate diagnosis is of paramount importance to avoid late sequel of the hip joint. To date, hip ultrasound (US) is the preferred diagnostic tool. The favored US technique is the Graf method. Features of the bony roof, osseous rim, and cartilaginous roof together with angles and age of the infant all designate the type of the hip joint. DDH has five main types with additional subtypes, and first two of those (types I and II) are described as centered hips, whereas others (types D, III, and IV) are decentered hips. For centered joints with inadequate maturation including type IIa(−), type IIb, and type IIc stable hips, a device should be used to place the hips in crouching position until appropriate maturation. Decentered joints should be reduced by a harness in the first 3 weeks of harness application. Reduction can be monitored by anterior US scanning of the hip.

Learning Outcomes

The most important reference point of a sonogram is lower limb of os ilium.

Just a standard plane of US can obtain a reproducible ultrasonographic view.

At the standard plane, the silhouette of iliac bone should be parallel to the probe.

Three landmarks should be well visualized on a sonogram: lower limb of the ilium at the depth of acetabular fossa, the midpoint of ace-

İ. Demirkale (✉)
Orthopedics and Traumatology, Kecioren Education and Research Hospital, Ankara, Turkey
e-mail: drismail@yahoo.com

C. Yıldız
Orthopedics and Traumatology, Gulhane Military Hospital, Ankara, Turkey
e-mail: cyorto@yahoo.com

A. Atilla, MD
Orthopedics and Traumatology, Mevki Military Hospital, Ankara, Turkey
e-mail: dratilatilla@hotmail.com

F. Korkusuz (ed.), *Musculoskeletal Research and Basic Science*,
DOI 10.1007/978-3-319-20777-3_9

tabular roof, and the labrum.

The examiner has to check the classical shape of chondro-osseous junction to be in proper silhouette to rule out any tilting effect.

The alpha angle quantifies the bony socket, whereas the beta angle quantifies the cartilaginous acetabular roof.

There are five types: types I and II describe the centered joints, and type D, type III, and type IV describe the decentered joints.

A newborn hip that will become a type 1 mature hip should have at least 50° of alpha angle at birth.

Premature infant should be classified according to his or her calendar age.

Type I depicts a mature hip with a well-developed socket ($\alpha \geq 60°$) and an angular bony rim.

Type IIa is subject to physiological immaturity.

Type IIb means that bony socket is deficient ($\alpha = 50–59°$), and the baby is older than 12 weeks of age.

Type IIc is subject to "decentering phenomenon"; bony rim has lost its rotundity, and bony roof is severely deficient ($\alpha = 43–49°$).

The main difference between a type IIc and type D hip is the β angle (type D, $\beta > 77°$).

The position of the perichondrium leads to a distinction between type III and type IV; type IV has a perichondrium toward to the acetabulum.

Two hard copies, one of them is free of figured lines, and report of the sonogram including age, hip type, alpha and beta angles, and management strategy suggestion should be included for documentation.

The recommended management of type IIa(−) hips is an abduction orthosis especially in newborn girls.

Hip reduction can be assessed by an anterior approach such as the Suzuki method by measuring the femoral head coverage and reduction quality without weaning off the harness.

Clinical Relevance

A 5-week-old female infant was brought to outpatient clinic for suspicion of left-sided developmental dysplasia of the hip according to pediatricians' initial physical examination. On physical examination, the infant had a hip abduction asymmetry with a positive Barlow and Ortolani tests at the involved side. Immediately, lateral hip scanning was performed on the infant through the Graf method on a cradle while she was in lateral decubitus position. The hip was defined as centered hip; the bony rim was flattened (Fig. 9.1). The alpha and beta angles were measured, and it was found that bony roof was severely deficient ($\alpha = 49°$) and beta angle was 59°. The hip was ultimately classified as type IIc according to the Graf classification. Thereupon, a Pavlik harness was applied, putting the involved joint in 100° of flexion by tightening the anterior straps of the harness and in moderate abduction. At 1-week intervals, follow-up was scheduled, and at the end of 3 and 6 weeks, hip ultrasound was repeated. Pavlik harness was discontinued when the acetabulum demonstrated a mature hip ($\alpha = 61°$), and then the baby was put in an abduction brace for additional 6 weeks. The x-ray examination after 8 months of follow-up revealed a 25° of acetabular index angle (Fig. 9.2).

Recently, a well-done hip ultrasound is the gold standard in diagnosing hip pathologies in infancy [1]. An orthopedic surgeon should know at least main principles of lateral and anterior ultrasound scanning of an infantile hip and also can make a conclusion on an ultrasound image. The silhouette of iliac bone should be parallel to the probe, lower limb of the ilium at the depth of acetabular fossa, and the midpoint of acetabular roof and labrum

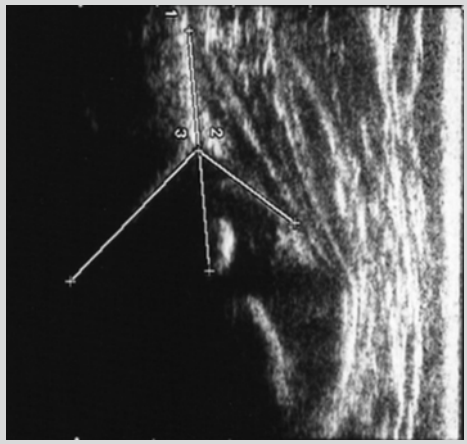

Fig. 9.1 Initial US image of the baby

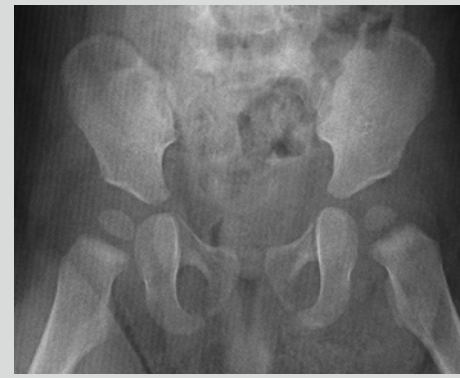

Fig. 9.2 Pelvis x-ray of the same child showing sufficiently developed acetabulum

should be clearly seen [2]. There are five types: types I and II describe the centered joints, and type D, type 3, and type IV describe the decentered joints.

All decentered hips including type D, type III, and type IV together with a centered but type IIc unstable hip should be reduced. Almost all type IIa(+) hips will spontaneously normalize until the end of 12 weeks of age [3]. However, the incidence of type IIa(−) hips through pursuance of type IIa hips is reported to be 15.6 %; thus, the recommended management of such hips is an abduction orthosis rather than wait-and-see regimen especially in newborn girls than boys [4].

The preferred treatment method in this age is application of Pavlik harness [5]. Follow-up through lateral scanning by the Graf method enables monitoring of the ossification of the acetabulum in centered hips. Many of Graf type III and type IV hips will reduce, and reduction quality can be checked through measurement of ischial limb-femoral distance by anterior scanning [6].

Introduction

Developmental dysplasia of the hip (DDH) is associated with specific suboptimal development affecting both the acetabulum and proximal femur, suggesting the need for concentric reduction for an acceptable hip development. Early diagnosis is the mainstay of treatment, and the gold standard for the diagnosis of DDH before 4 months of age is hip ultrasonography (HUS) especially in babies with positive risk factors [7].

Reinhard Graf was the one who first time introduced the use of HUS in screening and monitoring DDH in the late 1970s, and thereafter, HUS was widely accepted as a diagnostic tool in many countries [2, 8]. Following that, the technique has shown a progressive evolution, and Harcke, Terjesen, and Suzuki all described their own techniques [9–12]. All these HUS techniques intend to make an accurate and early diagnosis of DDH and to guide the treatment with having difference regarding image plane, direction of visualization, or focusing on morphology or stability. In the Graf method, the baby is placed on a cradle in lateral decubitus position, and the hip is scanned laterally, whereas in the Suzuki method, the baby is placed in supine position, and an anterior approach is used. The Harcke method uses a lateral approach on a baby in supine position and by applying the Barlow stress test; the hip is assessed both in neutral position and in flexion. Eventually, it's a dynamic four-step method and involves dynamic examination of the hip both in lateral and coronal views without measurements.

Morin et al. modified the Harcke method and measured the percentage coverage of the femoral head on a lateral coronal view in slight hip flexion [12]. The Terjesen method is also a modification of the Morin method in which head coverage is measured with the aid of a baseline parallel to the long axis of the laterally placed transducer, and it is different from the Morin method with regard to figured baseline which is parallel to the lateral iliac line. The Suzuki method intends to visualize both hips via an anterior approach by a caudally directed scanning plane to transect the center of the hip. The standard plane of this method is obtained when both pubic bones are displayed on the same view with the infants' hips in extension and then two lines are drawn. A (P) line is drawn along the anterior surface of the pubic bones, and a second line (E) is drawn from the lateral margin of the pubic bones. With a dislocated hip, femoral head crosses the P line, and in such case, the examination is repeated in abduction and flexion position. The transverse-neutral and coronal-flexion views can be combined to both detect direction of the displacement and evaluate acetabular dysplasia [13].

These four well-known procedures have their own advantages and disadvantages, but one must have in mind that a duly performed technique is the best whether an anterior or lateral technique was chosen. Among these, the Graf method is the most widely used for accurate and early diagnosis of a DDH with a well-defined standardization, and recent reports suggest the use of an anterior approach in management and follow-up of the patients with DDH [6].

Usually, suspicion of DDH begins with the very first physical examination of a pediatrician, and they consult babies with risk factors or having positive examination findings to pediatric orthopedic surgeons. According to one report, clinical examination alone in detecting DDH has a low specificity, so to prevent a misjudgment on the management of DDH, certification on the hard copy of a hip ultrasound image has a paramount importance [14]. That being said, in many cases, errors made in diagnosis or late diagnosis can lead to severe catastrophic results with a miserable lifetime quality of the patients [15]. Therefore, efforts to identify a baby with DDH, appropriate treatment, and prevention of hip dysplasia must, of necessity, become a major precedency of orthopedic surgeons.

To date, a well-done HUS is the gold standard in diagnosing hip pathologies in infancy [1]. The magnetic resonance imaging and computerized tomography can be used, but they are performed under anesthesia during infant age. Also radiation exposure is excessive at BT. Arthrography is useful but it is an invasive method. HUS visualizes chondral parts of the hip joint excellently. Currently, both radiologists and orthopedic surgeons perform HUS in these infants to screen DDH. Although a limited number of orthopedic surgeons perform HUS, more of them deal with the treatment of DDH. Thus, whether HUS is performed or not, an orthopedic surgeon should be very competent on the anatomy of newborn hip, know at least main principles of lateral and anterior ultrasound scanning of an infantile hip, and also can make a conclusion on an ultrasound image.

The Graf method has quantitative classification system and measures two angles, α and β; the Harcke and Terjesen methods determine the amount of the femoral head coverage by the osseous part of the acetabulum.

Ultrasonographic Anatomy of Newborn Hip Joint

The perichondrium of the cartilaginous acetabular roof, joint capsule, and acetabular labrum are echolucent structures, which means that the ultrasound beam can transmit through these structures. The proximal perichondrium is composed of the perichondrium, insertion of the capsule, and reflex head of the rectus femoris.

However, the bony parts also exist in the newborn hip. These are chondro-osseous junction between the shaft and neck of the femur, lower

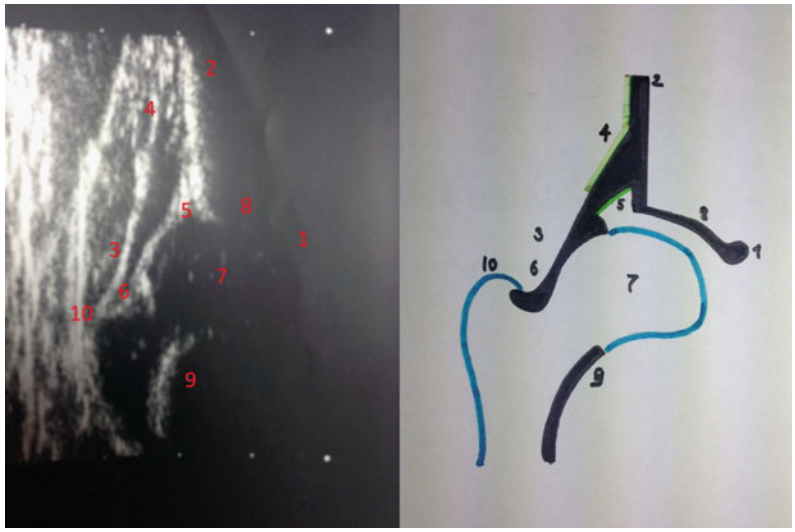

Fig. 9.3 Anatomical structures of infant hip: (**1**) Iliac bone ossific end, (**2**) Iliac bone, (**3**) Labrum, (**4**) Periosteum, (**5**) Perichondrium, (**6**) Joint capsule, (**7**) Femoral head, (**8**) Acetabulum, (**9**) Chondro-osseous junction and (**10**) Greater trochanter

limb of os ilium and os ischium, and upper part of os ilium just above the acetabulum, and these structures are seen as bright echoes leaving an acoustic shadow behind them. The most important reference point of a sonogram is the lower limb of os ilium and the hypoechoic triradiate cartilage that exists caudal to the lower limb (Fig. 9.3) [2]. When the examiner detects the lower limb of the ilium, then he/she has to move proximally to find out the point where the concavity of bony acetabulum turns to convexity of the ilium. This point is called as "osseous bony rim," which is the most lateral point of bony socket, and later it will be used to measure the cartilage roof angle.

The hypoechoic or anechoic structures are made up of hyaline cartilage, and they are found in triradiate cartilage, acetabular roof, femoral head, proximal femoral neck, and great trochanter. The femoral head is in "oval" shape, and its ossific center generally elicits at 5–7 weeks on sonograms; however, this center cannot be used as a reduction guide as it is not always at the center of the femoral head. Also if there is large ossific center, which curtains the lower limb of os ilium, a diagnosis cannot be made upon sonogram.

Graf Method

Using real-time 2D ultrasonography, the anatomical structure of the acetabulum in the standard projection of the Graf method is similar to that of an anteroposterior view of an x-ray. In the lateral decubitus position, the infant is placed in a cradle, and by a 5- or 7.5-MHz linear array probe, scanning of the hip is performed. For an accurate measurement, sonograms must be magnificated enough. The magnification factor should be 1:1.7 or more. Also a new probe-guiding system was introduced to avoid tilting effects especially for beginner sonographers. Positioning of the transducer is essential for an accurate scanning. It should be parallel to bolsters of the cradle and vertical to the spine.

Standard Plane

In order to obtain a reproducible ultrasonographic section, a standard plane of US should be used. At the standard plane, three structures have to be defined clearly:

- Lower limb of the ilium at the depth of acetabular fossa
- The midpoint of acetabular roof
- Acetabular labrum

At the standard plane, the silhouette of iliac bone should be parallel to the probe. Baseline is the point where the proximal perichondrium turns to the periosteum. It is the bony rim's highest point. Baseline starts from this point and goes parallel to echo of iliac bone. The measurement should be made at the standard plane. The order of anatomical structures that have to be identified are (1) chondro-osseous junction, (2) femoral head, (3) synovial fold, (4) joint capsule, (5) acetabular labrum, (6) acetabular roof, and (7) bony rim [2]. Then the standard plane should be assessed whether it is in the correct section. There can be three different sections: posterior, anterior, and middle [2]. In the midsection, the silhouette of the iliac bone is parallel to the monitor. When the iliac contour is concave, then the plane is defined as posterior (ilium leans to right) or anterior (ilium leans to left). When lower limb of the ilium, midsectional plane, and acetabular labrum are identified on a sonogram, then it is acceptable for reading. In addition to anterior and posterior sections, the transducer can be tilted, and in this case, serious misdiagnosis can be made. The transducer can be tilted in anteroposterior, posteroanterior, cranio-caudal, or caudo-cranial way. The latter is the most hazardous by assuming to have a poor bony socket. The examiner again has to check the classical shape of chondro-osseous junction to be in proper silhouette to rule out any tilting effect [2].

> The standard plane is like a page of a book. You have to take off a certain page. Other pages cannot be used.

Measuring the Angles

Two angles, both of which are independent from the position of the femur, are used to determine the depth of the acetabulum as well as coverage of the femoral head by the acetabulum. The alpha angle quantifies the bony socket, whereas the beta angle quantifies the cartilaginous acetabular roof. The alpha angle is formed by the angle between the acetabular roof line and the baseline and determines the hip type. The baseline is drawn from the point at the silhouette of the ilium where the periosteum of perichondrium begins and runs caudally. The acetabular roof line connects the inferior part of lower limb of the ilium and bony roof at the most caudal point of the ilium on the baseline. The cartilaginous roof line connects the center of the labrum and bony rim where the convexity turns to concavity (Fig. 9.4).

Classification

DDH can be simply classified as centered and decentered hips according to Graf classification [2]. In addition, there are five types: types I and II describe the centered joints, and type D, type 3, and type IV describe the decentered joints. This classification determines the severity of the pathology affecting the acetabulum. Before classifying a hip joint, the examiner should know the maturation potential of an acetabulum especially for an infant in 12 weeks of life [16]. Normally, the mean value of an alpha angle at birth is about 59° (range, 55–65°). A healthy infants' hip demonstrates a rapid maturation (increase in alpha angle) especially in the first 6 weeks of life, and then the acetabulum shows an upward ossification till the end of 12 weeks. The end of 12 weeks is a cut point between great maturation potential and a stepwise maturation. Thus, both the alpha angle at the time of US examination and the age of baby determine the type of the DDH and also optimal result of management of DDH. Thereby, a newborn hip that will become a type 1 mature hip should have at least 50° of alpha angle at birth [16]. This means that, from birth to 12 weeks of life, certain amount of ossification occurs each week in a term baby. However, the examiner should note that the baby could be a premature infant. In this case, premature infant should be

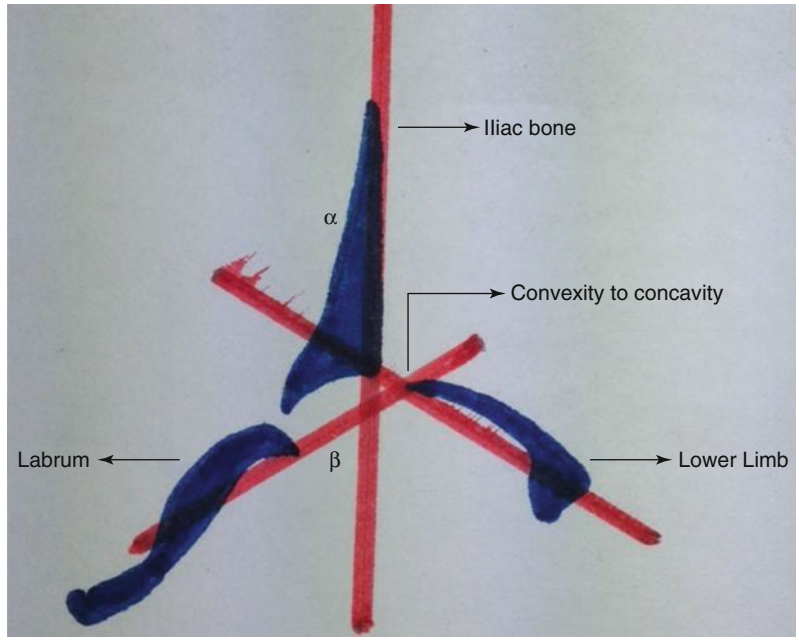

Fig. 9.4 Illustration of hip joint and the important points and lines that determine α and β angles

Table 9.1 The Graf classification

Type	Description	Bony roof/α angle	Cartilaginous roof/β angle	Bony rim
I	Mature hip	Good/α ≥ 60°	Covers head/Ia: β < 55 Ib: β > 55	Angular
IIa(+)	PI/0–12 weeks of age	Adequate/α 50–59	Covers head/β < 77	Rounded
IIa(−)	PI/>6–12 weeks of age	Deficient/ α 50–59	Covers head/β < 77	Rounded
IIb	Delay of ossification	Deficient/α 50–59	Covers head/β < 77	Rounded
IIc	Can be decentered	Severely deficient/α 43–49	Covers head/β < 77	Rounded/flattened
D	Decentering	Severely deficient/α 43–49	Not covers/β > 77	Rounded/flattened
IIIa	Decentered	Poor/α < 43	Superiorly oriented without echoes	Flattened
IIIb	Decentered	Poor/α < 43	Superiorly oriented echogenic	Flattened
IV	Decentered	Poor/α < 43	Inferiorly oriented	Flattened

Abbreviations: *PI* physiologically immature

classified according to his or her calendar age, and the age of the infant should be corrected. Consequently, features of the bony roof, osseous rim, and cartilaginous roof together with angles and age of the infant all designate the type of the hip joint (Table 9.1) [2].

Type I

As abovementioned, type I depicts a mature hip with a well-developed socket (α ≥ 60°) and an angular bony rim. The degree of ossification is consistent with a 12-week-old baby. Although cartilaginous acetabular roof adequately covers the femoral head, the labrum may have a short extension (β < 55°: type Ia) or broadly covers the head (β > 55°: type Ib). The latter may lead to femora-acetabular impingement in the future.

Type IIa

The joint is subject to physiological immaturity. However, bony socket is deficient (α = 50–59°), which defines that bony socket is underdeveloped with respect to age. Bony rim is rounded and cartilaginous roof covers the

femoral head. Hereupon, type IIa is subdivided into (−) and (+) types according to calendar age. The examiner calculates the approximate maturation potential of the hip, and if the result suggests that the hip will not reach a mature hip by the end of 12 weeks, then the hip is classified as type IIa(−) in contrast to type IIa(+) in which the hip has an adequate ossification potential.

Type IIb

The descriptions that belong to type IIa are similar to that of type IIb; however, the hip has no longer of an adequate ossification potential to reach a mature hip at the end of 12 weeks. In brief, bony socket is deficient ($\alpha = 50–59°$) and the baby is older than 12 weeks of age.

Type IIc

Although the cartilaginous roof still covers the head, bony rim has lost its rotundity, and bony roof is severely deficient ($\alpha = 43–49°$). Type IIc is further subclassified as stable and unstable. Owing to severe deficiency at the bony roof and incongruency between the head and acetabulum, the femoral head can be decentered. In this case, the hip is classified as type IIc unstable and can be described as "decentering phenomenon." However, classification is made when the hip is in resting position.

Type D

The bony roof is severely deficient ($\alpha = 43–49°$), and although cartilaginous roof still covers the head, it is inadequate due to cranially oriented labrum. So the main difference between a type IIc and type D hip is the β angle ($\beta > 77°$). Therefore, a type D hip can be defined as "decentering hip."

Type III

The bony socket has a poor development ($\alpha < 43°$), and the bony rim is flattened due to superior and posterior displacement of the head. This displacement leads to a superior orientation of cartilaginous acetabular roof. Over time, compression and shear forces on the hyaline cartilage tissue of acetabular roof by displaced femoral head lead to degeneration. The magnitude and duration of these eccentric forces affect morphologic features of the cartilage tissue. On sonogram, according to existence of degeneration, type III can be subdivided into type IIIa and type IIIb. When the hyaline cartilage still has a hypoechoic appearance similar to that of femoral head, then the hip is classified as type IIIa. If shearing forces lead to deformation at the cartilaginous roof, then sonogram detects echogenicity and classified it as type IIIb. Due to structural pathology at type IIIb hips, a proper treatment may not prevent secondary dysplasia of the hip. Thereof, regular follow-up of such hips is necessary until skeletal maturity.

Type IV

Type IV hip is a decentered joint; the bony roof is underdeveloped with an $\alpha < 43°$, and superior bony rim is flattened. The perichondrium is pushed caudally into the true acetabulum. This difference leads to a distinction between type III and type IV in which the contour of perichondrium is toward to the acetabulum.

Documentation

The hip type can be stated after defining structural properties of bony rim and cartilaginous and bony roof in a sonogram that is viewed on standard plane. The alpha and beta angles further confirm the hip type. A sonometer is a practical way of defining the type (Fig. 9.5). Two hard copies, one of them is free of figured lines, and report of the sonogram including age, hip type, alpha and beta angles, and management strategy suggestion should be included [2].

Management and Follow-Up

Diligent ultrasonographic examination of a hip with positive risk factors or with positive clinical findings is crucial in initiating the management of DDH. As the infant hip has a great potential for ossification, early diagnosis should be made to benefit from this potential [16]. The ossification stands for stimulative effect of the femoral head through the acetabulum, in other words

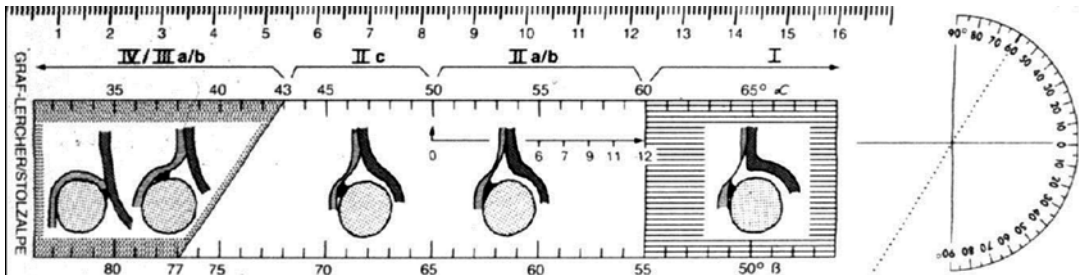

Fig. 9.5 Sonometer (Graf-Lercher/Stolzalpe)

Table 9.2 Treatment recommendations according to Graf classification

Type	Device/method	Duration
IIa(−)[a], IIb, IIc stable	Pavlik harness	Until maturation[b]
D, III, IV	i. Closed reduction	At least 8 weeks[c]
	ii. Abduction orthosis	

[a]Especially in newborn girls Omeroğlu et al. [4]
[b]Till an alpha angle of 60° by lateral scanning
[c]Abandon the closed reduction attempt if not reduced

"head in front of the door," so all decentered hips including type D, type III, and type IV together with a centered but type IIc unstable hip should be reduced properly followed by an adequate retention phase (Table 9.2) [2]. A retention device should place the hip joint to a maximum 45° of abduction and 90–100° of flexion. For centered joints with inadequate maturation including type IIa(−), type IIb, and type IIc stable hips, a device should be used to place the hips in crouching position until appropriate maturation [2].

Almost all type IIa(+) hips will spontaneously normalize until the end of 12 weeks of age [3]. However, the incidence of type IIa(−) hips through pursuance of type IIa hips is reported to be 15.6 %; thus, the recommended management of such hips is an abduction orthosis rather than wait-and-see regimen especially in newborn girls than boys [4].

The preferred orthosis in retention phase of treatment in this age is Pavlik harness [5]. With an attentive attention to the recommendations of Pavlik and using appropriate size of harness, Pavlik harness therapy has high satisfaction with low complication rate. Data from several studies have documented that prolonged harness treatment is necessary to provide enough time for dysplasia self-correction to occur [17–19]. Generally, 6–8 weeks of harness therapy is adequate for maturation [20].

Discontinuation of Pavlik harness therapy depends on two factors: hip stability confirmed by clinical examination and ultrasound findings. The Graf method may overestimate the number of unstable hips due to the position of the limb during lateral scanning [6]. Conversely, hip reduction can be assessed by an anterior approach such as the Suzuki method by measuring the femoral head coverage and reduction quality without weaning off the harness. Along with decentered hips, Graf type III hips were reported to wear short time with monitorization by anterior scanning compared to lateral scanning with the Graf method [6]. During follow-up of Pavlik harness therapy, subsequent monitoring with anterior scanning enables evaluation of hip reduction by demonstrating the positions of contour of the femoral head and chondro-osseous junction as well as ischial limb, which is the deepest part of the acetabulum in abducted position of the hip. To say that a hip is reduced, the center of the femoral head should be on the same horizontal plane with ischial limb. Immediately after harness application, many of Graf type III and type IV hips will reduce, and reduction quality can be checked through measurement of ischial limb-femoral distance by anterior scanning. This is not always the case; eccentric reduction can be seen in both types during the first 2–3 weeks of harness application. Under these

circumstances, Pavlik harness therapy should be ceased to avoid "Pavlik disease," which is the erosion of posterior and lateral parts of the acetabulum.

References

1. Dorn U, Neumann D (2005) Ultrasound for screening developmental dysplasia of the hip: a European perspective. Curr Opin Pediatr 17:30–33
2. Graf R (2006) Hip sonography: diagnosis and management of infant hip dysplasia. Springer, New York
3. Roovers EA, Boere-Boonekamp MM, Mostert AK et al (2005) The natural history of developmental dysplasia of the hip: sonographic findings in infants of 1–3 months of age. J Pediatr Orthop B 14: 325–330
4. Omeroğlu H, Caylak R, Inan U et al (2013) Ultrasonographic Graf type IIa hip needs more consideration in newborn girls. J Child Orthop 7: 95–98
5. Clarke NM (2014) Developmental dysplasia of the hip: diagnosis and management to 18 months. Instr Course Lect 63:307–311
6. Carlile GS, Woodacre T, Cox PJ (2014) Verification of hip reduction using anterior ultrasound scanning during Pavlik harness treatment of developmental dysplasia of the hip. J Orthop 11:174–179
7. Sezer C, Unlu S, Demirkale I et al (2013) Prevalence of developmental dysplasia of the hip in preterm infants with maternal risk factors. J Child Orthop 7:257–261
8. Omeroğlu H (2014) Use of ultrasonography in developmental dysplasia of the hip. J Child Orthop 8:105–113
9. Harcke HT, Clarke NMP, Lee MS et al (1984) Examination of the infant hip with real-time ultrasonography. J Ultrasound Med 3:131–137
10. Terjesen T, Bredland T, Berg V (1989) Ultrasound for hip assessment in the newborn. J Bone Joint Surg (Br) 71:767–773
11. Suzuki S, Kasahara Y, Futami T, Ushikubo S, Tsuchiya T (1991) Ultrasonography in congenital dislocation of the hip. Simultaneous imaging of both hips from in front. J Bone Joint Surg (Br) 73:879–883
12. Morin C, Harcke HT, MacEwen GD (1985) The infant hip: real-time US assessment of acetabular development. Radiology 157:673–677
13. Clarke NM, Harcke HT, McHugh P et al (1985) Real-time ultrasound in the diagnosis of congenital dislocation and dysplasia of the hip. J Bone Joint Surg (Br) 67:406–412
14. Dogruel H, Atalar H, Yavuz OY et al (2008) Clinical examination versus ultrasonography in detecting developmental dysplasia of the hip. Int Orthop 32:415–419
15. Eastwood DM (2003) Neonatal hip screening. Lancet 361:595–597
16. Tschauner C, Klapsch W, Baumgartner A et al (1994) Maturation curve of the ultrasonographic alpha angle according to Graf's untreated hip joint in the first year of life. Z Orthop Ihre Grenzgeb 132:502–504
17. Tucci J, Kumar S, Guille J et al (1991) Late acetabular dysplasia following early successful Pavlik harness treatment of congenital dislocation of the hip. J Pediatr Orthop 11:502–505
18. Alexiev VA, Harcke HT, Kumar SJ (2006) Residual dysplasia after successful Pavlik harness treatment: early ultrasound predictors. J Pediatr Orthop 26:16–23
19. Weinstein SL, Mubarak SJ, Wenger DR (2003) Developmental hip dysplasia and dislocation. Part I. J Bone Joint Surg Am 85:1823–1832
20. Carmichael KD, Longo A, Yngve D, Hernandez JA, Swischuk L (2008) The use of ultrasound to determine timing of Pavlik harness discontinuation in treatment of developmental dysplasia of the hip. Orthopedics 31(10)

Computerized Tomography in the Evaluation of Musculoskeletal System

10

Hatice Tuba Sanal and Sinan Akay

Abstract

With the advances in multidetector computerized tomography (MDCT) technology, indications for CT in the evaluation of musculoskeletal system have increased. Although magnetic resonance (MR) imaging of the musculoskeletal system has gained much attention over the years, indications for CT especially after MDCT got multiplied. While MR imaging is undoubtedly superior to CT in detecting soft tissue and bone marrow abnormalities with its inherited high-contrast resolution, MDCT is essential in several settings. With CT imaging, no absolute contraindications (such as cardiac pacemakers, electronic stimulators) have been identified as has been with MR imaging. The ease in availability of this modality has contributed to its indications mainly in the emergency departments especially with very short scanning times. CT is an excellent technique for detailed evaluation of skeletal trauma with the use of multiplanar reformations and three-dimensional-rendering techniques available, especially when complex fractures with articular involvement are suspected. Besides trauma patients, as an alternative to MR imaging in many situations, MDCT is particularly useful in patients who have metal hardware which otherwise metal artifact typically prohibits MR imaging evaluation. CT is also used to diagnose complications in fracture healing and selected bone tumors especially in evaluating the matrix mineralization and infectious diseases and to guide musculoskeletal interventions. The better delineation of skeletal structures adds to its advantages with multislice scanning and 3D-displaying capability.

H.T. Sanal, MD (✉)
Department of Radiology,
Gulhane Military Medical School,
Gn. Tevfik Sağlam Cad., Keciören-Etlik,
Ankara 06018, Turkey
e-mail: tubasanal@gmail.com

S. Akay, MD
Department of Radiology, Sirnak Military Hospital,
Sirnak, Turkey

F. Korkusuz (ed.), *Musculoskeletal Research and Basic Science*,
DOI 10.1007/978-3-319-20777-3_10

In this section, these and other indications for performance of CT of the musculoskeletal system, touching to the features of the modality, will be discussed.

Learning Outcomes

- To present some of the features of multidetector computerized tomography (MDCT), benefiting musculoskeletal imaging
- To display the optimum positioning and techniques in evaluating the related anatomic region
- To learn how to use MDCT efficiently for demonstrating bone, joint, and the other soft tissues with the aid of various softwares, after acquiring raw images following the examination

Terminology

Artifact Any discrepancy between the computerized tomography (CT) numbers in the reconstructed image and the true attenuation coefficients of the object.

Automatic tube current modulation Set of techniques that enable automatic adjustment of the tube current according to the size and attenuation characteristics of the body part being scanned and hence achieve constant CT image quality with lower radiation exposure.

Blurring effect The apparent streaking of rapidly moving objects in a still image or a sequence of images.

Contrast material Any internally administered substance that has a different opacity from the soft tissue on radiography, CT, or magnetic resonance (MR) imaging.

CT angiography An imaging modality that uses a CT scanner to produce detailed images of both blood vessels. A CT scan is then performed while the contrast flows through the blood vessels to the various organs of the body. After scanning, the images are processed using a special computer and software.

CT/MR arthrography A series of images acquired by CT/MR, after injection of a particular contrast medium into the joint.

Curved planar reformation A type of multiplanar reformation accomplished by aligning the long axis of the imaging plane with a specific anatomic structure, such as a blood vessel, rather than with an arbitrary imaging plane. This is particularly useful in displaying an entire vessel, ureter, or a long length of intestine.

Field of view (FOV) It is the diameter of body region area being imaged.

Gantry A frame housing the X-ray tube, collimators, and detectors in a CT, with a large opening into which the patient is inserted; a mechanical support for mounting a device to be moved in a circular path.

Image reconstruction Mathematical process that generates images from X-ray projection data acquired at many different angles around the patient. Image reconstruction has a fundamental impact on image quality and therefore on radiation dose.

Isotropic imaging Ideal case for imaging three-dimensional structures is to have resolution identical in all dimensions, easing MPR and 3D images obtained free from certain artifacts.

Kilovoltage (kVp) Electric potential difference or electromotive force, as measured in kilovolts.

Metal artifact Severe artifact due to presence of metal objects in scan field.

Milliampere (mA) A unit of electric current equal to 1,000th of an ampere.

Multidetector computed tomography (MDCT) Its two-dimensional detector array permits computed tomography scanners to acquire multiple slices or sections simultaneously and thus greatly increase the speed of image acquisition.

Multiplanar reformation (MPR) The process of using data from axial computed tomography images to create nonaxial two-dimensional images. MPR images are coronal, sagittal, oblique, or curved plane generated from a set of axial images.

Noise The presence of noise gives an image of a mottled, grainy, textured, or snowy appearance.

Picture archiving and communications systems (PACS) A medical imaging technology which provides economical storage of and convenient access to images from multiple modalities.

Postprocessing All procedures performed by specific computer systems after the image acquisition.

Spatial resolution The smallest discernible detail in an image.

Stairstep artifact It appears around the edges of structures in multiplanar and 3D-reformatted images when wide collimations and nonoverlapping reconstruction intervals are used.

Surface shading A surface-rendered image that provides a realistically looking 3D view of the surface of a structure.

Workstation Special computer designed for technical or scientific applications.

Clinical Relevance

1. *Is MDCT useful for evaluating multisystem trauma patients in the acute stage*?

   A 21-year-old male was admitted to the emergency department with multitrauma due to falling off a height. Head, shoulder, and left arm trauma signs were observed in addition to the extensive skin abrasions and ecchymoses at the left side of his body. His left elbow was prominently swollen, and elbow movements were painful and restricted on physical examination. The left elbow was splinted in order to decrease massive pain and to immobilize the joint just after the initial intervention in the emergency room. Multidetector computerized tomography (MDCT) was planned for his head, left shoulder, and elbow in order to evaluate probable pathologies after the initial radiograms. No fracture or soft tissue pathology was detected on the head and shoulder during computerized tomography (CT) examinations. However, on elbow CT, proximal radial and ulnar fractures plus radioulnar joint dislocation were observed (Fig. 10.1). The patient was operated the day after the trauma, and internal-fixating materials were implanted for stabilizing his fractures.

   Trauma remains the leading cause of death in people of age 45 and younger [1]. Multisystem trauma (polytrauma) is defined as injury to more than one body region such as the head, chest, abdomen,

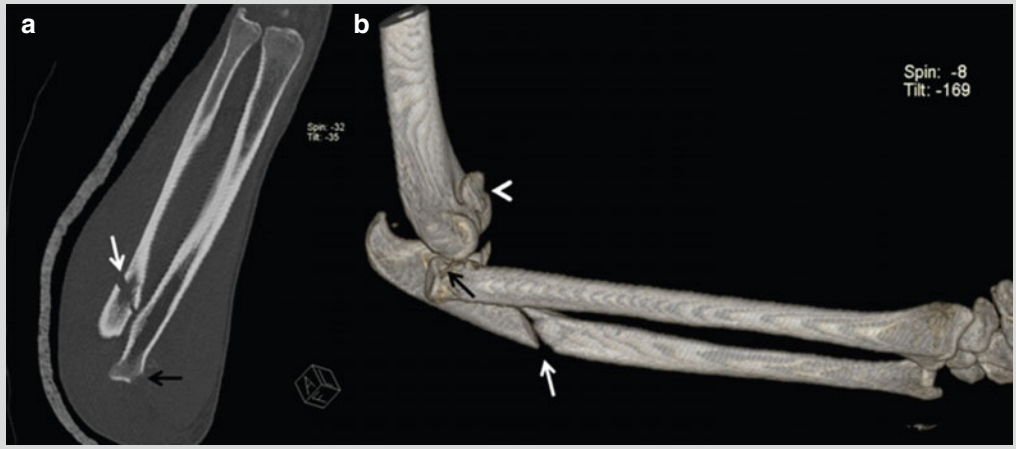

Fig. 10.1 On multiplanar reformatted oblique coronal image (**a**), proximal ulnar (*white arrow*) and radial head fractures (*black arrow*) are readily seen. Three-dimensional reconstructed image in bone window (**b**) demonstrates the two fracture lines, prominent elbow dislocation, and the free bone fragment (*arrowhead*) in front of the humerus

and extremities, which may be potentially fatal to the patient [2].

The introduction of MDCT led to further advantages in the setting of trauma. Scanning time was substantially reduced, and motion artifacts that were commonly observed with the slower scanners could be eliminated. Thinner slice collimation available allowed high-quality reformatted images in differently oriented planes whenever necessary [3].

In evaluating the multisystem trauma patients, time interval between the initial evaluation in the emergency room and the CT scanner becomes highly important. Dedicated trauma departments should have their own CT scanner available for the emergent multitrauma patients [4].

In the abovementioned case, after the initial evaluation and the stabilization of the patient in the emergency room, we were able to perform a multisystem CT examination in our dedicated CT scanner without any significant time loss. While lying in the CT gantry, owing to multitrauma and massive pain at his left elbow, a routine positioning to the patient could not be given. Nevertheless, although the patient was not in the proper position on the table, we were able to perform the CT examination and acquire qualified images without necessity of removing the splint.

2. *Is it possible to perform initial and control musculoskeletal CT examinations with reduced doses by using dose modulation strategies*?

Since its introduction in the 1970s, besides in the trauma setting, CT has played a major role in the diagnosis of many musculoskeletal diseases. Even though image quality is altered by metallic artifacts, CT also found indications in post-surgical imaging [5]. However, CT is a technique working on the principle of X-ray radiation that is responsible for the majority of medical irradiations [6].

In the last few years, MDCT has benefited from technological innovations, thereby considerably reducing the dose delivered to the patient. With these technological innovations and better control of the image acquisition parameters, it is now

possible to obtain CT images in lower doses [7].

There are some rules of thumb to reduce the radiation from CT in the evaluation of the diseases of the musculoskeletal system such as (1) comply with the diagnostic indications; (2) where possible, see if a non-radiating imaging method (i.e., ultrasound or MR imaging) can help to solve the clinical problem in question; (3) limit the CT coverage and number of acquisition phases during dynamic and perfusion examinations; (4) adopt the kilovoltage and milliampere according to the indications and morphology of each case; (5) reduce the kilovoltage during the exploration of the peripheral joints and arthro-CT; and (6) choose modern methods to reduce the dose (i.e., iterative reconstructions, automatic modulation of the milliamps, etc.) [7].

While evaluating the patients especially in pediatric age who are planned to perform initial or reexamination (postoperative or control) of CT scan, basic dose reduction strategies should always be in the clinicians' minds. Without sacrificing the image quality requisite for a proper diagnosis, one should care ALARA principle which describes the diagnostic X-ray utilization as "As Low As Reasonably Achievable" [8].

3. *Compared to the standard axial images, are multiplanar reformatted and/or three-dimensional-reconstructed images more beneficial for orthopedists in guiding preoperative session*?

Clinical applications of CT have increased extensively over the past decade and continue to widen. The introduction of three-dimensional (3D) reconstruction in CT technology has revolutionized medical imaging. With the anatomy displayed which the orthopedist may get more familiar with, this technique may have advantages in the preoperative planning of craniofacial surgery, assessment of complex fractures, and surgical treatment of dysplastic hips in children [9].

Three-dimensional CT imaging studies have come to stay, and with continued improvement in CT technology, it has now become an integral part of imaging studies of the musculoskeletal system [9]. Nevertheless, axial images should not be neglected, and these and three-dimensional images should be evaluated hand in hand.

The combination of axial, multiplanar reformatted CT and 3D reconstruction with volume rendering allows rapid and detailed examination of the musculoskeletal system. In a substantial number of cases, management may be altered with the findings seen better on the 3D images such as subtle fractures, complex injuries extending to joint spaces, and cases with metal hardware otherwise causing metallic streak artifacts and hence masking the pathologic conditions nearby. By displaying complex spatial information, 3D images are useful for conveying complicated anatomic information to orthopedists [10].

4. *Ultrasound or CT-guided biopsy in musculoskeletal mass lesions*: *which one should be selected*?

Soft tissue masses and bone lesions may require biopsy. The approach in performing these biopsies, in some ways, is not different from other nonmusculoskeletal biopsies and requires careful review of all the relevant clinical and radiological information [11].

The majority of musculoskeletal lesion biopsies are performed to determine whether there is an underlying neoplasm. In some cases where patients are unresponsive to conventional antibiotic therapy for treatment of bone or soft tissue infections, a biopsy may be performed to isolate the proper organism and direct a targeted antimicrobial therapy [11].

In the above terms, ultrasound is a commonly used modality for performing musculoskeletal soft tissue biopsies [12]. It can also be used for lesions near a bone surface or for a bone lesion with an extraosseous component [13]. Ultrasound is widely available, is minimally invasive, and offers real-time imaging. Its high spatial and contrast resolution also allows easier visualization of lesions, particularly small lesions that are difficult to visualize on noncontrast CT. Although CT or MR imaging can be used, the dynamic nature of the ultrasound allows easier and more comfortable patient and operator positioning. Ultrasound allowing real-time visualization of the needle provides a safe and satisfactory biopsy by avoiding nearby vital structures [14]. Furthermore, ultrasound-guided biopsies are free from ionizing radiation.

Computerized tomography-guided biopsies may be used for some bone lesions and soft tissue neoplasms. Computerized tomography, via cross-sectional images, displays excellent spatial localization of the lesion which is needed to determine the route that is safe, avoiding vital neurovascular structures nearby [15]. In general, avoiding crossing of more than one anatomic compartment is important in preserving a limb-salvage surgical plan; otherwise, the needle track is at risk of seeding tumor cells to multiple compartments [16].

Introduction

In the last two decades, computed tomography (CT) has brought a new insight into the radiography and magnetic resonance (MR) imaging-focused musculoskeletal examinations [17]. The advancements in the technology and the software systems have great impact on the increasing role of CT in musculoskeletal imaging. The importance of CT has increased further with the emergence of multidetector CT (MDCT) systems. It is now possible to get high-resolution images after a short scanning time with the isotropic spatial information that these systems can obtain. Decreased scanning time has allowed minimizing the problems that may arise secondary to the patient motion during imaging [18]. High-quality multiplanar reformatted (MPR) and three-dimensional (3D) images created at the separate workstations can easily be captured by the clinician compared with one single-plane image.

The picture archiving and communications systems (PACS) enable the postprocessing with interactive viewing and reformatting, using isotropic or near isotropic data sets that MDCT yields. These images can be permanently archived in PACS and be called any time when the comparison is needed in follow-ups [18].

While MRI is superior to CT in detecting and defining soft issue and bone marrow abnormalities given its inherited high-contrast resolution feature, MDCT is essential in several situations [5]. In trauma settings especially imaging complex skeletal injuries, fracture lines and their extensions are superbly defined by MDCT [19, 20]. Unlike MRI, for the evaluation of bone and soft tissue masses, CT can display and characterize mineralization, cortical disruption, and periosteal reaction more readily [20]. In postoperative evaluation of patients with metal armamentarium, MDCT allows imaging without generating significant metallic artifact [20]. The absolute contraindications such as cardiac pacemakers and electronic stimulators described for MR imaging are not applicable for CT, where this allows the technique a possible alternative to MR imaging in those settings.

In this paper, the utility of CT in imaging the musculoskeletal system will be provided by touching the technical aspects of MDCT.

MDCT Technique: Basics

The launch of MDCT into imaging stage in 1998 has opened a new page in radiological examinations. With the very fast image acquisition phase that MDCT can yield, total body scanning times have been reduced below 30 s [21]. Scanning speed is favorable especially when scanning large segments of the body or performing a dynamic imaging such as perfusion or CT angiography where image acquisition has to be fast [21].

Contrary to previous CT systems which have single detector, the X-rays pass through the patient body part to reach multiple channels with MDCT. The MDCT is called with the number of detectors it has, for example, if the detector row has four channels carrying information concurrently in each X-ray gantry rotation, the scanner is then called a four channel [21]. This means in each gantry rotation with X-rays passing through the relevant body part, more than one datum will be obtained, i.e., four in the previous example. Joined with the faster X-ray rotation speeds, CT data now can be collected faster and so the patient can be imaged rapidly than conventional single-slice helical CT [21, 22].

Projection data (PD) described by Dalrymple et al. [23] are the initial raw data collected by the CT detectors. Without any mathematical conversion in computerized media, these data from the body part cannot be viewed directly or used to create 3D images. Projection data are first used to generate axial images on the CT scanner. The spatial properties of PD are determined by the scan settings by the technologist or radiologist on the console, and once the data is obtained, it cannot be altered later. As long as the projection data are kept on the CT scanner and not deleted, (1) the thickness of the axial images (either thin or thicker slices), (2) the body part of interest (field of view, FOV), and (3) the reconstruction algorithms (i.e., bone or soft tissue) can be generated [18].

The flow of the information from the detectors can be picturized as shown below:

Isotropic Imaging

Thin sections are preferable for imaging musculoskeletal system in order to create multiplanar reformatted (MPR) and 3D images with superb spatial resolution [21, 24]. Isotropic imaging obtained with thin slices (i.e., 0.5 mm slice thickness) will yield MPR and 3D images with high spatial resolution and fine detail without possible artifacts such as "stairstep" and blurring effects [24]. Performing CT with thinner slices warrants creation of images in any plane with high spatial resolution. This issue particularly comes into account when imaging traumatized patient comfortably in any position she/he can bear, without giving a specific position in order to image the injured body part [24]. Complex joints such as the wrist and foot can be examined in any plane with multiplanar reformatted images without any sacrifice in the image detail, as a consequence of isotropic imaging with thinner slices [24]. Thinnest slice section issue has its own drawbacks, however, in terms of the noise of the image and the radiation dose for the patient, which will be discussed below.

Multiplanar Reformatting: MPR

Images at any plane can be reconstructed by the doctor himself on the workstations by interactive means, which by this way one can observe any point of interest in each plane. In order not to miss subtle fractures, the MPR images should be viewed as thin as possible to the point of apparent noise level which produces somewhat granulation on the image. When images become noisy, this problem may be reduced by fusing thin slices into much thicker images [18].

Three-Dimensional (3D) Imaging Methods (Surface Shading/Volume Rendering)

With the aid of improved software systems and powerful computer-based workstations, 3D imaging is now possible with isotropic volumetric data set. Three-dimensional images can be colored as well, and clinicians become more familiar with and easily perceive the anatomy like the one he expects on the operating table. Though 3D images may facilitate the orientation to the anatomy, axial and MPR images should not be neglected, and 3D imaging should stay as an adjunct [18]. Three-dimensional images readily show the extent of tendons and muscles and their relationship to bones and joints when injured (Fig. 10.2). Three-dimensional images are also subject to less metal artifact when imaging those with metal armamentarium in their postoperative stage [22, 25, 26].

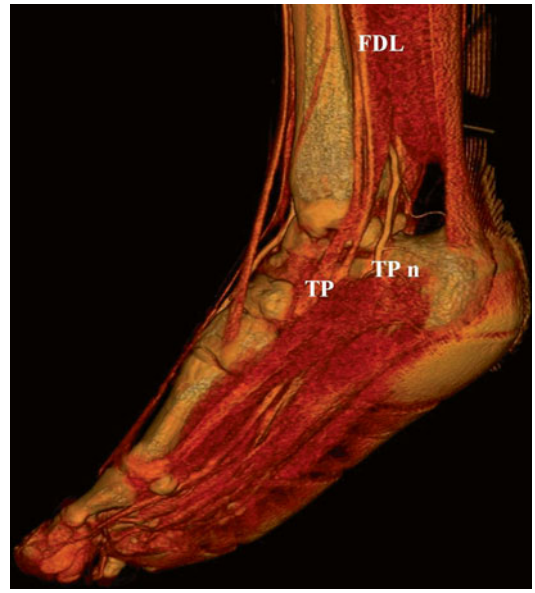

Fig. 10.2 It is possible to display the courses of the tendons, and their relationships with the bones as in the cadavers on 3D volume-rendered (*VR*) images by using advanced computer systems and softwares. *TP* tibialis posterior tendon, *FDL* flexor digitorum tendon, *TPn* tibialis posterior nerve

Radiation Dose

Multidetector CT being a high-dose imaging technique is well known [18]. The continuous recommendation for using the smallest slice thickness available to obtain isotropic data sets brings the concern for radiation dose to the patient. Especially when cervical vertebrae, facial bones and pelvis are examined with this technique, thyroid gland, lens and internal genitals which are sensitive to radiation, are subject to high doses during imaging. For this reason, the patient should be reevaluated for the indications of imaging the cervical vertebrae, skull, and pelvic region, and MDCT should not be used regularly for negligible trauma involving these regions [18].

The intensity of diagnostic X-rays from CT gantry can be reduced by decreasing the kilovolt and milliampere values when imaging the peripheral skeleton especially the forearm and leg since these structures are thin [18]. In the pediatric patient, radiation dose deserves much more importance; hence, it is wise to adhere the scanning parameters indicated in the literature for pediatric population [18]. Computerized tomography manufacturers also give hand to this problem by introducing new measures for reducing patient dose such as automatic tube current modulations which adjust the intensity of X-rays based on the thickness of the anatomy

being scanned. Nevertheless, MDCT should be handled as a high-dose technique, and the benefit-to-risk ratio to the patient with this examination should be thoroughly evaluated.

General Approach to the Musculoskeletal Imaging

Oblique Image Acquisition Principle

When isotropic imaging is not possible due to the limitations of the scanner or thick slices (>0.5 mm) have been selected instead of thinner slices, the quality of the following MPR images can be sustained by "obliquity principle" [24]. In order to visualize much of the joint surface, it is recommended that the affected extremity be placed in the gantry according to the following rules: (1) position the extremity obliquely (45° is optimal) and (2) in the center of the gantry (resolution is maximized in the center) [24].

Extended Anatomic Coverage

In order to assess the extension of a lesion and the anatomic regions it affects, a sufficient portion in the neighborhood should be incorporated into the area of interest (Fig. 10.3).

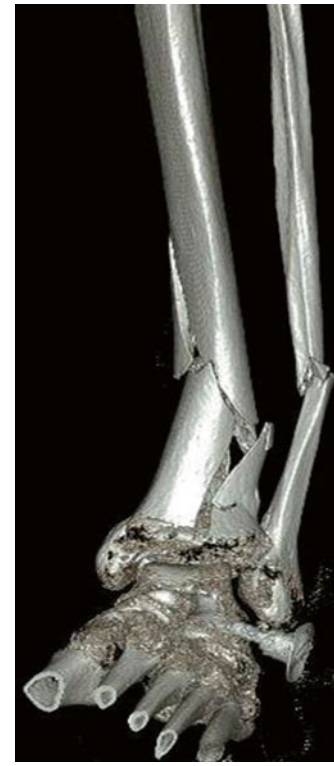

Fig. 10.3 Three-dimensional volume-rendered (*VR*) image with a large field of view that is acquired for demonstrating the fracture extension in a case with fragmented fracture at the tibia and fibula, with medial angulation of the long bones

Patients with Metal Hardware

Metal hardware such as prostheses and fixation devices causes artifacts in CT. The composition and thickness of the hardware, the geometry of the metal according to the body region, and the kilovoltage (kVp) and milliampere-second (mAs) values designated on the console by the imaging technician and the image reconstruction algorithms used are the factors affecting the intensity of the artifact created [27].

Hardwares made up of titanium causes less artifact compared to other metals [27]. The artifact created is also related to the thickness of the metal, and it is greatest at the thick portion of the metal hardware (Fig. 10.4) [27]. Selection of a "soft tissue" or smooth reconstruction filter especially for dense metal hardware is recommended while examining the images. It is also possible to play with the window settings interactively across the workstation, trying to get most diagnostic images in the neighborhood of the metal armamentarium.

Dual-Energy CT

This technique is based on the acquisition of two superimposable images with two different kilovoltages. Based on these native images, it is possible to reconstruct a virtual image corresponding to any voltage of the x tube. Several

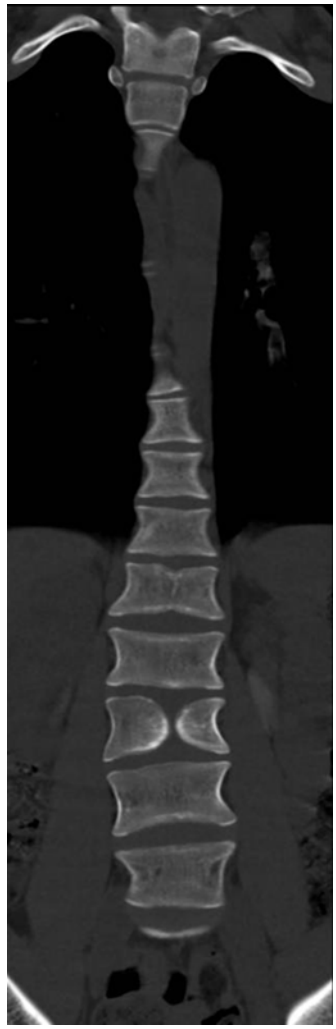

Fig. 10.4 Coronal multiplanar reformatted (*MPR*) image of a case with a butterfly vertebra at the thoracic spine

applications of the dual-energy CT in the osteoarticular clinical settings are now available for improvement in tissue characterization such as identifying subclinical tophus deposits by producing color displays for urate deposits [28, 29].

Applications with CT

Congenital Anomalies

It is possible with CT to examine cases with pectus deformities and skeletal dysplasia syndromes who may require large field of view to display the morphologic features of these disorders and associated deformities [5]. Owing to CT being a cross-sectional imaging modality free from superposition of structures as with conventional radiography and the possibility of displaying the images in various planes, vertebral anomalies can readily be seen with CT (Resim 3) [5].

Tarsal coalition is the fusion of the bones of the foot that may lead in deterioration of the foot dynamics and cause pain because of the abnormal differentiation and segmentation of primitive mesenchyme [20]. MDCT can be used to display the coalition in different planes and have an impact on decision making, either surgical resection or arthrodesis options [20]. The most common forms of coalition are ones between the talus and calcaneus and the calcaneus and navicular bone. Observing the reformatted images of the subtalar joint from anterior to posterior helps to examine the coalition which the coronal plane is the most valuable (Fig. 10.5). When the coalition is not osseous but fibrous or cartilaginous instead, findings like cyst formation and sclerosis can be seen as a consequence of osteoarthritis.

Trauma

Advanced trauma life-support guidelines on the initial assessment of patients with trauma propose radiographic examination as the initial modality; however, MDCT used at this stage is increasing in some centers [20]. The short examination time, patient comfort in the gantry, high sensitivity, and specificity compared to plain radiography make MDCT valuable in trauma occasions [20].

Fractures, dislocations, and joint abnormalities secondary to trauma can be readily displayed by MDCT. High spatial resolution allows to perceive and localize the tiny bone fragments and guides the surgeon before the operation [19]. Three-dimensional images, complementary to axial and reformatted images, have great impact on diagnosis and management of the spine and maxillofacial region trauma with complex anatomy [19, 25].

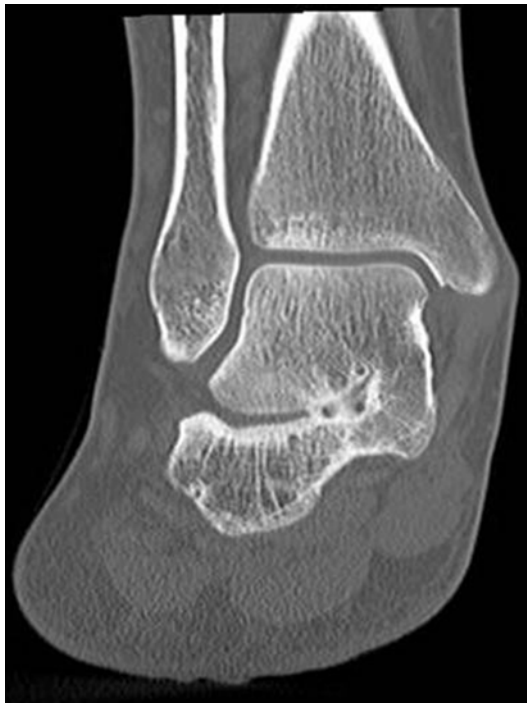

Fig. 10.5 Osseous coalition between the talus and calcaneus is readily seen on coronal reformatted image

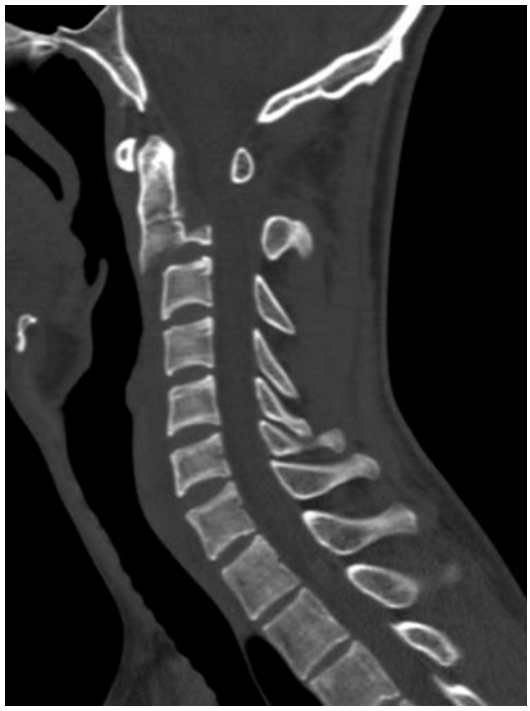

Fig. 10.6 Sagittal reformatted image of a case with unstable fracture involving the second cervical vertebra

Spinal trauma can result with permanent spinal cord injuries or even death, so it is important to identify fractures involving the vertebrae [17]. In multitrauma cases, MDCT images can be obtained from head to toe while the patient is lying in the gantry, and without changing position or at the expense of additional radiation, spine images can be reconstructed. With this approach, a 20 % reduction in the radiation dose for the patient can be achieved [17].

On Multiplanar reformatted images, obtained with thin slices and an overlap of 50 %, fractures are readily identified compared to radiographs (Fig. 10.6). Classification of spinal fractures and evaluation of the stability of the vertebral column can be done with high accuracy using MDCT. However, difficulty in identifying the injuries of ligaments and spinal cord is among the main restrains of CT. Ligamentous injury alone without an evident vertebral fracture has been noted previously [30]. As mentioned before, in the evaluation of cervical spinal trauma with CT, the radiation-sensitive organ, thyroid gland, is significantly radiated, and this issue is becoming more and more important in children.

It is important to know the extent of the fracture line to the glenohumeral joint when shoulder trauma is of concern [22]. In order to be free from artifact, and to reduce the radiation by automatic dose reduction system of the CT scanner, the other nontraumatic arm should be settled out of the field of interest, preferably overhead. Scanning should involve the shoulder joint from the acromioclavicular joint to the infrascapular region. A 2 mm section thickness with 50 % overlap yields optimum reformatted images for evaluating the shoulder and humeral fractures. Evaluating the three-dimensional images make the clinician more familiar with the anatomy (Fig. 10.7). However, it is advocated to evaluate 3D images in conjunction with axial and reformatted images. Volume-rendered imaging yields more favorable images with less artifact, when metal hardware is of concern. Nevertheless, the quality of 3D images is related at one hand with the software of the computing system available.

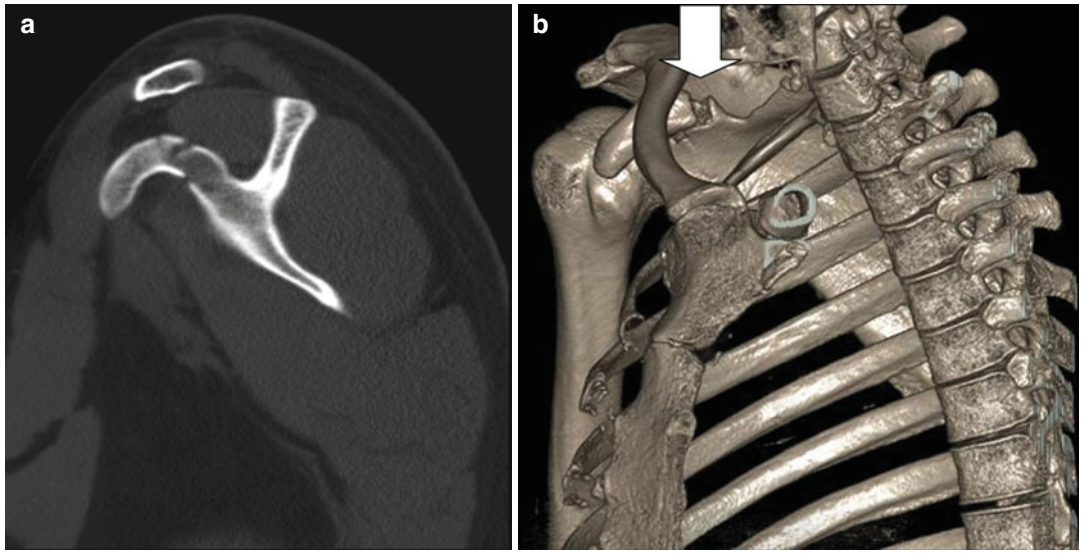

Fig. 10.7 On sagittal reformatted (**a**) and 3D (**b**) images, a case with coracoid process fracture is well seen

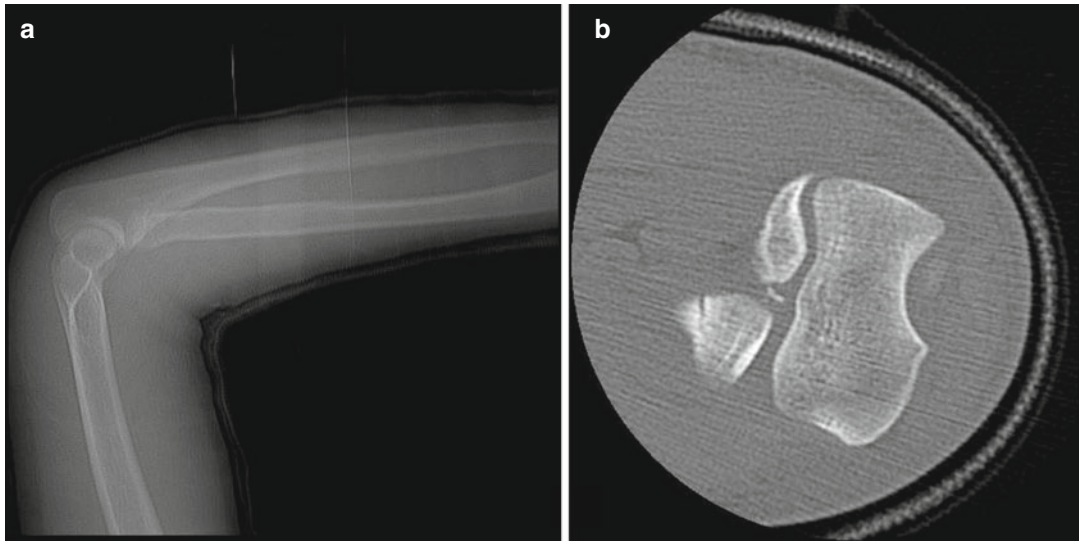

Fig. 10.8 A patient with elbow joint fracture is lying inside the gantry in "Superman" position while his flexed joint located at the center (**a**). Note the thin fracture line at the radial head and fractured piece in the radioulnar joint space (**b**)

High-quality multiplanar reformatted images ease to evaluate the fractures of the elbow and the free bony fragments in the joint [22]. Whenever possible, it is recommended to image the elbow joint, with patient in the "Superman position" and the shoulder stabilized with a pillow (Fig. 10.8). However, positioning the patient this way in multitrauma occasions is difficult, and in many cases, the patient lies in the gantry on supine, in a comfortable manner. A 1 mm section thickness with 50 % overlap yields optimum reformatted images for evaluating the elbow. As with other complex regions, evaluating the three-dimensional images make the clinician more familiar with the anatomy of the elbow (Fig. 10.9).

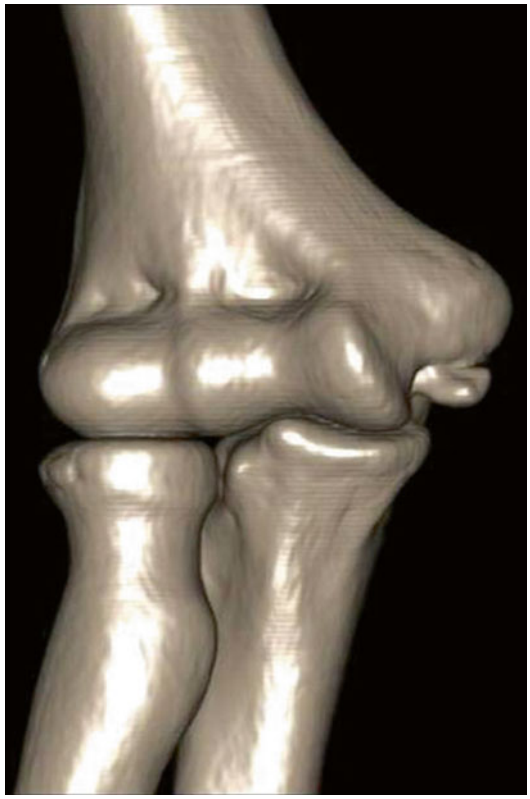

Fig. 10.9 On 3D image of a case with medial humeral condyle fracture, the rest of the bony structures are seen with their normal integrity

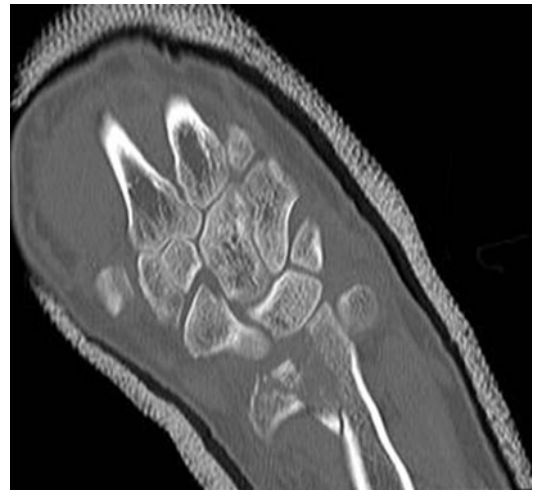

Fig. 10.10 Coronal multiplanar reformatted (*MPR*) image acquired with 0.5 mm slice thickness and 50 % overlap of a case with multifragmented fracture at the distal radius that reaches to the radiocarpal compartment. Note that the images have been acquired without the need for removing the plaster and while the patient is comfortably lying in the gantry

It is important to reveal fragments in the compartments and show the integrity of the wrist joint in the fracture scenarios [22]. Fractures can involve radiocarpal and radioulnar joints. The prognosis worsens when the ulnar styloid is fractured. For the most favorable images, the patient should lie in prone and the wrist in the center of the gantry. Slice thickness ideally less than 0.5 mm using small focal spot and bone algorithm yields optimum axial and MPR images. It is important to remember that the fracture can extend proximally, so adjusting the CT scan coverage beyond the fracture enabling assessment of the long bone axis eventually may affect treatment decision. In CT gantry, there is no need to take off the bandages or casts, and the images can be obtained in any position the patient feels comfort (Fig. 10.10).

Diagnosing the scaphoid fractures is important in terms of late complications such as avascular necrosis or nonunion [20]. When the radiographs are inconclusive or disconcordant with the clinics, it is recommended to examine the patient with MRI in acute cases of suspected scaphoid fractures [20]. MDCT is successful in revealing the complications and the method of choice in displaying displacement and the angulation of the fracture, according to the guidelines by the American College of Radiology [20].

Owing to its ringlike shape and the neighborhood anatomical structures superimposed, it may be difficult to discern fractures by the radiographs. It is crucial to evaluate all the links in the pelvic ring for stability. MDCT plays an important role with the availability of getting MPR and 3D images in pelvic ring fractures with substantial risk of mortality secondary to bleeding due to main vessels extending in the pelvis [22]. The entire pelvic ring can be screened with 3–4 mm slice thickness. In elder patients referred to CT imaging with hip pain after a fall, it is not rare to see pubic ramus or sacral fractures. Therefore, in patients who present with posttraumatic hip pain, it will be an appropriate approach to evaluate the

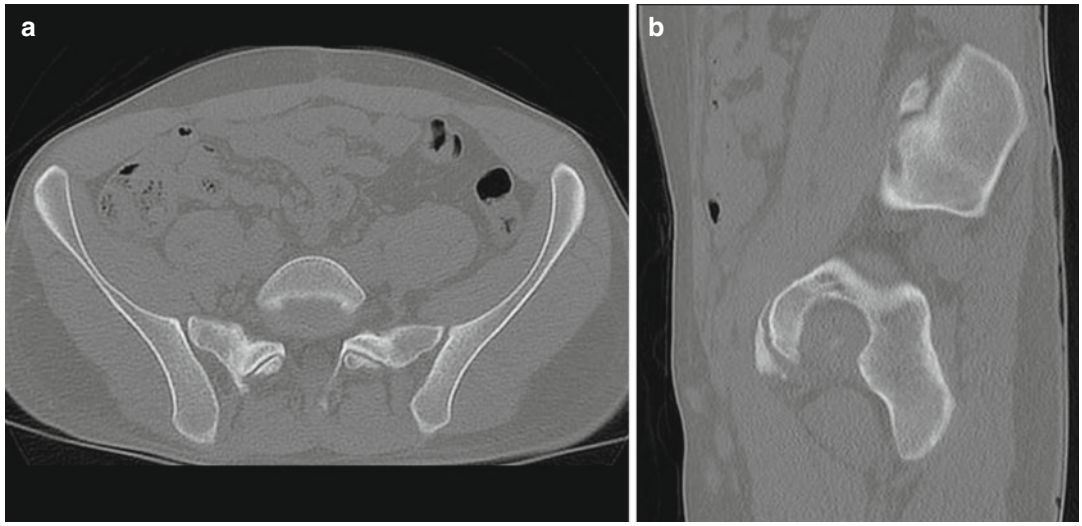

Fig. 10.11 Axial image acquired in 3 mm slice thickness for scanning the whole pelvis of a trauma patient that fell on his side (**a**). After the evaluation of these images, an acetabular fracture extending to the joint is seen on sagittal reformatted image, specifically acquired for hip joint in 2 mm slice thickness (**b**)

whole bony pelvis, but hip joint alone. For the hip joint, reformatted images obtained by 1 mm slice thickness with an overlap of 50 % will be optimal (Fig. 10.11). Haris et al. have classified the acetabular fractures based on CT images [31].

The proper classification of the tibial plateau fractures is important for proper treatment and good prognosis [22]. To evaluate the presence of depression, revealing the extent of the fracture in the long bone is important, and MDCT imaging with thin sections and large field of view enables optimum evaluation (Fig. 10.12). Images reformatted from 1 mm thick with a 50 % overlap provide proper 3D images of good quality.

The complex anatomy of the ankle joint and the tarsal bones can be scanned by CT while the patient lies comfortably in the gantry [22]. Axial images obtained by thin section, small focal spot, and bone reconstruction algorithm yield optimum MPR and 3D images and ease the evaluation of the tarsal bones, the ankle mortis, and the subtalar and Lisfranc joints (Fig. 10.13).

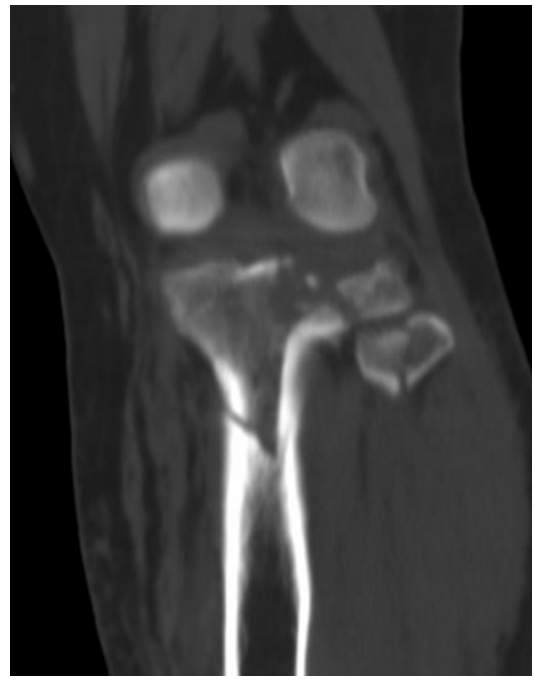

Fig. 10.12 On coronal reformatted image, the tibial fracture, classified as Schatzker type 6 is well seen. Additionally, a distinct fracture line at the fibula is observed

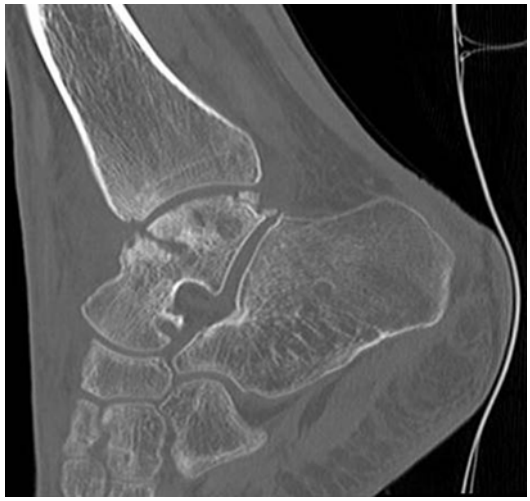

Fig. 10.13 The existence of old fracture lines that causes talar broadening is seen. Bones display osteoporotic appearance secondary to disuse

For the evaluation of the spine, sternum, and ribs, "curved planar reformatted" images are quite useful; even small fractures can be detected easily.

Postoperative Evaluation of Fracture Reductions

CT is advantageous in the postoperative period for the evaluation of the complex fractures and possible complications such as infection, broken rods/screws, particle disease, and osteolysis [26, 27].

Fracture Healing

Conventional radiographs often have limited value in showing the nonunion in the fracture lines. MDCT is more informative and hence in the detection of fracture healing has substituted radiographs in many centers [27]. MPR images enable thorough evaluation of the fractures, the stages of healing, and the callus formation. Besides, with conventional radiographs, it may

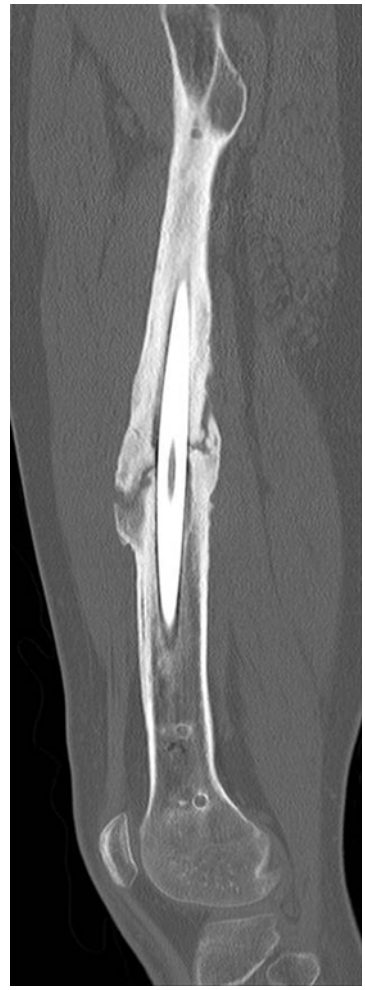

Fig. 10.14 Nonunion of a fracture in the diaphysis of the femur with an intramedullary nail

be difficult to assess the healing process in patients with metal protheses and other implanted metal hardware [27, 32] (Fig. 10.14).

Bone Tumors

Although MR imaging is undoubtedly superior in the detection of bone marrow pathologies, in the evaluation of matrix mineralization, CT is often needed (Fig. 10.15) [33]. MDCT is valuable in revealing bone destruction and periosteal

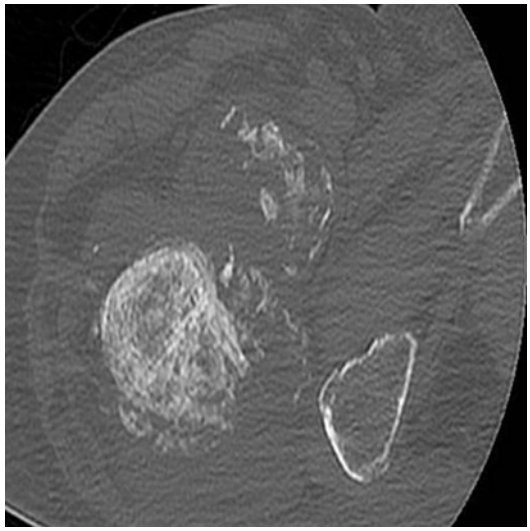

Fig. 10.15 The tumor located in the femoral trochanter with a soft tissue component displaying mineralization is seen

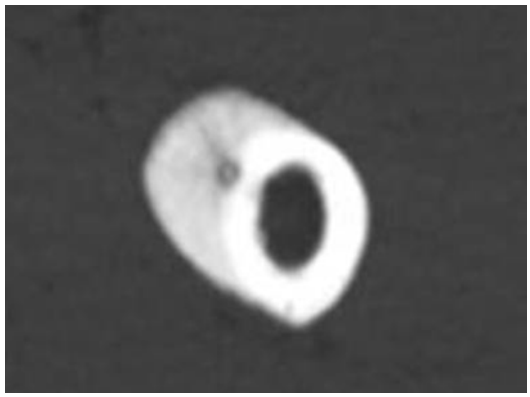

Fig. 10.16 Subperiosteally located nidus of the osteoid osteoma causing extensive periosteal reaction at the femoral diaphysis is seen

reaction which are not clarified or obvious by MR images or with radiography. For osteoid osteoma that originated in the complex anatomic regions such as the spine, CT has been advocated as the best imaging modality [34]. In these cases, before local ablative therapies, for displaying the location of the nidus and to guide ablation, CT is preferred (Fig. 10.16). Vertebral hemangiomas can be distinguished by their typical "polka-dot" appearance in the axial CT scans.

Infection

In infection cases, plain radiography, MRI, and scintigraphy remain the standard tests where CT can be added to the diagnostic algorithm in difficult cases (Fig. 10.17). CT is superior in demonstrating soft tissue mineralization that is difficult to discern on radiographies or MR images, accompanying chronic infections such as tuberculosis or fungus. Sequestration of chronic osteomyelitis can be readily observed on CT images. Besides MDCT guides to biopsy and therapeutic injections with the extreme accurate placement of needles with the cross-sectional images it yields [20].

Arthrographic Examinations

MR arthrography (MRA) better reveals internal derangements of joint structures with the aid of stretching the joint capsule by the diluted contrast material [20]. However, CT arthrography (CTA) has a number of benefits over MRA such as; i) not possessing the same absolute contraindications that MR has and ii) being much quicker with higher spatial resolution and minimized metallic artifacts. Its specificity and sensitivity is around 90 % in demonstrating the recurrent meniscal tears. CTA is successful in shoulder joint by demonstrating the rotator cuff, labral pathologies and articular surfaces. Ligament tears, triangular fibrocartilage complex injuries, and cartilage lesions can be equally displayed by CTA [34, 35].

CT-Guided Biopsies

Although ultrasound is widely available and minimally invasive and offers real-time and multiplanar imaging, CT may also be used as a guide for biopsies. CT provides excellent spatial localization of the lesion which helps to determine the route that is safe to avoid vital neurovascular structures [15].

When placing the patient on the CT table, correct positioning is very important as it will allow

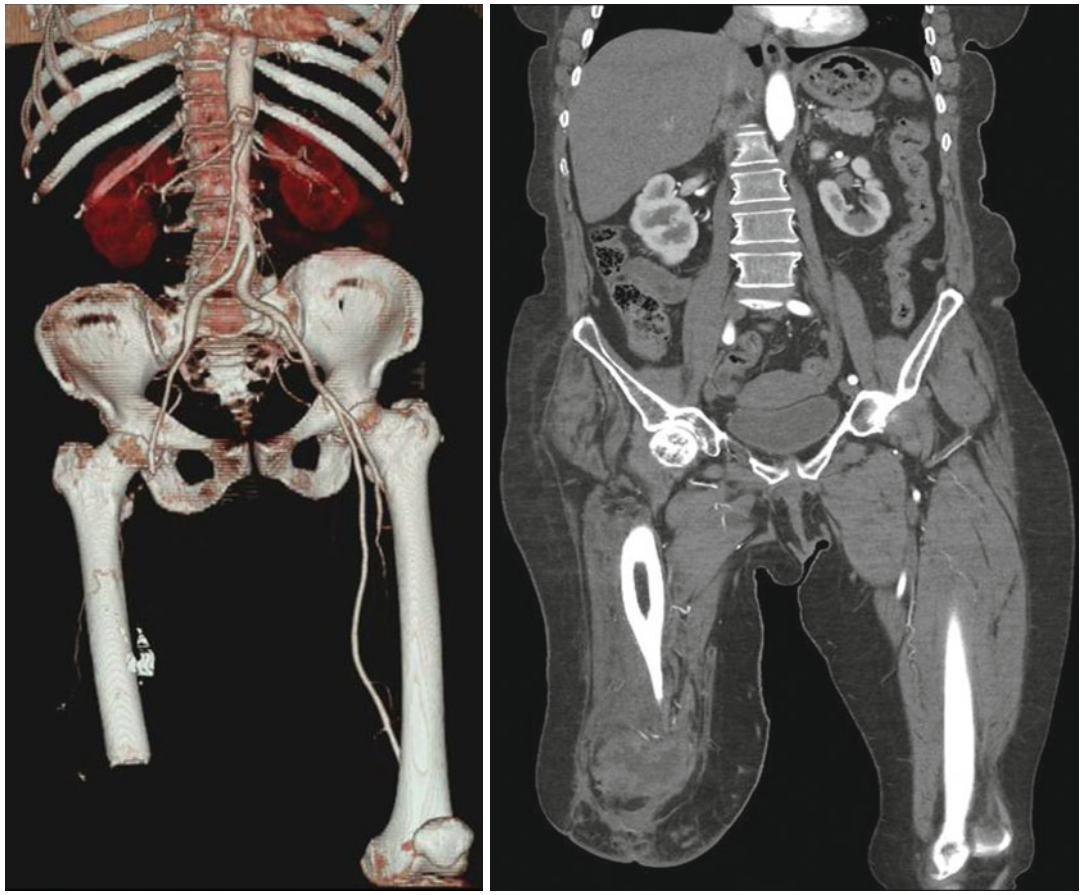

Fig. 10.17 A case with right above-knee amputation secondary to diabetes mellitus. On multidetector computed tomography angiography performed for the integrity of the lower extremity arteries, an area consistent with an abscess at amputation site with peripheral and thick contrast enhancement is observed

good access to the lesion while optimizing patient and operator comfort. Proper positioning will also enable the needles to fit through the gantry when confirming the needle tip's position. Some lesions are difficult to visualize on ultrasound as they have similar echogenicity to the neighboring structures such as the muscle. These lesions are often much better depicted on cross-sectional modalities, i.e., MR imaging and CT, and biopsy is much more favorable since the correlation of the lesion's location is much easier.

Conclusion

Though MR imaging of the musculoskeletal system stays in a central location with its inherited improved characterization of soft tissues, MDCT's indications over MRI are growing. These indications are exampled above. With the evolutions made in MDCT technology and the dose issues with the additive clinical experience, we believe that the indications for MDCT may increase.

References

1. Mutschler W, Kanz KG (2002) Interdisciplinary shock room management: responsibilities of the radiologist from the trauma surgery viewpoint. Radiologe 42:506–514
2. Trentz O (2000) Polytrauma: pathophysiology, priorities and management. In: Rüedi T, Murphy WM (eds) AO principles of fracture management. Thieme, Stuttgart, pp 661–673

3. Dawson P, Lees WR (2001) Multi-slice technology in computed tomography. Clin Radiol 56:302–309
4. Körner M, Linsenmaier U (2009) CT management of multisystem trauma. In: Reiser MF, Becker CR, Nikolaou K, Glazer G (eds) Medical radiology. Diagnostic imaging. Multislice CT. Springer, Berlin, p 589
5. Fayad LM, Bluemke DA, Fishman EK (2005) Musculoskeletal imaging with computed tomography and magnetic resonance imaging: when is computed tomography the study of choice? Curr Probl Diagn Radiol 34:220–237
6. Iochum S, Ludig T, Walter F, Fuchs A, Blum HP (2001) Intérêt de la technique de rendu volumique en pathologie ostéoarticulaire. J Radiol 82:221–230
7. Gervaisea A, Teixeiraa P, Villanic N, Lecocqa S, Louisa M, Bluma A (2013) CT dose optimisation and reduction in osteoarticular disease. Diagn Interv Imaging 94:371–388
8. Bushong SC (2008) Concepts of radiologic science in radiologic science for technologists. Mosby Elsevier, St. Louis, p 12
9. Alam A, Chander BN (2005) Three dimensional spiral CT imaging of the musculoskeletal system: application and advantages. MJAFI 61:133–138
10. Kuszyk BS, Ney DR, Fishman EK (1995) The current state of the art in three-dimensional oncologic imaging: an overview. Int J Radiat Oncol Biol Phys 33:1029–1039
11. Le HB, Lee ST, Munk PL (2010) Image-guided musculoskeletal biopsies. Semin Interv Radiol 27: 191–198
12. Rubens DJ, Fultz PJ, Gottlieb RH, Rubin SJ (1997) Effective ultrasonographically guided intervention for diagnosis of musculoskeletal lesions. J Ultrasound Med 16:831–842
13. Ahrar K, Himmerich JU, Herzog CE et al (2004) Percutaneous ultrasound-guided biopsy in the definitive diagnosis of osteosarcoma. J Vasc Interv Radiol 15:1329–1333
14. Kandarpa K, Aruny JE (2002) Handbook of interventional radiologic procedures, 3rd edn. Lippincott Williams and Wilkins, Philadelphia, p 765
15. Peh WCG (2006) CT-guided percutaneous biopsy of spinal lesions. Biomed Imaging Interv J 2:e25
16. Schwartz HS, Spengler DM (1997) Needle tract recurrences after closed biopsy for sarcoma: three cases and review of the literature. Ann Surg Oncol 4:228–236
17. Ohashi K, El-Khoury GY (2009) Musculoskeletal CT: recent advances and current clinical applications. Radiol Clin N Am 47:387–409
18. Geijer M, El-Khoury GY (2006) MDCT in the evaluation of skeletal trauma: principles, protocols, and clinical applications. Emerg Radiol 13:7–18
19. Imhof H, Mang T (2006) Advances in musculoskeletal radiology: multidetector computed tomography. Orthop Clin North Am 37:287–298
20. West ATH, Marshall TJ, Bearcroft PW (2009) CT of the musculoskeletal system: what is left is the days of MRI? Eur Radiol 19:152–164
21. Rydberg J, Liang Y, Teague SD (2004) Fundamentals of multichannel CT. Semin Musculoskelet Radiol 8:137–146
22. Buckwalter KA, Farber JM (2004) Application of multidetector CT in skeletal trauma. Semin Musculoskelet Radiol 8:147–156
23. Dalrymple NC, Prasad SR, Freckleton MW, Chintapalli KN (2005) Informatics in radiology (infoRAD): introduction to the language of three-dimensional imaging with multidetector CT. RadioGraphics 25:1409–1428
24. Buckwalter KA, Rydberg J, Kopecky KK, Crow K, Yang EL (2001) Musculoskeletal imaging with multislice CT. AJR Am J Roentgenol 176:979–986
25. Choplin RH, Farber JM, Buckwalter KA, Swan S (2004) Three-dimensional volume rendering of the tendons of the ankle and foot. Semin Musculoskelet Radiol 8:175–183
26. Farber JM (2004) CT arthrography and postoperative musculoskeletal imaging with multichannel computed tomography. Semin Musculoskelet Radiol 8:157–166
27. White LM, Buckwalter KA (2002) Technical considerations: CT and MR imaging in the postoperative orthopedic patient. Semin Musculoskelet Radiol 6:5–17
28. Karcaaltincaba M, Aktas A (2011) Dual energy CT revisited with multidetector CT: review of principles and clinical applications. Diagn Interv Radiol 17:181–194
29. Choi HK, Al-Arfaj AM, Eftekhari A, Munk PL, Shojania K, Reid G et al (2009) Dual energy computed tomography in tophaceous gout. Ann Rheum Dis 68:1609–1612
30. Chiu WC, Haan JM, Cushing BM et al (2001) Ligamentous injuries of the cervical spine in unreliable blunt trauma patients: incidence, evaluation, and outcome. J Trauma 50:457–463
31. Harris JH, Lee JS, Coupe KJ et al (2004) Acetabular fractures revisited : part 2, a new CT-based classification. AJR Am J Roentgenol 182:1367–1375
32. Grigoryan M, Lynch JA, Fierlinger AL et al (2003) Quantitative and qualitative assessment of closed fracture healing using computed tomography and conventional radiography. Acad Radiol 10:1267–1273
33. Mori T, Fujii M, Akisue T et al (2005) Three-dimensional images of contrast-enhanced MDCT for preoperative assessment of musculoskeletal masses: comparison with MRI and plain radiographs. Radiat Med 23:398–406
34. Moser T, Dosch JC, Moussaoui A, Dietemann JL (2007) Wrist ligament tears: evaluation of MRI and combined MDCT and MR arthrography. AJR Am J Roentgenol 188:1278–1286
35. Schmid MR, Schertler T, Pfirrmann CW et al (2005) Interosseous ligament tears of the wrist: comparison of multidetector row CT arthrography and MR imaging. Radiology 237:1008–1013

The Role of Magnetic Resonance Imaging in the Evaluation of Musculoskeletal System

11

Emrah Özcan and Hatice Tuba Sanal

Abstract

Last two decades, magnetic resonance (MR) imaging has emerged as one of the main modalities in musculoskeletal imaging. With MR imaging, there is no emission of damaging ionizing radiation, and hence, this is one of the most important feature of this technique. With the excellent soft tissue contrast resolution it displays, MR imaging is being used as the primary modality in joint imaging and tumour staging. With the advances in coil technology, its usage accelerated in the relatively small joints such as elbow, wrist and hand.

In occult trauma cases where radiograms and computerized tomography are incapable of showing the marrow changes, MR images are superb with the soft tissue resolution it yields. MR imaging is also irreplaceable in the evaluation of internal derangements of joints, showing delicate soft tissue structures.

In this section, these and other indications for MR imaging in the evaluation of musculoskeletal system diseases, touching to some of the basic features of the modality, will be discussed.

Learning Outcomes

To have an understanding of:

1. The basic physics of magnetic resonance (MR) imaging
2. The advantages and disadvantages of MR imaging technique as compared to other imaging modalities
3. The basic MR imaging sequences and plans used for evaluating musculoskeletal system
4. The applications of MR imaging on internal derangements of joints, characterization and staging of bone and soft tissue tumors, and evaluation of bone marrow with its superior soft tissue resolution

E. Özcan, MD (✉)
Radiology Department, Hakkari Military Hospital, Hakkari, Turkey
e-mail: dremrahozcan@gmail.com

H.T. Sanal, MD
Radiology Department, Gülhane Military Medical Academy, Ankara, Turkey

F. Korkusuz (ed.), *Musculoskeletal Research and Basic Science*,
DOI 10.1007/978-3-319-20777-3_11

Terminology

Coil Radio-frequency coils are used to transmit/receive electromagnetic radiation needed for image acquisition.

Contrast resolution It is the ability to distinguish between differences in intensities on an image.

Diffusion-weighted imaging It is a form of MR imaging based upon measuring the random Brownian motion of water molecules within a voxel of tissue. The relationship between histology and diffusion is complex; however, generally densely cellular tissues or those with cellular swelling exhibit lower diffusion coefficients, and thus diffusion is particularly useful in tumor characterization and cerebral ischemia.

Gradient echo sequences The images have advantage on showing the hemorrhage of the tissues markedly according to this sequence's formation principles.

Fourier transform It is a mathematical procedure that allows spatial information reconstructed from the raw data.

MR spectroscopy It allows analysis of the chemical species given in a volume such as ^{31}P state of muscle.

Multiplanar imaging A technique used in two-dimensional tomographic imaging (computed tomography and magnetic resonance) to generate sagittal, coronal, and oblique views.

Partial volume artifact It is caused as a result of two different tissues in a particular voxel.

Proton A positively charged elementary particle of all atomic nuclei. Magnetic resonance imaging signal is created as a result of interactions between RF pulses and hydrogen protons.

Radio-frequency wave It is a rate of oscillation in the range of around 3 kHz–300 GHz, which corresponds to the frequency of radio waves, and the alternating currents which carry radio signals. RF waves are used to react with hydrogen protons.

Spatial resolution The measure of how closely lines can be resolved in an image.

Spin echo sequences It is the most commonly used pulse sequence. The pulse sequence parameters can be adjusted to give an image, its T1-weighted, proton or spin density, and T2-weighted features.

Tesla It is the unit of magnetic flux density in the International System of Units. One tesla is equal to one weber per square meter, and it was named in 1960 in the honor of Nikola Tesla. It is used to describe for MR machine magnetic field power such as 1, 5, or 3 tesla.

TE (time to echo) The time between the application of radio-frequency excitation pulse and the peak of the signal induced in the coil. It is measured in milliseconds. The amount of T2 relaxation is controlled by TE.

TR (time to repetition) It is the time from the application of an excitation pulse to the application of the next pulse. It determines how much longitudinal magnetization recovers between each pulse. It is measured in milliseconds.

T1-weighted imaging It is one of the basic pulse sequences in MR imaging and demonstrates the differences in the T1 relaxation time of tissues.

T2-weighted imaging It is one of the basic pulse sequences in MR imaging. The sequence weighting highlights the differences in the T2 relaxation time of tissues.

Clinical Relevance

1. *Before performing MRI, the patient should be questioned for metallic foreign bodies or metal prothesis. If necessary, radiography should be obtained before MRI.*

   Magnetic resonance imaging is widely used in many clinical settings. The presence of implanted metallic objects may either render MR imaging unsafe or greatly limit its diagnostic utility. This presents a tremendous clinical challenge because there are many subjects with implanted devices in the population, who may require MR imaging evaluation.

   Ferromagnetic objects can experience strong forces that originate from the static magnetic field [1]. The forces are strongest in regions near the magnet where the field strength changes rapidly over a small distance. Unfortunately, over a small distance (tens of centimeters), forces can change from negligible to strong enough to cause a missile effect on the object.

   Some implants can cause heating because of interaction with radio-frequency fields. The most common example is guidewires [2, 3]. Although extensive research has characterized device safety and in some cases improved the ability to detect unsafe devices, no current methods exist to alter the MR imaging safety of ferromagnetic objects that may experience significant forces or implants causing heat.
2. *Follow-up of the patients with musculoskeletal tumor history and MR imaging with contrast material injection should be performed. Contrast enhancement of a suspected lesion is important to evaluate the residual or recurrent tumor.*

   Magnetic resonance imaging provides several advantages over other imaging modalities in the evaluation of recurrent tumors in the soft and bone tissues. Exquisite soft tissue contrast resolution better facilitates evaluation of the extent of the disease and its proximity to vital structures (such as neurovascular bundles), in comparison to CT [4]. Magnetic resonance imaging can be used as the primary imaging modality in the evaluation for recurrent/residual tumor or can be used as an adjunct to ultrasound. The typical MR appearance of a recurrent soft tissue neoplasm is a mass lesion demonstrating high signal intensity on T2-weighted sequence and enhancement after the administration of intravenous contrast media [5]. The familiarity with the appearance and behavior of post-therapeutic changes, the typical appearance of recurrence, and the knowledge of common variants aid in the early detection of recurrent soft tissue neoplasms.
3. *In occult fractures, MR imaging should be performed after radiography.*

   Radiographically, occult and subtle fractures are a common diagnostic challenge in daily practice. Indeed, fractures represent up to 80 % of the missed diagnoses in the emergency department [6]. Failure to recognize the subtle signs of osseous injury is one of the reasons behind this major diagnostic challenge [7]. The diagnostic performance of MR imaging in the detection of occult fractures has been shown to be comparable or better than CT in various papers. Indeed, while the specificity of both CT and MR imaging for the diagnosis of a fracture can be as high as 100 %, the sensitivity was reported to be higher for MR imaging [8–11].
4. *Magnetic resonance imaging is the primer imaging modality for joint diseases.*

   Magnetic resonance imaging may be one such indicator since it is more sensitive than conventional radiographs in demonstrating joint effusion and pathology in the synovial tissue, cartilage, and bone [12].

Introduction

As a consequence of the huge evolution in technical research and development in medicine, we now reap the benefits of magnetic resonance (MR) imaging. Magnetic resonance imaging allows a noninvasive means to assess the internal architecture of the musculoskeletal (MSK) system, so it has a growing role in the evaluation. Not working on the principle of ionizing radiation and so its safely application on children and pregnant cases repeatedly without any known harmful effects, it is one of the most important features of this technique. Owing to its excellent soft tissue resolution that it displays, MR imaging is now being used as the primary modality in joint imaging and tumor staging.

In occult trauma cases where direct graphies and computerized tomography are incapable of showing the bone marrow, MR images are superior in displaying the marrow changes early with the inherited high soft tissue resolution. MR imaging is also superb in the evaluation of internal derangements of the joints. In this section, these and other indications for the performance of MR imaging in the evaluation of musculoskeletal system, touching to some basic features of the modality, will be discussed.

Magnetic Resonance Imaging: Basic Features

Briefly, while the patient lies in the magnet of the MR machine, images of the proper anatomy are obtained via the signals after a complex interaction between the appropriate radio-frequency (RF) waves and the hydrogen protons in the cells. The main and the most important part of an MR device is its main magnet, which is given in tesla. In most of the clinical practices, the magnets have field strengths around 1.5 tesla. One can compare the huge strength of the magnet of an MR machine with that of the earth's, which is between 30 and 70 microtesla. With the use of 3 tesla devices in clinical practice, the images' spatial and contrast resolutions have been remarkably advanced proportional to the magnetic field strength.

Apart from the magnet, the coils are another piece of the MR machine. There are coils such as *volume*, *shim*, *gradient*, and *surface* used for different purposes. *Volume coils* have a major role in sending RF pulses to the patient and then gathering the signals, as a consequence of the interaction between RF pulses and protons.

The excellent soft tissue contrast resolution is the most striking feature of MR imaging giving a new insight to musculoskeletal system evaluation. While the extremity of interest is lying in the bore of the magnet, the technique allows imaging in various planes without changing the position of the extremity, providing a multiplanar imaging [13].

The large magnetic field of the MR imaging system can attract metallic objects and influence the working principles of mechanical and electrical devices such as computers, pacemakers, or neurostimulators. The bore of the magnet may exclude MR imaging an appropriate modality for claustrophobic patients. The metallic composition of the prothesis should be interrogated before MR imaging as certain metals are not compatible with safety. Certain Web sites may be visited in terms of MR compatibility and safety screening of metal prothesis [14–16].

The features of protons in the body that aid in obtaining MR images lie on the fact that they act like little magnets and perform a motion that resembles the wobbling of a spinning top which is called precession. When the body is positioned in the magnet, these protons align either parallel or antiparallel to the direction of the main magnet that only a few more protons prefer parallel aligning. As the protons aligning opposite directions cancel each other's magnetic vectors, a few more protons pointing the main magnetic field create a net magnetic vector longitudinal to the external magnetic field. At this time, an RF pulse transmitted through the coil, with the same frequency as the precessing protons, transfers energy to the protons. This results in decreasing the longitudinal magnetization of the protons and introduces a new magnetic vector, i.e., the transversal magnetization meaning precession of the protons in synchrony. When the RF pulse is switched off, the diminished longitudinal magnetization increases again which this longitudinal relaxation is described by a time constant T1. Simultaneously, transversal magnetization decreases and eventually disappears, which this transversal relaxation is described by a time constant T2. For a simple comparison, one can derive the T1 or T2 weightings of a particular MR image, by observing the physiologic fluid (i.e., cerebrospinal fluid, urine in bladder, etc.). While the fluid is in white tone with a T2-weighted image, it is

darker on T1-weighted image. In broadest terms, T1-weighted images are good for viewing the anatomy, and T2-weighted images are best for perceiving the pathology.

A pulse sequence is the strength, order, duration and repetition of RF pulses and magnetic gradients used to generate an MR image. In musculoskeletal system imaging, spin echo (SE) and gradient recalled echo (GRE) sequences are most commonly used. The latter one is sensitive to the susceptibility effects of iron atoms contained within hemosiderin [17] and shows strikingly the hemosiderin component of the *pigmented villonodular synovitis*, a rare proliferative disorder of the synovial membrane [18].

On T2-weighted imaging, water and to some extend fat show high signal intensity. Thus, in order to make watery milieu of edema conspicuous in the fatty bone marrow, fat suppression techniques are applied to the T2-weighted images.

Gadolinium, a paramagnetic substance, is used as an MR contrast agent which changes the signal intensity by reducing T1 significantly and T2 slightly, with an overall effect of high intensity best perceived on fat-saturated T1-weighted MR images. Gadolinium-based contrast agents are not totally innocent that in patients with advanced renal failure (those currently requiring dialysis or with a glomerular filtration rate [GFR] ≤15 ml/min), serious and sometimes fatal condition can happen called *nephrogenic systemic fibrosis*. Hence, physicians are advised in administering the minimal needed dose of contrast agent if MR imaging with contrast is necessary [19]. Gadolinium can be used via intravenous injections for evaluating musculoskeletal neoplasms both in characterization and observing the response to therapy [20]. Infectious and inflammatory processes of the bone and joints can also benefit with the contrast medium application.

MR arthrography is a technique performed after injection of diluted gadolinium contrast solution within the joint under fluoroscopy or computed tomography. Injecting contrast agent directly to the joints, the tension is created which aids in better visualization of the structures within the joints such as articular cartilage losses, partial ligament or tendon tears, and labral and triangular fibrocartilage tears [21]. After injection, images should be obtained within 30 min in order to benefit much from the contrast while it is still in the joint and not yet absorbed via the synovium [20]. For intra-articular detail, fat-suppressed, T1-weighted images are useful, and for evaluating pathologies about the joints, such as paralabral cysts of the shoulder and hip joints, fat-suppressed T2-weighted images are useful [20]. This method is minimally invasive; however, a dedicated time in MR machine is needed, with an increase in time and cost.

Applications

Tumor Imaging

High-resolution soft tissue images acquired by MR imaging provide very important information about the musculoskeletal tumors. Basically, the age of the patient, the clinical symptomatology, and the findings on direct radiography have all important role on the diagnosis of musculoskeletal tumors. Magnetic resonance imaging can display the origin of the tumor (i.e., cortical, juxtacortical, intramedullary, soft tissue), the extent of the tumor in the bone marrow, and the soft tissue component, if present [22] (Fig. 11.1). Necrosis, fat, and hematoma located within mass can be demonstrated by specific signal characteristics on the MR image. Fat tissue shows high signal intensity on T1-weighted images. Similarly, the fatty composition of the bone marrow shows high signal intensity on T1-weighted images. Thus, tumoral lesions that infiltrate the bone marrow can be visualized strikingly owing to the contrast created by hypointensity of the tumoral process and the fatty bone marrow, on T1-weighted images (Fig. 11.2).

While sagittal and coronal images may provide a broad perspective pertaining to the extension of the tumoral lesion with its full length in the bone marrow, axial images may display a better visualization of its neurovascular involvement.

Vascularity and permeability of the tumoral lesion may be assessed by using the paramagnetic contrast agents. Edema and cystic lesions show high signal intensity on T2-weighted images. Though dependent on their pathology, in general, musculoskeletal tumors are hypointense on T1-weighted images and hyperintense on T2-weighted images. In this content, a fibrous tumor with a high collagen content may display hypointense signal on T2-weighted images.

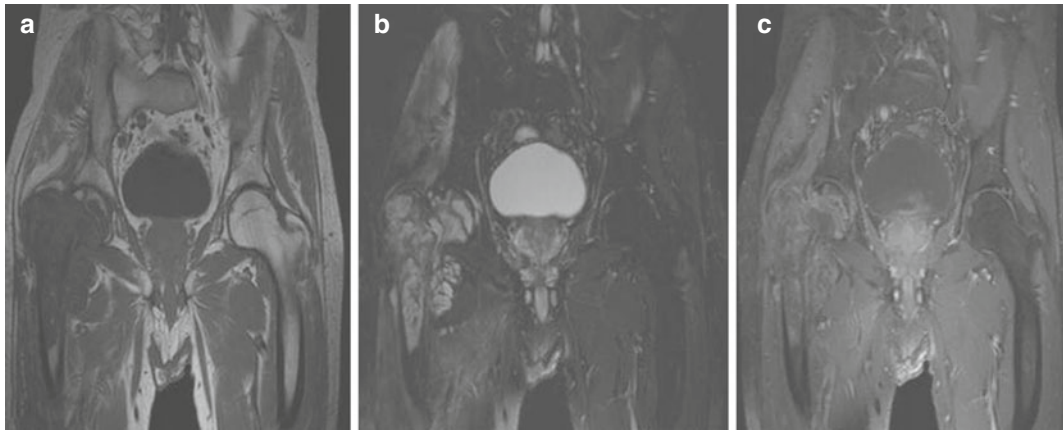

Fig. 11.1 Chondrosarcoma located in the right femur. Coronal images with T1-weighted (**a**), fat saturated (FS) T2-weighted (**b**), and contrast enhanced FS T1-weighted images (**c**). Note the associated soft tissue mass in the medial aspect of the femoral neck

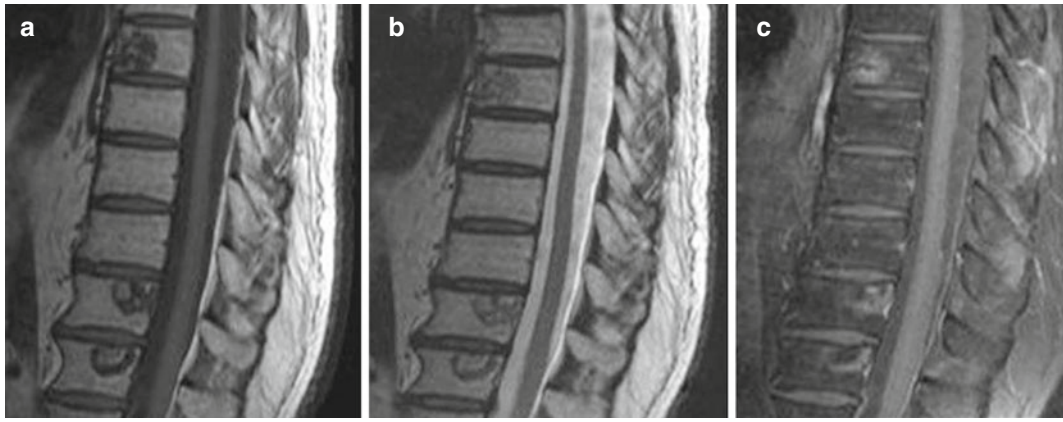

Fig. 11.2 Dorsal and proximal lumbar spine obtained in the sagittal plane with T1-weighted (**a**), T2-weighted (**b**) and contrast enhanced FS T1-weighted images (**c**). Multiple metastatic lesions in the vertebrae in a case with known prostate cancer

Some tumoral lesions are observed with their specific findings on MR images. For example, the cortex and medullary cavity of an osteochondroma is continuous with that of the involved bone. The thickness and morphology of the cartilage cap as well as an accompanying bursa formation can be defined on fluid-sensitive sequences (Fig. 11.3). Fluid-fluid (blood/serum) levels of an aneurysmal bone cyst (differential diagnoses should also include some other lesions as well as telangiectatic osteosarcoma), the periosteal reaction, and sclerosis around the nidus of an osteoid osteoma and its reactive edema are called "Aunt Minnie lesions" diagnosed on MR images.

Dynamic contrast-enhanced MR imaging can be referred for (1) determining the most appropriate route for biopsy sampling by evaluating the viable tumor tissue before intervention, (2) evaluating the change in tumoral size and necrosis as a means of treatment response after chemotherapy, and (3) assessing the residual and recurrent tumoral masses after the surgery.

Bone marrow involvement and the soft tissue component around the tumors can be shown to a better extent with MR imaging than with CT, owing to the inherited high soft tissue resolution of the previous technique. However, calcification in the tumoral tissue, cortical bone destruction, and periosteal reaction are perceived better with CT. In the complex anatomic regions such as the spine, tumor

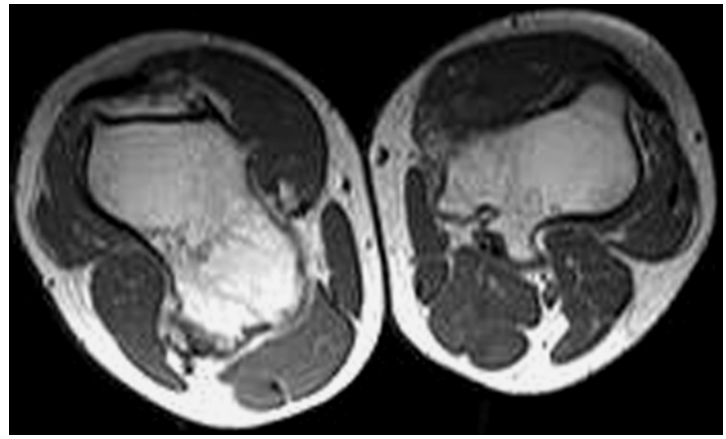

Fig. 11.3 Transverse T1-weighted MR image of both thigh. The cortical and marrow continuity of the lesions with the underlying bone is well seen. Note the compression of the popliteal vascular structures by these lesions

extension into the canal, accompanying soft tissue and bony invasion, can be evaluated on MR images.

Spinal Column Imaging

Magnetic resonance imaging is a highly referred modality in evaluating the discal pathologies of the vertebral column. Degeneration of an intervertebral disc and its other pathologies such as bulging and protrusion and their relation with that of thecal sac and the nerves can be readily seen on MR images [23] (Fig. 11.4). While the sensitivity of MR imaging is higher than that of CT for discal pathologies, it is comparable in the evaluation of spinal stenosis [24]. In addition, granulation tissue in the postoperative setting can be easily distinguished from recurrent/residual disc herniation on fat-suppressed T1-weighted images after contrast media administration. Granulation tissue shows contrast enhancement in contrast to recurrent/residual disc herniation [25].

Magnetic resonance myelography is a noninvasive means in demonstrating spinal canal narrowing by using coronal T2-weighted sequences, without any interventional procedure and necessitating the use of intrathecal contrast agents.

Spinal cord tumors, spondylitis – spondylodiscitis – and accompanying any abscess formation can be evaluated in detail with MR imaging, especially on post-contrast images [26] (Fig. 11.5). Spinal involvement secondary to specific infectious agents such as *Brucella* and tuberculosis, which are frequently seen in our country, can be evaluated on MR imaging.

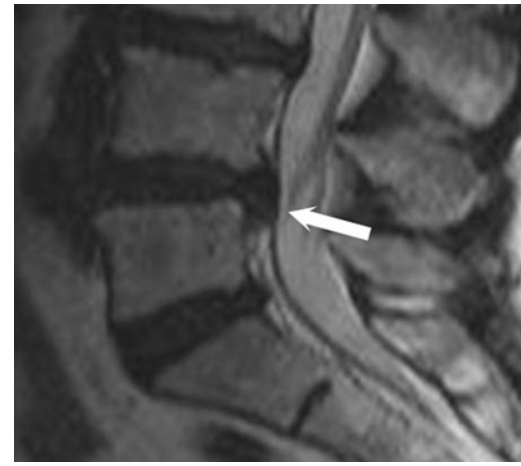

Fig. 11.4 Sagittal T2-weighted image of L4–5 disc extrusion (*arrow*)

Compression fractures of the vertebrae particularly seen in osteoporotic patients, the extension of the fractured bony fragments into the spinal canal, and the differentiation from malignant vertebral compression fractures can be made with high accuracy with MR imaging. In these patients, diffusion-weighted images added to the conventional sequences may be of help in making a distinction between these two processes, which in malignities, diffusion restriction can be observed.

Imaging in Trauma

Radiography for occult fractures of the spine CT is the preferred imaging modalities. However, MR imaging is particularly needed for the evaluation of trauma effects on soft tissues, such as

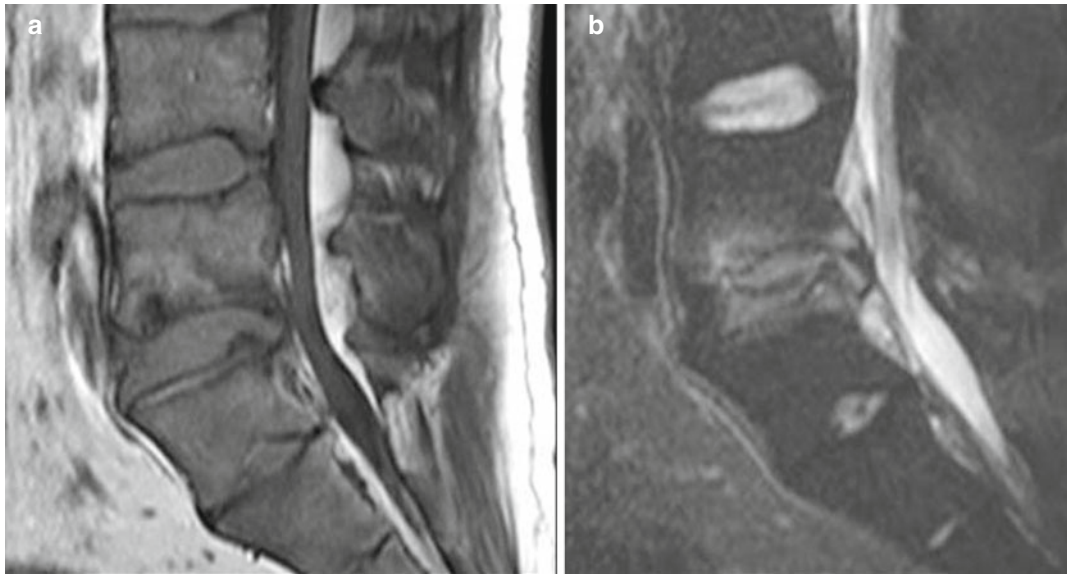

Fig. 11.5 Distal lumbar spine on sagittal plane with T1-weighted (**a**) and FS T2-weighted (**b**) images. There are irregularities at the end- plates of L4 and L5 vertebrae with hyperintense signal intensities both on the end-plates and the intervertebral disc (**b**), corresponding to vertebral osteomyelitis and discitis

tendons, ligaments, and muscle compartments. Bone marrow edema like intensity changes, i.e., high signal intensity on fluid-sensitive sequences and low intensity on T1-weighted images, is observed after trauma, secondary to the contusion of the trabeculae and hemorrhage. Bone marrow edema associated with occult fractures can readily be demonstrated on fat-saturated sequences. Fracture lines can easily be perceived on T1-weighted images with their linear low signal intensities [27]. Especially for the early diagnosis of scaphoid and femoral neck fractures, which are not seen on radiograms, MR imaging helps to identify the fracture lines and bone marrow edema with the high soft tissue resolution that this method yields (Fig. 11.6) [10].

Imaging Particular Joints

Temporomandibular Joint Imaging

The temporomandibular joint (TMJ) has a fibrous disc that resembles the meniscus of the knee, both in appearance and tissue composition. The disc looks like a bow tie on sagittal images with the triangles of the bow called "anterior or posterior band." The posterior band of the disc is much greater than the anterior band. A thin intermediate zone lies in between these two bands. The joint is evaluated while the patient is of open and closed mouth positions. The fibrocartilaginous disc is seen with low signal intensity on both sagittal T1- and T2-weighted images. The disc dislocations can be assessed at an open mouth position by evaluating the mandibular condyle-articular eminence relationship with the disc. Coronal images may show articular surfaces and so can reveal degenerative changes, if there is any [28].

Knee Imaging

The internal derangements of the joint that necessitates MR imaging may involve the menisci, ligaments (cruciate, collateral, patellar ligament), cartilage surfaces, and bone.

The normal meniscus is of low intensity on both T1- and T2-weighted sequences owing to its fibrocartilaginous tissue composition. Degeneration of the meniscus shows high signal intensity that does not extend to the articular surface on fluid-sensitive sequences. If this high signal intensity reaches to the articular surface, we should describe this as a tear that may be evaluated in more detail on coronal and sagittal proton-weighted images (Fig. 11.7). The two most important criteria for meniscal tears are an abnormal

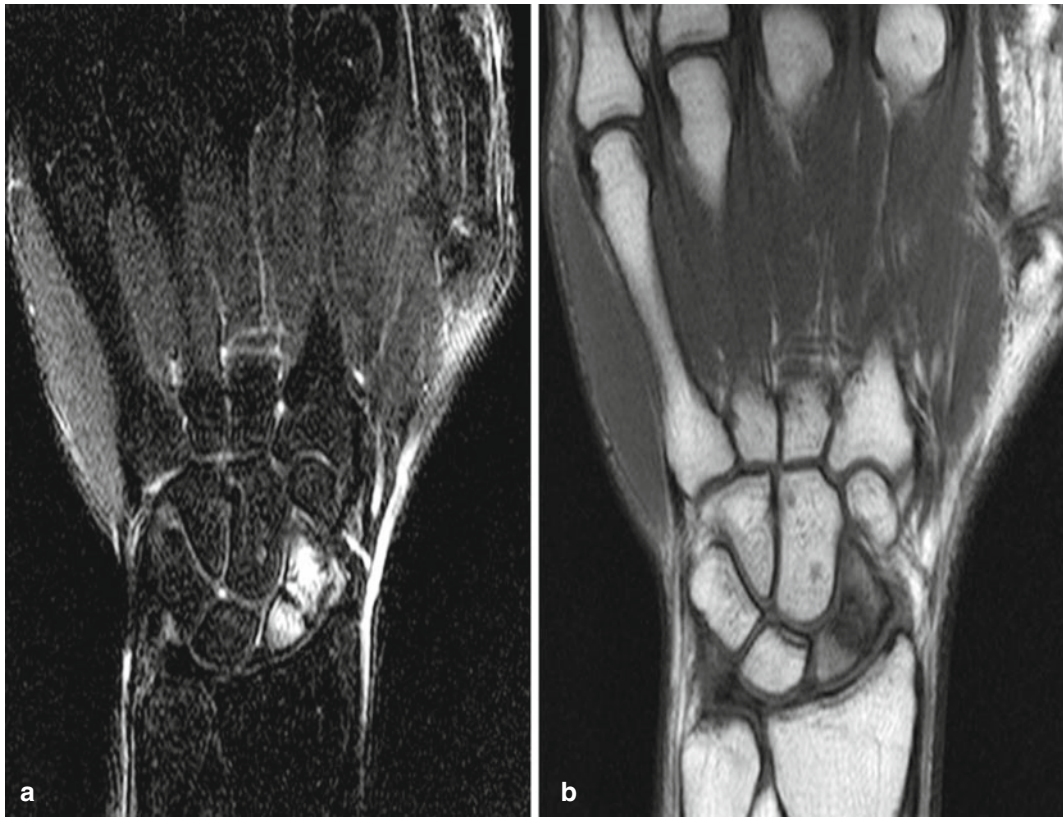

Fig. 11.6 Scaphoid fracture and accompanying edema, FS T2-weighted images (**a**) and T1-weighted images (**b**)

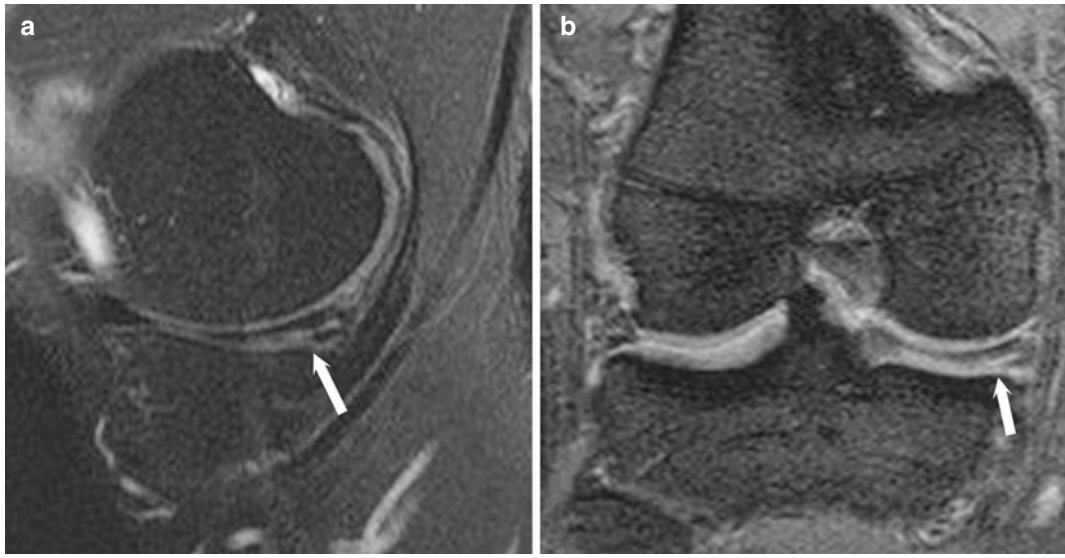

Fig. 11.7 Sagittal (**a**) and coronal (**b**) FS T2-weighted image. Medial meniscus tear of the dorsal horn extending lower articular surface (*arrow*) is observed

shape of the meniscus and high signal intensity unequivocally contacting the surface on proton-weighted images. Meniscal tears can be described roughly as longitudinal and vertical according to the orientation of the collagen bundles of the meniscus itself. A combination of these types can be reported as complex tears.

The anterior and posterior cruciate ligaments are revealed with their low signal intensity and in the sagittal images throughout their length. When completely torn, the ligaments are not observed with their full continuity (Fig. 11.8). Gradient echo sequences are helpful in evaluating the cartilage. Subchondral bone marrow edema with cartilage defects can be strikingly observed on fluid-sensitive sequences [29]. The patellar and quadriceps tendons show low signal intensity like other tendons, and the degeneration and surrounding inflammation are revealed with the high intensity on T2-weighted images.

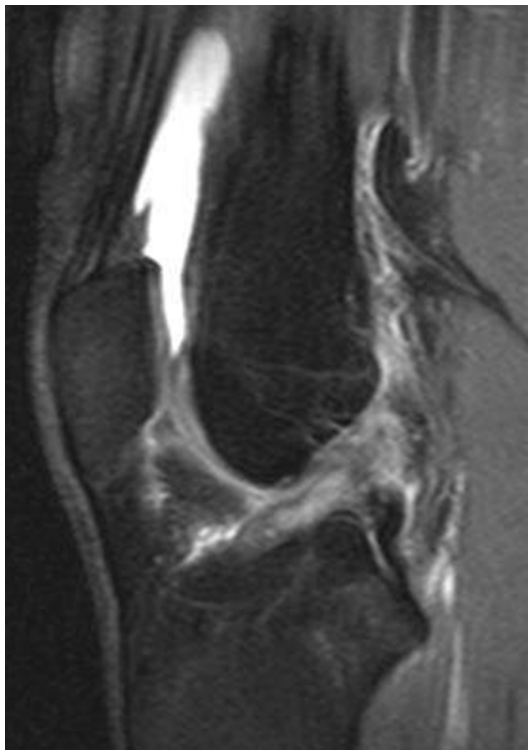

Fig. 11.8 Anterior cruciate ligament tear. Ligament is not visualized with its normal signal intensity and contour

Shoulder Imaging

Shoulder joint is the third most common site of musculoskeletal pain occurring in 7–25 % of general population [30]. The shoulder MR imaging is often referred for evaluating the rotator cuff lesions. With MR imaging, the rotator cuff, long head of the biceps tendon, glenoid labrum, cartilage, acromioclavicular joint, adjacent muscle, and bone structures are evaluated. Rotator cuff pathologies are commonly encountered in patients with shoulder impingement syndrome. Especially examining simultaneously the oblique, sagittal, and coronal fat-suppressed fluid-sensitive sequences reveals the partial- or full-thickness tendon tears in their high signal intensity (Fig. 11.9). Rotator cuff tears can be observed as:

A. Partial articular-sided tear
B. Partial bursal-sided tear
C. Complete tear [31]

A painful shoulder syndrome may result from other components of the joint such as the muscle, tendon, or articular capsule pathologies while not always being related to rotator cuff tendon degeneration or tears.

Glenoid labrum tears and SLAP (superior labrum anterior to posterior) lesions can be visualized if there is ample joint effusion making

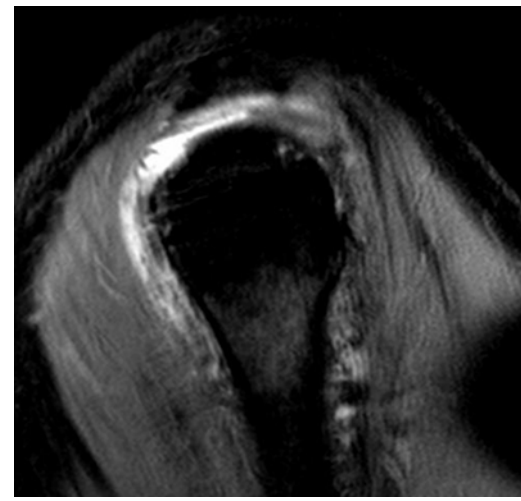

Fig. 11.9 Sagittal FS proton image that shows rupture of supraspinatus tendon and migration of ruptured part to coracoacromial arch

these pathologies easy to recognize on fluid-sensitive sequences; however, as mentioned earlier, MR arthrography may be needed when there is not enough joint fluid to demonstrate the labral and ligamentous pathologies and the extent of partial articular-sided rotator cuff tears [30].

Wrist Imaging

Magnetic resonance imaging is widely used mainly for evaluating the pathologies of triangular fibrocartilage complex (TFCC), median nerve in aiding the diagnosis for carpal tunnel syndrome, carpal bones for avascular necrosis, ligaments and tendons for their tears, and synovitis. The possible causes of carpal tunnel syndrome in the flexor retinaculum such as ganglia, tenosynovitis, bursitis, and other tumors may be evaluated. Median nerve located in the flexor retinaculum is ovoid in shape and intermediate in signal intensity. For early diagnosis of occult scaphoid fractures and in the chronic setting for the demonstration of possible avascular necrosis, MR imaging is superior to radiographies.

Ankle Imaging

Critical diagnostic information can be obtained on the bones, ankle mortise, ligaments, and tendons with MR imaging.

In clinically unequivocal cases and with chronic ankle pain, the ligaments can be evaluated. Extending between adjacent bones, the ligaments reveal low signal intensity on both T1- and T2-weighted images. Deltoid ligament is a broad ligament spanning on the medial aspect of the ankle beneath the flexor tendons. Thickening, loss of continuity, and high signal intensity on fluid-sensitive sequences may be observed after acute injury. Anterior talofibular ligament is the most common injured ligament in the supination and external rotation injuries of the ankle that can be depicted easily on axial plane. In the chronic stage, ondulations in the contour and thinning of the ligament may be observed (Fig. 11.10). Other pathologies for which MR imaging is referred are tendon changes (i.e., tendinosis, peri-/paratendinitis, tenosynovitis, rupture, entrapment), tarsal tunnel syndrome, osteochondral injury, Morton's neuroma, bone contusions, and synovial pathologies [32].

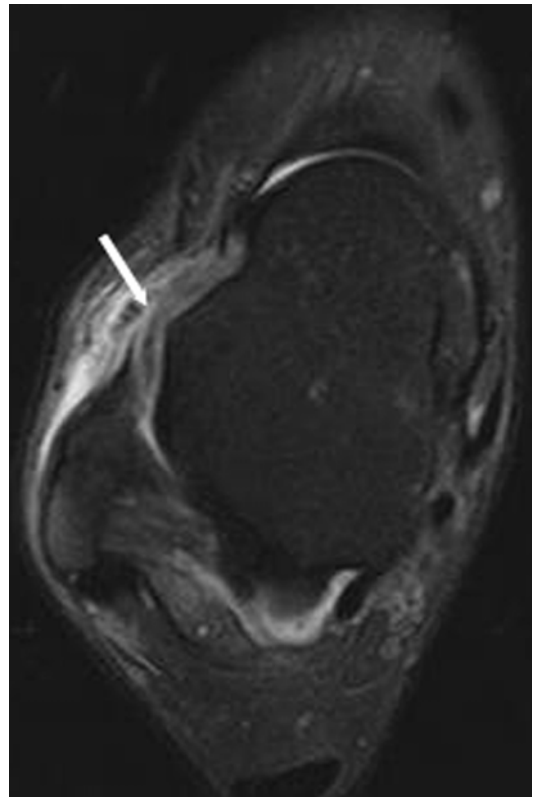

Fig. 11.10 Anterior talofibular ligament attachment tear (*arrow*) on axial FS T2-weighted image. We cannot see the ligament attachment to the talus, and edema in the capsule and extensor retinaculum is prominent

Elbow Imaging

Magnetic resonance imaging is helpful in demonstrating common pathologies of medial, lateral, collateral, and annular ligament tears, medial-lateral epicondylitis, biceps and triceps tendon tears, and ulnar nerve. Coronal fat-saturated fluid-sensitive sequences can show the whole extent of the lateral ligaments with extensor and flexor tendons important in the diagnosis of epicondylitis. The high signal intensity of the extensor or flexor tendons at the attachment site on the epicondyles may lead to the diagnosis of epicondylitis. Loss of the continuity and the presence of high signal intensity of the ligaments on fluid-sensitive sequences may be seen with tears [33].

Hip Imaging

With the use of gradient echo sequences that may reveal hip joint cartilage and the labrum, one can evaluate arthritis and impingement syndromes around the hip with detailed information. For pediatric hip joint, usage of superficial coils may help to provide optimal signal-to-noise ratio in demonstrating the relatively small parts of the joint. With MR imaging, the femoral head and neck shape, its location and relationship with the acetabulum, and the bone marrow changes can be evaluated in the pathologies of hip dysplasia. Early synovial changes observed in juvenile rheumatoid arthritis may be evaluated. In acute synovitis, one can see high signal intensity on T2-weighted images and contrast enhancement.

Early diagnosis of avascular necrosis of the femoral head can be diagnosed with great sensitivity with MR imaging. It has a characteristic appearance with a serpiginous, geographic border, hypointense on T1-weighted images, and hyperintense on T2-weighted images. Fragmentation and collapse of the femoral head that can be seen in the late stages of the disease can be observed especially in the coronal plane images [34].

A painful clinical syndrome, transient osteoporosis of the femoral head, shows diffuse hyperintensity on fluid-sensitive sequences mainly in the lateral aspect of the head and neck (Fig. 11.11).

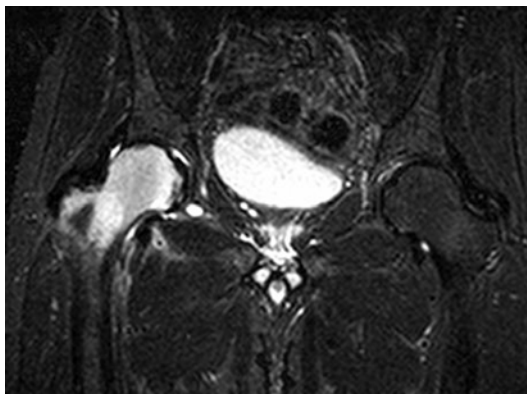

Fig. 11.11 Transient osteoporosis on right femoral neck on FS T2-weighted coronal image. Homogeneous high signal intensity is revealed

Conclusion

In the last two decades, MR imaging has placed among the main modalities in musculoskeletal imaging, together with direct graphies. With MR imaging, there is no emission of damaging ionizing radiation, and hence, this is one of the most important feature of this technique. With the excellent soft tissue resolution it displays, MR imaging is being used as the primary modality in joint imaging and tumor staging. In the last years with the advances in coil technology, its usage is also increased in the relatively small joints such as the elbow and wrist with high resolution. With the technological advances, one may expect to see more novelties in terms of coil technology and new sequences; new horizons are on the way of imaging musculoskeletal diseases.

References

1. Kanal E, Shellock F, Talagala L (1990) Safety considerations in MR imaging. Radiology 176:593–606
2. Wildermuth S, Dumoulin C, Pfammatter T, Maier S, Hofmann E, Debatin J (1998) MR-guided percutaneous angioplasty: assessment of tracking safety, catheter handling and functionality. Cardiovasc Intervent Radiol 21:404–410
3. Nitz WR, Oppelt A, Renz W, Manke C, Lenhart M, Link J (2001) On the heating of linear conductive structures as guide wires and catheters in interventional MRI. J Magn Reson Imaging 13:105–114
4. Aisen AM, Martel W, Braunstein EM et al (1986) MRI and CT evaluation of primary bone and soft tissue tumors. AJR 146:749–756
5. Griffiths HJ, Thompson RC, Nitke SJ et al (1997) Use of MRI in evaluating postoperative changes in patients with bone and soft tissue tumors. Orthopedics 20:215–220
6. Guly HR (2001) Diagnostic errors in an accident and emergency department. Emerg Med J 18(4):263–269
7. Sshwartz DT (2009) ACEP Scientific Assembly. Ten most commonly missed radiographic findings in the ED. Boston Convention and Exhibition Center. ACEP Scientific Assembly, October 8
8. Hakkarinen DK, Banh KV, Hendey GW (2012) Magnetic resonance imaging identifies occult hip fractures missed by 64-slice computed tomography. J Emerg Med 43:303–307
9. Liong SY, Whitehouse RW (2012) Lower extremity and pelvic stress fractures in athletes. Br J Radiol 85:1148–1156

10. Fredericson M, Jennings F, Beaulieu C, Matheson GO (2006) Stress fractures in athletes. Top Magn Reson Imaging 17(5):309–325
11. Memarsadeghi M, Breitenseher MJ, Schaefer-Prokop C et al (2006) Occult scaphoid fractures: comparison of multidetector CT and MR imaging—initial experience. Radiology 240(1):169–176
12. Poleksic L, Zdravkovic D, Jablanovic D, Watt I, Bacic G (1993) Magnetic resonance imaging of bone destruction on rheumatoid arthritis: comparison with radiography. Skelet Radiol 22:577–580
13. Edelman RR, Wielopolski PA (1996) Fast MRI. In: Edelman RR, Hessellink JR (eds) Clinical magnetic resonance imaging, 2nd edn. W.B. Saunders Company, Philadelphia, p 302
14. MRI safety (2006) Institute for Magnetic Resonance Safety, Education, and Research Web site. Available at: http://www.MRIsafety.com. Accessed 19 June 2006
15. American College of Radiology Web site. Available at: http://www.acr.org. Accessed 1 Aug 2006.
16. Institute for Magnetic Resonance Safety, Education, and Research Web site. Available at: http://www.IMRSER.org. Accessed 20 June 2006
17. Cheng A-L, Batool S, McCreary CR, Lauzon ML, Frayne R, Goyal M, Eric Smith E (2013) Susceptibility-weighted imaging is more reliable than T2*-weighted gradient-recalled echo MRI for detecting microbleeds. Stroke 44:2782–2786
18. Barile A, Sabatini M, Iannessi F, Di Cesare E, Splendiani A, Calvisi V, Masciocchi C (2004) Pigmented villonodular synovitis (PVNS) of the knee joint: magnetic resonance imaging (MRI) using standard and dynamic paramagnetic contrast media. Report of 52 cases surgically and histologically controlled. Radiol Med 107(4):356–366
19. Aydıngöz Ü (2006) The need for radiologists' awareness of nephrogenic systemic fibrosis. Diagn Interv Radiol 12:161–162
20. Berquist TH (2013) General technical considerations in musculoskeletal MRI, 6th ed. Lippincott Williams & Wilkins, Philadelphia, p 87
21. Blum A (2003) MR-arthrography: general principles and applications. J Radiol 84:639–657
22. Baweja S, Arora R, Singh S, Sharma A, Narang P, Ghuman S, Kapoor SK, Puri S (2008) Evaluation of bone tumors with magnetic resonance imaging and correlation with surgical and gross pathological findings. Indian J Radiol Imaging 16:611–618
23. Jensen MC, Brant-Zawadzki MN, Obuchowski N, Modic MT, Malkasian D, Ross JS (1994) Magnetic resonance imaging of the lumbar spine in people without back pain. N Engl J Med 331:69–73
24. Jarvik JG, Deyo RA (2002) Diagnostic evaluation of low back pain with emphasis on imaging. Ann Intern Med 137:586–597
25. Stadnik TW, Lee RR, Coen HL, Neirynck EC, Buisseret TS, Osteaux MJ (1998) Annular tears and disk herniation: prevalence and contrast enhancement on MR images in the absence of low back pain or sciatica. Radiology 206:49–55
26. Stone JA (2003) MR myelography of the spine and MR peripheral nerve imaging. Magn Reson Imaging Clin N Am 11:543–558
27. Grangier C, Garcia J, Howarth NR (1997) Role of MRI in the diagnosis of insufficiency fractures of the sacrum and acetabular roof. Skeletal Radiol 26:517–524
28. Emshoff R, Brandlmaier I, Gerhard S, Strobl H, Bertram S, Rudisch A (2003) Magnetic resonance imaging predictors of temporomandibular joint pain. J Am Dent Assoc 134:705–714
29. Hodler J, Resnick D (1996) Current status of imaging of articular cartilage. Skeletal Radiol 25:703–709
30. Beltran J, Rosenberg ZS, Chandnani VP, Cuomo F, Beltran S, Rokito A (1997) Glenohumeral instability: evaluation with MR arthrography. Radiographics 17:657–673
31. Snyder SJ (2003) Shoulder arthroscopy. Lippincott Williams & Wilkins, Philadelphia, pp 207–210
32. Hobby JL, Tom BD, Bearcroft PW, Dixon AK (2001) Magnetic resonance imaging of the wrist: diagnostic performance statistics. Clin Radiol 56:50–57
33. Rosenberg ZS, Beltran J, Bencardino JT (2000) From the RSNA refresher courses. Radiological Society of North America. MR imaging of the ankle and foot. Radiographics. Spec No:S153–79
34. Kijovsky J (2005) Magnetic resonance imaging of the elbow. Part II: abnormalities of the ligaments, tendons, and nerves. Skelet Radiol 34(1):1–18

Bone Mineral Densitometry: Measurement and Evaluation Methods

12

M. Özdeş Emer, Semra İnce, and Nuri Arslan

Abstract

Bone mineral density (BMD) is described as the bone mass in a bone mass unit and is found to be lesser than the normal value in patients who have osteoporosis and development of fracture risk. Although indications for measuring BMD have been increasing day by day, using dual-energy X-ray absorptiometry (DXA) method to determine the risk of fracture is still controversial, and there are different approaches in the guidelines prepared by national and international associations. Quantitative computed tomography, quantitative ultrasound, single-photon absorptiometry, dual-photon absorptiometry, and DXA are the most common methods used for measuring BMD. DXA is considered as the gold standard for BMD measurement with its high-resolution power as well as its high image quality and short acquisition time.

Lumbar spine and proximal femur BMD measurement is accepted as the standard examination protocol. While femoral neck and whole hip BMD measurement is performed for determination of fracture risk, whole hip BMD measurement is recommended for monitoring disease progression and response to therapy. On the other hand, forearm BMD measurement is recommended for patients who cannot have hip and/or spine BMD measurement and also for patients being investigated due to hyperparathyroidism-induced osteoporosis.

The World Health Organization Fracture Risk Assessment Working Group on the BMD criteria defined osteoporosis in young adults with a BMD T score below 2.5 standard deviation value. It is sufficient to perform DXA study once in every 1–2 years to monitor the response to treatment, and it is necessary to take into account at least 5 % of BMD change in order to demonstrate the effectiveness of treatment.

In this section, we will discuss these and other indications for the application of DXA with a brief section on the specifications of the used methods.

M.Ö. Emer (✉) • S. İnce • N. Arslan
Nükleer Tip Anabilim Dali, Gülhane Askeri Tip Akademisi
ve Askeri Tip Fakültesi, Etlik, Ankara 06018, Turkey
e-mail: ozdesemer@gata.edu.tr

F. Korkusuz (ed.), *Musculoskeletal Research and Basic Science*,
DOI 10.1007/978-3-319-20777-3_12

Learning Targets

- Describing osteopenia and osteoporosis
- Classifying osteoporosis considering its etiological reasons
- Identifying the groups of people who are at risk
- Identifying the fractures caused by osteoporosis and mortality and morbidity from these fractures
- Apprehending main treatment options used in osteoporosis treatment
- Defining T and Z scores used in the evaluation of bone mineral density (BMD) measurements, as well as the normal and pathological values of these scores
- Learning main indications and measurement methods for BMD measurement
- Apprehending advantages and disadvantages of methods used in BMD measurement and being able to decide on the most suitable method when it is necessary

Osteoporosis is today's most common metabolic bone disease characterized by decreasing bone mass, deteriorating microarchitecture of bone tissue, and increasing bone fragility [1–4]. Osteoporosis differentiates into two main types, namely, primary and secondary, considering its etiological reasons [1]. While primary osteoporosis is characterized by the loss of bone mass by age, secondary osteoporosis has some diseases and drug use in its etiology [1]. Type 1 (primary) osteoporosis is seen often in postmenopausal women and probably caused by the decrease in estrogen secretion. Vertebral and wrist fractures are the most common in primary osteoporosis. On the other hand, senile or Type 2 (secondary) osteoporosis is associated with an increased level of parathyroid gland function in old people. Femoral, proximal humerus, tibial, and pelvic fractures are more common in Type 2 osteoporosis [1]. Steroid use, Cushing disease, sedentary lifestyle, and nutritional disorders (malabsorption syndromes such as celiac disease) may be listed among the reasons of secondary osteoporosis [1, 5, 6].

Bone mass is the most important element contributing to the bone strength. Bone fracturability (or strength) is directly proportional to the bone structure and its mineral (Ca, P) content. Fracture risk increases considerably as the bone mass decreases. Bone mineral mass indicates the amount of minerals in bones in terms of gram.

The most important health problems arising from osteoporosis are the fractures due to decreased bone strength and consequent mortality and morbidity. Mortality in 6 months following femoral neck fractures is reported as 12–20 %. While 20 % of these cases die in 1 year, 50 % face long-term dysmotility, and 20–25 % need nursing for a long period [1, 6, 7]. Vertebral fractures are typically seen in thoracolumbar intersection (T12–L1) and midthoracic area (T7 and T8), while they are multicentric in 20–30 % of the patients [1]. On the other hand, while vertebral fractures are much more common compared to femoral fractures, fortunately they cause less serious health problems.

Bone mineral density (BMD), which means bone mass in mineral grams per unit of bone volume, accounts for 60–70 % of bone strength, and thus, it is the most important determinant of bone fracturability [2, 5]. T and Z scores are used in the evaluation of BMD measurements. T score identifies the difference between the average BMD score of normal young adult (ages 20–30) population of the same sex and ethnic background as the patient and the BMD score of the scanned patient. Z score stands for the difference between the scanned patient's BMD value and the BMD value of a control group of the same age and sex as the patient [1, 5]. World Health Organization (WHO) criteria for the diagnosis of osteopenia and osteoporosis using T scores by BMD measurement are given in Table 12.1.

Table 12.1 World Health Organization (WHO) criteria for BMD measurement

	T score
Normal[a]	At or over −1,0 SD
Osteopenia (low bone mass)[b]	Ranges between −1.0 and −2.5 SD
Osteoporosis[c]	At or below −2.5 SD
Severe or established osteoporosis	The existence of one or more fractures due to a mild trauma (such as a fall while standing up) in addition to a T score below −2.5 SD

[a]Figure 12.1
[b]Figure 12.2
[c]Figure 12.3

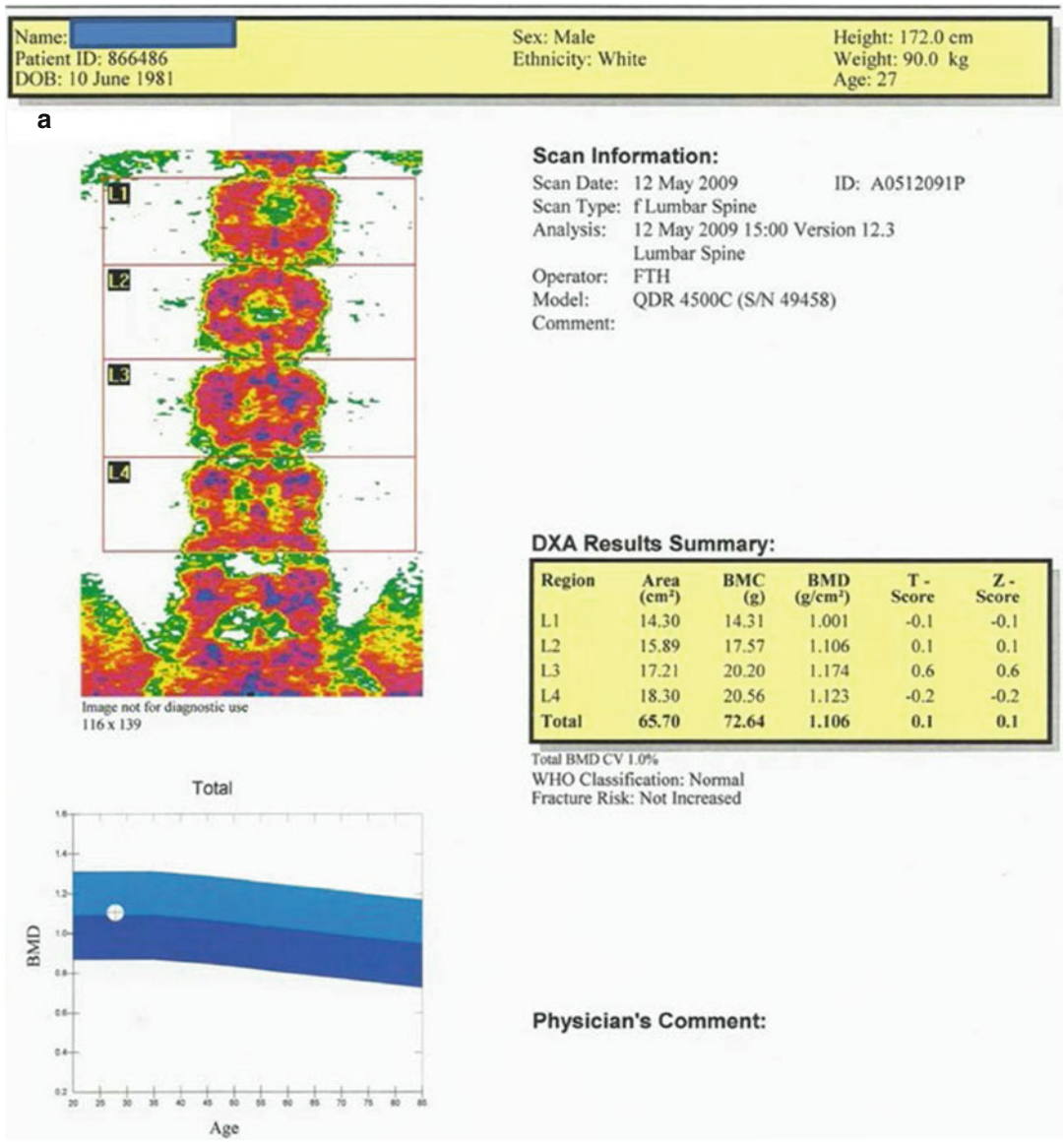

Fig. 12.1 (**a**) 27-year-old male patient suffering from hypogonadism. Average T and Z scores of L1–L4 vertebrae are calculated to be 0.1 and 0.1, respectively. The fracture risk is not increased, and Z score is to be evaluated as "within the expected range for this age" since the case is a male patient below 50 years of age. (**b**) The average T score for proximal femur in the same case is 0.4; Z score is 0.4. Fracture risk is not increased, and Z score is to be described as "within the expected range for this age" since the case is a male patient below 50 years of age

Name: [redacted]
Patient ID: 866486
DOB: 10 June 1981

Sex: Male
Ethnicity: White

Height: 172.0 cm
Weight: 90.0 kg
Age: 27

b

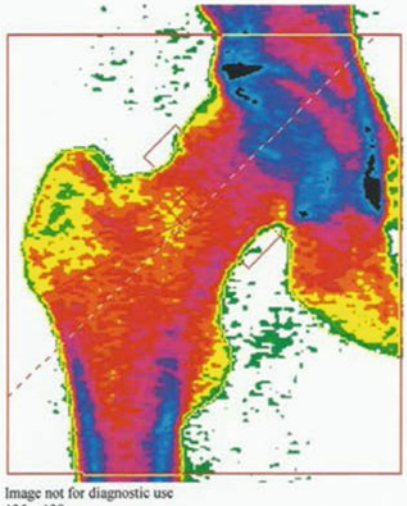

Image not for diagnostic use
125 x 139

Scan Information:

Scan Date: 12 May 2009 ID: A0512091Q
Scan Type: f Right Hip
Analysis: 12 May 2009 15:01 Version 12.3
Right Hip
Operator: FTH
Model: QDR 4500C (S/N 49458)
Comment:

DXA Results Summary:

Region	Area (cm^2)	BMC (g)	BMD (g/cm^2)	T - Score	Z - Score
Neck	5.85	6.41	1.095	1.2	1.3
Troch	15.23	11.98	0.787	0.1	0.1
Inter	34.18	42.00	1.229	0.2	0.2
Total	**55.26**	**60.39**	**1.093**	**0.4**	**0.4**
Ward's	1.12	1.00	0.895	0.8	0.9

Total BMD CV 1.0%
WHO Classification: Normal
Fracture Risk: Not Increased

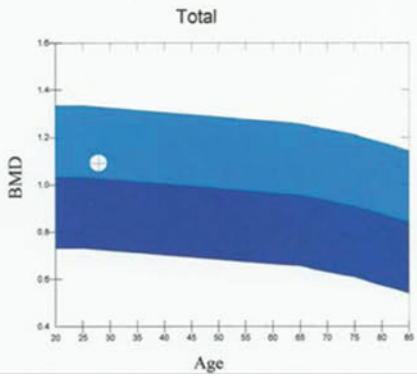

Physician's Comment:

Fig. 12.1 (continued)

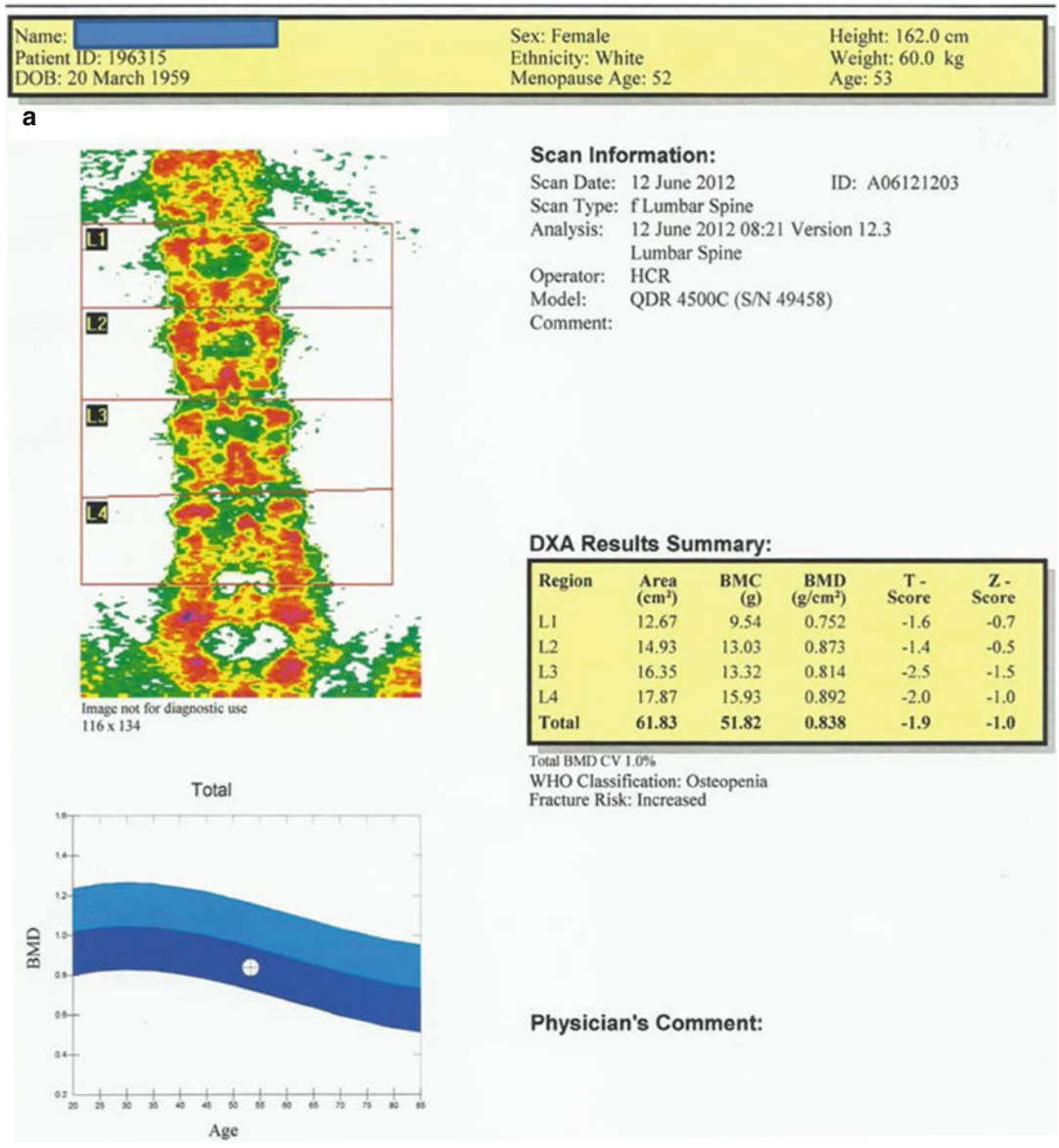

Fig. 12.2 (**a**) 53-year-old female patient. The average T score of L1–L4 vertebrae is −1.9, and Z score is −1.0. The BMD value is consistent with "osteopenia" range by WHO criteria and the fracture risk is increased. (**b**) The average T score for proximal femur in the same case is −1.2; Z score is −0.6. Although BMD value is consistent with "osteopenia" by WHO criteria, the fracture risk is increased

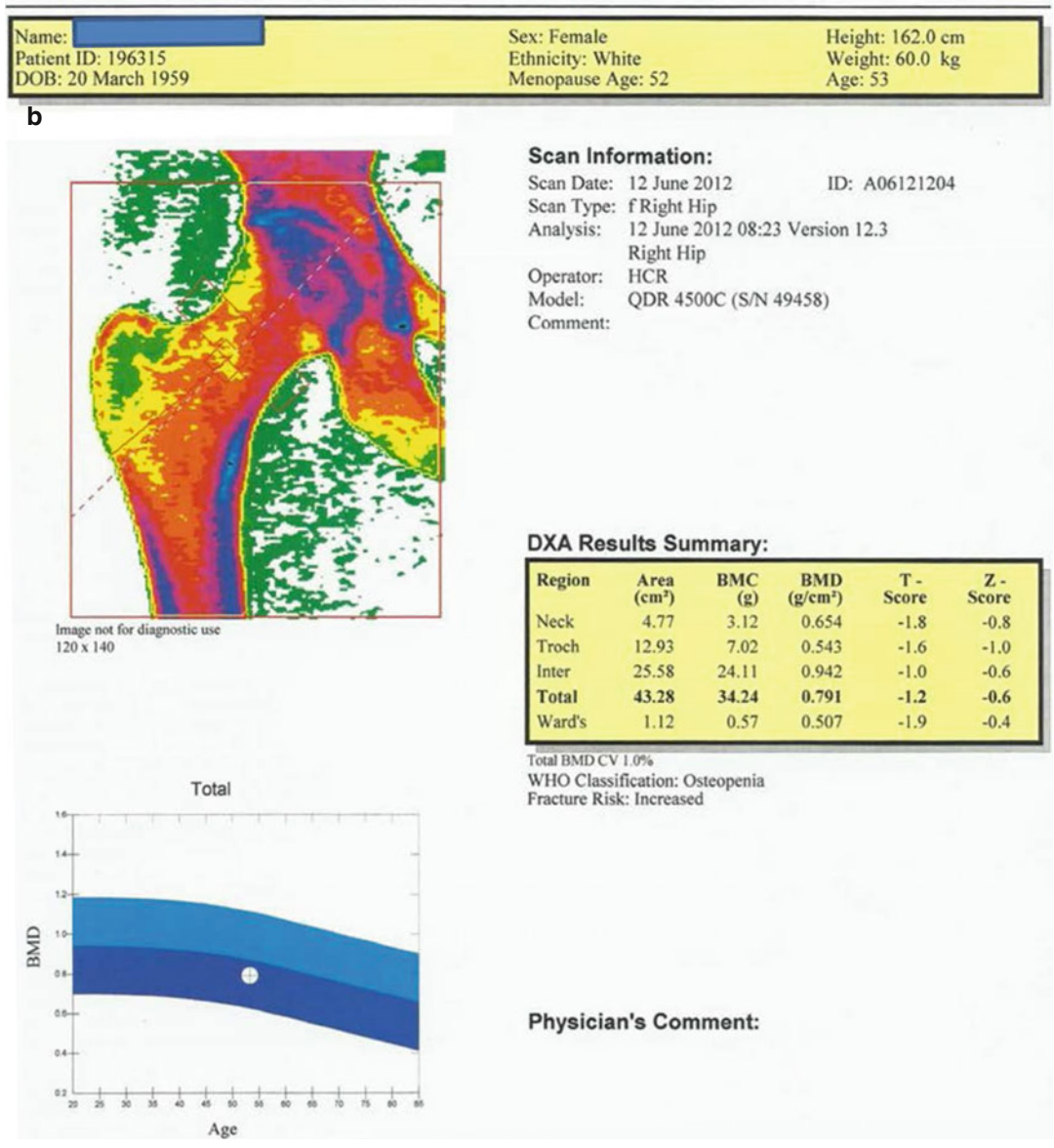

Fig. 12.2 (continued)

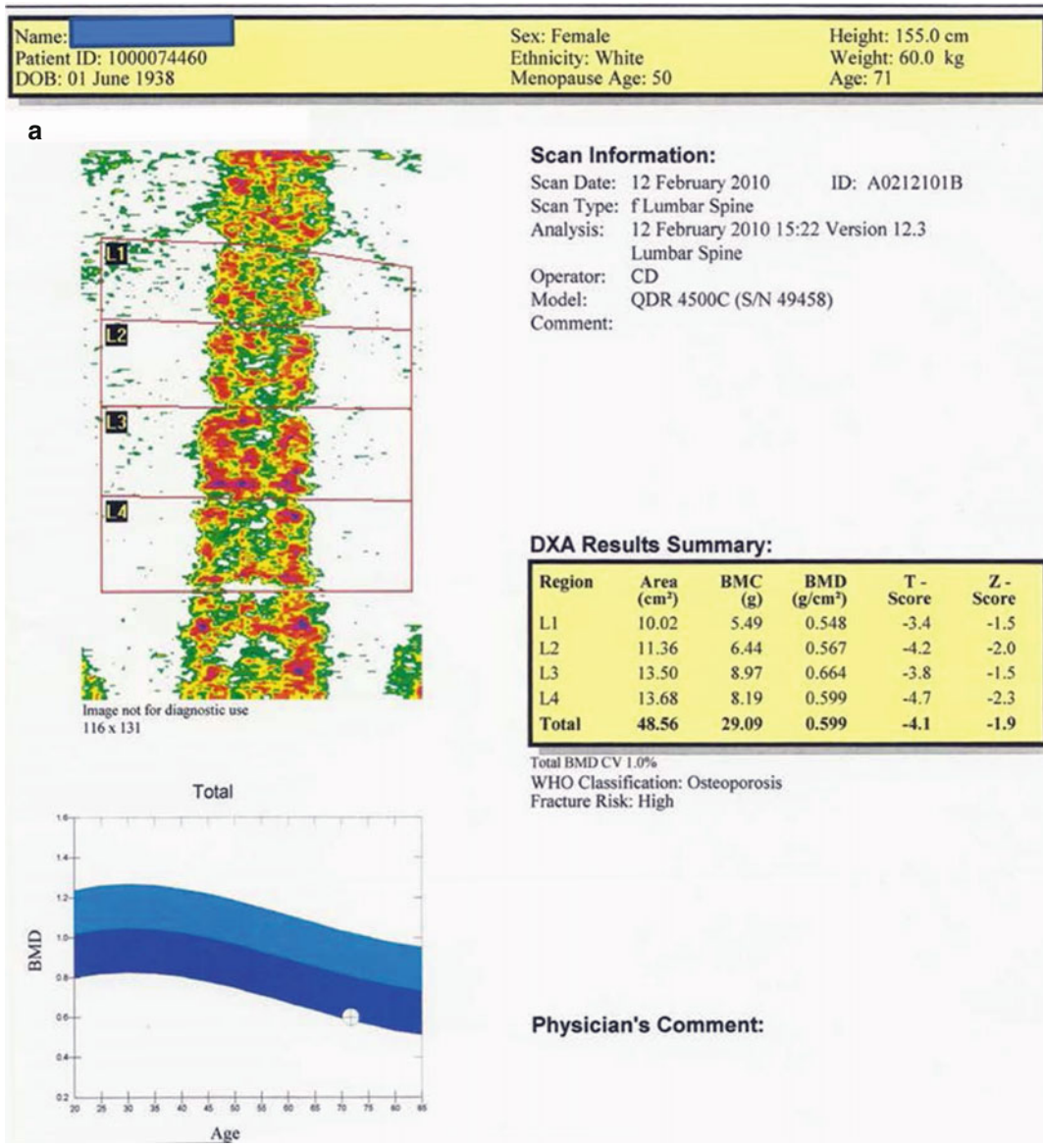

Fig. 12.3 (**a**) 71-year-old female patient. The average T and Z scores of L1–L4 vertebrae are −4.1 and −1.9, respectively. The BMD value of this case is consistent with "osteoporosis" by WHO criteria and the fracture risk is high. (**b**) The average T and Z scores for the proximal femur in the same case are −2.9 and −1.3, respectively. The BMD value is consistent with "osteoporosis" by WHO criteria, and the fracture risk is high

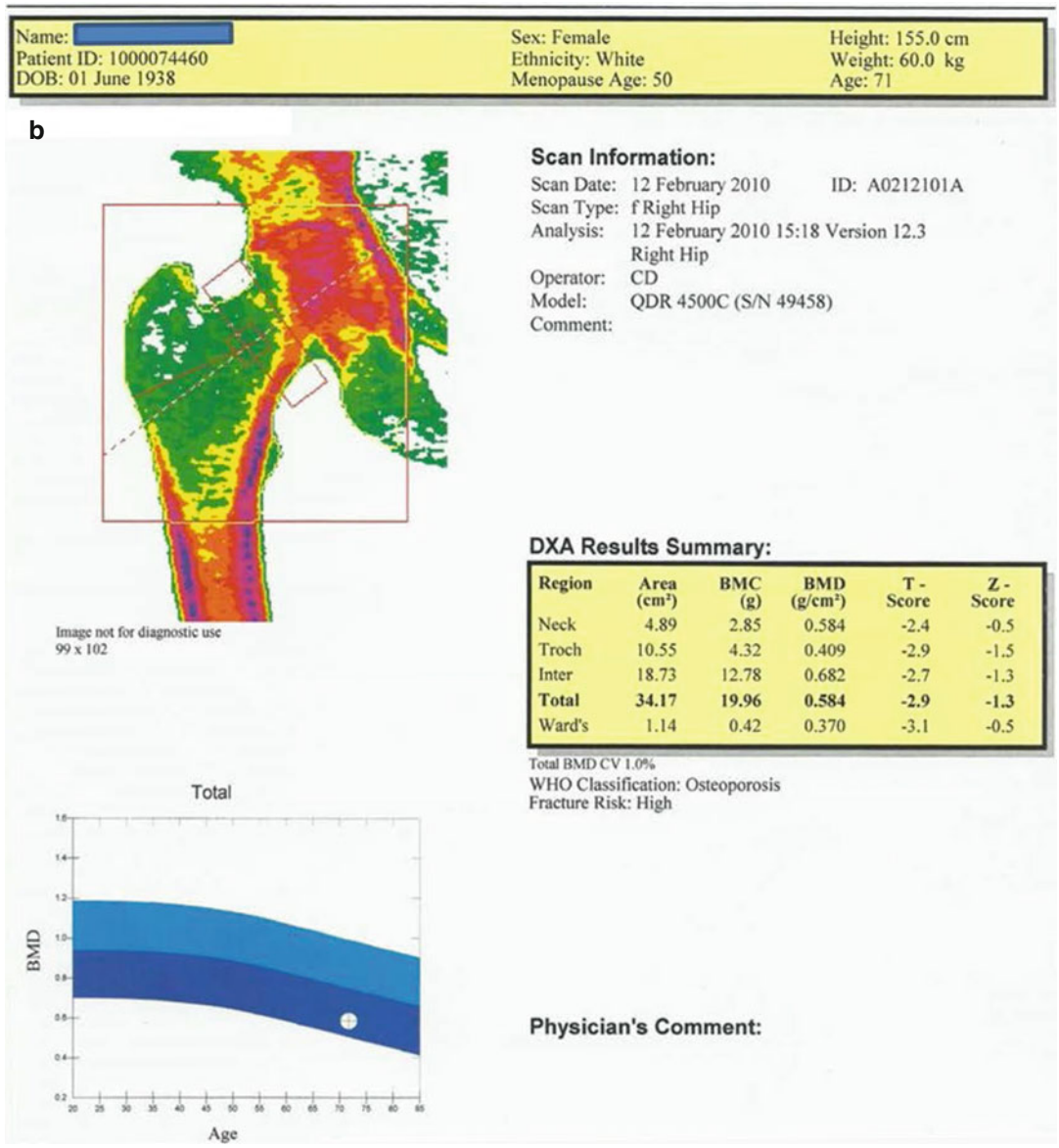

Fig. 12.3 (continued)

T score should be used for the diagnosis of osteoporosis in postmenopausal women and men over 50 years of age.

Z score should be used in premenopausal women, men under 50 years of age, and children.

The International Society for Clinical Densitometry (ISCD) states that:

Z score under −2 SD should be defined as "low bone mineral density below the expected range for chronological age."

Z score over −2 SD should be defined as "bone mineral density within the expected range for chronological age."

Z score is also especially important for the patients aged 75 years and over. ISCD also states that these populations cannot be diagnosed with osteoporosis only by using dual-energy X-ray absorptiometry (DXA) [1, 5, 8].

The proximal femur is not a reliable measurement location in pediatric patient group because of the variations in the development of skeletal system and a low level of repeatability in locating the field of interest. Lumbar vertebras (PA) and whole-body measurement excluding the head are the recommended locations for BMD measurement in children. Z score should be used instead of T score in the reports of pediatric patients. Besides that, the term "osteopenia" and, as long as there is no clinical history of fracture, the term "osteoporosis" should not be used in the pediatric patient group [9].

Patients with either osteoporosis or under the risk of developing fractures constitute the most important patient group for BMD measurement. BMD results must be comparatively evaluated in terms of age and sex for a more precise assessment. The fracture threshold for any individual is defined as 2.5 standard deviation (SD) below the BMD value of a young adult. While the fracture risk is almost nonexisting in an osteopenic patient with a T value of −1.1 SD, it is almost as much as an osteoporotic patient's risk in a person with a T value of −2.4 SD [2]. On the other hand, every unit of decrease in standard deviation increases the risk of femoral fracture 1.5–2 times [1, 5]. In addition to a low BMD value, the existence of femoral fracture or osteoporosis in the family, a low level of bone mass, use of steroids, smoking and alcohol habits, low calcium and vitamin D intake, and environmental factors increasing the risk of falling are defined as the risk factors for fractures [2]. Although the loss of BMD is related to the whole skeleton, it is more explicit in bones with higher trabecular density such as vertebras, femoral neck (Ward's triangle), and distal radius. BMD does not range in the same interval for the whole lifetime. It decreases in parallel with aging after the young adult age period. For example, BMD in the femoral neck decreases about 0.3 % every year in the third to fifth decades of a person's lifetime which means that a person's BMD value may decrease below the osteoporotic level due to age-associated bone loss even with no additional reason [2].

The main target in the treatment of low BMD is to get increase in bone mass to prevent fractures. Calcium and vitamin D should be taken both with diet and from sources external to diet. For the treatment of patients at the age of 80 and over, 1,500 mg calcium and 800 units of vitamin D intake is advised on a daily basis [2]. Bisphosphonates (alendronate, risedronate, ibandronate, and zoledronic acid) are also suggested in order to limit bone resorption and increase bone mass [2].

BMD measurement is advised for all menopausal women at the age of 65 and over and for all men over 70 years old regardless of risk factors, as well as for menopausal women aged below 65 years old with at least one risk factor, for premenopausal women over 40 years old with at least one history of a fracture associated with light trauma, and for all patients on osteoporosis treatment and on long-term steroid use [2]. In young people and in children, BMD should be measured if causes for secondary osteoporosis exist [9]. Main indications for BMD measurement are summarized in Table 12.2 [8, 10–13].

Table 12.2 Main indications in BMD measurement

Women aged 65 and older and men aged 70 and older, regardless of clinical risk factors
Younger postmenopausal women and men aged 50–69 with clinical risk factors listed below for fracture
Existence of osteopenia and/or vertebral pathology in radiology
History of fragility fracture (hip, vertebra, radius, proximal humerus fractures)
Smoking and increased alcohol consumption
History of osteoporotic fracture in family
Existence of significant shortening and thoracic kyphosis
Premature menopause (<45)
Prolonged secondary amenorrhea
Primary hypogonadism
Corticosteroid treatment (>5 mg/day or equivalent for ≥3 months)
Anorexia nervosa and malabsorption
Primary hyperparathyroidism

(continued)

Table 12.2 (continued)

Osteogenesis imperfecta
Hyperthyroidism
Long-term immobility
Cushing syndrome
Neoplasia (multiple myeloma and others)
Follow-up of treatment efficiency in patients being treated for osteoporosis
Cases that are not being treated but with possibility of bone loss that would require treatment
Women and men before 50 years of age with causes of secondary osteoporosis

Table 12.3 Commonly used BMD measurement methods

General classification	Method
Radiological methods:	Standard conventional radiography
	Bone radiometry
	Radiologic photodensitometry
	Digital image processing (DIP)
	Quantitative computed tomography (QCT)
Photon absorption techniques:	Single-photon absorptiometry (SPA)
	Dual-photon absorptiometry (DPA)
	Single-energy X-ray absorptiometry
	Dual X-ray absorptiometry (DXA)
Other methods:	Quantitative ultrasonography (QUS)
	Neuron activation analysis
	Magnetic resonance imaging
	Slit screening flography
	Bone biopsy

BMD Measurement Methods

The method of BMD measurement should be easy, cheap, reproducible, and specific, and it should provide sufficient and accurate information on the risk of fracture in advance. Other qualifications desired in the method are a low dose of radiation and comparability of the test to the standards of race, age, sex, and region in which the test is performed, providing sufficient and fast information for treatment follow-up and compatibility with other diagnostic tests (biochemical tests, biopsy, etc.) used for osteoporosis [14].

We will now examine briefly today's most commonly used BMD measurement methods listed in Table 12.3.

Quantitative Computed Tomography (QCT)

Computed tomography (CT) measures BMD in Hounsfield units as mg/cm^3 using single or dual energy [6]. One of the most important problems in QCT is that bone mineral content can be measured 15–20 % lower than its real value because of the increasing fat content in the bone marrow by age. Use of dual-energy technique provides more accurate results due to the capacity to correct the effect of fat in the bone marrow. Besides, this error associated with fat content is accepted as clinically insignificant since age is used to determine the risk of fracture [6].

It is important to be able to measure the BMD value of trabecular bone separately in patients with osteoporosis, since it is more sensitive in monitoring the changes in the course of disease and evaluation of response to the treatment [1, 5]. The overall sensitivity of QCT as an effective method in the estimation of vertebral fractures and in the measurement of bone loss with the capability of measuring trabecular and cortical bone density separately is higher than the overall sensitivity of DXA. The front part of the trabecular bone in vertebral corpus is used for analysis with QCT. It is also possible to measure trabecular bone selectively by excluding concentrations that can lead to a higher BMD value inaccurately, such as aortic calcification in the field of measurement [1]. Despite all these advantages, QCT is not often used in BMD measurement because of its high cost and higher radiation exposure (1.5–2.9 mSv) compared to other methods [5].

Quantitative Ultrasonography (QUS)

It is a method developed on the basis of physical changes that ultrasonic waves undergo while they pass through bone mass. Bone elasticity and hardness could be demonstrated by QUS. No radiation exposure, low cost, and ease of application are the advantages of QUS. The most important limit of QUS is that it can be used on superficial bones such as the patella, tibia, and calcaneus [15].

Single-Photon Absorptiometry (SPA)

One hundred fifty to 800 millicurie (mCi) I-125 (Iodine-125) source and 27–35 keV collimated X-rays photons are used for SPA. Similar to QUS, SPA is suitable for the measurement of superficially located bones with very few neighboring soft tissue [16]. Radiation dose to skin in SPA varies between 15 and 100 μSv [17]. It is most commonly used for the middle and distal section of radius and calcaneus. The most important disadvantage of this technique is the possibility of false measurement in the existence of prevailing soft tissue. On the other hand, although SPA can measure both cortical and trabecular bone density, the measurement results do not reflect accurately the vertebral and femoral density where the risk of fracture is the highest [16].

Dual-Photon Absorptiometry (DPA)

Gadolinium-153 (Gd-153) having 44 and 100 keV photons with 242 days physical half-life is used as a radioactive source in DPA. The basis of BMD measurement is the fact that the attenuation of each photon in soft tissue and bone is different. For this reason, it should be considered that false low BMD measurements could come up in the cases of laminectomy or lytic bone lesions, and false high BMD measurements could come up in the cases of pressure-related fractures, serious aortic calcification, myelographic contrast material use, and degenerative sclerotic changes [18]. The average dose being exposed in DPA is 12 mR. On the other hand, while both cortical and trabecular bone density can be measured by DPA in the vertebra and proximal femur, DPA of vertebra reflects mainly trabecular bone density.

Dual X-Ray Absorptiometry (DXA)

DXA is today's most commonly used method, and it is accepted as the golden standard in BMD measurement. X-ray tube radiating X-rays of two different energy levels, that is, 70 and 140 keV, is used as the radiation source in DXA. Patients are located between X-ray tube and detector. X-rays, after passing through the collimator system that helps their orientation to the selected field of interest, are absorbed at varying levels because of varying densities of the bone and soft tissue in the field of interest, and they reach to the detector on the patient (Fig. 12.4). Attenuation difference between the bone and soft tissue becomes more evident at low energy level. By entering the bone and soft tissue attenuation values in the system, it is possible to exclude the attenuation of soft tissues in the field of interest and to develop the attenuation profile of the interested bone [1, 5]. Radiation dose being exposed in the DXA technique (50 μSv) is 1/1,000 of conventional vertebral X-ray graphy [19]. High resolution and image quality as well as the short test duration (2–5 min) are the other advantages of this technique [5].

The loss of bone mineral is not the same in different parts of the body. Therefore, although the most suitable skeleton part to be used for measurement is not specified in diagnosing osteoporosis, lumbar spine and proximal femoral measurements are used in DXA as standard protocol [20, 21]. Routine DXA analysis of the femur (Fig. 12.5) gives us information about the BMD value of the femoral neck, trochanter, and Ward's triangle. Ward's triangle is defined as the lowest density area in the midpoint of the bottom edge of the triangle in the femoral neck. Whereas whole hip and femoral neck measurements provide the most valuable information in determining the fracture risk, total hip measurement is used for monitoring the course of disease and for the evaluation of the response to treatment since it provides a broader sampling area [6].

Use of peripheral skeleton areas for the diagnosis of osteoporosis has limited value. Among the peripheral measurements, only distal one third of the radius is valid according to World Health Organization's (WHO) criteria for diagnosing osteoporosis and osteopenia [22]. BMD measurement of the forearm may be preferred in cases where hip and/or vertebral measurements cannot be conducted or where results of the analysis cannot be evaluated. Besides that, forearm BMD measurement can also be performed in patients with acidic cirrhosis, in patients with hyperparathyroidism-associated osteoporosis,

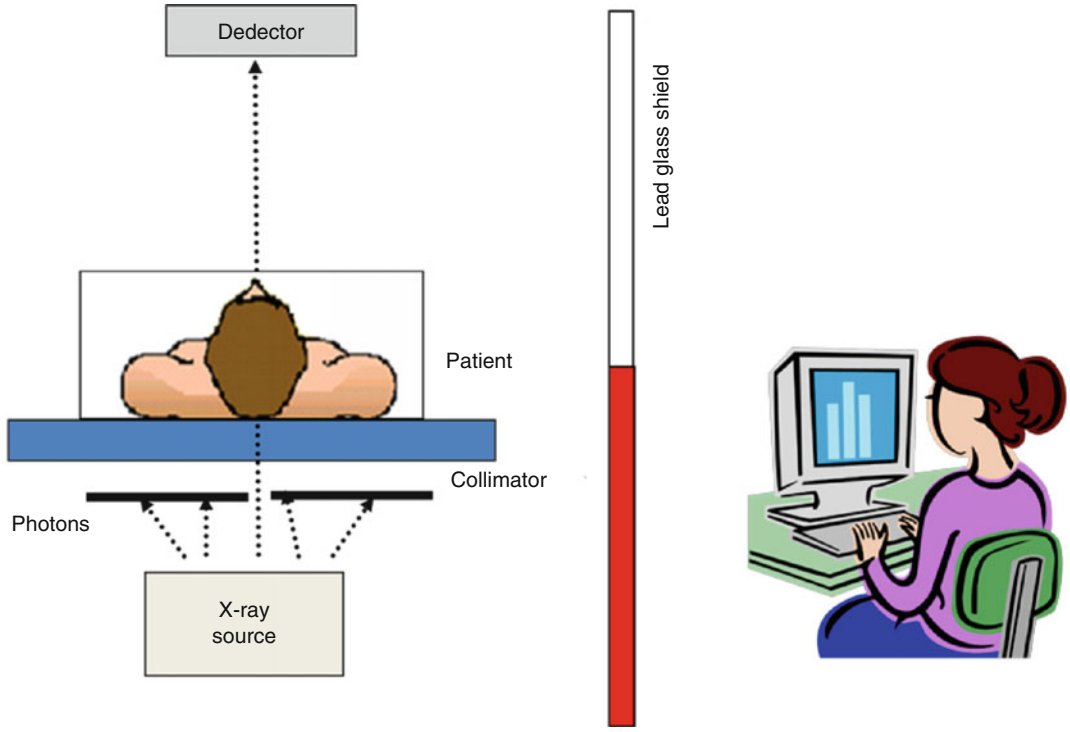

Fig. 12.4 DXA system composed of X-ray source and collimator system with the capacity to choose appropriate photons and detector

Fig. 12.5 Fields of interest in BMD measurement of the femoral neck

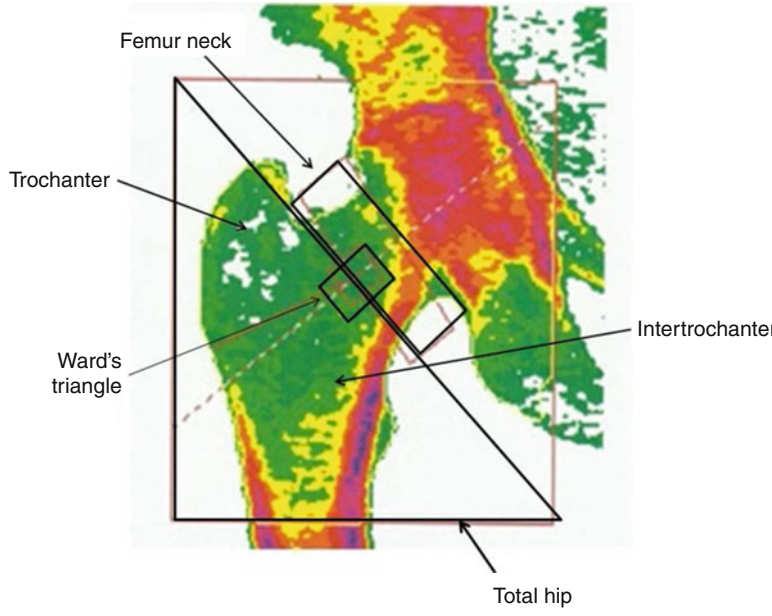

and in patients with extreme obesity who are over the limit of carrying capacity of DXA [22, 23].

BMD measurement should not be based upon the evaluation of only one or two vertebral corpus. The lesser the number of vertebral corpus analyzed, the higher the risk of false measurement. For this reason, the BMD value of lumbar vertebrae should be determined by tak-

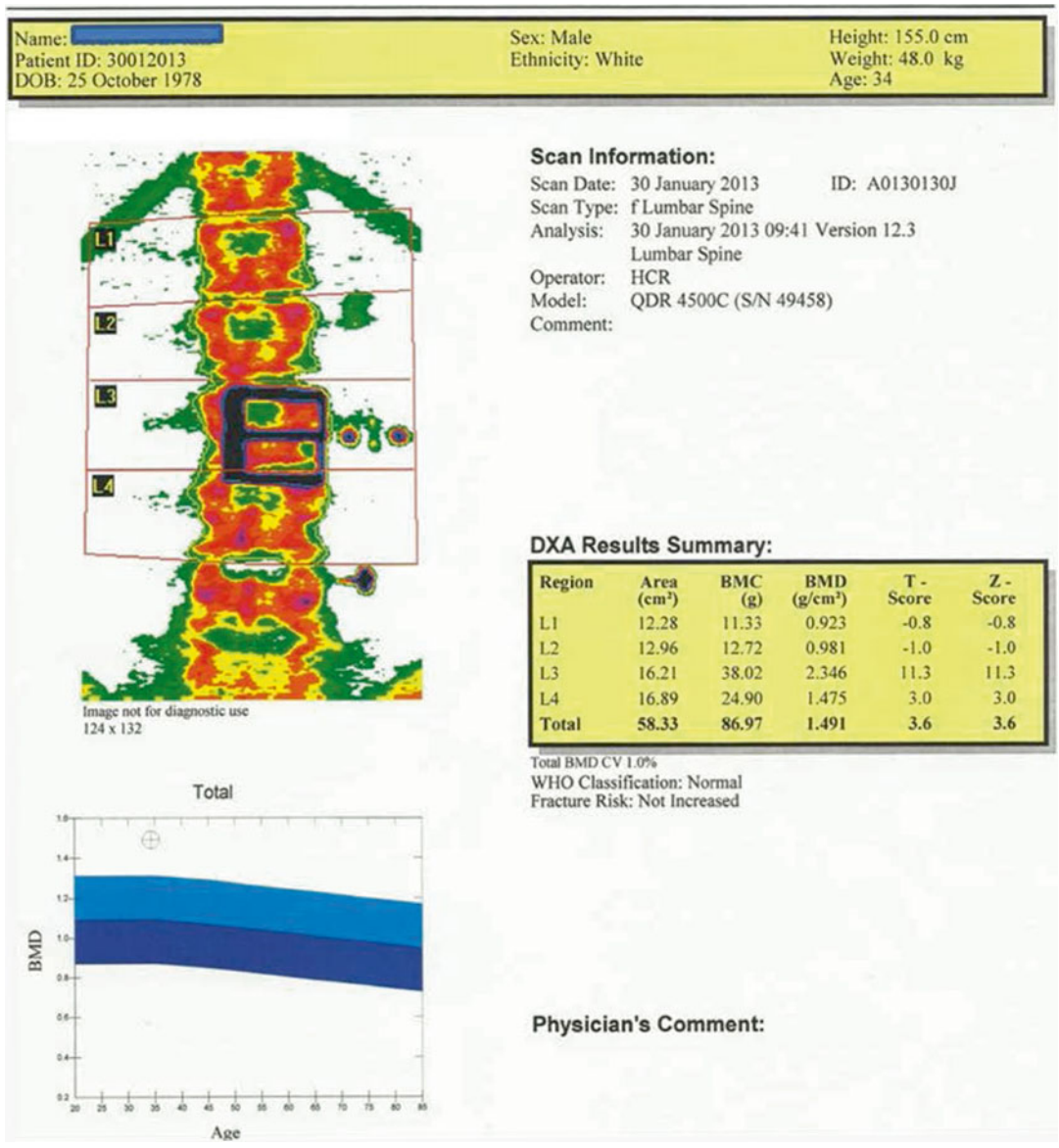

Fig. 12.6 The metal artifact and artificial increase in the BMD due to a belt buckle in a 34-year-old male patient

ing the average of the BMD values of L1–L4 vertebrae [6, 13].

BMD measurement of lumbar spine may score higher than its real value in the existence of morphological changes such as osteophytes overlapping with the vertebrae in the field of interest, severe scoliosis, old fractures and vertebral deformities, aortic calcification, reactive bone changes associated with degenerative facet, and disk, metallic, and radiopaque implants (Fig. 12.6) which may cause underestimation of the fracture risk [6, 14, 24]. Similarly, in obese patients, the excess of superimposed soft tissue would result in a BMD measurement value higher than actual since it would increase the amount of X-rays attenuated [5]. For these reasons, slower imaging speed should be preferred in obese patients or in the existence of very low BMD [6]. On the other hand, pressure fractures limit the vertebra field being measured and thus may cause false high BMD value often [6]. Also the existence of intestinal barium or recent injection of

radiopharmaceutical agent may end up with an incorrect BMD measurement [6].

In cases which scintigraphic scanning or radiopharmaceutical agent injection with the purpose of radionuclide treatment is delivered, BMD measurement should be postponed until ten physical half-life of used radionuclide passes.

It is also possible to evaluate vertebral corpus in lateral position for determining and fixing artifacts formed in anterior and posterior projection by degenerative changes and vascular calcifications. However, in this method, only L3 and L4 vertebrae could be evaluated because of the superimposition of the ribs and iliac crest [6].

One of the most important disadvantages of DXA is that it cannot differentiate between cortical and trabecular bones and it cannot distinguish the changes associated with bone geometry since it is a two-dimensional technique [1].

BMD measurement should be performed on the healthy side in patients with femoral prosthesis and on the forearm in patients with bilateral prosthesis.

While DXA can only measure the density in a defined area (g/cm^2) as it is a two-dimensional measurement, QCT is capable of volumetric measurement (mg/cm^3).

Although BMD measurement by DXA could be conducted every 1–2 years for monitoring the response to treatment, the frequency of measurement should be decided according to the patient's clinical symptoms. Follow-up could be conducted in postmenopausal women and men over 70 years of age once in 1–2 years for the evaluation of treatment efficiency and in longer intervals in clinically stable cases. However, closer follow-up (6-month intervals) is more suitable in patients who have secondary osteoporosis and who are on medications speeding up bone mineral loss such as corticosteroids. On the other hand, follow-up periods should be once in a year and twice in a year in patients who are on bisphosphonate and teriparatide therapy, respectively. The minimum follow-up interval for BMD measurements in children and adolescents should be at least 6 months [13].

DXA alone is not sufficient to determine fracture risk in patients with osteopenia. Therefore, other risk factors are needed to be determined to make a conclusion about fracture risk. The most important recent development about this issue is FRAX (WHO Fracture Assessment Tool). FRAX is an Internet software published by World Health Organization (WHO) which is used to identify the fracture risk in osteopenic cases. The hip is used for BMD measurement in FRAX as the best indicator for the fracture risk. The risk of hip fracture in 10 years and the risk of a major osteoporotic fracture could be calculated according to FRAX by answering the questionnaire. Its disadvantages are that it cannot evaluate risk depending on other body parts other than hips and it cannot be used in previously treated patients. FRAX should be considered in patients for whom DEXA T score is smaller than −2.5 SD and in the existence of fragility fracture [25].

The test's accuracy and its reproducibility are very important in clinicians determining the change and stability in the patient's BMD value. A crucial aspect in BMD measurement by DXA is accuracy [7]. Accuracy tells us about how close are the measurements to the real values. In the evaluation of measurements by DXA, for the difference to be significant, the least significant change (LSC) should be considered. LSC means that the difference between two measurements is significant with a 95 % possibility. In order to be able to talk about treatment efficiency in general, at least 5 % change in BMD is required. Vertebral measurement should be used in the evaluation of response to treatment. Peripheral measurements are not suitable for follow-up and response evaluation [26].

T score is not used in the follow-up; instead, definitely, change in g/cm^2 should be calculated.

In order to calculate LSC, first of all the coefficient of variation (CV) should be determined. CV is the criterion of reproducibility (precision), and it is the expression in percentage of the difference coming up in repeating measurements. For the calculation of CV, BMD measurements are conducted in 30 patients in maximum of 1-month intervals. This group is composed of 30 people and should be compatible with the patient group to be tested in terms of age and weight.

LSC is calculated by the equation below after CV in vivo is determined:

$$\mathrm{LSC}(\%) = \mathrm{Coefficient\ of\ Variation}(\mathrm{in\ vivo}) \times 2.77[7].$$

Higher reproducibility of DXA machine means that the possibility of obtaining the same results in repeating measurements conducted under the same conditions will be high. CVs of the DXA machines should be monitored for a healthy and reliable measurement. If the machine requires daily calibration, calibration steps should be followed precisely by the phantom provided by the producer company. Calibration should be carried out again by the phantom provided by the producer company when the BMD measurement machine is moved to a new location and also in cases of hardware/software updates or when a dramatic change occurs in the environment (temperature, humidity, etc.) [7].

Accuracy and reproducibility depend on several factors. Besides calibration of the scanner, the patient population and the region in which the measurement is made and the talent of the technician in patient positioning and in analyzing the test may affect the test results. Although it seems like a minor detail, it is recommended that the measurements are made in the same season because of small seasonal variations in BMD. Moreover, although both right and left femurs could be used for BMD measurement, the same side body site should be measured for reproducibility [27]. Results of BMD measurements by DXA are correlated with total body fat mass; therefore, it should be considered that the BMD measurements could be influenced by weight gain or weight loss [5, 6].

References

1. Guglielmi G, Muscarella S, Bazzocchi A (2011) Integrated imaging approach to osteoporosis: state-of-the-art review and update. Radiographics 31:1343–1364
2. Lentle B, Worsley D (2006) Osteoporosis redux. J Nucl Med 47:1945–1959
3. Melton LJ 3rd, Wahner HW (1989) Defining osteoporosis. Calcif Tissue Int 45:263–264
4. Frost HM (1985) The pathomechanics of osteoporosis. Clin Orthop 200:198–225
5. Link TM (2012) Osteoporosis imaging: state of the art and advanced imaging. Radiology 263:3–1
6. Lentle BC, Prior JC (2003) Osteoporosis: what a clinician expects to learn from a patient's bone density examination. Radiology 228:620–628
7. Erselcan T, Özen A, Yüksel D, Durmuş Altun G, Öztürk E, Balcı TA, Karayalçın B (2009) Procedure guideline for bone density measurement. Turk J Nucl Med 18:31–40
8. Cosman F, de Beur SJ, LeBoff MS, Lewiecki EM, Tanner B, Randall S, Lindsay R (2014) Clinician's guide to prevention and treatment of osteoporosis. Osteoporos Int 25:2359–2381
9. Blake GM, Fogelman I (2010) An update on dual-energy x-ray absorptiometry. Semin Nucl Med 40(1):62–73
10. Kanis JA, Delmas P, Burckhardt P, Cooper C, Torgerson D (1997) Guidelines for diagnosis and management of osteoporosis. The European Foundation for Osteoporosis and Bone Disease. Osteoporos Int 7:390–406
11. Kanis JA, McCloskey EV, Johansson H, Cooper C, Rizzoli R, Reginster JY, Scientific Advisory Board of the European Society for Clinical and Economic Aspects of Osteoporosis and Osteoarthritis (ESCEO) and the Committee of Scientific Advisors of the International Osteoporosis Foundation (IOF) (2013) European guidance for the diagnosis and management of osteoporosis in postmenopausal women. Osteoporos Int 24:23–57
12. Brown JP, Josse RG, Scientific Advisory Council of the Osteoporosis Society of Canada (2002) Clinical practice guideline for the diagnosis and management of osteoporosis in Canada. CMAJ 167(10 Suppl):S1–S34
13. The Society of Endocrinology and Metabolism of Turkey (2014) Diagnosis and treatment guideline for metabolic bone disorders, Ankara, pp 1–4
14. Lorente-Ramos R, Azpeitia-Armán J, Muñoz-Hernández A, García-Gómez JM, Díez-Martínez P, Grande-Bárez M (2011) Dual-energy x-ray absorptiometry in the diagnosis of osteoporosis: a practical guide. AAJR Am J Roentgenol 196:897–904
15. Gluer CC (1997) Quantitative ultrasound techniques for the assessment of osteoporosis: expert agreement on current status. The International Quantitative Ultrasound Consensus Group. J Bone Miner Res 12:1280–1288

16. Cameron JR, Sorenson J (1963) Measurement of bone mineral in vivo: an improved method. Science 142:230–232
17. Goodwin PN (1987) Methodologies for the measurement of bone density and their precision and accuracy. Semin Nucl Med 17:293–304
18. Wahner HW (1988) Comparison of dual-energy x-ray absorptiometry and dual photon absorptiometry for bone mineral measurements of the lumbar spine. Mayo Clin Proc 63:1075–1084
19. Fogelman I, Blake GM (2000) Different approaches to bone densitometry. J Nucl Med 41:2015–2025
20. Blake GM, Fogelman I (1997) Technical principles of dual energy x-ray absorptiometry. Semin Nucl Med 27:210–228
21. Black DM, Cummings SR, Genant HK, Nevitt MC, Palermo L, Browner W et al (1992) Axial and appendicular bone density predict fractures in older women. J Bone Miner Res 7:633–638
22. WHO Osteoporosis Study Group on Assesment of Fracture Risk and its Application to Screening for Postmenopausal Osteoporosis, Geneva (1994)
23. Labio ED, Del Rosario DB, Strasser SI, Mc-Caughan GW, Crawford BA (2007) Effect of ascites on bone density measurement in cirrhosis. J Clin Densitom 10:391–394
24. Kanis JA (2002) Diagnosis of osteoporosis and assessment of fracture risk. Lancet 359:1929–1936
25. Roux S, Cabana F, Carrier N, Beaulieu M, April PM, Beaulieu MC, Boire G (2014) The World Health Organization fracture risk assessment tool (FRAX) underestimates incident and recurrent fractures in consecutive patients with fragility fractures. J Clin Endocrinol Metab 99(7):2400–2408
26. Khan SN, Craig L, Wild R (2013) Osteoporosis: therapeutic guidelines. Guidelines for practice management of osteoporosis. Clin Obstet Gynecol 56(4): 694–702
27. Baim S, Wilson CR, Lewiecki EM, Luckey MM, Downs RW Jr, Lentle BC (2005) Precision assessment and radiation safety for dual-energy X-ray absorptiometry: position paper of the International Society for Clinical Densitometry. J Clin Densitom 8:371–378

13 Nuclear Medicine Techniques in the Diagnosis and Treatment of Diseases of the Musculoskeletal System

Murat Tuncel, Özgür Ömür, Ceren Deniz Kapulu, and Ömer Uğur

Abstract

Nuclear medicine techniques are increasingly used in the diagnosis and treatment of musculoskeletal system diseases. Among these, bone scintigraphy has been used for many years in the diagnosis and follow-up of benign and malignant diseases. The introduction of SPECT-CT improved the specificity of the test and increased utilization. Molecular imaging with FDG-PET-CT has now become indispensable in the staging and treatment follow-up of primary and secondary malignancies of skeletal system. Other radiopharmaceuticals like radiolabeled thymidine and tyrosine will help to better understand the molecular biology of diseases. Bone pain palliation and radiosynovectomy are the routinely used nuclear medicine therapies. The introduction of new radiopharmaceuticals used in conjunction with other methods of treatment will further improve the patient benefit.

Learning Outcomes

1. Learn the clinical applications of bone scintigraphy.
2. Understand the additional value of SPECT-CT and PET-CT in musculoskeletal diseases.
3. Learn nuclear therapy options in musculoskeletal diseases.

There are several alternative options in the treatment of musculoskeletal diseases. Orthopedic surgeons should decide the most appropriate treatment from these advanced and complicated methods using data obtained from the imaging modalities. Radiological imaging techniques such as computerized tomography (CT), magnetic resonance imaging (MRI), and

M. Tuncel (✉) • Ö. Ömür • Ö. Uğur
Hacettepe University Department of Nuclear Medicine, Ankara, Turkey
e-mail: muratmtx@yahoo.com; ougur@hacettepe.edu.tr

C.D. Kapulu
Ege University Department of Nuclear Medicine, İzmir, Turkey

F. Korkusuz (ed.), *Musculoskeletal Research and Basic Science*,
DOI 10.1007/978-3-319-20777-3_13

ultrasound reflect structural changes in the normal anatomy. Unlike the radiological methods, nuclear medicine imaging shows the metabolic and molecular properties of tissues.

Changes at biochemical and receptor levels occur before any changes in anatomy are detected. Also anatomic changes are not always disease specific and may not have clinical significance. For example, in a patient with Ewing's sarcoma, every lymph node that increase in size should not be interpreted as a sign of metastases, because in addition to the malignant disease many benign diseases, like sarcoidosis, may lead to an enlarged lymph node. Similarly some benign bone lesions in anatomic imaging may mimic malignancy. Molecular imaging techniques that provide tissue characterization by showing changes in the lesion metabolism and receptor status are needed when anatomic imaging cannot provide an adequate answer to the clinical question. Over the last two decades, increase in the utilization of SPECT (single-photon emission computerized tomography)-CT and PET (positron emission tomography)-CT imaging allowed physicians to answer the clinical questions by anatomic and metabolic imaging in a single examination.

Clinical Relevance

Does radionuclide therapy help for palliation of refractory metastatic bone pain?

A 67-year-old male patient with metastatic prostate cancer. Patient has suffered from intractable bone pain despite receiving analgesics, bisphosphonates, hormonal therapy, and external beam radiotherapy. He had normal renal functions and low-normal hematological parameters (Hb, 12 g/dl; total white cell count,5×10^3/μL; and platelet count, 154.000×10^3/μL). He could care for himself but unable to do active work (Karnofsky score >70) and had a life expectancy of >4 weeks. He had received 80 mCi of ^{153}Sm-EDTMP therapy for bone pain palliation. Three days after therapy, he had experienced increase in bone pain (flare phenomena) which resolves at the second week with a 50 % decrease in the pretherapy WHO pain score. He had mild decrease in the hematological parameters (Hb,10 g/dl; total white cell count, 3.5×10^3/μL; and platelet count, 100.000×10^3/μL) at 4 weeks which returned to baseline in the follow-up (Fig. 13.1).

Bone pain is a severe debilitating condition which frequently impairs the quality of life. Patients often receive analgesics, bisphosphonates, and external beam radiotherapy to provide symptomatic relief. However, each therapy has its side effect and not so effective in patients with widespread metastasis. Bone-seeking radiopharmaceuticals are one of the therapeutic options available for palliation of bone pain and should be used in conjunction with other therapy modalities in osteoblastic metastasis detected by bone scintigraphy. Approximately 60–80 % of these patients benefit from these therapy with mild transient hematological toxicity [96]. Although previous radiotracer like 89Sr, 153Sm-lexidronam, or 186Re-etidronate only provided bone pain palliation, recently introduced radium-223 chloride, an alpha-emitting radioisotope, was found to provide additional survival benefit in a phase 3 trial [97]. Ongoing studies with bone-seeking radiopharmaceuticals combined with other cytotoxic therapies will further clarify the potential patient benefit.

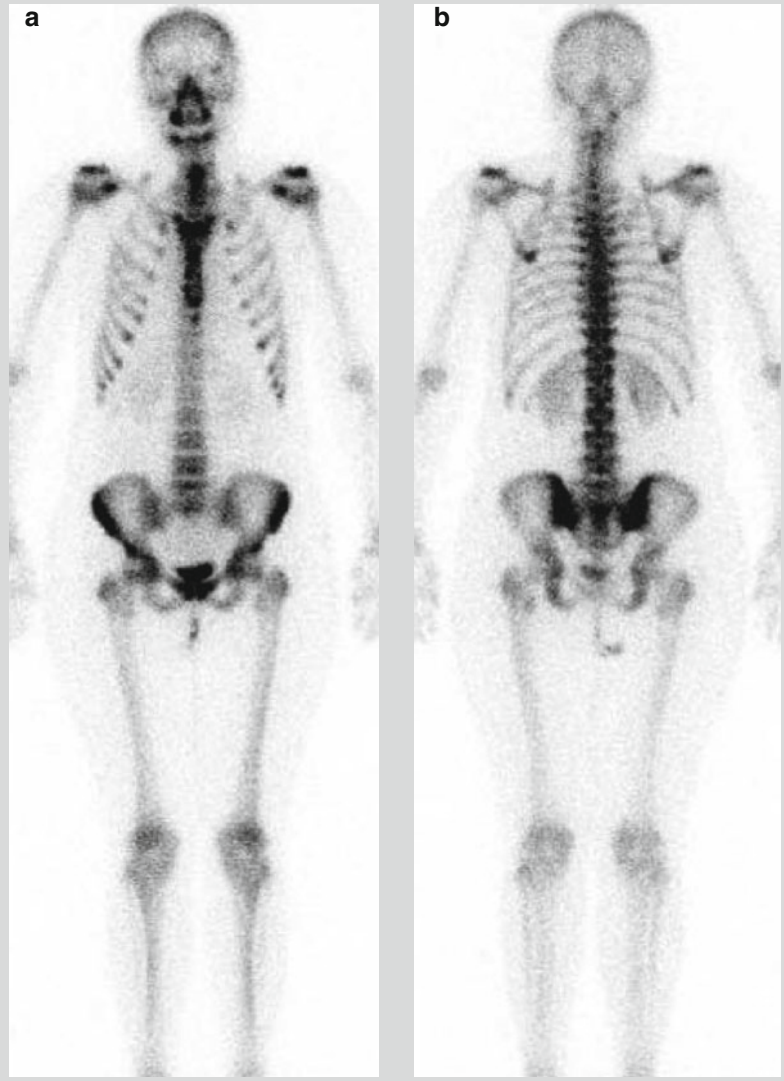

Fig. 13.1 Normal whole-body bone scintigraphy

A-Bone Scintigraphy (BS)

Plain radiographs provide assessment of anatomic structure of bone, whereas BS gives us the ability to detect bone's blood flow and metabolism. In addition to its high sensitivity, the visualization of the entire skeletal system in a single examination is another advantage of BS. However, the specificity of BS is low and needs to be correlated with other anatomic imaging modalities. In recent years, widespread use of SPECT-CT scanner allowed us simultaneous acquisition of 3D scintigraphic and CT data from the same region, and specific diagnosis can be reached in a single study.

Standard BS was performed as whole body for the investigation of metastatic disease. The three-phase BS consists of blood flow, blood pool, and delayed phases that shows blood flow and bone metabolism. Three-phase BS is used for localized involvement of bone lesions like osteomyelitis, tumors, or fractures [1, 2].

Indications of BS

1. Staging and follow-up of primary/metastatic bone tumors
2. Etiology bone pain that cannot be identified by radiography
3. Evaluation of patients with suspicion for fractures
4. Evaluation of bone and soft tissue infections.
5. Evaluation of joint involvement in patients with arthritis
6. Detection of prosthetic complications like aseptic loosening and infection
7. Assesment of bone graft viability
8. Investigation of maturation of soft tissue calcifications before surgery
9. Diagnosis of avascular necrosis (AVN)
10. Metabolic bone diseases
11. Reflex sympathetic dystrophy
12. Diagnosis and follow-up of Paget's disease
13. Evaluation of chronic back pain
14. Suspicion of child abuse
15. Evaluation of anormal and nonspecific bone pathologies detected on bone graphies [3]

Radiopharmaceuticals Used and Uptake Mechanisms

Tc-99m-labeled diphosphonates (e.g., methylene diphosphonate (MDP)) are used in bone scintigraphy [1–3]. After intravenous injection, radiopharmaceutical is biodistributed to the whole body via blood and passes to extravascular area by passive diffusion. Tc-99m-labeled phosphates are absorbed by chemical bonds to hydroxyapatite crystal found on bone surface. About 40–50 % of these compounds will be affixed to the bone by 4 h after injection. Excretion is primarily renal [4] and 70 % of the administered dose is eliminated by 6 h. The recommended dose for an adult patient is 20 mCi (740 MBq). The whole-body radiation dose from a Tc-99m MDP bone scan is approximately 0.01 rad/mCi (4.2 mSv); the urinary bladder is the critical organ because of renal excretion, receiving about 0.1–0.2 rad/mCi [3, 4].

The uptake of radiopharmaceutical in bone depends on blood flow and osteoblastic activity. There is a normal physiological activity in areas where bone turnover is increased like in joints, muscle insertion areas, and excretion pathways (mainly kidney and bladder and small amount by intestines). In areas where only osteoclastic activity is seen or in metabolically inactive sclerotic bone islands, normal radiopharmaceutical biodistribution is seen. Radiotracer uptake is increased in conditions where blood flow or bone metabolism is increased. Primary or secondary bone tumors, fractures, trauma, arthritis, degenerative joint changes, neuropathic joint pathologies, and pathological fractures due to osteoporosis were the conditions that osteoblastic activity could be seen [1–3].

Imaging Technique

BS has two main protocols, namely, three-phase and whole-body static images (2D imaging). In addition to these protocols, 3D SPECT or SPECT-CT imaging can be performed for suspected regions [1–3].

Standard BS

Whole-body images of skeleton were obtained 2–6 h after injection of radiotracer (Fig. 13.2).

Three-Phase BS

The area of interest was focused by gamma camera, and by using dynamic acquisition, blood flow (obtained as the tracer is injected) and blood pool phase that reflects soft tissue involvement (acquired immediately after the flow portion of the study and completed within 10 min of injection of the tracer) were acquired (Fig. 13.3). After 2–5 h whole-body images were taken as late images.

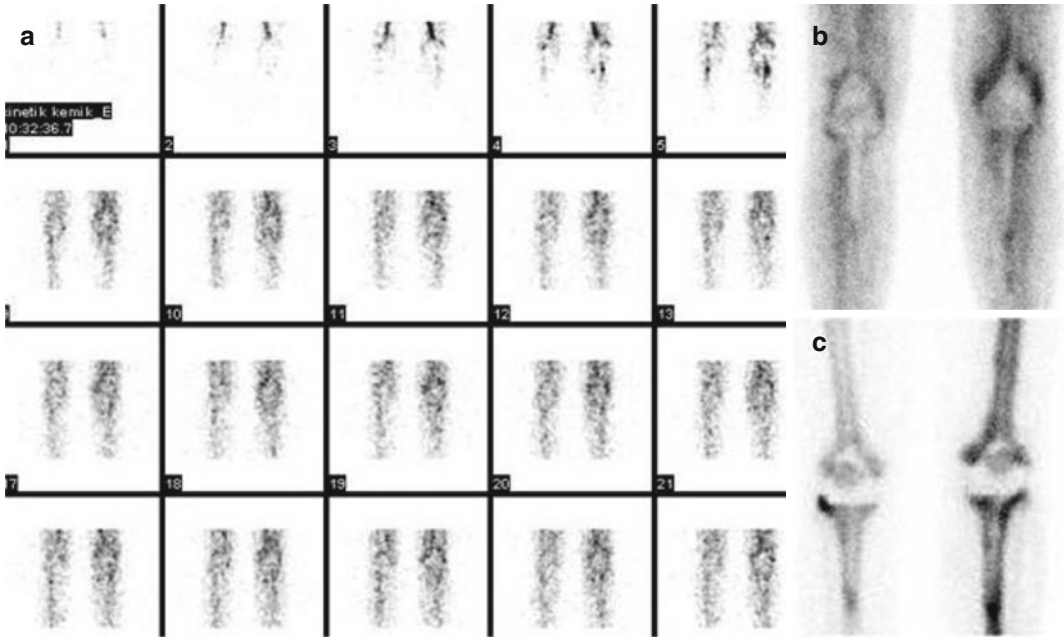

Fig. 13.2 Three-phase BS in a patient with knee prosthesis, (**a**) blood flow, (**b**) blood pool, (**c**) delayed phase

Patient Preparation

BS does not require specific preparation. Oral or i.v. hydration may increase the image quality by decreasing the background. Although radiation dose is lower than abdominal or thoracic CT, patient could further decrease this dose by excessive fluid intake and micturition. Patient should be asked for possibility of pregnancy. The main source of radiation to the fetus comes from the radioactivity from the bladder (17 mrad/mCi (4.6 μGy/MBq) at 8th week, 9.7 mrad/mCi (2.6 μGy/MBq) at 18th week). This risk can be decreased with hydration and frequent micturition [3, 5]. Although BS is not recommended for pregnant patient, if necessary one should know that radiation dose to fetus is low enough for BS to be used safely.

Interpretation of the Study Report

In normal BS, in addition to whole skeleton, normal mid radiotracer activity at soft tissue, kidney, bladder, and thyroid cartilage can be seen [1–3]. The areas that show high radiotracer activity than normal bone are called as hyperactive-hot focus. This finding can be seen in fractures, osteomyelitis, neoplastic diseases, and arthritis. Areas that show less uptake than normal are called hypoactive and cold focus. These can be seen in lytic lesions, tumor necrosis, early osteonecrosis, metallic foreign bodies, and after radiotherapy.

Another scintigraphic pattern is called superscan. This pattern is characterized by diffuse increased uptake in the whole skeleton and decreased activity in kidneys. It is commonly seen in patients with widespread bone metastases or hyperparathyroidism [3].

Clinical Applications

Detection and Follow-Up of Bone Metastases

BS is readily available, highly sensitive imaging modality for screening of bone metastases with

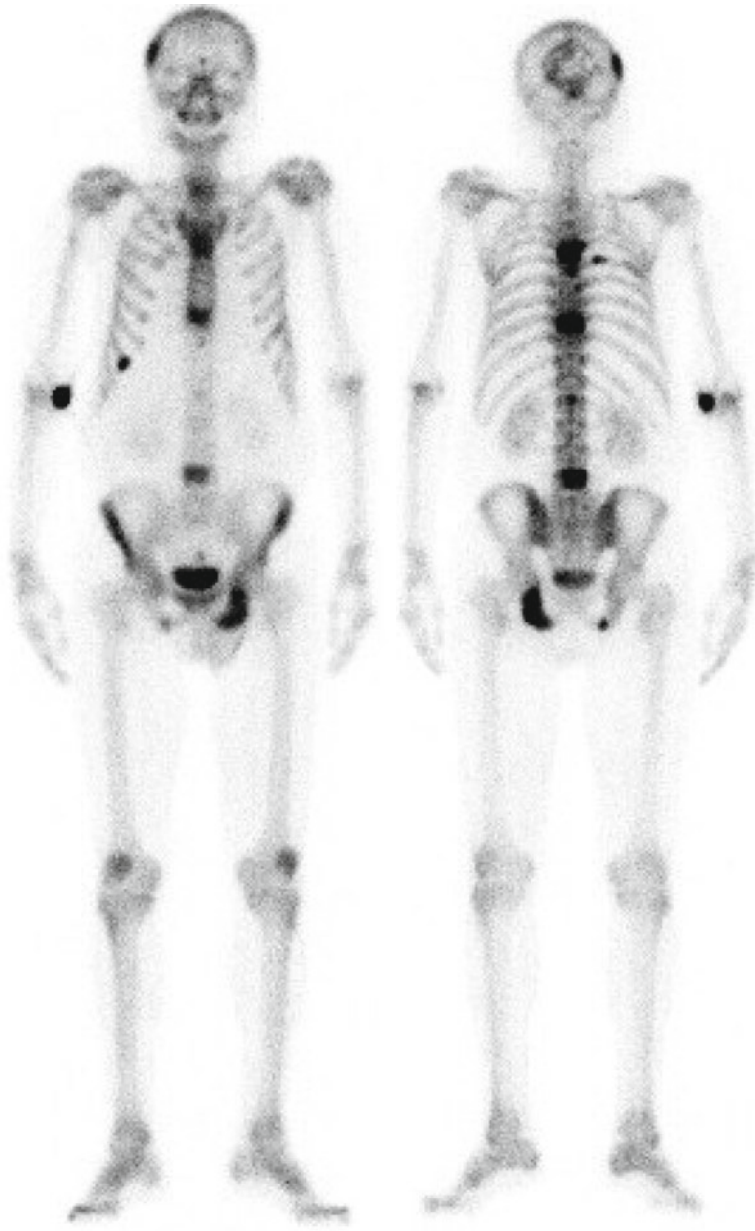

Fig. 13.3 Patient suffering from prostate cancer. Whole-body BS shows widespread bone metastases showing increased radiotracer uptake, PSA level: 2300 ng/ml

no absolute contraindications. It is 50–70 % more sensitive than radiographs in detecting skeletal metastases. This is because about 30–70 % of the bone mineral content must be lost before a metastasis is detectable on a radiograph [5, 6]. Contrary, 5–10 % change in the ratio of the lesion to normal bone is required to detect an abnormality on BS [6]. Also lesions in regions like sternum and scapula are also difficult to be detected by direct graphy due to overlapping bone structures. In general the sensitivity for bone scan in detecting bone metastases is between 62 and 100 % [6]. The success of BS is high in the detection of bone metastases from cancers like prostate which makes osteoblastic metastases or the metastases that lead to osteoblastic reaction. Asymmetric increased uptake throughout the skeleton is characteristic of bone metastases [6]. Other condi-

tions like fractures, degenerative disease, or other benign conditions that may lead to increased uptake may confuse the diagnosis, so correlation with other imaging modalities may help in the differential diagnosis. BS is probably not the procedure of choice for screening skeletal involvement in patients with multiple myeloma or lymphoma which usually make bone marrow or osteolytic metastases. However, combination of planar BS images with SPECT-CT can be used to improve the detection of lytic bone lesions.

SPECT imaging provides 3D images of a given lesion and results in overall improved sensitivity with the detection of 20–50 % more lesions in the spine when compared to planar images [6]. SPECT-CT can further improve accuracy by improving anatomic localization and by better evaluation of underlying bone pathology through CT data [7].

Whole-body imaging by BS is advantageous because about 90 % of patients with skeletal metastases present with multiple lesions. Detection of all metastatic sites could possibly effect patient management especially when local therapy is considered. Most of the metastatic lesions are in the axial skeleton. In patients with a known malignancy, 60–70 % of axial lesions are due to metastases, whereas about 30 % of lesions in the extremities or skull are due to metastases [1, 2]. In the evaluation of vertebral lesions, there are certain patterns of the radioactivity distribution which may help in the differential diagnosis, particularly when SPECT images are performed. Increased uptake beyond the vertebral body especially in facet joints is common due to degenerative changes [5]. Tracer uptake involving the vertebral body and extending to pedicles is usually indicative of metastatic disease [5, 6]. After chemotherapy for bone metastases, radiotracer uptake may increase in metastatic areas within 3 months after therapy. This is a sign of bone healing process after the death of tumor cells and called "flare phenomenon" [5]. It is commonly seen in breast or prostate cancer after chemo-/hormonotherapy and characterized by increase in the number and size of the pretherapy BS lesions. This phenomenon may lead to confusion in the differential diagnosis of progression or good therapy response. BS must be repeated 6 months after the end of therapy for differential diagnosis. Decrease in the number and intensity of lesions in the repeated scintigraphy is seen in good response, whereas progressive disease will show further progression [5].

BS in Prostate Cancer

Thirty-five percent of patients with prostate cancer have bone metastases in the first clinical presentation (Fig. 13.4) [8, 9]. Presence of bone metastases positively correlate with PSA (prostate-specific antigen) and Gleason score. Rate of bone metastases were 2.3 % for patients with PSA less than or equal to 10 ng/mL, 5.3 % for patients with PSA between 10.1 and 19.9 ng/mL, and 16.2 % for patients with PSA levels between 20 and 49.9 [6]. The rate of bone metastases increases to about 50 % when the PSA level is greater than 50 ng/mL [8–10]. Based upon the Gleason score, detection rates are 5.6 % of patients with a score of less than or equal to 7 and 29.9 % of patients with a score of 8 or greater [7–9]. Rate of bone metastases is low when PSA is below 10–20 ng/ml. BS should be limited to patients for initial staging with elevated PSA (greater than 10 ng/mL), high Gleason scores (8–10), locally advanced disease, elevated alkaline phosphatase, or bone pain symptoms. Patients who are receiving hormonal therapy (antiandrogen) may have bone metastases, even when their PSA is normal [11].

BS in Breast Cancer

Bone metastases occur in 70 % of patients during the course of disease in locally advanced breast cancers [12]. BS could detect metastases 2–12 months before the direct graphy (Fig. 13.5). However, as in other cancers specificity of the technique is low. The rate of positive BS changes with the stage of patient (2.5 % for stage 1, 7 % for stage 2, 16 % for stage 3, and may be as high as 14–28 % in stage IV disease [6, 12]). BS must be performed if the patient complains about bone pain, has elevated tumor markers, and has a stage of 3 or 4.

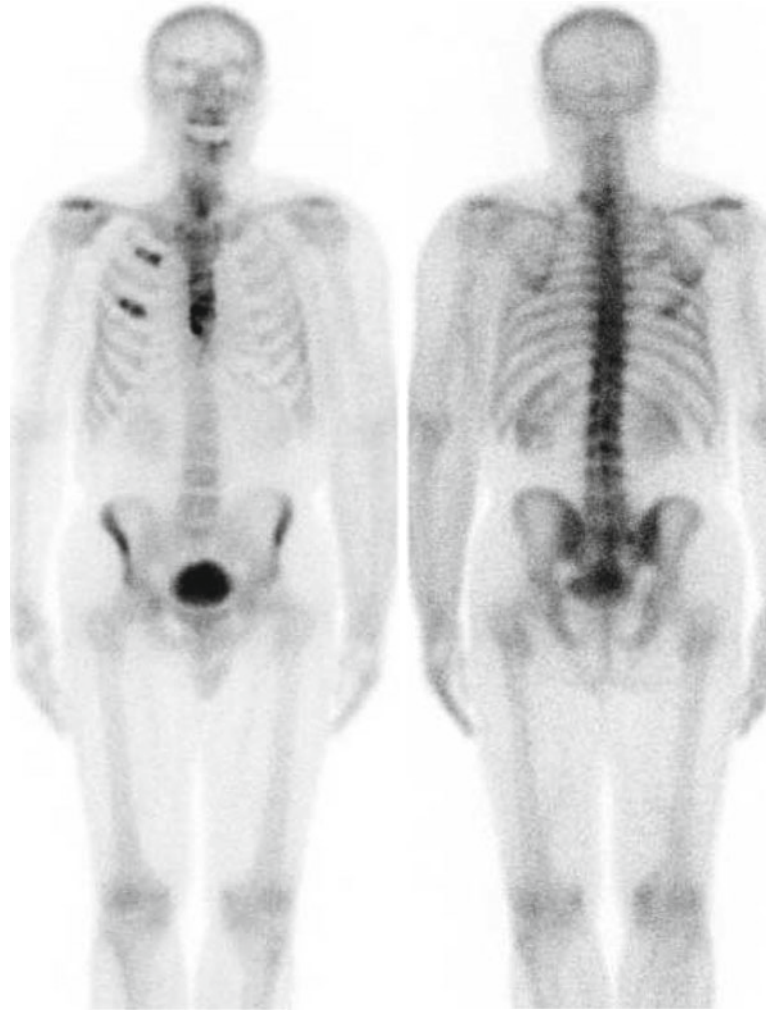

Fig. 13.4 Patient with rib metastases. Linear uptake in ribs is a sign of bone metastases

Recurrence was seen in 36 % of patients with locally advanced breast cancer during 4 years of follow-up and most of these were seen at bone. The rate of recurrence is higher in patients with lymph node metastases at the primary diagnosis. Although bone pain is a common symptom in these patients, up to 30–50 % of these patients can be asymptomatic. Increased radiotracer uptake in sternum is important for a patient with breast cancer as it has a 75 % likelihood of being a metastasis. There is also a strong correlation between the side of the sternal met, the side of the primary breast lesion, and the presence of internal mammary lymph node involvement.

BS also can be used in the therapy response evaluation of treatments like chemotherapy. However, low specificity of the BS due to benign changes and flare phenomenon limits its utilization. Due to its higher specificity, FDG (F-18-fluorodeoxyglucose)-PET-CT replaces BS in therapy response evaluation. However, BS is still used due to its readily availability and low cost. BS provides advantage in osteoblastic metastases where FDG shows lower sensitivity [5].

BS in Lung Cancer

Advanced lung cancers often metastasize to bone and BS is a routine imaging method for staging [1, 2]. BS is especially useful if curative surgery is planned. However, the utilization of BS is decreased with the increased availability of FDG-PET-CT in the staging of lung cancer. FDG-

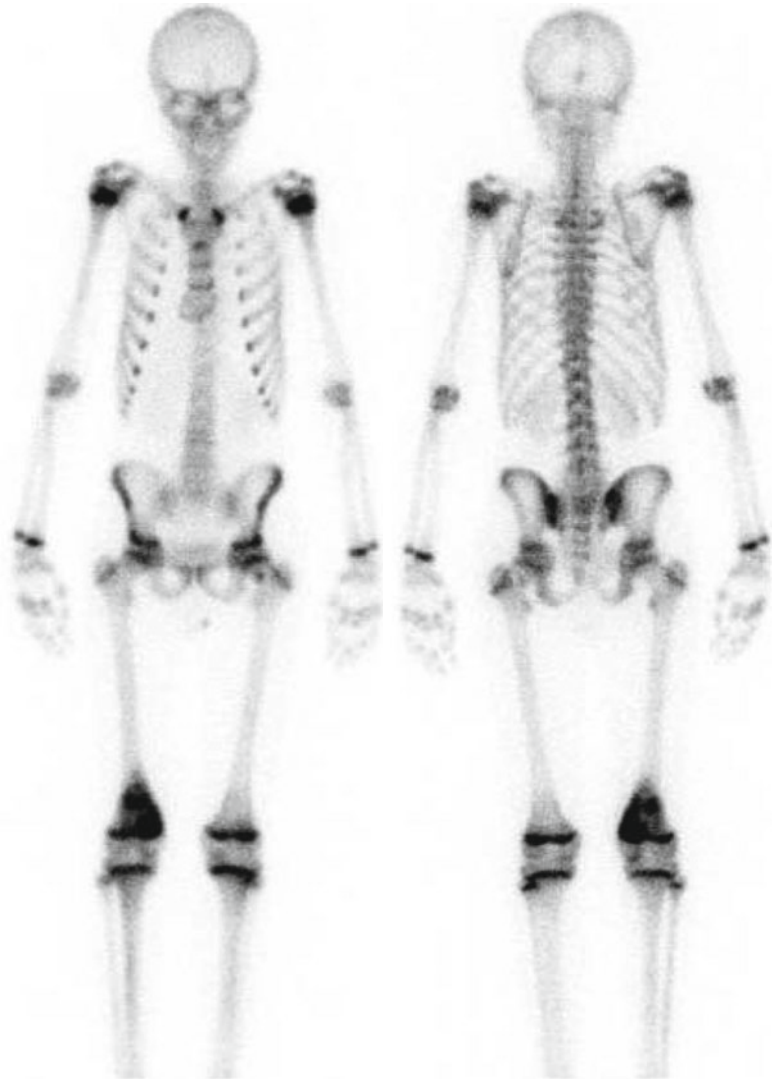

Fig. 13.5 Osteosarcoma in the right femur distal metadiaphyseal region

PET-CT not only detects early bone lesions (bone marrow, small sized cortical lesions etc) but also gives useful information about the lymph node and distant metastases [13, 14].

BS is not indicated in tumors which cause osteolytic metastases or bone metastases like renal cell cancer and multiple myeloma. It can be useful if patient is symptomatic and used with SPECT-CT that can detect osteolytic lesion and complications due to metastases like pathological fractures. MRI and FDG-PET-CT are the methodologies of choice for the staging of these tumors.

BS can be used as complementary to MIBG (metaiodobenzylguanidine) in patients with neuroblastoma and pheochromocytoma. MIBG is superior in detection of early bone marrow metastases, but BS may help in the tumors with no MIBG uptake.

Solitary Lesion on BS

A solitary rib lesion has about a 10 % probability of representing a metastasis in a patient with a known malignancy [15]. The chance of solitary lesion detected on BS to be malignant depends on the patient history, localization and shape of the

focus. For example, in patient with malignancy rate of solitary lesion in vertebra or pelvis to be malignant is as high as 60–70 %; however, this rate decreases if benign diseases like degenerative disease is detected by direct graphy. Similarly the rate of rib lesion to be malignant is low as 10 % especially in patient with trauma history. In a study held in Hacettepe University in patient with breast cancer patient, this rate was found to be as high as 26 % (Fig. 13.5) [16]. The percentage increased by the number of new lesions detected and reached 100 % when 5 new lesions were identified [17].

The Diagnosis, Staging, and Follow-Up of Primary Bone Tumors

MRI is the modality of choice in the preoperative detection of soft tissue involvement and lesion boundaries in primary bone tumors like osteosarcoma (OS) and Ewing's sarcoma (ES). Three-phase BS is a sensitive method for the detection of bone tumors; however, due to increased local blood flow and osteoblastic activity in late images, BS may overestimate lesion size. Due to its high sensitivity, BS mainly used for screening of bone metastases [18]. The most common malignant bone tumor in childhood and adolescence is osteosarcoma. Primary tumor and metastases show bone formation that can readily be detected by BS (Fig. 13.6). About 80 % of cases have localized tumor at presentation, whereas the remainder present with metastases most commonly to lungs and bones. Although radiotracer uptake within a pulmonary lesion is very specific for a metastatic focus of osteosarcoma, BS is less sensitive than CT in the detection of pulmonary

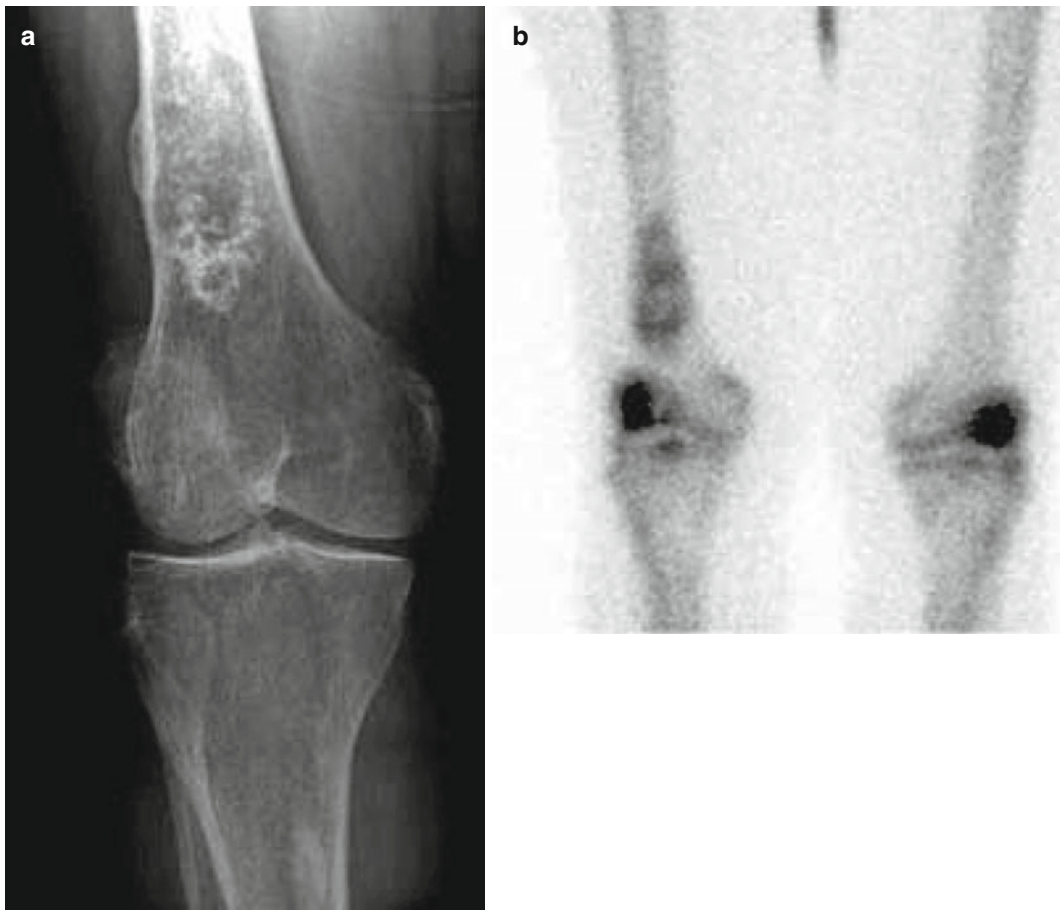

Fig. 13.6 Patient with an enchondroma in the right distal femur, (**a**) X-ray graphy, (**b**) bone scintigraphy

metastases especially when the metastases are small. Pulmonary metastases can be detected in 20 % (2D planar imaging BS) to 40 % (3D SPECT imaging) of patients [5]. BS could detect bone metastases with a high sensitivity of 80 %, but specificity may be low as 60 % because of benign changes that may mimic malignancy. Nonetheless, the presence of skeletal metastases is associated with a poor prognosis and will change treatment, and a baseline bone scan is generally recommended.

Ewing's sarcoma is the second most common malignant bone tumor. BS is also used for staging purposes; however, ES has the tendency to have early bone marrow metastases which decrease the sensitivity. FDG-PET and MRI are the modalities that has widespread application for bone metastases. ES and metastases are typically "hot" on blood pool and delayed bone scan images. On follow-up, the skeleton is the first site of metastatic disease in about 25 % of patients. Baseline and follow-up bone scans are therefore very useful in these patients. FDG-PEt also shows increased uptake in Ewing's sarcoma and is superior to bone scan for the detection of osseous metastases [19].

Early after chemoradiotherapy, benign reactive nonspecific radiotracer uptake on BS can be seen in the tumor bed. However, persistent uptake after 6–12 months raises the suspicion of local recurrence. CT and MRI could not be reliable in differentiation of necrosis/fibrosis from tumoral recurrence. Tl 201, Tc-99m sestamibi, and FDG-PET studies were useful in the evaluation of response [1–3]. There is a positive correlation between decrease in uptake and therapy response.

BS is not only used in bone tumors but also used in the evaluation of suspicious lesion detected on direct graphy. Although benign lesions show less and malignant lesion shows more uptakes, there is a significant overlap between benign-malignant lesions (Fig. 13.7). BS mainly gives information about lesion number and distribution.

In benign tumors, BS may also help in the differential diagnosis by showing the bone metabolism. Aneurysmal bone cyst show increased activity on all three phases. About two-thirds of the lesions will be photopenic centrally, surrounded by a "ring" of increased activity [20].

Bone islands (enostosis) are often confused with sclerotic bone metastases. Most of them show no radiotracer uptake; however, about 30 % of large bone islands may demonstrate mild increased uptake. Enchondroma is a benign neoplasm of the medullary canal composed of mature hyaline cartilage; they can have a very variable appearance on bone scan demonstrating very mild to prominent uptake of tracer.

Langerhans' cell histiocytosis is characterized by a varied and abnormal proliferation of histiocytes. The spectrum pathological entities included bone involvement (solitary and multifocal). Musculoskeletal manifestations occur 78 % of the time, and there is a predilection for marrow involvement with the flat bones of the skull and ileum being the most frequently involved.

On scintigraphy, up to 30–40 % of skeletal lesions may not be detected, and 10 % may appear cold [5]. Nonetheless, BS is considered to be complimentary to skeletal radiography in this disorder. Howarth et al. reported the sensitivity and specificity of the radiographic skeletal survey of 100 % and 61 %, respectively, compared to 91 % and 55 % for bone scintigraphy. For solitary lesions, radiographic sensitivity and specificity were 95 % and 73 %, respectively, compared with 88 % and 77 % for BS [21].

BS is most useful in two bone tumors. Among these osteoid osteoma is characterized as increased uptake in three phases. In the late phase, osteoid osteoma may be seen as more intense area in the middle as "double density" sign. BS provides whole-body screening and normal BS rules out osteoid osteoma diagnosis. BS is also used in other benign tumoral disorder like fibrous dysplasia. This entity may be 70–80 % monostatic and 20–30 % polyostotic. The diagnosis of monostotic form is late and most of these patients are asymptomatic (Fig. 13.8). Fibrous dysplasia is characterized by increased osteoblastic activity; however, these findings may be nonspecific. BS is helpful to screen polyostotic involvement and detection of biopsy site [1–3, 5, 6].

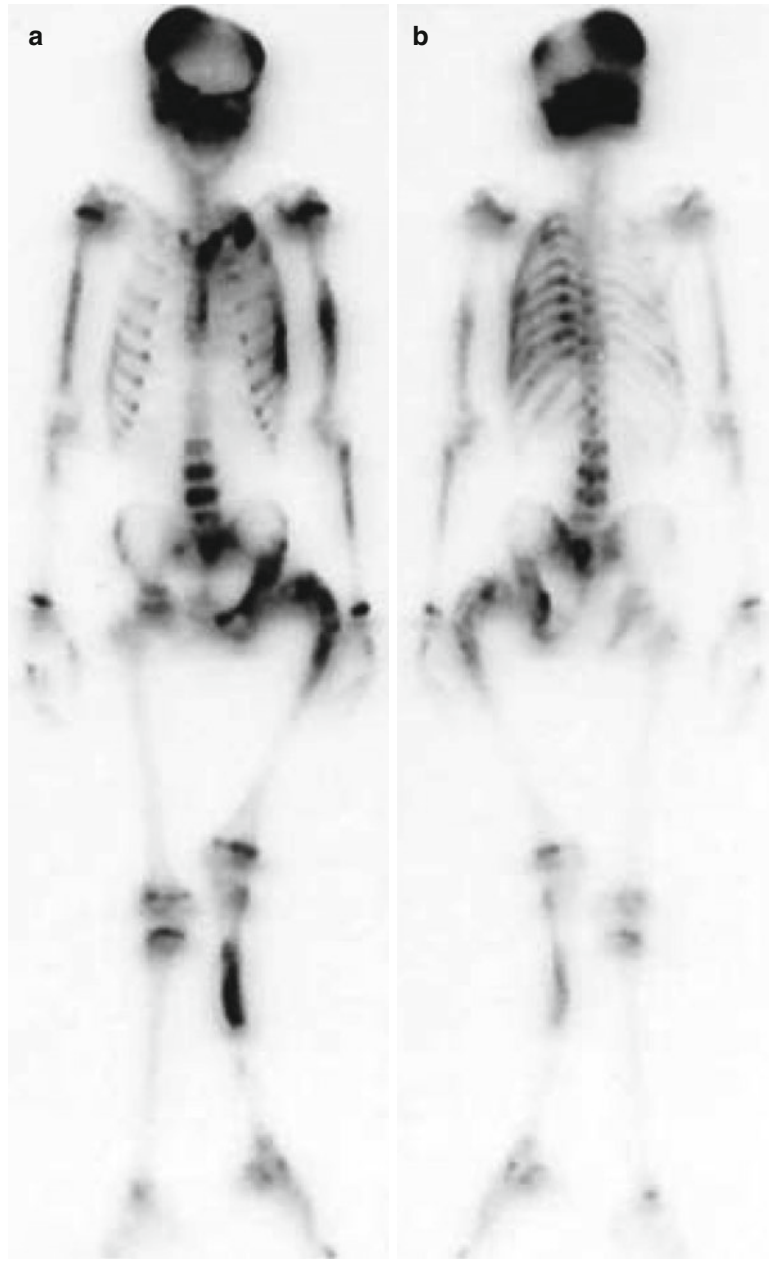

Fig. 13.7 A patient with fibrous dysplasia showing increased uptake on BS which produced left leg deformity

Bone Fracture

X-ray graphy is preferred for the initial diagnosis of acute trauma. It enables to see the anatomic fracture lines and help orthopedicians manage the patient with severe pain. However, it lacks enough sensitivity in small fractures and in bones with overlapping structures like scapula. BS is highly sensitive (>95 %) in detection of fractures [5]. About 80 % of bone scans will show increased activity at a site of fracture by 24 h and 95 % by 72 h, although patients over 75 years old and debilitated patients may not show activity for several days. A gradual decline in activity occurs over time with about 80 % of exams normalizing

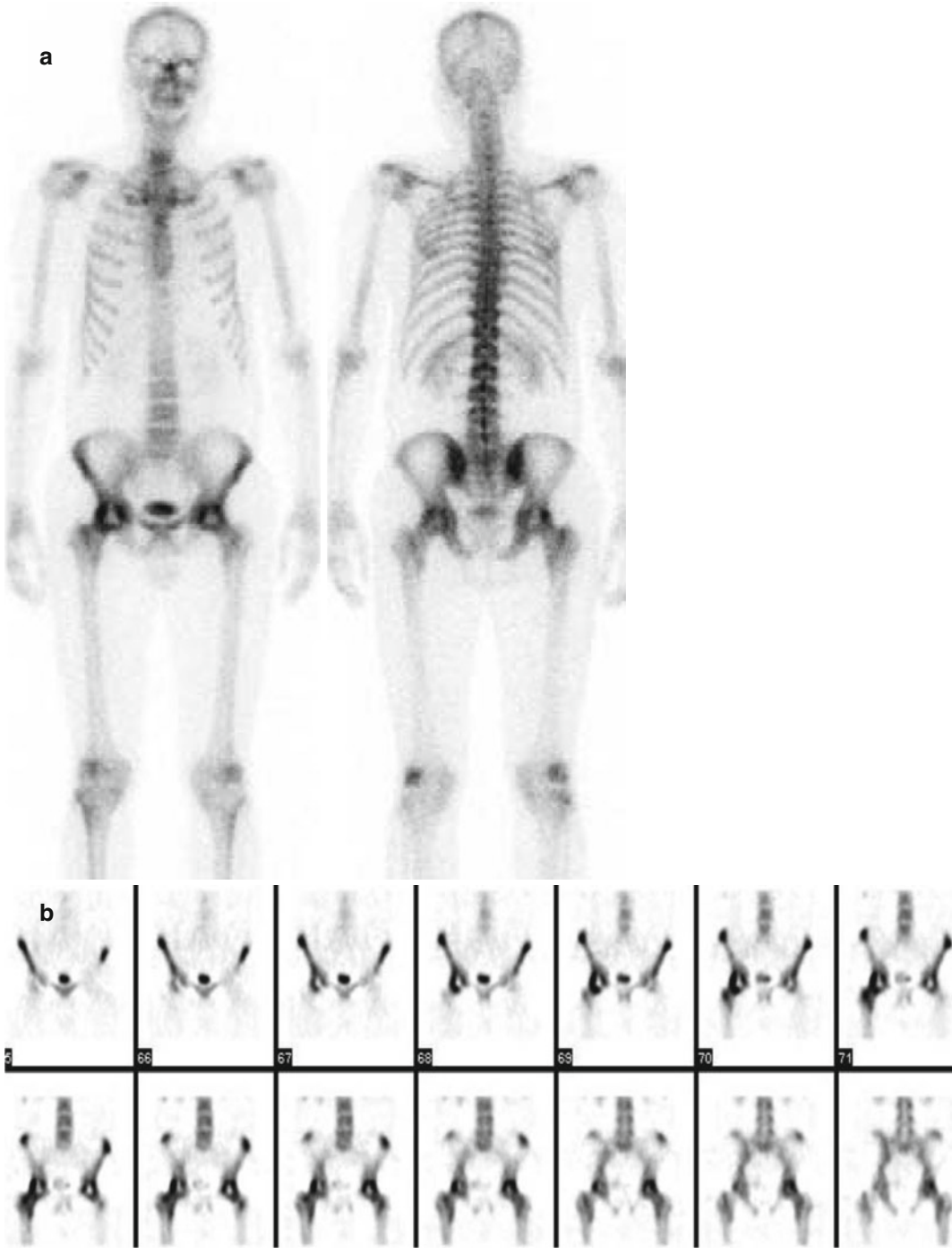

Fig. 13.8 Patient with avascular necrosis, (**a**) whole-body BS, (**b**) bilateral hypoactive areas in femoral heads in SPECT images

by 1 year and 90 % becoming normal by 2 years. The minimum time for normalization of activity is 6 months after properly fixed fracture [1, 2]. Nonunion occurs when there is failure of the fracture site to heal by 6–8 months following the injury. The tibia is the most frequent site of nonunion. Nonunion may occur secondary to an inadequate blood supply, osteoporosis, improper immobilization, or infection. Two types of nonunion have been described: reactive and atrophic. Reactive nonunion is characterized by persistent increased or normal uptake at the fracture site (80 %). This bone has potential for healing, and these fractures tend to show significant improvement following therapies like electrical stimulation. It is not possible to distinguish a reactive nonunion from a delayed union. Atrophic nonunion appears as a photon-deficient area between the fracture ends, which themselves may have increased activity. This group of fractures is usually not responsive to percutaneous electric stimulation. The etiology of the nonunion must be investigated with In-11-labeled leukocytes or Ga-67 to exclude infection.

Stress or Insufficiency Fracture or Shin Splints

Stress fractures occur due to repetitive trauma on normal bone. Bone adapts to stress with internal remodeling; however, if the trauma continues or high enough to exceed repair mechanisms, micro and gross fractures occur. Up to 40 % of patients with stress fractures can be asymptomatic [5]. Bone scan is much more sensitive than X-ray graphy for diagnosing stress fractures [5]. More than 80 % of stress fractures will not be evident on initial radiographs, while the sensitivity of bone scan for the diagnosis of stress fracture approaches 100 % [3]. On bone scan, stress fractures usually appear as solitary, focal, fusiform areas of increased tracer activity generally lasting for 10–12 weeks. SPECT imaging is much more sensitive than planar imaging for the detection of femoral neck stress fractures and can demonstrate fractures in patients with normal planar imaging [10].

Insufficiency fractures are common problem in elderly and debilitated patients. Most common cause of insufficiency fracture is osteoporosis. In these patients, proximal femur fracture is a diagnostic problem. Patient has history of pain and trauma history; however, X-ray graphy may be normal. These patients need urgent therapy before avascular necrosis or dislocation occurs. BS is preferred rather than X-ray graphies, and if the BS is not conclusive, MRI is the method of choice. In the sacrum, stress fractures are associated with osteoporosis or prior radiation therapy to the pelvis (an insufficiency fracture) [3]. The osteoporotic sacrum develops a characteristic "butterfly" or "Honda sign" fracture on BS. Plain films are typically normal but may show a sclerosis in sacral ala.

Shin splints (periosteal reaction) are due to abnormal movement of the either the soleus muscle tendon complex or posterior tibialis muscle which produces a periostitis-type lesion. They are characterized by abnormal linear (contrary to stress fracture not focal) uptake of tracer along the posteromedial tibial cortex. Shin splints have not been demonstrated to progress to stress fractures. Shin splints are mainly treated with anti-inflammatory drugs [22, 23]. However, stress fractures need longer immobilization.

Evaluation of Bone and Soft Tissue Infections

X-ray graphy is the first imaging modality in the suspicion of osteomyelitis. Most common problem is the early diagnosis. In the first 3 days, the radiological findings are nonspecific. Bone demineralization can be detected after 7 days, and after 14 days periosteal new bone formation can be seen. BS was shown to be positive 24–72 h after the beginning of infection [24]. Three-phase bone scintigraphy is performed in suspicion for osteomyelitis. BS could differentiate soft tissue infection vs osteomyelitis and acute vs chronic phase of new bone formation. Increased activity in blood flow and blood pool phases shows hyperemia and raises the suspicion of acute infection. Increased activity in late images show increased bone formation and osteoblastic activity. In patients with only soft tissue infections, there will be increased activity in the first two phases of three-phase BS, but late static images

will be normal and no increased osteoblastic activity. In osteomyelitis all three phases will be positive, and three-phase BS helps in the differential diagnosis of OM, cellulitis, and noninflammatory reactive bone pathologies (degenerative joint disease, chronic osteomyelitis). However, it is difficult to differentiate acute vs chronic OM and trauma-postoperative changes. In these patients, infection-specific radiotracers must be used. In complicated OM (diabetic foot or patients with prosthesis), Ga-67 scintigraphy and BS combination is useful [1, 2, 24]. Ga-67 is more specific than MDP in detection of infection. However, it also accumulates in the healing bone, so Ga-67 must be evaluated with BS. Ga-67 activity higher or more extended than the activity seen on BS is indicative of infection.

Radiolabeled leukocyte studies (In-111 or Tc-99m HMPAO) are more preferred for the diagnosis of complicated OM than Ga-67. There will be no significant leukocyte accumulation in fractures and prosthesis without infection. There is also accumulation of radiolabeled leukocytes imaging in bone marrow so the specificity and accuracy of the radiotracer is higher in peripheral extremities where bone marrow is less. When there is a problem in the differential diagnosis, bone marrow scintigraphy with Tc-99m nanocolloid could help to prevent interpreting physiological bone marrow activity as infection. Due to this limitation, Ga-67 or FDG-PET-BT must be preferred in vertebral osteomyelitis. Although BS activity remains high after therapy, infection-specific radiotracers return to normal faster than BS so can be used in the follow-up of antibiotic therapy.

Identification of Prosthetic Complications Like Loosening and Infection

X-ray graphy is the first imaging choice in the evaluation of prosthetic complications. It can help in the diagnosis of fractures, loosening, and identification of heterotopic ossification. BS when combined with Ga-67 and leukocyte scintigraphy is useful in the evaluation of prosthesis (Fig. 13.3) [1–3]. Prosthesis complications change with prosthesis type, postoperative time, age of the patient, etc.; however, there are some scintigraphic patterns that may help in the differential diagnosis. There is a high increased osteoblastic activity around prosthesis for 9–12 weeks, and moderate activity remains usually for 1 year. Tracer activity at trochanter major in hip prosthesis is a benign sign of remodeling; additionally mild radiotracer activity in the tip of prosthesis due to mechanic effect on small surface is a normal finding. BS is more sensitive than direct graphy in differential diagnosis of infection and loosening; however, specificity is similar. The sign of loosening is increased activity (higher than iliac crest activity) in the lateral aspect or tip of the diaphyseal component of prosthesis with accompanying radiolucency in X-ray graphy. This finding may overlap with infection; however, the uptake in the infection is higher, and increased activity in blood flow and blood pool phases are not observed in loosening unlike seen with infection. If the suspicion is high for infection Ga-67 and leukocyte, scintigraphy can be used with BS.

Viability of Bone Graft

Three-phase BS may evaluate viability of bone graft noninvasively and more sensitive than X-ray graphy [1–3]. BS findings change according to the graft type. In microvascularized autografts, perfusion is intact so BS show uniform uptake in three phases in viable graft. Vascular patency to the graft is characterized by normal or diffusely increased tracer uptake throughout the graft. When the vascularization of the grafts is injured, they do not concentrate tracer and will appear as photon-deficient areas on late bone images with reduced flow on the perfusion study. BS is most useful for predicting vascular patency and osseous metabolic activity when the scan is performed within 1 week of surgery (typically between 2 and 11 days after surgery). Scans performed later may be incorrectly interpreted as showing graft viability because of "periosteal creep" which is a new bone deposition on a nonviable graft. Allografts are devascularized when they are implanted so they are seen as hypoactive; in the repeated studies, graft shows progressive activity and revascularization progresses to the center. BS is a sensitive method in the revascularization monitorization than X-ray graphy [25].

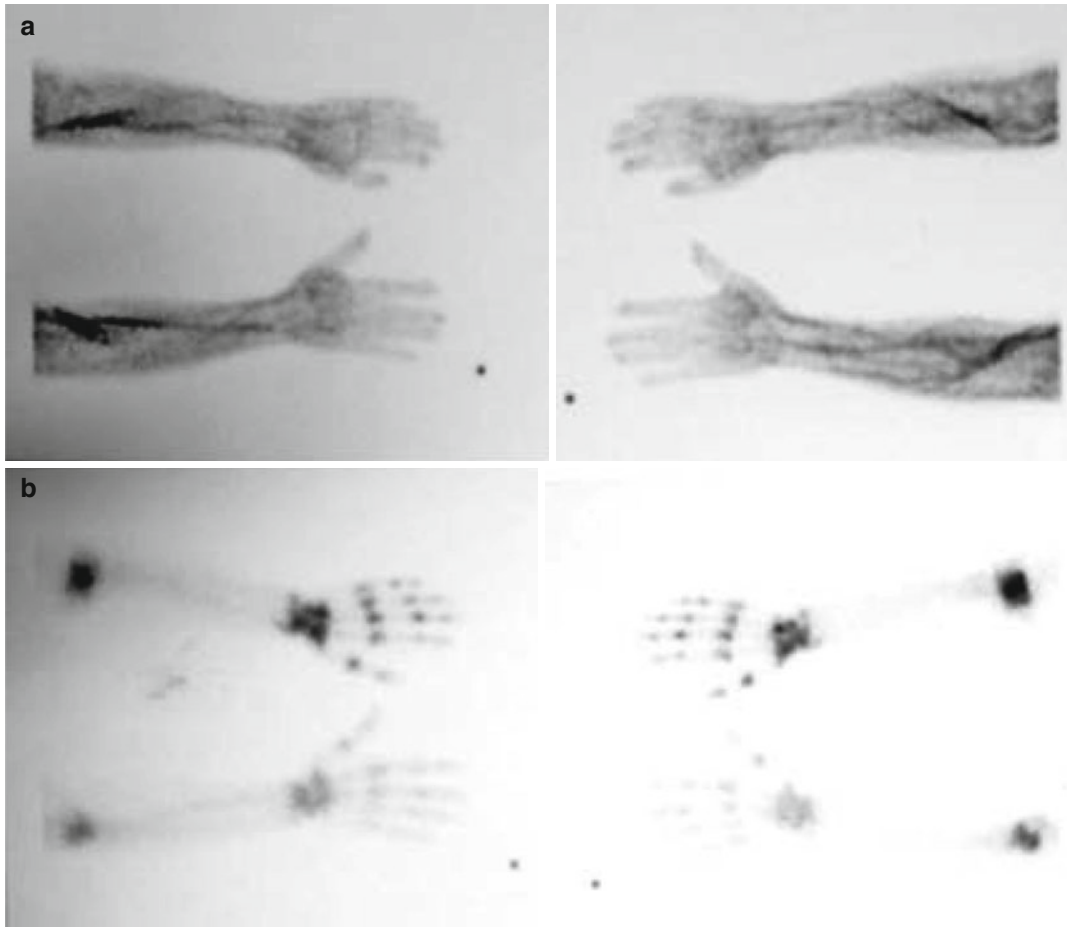

Fig. 13.9 Increased vascularity and periarticular uptake in a patient with reflex sympathetic dystrophy

Soft Tissue Calcifications

Myositis ossificans (MO) is a benign process characterized by heterotopic ossification usually within soft tissue (connective tissue, muscle, etc.). Three-phase BS is used for the evaluation of MO maturation. This entity is characterized by increased blood flow and osteoblastic activity before calcification is seen on X-ray graphy. The recurrence rate is higher if excised before maturation. When the activity in MO decrease to level in adjacent bone, maturation is completed [26].

Avascular Necrosis (AVN)

MRI and BS are used in the evaluation of femur head avascular necrosis. Osteonecrosis can be seen on BS before radiography. This enables physicians to early intervention that could prevent complications. SPECT images further help in detection of AVN by providing 3D and high-quality images (Fig. 13.9) [27]. In early phases, AVN is seen as hypoactive areas; in the healing phases, there is an increased activity starting from the periphery to the center.

In adults most of these patients referred to BS in the late phase and images show mainly increased uptake. Scintigraphy is sensitive but specificity must be increased with radiography by excluding activity due to nonspecific degenerative disease [28]. Patients with suspect of AVN should be evaluated by direct graphy, and if MRI is not available, BS with SPECT may be used. It must be remembered that BS may miss

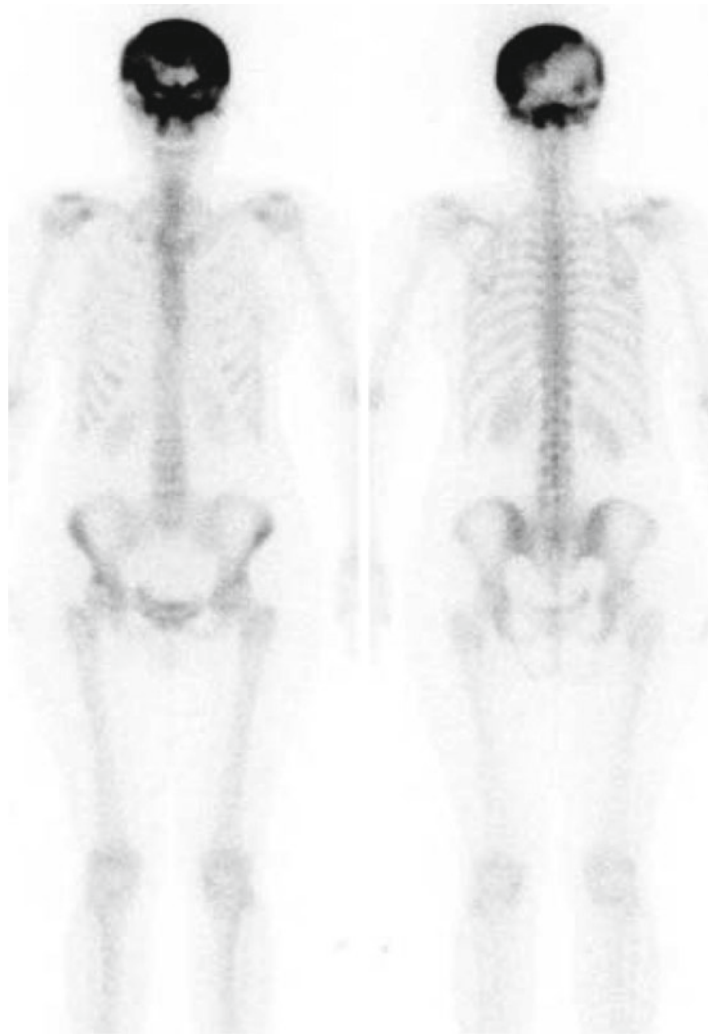

Fig. 13.10 Paget's disease in skull

small osteonecrosis. If the clinical suspicion is high, patient must undergo MRI.

Metabolic Bone Diseases

In metabolic bone diseases, there is an increase in bone turnover and Ca of the bone decreases so that these patients show increased skeletal uptake at BS. In these patients, BS may be helpful in detection of bone fracture and brown tumors which show increased radiotracer uptake [1, 2].

Reflex Sympathetic Dystrophy (RSD), Complex Regional Pain Syndrome

Due to classic scintigraphic pattern, BS is diagnostic in RDS [1–3, 17]. In 0–6 months increased blood flow and increased periarticular uptake in delayed phase. Six months to 1 year perfusion turns to normal but late images are permanent (Fig. 13.10) [29]. After 1 year, late images also turn to normal. This pattern is defined for hand and not seen in foot and knees so specificity of the method decreases in extremities in late stages. Scintigraphy also can be used for the therapy response.

Paget's Disease

Paget's disease is mainly asymptomatic and mostly presents itself above 40 years old. As 85 % of this disease is polyostotic, BS is an ideal imaging method for whole-body screening [1, 2, 30]. It has

higher sensitivity and specificity than X-ray graphy and may help in the therapy monitorization and detection of complications like sarcoma. The most commonly involved bones are the vertebral bodies (30–75 %), skull (25–65 %), pelvis (30–75 %), and proximal long bones (25–30 %) [1]. There are generally considered to be three phases: active lytic phase, mixed phase, and blastic phase; in early osteolytic active phase, BS shows high uptake that includes the whole bone, whereas in the late osteosclerotic phase, radiotracer activity decreases (Fig. 13.11). Sarcomatous degeneration occurs

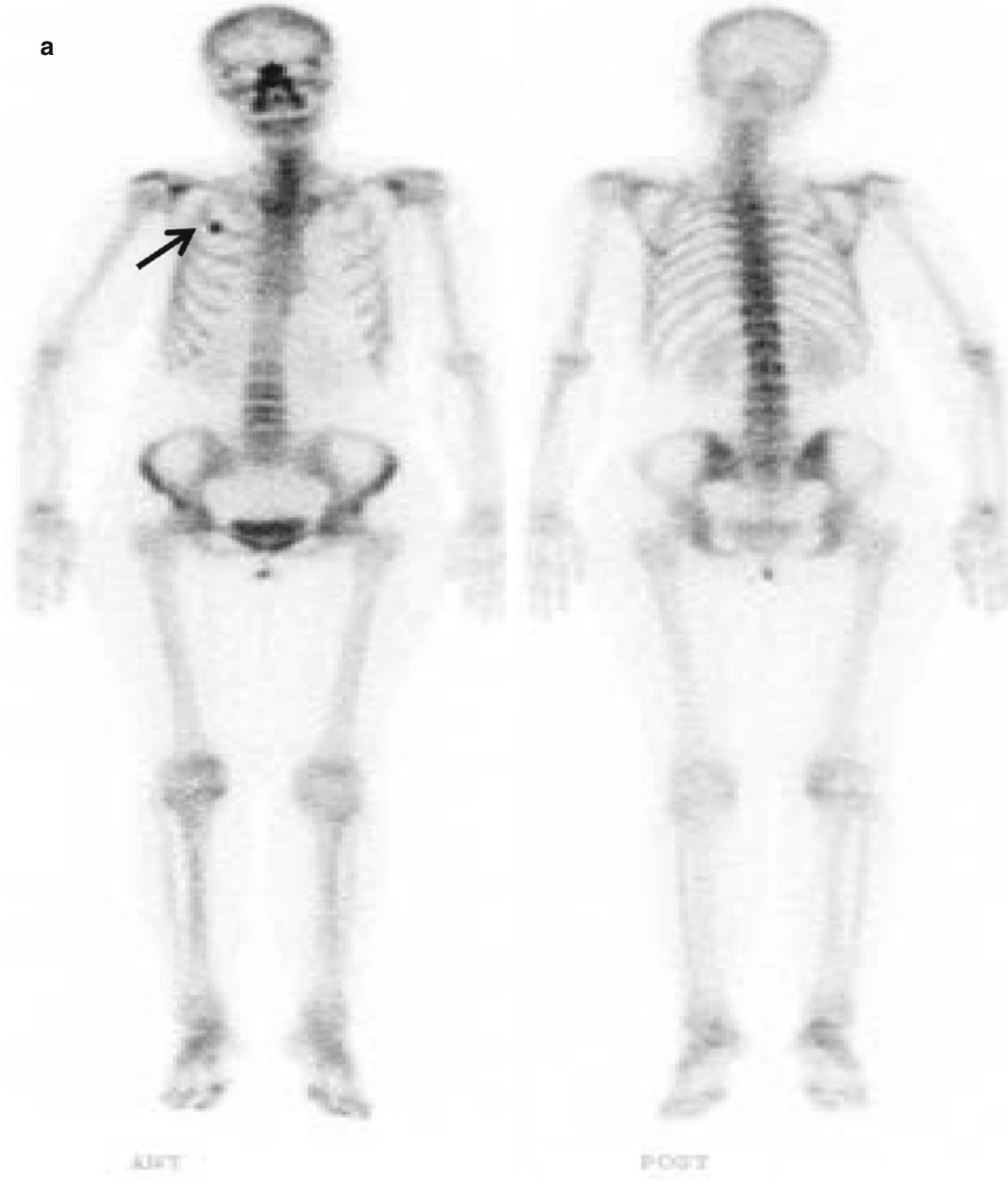

Fig. 13.11 A 40-year-old patient with breast cancer with mildly elevated tumor markers Ca 15-3: 27 U/mL (0–25). (**a**) Whole-body bone scintigraphy shows focal uptake in the right second rib (*black arrow*). (**b**, **c**) SPECT-CT images show benign fracture line that helped to exclude metastases (*white arrows*)

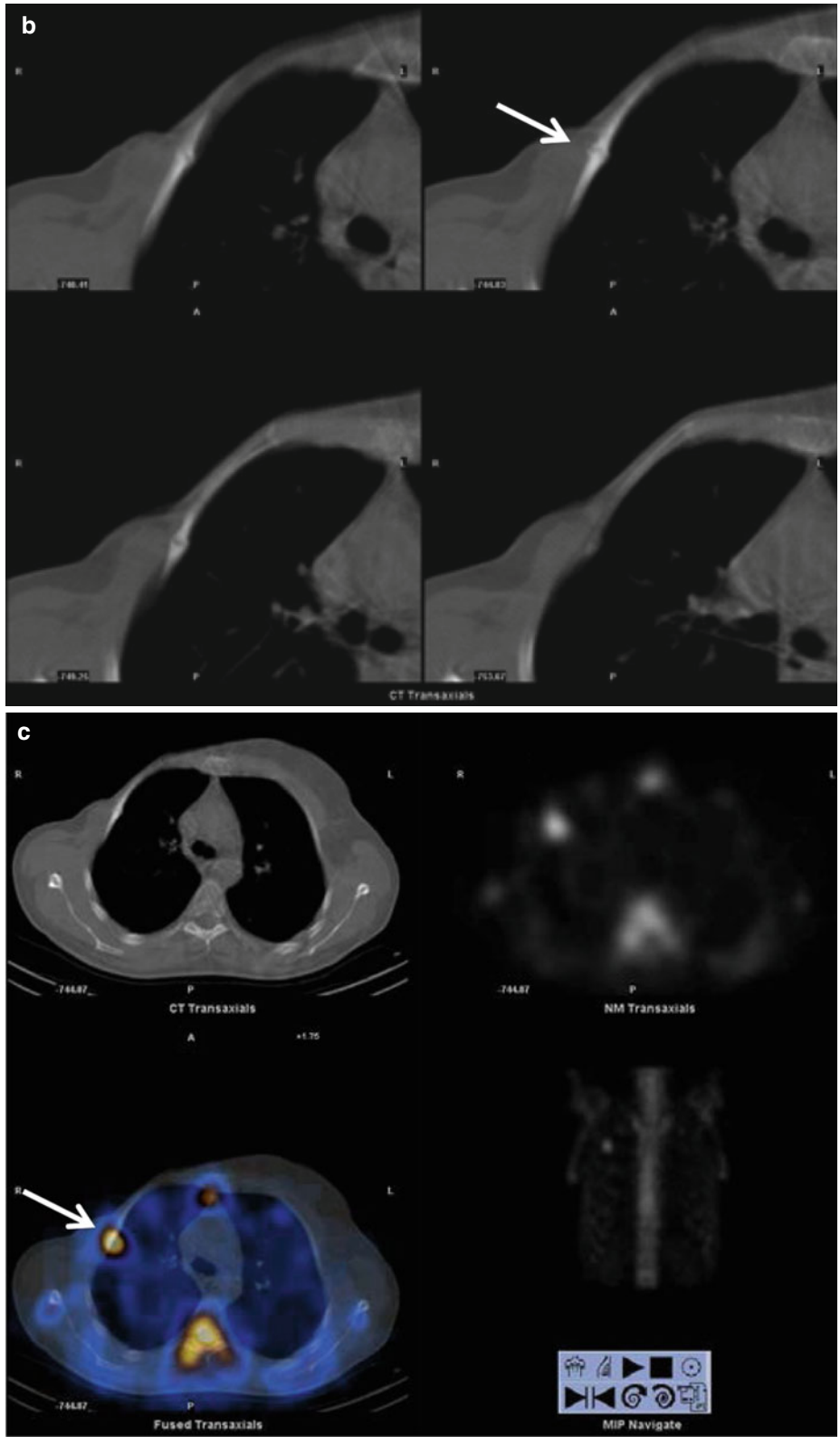

Fig. 13.11 (continued)

only rarely in pagetoid bone (about 1 % of patients). Increase in the activity of healed lesion may present a fracture or neoplastic transformation.

Detection of Compression Fractures and Evaluation of Back Pain

BS and MRI play a complementary role in chronic back pain in relation with patients' age and clinical presentation. In older patients, disc pathologies are a common source of pain, so in these patients MRI is used. BS is preferred in younger patients with no localized chronic back pain. SPECT imaging is highly sensitive in spondylosis and osteoid osteoma that may cause bone pain in this patient group. For the evaluation of bone grafts and pseudoarthrosis, CT and BS are preferred for the evaluation of osteoblastic activity and fractures. Increased osteoblastic activity in the lumbar fusion area after 1 year is compatible with pseudoarthrosis. BS as with MRI could also detect sacroiliitis which may cause back pain. BS is positive especially in the early period, and radiotracer activity decreases in the late phases. Vertebral compression fracture is a common problem in elderly. Radiological images have difficulty in detection of acute fracture from the old ones. Most elderly patients will have a positive bone scan by 48 h; however, the exam may not become positive for 3–7 days in up to 5–10 % of patients. By 1 year, about 60 % of compression fractures will normalize and 95 % will become normal by 3 years. When multiple fractures are present in different stages of healing, osteoporosis is the most likely diagnosis.

Facet syndrome is a disorder related to the lumbar facet joints that can produce both local and radiating pain associated with poorly defined or absent neurological findings. Although degenerative changes of the facets are commonly seen in these patients, there is poor correlation of symptoms with X-ray graphy or CT findings. SPECT bone imaging will usually detect an abnormality (sensitivity 100 %), but the exam suffers from a lack of specificity (70 %). Nonetheless, a normal exam confirms the absence of facet syndrome, and the examination can also demonstrate other, non-facet-related lesions [2].

B-SPECT-CT in Bone Diseases

Although BS has high sensitivity, it lacks specificity. This problem is recently solved by hybrid SPECT-CT which provides morphological and functional imaging.

SPECT-BT Applications in Benign Diseases

Most common benign applications of SPECT-CT are bone infections. Addition of SPECT-CT to planar imaging helps in the identification of exact localization of radiotracer uptake and characterization. CT part of SPECT-CT identifies infection-related osteolysis and sequestration of a bone segment. It also increases specificity by identification of degenerative changes [31]. In a study by Horger et al., the sensitivity of specificity of Tc-99m MDP BS in detecting OM is found to be 78 % and 50 %, respectively. The values increase to 78 and 86 % by addition of SPECT-CT [32].

Radiolabeled leukocyte imaging is routinely used in bone infections with high sensitivity and specificity. However, planar 2D imaging and inherent lack of landmark in scintigraphic imaging create problem in localization of uptake and decrease the test's accuracy. For the accurate localization, BS with Tc-99m MDP or anatomic imaging methods are needed for correlation. Addition of SPECT-CT increased the accuracy of radiolabeled leukocyte imaging by providing 3D imaging with fused anatomic localization at the same time.

Filippi et al. had found that SPECT-CT changed suspicious planar and SPECT interpretation of radiolabeled leukocyte imaging in 10/19 (52.6 %) areas in patients with diabetic foot. Addition of SPECT-CT ruled out OM in six patients, confirmed OM in one patient, and identified soft tissue infection in addition to bone infection in three patients [33]. The same authors in 28 patients (15 with suspicion of OM, 13 with orthopedic implant) found that SPECT-CT with Tc-99m HMPAO provided accurate anatomic localization of all positive foci and helped diagnosis in 10/28 (35.7 %) patients.

SPECT-BT helped in the differentiation of bone and soft tissue infection. It identifies struc-

tural changes after trauma. In patients with knee prosthesis, it could also identify synovial infection without prosthesis infection [34].

SPECT-CT has also additional value after spinal fixation. In a study by Damgaard et al., SPECT-CT was able to identify loosened screw in 6/9 patients suffering from pain after lumbar surgery [35]. Another application for SPECT-CT is patients suffering from pain of unclear etiology in extremities. Linke et al. evaluated contribution of SPECT-CT to three-phase BS in 34 patients evaluated as degenerative disease by planar and SPECT. SPECT-CT reclassified seven patients as having fracture and one as benign bone tumor. In 15 patients with a diagnosis of osteomyelitis, SPECT-CT reclassified 4 patient as osteoarthritis, 4 as fracture, and 1 as soft tissue infection. In eight patients with diagnosis of fracture, two evaluated as OM and two as osteoarthritis. Totally SPECT-CT changed diagnosis in 23/71 patients ($p < 0.01$) [36].

In addition to the studies above, SPECT-CT helped in the differential diagnosis of benign radiotracer uptake and increased the specificity and decreased the need of additional studies. In the literature, there are several benign lesions that were diagnosed with SPECT-CT like fibrous dysplasia, femoroacetabular impingement syndrome, osteochondral talar defect, osteopoikilosis, Paget's disease, and tarsal coalition [37–41].

SPECT-CT Applications in Oncology

One of the most common indications for BS is to rule out bone metastases. BS has a high sensitivity in detection of osteoblastic and mixed metastases, but specificity decreases due to traumatic and degenerative diseases which are commonly seen in this patient group (Fig. 13.12). In a study by Helyar et al., planar and SPECT BS classified 61 % lesion as unclear, whereas this values decreased to 8 % by SPECT-CT in patients with prostate cancer. Majority of unclear lesions are characterized as benign; SPECT-CT increased the concordance among different interpreters. (Kappa scores 0,43 for planar BS, 0,56 for SPECT and 0,87 for SPECT-CT) [42]. SPECT-CT helps to classify increased uptake as malignant by showing sclerotic metastases on CT and could detect additional lesions not detected by planar 2D images (Fig. 13.13). SPECT-CT could also give additional data by using CT data for the tumor types like renal cell cancer, leiomyosarcoma that leads to lytic metastases which show no uptake in BS [43]. SPECT-CT helps in the identification of benign bone diseases that can be due to cancer or its therapy like hypertrophic pulmonary osteoarthropathy and jaw osteonecrosis due to bisphosphonate therapy [44, 45].

SPECT-CT Radiation Dose

There are several SPECT-CT devices with different properties. The SPECT-CT device that authors use is a GE Hawkeye SPECT-CT system with low-dose CT (120–140 kV vs 1–2,5 mA). The additional radiation dose from SPECT-BT differs by body part, but average 1–2 mSv radiation dose is received by CT portion. This dose is lower than the radiation dose received from scintigraphic studies (5.9 mSv from BS and 6 mSv from leukocyte scintigraphy) [3, 46, 47].

C-Positron Emission Tomography in Musculoskeletal Diseases

X-ray graphy, CT, MRI, and BS are routinely used imaging methods in skeletal diseases. These modalities are helpful in diagnosis, staging, and follow-up. However, they have limitations in staging and the differential diagnosis of active disease or residual fibrotic tissue. PET-CT with metabolic imaging ability in addition to anatomic data from CT had found widespread application especially for tumor staging/restaging and tissue characterization. FDG-PET is the most commonly used radiotracer in oncological applications which is recognized by clinical guidelines. In addition to these oncological applications, FDG has been found to be helpful in musculoskeletal infections and vasculitis. However, due to its high cost, it has not been found cost-effective [48, 49].

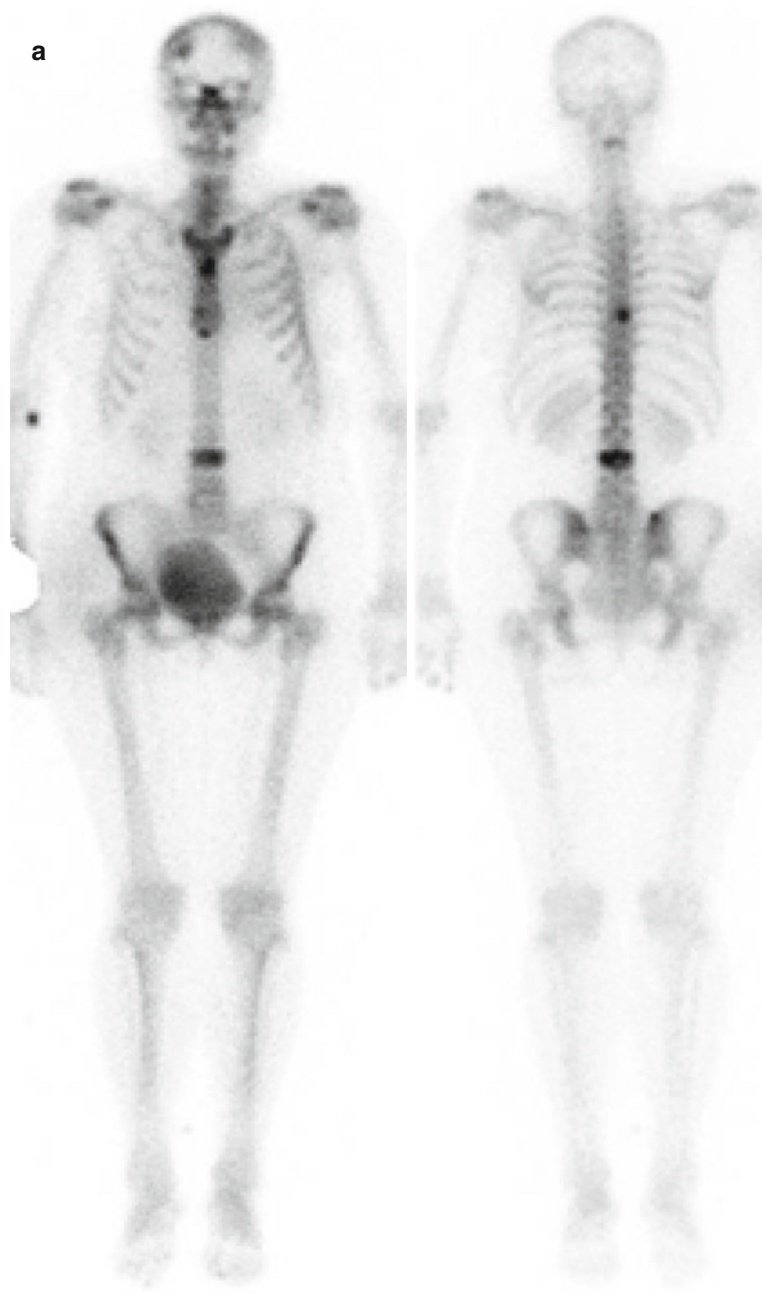

Fig. 13.12 A 35-year-old patient with breast cancer with elevated tumor markers (Ca 15-3: 39 U/mL (0–25) CEA:6 ng/ml (0–3,4). (**a**) Whole-body images show increased uptake in vertebras suspicious for bone metastases. (**b**, **c**) SPECT-CT images show the uptakes are due to sclerotic bone metastases and find additional lesions not detected by planar wholebody images (*white arrows*)

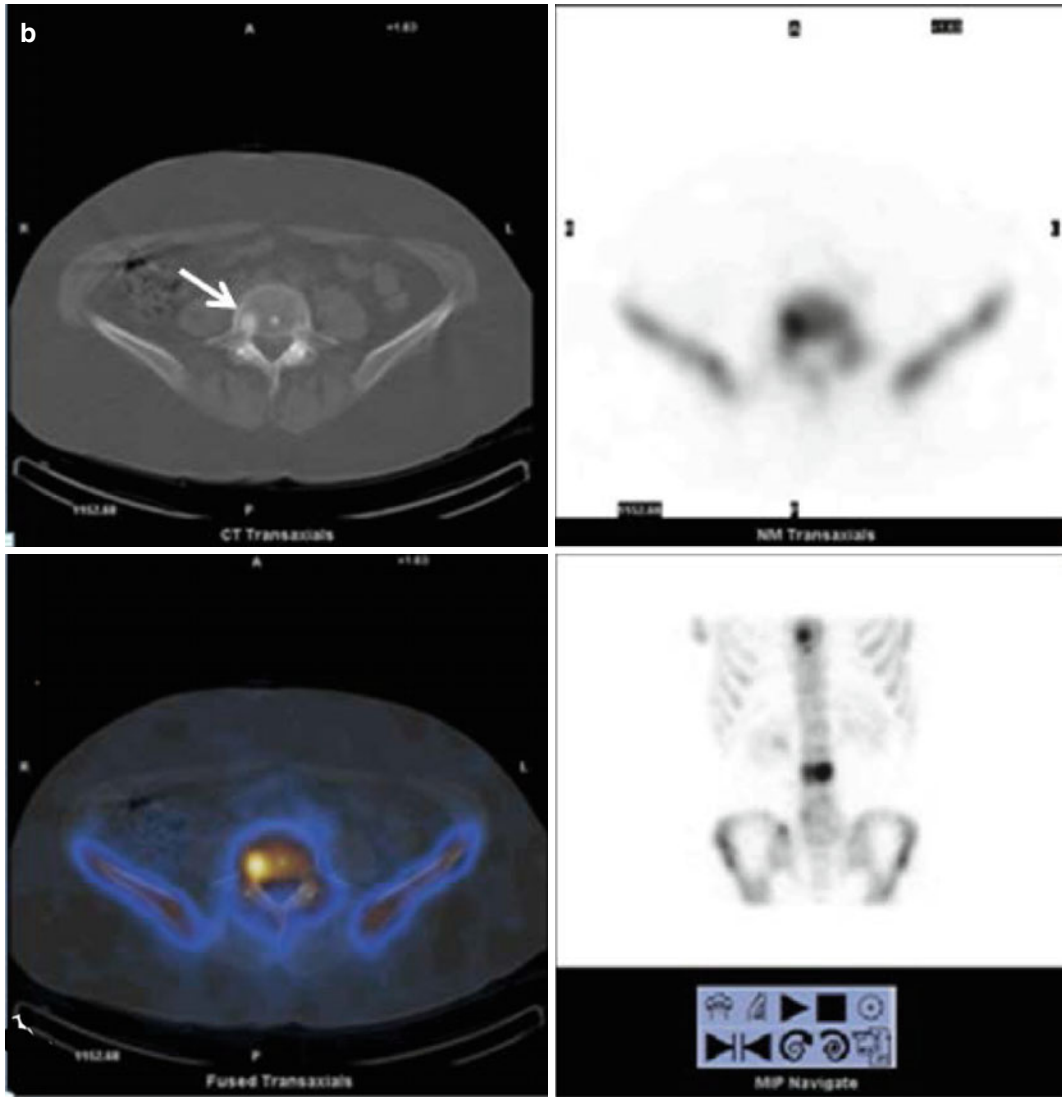

Fig. 13.12 (continued)

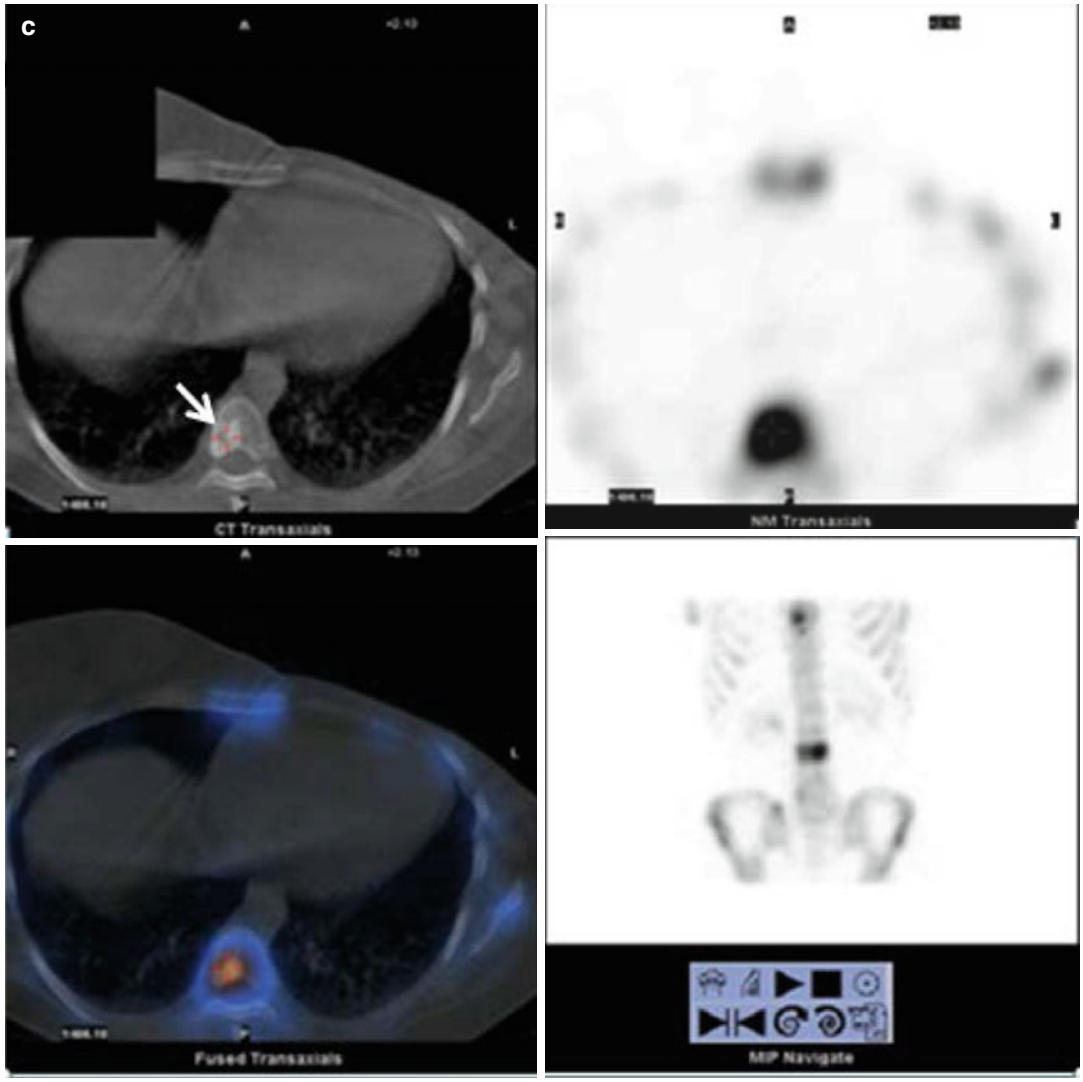

Fig. 13.12 (continued)

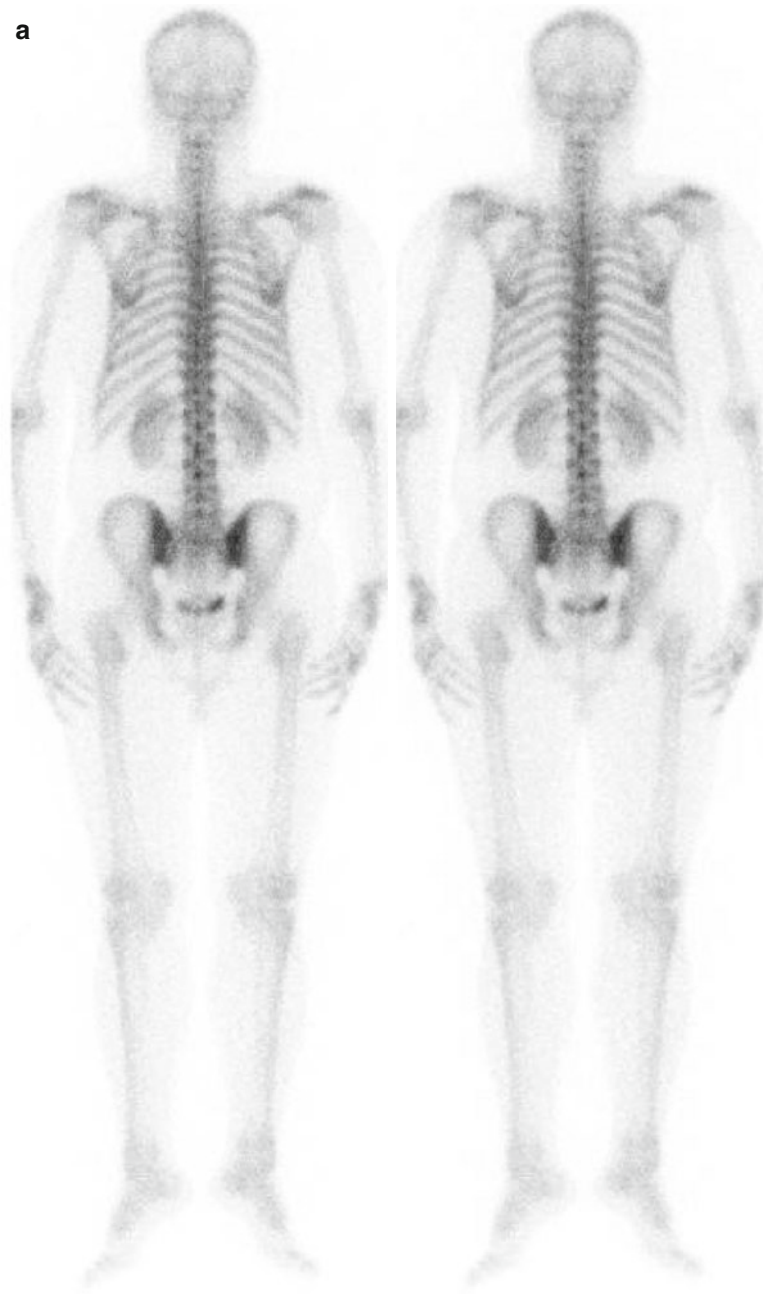

Fig. 13.13 A 65-year-old male patient with diagnosis of lung cancer. (**a**) Bone scintigraphy showed no sign of metastases. (**b**) NaF PET-CT images showed multiple metastatic increased activity on the left scapula, ribs, and pelvic bones (*black arrows*) with small sclerotic foci (*white arrows*)

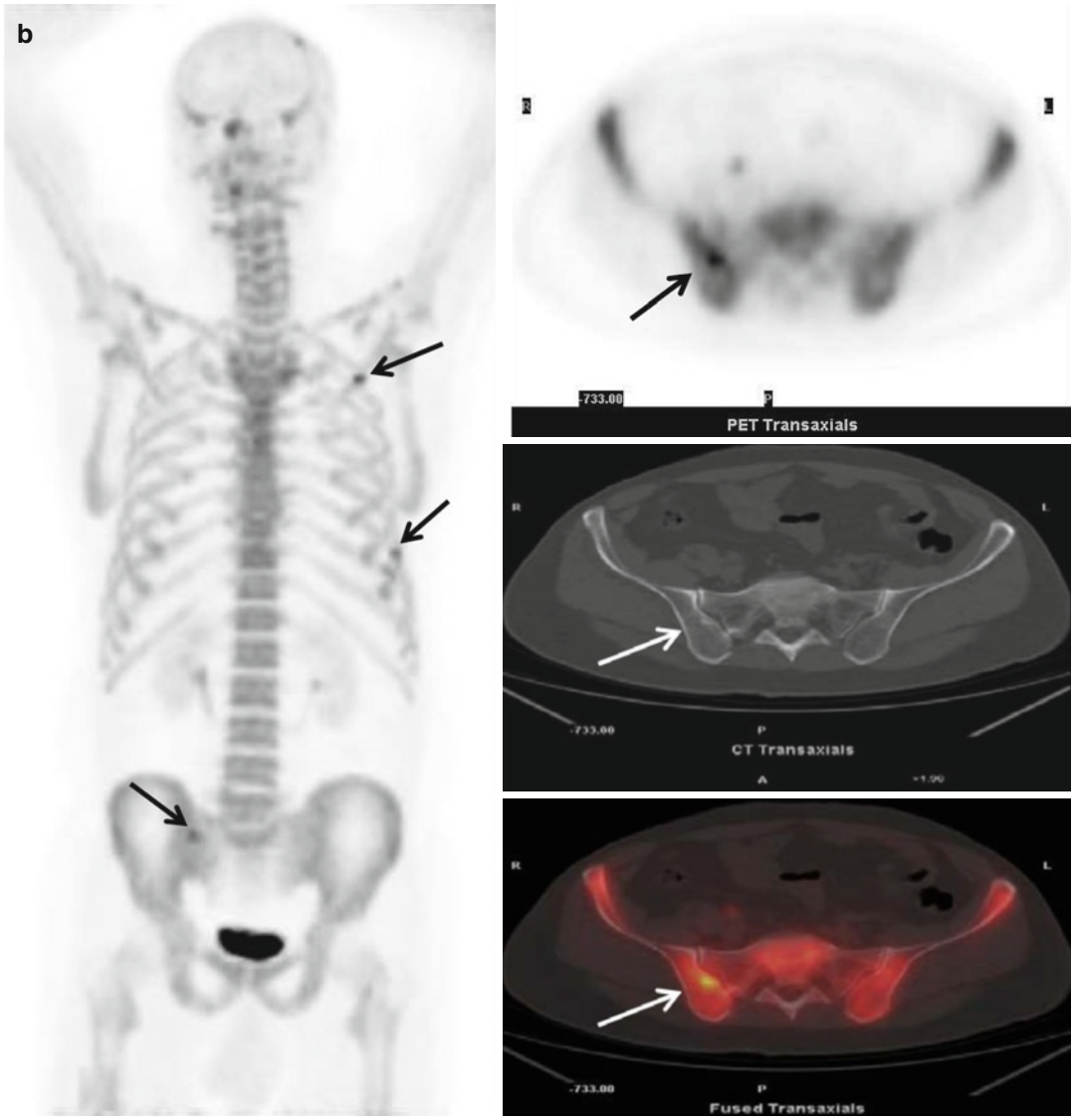

Fig. 13.13 (continued)

PET Radiopharmaceuticals in Musculoskeletal Diseases

^{18}F-FDG is a commonly used effective radiotracer in differential diagnosis of benign-malignant lesions and bone diseases. It is a glucose derivative and reflects the biodistribution and metabolism of glucose. After FDG enters to cell by glucose transporters, it is phosphorylated. Because of its ^{18}F-FDG PO4 bound, the FDG accumulates in the cell and does not enter glycolytic pathway like glucose. However, FDG is not malignancy specific and accumulates in cells with high metabolic activity like tumors or inflammatory cells like activated macrophages. New and more specific radiotracers are studied. C-11- and F-18-labeled thymidine analogs are developed to detect proliferative activity of musculoskeletal tumors [50, 51]. A tyrosine analog F-18 methyl tyrosine has been found to be more specific than FDG [52]. Similarly ^{18}F-NaF has been found to be superior to FDG in osteoblastic metastases [52, 53]. Recently Glu-NH-CO-NH-Lys-

(Ahx)-[(68)Ga(HBED-CC)]((68)Ga-PSMA) was introduced for detection of prostate cancer metastases. Radiotracer binds to prostate-specific membrane antigen that is highly expressed in prostate cancer cells and found to be superior to other PET tracers for this application [54].

PET in Non-tumoral Bone and Joint Diseases

Inflammatory Joint Disease

FDG-PEt also shows increased uptake in the inflamed synovium throughout the whole body and had good correlation with MRI or USG findings. The intensity of FDG uptake correlate with prognosis and can be used for response evaluation to TNF-α antagonists [55]. Tateishi et al. in a group of patients with rheumatoid arthritis found that uptake of FDG correlates with neutrophil number, plasma CRP, sedimentation, and joint complaints [56]. Similarly Beckers et al. found that PET findings are correlated with MRI and USG assessments of the pannus in RA, as well as with the classical serum parameter of inflammation, CRP, and the synovium-derived parameter, serum metalloproteinase-3 (MMP-3). PET was positive in 69 % of knees while MRI and USG were positive in 69 and 75 %. PET-positive knees exhibited significantly higher SUVs, higher MRI parameters, and greater synovial thickness compared with PET-negative knees. Changes in SUVs after 4 weeks were also correlated with changes in MRI parameters and in serum CRP and MMP-3 levels, but not with changes in synovial thickness [57].

Bone and Joint Infections

Osteomyelitis

The sensitivity and specificity of FDG-PET in acute and subacute bone infections changes between 94–100 % and 70–99 %, respectively [58]. The most problematic situation is low-grade chronic infections where other methods like leukocyte-labeled scintigraphy could not help the diagnosis. In this situation, the sensitivity of other scintigraphic methods decrease, whereas FDG-PET preserves its sensitivity due to macrophages that show high FDG metabolism. Guhlmann et al. found that for OM, the sensitivity, specificity, and accuracy of FDG-PET are 100 %, 92 %, and 97 %, respectively. In this patient group, accuracy of other scintigraphic methods like leukocyte-labeled scintigraphy was found to be 53–76 %. The biggest advantage of FDG-PET is that it can exclude OM when it is negative [59]. The tracer uptake in FDG-PET returns to normal after surgery and trauma faster than BS. Studies showed that if there is no underlying tumor or infection, FDG uptake decreases to normal in 4 months.

Infections Due to Joint Prosthesis

The differential diagnosis of loosening and infection is not easy. BS is a sensitive method for detection of bone infection; however, specificity is low. When combined with leukocyte imaging, it has a high accuracy in detection of infectious site. However, both these scintigraphic techniques are time consuming, and leukocyte labeling requires special preparations and laboratory conditions. The main problem with FDG-PET prosthesis imaging is that there are normal increased activities in periarticular area, femur head, and neck lasting for several years. Interpreters should know these patterns for proper interpretation [59, 60]. FDG-PET-CT is a sensitive method in detection of infections; however, when interpreted with certain criteria, specificity is high as 86 % in hip and 80 % in knee prosthesis [61, 62]. Chacko et al. in a review found that accuracy of FDG-PET in hip joints was higher than the knee due to more nonspecific uptake seen in knee joint 96 % vs 81 % [63]. In a study that compares FDG-PET with leukocyte scintigraphy and BS, FDG-PET showed 100 % sensitivity and 73 % specificity but had no additional value [62]. Consequently FDG-PET is not superior to BS and leukocyte imaging but can be preferred in places where leukocyte labeling is not available.

Vertebral Infections

Although bone scintigraphy has high sensitivity in detection of vertebral infections, it lacks specificity. Also infectious processes in disc space or epidural space cannot be detected by BS. Radiolabeled leukocyte scintigraphy has also low specificity due to physiological activity in vertebras. FDG-PET

was useful in patients with disc space infections where MRI is unclear. MRI has high accuracy in the evaluation of discitis, infection of vertebral corpus or epidural space. However, FDG-PET has found to have higher sensitivity which is 100 % and superior to MRI and BS. FDG-PET shows no increased uptake in endplate changes whereas positive in infectious changes. In this patient group, MRI shows 50 % sensitivity and 96 % specificity, whereas these values were 100 % for FDG-PET [64]. Schmitz et al. also showed high sensitivity rates and found that FDG-PET could show paravertebral extend better [65]. Although it has low specificity in the differential diagnosis of aseptic changes and infection, it could rule out degenerative diseases [65, 66].

PET in Musculoskeletal Tumors

In several studies FDG-PET was found to be useful in musculoskeletal tumors for staging and differentiation of high to low-grade, benign, to malignant tumors and to detect biopsy site [67, 68]. However, FDG-PET is not successful enough in differential diagnosis of low-grade malignant vs benign lesions which both show low-grade uptake. In aggressive benign tumors and acute inflammatory processes, false-positive reports for malignancy were also reported [49].

The sensitivity and specificity of FDG-PET (malignant criteria, tumor/background >3, and benign criteria, <1,5) for malignant musculoskeletal tumors are 93 % and 67 %, respectively [69]. FDG-PET is also used for the evaluation of neoadjuvant chemotherapy response and helps in prognostication [70]. The sensitivity of FDG for detection of recurrence after therapy is same with the combination of MRI, CT, and BS [71].

Plasmacytoma and Multiple Myeloma

The standard methods for the staging and therapy planning of malignant monoclonal gammopathies are X-ray graphy and MRI. It has been reported that FDG-PET is effective in the staging of multiple myeloma and more sensitive than X-ray graphy for detection of metabolically active foci [72]. In this patient group, FDG-PET was found to be more accurate for the differential diagnosis of fibrosis-malignant disease and decision for therapy follow-up.

In the evaluation of FDG-PET, lesions with SUV >2,5 were accepted to be positive. For the lesions with size <5 mm, activity above background was also accepted as active lesion. The biggest advantage of FDG-PET is that it could differentiate active myeloma (FDG positive) vs monoclonal gammopathy of undetermined significance (MGUS)) (FDG-PET negative). CT part of FDG-PET helped to identify small lytic lesions and increased the sensitivity and specificity. FDG-PET was found to be effective as MRI in whole-body imaging except vertebra. In multiple myeloma patients, the sensitivities of PET, MRI, CT, and X-ray graphy were found to be 86 %, 83 %, 70 %, and 47 %, respectively. FDG-PET was found to be more accurate than MRI for therapy response evaluation [73, 74].

Bone Metastases

Most common malignancy of bone is metastases from non-osseous malignancies. BS is a validated sensitive technique. However, it has lower sensitivity than MRI for the detection of axial metastases and osteolytic metastases [49, 75]. The main advantage of FDG-PET over BS is better detection of early bone marrow and osteolytic disease [49].

PET-CT could perform anatomic and metabolic imaging in a single device and by quantitative metabolic imaging capability help to differentiate benign-malignant lesions.

In breast cancer patients, metastases can be lytic, sclerotic, or mixed type. This pattern predicts the sensitivity of staging method. Cook et al. compared FDG-PET and BS in 23 breast cancer patients. Although FDG-PET detected more lesions, BS is superior in osteoblastic metastases. As accepted SUV was higher in osteolytic metastases when compared to osteoblastic ones (SUV: osteolytic, 6.6; mixed, 3.6; osteoblastic, 0.95) [76]. Uematsu et al. in 143

osteoblastic and 23 osteolytic metastases found that BS SPECT has a sensitivity of 87 %, whereas FDG has 17 % with similar specificities (99 %). The SPECT sensitivity in osteolytic lesions was 35 % and 92 % in osteoblastic metastases. The same values were 90 % and 6 % for FDG-PET [77]. Similarly Nakai et al. found that in lytic lesions FDG-PET has a sensitivity of 100 % and 56 % in sclerotic patients. BS SPECT values were 70 % and 100 %, respectively [78].

In malignancy like lung cancer producing osteolytic and bone marrow, Bury et al. found FDG to be more accurate than BS (accuracy: 96 % vs 66 %) [79]. The literature states that in lung cancer patients, BS after FDG-PET gives no additional information. In bone metastases from prostate cancer, the value of FDG-PET is low. In these osteoblastic metastases, F-18 florid PET-CT is preferred. There are several studies comparing BS, FDG-PET, and NaF PET in the detection of bone metastases [80, 81]. NaF PET has a sensitivity in the detection of osteoblastic and osteolytic metastases (Fig. 13.14). However, FDG-PET has poorer sensitivity in osteoblastic metastases. Another problem with the PET imaging is false positives. Fractures, infection, benign bone tumors with histiocytic, or giant cell may show increased uptake [75]. CT component of PET-CT could help to decrease the false positives. FDG-PET-CT also could be used for therapy response evaluation and superior to BS which shows increased uptake due to healing processes of bone after therapy. Decrease in FDG activity and increase in the sclerosis of bone metastases are signs of good response (Fig. 13.15).

Ga-68 PSMA is a new radiotracer with higher sensitivity and specificity than the other PET tracers like FDG and NaF PET. It is rather tumor specific, and interpreters do not face the common false positives due to benign lesions like fractures, benign bone tumors etc. that lead to increased uptake in NaF or FDG. In studies comparing Ga-68 PSMA with the commonly used radiotracers like Tc-99m MDP, NaF, FDG, and C-11 choline PET, Ga-68 PSMA has been found to be superior in detection of bone and soft tissue metastases [82] (Fig. 13.16).

PET in Childhood Musculoskeletal Tumors

Osteosarcoma and Ewing's sarcoma are the most common tumors of childhood. PET imaging is advantageous for detection of skip or distant metastases and differential diagnosis of recurrence vs fibrotic tissue [83]. Gerth et al. in patients with ES found that FDG-PET's sensitivity, specificity, and accuracy were 71 %, 95 %, and 88 % and for PET-CT 87 %, 97 %, and 94 %, respectively ($p < 0.0001$). Compared to PET, CT is superior in detection of pulmonary metastases [82, 84]. FDG-PET's sensitivity, specificity, and accuracy for detection of pulmonary metastases from malignant primary bone tumors were found to be 50 %, 98 %, and 87 % whereas for PET 75 %, 100 %, and 94 % [85]. When FDG-PET and BS are compared in bone metastases of ES patients, FDG-PET's sensitivity, specificity, and accuracy were 100 %, 96 %, and 97 % and for BS 68 %, 87 %, and 82 %. However, in OS patients, five metastases not detected by FDG were detected by BS [19]. Consequently CT is needed in detection of pulmonary metastases and FDG-PET can replace BS in ES; however, for OS patients, BS still holds its place for screening of bone metastases (Fig. 13.17).

FDG is also used for chemotherapy response evaluation. Byun et al. evaluated the potential of sequential FDG-PET-CT and MRI after one cycle of neoadjuvant chemotherapy to predict a poor histologic response in 30 patients with osteosarcoma treated with two cycles of neoadjuvant chemotherapy and surgery. All patients underwent PET/MRI before, after one cycle and after the completion of neoadjuvant chemotherapy, respectively. Imaging parameters [maximum standardized uptake value (SUVmax), metabolic tumor volume (MTV), total lesion glycolysis (TLG), and tumor volume based on magnetic resonance (MR) images (MRV)] and their % changes were calculated on each PET/MRI data set, and histologic responses were evaluated on the postsurgical specimen. Unlike the little volumetric change in MRI, PET parameters significantly decreased

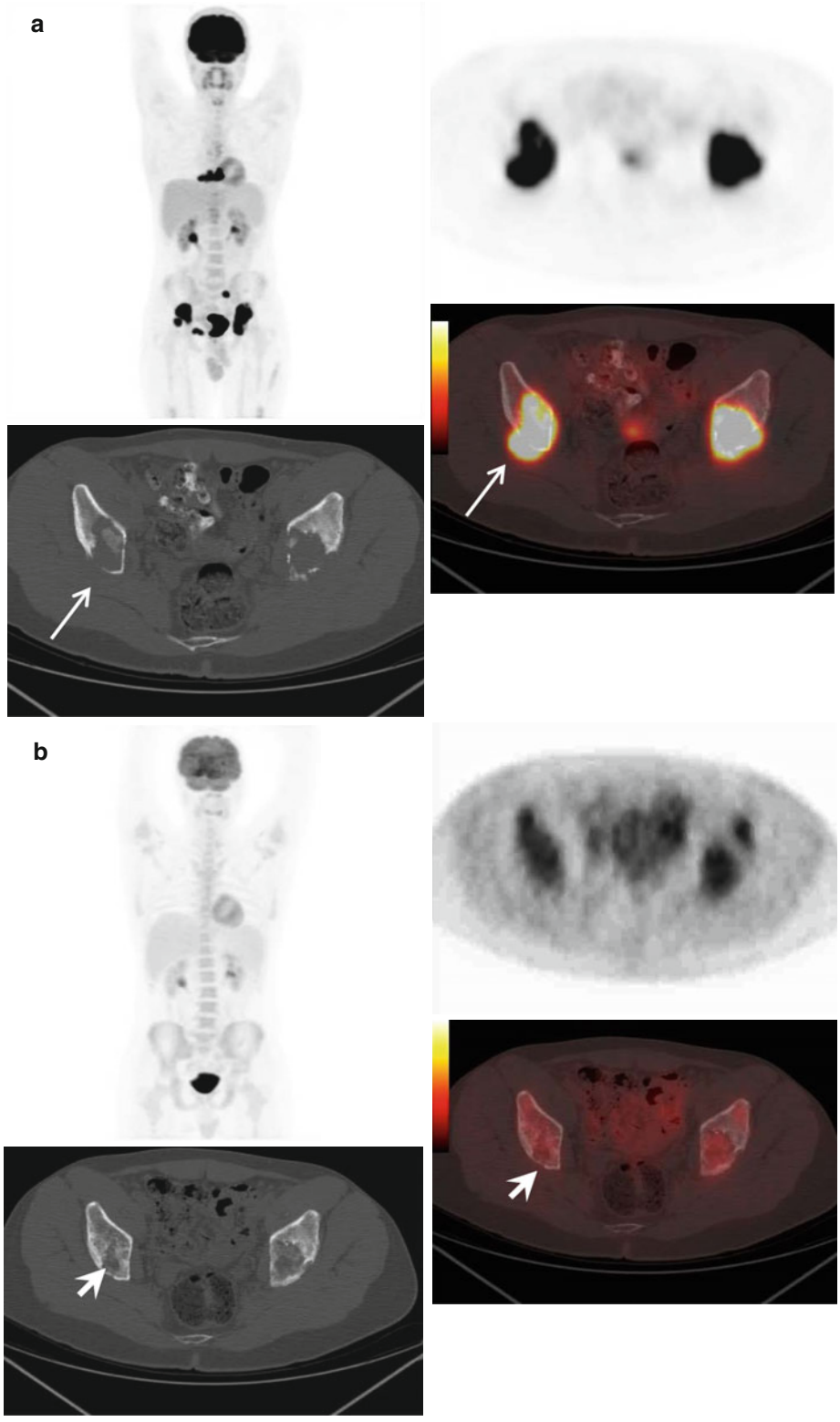

Fig. 13.14 A 50-year-old patient with diagnosis of lymphoma. (**a**) Pretherapy FDG-PET-CT images show lytic bone involvement with soft tissue component (*white arrows*). (**b**) Post-therapy FDG-PET-CT images shows decrease in FDG uptake, and lytic lesions heal with sclerosis (*white arrow heads*)

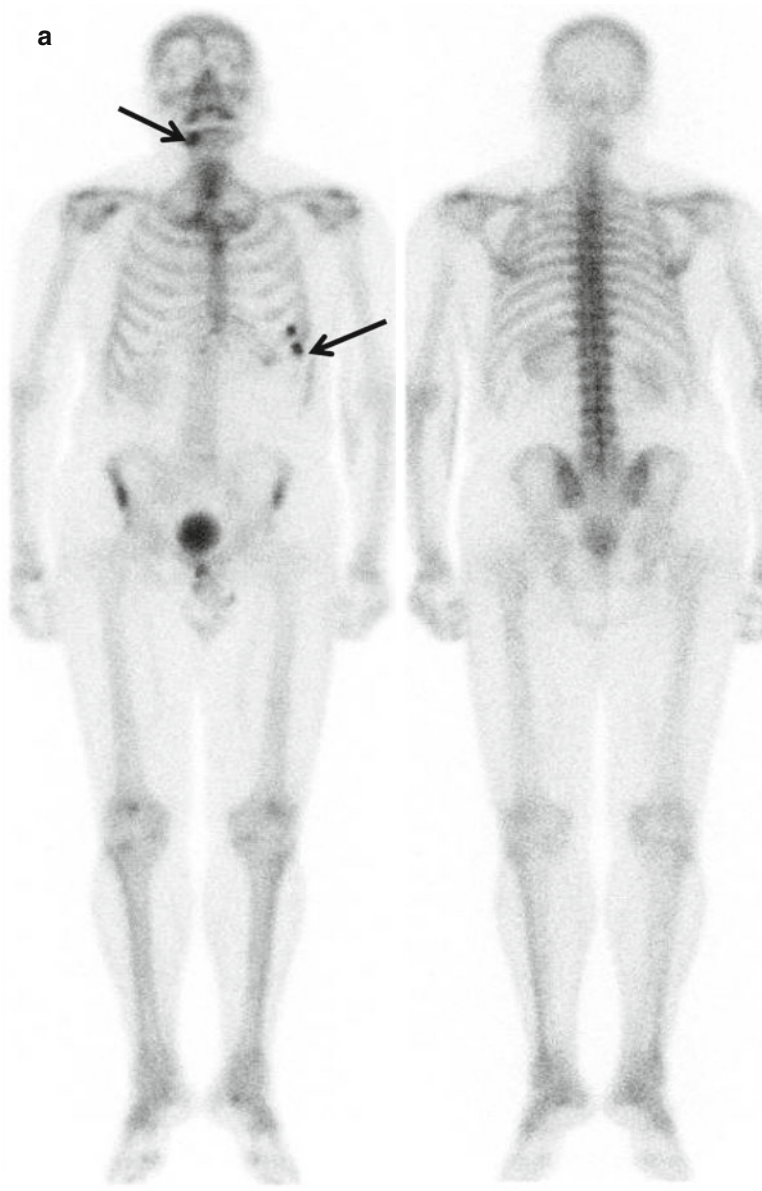

Fig. 13.15 A 70-year-old patient with a diagnosis of prostate cancer. He had rising PSA levels of 10 ng/ml after radical prostatectomy. (**a**) Bone scintigraphy showed increased uptake in the left sixth and seventh ribs due to trauma and in mandible due to recent dental implant (*black arrows*). There was no sign of metastases. (**b**) Ga-68 PSMA PET-CT showed metastases in the T4 vertebra (*black arrow*) with sclerosis on CT (*white arrows*) although unusual biopsy proved lung metastases with increased radiotracer uptake (*black arrow heads*)

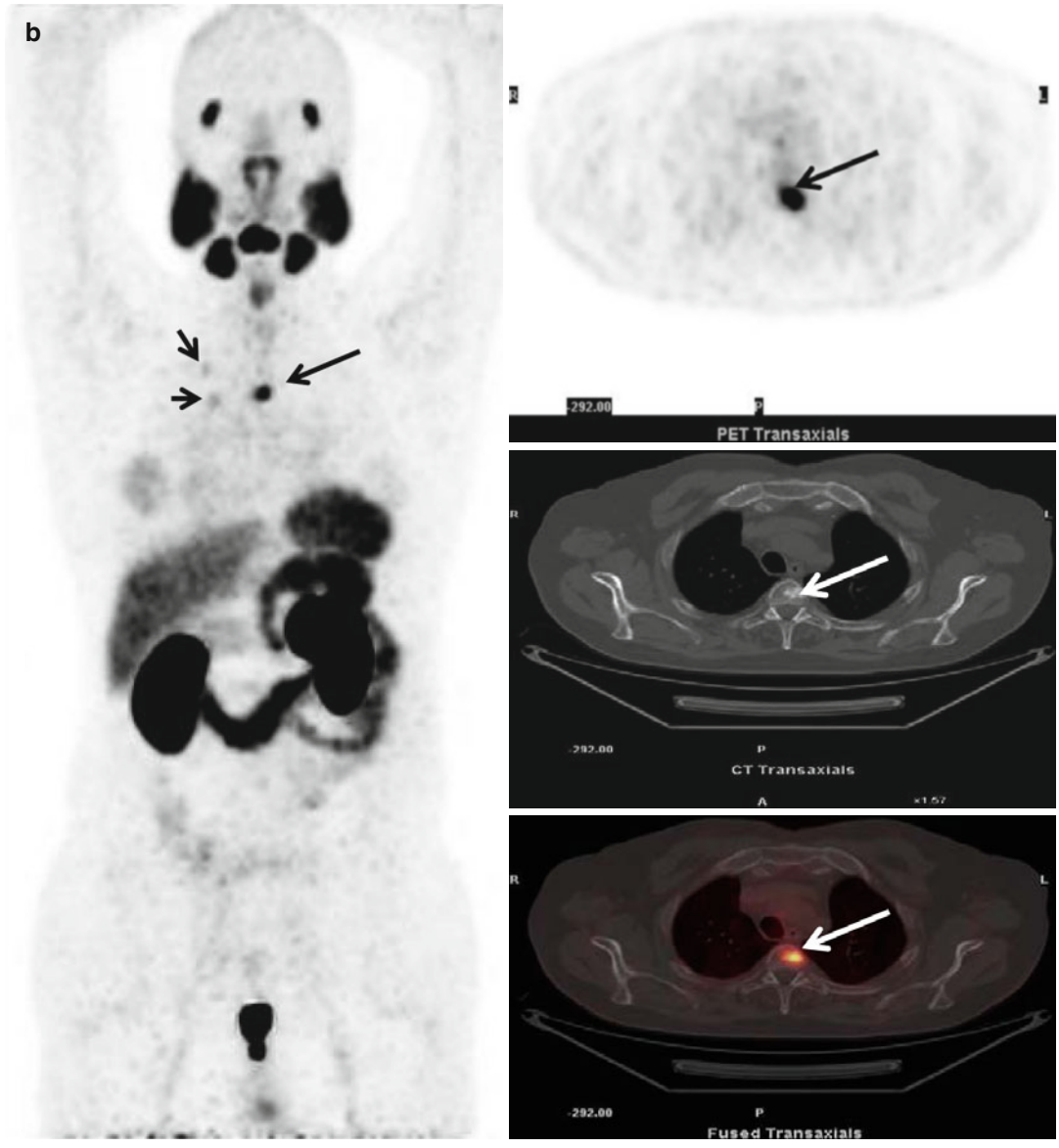

Fig. 13.15 (continued)

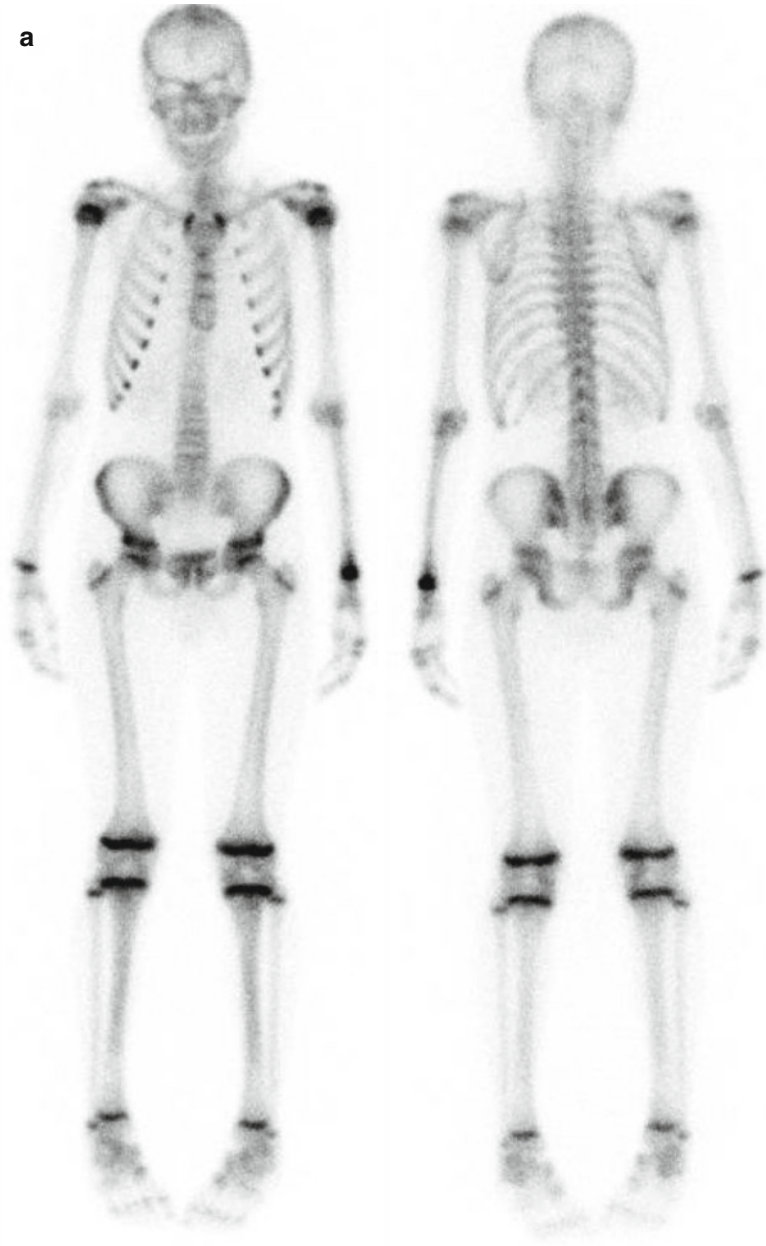

Fig. 13.16 A 14-year-old patient with diagnosis of soft tissue sarcoma. (**a**) Whole-body bone scintigraphy was normal. (**b**) FDG-PET-CT shows right axillary and supraclavicular lymph node metastases (*black arrow*) and intramedullary metastases in the humerus and right femur (*white arrow*)

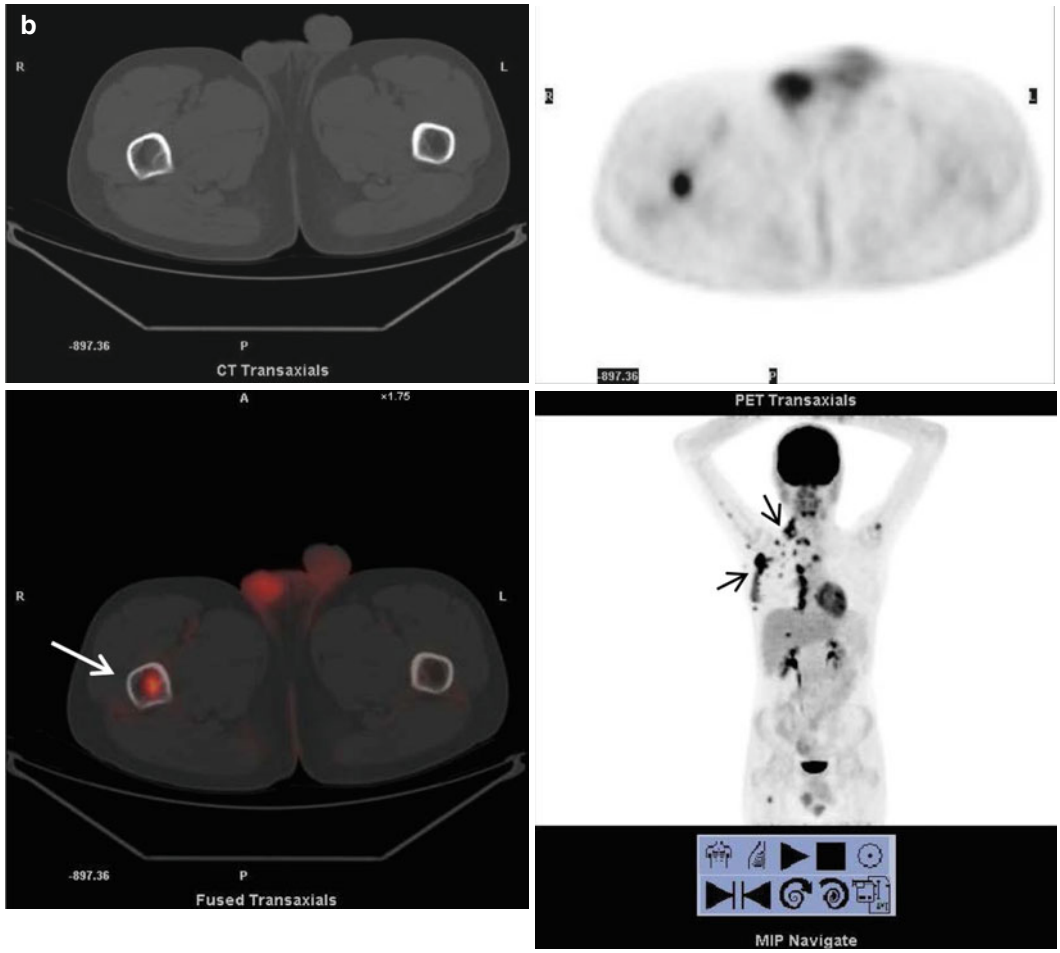

Fig. 13.16 (continued)

after one and two cycles of chemotherapy, respectively. After one cycle of chemotherapy, SUVmax, MTV, and TLG predicted the poor responders. Among these parameters, either MTV ≥47 ml or TLG ≥190 g after one cycle of chemotherapy was significantly associated with a poor histologic response on multivariate logistic regression analysis (OR 8.98, $p = 0.039$). The sensitivity, specificity, and accuracy of these parameters were 71 %, 85 %, and 77 %, respectively [86]. Hawkins et al. evaluated 36 patients with Ewing's sarcoma family of tumors (ESFTs). All patients received neoadjuvant and adjuvant chemotherapy. FDG-PET standard uptake values before (SUV1) and after (SUV2) chemotherapy were analyzed and correlated with chemotherapy response, as assessed by histopathology in surgically excised tumors. Good FDG-PET response was defined as SUV2 less than 2.5 or SUV2:1 ≤ 0.5. FDG-PET response by SUV2 or SUV2:1 was concordant with histologic response in 68 % and 69 % of patients, respectively. SUV2 was associated with outcome (4-year PFS 72 % for SUV2 <2.5 vs 27 % for SUV2 ≥2.5, $p = 0.01$ for all patients); FDG-PET imaging of ESFTs correlates with histologic response to neoadjuvant chemotherapy [87].

D-Radionuclide Methods in the Palliative Therapy of Painful Bone Metastases

Painful bone metastases are a life-debilitating condition in patients with advanced cancers. Analgesics, hormonal therapies, and bisphosphonates are also effective in bone pain palliation but have side effects like constipation, osteonecrosis, etc. [88–90]. External radiation therapy provides palliation starting from few days to 12–15 weeks in 75–90 % of cases; however, in patients with widespread bone metastases, effective palliation is not possible [91, 92].

In these patients, systemic radionuclide therapy provides palliation in all metastatic bone sites. After i.v. injection, radiotracers accumulate in the osteoblastic metastases and decrease the pain mediators by high radiation dose. The high specificity of the radiotracers to the osteoblastic bone metastases provides less toxicity to the nontarget organs.

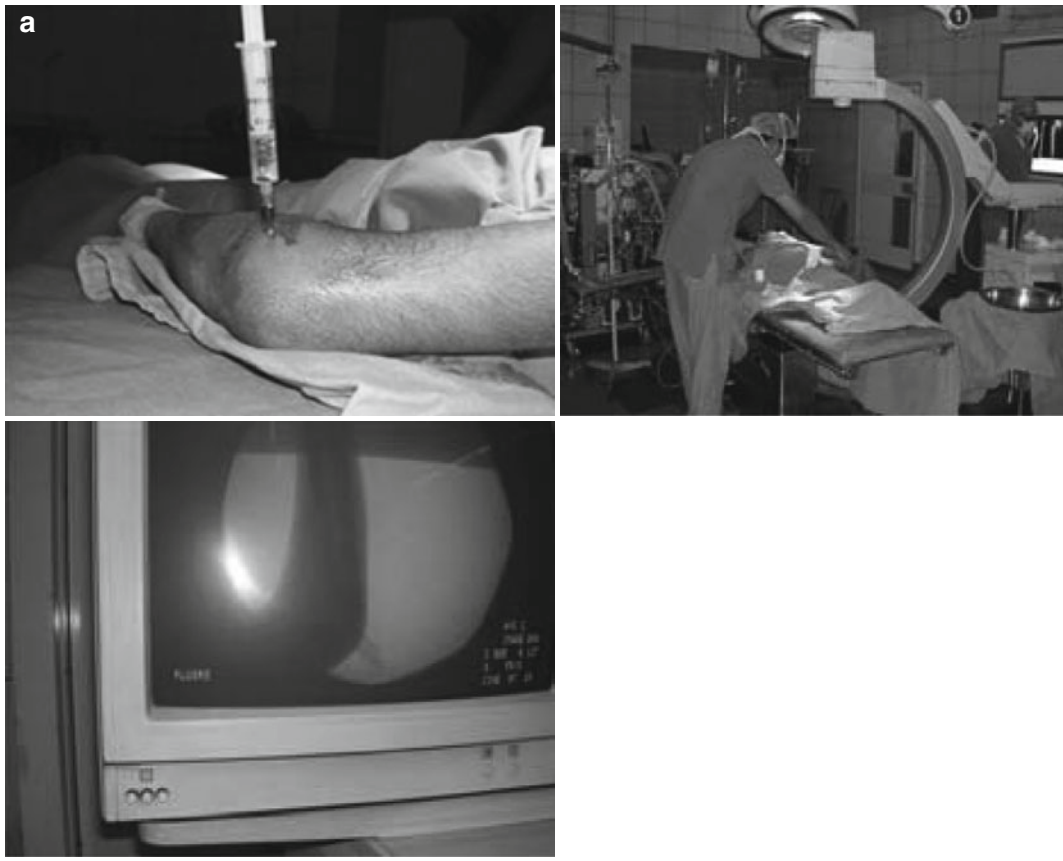

Fig. 13.17 Rh-186-sulfide application into the left elbow joint, (**a**) scope-guided intra-articular injection of radiotracer and (**b**) postinjection imaging to control absence of significant extra-articular leakage from the left elbow joint

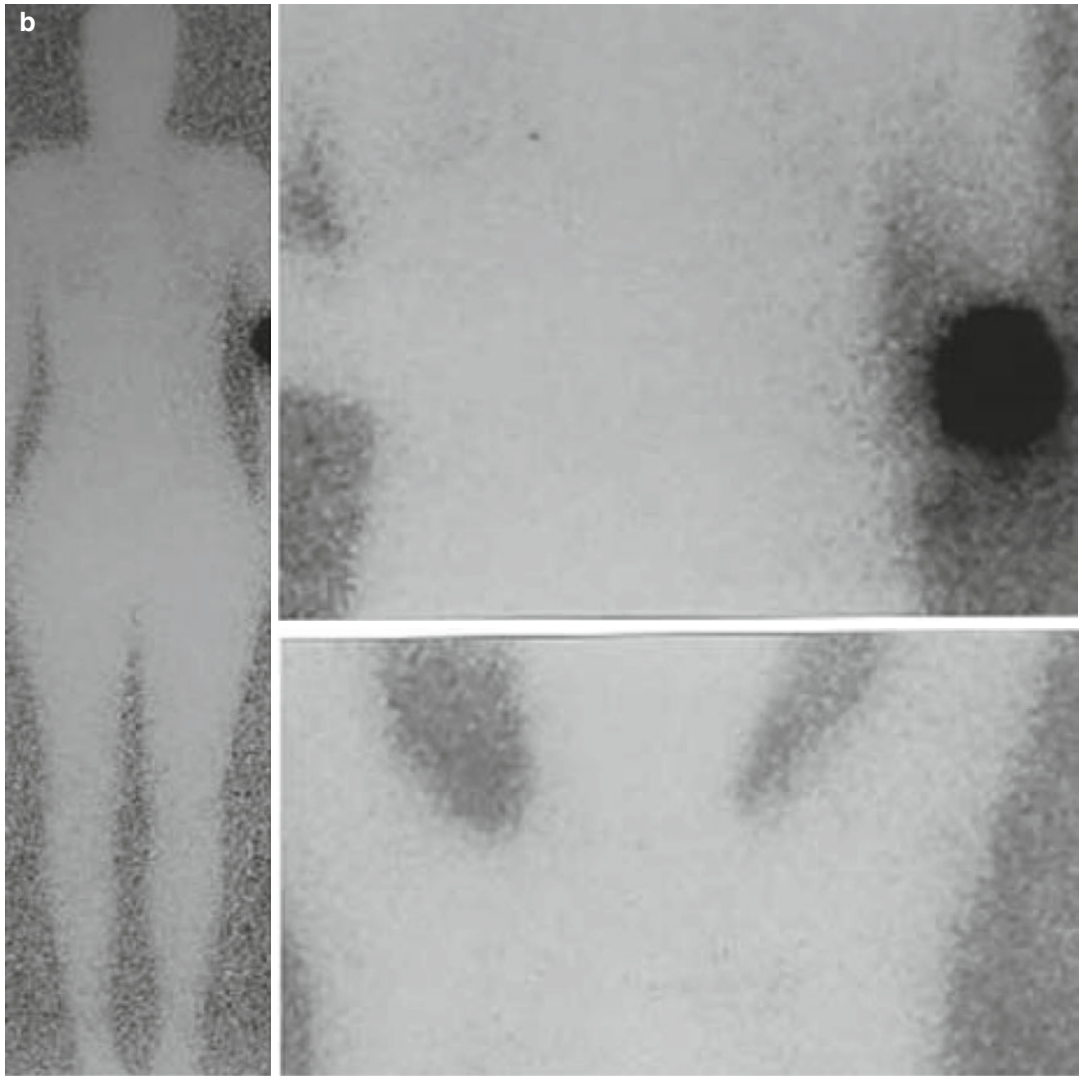

Fig. 13.17 (continued)

Indications

- Metastatic bone pain unresponsive to analgesics, chemotherapy, and hormonotherapy.
- Pain limits daily activities and needs regular analgesics.
- Multiple metastases impossible to control with local radiotherapy.
- Multiple osteoblastic metastases on BS.

Contraindications

1. *Absolute*
   Pregnancy and lactation
2. *Relative*
   (a) Hb <9 g/1
   (b) Total WBC $<4.0 \times 10^9$/l
   (c) Thrombocyte number $<100 \times 10^9$/l
   (d) GFR <30 ml/min

(e) Acute spinal compression or pathological fractures
(f) A life expectancy less than 4 weeks [93, 94]

There are several radiopharmaceuticals approved for therapy. ^{89}Sr-strontium chloride, ^{153}Sm-lexidronam (EDTMP), and ^{186}Re-etidronate (HEDP) were the radiotracers used for several years. Recently Ra-223 dichloride was introduced and found widespread application. The effectiveness of radiotracer depends on the concentration on bone metastases, retention time, particle type, and energy. Tables 13.1 and 13.2 summarize the properties of different radiotracers.

Patient Preparation

Increased uptake in the osteoblastic metastases should be confirmed with BS performed within 8 weeks of therapy. Hematological and biochemical profiles should be controlled. Radionuclide therapy can be combined with local-external radiotherapy. However, wide-field external therapy in 3 months is relatively contraindicated due to bone marrow suppression risk [95, 96]. Myelosuppressive chemotherapy must be stopped 4 weeks before therapy and not be performed after 6–12 weeks. At present, there is no evidence of competition between bisphosphonates and ^{153}Sm-lexidronam, ^{186}Re-etidronate, or ^{89}Sr. Therefore, they may be used concomitantly.

Patient Information and Instruction

Patient should be informed that this therapy is a palliative therapy and could not cure metastatic bone lesion. Patients should be told that 60–80 % of patients benefit from ^{89}Sr, ^{153}Sm-lexidronam, or ^{186}Re-etidronate therapy. Patients receiving Xofigo must be instructed that this therapy may produce survival benefit in patients with castration-resistant prostate cancer [97]. Patients should be warned of the risk of temporary increase in bone pain (flare) in 72 h. This phenomenon is usually mild and self-limiting and associated with good clinical response. The patient should be told that pain reduction is unlikely within the first week and could occur as late as 4 weeks or longer after injection, particularly for long-lived isotopes. Patients should continue prescribed analgesics until bone pain decreases. Patients should also be informed on the duration of the analgesic effect, generally of 2–6 months, and that retreatment is possible. In recurrent pain, if the bone marrow reserve is available, therapy can be repeated in 12 weeks. However, the success of therapy decreases with each therapy.

Precautions After Therapy

Urinary radiopharmaceutical excretion is of particular concern during the first 2–3 days post-administration. Patients should be advised to observe hygiene to avoid contamination. Patients should be warned to avoid soiling underclothing or

Table 13.1 Radiotracers used for bone pain palliation

Radiopharmaceutical	Half-life (day)	Maximum β energy (MeV)	Maximum penetration (mm)	Gamma photon energy (keV)	Alpha energy (Mev)
Sr-89 chloride	50,5	1,46	6,7	–	
Re-186 HEDP	3,8	1,07	4,7	137	
Sm-153 EDTMP	1,95	0,8	3,4	103	
Ra-223 dichloride	11.4				28 Mev

Table 13.2 Radiation dose to some critic organs (mGy/MBq)

Radiopharmaceutical	Bone	Bone marrow	Bladder
Sr-89 chloride	17	11	1,3
Re-186 HEDP	1,4	1,3	0,54
Sm-153 EDTMP	6,8	1,5	0,1
Ra-223 dichloride	1,152	138	4

areas around toilet bowls for 1-week postinjection and that significantly soiled clothing should be washed separately. Incontinent patients should be catheterized before radiopharmaceutical administration for radioprotection of caring person.

Side Effects

Early

1. "Flare" phenomena: increase of pain symptoms, in about 10 % of the patients, usually within 72 h, typically transient, usually mild, and self-limiting.
2. When cervicodorsal spinal metastases are present, an increase rate of spinal cord compression is possible. Prophylactic corticosteroids may be considered to prevent neurological symptoms.
3. A decrease of thrombocyte and leukocyte count in peripheral blood, as a result of myelosuppression, is frequently observed and has a nadir of 3–5 weeks (^{153}Sm-lexidronam, ^{186}Re-etidronate) or 12–16 weeks (^{89}Sr). The occurrence of grade 3 or 4 toxicity is dependent on previous myelosuppressive therapy (chemotherapy, wide field radiation therapy etc.) and bone marrow involvement. Hematological toxicity is usually temporary with complete or partial recovery over the next 3 months. The rate of recovery depends on the amount of administered activity and the bone marrow reserve.
4. Calcium-like flushing sensation, described with the use of ^{89}Sr; radiotracer should be infused slowly.

Late

Transient bone marrow suppression can be seen for 4–6 weeks. The recovery depends on the bone marrow reserve of the patient. Patient must be followed-up for recovery of hematological parameters.

E-Radiosynovectomy

Radiosynovectomy is performed by intra-articular injection of radionuclide having beta radiation like Y-90 labeled with citrate and silicate. The main aim is to destroy hypertrophied synovium by local high radiation. Most commonly used in rheumatoid arthritis and chronic hemophilic synovitis [98, 99].

Indications

- Rheumatoid arthritis
- Spondyloarthropathy (e.g., reactive or psoriatic arthritis)
- Other inflammatory joint diseases, e.g., Lyme disease
- Behcet's disease
- Persistent synovial effusion
- Hemophilic arthritis
- Calcium pyrophosphate dihydrate (CPPD) arthritis
- Pigmented villonodular synovitis (PVNS)
- Persistent effusion after joint prosthesis

Contraindications

1. *Absolute*
   - Pregnancy
   - Breast-feeding
   - Local skin infection
   - Ruptured popliteal cyst (knee)
   - Periarticular sepsis, cellulitis, septic arthritis, and bacteremia

2. *Relative*
   - The radiopharmaceuticals should only be used in children and young patients (<20 years) if the benefit of treatment is likely to outweigh the potential hazards.
   - Extensive joint instability with bone destruction.
   - Evidence of significant cartilage loss within the joint.

Ideal Radioisotope Properties

1. The beta-particle energy of radionuclide must be high to penetrate the synovial tissue but also low enough not to harm the adjacent cartilage and bone. By this principle, radionuclides with higher beta-particle energy were used for larger joints like knee, and lower energy particles were used for smaller joints like metacarpal joints.
2. Radionuclide must be applied as a colloidal solution attached with a particle that can be phagocyted. Particle must be small enough to phagocyted but large enough not to escape from the joint. Ideal particle size is 5–10 nm [99].
3. Radiotracer must be chemically pure and nontoxic and does not lead to granulation tissue.
4. Half-life must be short enough to decrease the dose if the radiotracer escapes from the joint by time.

Radionuclides Used in Radiosynovectomy

Y-90-sitrat and Y-90-silikat: Used for knee joint; ^{90}Y emits a beta particle with a maximum energy of 2.27 MeV, a mean energy of 0.935 MeV, and an average soft tissue range of 3.6 mm. The physical half-life is 2.7 days.

Re-186-sulfide: Used for shoulder, elbow, wrist, ankle, and subtalar joints. ^{186}Re emits a beta particle with a maximum energy of 1.07 MeV, a mean energy of 0.349 MeV, an average soft tissue range of 1.1 mm, and 9 % abundant gamma emission with a photopeak of 0.137 MeV. The physical half-life is 3.7 days.

Er-169 citrate: Used for metacarpophalangeal, metatarsophalangeal, and digital interphalangeal joints. ^{169}Er emits a beta particle with a maximum energy of 0.34 MeV, a mean energy of 0.099 MeV, and an average soft tissue range of 0.3 mm. The physical half-life is 9.4 days

Injection Technique

Intra-articular injection was performed under local anesthesia and aseptic conditions. After the punction, the radioactivity is injected when the needle tip is in the joint space (Fig. 13.18a). Before the needle is withdrawn, injector is rinsed with local anesthesia or steroid to prevent skin contamination from the possible drops to skin during withdrawal. After the injection to the joint, passive extension and flexion movements must be performed to provide homogenous distribution. Treated joint should be immobilized at least for 48 h to decrease escape from joint, and whole-body bremsstrahlung images must be obtained (Fig. 13.18b).

Therapy Response Evaluation

Patients should be told that 60–80 % of patients benefit from therapy, and response is unlikely within 14 days of injection and may be delayed until up to 1 month. Patients should be warned of the risk of a temporary increase in synovitis following treatment. The amount of effusion, pain, range of motion, synovial thickness as measured with USG or MRI, or inflammatory activity detected by scintigraphy may be used for response evaluation. Treatment failure is likely if no response is detected by 6 weeks postinjection. Patients who have failed to respond to the first radionuclide injection may be retreated 3–6 months later.

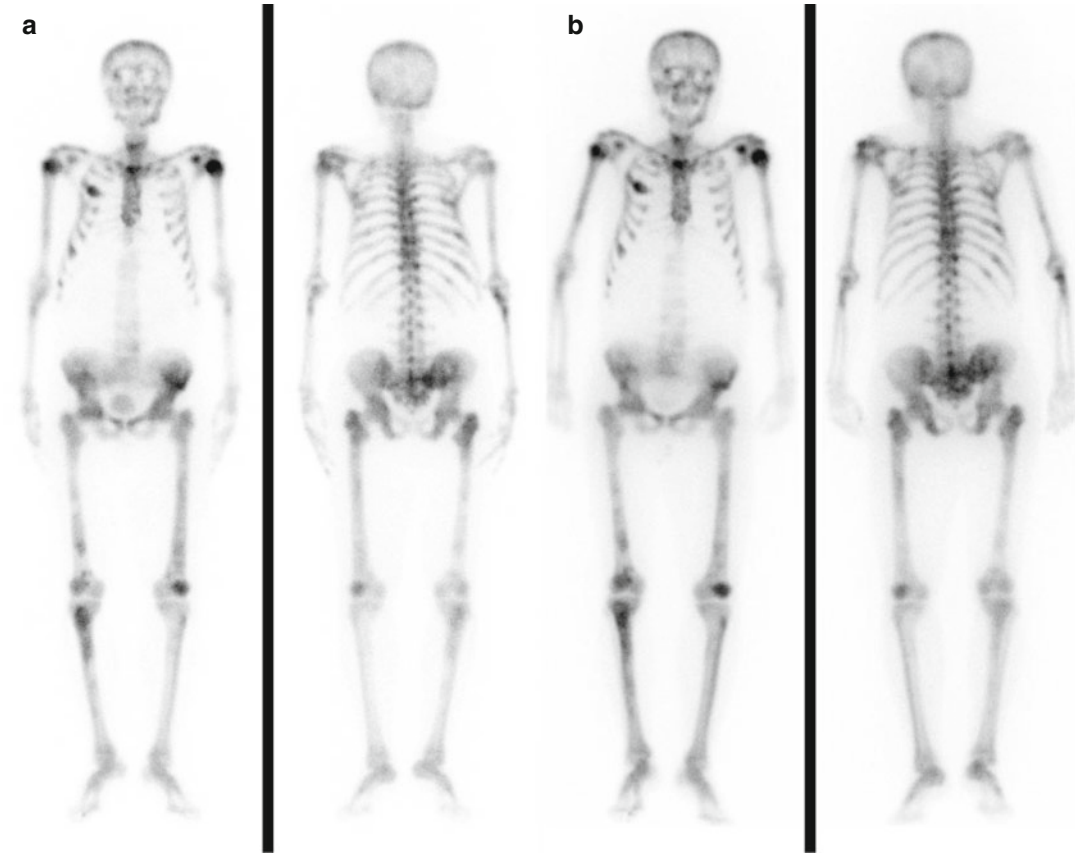

Fig. 13.18 (**a**) Whole-body bone scintigraphy after injection of 20 mCi Tc-99m MDP shows increased uptake in diffuse metastatic disease in axial and appendicular skeleton, (**b**) images after 80 mCi 153Sm-EDTMP therapy show similar increased uptake in metastatic sites

Early Local Complications

Radiation synovitis: Spontaneously regresses; steroid may be coinjected to prevent this complication.

Late Complications

1. Skin ulceration
2. Necrosis in periarticular tissue

   Wrong injection of radiotracer into periarticular joint is the most serious complication of radiosynovectomy. Treatment may be conservative or surgery may be needed depending on the necrosis.
3. Temporary lymphedema: Rare mostly seen after ankle treatments.

References

1. Light TR (1996) Musculoskeletal introduction: clinical applications of musculoskeletal nuclear medicine. In: Henkin RE, Boles MA, Wagner RH et al (eds) Nuclear medicine. Mosby-Yera Book, St. Louis, pp 1123–1156
2. Thrall JH, Ziessman HA (2001) Skeletal system. In: Thrall JH, Ziessman HA, eds. Nuclear medicine: the requisites. 2nd ed. St Louis, Mo: Mosby, p. 110–144.
3. Bombardieri E, Aktolun C, Baum RP et al (2003) Bone scintigraphy: procedure guidelines for tumour imaging. Eur J Nucl Med Mol Imaging 30(12):BP99–BP106
4. Wong KK, Piert M (2013) Dynamic bone imaging with ^{99m}Tc-labeled diphosphonates and ^{18}F-NaF: mechanisms and applications. J Nucl Med 54:590–599
5. Love C, Din AS, Tomas MB et al (2003) Radionuclide bone imaging: an illustrative review. Radiographics 23:341–358

6. Even-Sapir E (2005) Imaging of malignant bone involvement by morphologic, scintigraphic, and hybrid modalities. J Nucl Med 46:1356–1367
7. Römer W, Nömayr A, Uder M et al (2006) SPECT-guided CT for evaluating foci of increased bone metabolism classified as indeterminate on SPECT in cancer patients. J Nucl Med 47:1102–1106
8. Hage WD, Aboulafia AJ, Aboulafia DM (2000) Incidence, location, and diagnostic evaluation of metastatic bone disease. Orthop Clin N Am 31:515–528
9. Cornud F, Oven R (2002) Role of imaging in the diagnosis and staging of prostatic adenocarcinomas. J Radiol 83:863–880
10. Hricak H, Choyke PL, Eberhardt SC et al (2007) Imaging prostate cancer: a multidisciplinary perspective. Radiology 243:28–53
11. Caglar M, Tuncel M (2002) Preserved value of bone scintigraphy for the detection of skeletal metastases in prostate cancer patients with low prostate-specific antigen levels: effect of hormonal therapy and poor histologic differentiation. Clin Nucl Med 27(7):532–533
12. Citrin DL, Tormey DC, Carbone PP (1977) Implications of the 99mTc diphosphonate bone scan on treatment of primary breast cancer. Cancer Treat Rep 61:1249–1252
13. Hsia TC, Shen YY, Yen RF et al (2002) Comparing whole body 18F-2-deoxyglucose positron emission tomography and technetium-99m methylene diophosphate bone scan to detect bone metastases in patients with non-small cell lung cancer. Neoplasma 49(4):267–271
14. Lee JW, Lee SM, Lee HS et al (2012) Comparison of diagnostic ability between (99m)Tc-MDP bone scan and (18)F-FDG PET/CT for bone metastases in patients with small cell lung cancer. Ann Nucl Med 26(8):627–633
15. Tumeh SS, Beadle G, Kaplan WD (1985) Clinical significance of solitary rib lesions in patients with extraskeletal malignancy. J Nucl Med 26:1140–1143
16. Kara G, Bozkurt MF, Ozcan PP et al (2003) Solitary rib lesions in bone scans of patients with breast carcinoma. Nucl Med Commun 24(8):887–892
17. Jacobson AF, Stomper PC, Jochelson MS et al (1990) Association between number and sites of new bone scan abnormalities and presence of skeletal metastases in patients with breast cancer. J Nucl Med 31:387–392
18. Ho YY (2005) Review of non-positron emission tomography functional imaging of primary musculoskeletal tumours: beyond the humble bone scan. Australas Radiol 49:445–459
19. Franzius C, Sciuk J, Daldrup-Link HE et al (2000) FDG-PET for detection of osseous metastases from malignant primary bone tumours: comparison with bone scintigraphy. Eur J Nucl Med 27(9): 1305–1311
20. Solav S (2004) Bone scintiscanning in osteolytic lesions. Clin Nucl Med 29(1):12–20
21. Howarth DM, Mullan BP, Wiseman GA et al (1996) Bone scintigraphy evaluated in diagnosing and staging Langerhans' cell histiocytosis and related disorders. J Nucl Med 37(9):1456–1460
22. Rupani HD, Holder LE, Espinola DA et al (1985) Three-phase radionuclide bone imaging in sports medicine. Radiology 156:187–196
23. Holder LE, Michael RH (1984) The specific scintigraphic pattern of "shin splints in the lower leg": concise communication. J Nucl Med 25:865–869
24. Palestro CJ, Torres MA (1997) Radionuclide imaging of orthopedic infections. Semin Nucl Med 27:334–345
25. Palestro CJ et al (1995) Radionuclide imaging after skeletal interventional procedures. Semin Nucl Med 25:3–14
26. Peller PJ, Ho VB, Kransdorf MJ (1993) Extraosseous Tc-99m MDP uptake: a pathophysiologic approach. Radiographics 13(4):715–734
27. Savelli G, Maffioli L, Maccauro M et al (2001) Bone scintigraphy and the added value of SPECT (single photon emission tomography) in detecting skeletal lesions. Q J Nucl Med 45:27–37
28. DeSmet AA, Dalinka MK, Alazraki N et al (2000) Diagnostic imaging of avascular necrosis of the hip. Radiology 215(suppl):247–254
29. Fournier RS, Holder LE (1998) Reflex sympathetic dystrophy: diagnostic controversies. Semin Nucl Med 28:116–123
30. Wellman HN, Schauwecker D, Robb JA et al (1977) Skeletal scintimaging and radiography in the diagnosis and management of Paget's disease. Clin Orthop 127:55–62
31. Madsen JL (2008) Bone SPECT/CT detection of a sequestrum in chronic infected nonunion of the tibia. Clin Nucl Med 33:700–701
32. Horger M, Eschmann SM, Pfannenberg C et al (2007) Added value of SPECT/CT in patients suspected of having bone infection: preliminary results. Arch Orthop Trauma Surg 127:211–221
33. Filippi L, Uccioli L, Giurato L et al (2009) Diabetic foot infection: usefulness of SPECT/CT for 99mTc-HMPAO-labeled leukocyte imaging. J Nucl Med 50:1042–1046
34. Filippi L, Schillaci O (2006) Usefulness of hybrid SPECT/CT in 99mTcHMPAO- labeled leukocyte scintigraphy for bone and joint infections. J Nucl Med 47:1908–1913
35. Damgaard M, Nimb L, Madsen JL et al (2010) The role of bone SPECT/CT in the evaluation of lumbar spinal fusion with metallic fixation devices. Clin Nucl Med 35:234–236
36. Linke R, Kuwert T, Uder M et al (2010) Skeletal SPECT/CT of the peripheral extremities. AJR Am J Roentgenol 194:329–335
37. Mulholland NJ, Gnanasegaran G, Mohan HK et al (2008) Recognition of the femoroacetabular impingement syndrome on MDP SPECT CT. Clin Nucl Med 33:125–127

38. Tuncel M, Kiratli PO, Gedikoglu G (2012) SPECT-CT imaging of poliostotic fibrous dysplasia. Rev Esp Med Nucl Image Mol 31(1):47–48
39. Tuncel M, Caner B (2012) Osteopoikilosis: a major diagnostic problem solved by bone scintigraphy. Rev Esp Med Nucl Image Mol 31(2):93–96
40. Scharf S (2009) SPECT/CT imaging in general orthopedic practice. Semin Nucl Med 39:293–307
41. Gnanasegaran G, Barwick T, Adamson K et al (2009) Multislice SPECT/CT in benign and malignant bone disease: when the ordinary turns into the extraordinary. Semin Nucl Med 39:431–442
42. Helyar V, Mohan HK, Barwick T et al (2010) The added value of multislice SPECT/CT in patients with equivocal bony metastases from carcinoma of the prostate. Eur J Nucl Med Mol Imaging 37:706–713
43. Bailey E, HoShon I, Roach P (2007) Additional benefit of SPECT/CT in bone scanning of metastatic renal cell carcinoma. Clin Nucl Med 32:411–414
44. Russo RR, Lee A, Mansberg R et al (2009) Hypertrophic pulmonary osteoarthropathy demonstrated on SPECT/CT. Clin Nucl Med 34:628–631
45. Dore F, Filippi L, Biasotto M et al (2009) Bone scintigraphy and SPECT/CT of bisphosphonate-induced osteonecrosis of the jaw. J Nucl Med 50:30–35
46. Sawyer LJ, Starritt HC, Hiscock SC et al (2008) Effective doses to patients from CT acquisitions on the GE Infinia Hawkeye: a comparison of calculation methods. Nucl Med Commun 29:144–149
47. Datz FL, Seabold JE, Brown ML et al (1997) Procedure guideline for technetium-99m-HMPAO-labeled leukocyte scintigraphy for suspected infection/inflammation. Society of Nuclear Medicine. J Nucl Med 38:987–990
48. Duet M, Pouchot J, Liote F et al (2007) Role for positron emission tomography in skeletal diseases. Joint Bone Spine 74:14–23
49. Buck AK, Schirrmeister H, Reske SN (2004) Musculoskeletal tumors. In: Oehr P, Biersack HJ, Coleman E (eds) PET and PET-CT in oncology. Springer, Berlin, pp 275–289
50. Shields AF, Grierson JR, Dohmen BM et al (1998) Imaging proliferation in vivo with F-18 FLT and positron emission tomography. Nat Med 4:1334–1336
51. Watanabe H, Inoue T, Shinozaki T et al (2000) PET imaging of musculoskeletal tumors with fluorine-18 alpha-methyltyrosine: comparison with fluorine-18 fluorodeoxyglucose PET. Eur J Nucl Med 27:1509–1517
52. Schirrmeister H, Glatting G, Hetzel J et al (2001) Prospective evaluation of clinical value of planar bone scans, SPECT, and (18) F labelled NaF PET in newly diagnosed lung cancer. J Nucl Med 42:1800–1804
53. Palmedo H, Schaible R, Textor J (2002) PET with 18F fluoride compared to bone scintigraphy in the diagnosis of bone metastases: results of a prospective study. J Nucl Med 43(suppl):1150
54. Afshar-Oromieh A, Malcher A, Eder M et al (2013) PET imaging with a [68Ga]gallium-labelled PSMA ligand for the diagnosis of prostate cancer: biodistribution in humans and first evaluation of tumour lesions. Eur J Nucl Med Mol Imaging 40(4): 486–495
55. Beckers C, Ribbens C, Andre B et al (2004) Assessment of disease activity in rheumatoid arthritis with (18)F-FDG PET. J Nucl Med 45:956–964
56. Tateishi U, Imagawa T, Kanezawa N et al (2010) PET assessment of disease activity in children with juvenile idiopathic arthritis. Pediatr Radiol 40(11):1781–1788
57. Beckers C, Jeukens X, Ribbens C et al (2006) (18) F-FDG PET imaging of rheumatoid knee synovitis correlates with dynamic magnetic resonance and sonographic assessments as well as with the serum level of metalloproteinase-3. Eur J Nucl Med Mol Imaging 33:275–280
58. Stumpe KD, Dazzi H, Schaffner A et al (2000) Infection imaging using whole-body FDG-PET. Eur J Nucl Med 27:822–832
59. Guhlmann A, Brecht-Krauss D, Suger G et al (1998) Chronic osteomyelitis: detection with FDG PET and correlation with histopathologic findings. Radiology 206:749–754
60. Zhuang H, Chacko TK, Hickeson M et al (2002) Persistent non-specific FDG uptake on PET imaging following hip arthroplasty. Eur J Nucl Med Mol Imaging 29:1328–1333
61. Vankuickenborne B, Maes A, Nuyts J et al (2003) The value of 18-F-FDGPET for the detection of infected hip prosthesis. Eur J Nucl Med 30:705–715
62. van Acker F, Nuyts J, Maes A et al (2001) FDG-PET, Tc-99m HMPAO white blood cell SPECT and bone scintigraphy in evaluation of painful total knee arthroplasties. Eur J Nucl Med 28:1496–1504
63. Chacko TK, Zhuang H, da Nakho KZ et al (2003) Applications of fluorodeoxyglucose positron emission tomography in the diagnosis of infection. Nucl Med Commun 24:615–624
64. Gratz SI, Dörner J, Fischer U et al (2002) 18-F-FDG hybrid PET in patients with suspected spondylitis. Eur J Nucl Med 29:516–524
65. Schmitz A, Risse JH, Grunwald F et al (2001) Fluorine-18 fluorodeoxyglucose positron emission tomography findings in spondylodiscitis: preliminary results. Eur Spine J 10:534–539
66. Stumpe KDM, Zanetti M, Weishaupt D et al (2002) FDG positron emission tomography for differentiation of degenerative and infectious endplate abnormalities in the lumbar spine detected on MR imaging. Am J Roentgenol 179:1151–1157
67. Lucas JD, O'Doherty MJ, Cronin BF et al (1999) Prospective evaluation of soft tissue masses and sarcomas using fluorodeoxyglucose positron emission tomography. Br J Surg 86:550–556
68. Eary JF, Conrad EU, Bruckner JD et al (1998) Quantitative (F18) fluorodeoxyglucose positron emission tomography in pretreatment and grading of sarcoma. Clin Cancer Res 4:12115–12120
69. Schulte M, Brecht-Kraus D, Heymer B et al (2000) Grading of tumors and tumor like of bone: evaluation by FDG-PET. J Nucl Med 41:1695–1701

70. Franzius C, Sciuk J, Brinkschmidt C et al (2000) Evaluation of chemotherapy response in primary bone tumors with F-18 positron emission tomography compared with histologically assessed tumor necrosis. Clin Nucl Med 25:874–881
71. Franzius C, Daldrup-Link HE, Wagner-Bohn A et al (2002) FDG PET for detection of recurrences from malignant primary bone tumors: comparison with conventional imaging. Ann Oncol 13:157–160
72. Bredella MA, Steinbach L, Caputo G et al (2005) Value of FDG PET in assessment of patients with multiple myeloma. Am J Roentgenol 184:1199–1204
73. Durie BG, Waxman AD, D'Agnolo A et al (2002) Whole-body (18)F-FDG PET identifies high-risk myeloma. J Nucl Med 43:1457–1463
74. Wiesenthal AA, Nguyen BD (2007) F-18 FDG PET/CT staging of multiple myeloma with diffuse osseous and extramedullary lesions. Clin Nucl Med 32:797–801
75. Nakamoto Y, Osman M, Wahl RL (2003) Prevalence and patterns of bone metastases detected with positron emission tomography using F-18 FDG. Clin Nucl Med 28:302–307
76. Cook GJ, Houston SI, Rubens R et al (1998) Detection of bone metastases in breast cancer by 18FDG-PET: differing metabolic activity in osteoblastic and osteolytic lesions. J Clin Oncol 16:3375–3379
77. Uematsu T, Yuen S, Yukisawa S et al (2005) Comparison of FDG PET and SPECT for detection of bone metastases in breast cancer. AJR Am J Roentgenol 184:1266–1273
78. Nakai T, Okuyama C, Kubota T et al (2005) Pitfalls of FDG-PET for the diagnosis of osteoblastic bone metastases in patients with breast cancer. Eur J Nucl Med Mol Imaging 32:1253–1258
79. Bury T, Barreto A, Daenen F et al (1998) Fluorine-18 deoxyglucose positron emission tomography for the detection of bone metastases in patients with non-small cell lung cancer. Eur J Nucl Med 25:1244–1247
80. Hetzel M, Arslandemir C, König HH et al (2003) F-18 NaF PET for detection of bone metastases in lung cancer: accuracy, cost-effectiveness and impact on patient management. J Bone Miner Res 18:2206–2214
81. Even-Sapir E, Metser U, Flusser G et al (2004) Assessment of malignant skeletal disease: initial experience with 18F-fluoride PET and 18-fluoride PET/CT. J Nucl Med 45:272–278
82. Afshar-Oromieh A, Zechmann CM, Malcher A et al (2014) Comparison of PET imaging with a (68) Ga-labelled PSMA ligand and (18)F-choline-based PET/CT for the diagnosis of recurrent prostate cancer. Eur J Nucl Med Mol Imaging 41(1):11–20
83. McCrarville B (2006) The role of positron emission tomography in pediatric musculoskeletal oncology. Skeletal Radiol 35:553–554
84. Gerth HU, Juergens KU, Dirksen U et al (2007) Significant benefit of multimodal imaging: PET/CT compared with PEt alone in staging and follow-up of patients with Ewing tumors. J Nucl Med 48:1932–1939
85. Franzius C, Daldrup-Link HE, Sciuk J, Rummeny EJ et al (2001) FDG PET for detection of pulmonary metastases from malignant primary bone tumors: comparison with spiral CT. Ann Oncol 12:479–486
86. Byun BH, Kong CB, Lim I et al (2014) Early response monitoring to neoadjuvant chemotherapy in osteosarcoma using sequential ^{18}F-FDG PET/CT and MRI. Eur J Nucl Med Mol Imaging 41(8):1553–1562
87. Hawkins DS, Schuetze SM, Butrynski JE et al (2005) [18F]Fluorodeoxyglucose positron emission tomography predicts outcome for Ewing sarcoma family of tumors. J Clin Oncol 23(34):8828–8834
88. Bonica JJ (1985) Treatment of cancer pain: current status and future needs. In: Fields HL (ed) Advances in pain research and therapy, vol 9. Raven, New York, pp 589–616
89. Resche I, Chatal JF, Pecking A et al (1997) A dose-controlled study of 153Sm EDTMP in the treatment of patients with painful bone metastases. Eur J Cancer 33:1583–1591
90. Taylor AJ Jr (1994) Strontium-89 for the palliation of bone pain due to metastatic disease. J Nucl Med 35:2054
91. Tong D, Gillick L, Hendrickson FR (1982) The palliation of symptomatic osseous metastases. Final results of the study by Radiation Oncology Group. Cancer 50:893–899
92. McEwan AJ, Porter AT, Venner PM et al (1990) An evaluation of the safety and efficacy of treatment with strontium-89 in patients who have previously received wide field radiotherapy. Antibodies Immunoconj Radiopharm 13:91–98
93. Bodei L, Lam M, Chiesa C et al (2003) EANM procedure guidelines for treatment of refractory metastatic bone pain. Eur J Nucl Med 30:7–11
94. McEwan AJB (2004) Palliation of bone pain. In: Ell PJ, Gambhir SS (eds) Nuclear medicine in clinical diagnosis and treatment, vol 1. Elsevier Limited, Philadelphia, pp 407–422
95. Porter AT, McEwan AJ, Powe JE et al (1993) Results of a randomized phase-III trial to evaluate the efficacy of strontium-89 adjuvant to local field external beam irradiation in the management of endocrine resistant metastatic prostate cancer. Int J Radiat Oncol Biol Phys 25:805–813
96. McEwan AJB (1996) Unsealed source therapy of painful bone metastases: an update. Semin Nucl Med 27:165–182
97. Parker C, Nilsson S, Heinrich D et al (2013) Alpha emitter radium-223 and survival in metastatic prostate cancer. N Engl J Med 369(3):213–223
98. Harbert JC (1996) Radionuclide therapy in joint diseases. In: Harbert JC (ed) Nuclear medicine diagnosis and therapy. Thieme Medical Publishers, New York, pp 1093–1110
99. Schneider P, Farahati J, Reiners C et al (2005) Radiosynovectomy in rheumatology, orthopedics, and hemophilia. J Nucl Med 46(Suppl 1):48S–54S

Part III

Musculoskeletal Tissues and Their Functions

A. Gürsel Leblebicioğlu

Genetic Basis of Orthopedic Diseases

14

Rüştü Nuran, Onur Başçı, and Mustafa Karahan

Abstract

Genetics is a diverse subject concerned with variation and heredity in all living organisms. In clinical practice, the main significance of genetics is in elucidating the role of genetic variation and mutation in the etiology of a large number of disorders.

Genetic basis of orthopedic disorders is very complicated; to have a common idea, the relationship between osteoblast and osteoclast is the key point.

Learning Outcomes

After you have studied this chapter, you will have an understanding of:

1. The genetic disorders involving the skeletal systems
2. The pathogenesis of skeletal disorders on the molecular and genetic basis
3. The classification of skeletal disorders
4. The ongoing process of bone resorption and bone formation
5. Active signaling pathway for osteoblasts and osteoclasts
6. Clinically important orthopedic disorders and the key genes involved

R. Nuran, MD (✉)
Department of Orthopedics, Acibadem Hospital Group, Istanbul, Turkey
e-mail: drrustunuran@gmail.com

O. Başçı, MD
Department of Orthopedics, 9 Eylul University, Izmir, Turkey

M. Karahan, MD
Department of Orthopedics, Acibadem University, Istanbul, Turkey
e-mail: mustafa@karahan.dr.tr; drmustafakarahan@gmail.com

F. Korkusuz (ed.), *Musculoskeletal Research and Basic Science*,
DOI 10.1007/978-3-319-20777-3_14

Terminology

Allele Different forms of a gene found at a particular position on a chromosome.

Autosome Any chromosome other than the sex chromosomes X and Y; 22 pairs in the human karyotype.

Chromosome Rodlike structures that carry the genes, consisting of long strands of DNA in a protein framework. In nondividing cells, they are not individually distinguishable in the nucleus, but at mitosis or meiosis, they become condensed into visible strands that stain deeply with basic stains.

Congenital Present at birth; may or may not have a genetic cause.

Deletion The loss of a segment of DNA from a chromosome. It may be of any length, from a single base to a large part of the chromosome.

Diploid Having two copies of each chromosome; the normal constitution of most human somatic cells.

Dominant A characteristic that is apparent when there is only one copy of the particular gene present, or in the case of a genetic disease when only one copy is altered.

Familial A trait that occurs more often in the relatives of an affected person than in the general population, e.g., diabetes and coronary heart disease.

Gene The unit of inheritance, consisting of a sequence of DNA.

Genome All the genes present on a set of chromosomes.

Genotype The genetic constitution of an individual.

Haploid The normal number of chromosomes present in an egg or sperm. In humans, the haploid number of chromosomes is 23.

Heterozygote An individual having different forms of a gene (allele) at a certain position on a pair of chromosomes.

Homozygote An individual having two identical forms of a gene (allele) at a certain position on a pair of chromosomes.

Hyperostosis Thickening of cortical (compact) bone from deposition of osseous tissue along the subperiosteal and/or endosteal surfaces.

Karyotype The classified chromosome complement of an individual or cell.

Locus The precise location of a gene or DNA marker on a chromosome.

Macrocephaly Enlarged head.

Mendelian disorder Inherited disorder due to a defect in a single gene.

Metaphyseal dysplasia Abnormal bone development between the diaphyses (shaft) and epiphyses of long bones.

Missense mutation A nucleotide substitution that results in an amino acid change.

Multifactorial inheritance Due to the interaction between a number of genes and environmental factors.

Mutation A permanent change or alteration in the structure of DNA.

Nonsense mutation Results in a premature stop codon and truncation of the protein.

Osteosclerosis Increased density of trabecular (spongy) bone.

Pedigree A graphic representation of a person's family, also known as a family tree.

Phenotype The observable or clinical characteristics of an individual.

Polydactyly Excess digits.

Polymorphism The existence of genes at a particular position on a chromosome with an altered DNA sequence, usually non-pathological.

Recessive A characteristic that is only apparent when there are two copies of a particular gene present, one from each parent.

Single gene disorder A disease whose inheritance is controlled by one pair of genes (one on each homologous chromosome).

Somatic cell Any cell in the body except the eggs or sperm.

Somatic mutation A gene fault that occurs after fertilization and is found only in cells that are derived from the originally mutated cell.

Syndactyly Fusions of the digits (fingers or toes).

Syndrome A collection of physical findings that occur together frequently enough to be recognized as a distinct clinical entity.

Clinical Relevance

What is the exact influence of genetic differences in fractures related with osteoporosis? (Figure 14.1)

A 65-year-old female patient, who has a 68-year-old sister operated because of a femoral neck fracture due to osteoporosis, approached the outpatient clinic for bone mass density tests and asking if she is genetically prone to fracture due to osteoporosis because of her sister.

What we have in our hands about the genetic basis of osteoporosis is very limited, involving many functional variants [20]. This is similar for other complex human diseases representing serious health problems like diabetes and obesity. Recent advances in next-generation sequencing technologies have greatly enhanced our ability to discover functional rare variants. But on the other hand; these technologies are very expensive to be applied for whole population [21].

It is estimated that osteoporosis affects more than 75 % of women 70 years of age. Fractures related to osteoporosis result in significant morbidity and increased mortality. It is generally classified as primary or secondary (due to endocrine dysfunction, medications, and inflammatory disorders).

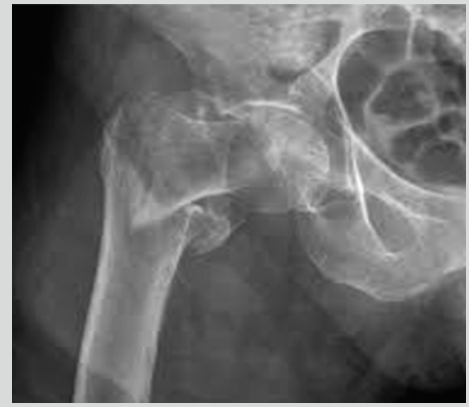

Fig. 14.1 X-ray of a 68-year-old female patient. Right hip fracture due to severe osteoporosis

According to bone mass density, genetic variations are estimated to be more than 70 % to cause such differences [22]. And according to the femoral neck geometry and bone turnover, these variations are between 50 and 80 % [23]. Besides, the heritability of fracture itself is relatively low, close to 25 % due to fall-related factors such as vision, balance, and strength [24].

Genetic disorders involving the skeletal system with their great variety in number occur due to any kind of mutation in skeletal development.

The recent years have witnessed major advances in our understanding of the genetic basis for many skeletal disorders. By means of technological improvement, the responsible gene for each disorder has been mapped, and the exact locus has been defined, the mutations clearly shown, and the functional significance of mutations determined; these are all important steps to clarify the molecular basis for pathogenesis.

In this chapter, we focus on our current understanding of the genetic basis and pathogenic mechanisms for disorders of bone homeostasis.

For researchers who are interested in genetics, Online Mendelian Inheritance in Man (http://www.ncbi.nlm.nih.gov/omim) and the human genome database are important and serve as a database.

From these databases, we have a long list of genes involved in skeletal disorders (Table 14.1).

Classification of Genetic Diseases

Almost all disorders occur as a result of multifactorial reasons or the interaction between the environment and genes; the relative role of genetics could be small or large mainly depending on the outcome of mutation.

Disorders in which genetic factors play a major role, partially or completely, are divided into four main groups.

Table 14.1 Name of the genes and their function with the skeletal disorders involved

Gene	Disease	Gene function
ARSE	Chondrodysplasia punctate	Unknown
ANKH	Premature osteoarthrosis with chondrocalcinosis	Transport molecule
Cathepsin K	Pyncodysostosis	
CBFA1	Cleidocranial dysplasia	Transcription molecule
C7orf2	Preaxial polydactyly	Signaling molecule
COL1A1, *COL1A2*	Osteogenesis imperfecta I–IV	Structural molecule
COL2A1	Achondrogenesis II	Structural molecule
	Hypochondrogenesis	
	Kniest dysplasia	
	Spondyloepiphyseal dysplasia congenital	
	Stickler's syndrome 1	
COL9A2	Multiple epiphyseal dysplasias	Structural molecule
COL10A1	Schmid metaphyseal chondrodysplasia	Structural molecule
COMP	Multiple epiphyseal dysplasias	Structural molecule
	Pseudoachondroplasia	
DTDST	Diastrophic *dysplasia*	Transport molecule
	Ehlers-Danlos syndrome (autosomal recessive)	
	Achondrogenesis 1 B	
	Atelosteogenesis II	
EBP	Chondrodysplasia punctate, x-linked type 2	Signaling pathway molecule
EVC	Ellis-van Creveld syndrome	Unknown
FBLN1	Complex synpolydactyly (one form)	Structural molecule
FGFR3	Achondroplasia	Cell-signaling molecule
	Hypochondroplasia	
	Thanatophoric dysplasias I–II	
FGFR2	Apert syndrome	Cell-signaling molecule
	Crouzon syndrome	
	Pfeiffer syndrome (most)	
FGFR1	Pfeiffer syndrome (some)	Cell-signaling molecule
GLI3	Greig cephalopolysyndactyly	Transcription factor
	Pallister-Hall syndrome	
	Postaxial polydactyly type A/B	
HOXA13	Hand-foot-genital syndrome	Transcription factor
HOXD13	Synpolydactyly	Transcription factor
	Brachydactyly D/E and A1	
LMX1B	Nail-patella syndrome	Transcription factor
MATN3	Ehlers-Danlos syndrome (autosomal dominant)	Structural molecule
	Hand osteoarthrosis	
MSX2	Boston-type craniosynostosis	Transcription factor
OFD1	Oral-facial-digital type I syndrome	Unknown
P63	Split hand/split foot	Cell-signaling protein
	Ectrodactyly-ectodermal dysplasia	
	ADULT syndrome	
PEX7	Chondrodysplasia punctate type I	Transcription factor

Table 14.1 (continued)

Gene	Disease	Gene function
PTH	Jansen's metaphyseal chondrodysplasia	Cell-signaling factor
ROR2	Brachydactyly type B	Cell-signaling factor
	Robinow syndrome	
SALL1	Townes-Brocks syndrome	Transcription factor
SEDL	X-linked spondyloepiphyseal dysplasia	Transport molecule
SHOX	Leri-Weill dyschondrosteosis	Transcription factor
	Idiopathic short stature (some)	
	Langer mesomelic dysplasia	
	Turner syndrome (part of)	
SOST	Bone dysplasia sclerosteosis	Unknown
SOX9	Campomelic dysplasia	Transcription factor
TBX3	Ulnar-mammary syndrome	Transcription factor
TBX5	Holt-Oram syndrome	Transcription factor
TGFB1	Camurati-Engelmann disease	Signaling molecule
TWIST	Saethre-Chotzen syndrome	Signaling molecule
WISP3	Spondyloepimetaphyseal dysplasia with progressive osteoarthropathy	Unknown

(a) *Single gene disorders*
Single gene disorders occur as a result of mutation in a single gene. They have a distinctive and characteristic pedigree. Many of these disorders are very rare; but as a group, they are responsible of a significant portion of morbidity and mortality in neonatal period. The incidence of serious single gene disorders in a study conducted in more than a million live births in the pediatric age group is 0.36 % and 6–8 % in hospitalized children involved [2, 9, 13].

(b) *Chromosomal disorders*
The main problem is an extra or a missing chromosome in the genomic structure. For example, although there is no pathology in genes of chromosome, an extra chromosome 21 causes Down's syndrome. The incidence of chromosomal disorders is 7:1,000 of live births and is responsible for half of the abortions in the first trimester [2, 9].

(c) *Multifactorial diseases*
Multifactorial diseases are responsible for great variety of congenital malformations. Disorders result from a combination of mutations in the gene, which in total lead to a serious error, and with the influence of environmental factors, the patient becomes prone to disorder. Multifactorial diseases affect 5 % of children in the entire population and 60 % of the entire population [2, 9, 13].

(d) *Mitochondrial diseases*
Mitochondrial DNA (mtDNA) is a circular DNA molecule, which is located in the mitochondria instead of the cell nucleus. All mitochondria in the zygote come from ovum not from sperm, so mutations in mtDNA will affect all children of that mother [9, 13].

Because of their great variety, the main challenge is to classify these disorders.

The Nosology and Classification of Genetic Skeletal Disorders is an important issue especially for naming the disorder correctly and for classifying them according to clinical, radiological, and also molecular pathways. According to molecular, biochemical, and radiographic criteria, at the end, 40 groups including 456 conditions were defined [17].

With the help of further revisions, the groups 1–8 were classified based on the underlying gene causing the disorder or affecting the pathway of molecular events.

Groups 9–17 were listed according to the specific localization of the disorder in the bone segment (epi-, meta-, or diaphysis). In groups 18–20, clinical features of the disorders were important:

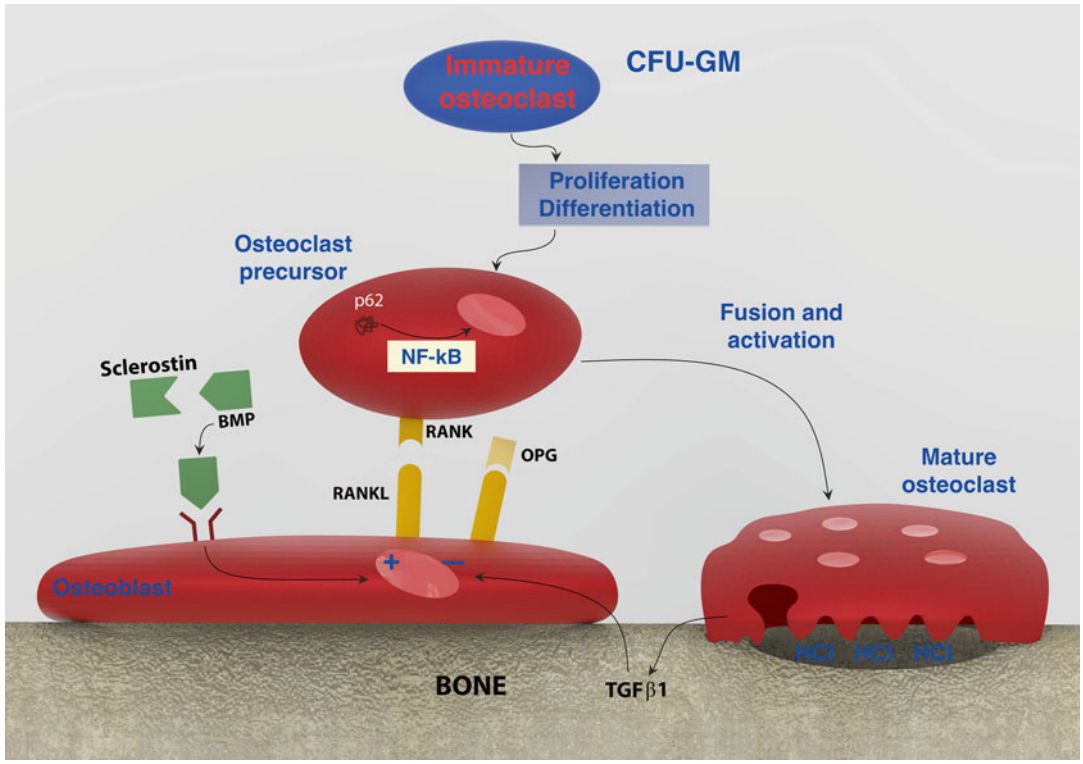

Fig. 14.2 Bone homeostasis: life cycle of osteoclast and the affect of osteoblast. The earliest osteoblast precursor is granulocyte-macrophage colony forming unit (CFU-GM); these cells proliferate and differentiate; after that they fuse to form multinucleated osteoclasts and finally activated to form bone-resorbing osteoclasts. NF-κB is an important transcription factor involved in osteoclast differentiation; this transcription factor plays a critical role in the expression of different cytokines which are important in differentiation process, IL-1, TNF-α, IL-6, and RANK ligand. RANKL produced by osteoblasts is important for osteoclast formation. RANKL also binds to osteoprotegerin (OPG) which is a member of TNF receptor family that inhibits osteoclast formation and bone resorption. Mutations in gene p62(sequestosome-1) or OPG (osteoprotegerin) have been associated with diseases of aberrant bone formation. Mutations in gene sclerostin have been associated with high bone mass

macroscopic appearance of the bones or the type of deformities involved. Groups 21–25 and group 28 were based on bone mineralization, whereas group 27 includes lysosomal disorders with skeletal manifestations, and group 29 includes disorders like exostoses and enchondromas and also known as "disorganized development of skeletal components." Group 30 is known as "overgrowth syndromes," whereas we have mainly inflammatory arthropathies in group 31. Groups 32–40 include disorders of embryonic development such as hypoplasia and dysostoses [17].

On the other side, for a different classification methodology, bone resorption and bone formation are two basic functional processes in developing skeleton. Osteoblasts and osteoclasts are two main cell types responsible for bone formation and bone resorption processes. And this classification method is based on the interactions between basic precursor cells of the bone, osteoblast and osteoclast. They maintain the balance between bone resorption and bone formation.

Osteoblasts, originated from mesenchymal precursors, work under the influence of many factors especially parathyroid hormone (PTH), vitamin D, and bone morphogenetic proteins (BMPs) which are one of the well known. Osteoblasts synthesize and secret bone matrix and also control osteoclast (Fig. 14.2).

Table 14.2 Bone formation and resorption are continuous processes; bone mass continues to increase during childhood; at its maximum level at third decade of life, after that there is a decline

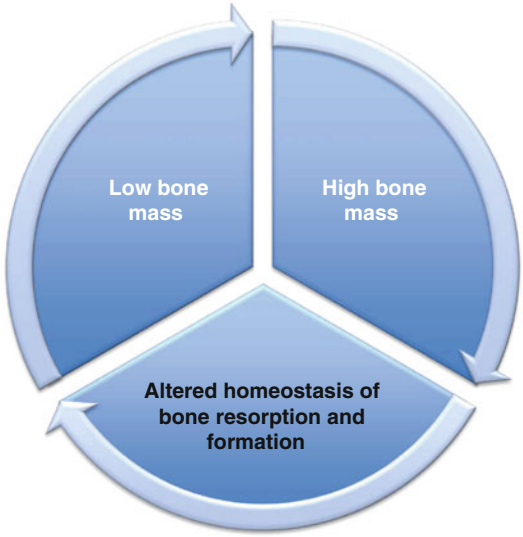

These processes are controlled by osteoblasts and osteoclasts, and there is a complex signaling pathway between these two. Any kind of interference to these processes will result in skeletal disorders either by causing low or high bone mass

Osteoclasts, originated from monocyte lineage, are important for bone demineralization. Proper regulation of osteoclasts and osteoblasts is critical for balance between bone formation and bone resorption. Because of genetic disorders, this balance is affected, causing low bone mass (osteoporosis), high bone mass (osteopetrosis), or altered bone homeostasis (Table 14.2) [4].

Low Bone Mass

Osteoporosis

Osteoporosis is one of the most common diseases of the bone and is characterized mainly by low bone mineral density (BMD), change of bone structure, and increased fracture risk. Osteoporosis creates serious social problems affecting wide range of population.

Vitamin D receptor (VDR) gene, because of its role in calcium metabolism and osteoblast cell function, is one of the first candidate genes [5]. LRP5, known as low-density lipoprotein (LDL) receptor-related protein 5, is a co-receptor for Wnt signaling and is important for osteoblastic processes. Mutations in LRP5 are responsible for autosomal recessive type of osteoporosis [11]. LRP5 is a co-receptor for Wnt; mutations will result in inactivation of osteoblast production leading to osteoporosis [8].

Despite all genetic information, identification of the key gene causing osteoporosis is still a big mystery. In addition to genetic factors, environmental factors still play a big role in osteoporosis.

High Bone Mass

Osteopetrosis is a result of decreased resorption and increased formation of the bone.

Decreased Bone Resorption

Autosomal Recessive Osteopetrosis

In autosomal recessive Albers-Schonberg disease or "marble" bone disease, bony deformities, macrocephaly, progressive hearing and vision loss, hepatosplenomegaly, and severe anemia are characteristic features of this disorder. The key gene is known to be TCIRG1/ATP6i, encoding a regulatory subunit of the H^+- ATPase pump, which results impaired bone demineralization [6].

Autosomal Dominant Osteopetrosis

Autosomal dominant Albers-Schonberg disease is clinically less severe than the autosomal recessive form. Classified in two types: type I is with cranial sclerosis and facial paralysis, and in this group, fractures and osteomyelitis of the mandible are common. In type II, in addition to sclerosis which is more common at the base, there is vertebrae end plate thickening causing "sandwich" appearance. The "bone within a bone" appearance is typical for osteopetroses. The key gene is ClCN7 with a locus at chromosome 16p13.3, important for the Cl^- channels located between osteoclast and bone junction [1, 3].

Increased Bone Formation

Van Buchem's Disease and Sclerosteosis

The onset is generally at puberty with osteosclerosis of the skull, mandible, and clavicle. Due to

osteosclerosis, optic atrophy and deafness are characteristic. Locus at the chromosome 17q12-q21 is the key area, and the name of the gene is sclerostin (SOST); due to mutations, the expression of sclerostin is suppressed [16].

Craniometaphyseal Dysplasia

The "Erlenmeyer flask" appearance due to widened metaphyses is characteristic. This disorder is usually autosomal dominant; hyperostosis of cranial bones will cause compression of cranial nerves which will lead to facial nerve palsy and hearing problems. The key gene is ANKH, encoding a transmembrane protein of osteoblasts important in inorganic pyrophosphate transport [12, 15].

Altered Homeostasis of Bone Formation and Resorption

Paget's Disease

Paget's disease is one of the most common chronic skeletal disorders affecting almost 3 % of mainly white population over 60 years of age. The disease is characterized by focal areas of increased bone resorption and formation mainly in the pelvis, spine, femur, skull, and tibia.

The genetic transmission of Paget's disease could be autosomal dominant or autosomal recessive. With whole genomic screening, a variety of susceptible loci on chromosomes are detected, and the most common ones are on chromosome 18q21-q22 (PDB2) and 5q35-qter (PDB3) [7, 10].

In addition to genetic background with the latest evidences, there is also a viral etiology for Paget's disease due to osteoclasts having nuclear and cytoplasmic inclusions like in paramyxovirus nucleocapsids [14].

Familial expansile osteolysis, although histologically similar to Paget's disease, generally starts at the second decade and known to be more severe, and the bones involved are more peripheral; early onset of deafness and loss of dentition are characteristic features for this disorder. The key gene is TNFRSF11A, encoding RANK. As a result, RANK will accumulate intracellularly and will lead to increased NF-κB activation [18].

Juvenile Paget's disease, also known as hereditary hyperphosphatasia, is an autosomal recessive disease affecting infants and children causing pain and bony deformities. There is ongoing bone turnover process, so the structure of the bones is weak and disorganized with increased fracture risk. Histologically, the number of osteoclast and osteoblast are both increased, and serum alkaline levels also increase (hyperphosphatasia). Genetically, the key gene is the TNFSFR11B gene which is located on chromosome 8q24, encoding osteoprotegerin, a receptor for RANKL [19]. As a result; osteoclast activation and bone resorption are both suppressed.

References

1. Benichou O, Cleiren E, Gram J (2001) Mapping of autosomal dominant osteopetrosis type II (Albers-Schonberg disease) to chromosome 16p13.3. Am J Hum Genet 69:647–654
2. Childs B (1982) Genetics in the medical curriculum. Am J Med Genet 13:319–324
3. Cleiren E, Benichou O, Van Hul E (2001) Albers-Schonberg disease (autosomal dominant osteopetrosis, type II) results from mutations in the ClCN7 chloride channel gene. Hum Mol Genet 10:2861–2867
4. Colbert RA (2007) Skeletal disorders. Genes and common diseases. Genetics in modern medicine by Alan Wright and Nicholas Hastie. Cambridge University Press, Cambridge, UK
5. Cooper GS, Umbach DM (1996) Are vitamin D receptor polymorphism associated with bone mineral density? A meta-analysis. J Bone Miner Res 11:1841–1849
6. Frattini A, Orchard PJ, Sobacchi C (2000) Defects in TCIRG1 subunit of the vacuolar proton pump are responsible for a subset of human autosomal recessive osteopetrosis. Nat Genet 25:343–346
7. Hocking LJ, Herbert CA, Nicholls RK (2001) Genome wide search in familial Paget disease of bone shows evidence of genetic heterogeneity which candidate loci on chromosome 2q36, 10p13 and 5q35. Am J Hum Genet 69:1055–1061
8. Kato M, Patel MS, Levasseur R (2002) Cbfa1-independent decrease in osteoblast proliferation, osteopenia, and persistent embryonic eye vascularization in mice deficient in Lrp5, a Wnt receptor. J Cell Biol 157:303–314
9. King RA, Rotter JI, Motulsky AG (1992) The genetic basis of common diseases. Oxford University Press, Oxford

10. Laurin N, Brown JP, Lemainque A (2002) Recurrent mutation of the gene encoding sequestosome 1 in Paget disease of bone. Am J Hum Genet 70:1582–1588
11. Mizuguchi T, Furuta I, Watanabe Y (2004) LRP5, low-density-lipoprotein-receptor related protein 5, is a determinant for bone mineral density. J Hum Genet 49:80–86
12. Nurnberg P, Thiele H, Chandler D (2001) Heterozygous mutations in ANKH, the human ortholog of the mouse progressive ankylosis gene, result in craniometaphyseal dysplasia. Nat Genet 28:37–41
13. Nussbaum R, McInnes R, Willard H (2001) Thompson & Thopmson Genetics in medicine, 6th edn. Saunders, USA, 1–3
14. Reddy SV, Kurihara N, Menaa C, Roodman GD (2001) Paget's disease of bone: a disease of the osteoclast. Rev Endocr Metab Disord 2:195–201
15. Reichenberger E, Tiziani V, Watanabe S (2001) Autosomal dominant craniometaphyseal dysplasia is caused by mutations in the transmembrane protein ANK. Am J Hum Genet 68:1321–1326
16. Van Hul W, Balemans W, Van Hul E (1998) Van Buchem disease (hyperostosis corticalis generalisata) maps to chromosome 17q12-q21. Am J Hum Genet 62:391–399
17. Warman ML, Cormier-daire V, Hall C, Krakow D, Lachman R (2011) Nosology and classification of genetic skeletal disorders. Am J Med Gen A 155(5): 943–968, Revision
18. Whyte MP, Mills BG, Reinus WR (2000) Expansile skeletal hyperphosphatasia: a new familial metabolic bone disease. J Bone Miner Res 15:2330–2344
19. Whyte MP, Obrecht SE, Finnegan PM (2002) Osteoprotegerin deficiency and juvenile Paget's disease. N Engl J Med 347:175–184
20. Bodmer W, Bonilla C (2008) Common and rare variants in multifactorial susceptibility to common diseases. Nat Genet 40:695–701
21. Cirulli ET, Goldstein DB (2010) Uncovering the roles of rare variants in common disease through whole-genome sequencing. Nat Rev Genet 11:415–425
22. Ralston SH (2003) Genetic determinants of susceptibility to osteoporosis. Curr Opin Pharmacol 3: 286–290
23. Arden NK, Baker J, Hogg C, Baan K, Spector TD (1996) The heritability of bone mineral density, ultrasound of the calcaneus and hip axis length: a study of postmenopausal twins. J Bone Miner Res 11:530–534
24. Calbert R (2007) Skeletal disorders. Genes and common diseases. In: Wright A, Hastie N (eds) Oral herbal therapies for treating osteoarthritis. The Cochrane Collaboration, Cambridge University Press, Cambridge, UK, pp 406–426

Stem Cell Therapy and Orthopedics

15

Sevil Köse, Duygu Uçkan Çetinkaya, Gaurav Sharma, Tae Kyun Kim, Petek Korkusuz, and Feza Korkusuz

Abstract

Stem cells obtained from various sources in the body and during different stages of development form the basis of cellular therapy and are often studied in the field of orthopedic regenerative medicine. Parameters such as potential, source, route of administration, and desired dose of stem cells to be used should be selected according to the type of regeneration, and research and application should be conducted with this in mind. This chapter details the general characteristics of stem cells, sources of stem cells, and the advantages and disadvantages of the various sources of stem cells. Detailed specifications of adult stem cells in the group of mesenchymal stem cells, which have more advantages in the field of orthopedics than other stem cells, are provided. Briefly, induced pluripotent stem cells and tissue engineering studies are discussed and examples of orthopedic studies with stem cells are provided.

S. Köse, MS • D.U. Çetinkaya, MD, PhD
Hacettepe University Medical Faculty,
Stem Cell Research and Application Center,
Sihhiye, Ankara 06100, Turkey
e-mail: sevilarslan@hotmail.com;
duyguc2008@gmail.com

G. Sharma, MD
International Research Fellow, Knee Surgery & Sports Medicine, Seoul National University Bundang Hospital, Korea
e-mail: sharmagaurav850@gmail.com

T.K. Kim, MD, PhD
Professor, Department of Orthopaedic Surgery, Seoul National University College of Medicine, Seoul, Korea

Director, Knee Surgery & Sports Medicine, Seoul National University Bundang Hospital, Korea
e-mail: osktk2000@yahoo.com

P. Korkusuz, MD, PhD (✉)
Department of Histology and Embryology, Hacettepe University Medical Faculty, Sihhiye, Ankara 06100, Turkey
e-mail: petek@hacettepe.edu.tr

F. Korkusuz, MD, PhD
Department of Sports Medicine, Hacettepe University Medical Faculty, Sihhiye, Ankara 06100, Turkey
e-mail: feza.korkusuz@gmail.com

F. Korkusuz (ed.), *Musculoskeletal Research and Basic Science*,
DOI 10.1007/978-3-319-20777-3_15

Definitions

Stem cells: Undifferentiated cells that can differentiate into specialized cells and divide to produce more stem cells.

Totipotent stem cells: Cells that can differentiate into embryonic and extraembryonic cell types.

Pluripotent stem cells: Cells that can differentiate into all cells of an embryo, that is, cells derived from any of the three germ layers.

Multipotent stem cells: Cells that can differentiate into a number of cell types, but only those of a closely related family of cells.

Unipotent stem cells: Cells that have the property of self-renewal but can produce only one cell type, their own.

Induced pluripotent stem cells: Adult cells reprogrammed with different techniques to give rise to pluripotent capabilities.

Self-renewal: Process by which stem cells divide to make more stem cells, perpetuating the stem cell pool throughout life.

Stemness: All of the essential characteristics of a stem cell, such as self-renewal and differentiation, that distinguish it from ordinary cells.

Quiescence: Reversible growth/proliferation arrest, thought to represent a homogenous state induced by diverse anti-mitogenic signals, allowing stem cells to protect their pools in the body.

Tissue engineering: A scientific branch involving combined use of cells, engineering and materials methods, and suitable biochemical and physicochemical factors to improve or replace biological functions.

Introduction

Bone regeneration is a major concern in orthopedic, trauma, spine and maxillofacial surgery. Current treatment options such as bone grafts and protein-based therapies do not provide a satisfactory solution for large bone defects. In recent years, stem cell-based therapies for the repair of massive bone loss have emerged as an alternative to existing solutions. Different potential stem cells from various sources are being studied for this purpose. The use of tissue-specific adult stem cells with the aim of bone regeneration offers many advantages. Mesenchymal stem cells (MSCs) have emerged as the most interesting cell type.

Features such as migration to damaged areas, angiogenesis support, fibrosis obstructions, and anti-inflammatory and restorative cytokine and chemokine secretions, including connective tissue cell (especially fat, bone, and cartilage) differentiation of MSCs, ensure that the stem cells' contribution is important in the regeneration process. These stem cells, which are multipotent, can be isolated from many locations, such as dental pulp, bone marrow, fat and muscle tissue, umbilical cord, and placenta. Because of their minimal count in tissues, they should be replicated in vitro. They can be used directly or differentiated into the desired cell type. Tissue scaffolds and soluble factors that affect the biological properties of the carrier system can be used in the form of combination therapy. In addition, it is possible to regenerate bone or cartilage to ensure efficient transcription of genes in vivo by genetic engineering practice and rapid bone formation and fracture repair. Thus, obtained stem cells with both autocrine effects and paracrine effects on host damaged stem cells can provide multiple dimensional regenerations.

The development of tissue engineering applications has made stem cell therapy more effective. Biomaterials keep cells in damaged areas and protect from scar tissue and host inflammation. Thus, the therapeutic potential of stem cells is made possible. In this review, sources of stem cells, their therapeutic potential, orthopedic stem cell therapy, and tissue engineering issues are summarized.

Stem Cells

Stem cells renew themselves and are capable of differentiating into specific cells. They have typical capacities according to obtained tissues and their potential. According to the potential stem

cells, totipotent stem cells can differentiate into embryonic and nonembryonic cells (16-cell embryo); pluripotent stem cells can differentiate into all cell types found in tissues belonging to the three germ layers (e.g., inner cell mass derived from embryonic stem cells); multipotent stem cells can differentiate into all cell types that belong to the origin of their germ (e.g., MSCs can differ mesoderm-derived cells (bone, cartilage, fat)); and unipotent (nullipotent) stem cells can form only a single cell type (e.g., oogonia is generated by oocyte cells) [1].

Another feature of stem cells, remaining silent (quiescence), prevents depletion of adult stem cells in tissues. In case of damage, stem cells in this quiet state are activated *via* symmetric or asymmetric division and differentiated tissue-specific cell regeneration is achieved. Isolated and cultured stem cells have the tendency to create clones (clonogenicity). Formed by a single cell, clones that include undifferentiated stem cells are proof of the self-renewal property [2].

Migration is one of the features that contributes to the regenerative potential of stem cells. With this feature, the stem cells migrate to the damaged microenvironment and contribute to repair. Migration of stem cells between different microenvironments is a critical factor in the determination of their self-renewal and differentiation features [2] (Fig. 15.1).

Stem Cells According to Sources and Potentials

Embryonic Stem Cells (ESCs)

Embryonic stem cells (ESCs): Each cell of the blastocysts (inner cell mass) formed on day 5 after formation of the zygote is called an ESC. These cells are pluripotent and differentiate into all cells of the body. In addition, they have the advantage of the ability to expand and differentiate in vitro and can also be genetically modified. However, the clinical use of ESCs is hindered on a large scale because of high risk of developing cancer, and there are ethical and legal problems associated with the use of human embryonic stem cells [3].

In vitro studies with embryonic stem cells have been especially concerned with spinal cord injuries. Embryoid bodies were developed from ESCs and neuronal progenitor cells were then obtained with a protocol developed by David Gottlieb, PhD, of Washington University (St. Louis, MO, USA) [4]. Retinoic acid treatments resulted in nestin-positive neural progenitor cells that could be differentiated into neurons, astrocytes, and oligodendrocyte cells [5]. Obtained neural progenitors were marked and injected directly into the injured spinal cords of rats. Two weeks after transplantation oligodendrocyte, astrocyte, and neuron differentiations were observed. In addition, a better Basso, Beattie,

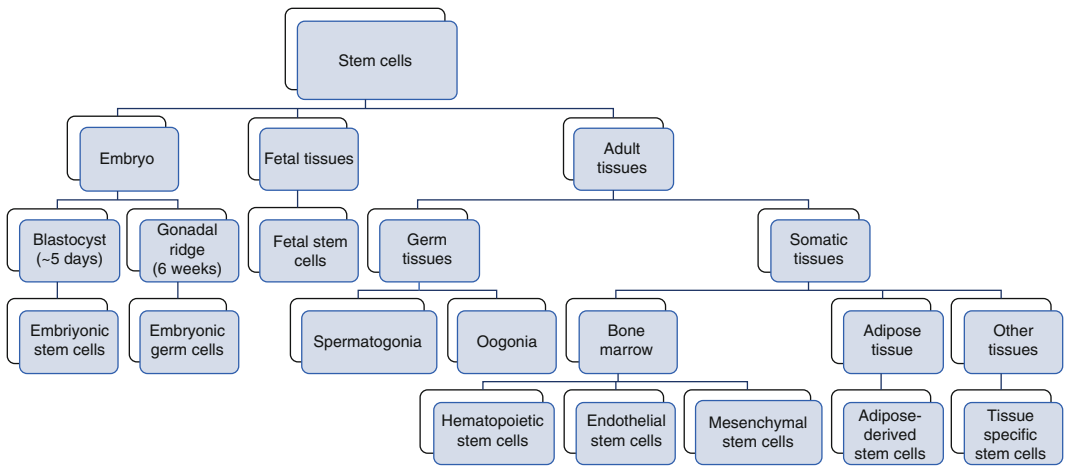

Fig. 15.1 Stem cells according to sources

Bresnahan (BBB) locomotor rating scale scoring was obtained in transplanted animals.

Despite the positive results of animal experiments with ESCs, the risk of forming tumors, immunological responses, use of short-lived experimental animals, and unavailability of human ESCs make clinical use of these cells impossible today.

Fetal Stem Cells (FSCs)

Fetal stem cells (FSCs) are obtained aborted fetuses, aged 5 to 9 weeks. These cells are pluripotent/multipotent and have self-renewal features. Because of these properties, they are an alternative to ESCs. Clinical use is limited, however, because of the risk of tumor formation. Appropriate sources of fetal tissue include donations following spontaneous abortion, but there are ethical issues that must be considered [6] (Fig. 15.2).

Adult Stem Cells (ASCs)

MSCs

General Characteristics of MSCs

General Characteristics of MSCs: MSCs, especially connective tissue-derived cells (bone, cartilage, fat, tendon, stroma), differentiate into many tissue cells (heart, liver, pancreas, nervous system cells) and/or synthesize soluble factors that contribute to tissue/organ regeneration. MSCs expand in vitro by protecting their stem cell properties and support hematopoiesis; when they are transplanted they are not rejected by immunosuppressive properties. Thus, these cells have possible applications in many clinical areas [7].

MSCs are the main cells of connective tissue. These cells were first identified in 1976 by Friedenstein [8], who, using fetal calf serum, showed that cell colonies are adhesive and morphologically resemble fibroblasts in bone marrow culture. These cells can differentiate into bone, fat, and cartilage cells. Previously, these cells were called colony-forming unit fibroblasts (CFU-F) and bone marrow stromal fibroblasts, but they are now known as mesenchymal stem/stromal cells.

Bone marrow, one of the richest sources of stem cells in organisms, hosts hematopoietic, endothelial, and mesenchymal stem/progenitor cells originating from the mesoderm [9]. Different studies indicate that an average of 2 to 100 MSCs have been identified in the 1×10^6 mononuclear cells (MNCs) in bone marrow aspiration. MSCs can be isolated from many tissues other than bone marrow. Enzymatic methods are used for the isolation of MSCs in solid tissues. MSCs can be isolated and expanded because of the adhesion properties from bone/periosteum, muscle tissue, dental pulp and maxillofacial tissues, liver,

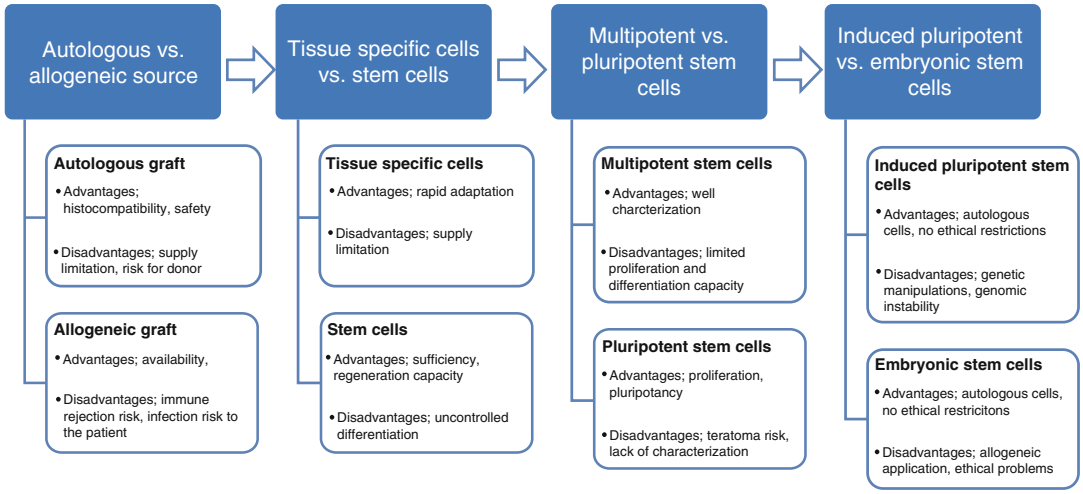

Fig. 15.2 Cell sources for tissue engineering: advantages and disadvantages

lipoaspiration materials, umbilical cord blood, cord stroma, placenta, amniotic fluid, and synovial fluid, and even stimulation through the peripheral blood. They have many properties such as adherence to plastic tissue culture dishes, showing fibroblastoid morphology, differentiation, and surface markers, and these features are independent of the tissues they were obtained from. These properties are substantially similar, but the differentiation capacity and functional characteristics may show some changes according to origin of tissue type [10].

Molecular Surface Properties of MSCs

In cultures with a heterogeneous cell population, MSCs can be distinguished from other cells by their cell surface molecules, which are different from other hematopoietic stem cells (HSC) and/or tissue-specific antigens. In contrast, being involved in adhesion, cell-cell and cell-extracellular matrix are known to be expressed high. However, a specific antigen has not been described for MSCs [11].

Molecular cell surface properties of bone marrow-derived and cultured MSCs have been studied in detail by flow cytometry. According to this technique, the hematopoietic antigen (e.g., CD45, CD34, CD14, CD11b, HLA class II, CD79α, CD19) positivity rate must not exceed 2 % in the cell population. However, stroma-associated antigens (CD73, CD90, CD29, CD44) must be positive.

According to the International Society for Cellular Therapy (ISCT) criteria, for the antigens CD105 (endoglin), CD73 (ecto-5′-nucleotidase), and CD90 (Thy-1), more than 90 % must be positive in an MSC population [10].

Secretory and Immunomodulatory Properties of MSCs

MSCs, which are found in various tissues as support cells, synthesize a large number of bioactive molecules, cytokines, chemokines, enzymes, and extracellular matrix proteins in relation to these features. MSCs release growth factors required for hematopoietic cells in bone marrow such as macrophage colony-stimulating factor (M-CSF), Flt-ligand, and stem cell factor (SCF). Furthermore, not only interleukin-6 (IL-6), IL-7, IL-8, IL-11, IL-12, IL-14, and IL-15 cytokines but also MSCs synthesize chemokines, including stromal-derived factor-1alpha (SDF-1alpha)/CXCL12 and monocyte chemoattractant protein (MCP)-1 [12].

MSCs transplanted into the injured area of the spinal cord have been shown to reduce apoptosis in neuronal cells [13]. Other studies have shown that neurotrophins such as brain-derived neurotrophic factor (BDNF) and nerve growth factor-β (NGF-β) are released by the MSCs that increase the life of the neuronal cells [14–16]. In addition, in vitro cocultures obtained from 25 different bone marrow MSCs and neuronal stem cells obtained from the cerebral cortex of mice showed that increased survival and migration properties have been observed for neuronal cells [17].

One of the most advantageous in vivo applications of MSCs is that immunogenicity of these cells is low and has inhibitory properties on the immune system. Besides these immune-regulating properties, they exert anti-inflammatory effects. They also prevent alloreactive T-cell activation and further reactions, inhibit activated B lymphocytes, and stimulate regulatory T cells. Thus, an immunosuppressive effect was shown resulting from the inhibiting lymphocyte proliferation in animals and humans. A dose-dependent stimulating effect probability is shown on the immune system in some circumstances [18]. In addition, the immunomodulatory effects of MSCs, antiapoptotic factors, and angiogenic and antifibrotic properties are also available. These features help explain their role in wound healing [19]. MSCs also prevent scar tissue formation with their antifibrotic property in spinal cord injury and inhibit the axonal regeneration [19].

Differentiation Potential of MSCs

The most interesting feature of MSCs, especially for applications in regenerative medicine, is the potential to differentiate into a variety of cell types in appropriate microenvironments, including connective tissue. Several researchers have stimulated in vitro osteogenic, adipogenic, chondrogenic, and myogenic differentiation with appropriate signals and demonstrated generated hematopoietic stroma. In the field of regenerative medicine, "stem cell plasticity" is the ability of a cell to differentiate into tissues other than that from which it originated [10]. Myoblast cell [20] and hepatic [21], cardiac [22], renal [23], and neu-

ral cell [24] differentiations have been shown in the studies with bone marrow-derived stem cells.

MSCs migrate to sites of inflammation in the body and differentiate to damaged cells and are helpful in healing wounds. The same property is realized for transplanted MSCs in the damaged area. Rat bone marrow stromal cells transplanted to spinal cord injury patients differentiated into neurons [25] and astrocytes [26], and functional improvement was documented based on BBB behavioral rating scoring [27].

Contribution of MSCs to Repair Damaged Tissue

Effective mechanisms of MSCs for improvement in damage, differentiation to mature functional cells, cell function recovery after damaged cell-MSC fusion, cell-cell and cell-extracellular matrix relationship with MSCs, release of the soluble factors (growth factors, cytokines, chemokines, etc.), paracrine factors, and the enzyme or immunomodulatory, anti-inflammatory, anti-apoptotic, and angiogenic effects can be considered [28].

Migration is required of MSCs from their niche into the damaged tissues. The signal for migration of cells has been shown to come from the damaged tissue microenvironments. Soluble factors like SDF-1/CXCL12, MCP-1, and complement C3 fraction released in the damaged area are known to have important roles in migration [29].

In spinal cord injury, a major problem is damage to cells forming the layer of myelin (oligodendrocytes and Schwann cells) and the transmission of pulses in the myelin sheath surrounding axons [30]. In studies, MSCs have been shown to prevent myelin loss and to promote myelination in spinal cord injury. Akiyama et al. [31] showed that bone marrow stromal cells differentiate into cells that express myelin and a myelin layer reformed around demyelinated axons [31]. In this study, the pulse transmission rate of the demyelinated axons was increased compared with the control group, as determined by in vitro electrophysiological methods. These results were supported in other studies carried out by Akiyama. Bone marrow-derived stromal cells differentiated especially into Schwann cells have been proven in another study [32].

Tracking of MSCs in Tissue

Clinical benefits were obtained with MSC infusion or tissue implantation in in vivo applications, but the fate of these cells after infusion, migration to damaged tissue and placement or accumulation in that area, proliferation, and differentiation features have not been studied in detail. In most studies, after cell infusion, difficulties are encountered in determining the presence of cells in tissue or blood.

Demonstration of different sex cells of the donor or use of species-specific markers (e.g., beta-2-microglobulin for human cells in animal tissues) are among the methods applied for the purpose of tracking MSCs in tissue. Tagging cells with fluorescent dye is one of the easiest methods of tissue tracking [33]. Temporary fluorescent markers such as CFSE, DiL, and DiO can also be used for short-term experimental studies [34]. Genetic marking with green fluorescent protein (GFP) is the preferred method because it is permanent. *In vivo* tracking of luciferase-labeled MSCs with a bioluminescence device and labeling with superparamagnetic iron oxide nanoparticles and imaging in vivo under magnetic resonance are other commonly used methods [35].

Advantages of Clinical Use of MSCs

The advantages of MSCs in clinical practice are as follows:

- Because of differentiation of connective tissue stromal cells, MSCs provide support related to the development and function of tissue cells.
- With their differentiation capacities, MSCs can become mesenchymal tissue cells such as muscle, fat, bone, cartilage, stromal cells, tendons, and ligaments and have differentiation capability for other tissue cells (transdifferentiation; neurons, hepatic, pancreatic, etc.) [36].
- MSCs are capable of fusion with damaged cells.
- MSCs contribute to the repair of damaged cells and tissues by growth factors, cytokines, and chemokines such as exosomes directly or *via* secreted soluble factors.
- With migration characteristics, MSCs have access to damaged tissue.

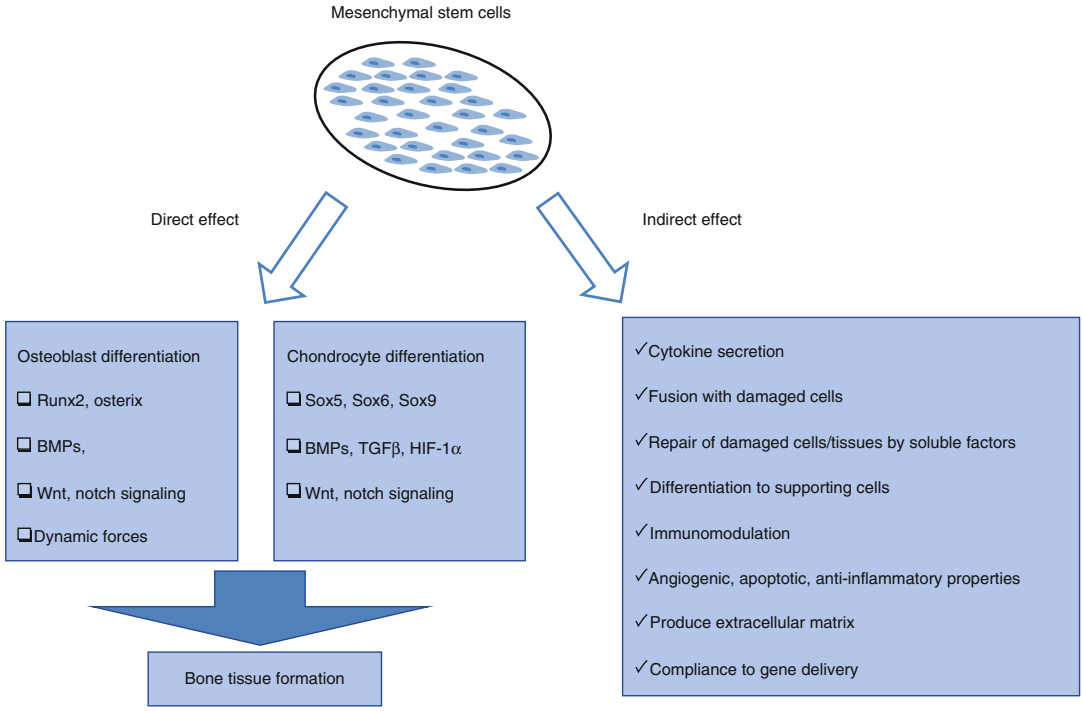

Fig. 15.3 Potential regenerative properties of mesenchymal stem cells for tissue damage

- MSCs are immunosuppressive and nonimmunogenic and because of these characteristics do not require HLA compatibility for clinical use.
- Because of their angiogenic, apoptotic, and anti-inflammatory properties, MSCs contribute to tissue repair [37] (Fig. 15.3),

Induced Pluripotent Stem Cells

Induced pluripotent stem cells (iPSCs) are cells that have gained pluripotency characteristics by the application of various methods and factors. The term iPSC was used for the first time in 2006 by Shinya Yamanaka of Kyoto University. Yamanaka et al. obtained ECS-like cells with retroviral transfection of four pluripotency genes (Oct4, Sox2, KLF-4, c-Myc) from skin fibroblast cells. Yamanaka and John Gurdon, who laid the foundation of cloning, showed terminally differentiated cells can gain pluripotency and were awarded the Nobel Prize for medicine in 2012 [38].

In the years since, the number of studies with iPSCs has increased rapidly. Improvements such as increased efficiency of forming cells, use of tissue-specific multipotent stem cells rather than terminally differentiated cells, and more convenient methods of clinical use instead of viral transfer increase the chances of clinical use of these cells. The greatest advantage of these cells is the absence of immunological incompatibility problems. Genetic corrections derived from pluripotent stem cells can be performed and can be differentiated to desired cells. Although iPSCs have many advantages compared with embryonic cells, there are challenges that must be overcome before clinical application. First, using nonviral methods, iPSC efficiency should be improved. In addition, the methods used must not create susceptibility to tumor formation. Xenogenic factors should not be used to avoid immunological reactions [39].

iPSCs are used in orthopedics to differentiate into bone and cartilage cells. iPSCs are expanded on tissue scaffolds and differentiated into osteogenic and chondrogenic cells. Prepared cell-

containing tissue scaffolds are injected into immunosuppressed mice, and bone and cartilage tissue formation are monitored. In addition to direct differentiation, iPSCs can be differentiated into MSCs before bone and cartilage cell differentiation. Thus, it is argued that a more controlled protocol be followed [40].

Tissue Engineering

The main goal of tissue engineering is to create tissues or organs for use in case of loss or damage. Tissue engineering includes four stages: the first using only biomaterials; the second using only cells (directly or with genetic modifications (gene therapy)); the third using biomaterials with adhesion and expansion biosignals; and the fourth using biomaterials, biosignals, and cells together. For the purpose of cell growth for guiding new tissue or organs and providing mechanical support, three-dimensional scaffolds can be produced from biomaterials. In addition, bioreactors can be used to mimic a tissue microenvironment [41].

Tissue scaffolds are produced to mimic extracellular matrix and they should provide a suitable surface for appropriate cell growth and adhesion, mechanical strength, and effective environmental and tissue interactions. Selection of biocompatible and biodegradable materials is important [41].

Cartilage, bone, and tendon regeneration is often studied in tissue engineering applications. Scaffolds with different properties for each application (size, three-dimensional structure, surface pattern, porosity, mechanical strength, etc.) should be used.

A tissue scaffold should have the following properties:

- It should promote cell adhesion and survival.
- It must have suitable porosity to support the expansion of the cells and formation of extracellular matrix.
- Its structure should permit nutrients to reach the cells and metabolites to be removed.
- Tissue scaffold degradation rate and new extracellular matrix formation rate must be the same.
- It must have mechanical strength appropriate to the damaged area [42] (Fig. 15.4).

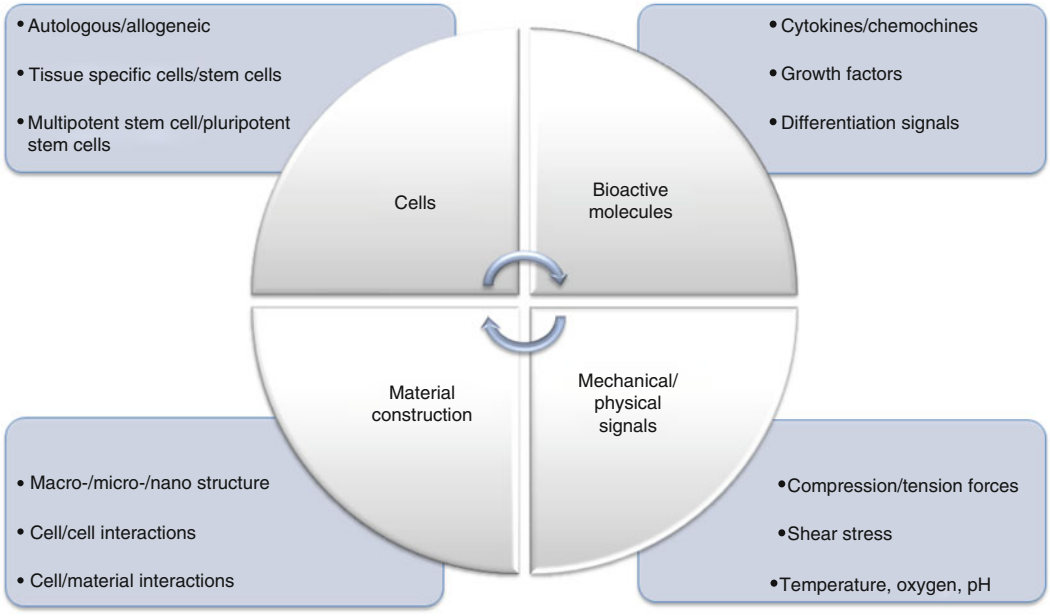

Fig. 15.4 The components of functional tissue regeneration

Cellular Therapy in Orthopedic Research

Articular Cartilage

Despite being prone to damage, the repair capacity of articular cartilage is low. Traumatic injury causes arthritic changes over the years. The treatment protocol includes infiltration or introduction of bone marrow stem cells to the damaged area with penetration of the subchondral bone so that localized cartilage is repaired. The microfracture technique is frequently used, however, it results in formation of a fibrous structure that has weak mechanical properties compared with normal cartilage. Nevertheless, use of this technique for the treatment of osteochondritis dissecans or traumatic osteochondral lesions has shown good outcomes at mid-term follow-up [43].

More recently in clinical applications, the regeneration of normal articular cartilage with autologous chondrocyte implantation (ACI) has been achieved [44]. Chondrocytes, mesenchymal stem cells, periosteum-containing chondroblasts, and osteochondral autograft (mosaicplasty) transplantation to articular cartilage defects of animal models provided better recovery compared with controls. Mosaicplasty showed better results compared with periosteal grafts [45].

Bone

Trauma and certain pathological conditions may cause large losses that require bone tissue or patch transfusions with the aim of preserving the structural integrity. The use of autologous or allogeneic bone graft can cause morbidity and infection. Mouse, rat, rabbit, dog, and human bone marrow cell isolation and expansion methods have improved, and bone formation was observed in ectopic implantation with ectopic hydroxyapatite or suitable carriers [46]. There is also expansion of bone marrow osteoprogenitor cells. Therefore, the use of autologous human stromal progenitors has been developed for the regeneration of large bone defects [47].

For successful bone tissue engineering, osteoproduction, osteo-induction, osteo-conduction, and mechanical stimulation are required. Osteoproduction is the ability to secrete bone materials from the cells. Healing of critical-size bone has been provided with bone marrow-derived MSCs [48, 49]. In recent years, the muscle-derived stem cells have been used as a source of osteoproducing cells. The rate of bone healing has increased with the use of factors such as TGF-β and analogs (bone morphogenetic proteins (BMPs)) in clinic. Osteo-conduction is the restructuring of bone cells in the damaged area. Grafts can serve as scaffolds. Mechanical stimulation is beneficial as it promotes cell proliferation and differentiation [50].

Growth factors have a short half life, and effective doses cannot be contained in the damaged area. These factors that impact the damaged area can be provided with gene therapy for a longer time-period. In this strategy, genes encoding the desired protein are isolated and transferred to the host cell *via* viral or nonviral methods. The advantage of these genetically modified cells is that they secrete autocrine growth factor and respond to the effects thereof. In gene therapy studies, BMP-2 and IGF growth factors have especially been shown to be effective in fracture wound healing [51]. However, no gene therapy applications for tissue repair are clinically applicable.

Tendons and Ligaments

Tendon and ligament tissue is of lower quality after injury. Autograft, allograft, and resorbable biomaterials are used for functional tissue restoration. However, donor site morbidity, scar formation, and tissue rejection problems can be seen after these treatments [52]. In animal experiments performed with tissue scaffolds (usually collagen-based) with MSCs, improvement of tendon repair was observed [53].

Meniscus

Standard treatment protocols in meniscal tears provide limited results. Also, meniscectomy leads to osteoarthritis [54]. In the context of cel-

lular therapy in meniscal tear, devitalized meniscal tissue has been maintained with a combination of meniscal matrix and chondrocytes. Increase of adhesion and new cartilage matrix synthesis was observed with time in histological and biomechanical analysis [55]. In pig studies, use of autologous bone marrow-derived MSCs resulted in repair of avascular meniscal lesions. Compared with surgical methods, cellular therapy for repair of one-third meniscal tears in the avascular portion gave better results [56].

Intervertebral Disc

Degeneration of the intervertebral disc can cause back pain and morbidity. Many patients are treated by conventional means and, in about 90 %, control of the back pain is achieved. When this treatment for discogenic back pain fails, surgical options are limited and are usually invasive. Discectomy with fusion is often performed, along with disk replacement [57].

These treatments all aim to relieve symptoms in disc regeneration, but the underlying cause is ignored. Cell-based tissue engineering containing autologous disc cells, chondrocytes, and MSC transplantation into the intervertebral disc offer better treatment alternatives compared with surgical methods. Cell transplantation increases disk regeneration by increasing proteoglycan production and also slows degeneration. Degeneration of the disc was found to slow with transplantation of autologous disc cells produced from costal cartilage and chondrocyte in animal experiments [58]. In another study, MSCs in hyaluronan gel injected into the damaged discs of rats were able to maintain their survival, proliferate, and produce extracellular matrix [59].

Spinal Fusion

Use of autologous bone is still regarded as the best method to achieve spinal fusion. However, there may be a 5–35 % rate of nonunion [60]. Use of suitable carriers to ensure release of BMP with autologous bone grafts and fusion was determined to be more successful [61]. However, this practice is expensive and side effects have limited the use. Mesenchymal stem cells have been used in conjunction with ceramic scaffolds, and fusion was achieved more successfully than with autologous bone [62].

Spinal Cord

With stem cell therapy, use of pluripotent cells to differentiate into neuronal cells will have an important place in the treatment of spinal cord injuries. However, the repair of spinal cord injury is complex, involving repair of the local spinal reflex arc and merger of axon endings. Gliosis may prevent the coming together of axons [63]. In recent years, with stem cell applications in mouse models of spinal cord injury, axonal regeneration and functional recovery have been achieved. Remyelination of demyelinating axons has been provided with direct injection of bone marrow-derived MSCs to the injury [64].

Epiphyseal Plate

In epiphyseal plate injuries, bony bridges can form between the epiphysis and metaphysis. In 25–35 % of injuries, shortening or angular deformities occur. Correction in older children is obtained by epiphysiodesis, osteotomy, or stapling. However, treatment is more difficult in younger patients. With removing bony bridges and adding adipose tissue, polymeric silicon, or muscle, partial success with interpositional patching has been achieved. These inert fillers do not stimulate growth in the physis but only prevent reformation of bony bridges [65]. In the context of cellular therapy, chondrocytes and MSCs have been transferred to the physeal defect in experimental animals and growth arrest has been prevented. When applied with TGF-β, decreased angular deformity was observed. In this study, donor MSC differentiation into chondrocytes and physis improvement were hypothesized.

References

1. McCulloch EA, Till JE (2005) Perspectives on the properties of stem cells. Nat Med 11(10):1026–1028
2. Weissman IL (2000) Stem cells: units of development, units of regeneration, and units in evolution. Cell 100(1):157–168
3. Thomson JA, Itskovitx-Eldor J, Shapiro SS et al (1998) Embryonic stem cell lines derived from human blastocysts. Science 282:1145–1147
4. Baın G, Kıtchens D, Yao M et al (1995) Embryonic stem cells express neuronal properties *in vitro*. Dev Biol 168:342–357
5. Lıu S, Qu Y, Stewart T et al (2000) Embryonic stem cells differentiate into oligodendrocytes and myelinate in culture and after spinal cord transplantation. Proc Natl Acad Sci U S A 97:6126–6131
6. O'Donoghue K, Fisk NM (2004) Fetal stem cells. Best Pract Res Clin Obstet Gynaecol 18(6):853–857
7. Barry FP, Murphy JM (2004) Mesenchymal stem cells: clinical applications and biological characterization. Int J Biochem Cell Biol 36:568–584
8. Friedenstein AJ (1980) Stromal mechanisms of bone marrow: cloning in vitro and retransplantation in vivo. In: Thienfelder S, Rodt H, Kolb HJ (eds) Immunology of bone marrow transplantation. Springer, Berlin, pp 19–20
9. Aubin JE (1998) Bone stem cells. J Cell Biochem Suppl 30–31:73
10. Pittenger MF, Mackay AM, Beck SC (1999) Multilineage potential of adult human mesenchymal stem cells. Science 284:143
11. Docheva D, Popov C, Mutschler W, Schieker M (2007) Human mesenchymal stem cells in contact with their environment: surface characteristics and the integrin system. J Cell Mol Med 11(1):21–38
12. Fox JM, Chamberlain G, Ashton BA, Middleton J (2007) Recent advances into the understanding of mesenchymal stem cell trafficking. Br J Haematol 137(6):491–502
13. Haynesworth SE, Baber MA, Caplan AI (1996) Cytokine expression by human marrow-derived mesenchymal progenitor cells in vitro: effects of dexamethasone and IL-1 alpha. J Cell Physiol 166(3):585–592
14. Auffray I, Chevalier S, Froger J, Izac B, Vainchenker W, Gascan H, Coulombel L (1996) Nerve growth factor is involved in the supportive effect by bone marrow-derived stromal cells of the factor-dependent human cell line UT-7. Blood 88:1608–1618
15. Labouyrie E, Dubus P, Groppi A, Mahon FX, Ferrer J, Parrens M, Reiffers J, De Mascarel A, Merlio JP (1999) Expression of neurotrophins and their receptors in human bone marrow. Am J Pathol 154:405–415
16. Chen X, Li Y, Wang L, Katakowski M, Zhang L, Chen J, Xu Y, Gautam SC, Chopp M (2002) Ischemic rat brain extracts induce human marrow stromal cell growth factor production. Neuropathology 22:275–279
17. Bai L, Caplan A, Lennon D, Miller RH (2007) Mesenchymal stem cell signals regulate neural stem cell fate. Neurochem Res 32:353–362
18. Nauta AJ, Kruisselbrink AB, Lurvink E, Willemze R, Fibbe WE (2006) Mesenchymal stem cells inhibit generation and function of both CD34+-derived and monocyte-derived dendritic cells. J Immunol 177(4):2080–2087
19. Jaquet K, Krause KT, Denschel J, Faessler P, Nauerz M, Geidel S, Boczor S, Lange C, Stute N, Zander A, Kuck KH (2005) Reduction of myocardial scar size after implantation of mesenchymal stem cells in rats: what is the mechanism? Stem Cells Dev 14(3):299–309
20. Beier JP, Bitto FF, Lange C, Klumpp D, Arkudas A, Bleiziffer O, Boos A, Horch RE, Kneser U (2011) Myogenic differentiation of mesenchymal stem cells co-cultured with primary myoblasts. Cell Biol Int 35:397–406
21. Mohsin S, Shams S, Ali Nasir G, Khan M, Javaid Awan S, Khan SN, Riazuddin S (2011) Enhanced hepatic differentiation of mesenchymal stem cells after pretreatment with injured liver tissue. Differentiation 81(1):42–48
22. Huang Y, Jia X, Bai K, Gong X, Fan Y (2010) Effect of fluid shear stress on cardiomyogenic differentiation of rat bone marrow mesenchymal stem cells. Arch Med Res 41(7):497–505
23. Asanuma H, Meldrum DR, Meldrum KK (2010) Therapeutic applications of mesenchymal stem cells to repair kidney injury. J Urol 184(1):26–33
24. Song S, Song S, Zhang H, Cuevas J, Sanchez-Ramos J (2007) Comparison of neuron-like cells derived from bone marrow stem cells to those differentiated from adult brain neural stem cells. Stem Cells Dev 16(5):747–756
25. Chopp M, Zhang XH, Li Y, Wang L, Chen J, Lu D (2000) Spinal cord injury in rat: treatment with bone marrow stromal cell transplantation. Neuroreport 11(13):3001–3005
26. Zurita M, Vaquero J (2006) Bone marrow stromal cells can achieve cure of chronic paraplegic rats: functional and morphological outcome one year after transplantation. Neurosci Lett 402(1–2):51–56
27. Horwitz EM, Prockop DJ, Fitzpatrick LA, Koo WW, Gordon PL, Neel M, Sussman M, Orchard P, Marx JC, Pyeritz RE, Brenner MK (1999) Transplantability and therapeutic effects of bone marrow-derived mesenchymal cells in children with osteogenesis imperfecta. Nat Med 5:309–13
28. Stappenbeck TS, Miyoshi H (2009) The role of stromal stem cells in tissue regeneration and wound repair. Science 324(5935):1666–1669
29. Xu F, Shi J, Yu B, Ni W, Wu X, Gu Z (2010) Chemokines mediate mesenchymal stem cell migration toward gliomas in vitro. Oncol Rep 23(6):1561–1567
30. Blakemore WF (1977) Remyelination of CNS axons by Schwann cells transplanted from the sciatic nerve. Nature 266:68–69

31. Akiyama Y, Radtke C, Kocsis JD (2002) Remyelination of the rat spinal cord by transplantation of identified bone marrow stromal cells. J Neurosci 22(15):6623–6630
32. Zhao FQ, Zhang PX, He XJ, Du C, Fu ZG, Zhang DY, Jiang BG (2005) Study on the adoption of Schwann cell phenotype by bone marrow stromal cells in vitro and in vivo. Biomed Environ Sci 18(5):326–333
33. Halabian R, Mohammadi Mohammad H, Salimi M, Amani M, Mohammadi Roushandeh A, Aghaeipour M, Amirizadeh N, Ebrahimi M, Jahanian N, Habibi RM (2010) Genetically engineered mesenchymal stem cells stably expressing green fluorescent protein. Iran J Basic Med Sci 13(2 (45)):24–30
34. Metzele R, Alt C, Bai X, Yan Y, Zhang Z, Pan Z, Coleman M, Vykoukal J, Song YH, Alt E (2011) Human adipose tissue-derived stem cells exhibit proliferation potential and spontaneous rhythmic contraction after fusion with neonatal rat cardiomyocytes. FASEB J 25:830–9
35. Gangrade N, Price JC (1991) Poly(hydroxybutyrate-hydroxyvalerate) microspheres containing progesterone: preparation, morphology and release properties. J Microencapsul 8:185–202
36. Zhang Y, Shen W, Hua J, Lei A, Lv C, Wang H, Yang C, Gao Z, Dou Z (2010) Pancreatic Islet-like clusters from bone marrow mesenchymal stem cells of human first-trimester abortus can cure streptozocin-induced mouse diabetes. Rejuvenation Res 13:695–706
37. Ling X, Marini F, Konopleva M, Schober W, Shi Y, Burks J, Clise-Dwyer K, Wang RY, Zhang W, Yuan X, Lu H, Caldwell L, Andreeff M (2010) Mesenchymal stem cells overexpressing IFN-β inhibit breast cancer growth and metastases through Stat3 signaling in a syngeneic tumor model. Cancer Microenviron 3(1):83–95
38. Takahashi K, Yamanaka S (2006) Induction of pluripotent stem cells from mouse embryonic and adult fibroblast cultures by defined factors. Cell 126(4):663–676
39. Yamanaka S (2012) Induced pluripotent stem cells: past, present, and future. Cell Stem Cell 10(6):678–684
40. Bilousova G, Jun du H, King KB, De Langhe S, Chick WS, Torchia EC, Chow KS, Klemm DJ, Roop DR, Majka SM (2011) Osteoblasts derived from induced pluripotent stem cells form calcified structures in scaffolds both in vitro and in vivo. Stem Cells 29(2):206–216
41. Nerem RM (1991) Cellular engineering. Ann Biomed Eng 19:529–545
42. Langer R, Vacanti JP (1993) Tissue engineering. Science 260:920–926
43. Buckwalter JA, Mankin HJ (1998) Articular cartilage: degeneration and osteoarthritis, repair, regeneration and transplantation. Instr Course Lect 47: 487–504
44. Bentley G, Greer RB 3rd (1971) Homotransplantation of isolated epiphyseal and articular cartilage chondrocytes into joint surfaces of rabbits. Nature 230:385–388
45. Hui JH, Chen F, Thambyah A, Lee EH (2004) Treatment of chondral lesions in advanced osteochondritis dissecans: a comparative study of the efficacy of chondrocytes, mesenchymal stem cells, periosteal graft, and mosaicplasty (osteochondral autograft) in animal models. J Pediatr Orthop 24:427–433
46. Goshima J, Goldberg VM, Caplan AI (1991) Osteogenic potential of culture-expanded rat marrow cells as assayed in vivo with porous calcium phosphate ceramic. Biomaterials 12:253–258
47. Jaiswal N, Haynesworth SE, Caplan AI, Bruder SP (1997) Osteogenic differentiation of purified, culture-expanded human mesenchymal stem cells in vitro. J Cell Biochem 64:295–312
48. Bruder SP, Kurth AA, Shea M et al (1998) Bone regeneration by implantation of purified culture-expanded human mesenchymal stem cells. J Orthop Res 16:155–162
49. Bruder SP, Fink DJ, Caplan AI (1994) Mesencymal stem cells in bone development, bone repair and skeletal regeneration therapy. J Cell Biochem 56:283–294
50. Wiesmann HP, Joos U, Meyer U (2004) Biological and biophysical principles in extracorporal bone tissue engineering: part II. Int J Oral Maxillofac Surg 33:523–530
51. Jullig M, Zhang WV, Stott NS (2004) Gene therapy in orthopaedic surgery: the current status. ANZ J Surg 74:46–54
52. Brown TD, Fu FH, Hanley EN Jr (1981) Comparative assessment of the early mechanical integrity of repaired tendon Achillis ruptures in the rabbit. J Trauma 21:951–957
53. Awad HA, Boivin GP, Dressler MR et al (2003) Repair of patellar tendon injuries using a cell-collagen composite. J Orthop Res 21:420–431
54. Allen PR, Denham RA, Swan AV (1984) Late degenerative changes after meniscectomy: factors affecting the knee after operation. J Bone Joint Surg (Br) 66-B:666–671
55. Peretti GM, Caruso EM, Randolph MA, Zaleske DJ (2001) Meniscal repair using engineered tissue. J Orthop Res 19:278–285
56. Dutton A, Hui JPP, Lee EH, Goh J (2004) Enhancement of meniscal repair using mesenchymal stem cells in a porcine model. In: Proceedings of 5th combined meeting of the orthopaedic research societies of USA, Canada, Japan & Europe. International combined orthopaedic research societies
57. Lee EH, Hui JH (2006) The potential of stem cells in orthopaedic surgery. J Bone Joint Surg (Br) 88(7):841–851
58. Brisby H, Tao H, Ma DD, Diwan AD (2004) Cell therapy for disc degeneration: potentials and pitfalls. Orthop Clin N Am 35:85–93
59. Crevensten G, Walsh AJ, Ananthakrishnan D et al (2004) Intervertebral disc cell therapy for regeneration: mesenchymal stem cell implantation in rat intervertebral discs. Ann Biomed Eng 32:430–434

60. Steinmann JC, Herkowitz HN (1992) Pseudarthrosis of the spine. Clin Orthop 284:80–90
61. Itoh H, Ebara S, Kamimura M et al (1999) Experimental spinal fusion with use of recombinant human bone morphogenetic protein 2. Spine 24:1402–1405
62. Cui Q, Ming Xiao Z, Balian G, Wang GJ (2001) Comparison of lumbar spine fusion using mixed and closed marrow cells. Spine 26:2305–2310
63. Barami K, Diaz FG (2000) Cellular transplantation and spinal cord injury. Neurosurgery 47:691–700
64. Akiyama Y, Radtke C, Honmou O, Kocsis JD (2002) Remyelination of the spinal cord following intravenous delivery of bone marrow cells. Glia 39:229–236
65. Mizuta T, Benson WM, Foster BK, Paterson DC, Morris LL (1987) Statistical analysis of the incidence of physeal injuries. J Pediatr Orthop 7:518–523

Platelet-Rich Plasma

16

Taner Özgürtaş, Burkay Utku, and Cemil Yildiz

Abstract

PRP is the acronym for *p*latelet-*r*ich *p*lasma. PRP is basically the process of enrichment of platelets, having the capability of healing by their granule constituents. The expected utility of PRP is its application to the area of lesion as a concentration of growth factors found in alpha granules. PRP has gained growing attention in the fields of soft tissue and wound healing, fracture treatment, arthritis, tissue engineering, and angiogenesis. Theoretically, it seems reasonable to expect favorable results from the application of platelets, containing growth and mitogenic factors, to the area of lesion. But larger controlled prospective studies are needed for clear assessments and classical approaches about this issue.

Platelet-rich plasma (PRP) is also known as autologous platelet gel, plasma rich in growth factor (PRGF), and platelet concentrate (PC) and is used as a treatment modality in musculoskeletal medicine. The aim of this treatment is the quick return of the patient to his/her daily activities via complementary or supporting interventions with or without surgical treatment. PRP treatment was used for the first time by Ferrari M. et al. in 1987 in cardiac surgery [1]. In the early 2000s, it attracted attention of other branches and was mostly used by maxillofacial surgeons [2]. In 2008, its use in some orthopedic disorders was approved by FDA in the USA [3].

Platelets are also natural sources of growth factors besides its commonly known role in hemostasis. PRP is basically the process of enrichment of platelets. Platelet count in the blood of a healthy human is approximately $150–400 \times 10^3$ per mm^3. Platelet count can be enriched to two- to fivefold according to the preparation technique of PRP, and it is applied to the lesion area [4].

T. Özgürtaş (✉)
Division of Biochemistry,
University of Gülhane Military Medical
Academy and Faculty, Ankara, Turkey
e-mail: chem352000@yahoo.com

B. Utku, M.D.
Sports Medicine Department,
ATATÜRK Education and Research Hospital,
Ankara, Turkey
e-mail: burkay.utku@gmail.com

C. Yildiz
Division of Orthopaedics and Traumatology,
University of Gülhane Military Medical
Academy and Faculty, Ankara, Turkey
e-mail: cyorto@yahoo.com

F. Korkusuz (ed.), *Musculoskeletal Research and Basic Science*,
DOI 10.1007/978-3-319-20777-3_16

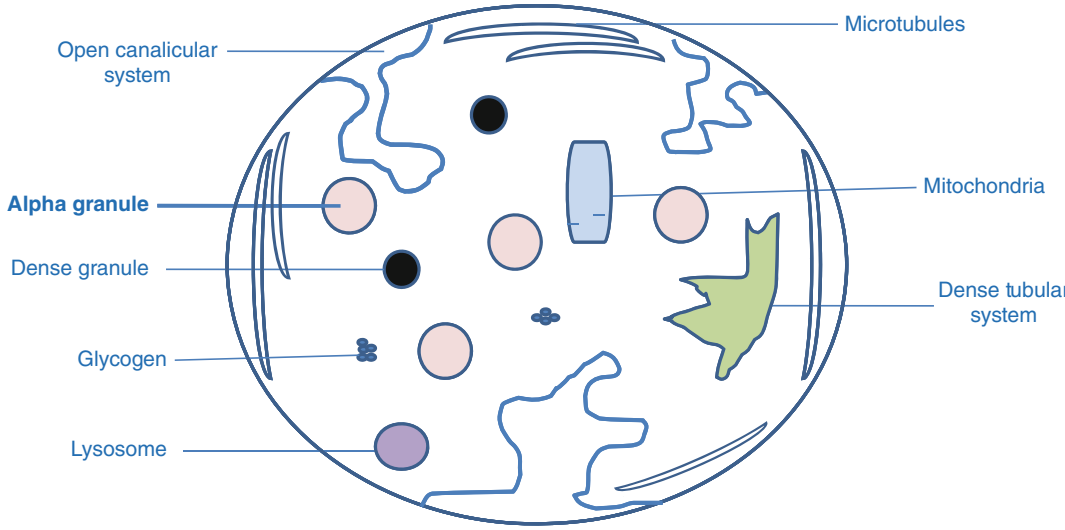

Fig. 16.1 Structure and organelles of platelets

Structure of Platelets

Platelets can be observed via light microscope. However, electron microscope is required to see their structural features. The presence of some granules, providing different features to these cells, was proved via electron microscopy and cytopathological applications performed between the years 1966 and 1980 [5–7] (Fig. 16.1). Alpha granules are specific only to platelets and have the highest number among all granules. Protein profile of platelets may be thought as limited and static because of not having nucleus. However, the proteomics studies showed that alpha granules included more than 300 different proteins [8]. Some of these are inherited from megakaryocytes, and some are taken to the inside of platelets from plasma. It can be seen that many proteins of different groups are present, considering the contents of alpha granules. These are adhesive proteins, coagulation and fibrinolysis factors, proteases and antiproteases, growth and mitogenic factors, chemokines and cytokines, antimicrobial proteins, and membrane proteins (Table 16.1) [9]. Growth factors are the key mediators, playing an important role in wound healing and regeneration, consisting of processes such as chemotaxis, proliferation, differentiation, and angiogenesis. Growth factors stored in alpha granules of the platelets are transforming growth factor-β (TGFβ), basic fibroblast growth factor (bFGF), epidermal growth factor (EGF), hepatocyte growth factor (HGF), insulin-like growth factor1 (IGF-1), vascular endothelial growth factor (VEGF), and platelet-derived growth factor (PDGF). Growth factor amounts of activated PRP and platelet-poor plasma were compared, and all growth factor concentrations were many times more higher in activated PRP except HGF and IGF-1. HGF and IGF-1 are also found in plasma as well as in platelets [10, 11]. Dense granules and lysosomes are also found in platelets besides alpha granules. Lysosomes contain enzymes related with cell metabolism. Dense granules contain mediators of coagulation process such as adenine nucleotides, ATP, ADP, serotonin, pyrophosphate, calcium, and magnesium. Platelets, previously supposed to play a role only in hemostasis, are thought to have many new functions in terms of this new information such as wound healing, angiogenesis, bone formation, and functions related with the immune system [12].

Preparation of PRP

Many protocols are being developed for obtaining PRP, and all methodologies have similar principles:

1. Anticoagulant is added into blood collection tubes. Citrate-phosphate dextrose, anticoagulated citrate-dextrose A (ACD-A), or trisodium citrate is preferred. ACD-A anticoagulant is also preferred for preserving

Table 16.1 Mediators found in alpha granules of platelets

Group	Mediators	Functions
Adhesive proteins	VWF, TSP-1, TSP-2, laminin-8	Hemostasis and coagulation, cell-to-cell contact
Coagulation factors and inhibitors	Factor V/Va; protein S; protease nexin-1, 2; protein C inhibitor	Thrombin generation and cell proliferation
Fibrinolytic factors and inhibitors	Plasminogen, PAI-1, u-PA, α2-macroglobulin	Plasmin production and vascular remodeling
Proteases and inhibitors	MMP-1, -2, -4, -9; TIMPs-1,4; C1 inhibitor, α1-antitrypsin	Angiogenesis and vascular remodeling
Growth and mitogenic factors	PDGF, IGF-1, EGF, VEGF, bFGF, HGF, BMP-2, CTGF	Chemotaxis, proliferation, differentiation, angiogenesis
Chemokines and cytokines	TGF-β1, β2, IL-1, RANTES, IL-8, MIP-1α, MIP-2, SDF-1α, PF4, angiopoietin-1, endostatin	Angiogenesis, chemotaxis, vascular remodeling, bone formation, cellular interactions
Antimicrobial proteins	Thrombocidins, quinocides	Bactericidal and fungicidal effect
Others	Chondroitin sulfate-4, immunoglobulins G and M, amyloid β-protein precursor, complement factor H	Various effects

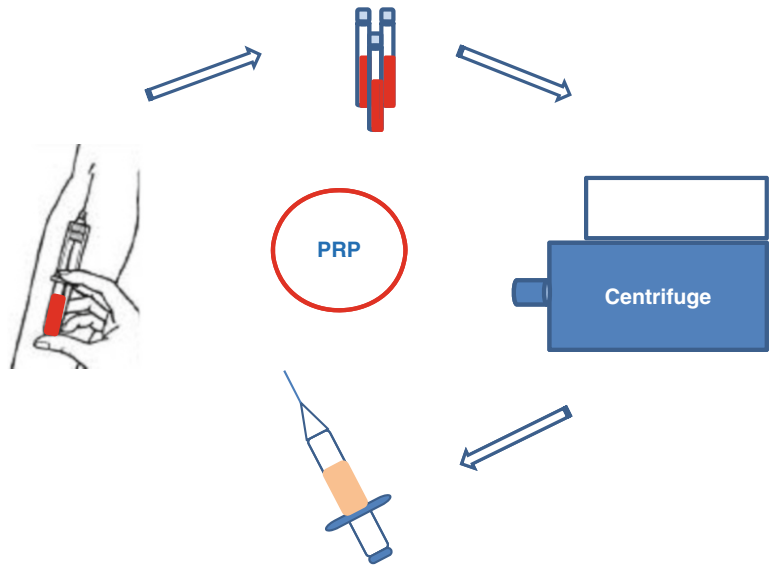

Fig. 16.2 Centrifuge method for PRP preparation

apheresis platelets. Dextrose is a source for platelets, and phosphate is used as a buffer solution. However, a commonly used anticoagulant, EDTA, is not preferred because EDTA-bound platelets are rapidly removed from plasma and it may harm the platelet surface integrity; therefore, a complete cell viability is essential for growth factor secretion of the platelets [4].

2. Collected blood is centrifuged. In the first centrifugation, blood is collected into layers (Figs. 16.2 and 16.3). Then, the layers are collected according to the type of PRP preferred (leukocyte-reduced or leukocyte-platelet-rich plasma). For leukocyte-reduced PRP, superficial buffy coat (BC) and plasma above the BC are collected, and a second hard-spin centrifugation is applied. In the final product, upper part of the plasma, called as platelet-poor plasma (PPP) is discarded. For obtaining leukocyte-platelet-rich plasma (L-PRP), BC, superficial red blood cells, and plasma above the BC are collected. After a second hard spin, BC and a few milliliters above the BC are collected with eye-balling. However,

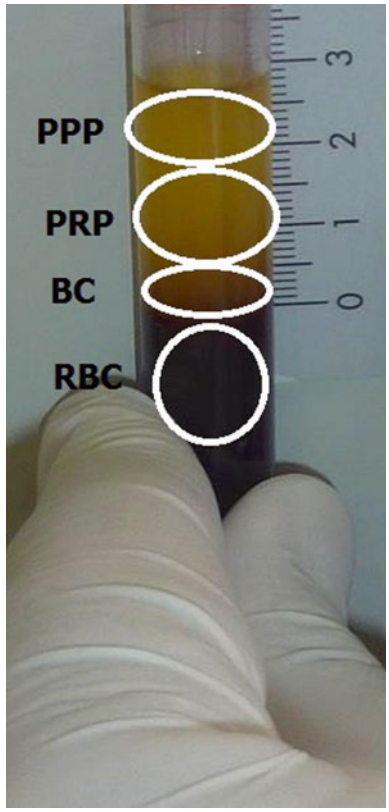

Fig. 16.3 Leukocyte-reduced platelet-rich plasma. After a soft-spin centrifugation, blood is separated into different layers. *RBC* red blood cells, *BC* buffy coat, *PRP* platelet-rich plasma, *PPP* platelet-poor plasma

in Anitua methodology, one-spin centrifuge is being used, and after a soft spin (460–580 g, 8 min), the lower part of the plasma above the BC is collected and named as plasma rich in growth factors (PRGF) [4, 13–15].

3. PRP can be activated and platelet-rich fibrin (PRF) can be obtained if needed. For activating and aggregating platelets, ADP, thrombin, collagen, arachidonic acid, and calcium chloride can be used in different doses. Platelet degranulation mostly occurs in 10 min and finishes in 1 h. PRF is obtained (Fig. 16.4) [15, 16].

In PRP applications, a gelous cement may be obtained from activated samples and applied to the area of lesion. The PRP method is the in vitro imitation of in vivo coagulation process and application to the area of lesion.

Application and Outcomes

The expected outcome of PRP is its application to the area of lesion as a concentration of growth factors found in alpha granules (Fig. 16.5). With this method, it is possible to apply many growth factors together much more cheaply compared to the cost of a single recombinant growth factor [17]. Additionally, the fibrous network, created by the activated platelets in PRP, is thought to have a contribution in the healing process via formation of regenerative matrix support [18]. PRP enhances the wound healing process and epithelization two to threefold and decreases scar formation via its content of platelet-derived growth factor (PDGF) and epidermal growth factor (EGF) [19]. In some animal studies, the growth factors released from PRP were shown to have favorable contributions to the osteoblasts or stromal cells, the vital cells of solid tissue [20]. In an in vitro study, it was stated that PRP favorably affected the development of chondrocytes and showed anabolic effects on chondrocytes, while PRP formulations having high leukocyte count might have an increased catabolic effect [21]. Ultrasonography-aided intratendineal application of PRP contributes to rapid healing of tendons [22]. In addition to these data, it is supposed that the application of autologous PRP remarkably eliminates the risk of cross reactivity, immune reactions, and disease contamination [23].

Today, there are some studies indicating that PRP applications have no favorable effects either [24]. The reason of this confused situation may be due to some individual differences (age, sex, different daily habits, smoking, obesity, nutrition differences, chronic diseases, use of drugs, etc.) as well as the differences in concentrations of platelets during application and growth factors released by these platelets. Lack of standardization in these applications is another significant factor, preventing data collection properly in a common source.

Theoretically, it seems reasonable to expect favorable results from the application of platelets, containing growth and mitogenic factors, to the area of lesion. In addition, these are autologous applications prepared rapidly and easily. However, larger controlled prospective studies are needed for clear assessments and classical approaches about this issue.

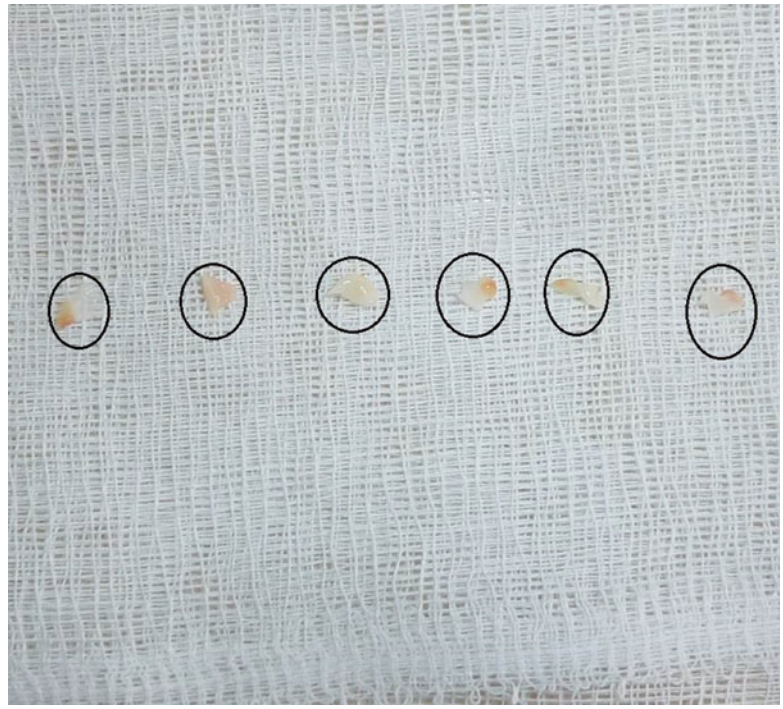

Fig. 16.4 Platelet-rich fibrin (PRF) obtained by adding 10 % calcium into PRP. After 10 min, PRF is ready for use as a source of growth factors

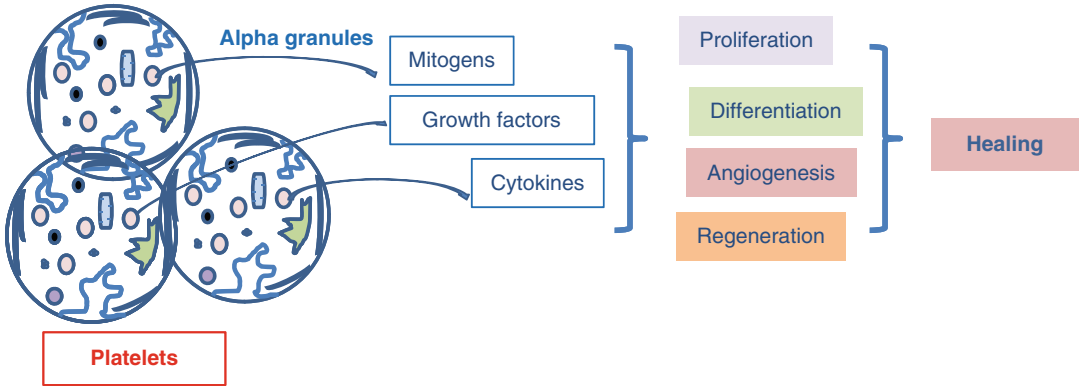

Fig. 16.5 Alpha granule contents in platelets and their possible effects

References

1. Ferrari M, Zia S, Valbonesi M, Henriguet F, Venera G, Spagnolo S, Grasso MA, Panzani I (1987) A new technique for hemodilution, preparation of autologous platelet-rich plasma and intraoperative blood salvage in cardiac surgery. Int J Artif Organs 10(1):47–50
2. Sonnleitner D, Huemer P, Sullivan DY (2000) A simplified technique for producing platelet-rich plasma and platelet concentrate for intraoral bone grafting techniques: a technical note. Int J Oral Maxillofac Implants 15(6):879–882
3. Recombinant and autologous platelet-derived growth factors as a treatment of wound healing and other conditions. Current procedural terminology of american medical association, June 2012. http://www.bcbsks.com/customerservice/providers/MedicalPolicies/policies/policies/Recombinant_AutologousPlatelet-DerivedGrowthFactors_Treatment_WoundHealing_OtherConditions_2014-02-05.pdf
4. Dohan Ehrenfest DM, Rasmusson L, Albrektsson T (2009) Classification of platelet concentrates: from pure platelet-rich plasma (P-PRP) to leukocyte- and platelet-rich fibrin (L-PRF). Trends Biotechnol 27:158–167

5. Bentfeld-Barker ME, Bainton DF (1982) Identification of primary lysosomes in human megakaryocytes and platelets. Blood 59(3):472–481
6. Tranzer JP, Da Prada M, Pletscher A (1966) Ultrastructural localization of 5-hydroxytryptamine in blood platelets. Nature 212(5070):1574–1575
7. Siegel A, Luscher EF (1967) Non-identity of the alpha-granules of human blood platelets with typical lysosomes. Nature 215(5102):745–747
8. Bentfeld-Barker ME, Bainton DF (1982) Identification of primary lysosomes in human megakaryocytes and platelets. Blood 59(3):472–481
9. Coppinger JA, Cagney G, Toomey S, Kislinger T, Belton O, McRedmond JP, Cahill DJ, Emili A, Fitzgerald DJ, Maguire PB (2004) Characterization of the proteins released from activated platelets leads to localization of novel platelet proteins in human atherosclerotic lesions. Blood 103:2096–2104
10. Weibrich G, Kleis WK, Kunz-Kostomanolakis M, Loos AH, Wagner W (2001) Correlation of platelet concentration in platelet-rich plasma to the extraction method, age, sex, and platelet count of the donor. Int J Oral Maxillofac Implants 16:693–699
11. Jakse N, Tangl S, Gilli R, Berghold A, Lorenzoni M, Eskici A, Haas R, Pertl C (2003) Influence of PRP on autogenous sinus grafts. An experimental study on sheep. Clin Oral Implants Res 14:578–583
12. Nurden AT (2011) Platelets, inflammation and tissue regeneration. Thromb Haemost 105(1):S13–S33
13. Anitua E, Andía I, Sanchez M, Azofra J, del Mar Zalduendo M, de la Fuente M, Nurden P, Nurden AT (2005) Autologous preparations rich in growth factors promote proliferation and induce VEGF and HGF production by human tendon cells in culture. J Orthop Res 23(2):281–286
14. Anitua E, Muruzabal F, Alcalde I, Merayo-Lloves J, Orive G (2013) Plasma rich in growth factors (PRGF-Endoret) stimulates corneal wound healing and reduces haze formation after PRK surgery. Exp Eye Res 115:153–161
15. Bausset O, Giraudo L, Veran J, Magalon J, Coudreuse JM, Magalon G, Dubois C, Serratrice N, Dignat-George F, Sabatier F (2012) Formulation and storage of platelet-rich plasma homemade product. Biores Open Access 1(3):115–123. doi:10.1089/biores.2012.0225
16. Rodrigues SV, Acharya AB, Thakur SL (2012) Platelet-rich plasma. A review. N Y State Dent J 78(1):26–30
17. Kerstin Jurk K, Kehrel BE (2005) Platelets: physiology and biochemistry. Semin Thromb Hemost 31(4):381–392
18. Minor AH, Burnett L (1952) Method for separating and concentrating platelets from human blood. Blood 7(7):693–699
19. Sanchez AR, Sheridan PJ, Kupp LI (2003) Is platelet-rich plasma the perfect enhancement factor? A current review. Int J Oral Maxillofac Implants 18:93–103
20. El-Sharkawy H, Kantarci A, Deady J, Hasturk H, Liu H, Alshahat M et al (2007) Platelet-rich plasma: growth factors and pro- and anti-inflammatory properties. J Periodontol 78:661–669
21. Anitua E, Andia I, Ardanza B, Nurden P, Nurden AT (2004) Autologous platelets as a source of proteins for healing and tissue regeneration. Thromb Haemost 91:4–15
22. Hanna R, Trejo PM, Weltman RL (2004) Treatment of intrabony defects with bovine-derived xenograft alone and in combination with platelet-rich plasma: a randomized clinical trial. J Periodontol 75:1668–1677
23. Cavallo C, Filardo G, Mariani E, Kon E, Marcacci M, Pereira Ruiz MT, Facchini A, Grigolo B (2014) Comparison of platelet-rich plasma formulations for cartilage healing: an in vitro study. J Bone Joint Surg Am 96(5):423–429
24. Dallaudiere B, Pesquer L, Meyer P, Silvestre A, Perozziello A, Peuchant A, Durieuş MH, Loriaut P, Hummel V, Boyer P, Schouman-Claeys E, Serfaty JM (2014) Intratendinous injection of Platelet-Rich Plasma under US Guidance to treat tendinopathy: A long-term pilot study. J Vasc Interv Radiol 5: 1051–1057

Development of the Musculoskeletal System

17

Barış Baykal and Petek Korkusuz

Abstract

Development of the musculoskeletal system is a complex series of events during the intrauterine life. In this section, we discuss the development of the musculoskeletal system, give brief information on the molecules affecting the development, and give some information on anomalies regarding the musculoskeletal system.

Introduction

Development of the musculoskeletal system involves intricate events that occur during the fourth to eighth week of development. During this period, interactions between various tissues cause the formation of musculoskeletal system of the human body. In this section, we aimed to discuss the development of the musculoskeletal parts of the body, which are the areas of interest of orthopedic surgeons. We will first discuss the formation and histogenesis of embryonic structures and tissues, the formation of axial musculoskeletal components, and then the formation of the limbs.

B. Baykal, MD
Department of Histology and Embryology, Gulhane Military Medical Academy, School of Medicine, Ankara, Turkey

P. Korkusuz, MD, PhD (✉)
Department of Histology and Embryology, Hacettepe University Faculty of Medicine, Ankara, Turkey
e-mail: petek@hacettepe.edu.tr

Formation of the Trilaminar Germ Disc and Its Derivatives

On the third week of development, a thickened linear band of epiblast, termed as primitive streak, appears in the medial plane of the dorsal aspect of the bilaminar embryonic disc. The cranial end of the primitive streak proliferates and forms the primitive node. Cells leave the primitive streak from its deep surface to form the mesoblast, which forms the mesenchyme, a loose embryonic connective tissue. At this point, the trilaminar germ disc is formed. Some mesenchymal cells migrate cranially from the primitive node and form the notochord, a rodlike process, which lies in the midline of the trilaminar germ disc from the primitive node to the prechordal plate between the endoderm and ectoderm [1]. Notochord is the first structure of the future axial skeleton. During development, the notochord becomes a slender rod of cells running the length of the embryo between the neural tube and the developing gut [2].

F. Korkusuz (ed.), *Musculoskeletal Research and Basic Science*,
DOI 10.1007/978-3-319-20777-3_17

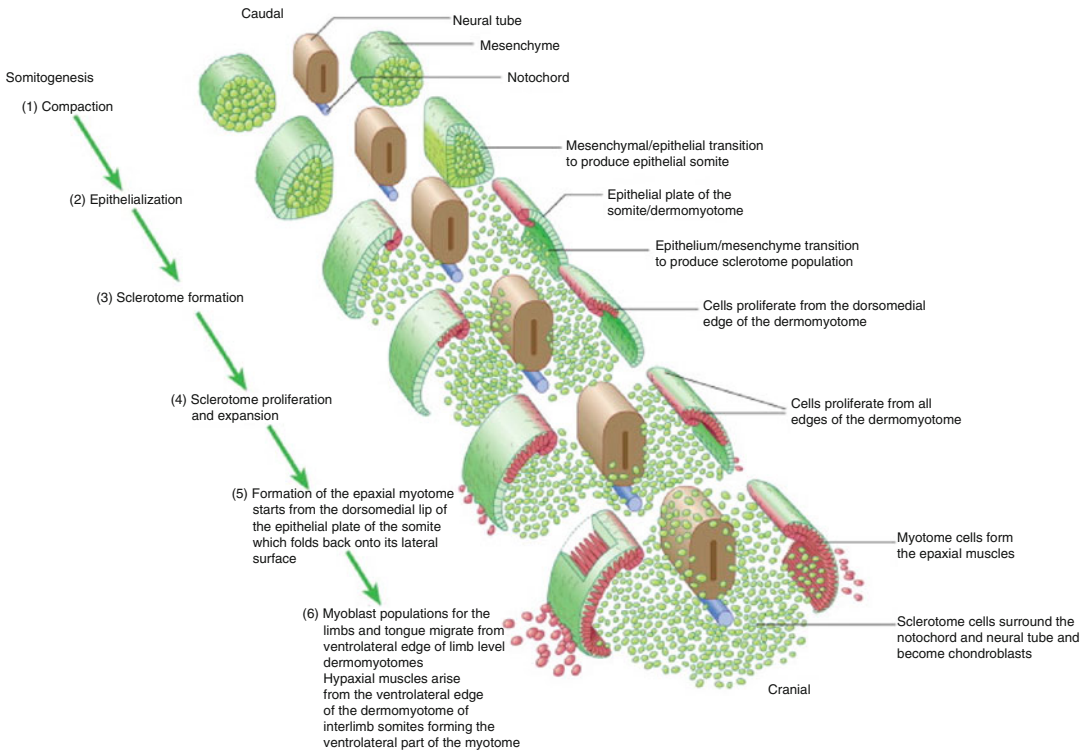

Fig. 17.1 The stages of somitogenesis. Development occurs in a craniocaudal order. The more cranially placed somites (at the *lower right* of the figure) are further developed than those caudally placed (at the *upper left* of the figure). The stages in somitogenesis are given on the *left* of the figure; more detailed information is given on the *right* (This figure was published in Gray's Anatomy, 40th Edition, Standring et. al., Development of the Back, 764, Copyright Elsevier (2008) [9]. Reproduction of this material is granted by Elsevier)

Mesoderm is laid down during gastrulation in an unsegmented manner, and mesodermal cells spread laterally between the ectoderm and endoderm forming a continuous layer [3, 4]. A thickened column of mesenchymal cells, termed as paraxial mesoderm, forms near the neural tube. Another compaction, the intermediate mesoderm, forms lateral to the paraxial mesoderm [3]. Lateral to the intermediate mesoderm is the lateral plate mesoderm, which is divided into somatic mesoderm and splanchnic mesoderm layers [1].

Compaction occurs in the paraxial mesoderm on both sides of the notochord, and spherical masses called somites are formed [2, 4–6]. The somites develop stepwise in a rostral to caudal direction along the body axis. Thus, the caudal-most somites are last formed [4]. As a result of this segmentation in the paraxial mesoderm, 42–44 pairs of somites (4 occipital, 8 cervical, 12 thoracic, 5 lumbar, 5 sacral, 8–10 coccygeal) are formed between the 19th and 32nd day of development. After that, the first of four occipital and the last seven or eight coccygeal somites regress and disappear. The early differentiation of all the persisting somites (the second occipital to the third or fourth coccygeal) is similar in the human embryo [2]. Early somites have an epithelial structure [7]. An epithelial/mesenchymal transition and dissociation takes place on the ventral and ventromedial walls of the somite, which gives rise to the mesenchymal sclerotome [4, 7]. The epithelial structure of the dorsal part of the somite is maintained, and the remaining cells on the dorsal epithelial part are called the dermomyotome [2, 4] (Figs. 17.1 and 17.2). Tendons associated with trunk muscles derive from the dorsal-most part of the sclerotome, termed as syndetome [8].

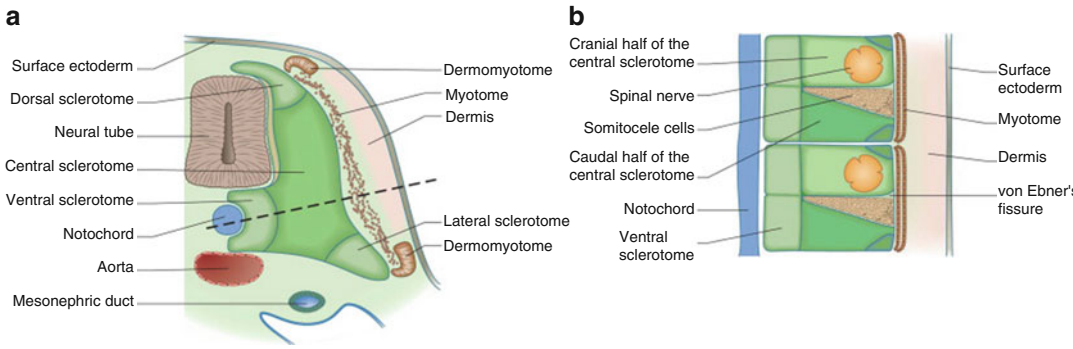

Fig. 17.2 Later development of the sclerotome. Transverse (**a**) and longitudinal (**b**) section through *dotted line* indicated in (**a**) showing the sclerotomal subdivisions (This figure was published in Gray's Anatomy, 40th Edition, Standring S. et. al., Development of the Back, 765, Copyright Elsevier (2008) [9]. Reproduction of this material is granted by Elsevier)

Table 17.1 Myotomes and their derivatives [11]

Myotome	Structure
Epaxial divisions of the myotomes	Extensor muscles of the neck, vertebral column, and lumbar region (deep muscles of the back that are attached to the vertebrae [7])
Sacral and coccygeal myotomes	Dorsal sacrococcygeal ligament
Hypaxial divisions of the cervical myotomes	Scalene, prevertebral, geniohyoid, and infrahyoid muscles
Thoracic myotomes	Lateral and ventral flexor muscles of the vertebral column
Lumbar myotomes	Quadratus lumborum muscle
Sacrococcygeal myotomes	Muscles of the pelvic diaphragm and probably the striated muscles of the anus and sex organs
Ventral portions of the last six or seven thoracic myotomes	Rectus abdominis muscle [2]

The sclerotome is the source of the vertebral column, ribs, tendons, and meninges, and the dermomyotome generates the vertebral and limb muscles, dermis, endothelial cells, and cartilage of the scapula blade [4, 5]. Each sclerotome has several portions: the central sclerotome (the main mass, close to the dermomyotome), the ventral sclerotome (close to the notochord), dorsal sclerotome, and lateral sclerotome (portions adjacent to the dermomyotome) [9] (Fig. 17.2).

A separate layer termed as the myotome is formed by the mesenchymal cells arising from the dorsomedial and ventrolateral borders of the dermomyotome [3] (Fig. 17.2). The cells produced by the myotome give rise to skeletal muscle dorsal to the vertebrae [9] (Table 17.1). At limb levels, cells from the ventrolateral edges of the dermomyotome loose their epithelial characteristics and migrate into the limb bud [9].

Differentiation of Muscle Cells

There are three types of muscle cells in the human body: smooth muscle, cardiac muscle, and striated muscle. Only the development of the striated muscle, which is one of the main interest areas of this book, will be discussed in this section.

Skeletal muscle of the trunk and limbs is derived from the myotomes of the somites [10]. As stated above, each somite has a myotome part. Each myotome divides into an epaxial (dorsal) division and a hypaxial (ventral) division [11]. These two divisions are innervated by the dorsal primary ramus and the ventral primary ramus, respectively, which are formed by the division on the spinal nerve that comes from the corresponding level of the developing spinal cord [11]. Even though muscles without an innervation will develop completely, a muscle that never had a nerve supply does not attain

its full differentiation at the fiber level and disappears with time [2]. The myotomes and the muscles derived from them are listed in Table 17.1 [11]. The first myotomes begin to differentiate into skeletal muscles early in the fifth week, and nearly all the skeletal muscles are present in a fetus of 8 weeks [2].

The structural units of skeletal muscle are called muscle cells or muscle fibers or myofibers [12]. The formation of new muscle fibers is termed as myogenesis. Prenatal myogenesis is divided into primary and secondary (fetal myogenesis), by which primary muscle fibers (during the embryonic stage) and secondary muscle fibers (during the fetal stage) develop respectively [13]. Myogenic precursors are derived from the cells that delaminate from the epaxial (adjacent to the neural tube) and hypaxial (adjacent to the lateral mesoderm) lips of the dermomyotome [7]. Myogenic precursor cells proliferate to increase their number. Under proper induction, myogenic precursors differentiate into myoblasts [13]. Myoblasts are mononucleated cells [2]. Under the influence of environmental signals, myoblasts align with each other, and their nuclei and cell bodies elongate in a direction parallel to the long axis of the embryo and proliferate by repeated mitotic divisions [2, 13]. Subsequently, they fuse with each other to form syncytia. Each syncytium turns into a tube (myotube) with continuous cytoplasm. The formation of myotubes begins at about the fifth week of embryonic development. The numerous nuclei within each syncytium are centrally located. Myofilaments of actin and myosin are laid down within the cytoplasm of each myotube and are oriented parallel to the long axis of the tube side by side. Thus, the myotube becomes a muscle fiber [2]. The myotubes become invested with external laminae during their development, and the external laminae segregate them from the surrounding connective tissue. The perimysium and epimysium layers of the fibrous sheath of the muscle are produced by fibroblasts; the endomysium is formed by the external lamina and reticular fibers [11]. The nuclei of the muscle fibers do not divide mitotically or amitotically. For the muscle fibers to grow in length, incorporation of new myoblasts into the syncytia is required [2]. The majority of muscle fibers are formed by secondary myogenesis. For this reason, the fetal stage is critical for skeletal muscle development [13]. Development of primary myotubes is autonomous, but the development of secondary myotubes, which form the majority of muscle cells of the adult, is dependent on innervation. Also, new muscle fibers cannot be generated in the absence of muscle contraction even if the nerves are present [14]. The persisting population of myoblasts found in close relationship to muscle fibers is the sources of subsequent generations of myotubes [2].

Development of Cartilage Tissue

The mesenchymal cells proliferate and condense in areas where the cartilage is going to form [15, 16]. These areas are termed chondrification centers [15]. Mesenchymal cells take round shape with round or oval nuclei and a low cytoplasm to nucleus ratio. The cells differentiate into chondroblasts, which secrete the extracellular matrix (type II collagen fibers, type IX collagen, and cartilage proteoglycan core protein) of the cartilage tissue [16]. There are three types of cartilages: hyaline cartilage (e.g., in synovial joints), fibrocartilage (e.g., in intervertebral discs), and elastic cartilage (e.g., in auricle of the ear) [15]. In areas of hyaline cartilage, continuous secretion of matrix separates the cells of condensed chondrification centers, thus taking the typical appearance of hyaline cartilage [16]. Hyaline cartilage is the most widely distributed type of cartilage and an example is the articular cartilage [15]. In areas of fibrocartilage formation, many of the cells differentiate into fibroblasts and secrete collagen. Chondroblastic activity appears only in isolated groups or rows of cells which become surrounded by dense bundles of collagen fibers secreted by the fibroblasts [16]. Fibrocartilage is found in intervertebral discs [15]. In areas of elastic cartilage formation, elastic fibers are secreted by the chondroblasts [16]. Elastic cartilage exists in auricles of the external ears [15].

The condensed mesenchyme surrounding the developing cartilage differentiates into a bilayered perichondrium [16]. The articular cartilage is not surrounded by perichondrium [2]. The cells of the outer layer of the perichondrium differentiate into fibroblasts and secrete a dense collagenous matrix. The cells of the inner layer differentiate into chondroblasts or prechondroblasts, which are in a resting state [16].

Development of Bone Tissue

Two types of bone formation (ossification) occur in the embryo. In intramembranous ossification, the mesenchyme condenses and becomes highly vascular [15]. Some cells differentiate into osteoprogenitor cells [16]. Osteoprogenitor cells proliferate around the branches of the capillary network and differentiate into osteoblasts (bone-forming cells) [15, 16]. Osteoblasts begin to deposit osteoid (unmineralized matrix), in which calcium hydroxy apatite is later deposited. As the osteoblasts deposit the matrix around their cell membrane, they are trapped and become osteocytes. During this process and afterwards, osteocytes remain connected to each other via their fine processes [16]. The space occupied by the osteocytes is called lacunae and the tubular spaces occupied by their processes are called canaliculi [15, 16]. As the bone spicules grow in size by the addition of newly synthesized matrix, they form a network of trabeculae [16] (Fig. 17.3).

In endochondral bone formation, first, a model of hyaline cartilage is formed in the area where the bone is to form [15]. The deep layers of the perichondrium around this model contain osteoprogenitor cells. These cells differentiate into osteoblasts [16]. Osteoblasts form a layer of bone tissue that surrounds the central shaft of the cartilage model (i.e., the diaphysis of the future bone) [15]. This layer of the bone is termed as the bony collar (periosteal bone) and is the first sign of ossification. From this point on, the role of the perichondrium has changed and it is now the periosteum [17]. The bony collar is thought to act as a diffusion barrier which impedes nutrient movement from the capillary network residing outside the cartilage model and thus triggers the events in endochondral ossification by virtue of nutrient deprivation [18, 19]. Concurrently with the formation of the bony collar, the chondrocytes within the center of the cartilage model begin to enlarge, their cytoplasms become vacuolated, and they accumulate glycogen [16, 17]. The matrix between these hypertrophic cells is compressed and resorbed and thus, perforated septa of thin

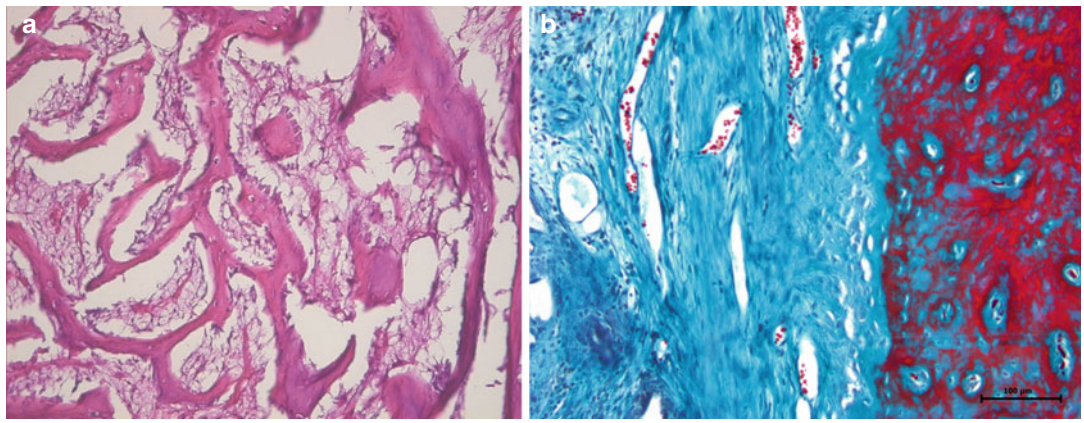

Fig. 17.3 Intramembranous ossification. (**a**) Acidophilic bone trabeculae lined by osteoblastic cells, hematoxylin and eosin 200×. (**b**) Mature calcified bone is in red. Collagenous connective tissue that surrounds the osteoid is in *blue*, Masson's trichrome 200×

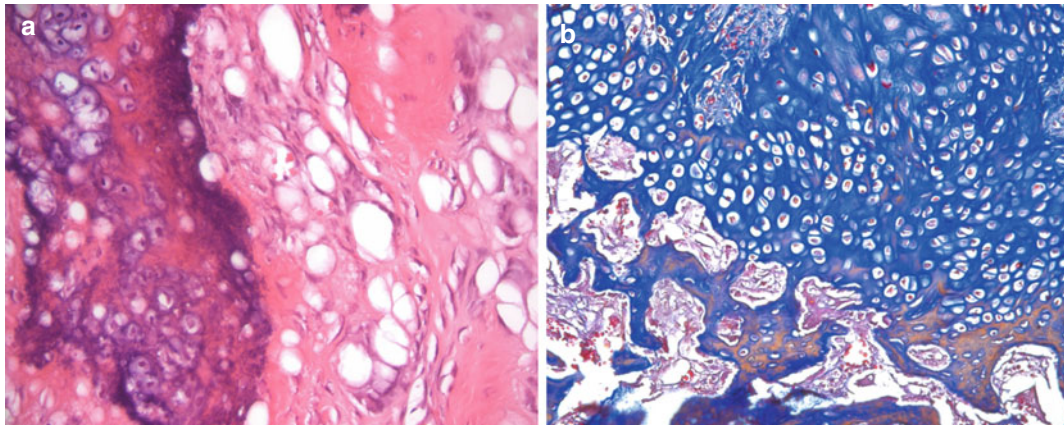

Fig. 17.4 Endochondral ossification. (**a**) Calcified cartilage is basophilically stained at the *left side*; new bone spicule is in *pink* (acidophilic) at the *right side* of the micrograph, hematoxylin and eosin 200×. (**b**) The cartilage is in *blue* at the *upper part*, and the new remodeling bone trabeculae with removal of cartilage residues are *reddish* at the *bottom*, Mallory trichrome 200×

irregular cartilage plates are formed. The cells begin to synthesize alkaline phosphatase, and the surrounding cartilage undergoes calcification [17]. The cells degenerate and leave behind enlarged lacunae. Blind-ended capillary sprouts (osteogenic or periosteal buds) originating from the periosteum invade the lacunae [16]. Osteogenic buds are accompanied by osteoprogenitor cells, and osteoclasts [16]. The blood vessels branch and project toward the borders of the primary ossification center [20]. Osteoprogenitor cells differentiate into osteoblasts, which attach themselves to the delicate residual walls of calcified cartilage and begin to deposit osteoid. A continuous lining of the bone forms over the cartilage residue [16]. A network of trabeculae forms by the addition of new osteoid over the previously formed spicules with cartilage cores (mixed spicules) [17]. At the same time, remodeling and removal of cartilage residues takes place by the action of osteoclasts [16, 17, 20] (Fig. 17.4). This area of the long bone, which is the first place of bone formation, is termed as primary ossification center [16, 17, 20]. Primary ossification center enlarges to the both ends of the bone until it reaches the future area of epiphyseal cartilage. Epiphyseal cartilages remain cartilaginous and persist until longitudinal growth ends in early adulthood [17]. The bony collar also extends to the both ends of the shaft of the long bone [16]. It is soon remodeled into compact bone. Secondary ossification centers appear in epiphyses of long bones shortly after birth [17]. In order for the embryo to grow in length, the cartilaginous model does not entirely turn into a bone. As the ossification front reaches near the ends of the cartilage model, the chondrocytes near the ossification front proliferate prior to undergoing hypertrophy and push out the cartilaginous ends of the bone [21]. These areas between the epiphyses and diaphyses of long bones are called epiphyseal growth plates [20]. Epiphyseal growth plate is formed of five zones: zone of reserve cartilage, zone of proliferation, zone of hypertrophy, zone of calcified cartilage, and zone of resorption. As ossification occurs by the events that occur in the last three zones, cartilage cells in the reserve cartilage that are nearest to the zone of proliferation proliferate and maintain the thickness of the proliferation zone [17].

The development of skeletal elements starts along a common pathway which diverges into osteogenic or chondrogenic programs depending on the nature of their local microenvironment [22] (Table 17.2). The long bones other than the clavicle are of endochondral origin [2].

Table 17.2 Molecular aspects of musculoskeletal development [22]

Molecule	Properties
Transforming growth factor-β	"Stimulates the synthesis of fibronectin and finally N-CAM" "Maintains the aggregated state of the cells in the preskeletal condensation"
RUNX-2	Starts the osteogenic program "Differentiation of mesenchymal cells into osteoblasts"
SOX-9	Starts the chondrogenic program Differentiation of mesenchymal cells into chondroblasts [20]
Indian hedgehog (Ihh), BMP-6	Induces hypertrophy of chondrocytes in the cartilage model of the future bone
Vascular endothelial growth factor	Secreted by the chondrocytes in the cartilage model of the future bone "Stimulates the ingrowth of blood vessels into the hypertrophic cartilage"
FGF-18	Secreted by the perichondrium "Inhibits the maturation of the chondrocytes around the periphery of the mass of cartilage"
RUNX-2, RUNX-3, Ihh	Periosteal bone (bony collar) formation
FGF, transforming growth factor-β	Keep the proliferating myogenic cells in the cell cycle
Insulin-like growth factor	Induces the postmitotic myoblasts to synthesize the major contractile proteins actin and myosin
Myf-5, MyoD	Commit certain cells of the dermomyotome to form muscle
Myostatin	"Arrests muscle growth when a muscle has attained its normal size"
Wnt	Activation of myogenesis [3]
Myogenin	Necessary for the fusion of myoblasts into myotubes [13]
Sonic hedgehog	Secreted by the notochord Induces the early somite to form the sclerotome, which induces the development of the vertebrae
Myf-5, Myf-6	Secreted by the myotomes of the thoracic-level somites "Stimulate the formation of the growth factors, platelet-derived growth factor (PDGF) and fibroblast growth factor (FGF), and cause proximal rib growth in the sclerotome"
BMP	Secreted by somatopleural mesoderm adjacent to the area of rib development "Formation of the distal portion of the ribs"
BMP-5, BMP-7	"Endogenous regulators of chondrogenesis and skeletal development" [15]

Development of the Joints

The joints begin to develop during the sixth week. Areas of condensed mesenchymal cells are observed between the neighboring developing bones [15]. These areas are termed interzonal mesenchyme and are the sites of future joints. In areas where fibrous joints will form, the interzone is converted into collagen [23] (Fig. 17.5). In synchondroses, the interzonal mesenchyme differentiates into hyaline cartilage, and in symphyses, it differentiates into fibrocartilage. In developing synovial joints, an intermediate zone appears in the interzonal mesenchyme and splits it into two dense layers [23]. The interzonal mesenchyme becomes cartilaginous like the developing bones, but cavitation takes place, and thus the joint cavity is formed [2, 23]. The mesenchyme around the cavity forms the joint capsule. The developing joints resemble adult joints by the end of the eighth week [15].

Development of the Axial Skeleton and Related Musculature

The dissociated cells of the sclerotome proliferate. A fissure that is initially filled with extracellular matrix and a few cells appears within

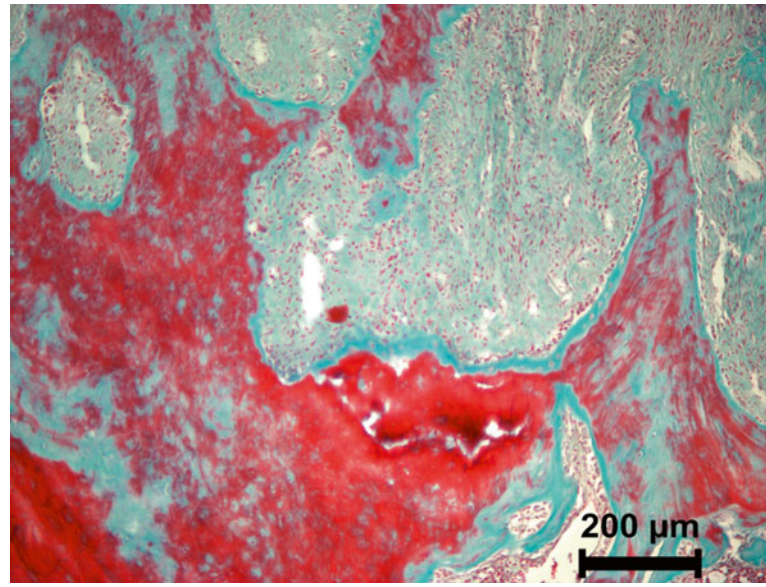

Fig. 17.5 In rat cranial suture as an example of fibrous joint, the interzone is converted into collagen. Collagen-rich connective tissue is in *green*, and cranial bone is in *red*, Masson's trichrome 100×

the sclerotome and divides it into two halves [9]. The cranial half is formed of loosely packed cells, and the caudal half is formed of densely packed cells [15]. The ventral sclerotomal cell populations on both sides of the notochord surround the notochord by migrating medially and form the perinotochordal sheath, which is an axial cell population within the extracellular matrix of the perinotochordal space. These cells undergo chondrogenic differentiation and form the cartilaginous model of the vertebral centrum [9] (Fig. 17.1). For the formation of each vertebra, the caudal half and the cranial half of two successive sclerotomes fuse [9]. The mesenchyme inside the sclerotomic fissure increases greatly in density and forms the future annulus fibrosus of the intervertebral disc [2, 9]. The notochord in the center of the developing intervertebral disc forms the nucleus pulposus [2] (Fig. 17.6). The central sclerotome gives rise to the pedicles and ventral parts of the neural arches and the proximal ribs. The dorsal sclerotomal cells form the dorsal part of the neural arches [9]. To form the neural arches and the costal processes, paired concentrations of mesenchymal cells extend dorsally and laterally from the body of the vertebrae. The costal processes of thoracic vertebrae form the ribs [2]. Distal ribs and endothelial cells of the blood vessels originate from the lateral sclerotomal cells [9]. The distal part (shaft) of each rib is derived from the lateral part of the adjacent cranial somite due to the resegmentation of the somites during the formation of the vertebrae. The ribs separate from the vertebrae by the time when ossification in the vertebrae begins [22]. The costal processes of the cervical vertebrae become the anterior part of the transverse foramen, and the costal processes of the lumbar vertebrae become the transverse processes of the lumbar vertebrae and the lateral part of the sacrum. The coccygeal vertebrae can be observed as a prominent tail at the fifth week. The tail regresses, and the four to five rudimentary vertebrae fuse with each other and become the coccyx [2]. Dorsal trunk muscles (epaxial muscles) originate from the dorsomedial lip of the dermomyotome [9]. They further divide into a medial (deep) and a lateral (superficial) group

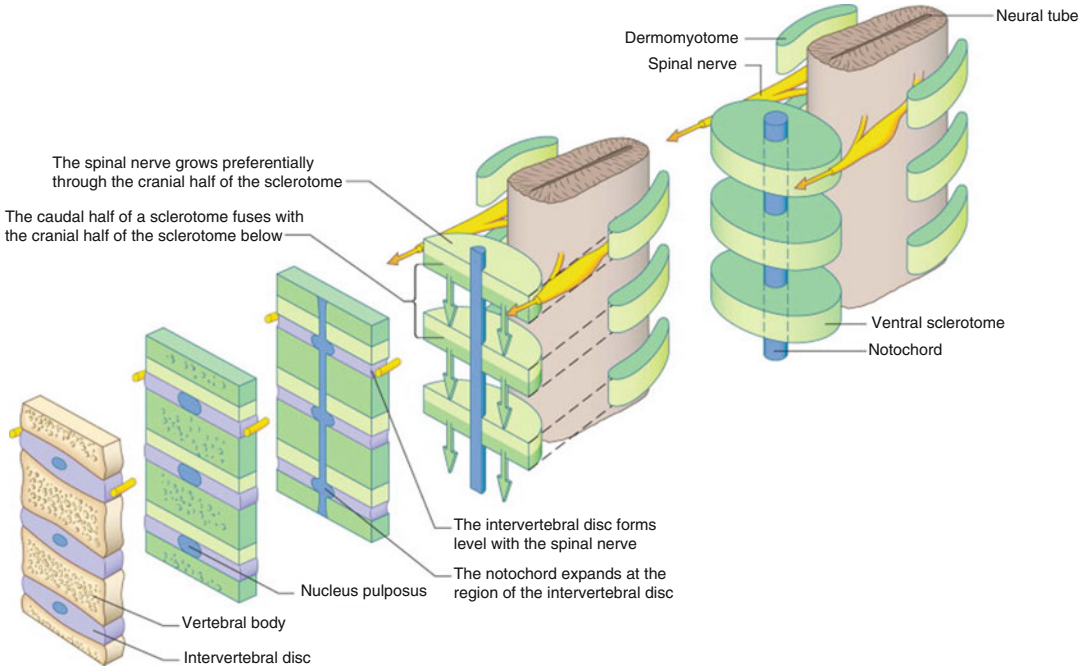

Fig. 17.6 Formation of vertebrae and intervertebral discs from the mesenchymal sclerotomes. Each vertebra is formed from the cranial half of one bilateral pair of sclerotomes and the caudal half of the next pair of sclerotomes (This figure was published in Gray's Anatomy, 40th Edition, Standring et. al., Development of the Back, 766, Copyright Elsevier (2008) [9]. Reproduction of this material is granted by Elsevier)

of muscles. The medial group forms the short oblique muscles of the vertebral column. The lateral group gives rise to the extensors of the vertebral column [2]. Ventrolateral trunk muscles (hypaxial muscles) originate from the ventrolateral edge of the dermomyotome [9]. The progenitors of axial muscles differentiate largely in situ by the influence of the neural tube and notochord. They initially differentiate into mononucleated myocytes by the expression of myogenic determination factors (Myf-5, MyoD) at or before the onset of myotome formation. The syndetome of the somites gives rise to the tendons of the epaxial muscles. The tendons of the hypaxial musculature arise from lateral plate mesoderm [22]. The layered muscles of the thorax and abdomen are formed by the extension of the hypomeres into the lateral and ventral body wall [2]. Some of the anomalies of the axial skeleton and related musculature are summarized in Table 17.3.

Development of the Limbs

Specific regions of the somatopleuric mesenchyme, which is located in the lateral body wall, are the origin of the limbs [23]. In these regions (the lower five cervical and the first thoracic myotomes for each upper limb and the second and fifth lumbar and the upper three sacral myotomes for each lower limb bud), near the end of the fourth week, somatopleuric mesenchyme proliferates extensively and gives rise to limb buds, which are the first visible signs of limb development [2, 23]. The limb buds appear during the fourth week [2]. They consist of a core of condensed mesenchyme and rimmed by a longitudinal ridge of high columnar epithelial cells. This ridge is termed the apical ectodermal ridge [2, 23]. The mesenchyme induces the development and maintenance of the apical ectodermal ridge [2]. Apical ectodermal ridge controls the growth of the limb bud [23]. At the posterior margin of

Table 17.3 Anomalies of the axial skeleton and related musculature [22]

Anomaly	Description
Spina bifida occulta	Incomplete closure of the bony roof of the spinal cord due to a defect in neural arches of the vertebrae
Spondylocostal dysostosis	"Abnormal segmentation of the vertebrae"
Hemivertebrae	Failure of formation of one half of a vertebra. The formed side has a unilateral pedicle. Causes scoliosis [25]
Butterfly vertebrae	Sagittally cleft vertebrae, possibly due to midline fusion defect
Block vertebrae	"Fused vertebrae"
Congenital scoliosis	Lateral curvature of the vertebral column, commonly caused by the presence of hemivertebrae
Klippel–Feil syndrome (brevicollis)	Characterized by a short neck, a low hairline, and limited neck motion due to fusion of one or more cervical vertebrae
Accessory ribs	Formation of extra ribs especially in the upper lumbar and lower cervical levels
Forked (fused, bifid, bifurcated) ribs	Fusion of some portions of two ribs due to misexpression of specific Hox genes
Prune belly syndrome	"Absence of the abdominal musculature"
Muscular dystrophy	"A family of genetic diseases characterized by the repeated degeneration and regeneration of various groups of muscles during postnatal life"
Myotubular myopathy	Persistence of fetal myotubes in extrauterine life. Primarily affects skeletal muscles. Causes muscle weakness and hypotonia [26, 28]
Congenital torticollis (wryneck)	Lateral bending of the head to the affected side and a slight turning away of the head from the affected side due to the shortening of the sternocleidomastoid muscle [11]

the limb bud, mesenchymal cells aggregate to form the zone of polarizing activity, which controls the normal patterning of the limbs along the anteroposterior axis [23, 27]. The early limb bud does not include any nerves. Initially, the mesenchyme of the limb bud consists of cells derived from the lateral plate mesoderm, which are the source of the connective tissues of the limb (cartilage, bone, tendon, and loose connective tissue) [23]. The skeletal muscles of the limb buds develop from the myotome cells, which migrate from the adjacent somites [2]. The nerves of the limbs originate from the cells that migrate from the neural crest [27].

In an early limb bud, one chondrogenesis center forms. During the lengthening and widening of the limb bud, the next two centers and more distally five centers of chondrogenesis appear [23]. The distal ends of the limb buds flatten [2]. Hand plates take paddle-like shape and foot plates take flipper-like shape [23]. The mesenchymal tissue in the hand and foot plates condenses to form digital rays. The tip of each digital ray has an apical ectodermal ridge, which induces development of the mesenchyme into the mesenchymal primordia of the bones (phalanges) in the digits [27]. A longitudinal condensation of mesenchyme forms in the future digit, and precartilaginous matrix is laid down. Then, segmentation occurs in the early digital ray to form specific phalangeal segments [24]. The loose mesenchyme between the digital rays undergoes tissue breakdown via apoptosis, and separate digits are formed by the end of the eighth week [27]. By the seventh week, the upper limbs make a 90° medial rotation on their longitudinal axes, and the lower limbs make a 90° medial rotation on their longitudinal axes [27].

Scapula is derived from lateral plate mesoderm except the blade part, which arises from the cells of the dermomyotome. Lateral plate mesoderm gives rise to the three bones of the pelvis [24]. Some of the molecules that effect limb development and their properties are summarized in Table 17.4 and some of the limb anomalies are summarized in Table 17.5.

Table 17.4 Molecular aspects of limb development [24]

Molecule	Source	Function
Tbx5	"Area of the future forelimb"	"Stimulates the expression and secretion of fibroblast growth factor-10 (FGF-10) by the local mesodermal cells" Beginning of limb development Limb muscle patterning
Tbx4	"Area of the future hindlimb"	"Stimulates the expression and secretion of fibroblast growth factor-10 (FGF-10) by the local mesodermal cells" Beginning of limb development Limb muscle patterning
Fibroblast growth factor-10 (FGF-10)	Local mesodermal cells of the future fore- and hindlimbs	"Stimulates the overlying ectoderm to produce FGF-8" Beginning of limb development
Gli-3	Anterior part of the early limb field	"Fixation of the anteroposterior axis"
Hand-2	Posterior part of the early limb field	"Fixation of the anteroposterior axis"
Radical fringe	Dorsal ectoderm of the limb bud	Determination of the position of the apical ectodermal ridge
Engrailed-1 (En-1)	Ventral ectoderm of the limb bud	Determination of the position of the apical ectodermal ridge
Hoxb8	Highest concentration at the location of future zone of polarizing activity	Determination of the location of zone of polarizing activity
FGF-4, FGF-9, FGF-17	Apical ectodermal ridge	Promotion of outgrowth
Sonic hedgehog (shh)	Zone of polarizing activity	"Organizes tissues along the anteroposterior axis" "Maintains the structure and function of the apical ectodermal ridge" Digit identity determination "Plays a pivotal role in digit patterning" [23]
Pitx-1	"Area of the future hindlimb"	Determination of hindlimb identity
Gremlin	"Posterior part of the limb bud"	Fixation of the anteroposterior axis "Functions as an apical ectodermal ridge maintenance factor" [23]
Wnt-7a	Dorsal ectoderm of the limb bud	Prevents differentiation of mesenchymal cells into cartilage "Acts as a dorsalizing signal" [23] Determination of dorsoventral axis
Hox family		"Involved in patterning of the proximodistal axis of the limb"
BMP-2, BMP-4, BMP-7, Msx-1, Msx-2	interdigital spaces	Initiatiation of interdigital cell death
Pbx-1, Pbx-2		Possible role in connection of limbs with their respective girdles
Wnt-14	Areas of joint formation	Formation of interzones of the joints [29]
Noggin	Areas of joint formation	Formation of interzones of the joints [30]
Scatter factor (hepatic growth factor)	"Proximal cells of the limb-forming area"	Stimulates the cells that originate from the ventral part of the dermomyotome to migrate toward the limb Formation of limb muscles
Wnt-6	Ectoderm of the limb bud	"Differentiation of the premuscle cells into muscle"

Table 17.5 Limb anomalies [24]

Anomaly	Description
Split hand–split foot malformation (ectrodactyly)	"Reduced number of digits and a wide separation between the anterior and posterior digits"
Intrauterine amputations	Loss of parts of digits or even hands or feet presumably caused by tears in the amnion
Clubfoot (talipes equinovarus)	Fixation of the ankle joint in inverted position due to the abnormal shortening of the muscles that invert the foot and the lengthening of their antagonists [2]
Amelia	Absence of an entire limb (Fig. 17.7a)
Meromelia	Absence of a part of a limb (Fig. 17.7b)
Macromelia (macrodactyly)	Enlarged limb or digit over the normal size (Fig. 17.8a, b)
Polydactyly	Presence of supernumerary digits
Syndactyly	Fusion of digits
Hemimelia	"Deficiencies of preaxial or postaxial limb components"
Brachypodism	"Shortening of the limb and the lack of development of certain joints"
Achondroplasia	Most common form of dwarfism resulting from mutations of the FGF receptor 3 gene and characterized by short stature secondary to limb shortening, midface hypoplasia, disproportionately large head, and pronounced lumbar lordosis [22]
Thanatophoric dysplasia	Severe shortening of the extremities and very narrow thorax. Usually death occurs in infancy due to respiratory insufficiency [22]
Campomelic dysplasia	"Characterized by pronounced bowing of the limbs, a variety of other skeletal anomalies, and sex reversal in XY males, resulting from a disruption of SOX-9 in sexual differentiation" [22]
Oligodactyly	Formation of fewer than five digits [23]
Arthrogryposis	"Multiple congenital joint contractions" [11]
Thumb hypoplasia	"Congenital underdevelopment of the thumb, which can range from a slight decrease in thumb size to complete absence" [31] (Fig. 17.8c, d)

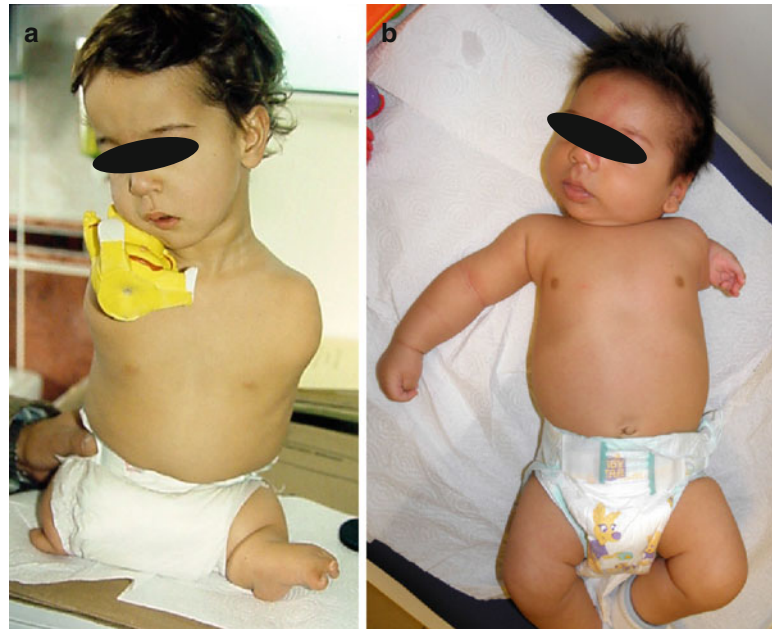

Fig. 17.7 Amelia (absence of an entire limb) (**a**) and meromelia (absence of a part of a limb) in upper and/or lower limbs (**b**) (Courtesy of Professor A. Gursel Leblebicioglu MD, Hacettepe University Faculty of Medicine Department of Orthopedic Surgery and Traumatology)

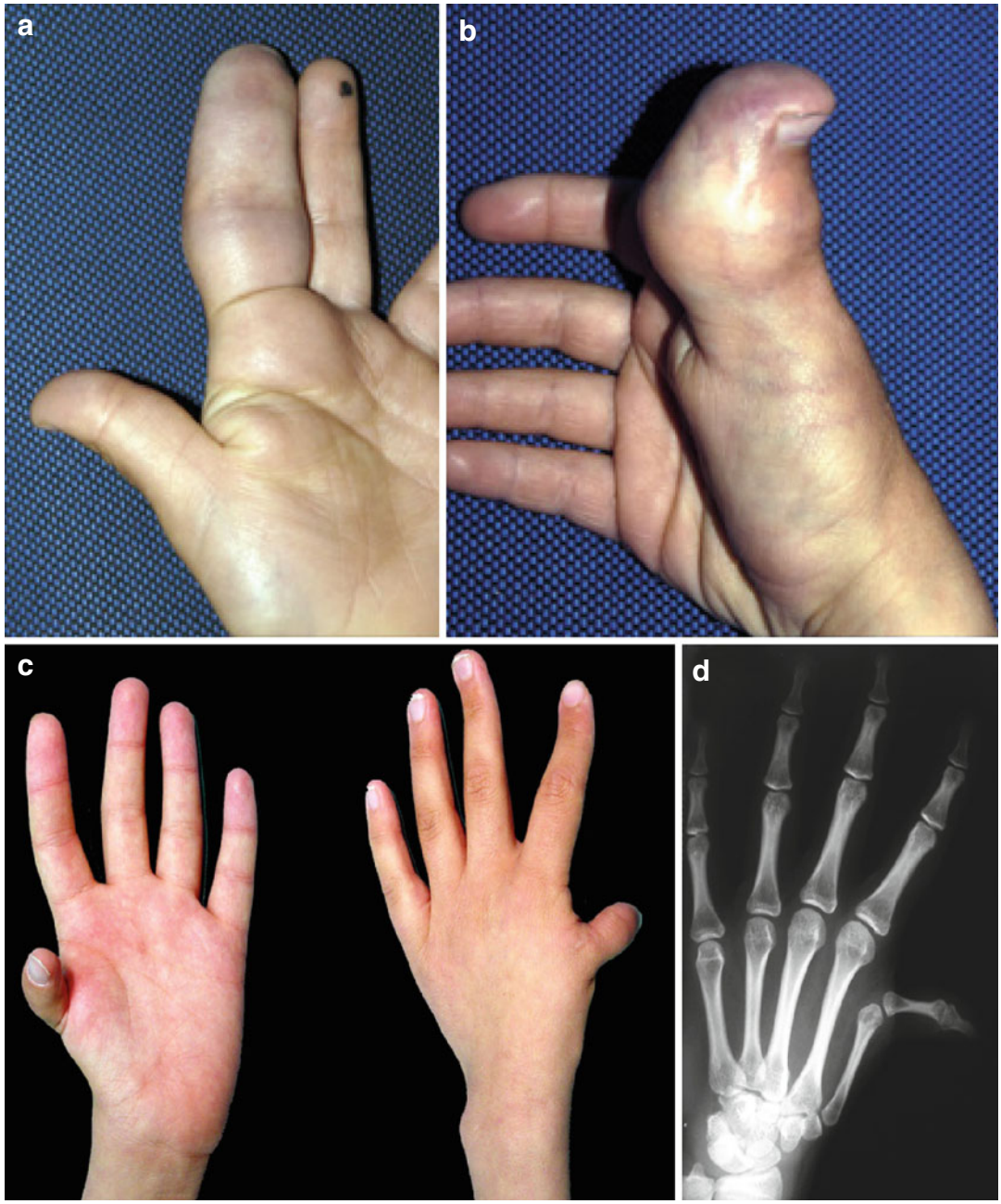

Fig. 17.8 (**a**, **b**) *Upper panel*: macrodactyly; (**c**, **d**) *lower panel*: thumb hypoplasia (Courtesy of Professor A. Gursel Leblebicioglu MD, Hacettepe University Faculty of Medicine Department of Orthopedic Surgery and Traumatology)

References

1. Moore KL, Persaud TVN, Torchia MG (2013) Third week of development. In: Moore KL, Persaud TVN, Torchia MG (eds) Before we are born: essentials of embryology and birth defects. Saunders, Philadelphia, pp 35–47. Electronic version
2. Iannotti JP, Parker RD (2013) Embryology. In: Iannotti JP (ed) Netter collection of medical illustrations: biology and systemic diseases. Saunders, Philadelphia, pp 1–22. Electronic version
3. Carlson BM (2014) Establishment of the basic embryonic body plan. In: Carlson BM (ed) Human embryology and developmental biology. Saunders, Philadelphia, pp 92–116. Electronic version
4. Kalcheim C, Ben-Yair R (2005) Cell rearrangements during development of the somite and its derivatives. Curr Opin Genet Dev 15(4):371–380
5. Christ B, Ordahl C (1995) Early stages of chick somite development. Anat Embryol 191(5):381–396
6. Gossler A, de Angelis MH (1997) Somitogenesis. In: Roger AP, Gerald PS (eds) Current topics in developmental biology. Academic, New York, pp 225–287
7. Hill JA, Olson EN (2012) Skeletal muscle development. In: Hill JA (ed) Muscle: fundamental biology and mechanisms of disease. Elsevier, San Diego, pp 749–762. Electronic version
8. Brent AE, Schweitzer R, Tabin CJ (2003) A somitic compartment of tendon progenitors. Cell 113(2):235–248
9. Standring S et al (2008) Development of the back. In: Standring S (ed) Gray's anatomy. Churchill Livingstone, Spain, pp 763–773
10. Tajbakhsh S, Buckingham M (1999) The birth of muscle progenitor cells in the mouse: spatiotemporal considerations. In: Charles PO (ed) Current topics in developmental biology. Academic, London, pp 225–268
11. Moore KL, Persaud TVN, Torchia MG (2013) Muscular system. In: Moore KL, Persaud TVN, Torchia MG (eds) The developing human. Saunders, Philadelphia, pp 363–370. Electronic version
12. Ross MH, Pawlina W (2011) Muscle tissue. In: Ross MH, Pawlina W (eds) Histology: a text and atlas. Lippincott Williams & Wilkins, China, pp 310–351
13. Yan X et al (2013) Developmental programming of fetal skeletal muscle and adipose tissue development. J Genom 1:29–38
14. Harris AJ (1981) Embryonic growth and innervation of rat skeletal muscles. I. Neural regulation of muscle fibre numbers. Philos Trans R Soc Lond B Biol Sci 293(1065):257–277
15. Moore KL, Persaud TVN, Torchia MG (2013) Skeletal system. In: Moore KL, Persaud TVN, Torchia MG (eds) Before we are born: essentials of embryology and birth defects. Saunders, Philadelphia, pp 223–246. Electronic version
16. Standring S et al (2008) Functional anatomy of the musculoskeletal system. In: Standring S (ed) Gray's anatomy. Churchill Livingstone, Spain, pp 81–125
17. Ross MH, Pawlina W (2011) Bone. In: Ross MH, Pawlina W (eds) Histology: a text and atlas. Lippincott Williams & Wilkins, China, pp 218–253
18. Caplan AI (1988) Bone development. Ciba Found Symp 136:3–21
19. Bianco P et al (1998) Bone formation via cartilage models: the "borderline" chondrocyte. Matrix Biol 17(3):185–192
20. Kierszenbaum AL, Tres LL (2012) Osteogenesis. In: Kierszenbaum AL, Tres LL (eds) Histology and cell biology: an introduction to pathology. Saunders, Philadelphia, pp 151–168. Electronic version
21. Gilbert S (2000) Osteogenesis: the development of bones. In: Developmental biology. Sinauer Associates, Sunderland, p 11
22. Carlson BM (2014) Integumentary, skeletal, and muscular systems. In: Carlson BM (ed) Human embryology and developmental biology. Saunders, Philadelphia, pp 156–192. Electronic version
23. Standring S et al (2008) Development of the limbs. In: Standring S (ed) Gray's anatomy. Churchill Livingstone, Spain, pp 899–904
24. Carlson BM (2014) Limb development. In: Carlson BM (ed) Human embryology and developmental biology. Saunders, Philadelphia, pp 193–215. Electronic version
25. Sponseller PD, Ting BL (2011) Congenital scoliosis. In: Herkowitz HN et al (eds) Rothman-Simeone the spine. Saunders, Philadelphia, pp 374–384. Electronic version
26. Spiro AJ, Shy GM, Gonatas NK (1966) Myotubular myopathy. Persistence of fetal muscle in an adolescent boy. Arch Neurol 14(1):1–14
27. Moore KL, Persaud TVN, Torchia MG (2013) Development of limbs. In: Moore KL, Persaud TVN, Torchia MG (eds) The developing human. Saunders, Philadelphia, pp 371–387. Electronic version
28. Stickland NC (1981) Muscle development in the human fetus as exemplified by m. sartorius: a quantitative study. J Anat 132(Pt 4):557–579
29. Hartmann C, Tabin CJ (2001) Wnt-14 plays a pivotal role in inducing synovial joint formation in the developing appendicular skeleton. Cell 104(3):341–351
30. Khan IM, Redman SN, Williams R, Dowthwaite GP, Oldfield SF, Archer CW (2007) The development of synovial joints. Curr Top Dev Biol 79:1–36
31. Soldado F, Zlotolow DA, Kozin SH (2013) Thumb hypoplasia. J Hand Surg Am 38(7):1435–1444

Bone

18

Önder Kalenderer and Ali Turgut

Abstract

Bone is a hard tissue that; protects the body organs, produce blood cells, and stores minerals. In a new-born body there is more than quantity of 270 bones and during different life stages this number decreases to 206 by coalisions in mature skeleton.

Bone tissue is basically divided into three types as long, short and flat according to its shape. Long and short bones are derived by cartilage model as endochondral ossification, flat bones are formed by concentration of mesenchymal tissues (intramembranous ossification). The hard outer portion that contains lower amount of space is called cortex and more soft and spongy structure that is biologically more active is the inner part and called trabecular bone. Bone tissue as the basis contains three type of cells that are; osteoblasts, osteoclasts and osteosits. Osteosits are the main types (larger amount) of cells in the mature skeleton that consist of trapped former osteoblast in the newly formed matrix. Osteoblasts are cells that are responsible for bone production while osteoclast are bone destructor. Bone matrix is developed by organic and inorganic component. Organic matrix is 40 % of dry weight of bone tissue and 90 % of this type of matrix is formed by collagens (mainly type 1). 60 % of the dry weight of the bone is inorganic matrix that contains calcium hydroxyapatite and calcium phosphate.

Bone's hard and mineralized nature is closely associated with the dynamic and self-renewal behavior. This dynamic structure; ensures the continuum of structural integrity, mechanical resistance and contributes to heal without scar tissue. This is achieved through the construction and destruction of the bone regularly. When the balance of construction and

Ö. Kalenderer (✉) • A. Turgut
Department of Orthopaedics and Traumatology,
Tepecik Training and Research Hospital,
İzmir, Turkey
e-mail: okalenderer@gmail.com

F. Korkusuz (ed.), *Musculoskeletal Research and Basic Science*,
DOI 10.1007/978-3-319-20777-3_18

destruction of bone fails, diseases such as osteoporosis, osteopetrozis can be seen. Cortical and trabecular bone remodels by osteoblastic and osteoclastic activities throughout life. All bone tissue can completely refresh itself in 4 – 20 years.

The bone is a hard tissue which protects and supports the organs in the body, produces red and white blood cells, and stores minerals. In a moving organism, bone tissue resists to fractures and failures ideally with a low weight. It consists of bone marrow, endosteum, periosteum, blood vessels, nerves, and cartilage tissue. There are more than 270 bones in human body at birth, but by coalition in various stages of life, this number decreases to 206 in adulthood. The biggest bone is the femur in the human body, while the smallest ones are located in the middle ear [1].

Functions of the Bone

The bone's functions can be divided into 11 subtitles. These functions are [2, 3]:

Protection function: The skull bones protect the brain and the ribs protect the heart and lungs.
Structural support function: The bone forms the basic structure of the skeleton supporting the body.
Motion function: The bones act with the muscles, tendons, and nerves to move the separate parts of the body independently.
Sound transmission: The bones are an important transmitter for hearing.
Blood production: Long bone marrow produces blood in the channel.
Mineral storage: The bone serves a repository function especially for calcium and phosphorus.
Growth factor storage: Mineralized bone matrix contains growth factors such as insulin-like growth factor (IGF), transforming growth factor (TGF), and bone morphogenetic protein (BMP).
Oil storage: Yellow bone marrow stores fatty acids.
Acid-base balance: The bone helps in maintaining blood pH balance by increasing or decreasing the release of alkaline salt.
Detoxification: Bone tissue absorbs heavy metals.
Endocrine effects: The bone reduces the absorption of phosphate via the kidneys by secretion of fibroblast growth factor 23 (FGF-23). Bone cells can also be effective in regulating blood glucose and fat storage by secretion of osteocalcin (increases insulin levels and decreases fat storage) [4].

Anatomy

Bone tissue is mainly divided into three, according to its shape as long, short, and flat bones. The long and short bones are formed by endochondral ossification through the cartilage model, and flat bones are formed by condensation of mesenchymal tissue (intramembranous ossification) [5]. Long bones such as the femur, humerus, and tibia are divided into three regions as epiphysis, metaphysis, and diaphysis. These three regions are separated according to their geometry and structure. Epiphysis and metaphysis consist of cancellous bone surrounded by a thin cortical bone and are separated from each other by physis in the people who continue to grow. Physis scar line or epiphyseal line exists after the closure of the physis (growth plate). Cortical bone (diaphysis) is a tubular structure with a thin cancellous bone which is surrounded by a thick cortical bone, and there is a channel in the middle. The inside of the cortical bone is called as endosteal face, while the outer surface other than the joint surface is called periosteal face. The bone tissue just below the articular cartilage of long bones is called as subchondral bone. Cartilage cells surround the subchondral bone [5].

All bone surfaces are surrounded by specialized cells or tissues. Periosteal face is covered with periosteal membrane. In the outer part, there is fibrous connective tissue, while the interior part consists of unchanged native/undifferentiated

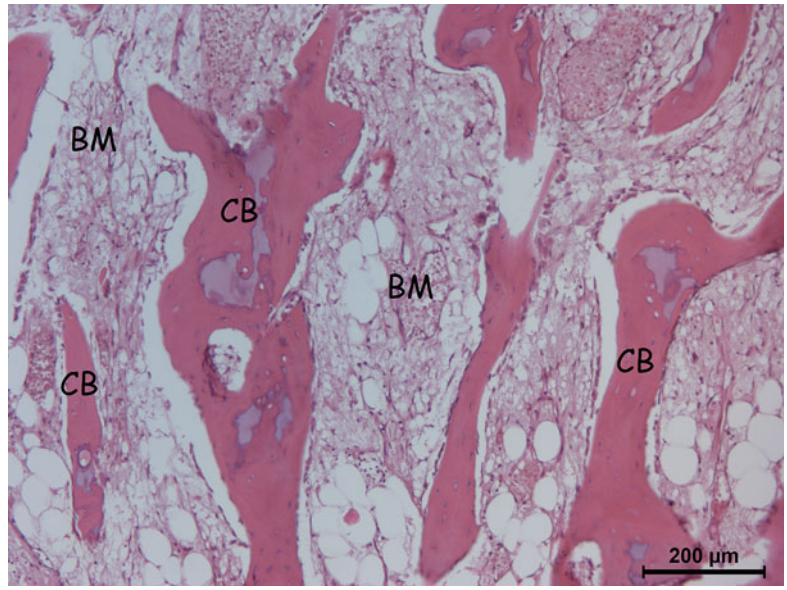

Fig. 18.1 Microscopic appearance of cancellous bone and bone marrow. *BM* bone marrow, *CB* cancellous bone

progenitor cells which form the bone during growth and fracture healing.

Vertebra, sternum, carpal, and tarsal bones are examples of short bones and are mainly composed of very fine cancellous and thin cortical bone. The bone is a hard tissue but contains gaps between the hard components. Lamellar bone is a tissue where collagen and osteoblasts are regularly inhabited and consists of two parts as cortical and trabecular. Braided (woven) bone is an irregular, weak, and more flexible bone tissue which can be formed during pathological conditions, embryonic development, and fracture healing [6].

Cortical Bone

Cortical bone is the part that contains less space which forms the hard outer part of the bone. The porosity is from 5 to 30 %. It looks straight, white, and tough. Macrostructure varies according to anatomic location. Cortical bone which is located in diaphysis is load-bearing and has a cylindrical structure surrounding the medullary channel. In metaphysis, epiphysis, and flat bone, cortical bone component acts as a shield for cancellous portion which is the part that is mainly load bearing. Although carrying a small portion of the load in this area, it distributes the forces which are mainly acting on trabecular bone. Cortical bone makes up about 80 % of bone tissue in adult skeleton [7, 8].

Trabecular Bone

Trabecular bone is also known as cancellous bone. It is the part of the bone which is biologically more active and more flexible and has more remodeling capacity to stress. Osteons and Haversian systems are found in cortical bone, whereas trabecular bone does not involve them [7, 8].

Tissue Organization

Cortical and cancellous bone is not only separated from each other by macroscopic appearance but also with microscopic structure and tissue organization. Bone tissue is primarily formed by extracellular matrix that consists of the collagen and inorganic minerals. Osteocytes are cells that are embedded within the matrix. Amount of space for osteocytes and their cellular extensions in the matrix is important for tissue structure and function (Fig. 18.1) [5].

Cancellous Bone

Bone tissue is formed in a place which does not contain any prior bone tissues. Embryos, bone growth, fracture callus, heterotopic ossification, Paget's bone, and the bone which is generated by tumors can be given as an example. Collagen and minerals are located randomly. Osteocyte organization is not clear. Cancellous bone remodels with removal of primary bone tissue and replacement with secondary bone formation. This formed new bone tissue is named as lamellar bone [5].

Lamellar Bone

This tissue is well organized with lamellar layers in contrast to irregular cancellous bone tissue. Lamellas are 3–7 μ thick layer that can be seen with polarized light microscopy. The layered appearance is not understood exactly; it is thought to be related to configuration of collagen fibers and extracellular matrix. Lamellas are formed after the elimination of an existing bone and as a result of remodeling process. In other words, the secondary bone tissue is such always in lamellar form. On the other hand, primary bone tissue is usually cancellous, but sometimes, it can be in lamellar bone form. For example, during environmental bone growth, environmental lamellas can be created by periosteal cells. Cancellous bone is formed faster than lamellar bone and contains less mineralized smaller crystals than lamellar bone, thereby more easily removed during remodeling. Lamellar bone consists of a process slower and more regular than cancellous bone, and mechanical properties are very important for mature bone. Lamellar tissue varies in cortical and cancellous bone.

Lamellar Cortical Bone

Cortical bone is organized into dense cylindrical lamellar structures – osteons which are also referred to as the Haversian system. Osteons are usually 3–6 mm in length and in diameter of 150–300 μ. In the center of osteons, there is a cylindrical cavity called the Haversian canal which vessels and poor myelinized nerve fibers pass through. Haversian canals are connected to each other or to surface of the bone by the Volkmann channels. The Haversian and Volkmann channels contribute a small amount to the porosity of cortical bone tissue. Each osteon is surrounded by cement lines (Figs. 18.2 and 18.3).

Lamellar Cancellous Bone

As in cortical bone, spongiosa is also subject to be organized into lamellae surrounded by cement lines [7].

Lacunae/Canaliculi

Gaps in the bone tissue are important for the mechanical properties and behavior. Cancellous or cortical bone tissue all contain osteocytes buried in the mineralized matrix. Osteocytes are present in the ellipsoidal cavity which is called lacunae. There are approximately 15,000 units of lacunae in each 1 mm bone tissue, and they constitute of 1 % of the bone. Recent studies report that the number and size of the lacunae can vary depending on bone health and the anatomical location. Most of the crack ends in lacuna, and starting from this point, it can be thought that lacunae stop the cracks and inhibit the progress of the cracks. Lacunae connect with each other, Haversian system, and bone surface by means of the canaliculi. Osteocyte cell extensions pass through in the canaliculi to connect with other osteocytes and bone cells on the surface. This network allows osteocytes for nutrients and oxygen, and again, this network removes waste. This network is very important that the mineralized matrix is not permeable to nutrients (Fig. 18.4).

Cement Lines

Cement lines are located in both cortical and secondary cancellous bones. Their thickness is 1–2 μ, and they contain small amount of collagen

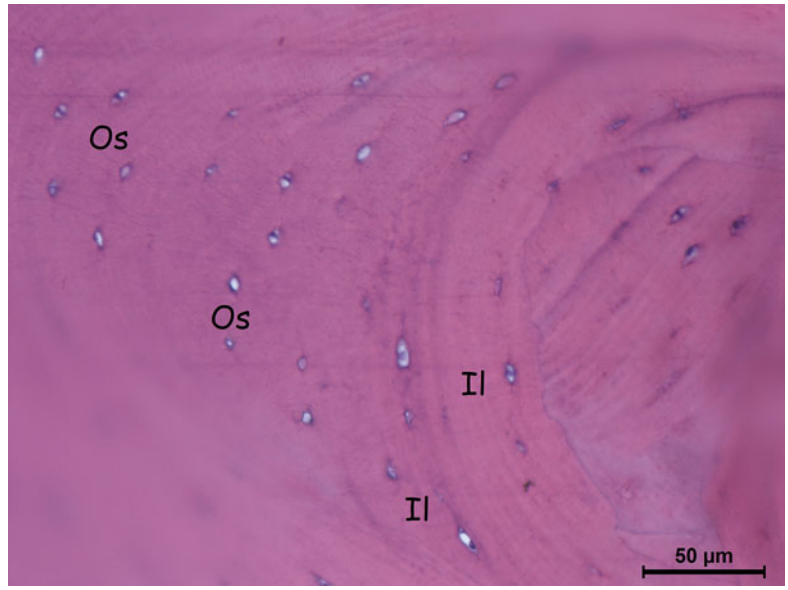

Fig. 18.2 Lamellar cortical bone's cross section (osteocytes, interstitial lamellae). *Os* osteocytes, *IL* interstitial (intermediate) lamellae

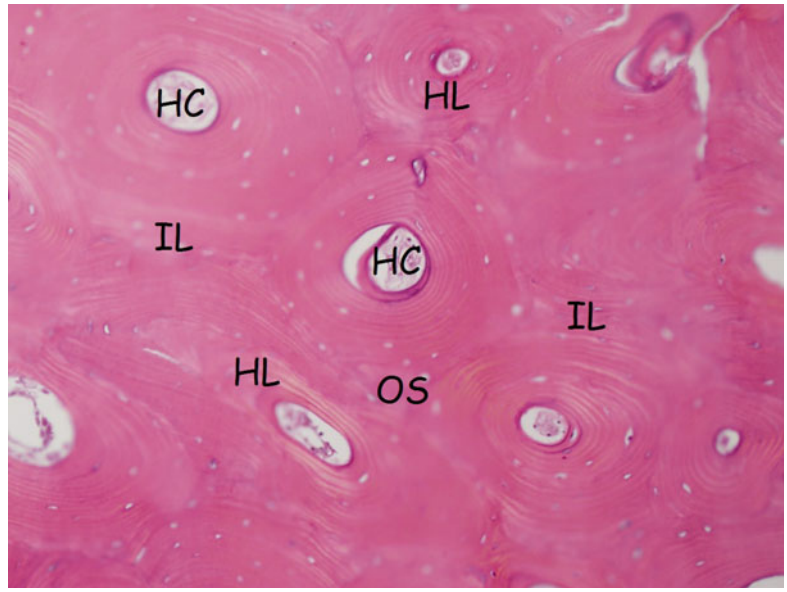

Fig. 18.3 Haversian system: osteon, Haversian canal, and Haversian and interstitial lamellae. *HC* Haversian canal, *HL* Haversian lamella, *OS* osteon (Haversian system), *IL* interstitial (intermediate) lamella

than the surrounding bone tissue. Cement lines form the boundaries of the reformed bone. Although their formation objectives are not clear, they are considered to be effective in stopping the progression of cracks as lacunae do. Osteocyte extensions rarely exceed the cement lines. This means that nutrients and chemical signals cannot pass effectively to osteon to another or to a trabecular package to another [5, 7].

Cellular Biology

Osteoblasts

They are tasked with bone formation. Overall, they are rounded and are arranged on the bone surface. Cellular structures according to the secretory structure expanded cisternal to include a well-developed Golgi apparatus. Newly formed

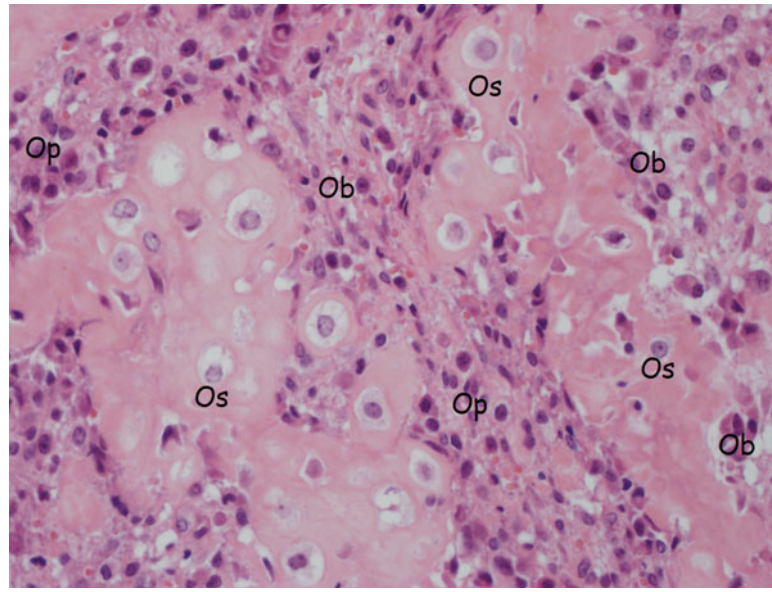

Fig. 18.4 Bone cells (osteocytes, osteoblasts, osteoprogenitor cells). *Os* osteocytes, *Ob* osteoblasts, *Op* osteoprogenitor cells

bone is not mineralized, and this bone is called osteoid. Osteoid's quality is closely related to bone-forming osteoblasts. Some of the osteoblasts switch into osteocytes by embedding into matrix after active bone production. Others come to align to the bone surface. These arrays of cells are flat-shaped surface and comprise a small amount of organelles [6].

Osteocytes are believed to be the last step in osteoblast differentiation. These cells are found buried in the osteocytic lacunae. Osteocytic lacunae are connected with each other by canaliculi with cytoplasmic continuation, and these canaliculi are important in the food and oxygen uptake from the capillary circulation. Surface area of osteocytes is quite large because of multiple cytoplasmic processes. In addition, these cytoplasmic bundles contain well-developed actin filament to detect mechanical stress. Given these features, osteocytes are believed to play a role in bone metabolism with mechanical stress detection and transmission. Recent studies of osteocytes showed that they release the channel that is activated by stress and shear stress-responsive elements [9].

Osteoblasts produce collagen, non-collagenous proteins (osteocalcin, bone sialoprotein, osteopontin, osteonectin), and several proteoglycans (decorin and the biglycan). Osteoblasts can also produce cytokines like insulin-like growth factor 1–2 (IGF), transforming growth factor (TGF), and bone morphogenetic protein 3 (BMP). These growth factors are important in the differentiation and function of osteoblasts and are stored in calcified bone matrix. Bone matrix is a storage location not only for calcium and phosphate but also for growth factors [8]. Significant alkaline phosphatase activity is available in plasma membranes of osteoblasts. More recently, experimental studies of mouse with defective tissue nonspecific alkaline phosphatase (TNAP) showed that TNAP's behavior was like pyrophosphatase hydrolyzing pyrophosphate which acts as a calcification inhibitor and was found to increase the inorganic phosphate required for calcification. Although alkaline phosphatase activity in the plasma membrane of osteoblast is quite effective, it has little effect at the membrane which faces the osteoid tissue and at osteocytes' membrane [10]. This histochemical evidence shows that the distribution of alkaline phosphatase is not always associated with calcification regions. Osteoblasts and bone matrix proteins' interaction is very important in osteoblast differentiation and function.

Osteoblast cells are also important in osteoclast differentiation and activation, as they are

effective in bone formation. Macrophage colony-stimulating factor (M-CSF) and nuclear factor kappa-B ligand (RANKL) which are essential in osteoclastogenesis are created by osteoblasts. In addition, osteoprotegerin (OPG) and trap receptor for RANKL are also synthesized by osteoblasts. Bone resorption formed by osteoclasts has to be connected to balance in RANKL and OPG which are released by osteoblasts [6]. On the other hand, the destructive agent, collagen matrix metalloproteinase 13 (MMP-13), is secreted by osteoblasts and osteocyte cells [9]. MMP-13 activity is stimulated by activator protein 1 and RUNX2 which are activated by parathyroid hormone (PTH) in osteoblasts [11].

Osteoblasts are formed from mesenchymal stem cells. These stem cells can return to chondrocytes, osteoblasts, myoblast, and adipocytes. This transformation is regulated by specific transcription factors. Transformation of chondrocytes is regulated by SOX 5, 6, and 9; PP and MyoD regulate transformation to adipocytes and myoblasts, whereas RUNX2/CBFA and osterix/Sp 7 activate the conversion of osteoblasts. In low-stress and high-oxygen-pressure condition, conversion to osteoblasts does occur, while in medium-stress and low-oxygen environment, conversion to chondroblasts does occur, and finally, in high-stress environments, differentiation is mainly to fibrous tissue. RUNX2 participates in the gene expression of osteopontin, bone sialoprotein, dentin sialoprotein, and TGF receptor 1, and RUNX2 is a transcriptional factor which connects to the structure that supports the formation of osteocalcin [11].

Osteoblast differentiation and function is regulated by 1,25-(OH)2D3, hormones like PTH and estrogen, and cytokines such as bone morphogenetic proteins (BMP).

Receptors found in osteoblasts and functions of them are summarized below [6, 11]:

1. Parathormone: Osteoclastic activity with continuous stimulation and increased osteoblastic activity in intermittent stimulation. Activates adenylate cyclase.
2. 1,25-(OH)2 vitamin D3: Activates matrix, alkaline phosphatase, and osteocalcin synthesis.
3. Glucocorticoids: Inhibit DNA synthesis, collagen production, and protein production.
4. Prostaglandines: Activate adenylate cyclase formation and bone resorption.
5. Estrogens: Activate bone formation and inhibit bone resorption. Increase mRNA levels for alkaline phosphatase synthesis. Inhibit activation of adenylate cyclase.

Osteocytes

They constitute 90 % of the mature skeleton. They are seen as the producing osteoblasts surrounded by newly formed osteoid. They are less effective in production of the bone than active osteoblasts. They are important for extracellular concentrations of calcium and phosphorus. They are stimulated by calcitonin and directly inhibited by PTH [6].

Osteoclasts

Osteoclasts, which are responsible for bone resorption, are multicellular giant cells. They are found in Howship's lacunae which are formed by their resorptive activity. Active ones are in contact with calcified bone surface. They are separated from other bone cells by their size and being multinucleated cells (Fig. 18.5) [12].

They have many mitochondria around the nucleus, endoplasmic retinaculum, and well-developed Golgi apparatus. In addition, they also contain the vesicles, lysosomes, tubular lysosomes, and vacuoles. The presence of these structures demonstrates that osteoclasts are important for energy generation, protein synthesis, and production of lysosomal enzymes [13].

Plasma membrane of active bone-resorbing osteoclasts is divided into three regions as clear zone, indented area, and basolateral membrane [14]. Clear region functions in attachment of osteoclast to the bone matrix and separates bone-resorbing compartment and extracellular fluid of cells from each other. This compartment provides effective situation for bone resorption [15]. The attachment of osteoclasts to bone matrix is

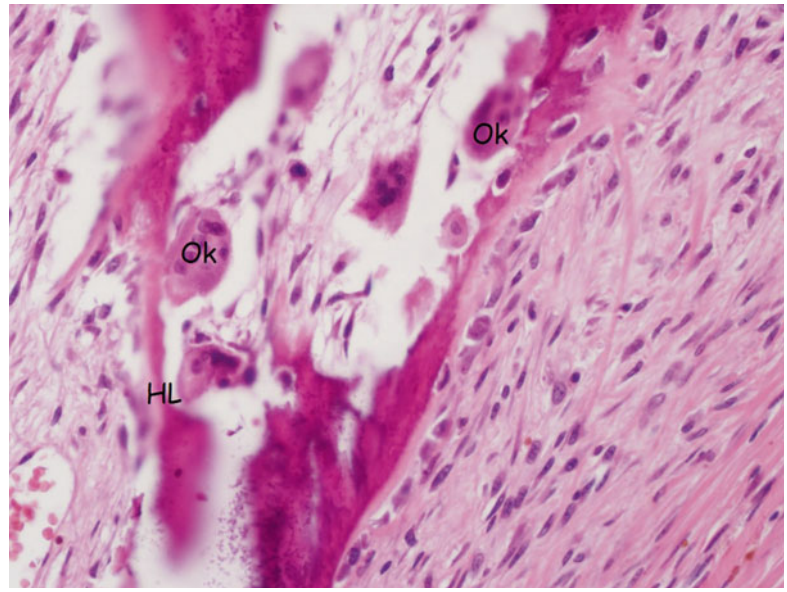

Fig. 18.5 Osteoclast and Howship's lacuna. *Ok* osteoclasts, *HL* Howship's lacuna

provided with the vitronectin and integrin receptors. Another ligand is considered to be osteopontin. The cell matrix interaction activates c-Src, a non-receptor-type tyrosine kinase. Absence of c-Src activity generates a phenotype of osteopetrosis. There are many osteoclasts with non-recessed surface in this type of osteopetrosis. The face of the plasma membrane that is toward to osteoclast bone matrix is a recessed portion. Bone resorption is associated closely with the recessed surface.

Bone resorption would be the dissolution of degradation products such as hydroxyapatite and organic components of bone matrix. Carbonic anhydrase which converts CO_2 and H_20 to H^+ and HCO_3^- in the cytoplasm and vacuolar H^+-ATPase in indented surface is involved in acidification in Howship's lacuna. H^+ ATPase is abnormal in osteopetrosis. Mitochondria in osteoclasts are believed to provide ATP for the transport of H^+ [14]. The balance of ions in the cytoplasm is provided with chloride channels. Defect of these channels has been shown to cause osteopetrosis in rat experiments. Extracellular digestion of the organic components is provided by lysosomal enzymes such as cathepsin K. Cathepsin K can break down collagen fibers in an acidic environment. Tartrate-resistant acid phosphatase is released in Howship's lacuna, and these enzymes are used as markers for osteoclasts. Basolateral plasma membrane is believed to be important for receiving calcitonin and cytokine stimulation. This area is also important in the cell-cell stimulation with osteoblast cells.

Calcitonin is a hormone whose receptor is on osteoclasts and that inhibits osteoclasts. This hormone breaks down actin filaments, eliminates the clear zone, and separates osteoclasts from the bone by retracting them [14, 15].

Osteoclasts are derived from precursor monocyte/macrophage cells and hematopoietic stem cells [16]. Macrophage colony-stimulating factor (M-CSF) is important for third derivation. Morphological findings support that osteoclasts and preosteoclasts are always in relationship with ALP-positive osteoblasts, and therefore, cell-cell relationship with osteoblasts is important for osteoclast differentiation. One of the most interesting findings in osteoclast differentiation is the effect of RANK/RANKL system. RANKL which is a member of the tumor necrosis factor family is produced by activated T cells and osteoblasts. RANKL takes a role in differentiation by binding to RANK on osteoclast precursors and osteoclasts. 1,25-(OH)2D3, prostaglandin E2, interleukin 1, PTH, and PTH-related protein, which are the

stimulators of osteoclastogenesis, promote the formation of RANKL on osteoblasts. Conversely, osteoprotegerin (OPG), the soluble receptor form of TNF, inhibits RANKL. Estrogen, TGF, and BMP increase the formation of OPG. RANKL/RANK signaling is regulated by the TNF receptor-associated factor on osteoclasts [16].

Parathyroid hormone-related peptide which is secreted by the tumor cells forms RANKL. RANKL binds to specific receptors on osteoclasts, and then mature osteoclast formation occurs, and this process leads to the activation of bone resorption [14].

Extracellular matrix containing heparan sulfate and fibronectin is important for the connection between osteoclast and osteoblast cells. This connection is important for cell stimulation [10].

Bisphosphonate group of drugs is classified as nitrogen containing and nonnitrogen containing. Antiresorptive effects of nitrogen-containing bisphosphonates are 1000 times more than the nonnitrogen-containing bisphosphonates. Nonnitrogen-containing bisphosphonates create apoptosis by nonfunctional adenosine triphosphate (ATP), whereas nitrogen-containing bisphosphonates (zoledronate, alendronate, etc.) inhibit farnesyl pyrophosphate synthetase enzyme which is on mevalonate pathway [6, 16].

Molecular Structure

Matrix

Most of the bone consists of a matrix. Matrix has two components, including organic and inorganic.

Inorganic Matrix

Inorganic matrix is the mineral part of the bone and formed by calcium hydroxyapatite and calcium phosphate. It constitutes 60 % of the dry weight of the bone [6].

Organic Matrix

Organic matrix constitutes 40 % of the dry weight of the bone. Ninety percent of organic matrix consists of collagen and the very large amount of collagen is type 1. Other components are proteoglycans, non-collagenous matrix proteins (osteocalcin), growth factors, and cytokines.

The following section will provide more detailed information on the matrix.

Extracellular Matrix

Bone tissue is relatively less cellular than the other tissues. Extracellular matrix (ECM) comprises the majority of bone tissue. ECM is composed of mineral, protein, water, salts, lipids, glycoproteins, and proteoglycans and primarily consist of osteoblasts, the cells that form the bone. The bone is composed of different types of ECM, and these types are mineralized ECM, osteoid (non-mineralized) ECM, and lacunar ECM (matrix which surrounds osteocytes). Lacunar matrix is probably moving in the canalicular network of osteocytes [18].

Osteoid is a temporary matrix which forms mineralized bone. A small percentage of the volume of the bone is osteoid except for mineralization disorder diseases such as osteoporosis and osteomalacia. Although osteoid is generally present in the areas of formation of new bones, it can be seen as a thin layer on mature bone surface which assumed a critical role in the regulation of remodeling.

Mineralized Bone Extracellular Matrix Components

Mineralized bone matrix defines bone tissue material properties and accounts for the majority of bone matrix. Mature bone matrix contains significant inorganic components in addition to the organic components unlike lacunar and osteoid matrix. Mineral constitutes 60–70 % of the tissue, primarily calcium, phosphate, sodium, and other appropriate ions such as magnesium carbonate. The organic matrix constitutes 20–25 % of the tissue, and 90 % of organic matrix is type 1 collagen, whereas 10 % is non-collagenous proteins. Types 3, 5 and small amounts of other types of collagen may also be present. Bone

morphogenetic proteins (BMPs) and other growth factors are also found in the mineralized matrix. The remaining tissue volume is filled with water. All mineralized bone surfaces are covered with a thin layer of non-mineralized osteoid.

The mineralized matrix is known to provide mechanical functions for the material properties of the bone for a long time. The dynamic role of ECM in the regulation of bone cell behavior and interaction between bone matrix and bone cells had been understood in very recent studies. ECM acts as pier for cells, regulates behavior of osteocytes and osteoblasts, regulates the diffusion of macromolecules and ions, can be connected to the protease and growth factors, or can edit their activities. Detailed information about the bone matrix components will be given in the section below [19].

Collagen

Collagen is the most abundant protein in mammals. There are over 20 different types of collagen according to their structure and function. Type 1 collagen is the most common type of collagen in bone tissue. Immature cancellous bone and lamellar bone contain lower amounts of type 3 and 5 collagen. Type 10 collagen is particularly found in hypertrophic chondrocytes in the growth plate and functions in the calcification of cartilage. Type 1, 3, and 5 collagens have three-helical structure, and they are the proteins that are converted into fibrils. The conversion of type 1 collagen to fibrils contributes to the uniform tensile strength of the bone. Non-fibrillar collagen types are also available. Some of these collagen types can contain short three-helical structure. Fibrillar collagens can interact among themselves. Type 5 collagen interacts with type 1 collagen and generally believed to be related to the regulation of the resulting fibril size. Mutations of type 5 collagen were found to cause irregularity of the type 1 in the rat experiment models. Type 3 collagen's precise functions are not fully understood, and they are located in regions close to the bone and soft tissue adhesion points, and mutation among type 3 collagen constitutes a serious form of Ehler-Danlos syndrome [19].

Inorganic Matrix and Mineralization

The bone comprises 50–70 % of mineral, 20–40 % of the organic matrix, 5–10 % of water, and about 2–3 % of oil/fat. Mineralized bone portions provide resistance to compression forces. Mineralized portion mainly consists of calcium phosphate (hydroxyapatite) (CA10(PO4)6(OH)2) and contains a small amount of carbonate, magnesium, and acid phosphate without hydroxyl groups. Hydroxyapatite crystals in the bone are very small and are more soluble compared to those found in nature.

Matrix maturation is associated with the synthesis of alkaline phosphatase, osteocalcin, osteopontin, and bone sialoprotein. It is believed that these calcium- and phosphate-binding proteins take role in mineral deposition by adjusting the amount and size of formed hydroxyapatite crystals. While mineral provides mechanical resistance and strength against force to the bone, the organic matrix gives elasticity and flexibility. Mineral is stored in holes located at the ends of the collagen fibrils. This process is facilitated by the bone extracellular matrix vesicles. These vesicles are generated by chondrocytes and osteoblasts and provide a safe environment in order to create crystal by accumulation and subsidence of calcium and phosphate ions. Normally, extracellular fluid is not saturated with hydroxyapatite excessively; hydroxyapatite therefore does not subside spontaneously. Matrix extracellular vesicles include inorganic phosphate which is successful in the subsidence of proteins, acidic phospholipid, calcium, and hydroxyapatite crystals. These vesicles are not specially located in the collagen fibril ends, so their effect is not very clear at this location. There is not enough evidence about noncrystalline calcium phosphate clusters' (amorphous calcium phosphate) formation in the bone before turning into hydroxyapatite. Hydroxyapatite crystals' expanding and heterogeneity are reduced as the bone matured. This expansion is formed by crystal growth and

coalescence. Dentin matrix protein 1 and bone sialoprotein have been confirmed as mineralization enhancers. Type 1 collagen has no effect on mineralization increase. Phosphoprotein kinase and alkaline phosphatase regulate the mineralization process. Alkaline phosphatase can increase the regional phosphorus density, can remove the inhibitors that prevent hydroxyapatite crystal growth containing phosphate from the medium, or can arrange phosphoproteins for activator positions [18–20].

Vitamin D has an indirect effect on mineralization. After vitamin D had been absorbed from gastrointestinal system or created on the skin, 25-hydroxyvitamin D is synthesized on the liver, and then biologically active 1,25-dihydroxyvitamin D (1,25-(OH)2D) is formed on the kidneys. 1,25-Dihydroxyvitamin D is very important in maintaining adequate serum calcium and phosphorus levels for passive mineralization of non-mineralized bone matrix. This process is primarily provided by 1,25-dihydroxyvitamin D by increasing the absorption of calcium and phosphorus from the intestine. 1,25-Dihydroxyvitamin D also increases the conversion to osteoblast and activates osteoblasts to form bone-specific alkaline phosphatase, osteocalcin, osteonectin, osteopontin, and cytokines. 1,25-Dihydroxyvitamin D is also effective in the proliferation and apoptosis of other skeletal cells including hypertrophic chondrocytes. Fluoride for hydroxide groups and strontium for calcium are available as backup in mineralized matrix [19].

Non-collagenous Matrix Proteins

Vitamin K Dependent

Osteocalcin (bone Gla protein or proteins containing gamma-carboxyglutamic acid) is one of the most abundant non-collagenous bone proteins. Osteocalcin is considered as an indicator of osteoblast differentiation because it is created by mature osteoblasts intensely. Its amount can be measured in urine, and its level is increased with an increase in bone formation or degradation. Osteocalcin is a member of protein group which is produced as a result of gamma-carboxylation's posttranslational modification of vitamin K-dependent glutamic acid residues.

Adhesive Proteins

Fibronectin and vitronectin are in this group. They enable interaction between extracellular matrix and cells. Adhesive extracellular matrix proteins interact with the bone cells by binding to the transmembrane protein receptors named integrin. This interaction is important for both the osteoblast and osteoclast functions. In studies, it has been shown that fibronectin blockade has caused the failure of the rescue of osteoblasts. This indicates that fibronectin is important in osteoblasts' adhesion and osteoblasts' survival.

While fibronectin is important in the adhesion of osteoblasts, vitronectin is more important in the adhesion of osteoclasts. Vitronectin provides osteoclast adhesion via α-v/β-3 integrin receptors. Osteoclastic function is decreasing in the absence of vitronectin, and it may be important in clinical drug development.

Matricellular Proteins

In this group, thrombospondin, osteopontin, tenascin, and osteonectin are available. Osteopontin (bone sialoprotein 1) is believed to be important in the function of phagocytic cells like macrophages and osteoclasts. Osteopontin is a chemotactic factor for osteoclasts [20].

Proteoglycans

Proteoglycans are molecules formed by a combination of protein and sugar. They are formed as adding glycosaminoglycan chains to a linear root protein by posttranslational carboxylation. The most characterized proteoglycan is aggrecan which has structural tasks in articular cartilage. Proteoglycans are found in cartilage tissue more than bone tissue. Some of the other proteoglycans

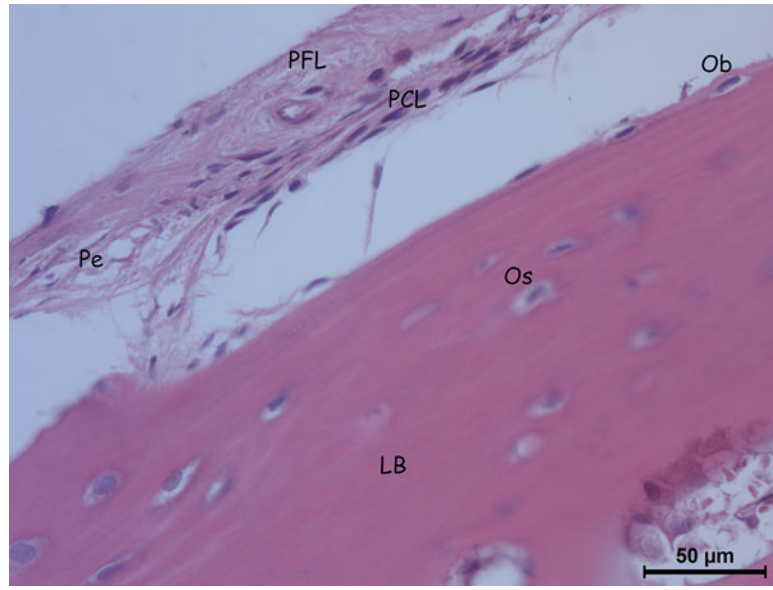

Fig. 18.6 Periosteum and its layers. *Pe* periosteum, *PFL* periosteum fibrous outer layer, *PCL* periosteum cambium (inner) layer, *Os* osteocytes, *Ob* osteoblasts, *LB* lamellar bone

in bone tissue are perlecan, decorin, biglycan, and syndecan. They have biophysical and biochemical functions.

Periosteum

It is the connective tissue surrounding the bone. They are thicker and more active in children. The inner side is called as cambium; this portion is rich in blood vessels having a loose structure. Cambium layer contains cells which may develop into osteoblasts, and the cells provide bone growth in width and form periosteal callus. Femoral neck does not involve cambium layer, so periosteal callus formation cannot be seen after this region's fractures. The outer layer of the periosteum is poor for blood vessels and this layer's structure is fibrous. This outer layer of periosteum is continued by the joint capsules (Fig. 18.6) [6].

Bone Marrow

Red bone marrow is the source of precursor cells to hematopoiesis (it includes 40 % water, 40 % fat, and 20 % protein). Red marrow changes into inactive yellow marrow with aging (it includes 15 % water, 80 % fat, and 5 % protein). These changes occur for appendicular skeleton before axial skeleton [6, 13].

Regulation of Bone Formation and Function

Hard and mineralized nature is closely related to the self-renewal and dynamic structure of the bone. This dynamic structure allows ensuring continuity of structure and mechanical strength and contributes to the scar-free healing. These events are achieved by regular bone formation and degradation. When the bone's formation and resorption balance is broken, characteristics of the bone are also deteriorated, and diseases such as osteopetrosis and osteoporosis occur [21].

Physiological, pharmacological, or pathological factors control the bone formation and destruction. The net effect determines bone mass and the placement of this mass. Systemic factors which control the resorption of the bone by serum calcium level and osteoclastic activity are well understood.

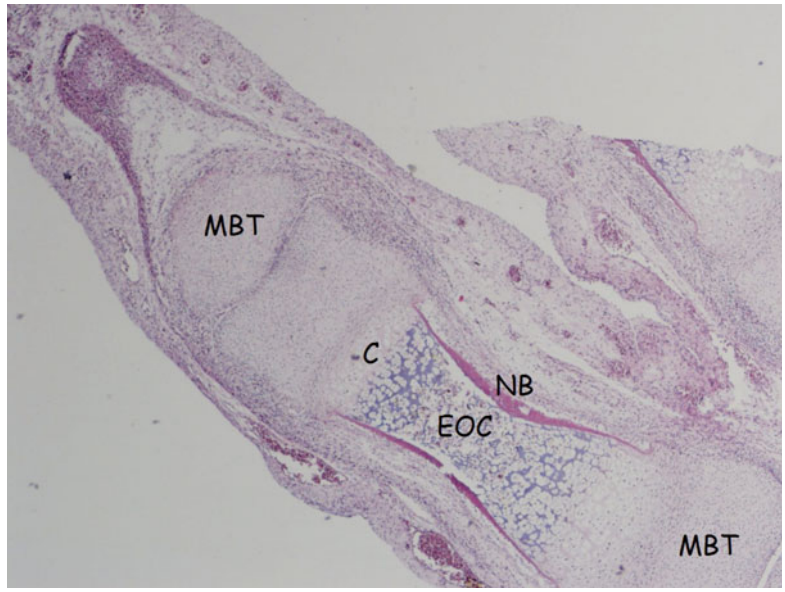

Fig. 18.7 Endochondral ossification center. *MBT* mesenchymal tissue which will become cartilaginous tissue, *C* cartilage, *EOC* endochondral ossification center, *NB* new bone

Osteoclastic resorption and release of calcium from the bones are enhanced by factors such as vitamin D and continuous secretion of parathyroid hormone but reduced by calcitonin. Systemic control of bone formation is less well understood. Intermittent release of parathyroid hormone, leptin protein which is formed by white adipose tissue, is seen as an important factor in osteoblastic bone formation [6, 21].

Pharmacologically, it is obvious that steroid usage reduces the bone formation and increases the destruction. Bisphosphonates are being used in the treatment of conditions such as osteoporosis, metastatic bone disease, and Paget's disease by decreasing osteoclastic bone resorption. The intermittently used parathyroid hormone preparations are used to increase bone formation [6].

Types of Bone Formation

Enchondral Ossification

Undifferentiated cells are transformed into chondrocytes, and cartilage matrix is created. The resulting matrix is mineralized and after invaded by blood vessels. Osteoprogenitor cells come to the place then. Osteoclasts break down the calcified cartilage and osteoblasts form bone tissue. Cartilage tissue is replaced by bone tissue in this type of ossification; cartilage is not turned to bone tissue. Embryonic long bone formation, longitudinal growth of the physis, fracture callus formation, and the bone which is formed by demineralized bone matrix can be given examples for endochondral ossification. There is defect of endochondral ossification in achondroplasia (Fig. 18.7) [6].

Intramembranous Ossification

Undifferentiated mesenchymal cells are combined in layers, are transformed to become osteoblasts, and mineralized by forming the organic matrix. There is no cartilage model. Flat embryonic bone formation, the bone formed in the stable distraction osteogenesis (if it is unstable, then it would be as endochondral ossification), and blastema which occurs after long bone amputation in children can be given as examples for intramembranous ossification. Intramembranous ossification is defective in Cleidocranial dysostosis (Fig. 18.8) [6].

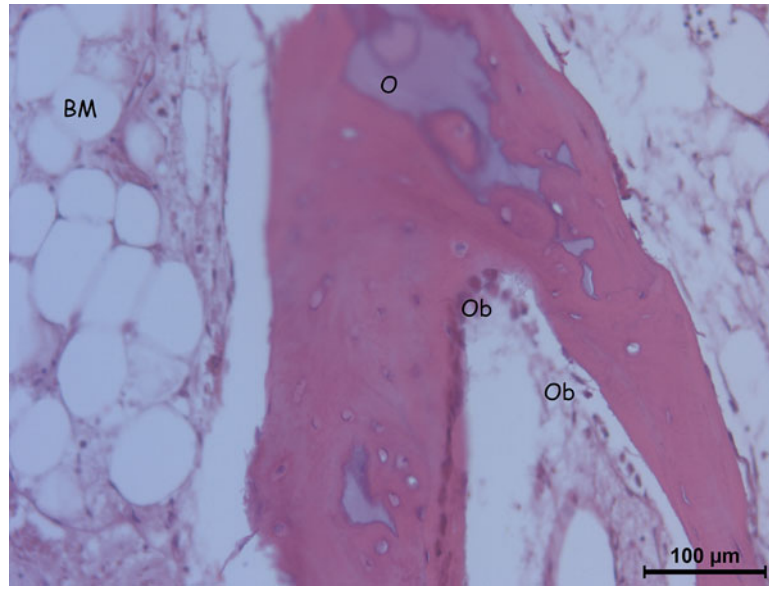

Fig. 18.8 Intramembranous ossification: bone marrow, osteoblasts, and osteoid tissue in each other. *O* osteoid, *BM* bone marrow, *Ob* osteoblasts

Appositional Ossification

Osteoblasts are arranged on the bone surface to form new bone. Periosteal growth in width can be given as an example for appositional ossification. Appositional ossification is defective in Paget's disease, infantile hyperostosis, and melorheostosis [6].

Remodeling of the Bone

Cortical and trabecular bone continues to remodel throughout life by osteoblastic and osteoclastic activity. Whole bone tissue is completely renewed in time periods ranging from 4 to 20 years. This cycle is about 5 % per year in adult bone, but this case varies depending on the age and bone layout. Changing is fastest in the pediatric age group (25 % trabecular bone, 20 % cortical bone). Bone tissue fragility is increased with age because of the mineral phase changes. Remodeling degradation occurs such as Paget's disease due to decreasing osteoclastic activity, and as a result, a pathological bone tissue occurs [6, 22].

Wolff's law: Increased mechanical loading generates bone gain, while decreasing the effect of mechanical loading causes bone loss. This loss is often reversible [6].

Piezoelectric: Remodeling occurs according to the electrical load. The compression side of the bone is electronegative, while pulling side is electropositive. Electronegativity increases the osteoblastic activity, and electropositivity leads to increased osteoclastic activity [6].

Hueter-Volkmann's law: Remodeling is carried out by hormones and cytokines. Compression reduces growth, while pulling activates growth. This law is based on the longitudinal growth of the physis, remodeling, and fracture healing. This law may be important in Blount disease and scoliosis [6].

Remodeling in cortical bone: Osteoclastic tunneling (cutting cones) concept emerges in this system. Osteoclasts and osteoblasts act simultaneously. Osteoblasts which are located at the back form new bone, while foremost osteoclasts break down the bone. Capillaries are available immediately behind the osteoclasts [23].

Remodeling in trabecular bone: Firstly, osteoclasts break down the bone and then osteoblasts produce new bone tissue.

Measures of Bone Formation and Resorption

Assessment of bone formation and resorption may provide some clinical benefits. During bone formation, increased levels of serum osteocalcin are obtained. Osteocalcin is specific to bone tissue because it is primarily formed by the osteoblasts. However, it is important to remember that after degradation of the bone, osteocalcin which is found in bone matrix is released and this event also increases the serum level of osteocalcin. As a result, it can be stated that increased osteocalcin levels show the increase in bone turnover. N-terminal and C-terminal propeptide levels are increased in serum and urine which are present in the structure of the collagen molecule that is formed by osteoblasts. The most important measure of bone resorption is N-telopeptide of type 1 collagen which is the degradation product of mature collagen. Again, pyridinoline is the degradation product of collagen cross-links. Hydroxyproline is only found in the structure of collagen, and the increase of its level in the urine is the most specific evidence of bone resorption. Levels of tartrate-resistant acid phosphatase and cathepsin may give an idea of osteoclastic activity [6, 23].

Innervation and Circulation of the Bone

Maintaining the blood circulation is critical for fracture healing, bone marrow function, and maintenance of bone tissue. Bone tissue receives 5–10 % of the blood which is pumped by the heart. Blood circulation of the scaphoid, talus, femoral neck, odontoid bone, and fifth metatarsal is troublesome. The circulation of the long bones is provided from three sources: (1) nutritional arteries, (2) metaphysis-epiphysis system, and (3) periosteal arteries. Nutritional artery and metaphyseal arteries form the medullary canal arterial system by anastomosing each other. Periosteal system consists of branches of the nutritional artery and muscle vessels. Normally, the inner two-thirds of the bone cortex is supplied by medullary system, whereas the outer one-third cortex by external periosteal system. Normally, arterial blood flow is centrifugal (inside out), and venous blood flow is centripetal (outside inward). Cortical bone is being supplied by the vessels with the help of Volkmann channels and Haversian system. Trabecular bone is supplied by diffusion from space of bone marrow. When the bone suffers a fracture, external periosteal system takes the primary role in blood supply of the bone because of injured medullary system. After explaining this information, the importance of soft tissue care in fracture treatment is clear. The nerves of periosteum pass along the bone and accompany the blood vessels in Haversian and Volkmann canals [6, 24].

The Mechanical Properties of the Bone

It is important to know the structural and material properties of the bone in the understanding of its mechanical and physiological role. The structural properties of the bone depend on its shape, size, and architecture, and material properties depend on the organic and inorganic matrix components.

Overall, two main tissue components of bone mineral and organic matrix determine material properties. Mineral content predominantly determines the capacity of the tissue strength and resistance to compression strength. Collagens which are a component of the organic matrix primarily provide the ability to withstand against stress. Increase in mechanical properties is provided as the bone ages (time goes by through the construction) because of increased mineral content in both cortical and trabecular components. If it is necessary to give an example about the importance of tissue type on bone property, trabecular bone is weaker than lamellar bone tissue because in trabecular bone tissue, collagen and mineral distribution is less durable than lamellar bone. Cancellous bone increases its durability by turning into lamellar bone under normal conditions [23].

Trabecular bone tissue deficiency affects the material properties negatively, and this may be important in osteoporotic and stress fractures [22].

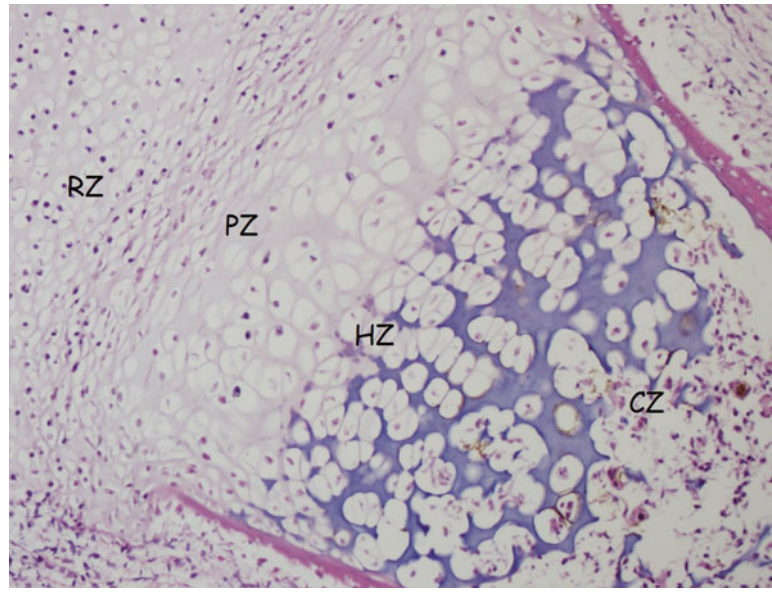

Fig. 18.9 Physis and its components. *RZ* recreation zone, *PZ* proliferation zone, *HZ* hypertrophy zone, *CZ* calcification zone

Cement lines formed in reshaping process which are present in osteocyte lacuna play a role in the mechanical behavior of bone tissue. The small amounts of minerals and collagen in the cement lines show a similar mechanism on preventing failure cracks of the bone as drill holes which are created to limit the fracture line during clinical applications of osteotomies [22, 23].

Physis

There are two types of physis as horizontal (physis) and spherical (epiphysis) in immature bone. Blood flow of the growth plate is provided mainly by perichondrial arteries. More physis will be discussed in detail which is more organized. Physis consists of three layers as reserve, proliferative, and hypertrophic portions (Fig. 18.9).

Reserve zone: The cells store fat, glycogen, and proteoglycan in this zone. The oxygen pressure is low. Diseases such as the Gaucher disease, diastrophic dysplasia, Kniest syndrome, and pseudoachondroplasia may affect this region.

Proliferative zone: Chondrocyte stacks are formed by cellular proliferation and matrix production, and as a result, longitudinal growth occurs. Calcification is inhibited by increased proteoglycan level and oxygen pressure. This zone is affected by various diseases such as achondroplasia, hypochondroplasia, and gigantism. Growth hormone shows its effects on this zone.

Hypertrophic zone: This zone consists of three layers as maturation, degeneration, and provisional calcification.

Maturation region: In this region, chondrocytes begin to grow and matrix is prepared for calcification.

Degeneration region: In this region, chondrocyte size increases up to five times. The matrix is prepared for calcification.

Provisional calcification region: Chondrocytes are at the largest states. Chondrocyte death leads to calcium release from the cell. As a result, matrix calcification occurs. Type 10 collagen is so important in mineralization which is formed by these hypertrophic chondrocytes.

Hypertrophic zone of physis is affected several diseases such as slipped capital femoral epiphysis (SCFE) which is not linked to kidney failure, rickets (provisional calcification zone), enchondroma, spondyloepiphyseal dysplasia, Schmid disease, Kniest syndrome, pseudoachondroplasia, and type 1 Salter-Harris epiphyseal

Physis

	Function	Blood supply	Oxygen pressure	Glycogen	Cell respiration	Local factors	Systemic factors
Reserve zone	Matrix production, storage	None	Low	High	Anaerobic	IL-1	PTH, CS
Proliferation zone	Cell proliferation, matrix production	Excellent	High	High (lower than reserve zone)	Aerobic	FGF, PDGF, TGF-β, BDGF, IL-1	PTH, TH
							GH, CS,
							Somatomedin, insulin, 24,25-(OH)2D3, vit. C
Maturation zone	Preparation of matrix for calcification	Good	Low	Fair	Aerobic-anaerobic	FGF, PDGF, TGF-β, BDGF, prostaglandin, IL-1	PTH, TH
							CS, calcitonin, 1,25-(OH)2D3, 24,25-(OH)2D3, vit. A, vit. C
Degeneration zone	Preparation of matrix for calcification	Fair	Low	Low	Anaerobic	TGF-β, BDGF, prostaglandin, IL-1	PTH,K.S., calcitonin, 1,25-(OH)2D3, 24,25-(OH)2D3, vit. A, vit. C
Provisional calcification zone	Matrix calcification	None	None	None	Anaerobic	TGF-β, BDGF, prostaglandin	PTH, KS, calcitonin, 1,25-(OH)2D3, 24,25-(OH)2D3, vit. A, vit. C
Primary spongiosa	Bone formation	Good	Fair	?	Aerobic-anaerobic	EGF, prostaglandin	PTH, CS, calcitonin
Secondary spongiosa	Remodelation	Excellent	High	?	Aerobic	EGF, prostaglandin, IL1	PTH, CS, calcitonin

BDGF bone-derived growth factor, *EGF* epidermal growth factor, *FGF* fibroblast growth factor, *IL-1* interleukin 1, *PDGF* platelet-derived growth factor, *TGF-β* transforming growth factor-β, *GH* growth hormone, *CS* corticosteroid, *PTH* parathormone, *TH* thyroid hormone

fractures. Hypertrophic zone expands in rickets disease and at the recovery phase of physis injury.

There are two layers named as primary and secondary spongiosa at the region where physis is in combination with primary ossification center. Primary spongiosa becomes mineralized to form woven bone and continues as the secondary spongiosa. Metaphyseal corner fractures and scurvy affect primary spongiosa layer, whereas secondary spongiosa layer is affected by SCFE that is related with renal failure [25].

Fracture Healing

Bone fracture healing process involves the stages that the injured bone returns to its pre-injury situation. This process is divided into four stages as inflammation, soft callus, hard callus, and remodeling phases [26].

Inflammatory phase: Fracture hematoma occurs after the rupture of blood vessels; after physiological coagulation cascade, torn vessels become thrombosed, and as a result of ischemia, the fractured bone ends become necrotic. Increased capillary permeability causes the local inflammation. Macrophages, neutrophils, and degranulating platelets multiply at the fracture site, and cytokines such as platelet-derived growth factor; transforming growth factor-β; interleukins 1, 6, 10, and 12; and tumor necrosis factor-α are secreted by these cells. A portion of these cytokines multiply as early as in first 24 h in the injury field. Inflammatory molecules can directly regulate the fracture healing. The absence of TNF-α may delay endochondral and intramembranous bone formation. Inhibition of cyclooxygenase (COX-2) has been found to adversely affect the fracture healing by inactivation of osteoblast differentiation over RUNX2 and osterix. Cyclooxygenase inhibitors (NSAIDs) adversely affect the early fracture healing by suppressing the inflammation.

Soft callus phase: Sources of the stem cells in fracture healing are periosteum, endosteum, bone marrow, surrounding muscles, and the circulatory system. Mesenchymal cells are stacked in the field of fracture after injury in response to growth factors and cytokines. Depending on the mechanical condition, mesenchymal cells develop into chondroblasts or osteoblasts. Overall mechanical instability provides chondrocyte transformation and endochondral bone formation, while the mechanical stability provides osteoblastic transformation and intramembranous ossification.

Hard callus and remodeling phases: Soft callus slowly turns into a hard callus with the endochondral ossification process. Chondrocytes in fracture callus form cartilage matrix and by entering to the maturation period differentiates into hypertrophic chondrocytes. These chondrocytes release type 10 collagen, proteases such as MMP13 (which breaks down the extracellular matrix), and vascular endothelial growth factor (for vascularization). The cartilage becomes calcified in the junction of mature chondrocytes and newly formed bone. Chondrocytes undergo apoptosis and invasion of new blood vessels takes place. Newly formed woven bone changes into lamellar bone by remodeling. Remodeling phase continues until occurrence of medullary cavity [27].

References

Introduction and Functions of Bone

1. Marieb EN, Hoehn K (2007) Human anatomy & physiology. 7th ed. Benjamin-Cummings Publishing Company
2. Derrickson BH, Tortora GJ (2005) Principles of anatomy and physiology. Wiley, New York

Anatomy

3. Brinker MR, O'Connor DP (2012) Basic Sciences. In: Miller MD, Thompson SR, Hart J, editors. Miller's Review of Orthopaedics. 6th ed. Saunders. p.1–10
4. Miller JD, McCreadie BR, Alford AI, Hankenson KD, Goldstein SA (2007) Form and Function of Bone. In: Einhorn TA, O'Keefe RJ, Buckwalter JA, editors. Orthopaedic Basic Science, Foundations of Clinical Practice. 3rd ed. AAOS. p.129–159

5. Crock HV (1996) An atlas of the vascular anatomy of the skeleton and spinal cord. Mosby, St. Louis, pp 131–303
6. Fawcett DW (1994) Bloom and Fawcett: a textbook of histology, 12th edn. Chapman and Hall, New York, pp 194–204
7. Hancox NM (1972) Biology of bone. Cambridge University Press, London, pp 18–35

Histology

8. McKee MD, Addison WN, Kaartinen MT (2005) Hierarchies of extracellular matrix and mineral organization in bone of the craniofacial complex and skeleton. Cells Tissues Organs 181:176–188
9. Bennett JH, Moffatt S, Horton M (2001) Cell adhesion molecules in human osteoblasts: structure and function. Histol Histopathol 16:603–611
10. Boskey AL (1996) Matrix proteins and mineralization: an overview. Connect Tissue Res 35:357–363
11. Anderson HC (1995) Molecular biology of matrix vesicles. Clin Orthop Relat Res 314:266–280
12. Duplomb L, Dagouassat M, Jourdon P, Heymann D (2007) Concise review: Embryonic stem cells: A new tool to study osteoblast and osteoclast differentiation. Stem Cells 25(3):544–552
13. Eriksen EF, Axelrod DW, Melsen F (1994) Bone histomorphometry. Raven Press, New York, pp 1–12
14. Roodman GD (1999) Cell biology of the osteoclast. Exp Hematol 27:1229–1241
15. Boyle WJ, Simonet WS, Lacey DL (2003) Osteoclast differentiation and activation. Nature 423:337–342
16. Blair HC, Athanasou NA (2004) Recent advances in osteoclast biology and pathological bone resorption. Histol Histopathol 19:189–199
17. Bart C (2008) Normal bone anatomy and physiology. Clin J Am Soc Nepro 3(supplement 3):131–139
18. Hock JM, Centrella M, Canalis E (2004) Insulin-like growth factor I (IGF-I) has independent effects on bone matrix formation and cell replication. Endocrinology 122:254–260
19. Rubin J, Rubin C, Jacobs CR (2006) Molecular pathways mediating mechanical signaling in bone. Gene 367:116
20. Anderson HC (1995) Molecular biology of matrix vesicles. Clin Orthop Relat Res (314):266–280
21. Noble BS, Reeve J (2000) Osteocyte function, osteocyte death and bone fracture resistance. Mol Cell Endocrinol 159:7–13

Mechanical Properties of Bone

22. Cullinane DM, Einhorn TA (2002) Biomechanics of bone. In: Bilezikian JP, Raisz LG, Rodan GA (eds) Principles of bone biology, 2nd edn. Academic Press, San Diego, pp 17–32
23. Hayes W (1991) Biomechanics of cortical and trabecular bone: implications for assessment of fracture risk, basic orthopaedic biomechanics. Raven Press, New York, pp 93–142
24. Ammann P, Rizzoli R (2003) Bone strength and its determinants. Osteoporos Int 14(suppl 3):S13–S818

Physis

25. Brinker MR, O'Connor DP (2012) Basic Sciences. In: Miller MD, Thompson SR, Hart J, editors. Miller's Review of Orthopaedics. 6th ed. Saunders. p.1–10

Fracture Healing

26. Lu C, Meinberg E, Marcucio R, Miclau T (2011) Fracture repair and bone grafting. John M. Flynn Editor in Orthopaedic knowledge update 10 American Academy of Orthopaedic Surgeons, p 11–21
27. Brinker MR, O'Connor DP (2012) Basic Sciences. In: Miller MD, Thompson SR, Hart J, editors. Miller's Review of Orthopaedics. 6th ed. Saunders. p.1–10

Fracture Healing

19

Mehmet Arazi and Mehmet Kerem Canbora

Abstract

Fracture healing, an extremely complicated and also a perfect process, has been successfully attracting man's attention for many years. Although a great number of mechanisms regarding the process have been figured out, much still remains unknown. Fracture healing is a unique process like no other, which develops without the formation of fibrous scar tissue and can be defined as the regeneration of a variety of tissues. To obtain full functional bone regeneration, it is necessary to progress of anatomical, biochemical, and biomechanical processes with excellent compatibility. In recent years, mesenchymal stem cells and many molecular and chemical pathways which have an important role in bone repair have been well defined. However, fracture repair continues to be an equation with several unknowns.

Learning Outcomes

After you have studied this chapter, you will have an understanding of (1) the histopathological periods of fracture healing; (2) the histo-biological characteristics of fracture healing; (3) the types of bone healing; (4) the osteogenic, osteoinductive, and osteoinductive stimulation methods of bone healing; and (5) the effect of fracture fixation methods on fracture healing.

Terminology

Absolute stability In contrast to relative stability, rigid osteosynthesis applied to the fracture line leads to direct bone healing. This is known as *absolute stability*.

Apoptosis Apoptosis is the process of programmed cell death.

M. Arazi (✉)
Department of Orthopaedics and Trauma Surgery, Farabi Klinik, Konya, Turkey
e-mail: mehmet.arazi@gmail.com

M.K. Canbora
Department of Orthopaedics and Trauma Surgery, Haydarpasa Numune Education and Research Hospital, Istanbul, Turkey
e-mail: kerem.canbora@gmail.com

F. Korkusuz (ed.), *Musculoskeletal Research and Basic Science*,
DOI 10.1007/978-3-319-20777-3_19

Autocrine A form of cell signaling where the active signaling molecule is secreted by a cell and afterward received by the receptors of that same cell.

Bone morphogenetic proteins The BMPs are known to play a critical role in bone healing by means of their ability to stimulate differentiation of mesenchymal cells to an osteochondroblastic lineage. The BMPs are members of the TGF-β superfamily.

Chondrocyte Cells of the cartilage. Chondroblast defines immature chondrocyte.

Collagen Collagen is the main structural protein of the various connective tissues in animals. As the main component of connective tissue, it is the most abundant protein in mammals, making up from 25 to 35 % of the whole-body protein content.

Cytokine Cytokines are a category of small proteins that are important in cell signaling. They include chemokine, interferon, interleukins, lymphokines, and tumor necrosis factor. Tumor necrosis factor-α (TNF-α) and interleukin-1 (IL-1), IL-6, IL-11, and IL-18 are cytokines that are responsible for initial pro-inflammatory response at fracture healing.

Demineralized bone matrix A form of allogenic bone type produced by extraction of allograft. DBM is used every area where allogenic grafts are used.

Distraction osteogenesis A surgical process used to reconstruct skeletal deformities and lengthen the long bones of the body. A corticotomy is used to create the gap formation between two segments of the bone. So the new bone formation in the gap is formed after osteotomy.

Dynamization In order to increase fracture healing and increase the callus integrity, external or intramedullary fixation device stimulates micro-movement between the fracture ends under controlled loading.

Endochondral ossification Involves the replacement of a cartilage model by the bone. This process contributes to longitudinal growth.

Extracellular matrix Collection of extracellular molecules secreted by chondrocytes that provide structural and biochemical support.

Hard callus From 2 to 3 weeks onward, a process begins whereby the fragile cartilage material of the soft callus is transformed completely into hard callus. Once the hard callus has formed at the former fracture site, then fracture union is said to have occurred.

Haversian system Haversian system is a series of tubes around narrow channels formed by lamellae. This is the region of the bone called compact bone.

Intramembranous ossification During fracture healing process, direct conversion of mesenchymal tissue into the bone is called intramembranous ossification. It also occurs without cartilage model (unlike enchondral ossification).

Osteoblast A large cell that is responsible for the synthesis and mineralization of the bone during both initial bone formation and later bone remodeling.

Osteocalcin Osteocalcin is the most abundant non-collagenous protein in the bone. Osteocalcin can be used as a marker of bone turnover.

Osteoclast Multinucleated, irregular giant cells which are responsible for resorption of the bone.

Osteoconduction Osteoconduction occurs when the bone graft material serves as a scaffold for new bone growth.

Osteogenesis A process of laying down new bone material by cells called osteoblasts. In other words, osteogenesis means bone tissue formation.

Osteogenic Osteogenic materials are derived from or made up of bone-forming tissue such as osteoblasts, primitive mesenchymal cells, and osteocytes. This osteogenic cell induces or supports the formation of the bone.

Osteoinductive Is a process that supports the mitogenesis of undifferentiated perivascular mesenchymal cells, leading to form new bone.

Osteopontin Osteopontin is known as a highly phosphorylated bone sialoprotein that is a prominent component of the mineralized extracellular matrices of the bones.

Periosteum The double-layered fibrous membrane covering the surface of the bones. The inner cambium layer has osteogenic and chondrogenic potential.

Platelet Blood cells whose function (along with the coagulation factors) is to stop bleeding.

Proteoglycan Heavily glycosylated proteins that consist of glycosaminoglycan (GAG) chains attached to a core protein.

Relative stability Flexible stabilization of the fracture that leads to micro-movement in the fracture line induces callus formation. This is known as relative stability.

Soft callus Soft callus is a temporary formation of fibroblasts and chondroblasts which forms at the area of a bone fracture as the bone attempts to heal itself. Following healing process, soft callus is eventually replaced by the bone.

Clinical Relevance

Is it possible to remove external fixator components smartly?

In order to promote healing of the fracture, progressive destabilization was used for this 21-year-old man with a compound tibial shaft fracture after a gunshot injury which was treated with external fixation. In clinical setting, different methods are used for enhancement of fracture healing process under external fixation [64]. Especially in the treatment of fresh fractures, the external fixator system which can increase movement and loading on fracture ends in the advanced stages of fracture healing has a positive effect on fracture healing and increases the callus integrity [63]. Dynamization [62] and progressive destabilization [6] are commonly used techniques.

You can see the clinical pictures of the patients' leg before (A) and after (B) the destabilization process (Fig. 19.1). The second bar was removed from the external fixator system, and the first bar was elevated from the skin in order to decrease the system stability. All these manipulations decrease system stability, and the ends of the fracture expose more compressive forces with full weight-bearing. It is very well known that compressive forces and controlled micromotions at the fracture site help to fracture healing process [55]. Both dynamization and destabilization increase the rate of maturation of the fracture, and the risk of refracture seen in early removal of the fixator is decreased.

Introduction

Fracture healing and bone repair, an extremely complicated and also a perfect process, have been successfully attracting man's attention for many years. Although a great number of mechanisms regarding the process have been figured out, much still remains unknown. The healing process starts following an injury. The primary causes of bone injury include trauma, infection, and oncological and metabolic events. In contrast to the healing of soft tissue where injured tissue is replaced by fibrous scar tissue, bone healing occurs through the

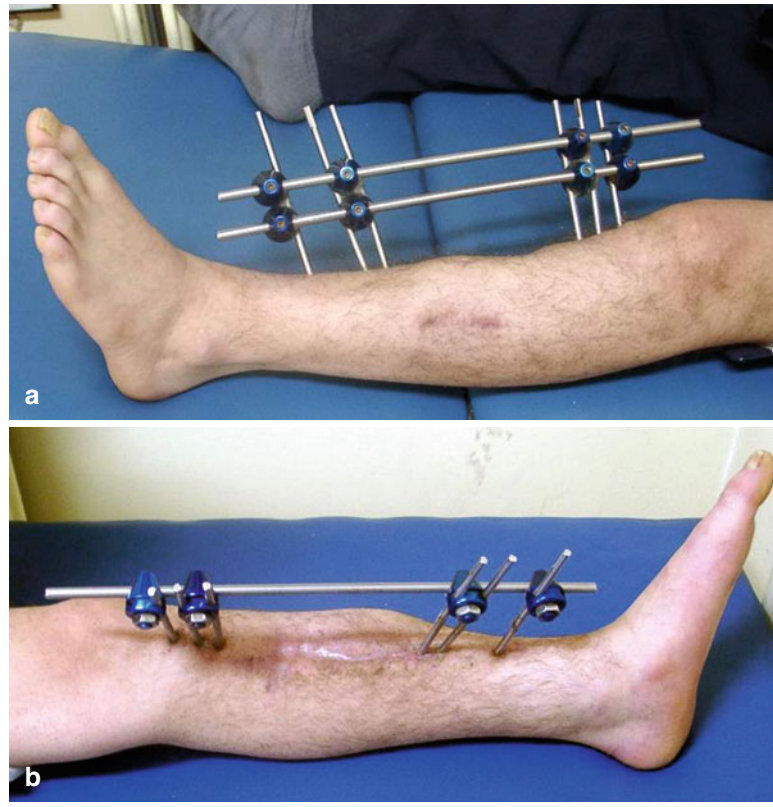

Fig. 19.1 A monolateral external fixator showing progressive destabilization process for enhancing fracture healing, before (**a**) and after (**b**) removal of some components of the external fixator

regeneration of a normal bone tissue. In other words, there is no place for a scar tissue in fracture healing. Moreover, a nonunion occurs as a result of formation of fibrous scar tissue. Thus, fracture healing can be defined as tissue regeneration. In this repair process, there is a cyclical effect created not only by growth factor stimulation but also by the division and differentiation of different cells exposed to inflammation and chemotaxis [1–5].

Fracture repair is closely related to the external factors such as mechanical environment of the fracture site and the type of fixation method. Although most of the factors affecting healing have been revealed in studies, what provides the ideal fracture fixation is still unknown. While the healing process is negatively affected if there is abnormal or gross motion of the fracture ends following reduction or excessive distraction, controlled micro-movement or periodic distraction can accelerate this process [5, 6]. While motion of the fracture site results in healing with the cartilage structure called as *endochondral ossification* (secondary or indirect healing), on the other hand, absolute lack of movement in the fracture area is characterized by direct bone formation called as *intramembranous ossification* (primary or direct healing). The vast majority of fractures heal with a combination of these two types of ossifications [4–7]. Endochondral and intramembranous ossifications also occur in the development of long bones. By expanding the bone while growing, the mesenchymal cells in periosteum are differentiated from osteoblasts with intramembranous ossification. In contrast, during the fracture healing and callus distraction, the mesenchymal cells in periosteum are differentiated from chondrocytes, and generally, endochondral ossification occurs [4, 5].

The Histopathological Periods of Fracture Healing

Fracture healing, which is a very complex process, can generally be examined as three overlapping stages. These are *the inflammatory*, *the repair* (soft and hard callus), and *the remodeling* stages. Bone tissue is extremely strong as a structure but fractures occur by excessive forces. When there is a fracture, not only bone tissue is injured, but also the periosteum, muscle tissues, and endosteal and periosteal vascular structures are damaged. The cortex, periosteum, bone marrow, and surrounding soft tissue in the field of injury all contribute to the healing process. A fracture, which is a mechanical event, triggers a reduction in local oxygen and nutrients at the site and secretion of various factors to the area, which will lead to biological events [4, 5].

The inflammatory stage starts with following trauma and the hematoma which is necessary to healing process formed with the cells containing bone marrow of peripheral and intramedullary origin. The major actors in the inflammatory process are cytokines, platelets, bone morphogenetic protein (BMP), and mesenchymal stem cells (MSCs). The inflammatory phase continues for approximately 1 week and progresses with cellular accumulation and macrophages and thrombocytes coming quickly to the injury site. Many growth factors are expressed from the cells. Primarily, these may include platelet-derived growth factor (PDGF), transforming growth factor-β (TGF-β), interleukin-1 and interleukin-6, and cytokines such as prostaglandin E_2 [3–5].

The initial pro-inflammatory response includes tumor necrosis factor-α (TNF-α) and interleukin-1 (IL-1), IL-6, IL-11, and IL-18 secretion. These pro-inflammatory cytokines are not only expressed from the macrophages but are also secreted from the MSCs in the periosteum. The secretions peak in the first 24 h after any fracture, and while the levels reduce during the period of cartilage formation, an increase is seen again during the bone remodeling phase [8]. These factors contribute to the accumulation of inflammatory cells and angiogenesis. In addition, cytokines play a role in endochondral bone formation and in the regulation of remodeling.

TNF-α is expressed from the macrophages and the other inflammatory cells, and it is believed that it plays a role in the formation of secondary inflammatory signals and the accumulation of chemotactic factors. IL-1 and IL-6 are the most important interleukins in fracture healing. In addition to the primary cartilaginous callus production of these two interleukin molecules and the angiogenesis-stimulating effects in the injury area, IL-6 also stimulates osteoblast and osteoclast differentiation [3]. All these factors play an active role in starting of the repair process with activation of the cells in the bone marrow, periosteum, and fracture hematoma [3, 5, 9–15].

In the early stage of bony formation, periosteal pre-osteoblasts and local osteoblasts differentiate to new bone with the expression of osteocalcin gene. As mesenchymal cells and fibroblasts proliferate with early new bone formation, they swap with fracture hematoma. The stem cells, which play an effective role in fracture healing, are believed to originate from the bone marrow, periosteum, local muscle, soft tissues, and vascular tissues [4–6, 11]. After maturation of fracture hematoma, a newly formed blood vessel network advances to the healing fracture callus. This vessel network forms a source for the growth factors and progenitor cells which differentiate the mesenchymal cells. The collagenous matrix develops in fracture hematoma and it contains major collagen types. These collagens are Type I and Type II collagens and are responsible for the continuity of the non-cartilaginous and cartilaginous extracellular matrix (ECM), respectively [5, 12]. In *the soft callus* period, which can last up to 3 weeks, the mesenchymal cells are differentiated from the chondrocytes which will create cartilaginous callus formation. Mature and hypertrophic chondrocytes release Type X collagen and proteases which fragment ECM. At the same time, hypertrophic chondrocytes express transcription factor called as *runx2* which regulates ECM proteins such as osteocalcin and osteopontin which are necessary for ossification [4, 5, 12, 16–19].

The differentiation of the hypertrophic cartilage to the bone is noticeable in the advanced stages of fracture healing. This final stage is known as *the hard callus* period, and soft callus tissue gradually changes to hard callus tissue which will be solid. In this period, the chondrocyte differentiation, apoptosis, ECM fragmentation, revascularization, and bone formation occur [5]. Consequently, cartilage tissue in the medium becomes calcified. At this point, new blood vessels enter the medium, and transformation of the cartilage to bone tissue continues. Finally, matured new bone cannot be distinguished from the original bone, and this period is called as remodeling stage of fracture healing [3–5, 12, 13, 20].

Histo-biological Characteristics of Fracture Healing

For an ideal fracture healing, there are four main biological requirements [5, 9, 14]. Firstly, it is necessary to have a series of *the progenitor or MSCs* in the right place at the right time. These cells also originate from trabecular bone, surrounding soft tissue including synovia and synovial fluid, the hematopoietic system, bone marrow, and particularly the deep layers of the periosteum, and they play an important role in fracture healing process [5]. Previous studies have supported that osteoblasts and osteocytes, which have a role in the formation of new bone, originate from periosteum, bone marrow, and endosteum, while chondrocytes within the fracture callus primarily originate from the periosteum [5, 15, 16]. Traumatic damage or subtraction of the periosteum leads to the loss of the local source of the multipotent MSCs. Absence of these cells consequences a delay in fracture healing. For bone regeneration, it is necessary to have an accumulation of MSCs that they proliferate and that they differentiate to osteogenic cells. Recent publications have emphasized that accumulation of the circulating systemic MSCs, particularly at the inflammatory response stage, plays an extremely important role in repair process [17–19]. In other words, as a response to the signaling associated with tissue damage, MSCs are sent to the fracture site and participate in the repair process. Primary source of these MSCs originating in the bone marrow is the periosteum cambium layer in fracture healing. Buckwalter et al. demonstrated that, if periosteum is removed, the fracture callus capacity is reduced [20].

The osteoprogenitor cells also produce some molecules such as BMPs, stromal cell-derived factor 1 (SDF-1), and hypoxia-inducible factor-1 α (HIF-α) [3]. These molecules also play an important role in bone repair. While BMP-2 is crucial in bone repair, other BMPs such as BMP-7 are more important in the accumulation of the progenitor cells. In an experimental rat model, the levels of BMP-2, BMP-4, and BMP-7 showed an increase in the early stages of intramembranous ossification [21].

The second requirement for bone repair is *the structure of ECM* that will create the scaffold to which the progenitor cells can attach. ECM is a dynamic structure and shows continuous changes in order to provide differentiation by gathering together progenitor cells in the bone regeneration process. The main structure of ECM is formed by collagens in cartilage and bone tissues [5]. The main collagen components are Types II, IX, X, and XI for the cartilage matrix and Types I and VI for of the bone matrix. During the bone healing process, ECM keeps on remodeling constantly. This cascade is primarily organized due to the resorption of mineralized cartilage started by macrophage colony-stimulating factor (M-CSF), receptor activator of nuclear factor kappa-B ligand (RANKL), osteoprotegerin, and TNF-α. The most important role of TNF-α is to trigger chondrocyte apoptosis. The absence of TNF-α results in a delayed resorption of mineralized cartilage and prevention of the formation of new bone. Some studies showed that while the level of RANKL is very low in intact bone, it is very high in levels after any fracture [8, 12]. In time, the cartilage tissue is replaced with bone tissue, and this substitution occurs in endochondral ossification; this is one of the most spectacular examples of tissue remodeling [5]. The fracture can gain a more stable structure from soft callus formed from cartilaginous callus in areas of relatively weak mechanical stability. This central

hard callus and the bridging which is formed allow weight-bearing on the fracture and ultimately represent a semirigid structure.

The third requirement is *some molecular structures* which play an effective role in the process of cartilage formation and ossification at different times. Runx2, BMP, TGF-β, and IGF are well-known molecular structures which play a role in osteoblast differentiation [5, 12]. Of these factors, there is a greater understanding of the importance of factor runx2, which plays a direct role in osteoblast differentiation.

The final requirement is to have *sufficient blood supply* in the region. For successful fracture healing, it is necessary to have a good blood supply and revascularization. Endochondral fracture healing does not remain only within the angiogenesis pathways but also includes cartilaginous degradation to remove the ECM and cells and chondrocyte apoptosis which is necessary for the development of blood vessels at the fracture site [5]. Nowadays, the effect of vascularization of the injured area on repair is a well-known issue. Because of this, it has been attempted to make the surgical methods used for fracture fixation and implant designs appropriate to protect of vascularization in the last few decades [22, 23]. In the endochondral ossification process, the replacement of the hypertrophic cartilage structure with bone tissue requires good vascularization of the environment. The vascular ingrowth within the developing callus tissue is regulated by fibroblast growth factor (FGF), vascular endothelial growth factor (VEGF), and angiopoietins 1 and 2 [3]. The two molecular pathways regulating the vascularization process are the angiopoietin-dependent pathway and the VEGF-dependent pathway [10]. As angiopoietins 1 and 2 are primary vascular morphogenetic proteins, they are expressed in the early stages of the healing cycle. In contrast, VEGF is expressed in the advanced stages of endochondral bone formation. VEGF plays a key role in the regulation of vascular regeneration and is thought to be the most effective factor [3, 24]. VEGF is expressed from both osteoblasts and hypertrophic chondrocytes. Thus, the opportunity is provided for transformation of the avascular cartilaginous matrix to vascularized bone tissue and blood vessel invasion. At the same time, VEGF is an essential mediator in the neo-angiogenesis and revascularization of the fracture site. In addition to VEGF, some other molecules such as TGF, BMP, FGF, and PDGF also play a regulatory role in the vascularization process [4, 5, 24].

Types of Bone Healing

There are two different ways of healing as *direct* (primary) and *indirect* (secondary) bone healing [3–5]. Direct healing is achieved by cortical healing cycle after complete anatomic reduction of the ends of fracture. The continuity of the fractured cortexes helps to intersect conic extensions. The bone structure formed without remodeling allows anatomic lamellar bone and rapid Haversian regeneration. If there is any form of movement in the fracture line, indirect fracture healing occurs.

Indirect (Secondary) Fracture Healing

Indirect fracture healing is the most commonly seen form of fracture healing. It can be summarized as a combination of endochondral and intramembranous ossification and subsequent callus formation [3]. This process develops with micro-movements of fracture ends and is accelerated by weight-bearing. The fracture healing which is seen in conservative treatment methods, intramedullary nailing, and external fixation or minimally invasive percutaneous osteosynthesis (MIPO) is called as indirect fracture healing [5, 24] (Fig. 19.2a–c).

Indirect fracture healing starts with the collection of fracture hematoma following a fracture. In contrast to the known negative effects of extended and chronically expressed inflammatory cytokines on the bone, joint, and implant materials, after an acute injury, pro-inflammatory molecules expressed short-term and, at a high rate, have a critical and positive effect on tissue regeneration [9]. The acute inflammatory response peaks within 24 h and is completed within 7 days.

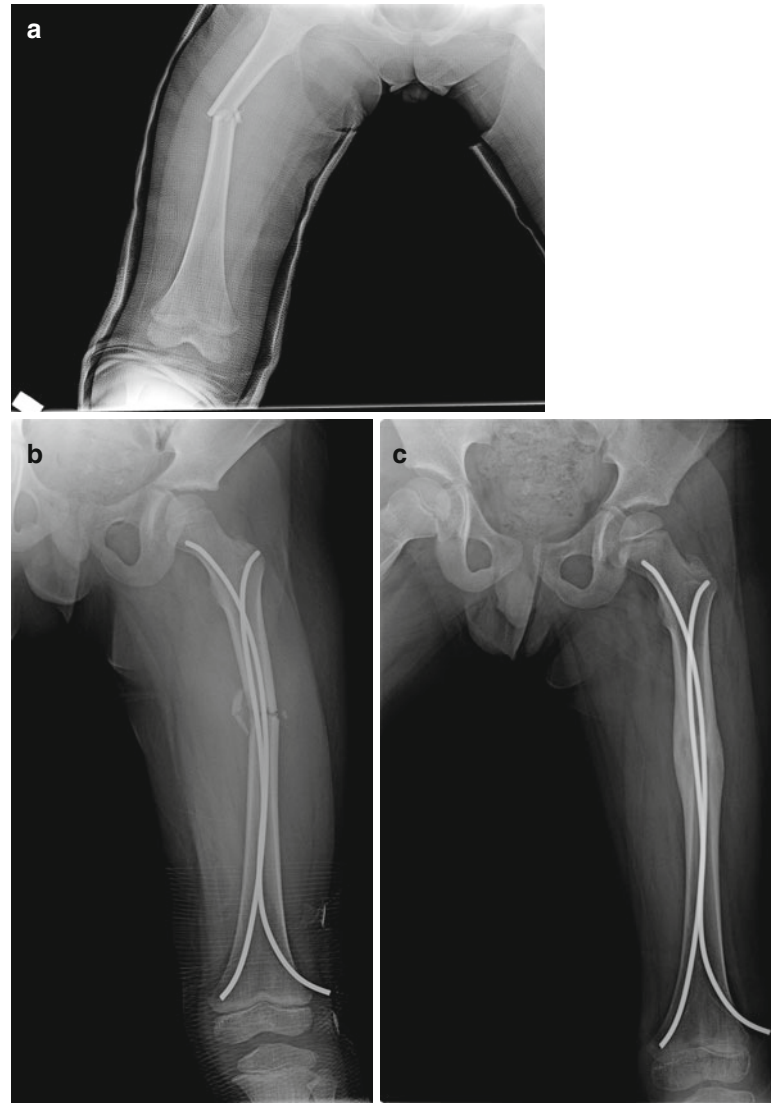

Fig. 19.2 A femoral shaft fracture in an 8-year-old boy (**a**) was treated by closed intramedullary nailing with elastic nails (**b**). Note the aberrant callus formation at 6-month follow-up radiograph that suggests indirect bone healing (**c**)

Following the inflammatory stage, indirect healing continues with the MSCs and the formation of cartilage callus followed by periosteal callus. Both intramembranous and endochondral ossification occur in indirect bone healing. In time, the cartilage callus is replaced with the mineralized and resorbed bone callus formation. Intramembranous bone formation occurs with osteogenic differentiation of periosteal MSCs without the cartilage stage. Endochondral ossification, however, requires the formation of chondro-progenitor cartilage callus [2].

At advanced stages, the bone regeneration process in a well-vascularized environment requires the transformation of primary soft callus to hard callus by resorption. This stage of fracture healing includes a combination of cell proliferation and differentiation and an increase in the number of cells and matrix deposition [3]. The chondrocytes of the fracture callus become hypertrophic with proliferation, and thus, the ECM becomes calcified. Due to the replacement of woven calcified cartilage with advanced formation of hard callus, the callus becomes stiff and mechanically rigid. Although hard callus

provides a rigid structure for biomechanical stability, the biomechanical properties of normal bone cannot be completely regenerated. The secondary resorption stage of the fracture healing cascade starts for a strong bony structure. In this stage, the hard callus is remodeled to lamellar bone with a medullar cavity in the center. While this stage is biochemically regulated by IL-1 and TNF-α is expressed at high rates, it has been observed that the expression of TNF-β is reduced at the same time [3, 5].

The process of remodeling occurs through the balance between resorption of the hard callus by osteoclasts and deposition of the lamellar bone. Although this process starts within 3–4 weeks of the fracture, the complete regeneration of the bone structure continues for years. Axial bone remodeling occurs with stimulation of osteoblastic activity and osteoclastic activity with the formation of electropositivity on the convex side and electronegativity on the concave side, respectively [20]. Thus, step by step, external callus is replaced with lamellar bone. In contrast, the remodeling of internal callus occurs with the formation of the new medullar cavity in the bone diaphysis [1, 3, 9]. Appropriate blood flow and a gradual increase in mechanical stability are indispensable components of successful bone remodeling.

Direct (Primary) Fracture Healing

Direct healing occurs outside of the natural process of fracture healing. For this healing model, anatomic reduction without any space between the fracture ends and rigid fixation are absolute conditions. When these conditions are met, the bone will become lamellar bone over time. Finally, it can be said that from the formation of direct healing, Haversian canals and revascularization are able to be formed. This process can take months or even years.

Direct healing may be in the form of *contact healing* or *gap healing* [1–5, 25–27]. In both processes, the structure is reformed by direct anatomic correction and biomechanically sufficient lamellar bone. For direct bone healing, anatomic restoration of fracture fragments is essential. After anatomic placement, the rigid fixation applied significantly reduces the strain between the fracture fragments. Obtaining bone continuity mechanically makes it possible to bring the bone together as a single entity from one cortex to the other [23, 28].

When the gap between the bone ends is <0.01 mm and the strain between the fragments is <2 %, the fracture is defined as *contact healing* [3] (Fig. 19.3a–c). In these conditions, intersecting conic extensions are formed from osteons in the region closest to the fracture site. By crossing the fracture line, the intersecting conic extensions include osteoclasts, and longitudinal cavities are formed in the bone. These cavities are filled with osteoid tissue formed by osteoblasts. The result is the simultaneous restoration of the Haversian systems and bone union. The newly formed Haversian systems allow for the penetration of blood vessels which carry osteoblastic precursors. The bridging osteons mature by directly remodeling as lamellar bone. Ultimately, fracture healing occurs without the formation of periosteal callus.

In the second form of direct healing, *gap healing*, bone union and the remodeling of the Haversian system are different. This situation occurs when there is successful anatomic and stable placement. In this system, the long bone vertical axis is primarily filled with developed lamellar bone. The primary bone structure changes step by step with longitudinal revascularized osteons produced by lamellar bone. This lamellar bone consisted of long vertical axises and it is mechanically weak. The initial process takes 3–8 weeks. Although it is not dense until endochondral remodeling, this stage is necessary for the complete restoration of anatomic and biomechanical properties [26, 28].

Stimulation of Fracture Healing

For many years, scientists have hoped to accelerate fracture healing, and various studies have been conducted related to this. Generally, the methods used to enhance process of the fracture healing can be classified under the two subheadings of

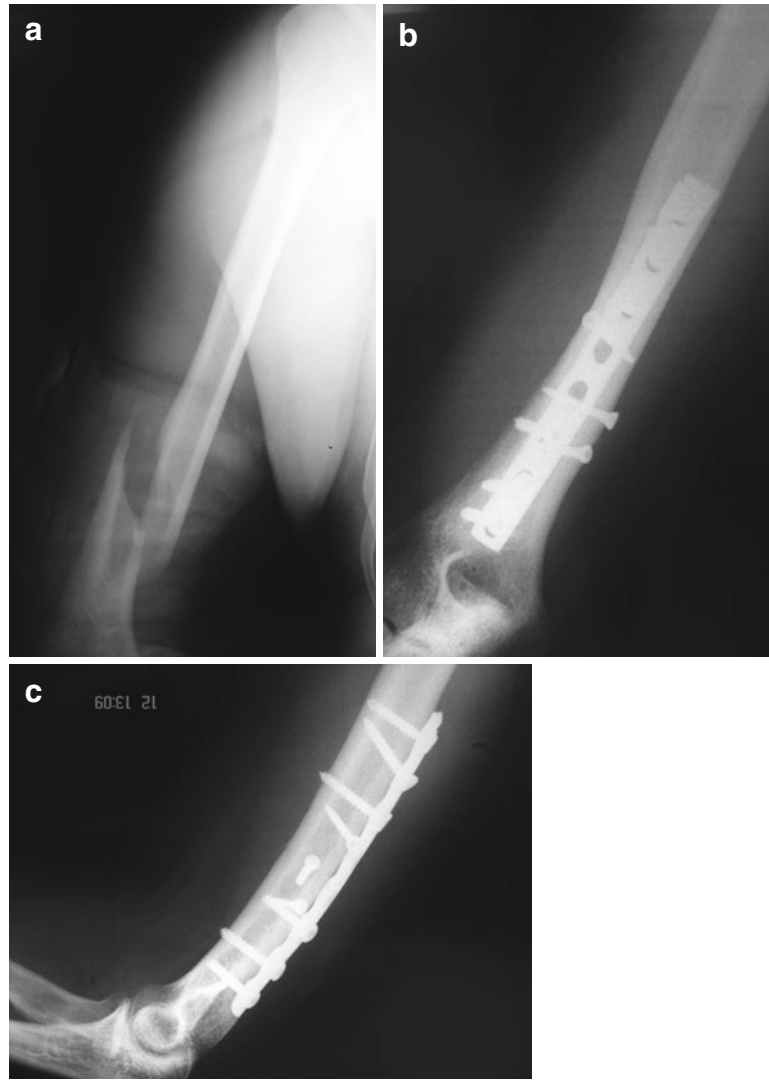

Fig. 19.3 A closed fracture of the distal part of humeral shaft (**a**) was treated by conventional open reduction and internal fixation with a dynamic compression plate (**b**). Excellent direct bone healing was achieved after anatomical reduction and rigid fixation of the fracture, and there is no visible callus formation at the last follow-up x-ray (**c**)

biological and *physical* methods. Biological stimulation is provided with osteoinductive, osteoconductive, or osteogenic factors [1–6, 11, 13, 14, 20, 25, 28]. While the osteoinductive effect has the meaning of stimulating bone formation, the osteoconductive effect is stated for the factors forming an appropriate skeletal frame for fracture healing. The osteogenic effect is stated to mean the factors stimulated for osteogenesis directly from the cells [4, 12, 29]. In addition, the electrical effect and the application of ultrasound can be included in the physical modalities used on the fracture site [2–5, 20, 28].

Autogenous Bone Grafts

Nowadays, autogenous bone grafts are the gold standard graft source [5]. Osteoinductive growth factors are included in osteogenic stem cells which are present in the bone marrow and osteoconductive ECM. Autogenous bone grafts have all these properties together. Osteoinduction occurs through differentiation of MSCs accumulated from the surrounding soft tissue from progenitor cells which make the bone. Osteoconductive materials support osteoprogenitor formation from vascularization as a

structural scaffold. Osteogenesis is defined as the process of bone formation. Osteogenic materials, in the context of bone grafting, include live cells such as osteocytes, osteoblasts, and primitive mesenchymal cells which have the capability to differentiate bone. The disadvantages of autogenous bone grafting can include morbidity of the host site, nerve, or artery injuries and infection while harvesting the graft (at rates of 8–30 %) [3–5, 30]. These disadvantages have increased the interest in alternative bone graft sources.

As autogenous cancellous bone grafts have a wider surface area than that of active osteoblasts, the formation of new bone is induced more from cortical bone. Bone formation and resorption occur simultaneously. While osteoclasts resorb dead trabecular bone, osteoblasts express osteoid laydown on the necrotic bone surface. This process is known as "creeping substitution" [5]. As a result, spongious grafts cannot provide immediate structural support to the bone. However, with swift incorporation, the host bone and bone marrow change places within 1 year. With these properties, spongious autogenous bone grafts are an excellent treatment choice in conditions which do not require structural support [3–5].

Autogenous cortical bone grafts are generally taken from the ribs, the fibula, or the ilium, either together with vessel pedicles or isolated. The majority of autogenous cortical grafts are osteoconductive and very few are osteoinductive. As the thickness of the cortical bone does not allow the continuation of life in osteocytes after transplantation, the osteogenic properties are very limited. Revascularization is very slow because of the cortical bone density. The functions of vascularized grafts are independent of the host vascularization because of their own blood vessels. Vascular penetration occurs through invasion of the Volkmann and Haversian canals and by peripheral osteoblastic resorption. Autogenous cortical bone grafts without blood vessels can be used in segmental bone defects which urgently require up to 6 cm of structural support. In large defects of more than 12 cm, vascularized grafts should be selected [3–5, 31].

Autologous Bone Marrow

Autologous bone marrow contains osteogenic precursor cells, and the usage as a graft depends on the number of osteoprogenitor cells. It has been shown in various experimental animal studies and clinical applications that bone marrow has the potential to be an osteogenic material and can be applied in the treatment of problems related to the bone union [29, 30, 32, 33]. New bone formation and accelerated fracture repair are brought about through this effect of bone marrow associated with the probable activities of the stem cells within and their stimulating factors. With blood loss or bone marrow aspiration, it has been determined that a secondary osteogenic peptide is expressed in the organism [29]. An experimental rabbit model study has also shown that in cases of delayed union or nonunion, autologous bone marrow accelerated fresh fracture healing and the healing of bone defects [32]. It is thought that there will be increasing use of autologous bone marrow in bone engineering in the future.

Distraction Osteogenesis (DO)

DO which is formed through low-energy gradual distraction of the vascularized surfaces of the osteotomy line with mechanical tension is defined as the new bone formation in the gap formed after an osteotomy. This method was presented for orthopedic reconstructive surgery by Gavril Ilizarov [34]. The mechanical stresses during distraction lead to the activation of various osteogenic pathways. This activation results in the stimulation of proliferative and biosynthetic cellular functions, known as *mechanotransduction*. Mechanotransduction leads to the temporary and spatial expression of various cytokines, such as BMP, FGF, IGF, TGFB, VEGF, and HIF, metalloproteinase, and ECM proteins [35–37]. When distraction forces are applied to these molecules, they upregulate, and at the end of the distraction phase, they downregulate. New bone is formed and remodeled in response to the balanced anabolic and catabolic reactions to biological, chem-

ical, and mechanical stimulations made in the distraction gap during DO. Bending or fracture of the regenerate formed when mechanical force is applied at the physiological level of the bone led to the emergence of external fixator. Bone regeneration formed during DO occurs as a response to longitudinal mechanical loading applied to the callus. The regenerate which fills the distraction gap is mostly formed through intramembranous ossification [38, 39]. Endochondral bone formation, however, may be seen in cases where new bone formation is delayed because of impaired blood circulation or stable external fixation in experimental models of DO.

Bone regeneration during DO uses the same processes which occurred in bone healing. However, the tissue healing during DO is different in a molecular and cellular sense. For example, the regenerative processes of both DO and bone healing include both intramembranous and endochondral bone formation. While endochondral bone formation is predominant in bone healing, intramembranous ossification is predominant in DO [40]. Both bone healing and DO are driven by the activities of molecule mediators of inflammation, TGF-β superfamilies' morphogenes, and angiogenesis mediators. The main difference between the two processes is the level and timing of the expression of skeletal growth factors such as IL-1, IL-6, and TGF-β.

Allogenic Bone

In contrast to the limitations such as potential morbidity in the iliac wing after harvesting autologous bone graft and the restricted capacity of the bone to be used, allogenic graft materials have attracted interest as no morbidity is created in the donor site, and they can be adapted to the measurements of the defect. The primary areas of use are orthopedic applications such as spinal surgery and arthroplasty. In these applications, the majority is used fresh frozen, frozen, or demineralized [5]. In comparison with autologous bone grafts, the potential risk of disease transmission reduced mechanical and biological properties, and higher costs are the main disadvantages of allogenic bone. On the top of that, the usage of allogenic bone is extremely limited in fresh fractures or nonunion cases. Sterilization methods such as fresh frozen and frozen and storage conditions are especially important. For example, the fresh frozen method reduces the osteoinductive potential of the allograft because of the induced death of the osteogenic cells. In contrast, sterilization by freezing at −60 °C or below reduces immunogenicity without changing the biomechanical properties [41]. Although the structural support provided by the allografts in particle form is weak, while there are properties of rapid revascularization and incorporation to the host bone in cortical allografts, incorporation to the host bone is extremely slow [41].

Demineralized Bone Matrix

Demineralized bone matrix (DBM) is an allogenic bone type produced by extraction of allograft [4, 5]. Using of DBM has been researched and becomes widespread in every area where allogenic grafts are used. Although DBM includes Type 1 collagen, non-collagen proteins, and osteoinductive growth factors, it does not provide structural support to the bone. DBM contains some carriers such as hyaluronic acid, glycerol, and gelatin. In the demineralization process, the osteoinductive glycoproteins including BMPs activate formative cells in host bone [5]. DBM has greater osteoinductive potential compared to conventional allografts because of the growth factors that can be biologically derived.

Mesenchymal Stem Cells

New bone formation after a fracture requires the differentiation of MSCs from osteoblasts. The clinical use of MSCs which play a key role in the process of fracture healing can be explained by the capacity to be able to be differentiated from osteoblasts in particular. The primary advantage of allogenic transplantation of MSCs is that it

does not require immunosuppression of the host [42–44]. MSCs are non-immunogenic and can be obtained from several sources. The side effects related to the use of MSCs are not seen during and after application. In addition, although the use of MSC especially in bone defects has yielded promising results in clinical practice, further researches are really needed.

Bone Graft Substitutes

An ideal substitute of bone graft must provide bridging for osteoinduction, growth factors to osteoinduction, and progenitor cells to osteogenesis [2, 4, 5, 20, 45–48]. Each of these materials must provide at least one of the abovementioned criteria. The effective use of the bone substitutes will avoid the limitations of autogenous bone graft usage.

Calcium sulfate, otherwise known as plaster of Paris, has been an extremely biocompatible substitute of bone graft. The osteoconductive function is seen through the filling of the bone cavities with matrix. Due to osteoblasts being associated with *calcium sulfate* and osteoclasts being reabsorbed and lacuna which are seen in the normal bone [4, 5]. The resolution of calcium phosphate makes the microenvironment acidic. This restricts bacterial activity. Using of calcium sulfate is being researched especially for acetabular fractures, nonunion, and defective cases. In recent years, manufacturers have focused on the combination of DBM and calcium sulfate [5].

Calcium phosphate ceramic is an osteoconductive and extremely biocompatible material. In metallurgy, it is obtained in pellet form by a process of heating shoots in natural powder form or milled [45]. A good osteoconductive skeletal material must have biomechanical properties similar to those of the surrounding bone. Most ceramic materials provide the facility of osteoconduction. However, its fragility and weak tensile strength limit its use as a bone graft [5, 45]. *Hydroxyapatite* (HA) and *tricalcium phosphate* are the most frequently used forms of phosphate ceramics and are generally used as implant coating or defect filling [45]. These materials have a similar composition and crystallinity to the mineral phase of the bone. Due to osteoinductive properties, the regeneration of bone morphology and strength is made through osteoclastic resorption and osteoblastic location change [5, 46]. HA is a ceramic with slow resorption and encourages osteointegration. The hydrothermal process applies hydroxyapatites in a form similar to that of human trabecular bone structure. There have been studies which have reported that resorption is very limited over time. HA is used on the outer surface of external fixation pins, which have been shown to have greater pulling force compared to standard pins [46]. *Calcium phosphate cement* is used for filling of bone defects which form in acute fractures [4, 5, 47]. This material, which contains a combination of inorganic calcium and phosphate, can be injected into the fracture site. Within 12 h of the injection, the internal formation is completed, and final compression strength is reached to 55 MPa. In a study where the paste form under the commercial name, Norian SRS (Norian, Cupertino, CA, USA), was used on radius distal-third fractures, improvements were reported in the functional and radiological results [47]. Its use is recommended in fractures of distal third of the radius, calcaneus, and intra-articular such as the tibial plateau and also to fill cavities and to increase implant stability in unstable intertrochanteric fractures.

Growth Factors

In recent years, interest has increased in the forms of growth factors used in humans of BMP-2, BMP-7, and BMP-14 [4, 5, 48]. BMP-2, BMP-7, and GDF-5 are members of the TGF-β supergene family. BMP-2 and BMP-7 are more osteogenic than GDF-5 [5]. Promising results have been obtained in some prospective blinded studies related to the use of recombinant human BMP-2 with autogenous grafts in both lumbar interbody fusion and in cases of tibial nonunion [49]. It is known that BMPs, which are members of the TGF-β superfamily, are glycoproteins without collagen. Their effects are shown with autocrine

and paracrine mechanisms [50]. In contrast to the difficult form of induced BMP-6 and BMP-9 osteoblastic differentiation, BMP-6 can promote terminal differentiation of osteoblasts and most osteoblastic precursors of BMPs [51]. At the same time, BMPs stimulate the synthesis and expression of IGF and VEGF. BMP-2 and BMP-7 (*osteogenic protein-1*, *OP-1*) are the most often used in clinical applications. The signaling cycle of BMPs originates from human fracture callus and, via this signaling medium, plays a regulatory role in the repair process. In the last 20 years, researchers have investigated the use of recombinant human BMP (*rhBMP*) in various musculoskeletal events. In a wide prospective, controlled, randomized, partially blind, multicenter study, the use of rhBMP-7 (OP-1) was compared with iliac crest bone graft in cases of tibial nonunion. It was reported that the use of OP-1 achieved an equivalent effect to that of autogenous bone graft [52]. *rhBMP-2* and BMP-7 are currently commercially available.

Transforming growth factor beta (*TGF-β*) expressed from thrombocytes plays a role in MSC stimulation and in increasing the synthesis of collagen and other extracellular matrix proteins and in the differentiation process [53]. In addition, TGF-β seems to have a function as a chemotactic stimulator for fibroblasts, macrophages, and mesenchymal cells. Although TGF-β plays an important role in the consolidation phase of fracture healing, the main effects are seen at the initial stage of callus formation.

The Effect of Fracture Fixation Methods on Fracture Healing

Fracture healing is affected positively by certain amount of movement in the fracture line. However, it is not completely clear how much movement is necessary. The role of the motion is definite at the beginning and the advanced stages of the healing process. The movement between the fracture fragments is closely related to the whole structure, in other words to the bone and implant function.

Intramedullary Nailing

Intramedullary nailing is one of the most frequently applied fixation methods in modern fracture treatment. In this type of fixation, axial load is shared between the bone and the implant, and secondary bone healing occurs due to relative stability. At the same time, it provides good bone alignment and the possibility of early weight-bearing. Another advantage of intramedullary nailing is that minimally invasive methods can be applied without soft tissue damage on the fracture site. Nails can be used cannulated or not. Although this subject is highly controversial, limited reaming is widely recommended. The use of reaming and wide nails forms the most solid structure in a mechanical sense. However, excessive reaming can severely disrupt the vascular nutrition in the healing bone [5, 23]. In clinical setting, a reamed and statically locked nailing is commonly preferred for uncomplicated healing. The resistance to torsional and axial compressive forces of the locking screw fixation system is significantly increased and makes early weight-bearing possible, even in lower extremity fractures [54] (Fig. 19.4a–d).

Plate Fixation

Bone plates are widely used for internal fixation of fractures for many years, and they showed a great revolution from their invention [23]. From a biomechanical aspect, the total load on the fracture is beared between the bone and the plates. This is different from the intramedullary nailing in that the plate itself carries the load [4, 5, 23]. This increases the load on the plate to a thoughtfully rate. Following plate-screw fixation of lower extremity fractures in particular, it is necessary to have a period of non-weight-bearing. There are three main interfaces which are affected by the mechanics of plate-screw fixation; these are the screw-plate, screw-bone, and plate-bone interfaces [5]. Any change in these interfaces changes the mechanical behavior of the bone to which the plate is applied to a significant degree. Each component

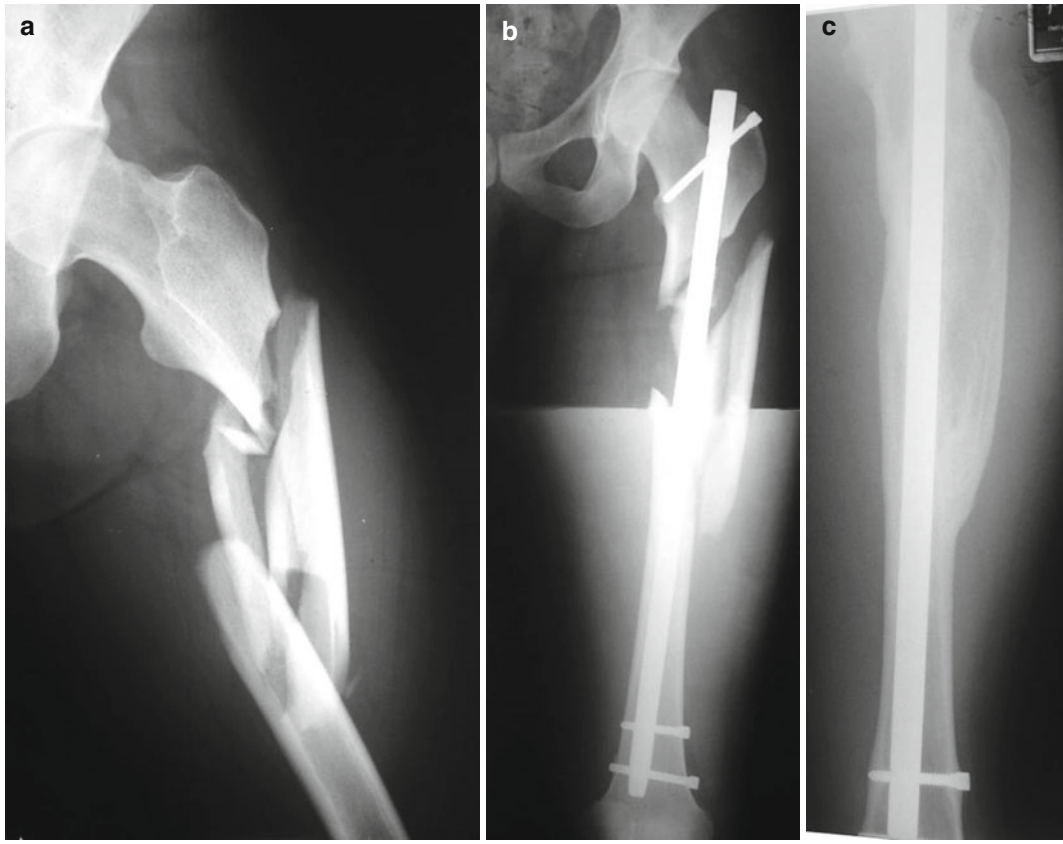

Fig. 19.4 A 27-year-old man was brought to our clinic after a serious car accident with a closed and comminuted fracture of the femoral shaft (**a**). We treated him with a closed intramedullary statically locked nailing (**b**). A full remodeling of the fracture can be seen at the 3-year follow-up x-ray (**c**). The use of closed reduction of this complicated fracture leads to spectacular bone healing due to prevention of fracture hematoma and protection of the soft tissues around the fracture. This is an excellent example for indirect or secondary bone healing

of the screw-plate-bone triad has an important role in the whole fixation scaffold. Insufficient grip of screws in osteoporotic bone leads to plate fixation failure and finally nonunion.

Plates are placed in different locations on each bone. Plates should be placed generally with the most appropriate side to the surrounding bone and as far as possible on the concave side [5]. Resistance to tensile force increases the chance of full bone union by continuing contact between fracture ends. For example, in the plate-screw technique in femoral shaft fractures, the plate should be placed on the lateral surface of the femur. This method is known as the "tension band" effect and is recommended for direct bone healing of the opposing cortexes. Weakening with loading on the bone below the plate in bone plating is known as "stress shielding" [5]. In this case, the response of the bone above the plate will be a reduction in mass and geometry and a significant weakening of the mechanical properties. Therefore, the removal of some plates is recommended after union.

Minimally Invasive Plate Osteosynthesis (MIPO)

MIPO is a relatively new method of indirect reduction to the fracture line which is applied through intervention with the bone and soft tissue by using small surgical instruments. Thus, surgical trauma is minimized. Previously, with a

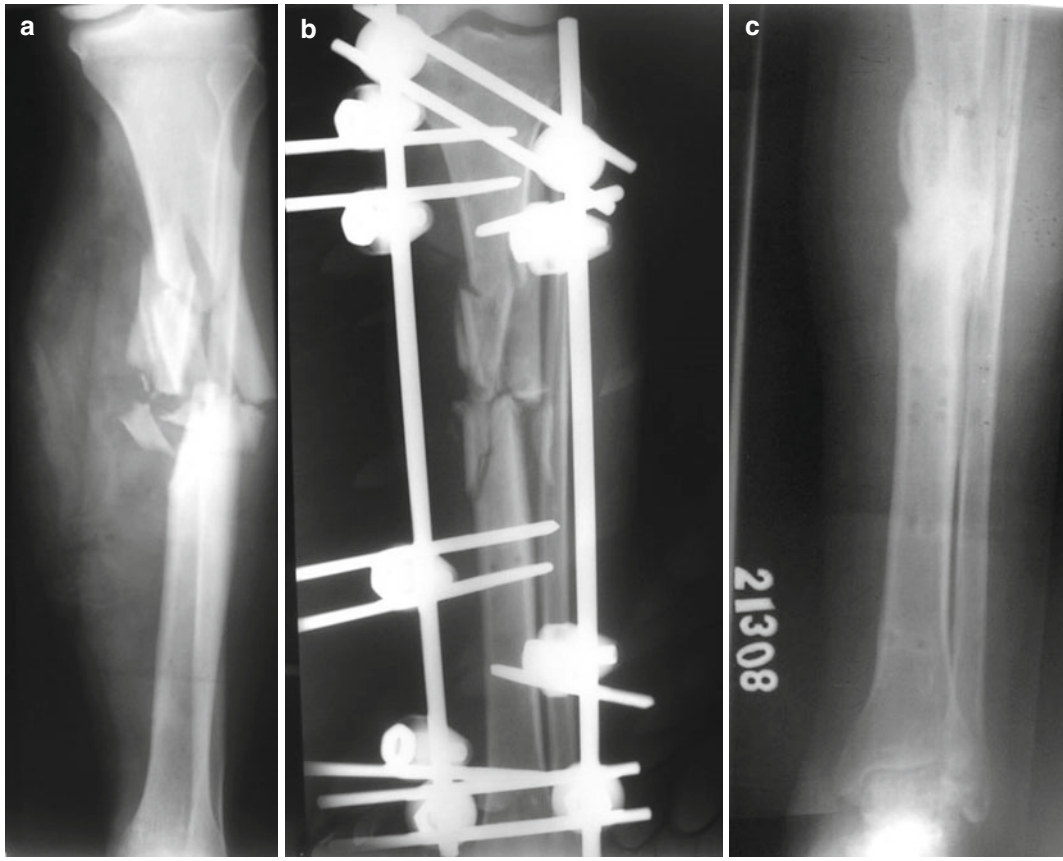

Fig. 19.5 Open fractures generally need an external fixation for safe bone healing. This is a 54-year-old man admitted to our clinic after farm injury with an open tibial shaft fractures (**a**). The fracture was treated with a monolateral external fixator after a radical debridement and copious irrigation (**b**). We used an autogenic bone grafting after wound healing to the enhancement of fracture healing, and complete healing was achieved with callus formation suggesting indirect bone healing (**c**)

conventional anatomic reduction and rigid fixation, it was aimed to have maximum stability in the fracture line. This philosophy of fixation led to severe soft tissue damage, loosening of the implant, and delayed union. Flexible stabilization, by leading to micro-movement in the fracture line, induces callus formation [55–59]. This is known as *relative stability*. In contrast to this, rigid osteosynthesis applied to the fracture line leads to direct bone healing, and this is known as *absolute stability*. When there is less than 2 % tension in the fracture line, callus tissue forms, and at 10–30 % tension, fibrous union occurs [57, 58, 60]. In other words, while strain or tension values of up to 2 % are well tolerated by lamellar tissue, strain of 10–30 % results in resorption in the fracture area. Lower tension in the fracture line of fragmented fractures in particular allows for flexible fixation to be applied.

The current use of new plating methods in fracture repair aims to protect the vascularization by limiting the periosteal dissection via indirect reduction. The aim of indirect reduction is only the achievement of alignment, rotation, and correct length of fragments. A balance between maximum stability and excellent mechanics can be obtained with this method. It is not necessary to have complete fit of the plate on the bone surface in MIPO with an internal fixator. Thus, by forming minimal contact on the

bone surface, the damage to blood circulation is minimized. As a result, there is minimal surgical trauma and stable fixation is maintained with bleeding bone [22, 60, 61].

In minimally invasive fracture surgery, bridging plates, subcutaneous or submuscular plates, or closed methods using intramedullary nails and external fixators can be used. The primary advantages of MIPO are high union and low infection rates, use in multiple trauma cases, allowing early movement of the extremity, and less need for grafting compared to the conventional plating. However, problems encountered with MIPO include problems in coronal and sagittal alignment, difficulties in restoration of length and rotation, and delayed union [61].

External Fixation

External fixation methods are used for fracture fixation and at the same time in distraction osteogenesis (DO) [5, 34]. Direct bone contact is obtained between the fracture ends, and the weight of the fixation device is shared over only one part. However, in cases where it cannot be completely placed on the cortexes such as in multi-fragmented fractures, the external fixation devices bear the whole load. Using different configurations of external fixation devices allows for an almost unlimited combination (Fig. 19.5a–c).

In addition, external fixators are devices which allow adjustment of the degree of fixation in the healing period. Especially in the treatment of fresh fractures, systems which can increase movement and loading on fracture ends in the advanced stages of fracture healing have a positive effect on fracture healing and increase the callus integrity. A widely used method for this purpose is dynamization [2, 5, 62–64]. Dynamization of the external fixation device stimulates micro-movement between the fracture ends. Parallel to the micro-movement, an increase in the blood circulation in the fracture field has been shown to lead to an increase of 25 % in callus volume [5]. Another alternative to dynamization which can be used in monolateral or circular type of external fixator devices is *progressive destabilization* [6]. In the destabilization technique, after the visualization of callus in the fracture ends, by gradually removing the parts of the fixator to reduce the stability of the fixator, the amount of loading and micro-movement coming on to the fracture ends is progressively increased (Fig. 19.1a, b). Both dynamization and destabilization increase the rate of maturation of the fracture, and the risk of refracture seen in early removal of the fixator is decreased.

Conclusion

Bone injuries and fractures are a significant workload in orthopedics and traumatology. Each year, many new fractures occur. Bone healing is a process like no other, which develops without the formation of fibrous scar tissue and can be defined as the regeneration of a range of tissues. To obtain full functional bone regeneration, it is necessary to have progress of anatomical, biochemical, and biomechanical processes with excellent compatibility. In recent years, mesenchymal stem cells and many molecular and chemical pathways which have an important role in bone repair have been well defined. However, fracture repair continues to be an equation with several unknowns.

References

1. McKibbin B (1978) The biology of fracture healing in long bones. J Bone Joint Surg Br 60:150–162
2. Einhorn TA (1995) Enhancement of fracture-healing. Current concepts review. J Bone Joint Surg Am 77:940–956
3. Marsell R, Einhorn TA (2011) The biology of fracture healing. Injury 42(6):551–555
4. Kakar S, Einhorn TA (2008) Biology and enhancement of skeletal repair. In: Browner BD, Jupiter JB, Levine AM, Trafton PG, Krettek C (eds) Skeletal trauma, 4th edn. WB Saunders Co, Philadelphia
5. Miclau T, Bozic KJ, Tay B et al (2007) Bone injury, regeneration and repair. In: Einhorn TA (ed) Orthopaedic basic science. American Academy of Orthopaedic Surgeons, Rosemont, pp 331–348
6. Arazi M, Yalcin H, Tarakcioglu N et al (2002) The effects of dynamization and destabilization of the external fixator on fracture healing: a comparative biomechanical study in dogs. Orthopedics 25(5):521–524

7. Panjabi MM, Soutwick WO (1977) The four biomechanical stages of fracture repair. J Bone Joint Surg Am 59:188–192
8. Gerstenfeld LC, Cho TJ, Kon T et al (2003) Impaired fracture healing in the absence of TNF-alpha signalling: the role of TNF-alpha in endochondral cartilage resorption. J Bone Miner Res 18:1584–1592
9. Gerstenfeld LC, Cullinane DM, Barnes GL et al (2003) Fracture healing as a post-natal developmental process: molecular, spatial, and temporal aspects of its regulation. J Cell Biochem 88(5):873–884
10. Kon T, Cho TJ, Aizawa T et al (2001) Expression of osteoprotegerin, receptor activator of NF-kappaB ligand (osteoprotegerin ligand) and related proinflammatory cytokines during fracture healing. J Bone Miner Res 16(6):1004–1014
11. Barnes GL, Kostenuik PJ, Gerstenfeld LC (1999) Growth factor regulation of fracture repair. J Bone Miner Res 14:1805–1815
12. Haynesworth SE, Goshima J, Goldberg VM et al (1992) Characterization of cells with osteogenic potential from human marrow. Bone 13:81–88
13. Linkart TA, Mohan S, Baylink DJ (1996) Growth factors for bone growth and repair: IGF, TGF beta and BMP. Bone 19:1–12
14. Bruder SP, Fink DJ, Caplan AI (1994) Mesenchymal stem cells in development, bone repair, and skeletal regeneration therapy. J Cell Biochem 56:283–294
15. Ozaki A, Tsunoda M, Kinoshita S et al (2000) Role of fracture hematoma and periosteum during fracture healing in rats: interaction of fracture hematoma and the periosteum in the initial step of the healing process. J Orthop Sci 5:64–70
16. Lee JY, Qu-Petersen Z, Cao B et al (2000) Clonal isolation of muscle-derived cells capable of enhancing muscle regeneration and bone healing. J Cell Biol 150:1085–1100
17. Granero-Molto F, Weis JA, Miga MI et al (2009) Regenerative effects of transplanted mesenchymal stem cells in fracture healing. Stem Cells 27(8): 1887–1898
18. Elena J, Xuebin Y (2011) Mesenchymal stem cells and bone regeneration: current status. Inj Int Care Injured 42:562–568
19. Robert B, Elena J, Dennis MG (2007) The role of mesenchymal stem cells in maintenance and repair of bone. Inj Int Care Injured 38S1:26–32
20. Buckwalter JA, Einhorn TA, Marsh LJ (2001) Bone and joint healing. In: Rockwood CA Jr, Green DP, Bucholz RW (eds) Fractures in adults, 5th edn. Lippincott, Philadelphia
21. Bostrom MP (1998) Expression of bone morphogenetic proteins in fracture healing. Clin Orthop 355S: 116–123
22. Krettek C, Schandelmaier P, Miclau T et al (1997) Minimally invasive percutaneous plate osteosynthesis (MIPPO) using the DCS in proximal and distal femoral fractures. Injury 28:A20–A30
23. Perren SM (2002) Evolution of the internal fixation of long bone fractures. The scientific basis of biological internal fixation: choosing a new balance between stability and biology. J Bone Joint Surg Br 84(8): 1093–1110
24. Gerber HP, Vu TH, Ryan AM, Kowalski et al (1999) VEGF couples hypertrophic cartilage remodeling, ossification and angiogenesis during endochondral bone formation. Nat Med 1999:623–628
25. Dimitriou R, Tsiridis E, Giannoudis PV (2005) Current concepts of molecular aspects of bone healing. Inj Int Care Injured 36:1392–1404
26. Einhorn TA (1998) The cell and molecular biology of fracture healing. Clin Orthop Relat Res 355(Suppl): 7–21
27. Lobenhoffer P, De Simoni C, Stabuli AE (2002) Open-wedge high tibial osteotomy with rigid plate fixation. Tech Knee Surg 1(2):93–105
28. Greenbaum MA, Kanat IO (1993) Current concepts in bone healing. Review of the literature. J Am Podiatr Med Assoc 83(3):123–129
29. Muschler GF, Nitto H, Boehm CA et al (2001) Age- and gender-related changes in the cellularity of human bone marrow and the prevalence of osteoblastic progenitors. J Orthop Res 19:117–125
30. Connolly JF (1998) Clinical use of marrow osteoprogenitor cells to stimulate osteogenesis. Clin Orthop 355(Supp):257–266
31. Gazdag AR, Lane JM, Glaser D et al (1995) Alternatives to autogenous bone graft: efficacy and indications. J Am Acad Orthop Surg 3:1–8
32. Sharma S, Garg NK, Veliaht AJ et al (1992) Percutaneous bone-marrow grafting of osteotomies and bony defects in rabbits. Acta Orthop Scand 63(2): 166–169
33. Arazi M, Öğün TC, Mutlu M et al (2000) Percutaneous autogenous bone-marrow injection in delayed union and nonunion of long bone fractures: a preliminary report. Acta Orthop Traumatol Turc 34:267–272
34. Ilizarov GA (1992) Transosseous osteosynthesis. Springer, Berlin
35. Ai-Aql ZS, Alagl AS et al (2008) Molecular mechanisms controlling bone formation during fracture healing and distraction osteogenesis. J Dent Res 87:107–118
36. Haque T, Amako M, Nakada S et al (2007) An immunohistochemical analysis of the temporal and spatial expression of growth factors FGF 1, 2 and 18, IGF 1 and 2, and TGFbeta1 during distraction osteogenesis. Histol Histopathol 22:119–128
37. Haque T, Hamade F, Alam N et al (2008) Characterizing the BMP pathway in a wild type mouse model of distraction osteogenesis. Bone 42:1144–1153
38. Aronson J, Good B, Stewart C et al (1990) Preliminary studies of mineralization during distraction osteogenesis. Clin Orthop Relat Res 250:43–49
39. Fink B, Pollnau C, Vogel M et al (2003) Histomorphometry of distraction osteogenesis during experimental tibial lengthening. J Orthop Trauma 17:113–118
40. Einhorn TA (1998) The cell and molecular biology of fracture healing. Clin Orthop Relat Res 355(Suppl): S7–S21

41. Pelker RR, Friedlaender GE, Markham TC et al (1984) Effects of freezing and freeze drying on the biomechanical properties of rat bone. J Orthop Res 1:405–411
42. Griffin M, Iqbal SA, Bayat A (2011) Exploring the application of mesenchymal stem cells in bone repair and regeneration. J Bone Joint Surg Am 79:1699–1708
43. Javazos EH, Beggs KJ, Flake AW (2004) Mesenchymal stem cells: paradoxes of passaging. Exp Hematol 32:414–425
44. Kylushenkova E, Mesca JD, Zernetkina V et al (2005) T cell responses to allogeneic human mesenchymal stem cells: immunogenicity, tolerance, and suppression. J Biomed Sci 12:47–57
45. Horstmann WG, Verheyen CC, Leemans R (2003) An injectable calcium phosphate cement as a bone graft substitute in the treatment of displaced lateral tibial plateau fractures. Injury 34:141–144
46. Fleming JE Jr, Cornell CN, Muschler GF (2000) Bone cells and matrices in orthopaedic tissue engineering. Orthop Clin North Am 31:357–374
47. Sanchez-Sotelo J, Munuera L, Madero R (2000) Treatment of fractures of the distal radius with a remodellable bone cement: a prospective, randomized study using Norian SRS. J Bone Joint Surg Br 82:856–863
48. Damien CJ, Parsons JR (1991) Bone graft and hone graft substitutes: a review of current technology and applications. J Appl Biomater 2(1):87–208
49. Burkus JK, Sandhu HS, Gornet MF et al (2005) Use of rhBMP-2 in combination with structural cortical allografts: clinical and radiographic outcomes in anterior lumbar spinal surgery. J Bone Joint Surg Am 87:1205–1212
50. Csimma C, Genant HK, Valentic-Opran A (1997) Recombinant human bone morphogenetic protein-2 for treatment of open tibial fractures. A prospective, controlled, randomized study of four hundred and fifty patients. J Bone Joint Surg Am 79:1699–1708
51. Cheng H, Jiang W, Phillips FM et al (2003) Osteogenic activity of the 38. fourteen types of human bone morphogenetic proteins (BMPs). J Bone Joint Surg Am 85-A(8):1544–1552
52. Friedlaender GE, Perry CR, Cole JD et al (2001) Osteogenic protein-1 (bone morphogenetic protein-7) in the treatment of tibial nonunions. J Bone Joint Surg Am 83-A(Suppl 1 (Pt 2)):S151–S158
53. Lind M, Schumacker B, Soballe K et al (1993) Transforming growth factor β enhances fracture healing in rabbit tibiae. Acta Orthop Scand 64: 553–556
54. Arazi M, Oğün TC, Oktar MN, Memik R, Kutlu A (2001) Early weight-bearing in statically locked reamed intramedullary femoral nailing: is it a safe procedure? J Trauma 50(4):711–716
55. Goodship AE, Kenwright J (1985) The influence of induced micromovement upon the healing of experimental tibial fractures. J Bone Joint Surg [Br] 67: 650–655
56. Ganz R, Mast J, Weber B et al (1991) Clinical aspects of "bio-logical" plating. Injury 22:4–5
57. Perren SM (2002) Evolution of the internal fixation of long bone fractures. Review article. J Bone Joint Surg [Br] 67:650–655
58. Hente R, Lechner J, Fuechtmeier B et al (2001) Der Einfluss einer zeitlich limitierten kontrollierten Bewegung auf die Fraktureilung. Hefte Unfallchirurg 283:23–24
59. Mast JW, Jakob R, Ganz R (eds) (1989) Planning and reduction technique in fracture surgery. Springer, Berlin
60. Khong KS, Kotlanka R, Ghista DN (2007) Mechanobiology. In: Tong GO, Bavonratanavech S (eds) AO manual of fracture management, minimally invasive. Plate osteosynthesis (MIPO). Thieme, Stuttgart, pp 8–21
61. Farouk O, Krettek C, Miclau T et al (1997) Minimally invasive plate osteosynthesis and vascularity: preliminary results of a cadaver injection study. Injury 28(Suppl I):S-A7–S-A12
62. De Bastiani G, Aldegheri R, Renzi Brivio L (1984) The treatment of fractures with a dynamic axial fixator. J Bone Joint Surg Br 66:538–545
63. Egger EL, Gottsauner-Wolf F, Palmer J, Aro HT et al (1993) Effects of axial dynamization on bone healing. J Trauma 34(2):185–192
64. O'Sullivan ME, Chao EYS, Kelly PJ (1989) Current concepts: the effects of fixation on fracture healing. J Bone Joint Surg (Am) 71:306–310

Gene-Based Approaches to Bone Regeneration

20

Gözde Kerman, Anthuvan Rajesh, K.C. Remant, and Hasan Uludağ

Abstract

Bone, despite its strength, is a fragile tissue that often fails under a variety of conditions. While biological therapies for stimulation of bone formation and repair have advanced to clinical practice, gene delivery is alternatively explored to provide more cost-effective and efficacious therapies. Due to safety concerns associated with viral gene carriers, non-viral gene carriers are actively developed to realize the dream of safe and efficient bone repair based on gene therapy. This chapter will summarize the recent gene therapy attempts, focusing on outcomes in key studies involving animal models. Carriers derived from synthetic materials will be first reviewed, followed by efforts to utilize gene activated matrices. Direct injection of genes and gene-modified matrices will be subsequently summarized, followed by physical methods of forced gene expression, electroporation and sonoporation, with select examples. We conclude with the authors' perspective on the future of gene therapy for bone repair.

Introduction

The bone is an important tissue of the body that can physically protect internal organs, provide a space to support hematopoiesis, and serve as a reservoir to maintain blood calcium homeostasis. Structurally, bones can be classified into two categories, namely, *cortical* and *cancellous* bones [90]. While a compact structure and uniform microscopic channels are present in cortical bones, nonuniform convolutions of lamellae are the property of cancellous (or trabecular) bones [29, 30]. Developmentally, bone formation happens in two distinct processes. One process is the *endochondral ossification*, where a cartilaginous

G. Kerman • A. Rajesh • K.C. Remant
Department of Chemical and Materials Engineering, Faculty of Engineering, #2-020 RTF, Edmonton, AB T6G 2G6, Canada

H. Uludağ, PhD (✉)
Department of Chemical and Materials Engineering, Faculty of Engineering, #2-020 RTF, Edmonton, AB T6G 2G6, Canada

Department of Biomedical Engineering, Faculty of Medicine & Dentistry, Edmonton, AB T6G 2G6, Canada

Faculty of Pharmacy and Pharmaceutical Sciences, University of Alberta, Edmonton, AB T6G 2G6, Canada
e-mail: huludag@ualberta.ca

F. Korkusuz (ed.), *Musculoskeletal Research and Basic Science*,
DOI 10.1007/978-3-319-20777-3_20

template precedes the formation of a calcified mature bone structure. Formation and elongation of most load-bearing bones in the body occurs by this process. The other process occurs without a cartilaginous template and is termed *intramembranous ossification*. Skull bones, for instance, are formed by this process.

Structural integrity and shape of the bone are constantly maintained by dissolution (or resorption) and removal of old matrix and in situ synthesis of new bone. The primary players in this process constitute two major cellular components of bone tissue, namely, the "bone-forming" *osteoblasts* and the "bone-resorbing" *osteoclasts*. Osteoblasts are derived from mesenchymal stem cells (MSCs) and are responsible for synthesizing organic extracellular matrix and controlling matrix mineralization [75]. Osteoclasts, on the other hand, are multinucleated cells derived from differentiation of hematopoietic precursor cells in the monocyte-macrophage lineage, under the influence by macrophage colony-stimulating factor and nuclear factor-κB ligands. These cells continuously resorb the formed bone [107]. Although bone resorption and formation appear as two independent processes, in reality, there are closely connected within temporary anatomical structures termed *basic multicellular units* (BMUs). A developed BMU supports osteoblasts, osteoclasts, connective tissue, and a dedicated source of blood supply. As the osteoclasts resorb bone, the entire BMU is postulated to advance alongside the bone with the resorbed bone replaced by osteoblasts synthesizing the bone matrix. Osteoblasts directly regulate bone matrix synthesis and mineralization, in addition to indirectly regulating osteoclast-mediated bone resorption via paracrine control [95].

Bone tissue has regenerative capabilities that allow majority of fractures and/or tissue loss to heal on its own or recover after noncritical orthopedic procedures [26]. Following a fracture, the tissues surrounding the fracture site – the cortical bone, periosteum, external soft tissues, and bone marrow – contribute to the healing process by formation of a connective tissue *callus*. A combination of endochondral and intramembranous ossification followed by bone remodeling completes the process of fracture repair [25]. Despite the excellent repair potential of bone tissue, in situations where trauma results in a critical-sized bone defect, complete regeneration cannot occur [46]. Severe trauma may lead to permanent impairment of blood supply, ischemia, and osteonecrosis and ultimately result in bone loss. In addition, the process of bone healing is impaired in conditions such as excessive alcohol intake [16], diabetes [36], smoking [63], old age [43], and osteoporosis [41]. Fractures in these clinical settings do not heal properly or in time and often result in *nonunion* and/or *malunion*. Therapeutic stimulation of bone healing is expected to offer significant clinical benefit in such scenarios.

The process of fracture healing is a specialized postnatal repair response that recapitulates embryological skeletal development [33]. Adequate bone repair comprises three essential elements: osteoconduction, osteoinduction, and vascularization [73]. Osteoconduction is the growth of bone from existing bone and can be facilitated by the application of a scaffold in the defect site. The implanted scaffold in this case offers a bridging structure to connect the fractured bone ends and support cell attachment [10]. Osteoinduction, on the other hand, is a more complex biological process (reviewed elaborately in [21, 39, 79]), involving (1) recruitment of mesenchymal osteoprogenitor cells (e.g., MSCs), (2) transformation of undifferentiated mesenchymal cells into "bone-forming" osteoblasts, and (3) formation of new mineralized bone tissue by the differentiated osteoblasts. Vascularization involves growth of new blood vessels to perfuse the regenerating tissue. Aside from nutrient transport and waste removal, the vasculature plays a crucial role in bone formation via production of growth factors that control the recruitment, proliferation, differentiation, function, and/or survival of osteoblasts, osteoclasts, and other supporting cells [96]. The objectives of therapeutic bone regenerative strategies are to provide these three elements in the appropriate order and proportion to promote bone repair. The readily available materials which accommodate these characteristics and used clinically for bone regeneration include autologous bone grafts and

allogeneic banked bone grafts [12]. However, limited availability of autologous transplantable bone tissue, donor site morbidity, shortage of allogeneic donors, and concerns associated with allogeneic tissue transplantation have imposed serious limitations on the sustained use of these materials [35]. Conversely, several synthetic bone substitutes have been developed for clinical application [105], but they are unable to match the autograft in osteogenic capacity [12]. This calls for closer understanding of the physiology of fracture healing and repair, in order to develop efficient therapeutic alternatives.

Ongoing research demonstrates that bone regeneration is initiated and controlled at the molecular level by the coordinated play of several factors broadly categorized into three types: (1) proinflammatory cytokines, (2) bone morphogenetic proteins (BMPs) and related growth factors, and (3) proangiogenic factors. The proinflammatory cytokines are derived from macrophages at the injury site and primarily include interleukin-1 (IL-1), IL-6, and tumor necrosis factor-α (TNF-α). These cytokines initiate the repair response by chemotactic recruitment of inflammatory and endogenous fibrogenic cells, promote extracellular matrix synthesis, and trigger angiogenesis [86]. Growth factors derived from degranulating platelets in the injury site such as platelet-derived growth factor (PDGF) and transforming growth factor-β (TGF-β) are chemotactic and/or mitogenic for macrophages and osteoblasts. The osteoblasts, chondrocytes, and a subset of mesenchymal cells secrete several structurally and functionally related protein factors termed BMPs. BMPs constitute a group of crucial morphogenetic signals controlling important steps in cartilage and bone formation, such as chemotaxis, mesenchymal and osteoprogenitor cell proliferation/differentiation, angiogenesis, and controlled synthesis of extracellular matrix [13, 21]. BMPs also stimulate the synthesis and secretion of other bone and angiogenic growth factors such as insulin-like growth factor (IGF) and vascular endothelial growth factor (VEGF), respectively [21]. Almost all of these growth factors have been studied as potential therapeutic agents to enhance the repair of bone [70].

Several growth factors in the form of recombinant proteins have been investigated as therapeutic agents for bone regeneration and fracture repair. However, a major concern is the adequacy of a single dose of exogenous protein to elicit a sustained clinical response in patients, especially in situations wherein viability of the host bone and surrounding soft tissues is compromised. To tackle this potential concern, a better strategy for therapeutic delivery is gene therapy. Gene therapy involves delivery of genetic information to particular cells, which then synthesize the protein in situ. Firstly, gene therapy can be applied either regionally or systemically. Secondly, the therapeutic gene can be introduced into cells in situ, at the specific anatomic site of interest. Alternatively, the therapeutic gene can be introduced ex vivo, in which cells are harvested from the patient, the deoxyribonucleic acid (DNA) is transferred to these cells in culture, and the genetically modified cells are then administered back to the patient [73, 98]. Based on the therapeutic application, both short-term and long-term protein expressions are desirable following gene therapy. For instance, chronic diseases, such as osteoporosis or rheumatoid arthritis, would probably require long-term expression. Fracture or small bone defect repair may only require short-term protein production. The duration of protein synthesis after gene therapy depends on the techniques used to deliver the gene to the cells (either ex vivo or in situ). The rest of the chapter discusses various gene therapy approaches for bone repair and regeneration.

Overview of Therapeutic Approaches

Gene therapy has become a promising research area for bone regeneration [115, 119]. Successful studies on modified osteogenic cells, which were delivered by using biomaterials for triggering bone repair, have been reported for years. Plasmid deoxyribonucleic acids (pDNA) encoding for BMPs and other growth factors were explored for accelerating the healing process and period. Administration of pDNA coding for “therapeutic

proteins" by the host cells is a process of *positive gene expression*, where the introduced factors are expected to stimulate bone formation. *Negatively regulated protein expression* refers to situation where application of genetic elements is intended for hindering osteogenesis. Ribonucleic acid interference (RNAi) mechanism can provide a means to suppress translation of desired proteins and prevent protein expression, therefore hindering osteogenesis usually [94]. The short interfering RNA (siRNA), in this case, can act as a pharmacological agent to suppress the expression of desired proteins. Most therapeutic approaches, however, are intended to stimulate bone formation directly, and negative regulation could be employed to inhibit the inhibitors of bone formation, so as to ultimately enhance the bone formation. Plasmids are the preferred expression vectors [73] due to reduced manufacturing expenditures and good safety properties when compared to viral vectors [109]. Storage conditions of pDNA are important for transfection efficiency [18, 47, 77, 102], and activity loss in gene delivery systems can be reduced by lyophilization or low storing temperature [18, 20, 47, 102]. Degradation rate of the scaffolds can effect pDNA release [58] and possibly influence the induction of new bone tissue.

MicroRNAs (miRNAs) are small single-stranded RNA molecules that are responsible for coordination of protein expression by reducing level of target messenger RNA (mRNA) or binding to 3′ untranslated region of target mRNA and constraining mRNA translation [45]. Endogenous expression of multiple growth factors can be regulated by overexpression or inhibition of miRNAs [114]. For tailoring bone regeneration, select miRNAs may have a role by adjusting osteogenesis and/or endogenous angiogenesis [69]. Gene expression at the time of MSC differentiation to osteoblasts can be induced by miRNAs [106]. miRNAs can therefore serve as an alternative to gene delivery approaches for protein expression.

Tissue-engineered bone grafts that are derived from gene therapy approaches have been also used in curative bone regeneration [71, 72]. In this approach, the cells intended for the engineered tissue are modified by genetic means for enhanced osteogenesis. In contrast to relying on in situ *gene* uptake and expression, this approach allows ex vivo gene transfer for better control of cell modification.

Nonviral Approaches to Gene Delivery in Animal Models

Multiple approaches have been used to induce bone regeneration by using gene medicines. A common model used to evaluate gene medicines, for example, is calvarial osteotomy model (Table 20.1), where different approaches for gene-based bone repair can be readily seen; one can find the use of gene expression vectors with and without a carrier, as well as direct in situ administration, and indirect delivery via modified cells. Below, the bone tissue gene therapy paradigm is presented in detail.

Synthetic Carriers Used in Gene Delivery

Gene therapies are intended to maintain optimal doses and local concentration of therapeutic proteins over a period of time under a minimal side effect which demonstrates the superiority of gene delivery over conventional protein delivery [81]. Significant achievements in gene delivery for bone regeneration and their intraosseous expression using both viral vectors, derived from adenovirus, retrovirus, lentivirus, and synthetic vectors, liposomes, and cationic polymers/dendrimers, have been reported elsewhere [4, 6, 40, 49]. Both ex vivo and in vivo approaches to delivery have been attempted with both types of vectors (Fig. 20.1) [92].

Nonviral gene delivery has been recently emphasized in the field due to facile chemical strategies, stability for long-term storage and reconstitution, safe toxicity profiles, and unlimited capacity of gene sizes (cargo). In gene therapy of the bone, two fundamental (indispensible) aspects of the therapy are *carrier vectors* (i.e., cationic molecules with enough binding capacity to protect nucleic acids and facilitate intracellular trafficking) and

Table 20.1 Selected studies using gene therapy to promote bone regeneration in calvarial critical-sized bone defect models

Animal	Gene	Scaffold	Vector	Outcome	Reference
No carrier					
Rat	BMP-2	Triacrylate/amine-gelatin	Free plasmid	Minimal to no effect on bone formation	Chew et al. [19]
Synthetic carrier					
Rat	PDGF-B	Collagen	PEI	14- and 44-fold higher new bone volume/total volume in treated calvarial defects compared to empty defects or empty scaffolds after 4 weeks of implantation	Elangovan et al. [27]
Rabbit	BMP-2	Porous HA	Cationic liposomes (SuperFect™, QIAGEN GmbH)	Robust bone formation in the cranial defect in animals treated with BMP-2 gene without HA; complete ossification observed at 9 weeks	Ono et al. [83]
Mouse	caALK6 and Runx2	PEG-block catiomer	Linear PEI (Fermentas) and FuGENE6 (Roche)	Bone formation covering entire lower surface of the implant at 4 weeks	Itaka et al. [50]
Rat	BMP-2	PFF	TAPP complexed with GMP	No enhanced bone formation (via micro-CT and histology) at 12 weeks postimplantation	Chew et al. [19]
Rat	BMP-4	PLGA	PEI	Enhanced bone regeneration at defect edges measured via histological and micro-CT evaluation; increase in osteoid and mineralized tissue density	Huang et al. [48]

HA hydroxyapatite, *PEG* poly(ethylene glycol), *PEI* polyethylenimine, *caALK6* activin receptor-like kinase 6, *Runx2* runt-related transcription factor 2, *PFF* 1⁄4 poly(propylene fumarate), *TAPP* triacrylate/amine polycationic polymer, *GMP* gelatin microparticles, *MSC* mesenchymal stem cell

biomaterial scaffolds (i.e., a three-dimensional construct to deliver complexes to repair sites, control release kinetics of complexes, and provide a milieu for osteoinduction). Effective nonviral vectors are generally constructed from cationic polymers, dendrimers, or lipids, but cationic polymers are the most attractive candidate [78, 80, 85, 89]. The common cationic polymers employed in these approaches comprise of polyethylenimine (PEI), poly(L-lysine) (PLL), poly[2-(dimethylamino)ethyl methacrylate] (PDMAEMA), poly(amidoamine) (PAMAM), and chitosan (CS) (Fig. 20.2a) [78, 80, 85].

Electrostatic interaction between cationic primary amines of polymers and anionic phosphate of polynucleotides forms the foundation of nonviral gene delivery. It leads to formation of condensed polyionic complexes (polyplexes) and protects the encapsulated cargo from enzymatic and nonenzymatic degradation, avoids the clearance through the reticuloendothelial system (RES), enhances cellular uptake via interactions with anionic cell surface proteoglycans, and finally increases half-life in the cytoplasm [3, 24, 99]. Many studies have shown that factors such as size, surface charge, chemical composition, degradability, and stimulus sensitivity affect cellular uptake and intracellular trafficking [17, 56]. The widely accepted benefit of cationic polymers in gene delivery is thought to be derived from their extraordinary cationic charge density and buffering capacity. Buffering capacity

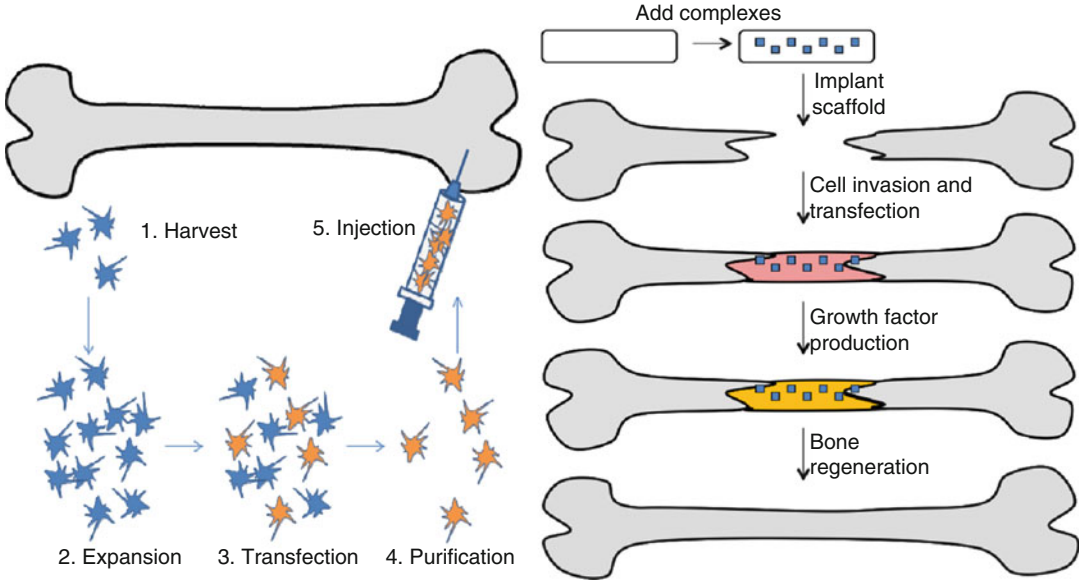

Fig. 20.1 Gene delivery approaches to the bone. In vivo approach (*right*) relies on the introduction of the therapeutic genes directly in suspension form or via gene-activated matrix (as shown). Ex vivo approach (*left*) relies on modified primary cells and subsequent implantation to the repair site (Adapted from Rose et al. [92] with permission)

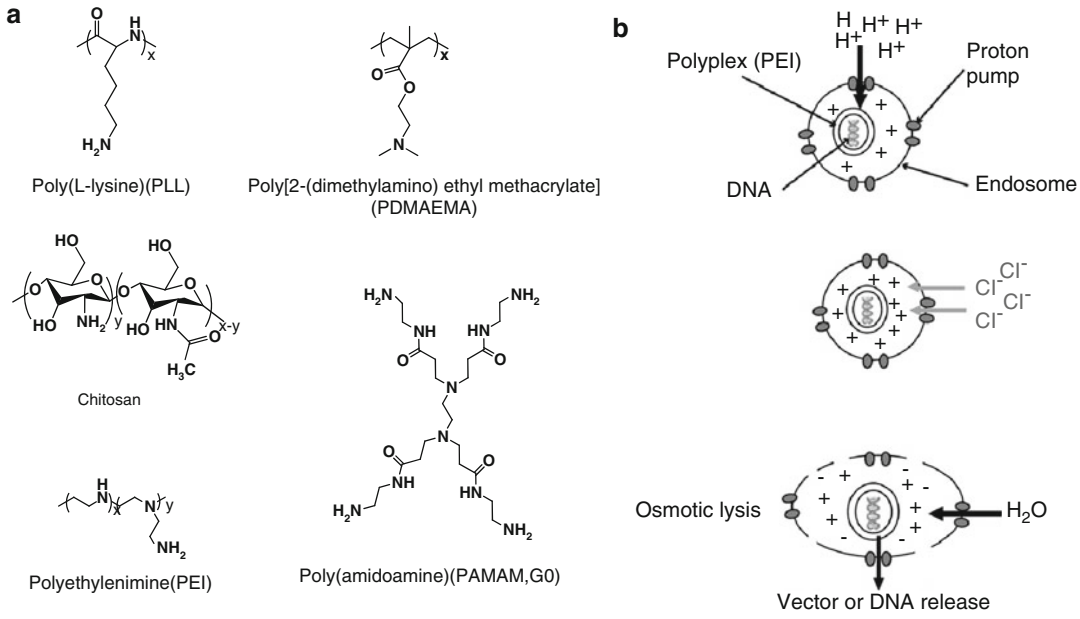

Fig. 20.2 (**a**) Chemical structure of common synthetic cationic polymers/dendrimers used in nonviral gene delivery. (**b**) Schematic representation of proton-sponge effect of the cationic polyplexes (The figure is adapted from Ref. [80] with permission)

is a specific feature of cationic polymers that enables "proton-sponge" effect (Fig. 20.2b) [108]. In PEIs particularly, secondary and tertiary amines generate buffering capacity over a wide range of pH values and facilitate endosomal escape. It has been reported that the gene delivery efficiency of cationic polymers depends on degree of polymerization (molecular weight), branching (topology), and the buffering capacity, which is a function of cationic charge density. As an example, Godbey et al. reported that, under in vitro condition, transfection efficiency of PEIs increases with molecular weight (MW) (70 kDa PEI >10 kDa PEI >1.8 kDa PEI) [42]. However, in vivo efficiency decreases with MW (25 kDa PEI >50 kDa PEI >800 kDa PEI) [1]. Despite intensive activity, however, concrete relationships among structure-property-functional performance remain incompletely described [37]. In the last few years, PEIs and its derivatives are investigated in gene delivery for bone regeneration studies in both ex vivo and in vivo models [27, 93]. The efficacy of native polymers is generally improved by hydrophobic modification using aliphatic lipid molecules [93]. The effect of MW in transfection efficiency was also observed in PLL, a widely used biodegradable polypeptide. Low MW PLL (<3 kDa) cannot even form complexes with DNA, whereas the efficacy of PLL 211 kDa/DNA complexes was 20-fold higher than PEI-20 kDa/DNA complexes, but the intolerable toxicity of higher molecular weight PLL limits its frequent application [64]. The amines of PLLs are completely protonated at physiological pH indicating inefficient buffering capacity, an essential mechanism for endosomal escape [2]. Dendrimers are another class of synthetic polymers with spherical highly branched geometry that comprises of primary amines on the surface to participate in DNA binding and buried tertiary amines to generate the proton-sponge effect. The particular interest in PAMAM is due to their customizable structure with reasonable functionality, which provides enough space for tailoring of appropriate ligand [23]. Like linear polymers, transfection efficacy of PAMAM dendrimers is also proportional to MW (i.e., the generation number) [61]. The CS, on the other hand, is a natural cationic polysaccharide polymer with a good biocompatibility and mucoadhesive and immunogenic properties that are obtained by partial deacetylation of chitin derived from crustacean shells [7].

Calcium phosphate (CaP) is one of the most studied inorganic materials employed to fabricate gene-activated matrix (GAM) for bone tissue engineering [9, 62, 113]. CaP/DNA coprecipitation technique has been used since 1970 for in vitro gene delivery due to its simplicity and nontoxic profiles [22]. CaP complexes of DNAs are tight and compact that likely keep DNA intact at transplanted or injected site; this increases its bioavailability, which is greater than common polymeric carriers [34]. These complexes display enough resistance against serum DNases that is the cause for higher efficacy [62].

In recent years, multiple strategies are being actively pursued in designing second-generation polymeric carriers via chemical modification [56, 118] and by engineering prefabricated nanostructured carriers [101]. Chemical modification alters the physicochemical properties of native polymers and generates new chemical functionalities that can further alter the physical and biological properties of native polymers. Despite extensive work in cell culture, the potential of the vast array of second-generation polymers remains to be fully explored in bone regeneration.

Gene-Activated Matrices (GAMs) for Gene Delivery

Controlled release of an expression vector (pDNA) to surrounding tissues can be achieved by a GAM. Diverse materials such as collagen, CS, silk, synthetic polymers, minerals, and their composites can be utilized as the basis of GAM. The specific examples from published studies were provided below. For enhancing GAM's transfection effectiveness in cells and triggering more effective bone regeneration in vivo, researchers have utilized PEI [48], CaP precipitates [28], or liposomes [74] as the pDNA carriers, although pDNA without any carriers were also attempted [94].

In a recent study, collagen scaffolds were used to deliver PEI/pDNA complexes encoding PDGF-B for bone regeneration in a rat calvarial

model [27]. Bone bridges were established at critical-sized defects in rats that were healed with scaffolds involving PEI/pDNA complexes alone. Trabecular bone volume fraction, degree of trabecular connectivity, and connectivity density were significantly higher in complex-enclosed scaffolds than the control interventions. A collagen sponge incorporating pDNA encoding parathyroid hormone (PTH) 1–34 or BMP-4 was explored by Fang et al. [31]. Osteogenic stimulation was obtained in segmental defect models in rats with desired consequences. In another study, the osteogenic potential of BMP-2 gene/fibronectin/apatite composite layer on hydroxyapatite (HA) ceramic scaffolds was investigated. The scaffolds were implanted into rats subcutaneously [110], and gene expressions for BMP-2 and alkaline phosphatase (ALP) were found to be increased upon application of composite layer-coated scaffolds. Administration of PEI-condensed pDNA encoding for BMP-4 from poly(lactic-co-glycolic acid) scaffolds was studied in rat cranial critical-sized defect models [48]. Bone regeneration was significantly enhanced at defect edges according to histological and microcomputed tomography evaluation in this approach. Increase in osteoid and mineralized tissue density was also obtained. Bone defects in a very large animal (horses) were repaired with collagen matrix containing human PTH (1–34) expression vector [5]. Enhanced bone formation in cortical defects was observed in human PTH-collagen matrix group.

Most GAM explored the delivery of a BMP-2 expression vector by using a carrier (or transfection agent). HA ceramic buttons with a layer containing BMP-2 gene and fibronectin were utilized to treat bone defects on cranium of rats [116]. Results showed that expressions of BMP-2, ALP activity, and osteocalcin were elevated in the HA-BMP-fibronectin group, with increased bone formation. An alginate hydrogel containing BMP-2 expression vector and goat multipotent stromal cells was implanted intramuscularly in goats [112]. Bone induction was observed at the implanted ectopic sites, and goat multipotent stromal cells/BMP-2 pDNA treatment resulted with higher collagen deposition and bone formation. A BMP-2 expression vector was also implanted in dorsal muscles of rats by using HA fibers [82]. The HA fibers incorporating high doses (50 or 100 μg) of BMP-2 expression vector induced more bone mineral content than other implant groups at 4 weeks. The HA fiber containing 50 μg dose of BMP-2 expression vector led to higher osteogenesis as compared to other groups according to radiographic analyses at 8 and 12 weeks. Alternatively, a pDNA encoding BMP-2 in triacrylate/amine polycationic polymer (TAPP) was applied with gelatin microparticles buried within scaffolds in a critical-sized rat cranial defect model [19]. Unlike other studies, the TAPP/pDNA polyplexes did not cause higher bone formation rate than other groups. The reason for this lack of effect could be due to polycationic polymers that had slow degradation rate to trigger sustained pDNA release from scaffolds. Also, in situ cytotoxicity of the polymers might have prevented bone induction, which should be evaluated in conjunction with osteogenesis studies. Bovine atelocollagen and pDNA that encodes human BMP-2 with CaP combination were investigated for treatment of critical-sized segmental bone defects in rats [28]. Bone defects were started to be healed and improved bone strength was obtained in BMP2/CaP-collagen group. Finally, a unique gene formulation was developed by coating preformed cationic PEI/pDNA polyplex with anionic peptide-PEG copolymers for development of so-called copolymer-protected gene vector (COPROG) [100]. Kirschner wires were then coated with COPROG/BMP-2 pDNA and applied in rat tibias intramedullary. Based on biomechanical analysis, the highest load was obtained with the BMP-2 gene delivery group, indicating the feasibility of turning a fracture stabilization device into a plasmid (gene) delivery system.

In addition to these osteogenic genes that were intended to directly stimulate osteogenic events, genes for cytokines involved in angiogenesis were also delivered for indirect stimulation of bone induction. A pDNA coding for human VEGF-165 was coated on collagen sponges (using no carriers or transfection agents) and applied to critical-sized defects in rabbits [38]. More bone formation and endothelial area were observed in the VEGF gene-delivered group, presumably linking enhancing angiogenic activity to bone deposition ultimately.

The synthetic siRNA has been alternatively used to silence specific targets and stimulate bone formation. Dioleoyl trimethylammonium propane (DOTAP)-based cationic liposomes were used in rats to deliver a siRNA that targeted casein kinase-2 interacting protein-1 (encoded by Plekho1) [117]. The mass (given by bone mineral density) and micro-architecture of bone were augmented in treated groups. Implantation of silk fibroin-CS scaffolds with a siRNA against guanine nucleotide-binding protein alpha-stimulating activity polypeptide 1 and prolyl hydroxylase domain-containing protein 2 was studied in the periosteum of sheep [91]. An increase in induced bone volumes was observed in the siRNA treatment groups.

In other studies, transfected cells/scaffold combinations were investigated which functions differently from the principle of GAMs. The basic fibroblast growth factor (bFGF)-transfected MSC containing beta-tricalcium phosphate ceramics (beta-TCP) were applied to critical-sized segmental bone defects of rabbits [44]. The results demonstrated that capillary-bone regeneration was higher in bFGF-transfected MSC/beta-TCP group. Arthrodesis at the dorsal spine of rats was treated with devitalized bone matrix which was soaked with bone marrow cells [8]. In a controlled design, one defect site had marrow cells transfected with complementary DNA (cDNA) encoding LIM mineralization protein-1 (LMP-1), and the other site had cells transfected with a reverse copy of the cDNA (as a control). Spine fusion and bone formation were significantly induced by marrow cells transfected with LMP-1 group, but not in the control group.

Direct Injection of Genes and Gene-Modified Cells

Direct injection of expression vectors to wound sites was proposed as a simple, clinically convenient way for bone induction and repair [73]. A significant concern with direct injection approach is the dissemination of the expression vectors to neighboring tissues and haphazard ossification [87]. The optimal timing of injection needs to be evaluated for each gene, that is, the timing of injection after a bone defect might be evaluated. The persistence of gene expression might be additionally difficult to control, but these are important variables to understand for an efficacious therapy [54]. Examples of studies that employed direct injection of pDNA or cells modified with therapeutic genes are below.

A pDNA encoding for osteogenic protein-1 (OP-1; BMP-7) with a collagen carrier was injected to rats as a model for posterolateral lumbar interbody arthrodesis [11]. Based on the radiological and histological results, bone formation was evident in pDNA/collagen-applied groups. A calcium phosphate/pDNA nanoparticle formulation encoding for BMP-2 was also found to be functional when injected subcutaneously in alginate hydrogels in mice [60]; bone formation was evident when pre-osteoblast cells were injected along with such a BMP-2 gene expression system. Beyond the delivery of BMP genes, the effect of tumor necrosis factor (TNF)-related apoptosis-inducing ligand (TRAIL) gene delivery on osteosarcoma and Ewing's sarcoma was investigated in mice [88]. Bone fractures are usual consequences of tumor expansion and broad bone disruption of Ewing's sarcoma [66], so that gene therapy could be beneficial at sites of localized, excessive bone resorption. Lipophosphoramide/DNA injections were undertaken as TRAIL therapy into retro-orbital veins of osteosarcoma and Ewing's sarcoma models. Overexpression of TRAIL was confirmed in plasmid construct-applied groups, and tumor incidence and osteolytic lesions were decreased in TRAIL-applied groups.

Gene-modified cells were also applied directly for bone regeneration. Healing of bone defects in the rabbit tibia was explored with fibroblasts that were transfected with VEGF [67]. More ossification as bone bridges and vessel formation were observed in VEGF fibroblast group. Bone marrow-derived MSCs (BM-MSCs) that were transfected with osterix (OSX) gene were also injected to distraction gaps in the mandibles of rabbits [65]. Increased bone development in distracted callus and also higher bone sialoprotein expression were observed in OSX-modified BM-MSCs treatment groups.

Electroporation and Sonoporation in Gene Expression

Utilization of electrical pulses for creating pores across plasma membrane is the process of *electroporation* [97], which can enable pDNA transfer into a cell without the need for a carrier. The operational parameters of pulses are important for effectiveness of transfection in this approach. Similarly, ultrasound-applied gene transfer (*sonoporation*) can serve for the same end by relying on microbubble-induced cell permeabilization for pDNA uptake [67, 68, 76]. Easier clinical translation and decreased invasiveness of sonoporation make it superior to electroporation [15]. Assimilating pDNA by electroporation or sonoporation percutaneously can be hard because of restriction by dense tissues enclosing human bones [94]. Studies involving electroporation and sonoporation showed that bone formation could occur especially in ectopic sites of bone in mice and rats following gene delivery [51–53, 57, 59, 84, 103]. A collagen sponge with pDNA encoding BMP-9 was injected into nonunion fractures of mice in one study [55]. After implantation, electroporation was undertaken and bone bridging was observed in electroporated BMP-9 group by histological analysis and microcomputed tomography. Feichtinger et al. investigated injection of BMP2/7 co-expressing pDNA with ultrasound application transcutaneously for bone regeneration in mice and rats [32]. Assessment of gene transfer effectiveness was performed with bioluminescence activity, which resulted with success rates of 85 % at 2 W/cm^2 and 100 % at 4 W/cm^2. In addition, sonoporation caused higher bone regeneration percentages according to microcomputed tomography consequences.

Perspective

Obtaining convenient means for harmless and effective gene delivery is difficult in functional bone regeneration, despite the availability of a spectrum of delivery agents. The spectrum of carriers functional for gene delivery is encouraging, but concerted efforts to understand and overcome factors limiting gene expression are continuously needed. The biocompatibility and mechanical properties of materials need to be evaluated on one hand [111], while the in situ residence of pDNA (or other expression vectors) at the defect site needs to be ensured in a functional state [60]. Animal models are essential to explore the proof of principle for the newly developed therapies, but investigation of therapeutic features beyond functional outcomes (e.g., biocompatibility, immune response, etc.) must be also incorporated in such studies. Minimal immunogenicity associated with nonviral approaches of gene delivery makes it safer than the viral approaches of gene delivery [14]. Delivering growth factors in gene form may become more practical over utilization of high doses of protein, to better sustain protein presence at the site [104] and possibly overcome adverse effects associated with high protein doses locally. Since most clinical cases requiring bone repair are non-life threatening, it is likely that the nonviral approach will gain the upper hand on the long run (i.e., viral delivery is difficult to justify in such clinical scenarios). Studies in larger animal models (as compared to rodents) will be required to better realize the potential of gene-induced bone repair in slower-growing or nongrowing organisms reminiscent of humans.

Acknowledgments The studies in the author's lab were supported by operating grants from NSERC and CIHR and infrastructure grants from Alberta Innovates – Health Solutions.

References

1. Abdallah B, Hassan A, Benoist C, Goula D, Behr JP, Demeneix BA (1996) A powerful nonviral vector for in vivo gene transfer into the adult mammalian brain: polyethylenimine. Hum Gene Ther 7(16):1947–1954
2. Akinc A, Langer R (2002) Measuring the pH environment of DNA delivered using nonviral vectors: implications for lysosomal trafficking. Biotechnol Bioeng 78(5):503–508
3. Alexis F, Pridgen E, Molnar LK, Farokhzad OC (2008) Factors affecting the clearance and biodistribution of polymeric nanoparticles. Mol Pharm 5(4): 505–515

4. Aronovich EL, McIvor RS, Hackett PB (2011) The sleeping beauty transposon system: a non-viral vector for gene therapy. Hum Mol Genet 20(R1):R14–R20
5. Backstrom KC, Bertone AL, Wisner ER, Weisbrode SE (2004) Response of induced bone defects in horses to collagen matrix containing the human parathyroid hormone gene. Am J Vet Res 65(9): 1223–1232
6. Baltzer AW, Lattermann C, Whalen JD, Wooley P, Weiss K, Grimm M, Ghivizzani SC, Robbins PD, Evans CH (2000) Genetic enhancement of fracture repair: healing of an experimental segmental defect by adenoviral transfer of the BMP-2 gene. Gene Ther 7(9):734–739
7. Bhattarai N, Gunn J, Zhang M (2010) Chitosan-based hydrogels for controlled, localized drug delivery. Adv Drug Deliv Rev 62(1):83–99
8. Boden SD, Titus L, Hair G, Liu Y, Viggeswarapu M, Nanes MS, Baranowski C (1998) Lumbar spine fusion by local gene therapy with a cDNA encoding a novel osteoinductive protein (LMP-1). Spine 23(23): 2486–2492
9. Bonadio J, Smiley E, Patil P, Goldstein S (1999) Localized, direct plasmid gene delivery in vivo: prolonged therapy results in reproducible tissue regeneration. Nat Med 5(7):753–759
10. Bose S, Roy M, Bandyopadhyay A (2012) Recent advances in bone tissue engineering scaffolds. Trends Biotechnol 30(10):546–554
11. Bright C, Park YS, Sieber AN, Kostuik JP, Leong KW (2006) In vivo evaluation of plasmid DNA encoding OP-1 protein for spine fusion. Spine 31(19):2163–2172
12. Bueno EM, Glowacki J (2009) Cell-free and cell-based approaches for bone regeneration. Nat Rev Rheumatol 5(12):685–697
13. Cao X, Chen D (2005) The BMP signaling and in vivo bone formation. Gene 357(1):1–8
14. Carofino BC, Lieberman JR (2008) Gene therapy applications for fracture-healing. J Bone Joint Surg Am 90(Suppl 1):99–110
15. Cemazar M, Golzio M, Sersa G, Rols MP, Teissié J (2006) Electrically-assisted nucleic acids delivery to tissues in vivo: where do we stand? Curr Pharm Des 12(29):3817–3825
16. Chakkalakal DA (2005) Alcohol-induced bone loss and deficient bone repair. Alcohol Clin Exp Res 29(12):2077–2090
17. Chen DJ, Majors BS, Zelikin A, Putnam D (2005) Structure-function relationships of gene delivery vectors in a limited polycation library. J Control Release 103(1):273–283
18. Cherng JY, Talsma H, Crommelin DJ, Hennink WE (1999) Long term stability of poly((2-dimethylamino) ethyl methacrylate)-based gene delivery systems. Pharm Res 16(9):1417–1423
19. Chew SA, Kretlow JD, Spicer PP, Edwards AW, Baggett LS, Tabata Y, Kasper FK, Mikos AG (2011) Delivery of plasmid DNA encoding bone morphogenetic protein-2 with a biodegradable branched polycationic polymer in a critical-size rat cranial defect model. Tissue Eng A 17(5–6):751–763
20. del Pozo-Rodríguez A, Solinís MA, Gascón AR, Pedraz JL (2009) Short- and long-term stability study of lyophilized solid lipid nanoparticles for gene therapy. Eur J Pharm Biopharm 71(2): 181–189
21. Dimitriou R, Tsiridis E, Giannoudis PV (2005) Current concepts of molecular aspects of bone healing. Injury 36(12):1392–1404
22. Dorozhkin SV (2011) Biocomposites and hybrid biomaterials based on calcium orthophosphates. Biomatter 1(1):3–56
23. Dufes C, Uchegbu IF, Schatzlein AG (2005) Dendrimers in gene delivery. Adv Drug Deliv Rev 57(15):2177–2202
24. Dykxhoorn DM, Palliser D, Lieberman J (2006) The silent treatment: siRNAs as small molecule drugs. Gene Ther 13(6):541–552
25. Einhorn TA (1998) The cell and molecular biology of fracture healing. Clin Orthop Relat Res Oct (355 Suppl):S7–S21
26. Einhorn TA (2005) The science of fracture healing. J Orthop Trauma 19(10 Suppl):S4–S6
27. Elangovan S, D'Mello SR, Hong L, Ross RD, Allamargot C, Dawson DV, Stanford CM, Johnson GK, Sumner DR, Salem AK (2014) The enhancement of bone regeneration by gene activated matrix encoding for platelet derived growth factor. Biomaterials 35(2):737–747
28. Endo M, Kuroda S, Kondo H, Maruoka Y, Ohya K, Kasugai S (2006) Bone regeneration by modified gene activated matrix: effectiveness in segmental tibial defects in rats. Tissue Eng 12(3):489–497
29. Enlow DH (1963) Principles of bone remodeling. Charles C Thomas, Springfield
30. Enlow DH (1968) The human face: an account of the postnatal growth and development of the craniofacial skeleton. Harper and Row, New York. Evans C (2011) Gene therapy for the regeneration of bone. Injury 42(6):599–604
31. Fang J, Zhu YY, Smiley E, Bonadio J, Rouleau JP, Goldstein SA, McCauley LK, Davidson BL, Roessler BJ (1996) Stimulation of new bone formation by direct transfer of osteogenic plasmid genes. Proc Natl Acad Sci U S A 93(12):5753–5758
32. Feichtinger GA, Hofmann AT, Slezak P, Schuetzenberger S, Kaipel M, Schwartz E, Neef A, Nomikou N, Nau T, Van Griensven M, McHale AP, Redl H (2014) Sonoporation increases therapeutic efficacy of inducible and constitutive BMP2/7 in vivo gene delivery. Hum Gene Therapy Methods 25(1):57–71
33. Ferguson C, Alpern E, Miclau T, Helms JA (1999) Does adult fracture repair recapitulate embryonic skeletal formation? Mech Dev 87(1–2):57–66
34. Fu H, Hu Y, McNelis T, Hollinger JO (2005) A calcium phosphate-based gene delivery system. J Biomed Mater Res A 74(1):40–48

35. Gamradt SC, Lieberman JR (2004) Genetic modification of stem cells to enhance bone repair. Ann Biomed Eng 32(1):136–147
36. Gandhi A, Liporace F, Azad V, Mattie J, Lin SS (2006) Diabetic fracture healing. Foot Ankle Clin 11(4):805–824
37. Gebhart CL, Kabanov AV (2001) Evaluation of polyplexes as gene transfer agents. J Control Release 73(2–3):401–416
38. Geiger F, Bertram H, Berger I, Lorenz H, Wall O, Eckhardt C, Simank HG, Richter W (2005) Vascular endothelial growth factor gene-activated matrix (VEGF165-GAM) enhances osteogenesis and angiogenesis in large segmental bone defects. J Bone Miner Res 20(11):2028–2035
39. Gerstenfeld LC, Cullinane DM, Barnes GL, Graves DT, Einhorn TA (2003) Fracture healing as a postnatal developmental process: molecular, spatial, and temporal aspects of its regulation. J Cell Biochem 88(5):873–884
40. Ghosh SS, Gopinath P, Ramesh A (2006) Adenoviral vectors: a promising tool for gene therapy. Appl Biochem Biotechnol 133(1):9–29
41. Giannoudis P, Tzioupis C, Almalki T, Buckley R (2007) Fracture healing in osteoporotic fractures: is it really different? A basic science perspective. Injury 38(Suppl 1):S90–S99
42. Godbey WT, Wu KK, Mikos AG (1999) Size matters: molecular weight affects the efficiency of poly(ethylenimine) as a gene delivery vehicle. J Biomed Mater Res 45(3):268–275
43. Gruber R, Koch H, Doll BA, Tegtmeier F, Einhorn TA, Hollinger JO (2006) Fracture healing in the elderly patient. Exp Gerontol 41(11):1080–1093
44. Guo X, Zheng Q, Kulbatski I, Yuan Q, Yang S, Shao Z, Wang H, Xiao B, Pan Z, Tang S (2006) Bone regeneration with active angiogenesis by basic fibroblast growth factor gene transfected mesenchymal stem cells seeded on porous beta-TCP ceramic scaffolds. Biomed Mater 1(3):93–99
45. Hobert O (2008) Gene regulation by transcription factors and microRNAs. Science 319(5871): 1785–1786
46. Hollinger JO, Kleinschmidt JC (1990) The critical size defect as an experimental model to test bone repair materials. J Craniofac Surg 1(1):60–68
47. Höbel S, Prinz R, Malek A, Urban-Klein B, Sitterberg J, Bakowsky U, Czubayko F, Aigner A (2008) Polyethylenimine PEI F25-LMW allows the long-term storage of frozen complexes as fully active reagents in siRNA-mediated gene targeting and DNA delivery. Eur J Pharm Biopharm 70(1): 29–41
48. Huang YC, Simmons C, Kaigler D, Rice KG, Mooney DJ (2005) Bone regeneration in a rat cranial defect with delivery of PEI-condensed plasmid DNA encoding for bone morphogenetic protein-4 (BMP-4). Gene Ther 12(5):418–426
49. Ishihara A, Shields KM, Litsky AS, Mattoon JS, Weisbrode SE, Bartlett JS, Bertone AL (2008) Osteogenic gene regulation and relative acceleration of healing by adenoviral-mediated transfer of human BMP-2 or -6 in equine osteotomy and ostectomy models. J Orthop Res 26(6):764–771
50. Itaka K, Ohba S, Miyata K, Kawaguchi H, Nakamura K, Takato T, Chung UI, Kataoka K (2007) Bone regeneration by regulated in vivo gene transfer using biocompatible polyplex nanomicelles. Mol Ther 15(9):1655–1662
51. Kawai M, Bessho K, Kaihara S, Sonobe J, Oda K, Iizuka T, Maruyama H (2003) Ectopic bone formation by human bone morphogenetic protein-2 gene transfer to skeletal muscle using transcutaneous electroporation. Hum Gene Ther 14(16):1547–1556
52. Kawai M, Bessho K, Maruyama H, Miyazaki JI, Yamamoto T (2005) Human BMP-2 gene transfer using transcutaneous in vivo electroporation induced both intramembranous and endochondral ossification. Anat Rec A: Discov Mol Cell Evol Biol 287(2):1264–1271
53. Kawai M, Bessho K, Maruyama H, Miyazaki J, Yamamoto T (2006) Simultaneous gene transfer of bone morphogenetic protein (BMP)-2 and BMP-7 by in vivo electroporation induces rapid bone formation and BMP-4 expression. BMC Musculoskelet Disord 7:62
54. Kimelman N, Pelled G, Gazit Z, Gazit D (2006) Applications of gene therapy and adult stem cells in bone bioengineering. Regen Med 1(4):549–561
55. Kimelman-Bleich N, Pelled G, Zilberman Y, Kallai I, Mizrahi O, Tawackoli W, Gazit Z, Gazit D (2011) Targeted gene-and-host progenitor cell therapy for nonunion bone fracture repair. Mol Ther 19(1): 53–59
56. Kircheis R, Wightman L, Wagner E (2001) Design and gene delivery activity of modified polyethylenimines. Adv Drug Deliv Rev 53(3):341–358
57. Kishimoto KN, Watanabe Y, Nakamura H, Kokubun S (2002) Ectopic bone formation by electroporatic transfer of bone morphogenetic protein-4 gene. Bone 31(2):340–347
58. Kolk A, Haczek C, Koch C, Vogt S, Kullmer M, Pautke C, Deppe H, Plank C (2011) A strategy to establish a gene-activated matrix on titanium using gene vectors protected in a polylactide coating. Biomaterials 32(28):6850–6859
59. Kotajima S, Kishimoto KN, Watanuki M, Hatori M, Kokubun S (2006) Gene expression analysis of ectopic bone formation induced by electroporatic gene transfer of BMP4. Ups J Med Sci 111(2):231–241
60. Krebs MD, Salter E, Chen E, Sutter KA, Alsberg E (2010) Calcium phosphate-DNA nanoparticle gene delivery from alginate hydrogels induces in vivo osteogenesis. J Biomed Mater Res A 92(3): 1131–1138
61. Kukowska-Latallo JF, Bielinska AU, Johnson J, Spindler R, Tomalia DA, Baker JR Jr (1996) Efficient transfer of genetic material into mammalian cells using Starburst polyamidoamine dendrimers. Proc Natl Acad Sci U S A 93(10):4897–4902

62. Kuroda S, Kondo H, Ohya K, Kasugai S (2005) A new technique with calcium phosphate precipitate enhances efficiency of in vivo plasmid DNA gene transfer. J Pharmacol Sci 97(2):227–233
63. Kwiatkowski TC, Hanley EN Jr, Ramp WK (1996) Cigarette smoking and its orthopedic consequences. Am J Orthop (Belle Mead NJ) 25(9):590–597
64. Kwoh DY, Coffin CC, Lollo CP, Jovenal J, Banaszczyk MG, Mullen P, Phillips A, Amini A, Fabrycki J, Bartholomew RM, Brostoff SW, Carlo DJ (1999) Stabilization of poly-L-lysine/DNA polyplexes for in vivo gene delivery to the liver. Biochim Biophys Acta 1444(2):171–190
65. Lai QG, Yuan KF, Xu X, Li DR, Li GJ, Wei FL, Yang ZJ, Luo SL, Tang XP, Li S (2011) Transcription factor osterix modified bone marrow mesenchymal stem cells enhance callus formation during distraction osteogenesis. Oral Surg Oral Med Oral Pathol Oral Radiol Endod 111(4):412–419
66. Lau YS, Adamopoulos IE, Sabokbar A, Giele H, Gibbons CLMH, Athanasou NA (2007) Cellular and humoral mechanisms of osteoclast formation in Ewing's sarcoma. Br J Cancer 96(11):1716–1722
67. Li R, Stewart DJ, von Schroeder HP, Mackinnon ES, Schemitsch EH (2009) Effect of cell-based VEGF gene therapy on healing of a segmental bone defect. J Orthop Res 27(1):8–14
68. Li YS, Davidson E, Reid CN, Mchale AP (2009) Optimising ultrasound-mediated gene transfer (sonoporation) in vitro and prolonged expression of a transgene in vivo: potential applications for gene therapy of cancer. Cancer Lett 273(1):62–69
69. Li Y, Fan L, Liu S, Liu W, Zhang H, Zhou T, Wu D, Yang P, Shen L, Chen J, Jin Y (2013) The promotion of bone regeneration through positive regulation of angiogenic-osteogenic coupling using microRNA-26a. Biomaterials 34(21):5048–5058
70. Lieberman JR, Daluiski A, Einhorn TA (2002) The role of growth factors in the repair of bone. Biology and clinical applications. J Bone Joint Surg Am 84-A(6):1032–1044
71. Lin CY, Chang YH, Kao CY, Lu CH, Sung LY, Yen TC, Lin KJ, Hu YC (2012) Augmented healing of critical size calvarial defects by baculovirus-engineered MSCs that persistently express growth factors. Biomaterials 33(14):3682–3692
72. Liu H, Peng H, Wu Y, Zhang C, Cai Y, Xu G, Li Q, Chen X, Ji J, Zhang Y, OuYang HW (2013) The promotion of bone regeneration by nanofibrous hydroxyapatite/chitosan scaffolds by effects on integrin-BMP/Smad signaling pathway in BMSCs. Biomaterials 34(18):4404–4417
73. Lu CH, Chang YH, Lin SY, Li KC, Hu YC (2013) Recent progresses in gene delivery-based bone tissue engineering. Biotechnol Adv 31(8):1695–1706
74. Lutz R, Park J, Felszeghy E, Wiltfang J, Nkenke E, Schlegel KA (2008) Bone regeneration after topical BMP-2-gene delivery in circumferential peri-implant bone defects. Clin Oral Implants Res 19(6):590–599
75. Manolagas SC (2000) Birth and death of bone cells: basic regulatory mechanisms and implications for the pathogenesis and treatment of osteoporosis. Endocr Rev 21(2):115–137
76. Mehier-Humbert S, Guy RH (2005) Physical methods for gene transfer: improving the kinetics of gene delivery into cells. Adv Drug Deliv Rev 57(5): 733–753
77. Meilander NJ, Pasumarthy MK, Kowalczyk TH, Cooper MJ, Bellamkonda RV (2003) Sustained release of plasmid DNA using lipid microtubules and agarose hydrogel. J Control Release 88(2): 321–331
78. Mintzer MA, Simanek EE (2009) Nonviral vectors for gene delivery. Chem Rev 109(2):259–302
79. Miron RJ, Zhang YF (2012) Osteoinduction: a review of old concepts with new standards. J Dent Res 91(8):736–744
80. Morille M, Passirani C, Vonarbourg A, Clavreul A, Benoit JP (2008) Progress in developing cationic vectors for non-viral systemic gene therapy against cancer. Biomaterials 29(24–25):3477–3496
81. Nikol S, Huehns TY (2001) Preclinical and clinical experience in vascular gene therapy: advantages over conservative/standard therapy. J Invasive Cardiol 13(4):333–338
82. Oda M, Kuroda S, Kondo H, Kasugai S (2009) Hydroxyapatite fiber material with BMP-2 gene induces ectopic bone formation. J Biomed Mater Res B Appl Biomater 90(1):101–109
83. Ono I, Yamashita T, Jin HY, Ito Y, Hamada H, Akasaka Y, Nakasu M, Ogawa T, Jimbow K (2004) Combination of porous hydroxyapatite and cationic liposomes as a vector for BMP-2 gene therapy. Biomaterials 25(19):4709–4718
84. Osawa K, Okubo Y, Nakao K, Koyama N, Bessho K (2009) Osteoinduction by microbubble-enhanced transcutaneous sonoporation of human bone morphogenetic protein-2. J Gene Med 11(7):633–641
85. Pack DW, Hoffman AS, Pun S, Stayton PS (2005) Design and development of polymers for gene delivery. Nat Rev Drug Discov 4(7):581–593
86. Pape HC, Marcucio R, Humphrey C, Colnot C, Knobe M, Harvey EJ (2010) Trauma-induced inflammation and fracture healing. J Orthop Trauma 24(9):522–525
87. Pelled G, Ben-Arav A, Hock C, Reynolds DG, Yazici C, Zilberman Y, Gazit Z, Awad H, Gazit D, Schwarz EM (2010) Direct gene therapy for bone regeneration: gene delivery, animal models, and outcome measures. Tissue Eng B Rev 16(1):13–20
88. Picarda G, Lamoureux F, Geffroy L, Delepine P, Montier T, Laud K, Tirode F, Delattre O, Heymann D, Rédini F (2010) Preclinical evidence that use of TRAIL in Ewing's Sarcoma and osteosarcoma therapy inhibits tumor growth, prevents osteolysis, and increases animal survival. Clin Cancer Res 16(8): 2363–2374
89. Putnam D (2006) Polymers for gene delivery across length scales. Nat Mater 5(6):439–451

90. Rho JY, Kuhn-Spearing L, Zioupos P (1998) Mechanical properties and the hierarchical structure of bone. Med Eng Phys 20(2):92–102
91. Ríos CN, Skoracki RJ, Mathur AB (2012) GNAS1 and PHD2 short-interfering RNA support bone regeneration in vitro and in an in vivo sheep model. Clin Orthop Relat Res 470(9):2541–2553
92. Rose L, Fitzsimmons R, El-Bialy T, Uludağ H (2011) Gene delivery for musculoskeletal diseases. In: Prokop A (ed) Intracellular drug delivery: fundamentals and applications, vol I. Springer, Dordrecht, Germany, pp 813–847
93. Rose LC, Kucharski C, Uludag H (2012) Protein expression following non-viral delivery of plasmid DNA coding for basic FGF and BMP-2 in a rat ectopic model. Biomaterials 33(11):3363–3374
94. Rose L, Uludağ H (2013) Realizing the potential of gene-based molecular therapies in bone repair. J Bone Miner Res 28(11):2245–2262
95. Rosenberg N, Rosenberg O, Soudry M (2012) Osteoblasts in bone physiology-mini review. Rambam Maimonides Med J 3(2):e0013
96. Santos MI, Reis RL (2010) Vascularization in bone tissue engineering: physiology, current strategies, major hurdles and future challenges. Macromol Biosci 10(1):12–27
97. Satkauskas S, Ruzgys P, Venslauskas MS (2012) Towards the mechanisms for efficient gene transfer into cells and tissues by means of cell electroporation. Expert Opin Biol Ther 12(3):275–286
98. Scaduto AA, Lieberman JR (1999) Gene therapy for osteoinduction. Orthop Clin N Am 30(4):625–633
99. Schaffer DV, Fidelman NA, Dan N, Lauffenburger DA (2000) Vector unpacking as a potential barrier for receptor-mediated polyplex gene delivery. Biotechnol Bioeng 67(5):598–606
100. Schwabe P, Greiner S, Ganzert R, Eberhart J, Dähn K, Stemberger A, Plank C, Schmidmaier G, Wildemann B (2012) Effect of a novel nonviral gene delivery of BMP-2 on bone healing. Sci World J 2012:560142
101. Sethuraman VA, Na K, Bae YH (2006) pH-responsive sulfonamide/PEI system for tumor specific gene delivery: an in vitro study. Biomacromolecules 7(1):64–70
102. Sharma VK, Thomas M, Klibanov AM (2005) Mechanistic studies on aggregation of polyethylenimine-DNA complexes and its prevention. Biotechnol Bioeng 90(5):614–620
103. Sheyn D, Kimelman-Bleich N, Pelled G, Zilberman Y, Gazit D, Gazit Z (2008) Ultrasound-based nonviral gene delivery induces bone formation in vivo. Gene Ther 15(4):257–266
104. Southwood LL, Frisbie DD, Kawcak CE, McIlwraith CW (2004) Delivery of growth factors using gene therapy to enhance bone healing. Vet Surg 33(6):565–578
105. Szpalski C, Wetterau M, Barr J, Warren SM (2012) Bone tissue engineering: current strategies and techniques – part I: Scaffolds. Tissue Eng B Rev 18(4):246–257
106. Taipaleenmäki H, Bjerre Hokland L, Chen L, Kauppinen S, Kassem M (2012) Mechanisms in endocrinology: micro-RNAs: targets for enhancing osteoblast differentiation and bone formation. Eur J Endocrinol 166(3):359–371
107. Teitelbaum SL (2000) Bone resorption by osteoclasts. Science 289(5484):1504–1508
108. Thomas M, Klibanov AM (2002) Enhancing polyethylenimine's delivery of plasmid DNA into mammalian cells. Proc Natl Acad Sci U S A 99(23): 14640–14645
109. Verma IM, Weitzman MD (2005) Gene therapy: twenty-first century medicine. Annu Rev Biochem 74:711–738
110. Wang X, Oyane A, Tsurushima H, Sogo Y, Li X, Ito A (2011) BMP-2 and ALP gene expression induced by a BMP-2 gene-fibronectin-apatite composite layer. Biomed Mater 6(4):045004
111. Wegman F, Öner FC, Dhert WJ, Alblas J (2013) Non-viral gene therapy for bone tissue engineering. Biotechnol Genet Eng Rev 29:206–220
112. Wegman F, Geuze RE, van der Helm YJ, Cumhur Öner F, Dhert WJ, Alblas J (2014) Gene delivery of bone morphogenetic protein-2 plasmid DNA promotes bone formation in a large animal model. J Tissue Eng Regen Med 8(10):763–770
113. Xie Y, Chen Y, Sun M, Ping Q (2013) A mini review of biodegradable calcium phosphate nanoparticles for gene delivery. Curr Pharm Biotechnol 14(10): 918–925
114. Yau WW, Rujitanaroj PO, Lam L, Chew SY (2012) Directing stem cell fate by controlled RNA interference. Biomaterials 33(9):2608–2628
115. Ye JH, Xu YJ, Gao J, Yan SG, Zhao J, Tu Q, Zhang J, Duan XJ, Sommer CA, Mostoslavsky G, Kaplan DL, Wu YN, Zhang CP, Wang L, Chen J (2011) Critical size calvarial bone defects healing in a mouse model with silk scaffolds and SATB2-modified iPSCs. Biomaterials 32(22):5065–5076
116. Zhang W, Tsurushima H, Oyane A, Yazaki Y, Sogo Y, Ito A, Matsumura A (2011) BMP-2 gene-fibronectin-apatite composite layer enhances bone formation. J Biomed Sci 18:62
117. Zhang G, Guo B, Wu H, Tang T, Zhang BT, Zheng L, He Y, Yang Z, Pan X, Chow H, To K, Li Y, Li D, Wang X, Wang Y, Lee K, Hou Z, Dong N, Li G, Leung K, Hung L, He F, Zhang L, Qin L (2012) A delivery system targeting bone formation surfaces to facilitate RNAi-based anabolic therapy. Nat Med 18(2):307–314
118. Zintchenko A, Philipp A, Dehshahri A, Wagner E (2008) Simple modifications of branched PEI lead to highly efficient siRNA carriers with low toxicity. Bioconjug Chem 19(7):1448–1455
119. Zou D, Zhang Z, He J, Zhu S, Wang S, Zhang W, Zhou J, Xu Y, Huang Y, Wang Y, Han W, Zhou Y, Wang S, You S, Jiang X, Huang Y (2011) Repairing critical sized calvarial defects with BMSCs modified by a constitutively active form of hypoxia inducible factor-1 alpha and a phosphate cement scaffold. Biomaterials 32(36):9707–9718

Growth Plate

21

Güney Yılmaz and Muharrem Yazıcı

Abstract

The growth plate, which is seated between the metaphysis and the epiphysis, is responsible for longitudinal and circumferential growth of long bones. This structure is composed of three distinct histological layers with different cellular organization and function. The systemic hormones in the circulation, locally produced growth hormones with peptide structure and biomechanical forces control the cellular activity in growth plate. These control mechanisms enable equal limb lengths at the end of the growth period. The modulation of the proliferation potential of the growth plate cells by means of different surgical techniques has been used in the treatment of limb length differences and deformities of the long bones and the spine.

Learning Outcomes

- Define the structure and the physiology of the growth plate
- Identify the basic principles behind growth of the long bones and its control mechanisms
- Appraise the basic principles of guiding growth plate activity as a treatment tool

The Growth Plate

The growth plate is an anatomic structure formed of hyaline cartilage and different histological layers, located between the primary and secondary ossification centers in the metaphyseal regions of the long bones. After the formation of the primary ossification center, ossification continues proximally and distally and the two growth plates grow away from each other [1]. The secondary ossification center emerges and after starting to cover the chondroepiphyseal area of both end regions, the growth plate remains present as a thin cartilage structure between the epiphysis and the metaphysis. The growth plate cartilage and fibrous components encircling the cartilage section are responsible for growth in the long bones both lengthwise and in diameter [2].

G. Yılmaz, MD • M. Yazıcı, MD (✉)
Hacettepe University, Faculty of Medicine,
Department of Orthopedics,
Sihhiye Ankara 06100, Turkey
e-mail: mimyazici@gmail.com

F. Korkusuz (ed.), *Musculoskeletal Research and Basic Science*,
DOI 10.1007/978-3-319-20777-3_21

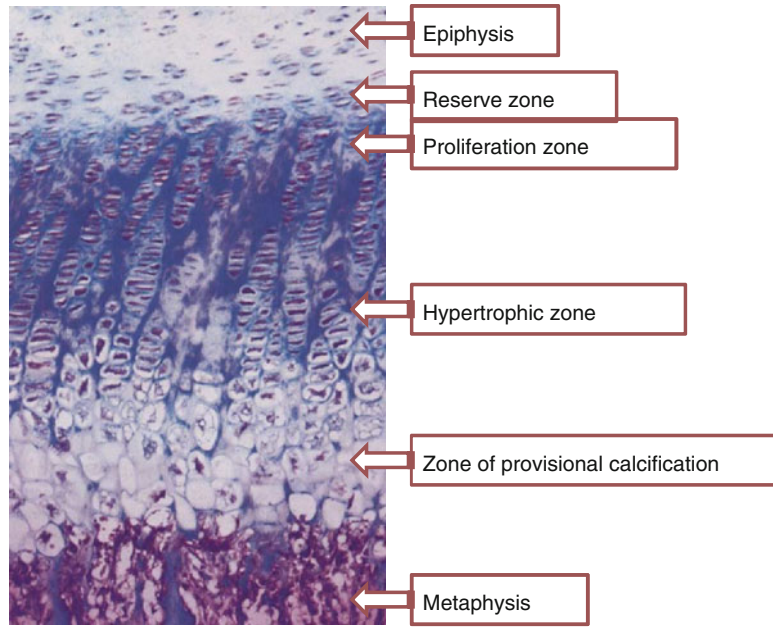

Fig. 21.1 The histologic structure of the growth plate

The pathologic conditions that can alter the anatomic integrity, physiological mechanisms, and hormonal and genetic control systems of the growth plate may cause serious orthopedic conditions like limb length differences, long bone deformities, and severe joint irregularities. Therefore, understanding the growth plate anatomy and physiology is crucial in order to diagnose the pathological conditions and in planning the treatment algorithm.

The longitudinal growth of the long bones is tightly controlled. This tight control ensures that when an individual reaches adolescence, the length of both extremities is equal or very close to be equal. Systemic hormones in circulation, locally produced peptide structure growth factors, and the biomechanical forces acting on the growth plate effect the gene expression of chondrocytes. These changes control chondrocyte size, extracellular matrix synthesis, enzyme and growth factor expression, and receptor expression. The process is completed with matrix calcification, chondrocyte apoptosis, and with enchondral bone formation [1].

Morphology and Physiology of the Growth Plate

Histologically, the growth plate is formed of fibrous, cartilage, and bone structures. The fibrous structure encircling the growth plate is formed of two different layers. The more superficial layer located at the convergence of the metaphysis and cartilage is the "LaCroix perichondrial ring," which includes dense fibrous tissue and provides mechanical support to the growth plate. It is formed of collagen fibers in a vertical, oblique, and circular fashion. The fibrous ring named the "Ranvier groove" or the "ossification groove" is in the section close to the growth plate and enables growth in width by providing progenitor cartilage cells for reserve zone [2, 3]. The Ranvier groove continues with the periosteum in the area close to the growth plate.

The cartilage component of the growth plate is formed from three main parts with different functional and histological properties; the reserve zone, proliferation zone, and hypertrophic zone. Within the hypertrophic zone, there are three different

zones: the maturation zone, the degeneration zone, and the zone of provisional calcification (Fig. 21.1).

Reserve Zone

This zone, which is the closest one to the epiphysis, contains chondrocytes, either singly or in pairs. These chondrocytes were recently shown to be effective in columnar and one-directional growth of the cells located deeper in the growth plate [4]. The size of the cells in reserve zone is similar to that of the cells in the proliferation zone. In cell staining studies, cytoplasms show strong positivity for glycogen. Electron microscopy studies have shown those cells to be rich in endoplasmic retinaculum, which is an indicator of protein synthesis [5]. The cells are scarcer compared to other zones and are separated from each other with a wider extracellular matrix. The oxygen density is low [6, 7]. Cartilage cells in the reserve zone pass to the proliferation zone with an unknown trigger mechanism.

Proliferation Zone

Cells in this zone have a smoother structure and settle as columns parallel to the long axis of the bone [5]. Oxygen density and the rate of cell metabolism are higher than in other zones. The basic function of this zone is the proliferation of cells, which is one of the basic mechanisms responsible for the longitudinal growth of the bone. The cell at the top of each column is a single cartilage cell displaying the properties of cartilage proliferation and thus it forms the true germinal layer of the growth plate [8]. Besides cell proliferation in this zone, it is also a zone of intense extracellular matrix synthesis [1]. Extracellular matrix synthesis helps cartilage cells separate from each other in the form of columns. The extracellular matrix is formed of collagens, proteoglycans, and other non-collagen proteins. Although the basic collagen of the growth plate is Type II collagen, Type IX and Type XI collagens are also intensively synthesized. Type IX collagen functions in the interaction of Type II collagen with the other matrix components surrounding. Mutations in Type II collagen are known to be related to skeletal dysplasia such as spondyloepiphyseal dysplasia, Kniest dysplasia, and Stickler syndrome.

Aggrecan is a basic proteoglycan of the cartilage matrix formed with the alignment of multiple keratan sulfate and chondroitin sulfate around a core protein [9]. It plays a key role in resistance of the cartilage against the compressive forces [10]. Decorin and biglycan are other matrix components with a proteoglycan structures. It is thought that decorin functions in the regulation of collagen fibril synthesis and biglycan in mineralization [11]. The most important non-collagen matrix protein is cartilage oligomeric matrix protein (COMP). It functions in binding of calcium to the extracellular matrix. Mutations are known to be related to pseudoachondroplasia and some forms of multiple epiphyseal dysplasias [12].

After a specific time period, either the number of cell divisions comes to an end or with the effect of local growth factors the chondrocytes lose their dividing capacity. The cells are differentiated by increasing their diameters and enter the hypertrophic zone [13].

Hypertrophic Zone

The cells that have been smoothed in the proliferation zone take on a spherical shape in the hypertrophic zone, which is the final zone, and their volume increases approximately fivefold compared to the proliferation zone [5]. Parallel to the increase in internal cell volume, an increase is seen in alkaline phosphatase enzyme activity and in the synthesis of Type X collagen, which is only found in the hypertrophic zone. Although the function of Type X collagen is not fully understood, it is known that mutations cause Schmid metaphyseal chondrodysplasia [14]. The dense cytoplasmic glycogen content, which is present at the beginning of the hypertrophic zone, decreases toward the middle of the hypertrophic

zone. Oxygen density is low associated with the scarce blood circulation. Under light microscopy, cell cytoplasm takes the form of a cavitary structure. This cavitary structure in the cell cytoplasm increases toward the lower layers of the hypertrophic zone and the nucleus of the cell starts to fragment. The vesicles, which have sprouted from the plasma membrane, accumulate within the matrix between the cartilage cell columns. In the same period, calcium starts to accumulate in these vesicles. Calcium phosphate, hydroxyapatite, and matrix metalloproteinase (MMP), which cause self and surrounding mineralization, are secreted from vesicles. Mineralization and low oxygen pressure attract primary spongious vessels to this zone [15]. Apoptosis starts in the chondrocytes, leaving a scaffold behind for bone formation. With lysosomal activity, endothelial and perivascular cells destroy the transverse cartilage septum, which is found at the very end of the hypertrophic zone [6]. The vast majority of this septum and the lacunae of the cartilage cells, which have undergone apoptosis, are filled with osteoblasts and osteoprogenitor cells. A trabecular network (primary spongiosa) is created from mineralized cartilage and bone matrix. Then, the metaphysis (secondary spongiosa) formed of lamellar bone develops on this covering [6].

Bone Growth and Control Mechanisms

The longitudinal growth of the bone is directly related to the proliferation rate of the cartilage cells in the growth plate. The rate of proliferation of the cartilage cells is controlled by the negative feedback cycle of parathyroid hormone-related peptide (PTHrP), Indian hedgehog (Ihh), and transforming growth factor-beta (TGF-β) expressed from the chondrocytes in the growth plate [11]. This feedback cycle controls the rate of cells, leaving the proliferation zone and turning into hypertrophic cells irreversibly. PTHrP delays hypertrophic transformation in chondrocytes, which have reached to the end of the proliferation zone. Cells, which have started hypertrophic transformation, express Ihh hand this goes back via the perichondrium causing the signal to be forwarded to the periarticular cells in order to the increase PTHrP production. TGF-β expressed from perichondrial cells has a role in the transmission of this signal and PTHrP production is increased [16, 17]. At the same time, by directly affecting cartilage cells, TGF-β can inhibit hypertrophic transformation [18]. The increase in PTHrP causes a decrease in hypertrophic transformation and a reduction in the density of cells that produce Ihh. Thus, the hypertrophic transformation is kept under control. Although it seems as if the basic control mechanism of cell proliferation in the growth plate is the feedback cycle of PTHrP, Ihh and TGF-β, cell proliferation can also be controlled by the local and systemic molecules such as fibroblast growth factor (FGF) and insulin-like growth factor I (IGF-I), which have previously shown to be effective on growth plate cell proliferation.

Chondrocyte hypertrophy has a significant role in longitudinal growth of the bone [19]. Forty-four to fifty-nine percent of the growth in the long bones occurs through chondrocyte hypertrophy and the remainder by extracellular matrix synthesis and chondrocyte proliferation. Hypertrophic chondrocyte dimensions in bones with different growth properties vary together with the growth capacity of the bone. The hypertrophic chondrocytes of the femur, which elongate faster than radius, have been shown to reach greater diameters [20, 21]. Although the reasons for these differences are not known, local, systemic, and genetic factors are thought to have an effect.

Another important function of hypertrophic cells is to prepare the extracellular matrix for calcification. Cartilage cells that have reached the final stage of hypertrophic transformation produce intense amounts of alkaline phosphatase and Type X collagen, which is only found in this zone. Alkaline phosphatase is essential for matrix calcification and is found in dense amounts within the vesicles expressed to the surrounding matrix from the hypertrophic chondrocytes. These vesicles are thought to be where the calcium hydroxy apatite nucleation first starts [22]. Alkaline phosphatase increases the density of phosphate ions, which are necessary

for calcification. A deficiency in alkaline phosphatase causes a reduction in matrix mineralization as in hypophosphatasia and the growth plate widens [22]. In the completion of cartilage maturation, bone morphogenetic proteins (BMPs) and receptors are thought to be effective [23, 24]. It has been shown that the cartilage cells undergo hypertrophic transformation when BMP is present in the environment. On the other hand, maturation has been shown to be prevented by BMP inhibition [25]. The other local and systemic factors that are effective on maturation are also thought to have an effect on the cartilage cells through BMP pathway.

Chondrocytes are metabolically active cells that synthesize the extracellular matrix. The matrix undergoes calcification starting from the vesicles expressed from the cartilage cells and these calcified areas function as a template to osteoblasts for bone formation. The calcium accumulation in the matrix vesicles is dependent on a family of calcium channel molecules, which is called Annexins. Both Type II and Type X collagen are effective in the calcification process, causing activation of Annexin-V.

While it was previously thought that a reduction of oxygen pressure in the environment and the necessary nutritional substances resulted in death of hypertrophic chondrocytes, today it is known that those cells also die as a result of a programmed process [26]. Although the physiological mechanisms regulating programmed cell death (apoptosis) in the growth plate have not yet been fully clarified, the relationship of the chondrocytes with the extracellular matrix, various growth factors, and cytokines are thought to affect the process. Extracellular matrix mineralization causes an increase in the phosphate ion concentration in the environment. In vitro studies have shown that increased phosphate ion concentration triggered apoptosis in mature cartilage cells [27].

Controlling the velocity of bone growth comprise a process containing several factors that are effective together. Genetic differences, systemic hormone levels, local effects of growth factors and cytokines, nutritional and vascular status of the growth plate, and the mechanical forces are effective at the cellular level and control the growth rate.

Several cellular events simultaneously occur within the growth plate during the longitudinal growth of bones. While the cells in the proliferation zone are being divided, cells in the hypertrophic zone expand and produce extracellular matrix. Cells in the provisional calcification zone complete their apoptosis process and are replaced by calcified cartilage. Of these cellular events, cartilage cell proliferation rate and extracellular matrix synthesis and expansion of the cells are the key mechanisms providing longitudinal growth.

Clinical Relevance

Guiding Growth Plate as a Means of Treatment Modality

The Hueter-Volkmann law explains the effects of mechanical forces on the growth plate. This describes how compressive forces on the growth plate decrease its activity and inhibits its growth. However, tensile, torsional, and bending forces are also known to have an effect on growth plate activity [28, 29].

Mechanical loading has been shown to have an effect on growth through cell proliferation, cell expansion, and transformation [30]. Compressive forces have been shown to reduce the number and ratio of proliferating chondrocytes in rabbit and rat growth plates [31]. On the other hand, reduction of the loads on the growth plate or the application of distraction forces causes widening of the growth plate [30]. The basic mechanisms achieving widening have been shown to be an increase in the number, height, and volume of chondrocytes [32] (Fig. 21.2).

The effect of mechanical forces on genes and proteins, which function in cartilage formation, has been studied in animal models. It has been shown in the growth plates of rat tibia that compressive forces decreases Type II collagen gene expression in the hypertrophic zone, and Type X collagen gene expression is limited in the lower layers of the hypertrophic zone [33]. However, in a

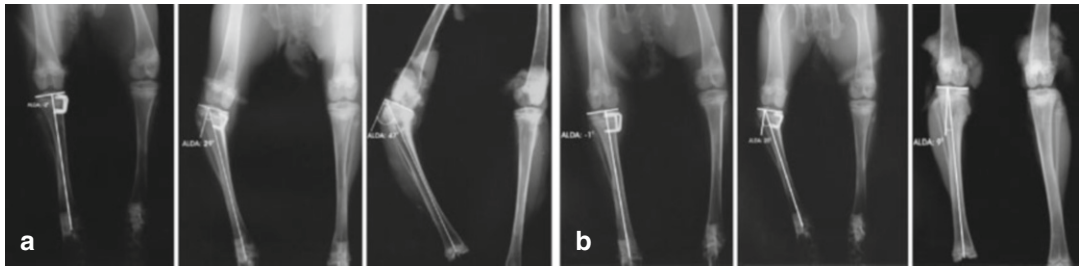

Fig. 21.2 The asymmetrical suppression of the activity of the growth plate in experimental models creates bone deformities (**a**). The deformity improves spontaneously after the suppression is removed (**b**)

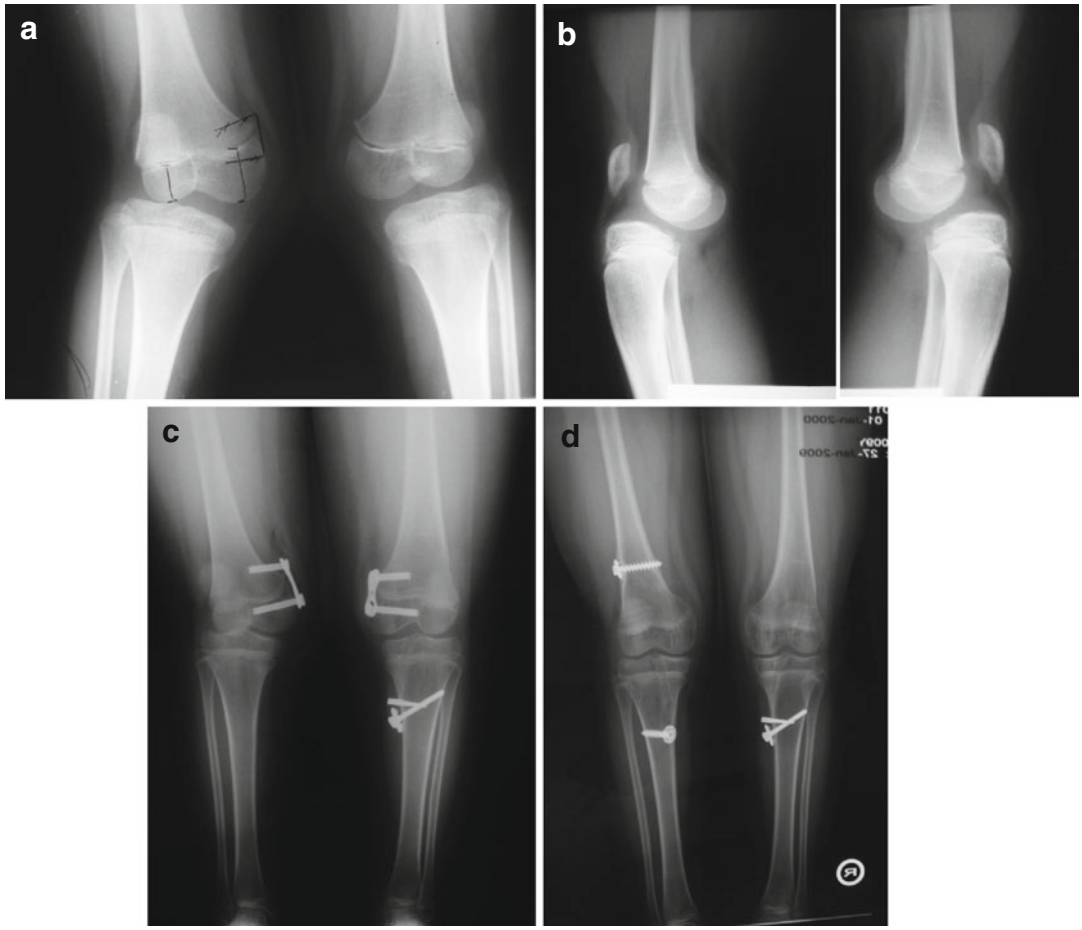

Fig. 21.3 Genu valgum deformity and knee subluxation in a child secondary to deficiency of anterior cruciate ligament (**a**, **b**). The end result obtained with ligament reconstruction and hemi-epiphysiodesis (**c**, **d**) (Courtesy Reha Tandogan, MD)

study where chickens roaming free within a cage were loaded with a sandbag, despite the narrowing of the area, where these two collagen types were synthesized, no difference was determined in the gene expression of those proteins [34].

Since the growth plate activity can be modulated by external forces, the growth plates, particularly in the pediatric age group, have been the focus of different treatment alternatives for various skeletal deformities in children (Figs. 21.3 and 21.4).

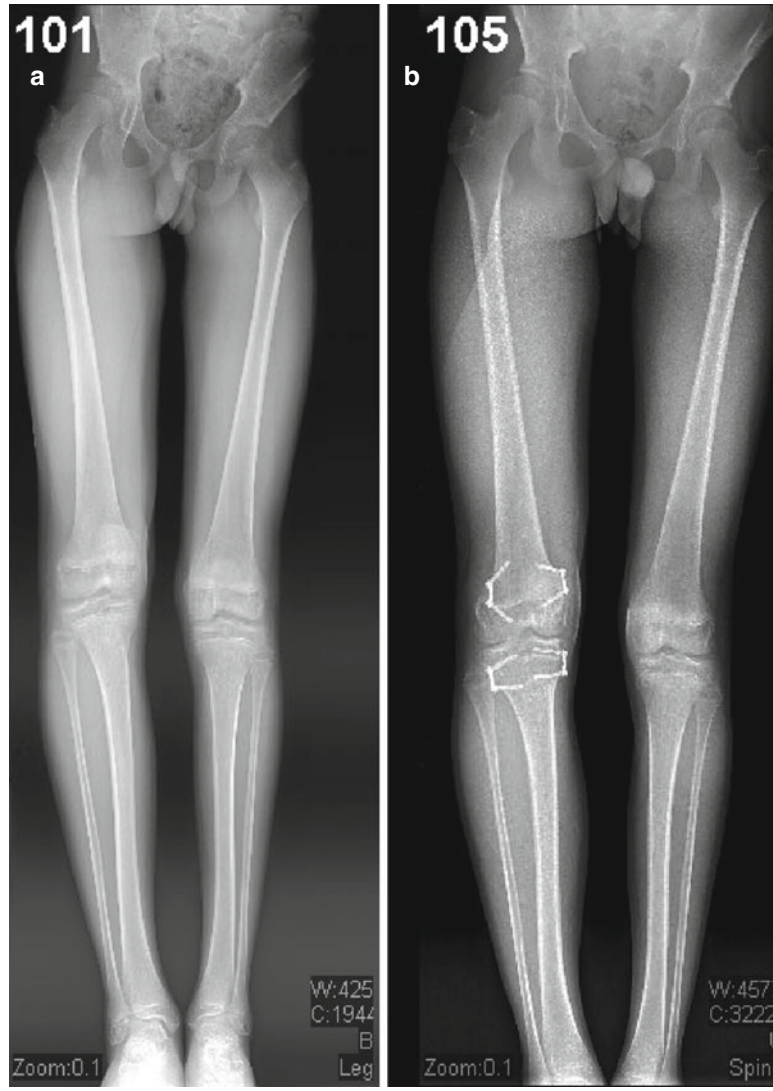

Fig. 21.4 In a case of hemihypertrophy (**a**) the equalization of limb lengths through epiphysiodesis both on the femur and tibia (**b**)

Phemister first described epiphysiodesis, or with its original name, "epiphysiodiaphyseal fusion," as a technique for treatment of limb length discrepancies [35]. In the light of Phemister's studies, Blount pioneered the application of hemi-epiphysiodesis with a staple in extremity deformities [36, 37], and the technique has been purified and become very popular using a two-hole plate and two-screw system (Fig. 21.5).

Following hemi-epiphysiodesis utilizing staple in rabbits, cellular activity was seen to slow down in the area where the staple was applied. And secondary to unilateral slowing of the cellular activity, an experimental bone deformity was created. After removal of the staple, cellular activity was seen to return to a normal level (Fig. 21.2) [38]. Similar results have been seen in pigs where plate-screw systems have been used [39]. Both techniques are known to be clinically effective in providing hemi-epiphysiodesis and correcting childhood skeletal deformities [40].

The basic logic in the correction of extremity deformities through growth plate modulation has also been applied to spine deformities. Longitudinal growth of the vertebral column occurs through the growth plates in the proximal and distal parts of the vertebral bodies. Distraction

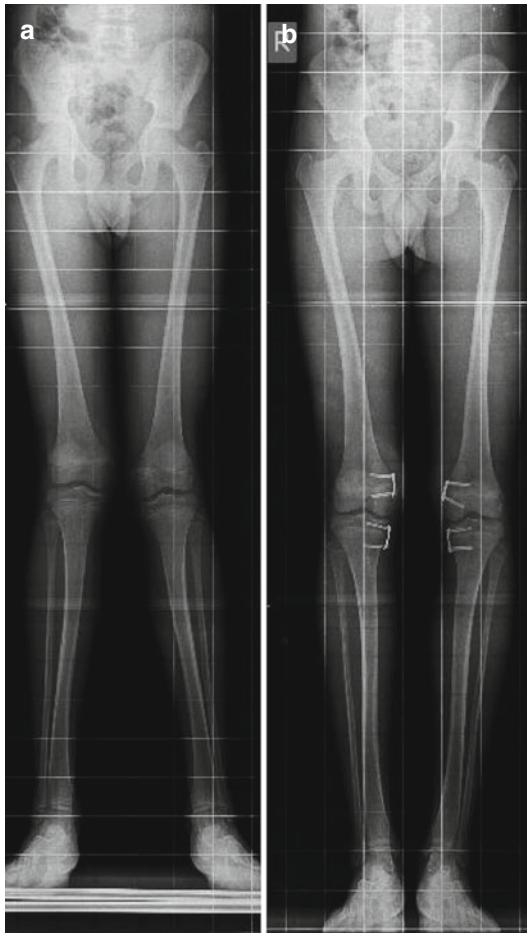

Fig. 21.5 A 13-year-old male patient with bilateral genu valgum deformity. (**a**) Treatment with medial femoral and tibial hemi-epiphysiodesis. Eighteen-month follow-up radiographs showing normal alignment (**b**)

or compression forces that will be effective on the growth plates have the potential to modulate the vertebral growth. In a porcine study, after instrumentation applied from the posterior without fusion, relatively more longitudinal growth was observed at the spinal levels under the effect of distraction forces than in the vertebral bodies, which were not under the effect of distraction forces [41]. Following anterior hemi-epiphysiodesis applied with a staple in the thoracic spine of pigs, there was a decrease in cartilage cell height and disc height in the growth plate, where the staple had been applied [42]. In another study of pigs, where a unilateral anterior staple was applied, suppression of the spinal growth was achieved on the instrumented side and a mean of 22.4° thoracic scoliosis was created [43]. The growth modulation effect obtained with a staple in the spine in animal studies was used in the treatment of idiopathic scoliosis, and in a study of 52 curvatures of 39 patients, curvature stabilization was obtained in 87% of the curves [44].

The process of the emergence of the skeletal system and its maturation are kept under tight control by genetic, hormonal, and environmental factors. Any deficiency in the control mechanisms causes a unilateral or bilateral breakdown in growth and this causes extremity deformities, limb length discrepancies, and joint irregularities. A good understanding of the functional mechanisms of the growth plate will assist in defining pathophysiology behind the clinical abnormalities and will also guide the clinicians for the best treatment algorithm.

References

1. van der Eerden BC, Karperien M, Wit JM (2003) Systemic and local regulation of the growth plate. Endocr Rev 24(6):782–801, Review
2. Shapiro F, Holtrop ME, Glimcher MJ (1977) Organization and cellular biology of the perichondrial ossification groove of Ranvier. J Bone Joint Surg 59A:703
3. Chung SMK, Batterman SC, Brighton CT (1976) Shear strength of the human femoral capital epiphyseal plate. J Bone Joint Surg 58A:94
4. Abad V, Meyers JL, Weise M, Gafni RI, Barnes KM, Nilsson O, Bacher JD, Baron (2002) The role of the restingzone in growth plate chondrogenesis. J Endocrinol 143(5):1851–1857
5. Brighton CT, Sugioka Y, Hunt RM (1973) Cytoplasmic structures of the epiphyseal plate chondrocytes: quantitative evaluation using electron micrographs of rat costochondral junctions with special reference to the fate of hypertrophic cells. J Bone Joint Surg 55A:771
6. Brighton CT (1987) Morphology and biochemistry of the growth plate. Rheum Dis Clin North Am 13(1):75–100
7. Brighton CT, Heppenstall R (1971) Oxygen tension in zones of the epiphyseal plate, the metaphysis, and diaphysis: an in vitro and in vivo study in rats and rabbits. J Bone Joint Surg 53A:719
8. Kember NF (1960) Cell division in endochondral ossification: a study of cell proliferation in rat bones

by the method of tritiated thymidine auto-radiography. J Bone Joint Surg 42B:824
9. Nap RJ, Szleifer I (2008) Structure and interactions of aggrecans: statistical thermodynamic approach. Biophys J 95(10):4570–4583
10. Roughley P, Martens D, Rantakokko J, Alini M, Mwale F, Antoniou J (2006) The involvement of aggrecan polymorphism in degeneration of human intervertebral disc and articular cartilage. Eur Cell Mater 11:1–7, discussion 7. Review
11. Ballock RT, O'Keefe RJ (2003) The biology of the growth plate. J Bone Joint Surg Am 85-A(4):715–726
12. Ballock RT, O'keefe RJ (2007) Growth and development of skeleton. In: Orthopaedic basic science foundations of clinical practice chapter 7, 3rd edn. American Academy of Orthopaedic Surgeons, IL, USA. pp 115–125
13. Minina E, Kreschel C, Naski MC, Ornitz DM, Vortkamp A (2002) Interaction of FGF, Ihh/Pthlh, and BMP signaling integrates chondrocyte proliferation and hypertrophic differentiation. Dev Cell 3(3): 439–449
14. Zhu Y, Li L, Zhou L, Mei H, Jin K, Liu K, Xu W, Tang J, Yang Y, Zhao R, He X (2011) A novel mutation leading to elongation of the deduced α1(X) chain results in metaphyseal chondrodysplasia type schmid. Clin Chim Acta 412(13–14):266–269. doi:10.1016/j.cca.2011.03.026, Epub 2011 Apr 5
15. Schipani E, Ryan HE, Didrickson S, Kobayashi T, Knight M, Johnson RS (2001) Hypoxia in cartilage: HIF-1alpha is essential for chondrocyte growth arrest and survival. Genes Dev 15(21):2865–2876
16. Serra R, Karaplis A, Sohn P (1999) Parathyroid hormone-related peptide (PTHrP)-dependent and -independent effects of transforming growth factor beta (TGF-beta) on endochondral bone formation. J Cell Biol 145(4):783–794
17. Alvarez J, Horton J, Sohn P, Serra R (2001) The perichondrium plays an important role in mediating the effects of TGF-beta1 on endochondral bone formation. Dev Dyn 221(3):311–321
18. Ballock RT, Heydemann A, Wakefield LM, Flanders KC, Roberts AB, Sporn MB (1993) TGF-beta 1 prevents hypertrophy of epiphyseal chondrocytes: regulation of gene expression for cartilage matrix proteins and metalloproteases. Dev Biol 158(2):414–429
19. Wilsman NJ, Farnum CE, Leiferman EM, Fry M, Barreto C (1996) Differential growth by growth plates as a function of multiple parameters of chondrocytic kinetics. J Orthop Res 14(6):927–936
20. Farnum CE, Wilsman NJ (2001) Converting a differentiation cascade into longitudinal growth: stereology and analysis of transgenic animals as tools for understanding growth plate function. Curr Opin Orthop 12(5):428–433
21. Eerola I, Elima K, Markkula M, Kananen K, Vuorio E (1996) Tissue distribution and phenotypic consequences of different type X collagen gene constructs in transgenic mice. Ann N Y Acad Sci 785:248–250
22. Anderson HC (1995) Molecular biology of matrix vesicles. Clin Orthop Relat Res 314:266–280, Review
23. Volk SW, Leboy PS (1999) Regulating the regulators of chondrocyte hypertrophy. J Bone Miner Res 14(4):483–486, Review
24. Enomoto-Iwamoto M, Iwamoto M, Mukudai Y, Kawakami Y, Nohno T, Higuchi Y, Takemoto S, Ohuchi H, Noji S, Kurisu K (1998) Bone morphogenetic protein signaling is required for maintenance of differentiated phenotype, control of proliferation, and hypertrophy in chondrocytes. J Cell Biol 140(2):409–418
25. Grimsrud CD, Romano PR, D'Souza M, Puzas JE, Schwarz EM, Reynolds PR, Roiser RN, O'Keefe RJ (2001) BMP signaling stimulates chondrocyte maturation and the expression of Indian hedgehog. J Orthop Res 19(1):18–25
26. Hatori M, Klatte KJ, Teixeira CC, Shapiro IM (1995) End labeling studies of fragmented DNA in the avian growth plate: evidence of apoptosis in terminally differentiated chondrocytes. J Bone Miner Res 10(12):1960–1968
27. Mansfield K, Rajpurohit R, Shapiro IM (1999) Extracellular phosphate ions cause apoptosis of terminally differentiated epiphyseal chondrocytes. J Cell Physiol 179(3):276–286
28. Arkın AM, Katz JF (1956) The effects of pressure on epiphyseal growth; the mechanism of plasticity of growing bone. J Bone Joint Surg Am 38-A(5):1056–1076
29. Moreland MS (1980) Morphological effects of torsion applied to growing bone. An in vivo study in rabbits. J Bone Joint Surg Br 62-B(2):230–237
30. Alberty A, Peltonen J, Ritsilä V (1993) Effects of distraction and compression on proliferation of growth plate chondrocytes. A study in rabbits. Acta Orthop Scand 64(4):449–455
31. Stokes IA, Clark KC, Farnum CE, Aronsson DD (2007) Alterations in the growth plate associated with growth modulation by sustained compression or distraction. Bone 41(2):197–205, Epub 2007 Apr 24
32. Stokes IA, Mente PL, Iatridis JC, Farnum CE, Aronsson DD (2002) Growth plate chondrocyte enlargement modulated by mechanical loading. Stud Health Technol Inform 88:378–381
33. Villemure I, Chung MA, Seck CS, Kimm MH, Matyas JR, Duncan NA (2005) Static compressive loading reduces the mRNA expression of type II and X collagen in rat growth-plate chondrocytes during postnatal growth. Connect Tissue Res 46(4–5):211–219
34. Reich A, Sharir A, Zelzer E, Hacker L, Monsonego-Ornan E, Shahar R (2008) The effect of weight loading and subsequent release from loading on the postnatal skeleton. Bone 43(4):766–774
35. Phemister DB (1933) Operative arrestment of longitudinal growth of bones in the treatment of deformities. J Bone Joint Surg Am 15:1–15
36. Blount WP (1971) A mature look at epiphyseal stapling. Clin Orthop Relat Res 77:158–163
37. Zuege RC, Kempken TG, Blount WP (1979) Epiphyseal stapling for angular deformity at the knee. J Bone Joint Surg Am 61:320–329

38. Aykut US, Yazici M, Kandemir U, Gedikoglu G, Aksoy MC, Cil A, Surat A (2005) The effect of temporary hemiepiphyseal stapling on the growth plate: a radiologic and immunohistochemical study in rabbits. J Pediatr Orthop 25(3):336–341
39. Burghardt RD, Kanellopoulos AD, Herzenberg JE (2011) Hemiepiphyseal arrest in a porcine model. J Pediatr Orthop 31(4):e25–e29
40. Wiemann JM 4th, Tryon C, Szalay EA (2009) Physeal stapling versus 8-plate hemiepiphysiodesis for guided correction of angular deformity about the knee. J Pediatr Orthop 29(5):481–485
41. Yilmaz G, Huri G, Demirkiran G, Daglioglu K, Ozkan C, Alanay A, Acaroglu E, Yazici M (2010) Growing rod instrumentation and vertebral body growth. A radiological investigation in immature pigs. Spine 35:730–733
42. Bylski-Austrow DI, Wall EJ, Glos DL, Ballard ET, Montgomery A, Crawford AH (2009) Spinal hemiepiphysiodesis decreases the size of vertebral growth plate hypertrophic zone and cells. J Bone Joint Surg Am 91(3):584–593
43. Wall EJ, Bylski-Austrow DI, Kolata RJ, Crawford AH (2005) Endoscopic mechanical spinal hemiepiphysiodesis modifies spine growth. Spine (Phila Pa 1976) 30(10): 1148–1153
44. Betz RR, D'Andrea LP, Mulcahey MJ, Chafetz RS (2005) Vertebral body stapling procedure for the treatment of scoliosis in the growing child. Clin Orthop Relat Res 434:55–60

Joint Cartilage

22

Rocky S. Tuan and Feza Korkusuz

Abstract

Joint cartilage is a highly specialized tissue that allows movement. Degeneration and injury impairs its functions. Chondrocytes and extracellular matrix determines utility. Thinning and loss of macromolecular structure of joint cartilage leads to degeneration. Changing load distribution aids recovering homeostasis to some extend. Disease modifying molecules help maintaining structure and function, however signaling molecules are still researched. This chapter also informs on mechanical and molecular determinants of joint cartilage, degeneration, and primary and posttraumatic osteoarthritis.

Learning Outcomes

After you have studied this chapter, you will have an understanding of (1) the structure and function of joint cartilage and chondrocytes, (2) the classification of layers of joint cartilage, (3) the chondrocyte–extracellular matrix interactions, (4) the structure and interactions of aggrecan, (5) the active signaling molecules maintaining autocrine homeostasis, (6) the cartilage mechanics and mechanisms of injury, (7) the synovial fluid and nutrition balance, and (8) the life-span changes and the pathogenesis of primary and secondary arthritis.

Terminology

Aggrecan A cartilage-specific proteoglycan core protein also named as chondroitin sulfate proteoglycan 1. The *ACAN* gene, a member of the lectican (chondroitin sulfate proteoglycan) family, codes this protein in humans. This proteoglycan withstands compression forces in the cartilage.

R.S. Tuan, PhD (✉)
Department of Orthopaedic Surgery,
Center for Cellular and Molecular Engineering,
University of Pittsburg, Pittsburg, PA, USA
e-mail: rst13@pitt.edu

F. Korkusuz, MD
Department of Sports Medicine, Hacettepe
University Medical Faculty, Ankara, Turkey
e-mail: feza.korkusuz@gmail.com

F. Korkusuz (ed.), *Musculoskeletal Research and Basic Science*,
DOI 10.1007/978-3-319-20777-3_22

Articulation Functional junctions between the joints.

Arthritis Inflammatory joint disorder that involves the synovium, all layers of joint cartilage, and subchondral bone.

Autocrine A form of cell signaling where the active signaling molecule is secreted by a cell and afterward received by the receptors of that same cell.

Bursae A sac lined with synovial membrane that contains synovial fluid. Bursae protect bony prominences (e.g., olecranon process of the elbow). They also cushion tendons so that they glide over the bones and joints.

Chondroitin (sulfate) A chain of glycosaminoglycan (GAG) that provides mechanical properties of joint cartilage.

Chondrocyte Cells of the cartilage. Chondroblast defines immature chondrocyte.

Condylar joint The ovoid-shaped bone ending covered with joint cartilage that fits into the ellipsoidal cavity of the other bone ending (e.g., the knee joint).

Diarthrotic joint Freely movable joint.

Extracellular matrix Collection of extracellular molecules secreted by chondrocytes that provide structural and biochemical support.

Glucosamine A dietary natural amino sugar that may decrease pain (placebo affect) in mild osteoarthritis [1]. **Caution**: Do not use together with warfarin (Coumadin).

Hinge joint A joint that permits movement only in a single plane. The convex and concave endings of the bones fit into each other (e.g., elbow joint).

Homeostasis A state of balance, whereby the internal conditions of tissues, organs, and/or organ systems remain stable and almost constant under external stimulations. A sensor to detect changes and a feedback mechanism are required to maintain homeostasis.

Hyaline (transparent) A type of cartilage that does not contain blood vessels and nerve endings.

Hyaluronan (hyaluronic acid) An extracellular matrix polysaccharide important for cell growth.

Joint capsule A two-layer structure that helps to keep the synovial joint in congruity. The outer layer of the joint capsule, consisting of dense connective tissue, which joins the periosteum. The inner layer consists of the synovial membrane. The skeletal muscles usually support this thin connective tissue.

Ligament A band of oriented fibrous tissue connecting the bones of a joint.

Periosteum The double-layered fibrous membrane covering the surface of the bones. The inner cambium layer has osteogenic and chondrogenic potential.

Proteoglycan Heavily glycosylated proteins that consist of glycosaminoglycan (GAG) chains attached to a core protein.

Spheroidal joint A ball and socket-type synovial joint (i.e., the hip and the shoulder joints).

Synarthrosis Immovable joints.

Synchondrosis Type of cartilaginous joint where bands of hyaline cartilage unite the bones (i.e., the physis).

Syndesmosis Type of fibrous joint: Dense connective tissue binds the bones to each other by sheets (e.g., distal tibiofibular joint).

Synovial fluid A viscous fluid composed of hyaluronan, lubricin, proteinases, and collagenases, which are essential for articular cartilage lubrication.

Synovial membrane or synovium A membrane that produces the synovial fluid. This membrane is assumed to contain regenerative cells.

Clinical Relevance

Do glucosamine, chondroitin, and/or hyaluronan help to relieve symptoms of arthritis? (Fig. 22.1)

A 65-year-old female patient approached the outpatient clinic with symptoms of knee pain. After physical examination and X-ray studies, the physician prescribed non-load-

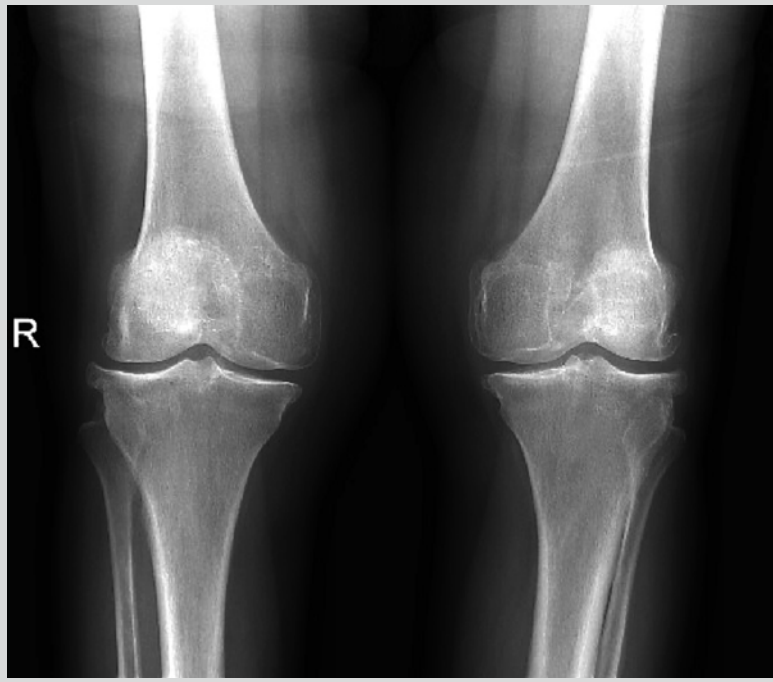

Fig. 22.1 Bilateral standing X-ray of a 65-year-old female patient. Mild to moderate radiological findings of osteoarthritis were recognized

bearing exercise and a dietary supplement containing glucosamine and chondroitin sulfate. The patient had to take the supplement for 3 months. At her control visit, when she reported partial relief of her pain symptoms, an intra-articular hyaluronan injection was proposed. While under treatment with exercise, glucosamine and chondroitin sulfate supplement, and intra-articular injections, the patient was followed up for 6 years until her joint replacement surgery was undertaken.

Oral glucosamine is a dietary supplement used to relieve pain in osteoarthritis (OA). Prescribed as a medicine in some European countries, controlled clinical trials indicate that this disease-modifying supplement is partially effective in the knee and hand but not in all types of OA [2]. More important is the patient's age, the disease severity, and the phenotype of the patient. Obese and severely osteoarthritic patients benefit less from this supplement. Oral glucosamine is not advised in diabetic patients although insulin resistance or endothelial dysfunction does not occur in healthy individuals [3]. Patients on warfarin (Coumadin) also should not use oral glucosamine. It should be noted that an updated intervention review [4] failed to show any benefit of glucosamine for pain, function, and stiffness scales though one formulation had better results than placebo. Another study found no evidence that oral herbal therapies improve joint structure and prevent joint space narrowing [5].

An algorithm recommended for the management of knee OA was recently defined [6]. Prescription of glucosamine sulfate and/or chondroitin sulfate with or without paracetamol is recommended at step one as background treatment according to this protocol. Intra-articular hyaluronan injection is advised at step two in persistently symptomatic patients in the same protocol. According to the recent OA Research Society International (OARSI) guidelines [7], the symptomatic efficacy of this type of supplementation is uncertain. American Academy of Orthopaedic Surgeons (AAOS)

guidelines concluded that these treatments do not provide evidence-based outcomes [8].

Intra-articular hyaluronan injection, which is also defined as viscosupplementation, decreases pain and improves function in knee OA [9].

Structure, Function, and Repair

The nineteenth century humanist, poet, essayist, and journalist Walter Whitman observed the way a joint of a finger is more complex than the most intricate machinery. Most orthopedic surgeons will concur with this observation. Artificial joints of today can partially fulfill requirements of the joints for a determined duration.

Joint cartilage is a highly specialized connective tissue tolerating broad range of motion between long bones. It generates a very low frictional surface and presents lubrication properties for millions of cycles through decades. This macroscopically shiny, light blue or opal tissue at young ages has distinctive structural features. Its thickness, cellular volume, extracellular matrix, and mechanical properties may vary between species, at different joints of the same kind and at different locations of the same joint [10]. The thickness of human knee joint cartilage is less than 10 mm. Six to eight times body weight is absorbed by this structure in a jogging human. Such an intensive load is very well distributed and absorbed in such a thin and small surface area. Macroscopically, the surface of joint cartilage is smooth and durable to deformation. Microscopically, this multilayered structure contains (a) one type of cells named chondrocyte, (b) is mostly of extracel-

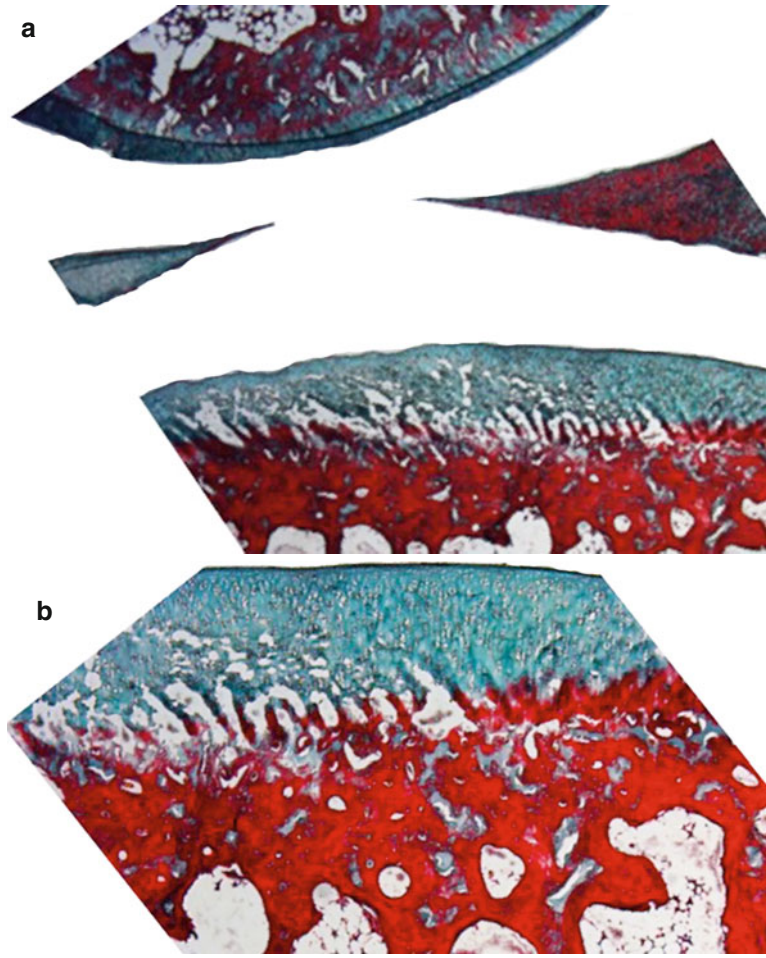

Fig. 22.2 Normal knee joint cartilage and meniscus of rabbit (**a**) Masson's trichrome 10× and (**b**) Masson's trichrome 40×

lular matrix, and (c) lacks blood and lymph vessels and nerve endings (Fig. 22.2) [11]. Chondrocytes are nourished from synovial fluid. They almost always metabolize through the anaerobic pathway and therefore have limited regeneration capacity. Their primary function is to maintain or restore the extracellular matrix. Chondrocyte function deteriorates with aging leading to cartilage degeneration. Thickness of the cartilage decreases and its molecular biologic structure weakens. The weakened microscopic molecular structure leads to abnormal fluid homeostasis depriving mechanical functions. Oriented fibers of joint cartilage act such as a natural sponge. Synovial fluid flows out of the sponge rapidly at initial loading. Micro- and nanopores of the sponge lock over each other when compressive loading continues and increases. A certain amount of synovial fluid is entrapped in the pores of the sponge-like structure of the cartilage even under excessive loads allowing it to properly function. Synovial fluid may not be attained in joint cartilage when this fiber structure of the extracellular matrix is disrupted, and chondrocytes are primarily responsible for regulating this homeostasis. The number and function of chondrocytes decrease with age leading to osteoarthritis (OA). Joint cartilage and subchondral bone degenerate in OA. Pain, limitation of joint motion, and deformity are its clinical findings. Fifty percent of practitioner visits of 65+-year-old patients are due to OA [12].

Ratio of chondrocyte to extracellular matrix is 1.65 % and 2.6 % at the superficial and middle–deep zones, respectively [13]. The superficial zone is also named as the fibrous or tangential zone. Superficial zone chondrocytes are fibroblast-like flattened cells aligned in the plane of the articular surface. Middle and deep zone chondrocytes function in their lacunae. Molecular mechanism of how chondrocytes control cartilage repair and/or regeneration is less known [14–16]. Regeneration and repair alter with age [17]. Proteolysis, glycation, and calcification are frequent features of aging. Cell density decreases. Abnormal secretory profiles and anabolic responses lead to biomechanical dysfunction and tissue destruction [17].

Eighty percent of wet weight of articular cartilage is of the synovial fluid. Synovial fluid and extracellular matrix determine the phenotype and endurance of joint cartilage. Synovial fluid containment capacity of joint cartilage is dependent on the macromolecule named aggrecan and the electrolyte containment of the synovial fluid. Collagen, proteoglycan, and glycoproteins establish 60 %, 25 %, and 15 % of the dry weight of joint cartilage, respectively. Collagen fibers are aligned longitudinally and are intense under the joint surface at the superficial zone. Resistance to tensional forces is generated by these fibers. In the middle and deep zones, collagen fibers keep chondrocytes in their lacunae. Proteoglycans and glycoproteins determine the synovial fluid containment of the cartilage. Type IX and XI collagens cross-link type II collagen and are responsible of cartilage integrity. Ninety to 95 % of joint cartilage structure is of type II collagen. Half-life of collagen is calculated as 3 months. Type VI collagen is mostly located around chondrocytes. Type X collagen is largely located near calcified and hypertrophic cartilage zones. Type X collagen is assumed to function at the calcification process of joint cartilage (Fig. 22.3).

Proteoglycan structure is of several glycosaminoglycan chains attached to a central protein chain. Glycosaminoglycan chains are of repeating disaccharides that contain amino glucose. Each disaccharide unit contains a negatively charged carboxyl or sulfate ring. Hyaluronic acid, chondroitin sulfate, keratan sulfate, and dermatan sulfate are major glycosaminoglycans. Keratan sulfate to chondroitin sulfate ratio increases with age as chondroitin sulfate degrades between globular domains two and three [18]. The big molecules of the 100 mg/ml dense proteoglycan are named as aggrecan. Decorin, biglycan, and fibromodulin are smaller proteoglycans. Type IX collagen is named as a glycosylated protein due to its glycosaminoglycan content (Fig. 22.4).

Keratan and chondroitin sulfates construct aggrecan structure [19]. Aggrecans fill 90 % of joint cartilages' interfibrillar space. Decorin, biglycan, and fibromodulin contain one, two, and several sulfate chains, respectively. These fill up the remaining interfibrillar space from the aggrecan. Aggrecan is attached to hyaluronic acid by non-covalent bindings. Aggrecan and hyaluronic acid are further attached to each other by connecting proteins. Aggrecan augments all proteoglycans, glycosaminoglycans, and collagen. Hyaluronan that expands from 100 to 10,000 nm establishes the central skeleton allowing about 300 aggrecan

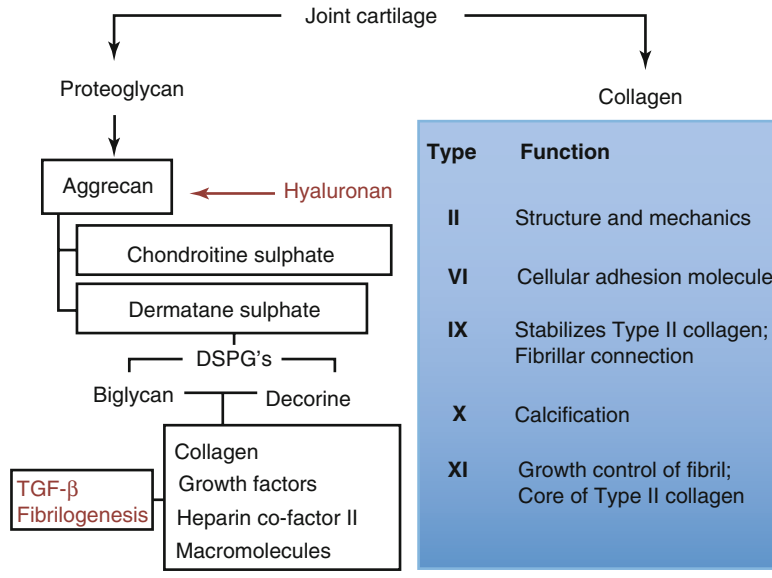

Fig. 22.3 Proteoglycan and collagen structure of joint cartilage

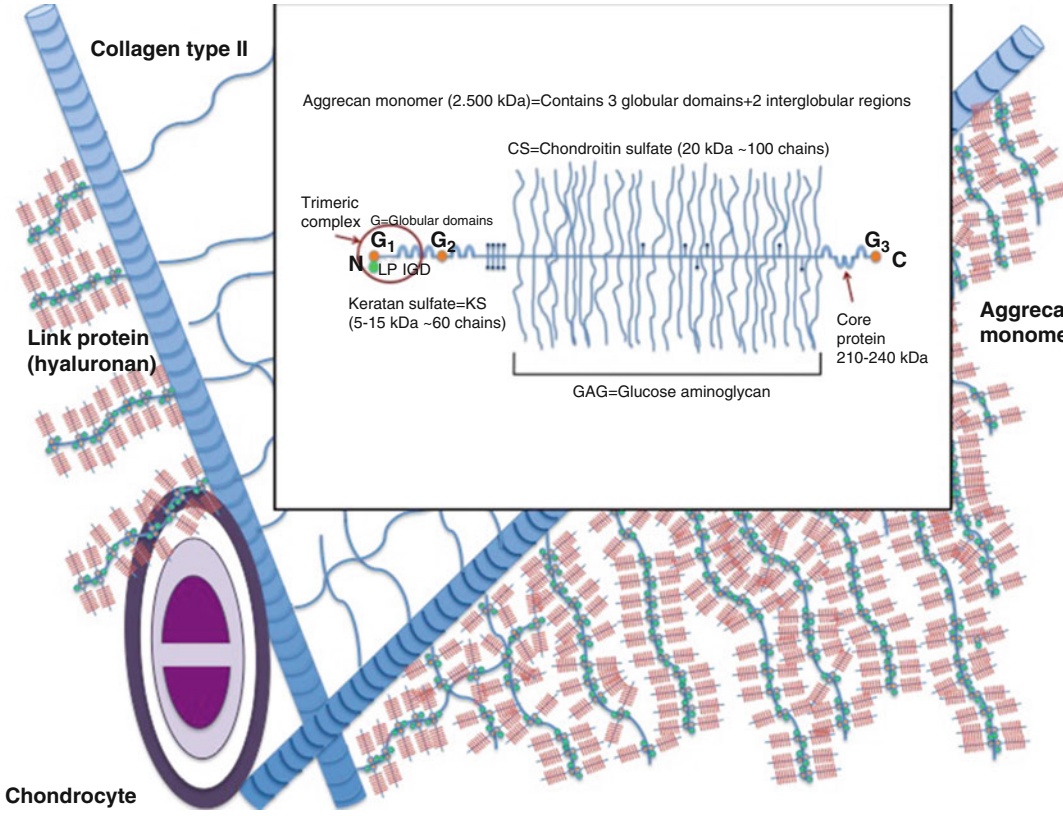

Fig. 22.4 Structure of aggrecan

attachment (Fig. 22.4). Small proteoglycans that do not attach to other proteins maintain chondrocyte homeostasis. Fibromodulin and decorin stabilize type II collagen and biglycan attaches to type VI collagen. Small proteoglycans furthermore regulate repair by attaching to transforming growth factor (TGF)-β. They also control degeneration triggering enzymes. Proteoglycans and connecting proteins are synthesized from the endoplasmic reticulum, whereas hyaluronan is assumed to be synthesized from the cell membrane.

Core protein of the aggrecan contains a single genetic code. Its three-dimensional structure is of three globular proteins and two other extensions. This structure is different in other species. The aggrecan monomer connects to the central hyaluronic acid skeleton through its N terminal. G1, G2, and G3 globular connection points separate this core protein to E1 and E2 sections. Aggrecan terminates at the G3 globular connection that is also named as the C terminal. The E1 and E2 sections are about 21 nm and 260 nm, respectively. Most of keratan sulfate and all of chondroitin sulfate are attached to the core protein E2 section. Globular connection points are of folding immunoglobulins and disulfide double loop repeating chains. They present CD44 staining and are immunogenic [20]. The three-dimensional G1 domain that is at the N terminal, which connects aggrecan to the central hyaluronic acid skeleton, is a complex structure [21]. G1 domain is stable for heat and proteinases. A disintegrin and metalloproteinase with thrombospondin motifs (ADAMTS) may catabolize this naturally stable trimeric complex and cause degeneration [22, 23]. ADAMTS are potential therapeutic targets for OA. Syndecans that fix ADAMTS to the cell membrane disintegrate by the inflammatory molecule interleukin-1 and lead to cartilage breakdown at synovial inflammation [24]. The G3 globular connection that is of ten cysteine molecules is defined in only 10–50 % of joint cartilage samples. The function of G3 globular connection is not clearly defined. G3 globular connection is assumed to regulate matrix organization, synthesis, intracellular translocation, and glycosylation.

Carbohydrate distribution of cartilage proteoglycans varies between chondroitin sulfate, keratan sulfate, and O-linked and N-linked oligosaccharides. Dimensions, quantity, pathway of sulfatization, and electrical charges of these proteoglycans change with age. Non-collagenous proteins and glycoproteins are oligosaccharides and monosaccharides. Ancorin CII and cartilage oligomeric matrix protein (COMP) connects chondrocytes to the extracellular matrix. COMP is specific to joint cartilage and increases in serum and synovial fluid with degradation [25]. Load-bearing exercise increases serum COMP levels [26]. Functions of non-collagenous proteins fibronectin and tenascin are still searched.

Joint Cartilage Layers

Superficial, intermediate, radiated, and calcified interconnecting zones of joint cartilage are defined (Fig. 22.5). Layers have different functions. Phenotype and metabolism of chondrocytes of these layers are different than each other. Each group of chondrocytes of a specific layer synthesizes different molecules. The thin fibril containing surface layer named as *lamina splendens* is constructed of tiny polysaccharides and contains almost no chondrocytes. Fibrocyte-like chondrocytes are aligned parallel to the joint surface just below the lamina splendens. The collagen content is high and the proteoglycan content is low of this layer. Lamina splendens controls synovial fluid in- and outflow. Penetration of toxic molecules and immune reactive cells of the synovium to the deeper cartilage layers is prevented by this lamina. Fibronectin and synovial fluid content of this layer is higher than the other layers. This layer is durable in shear force. Injury at the surface layer triggers inflammation and initiates immune response. Mechanical durability changes and deterioration or degeneration occurs after injury.

Endoplasmic reticulum and Golgi organ complex of the intermediate layer chondrocytes are better developed than the surface layer chondrocytes. Chondrocytes of the intermediate layer are spherical, and the collagen fibers are

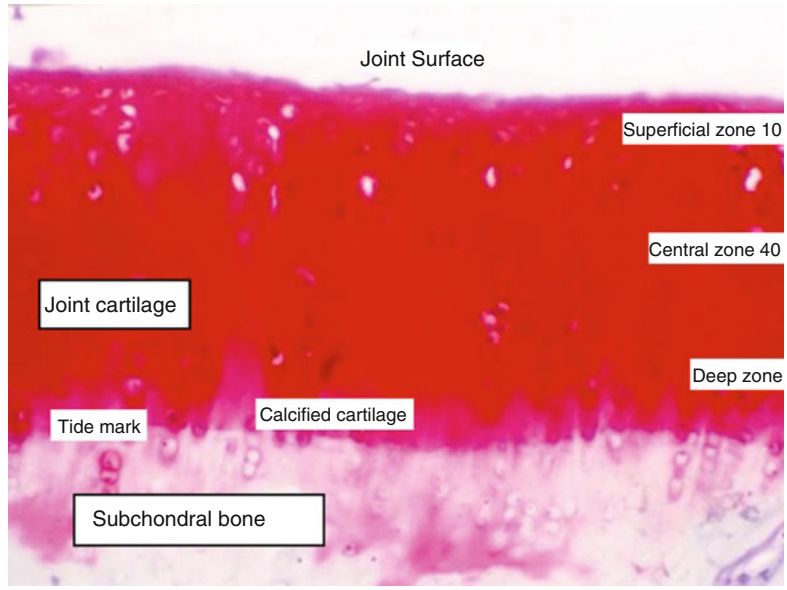

Fig. 22.5 Layers of joint cartilage

thicker than the surface layer. Some of these thick collagen fibers may reach the tidemark that separates subchondral bone and joint cartilage. Synovial fluid and collagen content of this layer is lower and the proteoglycan ratio is higher. Orientation of chondrocytes is perpendicular to the surface and their phenotype converts into oval. The intermediate layer due to the orientation of its fibers absorbs shear stress generated at joint movement.

The lower calcified cartilage layer is thin and separates joint cartilage from the subchondral bone. Chondrocyte content of this layer is lower compared to other layers. Active molecule synthesizing organelles of chondrocytes of this layer is less developed indicating lower molecular activity. Some chondrocytes of this layer are isolated in calcified lacunae. This layer regulates blood and other molecule penetration into the cartilage.

Extracellular Matrix and Chondrocyte Interaction

Homeostasis of the extracellular matrix structure and function is regulated and maintained by chondrocytes. Nutrients brought to the chondrocytes by the synovial fluid trespass the extracellular matrix. Some regulatory molecules, cytokines, and growth factors are stored in the extracellular matrix. Chondrocytes on the other hand synthesize the macromolecules of the extracellular matrix lifelong. Chondrocytes maintain the integrity of the extracellular matrix although less is known on the anabolic and catabolic metabolic pathways of maintenance. Inflammatory regulator interleukin-1 (Il-1) triggers extracellular matrix metaloproteases and increases catabolic macromolecules. Il-1 also affects transcription of extracellular matrix macromolecules. Insulin-like growth factor (IGF) and transforming growth factor beta (TGF-β) cytokines reduce catabolic activity by stimulating chondrocyte growth and extracellular matrix synthesis. Autocrine and paracrine cytokines act by binding chondrocyte membrane receptors. Catabolic cascade of the extracellular matrix is complex. Various cytokines including Il-1, stromelysin, aggrecanase, plasmin, and collagenase are involved in this cascade. Prostaglandin, TGF-β, tumor necrosis factor (TNF), metalloproteinase inhibitors, and tissue plasminogen stimulator and inhibitor turn the cascade on and off. Inhibition of Il-1 and TNF is investigated for treatment. Research on Il-6, Il-15, Il-17, Il-18, Il-21, leukemia inhibitory factor, and Il-8 chemokine is still ongoing [27].

Autocrine Regulation of Joint Cartilage

Chondrocytes are mainly isolated in their lacunae and autocrine molecules act less on these cells. Mechanical loads on the extracellular matrix improve autocrine stimulation. Effects of bone morphogenic protein (BMP), epidermal growth factor (EGF), platelet-derived growth factor (PDGF), parathyroid hormone-related protein (PTHrP), fibroblast growth factor (FGF), TGF-β, and IGF on chondrocytes are evaluated under mechanical loading. These hematopoietic cytokines are regenerative in most tissues; however, their molecular action mechanism in avascular joint cartilage is a research area. TNF-α, interleukins, and colony-stimulating factor (CSF) like cytokine levels increase after cartilage trauma and degenerative joint diseases.

IGF-1, TGF-β family, BMPs, and FGS family are most important regulatory autocrine growth factors.

(a) IGF: IGF-1 is released from the cartilage with systematic growth factor secretion. This is an anabolizing factor. IGF-2 is also isolated from joint cartilage and has similar anabolic effects. IFG-1 stimulates proteoglycan synthesis and chondrocyte proliferation. Metalloproteinase production is triggered by IGF-1. Metalloproteinases catabolize proteoglycans. Type II collagen synthesis is also stimulated by this mediator. Endochondral ossification of the physis is regulated by IGF-1. Growth hormone in acromegalia acts through this factor. Mitogenic activity of EGF and PDGF on joint cartilage is secondary to IGF-1.

(b) TGF-β: The TGF family has five isoforms. These polypeptides convert into their active form when they are released into the extracellular matrix. Temperature and pH of the environment determine TGF activity. TGF-β stimulates the DNA of chondrocytes and proteoglycan synthesis. TGF-β prevents extracellular matrix degeneration through its anti-catabolic activity. Proteoglycan synthesis increased, and inflammatory synovitis developed after intra-articular injection of TGF-β. TGF-β is accepted as a joint cartilage stimulant; however, it has adverse effects on synovial tissue. Effects of intra-articular PDGF injection have little effects on joint cartilage and synovium.

(c) FGF: Fibroblast growth factor (FGF) is another important signaling molecule of the joint cartilage. FGF-2 connects to heparin-like molecules frequently. FGF-2 is mitogenic to chondrocytes and synergistic with IGF-1. Opposite to IGF-1 and TGF-β, proteoglycan synthesis is suppressed with this molecule. It stimulates chondral growth when injected into the joint space of young rats. TGF-β secretion is stimulated by FGF. This molecule has a homing effect on mesenchymal stem cells at defect sites and stimulates cartilage restoration.

(d) BMP: Bone morphogenic proteins are a subgroup of the TGF-β family. They stimulate chondrogenesis of mesenchymal stem cells. All stages of endochondral ossification are observed when BMP is injected ectopically. BMP-1 is proteolytic on the extracellular matrix of joint cartilage. BMPs 2, 3, and 4 stimulate proteoglycan synthesis of joint cartilage. BMP-6 is secreted from hypertrophic chondrocytes [28].

Biomechanics of Joint Cartilage

Joint cartilage is almost always under static and dynamic loads. Physiologic loads on joint cartilage can rise up to 15–20 MPa while climbing stairs. Such load on a very short duration applies 1–3 % compression to the joint cartilage. Static loads up to 5–30 min affect 35–45 % of joint cartilage. Structural integrity of the extracellular matrix defines resistance to compression, tension, and sheer forces. Chondrocytes regulate integrity of synthesis and organization of proteoglycans, collagen, glycoproteins, and other molecules precisely to protect extracellular matrix durability. Up to 0.5 and 1 MPa compression, 0.25 MPa sheer and 10–50 MPa tension forces maintain joint cartilage homeostasis. Collagen fibers resist sheer and tension forces,

while aggrecan constituted of glycosaminoglycan molecules resists to compression and synovial fluid flow into the tissue. Electrostatic and osmotic swelling is aggrecan related and determines 50 % of compressive load balance.

Mechanical loads on joint cartilage are important for the metabolic activity, cellular integrity, and synthesis of prostaglandin and nitric oxide like inflammatory mediator turnover in joint cartilage [29]. Immobilization on the other hand decreases extracellular matrix production and causes softening of the tissue [30]. Aggrecan content increases at the site where load increases. Excessive exercise causes cartilage destruction. Acute and/or chronic injury or excessive compression destructs joint cartilage. In vitro experiments revealed that static compression decreased extracellular matrix production reversibly. Intermittent compression and/or hydrostatic pressure on the other hand increase core protein synthesis of aggrecan and all other joint cartilage related proteins. Mechanical forces at around the microenvironment of chondrocyte stimulate production and/or destruction of the nearby extracellular matrix macromolecules. Chondrocytes react to mechanical stimulation. Newly synthesized proteoglycan, collagen, and other molecules' quality and functionality are affected by mechanical stimulation in line with the extracellular matrix. Extracellular matrix that cannot resist to mechanical loads will be injured.

Resistance to synovial fluid flow determines resistance to pressure under loads. Behavior of chondrocytes under physiologic loads and how they are stimulated to maintain tissue integrity is a field of research. Chondrocytes function in an osmotic and mechanically active microenvironment. Chondrocyte metabolism is exerted by diffusion, and physiologic mechanical stimulation assists anabolism and catabolism. Chondrocytes respond directly to environmental changes. Physiologic loads differentiate cell into chondrocytes from embryogenesis to adulthood. Immobilization on the other hand causes severe proteoglycan lose and ends up with structural deformity [30].

Mechanical loads that affect joint cartilage are quite complex. Compressive loads on one site generate tension and sheer stresses at another site of joint cartilage. Hydrostatic pressure alterations also change chondrocyte behavior. Research on chondrocyte signaling molecules at combined mechanic and hydrostatic loading may elaborate new information. Physiologic increase in hydrostatic pressure leads to the increase of anabolism of chondrocytes in a few seconds. Static or dynamic loading of joint cartilage increases complexity. Transport of nutrients and cytokines is limited under static loads. Intercellular ionic state also changes with static loads. Sodium concentration increases and pH decreases outside the chondrocyte under static axial load. This change adversely affects extracellular matrix production. Combined increase of extracellular potassium and pH on the other hand increases extracellular matrix synthesis. Dynamic loading generates action potential at tissues. Flow in ions under dynamic loads leads to electric charges. Such charges influence chondrocyte metabolism. Chondrocytes are sensitive to shape and function optimal as long as they can preserve their oval phenotypes. This finding is an indirect proof of the presence of mechanoreceptors in these cells. Mechanoreceptors, which may be of protein, can be located on the membrane or cytoplasm of chondrocytes. The function of these mechanoreceptors should be the conversion of mechanical information into biomechanical function.

The upper most layer of joint cartilage decreases friction and allows lubrication. The friction coefficient of this layer of joint cartilage is between 0.02 and 0.04 [31]. Lubrication is attained by four main mechanisms. These are (a) boundary, (b) hydrostatic, (c) hydrodynamic, and (d) elastohydrodynamic mechanisms. All mechanisms are active at the same time during joint cartilage lubrication. Atomic force microscopic assessment [32] revealed sensitivity of 800 nm to 2 mm thick lamina splendens toward protease-containing enzymes.

Role of Synovial Fluid, Proteoglycans, and Collagen at Solution Exchange

Fluid flow along the extracellular matrix is essential for joint cartilage function. Regulatory factors, cytokines, and nutrients reach cells by this

flow. Regulatory factors function in a dose and time-dependent manner. They are synthesized in micro- or even nano-quantities, act in less than minutes, and disappear after conducting their function. Concentration of the fluid directly defines extracellular molecule transfer. Ions of the cartilage matrix are primary determinants of osmotic pressure. This pressure preserves fluid of joint cartilage under mechanical loads.

From the mechanical point of view, it is assumed that the intra- and extra-fibrillar areas form two different compartments [33]. Intrafibrillar fluid flow is slower than extra-fibrillar fluid flow. Smaller molecules are transferred in the intrafibrillar area. The extra-fibrillar area holds more fluid due to its proteoglycan content. Loss of proteoglycans in pathologic conditions decreases fluid preservation, and adaptation to loads is adversely affected. Collagen is highly selective to the calcium ion. In an experimental study [33], the calcium content of intrafibrillar calcium concentration increased up to 7.1 in proteoglycan depleted bovine cartilage. Concentrations of sodium, chloride, and bicarbonate change with pressure. For example, extra-fibrillar fluid content increases from 0.2 to 0.6 mEq/g with the increase in pressure. Likewise, sodium and calcium percentage increases from 1.7 to 3.2 and 6.4 to 23.9, respectively, whereas chloride and bicarbonate percentage and pH decrease from 0.7 to 0.5, 0.5 to 0.4, and 7.2 to 6.8, respectively. The fibers of the interfibrillar area cover or leave spaces in between each other (Fig. 22.6). The gap between fibers is less than 0.6 nm. The gap area is about 20 % of all the surface area of joint cartilage. Serum albumin and polyethylene glycol of 6.000–20.00 Da molecular weight contain the intrafibrillar space. Fluid content of joint cartilage decreases when pressure is applied. It is assumed that large channels open under long-lasting static loads in order to retake the lost fluid. The diffusion constant between joint cartilage and synovial fluid is 0.45 that changes due to anionic, cationic, and neutral conditions. Dissolution of ions compared to free fluid is slower. Diffusion space in the cartilage is narrow. Molecules of the synovial fluid are almost the same size as of the gaps of joint cartilage. Interaction between these

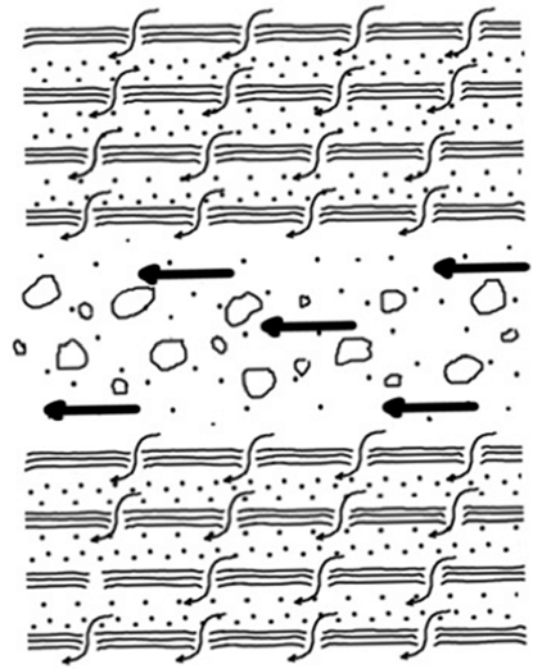

Fig. 22.6 Interfibrillar synovial fluid flow

groups is constant. All these factors are causes of slow synovial fluid and ionic exchange in joint cartilage. Smaller molecule decrease of diffusion constant is geometrically presented [33]. Cyclic loading slows down transportation of small molecules but improves speed of flow of larger molecules such as growth factors, hormones, and enzymes. Synovial fluid flow is important for joint cartilage nutrition. Decrease of motion leads to accumulation of molecules such as lactate and carbon dioxide and may increase tissue degradation.

Geometry of the glycosaminoglycan matrix affects anisotropic hydrolytic permeability of joint cartilage [34]. Intense fibrillar glycosaminoglycan structure is a resistance barrier toward fluid flow. If the glycosaminoglycan matrix had been irregular, then hydrolytic permeability would have been isotropic. Under mechanical loads however, hydrolytic permeability is anisotropic, and geometry is assumed to play an important role in synovial fluid flow [34]. Glycosaminoglycan fiber geometry and direction determine synovial fluid flow and tissue deformation. Important mechanical properties of joint

cartilage such as hardness and lubrication capacity are determined by this geometry [35].

Proteoglycan and glycosaminoglycan structures of joint cartilage present biphasic indentation [36]. The Poisson ratio of joint cartilage is between 0.13 and 0.45. Previously, this ratio was measured in laboratory studies as 0.40 and 0.49. This ratio defines how joint cartilage can function under frictional forces throughout decades. Patellar notch joint cartilage thickness permeability is several times higher than that of other locations [36].

Effects of Static and Dynamic Loading on Matrix Metabolism

Collagen fibers resist against tensional forces, whereas the tough and intense structure of proteoglycans allows them to electrostatically bind to glycosaminoglycans and increase strength toward compression [37]. Continuous production and degradation of proteoglycans, collagen, and other matrix molecules preserves mechanical properties of joint cartilage. Density and structure are controlled by molecular biological and cellular harmony under physical conditions.

Loads on the joint and motion may exacerbate complex metabolic activity. Proteoglycan synthesis increases to some extend with increased dynamic load. Static or impact loads however injure joint cartilage. Rupture of the anterior cruciate ligament deteriorates matrix metabolism and may cause osteoarthritis [38]. Physiological loads may lead to structural adaptation when skeletal muscles of the knee joint are trained. Structural adaptation due to mechanical stimulation is difficult to monitor in vivo. Indirect methods include measuring joint cartilage metabolites and growth factors of the serum or synovial joint.

Cartilage compression causes matrix and cellular deformation. Synovial fluid flow, ion concentration, and osmotic pressure change with compression. All mechanical, chemical, and electrical changes affect matrix metabolism alone or together. These stimulations naturally combine during joint loading, and it is difficult to isolate the one that is dominating changes. Pro-viscoelastic and electromechanical theoretical models are used to define cartilage response under static and dynamic loading. Patellar and hip joint nodular pressure is between 3 and 18 MPa. External forces and their directions and intensities change continuously. Thickness difference of joint cartilage at different sites makes load distribution calculations more complex. Synovial fluid flow in the cartilage is different under static and dynamic loads. Synovial fluid is released from joint cartilage under static loads, whereas under dynamic loads, it moves in- and outward. Less synovial fluid is released from the tissue as the frequency of cyclic loads increases. Synovial fluid outflow from joint cartilage decreases as faster as the loading occurs. This is defined as a tissue preventive homeostatic mechanism. Proteoglycan synthesis ceases under static loads. Proteoglycan synthesis increased when 0.2 Hz tension is applied to chondrocytes in culture [39]. Hydrostatic pressure inside the tissue increases with the frequency of dynamic loading. Mechanical loading plays a role not only in the anabolism but also catabolism of joint cartilage. It is assumed that proteoglycan synthesis decreases at the area where static load peaks but increases at the adjacent area where loads are slightly lower. Production and degradation are hand in hand in such sites. Acute and extreme intensive load will rupture the collagen matrix that will terminate with injury.

Decrease of stiffness under pressure is the first sign of joint cartilage degeneration. The relation of stiffness to degeneration is investigated by histology and biochemical measures in 24 cadaver knees using a handheld indentation probe [40]. Correlation between Mankin scores and cartilage stiffness was presented in the femoral condyles and lateral patellar cartilage but not in the medial patellar cartilage in this study. Instant pressure and extracellular matrix integrity was correlated; however, a strong relation between stiffness and total proteoglycan and collagen could not be established [40].

Mechanical stimulation as in bone tissue is assumed to aid regeneration of joint cartilage tissue [41]. Chondrocytes that sense mechanical stimulus play important roles in regeneration. They stimulate intrinsic and extrinsic cellular

mechanisms for production and degradation of the extracellular matrix. Several regulators are involved in these critical mechanotransductional pathways [41]. Joint cartilage deforms with time. Mechanical stimulation whether static or low volume intermittent dynamic is distributed in synovial fluid that flows between the matrixes. Potential side effects of loads over the threshold are prevented by their distribution in synovial fluid. The porous hyperelastic matter physical model described this condition [42].

Physical Entities That Shape Cartilage Metabolism

The matrix itself is the primary regulator of joint cartilage synthesis. Stimulants that appear during the exchange of matrix take part in the regeneration phase [43]. The exchange of the matrix may however affect chondrocytes adversely. For example, decrease of proteoglycan density may change extracellular osmolarity and disturb the ionic content of the matrix. This may end in tissue deformation by the decrease of joint cartilage stiffness and synovial fluid loss under pressure.

Chondrocytes, different than other cells, are located in a denser proteoglycan matrix. The constant negative ionic structure of proteoglycans increases free cations and lowers anions next to chondrocytes. This dense inorganic ionic milieu is the reason of the higher osmotic pressure of joint cartilage tissue plasma compared to synovial fluid. Osmotic pressure is the determinant of hydrostatic pressure. Unloaded joint cartilage tissue hydrostatic pressure is therefore about 1–2 atm. The negative charge of the matrix determines the hydrogen ion and pH tissue distribution. Tissue hydrogen ion concentration is always higher than that of the intercellular fluid. Joint cartilage pH is therefore comparatively lower than other tissues. Lactate is another determinant of pH of live cartilage tissue. pH decreases in some locations of joint cartilage due to lactate.

Chondrocytes of the joint cartilage absorb high and different quantity of loads. The load, in a general sense, causes matrix deformation and increases hydrostatic pressure in tissue and its cells. For example, loads in the knee joint of a standing person increases up to 100–200 atm in milliseconds and decreases to 40–50 atm while resting. Proteoglycan density increases, and ionic structure around chondrocytes converts to negative due to synovial fluid outflow from the tissue under long-lasting loads.

Chondrocytes respond directly to loads. Cellular response to mechanical loads generates in hours regarding the load type. Mechanical loads that increase the hydrostatic pressure and do not cause excessive fluid outflow stimulate matrix production. Loads that cause excessive fluid outflow, on the other hand, cease matrix production. Hydrostatic pressure of joint cartilage increases with external loads. This hydrostatic pressure prevents fluid outflow by distributing external loads evenly but also causes macroscopic deformation of the tissue. Sulfates and amino acids enter the tissue at 5 to 15 MPa (50–150 atm) [44]. Twenty second pressure is sufficient to allow ion inflow. It is assumed that increase of hydrostatic pressure will decrease this inflow. It is also assumed that hydrostatic pressure stimulates cAMP secondarily. Apart from hydrostatic pressure, higher potassium concentration also stimulates extracellular matrix production [45]. The calcium content of the intercellular fluid has no effect on matrix production.

Dynamic loads cause fluid flow in cartilage tissue [46]. This fluid flow mechanically and physicochemically stimulates chondrocytes. Matrix production or degradation is managed by chondrocytes with this stimulation. Proteoglycan and protein synthesis increases with dynamic loading [46]. Fluid flow at microscopical levels is sufficient to initiate this stimulation. Unloading [30] or excessive loading [47] of joint cartilage will initiate degeneration. Synovial fluid content decreased, and proteoglycan production decreased significantly in excessive load-bearing knee cartilage after femoral valgus osteotomy in an experimental study [47]. Proteoglycan synthesis was high in less-load-bearing areas. Collagen density changes with proteoglycan production and degradation. Load changes therefore are important in biochemical and morphological changes in joint cartilage.

Intensity and type of physiologic load at joint cartilage mechanics needs to be determined. This may change between individuals and at different ages of the same individual. Another important concept may be the different sensing of loads at different layers of joint cartilage. Physiologic tension loads increase biosynthesis and exacerbate catabolic response at the deeper cartilage layers, whereas longer durations and intensive pressure cause tissue and cell damage [48]. Loads in the direction from subchondral bone to joint cartilage are determinants of degeneration at trauma-related arthritis [49]. Subchondral tensional forces may not be that important in the tibial plateau; however, in the ankle joint, even small amounts of such forces are determinants of joint destruction [49].

Mechanical Determinants and Joint Cartilage

Joint cartilage is almost always under physiological loads. The type, direction, and magnitude of forces on joint cartilage may vary. Tensional forces on semielastic joint cartilage at an individual are different while standing for long durations or jogging. High-magnitude forces unevenly deform joint cartilage [50]. Joint cartilage, after a while, presents biphasic material properties, and elasticity is replaced with stiffness. A balance between elasticity and stiffness is established with time that determines the Young modulus and Poisson ratio [51]. Optical methods can be used to measure Young modulus and Poisson ratio of joint cartilage. The Poisson ratio of joint cartilage was found to be 0.185 ± 0.065 that was confirmed as 0.176 ± 0.106 by mechanical methods. Different parts of joint cartilage may present different Poisson ratios. The lowest Poisson ratio that was 0.070 ± 0.016 was at the femoral patellar grove across the patellar surface. Medial tibial plateau Poisson ratio was 0.236 ± 0.026, which was the highest [52]. Correlation of optical and mechanical measurements reveals that joint cartilage is isotropic. In homogeneous, lateral expansion of joint cartilage is observed at early periods of load release. Homogeneity is along the layers of joint cartilage. The surface layer expands less than that of the radial layer indicating matrix differences between these layers [51]. The linear transverse isotropic model therefore lacks to define joint cartilage balance under loadings [53]. The balance is almost always disturbed at the recovery phase of unloading, and injury is recorded during the stiff phase [54]. Injury of cartilage due to mechanical loading in osteoarthritic joints is more common compared to that of normal joints [55]. Skeletal muscle contraction on the other hand is important in maintaining joint cartilage homeostasis. Knee joint cartilage is preserved under extensive loads in athletes due to their strong skeletal muscles [56]. Biomechanical studies should take skeletal muscle strength into consideration of the knee joint.

Mechanical loads that injure the joint cartilage cause chondrocyte death [57]. High compressive loads create risers on the cartilage and chondrocyte death is next to these risers. Chondrocyte death is observed in far away locations than risers under low compressive loads [57]. Nitric oxide and leukotriene like biochemical triggering molecules are initiated with mechanical loads. Inflammation increases by leukotriene B4 secretion under dynamic loading [58]. Dynamic loading alters Il-1 beta synthesis and decreases nitric oxide and prostaglandin E2 synthesis of chondrocytes in culture [59].

The anisotropic structure of the extracellular matrix of joint cartilage will transfer loads in different forms to the microscopic level. Shear forces may harm joint cartilage severely depending on the age of the individual. Shear forces may cause severe disruption at the subchondral area in skeletally immature children, whereas similar forces may cause focal fissures in skeletally mature individuals [60]. Depending on the findings of that study, we can assume that the bone and joint cartilage junction is sensitive and determinant in acute load-related injuries. Another study [61] on joint cartilage and subchondral bone biomechanics revealed that tension forces at this location initiate micro fractures.

Joint cartilage absorbs and transfers loads while gliding. Load transfer occurs in 10–150 ms. The elastic modulus of joint cartilage determines this load transfer. Human joint cartilage elastic modulus is between 4.4 and 27.0 MPa when

loaded at every 20 ms [62]. This value increases at 32–75 % when the duration of load application increases to 2 s. When cyclic loads are continued for an hour, the elastic modulus will be between 0.18 and 0.36 MPa and 0.05 and 0.13 MPa in stiffer than 4 MPa and lower than 4 MPa joint cartilage samples, respectively. Surface tension of joint cartilage is also determined by tissue stiffness. Surface tension is usually as low as 0.02 MPa at low elastic modulus but increases up to 0.22 MPa when elastic modulus increases up to 18 MN/mm^2. Stiffer joint cartilage will allow higher synovial fluid adsorption [63]. Axial loads are mostly resorbed by meniscus in the knee joint. Medial and lateral collateral ligaments stabilize the joint at varus and valgus loads [64]. The anterior and posterior cruciate ligaments stabilize loads in the anterior–posterior directions. Isolated forces in one plane are rare in real life. Loads on the knee joint are complex and usually complex in various directions. The medial meniscus has to absorb large amount of loads in patients where the anterior cruciate ligament is missing. Meniscus repair or transplantations should therefore be undertaken after anterior cruciate ligament augmentation [64]. Mechanical basis of osteoarthritis is still an important area of research [65].

Joint biomechanical studies are undertaken at the microscopic levels recently. Computer simulations allow such evaluations. New technology to measure biomechanical outcomes of cartilage engineering is however still essential.

Degeneration and Osteoarthritis

Osteoarthritis is determined by the loss of structure and function of joint cartilage (Fig. 22.7) [66]. In osteoarthritis, thinning of joint cartilage is combined with molecular alterations. Degradation continues although joint cartilage tries to restore itself. Sclerosis of the subchondral bone, osteophyte, and cyst formation are observed along with remodeling. Pain, deformity, and loss of function are major symptoms. Swelling and crepitation can accompany. Osteoarthritis is most common in the ankle, knee, hip, spine, and hand joints. All other structures of the joint are involved in the disease. Fibrillation at the surface of the joint cartilage is the first finding. Proteoglycan content of the intermediate layers decreases afterward. Vascularization of the calcified cartilage and remodeling of the subchondral bone adjoin the scenario. Surface fibrillations convert to deeper risers with time. Irregular risers reach deeper

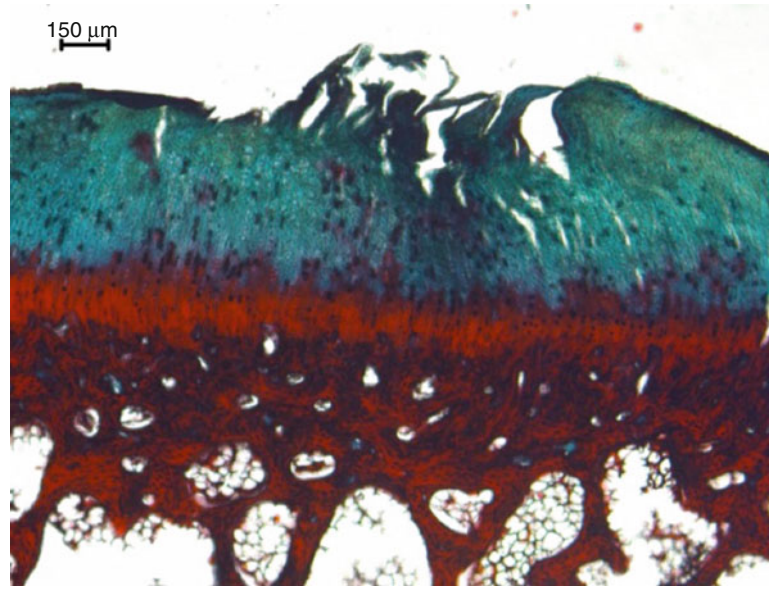

Fig. 22.7 Fibrillation at the joint surface of cartilage. Masson's trichrome 40×

layers of joint cartilage. Thinning and decrease of volume of the tissue is an obvious finding. Free cartilage particles may fall into the joint space. Necrotic and dense osteoid tissues appear at the last stage of the disease.

Macromolecular content of the extracellular matrix deteriorates at the initial stages. Synovial fluid content of the tissue decreases. Arachidonic acid stimulates prostaglandins and initiates inflammation at chondrocyte membranes (Fig. 22.8). Proteoglycan breakdown and synovitis are observed at the end-stage of the cascade. Established synovitis furthermore increases proteoglycan breakdown. Proteoglycan and aggrecan decrease is accompanied to loss of synovial fluid. The collagen content is stable at this stage. The glycosaminoglycan chain shortens. Aggrecan keeps more fluid with this change. More fluid in tissue decreases its mechanical durability. A high impact trauma or a rapid torsional stress may trigger these changes. Inflammation will fasten degradation of matrix macromolecules. Chondrocytes malfunction in such environment. Tension, osmolarity changes, current volume, and mediator secretions will be recognized by chondrocytes. Chondrocytes will proliferate and increase their metabolic activity. This proliferation is mitogenic, and growth factors will further stimulate cell and extracellular matrix production. Abnormal colonization of chondrocytes and increase of abundant extracellular matrix production will cause nitric oxide synthesis. Increase of nitric oxide will stimulate IL-1 and metalloproteinase synthesis that will trigger degradation of macromolecules. Fibronectin particles will furthermore increase IL-1 synthesis. Degraded type IX and XI collagens and other molecules will interrupt type II collagen integrity. Fluid of the aggrecan and tissue will keep increasing. Such surface changes will continue at the deeper layers of joint cartilage. Chondrocytes will decrease in number, while extracellular matrix production will keep increasing. Production and deprivation share the same time interval. Joint cartilage when treated appropriately has the chance to recover and regenerate at this stage. Changing the mechanical axis by osteotomy is proved to be effective in hip and knee joints. Chondrocyte proliferation and anabolic activity will halt in case of no intervention. Decrease of cytokine content

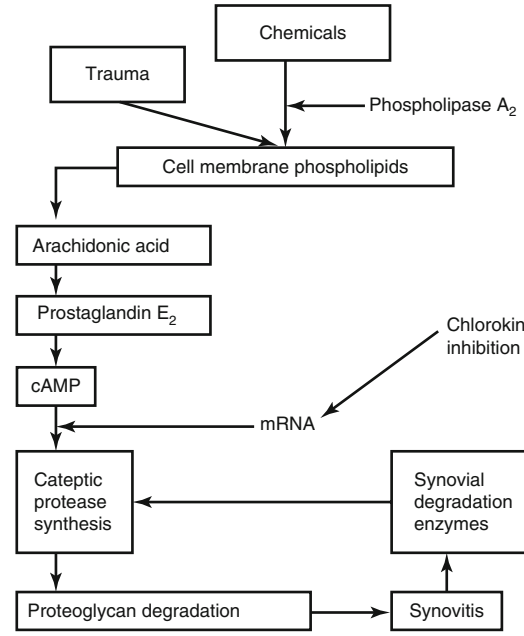

Fig. 22.8 Degenerative cascade of joint cartilage

and number of chondrocytes will deepen degeneration. Degrading molecules will inhibit anabolic decorin and insulin-like growth factor activity. Osteoarthritis of aging is established by molecular means at the end of this cascade.

Sclerosis and cysts appear in the subchondral area. Such changes are prone near the joint cartilage. The volume of subchondral tissue increases. Osteophytes are observed by radiology. New trabecular bone formation is the first sign of osteoarthritis. Rarely cysts appear first. The cartilage is totally destroyed at the final stage. Subchondral bone will touch the other joint surfaces. Shortening, deformity, and instability will establish when joint cartilage is eroded. Osteophytes usually accompany subchondral and metaphyseal bone changes. These intense chondrocyte containing bony projections is usually located at joint capsule attachments. Osteophytes that occur inside the joint are named as central osteophytes. The cartilage of capsular osteophytes is histologically alike joint cartilage. Some osteophytes are painful during physical examination. These may limit motion or may cause pain during motion. Osteophytes are located at the edges of the acetabulum or the femoral neck of the hip joint. In the shoulder joint, they are located below the

Table 22.1 Secondary arthritis initiators

1.	Joint injury (i.e., osteochondritis dissecans)
2.	Septic arthritis
3.	Aseptic necrosis
4.	Hemophilia
5.	Paget disease
6.	Gout arthritis
7.	Acromegalia
8.	Hemochromatosis–ochronosis
9.	Ehlers–Danlos syndrome
10.	Charcot disease

humeral head. One reason of osteophytes is joint cartilage degeneration and reorganization of the subchondral bone. Skeletal muscles, ligaments, synovium, and the joint capsule adjust to joint cartilage loss. Mild to moderate inflammation occurs in the synovial membrane. Interleukin produced by the synovial membrane increases joint cartilage degeneration. Cartilage islands begin to appear in the membrane. Capsule, ligaments, and tendons shorten with time and initiate contracture. This enhances range of movement loss that ends with skeletal muscle atrophy.

The cause of idiopathic or primary osteoarthritis is unknown. Osteoarthritis after trauma is named as posttraumatic. Secondary osteoarthritis may also develop after septic arthritis. Secondary osteoarthritis may accompany some developmental and hereditary diseases and/or disorders (Table 22.1). A study [67] defined genetic, estrogen-dependent, and age-dependent osteoarthritis.

Primary osteoarthritis develops in elderly. Accelerated shortening of telomeres was detected in osteoarthritis and other age-related diseases recently [68]. The prevalence increases over the age of 40. The pace of chondrocyte repair decreases in the elderly. Degeneration and degradation therefore increase with age. Family history of osteoarthritis, genetic background, and hormonal and metabolic status dominate the osteoarthritis process. Female sex and genetic background are defined for wrist and ankle osteoarthritis; however, the molecular pathways of such osteoarthritis are not yet defined. Inflammatory and immunogenic backgrounds are other ethiopathogenetic factors that may lead to primary osteoarthritis. Secondary osteoarthritis is defined in acromegalia; however, the hormonal relation is not determined. Etiopathology of alcaptonuric ochronosis and Paget disease is also unknown. Interleukins play important roles in such conditions. They initiate the osteoarthritic cascade.

A hypothesis is that inflammatory mediators are transmitted from the bone marrow to the joint cartilage. Immune response of the tissue is however not well known, as it has no vascular, nerve, and lymphatic endings. Pain is exacerbated by triggering local mediators that are received by pain processing centers of the brain [69].

Joint Injury and Posttraumatic Osteoarthritis

Injury at the meniscus, capsule, and ligaments may trigger joint cartilage degeneration. Degeneration cascade continues even if the primary injury site is repaired. Osteoarthritis generated after injury is named as posttraumatic arthritis and can be irreversible.

IL-1 [70], TNF, VEGF, and matrix metalloproteinase [71] produced at initial trauma may be responsible of degeneration [72]. Chondrocyte apoptosis and extracellular matrix destruction are observed. Caspase and aspartate-specific proteases are responsible of chondrocyte apoptosis. Inhibition of caspase can be reversed. N-acetylcysteine may prevent 70–80 % chondrocyte apoptosis. Collagen and extracellular matrix synthesis decreases, and type II collagen is replaced by collagen type I in some locations. Bone mineral density decreases and subchondral bone space increases with degeneration [73].

Acknowledgment Petek Korkusuz MD, PhD, provided histological pictures.

References

1. Yates AJ Jr, McGrory BJ, Starz TW et al (2014) AAOS appropriate use criteria: optimizing the nonarthroplasty management of osteoarthritis of the knee. J Am Acad Orthop Surg 22:261–267
2. Rovetta G, Monteforte P, Molfetta G, Balestra V (2004) A two-year study of chondroitin sulfate in erosive osteoarthritis of the hands: behavior of erosions,

osteophytes, pain and hand dysfunction. Drugs Exp Clin Res 30:11–16
3. Muniyappa R, Karne RJ, Hall G et al (2006) Oral glucosamine for 6 weeks at standard doses does not cause or worsen insulin resistance or endothelial dysfunction in lean or obese subjects. Diabetes 55:3142–3150
4. Towheed T, Maxwell L, Anastassiades TP et al (2005) Glucosamine therapy for treating osteoarthritis. Cochrane Database Syst Rev (2):1–84. Published by Wiley
5. Cameron M, Chrubasik S (2014) Oral herbal therapies for treating osteoarthritis. Cochrane Database Syst Rev (5):1–207. Published by Wiley
6. Bruyère O, Cooper C, Pelletier JP et al (2014) An algorithm recommendation for the management of knee osteoarthritis in Europe and internationally: a report from a task force of the European Society for Clinical and Economic Aspects of Osteoporosis and Osteoarthritis (ESCEO). Semin Arthritis Rheum 44:253–263
7. McAlindon TE, Bannuru RR, Sullivan MC et al (2014) OARSI guidelines for the non-surgical management of knee osteoarthritis. Osteoarthritis Cartilage 22:363–388
8. AAOS (2013) Treatment of osteoarthritis of the knee. Evidence-based guideline, 2nd edn. http://www.aaos.org/research/guidelines/treatmentofOsteoarthritisoftheKneeGuideline.pdf
9. Bellamy N, Campbell J, Welch V et al (2006) Viscosupplementation for the treatment of osteoarthritis of the knee. Cochrane Database Syst Rev (2):1–656. Published by Wiley
10. Hudelmaier M, Glaser C, Hohe J, Englmeier KH, Reiser M, Putz R, Eckstein F (2001) Age related changes in the morphology and deformational behavior of knee joint cartilage. Arthritis Rheum 44:2556–2561
11. Buckwalter JA, Mankin HJ (1997) Articular cartilage. Part I: tissue design and chondrocyte matrix interactions. J Bone Joint Surg 79-A:600–611
12. Pereira D, Peleteiro B, Araujo J, Branco J, Santos RA, Ramos E (2011) The effect of osteoarthritis definition on prevalence and incidence estimates: a systematic review. Osteoarthritis Cartilage 19:1270–1285
13. Hunziker EB, Quinn TM, Hauselmann HJ (2002) Quantitative structural organization of normal adult human articular cartilage. Osteoarthritis Cartilage 10:564–572
14. Li P, Raitcheva D, Hawes M, Moran N, Yu X, Wang F, Matthews GL (2012) Hylan G-F 20 maintains cartilage integrity and decreases osteophyte formation in osteoarthritis through both anabolic and anti-catabolic mechanisms. Osteoarthritis Cartilage 20:1336–1346
15. Schroeppel JP, Crist JD, Anderson HC, Wang J (2011) Molecular regulation of articular chondrocyte function and its significance in osteoarthritis. Histol Histopathol 26:377–394
16. Muddasani P, Norman JC, Ellman M, van Wijnen AJ, Im HJ (2007) Basic fibroblast growth factor activates the MAPK and NFkappaB pathways that converge on Elk-1 to control production of matrix metalloproteinase-13 by human adult articular chondrocytes. J Biol Chem 282:31409–31421
17. Lotz M, Loeser RF (2012) Effects of aging on articular cartilage homeostasis. Bone 51:241–248
18. Inerot S, Heinegård D, Audell L, Olsson SE (1978) Articular- cartilage proteoglycans in aging and osteoarthritis. Biochem J 169:143–156
19. Kiani C, Chen L, Wu YJ, Yee AJ, Yang BB (2002) Structure and function of aggrecan. Cell Res 12:19–32
20. Aruffo A, Stamenkovic I, Melnick M, Underhill CB, Seed B (1990) CD44 is the principle cell surface receptor for hyaluronate. Cell 61:1303–1313
21. Kohda D, Morton CJ, Parkar AA, Hatanaka H, Inagaki FM, Campbell ID, Day AJ (1996) Solution structure of the link module: a hyaluronan-binding domain involved in extracellular matrix stability and cell migration. Cell 86:767–775
22. Fosang AJ, Little CB (2008) Drug Insight: aggrecanases as therapeutic targets for osteoarthritis. Nat Clin Pract Rheumatol 4:420–427
23. Stanton H, Golub SB, Rogerson FM, Last K, Little CB, Fosang AJ (2011) Investigating ADAMTS-mediated aggrecanolysis in mouse cartilage. Nat Protoc 6:388–404
24. Pap T, Bertrand J (2013) Syndecans in cartilage breakdown and synovial inflammation. Nat Rev Rheumatol 9:43–55
25. Verma P, Dalal K (2013) Serum cartilage oligomeric matrix protein (COMP) in knee osteoarthritis: a novel diagnostic and prognostic biomarker. J Orthop Res 31:999–1006
26. Celik O, Salci Y, Ak E, Kalaci A, Korkusuz F (2013) Serum cartilage oligomeric matrix protein accumulation decreases significantly after 12 weeks of running but not swimming and cycling training – a randomised controlled trial. Knee 20:19–25
27. Kapoor M, Martel-Pelletier J, Lajeunesse D, Pelletier JP, Fahmi H (2011) Role of proinflammatory cytokines in the pathophysiology of osteoarthritis. Nat Rev Rheumatol 7:33–42
28. Rosier RN, OKeefe RJ (1998) Autocrine regulation of articular cartilage. In: Cannon WD (ed) Instructional course lectures, vol 47. American Academy of Orthopaedic Surgeons, Rosemont, pp 469–475
29. Guilak F, Fermor B, Keefe FJ, Kraus VB, Olson SA, Pisetsky DS, Setton LA, Weinberg JB (2004) The role of biomechanics and inflammation in cartilage injury and repair. Clin Orthop Relat Res 423:17–26
30. Üzümcügil O, Cila E, Ataoglu Ö, Atalay N, Balçik C, Korkusuz F (2001) Meniscal allografts role in preventing osteoarthritis. Acta Orthop Traumatol Turc 35:71–78
31. Mitchel N, Shepard N (1982) Structure and function of articular cartilage. In: Cruess RL (ed) The musculoskeletal system. Churchill Livingstone, New York, pp 255–287
32. Kumar P, Oka M, Toguchida J, Kobayashi M, Uchida E, Nakamura T, Tanaka K (2001) Role of uppermost superficial layer of articular cartilage in the lubrication mechanism of joints. J Anat 199:241–250
33. Maroudas A, Schneiderman R, Popper O (1992) The role of water, proteoglycan and collagen in solute transport in cartilage. In: Kuettner KE, Schleyerbach R,

Peyron JG, Hascall VC (eds) Articular cartilage and osteoarthritis. Raven Press, New York, pp 355–371
34. Quin TM, Dierickx P, Grodzinsky AJ (2001) Glycosaminoglycan network geometry may contribute to anisotropic hydraulic permeability in cartilage under compression. J Biomech 34:1483–1490
35. Kim YL, Bonassar LJ, Grodzinsky AJ (1995) The role of cartilage streaming potential, fluid flow and pressure in the stimulation of chondrocyte biosynthesis during dynamic compression. J Biomech 28:1055–1066
36. Mow VC, Gibbs MC, Lai WM, Zhu WB, Athanasiou KA (1989) Biphasic indentation of articular cartilage-II. A numerical algorithm and an experimental study. J Biomech 22:853–861
37. Sah RLY, Grodzinsky AJ, Plaas AHK, Sandy JD (1992) Effects of static and dynamic compression on matrix metabolism in cartilage explants. In: Kuettner KE, Schleyerbach R, Peyron JG, Hascall VC (eds) Articular cartilage and osteoarthritis. Raven Press, New York, pp 373–391
38. Korkusuz F (1990) Knee joint anterior cruciate ligament repair. Arthroplast Arthrosc Surg 2:68–71
39. DeWitt MT, Handley CJ, Oakes BW, Lowther DA (1984) In vitro response of chondrocytes to mechanical loading. The effects of short term mechanical tension. Connect Tissue Res 12:97–109
40. Franz T, Hasler EM, Hagg R, Weiler C, Jakob RP, Mainil-Varlet P (2001) In situ compressive stiffness, biochemical composition, and structural integrity of articular cartilage of the human knee joint. Osteoarthritis Cartilage 9:582–592
41. Grodzinsky AJ, Levenston ME, Jin M, Frank EH (2000) Cartilage tissue remodelling in response to mechanical forces. Annu Rev Biomed Eng 2:691–713
42. Oloyede A, Broom ND (1993) A physical model for the time-dependent deformation of articular cartilage. Connect Tissue Res 29:251–261
43. Sommarin Y, Larsson T, Heinegard D (1989) Chondrocyte and matrix interaction. Exp Cell Res 184:181–192
44. Hall A, Urban JPG, Gehl K (1991) The effects of hydrostatic pressure on matrix synthesis in articular cartilage. J Orthop Res 9:1–10
45. Daniel JC, Kosher RA, Hamos JE, Lash JW (1974) The influence of extracellular potassium on synthesis and deposition of matrix components by chondrocytes. J Cell Biol 63:843–854
46. Jin M, Frank EH, Quinn TM, Hunziker EB, Grodzinsky AJ (2001) Tissue shear deformation stimulates proteoglycan and protein biosynthesis in bovine articular explants. Arch Biochem Biophys 395:41–48
47. Wei L, Hjerpe A, Brismar BH, Svensson O (2001) Effect of load on articular cartilage matrix and the development of guinea-pig osteoarthritis. Osteoarthritis Cartilage 9:447–453
48. Guilak F, Meyer BC, Ratcliffe A, Mow VC (1994) The effect of matrix compression on proteoglycan metabolism in articular cartilage explants. Osteoarthritis Cartilage 2:91–101
49. McKinley TO, Bay BK (2001) Trabecular bone strain changes associated with cartilage defects in the proximal and distal tibia. J Orthop Res 19:906–913
50. Garcia JJ, Altiero NJ, Haut RC (2000) Estimation of in situ elastic properties of biphasic cartilage based on a transversely isotropic hypo-elastic model. J Biomech Eng 122:1–8
51. Jurvelin JS, Bushmann MD, Hunziker EB (1997) Optical and mechanical determination of Poisson's ratio of adult bovine humeral articular cartilage. J Biomech 30:235–241
52. Bursac PM, Obitz TW, Eisenberg SR, Stamenovic D (1999) Confined and unconfined stress relaxation of cartilage. J Biomech 32:1125–1130
53. Jurvelin JS, Arokoski JP, Hunziker EB, Helminen HJ (2000) Topographical variation of the elastic properties of articular cartilage in the canine knee. J Biomech 33:669–675
54. Armstrong CG, Lai WM, Mow VC (1984) An analysis of the unconfined compression of articular cartilage. J Biomech Eng 106:165–173
55. Day JS, Ding M, van der Linden JC, Hvid I, Sumner DR, Weinans H (2001) A decreased subchondral trabecular bone tissue elastic modulus is associated with pre-arthritic cartilage damage. J Orthop Res 19:914–918
56. Cole GK, Nigg BM, van den Bogert AJ, Gerrtsen KG (1996) Lower extremity joint loading during impact running. Clin Biomech 11:181–193
57. Ewers BJ, Dvoracek-Driksna D, Orth MW, Haut RC (2001) The extent of matrix damage and chondrocyte death in mechanically traumatized articular cartilage explants depends on rate of loading. J Orthop Res 19:779–784
58. Fermor B, Haribabu B, Weinberg JB, Pisetsky DS, Guilak F (2001) Mechanical stress and nitric oxide influence leukotriene production in cartilage. Biochem Biophys Res Commun 285:806–810
59. Chowdhury TT, Bader DL, Lee DA (2001) Dynamic compression inhibits the synthesis of nitric oxide and PGE2 by IL-1beta-stimulated chondrocytes cultured in agarose construction. Biochem Biophys Res Commun 285:1168–1174
60. Flachsmann ER, Broom ND, Oloyede A (1995) A biomechanical investigation of unconstrained shear failure of the osteochondral region under impact loading. Clin Biomech 10:156–165
61. Kelly PA, O'Connor JJ (1996) Transmission of rapidly applied loads through articular cartilage. Proc Inst Mech Eng H 210:27–37
62. Shepherd DE, Seedhom BB (1997) A technique for measuring the compressive modulus of articular cartilage under physiological loading rates with preliminary results. Proc Inst Mech Eng H 211: 155–165
63. Barker MK, Seedhom BB (2001) The relationship of the compressive modulus of articular cartilage with its deformation response to cyclic loading. Rheumatology 40:274–284
64. Bendjaballah MZ, Shirazi-Adl A, Zukor DJ (1997) Finite element analysis of human knee joint in varus-valgus. Clin Biomech 12:139–148
65. Moyer RF, Ratneswaran A, Beier F, Birmingham TB (2014) Osteoarthritis year in review 2014:

mechanics – basic and clinical studies in osteoarthritis. Osteoarthritis Cartilage 22:1989–2002
66. Miyaki S, Asahara H (2012) Macro view of microRNA function in osteoarthritis. Nat Rev Rheumatol 8: 543–552
67. Herrero-Beaumont G, Roman-Blas JA, Castañeda S, Jimenez SA (2009) Primary osteoarthritis no longer primary: three subsets with distinct etiological, clinical, and therapeutic characteristics. Semin Arthritis Rheum 39:71–80
68. Kuszel L, Trzeciak T, Richter M, Czarny-Ratajczak M (2015) Osteoarthritis and telomere shortening. J Appl Genet 56:169–176
69. Sofat N, Ejindu V, Kiely P (2011) What makes osteoarthritis painful? The evidence for local and central pain processing. Rheumatology (Oxford) 50: 2157–2165
70. Kraus VB, Birmingham J, Stabler TV et al (2012) Effects of intraarticular I11-Ra for acute anterior cruciate ligament knee injury: a randomized controlled pilot trial. Osteoarthritis Cartilage 20:271–278
71. Li H, Chen C, Chen S (2015) Posttraumatic knee osteoarthritis following anterior cruciate ligament injury: potential biochemical mediators of degenerative alteration and specific biochemical markers. Biomed Rep 3:147–151
72. Haller JM, McFadden M, Kubiak EN, Higgins TF (2015) Inflammatory cytokine response following acute tibial plateau fracture. J Bone Joint Surg Am 97:478–483
73. McKinley TO, Borrelli J Jr, D'Lima DD, Furman BD, Giannoudis PV (2010) Basic science of intra-articular fractures and posttraumatic osteoarthritis. J Orthop Trauma 24:567–570

Current Strategies in Osteochondral Repair with Biomaterial Scaffold

23

Kazunori Shimomura, Yu Moriguchi, Norihiko Sugita, Kota Koizumi, Yukihiko Yasui, Hideki Yoshikawa, and Norimasa Nakamura

Abstract

Osteoarthritis (OA) is a common disease defined as degenerative arthritis or joint disease involving degradation of articular cartilage and subchondral bone, and it could potentially affect the quality of life of elderly populations worldwide. The management of OA remains challenging and controversial. Although there are several clinical options for the treatment of OA, regeneration of the damaged articular cartilage has proven difficult due to the limited healing capacity. With the advancements in tissue engineering approaches including cell-based technologies and development of biomaterial scaffolds over the past decade, new therapeutic options for patients with osteochondral lesions potentially exist. This chapter will focus on the feasibility of tissue-engineered biomaterial scaffolds, which can mimic the native osteochondral complex, for osteochondral repair and highlight the recent development of these techniques toward tissue regeneration, which will contribute to osteochondral repair for the patients who are involved with an incurable OA treated by traditional procedures. Moreover, basic anatomy, strategy for osteochondral repair, and the design and fabrication methods of scaffolds as well as the choice of cells, growth

K. Shimomura, MD, PhD • Y. Moriguchi, MD, PhD
N. Sugita, MD • K. Koizumi, MD • Y. Yasui, MD
H. Yoshikawa, MD, PhD
Department of Orthopaedic Surgery, Osaka University Graduate School of Medicine, 2-2 Yamadaoka, Suita City, Osaka 565-0871, Japan
e-mail: kazunori-shimomura@umin.net; u_in_music@wj8.so-net.ne.jp; gsugita550503@gmail.com; cocacota@hotmail.co.jp; hikobosy@yahoo.co.jp; yhideki@ort.med.osaka-u.ac.jp

N. Nakamura, MD, PhD (✉)
Institute for Medical Science in Sports, Osaka Health Science University, 1-9-27 Tenma, Kita-ku, Osaka City, Osaka 530-0043, Japan

Center for Advanced Medical Engineering and Informatics, Osaka University, 2-2 Yamadaoka, Suita City, Osaka 565-0871, Japan
e-mail: norimasa.nakamura@ohsu.ac.jp

F. Korkusuz (ed.), *Musculoskeletal Research and Basic Science*,
DOI 10.1007/978-3-319-20777-3_23

factor, and materials will be discussed. Specifically, we focus on the latest preclinical animal studies using large animals and clinical trials with high clinical relevance. Accordingly, this will contribute to an understanding of the latest trends in osteochondral repair and future application of such clinical therapies in patients with OA.

Learning Outcomes

After you have studied this chapter, you will have an understanding of (1) the basic anatomy of osteochondral tissue; (2) the strategy for osteochondral repair; (3) the design and fabrication methods of scaffolds; (4) the choice of cells, growth factor, and materials; and (5) the latest preclinical animal studies and clinical trials.

Terminology

Osteoarthritis Degenerative arthritis or joint disease involving degradation of articular cartilage and subchondral bone.

Scaffold An artificial material supporting 3D tissue formation, in which cells are usually seeded.

Growth factor A protein or hormone stimulating cellular growth, proliferation, and cellular differentiation.

Chondrocyte Cells found in cartilage.

Mesenchymal stem cell Multipotent stromal cells that can differentiate into a variety of cell types, including osteoblasts (bone cells), chondrocytes (cartilage cells), and adipocytes (fat cells).

Induced pluripotent stem (iPS) cell A type of pluripotent stem cell that can be generated directly from adult cells. Typically, adult cells can be converted into pluripotent stem cells by the introduction of four specific transcription factors.

Chondrogenesis The process by which the cartilage is developed.

Osteogenesis The process by which the bone is developed.

Clinical Relevance

Is a biological joint replacement available in the near future?

A 73-year-old female patient came in the outpatient clinic with symptoms of knee pain. The X-ray of this patient showed a severe OA (Fig. 23.3b). As conservative treatments including physiotherapy and pharmacologic therapies were failed, a total knee replacement was performed for the patient. At 6 months postoperatively, the patient was pain-free and has acquired normal gait. Today, the joint replacement should be a gold standard treatment for the patients with terminal OA, but there exist several risks and complications including infection, loss of motion, and revision surgeries [90, 98]. Also, patients may lose their normal joint movements and structures such as the cartilage, bone, and ligaments after the joint replacement. With the recent advancements in tissue engineering approaches, there have been many promising scaffolds developed for osteochondral repair, some of which are already at the stage of clinical trials [29, 55]. Therefore, the application of these technologies to osteochondral lesions could be expected in the near future, and it will contribute to restore normal structures and functions by biologically replacing the damaged tissues.

Introduction

Osteoarthritis (OA) is a common disease causing joint pain, joint deformity, and functional disability. Globally, approximately 250 million people are potentially affected with OA [120]. Overall, OA affects 13.9 % of adults aged 25 years and older and 33.6 % of those 65 and older in the United States, consequently affecting the quality of life of elderly populations [26, 32, 58, 66]. Also, OA is associated with an extremely high economic burden. The costs due to hospital expenditures of total knee and hip joint replacements were estimated at $28.5 billion and $13.7 billion, respectively [78]. Current treatment strategies can be divided into nonsurgical (conservative) and surgical therapies according to the severity of OA [125–127]. In the early stage of OA, pharmacologic and/or physical therapies as conservative treatments are typically selected for the purpose of reducing pain and, in some cases, attempting to delay the progressive structural deterioration in affected joints. Surgical therapies such as joint replacement and osteotomy are available for patients who fail to respond to more conservative measures. These treatments are well established and effective for reducing pain and improving quality of life. Regardless of these therapeutic options, however, there is no method available that facilitates complete healing of the articular cartilage [6, 7, 15, 44, 47, 108]. Recently, several biological approaches, such as the use of tissue-engineered materials, have been tested to overcome such potential problems (Fig. 23.1). This chapter will focus on the feasibility of tissue-engineered materials in osteochondral repair and highlight recent advances in the biological repair of osteochondral lesions.

Anatomy of the Cartilage, Subchondral Bone, and Their Interface

The osteochondral complex consists of both the articular cartilage and underlying subchondral bone. Biochemically, cartilage tissue is largely comprised of water, chondrocytes, type II collagen, and proteoglycan [50, 81, 122]. The cartilage can be differentiated into four distinct zones: the superficial, middle, deep, and calcified cartilage zones (Fig. 23.2) [65]. Each zone is defined by a particular composition and organization of cells and extracellular matrix (ECM) molecules. The differential proportions in ECM composition influence the mechanical properties of each zone of the cartilage. For example, the superficial zone is strong in tension along the alignment of its collagen fibrils, thereby assisting in the resistance of shear forces at the surface. By comparison, the deep zone has more compressive strain.

Subchondral bone is a complex tissue consisting of water, collagen type I, and hydroxyapatite, with the two latter components providing the tissue's stiffness and compressive strength [9, 81, 122]. The compressive modulus of subchondral

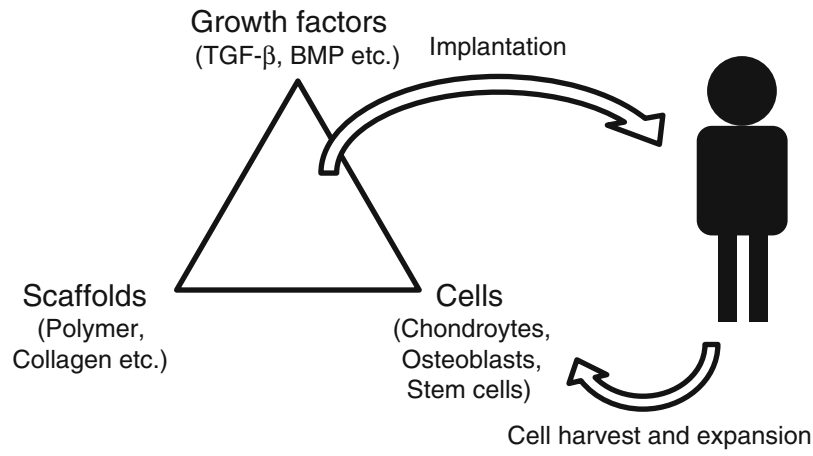

Fig. 23.1 Basic concept of tissue engineering. The use of a combination of cells, scaffolds, and growth factors improves or restores biological function

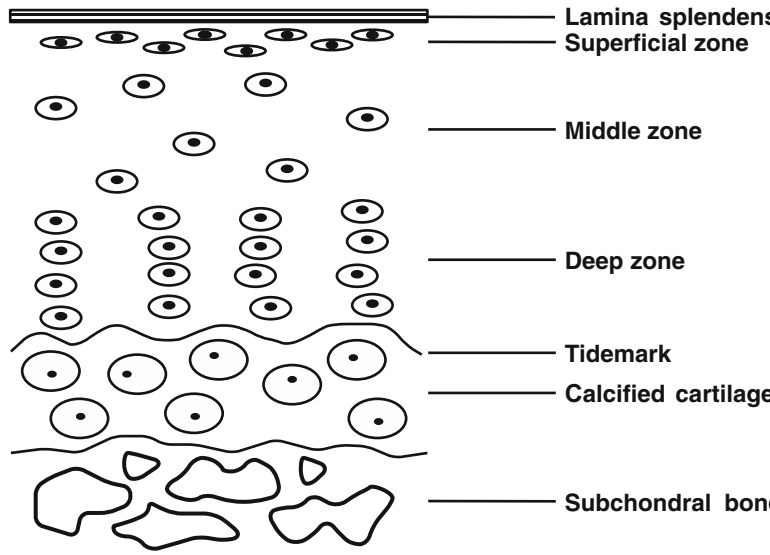

Fig. 23.2 Schematic drawing of the different zones of articular cartilage and subchondral bone

bone is higher than that of the cartilage. The different morphological compositions and mechanical properties of subchondral bone and cartilage indicate the complexity of the tissue interface.

The osteochondral interface is described by the interaction of calcified cartilage and the underlying subchondral bone [16]. Structurally, collagen fibers extend from the deep zone to calcified cartilage through a wavy tidemark, which enables the dispersal of force through the vertical orientation of collagen fibrils [83]. However, despite the fact that calcified cartilage is mineralized tissue, its mechanical strength is lower than that of the subchondral bone [72]. Calcified cartilage is interdigitated with subchondral bone, but fibers do not extend across the zone into the bone [23, 83]. The wavy tidemark and vertically oriented fibers at the tidemark, as well as interdigitations present at the interface, may allow for reducing stress concentrations, as well as better integration with the underlying subchondral bone [81, 83].

Characteristic of Osteoarthritic Joint

An osteoarthritic joint is characterized by degenerative changes, such as articular cartilage loss, subchondral bone thickening, and osteophyte formation [12, 39, 64, 77, 96]. The primary morphologic changes include thinning, fissuring, and fragmentation of articular cartilage. With the progression of the disease comes a continuous loss of articular cartilage, accompanied with the decrease of collagen type II and aggrecan [31, 76], leading to exposure of subchondral bone. Secondary changes are frequently seen in the underlying bone, such as sclerosis, cystic change, and new bone formation (Fig. 23.3a, b). These changes are considered to be triggered by a multitude of factors, including aging, trauma, obesity, mechanical overload, congenital disorder, and infection, which do not heal spontaneously once damaged.

Strategy for Osteochondral Repair

For an ideal repair of osteochondral lesions, it is important to regenerate subchondral bone and to facilitate zonal restoration of the cartilage and subchondral bone, layer by layer, mimicking the natural articular structure [37, 46, 53, 74, 85, 86, 102]. As a strategy to regenerate these structures in a layer-by-layer fashion, biphasic or triphasic constructs have been developed due to both mechanical and biological reasons, including the acquisition of initial mechanical strength, mimicking a natural articulate structure, a uniform tidemark at the osteochondral junction, and an integration of the biphasic implant with host tissue to sustain biological function (Fig. 23.4a–d) [2, 4, 18, 36, 43, 47, 69, 82, 84, 107, 110]. For satisfying the biological requirements, an

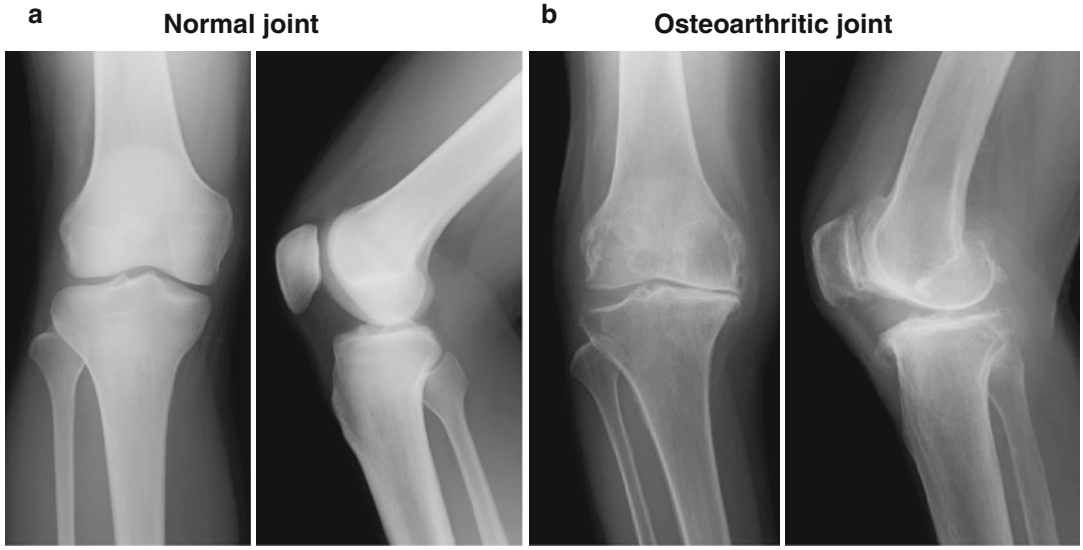

Fig. 23.3 Radiography of (**a**) normal healthy knee joint and (**b**) osteoarthritic knee joint. In osteoarthritis, the loss of the cartilage (joint space narrowing) and subchondral bone change such as sclerosis, cystic change, and new bone formation (osteophyte) are frequently seen

osteochondral implant should ideally have a rigid osseous layer to support the overlying cartilage and integrate with the native bone and a chondral layer to allow the seeding and proliferation of chondrocytes or mesenchymal stem cells (MSCs) and subsequent deposition of cartilaginous ECM. Also, for the successful osteochondral repair, the integration between the implant and host tissue should be one of crucial factors. Our previous study showed that the tissue integration to native surrounding osteochondral tissue after the implantation of biphasic construct could influence the quality and maturation of repair tissue [109]. In case of the failure of integration with the adjacent host cartilage, the repair tissue might evolve into a pathological condition such as OA due to mechanically unstable condition, which potentially raises concerns regarding the long-term durability of the repair tissue.

Design and Fabrication of Biomaterial Scaffold

In general, osteochondral tissue engineering strategies can be categorized into monophasic (Fig. 23.4b) and biphasic (Fig. 23.4c) depending on the biological and biomechanical characteristics of the scaffold. As mentioned above, a successful tissue engineering approach for osteochondral repair involves the design of a biphasic scaffold with the potential to regenerate both the cartilage and subchondral bone. The fabrication of the majority of scaffolds is performed through independent processes, whereby different scaffolds for the two sides are created and then combined, or via a simultaneous process through which a single scaffold is created and cultured simultaneously for both sides [67, 81]. A biphasic construct developed independently allows the cultivation of both chondrogenic and osteogenic cells in separate media and environmental conditions. However, these constructs must be hybridized into a single composite graft by connecting the two layers together. The potential disadvantage of this approach might be the difficulty in achieving a secure biological and mechanical integration between the two layers [67]. On the other hand, when the two layers are hybridized prior to culture, a complicated system will be required to promote osteo- and chondral differentiation separately in each layer. Due to the difficulty of two different cell cultures simultaneously, such pre-developed biphasic constructs are mainly used as a cell-free scaffold [53].

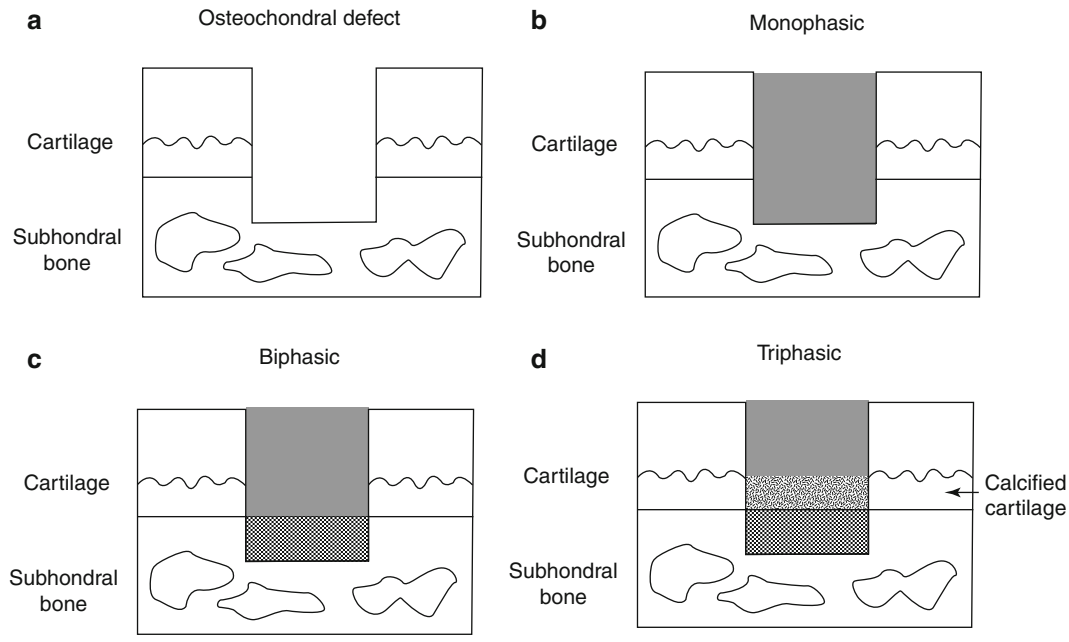

Fig. 23.4 Schematic drawing of (**a**) osteochondral defect and (**b**) implantation of monophasic scaffold, (**c**) biphasic scaffold, and (**d**) triphasic scaffold

Some research groups have raised the importance of an intermediate layer between the cartilage and subchondral bone layers to represent the tidemark or calcified cartilage; triphasic scaffolds were therefore developed (Fig. 23.4d) [53, 69]. However, the intermediate layer has unique osteochondral characteristics owing to the infiltration of the blood vessels, and thus, it may be difficult to mimic the unique structure with currently available biomaterial technologies. In fact, the superiority of triphasic scaffolds over biphasic for osteochondral repair has not yet been demonstrated and requires further investigation.

Most scaffolds have the pore structures inside, which would affect the regulation of cell invasion, vascularization, and tissue maturation [105]. The pore size and porosity should be controlled suitable for tissue engineering in the fabrication process of porous scaffolds. Regarding the effects of pore size on osteogenesis, the scaffold structure composed of porosity higher than 50 % and pores larger than 300 μm is recommended to achieve direct osteogenesis with enhanced vascularization [48]. On the contrary, the scaffold with smaller pores have been suggested for favorable chondrogenesis on 90–120 μm pores, in which MSCs proliferate and promote chondrogenesis in the scaffold [51].

Recent advances in computer-aided tissue engineering including three-dimensional (3D) printing technique enable the fabrication of multifunctional scaffolds that meet the microstructural, mechanical, and nutritional requirements based on optimized models [59, 63]. Moreover, these techniques will be expected to generate the custom-shaped engineered grafts from clinical imaging data with the use of CT or MRI, which fit the specific defect [79]. Therefore, the bioprinting technology should be a powerful tool for building tissues at cellular and organ levels.

Choice of Cells and Growth Factors

The most direct cell source may be the biopsy specimens taken from the patients, from which mature osteoblasts and chondrocytes may be obtained. However, as the number of cells obtained is usually limited, it is typically not enough to allow seeding onto the scaffolds. Also, expansion of primary cells may result in a loss

of differentiation capacity; for example, the expansion of articular chondrocytes can lead to dedifferentiation into fibroblast [13, 104, 115]. To overcome such potential problems with respect to dedifferentiation, three-dimensional (3D) culture can be used to retain the cellular phenotype and avoid dedifferentiation [116]. The most common method is the use of various scaffolds to produce a 3D culture condition [68, 128] and may be combined with the supplementation of growth factors [22], the use of bioreactor [35], the mechanical stimulation of the cells [33, 49], and the use of low oxygen tension [57] during cultivation. Also, even if chondrocytes lose their differentiated phenotype, dedifferentiated chondrocytes can regain their differentiated phenotype through the redifferentiation process of cultivation in a 3D scaffold combined with growth factors [3, 60].

As an additional option, stem cells may represent promising alternatives [113]. Specifically, mesenchymal stem cells (MSCs) have the capability to differentiate into a variety of connective tissue cell types, including the bone, cartilage, tendon, muscle, and adipose tissue [27, 108]. These cells may be isolated from various tissues, such as bone marrow, skeletal muscle, synovial membrane, adipose tissue, and umbilical cord blood [6, 7, 27, 52, 71, 99]. Moreover, allogeneic MSCs [25, 108] or induced pluripotent stem (iPS) cells [114, 119] may also be considered. However, there have not been much evidence using these cells forthcoming in terms of preclinical and clinical safety, and thus, further studies with such cells are likely necessary.

In addition, the use of a growth factor or its cocktail (combination), including insulin-like growth factor 1 (IGF-1), transforming growth factor beta 1 (TGF-β1), fibroblast growth factor 2 (FGF-2), and bone morphogenetic proteins (BMP-2, BMP-7), may support tissue maturation for the cartilage [10, 41, 87, 111]. Similar to the cartilage, the bone also possesses a large variety of growth factors that are involved in the regenerative process, including TGF-β; BMP-2, 4, 6, and 7; IGF-1 and 2; and platelet-derived growth factor (PDGF) [91, 97, 100].

On the other hand, some researchers have tested an acellular approach using a scaffold alone [29, 53]. Considering the time and cost-effectiveness, as well as safety issues associated with cell culture, this approach could represent a reasonable strategy in tissue engineering. Scaffolds should be developed to meet requirements such as the recruitment of enough tissue progenitor cells from the host tissue.

Choice of Materials

Several methods have been proposed to develop biphasic scaffolds with the hybridization of two distinct biomaterials, each of which being adequate to integrate with the respective surrounding tissue [67]. Many specific material types have been developed for both cartilage and bone regeneration, which are typically made of biocompatible and biodegradable polymers. For the cartilage layer, natural or synthetic polymer-based scaffolds are commonly used. More recently, scaffold-free implants have been developed and the potential feasibility tested. On the other hand, for a scaffold of the subchondral bone layer, it is important to choose materials with initial mechanical strength, good bone ingrowth, and integration of native surrounding bone. Ceramics, glasses, and metallic materials are commonly used. Also, natural or synthetic polymers, similar to cartilage layer, could be used alone or combined with ceramics [4, 18, 28, 54, 123, 124].

Natural Polymers

The materials of naturally derived polymers could provide a naturally occurring environment for the cells and tissues and thereby potentially facilitate cell proliferation and differentiation [42, 118]. Moreover, natural polymers usually contain specific molecular domains that can support and guide cells at various stages of their development [67, 81]; thus, biological interaction of the scaffold with the host tissue can be enhanced. However, they are, in general, biomechanically weak and less stiff than other materials [81]. As a source of materials, collagen, gelatin, glycosaminoglycan, chitosan, starch,

hyaluronic acid, alginate, and bacterial-sourced polymers (hydroxyalkanoates) are commonly used.

Synthetic Polymers

Biodegradable synthetic polymers offer several advantages over other materials for developing scaffolds in tissue engineering. The main advantages are being able to control mechanical properties (i.e., strength and stiffness) and degradation speed [38]. Synthetic polymers are also attractive because they can be fabricated into various shapes with a desired pore according to the speed of cell migration or tissue ingrowth [30]. Moreover, the progression of current techniques such as electrospinning methods and the 3D printer has enabled the simple design and fabrication of scaffolds, which mimic the original tissue structure [61–63]. On the other hand, synthetic polymers have limitations in bioactivity due to their hydrophobic surface not supporting cell attachment and proliferation [14, 89, 101, 106]. Surface treatment with chondroitin sulfate [17], silicate [20], and alkaline [89] could increase hydrophilicity and provide a suitable scaffold for tissue engineering. Also, these polymers, incorporated with growth factors such as TGF-β and BMP, would be helpful and convenient to support cell proliferation and differentiation, stimulating the repair of damaged tissue [93, 94]. As a source of biodegradable synthetic polymers, polyglycolic acid (PGA), poly(D,L-lactic-co-glycolic acid) (PLGA), poly-L-lactic acid (PLLA), polycaprolactone (PCL), and polyethylene glycol (PEG) have been commonly used.

Scaffold-Free Biomaterials

Polymer-based scaffolds have been reported to contribute to good osteochondral repair in vivo [2, 4, 43, 69, 84, 107]. Despite this, there remain several concerns associated with the long-term safety of these constructs due to the involvement of chemical or animal-derived materials. To overcome such potential problems, we have developed a scaffold-free three-dimensional tissue-engineered construct (TEC) composed of MSCs derived from the synovium and ECMs synthesized by the cells (Fig. 23.5a) [6, 7]. The feasibility of the resultant TEC to facilitate cartilage repair was demonstrated in a preclinical large animal model [5, 6, 108], and we have now proceeded clinical studies under the auspices of an approved first-in-man protocol [80]. These TECs are developed without an artificial scaffold, and thus, their implantation could eliminate or minimize the risk of potential side effects induced by extrinsic chemical or biological materials. Furthermore, such TEC are highly adherent to cartilage matrix and secure integration of the TEC until adjacent cartilage tissue is observed following implantation. Therefore, combined constructs of TEC and several materials for the subchondral bone layer may effectively repair an osteochondral lesion with zonal restoration, and TEC could be one of the strong candidates for a cartilage bioimplant. In our animal study, we have demonstrated that the combined bioimplant of TEC and ceramic-based artificial bone significantly accelerated and improved osteochondral repair (Fig. 23.5b, c) [109].

Ceramics and Glasses

Ceramics, such as hydroxyapatite (HA), or other calcium phosphates, such as tricalcium phosphate (TCP), and bioactive glasses, such as Bioglass®, are widely used for bone tissue engineering [45, 70, 117, 121]. These materials promote the formation of a bone-like tissue and enhance integration of the scaffold to the host tissue due to excellent osteoconductivity and osteoinductivity. Also, inclusion of growth factors in the scaffolds may be an interesting concept to explore and contribute to the maturation of bone tissue. Notably, the inclusion of BMP-2 in an HA-based scaffold was reported to promote subchondral bone as well as cartilage repair [117]. On the other hand, these scaffolds have low structural integrity being brittle and unsuitable for applications under mechanical stress, although they exhibit suitable stiffness [81]. The degradation behavior of these scaffolds

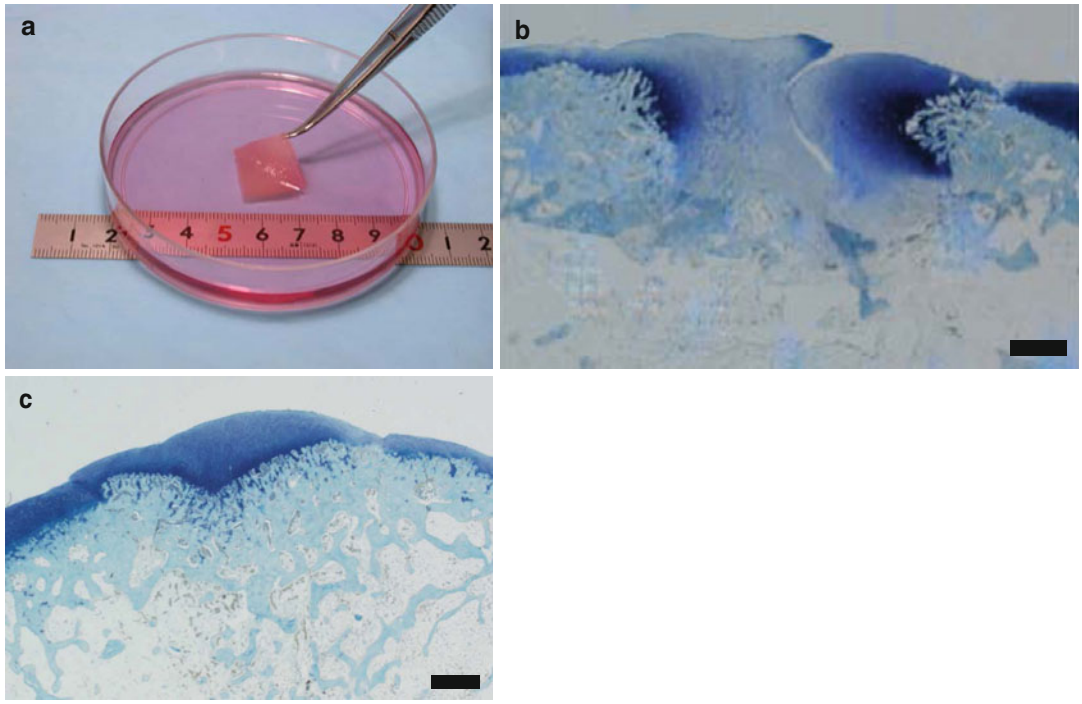

Fig. 23.5 (**a**) In vitro generated scaffold-free tissue-engineered construct (*TEC*) composed of MSCs derived from the synovium and ECMs synthesized by the cells. (**b**, **c**) Toluidine blue staining of repair tissues in osteochondral defect (**b**) untreated or (**c**) treated with the biphasic implant made of TEC and ceramic artificial bone using a rabbit model. The untreated repair tissue showed insufficient cartilage and subchondral bone repair with fibrous or fibrocartilaginous repair at 2 months postoperatively. The repair tissue treated with the implant showed complete osteochondral repair at 2 months postoperatively. Bar = 1 mm

can be controlled by changes in the porous structures, which can be tailored in terms of their degradation kinetics appropriate for bone tissue engineering. It is also well known that increasing porosity impairs further the mechanical properties of bioceramic scaffolds. This problem can be solved by modifying any porous scaffolds with infiltration or coating by biodegradable polymers [19, 73, 92].

Metallic Materials

Metals are widely used in orthopedic implants such as titanium, titanium alloys, stainless steels, and cobalt-chromium alloy. As an application of osteochondral bone repair, metallic materials withhold the capability of withstanding mechanical loading when used in the subchondral bone layer. On the other hand, the lack of degradation over time and the possibility of wear particle release or corrosion are disadvantages. As one of the examples, porous tantalum was reported to induce subchondral bone growth and showed integration to adjacent host bone in an in vivo rabbit study [11].

Preclinical Study and Clinical Trial

There have been many therapeutic procedures investigated to biologically repair damaged cartilage, some of which are already at the stage of clinical application. On the contrary, considering the higher incidence of OA, which involves subchondral bone pathology, by comparison to isolated chondral injury [8, 24, 26, 40, 88, 126], there is an urgent need to develop novel therapeutic methods for osteochondral repair with clinical relevance. In this regard, the number of animal

experiments and clinical trials to treat osteochondral lesions has been recently increased. We focus on the latest preclinical animal studies using large animal and clinical studies.

At first, in order to evaluate the feasibility and safety of new implants with clinical relevance, the selection of appropriate animal models is important. Due to the differences in matrix structure and composition, as well as in the natural osteochondral healing response and technical difficulty in creating the lesions of consistent size and location, the use of small animals such as rabbits, rats, and mice may not be appropriate [1, 21, 95]. Rather, in consideration of clinical relevance, it is preferable to utilize larger animal models, such as pigs, sheep, goats, and horses. Marquass et al. used an MSC-seeded combined implant with a collagen I hydrogel and β-TCP in an ovine osteochondral defect model and showed comparable repair quality to osteochondral autografts in terms of histology and biomechanical testing [69]. Miot et al. prepared engineered cartilage, which was generated from autologous chondrocytes cultured in hyaluronic acid scaffolds of different pre-culture periods, and implanted the engineered cartilage above the hydroxyapatite/hyaluronic acid sponges into goat osteochondral defects. They concluded that 2 weeks pre-culture of engineered cartilage achieved a suitable compromise between tissue maturity and structural/integrative properties of the repair tissue. These data demonstrate that the stage of development of engineered cartilage is an important parameter to be considered in designing cartilage repair strategies [75]. Kon et al. used an aragonite/hyaluronate biphasic scaffold for osteochondral defects in a goat model and showed that mechanical modification with drilled channels in the cartilage phase and impregnation of HA within the coral pores enhanced the scaffold's cartilage regenerative potential [56]. Schleicher et al. compared two biphasic scaffolds of either hydroxylapatite/collagen or allogenous sterilized bone/collagen and tested their integration in a sheep model. They showed that the latter scaffold proved to be stable and sufficiently integrated in the short term [103]. Sosio et al. treated the osteochondral lesions with a biphasic scaffold made of collagen type I and hydroxyapatite in a pig model, in which they compared the scaffold seeded with autologous chondrocyte with the unseeded scaffold [112]. Surprisingly, they showed that the unseeded scaffold exhibited better macroscopic and histological results than the cell-seeded scaffold. Kon et al. developed an acellular three-gradient multilayer scaffold made of collagen type I and nanoparticles of hydroxyapatite and tested the scaffold with or without autologous chondrocytes in sheep osteochondral defect model. They concluded that the scaffold contributed to the process of the bone and hyaline-like cartilage regeneration, regardless of the use of chondrocytes [54]. Also, they treated 27 patients with chondral or osteochondral lesions using an acellular scaffold [34, 53, 55] and demonstrated the safety and potential clinical benefit of the graded biomimetic osteochondral scaffold in promoting the bone and cartilage tissue with good clinical and magnetic resonance imaging results until the 5-year follow-up. Dhollander et al. treated 27 for cartilage lesions with an acellular osteochondral plug, which is composed of polylactide-co-glycolide copolymer, calcium sulfate, polyglycolide fibers, and surfactant (TruFit plug; Smith and Nephew, Andover, MA) [29]. In this clinical pilot study, a modest clinical improvement became apparent at 12 months of follow-up. Also, MRI data showed no deterioration of the repair tissue. However, 20 % of the patients had persistent clinical symptoms after surgery and had an additional surgery such as removal of the osteochondral plug remnants. The two latter studies were Level IV study, and further studies, which would be compared with conventional treatment such as bone marrow stimulation and osteochondral transplantation, are necessary. Also, in contrast with cell-free scaffolds, no clinical trial using cell-seeded scaffold has been reported, and these studies should be expected in the near future.

Future Directions

The management of OA remains challenging and controversial. Considering the steady progression of tissue engineering and cell-based

technologies over the past decade, we may have new therapeutic options for osteochondral repair in clinical practice. In this chapter, we have focused on biomaterial scaffold for osteochondral repair, including the concept, scaffold fabrication, in addition to the selection of cells and materials. There have been many promising scaffolds developed, some of which contribute to good osteochondral repair in vivo. Moreover, some of them are already at the stage of preclinical, large animal studies, as well as clinical trials. In addition, the recent work has been focused on not only investigating the effectiveness of materials or cells but also applying several new concepts and techniques such as mechanical [56], microstructural [30], and local microenvironment modification [94] for the design and fabrication of scaffolds. Therefore, the application of additional new implants to osteochondral lesions could be expected in the near future. On the other hand, the most suitable biomaterials for the cartilage or subchondral bone layers have not been fully investigated, while there are many biomaterials available for osteochondral repair. Therefore, the comparison of these materials should be performed to ultimately determine the ideal material. Further studies will be needed and should be conducted in a methodologically rigorous fashion.

Acknowledgments This study was supported by a grant from the New Energy and Industrial Technology Development Organization, Japan, Grant-in-Aid for Scientific Research (B), and Japan Society for the Promotion of Science, Japan.

References

1. Ahern BJ, Parvizi J, Boston R, Schaer TP (2009) Preclinical animal models in single site cartilage defect testing: a systematic review. Osteoarthritis Cartilage 17(6):705–713. doi:10.1016/j.joca.2008.11.008, S1063-4584(08)00353-1 [pii]
2. Ahn JH, Lee TH, Oh JS, Kim SY, Kim HJ, Park IK, Choi BS, Im GI (2009) Novel hyaluronate-atelocollagen/beta-TCP-hydroxyapatite biphasic scaffold for the repair of osteochondral defects in rabbits. Tissue Eng Part A 15(9):2595–2604. doi:10.1089/ten.TEA.2008.0511, 10.1089/ten.TEA.2008.0511 [pii]
3. Albrecht C, Schlegel W, Bartko P, Eckl P, Jagersberger T, Vecsei V, Marlovits S (2010) Changes in the endogenous BMP expression during redifferentiation of chondrocytes in 3D cultures. Int J Mol Med 26(3):317–323
4. Alhadlaq A, Mao JJ (2005) Tissue-engineered osteochondral constructs in the shape of an articular condyle. J Bone Joint Surg Am 87(5):936–944. doi:10.2106/JBJS.D.02104, 87/5/936 [pii]
5. Ando W, Fujie H, Moriguchi Y, Nansai R, Shimomura K, Hart DA, Yoshikawa H, Nakamura N (2012) Detection of abnormalities in the superficial zone of cartilage repaired using a tissue engineered construct derived from synovial stem cells. Eur Cell Mater 24:292–307. doi:vol024a21 [pii]
6. Ando W, Tateishi K, Hart DA, Katakai D, Tanaka Y, Nakata K, Hashimoto J, Fujie H, Shino K, Yoshikawa H, Nakamura N (2007) Cartilage repair using an in vitro generated scaffold-free tissue-engineered construct derived from porcine synovial mesenchymal stem cells. Biomaterials 28(36):5462–5470. doi:10.1016/j.biomaterials.2007.08.030, S0142-9612(07)00672-2 [pii]
7. Ando W, Tateishi K, Katakai D, Hart DA, Higuchi C, Nakata K, Hashimoto J, Fujie H, Shino K, Yoshikawa H, Nakamura N (2008) In vitro generation of a scaffold-free tissue-engineered construct (TEC) derived from human synovial mesenchymal stem cells: biological and mechanical properties and further chondrogenic potential. Tissue Eng Part A 14(12):2041–2049. doi:10.1089/ten.tea.2008.0015
8. Aroen A, Loken S, Heir S, Alvik E, Ekeland A, Granlund OG, Engebretsen L (2004) Articular cartilage lesions in 993 consecutive knee arthroscopies. Am J Sports Med 32(1):211–215
9. Arvidson K, Abdallah BM, Applegate LA, Baldini N, Cenni E, Gomez-Barrena E, Granchi D, Kassem M, Konttinen YT, Mustafa K, Pioletti DP, Sillat T, Finne-Wistrand A (2011) Bone regeneration and stem cells. J Cell Mol Med 15(4):718–746. doi:10.1111/j.1582-4934.2010.01224.x
10. Babensee JE, McIntire LV, Mikos AG (2000) Growth factor delivery for tissue engineering. Pharm Res 17(5):497–504
11. Bal BS, Rahaman MN, Jayabalan P, Kuroki K, Cockrell MK, Yao JQ, Cook JL (2010) In vivo outcomes of tissue-engineered osteochondral grafts. J Biomed Mater Res B Appl Biomater 93(1):164–174. doi:10.1002/jbm.b.31571
12. Barr RJ, Gregory JS, Reid DM, Aspden RM, Yoshida K, Hosie G, Silman AJ, Alesci S, Macfarlane GJ (2012) Predicting OA progression to total hip replacement: can we do better than risk factors alone using active shape modelling as an imaging biomarker? Rheumatology (Oxford) 51(3):562–570. doi:10.1093/rheumatology/ker382, ker382 [pii]
13. Benya PD, Shaffer JD (1982) Dedifferentiated chondrocytes reexpress the differentiated collagen phenotype when cultured in agarose gels. Cell 30(1):215–224. doi:0092-8674(82)90027-7 [pii]

14. Bhattarai SR, Bhattarai N, Viswanathamurthi P, Yi HK, Hwang PH, Kim HY (2006) Hydrophilic nanofibrous structure of polylactide; fabrication and cell affinity. J Biomed Mater Res A 78(2):247–257. doi:10.1002/jbm.a.30695
15. Brittberg M, Lindahl A, Nilsson A, Ohlsson C, Isaksson O, Peterson L (1994) Treatment of deep cartilage defects in the knee with autologous chondrocyte transplantation. N Engl J Med 331(14):889–895. doi:10.1056/NEJM199410063311401
16. Castro NJ, Hacking SA, Zhang LG (2012) Recent progress in interfacial tissue engineering approaches for osteochondral defects. Ann Biomed Eng 40(8):1628–1640. doi:10.1007/s10439-012-0605-5
17. Chang KY, Cheng LW, Ho GH, Huang YP, Lee YD (2009) Fabrication and characterization of poly(gamma-glutamic acid)-graft-chondroitin sulfate/polycaprolactone porous scaffolds for cartilage tissue engineering. Acta Biomater 5(6):1937–1947. doi:10.1016/j.actbio.2009.02.002, S1742-7061(09)00063-4 [pii]
18. Chen J, Chen H, Li P, Diao H, Zhu S, Dong L, Wang R, Guo T, Zhao J, Zhang J (2011) Simultaneous regeneration of articular cartilage and subchondral bone in vivo using MSCs induced by a spatially controlled gene delivery system in bilayered integrated scaffolds. Biomaterials 32(21):4793–4805. doi:10.1016/j.biomaterials.2011.03.041, S0142-9612(11)00310-3 [pii]
19. Chen QZ, Boccaccini AR (2006) Poly(D,L-lactic acid) coated 45S5 bioglass-based scaffolds: processing and characterization. J Biomed Mater Res A 77(3):445–457. doi:10.1002/jbm.a.30636
20. Chouzouri G, Xanthos M (2007) In vitro bioactivity and degradation of polycaprolactone composites containing silicate fillers. Acta Biomater 3(5):745–756. doi:10.1016/j.actbio.2007.01.005, S1742-7061(07)00016-5 [pii]
21. Chu CR, Szczodry M, Bruno S (2010) Animal models for cartilage regeneration and repair. Tissue Eng Part B Rev 16(1):105–115. doi:10.1089/ten.TEB.2009.0452
22. Chubinskaya S, Segalite D, Pikovsky D, Hakimiyan AA, Rueger DC (2008) Effects induced by BMPS in cultures of human articular chondrocytes: comparative studies. Growth Factors 26(5):275–283. doi:10.1080/08977190802291733, 795281645 [pii]
23. Clark JM, Huber JD (1990) The structure of the human subchondral plate. J Bone Joint Surg Br 72(5):866–873
24. Curl WW, Krome J, Gordon ES, Rushing J, Smith BP, Poehling GG (1997) Cartilage injuries: a review of 31,516 knee arthroscopies. Arthroscopy 13(4):456–460
25. Dashtdar H, Rothan HA, Tay T, Ahmad RE, Ali R, Tay LX, Chong PP, Kamarul T (2011) A preliminary study comparing the use of allogenic chondrogenic pre-differentiated and undifferentiated mesenchymal stem cells for the repair of full thickness articular cartilage defects in rabbits. J Orthop Res 29(9):1336–1342. doi:10.1002/jor.21413
26. Dawson J, Linsell L, Zondervan K, Rose P, Randall T, Carr A, Fitzpatrick R (2004) Epidemiology of hip and knee pain and its impact on overall health status in older adults. Rheumatology (Oxford) 43(4):497–504. doi:10.1093/rheumatology/keh086, keh086 [pii]
27. De Bari C, Dell'Accio F, Tylzanowski P, Luyten FP (2001) Multipotent mesenchymal stem cells from adult human synovial membrane. Arthritis Rheum 44(8):1928–1942. doi:10.1002/1529-0131(200108)44:8, <1928::AID-ART331>3.0.CO;2-P
28. Deng T, Lv J, Pang J, Liu B, Ke J (2012) Construction of tissue-engineered osteochondral composites and repair of large joint defects in rabbit. J Tissue Eng Regen Med. doi:10.1002/term.1556 [doi]
29. Dhollander AA, Liekens K, Almqvist KF, Verdonk R, Lambrecht S, Elewaut D, Verbruggen G, Verdonk PC (2012) A pilot study of the use of an osteochondral scaffold plug for cartilage repair in the knee and how to deal with early clinical failures. Arthroscopy 28(2):225–233. doi:10.1016/j.arthro.2011.07.017, S0749-8063(11)00994-7 [pii]
30. Duan P, Pan Z, Cao L, He Y, Wang H, Qu Z, Dong J, Ding J (2013) The effects of pore size in bilayered poly(lactide-co-glycolide) scaffolds on restoring osteochondral defects in rabbits. J Biomed Mater Res A. doi:10.1002/jbm.a.34683 [doi]
31. Duan Y, Hao D, Li M, Wu Z, Li D, Yang X, Qiu G (2012) Increased synovial fluid visfatin is positively linked to cartilage degradation biomarkers in osteoarthritis. Rheumatol Int 32(4):985–990. doi:10.1007/s00296-010-1731-8
32. Dunlop DD, Manheim LM, Song J, Chang RW (2001) Arthritis prevalence and activity limitations in older adults. Arthritis Rheum 44(1):212–221. doi:10.1002/1529-0131(200101)44:1, <212::AID-ANR28>3.0.CO;2-Q
33. El-Ayoubi R, DeGrandpre C, DiRaddo R, Yousefi AM, Lavigne P (2011) Design and dynamic culture of 3D-scaffolds for cartilage tissue engineering. J Biomater Appl 25(5):429–444. doi:10.1177/0885328209355332, 0885328209355332 [pii]
34. Filardo G, Kon E, Di Martino A, Busacca M, Altadonna G, Marcacci M (2013) Treatment of knee osteochondritis dissecans with a cell-free biomimetic osteochondral scaffold: clinical and imaging evaluation at 2-year follow-up. Am J Sports Med 41(8):1786–1793. doi:10.1177/0363546513490658, 0363546513490658 [pii]
35. Forsey RW, Tare R, Oreffo RO, Chaudhuri JB (2012) Perfusion bioreactor studies of chondrocyte growth in alginate-chitosan capsules. Biotechnol Appl Biochem 59(2):142–152. doi:10.1002/bab.1009
36. Gao J, Dennis JE, Solchaga LA, Goldberg VM, Caplan AI (2002) Repair of osteochondral defect with tissue-engineered two-phase composite material of injectable calcium phosphate and hyaluronan sponge. Tissue Eng 8(5):827–837. doi:10.1089/10763270260424187

37. Gomoll AH, Madry H, Knutsen G, van Dijk N, Seil R, Brittberg M, Kon E (2010) The subchondral bone in articular cartilage repair: current problems in the surgical management. Knee Surg Sports Traumatol Arthrosc 18(4):434–447. doi:10.1007/s00167-010-1072-x
38. Gunatillake PA, Adhikari R (2003) Biodegradable synthetic polymers for tissue engineering. Eur Cell Mater 5:1–16, discussion 16. doi:vol005a01 [pii]
39. Haverkamp DJ, Schiphof D, Bierma-Zeinstra SM, Weinans H, Waarsing JH (2011) Variation in joint shape of osteoarthritic knees. Arthritis Rheum 63(11):3401–3407. doi:10.1002/art.30575
40. Hjelle K, Solheim E, Strand T, Muri R, Brittberg M (2002) Articular cartilage defects in 1,000 knee arthroscopies. Arthroscopy 18(7):730-734. doi:S0749806302000257 [pii]
41. Holland TA, Bodde EW, Cuijpers VM, Baggett LS, Tabata Y, Mikos AG, Jansen JA (2007) Degradable hydrogel scaffolds for in vivo delivery of single and dual growth factors in cartilage repair. Osteoarthritis Cartilage 15(2):187–197. doi:10.1016/j.joca.2006.07.006, S1063-4584(06)00231-7 [pii]
42. Hsu FY, Hung YS, Liou HM, Shen CH (2010) Electrospun hyaluronate-collagen nanofibrous matrix and the effects of varying the concentration of hyaluronate on the characteristics of foreskin fibroblast cells. Acta Biomater 6(6):2140–2147. doi:10.1016/j.actbio.2009.12.023, S1742-7061(09)00564-9 [pii]
43. Hung CT, Lima EG, Mauck RL, Takai E, LeRoux MA, Lu HH, Stark RG, Guo XE, Ateshian GA (2003) Anatomically shaped osteochondral constructs for articular cartilage repair. J Biomech 36(12):1853–1864. doi:S0021929003002136 [pii]
44. Hunziker EB (2002) Articular cartilage repair: basic science and clinical progress. A review of the current status and prospects. Osteoarthritis Cartilage 10(6):432–463. doi:10.1053/joca.2002.0801, S1063458402908010 [pii]
45. Hutmacher DW (2000) Scaffolds in tissue engineering bone and cartilage. Biomaterials 21(24):2529–2543. doi:S0142961200001216 [pii]
46. Jiang CC, Chiang H, Liao CJ, Lin YJ, Kuo TF, Shieh CS, Huang YY, Tuan RS (2007) Repair of porcine articular cartilage defect with a biphasic osteochondral composite. J Orthop Res 25(10):1277–1290. doi:10.1002/jor.20442
47. Kandel RA, Grynpas M, Pilliar R, Lee J, Wang J, Waldman S, Zalzal P, Hurtig M, Team CI-BoST (2006) Repair of osteochondral defects with biphasic cartilage-calcium polyphosphate constructs in a sheep model. Biomaterials 27(22):4120–4131. doi:10.1016/j.biomaterials.2006.03.005, S0142-9612(06)00214-6 [pii]
48. Karageorgiou V, Kaplan D (2005) Porosity of 3D biomaterial scaffolds and osteogenesis. Biomaterials 26(27):5474–5491. doi:10.1016/j.biomaterials.2005.02.002
49. Kawanishi M, Oura A, Furukawa K, Fukubayashi T, Nakamura K, Tateishi T, Ushida T (2007) Redifferentiation of dedifferentiated bovine articular chondrocytes enhanced by cyclic hydrostatic pressure under a gas-controlled system. Tissue Eng 13(5):957–964. doi:10.1089/ten.2006.0176
50. Keeney M, Pandit A (2009) The osteochondral junction and its repair via bi-phasic tissue engineering scaffolds. Tissue Eng Part B Rev 15(1):55–73. doi:10.1089/ten.teb.2008.0388, 10.1089/ten.teb.2008.0388 [pii]
51. Kim K, Yeatts A, Dean D, Fisher JP (2010) Stereolithographic bone scaffold design parameters: osteogenic differentiation and signal expression. Tissue Eng Part B Rev 16(5):523–539. doi:10.1089/ten.TEB.2010.0171
52. Koga H, Shimaya M, Muneta T, Nimura A, Morito T, Hayashi M, Suzuki S, Ju YJ, Mochizuki T, Sekiya I (2008) Local adherent technique for transplanting mesenchymal stem cells as a potential treatment of cartilage defect. Arthritis Res Ther 10(4):R84. doi:10.1186/ar2460, ar2460 [pii]
53. Kon E, Delcogliano M, Filardo G, Busacca M, Di Martino A, Marcacci M (2011) Novel nano-composite multilayered biomaterial for osteochondral regeneration: a pilot clinical trial. Am J Sports Med 39(6):1180–1190. doi:10.1177/0363546510392711, 0363546510392711 [pii]
54. Kon E, Delcogliano M, Filardo G, Fini M, Giavaresi G, Francioli S, Martin I, Pressato D, Arcangeli E, Quarto R, Sandri M, Marcacci M (2010) Orderly osteochondral regeneration in a sheep model using a novel nano-composite multilayered biomaterial. J Orthop Res 28(1):116–124. doi:10.1002/jor.20958
55. Kon E, Filardo G, Di Martino A, Busacca M, Moio A, Perdisa F, Marcacci M (2013a) Clinical results and MRI evolution of a nano-composite multilayered biomaterial for osteochondral regeneration at 5 years. Am J Sports Med. doi:0363546513505434 [pii] 10.1177/0363546513505434 [doi]
56. Kon E, Filardo G, Robinson D, Eisman JA, Levy A, Zaslav K, Shani J, Altschuler N (2013b) Osteochondral regeneration using a novel aragonite-hyaluronate bi-phasic scaffold in a goat model. Knee Surg Sports Traumatol Arthrosc. doi:10.1007/s00167-013-2467-2 [doi]
57. Kurz B, Domm C, Jin M, Sellckau R, Schunke M (2004) Tissue engineering of articular cartilage under the influence of collagen I/III membranes and low oxygen tension. Tissue Eng 10:1277–1286. doi:10.1089/ten.2004.10.1277
58. Lawrence RC, Felson DT, Helmick CG, Arnold LM, Choi H, Deyo RA, Gabriel S, Hirsch R, Hochberg MC, Hunder GG, Jordan JM, Katz JN, Kremers HM, Wolfe F (2008) Estimates of the prevalence of arthritis and other rheumatic conditions in the United States. Part II. Arthritis Rheum 58(1):26–35. doi:10.1002/art.23176
59. Lee M, Wu BM (2012) Recent advances in 3D printing of tissue engineering scaffolds. Methods Mole Biol (Clifton, NJ) 868:257–267. doi:10.1007/978-1-61779-764-4_15

60. Levett PA, Melchels FP, Schrobback K, Hutmacher DW, Malda J, Klein TJ (2013) Chondrocyte redifferentiation and construct mechanical property development in single-component photocrosslinkable hydrogels. J Biomed Mater Res A. doi:10.1002/jbm.a.34924 [doi]
61. Li WJ, Cooper JA Jr, Mauck RL, Tuan RS (2006) Fabrication and characterization of six electrospun poly(alpha-hydroxy ester)-based fibrous scaffolds for tissue engineering applications. Acta Biomater 2(4):377–385. doi:10.1016/j.actbio.2006.02.005, S1742-7061(06)00021-3 [pii]
62. Li WJ, Mauck RL, Cooper JA, Yuan X, Tuan RS (2007) Engineering controllable anisotropy in electrospun biodegradable nanofibrous scaffolds for musculoskeletal tissue engineering. J Biomech 40(8):1686–1693. doi:10.1016/j.jbiomech.2006.09.004, S0021-9290(06)00318-6 [pii]
63. Lin H, Zhang D, Alexander PG, Yang G, Tan J, Cheng AW, Tuan RS (2013) Application of visible light-based projection stereolithography for live cell-scaffold fabrication with designed architecture. Biomaterials 34(2):331–339. doi:10.1016/j.biomaterials.2012.09.048, S0142-9612(12)01056-3 [pii]
64. Lynch JA, Parimi N, Chaganti RK, Nevitt MC, Lane NE, Study of Osteoporotic Fractures Research G (2009) The association of proximal femoral shape and incident radiographic hip OA in elderly women. Osteoarthritis Cartilage 17(10):1313–1318. doi:10.1016/j.joca.2009.04.011, S1063-4584(09)00114-9 [pii]
65. Madry H, van Dijk CN, Mueller-Gerbl M (2010) The basic science of the subchondral bone. Knee Surg Sports Traumatol Arthrosc 18(4):419–433. doi:10.1007/s00167-010-1054-z
66. Mannoni A, Briganti MP, Di Bari M, Ferrucci L, Costanzo S, Serni U, Masotti G, Marchionni N (2003) Epidemiological profile of symptomatic osteoarthritis in older adults: a population based study in Dicomano, Italy. Ann Rheum Dis 62(6):576–578
67. Mano JF, Reis RL (2007) Osteochondral defects: present situation and tissue engineering approaches. J Tissue Eng Regen Med 1(4):261–273. doi:10.1002/term.37
68. Marcacci M, Berruto M, Brocchetta D, Delcogliano A, Ghinelli D, Gobbi A, Kon E, Pederzini L, Rosa D, Sacchetti GL, Stefani G, Zanasi S (2005) Articular cartilage engineering with Hyalograft C: 3-year clinical results. Clin Orthop Relat Res 435:96–105. doi:00003086-200506000-00015 [pii]
69. Marquass B, Somerson JS, Hepp P, Aigner T, Schwan S, Bader A, Josten C, Zscharnack M, Schulz RM (2010) A novel MSC-seeded triphasic construct for the repair of osteochondral defects. J Orthop Res 28(12):1586–1599. doi:10.1002/jor.21173
70. Martin I, Miot S, Barbero A, Jakob M, Wendt D (2007) Osteochondral tissue engineering. J Biomech 40(4):750–765. doi:10.1016/j.jbiomech.2006.03.008, S0021-9290(06)00096-0 [pii]
71. Martin MJ, Muotri A, Gage F, Varki A (2005) Human embryonic stem cells express an immunogenic nonhuman sialic acid. Nat Med 11(2):228–232. doi:10.1038/nm1181, nm1181 [pii]
72. Mente PL, Lewis JL (1994) Elastic modulus of calcified cartilage is an order of magnitude less than that of subchondral bone. J Orthop Res 12(5):637–647. doi:10.1002/jor.1100120506
73. Miao X, Tan DM, Li J, Xiao Y, Crawford R (2008) Mechanical and biological properties of hydroxyapatite/tricalcium phosphate scaffolds coated with poly(lactic-co-glycolic acid). Acta Biomater 4(3):638–645. doi:10.1016/j.actbio.2007.10.006, S1742-7061(07)00172-9 [pii]
74. Minas T, Gomoll AH, Rosenberger R, Royce RO, Bryant T (2009) Increased failure rate of autologous chondrocyte implantation after previous treatment with marrow stimulation techniques. Am J Sports Med 37(5):902–908. doi:10.1177/0363546508330137, 0363546508330137 [pii]
75. Miot S, Brehm W, Dickinson S, Sims T, Wixmerten A, Longinotti C, Hollander AP, Mainil-Varlet P, Martin I (2012) Influence of in vitro maturation of engineered cartilage on the outcome of osteochondral repair in a goat model. Eur Cell Mater 23:222–236, vol023a17 [pii]
76. Mobasheri A (2012) Osteoarthritis year 2012 in review: biomarkers. Osteoarthritis Cartilage 20(12):1451–1464. doi:10.1016/j.joca.2012.07.009, S1063-4584(12)00897-7 [pii]
77. Mosher TJ, Walker EA, Petscavage-Thomas J, Guermazi A (2013) Osteoarthritis year 2013 in review: imaging. Osteoarthritis Cartilage 21(10):1425–1435. doi:10.1016/j.joca.2013.07.010, S1063-4584(13)00895-9 [pii]
78. Murphy L, Helmick CG (2012) The impact of osteoarthritis in the United States: a population-health perspective. Am J Nurs 112(3 Suppl 1):S13–S19. doi:10.1097/01.naj.0000412646.80054.21
79. Murphy SV, Atala A (2014) 3D bioprinting of tissues and organs. Nat Biotechnol 32(8):773–785. doi:10.1038/nbt.2958
80. Nakamura N, Hui J, Koizumi K, Yasui Y, Nishii T, Lad D, Karnatzikos G, Gobbi A (2014) Stem cell therapy in cartilage repair – culture-free and cell culture–based methods. Oper Tech Orthop 24(1):54–60. doi:10.1053/j.oto.2014.02.006
81. Nooeaid P, Salih V, Beier JP, Boccaccini AR (2012) Osteochondral tissue engineering: scaffolds, stem cells and applications. J Cell Mol Med 16(10):2247–2270. doi:10.1111/j.1582-4934.2012.01571.x
82. O'Shea TM, Miao X (2008) Bilayered scaffolds for osteochondral tissue engineering. Tissue Eng Part B Rev 14(4):447–464. doi:10.1089/ten.teb.2008.0327
83. Oegema TR Jr, Carpenter RJ, Hofmeister F, Thompson RC Jr (1997) The interaction of the zone of calcified cartilage and subchondral bone in osteoarthritis. Microsc Res Tech 37(4):324–332. doi:10.1002/(SICI)1097-0029(19970515)37:4<324::AID-JEMT7>3.0.CO;2-K,

10.1002/(SICI)1097-0029(19970515)37:4<324::AID-JEMT7>3.0.CO;2-K [pii]
84. Oliveira JM, Rodrigues MT, Silva SS, Malafaya PB, Gomes ME, Viegas CA, Dias IR, Azevedo JT, Mano JF, Reis RL (2006) Novel hydroxyapatite/chitosan bilayered scaffold for osteochondral tissue-engineering applications: scaffold design and its performance when seeded with goat bone marrow stromal cells. Biomaterials 27(36):6123–6137. doi:10.1016/j.biomaterials.2006.07.034, S0142-9612(06)00659-4 [pii]
85. Orth P, Cucchiarini M, Kohn D, Madry H (2013) Alterations of the subchondral bone in osteochondral repair – translational data and clinical evidence. Eur Cell Mater 25:299–316, discussion 314–296. doi:vol025a21 [pii]
86. Orth P, Meyer HL, Goebel L, Eldracher M, Ong MF, Cucchiarini M, Madry H (2013) Improved repair of chondral and osteochondral defects in the ovine trochlea compared with the medial condyle. J Orthop Res 31(11):1772–1779. doi:10.1002/jor.22418
87. Panseri S, Russo A, Cunha C, Bondi A, Di Martino A, Patella S, Kon E (2012) Osteochondral tissue engineering approaches for articular cartilage and subchondral bone regeneration. Knee Surg Sports Traumatol Arthrosc 20(6):1182–1191. doi:10.1007/s00167-011-1655-1
88. Peat G, McCarney R, Croft P (2001) Knee pain and osteoarthritis in older adults: a review of community burden and current use of primary health care. Ann Rheum Dis 60(2):91–97
89. Pena J, Corrales T, Izquierdo-Barba I, Serrano MC, Portoles MT, Pagani R, Vallet-Regi M (2006) Alkaline-treated poly(epsilon-caprolactone) films: degradation in the presence or absence of fibroblasts. J Biomed Mater Res A 76(4):788–797. doi:10.1002/jbm.a.30547
90. Ravi B, Escott B, Shah PS, Jenkinson R, Chahal J, Bogoch E, Kreder H, Hawker G (2012) A systematic review and meta-analysis comparing complications following total joint arthroplasty for rheumatoid arthritis versus for osteoarthritis. Arthritis Rheum 64(12):3839–3849. doi:10.1002/art.37690
91. Re'em T, Witte F, Willbold E, Ruvinov E, Cohen S (2012) Simultaneous regeneration of articular cartilage and subchondral bone induced by spatially presented TGF-beta and BMP-4 in a bilayer affinity binding system. Acta Biomater 8(9):3283–3293. doi:10.1016/j.actbio.2012.05.014, S1742-7061(12)00218-8 [pii]
92. Ren J, Zhao P, Ren T, Gu S, Pan K (2008) Poly (D,L-lactide)/nano-hydroxyapatite composite scaffolds for bone tissue engineering and biocompatibility evaluation. J Mater Sci Mater Med 19(3):1075–1082. doi:10.1007/s10856-007-3181-8
93. Reyes R, Delgado A, Sanchez E, Fernandez A, Hernandez A, Evora C (2012) Repair of an osteochondral defect by sustained delivery of BMP-2 or TGFbeta1 from a bilayered alginate-PLGA scaffold. J Tissue Eng Regen Med. doi:10.1002/term.1549 [doi]
94. Reyes R, Delgado A, Solis R, Sanchez E, Hernandez A, San Roman J, Evora C (2013) Cartilage repair by local delivery of TGF-beta1 or BMP-2 from a novel, segmented polyurethane/polylactic-co-glycolic bilayered scaffold. J Biomed Mater Res A. doi:10.1002/jbm.a.34769 [doi]
95. Rodrigues MT, Gomes ME, Reis RL (2011) Current strategies for osteochondral regeneration: from stem cells to pre-clinical approaches. Curr Opin Biotechnol 22(5):726–733. doi:10.1016/j.copbio.2011.04.006, S0958-1669(11)00068-1 [pii]
96. Roemer FW, Guermazi A (2012) Osteoarthritis year 2012 in review: imaging. Osteoarthritis Cartilage 20(12):1440–1446. doi:10.1016/j.joca.2012.07.008, S1063-4584(12)00896-5 [pii]
97. Rose FR, Hou Q, Oreffo RO (2004) Delivery systems for bone growth factors – the new players in skeletal regeneration. J Pharm Pharmacol 56(4):415–427. doi:10.1211/0022357023312
98. Sadoghi P, Liebensteiner M, Agreiter M, Leithner A, Bohler N, Labek G (2013) Revision surgery after total joint arthroplasty: a complication-based analysis using worldwide arthroplasty registers. J Arthroplasty 28(8):1329–1332. doi:10.1016/j.arth.2013.01.012
99. Sakaguchi Y, Sekiya I, Yagishita K, Muneta T (2005) Comparison of human stem cells derived from various mesenchymal tissues: superiority of synovium as a cell source. Arthritis Rheum 52(8):2521–2529. doi:10.1002/art.21212
100. Salgado AJ, Coutinho OP, Reis RL (2004) Bone tissue engineering: state of the art and future trends. Macromol Biosci 4(8):743–765. doi:10.1002/mabi.200400026
101. Sarasam AR, Krishnaswamy RK, Madihally SV (2006) Blending chitosan with polycaprolactone: effects on physicochemical and antibacterial properties. Biomacromolecules 7(4):1131–1138. doi:10.1021/bm050935d
102. Schek RM, Taboas JM, Segvich SJ, Hollister SJ, Krebsbach PH (2004) Engineered osteochondral grafts using biphasic composite solid free-form fabricated scaffolds. Tissue Eng 10(9–10):1376–1385. doi:10.1089/ten.2004.10.1376
103. Schleicher I, Lips KS, Sommer U, Schappat I, Martin AP, Szalay G, Hartmann S, Schnettler R (2013) Biphasic scaffolds for repair of deep osteochondral defects in a sheep model. J Surg Res 183(1):184–192. doi:10.1016/j.jss.2012.11.036, S0022-4804(12)01910-5 [pii]
104. Schnabel M, Marlovits S, Eckhoff G, Fichtel I, Gotzen L, Vecsei V, Schlegel J (2002) Dedifferentiation-associated changes in morphology and gene expression in primary human articular chondrocytes in cell culture. Osteoarthritis Cartilage 10(1):62–70. doi:10.1053/joca.2001.0482, S1063458401904820 [pii]
105. Seo SJ, Mahapatra C, Singh RK, Knowles JC, Kim HW (2014) Strategies for osteochondral repair: focus on scaffolds. J Tissue Eng 5:2041731414541850. doi: 10.1177/2041731414541850

106. Shafiee A, Soleimani M, Chamheidari GA, Seyedjafari E, Dodel M, Atashi A, Gheisari Y (2011) Electrospun nanofiber-based regeneration of cartilage enhanced by mesenchymal stem cells. J Biomed Mater Res A 99(3):467–478. doi:10.1002/jbm.a.33206
107. Sherwood JK, Riley SL, Palazzolo R, Brown SC, Monkhouse DC, Coates M, Griffith LG, Landeen LK, Ratcliffe A (2002) A three-dimensional osteochondral composite scaffold for articular cartilage repair. Biomaterials 23(24):4739–4751. doi:S0142961202002235 [pii]
108. Shimomura K, Ando W, Tateishi K, Nansai R, Fujie H, Hart DA, Kohda H, Kita K, Kanamoto T, Mae T, Nakata K, Shino K, Yoshikawa H, Nakamura N (2010) The influence of skeletal maturity on allogenic synovial mesenchymal stem cell-based repair of cartilage in a large animal model. Biomaterials 31(31):8004–8011. doi:10.1016/j.biomaterials.2010.07.017, S0142-9612(10)00858-6 [pii]
109. Shimomura K, Moriguchi Y, Ando W, Nansai R, Fujie H, Hart DA, Gobbi A, Kita K, Horibe S, Shino K, Yoshikawa H, Nakamura N (2014a) Osteochondral repair using a scaffold-free tissue-engineered construct derived from synovial mesenchymal stem cells and a hydroxyapatite-based artificial bone. Tissue Eng Part A. doi:10.1089/ten.tea.2013.0414 [doi]
110. Shimomura K, Moriguchi Y, Murawski CD, Yoshikawa H, Nakamura N (2014b) Osteochondral tissue engineering with biphasic scaffold: current strategies and techniques. Tissue Eng Part B Rev. doi:10.1089/ten.TEB.2013.0543 [doi]
111. Shintani N, Hunziker EB (2007) Chondrogenic differentiation of bovine synovium: bone morphogenetic proteins 2 and 7 and transforming growth factor beta1 induce the formation of different types of cartilaginous tissue. Arthritis Rheum 56(6):1869–1879. doi:10.1002/art.22701
112. Sosio C, Di Giancamillo A, Deponti D, Gervaso F, Scalera F, Melato M, Campagnol M, Boschetti F, Nonis A, Domeneghini C, Sannino A, Peretti GM (2014) Osteochondral repair by a novel interconnecting collagen-hydroxyapatite substitute: a large-animal study. Tissue Eng Part A. doi:10.1089/ten.TEA.2014.0129
113. Sundelacruz S, Kaplan DL (2009) Stem cell- and scaffold-based tissue engineering approaches to osteochondral regenerative medicine. Semin Cell Dev Biol 20(6):646–655. doi:10.1016/j.semcdb.2009.03.017, S1084-9521(09)00069-X [pii]
114. Takahashi K, Yamanaka S (2006) Induction of pluripotent stem cells from mouse embryonic and adult fibroblast cultures by defined factors. Cell 126(4):663–676. doi:10.1016/j.cell.2006.07.024
115. Takahashi N, Knudson CB, Thankamony S, Ariyoshi W, Mellor L, Im HJ, Knudson W (2010) Induction of CD44 cleavage in articular chondrocytes. Arthritis Rheum 62(5):1338–1348. doi:10.1002/art.27410
116. Takahashi T, Ogasawara T, Asawa Y, Mori Y, Uchinuma E, Takato T, Hoshi K (2007) Three-dimensional microenvironments retain chondrocyte phenotypes during proliferation culture. Tissue Eng 13(7):1583–1592. doi:10.1089/ten.2006.0322
117. Tamai N, Myoui A, Hirao M, Kaito T, Ochi T, Tanaka J, Takaoka K, Yoshikawa H (2005) A new biotechnology for articular cartilage repair: subchondral implantation of a composite of interconnected porous hydroxyapatite, synthetic polymer (PLA-PEG), and bone morphogenetic protein-2 (rhBMP-2). Osteoarthritis Cartilage 13(5):405–417. doi:10.1016/j.joca.2004.12.014, S1063-4584(04)00289-4 [pii]
118. Tan W, Twomey J, Guo D, Madhavan K, Li M (2010) Evaluation of nanostructural, mechanical, and biological properties of collagen-nanotube composites. IEEE Trans Nanobioscience 9(2):111–120. doi:10.1109/TNB.2010.2043367
119. Tsumaki N, Okada M, Yamashita A (2014) iPS cell technologies and cartilage regeneration. Bone. doi:10.1016/j.bone.2014.07.011
120. Vos T, Flaxman AD, Naghavi M, Lozano R, Michaud C, Ezzati M, Shibuya K, Salomon JA, Abdalla S, Aboyans V, Abraham J, Ackerman I, Aggarwal R, Ahn SY, Ali MK, Alvarado M, Anderson HR, Anderson LM, Andrews KG, Atkinson C, Baddour LM, Bahalim AN, Barker-Collo S, Barrero LH, Bartels DH, Basanez MG, Baxter A, Bell ML, Benjamin EJ, Bennett D, Bernabe E, Bhalla K, Bhandari B, Bikbov B, Bin Abdulhak A, Birbeck G, Black JA, Blencowe H, Blore JD, Blyth F, Bolliger I, Bonaventure A, Boufous S, Bourne R, Boussinesq M, Braithwaite T, Brayne C, Bridgett L, Brooker S, Brooks P, Brugha TS, Bryan-Hancock C, Bucello C, Buchbinder R, Buckle G, Budke CM, Burch M, Burney P, Burstein R, Calabria B, Campbell B, Canter CE, Carabin H, Carapetis J, Carmona L, Cella C, Charlson F, Chen H, Cheng AT, Chou D, Chugh SS, Coffeng LE, Colan SD, Colquhoun S, Colson KE, Condon J, Connor MD, Cooper LT, Corriere M, Cortinovis M, de Vaccaro KC, Couser W, Cowie BC, Criqui MH, Cross M, Dabhadkar KC, Dahiya M, Dahodwala N, Damsere-Derry J, Danaei G, Davis A, De Leo D, Degenhardt L, Dellavalle R, Delossantos A, Denenberg J, Derrett S, Des Jarlais DC, Dharmaratne SD, Dherani M, Diaz-Torne C, Dolk H, Dorsey ER, Driscoll T, Duber H, Ebel B, Edmond K, Elbaz A, Ali SE, Erskine H, Erwin PJ, Espindola P, Ewoigbokhan SE, Farzadfar F, Feigin V, Felson DT, Ferrari A, Ferri CP, Fevre EM, Finucane MM, Flaxman S, Flood L, Foreman K, Forouzanfar MH, Fowkes FG, Franklin R, Fransen M, Freeman MK, Gabbe BJ, Gabriel SE, Gakidou E, Ganatra HA, Garcia B, Gaspari F, Gillum RF, Gmel G, Gosselin R, Grainger R, Groeger J, Guillemin F, Gunnell D, Gupta R, Haagsma J, Hagan H, Halasa YA, Hall W, Haring D, Haro JM, Harrison JE, Havmoeller R, Hay RJ, Higashi H, Hill C, Hoen B, Hoffman H, Hotez PJ, Hoy D, Huang JJ, Ibeanusi SE, Jacobsen KH, James SL, Jarvis D, Jasrasaria R, Jayaraman S, Johns N, Jonas JB, Karthikeyan

G, Kassebaum N, Kawakami N, Keren A, Khoo JP, King CH, Knowlton LM, Kobusingye O, Koranteng A, Krishnamurthi R, Lalloo R, Laslett LL, Lathlean T, Leasher JL, Lee YY, Leigh J, Lim SS, Limb E, Lin JK, Lipnick M, Lipshultz SE, Liu W, Loane M, Ohno SL, Lyons R, Ma J, Mabweijano J, MacIntyre MF, Malekzadeh R, Mallinger L, Manivannan S, Marcenes W, March L, Margolis DJ, Marks GB, Marks R, Matsumori A, Matzopoulos R, Mayosi BM, McAnulty JH, McDermott MM, McGill N, McGrath J, Medina-Mora ME, Meltzer M, Mensah GA, Merriman TR, Meyer AC, Miglioli V, Miller M, Miller TR, Mitchell PB, Mocumbi AO, Moffitt TE, Mokdad AA, Monasta L, Montico M, Moradi-Lakeh M, Moran A, Morawska L, Mori R, Murdoch ME, Mwaniki MK, Naidoo K, Nair MN, Naldi L, Narayan KM, Nelson PK, Nelson RG, Nevitt MC, Newton CR, Nolte S, Norman P, Norman R, O'Donnell M, O'Hanlon S, Olives C, Omer SB, Ortblad K, Osborne R, Ozgediz D, Page A, Pahari B, Pandian JD, Rivero AP, Patten SB, Pearce N, Padilla RP, Perez-Ruiz F, Perico N, Pesudovs K, Phillips D, Phillips MR, Pierce K, Pion S, Polanczyk GV, Polinder S, Pope CA 3rd, Popova S, Porrini E, Pourmalek F, Prince M, Pullan RL, Ramaiah KD, Ranganathan D, Razavi H, Regan M, Rehm JT, Rein DB, Remuzzi G, Richardson K, Rivara FP, Roberts T, Robinson C, De Leon FR, Ronfani L, Room R, Rosenfeld LC, Rushton L, Sacco RL, Saha S, Sampson U, Sanchez-Riera L, Sanman E, Schwebel DC, Scott JG, Segui-Gomez M, Shahraz S, Shepard DS, Shin H, Shivakoti R, Singh D, Singh GM, Singh JA, Singleton J, Sleet DA, Sliwa K, Smith E, Smith JL, Stapelberg NJ, Steer A, Steiner T, Stolk WA, Stovner LJ, Sudfeld C, Syed S, Tamburlini G, Tavakkoli M, Taylor HR, Taylor JA, Taylor WJ, Thomas B, Thomson WM, Thurston GD, Tleyjeh IM, Tonelli M, Towbin JA, Truelsen T, Tsilimbaris MK, Ubeda C, Undurraga EA, van der Werf MJ, van Os J, Vavilala MS, Venketasubramanian N, Wang M, Wang W, Watt K, Weatherall DJ, Weinstock MA, Weintraub R, Weisskopf MG, Weissman MM, White RA, Whiteford H, Wiersma ST, Wilkinson JD, Williams HC, Williams SR, Witt E, Wolfe F, Woolf AD, Wulf S, Yeh PH, Zaidi AK, Zheng ZJ, Zonies D, Lopez AD, Murray CJ, AlMazroa MA, Memish ZA (2012) Years lived with disability (YLDs) for 1160 sequelae of 289 diseases and injuries 1990–2010: a systematic analysis for the global burden of disease study 2010. Lancet 380(9859):2163–2196. doi:10.1016/s0140-6736(12)61729-2

121. Yamasaki N, Hirao M, Nanno K, Sugiyasu K, Tamai N, Hashimoto N, Yoshikawa H, Myoui A (2009) A comparative assessment of synthetic ceramic bone substitutes with different composition and microstructure in rabbit femoral condyle model. J Biomed Mater Res B Appl Biomater 91(2):788–798. doi:10.1002/jbm.b.31457
122. Yang PJ, Temenoff JS (2009) Engineering orthopedic tissue interfaces. Tissue Eng Part B Rev 15(2):127–141. doi:10.1089/ten.teb.2008.0371
123. Zhang S, Chen L, Jiang Y, Cai Y, Xu G, Tong T, Zhang W, Wang L, Ji J, Shi P, Ouyang HW (2013) Bi-layer collagen/microporous electrospun nanofiber scaffold improves the osteochondral regeneration. Acta Biomater 9(7):7236–7247. doi:10.1016/j.actbio.2013.04.003, S1742-7061(13)00175-X [pii]
124. Zhang W, Chen J, Tao J, Hu C, Chen L, Zhao H, Xu G, Heng BC, Ouyang HW (2013) The promotion of osteochondral repair by combined intra-articular injection of parathyroid hormone-related protein and implantation of a bi-layer collagen-silk scaffold. Biomaterials 34(25):6046–6057. doi:10.1016/j.biomaterials.2013.04.055, S0142-9612(13)00529-2 [pii]
125. Zhang W, Moskowitz RW, Nuki G, Abramson S, Altman RD, Arden N, Bierma-Zeinstra S, Brandt KD, Croft P, Doherty M, Dougados M, Hochberg M, Hunter DJ, Kwoh K, Lohmander LS, Tugwell P (2007) OARSI recommendations for the management of hip and knee osteoarthritis, part I: critical appraisal of existing treatment guidelines and systematic review of current research evidence. Osteoarthritis Cartilage 15(9):981–1000. doi:10.1016/j.joca.2007.06.014, S1063-4584(07)00234-8 [pii]
126. Zhang W, Moskowitz RW, Nuki G, Abramson S, Altman RD, Arden N, Bierma-Zeinstra S, Brandt KD, Croft P, Doherty M, Dougados M, Hochberg M, Hunter DJ, Kwoh K, Lohmander LS, Tugwell P (2008) OARSI recommendations for the management of hip and knee osteoarthritis, part II: OARSI evidence-based, expert consensus guidelines. Osteoarthritis Cartilage 16(2):137–162. doi:10.1016/j.joca.2007.12.013, S1063-4584(07)00397-4 [pii]
127. Zhang W, Nuki G, Moskowitz RW, Abramson S, Altman RD, Arden NK, Bierma-Zeinstra S, Brandt KD, Croft P, Doherty M, Dougados M, Hochberg M, Hunter DJ, Kwoh K, Lohmander LS, Tugwell P (2010) OARSI recommendations for the management of hip and knee osteoarthritis: part III: changes in evidence following systematic cumulative update of research published through January 2009. Osteoarthritis Cartilage 18(4):476–499. doi:10.1016/j.joca.2010.01.013, S1063-4584(10)00046-4 [pii]
128. Zheng MH, Willers C, Kirilak L, Yates P, Xu J, Wood D, Shimmin A (2007) Matrix-induced autologous chondrocyte implantation (MACI): biological and histological assessment. Tissue Eng 13(4):737–746. doi:10.1089/ten.2006.0246

The Structure, Function, and Healing of the Meniscus

24

Elcil Kaya Biçer, Semih Aydoğdu, and Hakkı Sur

Abstract

The menisci have indispensable functions in the knee joint such as load bearing, shock absorption, articular nutrition, and joint lubrication, along with roles in maintaining joint stability and proprioception. Meniscal tissue loss results in early degenerative changes in the knee joint because of alterations in the loading pattern of articular cartilages. With the improved understanding of the fundamental roles of the menisci and the detrimental effects of their absence, repair of torn menisci, instead of amputation, is supported today. Its healing potential is directly related to its vascularization. The tears of the less-vascularized zone are suggested to be not only repaired but also augmented with various techniques. If it is indicated to perform a segmental meniscectomy in a knee without arthritic changes, it is possible to replace the removed part with a synthetic matrix graft. In patients who had a total meniscectomy, meniscal allograft transplantation can be regarded as a treatment option.

Learning Outcomes

- Basic embryologic, anatomic, histological, and biochemical functions of menisci
- Biomechanical characteristics and functions of the meniscus
- Types and features of meniscal injuries
- Healing of meniscal tears
- Treatment strategies of meniscal tears

Terminology

Aggregan Also known as chondroitin sulfate proteoglycan 1; a proteoglycan found in the extracellular matrix of chondral tissue that has a role in resisting compressive stresses in cartilage

Allograft Transplant of cells, tissues, or organs from a genetically nonidentical member of the same species

Biglycan A proteoglycan that consists of a small core protein with two glycosaminoglycan chains attached to it; found in the extracellular matrix of bone, cartilage, and tendon tissues

E.K. Biçer • S. Aydoğdu (✉) • H. Sur
Faculty of Medicine, Department of Orthopedics and Traumatology, Ege University,
Bornova, Izmir, Turkey
e-mail: semih.aydogdu@ege.edu.tr

F. Korkusuz (ed.), *Musculoskeletal Research and Basic Science*,
DOI 10.1007/978-3-319-20777-3_24

Bipedal walking Locomotion with two rear limbs

Chondrogenic Cartilage forming

Chondrification Conversion or formation of cartilage

Compressive stress Stress on materials leading to a smaller volume or shortening

Cytokine A small non-hormonal protein important in cellular signaling and immune response

Decorin A small proteoglycan structurally similar to biglycan, found in the connective tissue

Elastic return Returning to the original form of material after the stress has ceased. Materials deformed within their elastic ranges have this capacity

Endostatin A vascular endothelial growth factor inhibitor

Fibronectin A glycoprotein which is a major component of extracellular matrix and has roles in cellular processes including adhesion, growth, and differentiation

Fibromodulin A small proteoglycan probably having a role in the gathering of extracellular matrix

Gestational period The period which begins from fertilization and continues until birth

Glycosaminoglycan Long polysaccharide chains containing repeating disaccharide units. They are hydrophilic molecules and have roles in lubrication and shock absorption

Glycoprotein A protein which is glycosylated and mostly important in cellular interactions

Growth factor Group of proteins that have roles in cellular interactions, signaling, differentiation, proliferation, etc

Lubrication Process of reducing wear on the opposing chondral surfaces of the joint by interposing a lubricant substance

Major histocompatibility (MHC) antigens Human leukocyte antigens presented on the cell surface; help the immune system to discriminate self-antigens from foreign ones

Matrix metalloproteinases (MMP) Zinc-dependent endopeptidases which degrade extracellular matrix proteins

Mechanoreceptors Specialized sensory receptors responding to mechanical stimulus

Mitogenic Causing mitosis

MR arthrography MR imaging following the injection of contrast material into the joint. This is direct MR arthrography. When performing an indirect MR arthrography, the appropriate contrast material is given via intravenous route

Neuroanatomy Neural structure of an organ or a part of the body

Nitric oxide (NO) A free radical and is important in cellular signaling; a powerful vasodilator

Platelet- rich plasma (PRP) Blood plasma enriched with autologous platelets containing growth hormones and cytokines

Polymer A compound formed by the repeated units

Postovulatory The period after ovulation (discharge of an ovum)

Proinflammatory Tending to cause inflammation

Proprioception Perception of the position of body parts relative to each other

Proteoglycans Glycosylated proteins found in the connective tissue; their functions depend on the proteins or the attached glycosaminoglycans

Tensile properties Properties which show how the material will react to forces when applied in tension

Trephination Surgical procedure of drilling a hole in the tissue

Thrombospondins Multifunctional proteins secreted from platelets and have antiangiogenic properties

Vascularization Formation of blood vessels

Introduction

The fibrocartilage semilunar structures of the knee joint, the medial and lateral menisci, have important roles in load bearing/transmission, shock absorption, articular nutrition, and joint lubrication. They also provide important contributions to stability and proprioception of the knee joint [11, 17, 21, 36, 38, 59]. The menisci are regarded as one of the most frequently injured structures of the musculoskeletal system. If their lesions are not treated properly, serious morbidity and a long-term progression to degenerative changes are mostly inevitable. Thus, treatment of meniscal lesions is of paramount importance. Today, it is suggested to preserve meniscal tissue in every possible occasion. Up-to-date treatment methods are based on this principle [17, 20, 40].

Embryological Development of Menisci

Histological studies in the fifth- and eighth-postovulatory-week-old human embryos revealed that knee joint resembled its adult counterpart [19]. The formation of the lower limb buds, which do not have separate joint structures yet, occurs at the fourth postovulatory week. The interzone between the femur and the tibia which will develop into the future knee joint becomes recognizable following chondrification of a mesenchymal template. The femorotibial interzone contains three layers: first and third ones are the femoral and tibial chondrogenic layers. The second layer in between these two is less dense based on which both the menisci and the cruciate ligaments would be formed [8, 19].

Both medial and lateral menisci are recognizable in the embryonic knees at the age of seven and a half and eight (in terms of postovulatory weeks); however the orientation of cells in the lateral meniscus resembles their final appearance more than that of the medial meniscus. At the eighth postovulatory week, the menisci are definitely recognizable and more cellular [8, 19].

During gestation whole meniscal tissue is vascular. This abundant vascularity is present until the third postnatal month. Beginning from this time point, the blood vessels in the inner part gradually disappear [57]. In the beginning, the concentration of endostatin, which is a vascular endothelial growth factor inhibitor, is low throughout the whole meniscal tissue; but after the third postnatal month, the cells located at the inner parts of the menisci start to secrete endostatin, which then accumulates. This explains why the inner part of the meniscal tissue loses its vascularity [46]. Around the age of 11, the inner part of the menisci becomes avascular (Fig. 24.1) [57].

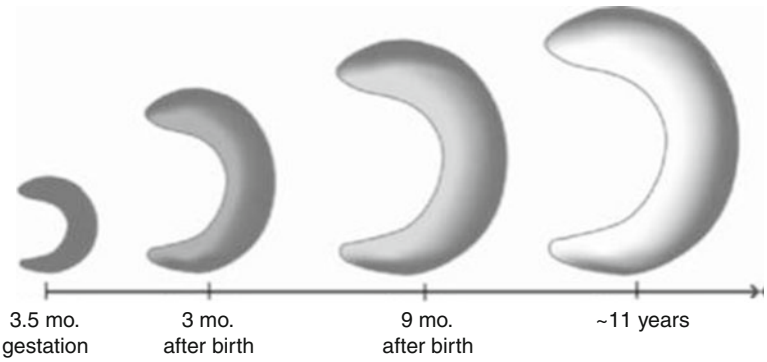

Fig. 24.1 Meniscus vascularity. During the gestational period, the whole meniscus is vascular. After birth, the inner part starts to lose its vascularity due to endostatin accumulation. Around the 11 years of age, the inner part becomes avascular (Reprinted from Springer Cellular and Molecular Bioengineering, Sanchez-Adams and Athanasiou [57], figure 3, with kind permission from Springer Science and Business Media)

During the gestational period, the developing menisci are highly cellular in the beginning and the nucleus–cytoplasm ratio is high. In time, these cells mature and the nucleus–cytoplasm ratio declines. While the number of cells decreases, their collagen production increases. Collagen fibers begin to orient in a circumferential manner. Locomotion and postnatal loading of the knee joint are thought to have important roles in the development of orientation of collagen fibers [8, 17].

Anatomy

Medial and lateral menisci which are located between femoral and tibial articular surfaces resemble a wedge in coronal plane. The two menisci are not completely identical. The medial meniscus has a crescent shape, anterior of which is wider when compared with its posterior part. However, the lateral meniscus is more circular, and its wideness remains the same throughout its anterior and posterior parts. The medial meniscus covers 60 % of the medial tibial plateau, whereas the lateral one covers 80 % of the lateral tibial plateau. Peripheral parts of the menisci are thick, convex, and continuous with the joint capsule. Their inner parts have thin, free ends. The upper surfaces of the menisci are concave which ease their articulation with the corresponding convex femoral articular surfaces. Their lower surfaces that attach to the tibia are flat. The congruency of the shapes of the menisci with their corresponding upper and lower articular surfaces diminish the friction emerging during joint motion [8, 17, 20, 57].

The anterior horns of both of the menisci are attached to each other via transverse intermeniscal ligament (Fig. 24.2). The anterior and posterior horns are attached to the tibia via insertional ligaments. The insertion site of the anterior horn of the medial meniscus is in the anterior intercondylar fossa which is just anterior to the anterior cruciate ligament (ACL). The posterior fibers of the anterior horn blend with the transverse meniscal ligament. The posterior horn is attached to the posterior intercondylar fossa which is situated between the posterior cruciate ligament (PCL) and the insertion site of the posterior horn of the lateral meniscus. The anterior horn of the lateral meniscus is attached close to the ACL, anterior to the tibial spines. The insertion sites of the anterior and posterior horns of the lateral meniscus are closer to each other when compared with that of the medial meniscus. The peripheral part of the medial meniscus is attached to the joint capsule via meniscotibial (coronary) ligaments. Also, the middle part of the medial meniscus is firmly attached to the deep part of medial collateral ligament. As a result of these anatomic characteristics, the mobility of the medial meniscus is limited. Unlikely, the lateral meniscus is not in relation with the lateral collateral ligament. In addition, there is the popliteal hiatus which is situated in the posterolateral part of the meniscus and constitutes one third of its posterior part with the popliteus tendon passing through and has no relation with the capsule. When compared with the medial meniscus, the lateral one is more mobile [11, 17, 20].

The posterior horn of the lateral meniscus is attached to the lateral part of the medial femoral condyle via anterior (Humphrey) and posterior (Wrisberg) meniscofemoral ligaments. The anterior meniscofemoral ligament passes anterior to PCL, and posterior to it, there is the posterior meniscofemoral ligament. The attachment site at the medial femoral condyle is in close proximity with the attachment site of PCL. As a result of studies conducted on cadaveric knees, a consensus has not been reached about the incidence and number of meniscofemoral ligaments. Though their function is not absolutely ascertained, it is suggested that they restrict the mobility of the lateral meniscus by pulling its posterior horn both anteriorly and medially throughout the range of motion [20, 22, 24].

The developmental variations of the lateral meniscus are more abundant than that of the

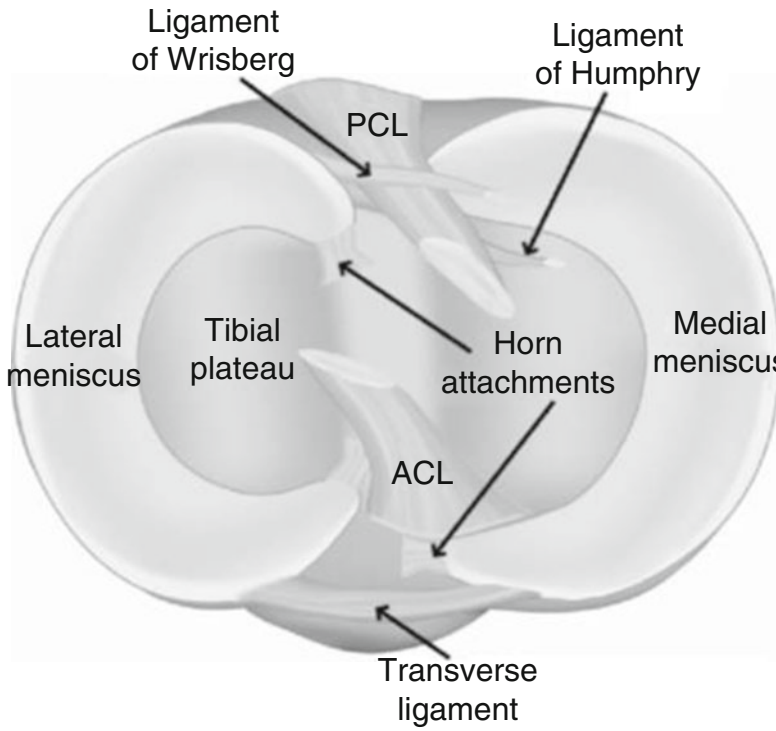

Fig. 24.2 The schematic axial showing the medial and lateral menisci. Anterior horns of the two menisci are attached to each other via the transverse meniscal ligament. The posterior horn of the lateral meniscus is attached to the lateral part of the medial femoral condyle via Humphrey and Wrisberg ligaments (Reprinted from Springer Cellular and Molecular Bioengineering, Sanchez-Adams and Athanasiou [57], figure 2 with kind permission from Springer Science and Business Media)

medial meniscus. Discoid meniscus is more commonly observed in the lateral meniscus. In the past, discoid meniscus was thought to be formed as a result of the cessation of development; however it was not possible to show that the meniscus possessed a discoid shape at any time during its development [8, 50].

Vascular Supply

The menisci of an adult knee are relatively avascular structures, and their vascular pattern is strongly related to its healing capacity. According to their vascularization, adult meniscus is divided into three zones. The outermost one third of it is regarded as the "red–red zone" which has an abundant blood supply. The middle one third part, named as the "red–white zone," has a scarce vascularization when compared with the red–red zone. The innermost one third is the avascular "white–white zone" (Fig. 24.3). When compared to its body, the insertion sites have richer vascularization [37].

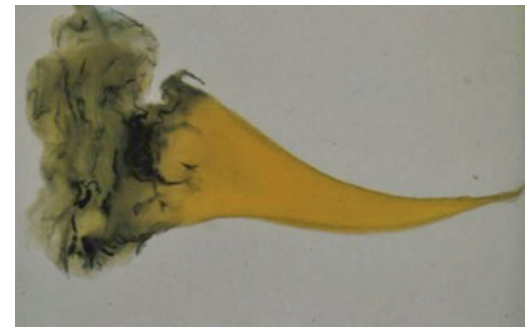

Fig. 24.3 Blood supply to adult's meniscus. Vascularization of the outer part of the meniscus from the perimeniscal plexus is observed (Reprinted from Arthroscopy: The Journal of Arthroscopic and Related Surgery, Stärke et al. [61], with permission from Elsevier)

Medial and lateral and superior and inferior geniculate arteries branching from the popliteal artery form a perimeniscal capillary plexus which

supplies the peripheral parts of the menisci. Both medial and lateral menisci have synovial folds over the peripheral parts of both femoral and tibial sides which possess short terminal vessels. Only the popliteal hiatus part of the lateral meniscus is devoid of this blood supply [9, 11, 21, 48].

Along with a few terminal branches of medial and lateral geniculate arteries, middle geniculate artery contributes to the vascularization of the menisci via the synovial folds of the anterior and posterior horns. These synovial vessels enter the tissue directly passing through the insertional ligaments and constitute short, terminal, endoligamentous vessels supplying the horns [7, 11].

The vascularization of the rest of the meniscal tissue is provided by either diffusion from the synovial fluid or mechanical pumping. Histological studies performed utilizing scanning electron microscopy revealed that there were canal-like structures opening to the surface of the menisci. The function of these canal systems has not been identified yet; nevertheless it is suggested that they had roles in the regulation of the hydrostatic pressure of the menisci and facilitation of liquid flow under loading conditions, providing supply to the avascular parts from the synovial fluid and blood vessels [1, 5].

In order to obtain diffusion from the synovial fluid, the menisci should be subjected to cyclic loading and stress relaxation provided by body weight and muscle force. During infancy since the menisci could not be exposed to loading conditions, it was claimed that diffusion from the synovial fluid did not contribute to their vascularization which was only supplied by blood vessels. Following the beginning of bipedal walking or after the muscles start to exert sufficient amount of forces on the menisci, the vascularization pattern changes. The menisci whole of which are supplied by blood vessels are replaced by adult-type menisci whose inner parts are avascular [21, 48].

Neuroanatomy of the Meniscus

Posterior articular branch of tibial nerve is responsible for most of the innervation of the meniscus. Medial articular branch of saphenous nerve also contributes to the innervation of the medial meniscus [15]. The larger nerves have a circumferential pattern in the perimeniscal tissue accompanying blood vessels. The smaller nerves or single axons have a radial course toward the outer one third of the meniscus. When compared with its middle part, the outer part of meniscal body is richer in nervous tissue, whereas the inner one third is devoid of it. Both the anterior and posterior horns possess more abundant neural tissue than the rest of the meniscus. As well as its vascularization, the majority of the nerves are observed in the horns and its periphery. The innervations of the medial and lateral menisci are alike [9, 15, 42].

Mechanoreceptors are specialized receptors that convert physical stimulus such as tension, compression, change of position, and acceleration to electrical neural stimulus. Mechanoreceptors are most commonly found in the horns of the menisci with the posterior horn having more than that of the anterior horn. In the horns and the periphery of the meniscus, three types of mechanoreceptors were identified. Type I (Ruffini) mechanoreceptors are responsible for the sensation of static joint positioning and changes in pressure. These are slowly adapting receptors with low threshold for activation. Type II (Pacini) mechanoreceptors are rapidly adapting receptors with also low threshold for activation which sense changes in tension and acceleration. Type III (Golgi) mechanoreceptors are slowly adapting receptors with high threshold for activation which are activated when the extremes of range of joint motion are achieved and initiate a protective reflex inhibition [1, 7, 9, 17, 21].

The proprioceptive information supplied from the menisci reaches the central nervous system which may contribute to the anteroposterior translation of femur over tibial plateau. In addition to the mechanical characteristics of menisci, their proprioceptive features may also have some effects in the knee joint stability. The proprioception of the knee joint was shown to decrease significantly in case of isolated meniscal injuries [1, 21, 30].

The presence of free nerve endings (nociceptors) was demonstrated in the periphery of

the menisci and their horns. They are activated by advanced tissue deformation, injuries, or inflammation and responsible for pain sensation [21, 42].

Histological and Biochemical Features of the Meniscus

The meniscal tissue which is fibrocartilage in nature is composed mainly of extracellular matrix and relatively scarce and scattered cells. There are three types of cells within the meniscal tissue. The cells located at the peripheral part are oval- or spindle-shaped cells which resemble fibroblasts morphologically. They possess thin, long, cytoplasmic processes which are used to communicate with other cells and extracellular matrix. These cells have abundant cytoplasm which is rich in granular endoplasmic reticulum and Golgi apparatus. They do not have pericellular matrix; instead, the collagen fibers of the extracellular matrix (which are mainly type I but to a lesser extent types III and V) surround these fibroblast-like cells. The cells of the inner menisci are more oval in shape and are surrounded by pericellular matrix. Owing to their resemblance to chondrocytes, they are called fibrochondrocytes or chondrocyte-like cells. The extracellular matrix around them contains mostly type II collagen, besides much less but significant amounts of type I collagen and glycosaminoglycan more than the outer menisci. Considering the fact that this part of the meniscus contains type II collagen and aggregan which is a proteoglycan, it resembles hyaline articular cartilage. The third type of cells is the ones located at the superficial part of the meniscus which is spindle shaped similar to the fibroblast-like cells but flatter than them and does not possess cytoplasmic processes. They are considered as progenitor cells with certain capabilities [25, 28, 37, 54].

Healthy meniscal tissue is composed of water (70–75 %), collagen (20–22 %), glycosaminoglycan (0.6–0.8 %), and deoxyribonucleic acid (DNA) (0.10–0.12 %) [28]. The collagen constituting meniscus is 90 % type I collagen and to a much lesser extent type II, III, V, and VI collagens. Type I and II collagens form the fibrillar skeleton of the meniscus. The functions of type III and V collagen are not clearly identified. However, type VI collagen is a matrix glycoprotein and responsible for the stabilization of the collagen skeleton and persistence of the attachment of fibrochondrocytes to matrix [54].

The orientation of collagen fibers is related to the mechanical properties of the menisci and their tearing patterns. The histological evaluation of meniscal sections revealed that it had three distinct layers. The superficial layer which exists both on the tibial and femoral surfaces is composed of a thin collagen fiber network whose fibers are approximately 30 nm in diameter. Underneath this reticular layer, there is a lamellar layer which also exists both on the femoral and tibial sides. The collagen fibers of the lamellar layer are radially oriented at the outer parts of the anterior and posterior horns; at the inner parts, they intersect at various angles. The main part of meniscal tissue is located between the two lamellar layers. The orientation of collagen fibers in this central layer is circumferential in the whole menisci. In addition, there are few radial fibers which connect the circumferential collagen fibers to each other (Fig. 24.4) [49, 54].

When the knee joint is subjected to axial loading, the menisci are compressed and pushed away from the center of the joint, which in turn leads to increased tensioning in their outer parts, named as “hoop stresses.” The tensioning is very well tolerated by the circumferentially oriented collagen fibers; however radial fibers are not durable enough. This phenomenon is considered in the etiology of longitudinal meniscal tears [49, 54].

The proteoglycans which are among the components of the organic part of noncollagen meniscal tissue are composed of a core protein and one or several glycosaminoglycan (GAG) chains attached to it. The amount of GAG of a meniscus is eight times that of articular cartilage [2]. The GAGs found in the meniscal tissue are chondroitin 6-sulfate (40 %), chondroitin 4-sulfate (20 %), dermatan sulfate (20 %), keratin sulfate (15 %), and hyaluronate (3 %) [28]. GAGs are negatively charged hydrophilic molecules; because of this property, the meniscal tissue is resistant to compressive stresses. The collagen network and GAGs

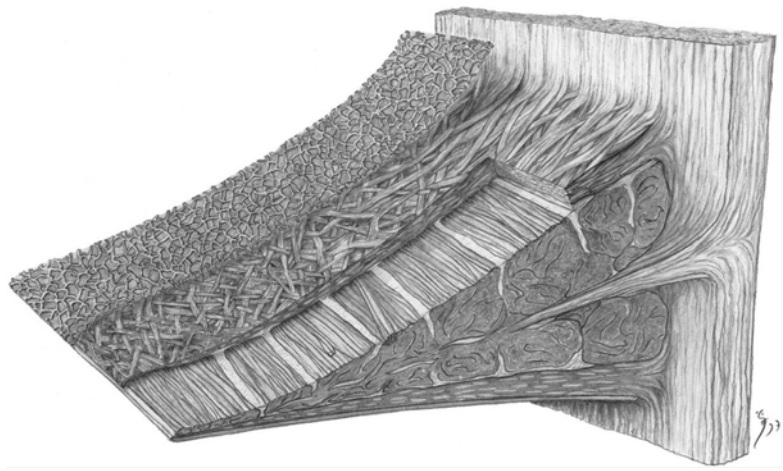

Fig. 24.4 Synoptic drawing of a meniscal section showing the superficial and lamellar layers both on the tibial and femoral surfaces and in between the central main layer. In the central layer, circumferentially oriented collagen fiber bundles are observed. A few radial fibers also intersect them (Reprinted from Springer-Verlag Anatomy and Embryology, Petersen and Tillmann [49], figure 5, with kind permission from Springer Science and Business Media)

of the menisci constitute a porous, permeable, solid matrix which is essential for the preservation of the hydrostatic pressure of tissue. In loading conditions, there is an influx of fluid into the tissue followed by the deformation of solid matrix which is responsible for the shock-absorbing property of the meniscus. The meniscal regions having the most abundant GAG content are subjected to the highest loading conditions [7, 17, 28, 54]. Aggregan is the main proteoglycan of the meniscal tissue and responsible for the viscoelastic, compressive properties. Decorin, biglycan, and fibromodulin are other proteoglycans found in low amounts in the meniscal tissue [17, 54, 58].

Matrix glycoproteins have a role in adhesion and connect cells to the components of extracellular matrix. They contribute to the structural and mechanical strength of the tissue. Type VI collagen, fibronectin, and thrombospondin are among the glycoproteins found in the meniscal tissue. Elastin is a noncollagen fibrillar protein found in the matrix of the meniscus which has a role in regaining the shape following deformation due to loading [1, 7, 17, 37, 54].

Biomechanical and Functional Properties of the Meniscus

The biomechanical features of the menisci are related to their anatomic and viscoelastic material characteristics which make them possess several important functions in the joint. Load bearing, shock absorption, and joint lubrication are among the functions of menisci. They also provide support to joint stability and have roles in proprioception [32, 54, 59].

The two incongruent joint surfaces, the distal femur and the proximal tibia, become congruent to each other as a result of meniscal function. They also have a role in load sharing. By means of menisci, the tibiofemoral contact area enlarges which in turn decreases the contact stress during loading. Since the menisci move together with the femur and tibia throughout the range of motion, they provide congruency of the tibiofemoral joint and participate in load sharing. This dynamic congruency also contributes to the joint stability and lubrication [68].

During loading, the menisci transmit 70 % of the load in the lateral compartment and 50 % in the medial compartment. In extension, they transmit 50 % of the load, whereas in 90° of flexion, they transmit 85 % of it and protect the articular cartilage against compressive stresses. The menisci are exposed to compressive, tensile, and shearing forces. By means of circumferential collagen fibers and the insertion characteristics of the anterior and posterior horns, vertical compressive stresses are converted to horizontal hoop stresses which prevent them from extrusion (Fig. 24.5). The tensile properties of the menisci facilitate load bearing and shock absorption functions [6, 37, 68].

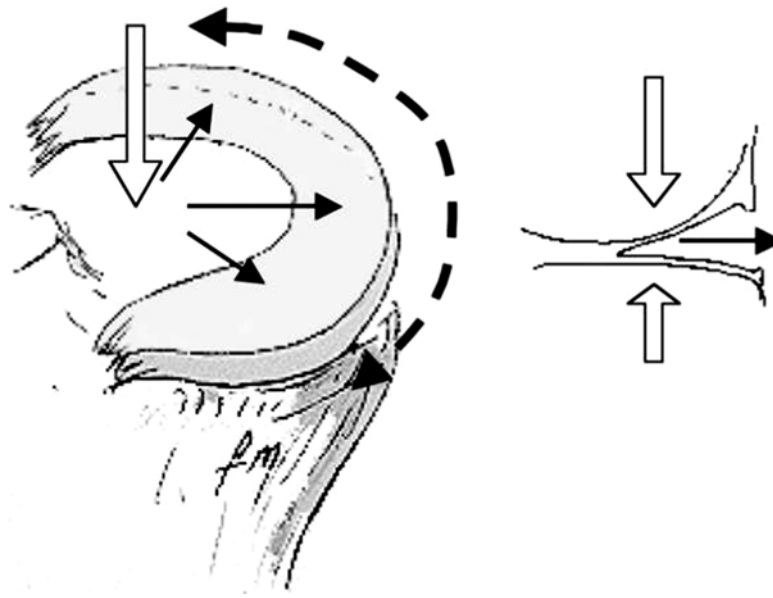

Fig. 24.5 A compressive force (*white arrow*) is converted a radially directed force (*black arrows*), which is taken up as hoop stresses (*dashed arrow*) within the meniscus (Reprinted from Boyd and Myers [6], with permission from Elsevier)

As well as other biological tissues, the menisci respond to loading in two steps. The first step is mechanical or elastic respond to loading. Compression of solid matrix and fluids inside the tissues leads to hydrostatic pressure increases. The second step is the efflux of liquids which is time dependent. Morphological changes which are biomechanically referred as "creep" occur in the meniscus facilitating the increase in the congruency and contact area between two corresponding joint surfaces. Efflux of liquid lowers the hydrostatic pressure of the meniscus which is called stress relaxation. The flow continues until a balance is reached between the applied pressure, hydrostatic pressure of the matrix, and tensile forces exerted by the collagen fibers [1]. When compared to the articular cartilage, its compressive stiffness and permeability are lower which is related to its shock absorption properties [32]. Though the exact mechanism of joint lubrication is not identified, it is considered to be related with the efflux of liquids from the meniscal tissue into the joint space. The menisci contribute to the nutrition of articular cartilage by pushing the synovial fluid against cartilage surfaces and protecting the synovial film layer over the articular cartilage [17, 32, 68].

It was demonstrated that under loading conditions, the anterior horn of the medial meniscus moved a mean of 7.1 mm, and the posterior horn 3.9 and 3.6 mm in the mediolateral direction with knee flexion; on the other hand the anterior horn of the lateral meniscus moved 9.5 mm, and the posterior horn 5.6 and 3.7 mm in the mediolateral direction. The results of this study showed that the lateral meniscus was more mobile than the medial one and the anterior horns were more mobile than the posterior ones. The mobility of the menisci throughout the range of motion increases the conformity of joint surfaces and protects them from injuries [68]. The higher incidence of meniscal tears occurring in the posteromedial part of the medial meniscus is explained by the fact that this part is more stagnant [6].

Partial or complete loss of the meniscus increases point loading which leads to early degeneration due to alterations of mechanical vectors. In a study conducted on cadaveric knees which evaluated the tibiofemoral contact mechanics, medial contact area and medial peak contact stress values were measured in the knees with intact meniscus or 50 %, 75 %, or total meniscectomized knees at extension and 30 and 60° of flexion. In case of an intact meniscus, the largest medial contact area was observed at extension;

with increasing flexion, medial contact area decreased. The comparison with the intact meniscus revealed that medial contact area decreased 20 % in the 50 % meniscectomized knees, 35 % in the 75 % meniscectomized knees, and 54 % in total meniscectomized knees. Medial peak contact stress increased 43 % in the 50 % meniscectomized knees, 95 % in the 75 % meniscectomized knees, and 136 % in total meniscectomized knees [34]. The type of meniscal tears is also important. The radial tears reaching the periphery of meniscus do not necessarily change the volume; however the ability to withstand hoop stresses is influenced which alters the functional capability of the meniscus [6].

Another important function of the meniscus is to contribute to the joint stability. The medial meniscus with its wedge shape limits the posterior movement of medial femoral condyle over tibial plateau which has limited influence on knee joint stability under normal circumstances. However, in knees with especially ruptured anterior cruciate ligaments, the medial meniscus provides important contributions to joint stability. With limiting anterior translation of tibia, the meniscus behaves as a secondary stabilizer of the knee joint in this plane [6, 20, 32, 54].

The menisci provide proprioceptive feedback with regard to the position sense of the joint via mechanoreceptors located in their structure. Besides the mechanical support to the stability of the knee joint, by means of proprioceptive reflex arc, the menisci also have functional contributions [21, 32, 54].

The Pathophysiology of Meniscal Injuries

The meniscal tears of young population generally occur as a result of sports injuries. In these patients, the mechanism of injury is mostly exposure to rotational torque to flexed knee under loading conditions. In this patient population, meniscal tears are frequently accompanied by anterior cruciate ligament ruptures or osteochondral injuries [20, 40].

Degenerative meniscal tears become more common with aging. The water content of degenerative meniscal tissue is increased, whereas cell count, collagen, and GAG contents are decreased. Mucinous type of degeneration is observed in the aging meniscus with a decrease in its elasticity and an increase in its friability which makes it vulnerable to tearing. Degenerated meniscus can be torn even with a minor trauma [20, 28].

Meniscal tears are classified as partial or complete tears according to their depth. Complete tears are further classified as stabile and unstable tears. Meniscal tears are also classified according to the type of tear: vertical/longitudinal, radial/transverse, or horizontal/complex tears. Radial tears of the posteromedial part of the medial meniscus are the most common. On the other hand, acute anterior cruciate ligament tears are generally accompanied by vertical longitudinal tears of the lateral meniscus. Degenerative complex tears are most commonly observed in the posterior horn [50].

Healing of the Meniscus

The healing capacity of meniscal tissue is limited. The healing rates of meniscal tears reported to have a range from 63 to 91 % in the literature [10]. Division of meniscal tissue according to its vascularization is relevant with its healing potential. The tears in the red–red zone which has the most abundant blood supply have the highest healing potential. The tears of the red–white zone have relatively good prognosis. Since the white–white zone is avascular, tears in this zone do not heal spontaneously. Even if they are surgically treated, healing would be suboptimal [37, 40].

As is the case in healing processes all around the body, inflammatory cells and mediators should reach the injured zone of the meniscus. Inflammatory cells form fibrin clots in the tears of the highly vascular other zone. This is the first step of healing. The fibrin clot forms a skeleton for the formation of matrix and is also chemotactic for the other mediators which will participate in the healing process. The vessels originating from the perimeniscal capillaries proliferate into the fibrin clot. Meanwhile undifferentiated mesenchymal cells also proliferate. The lesion is filled with a fibrovascular scar tissue which holds the wound edges together and is in continuation

with the neighboring meniscal tissue. In time, this tissue maturates to assume a normal fibrocartilage appearance [11, 50]. Nevertheless the newly formed healing tissue is not as durable enough as the healthy meniscal tissue [6].

Based on the understanding of the fact that the more the vascularization is, the better the healing, certain methods began to be applied in order to increase the vascularity of the avascular zone to treat the meniscal tears in this zone. These methods include trephination (forming channels connecting the avascular inner zone to the vascular outer zone), synovial abrasion, pediculated synovial grafts, rasping of the meniscus, exogenous fibrin clot, and bone marrow stimulation techniques [7, 14].

Today studies are being conducted on the utilization of growth factors and cytokines which control the mitogenic behavior of cells and their differentiation and also function as signaling molecules in order to augment the meniscal healing and regeneration. Proinflammatory cytokines such as tumor necrosis factor-alpha (TNF-α) or interleukin-1 (IL-1) were shown to have negative effect on meniscal healing [26, 62]. IL-1 stimulates the synthesis of nitric oxide (NO) and matrix metalloproteinases (MMP) which were shown to decrease the shear strength of repair and suppress cell accumulation and proliferation, therefore adversely affecting the meniscal repair process in vitro [26, 43, 51]. However, the inhibitory effects of IL-1 were shown to be antagonized by dynamic loading in in vitro conditions [43]. On the contrary, the growth factors including insulin-like growth factor (IGF), fibroblast growth factor (FGF), and platelet-derived growth factor (PDGF) have been shown to influence positively the proliferation of the cells of especially the avascular region of the menisci and the formation of new extracellular matrix [63–65]. Nevertheless, for today it seems that the introduction of these basic science findings into the clinical era necessitates further studies.

Utilization of platelet-rich plasma (PRP) has been proposed to augment meniscal healing along with a widespread effort to make it infiltrate into many fields of medicine; but despite the positive results obtained from a few experimental studies, controlled clinical trials favoring its use are lacking [29, 62, 67].

Treatment of Meniscal Tears

The evaluation of the location, type, and length of meniscal tear is essential to decide the proper treatment method. Before intervening with the meniscus, its upper and lower surfaces should be examined thoroughly arthroscopically. Partial tears which do not intersect the whole thickness of the meniscus or tears shorter than 8 mm seldom cause mechanical symptoms and have higher spontaneous healing potentials. Thus, in case of such stable tear, partial meniscectomy is not indicated; instead it should be treated conservatively [6].

Almost until 25–30 years ago, the choice of treatment in meniscal tears was mostly open total meniscectomy. Long-term deleterious effects of total meniscectomies have been shown; this type of treatment increased osteoarthritis risk by 14-fold [55]. In a cadaveric study performed in human knees, tibiofemoral contact mechanics was evaluated following serial meniscectomies. The results of this study revealed that the decrease in the contact area and the increase in the peak contact pressure were similar both in the segmental and total meniscectomized knees. This is because segmental meniscectomy disrupts the continuity of its peripheral part that contains circumferentially oriented collagen fibers resisting hoop stresses [34]. The current concept of treating meniscal tears includes the preservation of meniscal tissue as much as possible. Open procedures are replaced by arthroscopic interventions which are more favorable.

Clinical Relevance

Who is a proper candidate for arthroscopic partial meniscectomy (Fig. 24.6)?

A 26-year-old female patient attended the outpatient clinic with a symptom of pain in her right knee. She had suffered from two trauma incidents. The first trauma was 4 years ago and the second one was approximately 6 weeks ago. She defined the mechanism of trauma as jumping from a higher ground. Soon after the trauma, her right knee was swollen which lasted for about 2 weeks. She suffered from occasional locking, catching, and mild limping.

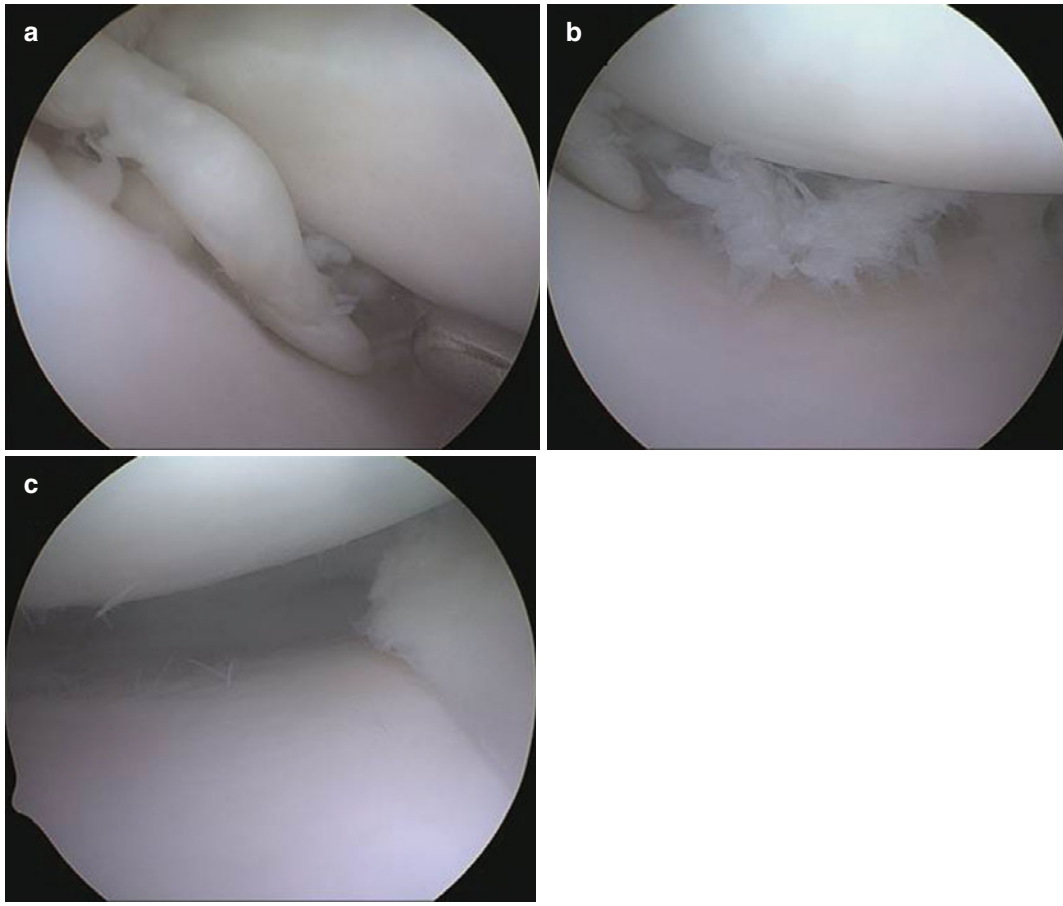

Fig. 24.6 Arthroscopic view of a right knee. (**a**, **b**) Complex tear of posterior horn of the medial meniscus. (**c**) Partial meniscectomy was performed

She was unable to kneel beyond 90°. Her physical examination revealed that her range of motion of her right knee was not limited. She had isolated medial joint line tenderness upon palpation. Specific meniscal tests were positive. On her magnetic resonance imaging sequences, the posterior horn of the medial meniscus was torn. Her arthroscopic examination revealed a complex tear of the posterior horn of the medial meniscus. Arthroscopic partial meniscectomy was performed. In the postoperative period, her pain subsided and her mechanical symptoms disappeared.

Today, arthroscopic partial meniscectomy is the most common treatment method performed for meniscal tears. It is effective in the elimination of mechanical symptoms caused by a torn meniscus. Meniscal tears which are amenable to repair including degenerative, complex tears are mostly treated with arthroscopic partial meniscectomy. Partial meniscectomies performed for the tears in the posterior root tears yield clinical results inferior to that of anterior root or bucket handle tears. Partial meniscectomies without protecting the meniscocapsular junction have similar results to total meniscectomies; that is why it is essential to protect the meniscocapsular junction in the treatment of meniscal tears [23, 41, 54].

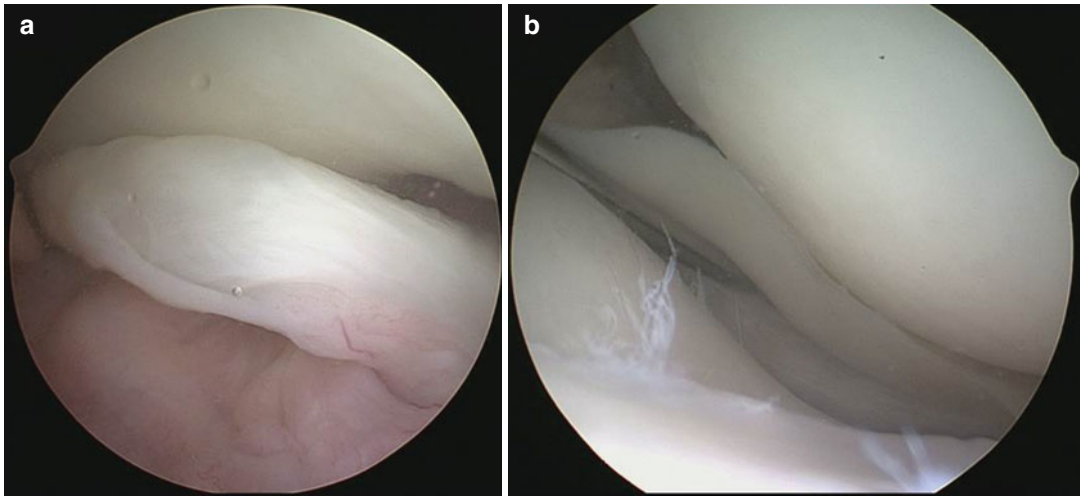

Fig. 24.7 Arthroscopic view of a left knee. (**a**) Torn segment is entrapped in the intercondylar notch. (**b**) This is a bucket handle tear of the left lateral meniscus. The torn segment is reducted

Meniscal Repair

In order to be able to conduct a repair, meniscal tear should be amenable to repair by physical and biological means. During arthroscopy, the tear is classified according to its location, type, and length. The tear should be reducible, and also the reduction should be preserved through the range of motion (Fig. 24.7). The examination of the remaining meniscal tissue is also important while deciding whether the tear is reparable or not. It should be intact and healthy. Single, peripheral, longitudinal, traumatic tears are almost always accepted as reparable with high success rate. The tears of the white–white zone, chronic degenerative tears, short longitudinal tears (less than 10 mm), and radial tears which do not reach the outer part are regarded as irreparable (Fig. 24.8) [45].

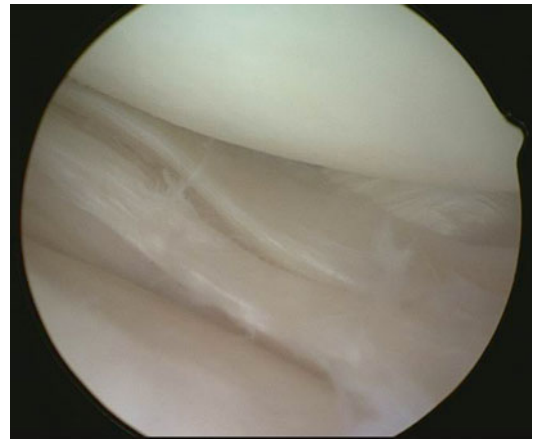

Fig. 24.8 Arthroscopic view of a left knee; a chronic, longitudinal tear in the white–white zone of the lateral meniscus treated with arthroscopic partial meniscectomy

Horizontal cleavage tears were used to be regarded as irreparable tears; because they are mostly degenerative tears of the avascular zone. However, newer studies have been published revealing favorable results of repairing horizontal cleavage tears with proper indications. Certain methods such as insertion of exogenous fibrin clot could accompany the repair procedure to enhance healing [31, 33].

Isolated meniscal repair should not be performed in an unstable knee which lacks an intact ACL. In this case, meniscal repair should be performed together with ACL reconstruction. If there is malalignment of the extremity accompanying the meniscal tear, a concomitant high tibial osteotomy should be planned. Patient compliance is also an important parameter to decide which patients are suitable candidates for this type of operation. It is not appreciated as a convenient option to perform meniscal repair in patients who are not willing to participate postoperative rehabilitation program [45].

Acute tears are more suitable to repair. It was shown that the clinical success rate of meniscal repair performed within 3 months after injury was 91 %, whereas the success rate dropped to 58 % when the procedure was performed 3 months after the injury [69].

Diagnosing and treating meniscal root tears are current topics with increasing popularity. Meniscal root tears are defined as direct avulsions of the roots from the tibial plateau or radial tears adjacent to the meniscal roots. Root tear is most prevalent in the posterior horn of the medial meniscus, because it is less mobile when compared to the rest. Patients mostly do not recall a trauma, but a subtle trauma history may be evident. Joint line tenderness is usually present, but mechanical symptoms are mostly lacking. Magnetic resonance imaging is useful in diagnosing these tears. In case of an acute root tear, or a chronic tear without the development of overt arthritic changes, a meniscal root repair might be suggested, as the integrity of the roots is important in resisting hoop stresses. It was shown that peak contact stresses were elevated in case of meniscal root tears. In order to prevent the development of degenerative changes or at least to postpone them, it is suggested to perform meniscal root repair for the patients with suitable indications [3, 4].

Meniscal Repair Techniques

Meniscal repair techniques have evolved in years, and open techniques were replaced by arthroscopy-assisted interventions. Arthroscopic meniscal repair can be performed utilizing three different techniques, namely, inside-out, outside-in, and all-inside techniques. In a systemic review which evaluated the outcomes of open techniques and the three types of arthroscopic repair techniques, at least 5 years postoperatively, similar failure rates (ranging from 22.3 to 24.3 %) were found [44].

Regardless of the technique used, however, the preparation of the meniscus has crucial importance in healing which includes debridement of unstable meniscal fragments or loose bodies and rasping of the two sites of the tear and also parameniscal synovium both in the meniscofemoral and meniscotibial regions [10]. The initial strength of the repair techniques should also be considered. Vertical mattress sutures are superior to horizontal mattress sutures regardless of the type of suture material; possibly because vertical sutures can capture a greater proportion of circumferentially oriented collagen fibers [10, 54, 61].

Arthroscopic Inside-Out Meniscal Repair

In this technique, the needles of the sutures are inserted inside the knee joint through cannula systems with arthroscopic assistance and can be placed through either the superior or inferior surfaces of the meniscus. There are two types of cannula systems: double- and single-lumen cannulas. Double-lumen cannulas are straight and let the surgeon place only horizontal sutures. While using these types of cannulas, the needles are bent prior to insertion. Single-lumen cannulas are zone specific and are preshaped having various curvatures which ease their use. According to their curvatures, the corresponding parts of the meniscus such as middle or posterior parts can be targeted. The meniscus can be sutured either horizontally or vertically with this cannula system. In this procedure, anterior portals are used. The arthroscope is usually introduced through the contralateral portal and the cannulas through the ipsilateral portal, but the reverse can also be suitable for certain tears. Following the insertion of needles, they are retrieved from a separate incision overlying the joint capsule. This is especially necessary for the repairs of the posterior meniscal tears. The incision is located posteromedially for the medial meniscal repairs and posterolaterally for the lateral meniscal repairs. Protection of neurovascular bundle with a retractor is very important in this step. The needles are inserted one by one, and the knots are tied over the joint capsule. This technique is especially chosen for tears of the posterior part of the meniscus (Fig. 24.9) [6, 10, 39].

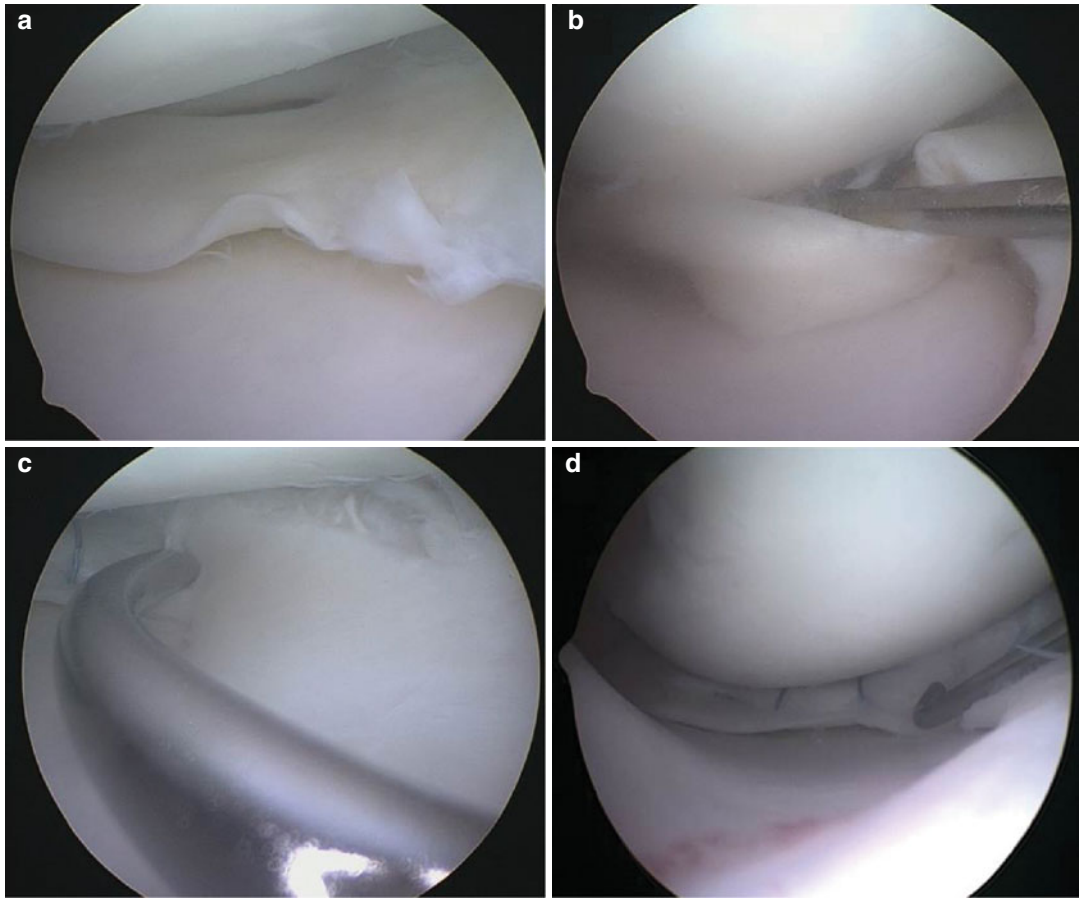

Fig. 24.9 Arthroscopic view of a right knee. (**a**, **b**) Longitudinal tear of posterior horn and middle part of the medial meniscus. (**c**, **d**) Arthroscopic inside-out meniscal repair of the torn segment

Arthroscopic Outside-In Meniscal Repair

This technique is suitable for repairing the tears in the anterior two thirds of the meniscus. Spinal needles or commercially available kits are used. With the arthroscopic assistance, a needle is passed from outside to inside the knee joint through the meniscal rim and the torn fragment. Suture material either braided or nonbraided is introduced through the needle. The second needle is also inserted parallel to the first one. For a vertical suture, the second needle should pass through the capsule above the first needle; for a horizontal suture, it should pierce the meniscus 5 mm away from the first meniscus. With a loop introduced into the joint through the second needle, the suture material is retrieved. Portal-sized mini incisions are made at the area of the needles to tie the knots over the joint capsule. In another described technique, the needles are inserted into the joint in the same manner. Two separate suture materials are introduced through these needles, and they are pulled outside the ipsilateral portal using a grasper. "Mulberry knot" is tied at the end of each suture. Subsequently the knots are placed over the meniscus by pulling the free ends of the sutures, and these ends are tied over the joint capsule [10, 39]. In a biomechanical study conducted on human menisci, horizontal loop and mulberry suture techniques were compared by means of pullout strength of meniscal repair. The findings of this study showed that the break load and the elastic return were not significantly different from each other [13].

Arthroscopic All-Inside Meniscal Repair

All-inside techniques have gained popularity since they were first introduced in the 1990s. In this technique, the peripheral rim of the meniscus and the torn fragment are held together utilizing certain devices such as hooks, arrows, and anchors (Fig. 24.10). The former generations of all-inside devices were associated with certain handicaps such as the inability to tension the knots following their placement and chondral injury. Today, fourth-generation devices have been introduced. Each has its own application technique, but the common denominator is that they are flexible and have low profile and the knots can be tensioned after placement. The risk of chondral injury is lower with these newer devices. All-inside techniques eliminated the need for separate incisions. With proper technique, the risk of neurovascular injuries is very low. Among the disadvantages of this technique, technical challenges especially when inserting a device posteriorly, the risk of cracking or misfiring of the device, and higher cost when compared to other sutures used for meniscal repair could be considered. All-inside meniscal repair is not suitable for the tears of the anterior part of either meniscus [6, 39, 54, 66]. The inside-out meniscal repairs are gold standard for these tears; however

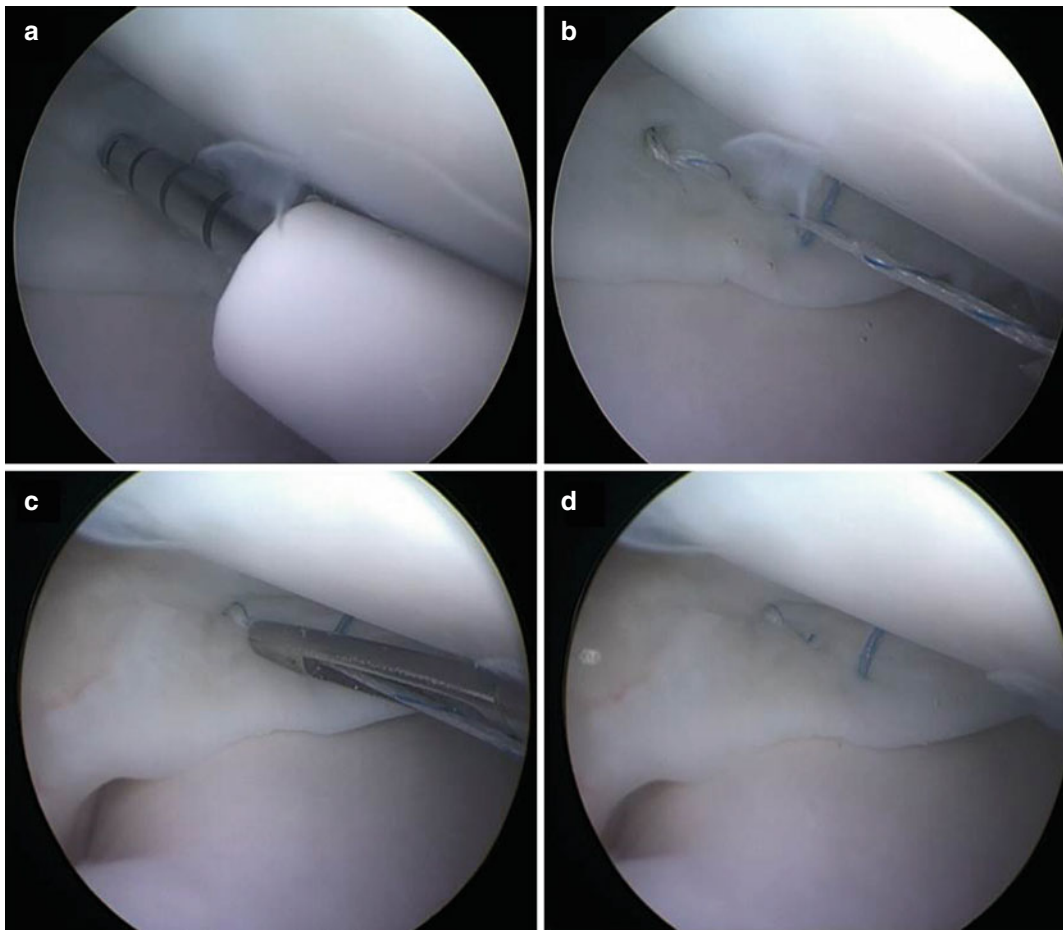

Fig. 24.10 Arthroscopic view of a right knee. (**a**) Insertion of an all-inside meniscal repair device (Smith & Nephew, Inc, Andover, USA). (**b**) Sliding of the prettied knot by pulling the free end of the suture material. (**c**) Cutting the suture material. (**d**) A vertical mattress suture at the medial part of the posterior horn of the medial meniscus is observed. Adjacent to this all-inside meniscal suture, an inside-out suture is visible

in a recent biomechanical study, the results of new generation all-inside meniscal devices were shown to be comparable with the vertical mattress inside-out meniscal repairs in cyclic loading conditions [56].

Replacement of Meniscus

Patients with irreparable meniscal tears, who have lost significant amounts of meniscal tissue with partial total meniscectomy and who underwent total meniscectomy with a pain in the ipsilateral compartment indicating that the degenerative changes have begun are candidates for meniscal replacement surgery. The meniscus is replaced with either meniscal allograft transplantation (MAT) or implantation of synthetic meniscal scaffolds [40].

Meniscal Allograft Transplantation (MAT)

The aim of MAT is to prevent chondral degeneration or at least slow down the process to reestablish the load bearing functions of the meniscus. For today, it is unclear that this goal is achieved with MAT though. In a properly selected patient group, it was shown that pain has subsided, functional improvements of the knee joint were achieved, and patients were satisfied with the outcome [27].

The suitable candidates for MAT are the patients below 50 years of age who have a prior history of meniscectomy or have an unrepairable meniscal tear but without advanced osteoarthritis. Posteroanterior standing radiographs with the knees flexed are obtained to evaluate the joint cartilage. Subchondral bone should not be visible, and the narrowing of the joint space should not be beyond 2 mm. There should not be chondral lesions any larger than 10–15 mm in diameter on the load-bearing joint surfaces and malalignment of the extremity. The joint should be stable. In case of a chondral lesion, autologous chondrocyte transplantation or autologous osteochondral tissue transfer can be performed concomitantly. If the knee joint is unstable, prior to meniscus transplantation, proper ligament reconstructions should be performed to obtain a stable knee. Meniscus transplantation and ACL reconstruction could be performed simultaneously. Malalignment should be corrected before transplantation. Isolated medial meniscus transplantation should not be done in a varus knee [45, 53, 54].

Two different MAT techniques were described. In the first technique, the outer rim of the meniscal allograft is sutured to the meniscal remnant either arthroscopically or with an open approach. In the second technique, the meniscal allograft is utilized with a tibial bone block. The attachments of the anterior and posterior horns of the transplant are preserved over the bone block which is inserted into a predrilled tunnel placed at the insertion sites of the anterior and posterior horns of the remnant and subsequently the allograft is sutured. The latter method is technically more challenging; also the graft size must be compatible with the recipient's knee. Nevertheless the latter technique is biomechanically superior [20].

The success of meniscus transplantation is related to several factors including tissue preservation, immunological compatibility of the donor and recipient, and maintenance of the integrity of the transplant for a long period both biologically and biomechanically. Meniscal allografts are available in fresh, cryopreserved, fresh frozen, and lyophilized forms. Unlike fresh frozen or lyophilized allografts, fresh and cryopreserved allografts contain living cells at the time of transplantation. Histological evaluation of fresh frozen meniscal allograft sections reveals that similar to the normal menisci tissue, there are fibrochondrocytes and fibroblasts, but as a result of rapid freezing process, these cells have lost their viability. Fresh allografts should be transplanted at most a few days after harvesting. How long the viability of cells in the fresh frozen or cryopreserved allografts does last is not known. Fresh allografts are associated with the risk of disease transmission. During the cryopreservation process, allograft tissue is frozen in glycerol, so the integrity of cellular membranes

and viability of cells are preserved. Before transplantation, allografts are left to melt down slowly. The preservation period of cryopreserved allografts is longer which gives sufficient amount of time to conduct serological tests. However, preservation of allografts with this technique is more expensive and difficult. Lyophilized allografts are prepared with freezing after vacuum dehydration. Before transplantation, allograft is left to melt down and rehydrated. Following transplantation, the graft provides a skeleton for the recipient's fibrochondrocytes to settle. These allografts can be preserved in the room temperature for a long time. Besides the risk of disease transmission, chondrocyte degeneration and synovitis and shrinkage of the lyophilized allograft have been observed. Considering the state-of-the art preservation conditions, utilization of fresh frozen meniscal allografts is suggested because they are cheaper and technically simpler. Secondary sterilization with gamma irradiation or ethylene oxide is not suggested because of the fact that the material properties of the meniscus can be altered in a dose-dependent manner. In addition, the by-products released while sterilizing with ethylene oxide may cause synovitis [7, 32, 52–54].

Frozen bone tissue stimulates immunogenic response. Thus the bone blocks of transplanted meniscus may increase the antigenic stimulus. Meniscal allografts are potentially regarded as immunogenic. It was shown that the cells of the meniscal tissue which was subjected to two cycles of freezing and melting contained class I and II major histocompatibility (MHC) antigens. The presence of these antigens shows that the tissue has the immunological response potential. The immune response developed by the recipient may influence the outcome of MAT. Synovitis, resistant effusions, delayed healing, and degeneration of either the allograft or the adjacent joint cartilage observed following MAT might be related to development of this immune response [52].

Histological evaluation of the tissue samples following MAT revealed that cells originated from synovial tissue were repopulated in the allograft and adjacent synovial tissue. These cells and fibrochondrocytes of the normal meniscal tissue have certain differences phenotypically. The repopulated cells remodel the extracellular matrix. Along with cellular repopulation and remodeling of extracellular matrix, the meniscus is prone to injuries. A subclinical immune response against the allograft develops though it is not directly relevant with the clinical outcome. Graft rejection has not been shown. Consequently postoperative immunosuppression is not necessary [52].

Surgical technique and compatibility of the graft size with the recipient are important factors influencing the success rate of transplantation. The insertion sites of the anterior and posterior horns influence the transmission of hoop stresses. Fixation of the horns to the proper locations securely is important in facilitating load transmission of the transplanted meniscus. If the morphology of the transplant is distorted due to improper fixation, the biomechanical functions of the meniscus are affected. The dimensions of the meniscal allograft should be matched to the dimensions of the recipient's knee. If the allograft is a match, it is safe to assume that it will be congruent with the femoral condyle. The congruence is necessary for the generation of hoop stresses and functionality of the meniscus. A standard method to measure the allograft size is not available, but knee radiographs are generally used for the measurement. If the allograft is smaller than it is supposed to be, it would be subjected to higher loads. On the other hand, if it is larger, it extrudes from the compartment disrupting the transmission of compressive loads [53].

Synthetic Meniscal Scaffolds

MAT is suitable for the patients who underwent total meniscectomy but not subtotal. If the peripheral part of the meniscus is intact in a knee with a prior subtotal meniscectomy and there is enough tissue at the anterior and posterior horns for attachment, a reconstructive procedure with synthetic meniscal scaffolds can be appropriate.

Synthetic meniscal implant comforting the empty space is sutured to the remaining meniscal tissue. When compared to MAT, synthetic scaffolds do not have disease transmission risk. The implants are cut and reshaped during surgery. This eliminates the size match problem and the necessity to wait for a properly sized allograft [40, 60].

The aim in using synthetic meniscal scaffolds is to form a skeleton for the meniscal cells to nest and regenerate new meniscal tissue inside which should be compatible with the mechanical features of native meniscus. Today two synthetic matrix skeleton options are available in the market to reconstruct the segmental meniscus defects: Menaflex®, also known as collagen meniscal implant (CMI) (ReGen Biologics, Inc., Hackensack, New Jersey, USA) and Actifit® (Orteq Bioengineering Ltd, London, UK). Both of these scaffolds have not gained US Food and Drug Administration (FDA) approval yet, but they have received the Conformité Européenne (CE) mark for use in Europe. Both of them can replace either medial or lateral meniscus. Meniscal replacement with scaffolds can be performed at the same time with meniscectomy or be delayed until the patient becomes symptomatic [40, 47, 60, 70].

Menaflex® is a biodegradable, biocompatible, highly porous scaffold made of type I collagen purified from bovine Achilles tendon enriched with glycosaminoglycans. These collagens are shaped to resemble a meniscus under appropriate temperature and pressure conditions. Actifit® is also biodegradable, biocompatible, and porous but polymeric scaffold made of aliphatic polyurethane. It has advantageous wear characteristics. Approximately in 5 years it degrades slowly, and via hydrolysis, it is decomposed into nontoxic components which are either safely excreted from the body or incorporated into the native tissue [40, 47, 60, 70].

The studies have showed that meniscus-like tissue had been developed in both of these implants and patients have experienced clinical and functional improvements. When compared with partial meniscectomy patients, these scaffolds were shown to be associated with good clinical results. In a recent systematic review on scaffolds for partial meniscectomy, it was concluded that histological, radiological, and clinical evaluations conducted in the postoperative period for both Menaflex® and Actifit® were found to be equivalent. However, better randomized controlled trials are needed to confirm their efficacy and to understand whether they reduce the chondral degradation and prevent development of osteoarthritis [40, 47, 60, 70].

There is a third type of implant: NUsurface® (Active Implants LLC, Memphis, USA) which is a total meniscal substitute. It is different from the former two meniscal implants because this is produced for replacements after total meniscectomies. NUsurface® is a polyethylene (Dyneema Purity®, DSM, Heerlen, the Netherlands) reinforced with polycarbonate urethane (PCU) meniscus implant which is discoid in shape and floats in the knee joint. Following the promising results of several animal studies, clinical phase I studies have begun which will give results in the next years [35, 70].

Tissue Engineering

The meniscus is a very complex tissue to reproduce with tissue engineering methods because of the variations in its anatomy with respect to its different parts, matrix molecules, and cells. With the increasing body of knowledge about the morphology of meniscal cells and their responses to growth factors, serious progresses have been achieved in the reproduction of the menisci [57].

Several natural or synthetic materials which can replace meniscal tissue which gives satisfactory results by all means have not been found yet by studies. Ideal meniscal skeleton should be a temporary supportive device which stimulates cellular growth, provides a convenient medium for growth, and should have appropriate biomechanical features. Its degradation products should be biocompatible. Its degradation rate should be long enough to allow new matrix to be synthesized and a functional tissue to develop [12, 37].

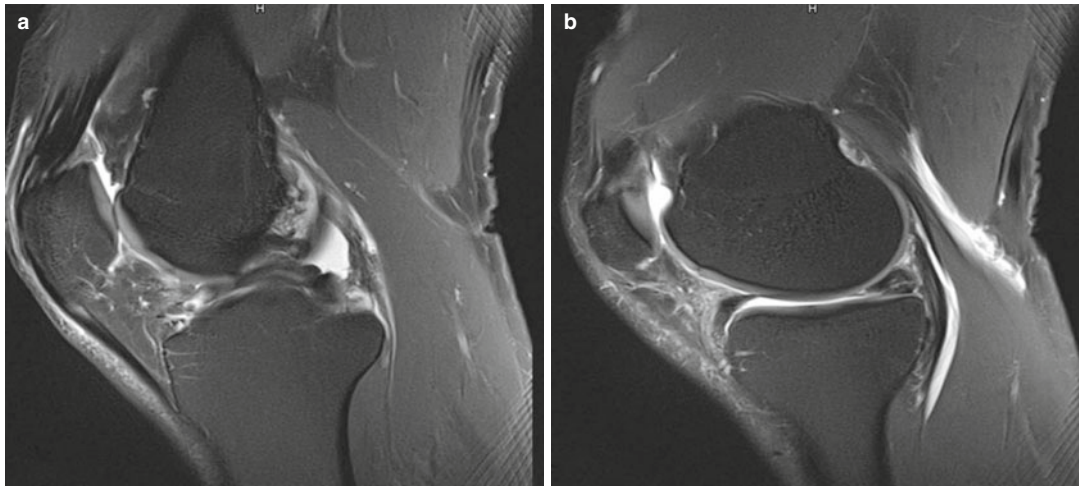

Fig. 24.11 Sagittal MRI sections of the same knee on T2 sequence. (**a**) A longitudinal medial meniscal tear which is specifically named as "bucket handle tear" is observed. The torn meniscal segment is displaced into the intercondylar notch and observed anterior to PCL which is referred to "double PCL sign." (**b**) The hyperintense signal change in the meniscal substance extending to the meniscal surface indicating a meniscal tear

The skeletal components used for the reproduction of the meniscus with tissue engineering are categorized into four groups: synthetic polymers, hydrogels, extracellular matrix components, and materials obtained from tissue. Synthetic polymers are materials which do not exist in the body under normal circumstances; at least they do not exist in the polymer forms. Polyurethane, polycaprolactone, polylactic acid, polyglycolic acid, and poly(lactic-co-glycolic) acid are polymers utilized with this purpose. Hydrogels are hydrophilic molecules which attract water. They may be synthetic such as poly(N-isopropylacrylamide) or natural such as alginate. Scaffolds made up of extracellular matrix components are materials which are formed from an abundantly found element of natural matrix such as collagen or hyaluronan. These skeletons are more biomimetic when compared to synthetic polymers and hydrogels. Materials obtained from tissue are submucosa of the small intestine, decellularized extracellular matrix tissue, or processed tissues such as silk [37].

Skeletons may be utilized with cells in order to provide cellular ingrowth inside the implant and improve the primary biomechanical stability. Thus a living, bioactive composite is obtained. Fibrochondrocytes originated from meniscal tissue, chondrocytes obtained from other cartilage sources of the body, dermal fibroblasts, and synovial cells can be utilized as a probable cell source [12].

Several growth factors are in use to prevent cells from losing their favorable features and stimulate them to differentiate into the phenotype anticipated. Insulin-like growth factor (IGF), bone morphogenetic protein-2 (BMP-2), platelet-derived growth factor (PDGF), and transforming growth factor-β (TGF-β) were studied to achieve this goal [12].

With regard to the developments in the bioreactor technology, scaffold-free structures can be formed and also growth factors can be added. Thus it is possible to produce cells similar to meniscal cells by means of their geometric, biomechanical, and biochemical characteristics from chondrocytes. When scaffold-free approach

is applied to tissue engineering, it is possible to obtain geometry similar to meniscus and matrix accumulation. These structures are heterogeneous in their physical and biomechanical features like native meniscal tissue. Nevertheless for today, natural meniscal tissue is still superior biomechanically. In the future, when optimum conditions are created, in vitro production of tissues which may be biomechanically competent with the natural meniscus is considered to be possible [57].

Radiologic Imaging

Magnetic resonance imaging (MRI) is used as a diagnostic tool to evaluate the menisci and diagnose their pathologies. The image of a healthy meniscus resembles a uniform triangle with low signal intensity (dark color). In a knee without a prior history of meniscal surgery, the diagnostic criterion for a meniscal tear is to show signal changes reaching the meniscal surface in at least one image or to observe abnormal meniscal morphology (Fig. 24.11). The sensitivity and specificity of MRI in the detection of meniscal tears are very high [16, 17]. The structural alterations in the meniscal histology with advancing age can be observed as changes in the signal intensities which may be misinterpreted as meniscal tears. That is why it is considered wise to evaluate the symptoms and clinical findings of the patients while commenting on MRI findings [18].

Postoperative imaging of the meniscal tissue is complicated. It is not appropriate to use classic diagnostic criteria when diagnosing a new tear at the meniscal repair site or at the partially resected meniscal region. A repaired or healing meniscal tissue may possess abnormal signal changes due to the granulation tissue reaching the meniscal surface on T1-weighted or proton density sequences for years. If there is effusion in the joint, the fluid may imbibe into the cleft formed by a tear and will be visible on T2-weighted images which is diagnostic for a new tear. Direct or indirect MR arthrography can be used to diagnose residual or recurrent tears in knees with a history of meniscal surgery that notwithstanding MR arthrography is an invasive procedure. Today utilizing frequency-selective fat suppression techniques may be helpful in distinguishing repaired tissue from a tear which reduced the necessity for invasive procedures [18, 54].

References

1. Aagaard H, Verdonk R (1999) Function of the normal meniscus and consequences of meniscal resection. Scand J Med Sci Sports 9(3):134–140
2. Adams ME, Muir H (1981) The glycosaminoglycans of canine menisci. Biochem J 197(2):385–389
3. Allaire R, Muriuki M, Gilbertson L, Harner CD (2008) Biomechanical consequences of a tear of the posterior root of the medial meniscus. Similar to total meniscectomy. J Bone Joint Surg Am 90(9):1922–1931
4. Bhatia S, Laprade CM, Ellman MB, Laprade RF (2014) Meniscal root tears: significance, diagnosis, and treatment. Am J Sports Med. doi:10.1177/0363546514524162
5. Bird MD, Sweet MB (1987) A system of canals in semilunar menisci. Ann Rheum Dis 46(9):670–673
6. Boyd KT, Myers PT (2003) Meniscus preservation; rationale, repair techniques and results. Knee 10: 1–11
7. Brindle T, Nyland J, Johnson DL (2001) The meniscus: review of basic principles with application to surgery and rehabilitation. J Athl Train 36(2):160–169
8. Clark CR, Ogden JA (1983) Development of the menisci of the human knee joint. Morphological changes and their potential role in childhood meniscal injury. J Bone Joint Surg Am 65(4):538–547
9. Day B, Mackenzie WG, Shim SS et al (1985) The vascular and nerve supply of the human meniscus. Arthroscopy 1(1):58–62
10. DeHaven KE (1999) Meniscus repair. Am J Sports Med 27(2):242–250
11. DeHaven KE, Arnoczky SP (1994) Meniscal repair part I: basic science, indications for repair, and open repair. J Bone Joint Surg Am 76:140–152
12. Drengk A, Stürmer KM, Frosch KH (2008) Current concepts in meniscus tissue engineering. Curr Rheum Rev 4(3):196–201
13. Fantasia F, Potalivo G, Placella G, Fantasia L, Cerulli G (2012) Meniscal sutures: biomechanical study of "mulberry" and horizontal loop techniques. J Orthop Traumatol 13(1):13–19
14. Freedman KB, Nho SJ, Cole BJ (2003) Marrow stimulating technique to augment meniscus repair. Arthroscopy 19(7):794–798

15. Freeman MA, Wyke B (1967) The innervation of the knee joint. An anatomical and histological study in the cat. J Anat 101(Pt 3):505–532
16. Fox MG (2007) MR imaging of the meniscus: review, current trends, and clinical implications. Radiol Clin N Am 45(6):1033–1053
17. Fox AJ, Bedi A, Rodeo SA (2012) The basic science of human knee menisci: structure, composition, and function. Sports Health 4(4):340–351
18. Fukuta S, Masaki K, Korai F (2002) Prevalence of abnormal findings in magnetic resonance images of asymptomatic knees. J Orthop Sci 7(3):287–291
19. Gardner E, O'Rahilly R (1968) The early development of the knee joint in staged human embryos. J Anat 102(Pt 2):289–299
20. Getgood A, Robertson A (2010) Mini-symposium: soft tissue surgery in the knee (v) meniscal tears, repairs and replacement – a current concepts review. Orthop Trauma 24(2):121–128
21. Gray JC (1999) Neural and vascular anatomy of the menisci of the human knee. J Orthop Sports Phys Ther 29(1):23–30
22. Gupte CM, Smith A, McDermott ID et al (2002) Meniscofemoral ligaments revisited. Anatomical study, age correlation and clinical implications. J Bone Joint Surg (Br) 84(6):846–851
23. Hede A, Larsen E, Sandberg H (1992) The long term outcome of open total and partial meniscectomy related to the quantity and site of the meniscus removed. Int Orthop 16(2):122–125
24. Heller L, Langman J (1964) The meniscofemoral ligaments of the human knee. J Bone Joint Surg (Br) 46:307–313
25. Hellio Le Graverand MP, Ou Y, Schield-Yee T et al (2001) The cells of the rabbit meniscus: their arrangement, interrelationship, morphological variations and cytoarchitecture. J Anat 198(Pt 5):525–535
26. Hennerbichler A, Moutos FT, Hennerbichler D et al (2007) Interleukin-1 and tumor necrosis factor alpha inhibit repair of the porcine meniscus in vitro. Osteoarthr Cartil 15(9):1053–1060
27. Hergan D, Thut D, Sherman O, Day MS (2011) Meniscal allograft transplantation. Arthroscopy 27(1):101–112
28. Herwig J, Egner E, Buddecke E (1984) Chemical changes of human knee joint menisci in various stages of degeneration. Ann Rheum Dis 43(4):635–640
29. Ishida K, Kuroda R, Miwa M et al (2007) The regenerative effects of platelet-rich plasma on meniscal cells in vitro and its in vivo application with biodegradable gelatin hydrogel. Tissue Eng 13(5):1103–1112
30. Jerosch J, Prymka M, Castro WH (1996) Proprioception of knee joints with a lesion of the medial meniscus. Acta Orthop Belg 62(1):41–45
31. Kamimura T, Kimura M (2011) Repair of horizontal meniscal cleavage tears with exogenous fibrin clots. Knee Surg Sports Traumatol Arthrosc 19(7):1154–1157
32. Kawamura S, Lotito K, Rodeo SA (2003) Biomechanics and healing response of the meniscus. Oper Tech Sports Med 11(2):68–76
33. Kurzweil PR, Lynch NM, Coleman S, Kearney B (2014) Repair of horizontal meniscus tears: a systematic review. Arthroscopy. doi:10.1016/j.arthro.2014.05.038. pii: S0749-8063(14)00499-X
34. Lee SJ, Aadalen KJ, Malaviya P et al (2006) Tibiofemoral contact mechanics after serial medial meniscectomies in the human cadaveric knee. Am J Sports Med 34(8):1334–1344
35. Linder-Ganz E, Elsner JJ, Danino A, Guilak F, Shterling A (2010) A novel quantitative approach for evaluating contact mechanics of meniscal replacements. J Biomech Eng 132(2):024501
36. Macconaill MA (1950) The movements of bones and joints; the synovial fluid and its assistants. J Bone Joint Surg (Br) 32-B(2):244–252
37. Makris EA, Hadidi P, Athanasiou KA (2011) The knee meniscus: structure-function, pathophysiology, current repair techniques, and prospects for regeneration. Biomaterials 32(30):7411–7431
38. Markolf KL, Mensch JS, Amstutz HC (1976) Stiffness and laxity of the knee – the contributions of the supporting structures. A quantitative in vitro study. J Bone Joint Surg Am 58(5):583–594
39. McCarty EC, Marx RG, DeHaven KE (2002) Meniscus repair: considerations in treatment and update of clinical results. Clin Orthop Relat Res 402:122–134
40. McDermott I (2011) Meniscal tears, repairs and replacement: their relevance to osteoarthritis of the knee. Br J Sports Med 45(4):292–297
41. McDermott ID, Amis AA (2006) The consequences of meniscectomy. J Bone Joint Surg (Br) 88-B(12):1549–1556
42. Mine T, Kimura M, Sakka A et al (2000) Innervation of nociceptors in the menisci of the knee joint: an immunohistochemical study. Arch Orthop Trauma Surg 120(3–4):201–204
43. McNulty AL, Estes BT, Wilusz RE, Weinberg JB, Guilak F (2010) Dynamic loading enhances integrative meniscal repair in the presence of interleukin-1. Osteoarthr Cartil 18(6):830–838
44. Nepple JJ, Dunn WR, Wright RW (2012) Meniscal repair outcomes at greater than five years: a systematic literature review and meta-analysis. J Bone Joint Surg Am 94(24):2222–2227
45. Noyes FR, Heckmann TP, Barber-Westin SD (2012) Meniscus repair and transplantation: a comprehensive update. J Orthop Sports Phys Ther 42(3):274–290
46. O'Reilly MS, Boehm T, Shing Y et al (1997) Endostatin: an endogenous inhibitor of angiogenesis and tumor growth. J Cell 88(2):277–285
47. Papalia R, Franceschi F, Balzani LD, D'Adamip S, Maffuli N, Denaro V (2013) Scaffolds for partial meniscal replacement: an updated systematic review. Br Med Bull 107:19–40. doi:10.1093/bmb/ldt007
48. Petersen W, Tillmann B (1995) Age-related blood and lymph supply of the knee menisci. A cadaver study. Acta Orthop Scand 66(4):308–312

49. Petersen W, Tillmann B (1998) Collagenous fibril texture of the human knee joint menisci. Anat Embryol (Berl) 197(4):317–324
50. Rath E, Richmond JC (2000) The menisci: basic science and advances in treatment. Br J Sports Med 34(4):252–257
51. Riera KM, Rothfusz NE, Wilusz RE, Weinberg JB, Guilak F, McNulty AL (2011) Interleukin-1, tumor necrosis factor-alpha, and transforming growth factor-beta 1 and integrative meniscal repair: influences on meniscal cell proliferation and migration. Arthritis Res Ther 13(6):R187
52. Rodeo SA, Seneviratne A, Suzuki K, Felker K, Wickiewicz TL, Warren RF (2000) Histological analysis of human meniscal allografts. A preliminary report. J Bone Joint Surg Am 82-A(8):1071–1082
53. Rodeo SA (2001) Meniscal allografts – where do we stand? Am J Sports Med 29(2):246–261
54. Rodeo SA, Kawamura S (2007) Form and function of the meniscus. In: Einhorn TA, O'Keefe RJ, Buckwalter JA (eds) Orthopedic basic science, 3rd edn. American Academy of Orthopaedic Surgeons, Rosemont, pp 175–189
55. Roos H, Laurén M, Adalberth T, Roos EM, Jonsson K, Lohmander LS (1998) Knee osteoarthritis after meniscectomy: prevalence of radiographic changes after twenty-one years, compared with matched controls. Arthritis Rheum 41(4):687–693
56. Rosso C, Müller S, Buckland DM et al (2014) All-inside meniscal repair devices compared with their matched inside-out vertical mattress suture repair: introducing 10,000 and 100,000 loading cycles. Am J Sports Med 42(9):2226–2233
57. Sanchez-Adams J, Athanasiou KA (2009) The knee meniscus: a complex tissue of diverse cells. Cell Mol Bioeng 2:332–340
58. Scott PG, Nakano T, Dodd CM (1997) Isolation and characterization of small proteoglycans from different zones of the porcine knee meniscus. Biochim Biophys Acta 1336(2):254–262
59. Seedhom BB, Dowson D, Wright V (1974) Proceedings: functions of the menisci. A preliminary study. Ann Rheum Dis 33(1):111
60. Spencer SJ, Saithna A, Carmont MR, Dhillon MS, Thompson P, Spalding T (2012) Meniscal scaffolds: early experience and review of the literature. Knee 19(6):760–765
61. Stärke C, Kopf S, Petersen W, Becker R (2009) Meniscal repair. Arthroscopy 25(9):1033–1044
62. Taylor SA, Rodeo SA (2013) Augmentation techniques for isolated meniscal tears. Curr Rev Musculoskelet Med 6(2):95–101
63. Tumia NS, Johnstone AJ (2004) Promoting the proliferative and synthetic activity of knee meniscal fibrochondrocytes using basic fibroblast growth factor in vitro. Am J Sports Med 32(4):915–920
64. Tumia NS, Johnstone AJ (2004) Regional regenerative potential of meniscal cartilage exposed to recombinant insulin-like growth factor-I in vitro. J Bone Joint Surg (Br) 86(7):1077–1081
65. Tumia NS, Johnstone AJ (2009) Platelet derived growth factor-AB enhances knee meniscal cell activity in vitro. Knee 16(1):73–76
66. Turman KA, Diduch DR, Miller MD (2009) All-inside meniscal repair. Sports Health 1(5):438–444
67. Wei LC, Gao SG, Xu M, Jiang W, Tian J, Lei GH (2012) A novel hypothesis: the application of platelet-rich plasma can promote the clinical healing of white-white meniscal tears. Med Sci Monit 18(8):HY47–HY50
68. Vedi V, Williams A, Tennant SJ, Spouse E, Hunt DM, Gedroyc WM (1999) Meniscal movement. An in-vivo study using dynamic MRI. J Bone Joint Surg (Br) 81(1):37–41
69. Venkatachalam S, Godsiff SP, Harding ML (2001) Review of the clinical results of arthroscopic meniscal repair. Knee 8(2):129–133
70. Vrancken AC, Buma P, van Tienen TG (2013) Synthetic meniscus replacement: a review. Int Orthop 37(2):291–299

A Fibroelastic Cartilage: Meniscus

25

Hasan Havıtçıoğlu, Ramadan Özmanevra, and Ahmet Karakaşlı

Abstract

The fibrocartilaginous menisci dwell between the articular surfaces of the knee and play a crucial role in healthy joint loading. They transmit forces, absorb shock, and enhance the stability of the joint. Traumatic injury and/or degenerative changes disrupt the mechanical function of these tissues. These changes can lead to the early onset and accelerate the development of osteoarthritis. The current standard treatment is meniscectomy, or resection of the damaged portion of the meniscus, a procedure that fails to regenerate normal knee mechanics or prevent the initiation of osteoarthritic cascades. Because of the high prevalence of meniscal injury, a repair strategy is needed that restores meniscus mechanical function in orthopedic medicine. To develop strategies and technologies for replacing damaged or diseased meniscus with tissue engineered, we have to understand the biomechanics of the menisci. The meniscus tissue biomechanics depends on the meniscus anatomy, microstructure, the amount of water it contains, biochemistry, and many features. Besides the properties of a biomechanical point of normal meniscal tissue allograft, the meniscus has also important biomechanical characteristics of degenerative meniscus mechanisms besides mechanisms of injury. Undoubtedly, this information may be important for artificial meniscus study.

Learning Outcomes

- Microstructure and composition of the meniscus
- Biomechanical properties of the meniscus
- Finite Element
- Degeneration and Functional biomechanics of the degenerative meniscus
- New treatment options

H. Havıtçıoğlu (✉) • R. Özmanevra • A. Karakaşlı
Department of Orthopedics and Traumatology,
Dokuz Eylul University, Faculty of Medicine,
Balçova, Turkey
e-mail: hasan.havitcioglu@deu.edu.tr;
hhvtci@gmail.com

F. Korkusuz (ed.), *Musculoskeletal Research and Basic Science*,
DOI 10.1007/978-3-319-20777-3_25

Terminology

Allograft Transplants of cells, tissues, or organs from a genetically nonidentical member of the same species.

Anisotropic A property of being directionally dependent, which implies identical properties in all directions.

Chondrocytes Cells found in cartilaginous tissue; they produce cartilaginous matrix.

Collagen Major insoluble fibrous protein in the extracellular matrix and in connective tissue.

Compression load A pushing or pressing force that is directed toward the center of an object.

Compressive stress Stress on materials leading to a smaller volume or shortening.

Convex Curving out or extending outward.

Finite element method A numerical technique for finding approximate solutions to boundary value problems for partial differential equations.

Glycosaminoglycan Long polysaccharide chains containing repeating disaccharide units. They are hydrophilic molecules. They play roles in lubrication and shock absorption.

Hyaline is a type of cartilage that founds as a supportive tissue.

Hoop Stress Force exerted circumferentially (perpendicular both to the axis and to the radius of the object) in both directions on every particle in the cylinder wall.

Innervation The distribution or supply of nerves to a part.

Lubrication Process of reducing wear on the opposing chondral surfaces of the joint by interposing a lubricant substance.

Menisectomy Surgical removal of all or part of a torn meniscus.

Osteoarthritis Also known as degenerative arthritis or degenerative joint disease or osteoarthrosis, it is a group of mechanical abnormalities involving degradation of joints including articular cartilage and subchondral bone.

Proprioception Perception of the position of body parts relative to each other.

Proteoglycans Glycosylated proteins found in the connective tissue.

Strain Relative change in shape or size implies that it is dimensionless and has no units.

Stress The applied force over a certain area that tends to deform an object or structure.

Tensile test A fundamental materials science test in which a sample is subjected to a controlled tension until failure.

Introduction

The menisci are a pair of semilunar fibrocartilaginous structures found between the femoral condyles and tibial plateau in the knee joint (Fig. 25.1). They play a central role in the knee. They provide joint stabilization, shock absorption, and load transmission [1–3]. They are wedge-shaped structures and there is a congruity between the tibial plateau and femoral condyles, allowing stable articulation and low contact pressures. It has been shown that approximately 50 % of the load through the knee is transmitted through the menisci. The shock-absorbing

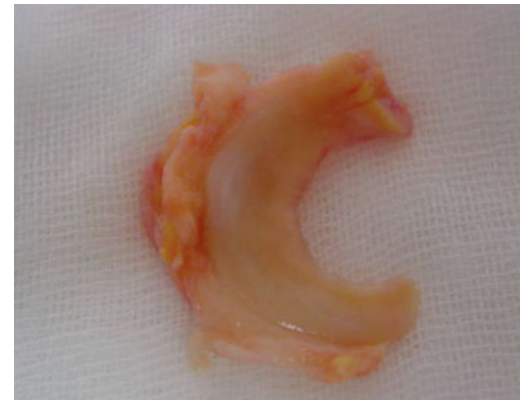

Fig. 25.1 The meniscus is a semilunar fibrocartilaginous structure

capacity of the menisci has been demonstrated by studies measuring the vibrations in the proximal tibia resulting from gait. By this way, it has been shown that shock absorption is approximately 20 % less in knees without menisci [4].

Traumatic injury and/or degenerative changes disrupt the mechanical function of these tissues. These changes can lead to the early onset and accelerate the development of osteoarthritis. The current standard treatment is meniscectomy, or resection of the damaged portion of the meniscus, a procedure that fails to regenerate normal knee mechanics or prevent the initiation of osteoarthritic cascades.

Microstructure and Composition

About 70–75 % of the wet weight of the meniscus consists of water [2, 5–7]. The dry weight consists of 60–70 % collagen, 1 % proteoglycans, and 8–13 % non-collagenous proteins (such as elastin). Collagens are primarily type I (90 %) with smaller amounts of II, III, V, and VI [6, 8]. The collagen fibres are mainly oriented circumferentially, with some radially oriented fibres (Fig. 25.2). This may be related to the mechanical forces that act on the menisci.

Fibrochondrocytes are the predominant cell type in the meniscus. They produce collagen and its extracellular matrix [8].

Along the inner avascular zone, cells are morphologically similar to articular chondrocytes but on the periphery, cells are more similar to fibroblasts. Arnoczky et al. demonstrated that the outer 10–30 % of the medial meniscus and 10–25 % of the lateral meniscus is vascular [9].

The medial and lateral geniculate arteries form a perimeniscal capillary plexus that supplies the outer surface of the menisci. The menisci have intrinsic innervation. Innervation is most abundant on the periphery and the anterior and posterior horns [10]. The meniscus does have an inherent ability to heal itself, but this is limited to the vascularized periphery [11].

Proprioception is believed that obtained from free nerve endings and they are activated on the anterior and posterior horns during flexion and extension of the knee [12, 13].

The unique architecture of the meniscus consists of circumferentially oriented collagen fibers interspersed with radial collagen fibers [2].

Biomechanics of the Menisci

The mechanical properties of this tissue are highly anisotropic (different in opposing directions), and strongly dependent on the prevailing fiber direction [14, 33]. This can be seen in the tensile stress–strain response of samples oriented in the circumferential direction as compared to those oriented in the radial direction.

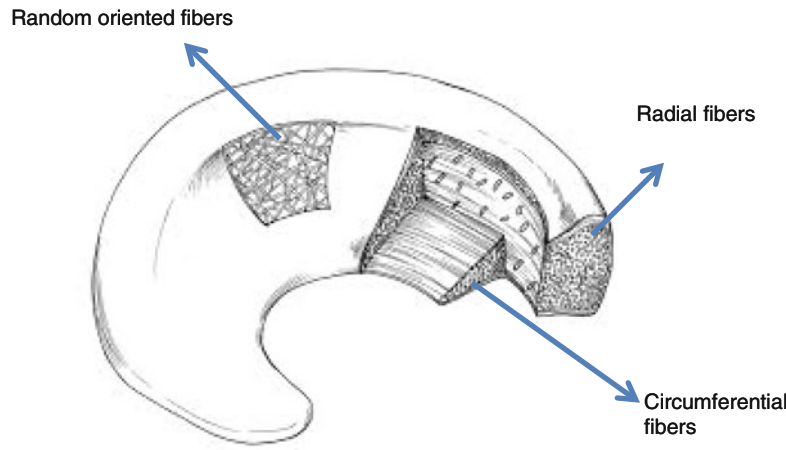

Fig. 25.2 Schematic diagram of the ultrastructure of collagen fibers of the meniscus

Circumferential samples show a pronounced "toe" region common to fiber-reinforced tissues, and a higher linear modulus thereafter. Radial samples are relatively linear in their stress–strain response, with a much lower modulus. The tensile properties of the meniscus range from 48 to 259 MPa in the circumferential direction and 3–70 MPa in the radial direction, depending on anatomic location and species [2, 14, 15, 33]. The compressive properties of the meniscus are low relative to articular cartilage (50–400 kPa, about one-half) [16]. The meniscus, less stiff in compression, is also much less permeable than articular cartilage [2], suggesting that the tissue is optimized to enhance congruency, load distribution, and shock absorption across the joint [33].

Load distribution over an incongruent joint surface is redistributed by the menisci by maintaining maximal congruency. The functionality of the menisci and their role in load transmission across the knee has been discussed by many authors [2, 17].

The main functions of the meniscus are to increase joint congruency, transmit and distribute compressive load between the femur and the tibial plateau, stabilize the joint, and improve articular cartilage nutrition and lubrication [7]. These functions are achieved by the unique load transfer that occurs between the (more hyaline) inner region and the (more fibrous) outer region of the meniscus. When the joint is loaded vertically, axial loads from the femoral condyles are redirected laterally .Lateral extrusion of the meniscus is resisted by the osseous anchorage of the anterior and posterior horns [33], generating hoop stresses within the dense network of circumferentially oriented collagen fibers [18]. Normally, the menisci transmit 50–100 % of the loads in the knee (multiples of body weight) [19], with tensile deformations limited to 2–6 % [20, 21].

The main role of the menisci in the knee joint is load bearing. When bearing load, the knee joint is subjected to compression. The compressive force through the joint is distributed over an articulating contact area resulting in contact stresses (contact pressure). The menisci optimize the way that load is transferred across the knee joint by increasing the congruency of the articulation. The areas of contact increase and, as a result, the contact pressure on the articulating surfaces decreases. As the femoral condyles bear down onto the menisci, the meniscal wedged cross section causes the menisci to extrude radially out of the joint; this causes their circumference to increase. Each meniscus attaches mainly to the tibia by anterior and posterior insertional ligaments. Thus, the bulk tissue resists radial displacement by developing circumferential tension (hoop stresses) (Fig. 25.3); this is due to the stiffness of the meniscal tissue, with the predominantly circumferential orientation of the collagen fibres.

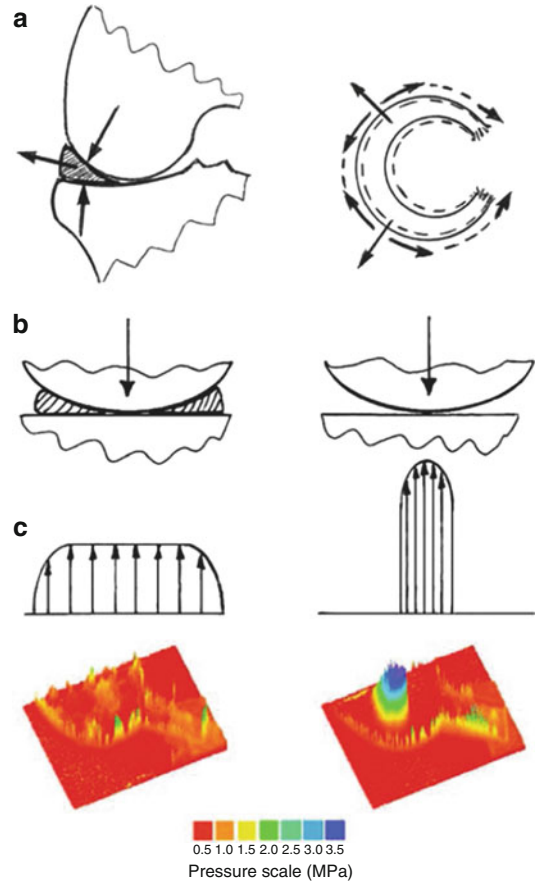

Fig. 25.3 (**a**) Load transfer through the knee joint. The menisci extrude under axial joint load. (**b**) Contact areas decrease and contact stresses increase following meniscectomy. (**c**) Contact stress distribution (in MPa) in the tibial cartilage of the intact and meniscectomized joint

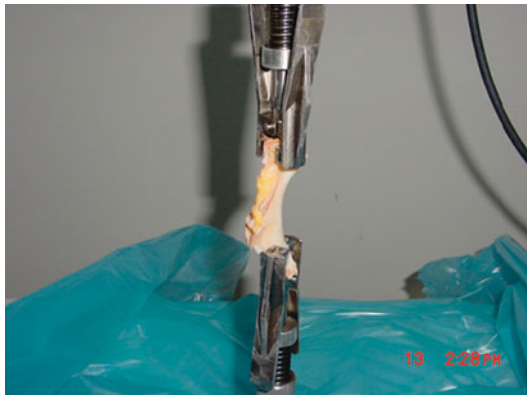

Fig. 25.4 Photograph of meniscus during the tensile test

The lateral meniscus is more mobile than the medial meniscus because it is not as tightly attached to the capsule as the medial meniscus. Also, the concave medial tibial plateau does not allow the posterior aspect of the medial meniscus to displace off the joint posteriorly in deep flexion; however, the convex posterior aspect of the lateral tibial plateau allows the lateral meniscus to displace posteriorly (go "downhill") in deep flexion. These key factors may explain the increased frequency of medial meniscal tears compared to lateral meniscal tears, at a ratio of 2:1 [22].

The variable effect and frequency of the various types of meniscal tear may depend on the resistance of the menisci to compressive loads by increasing their circumference and developing hoop stresses.

The menisci distribute contact forces over the articular surfaces effectively by increasing the contact surface of the joint. The menisci maintain maximal congruency by redistribution of the load, over an incongruent joint surface. The functionality of the menisci and their role in load transmission across the knee has been discussed by many authors [2, 17].

Havitcioglu et al. investigated the biomechanical properties of meniscus under pull-out and compression forces (Fig. 25.4) [23]. In compression–tensile tests, statistically significant difference was observed between force and displacement values [($p=0.037$) and ($p=0.045$), respectively] (Tables 25.1 and 25.2).

Table 25.1 Force and displacement values in compression tests

Force (N)	Displacement (mm)
4494.06	9.83
4498.75	7.21
4501.20	3.99
4495.94	8.43
4497.34	6.67

Table 25.2 Force and displacement values in pull-out tests

Force (N)	Displacement (mm)
17.50	6.60
24.06	6.04
21.40	5.09
55.93	16.6
105.05	14.37
29.21	11.10
22.18	3.87
29.21	4.08
46.56	9.34

Knowledge of the detail properties of the meniscus and cell culture biomechanics will help the artificial meniscus basic studies. Biomechanical knowledge of the properties of natural meniscus are light is keep for future studies.

Finite Element

With respect to meniscus biomechanics and its possible degeneration, finite element simulations help to understand the stress distribution in the human knee joint and prevent joint injuries and pathological degeneration of articular joints. Three-dimensional finite element models can also be used to estimate the consequences of surgical treatments such as total or partial meniscectomies. [24] considered the effect of meniscectomies on the human knee joint using the finite element method.

Some study was to develop a three-dimensional finite element model of the human tibio-femoral joint including the femur, tibia, cartilage layers, menisci, and main ligaments to estimate the con-

tact areas and pressure distributions between menisci and articular cartilage and the stress distribution in the articular cartilage to investigate the effect of meniscal tears and meniscectomies on these variables. This could help to explain the cartilage degeneration after a total or partial meniscectomy [25, 26].

A 3D model was developed of the tibio-femoral human knee joint including femur, tibia, cartilage layers, menisci, and joint ligaments and analyzed under axial compression forces. It allows a better understanding of the role of the menisci in the transmission of forces across the knee and to investigate the effect of meniscal tears and meniscectomies on the biomechanics of human knee joint [27].

Degeneration and Functional Biomechanics of the Degenerative Meniscus

Normal menisci are semilunar, fibrocartilage structures (Fig. 25.1). Deviations from this can occur due to disease, degeneration, traumatic injury, or abnormal development. Once torn, or damaged, the chondroprotective ability of the tissue is disrupted and the cascade toward osteoarthritis initiated [28]. Osteoarthritis leads to degenerative changes in the menisci with the surrounding cartilage, and this is related to 75 % of all meniscal tears and extrusions [29, 30].

Several authors suggested that damage in cartilage starts at its surface and extends through the thickness. This can be explained by a maximal shear stress criterion [31]. Moreover, loss of meniscal tissue frequently leads to long-term degenerative joint changes, articular cartilage degeneration, and osteoarthritis [32, 33].

Most authors agree that total meniscectomy leads to progressive articular wear after a few years. This is a fact that the global biomechanics of the knee is altered and the articular instability increases; so this state can be resulted a progressive and degenerative arthrosic pathology [17, 34].

With consider to meniscus biomechanics and its possible degeneration, finite element simulations help to understand the stress distribution in the human knee joint, so this will help us to prevent joint injuries and pathological degeneration of articular joints. Three-dimensional finite element models can also be used to predict the results of surgical treatments such as total or partial meniscectomies.

Wilson et al. considered the effect of meniscectomies on the human knee joint using the finite element method. They determined the stress and strain distributions and fluid velocities in the articular cartilage before and after meniscectomy, but only used an axisymmetric model [24]. In another study, Pena et al. investigated the effect of meniscal tears and meniscectomies on the human knee joint. They use a 3D finite element model that included the femur, tibia, cartilage layers, menisci, and ligaments. Three different situations were compared: a healthy tibio-femoral joint, a tibio-femoral joint with tears in one meniscus, and a tibio-femoral joint after meniscectomy. According to Pena et al., the minimal principal stresses corresponding to a compressive load at 0° flexion were obtained for the posterior zone of the medial meniscus and the corresponding region of the articular cartilage. The maximal contact stress in the articular cartilage after meniscectomy under an axial femoral compressive load was about twice that of a healthy joint [27]. This fact could partially explain the cartilage damage and degeneration that have been occurring after meniscectomy.

New Treatment Options

Meniscal Scaffold

To create the custom-made scaffold with definite pore dimension and consequently biomechanical features and the high biocompatibility of the whole tissues are important. Also, there are too many features important such as cell attachment. A biomaterial used as scaffold for meniscus tissue engineering purposes should present many features. The ideal meniscal scaffold should be (1) “cell-instructive”, promoting cell differentiation and proliferation if cell-seeded, or cell migration if cell-free; (2) “biomimetic”, mimicking

architecture, tribology and mechanical features of the native meniscus; (3) resilient and resistant to withstand mechanical forces acting in the joint while cells produce ECM (extracellular matrix); (4) biocompatible, not evoking any foreign-body reaction also with its degradation products; (5) slowly biodegradable, allowing to be gradually replaced by biologic tissue; (6) open, with high porosity, allowing diffusion of nutrients and catabolic substances; and (7) easy to handle, to be sutured and to be implanted by the surgeon [35, 36].

With the ultimate goal of designing the ideal scaffold for meniscus tissue engineering, many biomaterials have been evaluated, both natural and synthetic [37]. Natural materials used to date are as follows: *periosteal tissue* [38]; *perichondral tissue* [39]; small intestine submucosa (SIS) [40]; *acellular porcine meniscal tissue* [41]; and *bacterial cellulose* [42]. While these tissues have high biocompatibility, they do not allow varying structure geometry and initial mechanical properties because some of them cannot be employed for tissue engineering techniques [37]. A more attractive strategy is represented by isolated tissue components like collagens and proteoglycans [43, 44]. They maintain the high biocompatibility of the whole tissues while allowing to create custom-made scaffold with definite pore dimension and geometry and, consequently, biomechanical features.

However, these scaffolds have usually low biomechanical properties and are characterized by rapid biodegradation, consequently not long enough to be completely replaced by the newly formed tissue [37].

On the other hand, polymer materials can be manufactured in custom-made shapes of any geometrical structure, porosity and biomechanical properties, according to the characteristics of the host tissue and the seeded cells. In particular, it has been shown that for optimal ingrowth and incorporation of a meniscal scaffold, macropore sizes must be in the range of 150–500 μm [45]. The biodegradation rate can be also modulated by acting on polymer composition. The most used synthetic polymers are as follows: polyglycolic acid (PGA) [46]; poly(L)lactic acid (PLLA) [47]; poly-(lactic-co-glycolic acid) (PLGA) [48]; polyurethane [49, 50]; polyester carbon [51]; polytetrafluoroethylene [52]; and polycaprolactone (PCL) [53]. Possible disadvantages of the use of synthetic polymers for tissue engineering purposes are the low cell-adhesive properties, since they lack the cell-adhesion domains normally present on natural macromolecules, and already mild foreign-body reaction occurring after implantation [54, 55]. In order to improve biocompatibility and biodegradability of polymer scaffolds, a biopolymer, such as silk fibrous protein, has been suggested [56, 57].

An alternative strategy is represented by the use of hydrogel materials. Their semi-liquid nature allows engineering anatomic geometries derived from medical imaging techniques, such as computed tomography or magnetic resonance, by the use of custom-printed moulds [58]. Auspicious results were reported with alginate [58, 59] and polyvinyl alcohol (PVA) [60, 61].

Briefly, both natural materials and synthetic polymers present advantages and disadvantages. Most importantly, no biomaterial demonstrated to be superior to the others in terms of supporting cell proliferation and tissue growth. No clear advantage has been shown in terms of biomechanical properties suitable for implantation in the knee joint. A possible solution is represented by combining them, in order to couple the high cell affinity and biocompatibility of natural polymers with the superior mechanical strength and practicality planted of synthetic polymers. This strategy has been recently evaluated in two large animal studies on partial and total meniscus tissue engineering with a hybrid material composed of PCL and hyaluronic acid (HA) with good results [62, 63].

Meniscus Prosthesis

Biomaterial prostheses could have great potential. They are easy to produce and are available in unlimited numbers. Material composition, physical structure and size can be controlled, and immunologic problems can be prevented. Prostheses have been made of reconstituted

collagen, polyester–carbon fiber, fiber–teflon, and Dacron with polyurethane coating.

Klompmaker et al. showed that a meniscal replica can develop after implantation of a porous polymer prosthesis. When compared to meniscectomy, cartilage degeneration decreased [64].

Esposito et al. evaluated the ability of fibrochondrocytes preseeded on PLDLA/PCL-T [poly(L-co-D,L-lactic acid)/poly(caprolactone-triol)] scaffolds to stimulate regeneration of the whole meniscus. The aim of this study was to assess the usefulness of primary cultures of rabbit meniscus fibrochondrocytes grown on PLDLA/PCL-T (90/10) scaffolds for meniscus regeneration. At the end of the study, it has been shown that the PLDLA/PCL-T 90/10 scaffold has potential for orthopedic applications since this material allows the formation of fibrocartilaginous tissue, a structure of crucial importance for repairing injuries to joints, including replacement of the meniscus and the protection of articular cartilage from degeneration [65].

Studies have been reviewed of two types of scaffolds in the literature: CMI (Collagen Meniscus Implant—Ivy Sports Medicine GmbH, Germany); Actifit (Orteq, United KingdomGood). Clinical results have been documented both at histological and MRI evaluation. Safety and positive results have been shown for both scaffolds [66].

A. *The Menaflex CMI* is a porous collagen-glycosamino-glycan (GAG) matrix of defined geometry, density, thermal stability, and mechanical strength [67, 68]. The CMI is composed of about 97 % purified type I collagen (the most commonly found protein in the body). The remaining portion of the CMI consists of GAGs (glycoseaminoglycanes), which include chondroitin sulfate and hyaluronic acid [67, 69, 70]. The type I collagen is isolated and purified from bovine Achilles tendons from animals originating in the United States. It is implanted in the joint and fixed with sutures to the host meniscus [67].
B. *The Actifit meniscal implant* (Orteq Sports Medicine, London, UK) is a biodegradable, synthetic, acellular scaffold composed of aliphatic polyurethane. It has been designed to treat symptomatic, segmental defects of both medial and lateral menisci, thereby regenerate its biomechanical function and satisfactory clinical outcomes. It is a highly porous structure (approximately 80 %), allowing biological tissue ingrowth. In animal studies, removal of the material has been shown safely, as well as tissue ingrowth and vascularization [71].

A goal in the surgical management of meniscal tears or defects is to recreate a mechanically functional tissue in an attempt to halt disease progression. Use of scaffolds to facilitate tissue ingrowth into meniscal defects is one such option that is under investigation. Although not yet used clinically, cell-seeded scaffolds designed to be cultured in a laboratory setting prior to implantation have been developed for the treatment of meniscal defects [63, 72, 73.

A cell/scaffold combination could be a very promising alternative for repair of large meniscal defects [32]. For example, Ibarra and coworkers used fibrochondrocytes-seeded polyglycolic acid scaffolds to create tissue-engineered meniscal implants in sheep [74].

In another recent study by Peretti et al. [75] using a porcine model, meniscal tears in the avascular zone were repaired by using autologous chondrocyte seeded onto devitalized allogenic meniscal slices and cultured for 2.5 weeks prior to implantation in animals.

Both these studies and others reported in the literature [74–77] have provided histological evidence that cell therapy may be a good approach for treating meniscal cartilage lesions. However, these studies lack any evidence of biomechanical stability of the repair site and crucially they fail to identify the various factors contributing to the mechanism of repair. Since the long-term biochemical and biomechanical characteristics of a meniscus scaffold are ultimately determined by the cellular phenotype, a combination of a well-characterized cell population with a scaffold appears to be a logical option. Several candidate cell-types are of interest for meniscus tissue engineering. Of these, progenitor cells have the advantage to be easily expandable without the

loss of their differentiation potential. The authors present and discuss their current hypothesis for cell-based meniscus tissue engineering in combination with a scaffold.

Resources have thus far been largely directed to the sciences of polymer chemistry, cell biology, and cell–matrix interactions. Few resources, if any, have been used to standardize methods to assess the mechanical properties and functional performance of the candidate materials. Currently, information about the mechanical performance of materials intended for meniscal replacement such as their ability to provide knee joint stability and chondroprotection without damaging the articular cartilage is rarely reported in the scientific literature.

As a result, despite 20 years of tissue engineering innovation, only one scaffold for the treatment of meniscal defects has translated into clinical use in the United States—Menaflex™ (Regen Biologics, NJ, USA); yet, there have been no published reports that quantify the ability of the scaffold to mechanically function in the knee joint. Given that the scaffold is intended to function in the highly loaded environment of the knee, which is exposed to three to five times body weight during activities of daily living [78, 79] and subjected to millions of loading cycles each year, this lack of information negatively impacts regulatory decisions as to the safety and efficacy of an implant and suggests the urgent need to standardize tests aimed at evaluating functional performance.

Meniscus Allografts

Another approach to meniscus repair is allograft transplantation of a whole fresh-frozen or cryopreserved meniscus from a human donor. These tissue transplants are fixed to the tibial plateau via bone blocks or tunnels and can be derived from cadaveric sources. Whole meniscus transplants can restore some aspects of load transmission after total meniscectomy. However, in several studies, it has been shown that cartilage degeneration following implantation is most likely attributable to improper sizing of the implants [80–83]. A recent study showed that if allografts were more or less than 10 % of the original tissue size, the contact area of and resulting load transmission through cartilage and meniscus varied considerably from normal [84]. Additionally, non-anatomic positioning of meniscus transplants can significantly impact load transmission [85], and may explain some variation in clinical findings. Allografts also improve concerns regarding the methods of cryopreservation, graft sterility, and the proper method of fixation [81]. Clinical results of meniscal allografts suggest that function is only partially restored and that poor integration makes the grafts sensitive to premature failure [86]. These findings emphasize the need for a functional repair strategy short of total replacement for the clinical treatment of meniscal tears.

Future Options

Conservative and surgical modalities can be utilized in the treatment of the painful degenerative meniscal tear. Surgical approaches to the treatment of meniscal pathology can be categorized into partial menisectomy or repair with different techniques. Most of the time, treatment of meniscus lesions does not give satisfactory results because of unfavorable mechanical properties and the difficulty in obtaining these natural substitutes.

Currently, a number of researchers work on the development of different potential regenerative solutions for meniscal regeneration. Research potential for meniscus repair and regeneration is a wide spectrum from cell therapy to tissue therapy. Tissue engineering is going to become popular (cells, growth factors, and scaffolds). Meniscal scaffold and meniscal prosthesis with the literature will be mentioned in the following chapters. The use of prostheses, there are still no artificial materials with mechanical properties similar to those of the original meniscus. Although nonabsorbable synthetic materials allow cell invasion, collagen I and II deposition, and the formation of new tissue with fibrochondrocyte-like characteristics. Meniscal replacement using a porous

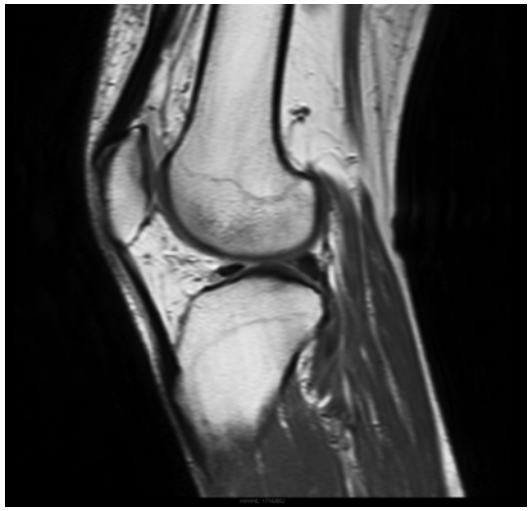

Fig. 25.5 Sagittal magnetic resonance image of the patient

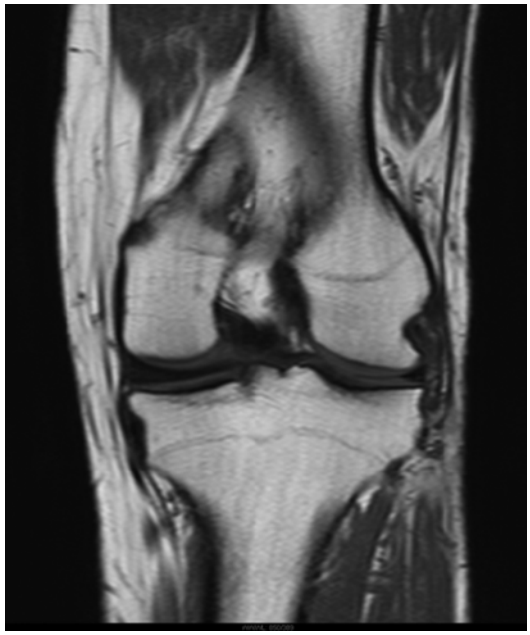

Fig. 25.6 Coronal magnetic resonance image of the patient

polymer prosthesis: a preliminary study in the dog. They are unable to confer long-term protection to articular cartilage after long periods alternative treatments, effects on articular cartilage, and future directions.

Clinical Relevance

What is the diagnosis and the most appropriate treatment? (Figs. 25.5 and 25.6)

A 39-year-old male, amateur football player, sustained an injury during game. He developed pain and swelling in his left knee. In his physical examination, specific meniscal tests were positive. His magnetic resonance imaging sequences revealed lateral meniscus tear. His arthroscopic examination revealed a bucket-handle tear of lateral meniscus. Arthroscopic partial meniscectomy was performed.

References

1. Arnoczky S, Dodds J, Wickiewics T (1996) Basic science of the knee. Lippincott-Raven Publishers, Philadelphia, p 29
2. Fithian DC MD, Kelly MA MD, Mow VC PD (1990) Material properties and structure-function relationships in the menisci. Clin Orthop Relat Res 252:19–31
3. Rath E, Richmond JC (2000) The menisci: basic science and advances in treatment. Br J Sports Med 34:252–257
4. Voloshin AS, Wosk J (1983) Shock absorption of meniscectomized and painful knees: a comparative in vivo study. J Biomed Eng 5:157–161
5. Arnoczky SP, Adams MF, DeHaven K et al (1988) The meniscus. In: Woo SI-Y, Buckwalter I (eds) NIAM5/AAOS workshop on the injury and repair of musculoskeletal soft tissues. Am Acad Orthop Surg, Park Ridge, 487–537
6. Adams ME, Hukins DWL (1992) The extracellular matrix of the meniscus. Knee meniscus: basic and clinical foundations. Raven Press, New York, pp 15–28
7. Ghosh P, Taylor TKF (1987) The knee joint meniscus. A fibrocartilage of some distinction. Clin Orthop 224:52–63
8. McDevitt CA, Weber RJ (1990) The ultrastructure and biochemistry of meniscal cartilage. Clin Orthop 252:8–18
9. Arnoczky SP, Warren RF (1982) Microvasculature of the human meniscus. Am J Sports Med 10:90–95
10. Fox AJ, Bedi A, Rodeo SA (2012) The basic science of human knee menisci: structure, composition, and function. Sports Health 4:340–351
11. Arnoczky SP, Warren RF (1983) The microvasculature of the meniscus and its response to injury—an experimental study in the dog. Am J Sports Med 11:131–141

12. O'Connor BL (1984) The mechanoreceptor innervation of the posterior attachments of the lateral meniscus of the dog knee joint. J Anat 138(Pt 1):15–26
13. O'Connor BL, McConnaughey JS (1978) The structure and innervation of cat knee menisci, and their relation to a "sensory hypothesis" of meniscal function. Am J Anat 153:431–442
14. Bullough PG, Munuera L et al (1970) The strength of the menisci of the knee as it relates to their fine structure. J Bone Joint Surg Br 52(3):564–567
15. Proctor CS, Schmidt MB et al (1989) Material properties of the normal medial bovine meniscus. J Orthop Res 7(6):771–782
16. Sweigart MA, Zhu CF et al (2004) Intraspecies and interspecies comparison of the compressive properties of the medial meniscus. Ann Biomed Eng 32(11):1569–1579
17. Macnicol MF, Thomas NP (2000) The knee after menisctomy. J Bone Joint Surg 82:157–159
18. Shrive NG, O'Connor JJ et al (1978) Load-bearing in the knee joint. Clin Orthop (131):279–287
19. Ahmed AM, Burke DL (1983) In-vitro measurement of static pressure distribution in synovial joints – part I: tibial surface of the knee. J Biomech Eng 105(3):216–225
20. Jones RS, Keene GC et al (1996) Direct measurement of hoop strains in the intact and torn human medial meniscus. Clin Biomech (Bristol, Avon) 11(5):295–300
21. Richards CJ, Gatt CJ et al (2003) Quantitative measurement of human meniscal strain. Trans Orthop Res Soc 28:649
22. Campbell SE, Sanders TG, Morrison WB (2001) MR imaging of meniscal cysts: incidence, location, and clinical significance. Am J Roentgenol 177:409–413
23. Havitcioglu H, Cecen B, Baktiroglu L, Erduran M, Karakasli A (2009) The biomechanical properties of meniscus. 14th Biomedical Engineering Meeting, at Izmir, Turkey, 20–22 May
24. Wilson W, van Donkelaar C, van Rietbergen B, Huiskes R (2003) Pathways of load-induced cartilage damage causing degeneration in the knee after meniscectomy. J Biomech 36:845–851
25. Andersson-Molina H, Karlsson H, Rockborn P (2002) Arthroscopic partial and total meniscectomy: a long-term follow-up study with matched controls. Arthroscopy 18:183–189
26. LeRoux MA, Setton LA (2002) Experimental biphasic fem determinations of the material properties and hydraulic permeability of the meniscus in tension. J Biomech Eng 124:315–321
27. Pen˜a E, Calvo B, Martı'nez MA, Palanca D, Doblare M (2005) Finite element analysis of the effect of meniscal tears and meniscectomies on human knee biomechanics. Clin Biomech 20:498–507
28. Messner K, Gillquist J (1993) Prosthetic replacement of the rabbit medial meniscus. J Biomed Mater Res 27:1165–1173
29. Berthiaume MJ, Raynauld JP, Martel-Pelletier J et al (2005) Meniscal tear and extrusion are strongly associated with progression of symptomatic knee osteoarthritis as assessed by quantitative magnetic resonance imaging. Ann Rheum Dis 64:556–563
30. Lange AK, Singh MAF, Smith RM et al (2007) Degenerative meniscus tears and mobility impairment in women with knee osteoarthritis. Osteoarthritis Cartilage 15:701–708
31. Donahue TLH, Hull ML, Rashid MM, Jacobs RC (2000) A finite element model of the human knee joint for the study of tibiofemoral contact. J Biomech Eng 124:273–280
32. Cook JL (2005) The current status of treatment for large meniscal defects. Clin Orthop Relat Res 435:88–95
33. Setton LA, Guilak F, Hsu EW, Vail TP (1999) Biomechanical factors in tissue engineered meniscal repair. Clin Orthop Relat Res 367(Suppl):S254–S272
34. McNicholas MJ, Rowley DI et al (2000) Total meniscectomy in adolescence. J Bone Joint Surg Br 82(2):217–221
35. Arnoczky SP (1999) Building a meniscus. Biologic considerations. Clin Orthop Relat Res 367(Suppl):S244–S253
36. van Tienen TG, Hannink G, Buma P (2009) Meniscus replacement using synthetic materials. Clin Sports Med 28:143–156
37. Buma P, Ramrattan NN, van Tienen TG, Veth RP (2004) Tissue engineering of the meniscus. Biomaterials 25:1523–1532
38. Walsh CJ, Goodman D, Caplan AI, Goldberg VM (1999) Meniscus regeneration in a rabbit partial meniscectomy model. Tissue Eng 5:327–337
39. Bruns J, Kahrs J, Kampen J et al (1998) Autologous perichondral tissue for meniscal replacement. J Bone Joint Surg Br 80:918–923
40. Cook JL, Tomlinson JL, Kreeger JM, Cook CR (1999) Induction of meniscal regeneration in dogs using a novel biomaterial. Am J Sports Med 27:658–665
41. Stapleton TW, Ingram J, Katta J et al (2008) Development and characterization of an acellular porcine medial meniscus for use in tissue engineering. Tissue Eng Part A 14:505–518
42. Bodin A, Concaro S, Brittberg M, Gatenholm P (2007) Bacterial cellulose as a potential meniscus implant. J Tissue Eng Regen Med 1:406–408
43. Mueller SM, Schneider TO, Shortkroff S et al (1999) Alpha-smooth muscle actin and contractile behavior of bovine meniscus cells seeded in type I and type II collagen-GAG matrices. J Biomed Mater Res 45:157–166
44. Pabbruwe MB, Kafienah W et al (2010) Repair of meniscal cartilage white zone tears using a stem cell/collagen-scaffold implant. Biomaterials 31:2583–2591
45. Klompmaker J, Jansen HW, Veth RP, Nielsen HK et al (1993) Porous implants for knee joint meniscus reconstruction: a preliminary study on the role of pore sizes in ingrowth and differentiation of fibrocartilage. Clin Mater 14:1–11
46. Vacanti CA, Langer R, Schloo B, Vacanti JP (1991) Synthetic polymers seeded with chondrocytes provide a template for new cartilage formation. Plast Reconstr Surg 88:753–759

47. Freed LE, Marquis JC, Nohria A et al (1993) Neocartilage formation in vitro and in vivo using cells cultured on synthetic biodegradable polymers. J Biomed Mater Res 27:11–23
48. Kang SW, Son SM, Lee JS et al (2006) Regeneration of whole meniscus using meniscal cells and polymer scaffolds in a rabbit total meniscectomy model. J Biomed Mater Res A 78:659–671
49. Heijkants RG, van Calck RV, De Groot JH et al (2004) Design, synthesis and properties of a degradable polyurethane scaffold for meniscus regeneration. J Mater Sci Mater Med 15:423–427
50. van Tienen TG, Heijkants RG, Buma P et al (2002) Tissue ingrowth and degradation of two biodegradable porous polymers with different porosities and pore sizes. Biomaterials 23:1731–1738
51. Wood DJ, Minns RJ, Strover A (1990) Replacement of the rabbit medial meniscus with a polyester-carbon fibre bioprosthesis. Biomaterials 11:13–16
52. Toyonaga T, Uezaki N, Chikama H (1983) Substitute meniscus of Teflon-net for the knee joint of dogs. Clin Orthop Relat Res 179:291–297
53. Lebourg M, Sabater Serra R, Más Estellés J et al (2008) Biodegradable polycaprolactone scaffold with controlled porosity obtained by modified particle-leaching technique. J Mater Sci Mater Med 19:2047–2053
54. Cao Y, Rodriguez A, Vacanti M et al (1998) Comparative study of the use of poly(glycolic acid), calcium alginate and pluronics in the engineering of autologous porcine cartilage. J Biomater Sci Polym Ed 9:475–487
55. Welsing RT, van Tienen TG, Ramrattan N et al (2008) Effect on tissue differentiation and articular cartilage degradation of a polymer meniscus implant: a 2-year follow-up study in dogs. Am J Sports Med 36:1978–1989
56. Mandal BB, Park SH, Gil ES, Kaplan DL (2011) Multilayered silk scaffolds for meniscus tissue engineering. Biomaterials 32:639–651
57. Mandal BB, Park SH, Gil ES, Kaplan DL (2011) Stem cell-based meniscus tissue engineering. Tissue Eng Part A 17:2749–2761
58. Ballyns JJ, Gleghorn JP, Niebrzydowski V et al (2008) Image-guided tissue engineering of anatomically shaped implants via MRI and micro-CT using injection molding. Tissue Eng Part A 14:1195–1202
59. Ballyns JJ, Wright TM, Bonassar LJ (2010) Effect of media mixing on ECM assembly and mechanical properties of anatomically-shaped tissue engineered meniscus. Biomaterials 31:6756–6763
60. Kobayashi M, Toguchida J, Oka M (2003) Preliminary study of polyvinyl alcohol-hydrogel (PVA-H) artificial meniscus. Biomaterials 24:639–647
61. Kobayashi M, Chang YS, Oka M (2005) A two year in vivo study of polyvinyl alcohol-hydrogel (PVA-H) artificial meniscus. Biomaterials 26:3243–3248
62. Chiari C, Koller U, Dorotka R et al (2006) A tissue engineering approach to meniscus regeneration in a sheep model. Osteoarthritis Cartilage 14:1056–1065
63. Kon E, Chiari C, Marcacci M et al (2008) Tissue engineering for total meniscal substitution: animal study in sheep model. Tissue Eng Part A 14:1067–1080
64. Klompmaker J, Veth RPH, Jansen HWB et al (1996) Meniscal replacement using a porous polymer prosthesis: a preliminary study in the dog. Biomaterials 17:1169–1175
65. Esposito AR, Moda M et al (2013) Biores Open Access 2(2):138–147
66. Filardo G, Andriolo L, Kon E et al (2014) Meniscal scaffolds: results and indications. A systematic literature review. Int Orthop. doi:10.1007/s00264-014-2415-x
67. Li S-T, Rodkey WG, Yuen D et al (2002) Type I collagen- based template for meniscus regeneration. In: Lewandrowski K-U, Wise DL, Trantolo DJ, Gresser JD, Yaszemski MJ, Altobelli DE (eds) Tissue engineering and biodegradable equivalents. Scientific and clinical applications. Marcel Dekker, New York, pp 237–266
68. Rodkey WG (2008) A look beyond the horizon. In: Feagin JA Jr, Steadman JR (eds) The crucial principles in care of the knee. Lippincott Williams & Wilkins, Philadelphia
69. Stone KR, Rodkey WG, Webber RJ et al (1990) Future directions: collagen-based prosthesis for meniscal regeneration. Clin Orthop Relat Res 252:129–135
70. Stone KR, Rodkey WG, Webber RJ et al (1992) Meniscal regeneration with copolymeric collagen scaffolds: in vitro and in vivo studies evaluated clinically, histologically, biochemically. Am J Sports Med 20:104–111
71. Tienen TG, Heijkants RG, de Groot JH et al (2006) Replacement of the knee meniscus by a porous polymer implant: a study in dogs. Am J Sports Med 34:64–71
72. Aufderheide AC, Athanasiou KA (2007) Assessment of a bovine co-culture, scaffold-free method for growing meniscus-shaped constructs. Tissue Eng 13(9):2195–2205
73. Weinand C, Peretti GM, Adams SB Jr et al (2006) An allogenic cell-based implant for meniscal lesions. Am J Sports Med 34(11):1779–1789, Epub
74. Hidaka C, Ibarra C, Hannafin JA, Torzilli PA, Quitoriano M, Jen SS et al (2002) Formation of vascularized meniscal tissue by combining gene therapy with tissue engineering. Tissue Eng 8(1):93–105
75. Peretti GM, Gill TJ, Xu JW, Randolph MA, Morse KR, Zaleske DJ (2004) Cell-based therapy for meniscal repair: a large animal study. Am J Sports Med 32(1):146–158
76. Ibarra C, Jannetta C, Vacanti CA, Cao Y, Kim TH, Upton JV et al (1997) Tissue engineered meniscus: a potential new alternative to allogeneic meniscus transplantation. Transplant Proc 29:986–988
77. Stone KR, Steadman JR, Rodkey WG, Li ST (1997) Regeneration of meniscal cartilage with use of a collagen scaffold. Analysis of preliminary data. J Bone Joint SurgAm 79(12):1770–1777

78. Heinlein B, Kutzner I, Graichen F, Bender A, Rohlmann A, Halder AM, Beier A, Bergmann G (2009) ESB Clinical Biomechanics Award 2008: complete data of total knee replacement loading for level walking and stair climbing measured in vivo with a follow-up of 6–10 months. Clin Biomech (Bristol Avon) 24(4):315–326, Epub
79. Mündermann A, Dyrby CO, D'Lima DD, Colwell CW Jr, Andriacchi TP (2008) In vivo knee loading characteristics during activities of daily living as measured by an instrumented total knee replacement. J Orthop Res 26(9):1167–1172
80. Garrett JC (1992) Meniscal transplantation. In: Aichroth PM, Canon WD (eds) Knee surgery, current practice. Raven Press Ltd, New York, pp 95–102
81. Jackson DW, McDevitt CA et al (1992) Meniscal transplantation using fresh and cryopreserved allografts. An experimental study in goats. Am J Sports Med 20(6):644–656
82. Elliott DM, Jones R et al (2002) Joint degeneration following meniscal allograft transplantation in a canine model: mechanical properties and semiquantitative histology of articular cartilage. Knee Surg Sports Traumatol Arthrosc 10(2):109–118
83. Mora G, Alvarez E et al (2003) Articular cartilage degeneration after frozen meniscus and Achilles tendon allograft transplantation: experimental study in sheep. Arthroscopy 19(8):833–841
84. Dienst M, Greis PE et al (2007) Effect of lateral meniscal allograft sizing on contact mechanics of the lateral tibial plateau: an experimental study in human cadaveric knee joints. Am J Sports Med 35(1):34–42
85. von Lewinski G, Kohn D et al (2008) The influence of nonanatomical insertion and incongruence of meniscal transplants on the articular cartilage in an ovine model. Am J Sports Med 36(5):841–850
86. Rath E, Richmond JC et al (2001) Meniscal allograft transplantation. Two- to eight-year results. Am J Sports Med 29(4):410–414

Skeletal Muscle; Structure, Function, and Repair

26

Hakan Ömeroğlu and Suna Ömeroğlu

Abstract

Skeletal muscle has a specialized structure due to its distinctive function. Skeletal muscle fibers (muscle cells) have cross-band appearance because of the intracellular contractile proteins called the myofilaments. Bundles of thick and thin myofilaments form myofibrils; bundles of myofibrils form muscle fibers; and finally, bundles of muscle fibers constitute skeletal muscle tissue. Thick myofilaments contain myosin protein and thin myofilaments contain mainly actin protein. Sarcoplasmic reticulum stores Ca^{2+} ions, which are essential for muscle contraction, and T-tubules provide the transmission of muscle innervation. Release of acetylcholine from the axon ending into the synaptic cleft initiates the depolarization of sarcolemma (muscle fiber membrane), and this leads to release of Ca^{2+} ions from the terminal sacs of sarcoplasmic reticulum into the sarcoplasm (cytoplasm). Ca^{2+} binds the troponin proteins found on the thin myofilaments. This initiates the attachment of actin to the binding site of myosin and thin myofilaments slide over thick myofilaments and the muscle contraction process occurs. Skeletal muscle injuries are due to direct (sharp, blunt, and penetrating) or indirect (rapid eccentric contraction) trauma. The repair process of skeletal muscle includes necrosis/degeneration, inflammation, proliferation and differentiation of certain cells, formation of scar tissue, and remodeling phases.

Learning Objectives

- Defining the macroscopic and microscopic structure of skeletal muscle
- Defining the contraction process in the skeletal muscle
- Defining the neural innervation of skeletal muscle

H. Ömeroğlu (✉)
Department of Orthopedics and Traumatology,
Eskişehir Osmangazi University Faculty of Medicine,
Eskişehir 26480, Turkey
e-mail: omeroglu.h@gmail.com; homer@ogu.edu.tr

S. Ömeroğlu
Department of Histology and Embryology,
Gazi University Faculty of Medicine,
Ankara 06100, Turkey

F. Korkusuz (ed.), *Musculoskeletal Research and Basic Science*,
DOI 10.1007/978-3-319-20777-3_26

- Explaining the mechanism and repair process of skeletal muscle injury
- Reviewing the clinical relevance of the skeletal muscle structure, contraction process, neural innervation, and skeletal muscle injuries

Introduction

Life is movement and movement is life is one of the well-known sayings of Orthopedics. Muscle tissue can be considered as the essential tissue producing movement in human body. *Muscle fibers* (*muscle cells*) are predominantly alike other cells in the body. This is because, muscle fibers contain highly specialized intracellular components, making them distinctive, in order to provide body movement as well as to change the shape and size of the internal organs [1, 2]. Muscle tissue is classified as *striated muscle* and *smooth muscle* according to the appearance of the muscle fiber at the light microscope level [2–4]. Striated muscle has muscle fibers having regularly repeated cross-band appearance, which is mainly due to intracellular contractile proteins called the *myofilaments*. Striated muscle is further classified into two groups according to the location as *skeletal muscle*, which contracts voluntarily, and *cardiac muscle*, which contracts involuntarily. More than 400 skeletal muscles make about 40–50 % of total body in an adult [2, 5, 6]. Smooth muscle contains muscle fibers, which do not have cross-band appearance, contracts involuntarily and is found in walls of blood vessels, viscera, and in dermis of the skin [2–4, 7].

In this chapter, the structure, function, and repair of skeletal muscle as well as the clinical relevance of the contents of these topics will be reviewed.

Structure of Skeletal Muscle

Macroscopic and Microscopic Structure

Skeletal muscle that is attached to bone provides movement of the skeleton and maintenance of body position and posture. Besides trunk and limbs, skeletal muscle is found in eye and ear [2]. Skeletal muscle is in pink-red color, due to its rich blood supply and oxygen-transporting proteins called the *myoglobins* [3].

Macroscopic arrangement of muscle fibers demonstrates a high level of organization. Organization of muscle fibers in relation to the force generation axis is called *muscle architecture*. Parallel or longitudinally arranged muscles, such as biceps brachi muscle, contain muscle fibers, which are parallel to the muscle force-generation axis. Unipennate muscles, for example vastus lateralis muscle, contain muscle fibers that are oriented at a single angle, generally varying between 0° and 30°, relative to the muscle force-generation axis. Finally, multipennate muscles, such as gluteus medius muscle, have fibers, which are positioned at several angles to the muscle force-generation axis [1, 5].

The vascular supply to skeletal muscle varies slightly in different muscles. The blood supply can be derived from a single penetrating main artery in some muscles. On the other hand, the blood supply can be derived from a series of penetrating arteries in some other muscles [5].

A skeletal muscle is composed of bundles of muscle fibers called the *fascicles*, which contain numerous muscle fibers. A muscle fiber is composed of longitudinally arrayed units called the *myofibrils*. A myofibril is composed of thick and thin myofilaments [1–5] (Fig. 26.1). There are investments of the skeletal muscle composed of connective tissue and needed for contractile force transmission [2, 3]. *Endomysium* is the name of the structure, including reticular fibers and basal lamina and surrounding individual muscle fibers (Fig. 26.1). Basal lamina plays a crucial role in muscle fiber repair following injury. Small capillaries and thin nerve branches are present in the endomysium. *Perimysium* is a dense collagenous connective tissue surrounding the bundles of muscle fibers (Fig. 26.1). There are nerves, arteries, and veins in the perimysium. *Epimysium* is a dense irregular collagenous connective tissue surrounding the entire muscle (Fig. 26.1). The main nutrient vessels and nerves of the muscle penetrate epimysium [1–5, 7].

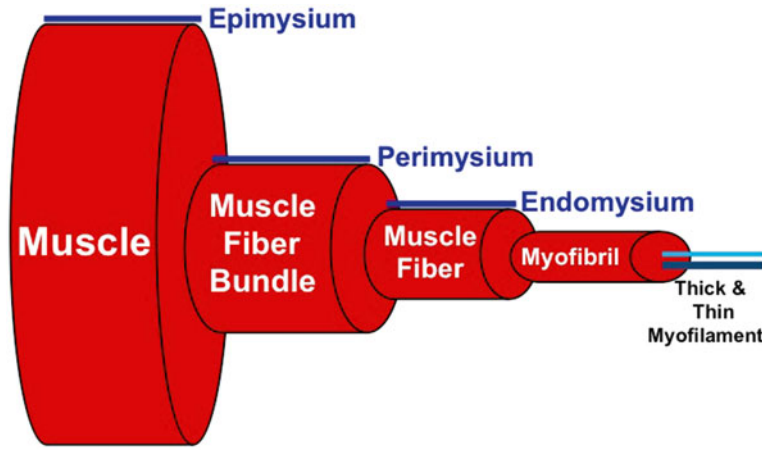

Fig. 26.1 Schematic drawing of the skeletal muscle organization

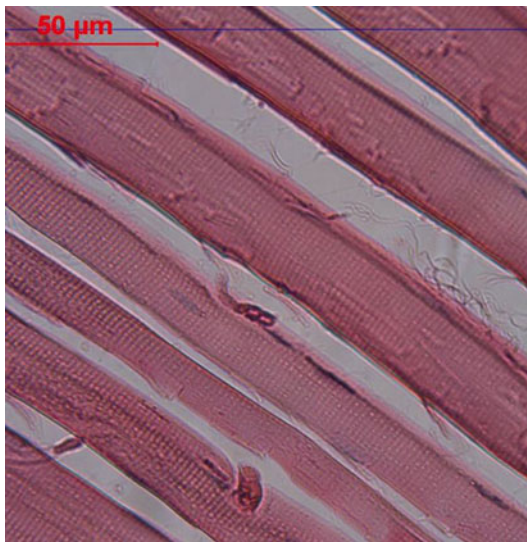

Fig. 26.2 Longitudinal section of a skeletal muscle at the light microscopy level. Cross-striations due to contractile proteins are seen (H.E., ×200)

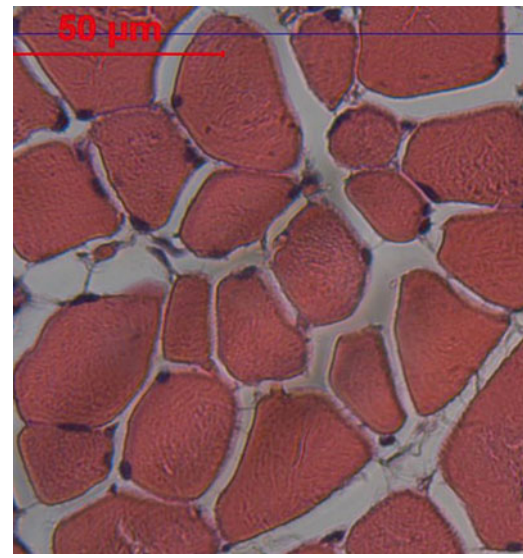

Fig. 26.3 Transverse section of a skeletal muscle at the light microscopy level. Peripheral localization of numerous nuclei in muscle fibers is seen (H.E, ×200)

Most of the skeletal muscles are derived from somatic mesoderm. In the embryo, a muscle fiber is formed by the fusion of a number of myoblasts, which are small, mononucleated, immature muscle cells and derived from pluripotent mesenchymal stem cells [2–5, 7]. Skeletal muscle fibers are long, cylindrical, multinucleated cells, and peripheral location of numerous nuclei just beneath the *sarcolemma* (*cell membrane*) is typical (Figs. 26.2 and 26.3). The diameter of a mature muscle fiber varies from 10 to 100 µm. The length of a mature muscle fiber is related with its location and varies from a few millimeters to about 1 m [1–4, 7]. Males have greater muscle mass than females. Size of the individual muscle fibers is larger in males due to bigger body size, more physical exertion, and hypertrophic effect of androgens on muscle fibers [5]. Experimental studies have shown that the length of muscle fibers is directly proportional with the skeletal muscle excursion (maximum contraction velocity). Besides, the diameter of the muscle fibers is directly proportional with the force generated by the skeletal muscle [1].

Satellite cells are small cells with single nucleus and localized in shallow depressions on muscle fibers' surfaces. They act like stem cells in the repair process and following a muscle injury, they proliferate to give rise to new myoblasts [2, 3, 5].

The structural and functional subunit of a muscle fiber is myofibril. Most of the muscle fiber cytoplasm (sarcoplasm) is filled with myofibrils, which are cylindrical in shape, arranged as parallel arrays extending the entire length of muscle fibers and having a diameter of 1–3 μm and a length of 1–2 cm [2–4, 8]. Myofibrils are composed of bundles of thick and thin myofilaments. Thick myofilaments, which are 1,5 μm long and 15 nm in diameter, are composed of the protein *myosin*. Each thick myofilament contains about 200–300 myosin proteins [2–5, 7]. Thin myofilaments, which are 1 μm long and 6–8 nm in diameter, are mainly composed of the protein called the *actin* and *troponin*, *tropomyosin*, as well [2–5, 7]. Each thick myofilament is equidistantly surrounded by six thin myofilaments in a mammalian skeletal muscle [3]. Accessory proteins, including titin, α-actinin, nebulin, tropomodulin, desmin, myomesin, C protein, and dystrophin regulate the spacing, attachment, and alignment of the myofilaments [2]. Myosin and actin constitutes more than half of the proteins found in the striated muscle [4].

Cross-striations of muscle fibers can be visible in unstrained preparations examined in polarizing microscope and look as repetitive light and dark bands. In polarizing microscopy, dark bands are anisotropic or double refractive and named as *A bands* (Fig. 26.4). A bands contain both thick and thin myofilaments. A band is bisected by a light region called the *H band* (Fig. 26.4). H band contains only thick myofilaments. H band is bisected by a narrow and dense line called the *M line* (Fig. 26.4). M line is formed by the linkage of adjacent thick myofilaments [1–4]. Light bands are isotropic and named as *I bands* (Fig. 26.4). I bands contain only thin myofilaments [1–4]. I band is bisected by a dense line called the *Z line* (*Z disk*) (Fig. 26.4). The segment of the myofibril between two adjacent Z lines is called the *sarcomere*. It is the basic contractile unit of striated muscle and its length is about 2–3 μm in resting mammalian muscle. Its length decreases during muscle contraction and increases in muscle stretching. The length of A band remains unchanged during resting, contraction, or stretching; however, the lengths of H and I bands change according to the status of the skeletal muscle [1–5, 7] (Fig. 26.4).

Most of the intracellular organelles of the muscle fiber are located around the nucleus and myofibrils. *Sarcoplasmic reticulum* is the intracellular organelle, placed around the myofibrils as a meshwork and forms a channel called the *terminal sac* at the A-I band junction. Terminal sac of sarcoplasmic reticulum is the main store of Ca^{2+}, which is the essential ion for initiating muscle contraction. *T tubules* are the tubular

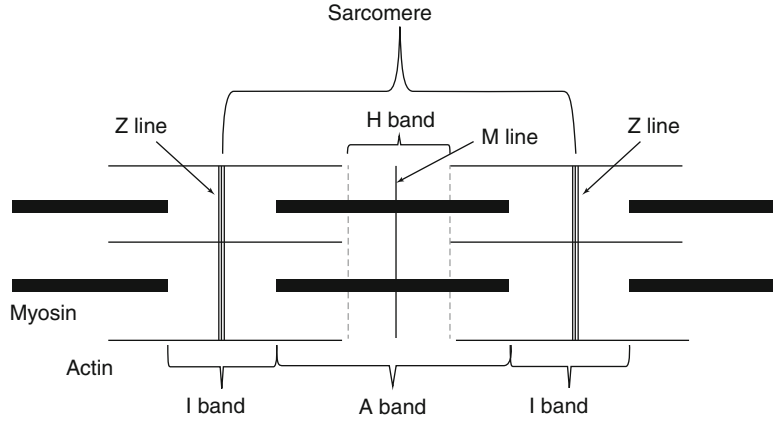

Fig. 26.4 Schematic drawing of a sarcomere

invaginations of the sarcolemma and located at the A-I band junction. They carry the impulses from sarcolemma to terminal sac. The complex of two neighboring terminal sacs and one T-tubule is called the *triad*. As the reactions initiating the contraction process need energy, variable numbers of mitochondria, 1 μm in width each, are located around the myofibrils and close to the Z line. Besides, numerous glycogen molecules are located close to myofibrils [1–5, 7].

Types of Muscle Fibers

Skeletal muscle fibers have a wide spectrum of morphologic, contractile, and metabolic properties. Several classification schemes have been defined for typing the muscle fibers [1] (Table 26.1). Fast contracting glycolytic muscle fibers are large in cross section, have the highest number of glycogen molecules and glycolytic enzymes, so are rich in ATP and adapted for sudden and stronger contraction to make the precise and rapid movements available, but fatigue rapidly. Such muscle fibers are mostly found in muscles controlling the movements of digits [1–3, 7]. Slow contracting oxidative muscles are small in cross section, contain abundant mitochondria, therefore are rich in oxidative enzymes and myoglobin, adapted for slow, weaker, repetitive contraction but have more resistance to fatigue. Such muscle fibers are found in limb and long back muscles [2, 3, 5, 7]. While the number of fast glycolytic muscle fibers is higher in sprinters, the number of slow oxidative muscle fibers is higher in long distance runners [5, 8].

Clinical Relevance

Muscle hypertrophy is the increase in the diameter and volume of muscle fibers due to several factors such as nutrition and exercise. *Muscle atrophy* is decrease in the diameter and volume of muscle fibers due to factors like aging and immobilization [4, 5, 8].

Muscle hyperplasia is the increase in the number of muscle fibers and does not occur in a healthy skeletal muscle [4].

Muscle dystrophies are a group of inherited disorders with progressive degeneration and weakness of skeletal muscles. Duchenne's and Becker's muscular atrophies are the most common types and due to absence of dystrophin in myofibrils as a result of mutation in encoding dystrophin [9].

In *pes equinovarus due to myelomeningocele*, the diameter of muscle fibers decreases except the gastrocnemius muscle and the most severe atrophy and fibrosis is seen in the long peroneal muscle [10].

The use of tourniquets on extremities during surgery can have adverse effects on the ultrastructure of muscle fibers distal to the tourniquet. Early ultrastructural findings of muscle atrophy can be seen in muscles distal to tourniquet if the tourniquet time exceeds 1 h [11]. Besides, post-ischemic reperfusion can be seen following the use of tourniquet. This increases the capillary permeability and leads to oxidative stress [11, 12].

The architecture of skeletal muscles can play an important role in *tendon transfers*. Theoretically, transferring the tendon of a skeletal muscle to the tendon of another skeletal muscle with similar architectural properties may obtain a better muscle function [1].

Table 26.1 Classification patterns for muscle fibers [1]

Basis for classification	Muscle fiber subgroups		
Metabolic	Slow contracting, oxidative	Fast contracting, oxidative glycolytic	Fast contracting glycolytic
Morphologic and physiologic	Slow contracting red	Fast contracting white	Fast contracting white
Z-line width	Wide	Intermediate	Narrow
Histochemical	Type 1	Type 2A	Type 2B
Immunohistochemical	Type 1	Type 2A and 2X	Type 2B

Contraction of Skeletal Muscle

Process of Muscle Contraction

The process of muscle contraction due to neural stimulation is called *excitation–contraction coupling* [1]. Contraction of skeletal muscle follows the *all-or-none law* and each contraction is followed by relaxation [3]. Onset of a nerve impulse at the neuromuscular junction is followed by the neurotransmitter (acetylcholine) release from the nerve ending. Acetylcholine initiates a sarcolemma depolarization and this impulse is transmitted along the sarcolemma to the T-tubules. The activation of T-tubules opens the Ca^{2+} channels found in the terminal sacs of the sarcoplasmic reticulum. Ca^{2+} ions are rapidly and enormously released into the sarcoplasm and bind to the troponin proteins on the thin myofilaments [1–5]. Binding of Ca^{2+} to troponin initiates the muscle contraction cycle, which simply includes the attachment of myosin binding site to actin followed by power generation, which leads to sliding of the thin myofilaments upon the thick myofilaments and shortening of sarcomere. Thus, when the muscle contraction occurs, the thin myofilaments move toward the center of sarcomere (*sliding filament theory*) [2–4, 7] (Fig. 26.5a, b). The reduced levels of Ca^{2+} around the myofibrils due to active drive of Ca^{2+} back into the terminal sac leads to the release of the bond between myosin and actin, which relaxes the muscle [3, 5]. Each series of attachment and release requires ATP to convert the chemical energy into movement [1, 3].

Clinical Relevance

İsometric contraction is the kind of contraction in which the force generated by the muscle is equal to the resisting load. The length of the muscle remains unchanged during isometric contraction [1, 5, 6].

Concentric contraction is the shortening of the muscle length during contraction as the force generated by the muscle is greater than the external force [1, 6].

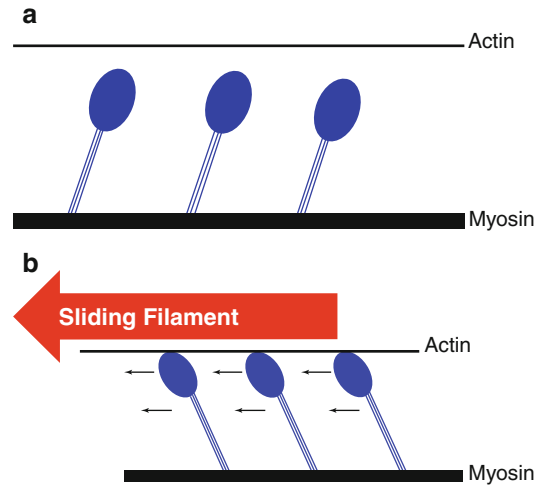

Fig. 26.5 Schematic drawing of the muscle contraction. (**a**) In resting muscle, myosin and actin are not bound to each other. (**b**) In muscle contraction, actin is bound to binding sites of myosin and thin myofilaments slide over the thick myofilaments

Eccentric contraction is the forced lengthening of the muscle during contraction due to the existence of external force higher than the maximum force generated by the muscle. Repeated exercises leading to eccentric contractions increase the muscle mass and strength. Muscle injury and tenderness are primarily related with the eccentric contraction [1, 6, 8].

Innervation of Skeletal Muscle

Types of Nerve Innervation

Each skeletal muscle fiber has at least two types of nerve innervation, namely, motor and sensorial. Muscle fibers need to be innervated by motor nerves in order to maintain their structural integrity. Otherwise, the muscle fiber undergoes structural changes that can only be reestablished by restoring the integrity of the innervating nerve [2].

Motor nerve fibers are composed of myelinated axons of α-motor neurons. A single motor neuron may innervate numerous muscle fibers. *Neuromuscular junction* (*motor end plate*) is

composed of axon ending of the neuron, synaptic cleft, and sarcolemma of the muscle fiber [2, 3]. The impulse from axon to sarcolemma is transmitted via synaptic cleft. Release of acetylcholine from axon ending of the neuron into the synaptic cleft is followed by the binding of acetylcholine to the specific receptors found in the sarcolemma. This binding leads to depolarization of the sarcolemma and this subsequently initiates the skeletal muscle contraction, which has previously been described [1–5]. Acetylcholinesterase enzyme inactivates the acetylcholine found in the synaptic cleft to end the muscle contraction [2, 4].

Muscles contain specialized sensorial receptors, which monitor the tension and position of the muscles during resting or contraction. *Muscle spindles* are specialized stretch receptor units of muscles, which are encapsulated and contain both sensorial (afferent) and motor (efferent) nerve fibers. Sensorial nerve fibers monitor the changes in the length of the muscle, and excessive stretching of the muscle is followed by a reflex contraction. Motor nerve fibers control the sensitivity of sensorial endings in the muscle spindle [2–4]. *Golgi tendon organs* (*neurotendinous spindles*) are specialized receptors located at the musculotendinous junction. They contain sensorial (afferent) nerve fibers, monitor the force of muscle contraction, and have inhibitory effect in case of strong muscle contraction [2–5].

Autonomic nerve fibers innervate the vessels found in the skeletal muscle [2, 3].

Clinical Relevance

Botulism is caused by the Clostridium botulinum bacteria and its toxin causes flask muscular paralysis by inhibiting the release of acetylcholine from axon ending into the synaptic cleft. Botulinum Toxin A has been used for the treatment of spastic contractures of muscles in cerebral palsy [1, 3, 8]. The temporary relaxing effect of the toxin on the contracted muscles improves the physiotherapy process.

Myasthenia gravis is an autoimmune disease, which is characterized by advanced weakness of the muscles due to blockage of the receptors in the sarcolemma by autoimmune antibodies. As the number of functioning neuromuscular junctions is considerably reduced, the muscle contraction is diminished in varying degrees [2–4, 8, 9].

Neurotoxins of some poisonous snakes and insects bind to acetylcholine receptors in the sarcolemma and cause flask paralysis in skeletal muscles [3].

Patellar tendon reflex test is an example of reflex muscle contraction initiated by muscle spindles [3].

Skeletal Muscle Injury and Repair

Skeletal muscle injuries are a common health problem in all kinds of sports. For example, about one-third of the injuries in elite football players are muscle injuries [13]. Skeletal muscle injuries can be due to direct or indirect trauma [15]. Direct trauma is caused by blunt, sharp, or penetrating external force [13]. Muscle injuries due to indirect trauma are mainly due to rapid eccentric muscle contraction and commonly seen in the musculotendinous junction, which is the weakest point of the skeletal muscle. Most of these injuries occur in biarticular muscles and skeletal muscles containing primarily fast contracting glycolytic muscle fibers [8, 13]. Several classifications for muscle injuries have been defined based on the amount of tissue damage as well as on the radiological examinations including ultrasonography (US) and magnetic resonance imaging (MRI). A recent and precise classification system for skeletal muscle injuries and disorders, based on a consensus statement between several sports medicine experts and including the type of macroscopic structural damage, clinical signs and symptoms, injury site and US/MRI findings, seems to cover almost all aspects of such problems [13] (Table 26.2).

The repair process of an injured muscle is similar to the repair process of other mesenchymal tissues [14] (Fig. 26.6). The repair process includes necrosis/degeneration, inflammation, proliferation and differentiation of certain cells,

Table 26.2 Classification of acute skeletal muscle disorders and injuries [13]

I. Indirect muscle disorder/injury
A. Functional muscle disorder
Type 1: Overexertion-related muscle disorder
Type 1A: Fatigue-induced muscle disorder
Type 1B: Delayed-onset muscle soreness
Tip 2: Neuromuscular muscle disorder
Type 2A: Spine-related neuromuscular muscle disorder
Type 2B: Muscle-related neuromuscular muscle disorder
B. Structural muscle injury
Tip 3: Partial muscle tear
Type 3A: Minor partial muscle tear
Type 3B: Moderate partial muscle tear
Tip 4: Subtotal or total muscular tear
Subtotal or complete muscular tear
Tendinous avulsion
II. Direct muscle injury
Contusion
Laceration

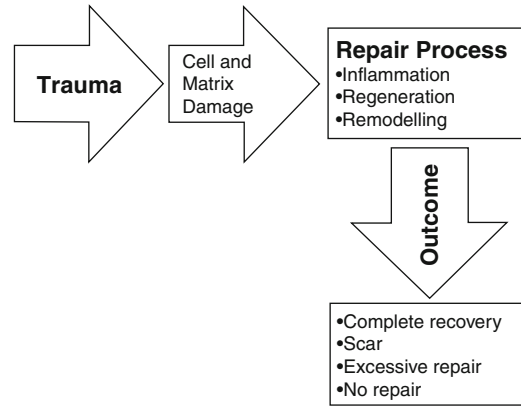

Fig. 26.6 Common repair process of mesenchymal tissues

formation of scar tissue, and remodeling [6, 15, 16]. Early phase of skeletal muscle repair is characterized by muscle necrosis followed by inflammatory response, including infiltration of the injury site first with polymorphonuclear neutrophils and then with macrophages. Cytokines and several growth factors are released from macrophages, fibroblasts, as well as from extracellular matrix as a response to muscle damage [6, 15, 16]. Some growth factors such as FGF (fibroblast growth factor), IGF (insulin-like growth factor), TGF-β (transforming growth factor-β), IL-6 (interleukin-6), hepatocyte growth factor (HGF), and platelet-derived growth factor (PDGF) activate the satellite cells to proliferate and differentiate into the muscle fiber precursor cells, myoblasts. Myoblasts then fuse to form new muscle fibers [6, 15, 16]. It is currently evident that satellite cells are essential and unable to be substituted in the skeletal muscle repair process [17]. At the early stages of regeneration phase, the newly formed muscle fibers are small in diameter and have centrally located nuclei [6, 16]. The newly formed muscle fibers increase in size and nuclei move to a peripheral position during remodeling phase. While the disrupted muscle fibers are regenerating, a connective scar tissue is formed by the fibroblasts. This scar tissue is reorganized and contracted during remodeling phase. However, formation of an excessive scar tissue due to excessive proliferation of fibroblasts influences the complete recovery from injury as such a repair tissue has lesser mechanical strength and impairs function [16]. At the end of repair process, the repaired muscle tissue is morphologically and functionally looks like a healthy muscle tissue under normal conditions [6, 15]. Denervation of muscle fibers due to damage of nerve branches within the muscle tissue has negative effects on muscle repair process [16].

The results of several studies have revealed that IGF, b-FGF, and nerve growth factor (NGF) have positive effects on skeletal muscle repair process by stimulating the proliferation and differentiation of precursor cells. Overproduction of TGF-β1 is responsible for tissue fibrosis; therefore, researchers have developed several drugs to inhibit TGF-β1 for lessening the amount of fibrosis during repair process of skeletal muscle [6, 16]. Several in vivo studies have been performed to deliver growth factors into the injured muscle by gene therapy [6]. There is currently insufficient evidence to recommend the use of platelet-rich plasma therapy for treating musculoskeletal soft tissue injuries [18].

Therefore, the key points to achieve effective and functional repair of skeletal muscle after

injury are to control inflammation by RICE (rest, ice, compression, elevation) approach, stimulate regeneration, protect the integrity of muscle innervation, and limit fibrosis as much as possible [16, 19].

Skeletal muscle has a close contact with bone and seems to contain highly osteoinductive potential, which may have significant roles in bone repair [20]. This is an area that needs more research in the next future.

References

1. Lieber R (2007) Form and function of skeletal muscle. In: Einhorn TA, O'Keefe RJ, Buckwalter JA (eds) Orthopaedic basic science: foundations of clinical practice, 3rd edn. American Academy of Orthopaedic Surgeons, Rosemont, pp 223–243
2. Ross MH, Kaye GI, Pawlina W (2003) Histology; a text and atlas with cell and molecular biology, 4th edn. Lippincott Williams & Wilkins, Baltimore
3. Gartner LP, Hiatt JL (2001) Color textbook of histology, 2nd edn. W.B.Saunders Co., Philadelphia
4. Junqueira LC, Carneiro J (2003) Basic histology; text & atlas, 10th edn. McGraw-Hill Co., New York
5. Heffner RR Jr (1997) Skeletal muscle. In: Sternberg SS (ed) Histology for pathologists, 2nd edn. Lippincott-Raven Publishers, Philadelphia, pp 197–220
6. Huard J, Li Y, Fu FH (2002) Muscle injuries and repair. Current trends in research. J Bone Joint Surg Am 84:822–832
7. Young B, Heath JW (2000) Wheater's functional histology; a text and colour atlas, 4th edn. Churchill Livingstone, Edinburgh
8. Brinker MD, O'Connor DP (2012) Basic sciences. In: Miller MD, Thompson SR, Hert JA (eds) Review of orthopaedics, 6th edn. Elsevier Saunders, Philadelphia, pp 1–142
9. Thompson GH, Berenson FR (2014) Other neuromuscular disorders. In: Weinstein SL, Flynn JM (eds) Lovell and Winter's pediatric orthopaedics, 7th edn. Lippincott Williams & Wilkins, Philadelphia, pp 587–628
10. Omeroglu S, Peker T, Omeroglu H, Gulekon N, Mungan T, Danisman N (2004) Intrauterine structure of foot muscles in talipes equinovarus due to high-level myelomeningocele: a light microscopic study in fetal cadavers. J Pediatr Orthop B 13:263–267
11. Omeroglu H, Erdogan D, Omeroglu S, Gunel U, Bicimoglu A (1997) Ultrastructural analysis of the alterations in skeletal muscle during tourniquet application on extremities (in Turkish). Acta Orthop Traumatol Turc 31:323–326
12. Sarban S, Atik OS, Erdogan D, Omeroglu S, Sayan H, Yanicoglu LP (1998) Histopathological findings in oxidative stress due to tourniquet use. Joint Dis Relat Surg 9(2):125–130
13. Mueller-Wohlfahrt H-W, Haensel L, Mithoefer K, Ekstrand J, English B, McNally S, Orchard J, van Dijk CN, Kerkhoffs GM, Schamasch P, Blottner D, Swaerd L, Goedhart E, Ueblacker P (2013) Terminology and classification of muscle injuries in sport: the Munich consensus statement. Br J Sports Med 47:342–350
14. Omeroglu H (2010) Composition, function, healing of the basic anatomic structures in the musculoskeletal system and the bone metabolism (in Turkish). TOTBID Derg 9:78–84
15. Cabral AJV, Machado V, Farinha R, Cabrita A (2008) Skeletal muscle regeneration: a brief review. Exp Pharmacol Health Sci 2:9–17
16. Baoge L, Van Den Steen E, Rimbaut S, Philips N, Witvrouw E, Almqvist KF, Vanderstraeten G, Vanden Bossche LC (2012) Treatment of skeletal muscle injury: a review. ISRN Orthop. doi:10.5402/2012/689012
17. Relaix F, Zammit PS (2012) Satellite cells are essential for muscle regeneration: the cell on the edge returns centre stage. Development 139:2845–2856
18. Moraes VY, Lenza M, Tamaoki MJ, Faloppa F, Belloti JC (2014) Platelet-rich plasma therapies for musculoskeletal soft tissue injuries. Cochrane Database Syst Rev 4, CD010071
19. Danna NR, Beutel BG, Campbell KA, Bosco JA 3rd (2014) Therapeutic approaches to skeletal muscle repair and healing. Sports Health 6:348–355
20. Liu R, Schindeler A, Little DG (2010) The potential role of muscle in bone repair. J Musculoskelet Neuronal Interact 10:71–76

Peripheral Nerve

27

A. Gürsel Leblebicioğlu, D. Burcu Hazer, Pierluigi Tos, Jörg Bahm, and Eftal Güdemez

Abstract

In order to understand peripheral nerve dysfunction, and to follow neuronal regeneration, basic sciences of the peripheral nerve should be understood completely. A surgeon who operates on "nerves" uses this knowledge, especially the organization of the peripheral nerve, in nerve reconstructions. When a nerve has been injured, the goal of surgical repair is generally to reapproximate the ends of the injured nerve. However, this cannot be possible in some occasions. If a primary suture is not feasible due to local tissue trauma, appropriate grafting of short and long defects is still the golden standard procedure. To bridge the nerve defects, the interfascicular autologous nerve grafting technique is still considered the "gold standard" but many other different "grafts" have been studied. In the presence of a critical motor target distance, one should consider distal motor nerve transfers. An alternative in late cases (after 6–12 months) is only provided by free muscle transfers, replacing the chronically denervated muscle with a newly denervating muscle, which the growing motor nerve should reach in the shortest time. Although nerve transfer surgery cannot

A.G. Leblebicioğlu, MD (✉)
Faculty of Medicine, Department of Orthopedic Surgery, Hacettepe University, Sıhhiye Ankara 06100, Turkey
e-mail: gurselleblebicioglu@ttmail.com

D.B. Hazer, MD
Faculty of Medicine, Department of Neurosurgery, Muğla Sıtkı Koçman University, Muğla 48000, Turkey
e-mail: burcuhazer@hotmail.com

P. Tos, MD, PhD
Department of Orthopaedics, Traumatology and Rehabilitation, Microsurgery Unit, AO Città della Salute e della Scienza, Orthopaedic and Trauma Center, Via Zuretti 29, Turin 10126, Italy
e-mail: Pierluigi.tos@unito.it

J. Bahm, MD
Euregio Reconstructive Microsurgery Unit, Franziskus Hospital, Morillenhang 27, Aachen 52074, Germany
e-mail: jorg.bahm@belgacom.net

E. Güdemez, MD
Koc University School of Medicine, Department of Orthopedics and Traumatology, KUH Hospital, Davutpaşa Cad., 4, Topkapı/Zeytinburnu 34010, İstanbul
e-mail: egudemez@ku.edu.tr

F. Korkusuz (ed.), *Musculoskeletal Research and Basic Science*,
DOI 10.1007/978-3-319-20777-3_27

fully replace functional restorations with tendon transfers, it has become a viable option in many cases. Overall, combination of nerve transfers with tendon transfers may provide better outcome.

Basic Science

Embryology

Neural Tube

The development of the nervous system begins at about 17 days following fertilization. At that time, a thickening of the ectoderm, called the neural plate, forms along the entire dorsal midline of the embryo and becomes largest near the future head of the developing embryo. The neural plate will differentiate into all of the neurons and most of the supporting cells of the nervous system (neuroglial cells) [32, 37].

The midline of the neural plate folds inward (invaginates) and forms a longitudinal neural groove. A concurrent proliferation of cells along the lateral margins of the neural plate produces thickened raised edges called neural folds. The neural groove continues to deepen as the neural folds become elevated. By the 20th day, the neural folds meet and fuse at the dorsal midline, and the neural groove becomes a neural tube. The neural folds first contact each other midway along the axis of the neural plate. Openings, or neuropores, at the cranial and caudal ends of the neural tube close during the fourth week.

Neural Crest

As the neural folds fuse longitudinally along the dorsal midline, cells at the tips of the neural folds develop into the neural crest that lies between the surface ectoderm and the dorsal surface of the neural tube. Most of the peripheral nervous system (PNS) develops from the neural crest, including the dorsal root ganglia of spinal nerves, ganglia of cranial nerves, and the somatic and visceral sensory neurons of spinal nerves and cranial nerves (V, VII, IX, and X). Some neural crest cells break away from the main tissue mass and migrate to other locations where they aggregate and differentiate into autonomic ganglia and postganglionic sympathetic and parasympathetic neurons near the vertebral column and in peripheral organs [18].

Besides forming dorsal root ganglia and associated glial cells, neural crest cells migrate around the central nervous system and develop into the spinal and cranial meninges. Migrating neural crest cells contribute to the formation of teeth and produce laryngeal cartilages, melanocytes, portions of the skull, connective tissues around the eye, intrinsic muscles of the eye, amphicytes, adrenal medullae, and Schwann cells [20].

By this time, neural crest cells have migrated to both sides of the spinal cord and have formed the dorsal root ganglia. The neural crest cells become the sensory neurons and glial cells (Schwann cells and satellite cells). Processes from these sensory neurons grow to the periphery to contact receptors and into the central nervous system through the dorsal roots of the spinal nerves. The axons of the developing motor neurons in each segment form a pair of ventral roots that grow away from the spinal cord. Distal to each dorsal root ganglion, motor efferent neurons of the ventral root and sensory afferent neurons of the dorsal root are bound together into a single spinal nerve [16, 43].

It has been suggested that normal development of the peripheral nerve network is based on incredible ability of axon wiring to locate and recognize their appropriate synaptic patterns. The axonal wiring occurs in two steps: the "pathfinding" and the "target selection" [54]. Developing axons choose specific routes in the embryos during pathfinding stage followed by growth cones navigating toward their targets [49]. Axons' targets sometimes may be far away from their soma and they generally pass through intermediate targets to form axon networks. In a previous study, it was suggested that outgrowth and termination of nerve fibers must be guided to

their respective end organs and other connection sites by selective chemical or electrical forces.

A Neuron

Structure of a Neuron

The nervous system in the body acts as an on-off button, which is responsible for coordination of voluntary and involuntary actions through a complex network. The basic element of this complex network is the nerve cell – or named as a "neuron." A neuron consists of a nerve cell body and its processes: a number of dendrites associated with the cell body and one long extension – an axon – terminating in peripheral synaptic terminals. Dendrites are thin structures that arise from the cell body, often extending for hundreds of micrometers and branching multiple times, giving rise to a complex "dendritic tree." An axon is a special cellular extension that arises from the cell body at a site called the axon hillock and travels for a distance, as far as one meter in humans or even more in other species. The cell body of a neuron frequently gives rise to multiple dendrites, but never to more than one axon, although the axon may branch hundreds of times before it terminates [24].

Electrical Activity in a Neuron

The cell body is the genomic and metabolic center of the neuron where synthesis of materials necessary for the maintenance of structural and functional integrity of the axon and its terminals occur. Considering the distance between cell body and axon, special network is required for transport named as retrograde and anterograde transport. By anterograde transport, variety of materials – neurotransmitters, their precursors, some enzymes – produced in the nerve cell body are carried outward along the axon at different rates. Axonal transport also includes whole organelles, such as mitochondria, glycoproteins, or proteins destined for incorporation in the cell membrane or for construction of the axonal cytoskeleton. In retrograde transport, the signal is transported from axon to the cell body, and it transports endosomes generated by endocytic activity at the nerve terminals [25]. All neurons are electrically excitable, maintaining voltage gradients across their membranes by means of metabolically driven ion pumps, which combine with ion channels embedded in the membrane to generate intracellular versus extracellular concentration differences of ions such sodium, potassium, chloride, and calcium. Changes in the cross-membrane voltage can alter the function of voltage-dependent ion channels. If the voltage changes in enough amount, an all-or-none electrochemical pulse called an action potential is generated, which travels rapidly along the cell's axon, and activates synaptic connections with other cells when it arrives [24].

Peripheral Nervous System

Peripheral nervous system, described as the part of the nervous system consisting of the nerves and ganglia outside of the brain and spinal cord. It consists of a dorsal root, dorsal root ganglia, ventral root, and the spinal nerve itself, finally named as the peripheral nerve. The cranial nerves are also part of the PNS with the exception of cranial nerve II, the optic nerve, along with the retina [9]. The ganglia of the cranial nerve originate in the CNS (except for nodosa ganglia, the ganglia of the Xth cranial nerve); however, their axons extend beyond the brain and are therefore considered part of the PNS.

Peripheral nerves are usually classified into three main categories, depending on fiber-type composition: (1) sensory, (2) motor, and (3) mixed nerves [24]. With only few exceptions (VIII cranial nerve and the mesencephalic root of the V cranial nerve), sensory nerve fibers originate from pseudounipolar neurons located in the sensory ganglia. On the other hand, motor nerve fibers originate from somatic and autonomic motor neurons located in the CNS. While somatic motor fibers directly reach the target skeletal muscle fibers, autonomic motor fibers create synapses in parasympathetic ganglion where the second-order autonomic neuron is located and the axon of which eventually reaches the target visceral organs [9].

Peripheral nervous system consists of somatic-sensory nervous system (31 pairs of spinal nerves and 11 pairs of cranial nerves) and autonomic nervous system [9]. The autonomic nervous system is composed of two divisions: the parasympathetic division derived from four of the cranial nerves (CN III, VII, IX, and X) and the S2–S4 sacral spinal cord levels, and the sympathetic division associated with the thoracic and upper lumbar spinal cord levels (T1-L2). The autonomic nervous system is a two-neuron chain, with the preganglionic neuron arising from the central nervous system and synapsing on a postganglionic neuron located in a peripheral autonomic ganglion. Postganglionic axons of the autonomic nervous system innervate smooth muscle, cardiac muscle, and glands. Basically, the sympathetic division mobilizes our body ("fight or flight") while the parasympathetic division regulates digestive and homeostatic functions. Normally, both divisions work in concert to regulate visceral activity (respiration, cardiovascular function, digestion, and associated glandular activity).

Nerve Fiber

Each nerve is a cordlike structure that contains many axons, also called nerve fibers. Within a nerve, each axon is surrounded by a layer of connective tissue called the endoneurium. The axons are bundled together into groups called fascicles, and each fascicle is wrapped in a layer of connective tissue called the perineurium, which is a lamellated sheath of considerable tensile strength. Because of the diffusion barrier in the perineurium, the interior of the fascicles, the endoneurial space, is chemically isolated from the surrounding tissues, thereby preserving a specialized ionic environment. Finally, the fascicles are embedded within an epineurium, which is a supporting and protective connective tissue carrying the main supply channels of the intraneural vascular system: the epineural vessels. Usually, several fascicles are grouped together in fascicular bundles constituting well-defined subunits of the nerve trunk. Schwann cells encircle the axonal projections and produce myelin, which facilitates the electrical conduction along the nerve [14, 19].

Nerve fibers can be myelinated or nonmyelinated. In the myelinated fiber, one axon is associated with only one Schwann cell of whose membrane is being wrapped spirally around the axon, producing a sheath of alternating layers of lipid and protein: the myelin sheath. In nonmyelinated fibers, however, one Schwann cell accumulates a great number of axons. The Schwann cells, being arranged in a longitudinal sequence along the axons surface, meet each other at the nodes of Ranvier, where finger-like cellular processes interdigitate. At this location, there is a space between the processes, allowing extracellular ions to reach the axon [17]. This is an important process in the so-called saltatory propagation of impulses from node to node. In between the nodes of Ranvier, the compact myelin and cytoplasm within a Schwann cell are arranged in a series of concentric subcellular compartments surrounding the axon, insulating it both morphologically and physiologically from the endoneurium [46]. The axon has a core of axoplasm surrounded by a continuous plasma membrane: the axolemma. The surrounding concentric layers of Schwann cell cytoplasm and myelin are bound peripherally by a continuous Schwann cell plasma membrane and its basal lamina. In literature, this basal lamina, together with the endoneurial reticular and collagen fibers providing the framework supporting the nerve fiber, has been referred to as the endoneurial tube or endoneurial sheath [31].

Nerve fibers of the PNS are classified according to their involvement in motor or sensory, somatic or visceral pathways [9]. Mixed nerves contain both motor and sensory fibers. Sensory nerves contain mostly sensory fibers; they are less common and include the optic and olfactory nerves. Motor nerves contain motor fibers. Most of the peripheral nerves in body contain both motor and sensory nerve fibers [9].

Ganglia

The cell bodies of peripheral neurons are present in nervous structures called ganglia. There are two types of ganglia: autonomic ganglia and somatic-sensory ganglia. Autonomic ganglia

possess sympathetic and parasympathetic postganglionic cells. Two types of somatic sensory ganglia exist: those associated with cranial nerves, i.e., cranial ganglia; and those associated with spinal nerves, i.e., spinal ganglia or dorsal root ganglia. The neurons in dorsal root ganglia are pseudounipolar neurons, and in this type of neurons, one single process, an axon, leaves the cell body and divides into two processes, one projecting to the CNS, and the other projecting to peripheral targets. Dorsal root ganglia neurons innervate muscle spindles and receptors in the skin [14]. The peripheral ganglia also contain glial cells such as satellite cells and Schwann cells (SCs). The glial cells regulate the neuronal environment by supporting and protecting the neurons. They can also produce neurotropic factors in response to neuronal injury. A ganglion also contains blood vessels and fibrobalsts. The entire ganglion is encapsulated in a connective tissue layer, which is continuous with the epineurium of the nerve.

Peripheral Nerve Injury

When a nerve has been injured, the goal of surgical repair is generally to reapproximate the ends of the injured nerve. Sometimes during repair after a nerve injury, a portion of the injured nerve, called a neuroma, needs to be excised, leaving a gap. When the nerve ends cannot be brought together, then a nerve graft may be necessary.

Nerve grafts are generally portions of a sensory nerve that are harvested from another part of the body to be used as graft material. Once the graft is in place, the regenerating nerve fibers grow from the proximal nerve stump, through the graft, through the distal nerve segment into the target muscles. Thus, patients may recover function in muscles following graft repair of nerve injuries. Sural nerve, superficial radial sensory, and medial antebrachial cutaneous nerve are common donor nerves for graft material.

Classification of nerve injury was described by Seddon in 1943 and by Sunderland in 1951 [41, 45]. The lowest degree of nerve injury in which the nerve remains intact but signaling ability is damaged is called neurapraxia. The second degree in which the axon is damaged but the surrounding connecting tissue remains intact is called axonotmesis. The last degree in which both the axon and connective tissue are damaged is called neurotmesis. Sunderland in 1951 reclassified nerve injury in detail related more to the anatomy of the nerve (Table 27.1).

Clinical Assessment of Nerve Injury

The location and extent of the injury must be located in the first place in peripheral nerve injury cases. The physical examination includes testing of all muscle groups innervated by related nerve.

Table 27.1 Peripheral nerve injury classification

Seddon	Sunderland	Tissue damage	Recovery
Neuropraxia	Grade 1	Myelin damage, conduction block	Less than 3 months, without surgical intervention
Axonotmesis	Grade 2	Myelin damage, axon damage	Usually recovers without surgical intervention, but slow due to scar tissue
Neurotmesis	Grade 3-Axon continuity is disrupted by loss of endonueral tube, but perineurium is intact	Myelin damage, axon damage, endoneurium	Slow recovery due to scar tissue, depends on the involved fascicles
	Grade 4-Neural fascicle is damaged but sheath continuity is maintained	Myelin damage, axon damage, perineurium	Surgical intervention is needed to remove scar tissue and nerve repair
	Grade 5-Substantial perineural hemorrhage and scarring occurs	Myelin damage, axon damage, epineurium	Surgical intervention is needed

All modalities of sensory function are tested also. An EMG is performed *2–3 weeks* after the injury. If an EMG remains normal in 3 weeks after the injury, then a Sunderland grade I injury is present and full recovery is expected. In the presence of axonal injury, there is spontaneous activity in EMG recordings. The presence or absence of a sensory nerve conduction potential can be used to determine if a lesion is likely to be proximal or distal to the dorsal root ganglion (DRG). A lesion proximal to the DRG, such as a brachial plexus avulsion from the spinal cord, will usually not disconnect the peripheral axon from the cell body. No Wallerian degeneration occurs in the sensory portion of the peripheral nerve and the sensory conduction potential remains intact. If, however, the lesion is distal to the DRG, there is sensory axonal Wallerian degeneration and loss of the sensory conduction action potential. The physician must determine if there is a root avulsion, because in that case there is no spontaneous recovery. Physical examination shows decreased or absent power in all muscles innervated by the avulsed root and sensory loss is present in dermatomal distribution.

To assess nerve regeneration clinically, ectopic mechanosensitivity can be used. Tapping regenerating axon of the nerve will produce a paresthesia felt in the distribution normally innervated by the nerve (Tinel's Sign). The *Tinel's sign* should move 1 mm/day distally in accordance with the advancing axonal growth cone. The EMG is more sensitive than physical examination for signs of muscle reinnervation, and it should be repeated when axonal regeneration has reached the target muscle.

Nerve Reconstruction

It is well known that any degree of tension at the suture site may decrease the possibility of nerve healing; the tension diminishes the extrinsic vascular supply and predisposes to failure of the repair by increasing scar formation between the nerve stumps.

To bridge the nerve defects, the interfascicular autologous nerve grafting technique is still considered the "gold standard" but many other different "grafts" have been studied and described to avoid, in particular circumstances and in short nerve gaps, the use of autologous nerves (to avoid donor site morbidity).

Techniques reported below are applied in different situations; different indications can justify to avoid classical nerve graft: kind of nerves (mixed, pure), level and kind ("dominant" hemipulp in sensory nerves in the hand), kind of injury (in emergency (neat/blunt), late reconstruction). The aim of the reconstruction should be the one with the maximum of the results with the minimum harm for the patients. In this small review, we report only the clinical use of these grafts.

Autogenous Nerve Grafts

It is currently accepted that the interfascicular autologous nerve grafting technique is the gold standard for nerve repair in presence of major loss of substance after injury. Nerve grafting provides continuity of the stumps, with minimal or no tension, and supports axonal regeneration by means of the Schwann cells and/or the inner surface of the Schwann cell columns, protecting against surrounding scar tissue formation.

Generally, it is in case of secondary procedures that grafts are mostly needed. In an open injury when the nerve repair was not carried out immediately because of the type of injury (blunt or crush injuries), or the lack of microsurgical expertise, or because of iatrogenic lesions, the nerve stumps retract, requiring secondary grafting. In closed injury, a stretching or blunt trauma often produce a neuroma in continuity that require secondary resection and nerve grafting.

Donor site morbidity is a significant factor when selecting an autologous nerve for grafting. The resulting functional deficit must be acceptable and limited to noncritical sensation areas. The choice of nerve graft is dictated by the length of the nerve gap, the cross-sectional area of the recipient nerve, the available expendable donor nerves for that particular nerve injury, the surgeon's and the patient's preference.

Although the sural nerve is the most commonly used autograft, there are many other

suitable nerves that can be used as interposition grafts, including: the medial and lateral cutaneous nerves of the forearm, the dorsal cutaneous branch of the ulnar nerve, the terminal branches of posterior and anterior interosseous nerve.

From the technical point of view, stitches (9 or 10–0) or glue are both useful for the coaptation of the fascicles; key points are the trimming of the nerve stumps and the positioning of grafts not only during the suture but also allowing each graft to have optimal contact of the total surface area with the surrounding tissues, then permitting better revascularization of the graft (this technique is preferable especially in large-diameter recipient nerves). No consensus exists on the maximal length that may be bridged with a nerve graft: many successful cases are reported even with 20-cm and longer nerve grafts.

Allogenic Nerve Grafts

During the 1980s and 1990s, many studies have been done on immunosuppressed allografts that functioned as a structural scaffold for regenerating host nerve fibers. As regeneration proceeds, donor antigenic determinants within the allograft, such as Schwann cells, are lost and replaced by host components. Mackinnon and colleagues in 2001 applied allografts in seven patients with a limited period of immunosuppression (6 months of cyclosporine A or tacrolimus and prednisone) [26]. All but one demonstrated a promising recovery in motor and sensory function. No other attempts have been done after that experience.

To avoid immunosuppression, researchers tried to decellularize the nerve allografts, giving the surgeon a scaffold similar to a nerve; methods to decellularize allografts include irradiation, freeze thawing, detergent-processing, and cold preservation. After these procedures in humans, allograft has shown promising outcomes in peripheral nerve repair from 5 to 50 mm in sensory, mixed, and motor nerves [6, 10]. The studies reported in literature are all done with the help of the company producing the allograft. If results are confirmed, this solution could be very useful in nerve gap repair. Concern remains about costs and storage of these allografts.

Nerve Substitutes

Many biological and synthetic conduits have been tested to bridge a peripheral loss of substances, arteries, veins, mesothelial chambers, predegenerated or fresh skeletal muscle, empty artificial tubes, resorbable or not, tubes filled with growth factors and/or Schwann cells. Nerve substitutes are "tubes" that are subdivided in "natural" or "autologous" conduits and "synthetic" conduits. Between synthetic materials in clinical settings, only resorbable conduits are employed at the moment. The maximum gap length to be bridged by tubulization should not exceed 30 mm because beyond that, regeneration capacity clearly deteriorates.

For certain indications, nerve conduits have become a useful tool to avoid donor site morbidity associated with autologous nerve grafting; both biologic or synthetic conduits give reasonable results only on short gaps (not longer than 2–3 cm) and in pure nerves, mostly sensory nerves. Best indications are sensory nerves of the all body, "nondominant" hemipulp in nerves of the hand, emergency reconstruction of blunt injury also for mixed nerves. Nerve tubes have been used for primary as well as secondary reconstruction. No data can suggest a better outcome between different natural or resorbable materials at the moment.

Natural

Autologous materials such as arteries, veins, predegenerated muscle, some in combination with muscle inlays, have been assessed clinically. Most used are veins filled or not with muscle. A recent prospective, randomized study comparing polyglycolic acid and autogenous vein scaffolds for reconstruction of digital nerve gaps showed that recovery after reconstruction with a vein conduit was equivalent to polyglycolic acid conduit repair with fewer postoperative complications [38].

Synthetic

A variety of alternatives to hollow biodegradable nerve conduits have been tested in experimental or clinical settings. Nonresorbable conduits made of silicone, Teflon, or Polysulfone, which can lead to secondary nerve compression and usually prevent nutrient diffusion into the lumen, are no longer employed in clinical setting.

Collagen conduits, polyglycolic acid conduits, polylactid acid conduits, caprolactone conduits, and chitosan conduits are the available materials on the market. No evidence indicates a beneficial use of one over the other at the moment.

End-to-Side Coaptation

The possibility to regain nerve function after damage even if the proximal stump is not available is the aim of this technique, based on the concept that collateral axonal sprouting from a healthy neighbor donor nerve can involve a distal stump of a transected nerve, if these are sutured in end-to-side.

End-to-side coaptation may be an effective means of nerve reconstruction when proximal nerve stump or donor nerves are not available; nevertheless, a discrepancy between experimental and clinical results still exists. It is largely agreed that at present end-to-side neurorrhaphy could not substitute standard techniques in most cases, as brachial plexus repair, but can be considered a valid therapeutic option in selected situations, optionally in combination with other strategies, or in case of failure of other previous attempts of nerve repair or whenever other options are feasible. Reports are done on sensory nerves, sensory nerves in the hand, brachial plexus, facial nerve.

Direct Muscular Neurotization

When the nerve has been avulsed from the muscle, Brunelli utilizes the "direct muscular neurotization" with direct implantation of the nerve into the muscle (a window in the epimisium is done and the fascicle is inserted directly into the muscle).

Restoration of Function in Upper Extremity with Nerve Transfers

Loss of contractility of skeletal muscles and other target organ changes are a major concern in peripheral nerve surgery. Time interval between denervation and reinnervation is a critical determinant of functional outcome. Slow pace of axonal regrowth and immediate changes taking place in target tissues following peripheral nerve injuries make fully satisfactory clinical results unlikely. Repair or reconstruction of peripheral nerve lesions at very proximal levels such as brachial or lumbosacral plexus injuries, results in negligible return of function in extremities. Lessening denervation-reinnervation interval may decrease target tissue changes, and may lead to a better outcome. The concept of transferring healthy peripheral nerves to the distal segments of the proximally injured nerves at a level closer to target tissues is not new, but gaining acceptance only recently. Earlier and pioneering reports on peripheral nerve transfers from healthy muscles to denervated muscles, or from healthy skin to denervated skin indicated favorable outcomes [2, 29, 50–52]. During the last couple of years, exploding number of laboratory and clinical studies with promising clinical outcomes has been reported [48]. Currently, refinement of previously described procedures continues while newer innovative nerve transfers are described.

The need for a single neurorrhaphy site, the possibility to operate outside the zone of injury, lesser need of dissection, and shortness of the distance over which axons has to generate are the three major benefits of peripheral nerve transfers.

Conditions of Nerve Transfers

- A purely motor nerve should receive a motor donor. The same is true for sensory nerves.
- Loss of the function of the donor nerve should be acceptable.
- Direct neurorrhaphy of the donor and recipient should be possible.
- Tension free coaptation is crucial.
- Transfer of synphasic and agonist nerves may provide a better outcome.

- Conditions of the wound and extremity should be suitable for nerve transfer surgery.
- Target muscles should be reinnervated ideally before 12–18 months (Tables 27.2 and 27.3).

Although nerve transfer surgery cannot fully replace functional restorations with tendon transfers, it has become a viable option in many cases. Tendon transfers and nerve transfers are not mutually exclusive. Combination of nerve transfers with tendon transfers may provide better outcome.

Problems of Very Proximal Nerve Injuries

Proximal nerve injuries present with the double problem of being close to the nerve cell bodies [which might undergo apoptosis in case of severe and extended axonal injury] and far from distal motor and sensitive targets. Muscle denervation atrophy is a critical issue, as shown by poor or absent recovery of intrinsic muscle function in the upper extremity after severe proximal median and/or ulnar nerve injury. This may cause high health care expenses and costs of lost production in the community [39].

Early primary repair surgery combined with any available and efficient muscle function preservation strategy [like external electrical stimulation], including any opportunity to perform distal motor nerve transfers to shorten the delay for reinnervation is thus of capital importance.

If a primary suture is not feasible due to local tissue trauma, appropriate grafting of short and long defects is still the golden standard procedure and extensive reconstructions like contralateral nerve transfers in case of multiple avulsion brachial plexus injuries show that reinnervation

Table 27.2 Reanimation of motor functions

Region	Recipient nerve	Donor nerve	Authors
Shoulder	Suprascapular nerve	Long thoracic nerve	
		Radial nerve	
		Intercostal nerves	
		Spinal accessory nerve	[3, 30, 44, 48]
	Axillary nerve	Radial nerve, triceps branch	[3, 22]
		Intercostal nerves	[28]
	Long thoracic nerve	Thoracodorsal nerve	[53]
		Intercostal nerves	
Elbow	Musculocutaneous nerve	Ulnar nerve fascicle to FCU	[34, 40, 42, 47]
	Musculocutaneus nerve branch to brachialis (Oberlin plus)	Median nerve fascicle to FCR or FDP, FDS	[8, 11, 13, 27, 23, 36]
		Anterior thoracic nerve	
		Medial pectoral nerve	[5]
		Intercostal nerves	
		Thoracodorsal nerve	[33]
Wrist hand	Nerve to ECRB	Nerve to FDS	[35]
	Posterior interosseous nerve	Nerve to FCR	[35]
	Ulnar, deep motor branch	Distal median, anterior interosseal nerve	[7, 12, 15]
	Ulnar, motor branch	Distal median, anterior interosseal nerve	[1]
	Ulnar, sensory fascicles	Median, superficial sensory branch	
		Iatrogenic Martin-Gruber anastomosis	

Table 27.3 Reanimation of sensory functions

Region	Recipient nerve	Donor nerve	Authors
Hand	Median nerve	Radial nerve	[21]
Thumb, ulnar			
Index, radial			
Fingers	Palmar digital nerves, thumb, index	Radial nerve distal sensory branches, thumb, index	[4]
Palm			
Hypothenar aspect	III. common digital	Superficial ulnar nerve	[12]

occurs over long distances including interpositional grafts or not.

Late sensitive reconstructions may provide acceptable results, probably because the end organs' survival is not as critical as in muscle tissue.

Our knowledge about denervated and reinnervated muscles is scarce: how long they are reinnervatable [2 years seems an accepted delay endpoint]; how much fibrosis will develop and contribute to "contractured," but still functional muscle bulk; how much strength may be recovered after intensive rehabilitation. According to the BRMC grading, only grades 3 or plus muscles will contribute to the functional balance between agonists and antagonists around the target joints of upper and lower limb.

So far, no evidence exists about tools to fasten nerve regeneration in critical repairs. Neither could we rely on nerve growth promoting factors in microsurgery, nor exist proven drug protocols [e.g., immunosuppressive therapy] to enhance the regeneration process. Imaging techniques are on the way to allow a view on the regenerating nerve within the postoperative follow-up through MRI tractography software.

Meanwhile, nerve surgeons only rely on the best microsurgical technique they can offer: early exploration, primary suture whenever feasible without excessive tension, eclectic interposition grafting: Whenever a critical motor target distance exists, one should consider distal motor nerve transfers. An alternative in late cases [after 6–12 months] is only provided by free muscle transfers, replacing the chronically denervated muscle with a newly denervating muscle, which the growing motor nerve should reach in the shortest time.

Very proximal nerve injuries remain challenging to the surgeon and to searchers who so far failed to provide additional biologic factors either to increase the regeneration process within the nerve or to decrease or delay the intramuscular changes in prolonged denervation.

References

1. Battiston B, Lanzetta M (1999) Reconstruction of high ulnar nerve lesions by distal double median to ulnar nerve transfer. J Hand Surg 24:1185–1191
2. Bedeschi P, Celli L, Balli A (1984) Transfer of sensory nerves in hand surgery. J Hand Surg Br 9:46–49
3. Bertelli JA, Ghizoni MF (2004) Reconstruction of C5 and C6 brachial plexus avulsion injury by multiple nerve transfers: spinal accessory to suprascapular, ulnar fascicles to biceps branch, and triceps long or lateral head branch to axillary nerve. J Hand Surg Am 29(1):131–139
4. Bertelli JA, Ghizoni MF (2011) Very distal sensory nerve transfers in high median nerve lesions. J Hand Surg 36:387–393
5. Brandt KE, Mackinnon SE (1993) A technique for maximizing biceps recovery in brachial plexus reconstruction. J Hand Surg 18:726–733
6. Brooks DN, Weber RV, Chao JD et al (2012) Processed nerve allografts for peripheral nerve reconstruction: a multicenter study of utilization and outcomes in sensory, mixed, and motor nerve reconstructions. Microsurgery 32(1):1–14
7. Brown JM, Yee A, Mackinnon SE (2009) Distal median to ulnar nerve transfers to restore ulnar motor and sensory function within the hand: technical nuances. Neurosurgery 65:966–977, discussion: 977–8
8. Carlsen BT, Kircher MF, Spinner RJ et al (2011) Comparison of single versus double nerve transfers for elbow flexion after brachial plexus injury. Plast Reconstr Surg 127:269–276
9. Catala M, Kubis N (2013) Gross anatomy and development of the peripheral nervous system. Handb Clin Neurol 115:29–41
10. Cho MS, Rinker BD, Weber RV et al (2012) Functional outcome following nerve repair in the upper extremity using processed nerve allograft. J Hand Surg Am 37(11):2340–2349
11. Estrella EP (2011) Functional outcome of nerve transfers for upper-type brachial plexus injuries. J Plast Reconstr Aesthet Surg 64:1007–1013
12. Flores LP (2011) Distal anterior interosseous nerve transfer to the deep ulnar nerve and end-to-side suture of the superficial ulnar nerve to the third common pal-

mar digital nerve for treatment of high ulnar nerve injuries: experience in five cases. Arq Neuropsiquiatr 69:519–524
13. Garg R, Merrell GA, Hillstrom HJ, Wolfe SW (2011) Comparison of nerve transfers and nerve grafting for traumatic upper plexus palsy: a systematic review and analysis. J Bone Joint Surg Am 93(9):819–829
14. Geuna S, Raimondo S, Ronchi G et al (2009) Histology of the peripheral nerve and changes occurring during nerve regeneration. Int Rev Neurobiol 87:27–46
15. Haase SC, Chung KC (2002) Anterior interosseous nerve transfer to the motor branch of the ulnar nerve for high ulnar nerve injuries. Ann Plast Surg 49:285–290
16. Hockfield S, McKay RD (1985) Identification of major cell classes in the developing mammalian nervous system. J Neurosci 5:3310–3328
17. Jessen KR, Mirsky R (2008) Negative regulation of myelination: relevance for development, injury, and demyelinating disease. Glia 56:1552–1565
18. Kaplan S, Odacı E, Unal B et al (2009) Development of the peripheral nerve. Int Rev Neurobiol 87:9–26
19. King R (2013) Microscopic anatomy: normal structure. Handb Clin Neurol 115:7–27
20. Le Douarin NM, Smith J (1988) Development of the peripheral nervous system from theneural crest. Annu Rev Cell Biol 4:375–404
21. Leechavengvongs S, Ngamlamiat K, Malungpaishrope K et al (2011) End-to-side radial sensory to median nerve transfer to restore sensation and relieve pain in C5 and C6 nerve root avulsion. J Hand Surg Am 36(2):209–215
22. Leechavengvongs S, Witoonchart K, Uerpairojkit C, Thuvasethakul P (2003) Nerve transfer to deltoid muscle using the nerve to the long head of the triceps, part II: a report of 7 cases. J Hand Surg Am 28(4):633–638
23. Liverneaux PA, Diaz LC, Beaulieu JY et al (2006) Preliminary results of double nerve transfer to restore elbow flexion in upper type brachial plexus palsies. Plast Reconstr Surg 117:915–919
24. Lundborg G (2004) Nerve injury and repair. In: Regeneration, reconstruction and cortical remodeling, 2nd edn. Elsevier, Philadelphia, pp 25–29
25. Lundborg G, Dahlin LB (1991) Structure and function of peripheral nerve. In: Gelberman RH (ed) Operative nerve repair and reconstruction. Lippincott, Philedelphia, pp 3–18
26. Mackinnon SE, Doolabh VB, Novak CB, Trulock EP (2001) Clinical outcome following nerve allograft transplantation. Plast Reconstr Surg 107(6):1419–1429
27. Mackinnon SE, Novak CB, Myckatyn TM et al (2005) Results of reinnervation of the biceps and brachialis muscles with a double fascicular transfer for elbow flexion. J Hand Surg 30:978–985
28. Malungpaishrope K, Leechavengvongs S, Witoonchart K, Uerpairojkit C, Boonyalapa A, Janesaksrisakul D (2012) Simultaneous intercostal nerve transfers to deltoid and triceps muscle through the posterior approach. J Hand Surg Am 37(4):677–682
29. Matloubi R (1988) Transfer of sensory branches of radial nerve in hand surgery. J Hand Surg Br 13:92–95
30. Merrell GA, Barrie KA, Katz DL et al (2001) Results of nerve transfer techniques for restoration of shoulder and elbow function in the context of a metaanalysis of the English literature. J Hand Surg Am 26(2):303–314
31. Millesi H, Terzis JK (1984) Nomenclature in peripheral nerve surgery. Committee report of the International Society of Reconstructive Microsurgery. Clin Plast Surg 11(1):3–8
32. Moore KL, Persaud TVN (1993) The nervous system. In: The developing human: clinically oriented embryology, 5th edn. Saunders Company, Philadelphia, pp 385–422
33. Novak CB, Mackinnon SE, Tung TH (2002) Patient outcome following a thoracodorsal to musculocutaneous nerve transfer for reconstruction of elbow flexion. Br J Plast Surg 55(5):416–419
34. Oberlin C, Beal D, Leechavengvongs S et al (1994) Nerve transfer to biceps muscle using a part of ulnar nerve for C5-C6 avulsion of the brachial plexus: anatomical study and report of four cases. J Hand Surg 19:232–237
35. Ray WZ, Mackinnon SE (2011) Clinical outcomes following median to radial nerve transfers. J Hand Surg 36:201–208
36. Ray WZ, Pet MA, Yee A et al (2011) Double fascicular nerve transfer to the biceps and brachialis muscles after brachial plexus injury: clinical outcomes in a series of 29 cases. J Neurosurg 114(6):1520–1528
37. Rice D, Barone S Jr (2000) Critical periods of vulnerability for the developing nervous system: evidence from humans and animal models. Environ Health Perspect 3:511–533
38. Rinker B, Liau JY (2011) A prospective randomized study comparing woven polyglycolic acid and autogenous vein conduits for reconstruction of digital nerve gaps. J Hand Surg [Am] 36:775–781
39. Rosberg H, Carlsson KS, Cederlun RI et al (2013) Costs and outcome for serious hand and arm injuries during the first year after trauma – a prospective study. BMC Public Health 13:501
40. Sedain G, Sharma MS, Sharma BS et al (2011) Outcome after delayed Oberlin transfer in brachial plexus injury. Neurosurgery 69:822–827 [discussion: 827–8]
41. Seddon HJ (1943) Three types of nerve injury. Brain 66(4):237–283
42. Shigematsu K, Yajima H, Kobata Y et al (2006) Oberlin partial ulnar nerve transfer for restoration in obstetric brachial plexus palsy of a newborn: case report. J Brachial Plexus Peripher Nerve Inj 1:3
43. Song A, Tracey DJ, Ashwell KW (1999) Development of the rat phrenic nerve and the terminal distribution of phrenic afferents in the cervical cord. Anat Embryol 200:625–643
44. Suzuki K, Doi K, Hattori Y, Pagsaligan JM (2007) Long-term results of spinal accessory nerve transfer to the suprascapular nerve in upper-type paralysis of brachial plexus injury. J Reconstr Microsurg 23(6):295–299

45. Sunderland S (1951) A classification of peripheral nerve injuries producing loss of function. Brain 74(4):491–516
46. Thomas PK, Ochoa J (1984) Microscopic anatomy of peripheral nerve fibers. In: Dyck PJ, Thomas PK, Lambert EH (eds) Peripheral neuropathy, 2nd edn. Saunders, Philadelphia, pp 39–96
47. Teboul F, Kakkar R, Ameur N et al (2004) Transfer of fascicles from the ulnar nerve to the nerve to the biceps in the treatment of upper brachial plexus palsy. J Bone Joint Surg Am 86(7):1485–1490
48. Terzis JK, Kostas I (2006) Suprascapular nerve reconstruction in 118 cases of adult posttraumatic brachial plexus. Plast Reconstr Surg 117(2):613–629
49. Tessier-Lavigne M, Goodman CS (1996) The molecular biology of axon guidance. Science 15;274(5290): 1123–1233. Review
50. Tung TH, Mackinnon SE (2010) Nerve transfers: indications, techniques, and outcomes. J Hand Surg 35:332–341
51. Turnbull F (1948) Radial-median anastomosis. J Neurosurg 5:562–566
52. Turnbull F (1963) Restoration of digital sensation after transference of nerves. J Neurosurg 20:238–240
53. Uerpairojkit C, Leechavengvongs S, Witoonchart K et al (2009) Nerve transfer to serratus anterior muscle using the thoracodorsal nerve for winged scapula in C5 and C6 brachial plexus root avulsions. J Hand Surg Am 34(1):74–78
54. Zou Y, Lyuksyutova AI (2007) Morphogens as conserved axon guidance cues. Curr Opin Neurobiol 17(1):22–28

Tendons and Ligaments

28

Nurettin Heybeli, Baran Kömür, Barış Yılmaz, and Olcay Güler

Abstract

Tendons and ligaments are complex structures and have different anatomical and dynamic properties. Injury of tendons and ligaments remodel with scar formation with differences in themselves. Although scarring depends on the quality and quantity of the injured tissues, it can be qualified with appropriate rehabilitation. In normal conditions, scar formation prevents returning of normal tendon function because of its structural and biological limitations. It has been shown that reconstruction of injured tendons and ligaments with allografts and autografts in different clinical and experimental studies. Despite of these developments, healing process of both biological and biomechanics of the tendons and ligaments is still have to be investigated.

N. Heybeli, MD, MSc (✉)
Department of Orthopaedics and Traumatology, Trakya University School of Medicine, Edirne, Turkey
e-mail: heybelin@yahoo.com; nurettin.heybeli@gmail.com

B. Kömür, MD
Department of Orthopaedics and Traumatology, Kanuni Sultan Suleyman Training Hospital, Istanbul, Turkey

B. Yılmaz, MD
Department of Orthopaedics and Traumatology, Fatih Sultan Mehmet Training Hospital, Istanbul, Turkey

O. Güler, MD
Department of Orthopaedics and Traumatology, Istanbul Medipol University School of Medicine, Istanbul, Turkey

Learning Outcomes

After you have studied this chapter, you will have an understanding of: (1) the structure and function of tendons and ligaments, (2) the classification, morphology, histology, microanatomy and cell biology, (3) vascularization and innervation, (4) functions, proprioception, (5) clinical injuries and healing periods, and (6) principles of reconstruction and grafting.

F. Korkusuz (ed.), *Musculoskeletal Research and Basic Science*,
DOI 10.1007/978-3-319-20777-3_28

Terminology

Allograft Transplant of an organ or tissue from one individual to another of the same species.

Autograft Transfer of tissue from one part of the body to another part of the body through surgical procedures.

Degeneration Condition of a tissue or an organ in which its vitality has become either diminished or perverted; a substitution of a lower for a higher form of structure.

Dislocation Displacement of a bone from its normal position.

Epitendon Structure surrounding fascicles.

Extracellular matrix Collection of extracellular molecules secreted by chondrocytes that provide structural and biochemical support.

Ligament A band of oriented fibrous tissue connecting bones of a joint.

Paratenon Structure that covers tendons.

Proprioception Feedback signals activate muscle contraction.

Sharpey's fibers Continuity of tendon fibrils, which extend along the periosteum.

Tenascin-C A molecule forming the elements of extracellular matrix.

Tendon Dense fibrous tissues of musculoskeletal system, which play fundamental roles in stability and mobility.

Tenosynovitis The disease of synovial sheath itself.

Clinical Relevance

Forty-two-year-old recreational soccer player, sudden popping during sports activity causing Achilles tendon rupture. Operative view: "Degenerated Achilles Tendon with Rupture" (Authors' Personal Archive).

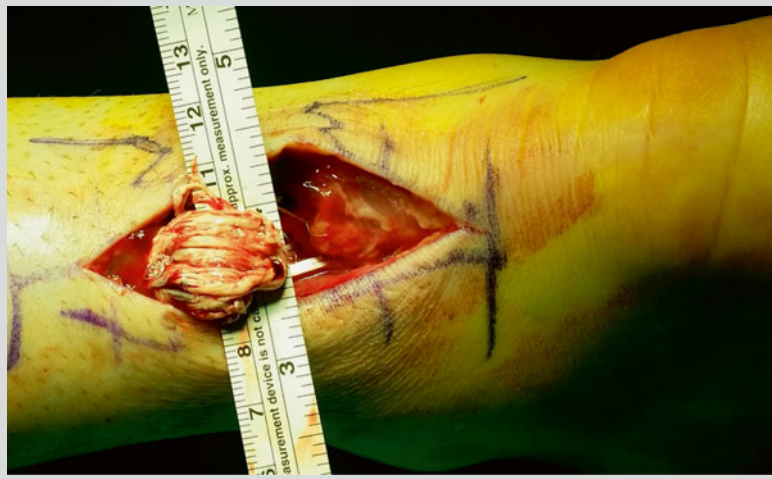

Tendons

Structure and Classification

Tendons and ligaments are similar structures in terms of their composition, organization, and mechanical properties. The distinction between them stems from their anatomical location; tendons form a link between muscle and bone while ligaments link bones to bones [1].

Tendons are dense fibrous tissues of musculoskeletal system, which play fundamental roles in stability and mobility. They vary according to their sites of distribution but all have an

attachment site to the bone and with the aid of this property, they bare high loads with minimal deformation. Tendons are composed of three components: tendon itself, muscle–tendon junction, and bony insertion. They have a complex structure and are composed mostly of connective tissue. Originating from their functional properties, they are very tough to carry hundreds and even thousands of Newtons. Most of them usually cross the joints to attach their distal sites, which increases the affectivity of muscles on joint movements. Additionally, tendons carry weights similar to the bones and therefore their mechanical properties are variable. Tendons are a part of bone–muscle–tendon unit. Therefore, the localization of tendons should be known to understand its structure since not all muscles have tendons [2]. Tendons are found in some group of muscles, which play active roles in joint movements while the presence of some tendons increases the movement distance of the muscle.

A tendon is a compositionally complex tissue with a predominantly mechanical function: translating muscular contractions into joint movements by transmitting forces from muscle to bone. Achilles tendon, for instance, is a special tendon that centralizes the power of a couple of muscles, and carries their weights. On the other hand, some tendons including posterior tibial tendon act by distributing the weight over more than one bone due to their sites of attachment. Although we know that most tendons originate from the muscle and attach to the bone, some tendons may act like sites of origin for muscles or two muscles may be attached with a tendon [3, 4].

Histologically, tendons consist of dense regular connective tissue fascicles encased in dense irregular connective tissue sheaths. Tendons are composed mostly of parallel arrays of collagen fibers closely packed together [5]. Structurally, tendons are composed of collagen fibrils and collection of these fibrils constitute bundles, collection of the bundles form fascicles, and finally, a group of fascicles come together to form a tendon. Connective tissues surrounding the tendons permit friction. Most tendons have a mesotendon that attaches to the surrounding connective tissue and ensheathes it. This structure is also responsible for the vascularization of the tendon [6]. In addition, tendons contain water representing the 55–70 % of the total wet weight. The water content in tendon could play an important role of healthy or pathological index for different clinical presentations.

In some body sites, surrounding connective tissue forms a sheath and ensheathes the tendon. Multiple bundles are composed of fibroblasts and dense linear collagen fibrils. These form the structure of a tendon and confer a fibrous appearance to it. The low-density connective tissue surrounds tendon fascicles on its own. This structure is then called endotendon. When tendon fascicles are surrounded by endotendon, tendon bundles are enabled to make small sliding movements. Endotendon tissue continues as an epitendon covering tendon surface. At the site where tendon joins muscle, epitendon is continuous with epimysium of the muscle. Muscle–tendon unit should transmit muscle contraction to the tendon. Attachment of a muscle to tendon occurs by interdigitation of collagen fibers of the muscular fibrous tissue layer with collagen fibrils of the tendon. Electron microscopic examination reveals the structure of muscle cells and tendon, which appear as interdigitated fingers of both hands. Collagen fibrils do not enter into the muscle cells, but they firmly attach underneath the cellular basement membrane. Normal tendon sliding movement, transfer of muscle power for joint movement, and vascularization of tendons depend on peritendinous connective tissues. This is also called as peritendon. These structures form a delicate organized structure, which is composed of loose connective tissue [7].

Attachment of tendons to bone is complex; collagen fibrils integrate into fibrocartilage, mineralize, and then unite with the bone. “Sharpey’s fibers”, continuity of tendon fibrils that extend along the periosteum with outer lamellar structure of bone, are important for tendon entry, which is known as enthesis. Attachment of tendon to bone resembles fibrous or indirect attachment seen in metaphysis or diaphysis of long bones, or fibrocartilagenous or direct attachment seen in attachment to epiphysis or apophysis of bones. In fibrous attachments, collagen fibers of the tendon are continuously attached to the periosteum during the entire bone development, while in fibrocartilagenous attachments, transition from tendon to bone is more gradual. This gradual transition observed in fibrocartilagenous attachments

includes four zones, namely; (1) tendon, (2) decalcified fibrocartilage, (3) calcified fibrocartilage, and (4) bone. With this organization, the load is evenly distributed at the site of attachment and coordination of collagen fibers is maintained with joint movements. In addition, compressive forces show variances inside a tendon depending on sites of attachment and this affects the structure of fibrocartilage. Therefore, a better protection against compressive forces is ensued [8].

Despite the fact that blood circulation is very important for tendon health, it is not as rich as the muscle and bone tissues. The vascularization of tendons is primarily from muscle–tendon unit, paratendon, and synovium at the site of attachment to tendon. Some tendons are supplied by paratendon surrounding it, as in the Achilles tendon, while others are supplied from a real synovial sheath surrounding them. Since there is a cartilagenous tissue at the site of attachment to bone and tendon, blood flow cannot directly pass through bone–tendon unit. Instead, they make indirect contacts through the vessels of periosteum. Diversely, tendons have a rich nervous network. They are usually innervated from the muscle with which they are interacted, or its local cutaneous nerves. Nerve endings are located at bone tendon units or underneath muscle tendon unit as Golgi organs, Pacinian corpuscles, or Ruffini corpuscles. Golgi organs are stimulated mechanically only with pressure or compression, and their functions differ according to the locations they are situated in. By this, they receive information from the power generated by the muscle itself. Pacinian corpuscles are fast-adapting mechanoreceptors, which contain capsular endings highly sensitive to deformations. By these mechanisms, they dynamically respond to deformation, but they are insensitive to continuous or constant changes. Ruffini endings are originated from a single axon with multiple thin capsular endings and they have slowly adapting mechanoreceptors. With these features, they are stimulated during deformation while they continuously receive information until they reach a constant level of stimulation. Free nerve endings are usually seen in myotendinous unit [9].

Tendons are classified according to their shape, localization, and anatomical structure. In this classification, tendons are divided into spherical and flat types while they do not have significant differences in terms of function and structure. In addition, spherical tendons have parallel collagen alignment, which helps them to give equal responses against tensile forces while flat longitudinal and oblique collagen alignments are found in flat tendons, which are more resistant against pressing and crossing forces [10].

Tendons can also be classified according to their localizations in multiple ways while the most reasonable classification would be according to their function as intra- and extraarticular. While tendons are mostly extraarticular, there are tendons located inside the joint, including the long head of biceps tendon, and popliteus tendon of the knee.

Anatomical localization of tendons can be classified as sheathed or unsheathed and synovium-covered or paratenon-covered. Actually, this anatomical classification should consider soft tissue protection and blood circulation of two tendon types.

Morphology, Histology, Microanatomy, and Cell Biology

The predominant cell type for tendons is fibroblasts. In addition to water, collagen, elastin, proteoglycan, and noncollagenous proteins unite to form macromolecular framework of dense fibrous tissues. These cardinal elements of tendon structure are not randomly aggregated at various ratios and types. Water is the main element of all structures, including tendons. The water content of tendon structure is 50–60 % and alterations in this ratio affect normal structure and function of tendon considerably. This fact becomes obvious in situations at which tendons are damaged in some ways [9, 10].

Collagen constitutes 70–80 % of the dry weight of tendon of which 95 % is collagen type 1 and 5 % is collagen type 3 [11, 12]. In addition, collagens type 5 and 6 are found in small amounts. Collagen molecule found in its structure is primarily found as triple helicals and one or more nonhelical structures integrating into the structure. Each individual chain characteristically contains glycine-x-y tripeptide sequence where x

is usually a proline, and y is hydroxyproline [13]. With this, the primary structure of collagen is glycine in 33 %, proline in 15 %, and hydroxyproline in 15 %. As a result, these collagen chains form a superhelical structure with linear stick shape, which is approximately 1.5 nm in diameter and 300 nm in length with 1050 amino acids [14]. Type 1 collagen is produced by tenocytes and forms 90 % of the cellular component of the normal Achilles tendon. But, type 3 collagen may affect the tensile strength of the tendon generally produced under pathological conditions [15].

Proteoglycans are other fundamental units of the structure, which constitute 1–5 % of the dry weight of tendons. Proteoglycans are macromolecular proteins and contain negatively charged glycosaminoglycans as carbohydrate chains. With the help of this organization, tendons are hydrated and maintain their viscoelastic structure. Proteoglycans also contain more than 30 molecules forming the elements of extracellular matrix. Among these molecules, decorin and tenascin-C are well-known. Decorin is the most abundant proteoglycan found in tendon, which takes role in surface attachment of collagen fibrils and fibrillogenesis inside collagen itself as seen by in vitro settings. Tenascin-C is found abundantly in osteotendinous and myotendinous areas, which contributes to the matrix structure and affects the cells found in extracellular matrix, which are in contact [16–18].

The predominant cell type in a mature tendon is tenocyte while they are named as tenoblasts in newborns. The substantial difference between tenoblasts and tenocytes is predominance of aerobic cycle in tenoblasts while tenocytes prefer anaerobic respiration over time. These conditions are explained by the decrease in the metabolic load of mature tenocyte, as well as ischemia and necrosis risk against loading. In addition, there are some recently described cells with complex structures organized within a tendon. It is thought that there are cytoplasmic connections between these cells ~~are~~ and these networks are sensitive to loading. Therefore, tendon cells respond to loading and similar other stimuli with coordination [19].

Most of the tendons move inside of vascularized tendon sheaths, which are lined with mesenchymal cells resembling synovium. The factor ensuing the sliding of tendon is hyaluronic acid synthesized by mesenchymal cells. This sliding function can be disturbed by inflammation caused by fibrous adhesions developed due to immobility after trauma or surgery.

Functions and Biomechanics

The common function of tendons independent from their shape and size while transmitting the muscle contraction force to the bone. In other words, the primary function of tendons is transmitting the load of weight endured by the muscle to bone. Therefore, tendons are more powerful than muscles and they are subject to intense pressure and tensile forces due to their characteristics. Tendons have stronger structure than muscles, in terms of the resistance that they show against tensile forces, are equal to bone tissue but more flexible and more extensible than the bone [20]. Therefore, tendons execute joint movements and help muscles affect a point further from itself. In addition, they are resistant to tensile forces, but are also flexible, which helps them elongate a little bit as an elastic tissue. With the help of these features, the force generated by the muscle is transmitted to bones, and they exhibit perfect interactions with joint areas and the surroundings of bones. The resilience of tendon against tensile forces is similar to the bone, for example, a tendon of 1 cm thickness can endure a load of 600–1000 kg. Some tendons can store elastic energy in elongation and shortening cycles. By this way, it is obvious that they carry 400–1800 times more elastic tensility stress/unit. In addition, due to their viscoelastic structure, in high-energy injuries or sudden direct trauma, they decrease the severity of muscle injury. Some tendons act to strengthen the capsule of synovial joint and provide joint surface [21, 22].

Some tendons contain bony or cartilaginous sesamoid bones. These bones enable the compatibility of tendon to bone surface. The most vulnerable site of tendon is its end on muscle side. Enthesis, on the other hand, which is the site of attachment to bone is very strong and is susceptible to calcification. The fibrous tendon to bone enthesis is established through a structurally continuous gradient from uncalcified tendon to calcified bone [23]. Depending on where they are located, as in

the case for Achilles tendon, they can take role in a single attachment site as a center of more than one muscle, or they may transmit the power of contraction of an individual muscle to more than one bone as in tibialis posterior tendon. Apart from all these, at joints including wrist and ankle, they enable the effect of muscle at a site distant from muscle attachment site, and passage through narrow sites of the body, or as in replacement of posterior tibial tendon around medial malleolus, it may change its way with the help of pulley and align its direction. Moreover, tendons act as dynamic stabilizers of joint in addition to their neurosensorial and proprioceptive functions. They function as the joint stabilizers of the force originating from the muscle and acting on the joint.

One of the most important biomechanical features of tendons is their nonlinear anisotropic behavior. The initial response of tendon to tensile forces is flattening of fibers. This feature is particularly due to the elastic properties of collagen and it constitutes the first section of force–deformation curve. Tendons demonstrate relatively higher compliance, particularly under conditions with lesser load. However, with increasing tensile strength, tendons increase in toughness and this toughness continues as long as a linear toughness is reached. At this step, elastic elongation and molecular separation occur due to separation of fibrils. After this level, energy is absorbed and tendons lose their tensile strength. In other words, the behavior of tendons might change depending on the increases in the rate of tensility. At higher levels of tensile forces, tendons get harder and as they gain tensility, they absorb more and more energy. On the other hand, to minimize the effect of injury, alterations occur at sites of tendon attachment to bones. With the help of this feature, they act at high toughness and power at sudden tensile forces. By this way, bone–tendon complex adapt and react to minimize trauma at high tensile forces [24, 25].

The position of tendon during endurance is particularly important during tendon ruptures. During oblique forces at eccentric positions, tendon ruptures are more common. In general, the final loading of tendon is more powerful than its own muscle or attachment site and thus, tendon avulsions are more common than tendon ruptures.

Since tendons are viscoelastic, their current and past characteristics are important. Therefore, their mechanic behaviors depend on the ratio of loading, limits of loading, loading histories, and environmental factors including heat and water content. In addition, tendons maintain biomechanical balance not only during normal daily activities and repeated displacements, but also during lower loads (i.e., static shape changes) or repeated lower loads (i.e., static position changes) [26]. This behavior pattern is important in clinics because deformation is reversible to some extent. However, joint laxity may ensue after pathological deformation-related injury, repair, or reconstruction.

In addition to their mechanical features, tendons take important roles in joint proprioception. Proprioception means that an extremity has a conscious perception in space. Central nervous system receives inputs from more than one centers and it describes these inputs as perception or sensation according to the movement of joint. Motor control of central nervous system centers gives response depending on visual, vestibular, cochlear, cutaneous, articular, or muscle-related information. At this point, tendons play active and important roles as well. Tendons function as trauma absorbers and maintain posture. Tendons are important to draw muscle from a small area, which helps changing the pulling direction of muscle and controlling the muscle from a distance [25].

Tendon Diseases and Injuries

Tendon diseases may involve any structure constituting a tendon and it may arise due to different reasons at different sites of a tendon (Table 28.1). Therefore, it is difficult to differentiate it. Moreover, the majority of tendon injuries occur due to excessive forces applied to vulnerable sites of muscle–tendon complex. These kinds of injuries show variations depending on anatomical localization, vascularity, skeletal maturity of patient, and the force being exposed to. Tendon does not rupture with the normal borders of physiological loads. However, tendon that has a deterioration of its structure, particularly as a result of aging and external injuries, can rupture without sudden and extreme loads [27, 28].

Table 28.1 Tendon injuries and diseases

Disease	Description	Example	Clinical findings
Ruptures	Disruption in the integrity of a tendon (partial or complete)	Shoulder tendon rupture—Achilles rupture	Pain (may be absent), loss of strength, feeling of emptiness on palpation
Paratenonitis	The disease of paratenon layer	Achilles paratenonitis	Pain, tenderness, swelling, crepitation, warmth (early term)
Tenosynovitis	The disease of synovial sheath itself	De Quervain disease	Pain, tenderness, swelling of the sheath, crepitation, warmth (early term)
Stenosing tenosynovitis	The disease of tendon and synovial sheath	Trigger finger	Pain, crepitation, nodule on palpation, triggering in the finger
Tendinosis	Degeneration of tendon structure (wear and tear)	Lateral epicondylitis, shoulder tendinosis	Pain, localized tenderness, nodule on palpation
Entesopathy	Problem in the attachment site of tendon to the bone	Achilles tendinosis	Tenderness, swelling at the site of attachment to bone, pain
Contracture	Hardening of tendon sheath and attachment of it to the surrounding tissues	Joint contracture	Restrictions in joint mobility

Depending on their types of occurrence, tendon injuries can be classified as direct and indirect mechanisms. Direct mechanism means that the injury occurs as a result of a trauma without being linked to a prior disease. They usually occur at hand–elbow region and the healing process in such injuries might change depending on the presence of paratendon or sheath. However, with indirect mechanisms, tendons are damaged from bone or muscle–bone unit. There is usually a pathological degeneration process prior to such injuries. Histological changes include tendinosis and exhibit increases in collagen degeneration, fibrillar disorientation, hypercellularity, vascular alterations, and glycosaminoglycans in between fibrils. Together with that, Achilles tendon injuries, which are particularly common in our daily life, may present with different clinical pictures. For instance, a young sportsman who has no prior Achilles tendon problem may have a direct trauma, which can cause tendon injury. In other way, a middle-aged sportsman with no prior sports carrier may experience Achilles tendon injury after physical activity, which usually demonstrates an "angiofibroblastic hyperplasia" assessed by pathological studies, which is a degenerative process and underlies the preexisting tendinosis. Similarly, supraspinatous tendon injuries, which are common in daily life and occur after degenerative processes, have histological alterations, including decreased cellularity, thinning of tendon fibrils and disorganization, presence of granulation tissue, glycosaminoglycan infiltration, fibrocartilaginous alterations, calcification, and partial tears. In addition, tendon degeneration originates mostly from multifactorial reasons and among them are mechanical compression, pressing, and tensile forces. In addition to them, ischemia, free oxygen radicals, hypoxia, pathological changes, tenocyte apoptosis, and fluoroquinolone use are among other potential mechanisms [14, 29–31]. In addition, in repaired complete ruptures, a hard and heterogeneous pattern of tendon structure may be a natural consequence of tendon healing [32].

Radiological examination of tendons is based on magnetic resonance (MR) imaging. MR imaging makes it possible to evaluate the presence of tendinous "degeneration", or of a tear partial or complete, the extent of tendon retraction in full thickness tears, and the presence of associated lesions.

It is obvious that excessive or oblique load-related tensile forces might cause disruptions in tendon structure. However, this damage is at microscopic level and it is usually repaired by tendon cells. With prolonged or repeated tensile

forces or compressions, repairing capacity might not reach damage rate, which causes accumulation of damage and partial or complete ruptures with pain. In addition to that, gene structures, structural reasons including nutrition and environment, decrease in blood flow, various rheumatic diseases, including gout and rheumatoid arthritis, directly affect tendon and decrease inflammation or repair abilities, causing accumulation of damage [33, 34]. Additionally, a high Body Mass Index (BMI) >25 and constitutional factors (such as the asymmetry of the lower limbs) may exert an excessive or abnormal load on tendons. Also, hypercholesterolemia appears to be associated with an increased risk of tendon rupture. Furthermore, clinical studies have pointed an association between diabetes and calcific tendinitis.

The fundamental manifestation of tendon diseases is pain and loss of function. Clinical examination may also show swelling and thickening. Generally, there is a local tenderness and pain increases with passive tension and active resistance. With predominant loss of strength, rupture of tendon should be thought. Severe paratenonitis demonstrates crepitation and triggering is also seen. Palpable tendon nodule is consistent with tendinosis. Degenerative changes are named as tendinosis and inflammatory changes are termed tendonitis, which separates these two terms. The difference between paratenonitis and tendinosis is difficult when cardinal signs of inflammation including swelling, redness, and increased heat are absent.

In conclusion, tendon injuries may occur as a result of direct or indirect mechanisms or rapid contraction due to overloading of muscle or sudden change in position of an extremity with rapid muscle contraction. We can classify all types of tendon injuries depending on the duration of lesion development. In this method, acute lesions are the ones with less than 2 weeks of duration, subacute lesions are between 2 and 4 weeks, and chronic lesions are more than 4 weeks [35].

Tendon Repair and Healing Periods

Healing process of tendon is slow and in case of injury, surgical repair methods cannot obtain mechanical features of tendon as in uninjured tendon [36]. Two separate models are proposed to explain tendon healing mechanisms. Extrinsic healing model describes the formation of granulation tissue with migration of cells and vessels from surrounding tissues while intrinsic healing model encompasses synovial fluid-supported healing with the healing capacity of cut edges of tendon. Both of these mechanisms are clinically seen in injured tendons, but extrinsic healing predominates in early period while intrinsic mechanisms take place in later phases.

Extrinsic mechanism encompasses the invasion of inflammatory healing tissue and fibroblasts into the injured area from outside the tendon. Extrinsic mechanism is held responsible for high cellularity, high water content in injury line and disorganized collagen matrix, and adhesion formation occurring initially. Adhesion formation is dependent on the severity of trauma, surgical trauma, lack of blood supply to the tendon, immobility of tendon, and loss of tendon sheath. In other words, prolongation of extrinsic mechanism during healing period causes adhesions of tendons, thus, suppressing extrinsic mechanism in tendon repair is important. On the contrary, intrinsic mechanism includes synovial fluid diffusion and intrinsic vascularization of tendon. With this mechanism, fibroplasia and new collagen formation can take place with no adhesions on superficial layer. In general, the mechanism is responsible for reorganization of collagen fibrils and their maintenance. Several growth factors operate in organization of cellular response and its activation during entire tendon repair process. These factors or cytokines bind to specific receptors found on cell surface, activating particular signalization events inside a cell. This starts with a cascade, which leads to transcription of specific regulatory genes. Elaboration of these factors occurs during entire remodeling process by cells localized at the border of injury and also with mechanical pressures on injured tendon. As a result, one of these two healing pathways predominates. Under some circumstances in which synovial sheath integrity is maintained and tendon mobility is ensued, intrinsic healing predominates and tendon adhesion occurs at a bottom level. If extrinsic healing predominates,

adhesions in tendon and surrounding tissues would be more prominent [37, 38]. In addition, tensile testing and clinical studies have sought to compare different suturing techniques, often focusing on strength, gapping resistance, glide and resultant mobility [39]. A strong tendon repair that reduces dehiscence and allows early movement may be all that is needed to produce good results [40].

The healing of tendon takes 6–8 weeks, which can be evaluated in three stages: inflammatory, proliferative, and remodeling. Inflammatory stage encompasses the time between days 1 and 5 after tendon injury. This stage is the time when tendon strength is minimum and is characterized by cellular migration and phagocyte activation. Hematoma formation occurs in tendon healing line due to the injuries to blood vessels. The clot that is formed causes the migration of inflammatory cells from the surrounding tissues, and elaboration of several proinflammatory and vasodilator molecules in addition to chemotactic factors. Fibronectin, which is also a chemotactic molecule, increases as well as cell surface integrins. Basic Fibroblast Growth Factor (bFGF) also operates in tendon healing and it is a growth factor that takes place in early mitogenic activities. It acts as a potent angiogenic factor at the same time. Erythrocytes, thrombocytes, neutrophils, monocytes, and macrophages migrate to the wound areas. Clot, cellular debris, and foreign molecules are phagocytozed. During the first week, the area of injury is filled with extrinsic peritendinous tissue, as well as epitenon and endotenon-originated cells. As the cells proliferate, phagocytosis increases and new collagen formation occurs. Fibroblasts populate in this area to initiate extracellular matrix synthesis. Angiogenic factors are released during this period and they initiate vascular network formation. DNA and extracellular matrix increase, both of which take place in maintenance and partial stability of wound area. It is possible that a combination of wrapping periosteum and injecting bone marrow to the tendon graft would have a synergistic effect (early and strong). To prove this hypothesis, future studies, which would combine both methods, are needed [41, 42].

During proliferative phase, clot organization occurs with cellular proliferation and matrix synthesis. With the organization of clot, fibroblasts come from parenchymal tissue and wounded tendon sheath, proliferate in the area of injury, and synthesize all components of extracellular matrix including collagen, and proteoglycans. Between days 7 and 10, vascularization increases rapidly in epitenon and endotenon. On day 7, collagen fibrils are visible. During initial phases, these components are randomly arranged in extracellular matrix (ECM) and type 3 collagen is primarily produced in this phase. A dense blood vessel network is formed and the wound seems to be scarred. At the end of this stage, repair tissue is highly cellular and the water content, as well as ECM component is increased. During this period, granulation tissue is seen at the site of repair. Matrix is unorganized as well. Tensile strength and proper organization of the tendon are not well constructed. With the synthesis of collagen, tendon strength increases gradually.

Remodeling is the terminal stage of tendon healing. After these stages, repair tissue is formed during the second week and this unites tendon endings together. During remodeling phase, cellularity, matrix synthesis, and type 3 collagen decrease, while type 1 collagen synthesis increases. Collagen synthesis occurs not only at the site of injury, but in the tendon as a whole. Between days 14 and 28, collagen synthesis is maximum. Type 1 collagen fibrils align as long as the entire axis of tendon longitudinally, and are responsible for mechanical force and tissue regeneration. As long as the remodeling phase continues, vascularity and cellularity decreases while collagen fibrils and cross bindings increase. At 20th week, minimal histological changes are seen in tissue during early tendon healing, while collagen content and tendon collagen fibril organization and diameter change substantially. While some tendon characteristics return back to their normal structure, this process usually takes months, and even years [43].

Taking into consideration the biomechanical properties of tendon in the healing process is critical for the management of tendon repair and healing. The scar tissue in the first stages of

the repair process is in insufficient state for stretching. For this reason, immobilization of the joints related to tendon in the process of repair and recovery is necessary for optimal healing. It has been mentioned that, in tendon healing process, the mechanical stimuli play an important role in the formation of scar tissue and collagen fibrils. To achieve this depends on the strength of the repaired or healing tendon tissue. Therefore, to obtain the strength of healing tissue was considered as main part in the development of tendon repair methods. Tendon-to-bone healing is vital to the ultimate success of the various surgical procedures performed to repair injured tendons. Achieving tendon-to-bone healing that is functionally and biologically similar to native anatomy can be challenging because of the limited regeneration capacity of the tendon–bone interface [44–48]. Beside the ruptures, the exposure of tendon to the degenerative process sometimes may result in malfunction, which can need medical treatment [49]. During this period, using of heparin is controversial [50].

An effective tendon repair can only be done by ensuing the balance between tendon stability and mobility. In other words, while efforts are made to increase stability of tendon, decreasing its mobility, which might lead to scarring and increased toughness, is an unwanted tendon healing state. On the other hand, early mobilization to prevent tendon adhesion after tendon repair might cause graft separation and formation of a hole in repair site. Therefore, during an ideal tendon repair, strong repair does not impair tendon blood supply, does not cause scarring or re-rupturing. An aggressive rehabilitation is also needed. In general, in order to prevent formation of holes during tendon repair, central and epitendinous sutures should be used in combination. It should be known that the strength of the repair performed is proportional to the number and width of the sutures passing through repair site. Together with this, the use of nonabsorbable central sutures, obtaining equal tensile strength at all sutures, and performing central sutures from dorsal aspect increase repair success of the tendon.

Various natural and synthetic materials have been used to construct extracellular matrices (ECMs) for in vitro cell culture and in vivo tissue regeneration. Some studies reported that they reduced the adhesion with the combination of HA and phosphatidylcolin. Moreover, in another study, lubricin was used with the aim of improving tendon gliding mechanism and was found successful. Endobutton-assisted modified Bunnell technique provides stronger fixation than conventional techniques. It may allow early range of motion and can be easily applied in minimally invasive and percutaneous methods, particularly for cases with poor quality Achilles tendon at the distal part of rupture [51–54].

Nitric oxide is generated after tendon injury. Reduced production of nitric oxide has been shown to result in reduced tendon healing and the addition of nitric oxide has been shown to enhance tendon healing and enhanced collagen synthesis. Also, endogenous oestrogen may improve healing of the tendons [55].

In addition, the advances in genetic engineering and the complications and deficiencies that still continue in tendon repair, pointed the researches to this direction [56]. Tang et al. cloned bFGF gene by transferring adeno-associated virus-2 vector to tendon fibroblasts. In this study, the obtained genes were incorporated in the ends of the cut tendon, expression of local bFGF was increased and thereby, it has been shown that, the strength of tendon repair tissue was higher in second and fourth weeks [57]. On the other hand, BMP-12 and N-butyl-2-cyanoacrylate was used for tenogenesis and found to be effective [58]. Also, use of HMG CoA reductase inhibitors (statins) can affect tendon healing [59]. Some studies emphasize that in the patients undergoing BMP-12, the resistance of repaired tendon was higher than the control group [60, 61]. Stem cells are promising in the management of tendinopathies and tendon ruptures, and this technology will probably grow to be an important therapeutic option in musculoskeletal regenerative medicine [62]. Recent studies reveal that bone marrow treatment can be more effective than stem cell treatment [63, 64].

In summary, today, all these challenges continue to be one of the most important issues that the orthopedic surgery is trying to manage. Thus, the innovations about the management of tendon healing and repair continue.

Ligaments

Structure and Classification

Tendons and ligaments are similar structures in terms of their composition, organization, and mechanical properties. The distinction between them stems from their anatomical location; tendons form a link between muscle and bone while ligaments link bones to bones.

Ligaments are defined as strong dense collagen bands, which connect two bones to each other, maintain passive stabilization, and prevent inappropriate movements of joints. Concerning the functions of joints where they localize, they usually cross over the joints or can bind to different points of the same bone. The anatomical place where they attach to bones is defined as enthesis. Size, shape, localization, and attachment pattern of each ligament are different from each other. As they structurally resemble tendons, ligaments also show unremarkable viscoelastic property contributing to length, load and load distribution. In this way, internal fibers cluster during the movement, and change their shapes on bones. In other words, tendons behave like an active driver of joint movement; on the other hand, ligaments resist in a passive way. Ligaments seem to be as structures restricting the joint movement; however, some ligaments are loose or tight depending on the position of bone and acting forces. They are dense collagen tissues with parallel fibers, and they are more hardly dissectible than tendons due to less space between fibers. Also, ligaments have more interfiber interactions than tendons, suggesting that ligaments have more complex structures than previously thought.

Ligaments in human body can be classified according to a variety of properties, including the bone attachments, anatomical shapes, and interactions with joints or each other. In addition, there is also a weaker secondary ligament structure called capsular ligament. These ligaments have less space between fibers due to their fusion on periarticular capsule of diarthroidal joints [2, 4].

In contrast to their white macroscopic appearance, ligaments were shown to be more vascular than previously thought. Ligaments are covered with layer rich in vessels called “epiligament”, and this structure receives more blood than ligament itself. Epiligament cannot be separated from true ligament, but it continues as periosteum at the enthesis region. Regional arteries supply blood to the superficial arterioles entering the surface of ligaments, give superficial branches to epiligament layers, and then enter the lower layers of ligament. These vessels are denser at the surfaces close to ligament insertions, but it shows variations. In spite of their scarceness, they play critical role in nutrition supply and water distribution inside ligaments. When epiligamental structure is taken off, fibrous structure that is organized hierarchically as fiber groups lying parallel to each other as collagen bands is seen. These bands seem to be connected to each other, and it is difficult to disconnect them. Epiligament structure also contains more cells and more sensory and proprioceptive nerves. Nerves course closely to the vessels and enthesis region has much more nerve fibers. Disturbances in the joint innervation secondary to aging or injury may play a role in the pathogenesis of osteoarthritis [14].

Nerves inside ligaments tend to be more abundant, especially at the sites where ligaments attach to bones. Both nociceptive pain sensors and proprioceptive nerve elements are present in ligaments, and this plays a role in the neuromuscular feedbacks from position sense of ligaments and functional joints.

Morphology, Histology, Microanatomy, and Cell Biology

Microscopically, ligaments are complex structures containing fibroblasts with surrounding matrices. Biochemically, it is composed of two-thirds of water while rest is solid. Solid component contains glycoproteins including

collagen, which constitutes 75 % of dry weight, proteoglycan, elastin, actin, laminin, and integrins; 85 % of collagen is type 1, while rest of them is type 3, 4, 5, 11, and 14. Thus, ligaments resemble the tendons in terms of histology, but some ligaments have higher elastin/collagen ratios than tendons. Proteogylcans, primarily decorin and biglycan, which are important in the interaction of fiber sliding and fiber space and water and growth factor retention, constitute 1 % of dry weight of ligament. Biglycan is present in ligaments more than tendons. Other proteoglycans like lumican, fibromodulin, and aggregan are seen in surfaces of tendons and ligaments exposed to friction. Recent studies have showed that collagen fibers are composed of smaller fibers. In molecular level, collagen is synthesized as procollagen molecules and released to extracellular space via microtubules. They are composed of fibers and fibrils, which have a triple helical structure after a modification by an extracellular enzyme called lysyl oxidase. Lysyl oxidase yields an intramolecular and intermolecular linkage. Formation of cross-links gives enormous strength to collagen fibers. This context of ligaments makes them more viscous and less strong and rigid. Cross-links that are relatively immature during growth and development period become more mature, insoluble, and strong. This process is also available for the healing period of injured ligaments [1].

Cells that are relatively lower in number than other tissues are responsible for the synthesis of matrix and constitute only a small percentage of ligament structure. Although these cells seem to be isolated in terms of physical and functional properties, they connect to nearby cells with long cytoplasmic processes and form a three-dimensional structure. This structure appears as collagen bands, which twist, similar to a wavy hair, along the long axis of ligaments under polarized light. These twists allow elastic deformation, which means elongation of ligaments without a permanent damage upon increasing loads. In addition, different fibers can have potential differences in terms of cell shapes and behaviors.

Compared to tendons, ligaments contain thin and long, but still mildly plump fibroblasts and fibrocytes. Moreover, ligaments have more complex morphology in bone insertion sites, and connection sites prior to soft central body, stress-bearing fibrocartilage, and calcified fibrocartilage as in the tendons [2, 6].

Functions and Biomechanics

One of the main functions of ligaments is the mechanical function. Ligaments stabilize joints passively and maintain a normal joints space against tensile forces. Tensile forces spread through different parts in each ligament depending on the position of the bone, and each part of a ligament is responsible for prevention of abnormal bone movements during different positions of joints. Compliance of collagen fibers to low loads is pretty good due to viscoelastic property of ligaments and presence of other matriceal elements. Thus, more the load causes more the elongation and stiffness of ligaments. At the end of these elongations, they continue to absorb the energy. As a result, ligaments are relatively stiff and strong against stress straining as in the tendons. With these properties, they are one of the most durable tissues of body. Since ligaments connect to bones at both tips, attachment areas are very important for their structural strength. One of the other functions of ligaments is their viscoelastic property (i.e., loading and relaxing). Ligaments absorb the forces on joints with their elastic structures. Also, they relax and undergo elastic deformation under repetitive or constant forces. However, excessive relaxing as a result of joint damage or during reconstructive surgery results in joint laxity. Thus, joint laxity causes a predisposition to joint deformities [25, 65].

Tense or functioning part of ligament is damaged during abnormal movements of bones. Joint position, magnitude, and direction of forces determine which fibers will be functioning at that time, and in which order they get injured after the upper limit of tension. In that case, fibers are relaxed at the beginning, and then tension begins to increase and ligament gets damaged after

upper limit of the tension. Ligaments responding to tension usually have different subdivisions forming functional bands at the normal range of movements of joints. This suggests that ligaments do not function as a single homogenous unit. In that case, in order to test the function of each part of ligament during physical examination, range of motions of joints should be tested. If abnormal movements are observed during the examination of all joint angles, it is thought that this structure is most probably fully damaged.

The third function of ligaments is its role in joint proprioception. Proprioception in the joints like knee is provided with joint capsule, muscle, and cutaneous receptors. When ligaments get tensed, feedback signals activate muscle contraction. It is thought that this situation plays role in sensation of position. The role of ligaments in proprioception is not clear yet. There is a positive correlation between the numbers of mechanoreceptors and proprioceptive function. On the other hand, normal aging process is associated with deficits in proprioception. The numbers of mechanoreceptors, especially Ruffini receptors, decreased with aging. Increased age was associated with changes in the morphology of mechanoreceptors. In conclusion, aging results in both diminished numbers and changed morphology of mechanoreceptors [66, 67].

Clinical Injuries

Ligaments are affected in accordance with the degree of injury in joint injuries; they may even tear off partially or totally. In this instance, fibers are not really torn off, but get tensed, and damaged partially or totally. With the increasing degree of force of injury, there will be more damaged fibers, causing more influence on laxity and stability of the injured joint. Such injuries are probably symptomatic. Moreover, the instability in combined ligament injury is a hurdle against spontaneous healing.

Ligament injuries cause symptoms depending on the affected part of ligament, and can be classified clinically. First-degree sprain is the partial tear of a part of a functional band. In this instance, bones have no or minimal dislocation. Second-degree sprain has disruptions of many but not all fibers. However, some regions are undamaged. Lastly, if there is no undamaged area, this is called third-degree sprain or complete injury.

Ligament injuries can occur with direct or indirect mechanisms as in tendon injuries. Direct mechanism causes an injury secondary to trauma without a preexisting disease. With indirect mechanism, there is a pathological degeneration process prior to injury, as in tendons; and this process usually results from multifactorial causes. Mechanical compression, tensile overload, and compression can be counted among those causes. It is very clear that excessive or oblique loads cause structural distortions in ligaments. In addition, symptoms of ligament and tendon injuries resemble each other regardless of whether it is caused by a direct or indirect mechanism and majority of symptoms are secondary to joint function affected anatomically. Sex also is an important factor in injury. Identifying the landing strategy differences between female and male college volleyball players may provide detailed perspective about the load distribution in lower extremity joints for determining major factors affecting the increased incidence of anterior cruciate ligament injuries in females [68].

Ligament Repair and Healing Periods

Healing of ligaments usually resemble each other. For instance, when we investigate the healing of medial collateral ligament (MCL) in rabbit models, three phases are seen; hemorrhage and inflammation phase, matrix and cellular proliferation phase, and remodeling and maturation phase. During the first phase, tips of torn ligament are retracted. A clot develops in the space between those two tips. And then, clot is resorbed, and replaced with a dense cellular infiltration. A remarkable hypertrophic vascular structure forms between the tips, and blood supply increases. Both vascularization and blood supply gradually decrease over time. In proliferation phase, a scar tissue is produced by hypertrophic fibroblastic cells; matrix that is rich in cells and composed of

collagenous connective tissue forms a bridge between torn MCL tips. This scar tissue is not organized in the beginning and contains much more blood vessels, adipocytes, inflammatory cells, and loose connective tissue than normal ligament matrix. A few weeks later, collagen shows a good arrangement along the long axis of ligament, but type 3 collagen presents more than type 1, type 5 is increased, and collagen fibrils are thin and abnormal. During the remodeling phase, matrix gradually replaces the abnormalities in scar tissue. However, there are still major differences in composition, architecture, and function. Continuing differences are changed proteoglycan and collagen types, insufficiency in collagen cross-links, thin collagen fibrils, changes in cell attachments, increased vascularity, abnormal innervation, increased cellularity, and incomplete resolution of matrix abnormalities [69].

Healing response of ligaments to any injury can be affected by several factors including age, genetics of patient, hormonal effects, presence of any comorbidity, and mechanical and biological quality of the tissue prior to injury and changes in neurovascular structure. However, the most important factor seems to be age. Changes in ligament structure during aging process are decisive for ligament injuries and healing response. Prior to skeletal maturity, ligaments are more viscous due to high water content, and have smaller cross-sectional area. This makes them more flexible. Joints are relatively free, and especially insertion sites are more prone to injuries due to their improper attachment to bones. After skeletal maturity, ligament cells begin to slow their metabolic functions. In this instance, ligaments are less viscous, and have reached maximum size and structural stiffness. However, both ligaments and ligament insertions start weakening with aging, and this results in gradual structural loss. Viscosity decreases, and collagen becomes cross-linked. Ligaments become less flexible, and joints become stiffer over time. At the same time, joints are deformed as a result of changes in bone shapes with aging, and ligaments can be deformed, and cause a pathological joint laxity [70–72]. Gender-specific and hormone-related variables and ligament injuries potentially affect the response to both these injuries. However, women tend to respond more severe inflammatory. Genetic factors are more common in some breeds than others like pathological scarring and keloid formation as playing a role in wound healing. The quality of the tissue before the injury may also play a role in wound healing and results. The presence of comorbidity, which leads to impaired inflammatory response and wound healing response due to the increase of growth factors, may also affect the results of healing. Also, the treatment of comorbidity may affect the healing process. Neural and vascular elements are likely to play an important role in the result of healing process. Indeed, some ligaments that have more angiogenesis capability and resulting in providing more blood, heal better than others by joints' proprioception, nociception, and vasoregulation [73]. Despite difficulties of important healing, several ligaments are known to have a natural healing potential with scar formation as in the tendons [74].

Ligament scars are collagen matrices build on fibrin clots with increasing amounts of fibrous matrix deposition, which are slowly remodelized to couple with early cellular division and main tense axis of the structure. Scar tissue has shown to have an absolute healing potential. Scar tissue that has a hypermetabolic and hypercellular structure responds to several variables. Joint movement and tissue loading are especially important among those variables. These scars that show limited healing even in months and years stop healing when 30–50 % of tissue quality is reached. Moreover, viscoelastic properties of ligament scars are abnormal. Also, scars undergo more deformation than normal ligaments even under low stress levels. Some ligaments have compensatory mechanisms for healing as they heal; but in others, they do not have such a mechanism, and it is thought that ligaments have different healing capacities [75]. In ligament injuries, space that occurs as a result of retraction of torn tips can reach to unbearable sizes depending on severity of injury and location of ligament, and can necessitate repair and restoration. Studies have showed that increased space between torn tips cause structurally weaker scars

due to probably increased number and size of critical defects [76].

Since surgical repair help to regain some functions in muscle–tendon units, suture of torn tips of ligamentous structures is preferred in acute ligament ruptures. Studies have shown that sutures of torn ligament tips provide more qualified repair than nonsurgical techniques. Although there are evidences regarding better functional results for acute suture repairs of some ligaments, this does not apply to all ligaments. In the opposite data, it is very clear that acute ligament suture repair does not change joint stability or repeated injury of ligament regardless of the aim of the procedure.

Despite the current discussions, with the exception of patients with severe combined injury and dislocation, acute suture repair of ligament injuries are about to be abandoned due to the tendency toward nonsurgical rehabilitation. Although the success of nonsurgical approach with increasing healing of injured tissues has not been proven, it is claimed that it obtains satisfactory clinical results with safer ways.

In conclusion, some ligament injuries are important because functional clinical outcomes can be obtained with appropriate aggressive treatment and natural healing processes. Moreover, new surgical and biological approaches are necessary. Reconstructive surgery has also improved from day to day to manage such conditions.

Principles of Reconstruction and Grafting for Tendons and Ligaments

For a long period of time, resources that contain dense connective tissue are used from time to time for tendon and ligament replacement depending on the size and location of injury. Under these circumstances, it is important to decide from where and whom this graft will be provided. Among these sources, autograft use from the similar person or allograft use from a different person of same species are common, but although xenograft use from another animal might be possible, it has lost its popularity recently due to the link with immunologic rejection. The cheapest and most appropriate two graft sources are tendon and fascia. In general, palmaris longus tendon grafts from upper extremity, hamstring and partial patellar tendon grafts from lower extremity, and fascial strips obtained from fascia lata can be used as tendons and ligaments. On the other hand, transfer of a ligament from a donor site without causing any functional problems at donor area seems to be impossible. Under such circumstances, or when tendons cannot be used as autografts or when such a condition is not preferred, tendon and ligament replacements developed with bioengineering methods gain popularity. At the same time, although autograft use seems to be more reasonable and safe for replacements, during tendon removal, pain, swelling, sensory disturbances due to neural damage, scarring, toughness, weakness, atrophy, tendinitis, and infection risks limit autograft use from time to time independent of which tendon was removed.

Autograft and allograft use are both very well in terms of results in damaged tendon and ligament repair. In addition to that, despite early and long-term successful results obtained, increased frequency of rupture and degeneration-related failures in long-term setting constitutes an important topic to study. In reality, despite superior clinical outcomes of autografts and allografts in functional stability, clinical and experimental studies indicate that their structure and function change with time. During the studies conducted up to now, including histopathological studies performed after replacement, it is well known that cellularity and collagen matrix architecture changes in transferred structure. It has been shown that cells and vessels grow toward the graft being transferred and contribute to remodeling. Transition of large collagen microfibrils into small little scar-like fibrils or shortening of normal fibrils are the main reasons why transferred tendon tissue looks less tough, weak, and vulnerable to damage. Consistent with this, grafts soften due to their water and proteoglycan content and this condition causes changes in their viscoelastic features. Under these circumstances, both autografts and allografts are subject to increased

potential of permanent deformation and increased deformation at permanent loading. With these results, joint mechanics change without causing prominent symptoms in joint laxity, and also lead to remodeling and cartilage degeneration. As a result, further studies investigating the success of autografts vs. allografts, and comparison of either one in terms of anatomical site used, type of injury, and surgical technique are needed [77].

References

1. Birch HL, Thorpe CT, Rumian AP (2013) Specialisation of extracellular matrix for function in tendons and ligaments. Muscles Ligaments Tendons J 3(1):12–22
2. Benjamin M, Ralphs JR (2000) The cell and biology of tendons and ligaments. Int Rev Cytol 196:85–130
3. Rodeo SA, Arnoczky SP, Torzilli PA, Hidaka C, Warren RF (1993) Tendon-healing in a bone tunnel. A biomechanical and histological study in the dog. J Bone Joint Surg Am 75:1795–1803
4. Vesentini S, Redaelli A, Gautieri A (2013) Nanomechanics of collagen microfibrils. Muscles Ligaments Tendons J 3(1):23–34
5. Cowin SC, Doty SB (2007) Tendon and ligament, tissue mechanics. Springer Science and Business Media, LCC, New York, pp 559–594
6. Tresoldi I, Oliva F, Benvenuto M, Fantini M, Masuelli L, Bei R, Modesti A (2013) Tendon's ultrastructure. Muscles Ligaments Tendons J 3(1):2–6
7. Benjamin M, Kaiser E, Milz S (2008) Structure-function relationships in tendons: a review. J Anat 212(3):211–228
8. Wang JH, Guo Q, Li B (2012) Tendon biomechanics and mechanobiology: a minireview of basic concepts and recent advancements. Hand Ther 25(2):133–140
9. Ackermann PW (2013) Neuronal regulation of tendon homoeostasis. Int J Exp Pathol 94(4):271–286
10. Thomopoulos S, Zampiakis E, Das R, Silva MJ, Gelberman RH (2008) The effect of muscle loading on flexor tendon-to-bone healing in a canine model. J Orthop Res 26(12):1611–1617
11. Nakamura N, Hart DA, Boorman RS, Kaneda Y, Shrive NG, Marchuk LL, Shino K, Ochi T, Frank CB (2000) Decorin antisense gene therapy improves functional healing of early rabbit ligament scar with enhanced collagen fibrillogenesis in vivo. J Orthop Res 18:517–523
12. O'Brien M (2005) Anatomy of tendons. In: Maffuli N, Renström P, Leadbetter WB (eds) Tendon injuries. Springer, London, pp 3–13
13. Karahan M, Erol B (2004) Muscle and tendon injuries in children and adolescents. Acta Orthop Traumatol Turc 38(Suppl 1):37–46
14. Reuther KE, Gray CF, Soslowsky LJ (2013) Form and function of tendon and ligament. In: O'Keefe RJ, Jacobs JJ, Chu CE, Einhorn TA (eds) Orthopaedic basic science, 4th edn. American Academy of Orthopaedic Surgeons, Rosemont, pp 213–228
15. Doral MN, Alam M, Bozkurt M, Turhan E, Atay OA, Dönmez G, Maffulli N (2010) Functional anatomy of the Achilles tendon. Knee Surg Sports Traumatol Arthrosc 18(5):638–643
16. September AV, Schwellnus MP, Collins M (2007) Tendon and ligament injuries: the genetic component. Br J Sports Med 41(4):241–246
17. Thorpe CT, Birch HL, Clegg PD, Screen HR (2013) The role of the non-collagenous matrix in tendon function. Int J Exp Pathol 94(4):248–259
18. Majima T, Marchuk LL, Sciore P, Shrive NG, Frank CB, Hart DA (2000) Compressive compared with tensile loading of medial collateral ligament scar in vitro uniquely influences mRNA levels for aggrecan, collagen type II and collagenase. J Orthop Res 18:524–531
19. Lo IK, Chi S, Ivie T, Frank CB, Rattner JB (2002) The cellular matrix: a feature of tensile bearing dense soft connective tissues. Histol Histopathol 17:523–537
20. Beredjiklian PK, Favata M, Cartmell JS, Flanagan CL, Crombleholme TM, Soslowsky LJ (2003) Regenerative versus reparative healing in tendon: a study of biomechanical and histological properties in fetal sheep. Ann Biomed Eng 31:1143–1152
21. Wang JH, Guo Q, Li B (2012) Tendon biomechanics and mechanobiology – a mini-review of basic concepts and recent advancements. J Hand Ther 25(2):133–141
22. Maganaris CN, Narici MV (2005) Mechanical properties of tendons. In: Maffuli N, Renström P, Leadbetter WB (eds) Tendon injuries. Springer, London, pp 14–21
23. Apostolakos J, Durant TJ, Dwyer CR, Russell RP, Weinreb JH, Alaee F, Beitzel K, McCarthy MB, Cote MP, Mazzocca AD (2014) The enthesis: a review of the tendon-to-bone insertion. Muscles Ligaments Tendons J 4(3):333–342
24. Killian ML, Cavinatto L, Galatz LM, Thomopoulos S (2012) The role of mechanobiology in tendon healing. J Shoulder Elbow Surg 21(2):228–237
25. Thomopoulos S, Genin GM (2013) Tendon and ligament biomechanics. In: Winkelstein BA (ed) Orthopaedic biomechanics. CRC/Taylor and Francis, Boca Raton, pp 49–74
26. Lephart SM, Henry TJ (1992) The physiological basis for open and closed kinetic chain rehabilitation for the upper extremity. J Sport Rehabil 1:188–196
27. Kim CH (2012) Spontaneous rupture of the extensor pollicis longus tendon. Arch Plast Surg 39:680–682
28. Chan KM, Fu SC (2012) Tendinopathies in sports: from basic research to the field. In: Doral MN, Tandoğan RN, Mann G, Verdonk R (eds) Sports injuries: prevention, diagnosis, treatment and rehabilitation. Springer, Berlin, pp 859–870

29. Meimandi-Parizi A, Oryan A, Moshiri A (2013) Role of tissue engineered collagen based tridimensional implant on the healing response of the experimentally induced large Achilles tendon defect model in rabbits: a long term study with high clinical relevance. J Biomed Sci 20(1):28
30. Blevins FT, Djurasovic M, Flatow EL, Vogel KG (1997) Biology of the rotator cuff tendon. Orthop Clin North Am 28:1–16
31. Sano H, Ishii S, Yeadon A, Backman Brunet JA, Uhthoff HK (1997) Degeneration at the insertion weakens the tensile strength of the supraspinatus tendon: a comparative mechanical and histologic study of the bone-tendon complex. J Orthop Res 15:719–726
32. Tan S, Kudaş S, Özcan AS, İpek A, Karaoğlanoğlu M, Arslan H, Bozkurt M (2012) Real-time sonoelastography of the Achilles tendon: pattern description in healthy subjects and patients with surgically repaired complete ruptures. Skeletal Radiol 41(9):1067–1072
33. Thomopoulos S (2014) Tendons and ligaments. In: Boyer MI (ed) Comprehensive orthopaedic review, 2nd edn. American Academy of Orthopaedic Surgeons, Rosemont, pp 105–111
34. Galloway MT, Lalley AL, Shearn JT (2013) The role of mechanical loading in tendon development, maintenance, injury, and repair. J Bone Joint Surg Am 95(17):1620–1628
35. Sharma P, Mafulli N (2005) Tendon injury and tendinopathy: healing and repair. J Bone Joint Surg Am 87:187–202
36. Çakmak S, Mahiroğulları M, Keklikçi K, Rodop O (2013) Regenerative applications in tendon repair. Turk Klin J Orthop Traumatol-Spec Top 6(1):60–65
37. Lo R, Majima T (2000) New directions understanding and optimizing ligament and tendon healing. Curr Opin Orthop 11:421–428
38. Lu HH, Thomopoulos S (2013) Functional attachment of soft tissues to bone: development, healing and tissue engineering. Annu Rev Biomed Eng 15:201–226
39. Rawson S, Cartmell S, Wong J (2013) Suture techniques for tendon repair; a comparative review. Muscles Ligaments Tendons J 3(3):220–228
40. Hill R, Chan S (2013) Flexor tendon injuries: a review. Int Musculoskelet Med 35(2):72–79
41. Karaoglu S, Celik C, Korkusuz P (2009) The effects of bone marrow or periosteum on tendon-to-bone tunnel healing in a rabbit model. Knee Surg Sports Traumatol Arthrosc 17(2):170–178
42. Sandra LC (1996) Tendon injuries: pathophysiology and treatment. In: Zachazewski JE, Magee DJ, Quillen WS (eds) Athletic injury and rehabilitation. W.B. Saunders, Philadelphia, pp 27–53
43. Maffulli N, Moller HD (2005) Optimization of tendon healing. In: Nicola M, Per R, Leadbetter WB (eds) Tendon injuries. Springer, London, pp 304–306
44. Atesok K, Fu FH, Wolf MR, Ochi M, Jazrawi LM, Doral MN, Lubowitz JH, Rodeo SA (2014) Augmentation of tendon-to-bone healing. J Bone Joint Surg Am 96(6):513–521
45. Nguyen TD, Liang R, Woo SL, Burton SD, Wu C, Almarza A, Sacks MS, Abramowitch S (2009) Effects of cell seeding and cyclic stretch on the fiber remodeling in an extracellular matrix-derived bioscaffold. Tissue Eng Part A 15:957–963
46. Andersson T, Eliasson P, Hammerman M, Sandberg O, Aspenberg P (2012) Low-level mechanical stimulation is sufficient to improve tendon healing in rats. J Appl Physiol 113:1398–1402
47. Maffulli N, Moller HD, Evans CH (2002) Tendon healing: can it be optimised? Br J Sports Med 36(5):315–316
48. Bluman EM, Allen SD, Fadale PD (2006) Tendon repair and regeneration. In: Walsh WR (ed) Repair and regeneration of ligaments, tendons, and joint capsule. Humana Press, New Jersey, pp 3–12
49. Kampa RJ, Connell DA (2010) Treatment of tendinopathy: is there a role for autologous whole blood and platelet rich plasma injection? Int J Clin Pract 64:1813–1823
50. Tatari H, Koşay C, Baran Ö, Özcan Ö, Özer E, Ulukuş C (2001) Effect of heparin on tendon degeneration: an experimental study on rats. Knee Surg Sports Traumatol Arthrosc 9(4):247–253
51. Huri G, Biçer ÖS, Ozgözen L, Uçar Y, Garbis NG, Hyun YS (2013) A novel repair method for the treatment of acute Achilles tendon rupture with minimally invasive approach using button implant: a biomechanical study. Foot Ankle Surg 19(4):261–266
52. Oryan A, Moshiri A, Meimandi Parizi AH, Raayat JA (2012) Repeated administration of exogenous sodium-hyaluronate improved tendon healing in an in vivo transection model. J Tissue Viability 21:88–102
53. Moro-oka T, Miura H, Mawatarl T, Kawano T, Nakanishi Y, Higaki H, Iwamoto Y (2000) Mixture of hyaluronic acid and phospholipid prevents adhesion formation on the injured flexor tendon in rabbits. J Orthop Res 18:835–840
54. Yagi M, Mitsui Y, Gotoh M, Sato N, Yoshida K, Nagata K (2012) Role of the hyaluronan-producing tenosynovium in preventing adhesion formation during healing of flexor tendon injuries. Hand Surg 17:13–17
55. Circi E, Akpinar S, Balcik C, Bacanli D, Guven G, Akgun RC, Tuncay IC (2009) Biomechanical and histological comparison of the influence of oestrogen deficient state on tendon healing potential in rats. Int Orthop (SICOT) 33:1461–1466
56. Whitlock PW, Seyler TM, Mannava S, Pohling GG (2012) A tissue-engineered approach to tendon and ligament reconstruction. In: Doral MN, Tandoğan RN, Mann G, Verdonk R (eds) Sports injuries: prevention, diagnosis, treatment and rehabilitation. Springer, Berlin, pp 1185–1192
57. Tang JB, Cao Y, Zhu B, Xin KQ, Wang XT, Liu PY (2008) Adeno-associated virus-2-mediated bFGF gene transfer to digital flexor tendons significantly increases healing strength: an in vivo study. J Bone Joint Surg Am 90:1078–1089

58. Oztuna V, Yilmaz A, Yilmaz C, Eskandari M, Ayan İ, Milcan A, Kuyurtar F (2005) The use of N-butyl-2-cyanoacrylate (Histoacryl) in primary tendon repair: a biomechanical study with sheep flexor tendons. Acta Orthop Traumatol Turc 39(3):258–262
59. Esenkaya İ, Sakarya B, Unay K, Elmali N, Aydin NE (2010) The influence of atorvastatin on tendon healing: an experimental study on rabbits. Orthopedics 33(6):398
60. Majewski M, Betz O, Ochsner PE, Liu F, Porter RM, Evans CH (2008) Ex vivo adenovlral transfer of bone morphogenetic protein 12 (BMP-12) cDNA improves Achilles tendon healing in a rat model. Gene Ther 15:1139–1146
61. Rui YF, Lui PP, Lee YW, Chan KM (2012) Higher BMP receptor expression and BMP-2-induced osteogenic differentiation in tendon-derived stem cells compared with bone-marrow-derived mesenchymal stem cells. Int Orthop 36:1099–1107
62. Ruzzini L, Longo UG, Rizzello G, Denaro V (2012) Stem cells and tendinopathy: state of the art from the basic science to clinic application. Muscles Ligaments Tendons J 2(3):235–238
63. Chong AK, Ang AD, Goh JC, Hui JH, Lim AY, Lee EH, Lim BH (2007) Bone marrow-derived mesenchymal stem cells influence early tendon-healing in a rabbit Achilles tendon model. J Bone Joint Surg Am 89(1):74–81
64. Kanazawa T, Soejima T, Noguchi K, Tabuchi K, Noyama M, Nakamura K, Shiba N (2014) Tendon-to-bone healing using autologous bone marrow derived mesenchymal stem cells in ACL reconstruction without a tibial bone tunnel-A histological study. Muscles Ligaments Tendons 4(2):201–206
65. Woo SL, An KN, Frank CB (2000) Anatomy, biology, and biomechanics of tendon and ligament. In: Buckwalter TA, Einhorn TA, Simon SR (eds) Orthopaedic basic science: biology and biomechanics of the musculoskeletal system, 2nd edn. American Academy of Orthopaedic Surgeons, Rosemont, pp 581–616
66. Aydoğ ST, Korkusuz P, Doral MN, Tetik O, Demirel HA (2006) Decrease in the numbers of mechanoreceptors in rabbit ACL: the effects of ageing. Knee Surg Sports Traumatol Arthrosc 14(4):325–329
67. Jung HJ, Fisher MB, Woo SL (2009) Role of biomechanics in the understanding of normal, injured, and healing ligaments and tendons. Sports Med Arthrosc Rehabil Ther Technol 1:9
68. Salci Y, Kentel BB, Heycan C, Akin S, Korkusuz F (2004) Comparison of landing maneuvers between male and female college volleyball players. Clin Biomech (Bristol, Avon) 19(6):622–628
69. Frank CB, Hart DA, Shrive NG (1999) Molecular and biomechanics of normal and healing ligaments: review. Osteoarthritis Cartilage 7:130–140
70. Hsu SL, Liang R, Woo SL (2010) Functional tissue engineering of ligament healing. Sports Med Arthrosc Rehabil Ther Technol 2:12
71. Ng GY, Oakes BW, McLean ID, Deacon OW, Lampard D (1996) The long-term biomechanical and viscoelastic performance of repairing anterior cruciate ligament after hemitransection injury in a goat model. Am J Sports Med 24:109–117
72. Thornton GM, Boorman RS, Shrive NG, Frank CB (2002) Medial collateral ligament autografts have increased creep response for at least two years and early immobilization makes this worse. J Orthop Res 20(2):346–352
73. Dunn MG, Liesch JB, Tiku ML, Zawadsky JP (1995) Development of fibroblast-seeded ligament analogs for ACL reconstruction. J Biomed Mater Res 29:1363–1371
74. Shino K, Oakes BW, Horibe S, Nakata NN (1995) Collagen fibril populations in human anterior cruciate ligament allografts: electron microscopic analysis. Am J Sports Med 23:203–208
75. Woo SL, Smith DW, Hildebrand KA, Zeminski JA, Johnson LA (1998) Engineering the healing of the rabbit medial collateral ligament. Med Biol Eng Comput 36:359–364
76. Kaplan N, Wickiewicz TL, Warren RF (1990) Primary surgical treatment of anterior cruciate ligament ruptures: a long-term follow-up study. Am J Sports Med 18:354–358
77. Ng GY, Oakes BW, Deacon OW, McLean ID, Lampard D (1995) Biomechanics of patellar tendon autograft for reconstruction of the anterior cruciate ligament in the goat: three-year study. J Orthop Res 13:602–608

Spinal Cord and Intervertebral Disc

29

Erdem Aktaş and Alpaslan Şenköylü

Abstract

The spinal cord is a part of the central nervous system (CNS) that extends longitudinally with its surrounding meninges within the vertebral canal down to the space between the first and second lumbar vertebrae. Its morphology is a tubular cord made up of nervous tissue and support cells. Cord includes 31 segments (12 thoracic segments, 5 lumbar segments, 5 sacral segments, and 1 coccygeal segment), which gives 31 pair of spinal nerves to the trunk and limb. It controls the voluntary muscles of the limbs and trunk, receives sensory information from these regions, and controls the viscera and blood vessels of the thorax, abdomen, and pelvis.

Intervertebral disc is a highly specialized and organized tissue including three components (Nucleus pulposus, annulus fibrosus, cartilaginous endplates). Each disc forms a fibrocartilaginous joint that provides flexibility and allows bending, flexion, and torsion of the vertebrae. There are a total of 23 discs in the human spine (6 in the cervical region, 12 in the thoracic region, and 5 in the lumbar region) that are located between vertebral bodies. Intervertebral discs have important roles; (1) protecting the spinal cord and nerve roots, (2) maintaining cervical and lumbar lordosis, and (3) absorbing energy and transmitting loads through the spinal column.

Learning Outcomes

After reading this chapter, the reader will be able

1. To describe development of spinal cord
2. To define gross anatomy of spinal cord and its membranes
3. To explain blood supply and its importance of spinal cord

E. Aktaş
Department of Orthopaedics and Traumatology, Oncology Hospital, Yenimahalle, Ankara, Turkey

A. Şenköylü (✉)
Department of Orthopaedics and Traumatology, Gazi University, Besevler 06510, Ankara, Turkey
e-mail: drsenkoylu@gmail.com; senkoylu@gazi.edu.tr

F. Korkusuz (ed.), *Musculoskeletal Research and Basic Science*,
DOI 10.1007/978-3-319-20777-3_29

4. To list main columns and their functions of spinal cord
5. To summarize autonomic nervous system
6. To identify upper motor neuron syndrome, spinal shock, and incomplete spinal cord syndrome
7. To recognize the structure of intervertebral disc
8. To list functions of intervertebral disc
9. To explain vascular and nerve supply of disc
10. To define aging disc concept and its clinical importance
11. To describe pathophysiology of degenerative disc disease and disc herniation

Spinal Cord

Spinal cord is a thick, cylindrical bundle of nervous tissue and supports cells that extend from the medulla oblongata. Cord is a part of the CNS that controls the voluntary muscles of the limbs and trunk, receives sensory information from these regions, and controls the viscera and blood vessels of the thorax, abdomen, and pelvis.

Development of the Spinal Cord

Nervous system consists of two systems: (1) Central nervous system (brain and spinal cord), (2) Peripheral nervous system (cranial and spinal nerves). Post conception day 20, the CNS develops as the neural plate from the part of ectoderm. At the third week, the midsagittal groove of this primitive structure deepens within the ectoderm and begins to fold onto itself and forms the neural tube. It closes and the neural crest forms dorsal to the neural tube. The notochord remains ventral. The neural tube forms the spinal cord, and the notochord forms the anterior vertebral bodies and intervertebral discs. The neural crest forms the peripheral nervous system including the pia mater, spinal ganglia, and sympathetic trunk. The spinal cord changes position with growth. At birth, the conus lies at the level of L3, whereas it moves to L1-2 by skeletal maturity (Fig. 29.1).

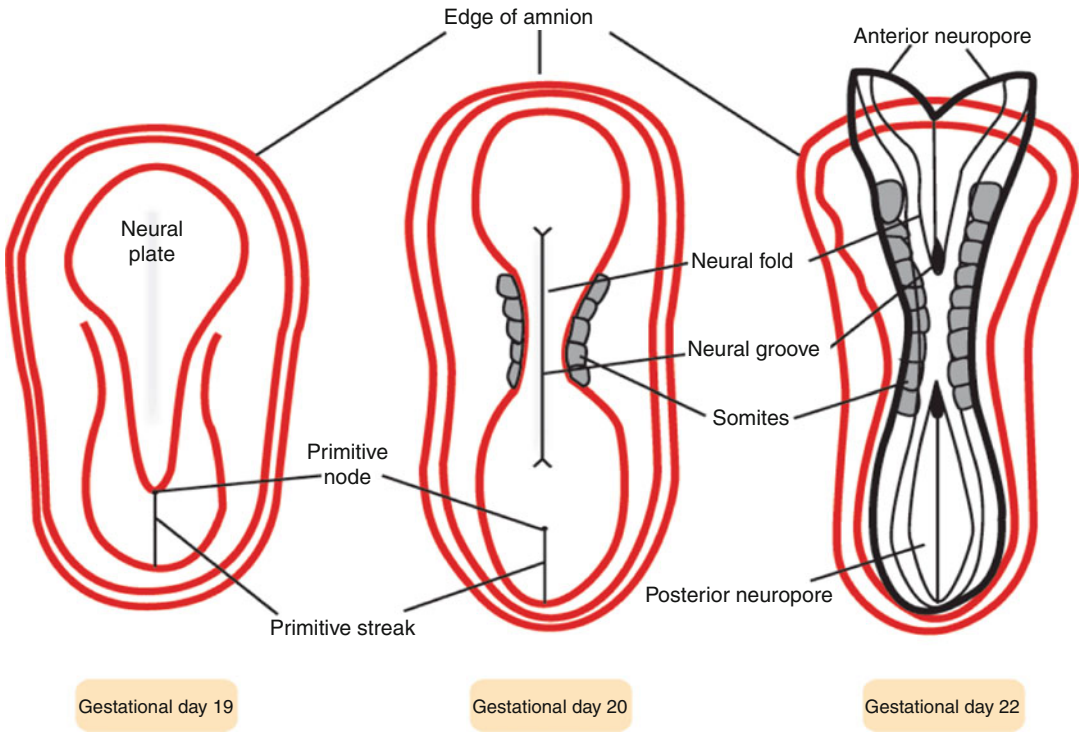

Fig. 29.1 Development of the spinal cord at gestational day 19, 20, and 22

Failure of the Ends of the Neural Tube to Close

(a) Cranially, may cause anencephaly
(b) Caudally, may cause spina bifida occulta, meningocele, myelomeningocele, and myeloschisis
(c) Persistence of the neurocentric canal causes diastematomyelia, which is a septum dividing the medullary canal into two parts on sagittal plain.

Gross Anatomy

The adult human spinal cord is made up of 31 segments (12 thoracic segments, 5 lumbar segments, 5 sacral segments, and 1 coccygeal segment). The spinal cord and its surrounding meninges lie within the vertebral canal and reaches down to the space between the first and second lumbar vertebrae. The average length of the spinal cord differs with gender. Average length in humans is 45 cm (18 in.) in males and 42–43 cm (17 in.) in females. It has a width, ranging from 13 mm (0.5 in.) thickness to 6.4 mm (0.25 in.).The average cross-sectional area of the cervical spinal cord in humans is 122 mm^2 at C4, while it is 110 mm^2 at C2 and 85 mm^2 at C7 [7, 35]. The cross-sectional area of the lumbar enlargement is about 50 mm^2, the sagittal diameter about 7 mm, and the transverse diameter 9 mm in human cadavers [17]. This cross-sectional area increases from C1 to C6 and then remains constant throughout the middle thoracic segments. It increases again from T12 to L4 and decreases rapidly below S1 [15]. There are four grooves in the spinal cord. The ventral median fissure lies on the ventral surface of the spinal cord as a midline deep longitudinal fissure. In humans, the average depth of the ventral median fissure is 3 mm and is deepest at C5 [7]. On the dorsal surface of the spinal cord lies the dorsal median sulcus. On the lateral side, there is a hollow ventrolateral sulcus and a deeper dorsolateral sulcus.

Meninges

Membranes that cover and protect the brain and spinal cord are named the meninges. There are three meninges according to their anatomical relation with the spinal cord and morphology.

1. *Pia mater*: Surrounds the brain and spinal cord, it is the innermost layer of the meninges.
2. *Arachnoid mater*: It is located between the more superficial dura mater and the deeper pia mater. It is separated from pia mater by the subarachnoid space. The subarachnoid space contains the cerebrospinal fluid (CSF). CSF exits the subarachnoid space and enters the blood stream via arachnoid villi that are small protrusions through the dura mater into the venous sinuses of the brain.
3. *Dura mater*: The outermost and thickest membrane of the three layers of the meninges. It is derived from the mesoderm.

Spinal Cord Blood Vessels

Three arteries, a single ventral spinal artery, and two dorsal spinal arteries supply the spinal cord. The ventral spinal artery originates from the vertebral artery and descends within the ventral median fissure of the spinal cord. The right and left dorsal spinal arteries originate either from the vertebral artery or its inferior posterior cerebellar branch, and descend in the dorsolateral sulcus of the spinal cord. They form anastomoses with the anterior and posterior segmental medullary arteries, which are branches from the vertebral, deep cervical, intercostal, and lumbar arteries (Fig. 29.2). The veins of the spinal cord form a

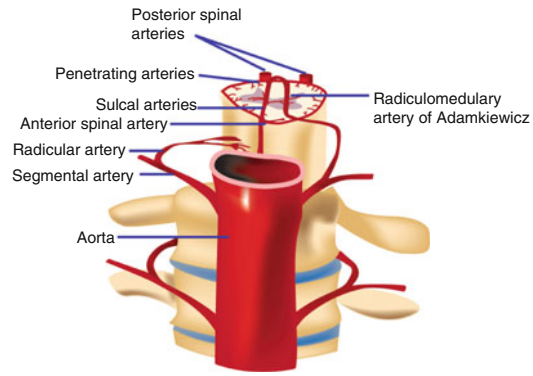

Fig. 29.2 Arterial supply to the spinal cord

surface plexus, which drain ventrally into the cerebellar veins and cranial sinuses and through the intervertebral veins and external venous plexuses to the azygous system.

The actual blood flow caudally through these arteries is inadequate to maintain the spinal cord beyond the cervical segments. The major contribution to the arterial blood supply of the spinal cord below the cervical region comes from the radially arranged posterior and anterior radicular arteries, which run into the spinal cord alongside the dorsal and ventral nerve roots. These intercostal and lumbar radicular arteries arise from the aorta, provide major anastomoses, and supplement the blood flow to the spinal cord. An animal study suggests that critical spinal cord ischemia after complete thoracoabdominal aortic segmental artery sacrifice does not occur immediately, but is delayed 1–5 h or longer after injury [5]. In humans, the largest of the anterior radicular arteries is known as the artery of Adamkiewicz (anterior radicularis magna artery), which usually arises between L1 and L2 [39]. Meticulous surgical technique has to be carried out, since impairment of blood flow through posterior and anterior radicular arteries can result in serious conditions, such as paraplegia due to spinal cord infarction. To further enhance the understanding of spinal cord circulation, a novel monitoring system for spinal cord blood flow has been recently developed in an animal model. The device is told to hold promise to detect imminent ischemia or ensure acceptable blood perfusion in the spinal cord [12].

Structures of the Spinal Cord

The caudal end of the spinal cord narrows and forms the conus medullaris. The conus medullaris runs as a long fibrous strand, called the filum terminale. The filum terminale is an elastic structure composed of longitudinally arranged collagen bundles and elastic fibers [6]. Filum terminale arises from the end of the spinal cord at the level of the L1 vertebra and attaches to the coccyx. In humans, the length of the filum terminale internum is about 15 cm, the mean initial diameter 1.5 mm, and the midpoint diameter is 0.75 mm [26]. At the level of S2 vertebra, it perforates the dura and continues as the filum terminale externum that terminates on the dorsal surface of the first coccygeal vertebra together with the coccygeal ligament. The spinal cord is mainly composed of gray matter and white matter.

Gray Matter

Depending on the level, the gray matter is oriented in the form of the capital letter H in transverse sections. It also looks like a butterfly on the same plain. The gray matter can be divided into dorsal and ventral horns and intermediate region between them. The dorsally projecting arms of the gray matter are called the dorsal horns, and the ventrally projecting arms are called the ventral horns. The central region that connects the dorsal and ventral horns is called the intermediate gray matter. Microscopic analysis of the spinal gray matter reveals a complex structure, characterized by layers of cells from dorsal to ventral. The spinal cord gray matter consists of glial cells, neuronal cells, dendrites, and axons. The spinal gray matter is divided into ten regions in transverse sections. Nine laminae are organized from dorsal to ventral whereas the tenth lamina consists of cells surrounding the central canal. Laminae 1–4 are the main cutaneous receptive regions; lamina 5 receives afferents from the viscera, skin, and muscles. Lamina 6 receives proprioceptive and some cutaneous afferents.

White Matter

The gray matter is surrounded by white matter. The white matter consists of longitudinally running axons and also glial cells. A large group of axons, which are located in a given area, is called as funiculus. Smaller bundles of axons, which share common features within a funiculus, are called as fasciculus. A group of nerve fibers with the same course, origin, termination, and function is a tract. A group of tracts with a related function is a pathway. The horns of gray matter divide the white matter into three columns: dorsal, lateral, and ventral. The lateral and anterior columns contain ascending and descending fiber groups. The ascending tracts include the spinothalamic,

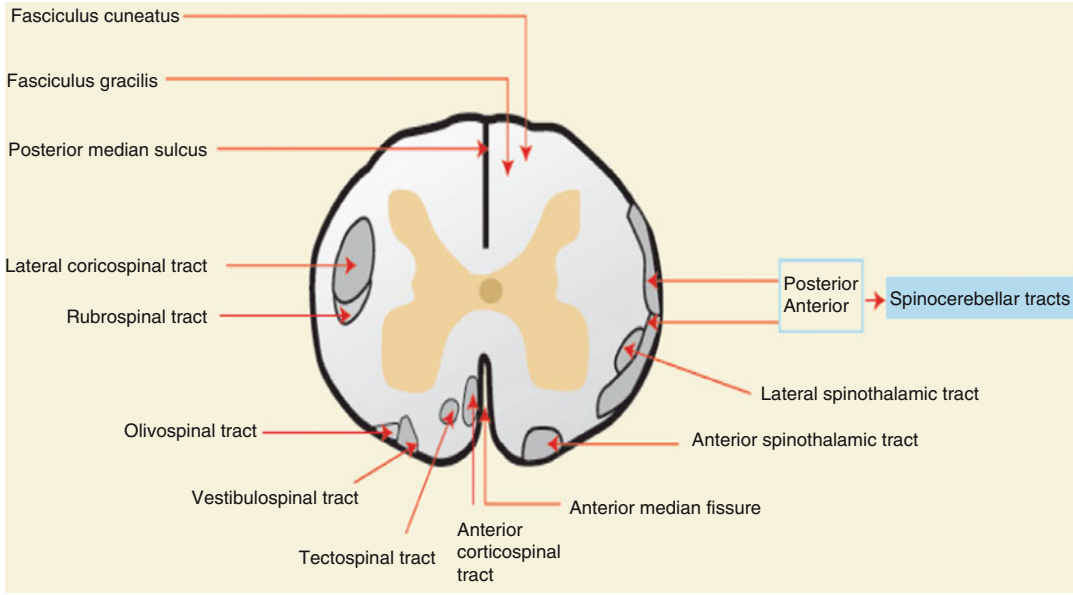

Fig. 29.3 Ascending and descending pathways of the spinal cord in cross-section

spinocerebellar, and spinotectal tracts and the descending tracts include the corticospinal, vestibulospinal, tectospinal, and reticulospinal tracts (Fig. 29.3).

During neural tube closure, the dorsal cells (alar lamina) become primarily sensory (afferent), and the ventral cells (basal lamina) become primarily motor (efferent) in function.

(a) *Dorsal Column*: transfer vibration, deep touch sensation, and proprioception
(b) *Anterolateral Column*: lateral spinotalamic tract transmits pain and temperature sensation
(c) *Ventral Spinotalamic Tract*: light touch sensation
(d) *Lateral Corticospinal Tract*: voluntary motor function

Spinal Nerves

Spinal nerves emerge the vertebral column between the adjacent vertebrae through the intervertebral foramina and send motor impulses from the CNS to muscles and target organs and carry sensory information from organs to the CNS. There are 31 pairs of spinal nerves: 8 cervical (C1–C8), 12 thoracic (T1–T12), 5 lumbar (L1–L5), 5 sacral (S1–S5), and 1 coccygeal (Co1). Spinal nerves emerge from the vertebral canal below their respective vertebrae, except from the cervical region. Although the first seven cervical spinal nerves emerge similarly above their respective vertebrae, because there are eight cervical spinal cord segments, but only seven cervical vertebrae, the nerve emerging between C7 and T1 is named the eighth cervical nerve. Each spinal nerve is attached to the spinal cord via anterior and posterior roots. Each root is compromised of seven to nine rootlets. Axons of motor neurons come together and form ventral rootlets whereas axons of sensory neurons form dorsal rootlets. Each dorsal nerve root contains a dorsal root (spinal) ganglion. These cells are the origin of peripheral and central nerve fibers. A transition zone is defined between the CNS and the peripheral nervous system at the attachment point of each rootlet to the spinal cord [9].

Ventral roots: Each ventral root can also be named the anterior root, radix anterior, radix ventralis, or radix motoria. They are attached to the spinal cord by a series of rootlets that emerge from the ventrolateral sulcus of the spinal cord.

The ventral roots predominantly consist of efferent somatic motor fibers (thick alpha motor axons and medium-sized gamma motor axons) derived from nerve cells of the ventral column.

Dorsal roots: There are 31 pairs of dorsal roots. Each dorsal root can also be named the posterior root, radix posterior, radix dorsalis, or radix sensoria. They are attached to the dorsolateral sulcus of the spinal cord by a series of rootlets. The dorsal roots contain sensory fibers from the skin, subcutaneous and viscera, skeletal muscles, tendons, and joints. It is estimated that there are 2–2.5 million afferent fibers in human adult dorsal roots on each side [31].

Dorsal root (spinal) ganglia: Each dorsal spinal root comprises dorsal root ganglion (DRG). The DRG consists of pseudounipolar neurons with single axon, cells that are primary sensory. They divide into peripheral and central branches, where the central branch enters the spinal cord via the dorsal roots. The peripheral branch carries sensory information from the body to the DRG cell body, whereas central branch carries information from the cell body of DRG neuron to the spinal cord.

Each spinal nerve consists of somatic and visceral fibers that can be classified according to their functions; as visceral efferent, somatic efferent, somatic afferent, and visceral afferent fibers.

Somatic afferent fibers: Exteroceptive fibers that carry impulses generated by external stimulations and somatic afferent fibers are peripheral continuation of DRG neurons. Their main objective is to carry sensory information from the skin, viscera, subcutaneous tissues, and deep tissues.

Somatic efferent fibers: compromised of axons from the ventral horn neurons. Their main objective is to carry motor impulses to the skeletal muscles.

Visceral afferent fibers: Interoceptive fibers that carry visceral sensation. They are made up of peripheral processes of DRG neurons. They constitute less than 10 % of afferent fibers in dorsal roots.

Visceral efferent fibers: Sympathetic or parasympathetic autonomic nerve fibers that carry motor impulses to glands, cardiac and smooth muscles.

Autonomic Nervous System

The autonomic nervous system is responsible for regulating vegetative functions and maintaining homeostasis in the body. The visceral efferent fibers are autonomic (sympathetic/parasympathetic) nerve fibers that carry motor impulses to glands and cardiac and smooth muscles. Despite visceral efferents that are divided into parasympathetic and sympathetic fibers, afferent fibers of the autonomic nervous system, which transmit sensory information from the internal organs of the body to the CNS, are conducted by general visceral afferent fibers. These are unconscious visceral motor reflex sensations from glands and organs that are transmitted to the CNS. The system is under the control of the hypothalamus and also works concordant with the endocrine system [22].

(a) *Sympathetic*: Fibers innervate tissues in almost every organ system. The system is composed of 22 ganglia (3 cervical, 11 thoracic, 4 lumbar, and 4 sacral). In the sympathetic system, two kinds of neurons are involved in the transmission of signals: preganglionic and postganglionic. Preganglionic neurons are shorter and originate from the thoracolumbar region levels, especially T1–L2, and travel to a ganglion. At the paravertebral ganglia, they synapse with a postganglionic neuron. At the synapses within the ganglia, preganglionic neurons secrete acetylcholine, which activates nicotinic acetylcholine receptors on postganglionic neurons. In response, postganglionic neurons secrete norepinephrine, which activates adrenergic receptors on the target tissues. The postganglionic neuron is longer and extends across the body. They provide several regulatory functions. The most prominent ones are pupil dilatation, increase in cardiac rate and force of contraction, dilatation of bronchioles, peristalsis inhibition, sweat secretion activation, and renin secretion activation [23]. Horner syndrome (miosis, ptosis, and anhidrosis) can be seen if damage to the sympathetic nervous system occurs.

(b) *Parasympathetic*: The parasympathetic system is responsible for stimulation of activities that occur when the body is at rest and the system uses acetylcholine and cholecystokinin as its neurotransmitter. Nerve fibers of the parasympathetic nervous system arise from the CNS. Parasympathetic preganglionic efferent fibers originate from the neurons of the sacral parasympathetic nucleus. The functions of the parasympathetic system are sexual arousal, digestion, salivation, lacrimation, urination, and defecation. Several cranial nerves have parasympathetic properties: the occulomotor nerve, facial nerve, glossopharyngeal nerve, and vagus nerve. Apart from cranial nerves, three spinal nerves in the sacrum (S2–4) also act as parasympathetic nerves, which are named as the pelvic splanchnic nerves.

Apart from these functions, sensory and motor fibers of the spinal nerves form a reflex arc. The reflex arc is polysynaptic and functions when afferent fibers impulses end up with a motor reaction before sending information to the brain. This maintains the posture of the body and helps movements to occur in harmony (Fig. 29.4).

Dermatomes

A dermatome is the area of skin supplied by a single spinal nerve. Although there are 31 pairs of spinal nerves in humans, there are only 30 dermatomes. Along the trunk, dermatomes have a segmental distribution represented as narrow bands of skin running almost horizontally, whereas in the limbs, due to the growth and rotation of limb buds during development, they are generally oriented longitudinally along the long axis of the limbs (Fig. 29.5).

Segmental Motor Distribution

Skeletal muscles are innervated by more than one spinal nerve with a segmental motor distribution (Table 29.1). Each spinal nerve supplies the muscles originating from the myotomes of the same segment. Although the segmental distribution is apparent in the distribution of peripheral nerves to the muscles, axons of the spinal nerves are redistributed into peripheral nerves in plexuses in the cervical, brachial, and lumbosacral regions.

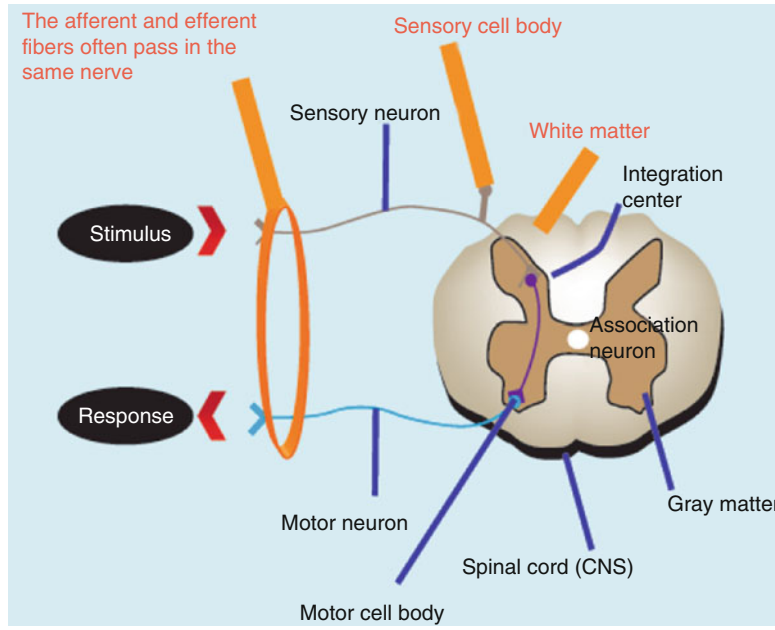

Fig. 29.4 Reflex arc of the spinal cord

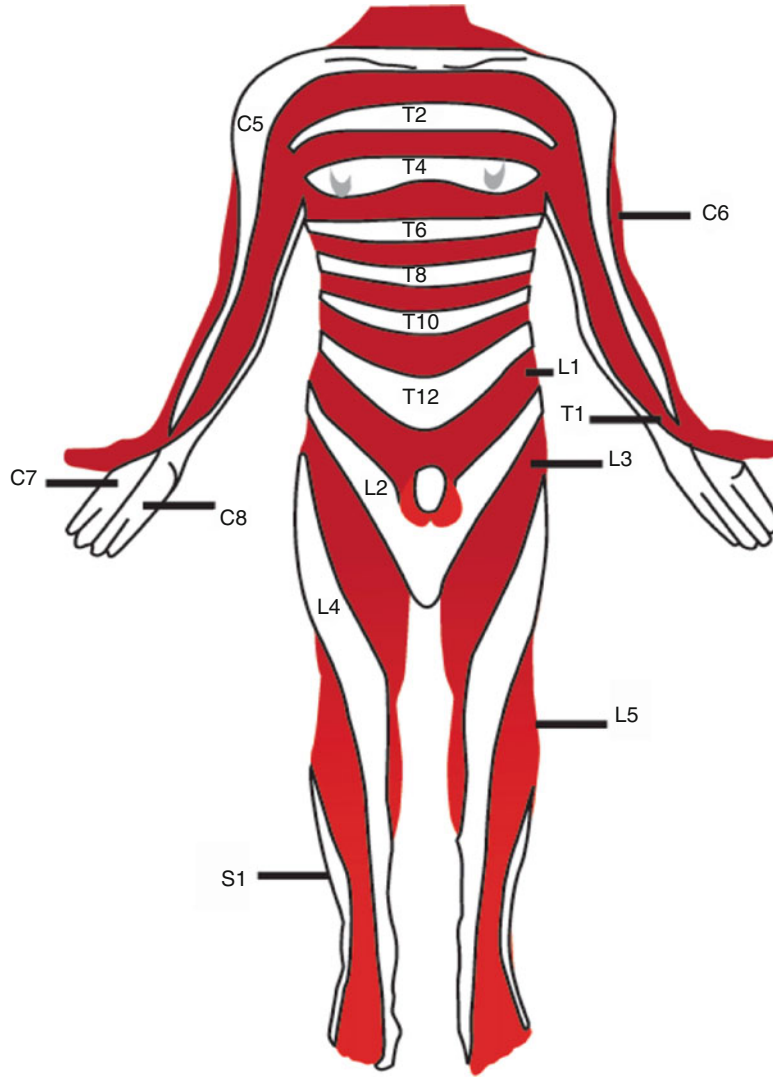

Fig. 29.5 Dermatomes of the human body. Areas of the skin supplied by afferent nerve fibers originating from posterior spinal root

Clinical Relevance

Upper Motor Neuron Syndrome

Damage of the descending motor pathways anywhere between the cerebral cortex and spinal cord can result in symptoms called the upper motor neuron syndrome. Acute manifestations are usually tended to be more severe on the extremities. In general, symptoms include: spasticity, hyporeflexia of superficial reflexes, Babinski sign, inability to form fine movements, and increase in deep tendon reflexes. Negative symptoms such as weakness, paresis, and fatigue can be observed. During acute manifestations, negative symptoms can be more prominent. In chronic entities, loss in fine movements of the hand is apparent.

Spinal Shock

The description of spinal shock is absence of spinal reflexes distal to the level of spinal cord injury. Four phases can be defined. Phase 1 (0–day 1) consists of areflexia or hyporeflexia, phase 2 (days 1–3) consists of recovery of initial reflex, phase 3 (weeks 1–4) consists of initial hyperreflexia, and phase 4 (1–12 months) includes hyperreflexia. Delayed plantar reflex is the first to be seen and is accepted to be a sign of bad prognosis if present more than 7 days [3].

Incomplete Spinal Cord Syndromes

Incomplete motor syndromes can be defined as spinal cord injury with some preserved motor or sensory function below the injury level. The American Spinal Injury Association (ASIA) classification has a high predictive value for identifying complete spinal cord (ASIA A) injuries (Table 29.2). Only 7 % of ASIA A converts to ASIA B [2].

Clinically, there are five different types of incomplete spinal cord syndromes: Central cord syndrome, anterior cord syndrome, Brown-Sequard syndrome, and posterior cord syndrome. Most common type is central cord syndrome. It is mostly seen in elderly patients and associated with an underlying cervical stenosis. Injury mechanism is, typically, minor head trauma with hyperextension of neck. Motor deficit is worse in upper extremities than lower extremities since upper extremities represented centrally in corticospinal tract. This incomplete spinal cord syndrome has a good prognosis although full functional recovery is rare at the end [11].

Table. 29.1 Motor innervation of the upper lower limbs and associated nerves, nerve roots

Action	Muscles	Nerves	Nerve roots
Finger extension	Extensor digitorum, extensor indicis, extensor digit minimi	Radial nerve (posterior interosseous nerve)	*C7*, C8
Wrist flexion and hand abduction	Flexor carpi ulnaris	Ulnar nerve	C7, *C8*, T1
Wrist flexion and hand abduction	Extensor carpi radialis	Radial nerve	C5, *C6*
Elbow flexion	Biceps, brachialis	Musculotaneous nerve	C5, C6
Hip flexion	Iliopsoas	Femoral nerve, and L1-L3 nerve roots	L1, L2, *L3*, L4
Knee extension	Quadriceps	Femoral nerve	L2, *L3*, *L4*
Knee flexion	Hamstrings	Sciatic nerve	L5, *S1*, S2
Leg abduction	Gluteus medius, gluteus minimus, tensor fasciae latae	Superior gluteal nerve	*L4*, *L5*, S1
Leg adduction	Obturator externus, adductor longus, magnus, and brevis, gracilis	Obturator nerve	*L2*, *L3*, L4
Toe dorsiflexion	Extensor hallucis longus, extensor digitorum longus	Deep peroneal nerve	*L5*, S1
Foot dorsiflexion	Tibialis anterior	Deep peroneal nerve	L4, L5
Foot plantar flexion	Triceps surae	Tibial nerve	S1, S2
Foot inversion	Tibalis posterior	Tibal nerve	L4, L5

Table 29.2 ASIA score

A	Complete	No motor or sensory function is preserved in the sacral segments S4–S5
B	Incomplete	Sensory function preserved but motor function is not preserved below the neurological level and includes the sacral segments S4–S5
C	Incomplete	Motor function is preserved below the neurological level, and more than half of key muscles below the neurological level have a muscle grade less than 3
D	Incomplete	Motor function is preserved below the neurological level, and at least half of key muscles below the neurological level have a muscle grade of 3 or more
E	Normal	Motor and sensory functions are normal

Intervertebral Disc

Intervertebral disc is a highly specialized and organized tissue that is located between vertebral bodies. There are a total of 23 discs in the human spine: 6 in the cervical region, 12 in the thoracic region, and 5 in the lumbar region. There is one disc between each pair of vertebrae, except for the first cervical segment, the atlas. Intervertebral discs have important roles: (1) protecting the spinal cord and nerve roots, (2) maintaining cervical and lumbar lordosis, and (3) absorbing energy and transmit loads through the spinal column. Each disc forms a fibrocartilaginous joint that provides flexibility and allows bending, flexion, and torsion of the vertebrae.

Structure

Intervertebral disc is 4 cm in diameter and 7–10 mm thick in the lumbar region and is comprised of three main components: (1) nucleus pulposus, (2) annulus fibrosus, and (3) cartilaginous endplates [28].

Annulus Fibrosus

A fibrocartilaginous tissue made up of 15–15 concentric lamellae that form a thick external ring surrounding a more gelatinous core, the nucleus pulposus. Fibers of the outer lamellae continue into the longitudinal ligaments and vertebral bodies. Elastin fibers lie between these lamellae, bind the lamellae together, and help the disc to return to its original form following movements (e.g., flexion and extension). This arrangement allows the discs to facilitate movement and flexibility within what would be an otherwise rigid spine [40].

The disc is compromised of relatively few cells that are organized in a specific manner. Number of cells makes up approximately 1 % of the total volume of the disc. The morphology of the cells tends to change according to their localization. Compared with those of the nucleus pulposus, which are more oval and chondrocyte-like, the cells of the annulus tend to be fibroblast-like, elongated, and aligned parallel to the collagen fibers [4]. Apart from their morphological difference, these two cell populations also behave differently in regard to their response to applied loads or in synthesizing different matrix molecules. Annulus fibrosus cells mainly produce type-I and type-II collagen, whereas type-III and type-VI collagen are also found predominantly.

Nucleus Pulposus

Although nucleus pulposus are closely linked structures, different from annulus fibrosus, which develop from the mesoderm, the nucleus pulposus derives from endoderm and is a remnant of the notochord. The central nucleus pulposus is made up of collagen and elastin fibers, where collagen fibers are organized randomly and elastin fibers are organized radially. These fibers are suspended in a mucoprotein gel, which helps distribute pressure and axial loading evenly. The nucleus of the disc acts as a shock absorber and relieves the magnitude of impact related with the body's activities. Although elastin constitutes 2 % of the dry weight of the annulus, it gives a big contribution to disc functions. The nucleus pulposus is a complex structure, consisting of notochord cells, chondrocyte-like cells, collagen fibrils, and proteoglycan aggrecan. Chondroitin sulfate and keratan sulfate are attached to each aggrecan molecule. Nucleus pulposus cells generally synthesize only type-II collagen. The nucleus pulposus is contained inferiorly and superiorly by cartilage endplates.

Cartilage Endplate

A thin horizontal layer made up of hyaline cartilage 0.6–1 mm thick, which occupies the central 90 % of the interface between the disc and the vertebral body. In early life, cartilage endplate functions as a growth plate for the adjacent vertebral body. During skeletal maturity, this unique structure regresses and by adulthood, the cartilage endplate ends up as a layer of hyaline cartilage with calcified cartilage adjoining the bone.

Blood Vessels and Nerve Supply of the Disc

Mainly restricted to the outer lamellae, blood vessels and nerves are present to a limited degree in the adult disc. Mechanoreceptors that are similar to Golgi apparatus, Ruffini receptors, Pacinian corpuscles are present in small numbers. Up till 12 months, blood vessels are present in the longitudinal ligaments adjacent to the disc and cartilage endplates, which are branches of the spinal artery. Nerves in the disc have been demonstrated, often accompanying these vessels. Apart from this, vessels also occur independently, being branches of the sinuvertebral nerve or derived from the ventral rami or gray rami communicantes. In the healthy adult, cartilaginous endplate is aneural and avascular. The recurrent sinovertebral nerve, as a meningeal branch of the spinal nerve, originates near the disc space. The nociceptive fibers from the ascending branch of the sinovertebral nerve innervate the adjacent outer layers of the annulus fibrosis.

Function

The intervertebral disc functions to: (1) support the axial load on the column and to distribute hydraulic pressure in all directions as it is delivered by body mass and gravity, thus providing the appropriate surface for shock absorbing, (2) assists in range of motion at the spine, and (3) separates the vertebrae from each and serves ligament functions between vertebrae corpus. Nucleus pulposus resists compressive loading and distribute them evenly to the adjacent endplate. On the other hand, annulus fibrosus stands against distractive and rotational loading.

The Aging Disc

Interestingly, the intervertebral disc in humans undergoes degenerative changes earlier in life than other tissues do. Degenerative changes begin at the end of first decade of life.

Age-related degeneration of intervertebral discs includes accumulation of degraded matrix molecules, declining nutrition, loss of viable cells, modification of matrix proteins, and fatigue failure of the matrix. Among these mechanisms, nutrition of the central disc that allows accumulation of cell waste products and degraded matrix molecules that impair cell nutrition, and cause a fall in pH levels that further compromises cell function appears to be most important [16].

With increasing age, the nucleus becomes more fibrotic and less gel-like. The number of vascular channels perforating the osseous vertebral endplate diminishes dramatically between 6 and 30 months of age. The progressive changes in disc histology that occur with age include increased number and extent of clefts and tears. The annular lamellae become irregular, bifurcating. Presence of granular material, disorganized elastin and collagen networks and neovascularization from the outer aspect of the annulus are also structural changes seen in the aging disc. Cell proliferation, cluster formation, and a greater level of cell death also occur, particularly in the nucleus [14]. Nerves and blood vessels are found to increase with the degeneration process. It has been reported that more than 50 % of cells in adult discs are necrotic [24].

These above-mentioned age-related degenerative changes contribute to some of the most common causes of disability for middle aged and older persons: spine stiffness, neck pain, and low back pain.

Clinical Significance

Degenerative Disc Disease

On MRI images, approximately 25 % of people show evidence of disc degeneration at one or more levels before age 40, whereas the rate is as high as 60 % beyond age 40. Clinical symptoms may not be relevant with radiological findings. The most common clinical symptom of degen-

erative disc disease is intermittent or continuous back pain accompanied with spasm of the back muscles. Clinical symptoms are mostly mild, whereas there tends to be prominent radiological changes compared within the healthy disc, especially changes in disc height [1, 8]. Abnormal mechanical loading is still argued as a prognostic factor in disc degeneration [34]. Acute injuries, chronic overloading resulting from long-term, highly specialized training, especially in elite athletes can cause the musculoskeletal system to become overloaded and lead to degenerative changes in the lumbar spine [25, 38]. Since microscopic and macroscopic changes are similar to those occurring with increasing age, it is difficult to differentiate degeneration of the aging intervertebral disc from degenerative disc disease resulting from a pathologic process. The homeostasis of the tissue is altered where the major reason in disc degeneration is the dehydrated nucleus pulposus and nutritional insufficiency. The aggrecan and collagen metabolism changes with aging. Keratan sulfate-to-chondroitin sulfate ratio increases as a consequence of decrease of chondroitin-4-sulfate and chondroitin-6-sulfate concentrations. Chondroitin-4-sulfate and chondroitin-6-sulfate are strongly hydrophilic whereas Keratan sulfate demonstrates a small hydrophilic potential and has less tendency to form stable aggregates with hyaluronic acid. As aggrecan is fragmented and its molecular weight and number decreased, the viscosity and hydrophilicity of the nucleus pulposus decreases. As the concentration of proteoglycans decreases, the ability of the intervertebral disc to maintain its function and absorb shock diminishes.

Gross pathology is increase in lamellar disorganization and fissures, vascularization, innervation, and sclerosis of the subchondral bone. The increased production of cytokines and matrix-degrading enzymes, especially matrix metalloproteinases (MMPs) and oxidative stress products are molecular changes seen in the molecular level. Matrix composition and organization can be altered as different types of collagen type-I, III, VI, and X, elastin, fibronectin, and amyloid is produced [13].

Especially at the advanced stages of the disease, increased cell death as a consequence of apoptosis and necrosis and cell-cluster formation can be observed throughout the process. The decrease in the number and activity of these cells depends mainly on insufficient nutrient transport, growth factors, abnormal mechanical loading, and genetic factors.

Advances in the field of radiology allow us to evaluate the intervertebral endplate cartilaginous structures using MRI, which is nowadays accepted as an important factor in disc degeneration etiology [21]. Vertebral endplate lesions, called Schmorl's nodes, occur when there is herniation of the nucleus pulposus through the cartilaginous and bony endplate into the vertebral body and occur in 76 % of individuals. Although these lesions are mostly incidental findings in asymptomatic patients, there is still a debate whether they are related to age or degeneration [20]. Researchers emphasize that apart from thoracolumbar region (T10–L1), Schmorl's nodes in the lower lumbar discs (L2–L5) are related to disc degeneration. Schmorl's nodes have been occasionally implicated in the etiology of chronic axial pain as well as in pathological osteoporotic fractures, suggesting that a reduction in disc height might be a pathologic feature but not a normal aging process [18].

Data from recent research suggests that degenerative disc alone is not associated with low back pain. By contrast, the combination of degenerative disc and endplate signal changes seen on MRI is highly associated with low back pain [36]. Although aging changes of the disc seem to be inevitable to distinguish pathological conditions, agents that accelerate these changes from benign conditions are important to select the most appropriate treatment option.

Nutritional Insufficiency, Abnormal Mechanical Loading, and Genetic Factors

The failure of nutritional supply to the disc cells is known to be one of the major causes of disc degeneration process. In regard, imaging studies are carried out to detect the nutritional status of

the intervertebral disc as post-contrast MRI imaging [10]. The activity of disc cells is very sensitive to extracellular oxygen and pH. A fall in nutrient supply that leads to a lowering of oxygen tension or of pH could affect the ability of disc cells to synthesize and maintain the disc's extracellular matrix. Matrix synthesis rates fall steeply at acidic pH and at low oxygen concentrations. Various systemic diseases, endplate calcification, smoking, and the overall nutritional status all appear to lead to a significant impact over the discs nutritional status. Atherosclerosis, sickle cell anemia, Caisson disease, and Gaucher's disease can disturb nutrient supply to the nucleus cells. Cells cannot survive prolonged exposure to low pH or glucose levels concentrations. This clinical entity can lead to disc degeneration.

In scoliotic discs, although the blood supply remains undisturbed, nutrients may not reach the disc cell because cartilaginous endplate calcification is intense [19].

Abnormal mechanical loads are also thought to provide a pathway to disc degeneration. Experimental overloading or injury to the disc initiates a pathway that leads to structural damage and finally to degenerative changes [33].

More recent work suggests that genetic components may have an important impact on the disc degeneration. Various genes have been identified to be associated with disc degeneration. A recent study identifies specific single nucleotide polymorphism associations of five genes in young adults with severe lumbar disc degeneration. These five genes (COL11A1, ADAMTS5, CALM1, IL1F5, and COX2) are shown to be important in the matrix metabolism, intracellular signaling, and inflammatory cascade [27]. Individuals with a polymorphism in the aggrecan gene were also found to be at risk for early disc degeneration. Mutations in structural matrix molecules such as aggrecan, collagen II, and collagen IX can lead to disc degeneration. Sulfatase-1 (SULF1) is known to play an important role in cell signaling involving cell growth, differentiation, proliferation, and migration. Abnormal SULF1 expression has been implicated in the development of various cancers and diseases of the skeletal and nervous systems. Findings from Tsai et al. show an upregulation of SULF1 in degenerative discs for the first time, and suggest that there is a link between SULF1 and disc degeneration [37].

Studies have reported findings from different twin studies indicating a strong familial predisposition for disc degeneration and herniation. The study showed heritability over 60 % and magnetic resonance images in identical twins were shown to be very similar with respect to the pattern of disc degeneration [30].

Herniated Nucleus Pulposus

Nucleus pulposus bulges out beyond the damaged outer ring, the annulus fibrosus of an intervertebral disc. Although trauma, lifting injuries have been implicated, disc herniation is usually due to degeneration of the annulus fibrosus. Majority of the tears are posterolateral due to the localization of the posterior longitudinal ligament in the spinal canal. Herniated discs are more vascularized and more highly innervated than normal discs. There is still a debate over the effect of cytokines on intervertebral disc herniation. Some studies implicate that herniated discs have higher levels of MMP8 and MMP7, interleukins, tumor necrosis factor Tumor necrosis factor-alpha, monocyte chemoattractant protein-1, and TNF-alpha stimulating gene-6 (TSG-6) compared to non-herniated discs, whereas some conclude there is significance between the two clinical entities [29, 32].

The degree of structural damage changes from protrusions where the outer annular lamellae remain intact to extrusions, where the outer annular lamellae is ruptured to sequestrations where herniation is completely detached from the body of the disc.

Depending on the location of herniation and the type of soft tissue that becomes involved, symptoms of a herniated disc can vary. Focal disc protrusions in the cervical spine can be found in individuals that do not have noticeable symptoms. On the other hand, even in the absence of nerve root compression, the tear in the annulus may result in the release of inflammatory chemical mediators, which may cause severe pain, unrelated with nerve

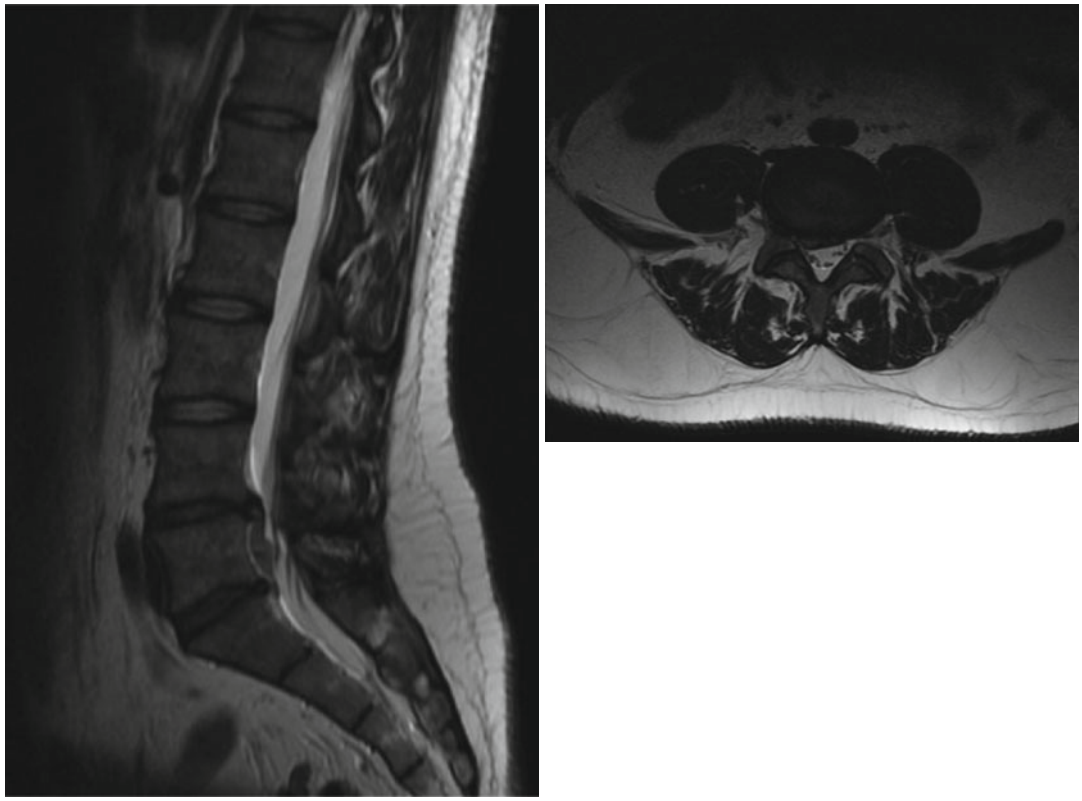

Fig. 29.6 Demonstrative T2-weighed MRI images of a 38-year-old male with complained of right sciatica and right ankle weakness. Midsagittal section of the patient shows loss of disc height and water content at L4–5 and L5–S1 levels. Both midsagittal and axial images of L4-5 level reveal a sequestrated disc occupied right lateral recess and compressed dural sac

compression. Typically, symptoms are experienced only on one side of the body and usually vary from no pain to little pain if the disc is the only tissue injured (Fig. 29.6). Severe to unrelenting pain can be experienced at the regions innervated by affected nerve roots if the herniated disc impinges nerve roots. In such conditions, symptoms can be numbness, tingling, muscular weakness, sciatica, paralysis, paresthesia, and affection of reflexes. If the herniation is large and presses on the spinal cord or the cauda equina, nerve damage can result in loss of bowel and bladder control and sexual dysfunction.

Disc in Spinal Deformities

Intervertebral discs from patients with spinal deformities such as kyphosis or scoliosis can show morphologic differences from unaffected individuals; hence, this may not cause pain in some people, while in others these conditions may cause chronic severe pain. One of the most apparent features in patients with scoliosis is varying degrees of ectopic calcification of the cartilage endplate and sometimes in the disc that interferes with the flow of nutrients and metabolites through the end plate into the disc. This is thought to be part of reason for major changes that take place in collagen turnover and low number of viable cells. In terms of collagen type, more type-I and minor collagens (III, VI, IX, and X) are present than usual in the scoliotic discs [41]. Gross remodeling of collagen bundles of annular lamellae can take place accompanied by very disorganized elastic fiber composition.

References

1. Adams A, Roche O, Mazumder A, Davagnanam I, Mankad K (2014) Imaging of degenerative lumbar intervertebral discs; linking anatomy, pathology and imaging. Postgrad Med J 90:511–519
2. Burns AS, Lee BS, Ditunno JF Jr, Tessler A (2003) Patient selection for clinical trials: the reliability of the early spinal cord injury examination. J Neurotrauma 205:477–482
3. Ditunno JF (2010) Outcome measures: evolution in clinical trials of neurological/functional recovery in spinal cord injury. Spinal Cord 48(9):674–684
4. Errington RJ, Puustjarvi K, White IR, Roberts S, Urban JP (1998) Characterisation of cytoplasm-filled processes in cells of the intervertebral disc. J Anat 192:369–378
5. Etz CD, Homann TM, Luehr M, Kari FA, Weisz DJ, Kleinman G, Plestis KA, Griepp RB (2008) Spinal cord blood flow and ischemic injury after experimental sacrifice of thoracic and abdominal segmental arteries. Eur J Cardiothorac Surg 33(6): 1030–1038
6. Fontes RB, Saad F, Soares MS, de Oliveira F, Pinto FC, Liberti EA (2006) Ultrastructural study of the filum terminale and its elastic fibers. Neurosurgery 58:978–984
7. Fountas KN, Kapsalaki EZ, Jackson J, Vogel RL, Robinson JS Jr (1998) Cervical spinal cord – smaller than considered? Spine 23:1513–1516
8. Frobin W, Brinckmann P, Kramer M, Hartwig E (2001) Height of lumbar discs measured from radiographs compared with degeneration and height classified from MR images. Eur Radiol 11:263–269
9. Fraher JP (2000) The transitional zone and CNS regeneration. J Anat 196:137–158
10. Galbusera F, Brayda-Bruno M, Wilke HJ (2014) Is post-contrast MRI a valuable method for the study of the nutrition of the intervertebral disc? J Biomech 47:3028–3034
11. Harrop JS, Sharan A, Ratliff J (2006) Central cord syndrome: pathophysiology, management and outcomes. Spine J 6:198–206
12. Hayatsu Y, Kawamoto S, Matsunaga T, Haga Y, Saiki Y (2014) Real-time monitoring of spinal cord blood flow with a novel sensor mounted on a cerebrospinal fluid drainage catheter in an animal model. J Thorac Cardiovasc Surg 148:1726–1731
13. Hou G, Lu H, Chen M, Yao H, Zhao H (2014) Oxidative stress participates in age-related changes in rat lumbar intervertebral discs. Arch Gerontol Geriatr 59:665–669
14. Johnson WEB, Eisenstein SM, Roberts S (2001) Cell cluster formation in degenerate lumbar intervertebral discs is associated with increased disc cell proliferation. Connect Tissue Res 42:197–207
15. Kameyama T, Hashizume Y, Sobue G (1996) Morphologic features of the normal human cadaveric spinal cord. Spine 21:1285–1290
16. Kepler CK, Ponnappan RK, Tannoury CA, Risbud MV, Anderson DG (2013) The molecular basis of intervertebral disc degeneration. Spine J 1:318–330
17. Ko HY, Park JH, Shin YB, Baek SY (2004) Gross quantitative measurements of spinal cord segments in human. Spinal Cord 42:35–40
18. Kulduk A, Senkoylu A, Altun N (2015) Biomechanical comparison of effects of the dynesys and coflex dynamic stabilization systems on range of motion and loading characteristics in the lumbar spine: a finite element study. Int J Med Robot Comput Assist Surg doi: 10.1002/rcs.1636 [Epub ahead of print]
19. Laffosse JM, Accadbled F, Bonnevialle N, Gomez-Brouchet A, de Gauzy JS, Swider P (2010) Remodelling of vertebral endplate subchondral bone in scoliosis: a micro-CT analysis in a porcine model. Clin Biomech 25:636–641
20. Mattei TA, Rehman AA (2014) Schmorl's nodes: current pathophysiological, diagnostic, and therapeutic paradigms. Neurosurg Rev 37:39–46
21. Moon SM, Yoder JH, Wright AC, Smith LJ, Vresilovic EJ, Elliott DM (2013) Evaluation of intervertebral disc cartilaginous endplate structure using magnetic resonance imaging. Eur Spine J 22: 1820–1828
22. Moore KL, Agur AM (2007) Essential clinical anatomy: third edition. Lippincott Williams & Wilkins, Baltimore, pp 34–35
23. Moro C, Tajouri L, Chess-Williams R (2013) Adrenoceptor function and expression in bladder urothelium and lamina propria. Urology 81:1–7
24. Paietta RC, Burger EL, Ferguson VL (2013) Mineralization and collagen orientation throughout aging at the vertebral endplate in the human lumbar spine. J Struct Biol 184:310–320
25. Ogurkowska M, Kawalek K (2014) Pathological changes in the lumbar intervertebral discs among professional field hockey players. J Sports Med Phys Fitness [Epub ahead of print]
26. Pinto FC, Fontes RB, Leonhardt Mde C, Amodio DT, Porro FF, Machado J (2002) Anatomic study of the filum terminale and its correlations with the tethered cord syndrome. Neurosurgery 51:725–729
27. Rajasekaran S, Kanna RM, Senthil N, Raveendran M, Ranjani V, Cheung KM, Chan D, Kao PY, Yee A, Shetty AP (2014) Genetic susceptibility of lumbar degenerative disc disease in young Indian adults. Eur Spine J (Epub ahead of print)
28. Roberts S, Menage J, Urban JPG (1989) Biochemical and structural properties of the cartilage end-plate and its relation. Spine 14(2):166–174
29. Roberts S, Caterson B, Menage J, Evans EH, Jaffray DC, Eisenstein SM (2000) Matrix metalloproteinases and aggrecanase: their role in disorders of the human intervertebral disc. Spine 25:3005–3013

30. Sambrook PN, MacGregor AJ, Spector TD (1999) Genetic influences on cervical and lumbar disc degeneration: a magnetic resonance imaging study in twins. Arthritis Rheum 42:366–372
31. Schoenen J, Grant G (2004) Spinal cord: connections. In: Paxinos G, Mai JK (eds) The human nervous system, 2nd edn. Elsevier Academic Press, San Diego
32. Scuderi GJ et al (2006) Cytokine assay of the epidural space lavage in patients with lumbar intervertebral disk herniation and radiculopathy. J Spinal Disord Tech 19:266–269
33. Sengupta DK, Fan H (2014) The basis of mechanical instability in degenerative disc disease: a cadaveric study of abnormal motion versus load distribution. Spine 39:1032–1043
34. Senkoylu A (2011) Evidence based medicine in the treatment of degenerative spine disease. Turk J Phys Med Rehabil 57(2):341–344
35. Sherman JL, Nassaux PY, Citrin CM (1990) Measurements of the normal cervical spinal cord on MR imaging. AJNR Am J Neuroradiol 11:369–372
36. Teraguchi M et al (2014) The association of combination of disc degeneration, endplate signal change, and Schmorl's node with low back pain in a large population study: the Wakayama Spine Study. Spine J. doi:10.1016/j.spinee.2014.11.012
37. Tsai TT (2014) Increased sulfatase 1 gene expression in degenerative intervertebral disc cells. J Orthop Res. doi:10.1002/jor.22766
38. Vadalà G et al (2014) Early intervertebral disc degeneration changes in asymptomatic weightlifters assessed by t1ρ-magnetic resonance imaging. Spine 39:1881–1886
39. Yoshioka K, Niinuma H, Ohira A, Nasu K, Kawakami T, Sasaki M, Kawazoe K (2003) MR angiography and CT angiography of the artery of Adamkiewicz: noninvasive preoperative assessment of thoracoabdominal aortic aneurysm. Radiographics 23(5):1215–1225
40. Yu J, Winlove CP, Roberts S, Urban JP (2002) Elastic fibre organization in the intervertebral discs of the bovine tail. J Anat 201:465–475
41. Yu J, Fairbank JC, Roberts S, Urban JP (2005) The elastic fiber network of the annulus fibrosus of the normal and scoliotic human intervertebral disc. Spine 30:1815–1820

Part IV

Basic Pathology

Ahmet Turan Aydin

Bone and Joint Infections

30

Akif Güleç, Oktay Adanır, Ender Alagöz,
Sever Çağlar, Ozan Beytemür, and Volkan Öztuna

Abstract

Infectious diseases have threatened human beings from ancient times. Bone and joint infections continue to be serious conditions for the orthopedic surgeons. The use of implants in modern orthopedic surgery and low blood supply to bone and joint tissues increase the risk for infection. Infection is an important cause of morbidity and mortality in orthopedic surgery. The pathogenesis of infection must be well understood by orthopedic surgeons for the eradication of infection. Recognizing unique characteristics of joint and bone infections mentioned earlier, the best way is prevention.

Perioperative antimicrobial administration 30–60 min before incision and inflation of tourniquet are the most effective issues. Evaluating the patient by considering patient-dependent factors and surgeon-dependent factors are important for the prevention of infections. Nutrition, immunological status, and infection at a remote site are patient related. Wound and skin cleaning, operating room condition, and surgical technique are surgeon related. We can state that it is much easier to prevent than it is to treat.

Pain is the most common symptom, which is localized to the site of infection. Redness, swelling sinus formation that are well-known characteristics of infection are not seen in many patients. Culture and direct microscopy of bacteria is the definitive diagnosis of an infection and antibiogram is an important part of medical treatment. Surgical intervention is

A. Güleç
Department of Orthopedics and Traumatology,
Bağcılar Education and Research Hospital,
Bağcılar/İstanbul, Turkey

O. Adanır (✉) • E. Alagöz • S. Çağlar
O. Beytemür
Department of Orthopedics and Traumatology,
Bağcılar Education and Research Hospital,
Bağcılar/İstanbul, Turkey
e-mail: droktayadanir@yahoo.com

V. Öztuna
Department of Orthopedic Surgery and Traumatology,
Mersin University Medical Faculty, Mersin, Turkey

F. Korkusuz (ed.), *Musculoskeletal Research and Basic Science*,
DOI 10.1007/978-3-319-20777-3_30

most important. Deficiency in humoral and cellular immunological system of the host can result in failure of antibiotic treatment of osteomyelitis. The use of rifampin combinations is crucial for success in the treatment of implant-related infections caused by staphylococcus.

Learning Outcomes

1. Properties and treatment algorithm of implant related infections
2. Patient and surgeon related factors in the development of surgical site infections
3. Diagnosis and treatment of osteomyelitis
4. General approach to diagnosis and treatment of infected total joint arthroplasties

Introduction

Infectious diseases have threatened human beings from ancient times; therefore pathogenesis, diagnosis, treatment, and avoidance from infections are the most common researched subjects in the medical literature. Discovery of antibiotics and prophylactic vaccines were the most important progressions about infectious diseases during the twentieth century. Severe acute respiratory syndrome (SARS) epidemic in recent years pointed out once again how infectious diseases can threaten human beings despite these advances [1].

Musculoskeletal infections are the most difficult infection type to treat and cause serious complications. Different clinical presentation of musculoskeletal infections, delay in treatment, random antibiotic use, difficulty in identification of bacteria, insidious clinic of some infections, formation of biofilm cause the treatment to be complex. Increasing number of elderly population gradually and trauma cases result in increase of implant usage. On the other hand, lifelong risk of hematogenous spread of bacteria to implant surface causes a lot of research to be made on implant-related infections [2]. Nowadays, a number of septic loosening after arthroplasty surgeries decreased compared with aseptic loosening, but are still the most serious complications after arthroplasty surgery [3].

The reported rate of infection in the first 2 years after surgery is less than 1% after total hip arthroplasty (THA) done in high technological operation rooms (hepa filtrate, laminar flow, and positive pressure). The reported rate for total knee arthroplasty (TKA) is less than 2%. Infection rate after revision cases is much more than primary arthroplasty cases and reported to be between 5% and 40% [4]. When all orthopedic implants are considered, the infection rate is approximately 5%. In open fractures, this rate is approximately 30%, and this rate falls with preemptive antimicrobial treatment [5].

The main purpose of this chapter is to provide understanding of the mechanism between the microbial pathogen and the host response [6].

Pathogenesis

Bone is very resistant to infection, therefore in order to produce an infection, the number of bacteria must be high. Ischemia and tissue necrosis developed after trauma to bone and soft tissues make the bone susceptible to development of infection.

Local Inflammation and Bone Injury in Osteomyelitis

Three mechanisms are said to be responsible of bone tissue damage [45]:

1. The damage that is caused by the endotoxins, which are secreted by the bacteria (bacterial lipopolysaccharides)
2. The trigger of bacteria on osteoclastic activity
3. The inhibition of bone matrix synthesis

The inflammatory response, triggered by the microorganisms in the role of bone injury is exposed clearly at present. Cytokines such as IL-1, IL-6, IL-11, nitric oxide, and TNF, secreted from the osteoblasts that were stimulated by the host macrophages and the bacterial lipopolysaccharides, play a role in these mechanisms [46–48].

The best response of this inflammatory process is the prevention of the bone injury with cyclooxygenase inhibitors and anti-IL-1 serum in in vitro experiments [49]. It was shown that the other branch of the inflammation, leukotrienes also increase the osteoclastic activity and with the inhibition of 5-lipoxygenase in the leukotriene pathway, the bone resorption is decreased [50]. Thus, a combination of antibiotics with anti-inflammatory agents would increase the success of the treatment in clinical applications.

Bacterial molecules such as lipopolysaccharides and gapstatin play a role not only in the bone resorption, but they also inhibit the collagen synthesis and block the mitotic reproduction of osteoblasts [45].

In addition, *S. Aureus* stimulates inflammation, thereby inhibiting the proliferation of T-lymphocytes by PG-E2 pathway [51]; it can also survive in neutrophils and monocytes that arrive in the region [52].

Surgical wound is the most common and easy way of entry for the bacteria. Soft tissue injury caused by surgical trauma leads to decreased blood flow to surrounding tissues, may lead to tissue necrosis and production of hematoma. In addition to the above-mentioned, in the presence of an implant like plate, screw, prosthesis, or bone cement, the minimum infective bacteria number necessary to produce an infection also decreased [7]. Infection risk in individuals with intact immune system requires much more bacterial load than individuals with local or systemic problems. It is not possible to know how many bacteria would cause an infection in which region. But, in experimental studies, this number can be adjusted. The unit used for this is the inoculum that is needed to form a disease in minimum 50 % (effective dose 50-ED50) of the experiment group, which is generally between 10^6 and 10^8 CFU/mL. It is believed that this number is lower in human beings [53]. In the light of this information, it is crucial to wash the open wound sites and the operation sites with bolus isotonic saline solution to decrease the number of bacteria, in clinical practice. It is obvious that the biomaterials used would be a medium for the colonization of microorganisms; however, a colonized microorganism accumulation is not sufficient to cause infection alone. In clinical practice, the implant itself is not the only factor, but the injury caused during the implantation process also plays a role in this course. In in vitro studies, it is reported that some metals in the medium did not increase the infection rates [54], but in in vivo studies, there might be different results according to the animal model used [55, 56].

Clinical Relevance

Bacteria can directly inoculate to an open wound or surgical wound, or it may also cause infection by hematogenous spread. When the bacteria settle to soft tissue or bone, one of the three situations described below happen [8–12].

1. Bacteria may be destroyed by host defense
2. Bacteria may live with the host symbiotically
3. Bacteria may multiply to produce infection, sepsis or even death

Which of the above would happen is related to:

(a) Number of bacteria
(b) Virulence of bacteria
(c) The response of the host immune system [13]

Because of the aforementioned reasons, irrigation of open fractures with liters of serum physiologic is a very effective way to decrease the number of bacteria in the contaminated wound. Additionally, frequent irrigation of the

wound during surgery also decreases the number of bacteria that can contaminate from skin or air. Irrigation during surgery also prevents tissue desiccation and lessens tissue necrosis. A good skin cleaning before surgery and use of iodine-based surgical drapes also prevent contamination of bacteria from skin. Wearing double gloves by the surgical team prevents contamination of the wound if one of the gloves is perforated. Operation room with a hepa filtrate, laminar flow, and positive pressure prevent contamination of the wound from air.

The capability of producing biofilm or capsule is an important virulence factor for the bacteria [14]. These properties prevent host cellular and humoral (anticore) immune system elements to reach the bacteria and also causes the host to secrete increased amount of cytokines. These cytokines produce additional tissue injury that attract pathogenesis to the area of interest. Pathogen can adhere to host tissue by secreting adhesin and can also produce additional tissue injury and damage to host cells by producing toxins. *Staphylococcus aureus* can degrade proteoglycan found in connective tissue by producing hyaluronidase and degrade clot by producing streptokinase. These factors increase the virulence of microorganisms [15–17].

Lymphocyte level below 1,500/mm^3 and albumin level below 3.5 g/dl are important parameters of malnutrition. Malnutrition is associated with immune system dysfunction. If the lymphocyte level is less than the threshold, blood transfusion or appropriate medication in order to increase lymphocyte level, also albumin replacement or hyperalimentation if albumin level is less than threshold, is very helpful to enhance host immune response. Another index to evaluate the nutritional status of the patient is nutritional index.

$$\text{Nutritional index}: \left(1.2\times\text{albumin} + 0.013\times\text{transferrin}\right) - 6.43$$

If the nutritional index is equal to zero or negative, oral or parenteral hyperalimentation must be given. If a patient loses more than 5 kg of weight before an elective surgery, a kind of supportive therapy must be considered. In trauma or infected cases, the basal metabolism rate can increase up to 30–50%, also 0.5C0 increase in body temperature increases the basal metabolism rate up to 12%. Alimentation must be adjusted in these situations. Malnutrition affects humoral and cellular immune response negatively. In malnutrition, chemotaxis of polymorphonuclear leukocytes, bacterial phagocytosis, and serum complement function deteriorate [18].

In the prevention of infection, both cellular and humoral immune system is very important. Also reticuloendothelial system organs like liver, spleen, and lymph nodes are important in the prevention of infection. If there is a defect in anyone of these, then opportunist microorganisms can produce infection. This defect can be congenital or acquired. Pseudomonas in heroin addicts, *Salmonella* and *S. aureus* in sickle cell anemia are the most seen organisms. Diabetes mellitus, alcoholism, hematological malignancies, and cytotoxic treatments cause neutrophil function defect and *S. aureus*, gram negative bacillus, aspergillus, and candida infections are mostly seen because of these defects. Immunoglobulins and complement systems are the important components of the humoral immunity. In hypogammaglobulinemic or post-splenectomy patients, encapsulated bacteria (*Pneumococcus*, *Haemophilus influenza*, *Streptococcus*, *Neisseria*) are commonly seen as infectious agents.

Lymphoma, systemic lupus erythematosus (SLE), steroid treatment, and malnutrition impair the cellular mechanism and cause mycobacterium, fungal, and herpes infections. Chronic granulomatous disease, hemophilia, hypogammaglobulinemia, sickle cell anemia, terminal complement pathway deficiency, and leucocyte adhesion disorders are the congenital disorders that increase the risk of infection. Acquired diseases are diabetes mellitus, rheumatoid arthritis, hematological malignancies, drugs that depress immune system, transplantation, collagen vascular diseases, uremia, malnutrition, and radiation therapy. The risk of infection in total joint replacement increases six times in diabetes mellitus and rheumatoid arthritis patients.

Host Response

The host responses to bacterial invasion with inflammatory reaction, first. Acute inflammatory reaction is a protective response that causes cell damage and also removes these residual necrotic tissues and cells. Also, the act that is named as repairing, which means the fulfilling of defect with fibrous scar tissue, and regeneration of parenchymal cells of damaged tissue, occurs concomitantly [19–21].

First and Congenital Immune Response

Either tissue damage or the bacteria itself activates the complement system. Complement activation causes vasodilatation, edema, and polymorphonuclear leucocyte migration. Polymorphonuclear leucocytes invade the bacteria by opsonin and provide a suitable environment for phagocytosis. Interleukin-1, interleukin-6, and tumor necrosis factor released by damaged tissue provide more polymorphonuclear cells and macrophage migration to the area. Activated phagocytic cells produce free oxygen radicals, which is essential for host immune response. Pain, swelling, erythema, and warmth are clinical evidences of vasodilatation and tissue edema.

Acquired Immune Response

T-lymphocytes are responsible for cellular immune response and B-lymphocytes for humoral. In acute inflammation, polymorphonuclear cells are predominant, whereas mononuclear cells (lymphocyte, macrophage, plasma cells) are predominant in chronic inflammation. Chronic inflammation is a prolonged inflammation in which acute inflammation, cell damage, and recovery progresses together.

If the infection is septic arthritis, bacteria damages the cartilage tissue by acting on glycosaminoglycan, which is a subunit of proteoglycan molecule. Glycosaminoglycan, which consists of chondroitin sulfate, keratan sulfate, dermatan sulfate, and hyaluronic acid, is a macromolecule that increases physical property of cartilage tissue, maintains retention of fluid, and provides strength to pressure. Damage to glycosaminoglycan causes cartilage destruction and collagen break and also secondary osteoarthritis.

Biofilm

Another virulence factor that is efficient in infections following orthopedic operations is the binding of the organism to biomaterials and organic tissues and its capacity to form biofilm. Biofilm is a gel-like polysaccharide-containing layer that is formed by the binding of bacteria to each other or to the materials. Biofilm structure is a barrier that blocks the host's immune system elements and the antibiotics to reach the organisms [57]. Eighty percent of biofilms found in a body are formed by *Staphylococci*. The reason is that these microorganisms are found in skin flora and they can accumulate along the catheters easily, and they can easily reach the deep tissues and the implants during the manipulations (Fig. 30.1).

Biofilms may be found on catheters, implants, heart valves, contact lenses, kidney stones, and organic tissues. All foreign bodies are recognized by the body and covered with a protein layer containing laminin, fibronectin, vitronectin, collagen, and fibrinogen. This structure called *slime factor* can bind the microorganism to both the implant and the organic tissues [58]. In addition, a group of protein called "microbial surface components recognizing adhesive matrix molecules" (MSCRAMM) on the surface of the *Staphylococci* makes a tight connection with this slime factor and forms glycocalyx (biofilm). Teichoic acid also plays a major role in this connection [59]. The main material of the biofilm layer is

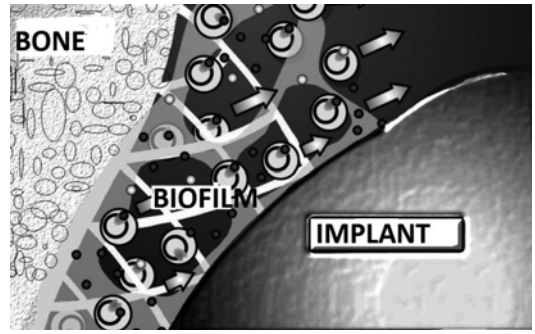

Fig. 30.1 Biofilm

N-Acetylglucosamine and it forms two different polysaccharide structures. Type 2 polysaccharide structure is responsible for the intercellular aggregation and is alternatively called polysaccharide intercellular adhesin (PIA). This structure is the component that has the ability to bind to the hydrophilic surfaces with physicochemical bonds [60]. To have knowledge about these molecules in *Staphylococcus* infections is important to develop new treatment modalities, because these structures may provide protective immunity when they are injected to individuals in their purified form (*Staphylococcus* vaccine) [61]. These researches are the basis of the policy for the development of vaccines against the nosocomial infections that may develop in patients that will stay for a long period at the hospitals.

The adhesion on implant generally happens in two steps. The first step is the holding of the microorganism on the surface with physicochemical gravity, such as hydrophobic forces and van der Waals forces (*adhesion phase*). The second step is the development of slime factor with special protein structures, and the continued accumulation of the bacteria (*accumulation phase*) [62]. Every step requires different molecules. The efficient structure in both periods is the "biofilm associated protein."

Biofilm formation is seen in infections where the implant is used. The implant is isolated and covered with a layer formed by macromolecules, then microorganisms attach to implant and to this layer. Glycocalyx formation occurs when the exopolymers cover the film layer that is formed by the macromolecules. Bacteria within this glycocalyx layer are protected from antibiotics, humoral and cellular immune system elements. Inside the biofilm layer there is not enough metabolite and waste products formed by bacteria also accumulate; therefore bacterial proliferation is decreased or sometimes proliferation does not occur. Bacteria inside the biofilm transform into an organized cell population and become structurally and functionally different. Genetic differentiation occurs with cell to cell signaling. Because of the after-mentioned reasons, in order to eradicate infection from infected implants, the biofilm layer and the implant must be removed from the area of infection. It should not be forgotten that the ability of *Staphylococcus* to form a biofilm is high.

Implant-related infections can occur by direct contamination during surgery or by hematogenous spread from a remote infection. Also infection can occur by direct or lymphatic spread from a nearby infection focus. Pathogenesis and duration of development of infection after arthroplasty vary according to the pathogenic microorganism. Therefore, prosthesis infections can be classified in three different categories:

(a) Acute infection
(b) Subacute infection
(c) Chronic infection

This classification also determines the approach to treatment. Early infection after surgery is defined as the emergence of signs of infection at the implant site within the first 3 months. Direct contamination during surgery is the reason for early infection and virulent microorganisms are mainly the causative agent (e.g., *S. aureus*). Intractable local pain, erythema, hematoma, and fever are the clinical findings. Subacute infection is seen 3–24 months after surgery. Mostly low virulence of microorganisms (coagulase-negative *Staphylococci*, *Propionibacterium* acnes) is the causative agent. Continuous or increasing pain and early loosening is seen; sometimes it is very difficult to discriminate from aseptic loosening, because signs and symptoms related to infection may not be seen. Chronic infection is defined as infection seen 2 years or more after surgery. Infectious agents in this period cause infection by hematogenous spread from teeth, skin, respiratory tract, and urinary tract infections. Hematogenous infection of the internal fixation devices is more rare. Similarly, in the early period (within 10 weeks) most commonly seen causative agents were *S. aureus* and gram (−) bacilli, while in the later period (after 10 weeks) low virulence microorganisms like coagulase negative *Staphylococci* are the causative agents [22–26].

Infection Prophylaxis

Antimicrobial prophylaxis is the most effective way to decrease infection prevalence after orthopedic surgery [27, 28]. First or second generation cephalosporins like cefazolin, cefamandole, or cefuroxime are used in orthopedic surgery. If the patient has an allergy to these drugs or if the hospital has a high prevalence of methicillin-resistant *S. aureus* infection then vancomycin or teicoplanin is used. In order to ensure an effective prophylaxis, a minimum inhibitory concentration level should be achieved during surgery. Risk of surgical site infection increases six times when prophylaxis was done 2 h prior to surgery or 3 h after surgery. Studies demonstrate that in order to obtain the most effective tissue concentration, antibiotic prophylaxis must be done 30–60 min prior to surgery or tourniquet application. Clindamycin may be used in the presence of penicillin allergy. An additional dose should be given every 4 h or when blood loss is more than 1,000 ml during surgery. Prophylaxis should not be given more than 24 h even in the presence of catheters and drains. Complications like drug-related fever, allergic reactions, thrombophlebitis, and superinfections can be seen if used more than 24 h. Risk of bacteremia has shown to increase in intensive care unit patients when antibiotics were used more than 4 days. In the presence of open fracture or during an elective surgery, irrigation with liters of serum physiologic is a very effective way to decrease the number of contaminated bacteria and so is an important step in infection prophylaxis. Irrigation during surgery also prevents tissue desiccation and lessens tissue necrosis. In Gustilo Anderson grade I and II open fractures, prophylactic treatment with cefuroxime or cefamandole for 1 day and in grade III open fracture, a preemptive treatment with an antistaphylococcal drug like i.v. amoxicillin/clavulanic acid or cefuroxime for 5–7 days is usually enough.

Most of the infections in orthopedic surgery are coagulase (−) *S. aureus* and *S. epidermidis*, which are originated from skin flora. Factors that can be managed by a surgeon in the prevention of infections are very important. The source of an infectious agent can either be patient or surgeon's skin flora. Skin hygiene is more important in orthopedic surgery than other surgical departments. It is impossible to sterilize the skin but it can be possible to minimize bacterial burden. One of the most important factors in the development of infection is the number of bacteria. Skin and hairy tissues are cleared by hexachlorophene, chlorhexidine, alcohol, or iodine. However, hairy follicles cannot be cleared as well and as time expands bacteria proliferates during surgery and the risk of contamination increases. Use of iodine-based surgical drapes also prevents the contamination of bacteria from hair follicles. In the past, disinfectants that can penetrate to hair follicles, sebaceous and sweat glands were used, but it must not be forgotten that absorption of these disinfectants lead to neurotoxicity. Bristles must be removed in the operating room just before the surgery. Removal of the bristles one day prior to surgery leads to microtrauma to skin, and bacterial colonization of this traumatized areas occur. Removal of bristles must be done with using clippers not with razor blades or other sharp objects.

As mentioned above, another source of microorganism contamination is the skin flora of the surgical team. Laceration of the gloves of the surgeon is seen to occur in 48 % of the cases in orthopedic surgery. Glove laceration is most commonly seen in the first and second fingers of the nondominant arm. It is appropriate to use double gloves and the usage of gloves that has an indicator to laceration is also helpful. Appropriate hand washing before surgery and usage of masks and caps that cover the whole face except the eyes is important in the prevention of contamination (Fig. 30.2). The usage of a large safety glasses also decreases contamination and protects the surgeon's conjunctiva from contamination with patient's blood and body fluids. "Body exhaust systems" can be used in order to decrease contamination (Fig. 30.3). Bacteria suspended in the air of the operating room is another source for bacterial contamination. Staff in the operating room is the source of these bacteria. A person can

release between 5,000 and 55,000 particles/min. There are 7,000 particles per liter of air in a conventional operating room theatre. This number and hence the contamination risk can be decreased significantly by the usage of HEPA filters, positive pressured theaters, and laminar flow. The air pressure in the operating room must be higher than in the corridors. Filtered clean air from HEPA filters must enter the operating room, then with the effect of positive pressure air travel from the operating room to corridors and must leave the operating theatre from the main entrance. For an effective system, windows in the operating rooms should not be openable, and an airlock system at the entrance of the operating theatre is required. A decreasing percentage of the surface of staff's skin that has contact with the air also lessens the amount of particles. Operating rooms must be 19 °C, corridors 21 °C, and resting rooms 23 °C. In past, UV light has been used to diminish the amount of bacteria but because of the adverse effects and its time-consuming effect, it is not recommended recently.

Fig. 30.2 Appropriate mask and cap usage to decrease contamination and particle release

Clinical Characteristics and Diagnosis of Osteomyelitis

Hematogenous osteomyelitis refers to a bone infection that is transported by blood from the region far away to the infectious area. That kind of osteomyelitis occurs mostly in children and sometimes after total joint arthroplasty operations. In children with incomplete skeletal maturation, because of decreased blood flow in the metaphyseal region, bacteria settle in this region. In some locations (e.g., proximal femur) the metaphyseal part of the bone is inside the joint so osteomyelitis in these regions can easily complicate with septic arthritis. Because of the avascular nature of the joint, drainage of the joint must be done in order to treat joint infections. Pathogenic microorganisms vary according to the

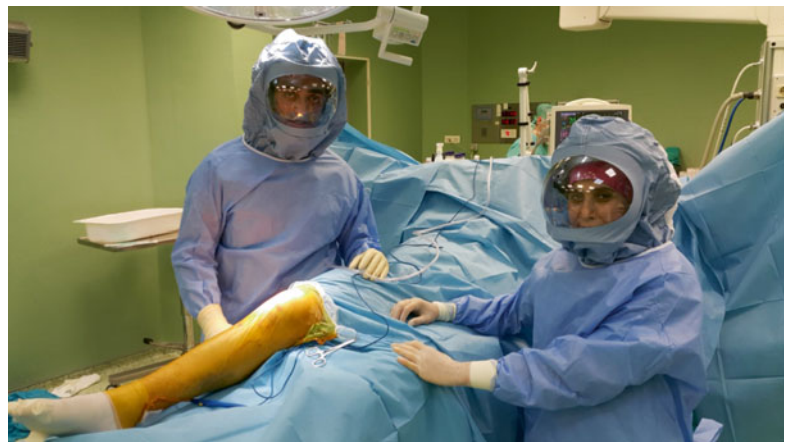

Fig. 30.3 Picture of a surgical team wearing body exhaust system

age of the child. In neonates and infants staphylococcus, between 6 months and 3 years old *H. influenza*, after 3 years old staphylococcus, and in adolescents staphylococcus species are the most commonly seen causative agents (Tables 30.1, 30.2, 30.3, and 30.4).

Joint aspiration, culture, and direct microscopy are very important tools for the diagnosis. Especially for septic arthritis 50,000/mm^3 or more leucocytes in direct microscopy is diagnostic. Local edema, warmth, redness, sensitivity, limitation of joint motion, and systemic fever can be clinical findings. Periosteal reaction, bone destruction, deterioration of trabecules, and increase in soft tissue density can be seen in direct radiological examination. Complete blood count, erythrocyte sedimentation rate (ESR), and C-reactive protein (CRP) are used both for the diagnosis and follow-up. CRP can elevate within hours in acute infection and can reach very high values within 48 h. After recovery of infection, CRP falls to normal values within weeks. CRP is a more precise diagnostic tool both for diagnosis and follow-up. ESR needs longer time to reach normal values.

Table 30.1 Most common causative agents for osteomyelitis according to age

Neonate and infant
Staphylococci
Streptococci
Gram (−) bacteria

Table 30.2 Most common causative agents for osteomyelitis according to age

6 months to 3 years old
Haemophilus influenzae Type B
Staphylococci
Streptococci

Table 30.3 Most common causative agents for osteomyelitis according to age

3 years old–Adolescent
Staphylococci
Streptococci

Table 30.4 Most common causative agents for osteomyelitis according to age

Adolescent
Staphylococci
Streptococci
Neisseria gonorrhoeae (rarely)

In the first 2 weeks, direct radiological examination findings may be less clear, so bone scintigraphy can be useful for the diagnosis of septic arthritis and osteomyelitis. Imaging with 99mTc-methylene diphosphonate (99mTc-MDP) is the initial method of choice. Scintigraphy shows osteoblastic activity and blood flow. The third phase is the phase that is 3 h after injection and shows bone involvement. Scintigraphy is a sensitive test in the diagnosis of septic arthritis and osteomyelitis. But in newborns, we should be aware of false (−) results. On the other side, in pre-existing chronic diseases of bone, especially in sickle cell anemia or bony metastases of tumors, we can see false (+) results. In the healing stage of bone fracture, increased uptake can be seen too. Ga 67(gallium citrate) can be used in musculoskeletal scintigraphic examinations. But it can take 2 days for results and it is time consuming. Using radioactive indium labelled leucocytes is rigorous and needs a long time.

CT and MRI are useful methods in the diagnosis and treatment of osteomyelitis. CT helps in surgical planning by imaging cortical bone and sequestrum. MRI is a more sensitive and specific method and helpful in surgical planning. It shows abscess in sinuses. It is not an expensive method anymore and there is no radiation exposure. However, it is not useful for cases where implants were used [29–31].

Treatment

After the diagnosis of septic arthritis or osteomyelitis, cultures from blood and deep soft tissues are taken; then drainage and debridement of the infected and necrotic tissues is planned immediately. In order to treat infection, all necrotic tissues must be removed. Necrotic tissue is a suitable environment for bacteria. Also host defense mechanisms try to remove necrotic mate-

rial. This causes continuous drainage from sinus tracts. Sometimes a sequestered fragment is removed from sinus opening after months.

Medical treatment without surgery can be done in children with acute osteomyelitis if it is diagnosed early. In order to be successful, diagnosis must be done early and antibiotics specific to the pathogenic microorganism must be given. In the treatment of acute osteomyelitis and septic arthritis, parenteral antibiotics are administered for the first 1–2 weeks followed by 4–5 weeks of oral antibiotics. However, the time of antibiotic administration must be longer in diabetics or in other immunocompromised patients. Response to treatment is followed with both clinical and laboratory findings. ESR and CRP levels must be followed during treatment, and if regression of the ESR and CRP levels is not seen, then antibiotics must be given for longer periods. Repeated surgical debridement of necrotic materials must be done in patients in whom improvement cannot be seen. It must be known that in order to control and treat implant-related infections, implants like plate, screw, prosthesis, or bone cement must be removed. In the presence of fracture, implant may be retained with antibiotic suppression until fracture healing occurs.

In the treatment of chronic infections with large necrotic soft tissues, rotational or free flaps, myocutaneous or fasciocutaneous composite greft usage can be successful after a radical debridement. These kinds of flaps and grefts fill the death spaces and also carry living tissue to infection areas thus increasing perfusion and helping fracture healing.

All necrotic bone must be removed. The bony defect formed after debridement can be filled with autogrefts or allogrefts. In large defects, distraction osteogenesis and filling the defect with segment transport can be done.

Local antibiotic treatments and vectors were developed to provide the antibiotics to reach to high concentration levels especially at the infection area, where systemic applications may cause toxic effects. These vectors are bone cement, synthetic and organic bone grafts, plaster of Paris, polylactate and polyglycolate membranes, Ca sulfate-phosphate, hydroxyapatite, and amylose-starch implants [63–68].

The use of the most frequent application method, methacrylate beads containing gentamicin, both provides to fill the dead areas and to keep the local antibiotic concentration at high levels [69]. With this method, it was shown that the local antibiotic concentration is 200 times higher than with systemic application [70]. Biosoluble vector systems are more advantageous, because they do not need to be extracted later.

Infection and Total Joint Replacement

Nowadays, infection rate after total joint replacement surgery is less than 1 % but it is still the most serious complication after arthroplasty. Infection can present like acute hematogenous osteomyelitis, chronic osteomyelitis, or septic arthritis [32].

Resting pain is the most frequent finding. Normally pain around the surgical wound diminishes within days. Continuous or even increasing pain after surgery is an important finding. Fever, chills, purulent drainage, and sinus formation are rarely seen after periprosthetic infections. Erythema around incision can be seen after total knee arthroplasty and it is not specific to infection. If other findings accompany erythema like pain, close follow-up for infection is necessary. Blood sample for complete blood count, ESR, and CRP are taken from the patient. These laboratory examinations are helpful for the diagnosis, but gram stain, direct microscopy, and the culture of the tissue specimen that are taken by surgery or aspiration are exact diagnostic methods. Aspiration of synovial fluid is a simple, quick, and definitive method. More than 1,700 leucocytes in 1 mm^3 of fluid and neutrophils >65 % is a potent indicator of infection. And these numbers are very much lower than the numbers used in the diagnosis of septic arthritis. Sensitivity of this method is 94 % and 97 % and specificity is 88 % and 98 %, respectively. In frozen sections of specimens that are taken during surgery, the

number of polymorphonuclear leucocytes seen in every field (at big magnification) is informative about infection. Polymorphonuclear leucocyte count in every field >5 increases the possibility of infection; >10 is a strong indicator of infection. Tissue specimens should not be taken from the region close to fracture, because it causes false (+) results. It must be taken from the granulation tissue close to the components of prosthesis (Fig. 30.4). If the implant has been removed, the sonication method that separates microorganisms apart the surface of the implant and subsequent culturing increases the sensitivity of culture. This method is gaining popularity nowadays.

Polymerase chain reaction (PCR) is the most efficient and fast technique for diagnosis. This method is efficient in detecting even a single molecule, but it is expensive. The principle of this method is replication of bacteria's DNA. Both blood serum and tissue samples can be used for PCR. Although it is a very efficient way, in the diagnosis of periprosthetic infections, culture of the tissue sample taken during surgery or fluid taken by aspiration are the mainly used methods.

Osteolysis, periosteal reaction, and focal lytic lesions around the prosthesis can be seen in direct graphies in periprosthetic infections. These findings are not specific to periprosthetic infection and can be seen in aseptic loosening. Scintigraphic methods can be conflicting, and MRI image quality is not good because of the implant [33, 34]. Leucocyte scintigraphy is a valuable and specific method that can be used in periprosthetic infections. Most commonly used leucocyte scintigraphies are indium-111 and Tecnetium-99m hexamethyl propylene amine oxide. Reported sensitivity of leucocyte scintigraphy is 80–90 % and specificity is 85–100 %. Nonspecific human immunoglobulin G scintigraphy is a new technique with high sensitivity and specificity, and it is successful in showing infection and inflammation.

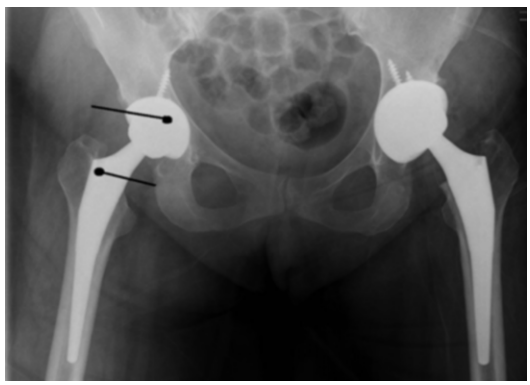

Fig. 30.4 Tissue specimen for PMNL count must be taken from granulation tissue nearby the components of the prosthesis

Once diagnosis is made as periprosthetic infection, it must be treated surgically. Fundamentals of the treatment are given in Table 30.5. All necrotic tissues must be excised and radical debridement must be done. In periprosthetic infections, all implants and bone cement must be removed, but in infected fracture cases, because infected nonunion is a worse situation than infected but healed fracture, it is wise to wait with antibiotic suppression until fracture healing occurs.

After tissue samples are taken surgically for culture, wide spectrum antibiotic administration is started. Causative organisms are presented in Table 30.6. After culture results, specific antibiotics to the causative pathogen is started and continued for at least 6 weeks. Before the decision of reimplantation of prosthesis, repetitive tissue

Table 30.5 Treatment principles of infected arthroplasty surgery

General principles of infection are applied
Surgical debridement of the infected area
Removal of infected, necrotic, and foreign material
Culture, biopsy
Parenteral antibiotics

Table 30.6 Most common microorganisms isolated in infected atrhroplasty cases

Causative agent	Incidence (%)
Coagulase (−) *Staf.*	20–25
S. aureus	20–25
Polymicrobial	14–19
Gram (−) bacillus	8–11
Streptococci	8–10
Aneorob	6–10
Enterococci	3
Others	10

specimens should be taken. Components of prosthesis are retained despite infection in two conditions: First, if surgery was done less than 3 months ago and second if signs of infection started less than 1 month ago. In these situations, debridement without prosthesis removal can be done but the possibility of failure in this condition is 50 %. Some reports suggest that if soft tissue is good enough and if used drugs are efficient on biofilm, success rate can reach nearly 70 % [35–39]. The two-stage revision, the most used method, consists of excision of components of prosthesis and using spacer with antibiotics following debridement. New prosthesis is implanted after at least 6 weeks of parenteral antibiotic treatment. If causative agents are difficult microorganisms to treat (MRSA, multiresistant bacteria, enterococcus, or fungi), then the duration of antibiotic usage must be 8 weeks or more. Single stage revision which means reimplantation of new prosthesis in the same surgical procedure after debridement and removal of the infected implants also can be applied. If soft tissues are good, the causative agent is not so virulent and if the patient has no comorbid diseases single stage revision can be done. But the success rate of single-stage revision is less than two-stage revision, which has a success rate of 90 %. If there are bony defects in association with a periprosthetic infection, three-stage revision can be done. In this situation, the second stage is the reconstruction of bony defects with grefts and the third stage is the reimplantation of a new prosthesis. Revision may not be considered in patients with high infection risk, in very old patients, and in bedridden patients with no functional expectations.

Antimicrobial Treatment

The list of recommended antibiotics is given in Tables 30.7 and 30.8. In two-stage revisions and in patients where only debridement is done without implant removal, the duration of antibiotic treatment is 3 months. Two to four weeks of intravenous antibiotics are given and continued with oral antibiotics until the whole treatment duration is 3 months. The duration of antibiotic treatment in infected trauma cases is 3 months if the implant is retained and 6 weeks if the implant is removed. In clinical and experimental studies on *Staphylococcus* infections related with implants, it has been seen that rifampin is very effective on slow growing *Staphylococcus* adhered to implant [40–44]. However, in order to prevent resistance development to rifampin it

Table 30.7 List of recommended antibiotics according to causative agent

Microorganism	Drug	Dosage	Route of administration
Staphylococci (methicillin sensitive)	2–4 weeks rifampicin plus nafcillin or	450 mg every 12 h	p.o/i.v.
	Flucloxacillin	2 g every 6 h	i.v.
	Then rifampicin plus	450 mg every 12 h	p.o.
	Ciprofloxacin	750 mg every 12 h	p.o.
	Or levofloxacin	750 mg every 12 h	p.o.
Staphylococci (methicillin resistant)	2 weeks Rifampicin plus vancomycin	450 mg every 12 h	p.o./i.v.
		1 g every 12 h	i.v.
	Then rifampicin plus ciprofloxacin	450 mg every 12 h	p.o.
		750 mg every 12 h	p.o.
	Or levofloxacin	500 mg every 12 h	p.o.
	Or teicoplanin	400 mg every 24 h	i.v./i.m.
	Or fucidic acid	500 mg every 8 h	p.o.
	Or co-trimoxazole	160/800 mg every 8 h	p.o.
	Or minocycline	100 mg every 12 h	p.o.
Streptococci	4 weeks pen. G	5 mil. Ü every 6 h	i.v.
	Or ceftriaxone	2 g every 24 h	i.v.
	Then amoxicillin	750–1,000 mg every 8 h	p.o.

Table 30.8 List of recommended antibiotics according to causative agent

Microorganism	Drug	Dosage	Route of administration
Enterococci (penicillin sensitive)	2–4 weeks pen. G or	5 mil. Ü every 6 h	i.v.
	Ampicillin or amoxicillin plus aminoglycoside	2 g every 4–6 h. Can be given once a day	i.v.
	Then amoxicillin	750–1,000 mg every 8 h	i.v.
Enterobacteriaceae (quinolone sensitive)	Ciprofloxacin	750 mg every 12 h	p.o.
Non-fermentative (e.g., *Pseudomonas aeruginosa*)	2–4 weeks cefepime or ceftazidime plus aminoglycoside	2 g every 8 h. Can be given once a day	i.v.
	Then ciprofloxacin	750 mg every 12 h	i.v.
Anaerobes	2–4 weeks Clindamycin	600 mg every 6–8 h	p.o.
	Then Clindamycin	300 mg every 6 h	p.o.
Mixed infections. (without MRSA)	2–4 weeks amoxicillin/clavulanic acidOr piperacillin/tazobactam Or imipenem Or meropenem Then different antimicrobial regimens according to sensitivity	2,2 g every 8 h 4,5 g every 8 h 500 mg every 6 h 1 g every 8 h	i.v. i.v. i.v. i.v.

Table 30.9 Patients at risk for hematogenous arthroplasty infections

Rheumatoid arthritis, SLE
Chronic diseases
Hemophilia
Type 1 diabetes
First 2 years after surgery
Malnutrition
Previous prosthesis infection
Immunocompromised patient

Table 30.10 Dental procedures with high bacteremia incidence

Dental extraction
Periodontal interventions
Dental implant surgery
Endodontic treatment
First orthodontic band application
Intraligamentary local anesthetic injections
Prophylactic washing for bleeding

must be combined with other drugs. In the beginning, a beta-lactam antibiotic (cefazolin, nafcillin, cloxacillin, floxacillin) or a glycopeptide (vancomycin or teicoplanin) is used for 2–4 weeks. Using quinolones combined with rifampin is a good choice for treatment against *Staphylococcus* infection but using quinolone alone decreases the effectiveness. Co-trimoxazole, minocycline, fucidic acid, and other antistaphylococcal drugs are the drugs that can be used with rifampin and the success rate is high.

Total joint arthroplasty can also be infected hematogenously. Table 30.9 shows patients that especially carry risk for total joint arthroplasty infections. Incidence of bacteremia of these patients has decreased substantially with prophylaxis before the interventions that carry high bacteremia risk. Tooth interventions that carry high bacteremia risk are shown in Table 30.10. Cephalexin, cephradine, or amoxicillin 2 g (oral) should be given 1 h before tooth intervention. If oral treatment is not possible, cefazolin 1 g (i.v./i.m.) or ampicillin 2 g (i.v./i.m.) should be given. If the patient is allergic to penicillin, clindamycin 600 mg (oral, i.v./i.m.) can be given.

References

1. Bloom BR (2003) Lessons from SARS. Science 300:701
2. Zimmerli W, Trampuz A, Ochsner PE (2004) Prosthetic-joint infections. N Engl J Med 351(16):1645–1654
3. Steckelberg JM, Osman DR (2000) Prosthetic joint infection. In: Bisno AL, Qaldvogel FA (eds) İnfections associated with indwelling medical devices, 3rd edn. American Society for Microbiology, Washington, DC, pp 173–209

4. Widmer AP (2001) New developments in diagnosis and tretment of infection in orthopedic implants. Clin Infect Dis 33(Suppl2):94–106
5. Droulche RO (2004) Treatment of infections associated with surgical implants. N Engl J Med 350: 1422–1429
6. Gross J M, Schwarz E M (2006) Orthopedic basic science, Chapter 16. Infections in Orthopaedics, 3rd edn. pp 311
7. Bleton C et al (1996) A model of experimental prosthetic joint infection due to methicillin-resistant Staphylococcus aureus: a microbiologic, histopathologic, and magnetic resonance characterization. J Infect Dis 174:414–417
8. Daum RS, Davis WH, Farris KB, Campeau RJ, Mulvihill DM, Shane SM (1990) A model of Staphylococcus aureus bacteremia, septic arthritis, and osteomyelitis in chickens. J Orthop Res 8:804–813
9. Passl R, Muller C, Zielinski CC, Eibl MM (1984) A model of experimental post-traumatic osteomyelitis in guinea. J Trauma 24:323–326
10. Rissing JP, Buxton Weinstein RS, Shockley RK (1985) Model of experimental chronic osteomyelitis in rats. Infect Immun 47:581–586
11. Tsukayama DT (1999) Pathophysiology of posttraumatic osteomyelitis. Clin Orthop Relat Res 360:22–29
12. Tsukayama Goldberg VM, Kyle R (2003) Diagnosis and management of infection after total knee arthroplasty. J Bone Joint Surg Am 85(Suppl 1):S75–S80
13. Morrissy Haynes DW (1989) Acute hematogenous osteomyelitis: a model with trauma as an etiology. J Pediatr Orthop 9:447–456
14. Gray ED, Peters G, Verstegen M, Regelmann WE (1984) Effect of extracellular slime substance from Staphylococcus epidermidis on the human cellular immune response. Lancet 1:365–367
15. Gristina AG, Oga M, Webb LX, Hobgood CD (1985) Adherent bacterial colonization in the pathogenesis of osteomyelitis. Science 228:990–993
16. Johnson GM, Lee DA, Regelmann WE, Gray ED, Peters G, Quie PG (1986) Interference with granulocyte function by Staphylococcus epidermidis slime. Infect Immun 54:13–20
17. Mayberry-Carson KJ, Tober-Meyer B, Lambe DW, Costerton JW (1992) Osteomyelitis experimentally induced with Bacteroides thetaiotaomicron and Staphylococcus epidermidis: influence of a foreign-body implant. Clin Orthop Relat Res 280:289–299
18. Gulec MA, Yuksel S, Albay C (2011) Enfeksiyonun Genel Prensipleri. Totbid Dergisi Cilt 10(Sayı 3): 185–188
19. Cierny G III, Mader JT (1987) Approach to adult osteomyelitis. Orthop Rev 16:259–270
20. McGuire MH (1989) The pathogenesis of adult osteomyelitis. Orthop Rev 18:564–570
21. Verdrengh M, Tarkowski A (1997) Role of neutrophils in experimental septicemia and septic arthritis induced by Staphylococcus aureus. Infect Immun 65:2517–2521
22. Zimmerli W, Ochsner PE (2003) Management of infection associated with prosthetic joints. Infection 31:99–108
23. Kaandrop CJ, Dinant HJ, Van de Laar MA et al (1997) İncidence and sources of native and prosthetic joint infection: a community based pprospective survey. Ann Rheum Dis 56:470–475
24. Law MD Jr, Stein RE (1993) Late infection in healed fractures after open reduction and internal fixation. Orthop Rev 22:545–552
25. Murdoch DR, Roberts SA, Fowler JV Jr et al (2001) İnfection of orthopedic prosthesis after Staphylococcus aureus bacteremia. Clin Infect Dis 32:647–649
26. Willenegger H, Roth B (1986) Treatment tactics and late results in early infection following osteosynthesis. Unfallchirurgie 12:241–246
27. Marculescu CM, Osmon DR (2005) Antibiotic prophylaxis in orthopedic prosthetic surgery. Infect Dis Clin N Am 19:931–946
28. Trampuz A, Widmer AF (2006) Ortopedik implantlarla ilişkili enfeksiyonlar. Curr Opin İnfect Dis Türkçe baskı Cilt 1(Sayı 3):158–167
29. Boyle WJ, Simonet WS, Lacey DL (2003) Osteoclast differentiation and activation. Nature 423:337–342
30. Faber C, Stallmann HP, Lyaruu DM et al (2003) Release of antimicrobial peptide Dhvar-5 from polymethylmethacrylate beads. J Antimicrob Chemother 51:1359–1364
31. Klemm K (2001) The use of antibiotic-containing bead chains in the treatment of chronic bone infections. Clin Microbiol Infect 7:28–31
32. Blom AW, Taylor AH, Pattison G, Whitehouse S, Bannister GC (2003) Infection after total hip arthroplasty: the Avon experience. J Bone Joint Surg (Br) 85:956–959
33. Kaim A, Ledermann HP, Bongartz G, Messmer P, Muller-Brand J, Steinbrich W (2000) Chronic posttraumatic osteomyelitis of the lower extremity: comparison of magnetic resonance imaging and combined bone immünoscintigraphy with radiolabelled monoclonal antibodies. Skelet Radiol 29:378–386
34. Mahomed NN, Barrett JA, Katz JN et al (2003) Rates and outcomes of primary and revision total hip replacement in the United States medicare population. J Bone Joint Surg Am 85:27–32
35. Douglas P, Asimus Swan J, Spigelman A (1997) Prevention of wound infections: a quality improvement project. J Qual Clin Pract 21:149–153
36. American Academy of Orthopaedic Surgions (2004) Antibiotic prophylaxis for dental patients xith total joint replacements. Document no. 1014
37. American Academy of Orthopaedic Surgions (2004) Anitiotic prophylaxis for urological patients with total joint replacements Document no. 1023
38. Maderazo EG, Juddson S, Pastlemak H (1988) Late infections of total joint prostheses: a review and recommendations for prevention. Clin Orthop Relat Res 229:131–142
39. Widmer AF, Frei R, Rajacic Z et al (1990) Correlation between in vivo and in vitro efficacy of antimicrobial agents against foreign body infections. J Infect Dis 162:96–102
40. Zimmerli W, Frei R, Widmer AF et al (1994) Microbiological tests to predict treatment outcome

in experimental device-related infections due to Staphylococcus aureus. J Antimicrob Chemother 33:959–967
41. Zimmerli W, Qidmer AF, Blatter M et al (1998) Role of rifampin for treatment of arthofedic implant-related staphylococcal infections: a ranromized controlled trial. Foreingn-body infection(FBİ) Stidy Group. JAMA 279:1537–1541
42. Widmer AF, Gaechter A, Ochsner PE et al (1992) Antimicrobial treatment of orhopedic implan-related infections with rifampin combinations. Clin Infect Dis 14:1251–1253
43. Schwank S, Rajacic Z, Zimmerli W et al (1998) İmpact of bacterial biofilm formation on in vitro and in vivo activities of antibiotics. Antimicrob Agents Chemother 42:895–898
44. Lafter RR, Graber P, Ochsner PE et al (2006) Outcome of prosthetic kneeassociated infection: evaluation of 40 consecutive episodes of a single center. Clin Microbiol Infect 12:433–439
45. Nair SP, Meghji S, Wilson M, Reddi K, White P, Henderson B (1996) Bacterially induced bone destruction: mechanisms and misconceptions. Infect Immun 64(7):2371–2380
46. Millar SJ, Goldstein EG, Levine MJ, Hausmann E (1986) Modulation of bone metabolism by two chemically distinct lipopolysaccharide fractions from Bacteroides gingivalis. Infect Immun 51(1): 302–306
47. Ishimi Y, Miyaura C, Jin CH et al (1990) IL-6 is produced by osteoblasts and induces bone resorption. J Immunol 145(10):3297–3303
48. Riancho JA, Salas E, Zarrabeitia MT et al (1995) Expression and functional role of nitric oxide synthase in osteoblast-like cells. J Bone Miner Res 10(3):439–446
49. Ishihara Y, Nishihara T, Maki E, Noguchi T, Koga T (1991) Role of interleukin-1 and prostaglandin in vitro bone resorption induced by Actinobacillus actinomycetemcomitans lipopolysaccharide. J Periodontal Res 26(3):155–160
50. Franchi-Miller C, Saffar JL (1995) The 5-lipoxygenase inhibitor BWA4C impairs osteoclastic resorption in a synchronized model of bone remodeling. Bone 17(2): 185–191
51. Yoon KS, Fitzgerald RH, Sud S Jr, Song Z, Wooley PH (1999) Experimental acute hematogenous osteomiyelitis in mice. Influence of staphylococcus aureus infection on T-cell immunity. J Orthop Res 17:382–391
52. Gresham HD, Lowrance JH, Caver TE, Wilson BS, Cheung AL, Lindberg FP (2000) Survival of Staphylococcus aureus inside neutrophils contributes to infection. J Immunol 164(7):3713–3722
53. Mader JT (1985) Animal models of osteomiyelitis. Am J Med 78(suppl 6B):213–217
54. Gristina AG, Rovers GD (1963) An in vitro study of the effects of metal used in internal fixation on bacterial growth. J Bone Joint Surg 45(A):1104
55. Darouiche RO, Landon GC, Patti JM et al (1997) Role of Staphylococcus aureus surface adhesins in orthopaedic device infections: are results model-dependent? J Med Microbiol 46(1):75–79
56. Öztuna V, Ersöz G, Coskun B, Kaya A, Çolak M, Kuyurtar F (2002) Farelerde oluşturulan osteomiyelit modellerinde yabancı cisim uygulanmasının lokal ve sistemik infeksiyon bulguları üzerine etkileri. Artroplasti-Artroskopik Cerrahi 13(2):94–98
57. Gracia E, Lacleriga A, Monzon M, Leiva J, Oteiza C, Amorena B (1998) Application of a rat osteomiyelitis model to compare in vivo and in vitro the antibiotic efficacy against bacteria with high capacity to form biofilms. J Surg Res 79(2):146–153
58. Herrmann M, Vaudaux PE, Pittet D et al (1988) Fibronectin, fibrinogen, and laminin act as mediators of adherence of clinical staphylococcal isolates to foreign material. J Infect Dis 158(4):693–701
59. Hussain M, Heilmann C, Peters G, Herrmann M (2001) Teichoic acid enhances adhesion of Staphylococcus epidermidis to immobilized fibronectin. Microb Pathog 31(6):261–270
60. Lew DP, Waldvogel FA (2004) Osteomyelitis. Lancet 364(9431):369–379
61. Maira-Litran T, Kropec A, Goldmann D, Pier GB (2004) Biologic properties and vaccine potential of the staphylococcal poly-N-acetyl glucosamine surface polysaccharide. Vaccine 22(7):872–879
62. Galliani S, Viot M, Cremieux A, Van der Auwera P (1994) Early adhesion of bacteremic strains of Staphylococcus epidermidis to polystyrene: influence of hydrophobicity, slime production, plasma, albumin, fibrinogen, and fibronectin. J Lab Clin Med 123(5):685–692
63. Gunal I, Seber S, Kiraz N, Turkay S, Oztuna V, Gokturk E (1996) In vitro evaluation of antibiotic diffusion from antibiotic impregnated xenografts. Rev Chir Orthop Reparatrice Appar Mot 82(1):59–62
64. Calhoun JH, Mader JT (1997) Treatment of osteomyelitis with a biodegradable antibiotic implant. Clin Orthop Relat Res 341:206–214
65. Dion A, Berno B, Hall G, Filiaggi MJ (2005) The effect of processing on the structural characteristics of vancomycin-loaded amorphous calcium phosphate matrices. Biomaterials 26(21):4486–4494
66. Huneault LM, Lussier B, Dubreuil P, Chouinard L, Desevaux C (2004) Prevention and treatment of experimental osteomyelitis in dogs with ciprofloxacin-loaded crosslinked high amylose starch implants. J Orthop Res 22(6):1351–1357
67. Kankilic B, Bilgic E, Korkusuz P, Korkusuz F (2014) Vancomycin containing PLLA/ß-TCP controls experimental osteomyelitis in vivo. J Orthop Surg Res 9(1):114
68. Ersoz G, Oztuna V, Coskun B, Eskandari MM, Bayarslan C, Kaya A (2004) Addition of fusidic acid impregnated bone cement to systemic teicoplanin therapy in the treatment of rat osteomiyelitis. J Chemother 16(1):51–55
69. Stabile DE, Jacobs AM (1990) Development and application of antibiotic-loaded bone cement beads. J Am Podiatr Med Assoc 80:354–359
70. Wahlig H, Dingeldein E, Bergmann R, Reuss K (1978) The release of gentamicin from polymethylmethacrylate beads. An experimental and pharmacokinetic study. J Bone Joint Surg 60:270–275

Rheumatoid Arthritis

31

Emel Gönen and Ajda Bal

Abstract

Rheumatoid arthritis is a chronic, systemic, inflammatory disease characterized by articular cartilage destruction, erosion, ligamentous laxity, and synovial enlargement. It causes serious deformities and disabilities by affecting especially the small and middle joints symmetrically.

Cartilage degradation is a result of the chemical effect of free oxygen radicals and lysosomal enzymes, which are secreted by the cytokine-activated neutrophils. T and B lymphocytes, monocytes/synovial macrophages, neutrophils, mast cells, and synovial fibroblasts are all thought to play a role in the pathogenesis. Synovial inflammation may cause restrictions in range of motion and disabilities via the cartilage degeneration, bone erosion, and loss of joint integrity, and the quality of the life of the patients may be impaired. Genetic, autoimmunity, and environmental factors are all thought to play a role in the etiology of the disease. An interaction between the disease and the locus of human leukocyte antigen (HLA) on chromosome 6p21, protein tyrosine phosphatase non-receptor type 22 (PTPN22), and anti-cyclic citrullinated peptide (anti-CCP) antibodies is shown. Autoimmunity has gained in importance since the existence of the autoantibodies for the antigenic areas on the Fc part of the human immunoglobulin (Ig) G molecules.

The need for orthopedic surgery has recently decreased with the help of both nonbiologic and biologic disease-modifying antirheumatic drugs (DMARDs) that are used in the treatment. Thirty percent of RA patients

E. Gönen (✉)
Department of Orthopedics and Traumatology,
Ankara Diskapi Research and Teaching Hospital,
Asmabahce, G-30, Koru, Ankara 06810, Turkey
e-mail: emelgonen@yahoo.com

A. Bal
Department of Physical Therapy and Rehabilitation,
Ankara Diskapi Research and Teaching Hospital,
Ankara, Turkey
e-mail: ajdabal@yahoo.com

F. Korkusuz (ed.), *Musculoskeletal Research and Basic Science*,
DOI 10.1007/978-3-319-20777-3_31

need major joint replacement surgeries such as hip and knees. Joint reconstruction, joint fusion, repair of tendon rupture, and tenosynovectomy are the reliable and effective options. When a surgical intervention is needed simultaneously, perioperative precautions have gained in importance because of the drugs that are still being used. Special preferences exist in terms of the appropriate surgical procedure, features of the implant, and sequence of the orthopedic surgical procedures.

Learning Outcomes

The target of this chapter is to reveal the physiopathology of the rheumatoid arthritis that is triggered by the inflammatory immunogenic mediators and to enlighten the etiology that is still complicated and needed to be ascertained. Besides, the findings of this disease, diagnosis tools, and the mechanism of the effect of pharmacologic agents used in treatment will also be mentioned. The understanding of this immunopathologic, humoral, and intracellular biochemical cascades will illuminate the aim and the principles of orthopedic surgical procedures besides the necessary precautions establishing a fundamental approach for an effective orthopedic surgery.

Terminology

Alleles Common shortening of the term "allelomorph." One of two or more forms of a gene arising by mutation and occupying the same relative position (locus) on homologous chromosomes.

Angiogenesis The process of *vascularization of a tissue involving invasion by proliferating endothelium.

Antibody A protein produced by certain white blood cells (plasma cells) in response to entry into the body of a foreign substance (antigen) in order to render it harmless.

Apoptosis The death of cells which occurs as a normal and controlled part of an organism's growth or development. Also called programmed cell death.

Arthritis Inflammatory joint disorder that involves the synovium, all layers of joint cartilage, and subchondral bone.

Autoimmunity A disorder of the body's defense mechanisms in which an immune response is generated against components or products of its own tissues, treating them as foreign material.

B lymphocyte A lymphocyte not processed by the thymus gland and responsible for producing antibodies. Also called B-cell.

Bursa A sac lined with synovial membrane that contains synovial fluid. Bursae protect bony prominences (e.g., olecranon process of the elbow). They also cushion tendons so that they glide over bones and joints.

Cartilage A skeletal connective tissue formed by groups of cells that secrete into the intercellular space a ground substance containing a protein, collagen (q.v.), and a polysaccharide, chondroitin sulfuric acid.

Chondrocyte Cells of cartilage. Chondroblast defines immature chondrocyte.

Chondroitin (sulfate) A chain of glucosaminoglycan (GAG) that provides mechanical properties of joint cartilage.

Co-stimulation The delivery of a second signal from an antigen-presenting cell to a T cell, which rescues an activated T cell from anergy, allowing it to produce the

lymphokines necessary for production of additional T cell.

Cytokines Any of a number of substances, such as interferon, interleukin, and growth factors, which are secreted by certain cells of the immune system and have an effect on other cells.

Effusion An escape of fluid into a body cavity.

Enthesopathy Any rheumatic disease resulting in inflammation of entheses (the site of insertion of tendons or ligaments into bones).

Erosive The ability of denudation that includes the physical breakdown, chemical solution, and transportation of material.

Granulocyte Any white blood cell that contains granular material (secretory vessels) and lysosomes in its cytoplasm. Neutrophils, basophils, and eosinophils are examples of granulocytes.

Hyperplasia The increased production and growth of normal cells in a tissue or organ.

Immunogenic Capable of stimulating an immune response.

Interleukin Any of a class of glycoproteins produced by leucocytes for regulating immune responses.

Joint capsule A two-layer structure that helps to keep the synovial joint in congruity. The outer layer of the joint capsule, consisting of dense connective tissue, joins the periosteum. The inner layer consists of the synovial membrane. Skeletal muscles usually support this thin connective tissue.

Ligament A band of oriented fibrous tissue connecting bones of a joint.

Macrophages A large, phagocytic, white blood cell, which occurs in large numbers at sites of infection where it is instrumental in removing foreign cells and cell debris.

Monocyte A large phagocytic white blood cell with a simple oval nucleus and clear, grayish cytoplasm.

Neuropeptides Any of a group of compounds which act as neurotransmitters and are short-chain polypeptides.

Osteoclast A large multinucleated cell of uncertain origin, which destroys bone cells and reabsorbs calcium.

Pannus A condition in which a layer of vascular fibrous tissue extends over the surface of an organ or other specialized anatomical structures.

Periosteum The double-layered fibrous membrane covering the surface of bones. The inner cambium layer has osteogenic and chondrogenic potential.

Plasma cells Antibody-producing cells found in blood-forming tissue and also in the epithelium of the lungs and gut. They develop in the bone marrow, lymph nodes, and spleen when antigens stimulate B lymphocytes to produce the precursor cells that give rise to them.

Pleurisy Inflammation of the pleurae, which impairs their lubricating function and causes pain when breathing.

Polymorphism The occurrence of a chromosome or a genetic character in more than one form, resulting in the coexistence of more than one morphological type in the same population.

Proliferation An increase in the size of a population of cells.

Proteoglycan Heavily glycosylated proteins that consist of glycosaminoglycan (GAG) chains attached to a core protein.

Synovial fluid A viscous fluid composed of hyaluronan, lubricin, proteinases, and collagenases, which are essential for articular cartilage lubrication.

Synovial membrane or synovium A membrane that produces the synovial fluid. This membrane is assumed to contain regenerative cells.

T lymphocytes A lymphocyte of a type produced or processed by the thymus gland and actively participating in the immune response. Also called T cell.

Introduction and Definition

Rheumatoid arthritis (RA), a chronic, systemic, and inflammatory disease, symmetrically involves particularly small- and medium-sized joints and is characterized by erosion and synovitis. RA may lead to serious deformities and disability. Symmetrical inflammatory synovitis in the small joints of hands and feet is the most prominent feature of RA. Synovial inflammation may cause restriction of the joint mobility and deformities by leading to cartilage destruction, bone erosion, and impairment in joint integrity and, consequently, may reduce patient's quality of life [1, 2].

The primary underlying pathology in rheumatoid arthritis is the erosion of the joint cartilage and subchondral bone by ectopic and hyperplastic synovium. B and T lymphocytes, macrophages, mast cells, and synovial fibroblasts, that are stimulated by both inflammation and immunity originated mediators and by the endothelial cells regulating vascular permeability, all play role in the etiopathogenesis. Tumor-like aggressiveness appears in type B synovitis that share the same character with the mesenchymal-derived fibroblasts. In the early periods, edema in synovium and an increase in the quantity and the thickness of type A and B synovitis inside intima after angiogenesis are observed. Type B synovium cells increase more than type A cells by time. Synovial hyperplasia, synovitis, and pannus form at late phase of the disease. Significant villi and pannus formation take place due to chronic synovial inflammation. Because of the villi formation and effusion of inflammatory fluid into the joint space, synovial membrane gets thickened and the capsule tightened. These changes cause pain. Along through the zone of cartilage-bone border, a destruction occurs involving invasion into the cartilage and bone, cartilage degradation, narrowing of joint space, and superficial cysts in subchondral bone [3, 4].

Epidemiology

Although RA is more prevalent in some populations, it can occur in all races and ethnic groups all over the world. Its worldwide prevalence is approximately 0.5–1 %. The risk of developing RA is two to ten times higher in the individuals having a first-degree relative with RA. It is threefold more prevalent in females than in males. Difference between genders decreases with increasing age [5, 6].

Etiology

Although the etiopathogenesis of the disease is unclear, genetic, environmental, and immunologic factors are blamed.

Genetic Predisposition

There are numerous data suggesting genetic predisposition in RA. Genetic factors are considered important in the development of RA because the studies in monozygotic twins have determined RA concordance to be 15–20 % [7].

A significant component of genetic risk factors that pose predisposition to RA is associated with human leukocyte antigen (HLA) locus on the chromosome 6p21. HLA encodes three classes of antigens. Class II antigens are encoded in the D region of HLA. This region, which is described as HLA-D, includes the subunits such as DR, DP, and DQ. The relation with *HLA-DRw4* gene in RA patients has been known since 1970. Previous studies have demonstrated that 28 % of control subjects and 70 % of RA patients express HLA-DRw4. Other studies have also defined the relation between HLADRB1 multiple alleles and RA. Thereafter, the "shared epitope" hypothesis has been propounded and it has been demonstrated that the array in the third hypervariable region (70–74 amino acids) of HLA structure discriminates disease-related alleles from those without RA risk. It has been tried to determine which allele is the most frequent in each population. HLA DRB1*0404 and HLA DRB1*0101 and HLA DRB1*0401 alleles have been determined particularly in Caucasians. The presence of both alleles poses a higher risk for the individual. It has been reported that the disease is severer and joint symptoms are more frequent in individuals carrying HLA DRB1*0401

and HLA DRB1*0404 alleles, whereas the disease slowly progresses in those carrying HLA DRB1*0101 allele [8, 9].

Relation with the protein tyrosine phosphatase non-receptor 22 (PTPN22) has become clearer in recent years. This protein, which encodes lymphoid-specific phosphatase, is expressed in hematopoietic tissues. Polymorphism of this gene plays a role in the pathogenesis of many autoimmune diseases. It has been proposed that PTPN22 is the major predisposing gene in RA. It is strongly associated with anti-cyclic citrullinated peptide (anti-CCP) antibody. PTPN22 polymorphism is a strong risk factor for development of RA in rheumatoid factor (RF)- and anti-CCP-positive cases [10].

Autoimmunity

The presence of autoantigens and their corresponding autoantibodies in the etiopathology of RA has made the autoimmunity critical in the etiology.

Rheumatoid factors are the autoantibodies that occur against antigenic sites in the Fc region of human immunoglobulin (Ig) G molecule. RFs in RA are produced by peripheral blood and synovial B cells. Synovial B lymphocytes are the main sources of RF in RA serum. Although autoantibodies are most frequently found in the form of Ig M, there are also Ig A, Ig G, and Ig E subtypes. The relevance of circulating RF in the pathogenesis is unclear; however, it is believed that their presence in the joint contributes to inflammatory reaction. The sensitivity and specificity of RF in diagnosis is 69 % and 85 %, respectively. RF positivity, the prevalence of which is about 3–5 % in healthy individuals, reaches to 10–30 % in elderly [1].

Antibodies against citrullinated peptides are defined to be quite specific markers for RA. In the studies, specificity and sensitivity of anti-CCP autoantibodies change between 91 % and 98 % and between 41 % and 67 %, respectively, in the diagnosis of RA. Anti-CCP autoantibodies are produced in early RA and in the preclinical course of the disease and have been reported to be effective both in diagnosis and determination of disease severity. Anti-CCP positivity is a critical progenitor marker in determining erosive disease [11, 12].

Environmental Factors

Infections

Although it has been focused on infectious reasons, which are believed to play a role in the etiology of RA, any microorganism could not be exposed clearly until today. Epstein-Barr virus (EBV) is one of the agents that have become prominent. The presence of elevated number of antibodies against this virus in RA patients and understanding that the virus can live for a long time in B lymphocytes in patients with impaired cellular immunity have led assignment of an etiological meaning to this infection. *Mycobacterium tuberculosis*, parvovirus B19, *Escherichia coli*, *Proteus mirabilis*, hepatitis B virus, human T-lymphotropic virus 1, and some retroviruses are also the other agents blamed in the etiology [13].

Gender and Hormones

Rheumatoid arthritis is more prevalent and severer in females. Dramatic improvement during pregnancy, exacerbation in the postpartum period, and the risk of RA's being two to three times higher in nulliparous women suggest likely hormonal effect. While female/male ratio is 3/1 in the premenopausal period, the incidence becomes equal in the postmenopausal period [14].

Diet

Although a certain group of foods is not blamed, it is thought that some dietary factors such as high-protein diet and selenium or cupper deficiency trigger arthritis attacks.

Smoking

Smoking influences the risk for disease development and disease severity. The risk for developing RA increases proportional to the number of package/year. The relation is dose-dependent and is more prominent in heavy smokers. While smoking increases the risk of RA if anti-CCP is positive, it does not influence the development of RA if anti-CCP is

negative. The risk increases in the presence of shared epitope alleles [15].

Trauma and Stress

It has been reported that trauma and stress trigger RA in some individuals and this has been attributed to the defects in the regulation of hypothalamo-hypophyseal-adrenal axis [13].

Pathogenesis

Humoral and cellular immune mechanisms act together in the pathogenesis of RA. T-cell activity causes sequential events that proceed to bone and cartilage destruction, whereas B lymphocytes proliferate into plasma cells and produce antibodies. Antibody production leads to immune complex formation, complement activation, and granulocyte migration, and thereby, inflammation causes irreversible tissue change (Fig. 31.1).

Synovial tissue is the main site of inflammation. Histologically, synovial cell hyperplasia and proliferation are seen in the joints involved. In the synovia, massive perivascular inflammatory cell infiltration consisting of CD4+ T cells, plasma cells, and macrophages, enhanced vascularity due to angiogenesis, neutrophils and organized fibrin clusters on synovial surface and in the joint space, and pannus tissue containing chronic synovitis characterized by osteoclast activity that causes synovial penetration and bone erosion in the underlying bone are seen [1].

In cellular immune mechanism, immune response begins with the activation of T lymphocytes by triggering antigen via antigen-presenting cell (APC). Here, T-cells are in the form of CD4+ T cells. For the immune response to begin, CD4+

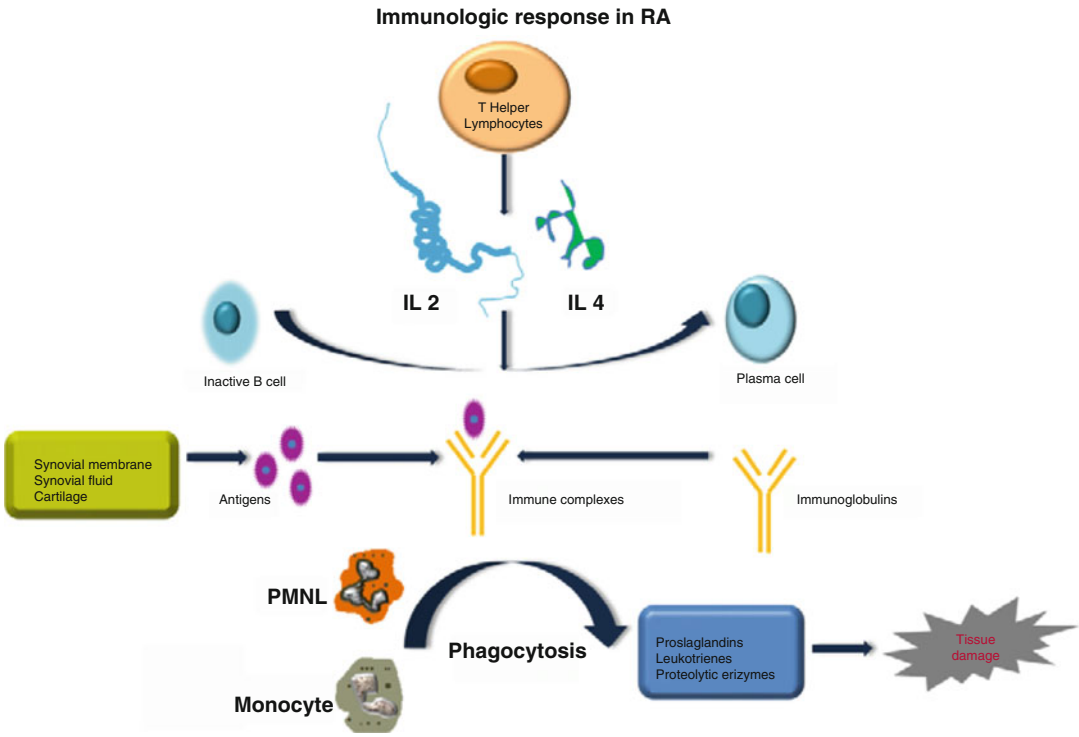

Fig. 31.1 Appearance of the immunologic response in RA: interleukin-2 (IL2) and interleukin-4 (IL4) cytokines that are released from T-helper lymphocytes proliferate and activate the B lymphocytes. Activated B cells transform into plasma cells that produce immunoglobulins (Ig). Ig combines with the antigens that are presented on the synovial membrane, synovial fluid, and joint cartilage of a RA patient by generating immune complexes. Polymorphonuclear leukocytes (PMNL) and monocytes phagocyte these immune complexes, and as a result, they trigger the production of prostaglandins (PG), leukotrienes (LT), and proteolytic enzymes which cause tissue damage

cells need to have recognized the antigen previously and interleukin 1 (IL-1) needs to be released by monocyte and macrophages. Immune response begins with the activation of CD4+ lymphocytes. T cells coming across the antigens alone are not enough to enhance immune response; at least a single co-stimulation is needed. CD80/86-CD28 co-stimulation pathway is well defined. Co-stimulation occurs when the molecules on APC surface (CD80 or CD86) bind to CD28 receptor molecule on T-cell surface. Cytotoxic-T-lymphocyte-associated antigen 4 (CTLA4) is the most important regulator of T-cell co-stimulation and this molecule is expressed by activated T cells and competes with CD28 for binding to CD80/86 on the APC surface, and accordingly, T-cell activation is weakened [7].

T cells play a primary role in the pathogenesis of RA by allowing secondary activation of endothelial cells, macrophages, and osteoclasts. These activated cells stimulate other T lymphocytes, macrophages, and fibroblasts by secreting the cytokines such as interferon gamma (IFN-γ) and interleukin 2 (IL-2). IFN-γ activates monocyte/macrophage cells. Activated macrophages continuously secrete IL-1 and tumor necrosis factor alpha (TNF-α). In RA, IL-1 and TNF-α, which are among inflammatory cytokines, are increased in the synovia, synovial fluid, and systemic circulation and enhance destruction and decrease production resulting in local and systemic bone loss. Among the factors that are effective in osteoclastic differentiation, receptor activator nuclear factor of kappa B ligand (RANKL), IL-1, and TNF-α are found in rheumatic synovia. IL-1 and TNF-α enhance the production of RANKL, which has an important role in osteoclastic differentiation. Fibroblasts and active T cells synthesize RANKL in rheumatic synovia, and accordingly, they enhance osteoclast migration and activation. On the other hand, IL-1 and TNF-α also enhance osteoblast apoptosis and consequently prevent bone formation by increasing bone destruction. IL-1 and TNF-α are the main cytokines that play a role in RA [16].

B lymphocytes, which are activated by helper T lymphocytes, change into plasma cells and secrete Ig and RF. In addition, B cells present antigen to CD4+ T cells. Secreted Igs unite with the antigens in the synovial membrane, synovial fluid, and articular cartilage and form immune complexes. Immune complexes activate complement and cause chemotactic factors to be released. Chemotactic factors allow polymorphonuclear leukocytes and monocytes to accumulate in this region by increasing the vascular permeability. These cells phagocyte immune complexes and allow production and release of prostaglandins, leukotrienes, free radicals, and proteolytic enzymes, which cause tissue injury. They lead to tissue destruction together with activated osteoclasts [1].

Humoral mechanism is responsible for the pathogenesis of secretion of RF and anti-CCP, formation of immune complex, and activation of complement.

Toll-like receptors (TLR) are the molecules that have critical role in natural (innate) immunity. They activate natural immunity against infections. They act as a bridge between natural immunity and adaptive immunity. It has been proven that TLRs play a critical role in the pathogenesis of RA by activating natural immunity [17].

It is believed that synovial macrophages are the inflammation-intensifying cells rather than inflammation-initiating cells. They are abundant in inflamed synovial membrane and cartilage-pannus junction. They act as antigen-presenting cells in the early phase of the disease. Although macrophages secrete substantial amount of inflammatory cytokines and proteases in destruction site, they contribute to tissue destruction by activating fibroblasts rather than being the primary factor [18].

It has been understood that synovial fibroblasts have an active role in the pathogenesis of RA. They cause excessive matrix destruction by secreting matrix destructive enzymes as well as by indirectly influencing osteoclast activation. They have important roles in the activation of synovial macrophages and their cellular differentiation. Synovial fibroblasts of RA prevent programmed cell death (apoptosis) of both T and B lymphocytes. Independent from T cells, synovial fibroblasts play a role in RF production via plasma cell activation.

Moreover, it has been suggested that synovial fibroblasts of RA have ability to migrate to different regions and can prevent arthritis to spread to other joints [19].

Clinical Findings

General Findings

Rheumatoid arthritis is the most frequent chronic inflammatory disease of the joints. The onset and progression of the disease vary among individuals. Slow and insidious onset in weeks and months is seen in 55–65 % of RA patients, whereas acute onset is seen in 8–15 % of the patients. The symptoms peak within several days and may be accompanied by fever and extra-articular organ involvement. Symmetrical pattern is less common in acute onset than in insidious onset. Onset is subacute in 15–20 % of the patients. Systemic complications are more common in this group than in the group with insidious onset.

Presenting symptoms may be systemic or articular. Some individuals may develop nonspecific complaints, such as fatigue, weakness, weight loss, low-grade fever, or extensive muscular pain, before articular symptoms.

Articular Symptoms

In anamnesis, patients frequently express involvement of a single joint at first and then the other joints. Typically, joint swelling and tenderness are present and restriction of joint mobility occurs in the long term. Although it is known that classical joint involvement is symmetrical, asymmetrical involvement as well is not rare. Symmetry becomes more prominent in advanced stages of the disease. It is thought that symmetrical joint involvement results from bilateral release of neuropeptides, such as substance P, from terminal nerve ends in the joints. Morning stiffness may appear before pain and is explained by accumulation of edema fluid in inflamed tissue during sleep [2].

Metacarpophalangeal (MCP) joints, proximal interphalangeal (PIP) joints, and wrists are the joints involved most frequently and earliest in RA (Fig. 31.2a, c). Symmetrical fusiform swelling in PIP joints and accompanying swelling in MCP joints are typical involvements in RA. Involvement of distal interphalangeal (DIP) joints alone is almost never seen and it is not the site of initial involvement. Involvement of DIP joint may be due to concomitant osteoarthritis particularly in elder RA patients. Studies, which radiologically monitored the wrist involvement in RA in the long term, have demonstrated that joint injury develops in the first 3 years, particularly in the first year, and that disease progression then slows down. While swelling, pain, and restriction of mobility are initially in the forefront due to synovial hypertrophy, typical deformities for RA are developed over time. Swan neck deformity results from hyperextension of PIP joint and flexion of DIP joint, whereas boutanniere deformity results from flexion of PIP joint and hyperextension of DIP joint (Figs. 31.2a, b, 31.3, and 31.4). Ulnar deviation and volar subluxation are the deformities that can be seen due to the involvement of MCP joints. Dorsal swelling in the wrist due to the inflammation of extensor tendon sheaths is one of the early signs of disease. In further stages, generally radial deviation and volar subluxation are developed (Fig. 31.4). Involvement of distal radioulnar joint causes instability and dorsal subluxation of the ulnar head. This together with erosive changes leads to the rupture of surrounding tendons (Fig. 31.5). Trigger finger is seen due to flexor tenosynovitis, which is encountered frequently [20].

Among the joints of foot, the most commonly involved one is the metatarsophalangeal (MTP) joint followed by in turn the subtalar and tibiotalar joints. They are the joints involved initially in 20 % of the patients. Involvement of these joints causes more pain and restriction of mobility as compared to the joints of upper extremity because they carry load. Foot deformities include claw toe deformity, hallux valgus, volar subluxation, and cock-up deformities in the PIP joint (Fig. 31.6). Valgus deformity and flattening of the medial

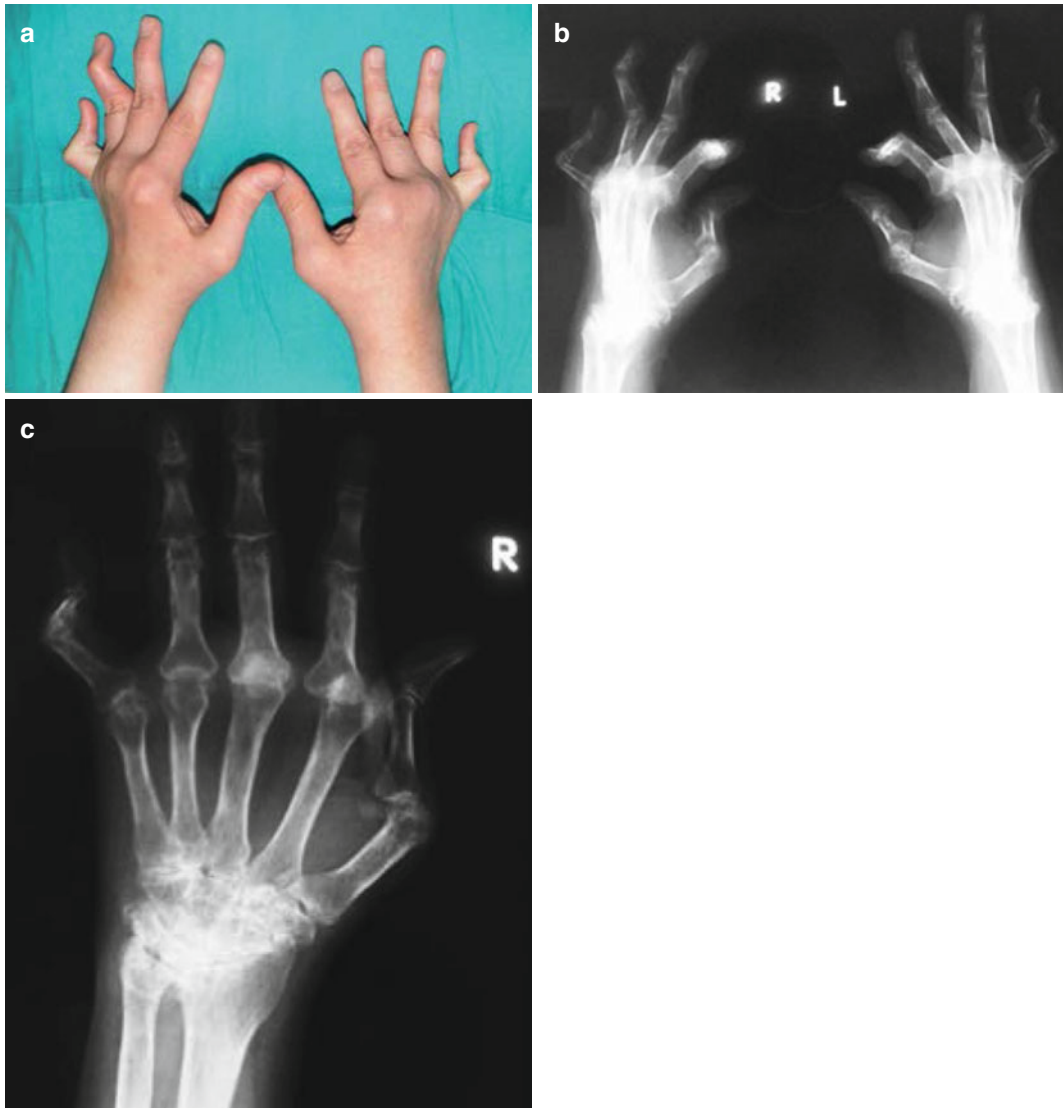

Fig. 31.2 (**a**–**c**) Hand involvement in a rheumatoid patient: inflamed synovia causes the tendon rupture and/or dislocation by weakening the ligaments. (**a**, **b**) Volar subluxation of the MCP joints, swan neck deformity of the fourth finger of the left hand and boutanniere deformity of the fifth fingers bilaterally. (**c**) Narrowing, erosion, and cysts of the wrist joint

longitudinal arch occur with the development of cartilage loss and erosion [2].

Complaints related to shoulder joint are seen in two-thirds of RA patients. Synovitis and erosion cause damage both in the glenoid fossa and humeral head. It has been observed that involvement of the shoulder joint is more common particularly in elder patients and in RF-positive cases. RA may involve all components of shoulder joints. Rupture may be seen in the long head of the biceps and the rotator cuff tendons may be involved. Pain is typical in the C4 region in involvement of the glenohumeral joint and in the C5 region in involvement of the rotator cuff.

The most common signs seen in the elbows include failure in complete extension of elbow due to synovitis or effusion, the presence of effusion-related periarticular cysts, and rheumatoid nodules. Limited supination may lead to disability in eating and other daily activities.

Hip joint is rarely involved in RA. Movement restriction may be seen in the abduction and rotation.

Knee involvement is common in RA; it may be the first joint involved in the early period and it is a good indicator of disease activity. Effusion and atrophy and flexion deformity due to dysfunction of quadriceps muscle may be seen in the knees. Baker's cysts, which can be palpated in the popliteal fossa, are the other common pathology. Baker's cysts, when ruptured, can cause swelling and pain in the calf. This needs to be discriminated from acute thrombophlebitis. Destruction of the knee joint may lead to involvement of lateral and cruciate ligaments and accordingly instability. Secondary osteoarthritis, which occurs due to progressive synovitis, is the other condition related to the knee joint [2].

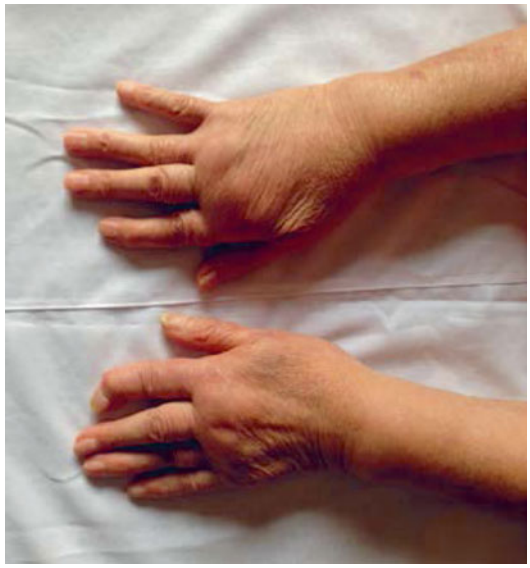

Fig. 31.3 Fusiform edema of the MCP and PIP joints is the typical involvement in RA accompanying volar subluxation of MCP joints and swanneck deformity of second finger

Although involvement of the cervical vertebrae is less common, it needs not to be ignored since it may cause life-threatening serious complications. Neck pain with movement and occipital headache are the clinical symptoms of neck involvement. The atlantoaxial joint is a synovial joint and may be exposed to proliferation and instability, similar to the other joints. Subluxation may develop due to erosion and ligament injury. The atlantoaxial subluxation is the enlargement of the space between the odontoid process of the axis and the arch of the atlas, which normally does not exceed 3 mm. In the presence of atlantoaxial subluxation, it is risky for the odontoid process to compress spinal cord during flexion of the neck. Head and neck pain, paresthesia, weakness, transient ischemic attack, and sphincter defect in the bladder and anus may appear. The presence of

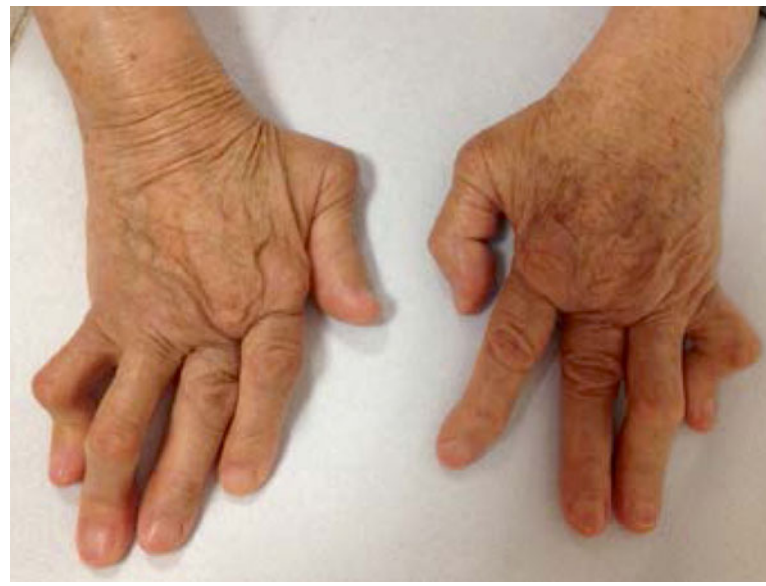

Fig. 31.4 Ulnar deviation of MCP joints with the swan neck deformity of the fourth and fifth fingers bilaterally in a RA patient

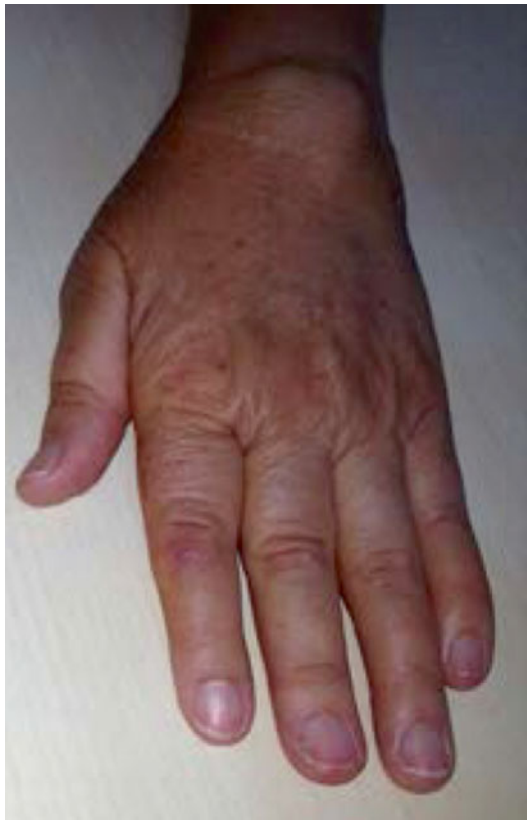

Fig. 31.5 Extensor tenosynovitis on the dorsal surface of the wrist in RA

subluxation should be definitely assessed prior to anesthesia. Lateral cervical radiographs in flexion position are recommended prior to surgery. In case subluxation is determined, preoperative measures that would prevent spinal cord injury should be taken. Sometimes, the odontoid moves to the superior aspect toward to the foramen magnum and may involve the medulla.

Moreover, RA may cause jaw pain and jaw opening defect by involving the temporo-mandibular joints, hoarseness or deepened voice by involving the cricoarytenoid joint, and hearing defects by involving small bones in the inner ear [1, 2].

Extra-articular Symptoms

Rheumatoid arthritis is a systemic inflammatory disease and has many extra-articular symptoms. These symptoms are more prevalent in patients with high RF-positive titers. Sometimes extra-articular involvement may appear before articular involvement.

Rheumatoid nodules occur in 20–30 % of RA patients. They are usually seen in the extensor surfaces of joints or in other regions that are exposed to mechanical pressure. Extensor surface of the elbow, dorsum of the hand, occipital region, sacrum, and the Achilles tendon are the regions where rheumatoid nodules are seen frequently (Fig. 31.7a, b). They are histologically composed of collagen necrotic part in the center, a middle layer consisting macrophages, and an outer layer consisting granulation tissue (Fig. 31.8). Rheumatoid nodules may be seen in many organs primarily in the lungs, sclera, and heart [2].

Pulmonary involvement of RA most commonly presents with pleurisy and is usually asymptomatic. It may occur either in the early or advanced stages. Pleural fluid is usually exudative and characterized by low glucose concentration. RA-induced interstitial pulmonary disease is more prevalent in individuals with long-term seropositive RA and in smokers. Diffuse interstitial fibrosis is the most common type of parenchymal involvement in RA. Nodular pulmonary disease usually occurs in those with rheumatoid nodules in the other regions of the body and in smokers. Pulmonary hypertension is less common [21]. Pericarditis is the most prevalent complication of cardiovascular involvement. Its prevalence is about 50 % in autopsy series. It is usually observed in seropositive patients with rheumatoid nodules. Myocardial involvement and related conduction defects are less common. Inflammation in RA patients enhances the risk of ischemic heart disease in association with cellular and humoral mechanisms. This risk is considered to be associated with disease severity and the presence of anti-CCP antibodies. Some studies have demonstrated that cardiovascular mortality and morbidity are decreased with methotrexate (MTX) and anti-TNF therapies.

Hematologically, anemia is quite prevalent in RA and is multifactorial. Normochromic and normocytic anemia is the most frequently encountered form. Iron-deficiency anemia may

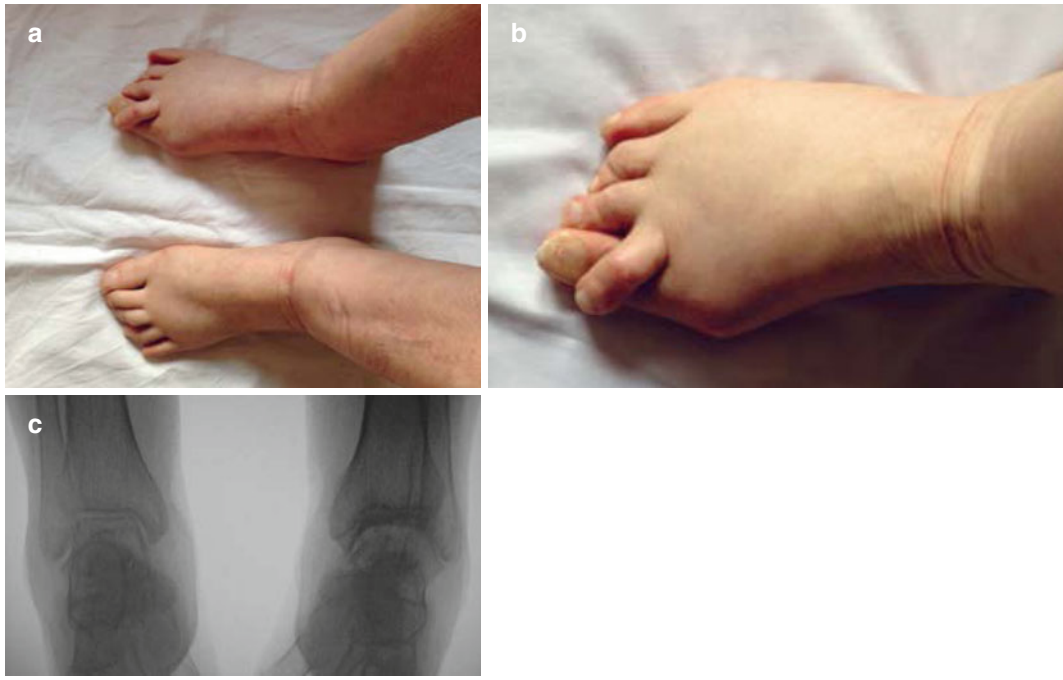

Fig. 31.6 (**a**–**c**) RA patient presenting hallux valgus deformity (**a**), cock-up deformity that is the result of overriding of the second finger by MTP joint extension, adduction, and lateral rotation on the first finger (**b**). Joint erosion of a patient with the tibiotalar joint involvement on the AP X-ray of the ankle (**c**)

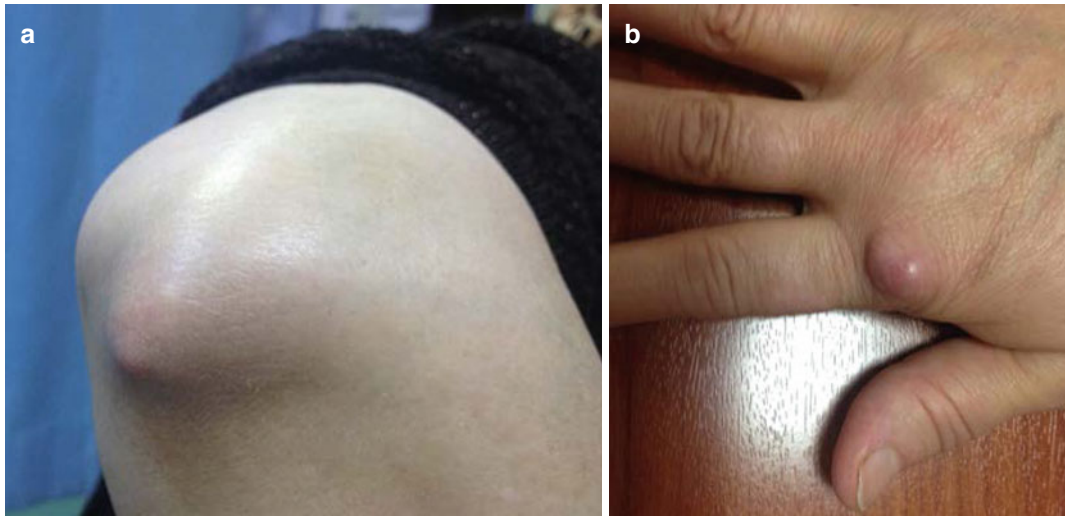

Fig. 31.7 (**a**, **b**) Rheumatoid nodules on the elbow extensory side of right elbow (**a**) and on the left hand (**b**)

result from gastrointestinal bleeding induced by nonsteroidal anti-inflammatory drugs (NSAIDs) and other drugs. Moreover, macrocytic anemia may develop secondary to folic acid deficiency and drug therapy. Thrombocytosis may be present in those with polyarticular involvement and active disease. Moreover, thrombocytopenia may be seen in patients with RA due to

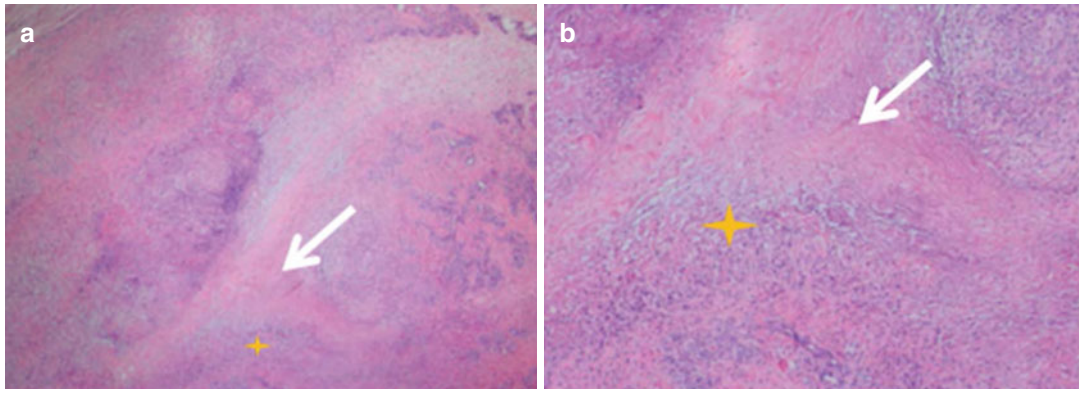

Fig. 31.8 (**a**, **b**) Histopathology of rheumatoid nodule: (**a**) necrotic area (*white arrow*) settling subcutaneously is surrounded by the histiocytes arranged as palisades (*yellow star*). HE ×50. (**b**) The histiocytes and myofibroblasts that show a palisadic order (*yellow star*) around the necrotic connective tissue (*white arrow*). HE ×100

immunosuppressive and cytotoxic drugs or due to treatment with gold, penicillamine, and sulfasalazine [21].

Muscular involvement in RA is usually in the form of atrophy and weakness in the muscles that are adjacent to the joints involved, primarily in the interosseous and quadriceps muscles. Besides, it may develop due to steroid use and neuropathy.

Rheumatoid vasculitis is the late-term finding of RA but not common. It is more prevalent in males, seropositive patients, patients with rheumatoid nodules, and patients with joint destruction. It is classically a vasculitis of the small vessels. Panarteritis is its pathological sign; all layers of the vascular wall are infiltrated by mononuclear cells. Proliferation in the intimal region causes thrombosis. Mostly, thrombosis in the capillary of the perionychium, infarction in the fingertips, and leg ulcers are developed.

There are four main reasons for neurological involvement in RA:

1. Spinal cord involvement due to cervical vertebral involvement
2. Entrapment neuropathy due to arthritis and tenosynovitis
3. Distal sensorial peripheral neuropathy in general
4. Mononeuritis multiplex resulting from the involvement of vasovasorum due to vasculitis. Mononeuritis multiplex is a sudden and painful involvement of the peripheral nerve [1].

Ocular involvement is seen in the late phase of the disease and in the form of keratoconjunctivitis sicca. Scleritis and episcleritis are rare. Loss of vision due to episcleritis does not occur; however, secondary cataract and related loss of vision may occur.

Renal involvement usually occurs due to amyloidosis, which is a complication of chronic RA, or treatment of the disease with D-penicillamine, cyclosporine, and NSAIDs rather than direct effect of RA.

Gastrointestinal involvement is not directly associated with RA. Duodenal ulcer and liver toxicity may occur due to the use of NSAIDs and some disease-modifying antirheumatic drugs (DMARDs) [21].

Felty syndrome is the presence of splenomegaly and leukopenia together with RA. This may be accompanied by anemia, thrombocytopenia, lymphadenopathies, and liver involvement. It is an important cause of mortality.

Secondary Sjögren's syndrome is a picture characterized by dry mouth and dry eye, which result from autoimmune destruction of exocrine glands primarily the lacrimal and salivary glands. It is thought to occur in 10 % of RA patients.

Secondary osteoporosis may develop due to inflammation, corticosteroid therapy, and immobility in long-lasting cases, and vertebral and non-vertebral fractures may be seen. The risk is twofold higher in both females and males. Risky

patients should be evaluated via bone mineral densitometry.

The risk of cancer is mildly increased particularly in RA patients with lymphoma. It is associated with disease severity and inflammatory activity.

Infections are increased due to the disease itself and to the treatment with glucocorticoids and immunosuppressive and biologic drugs. There is also risk for RA-induced septic arthritis and discrimination from acute arthritis flare-ups is of great importance to prevent joint loss [1].

Laboratory Findings

There is no test specific for the diagnosis of RA.

Rheumatoid factor, which is an autoantibody that reacts with the Fc region of Ig G, is positive in more than two-third (60–80 %) of the patients [22]. RF may be positive in 5 % of healthy subjects; its prevalence increases with age and reaches to 10–30 % over the age of 65 years. Articular and extra-articular symptoms are severer in individuals who have positive high titers. RF positivity is a constant finding in patients with rheumatoid nodules and vasculitis. The important issue in RA is the evaluation of RF together with clinical findings. In addition to RA, some diseases are also associated with RF. These diseases are systemic lupus erythematosus (SLE), Sjögren's syndrome, chronic liver disease, sarcoidosis, interstitial pulmonary fibrosis, infectious mononucleosis, hepatitis B, tuberculosis, leprosy, syphilis, subacute bacterial endocarditis, visceral leishmaniasis, schistosomiasis, and malaria [22].

Antibodies against citrullinated proteins such as filaggrin and its circular form are called as anti-citrullinated peptide antibody (ACPA). The most widely used one is anti-CCP antibody, the specificity and sensitivity of which are 88–96 % and 48–68 %, respectively, for the diagnosis of RA. When evaluated together with RF, specificity of anti-CCP antibody in diagnosing RA increases up to 98 %. A positivity by 70 % has been detected in early RA. It is well correlated with disease progression. There are studies suggesting that anti-CCP antibody is associated with erosive arthritis development and radiological damage and may be used in diagnosing early RA [23].

Typically, normochromic/normocytic or hypochromic/normocytic anemia may be seen in RA patients. These are chronic anemia diseases. Inadequate production in bone marrow occurs due to suppressing effect of inflammatory cytokines (IL-1, TNF-α, TNF-γ) on bone marrow. Sometimes, iron deficiency may accompany.

Blood leukocyte count is generally high in patients with active RA receiving steroids. Thrombocytes may be increased directly proportional with disease activity.

Erythrocyte sedimentation rate (ESR), C-reactive protein (CRP), and fibrinogen are correlated with the degree of disease activity. CRP is a better indicator of activity than ESR [24].

Hepatic and renal function tests should also be analyzed to evaluate liver and kidney involvement [22].

Radiological Findings

Radiological evaluation is generally performed by direct radiographs. Primarily, anteroposterior hand, wrist, and foot radiographs should be evaluated. Afterward, baseline radiographs are necessary to determine progression. Periarticular soft tissue swelling and enlargement in joint space are seen in the early period. This results from synovial inflammation and fluid production. Periarticular osteoporosis is also one of the early signs. Narrowing of the joint space, subchondral pseudocysts, and erosive changes are seen due to the destruction of cartilage by the pannus. Extreme irregularity on the joint surface, subluxations, general osteoporosis, joint deformities, fractures, degenerative and destructive changes, and bone ankylosis may be encountered in the late period (Figs. 31.9, 31.10, and 31.11a–c) [25]. For standardization of evaluation by direct radiography, indexes were developed first by Larsen and then by Sharp. Atlantoaxial radiograph is valuable in suspected conditions and chest X-ray is valuable for pulmonary involvement [26].

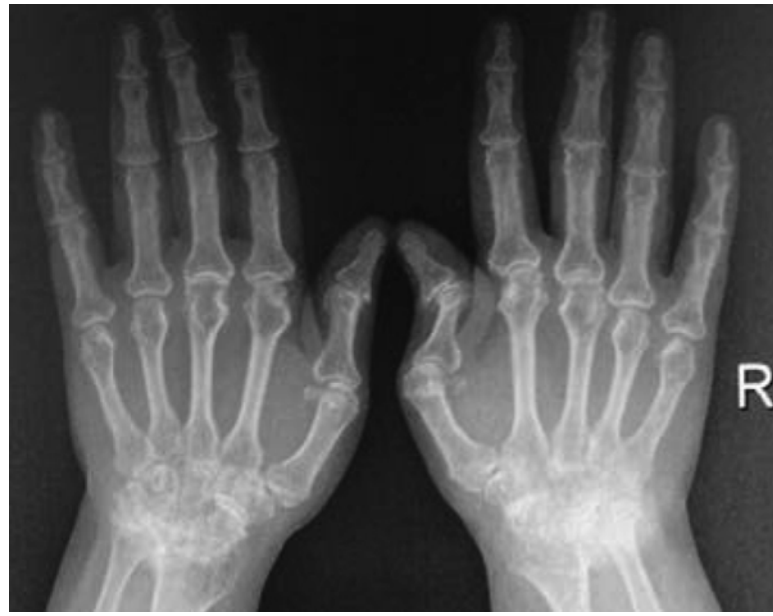

Fig. 31.9 Hand-wrist radiograph of a rheumatoid arthritis patient: narrowing, erosion, and cysts in the carpal joints; narrowing in the proximal interphalangeal joints; and subluxation in the first interphalangeal and metacarpophalangeal joints

Ultrasonography (US) is a more sensitive method than conventional radiography to detect small bone erosions and subclinical synovitis in the early period. Inflammation and fluid in the joints and in the bursa and tendon sheaths can be detected by US and enthesopathy can be assessed [27].

Magnetic resonance imaging (MRI) is more sensitive as compared to both physical examination and conventional radiography in detecting synovitis and erosions in the joints of hands and wrists in the early period of the disease. Bone edema is very early determinant of inflammation and can predict further erosions together with synovitis; thus, it has prognostic value. If a bone erosion is initially detected in a region via MRI, the risk of erosion in that region increases sixfold at the end of 1 year. The degree of synovitis is also an important indicator of prognosis in RA [25].

Diagnosis

There is no specific test for the diagnosis of RA. Diagnosis is established with the presence of symptoms and signs of RA and exclusion of other diseases. RA should be considered if RF and anti-CCP antibody are positive in a patient with symmetrical articular pain, swelling in the joints of hands and feet, and morning stiffness.

Diagnostic criteria for RA were first developed in 1958 by ACR (the American College of Rheumatology) and these criteria were then revised in 1987. These either did not establish definite diagnosis of RA or exclude RA. New criteria for RA classification were created in 2010 by EULAR (the European League Against Rheumatism) and ACR [28]. According to the most recent classification, diagnosis of RA is established in those with a score of 6 and higher (Table 31.1) [28].

Differential Diagnosis

In differential diagnosis, RA should be discriminated from generalized osteoarthritis (OA) since they are seen in the same age group and involve the joints of the hand. Different from RA, MCP and wrist are not involved in OA. It may be difficult to discriminate psoriatic arthritis from RF-negative RA. Other connective tissue diseases (SLE, scleroderma, Sjögren's syndrome) should also be considered in differential diagnosis. The other

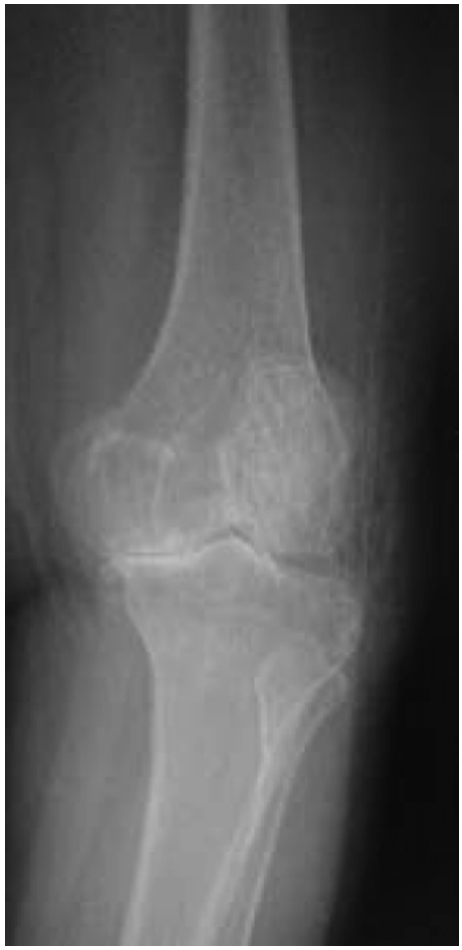

Fig. 31.10 Knee radiograph of a rheumatoid arthritis patient: concentric narrowing in the joint space, cysts, and subluxation

diseases that should be considered are as follows: spondyloarthropathies, vasculitis (polymyalgia rheumatica, giant-cell temporal arteritis), crystal arthropathies (gout, chondrocalcinosis), fibromyalgia syndrome, acute rheumatic fever, acute viral polyarthritis, palindromic rheumatism, relapsing symmetrical seronegative synovitis and peripheral edema, Lyme disease, sarcoidosis (chronic granulomatous form), familial Mediterranean fever, hypertrophic osteoarthropathy, hematological diseases (hemochromatosis, hemophilia), malignancies and paraneoplastic diseases (non-Hodgkin lymphoma, acute lymphoblastic lymphoma, myelodysplastic syndrome), multicentric reticulohistiocytosis, and pigmented villonodular synovitis [1].

Evaluation of the Disease

In general, the Disease Activity Score-28 (DAS-28), which is an EULAR disease activity index, and response criteria are used to evaluate disease activity. The DAS-28 ESR is a composite index that evaluates 28 joints and consists of number of swollen and tender joints and patient global assessment (PGA) (DAS-28 = 0.56*sqrt [number of tender joints]+0.28*sqrt [number of swollen joints]+0.70*ln[ESR] + 0.014*[PGA]) [29]. The DAS-28 < 2.6 is considered as remission, ≤3.2 is considered as low disease activity, <5.1 is considered as moderate disease activity, and >5.1 is considered as high disease activity [30]. In addition, the simplified disease activity index and the clinical disease activity index are also used to evaluate disease activity [31].

Health assessment questionnaire (HAQ), which is the most practical tool in daily practice and gives the most sensitive information on disease progression, is used to evaluate disability. It consists of 8 subtitles and 20 questions concerning health status and level of functionality. HAQ consists of dressing, eating, arising, walking, hygiene, grip, reaching, and daily activity subtitles and each question is rated between 0 and 3 [32, 33].

Generic measures such as the Short Form-36 and the Nottingham Health Profile can be used for quality of life [34].

Clinical Course and Prognosis

The course of RA is quite variable and it is difficult to estimate disease course for each patient. Disease activity shows continuous but alternating progression accompanied by various degrees of articular defects and functional restriction in many patients. Radiological progression is the fastest particularly in the first 2 years of disease and joint injury is usually completed in the first 5 years.

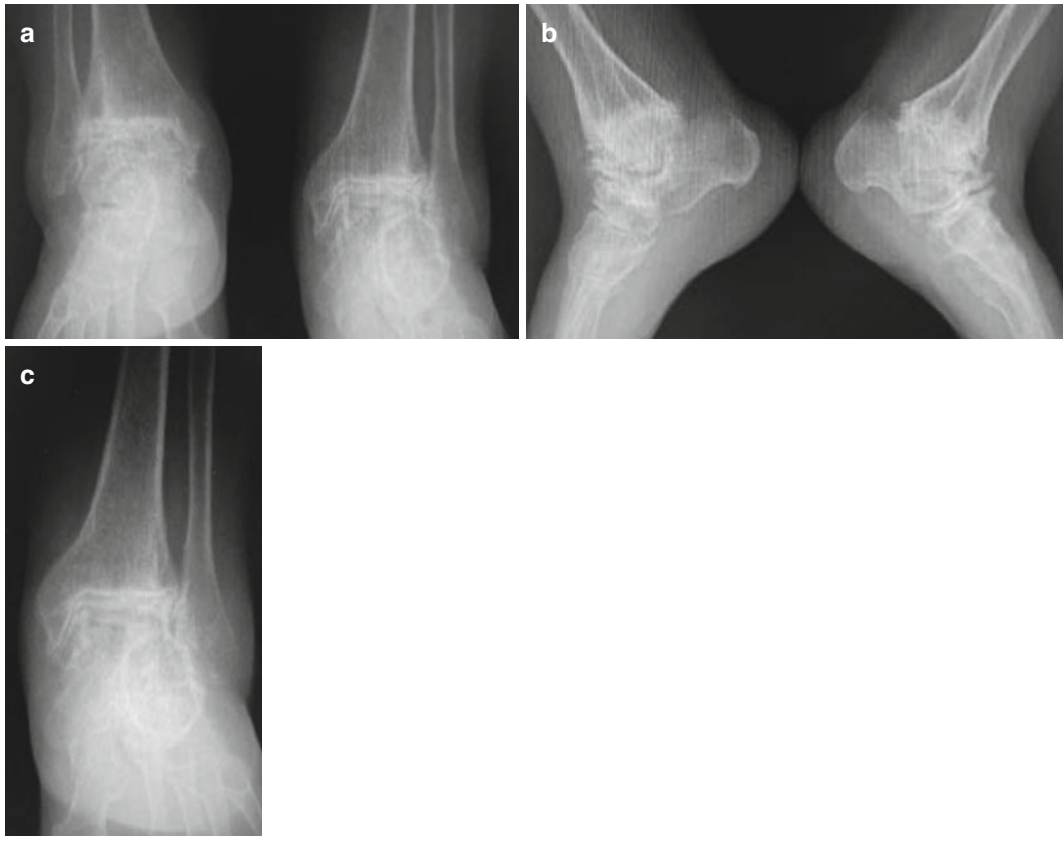

Fig. 31.11 (**a**–**c**) Ankle joint narrowing and degeneration on AP (**a**) and lateral radiographies (**b**)

Table 31.1 The 2010 ACR (the American College of Rheumatology) classification criteria for rheumatoid arthritis

	Score
A. Joint involvement	
1 great joint	0
2–10 great joints	1
1–3 small joints (great joint involvement yes/no)	2
4–10 small joints (great joint involvement yes/no)	3
>10 small joints	5
B. Serology (at least one test result is required)	
Negative RF or anti-CCP	0
Low-positive RF or anti-CCP	2
High-positive RF or anti-CCP	3
C. Acute-phase reactants (at least one test result is required)	
Normal CRP and ESR	0
Abnormal CRP or ESR	1
D. Duration of symptoms	
<6 weeks	0
>6 weeks	1

A score of 6 and higher is suggestive of definite diagnosis of rheumatoid arthritis
RF rheumatoid factor, *Anti-CCP* anti-cyclic citrullinated peptide, *CRP* C-reactive protein, *ESR* erythrocyte sedimentation rate

Patients with poor prognostic factors should be treated earlier and more aggressively. Indicators of poor prognosis for radiographic injury, disability, and mortality have been defined in RA. These indicators include permanent inflammation in more than 20 joints, high number of swollen joints, the presence of rheumatic nodules, the presence of high serum RF, the presence of articular erosions, disease onset at advanced age, high ESR and CRP, the presence of extra-articular involvement, and poor functional status at the time of diagnosis, the presence of HLA-DRB1*0401 or HLA-DRB1*0404, the presence of comorbid conditions, and low socioeconomic status and education level. Again, some studies have emphasized that the presence of Ig A RF and being young female are associated with poor prognosis and probability of articular destruction. Moreover, various studies emphasize that anti-CCP and anti-modified citrullinated vimentin antibodies as well, which are among new diagnostic autoantibodies, are the parameters that could be used in predicting aggressive destructive disease.

Recent studies have demonstrated that RA patients have enhanced mortality as compared to the normal population at the same age and gender. Standardized mortality rates have been found to be 1.98–3.08 in different studies. Disease severity, activity, and disability have been found to be associated with mortality [35].

Treatment

General Approach

The primary aim of treatment of RA, which is a chronic disease, is to relieve pain and inflammation, prevent articular destruction and related deformities, and provide a functional and independent life.

The opinion that has gained importance in recent years is the early diagnosis and early and aggressive use of disease-modifying drugs, as well as biologic drugs, when necessary, since the disease becomes destructive in a short time. Today, the aim should be remission or to provide low disease activity. Particularly, the first 2 years are important in terms of treatment. If this process is not well-observed, development of irreversible changes is quite likely [36, 37].

Treatment regimen can be listed as education of the patient and family, enabling patient collaboration and motivation, psychological support, occupational therapy, diet, resting and exercise, physical therapy and rehabilitation, drug therapy, and surgical methods.

Non-pharmacological Therapies

Patient Education

All patients should be educated about the disease, drugs and their side effects, non-pharmacological therapies, exercise and joint-protection programs, orthosis to be used, coping with stress, and diet as soon as they are diagnosed. These can be performed as one-to-one education by the doctor or as group meetings and via brochures and videos.

Exercise and Resting

RA may cause weakness, restriction in joint movements, contractures, muscular atrophy, and articular instability. Therefore, the basic aim of exercises is to enhance aerobic capacity, preserve joint range of motion, and increase muscle strength. Exercises should be planned individually for each patient according to the disease activity, deformities, and patient capacity.

Rheumatoid arthritis patients should be recommended resting in the active period and exercise in the inactive period. Based on the patient's situation, resting may be in the form of bed resting or, when necessary, local resting with splint and plasters. Bed resting should not be long lasting as it leads to decrease in muscle mass and active and passive exercise for joint range of motion should be recommended in this period.

Exercises such as walking, biking, and swimming would enhance aerobic capacity of patients. Such exercises should be recommended in the periods when the disease is not very active. Passive exercises for joint range of motion and isometric strengthening are suitable for inflamed joints. Isometric, isotonic, and isokinetic exercises can be given to strengthen non-inflamed joints [38].

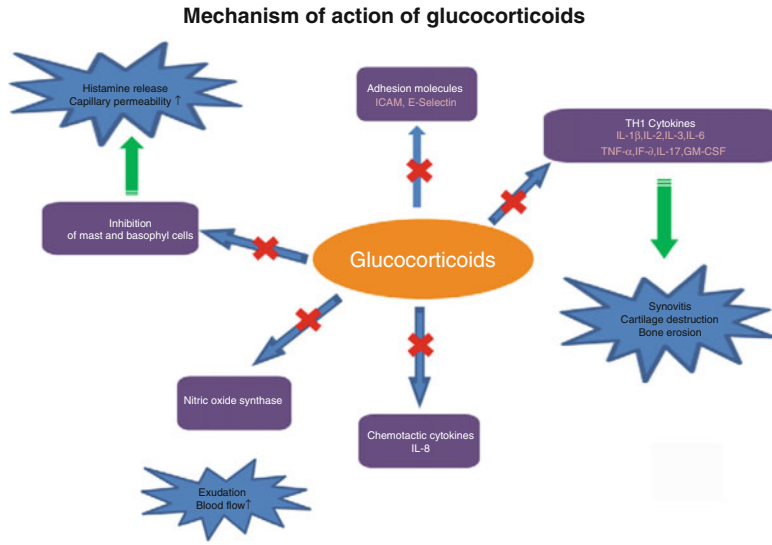

Fig. 31.12 Mechanism of action of glucocorticoids

Physical Therapy and Rehabilitation

The goals of physical therapy and rehabilitation are to reduce pain and inflammation and to preserve and enhance joint functions.

Cold compress may be effective in reducing pain and inflammation, particularly in the active joint. Hot compress may prepare contracted joint for exercise and may provide analgesia in the inactive joint. Electrotherapy is beneficial to relieve pain and improve muscle strength.

Corsets, kneepads, and splints are effective in supporting the joints during resting and in preventing deformities.

Walker, crutch, walking sticks, and wheelchair are used in patients with difficulty in walking due to lower extremity problem and balance problem.

Auxiliary tools such as elevated toilet seats and bath seats and fork and knife with thick holder are helpful in daily activities of patients [39].

Diet

Although there is no specific diet in the prevention and treatment of RA, it is thought that diets containing fish oil or eicosapentaenoic acid and docosahexaenoic acid might relieve the symptoms by reducing arachidonic acid metabolites and cytokines.

Pharmacological Therapies

Nonsteroidal Anti-inflammatory Drugs (NSAIDs)

These drugs show analgesic, anti-inflammatory, and antipyretic efficacy by inhibiting productions of prostaglandin, prostacyclin, and thromboxane over the cyclooxygenase enzyme. They reduce inflammation-related signs and symptoms. NSAIDs do not alter disease course. Gastrointestinal system (GIS) side effects being the leading, their side effects include nephrotoxicity, thrombocyte dysfunction, allergic rhinitis, and exacerbation of asthma.

Glucocorticoids

The aim of using systemic glucocorticoid therapy is to suppress inflammation and alter immune response (Fig. 31.12). Glucocorticoids lead to decrease in neutrophil concentration while suppressing their migration. They inhibit the quantity and the functions of the lymphocytes, macrophages, monocytes, fibroblasts, and endothelial cells. Low-dose prednisolone (5–7.5 mg) is considered beneficial in symptom control. Glucocorticoids are particularly used as a bridge therapy to relieve symptoms until the onset of DMARDs' action. In addition, long-term low-dose glucocorticoid has also joint injury-preventing effects. It has many dermatologic,

endocrine, bone, GIS, immunologic, cardiovascular, and ocular complications. 15 mg/kg or lower doses of prednisolone can be used intermittently when the disease cannot be controlled by other modalities, as shown in a Cochrane review that evaluated the effects of prednisolone and NSAIDs [40].

Nonbiologic Disease-Modifying Anti-rheumatic Drugs (DMARDs)

Effect of nonbiologic DMARDs in RA includes controlling the symptoms and signs of joint involvement, increasing the functional status and quality of life, and regressing the development of radiographic erosion. It should be considered as the first-line treatment and commenced in all patients in the shortest possible time after diagnosis. The next step is close monitoring of the patients and evaluating response to treatment [41].

Methotrexate

It is a folic acid antagonist. It has immunomodulatory and adenosine-mediated anti-inflammatory effect. Methotrexate reduces monocytic cell growth while increasing their apoptosis. It decreases the IL1, IL6, IL4, and IL10 secretion and gene expression of proinflammatory Th1 cytokines (IL2 and IFNγ) while increasing the IL1ra production. Methotrexate has indirect inhibitory effect on COX-2 synthesis, neutrophil chemotaxis, and synovial metalloproteinase production and stimulates tissue inhibitor of metalloproteinase [42].

It is recommended as the first-line therapy in RA (particularly in aggressive type). Starting dose is 7.5–10 mg/week. The dose is increased monthly by 2.5–5 mg until obtaining adequate clinical response. The usual maintenance dose is 15–20 mg/week. Nausea, loss of appetite, diarrhea, stomatitis, weight loss, dizziness, headache, and behavioral changes are seen in patients receiving MTX. Hepatotoxicity is dose-independent. Complete blood count and creatinine and transaminase levels should be monitored monthly in the first 6 months and then at 3-month interval over the course of treatment. Patients on MTX treatment should receive folic acid. It is known that folic acid reduces likely adverse events of MTX [43].

Sulfasalazine

It has been demonstrated to slow down the development of erosion in RA. Starting dose is 0.5 g/day and is increased to 2 g in 4 weeks by 0.5 g increases at weekly intervals. Therapeutic effect usually begins in 4–8 weeks. While nausea, abdominal pain, dizziness, headache, and skin rash are relatively frequent side effects, hemolysis, leukopenia, thrombocytopenia, and oligospermia are less common. Complete blood count should be monitored at 2–4-week interval in the first 3 months and thereafter every 3 months [43].

Antimalarials

Hydroxychloroquine (HCQ) and chloroquine are used in RA. They are preferred in nonerosive forms or in combined therapy. Clinical and laboratory effects have been demonstrated. They are unable to prevent radiological erosions. Their effect remains unclear. They are considered to suppress phospholipase A2, inhibit neutrophil chemotaxis, and prevent immune complex formation. Starting dose for HCQ is 200 mg/day. Maintenance dose is 400 mg/day. Toxic retinopathy is the most important side effect. Hence, ophthalmological examination should be performed at 12-week intervals [43].

Leflunomide

It is an immunomodulatory drug. It acts over activated lymphocytes by suppressing dihydrofolate enzyme. Maintenance dose is 10–20 mg/day. It has hepatic and GIS side effects and may cause dermatitis. Complete blood count and creatinine levels are monitored at monthly intervals in the first 6 months and thereafter every 2 months [42].

Gold

It is one of the old DMARDs used in the treatment of RA. Gold sodium thiomalate and gold sodium thioglucose are the intramuscular forms, whereas auranofin is the oral form. It has side effects such as allergic reaction, stomatitis,

proteinuria, and aplasia. It may be used in resistant patients [43].

Other Nonbiologic DMARDs

Azathioprine, cyclosporine, D-penicillamine, tacrolimus, and tetracycline derivatives are among the rarely used DMARDs due to side effects.

Biologic Disease-Modifying Antirheumatic Agents

Biologic agents have three mechanisms of action:

1. Reversing the functions of cytokines
2. Blocking the signals that are needed for T-cell activation
3. Decreasing B-cell concentration

Anti-TNF-α Agents

Because of the substantial groups of unresponsive patients to DMARDs therapy in RA, drugs targeting the cytokines have begun to be developed. TNF-α, IL-6, and IL-1, which have central role in the pathogenesis and key role in regulating inflammation, rank first among targeted cytokines. TNF is a cytokine effecting onto many different pathways such as bone and cartilage resorption; HLA class 2 expression; the induction of collagenase and PGE-2; chemotaxis by the induction of IL-8; increasing of the release of proinflammatory cytokines like IL-1, IL-6, and GM-CSF; activating the endothelial cells by the help of adhesion molecules, inducing macrophages and T and B cells; and eliciting the maturation and the activation of dendritic cells by changing their surface pattern. Anti-TNF-α drugs show their effects by inhibiting those functions (Fig. 31.13). Anti-TNF-α drugs relieve symptoms and signs, suppress structural injury, and improve physical function in RA patients. Its activity begins faster than classical DMARDs. They are more effective when used together with MTX. Those drugs are all indicated by alone or combined with Mtx at the beginning phase of the disease or nonresponsive to the other classical DMARDs in the treatment of the medium or severe active rheumatoid arthritis patients. Since TNF-α has an important role in inflammation mechanism, anti-TNF-α therapies are used in many inflammatory diseases. The main side effects related to anti-TNF-alpha include infection, autoimmune diseases, demyelinating disease, malignancies, and congestive heart failure. Since TNF-α is important in granuloma formation, tuberculosis reactivation is the main infection associated with anti-TNF-α. Autoantibodies (antinuclear antibody, anti-dsDNA, antiphospholipid antibody) may be developed after the use of anti-TNF-α. Treatment should not be commenced in patients with stage 3–4 congestive heart failure since it might be mortal; ejection fraction should be closely monitored in stage 1–2 patients and should not be restarted in the event of decrease [44].

Infliximab

It is a chimeric rat-human anti-TNF-α monoclonal antibody. It is usually used in patients with serious and active disease that do not respond to treatment. A dose of 3–5 mg/kg is administered in 2 h via IV route and infusion is repeated in the second and sixth weeks after the first administration and then every 4–8 weeks. Autoantibody development with treatment has been reported. Therefore, it is recommended to be used together with MTX. It has been observed that radiological progression is stopped with the use of infliximab.

Etanercept

It is a soluble TNF-α receptor fusion protein. Recommended dose is weekly 50 mg. It is administered via subcutaneous route.

Adalimumab

It is a monoclonal human anti-TNF-α antibody. It suppresses macrophage and T-cell functions via p55 and p75 surface receptors. It is used every 2 weeks at a dose of 40 mg [44].

Certolizumab Pegol

It is a human antibody against recombinant TNF, includes only Fab region, and is conjugated with

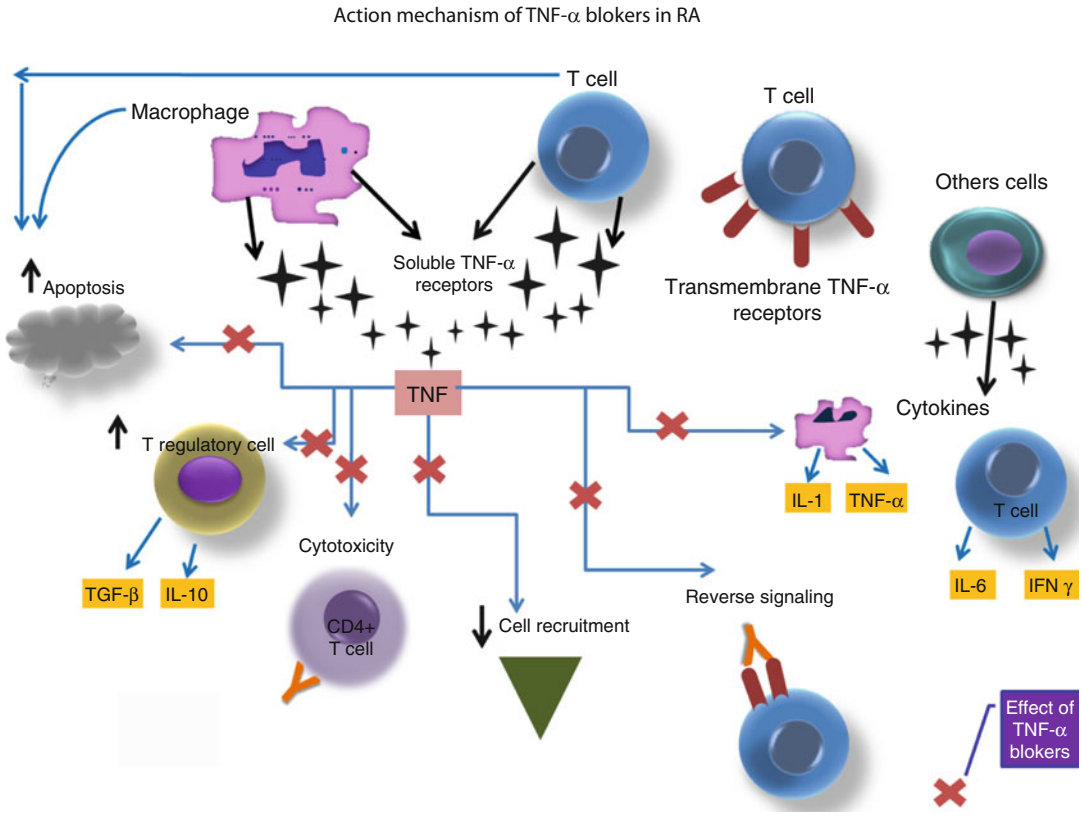

Fig. 31.13 Mechanism of action of TNF-α blockers in rheumatoid arthritis. TNF-α shows its effect by merging soluble TNF-α and transmembrane TNF-α receptors. TNF-α blocker drugs inhibit the effects of TNF-α that are shown on this diagram

polyethylene glycol to prolong its half-life. It is used at baseline and at the second and fourth weeks at a dose of 400 mg and thereafter at 2-week intervals at a dose of 200 mg via subcutaneous route together with MTX [43].

Golimumab

It is a pure human Ig G1 monoclonal antibody specific to both circulating and membrane-bound TNF. It is recommended as subcutaneous injections at a dose of 50 mg monthly together with MTX [43].

Anakinra

It is an IL-1 receptor antagonist. The proinflammatory effects of the IL-1 are inhibited by the IL-1 receptor antagonists (IL-1Ra) that occur naturally. IL-1Ra inhibits the PG and MMP synthesis of the synovial cells and chondrocytes and also blocks the infiltration of mononuclear cells to into the joint. IL-1 inhibitors are less effective than TNF inhibitors in the treatment of rheumatoid arthritis and the other inflammatory arthritis. It is recommended in combination with MTX or alone in severe cases that are unresponsive to treatment. Recommended dose is 100 mg/day via subcutaneous route [45].

Tocilizumab

Tocilizumab is an anti-IL-6 receptor antibody. IL-6 has the proinflammatory effects: It leads to hypergammaglobulinemia and resulting in increase in the autoantibody titers by activating the B cells. IL-6 increases the synthesis of acute-phase reactants by activating the hepatocytes. Besides, IL-6 causes the inflammatory response to lengthen by increasing the life time of the neutrophils that is reaching to inflammation area. It

also has the contribution to the prominence of vascular endothelial growth factor (VEGF), pannus formation, and neovascularization. Tocilizumab is an anti-IL-6 receptor antibody. It competes with IL-6 for binding to the receptor membranous and soluble IL-6. It is known to delay structural joint injury. It is administered every 4 weeks at a dose of 4 mg/kg as infusion [43].

Rituximab

It binds to CD20 on the surface of B lymphocytes. Thus it inhibits the CD20 and B-cell population selectively and temporarily. CD is a surface antigen that exists only in pre-B cells and mature B cells but not in plasma or stem cells. The depletion of B cells may affect the level of the autoantibodies like RF and anti-dsDNA. Rituximab causes B-cell depletion by three postulated mechanisms that are complement-mediated cytotoxicity, antibody-dependent cell-mediated cytotoxicity, and induction of apoptosis. First mechanisms are thought to be more dominant in vivo, probably depending on the cell's specific anatomical location. It is found to be effective in RA when used together with MTX. Onset of action may be delayed until 3 months. Two doses of 1,000 mg are administered via IV route at 2-week intervals and these cures are repeated every 6 months depending on patient status. Side effects such as infection, hepatitis, malignancy, and neurological symptoms may develop after rituximab therapy. Neurological signs should be monitored in terms of progressive multifocal leukoencephalopathy [43].

Abatacept

It is a recombinant human protein consisting of extracellular region of CTLA4 and Fc region of Ig G1 and is developed to prevent complement activation. Abatacept binds CD80/CD86 molecules located on the surface of antigen-presenting cells (APC) like natural CTLA4. Thus the co-stimulation of CD28 on the surface of T cells is hindered. As a result, T cells that are stimulated by CD80/CD86-CD28 co-stimulation pathway are inhibited. It is found to be effective in preventing progression of structural injury [46].

Tofacitinib

It is a newly developed agent and the inhibitor of Janus kinase 3, which influences JAK/STAT signal pathway. It is thought to suppress inflammation and joint injury [47].

Orthopedic Surgical Strategy

Rheumatoid arthritis has a poor prognosis causing disabilities in 80 % of the patients in 20 years. By the improvements in the medical treatments of RA, incidence of the hip and knee surgery has decreased by 40 %. It seems that 17 % of RA patients need orthopedic surgery within 5 years after the diagnosis [48]. Forty-one percent of these surgeries are noted to be total joint arthroplasties [49]. One out of three patients need major joint arthoplasties constituting majority of being the hip and knee replacements (Figs. 31.14 and 31.15) [48]. One may assume 8 years median time from the beginning of rheumatoid arthritis symptoms to the time for the first orthopedic surgery [49]. 4.5 procedures per 100 person-years are estimated as the rate of orthopedic surgery from the onset of disease [49]. The risk factors for having an orthopedic surgery for RA patients are nonsteroidal anti-inflammatory drugs (NSAID) in the previous 2 years, long-term disease, female sex, and the presence of extra-articular complications [49]. Being old, having a long-term disease, taking biologic therapies, anemia, high sedimentation rate, and illness scores are defined as the risk factors for the major joint arthroplasties [48, 49]. Biologic drug usage does not cause a decrease in the need for joint replacement surgery in patients with similar on-medication disease activity [50]. Biologic drug users have lower revision rates in spite of non-evolving durability of prosthesis [50].

Eighty percent of RA patients suffers from wrist involvement and the findings of wrist arthritis emerge in 95 % within 12 years. Distal radioulnar joint, being the first involved compartment, is affected in 31–75 % of these patients (Figs. 31.2 and 31.9). Extensor tendon ruptures are often added to the inflammatory circumstances that cause caput ulna syndrome [51]. Extensor tendon

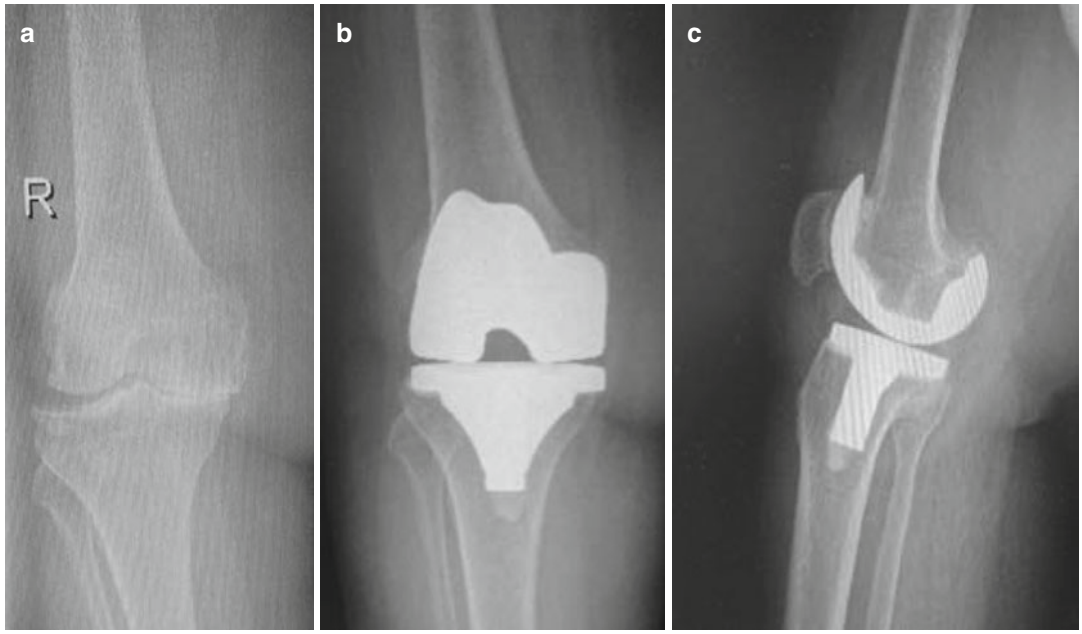

Fig. 31.14 (**a**–**c**) Pain and deformity due to the cartilage erosion of the knee joint (**a**) that require a total knee arthroplasty in a RA patient with the postoperative AP (**b**) and lateral radiographies (**c**)

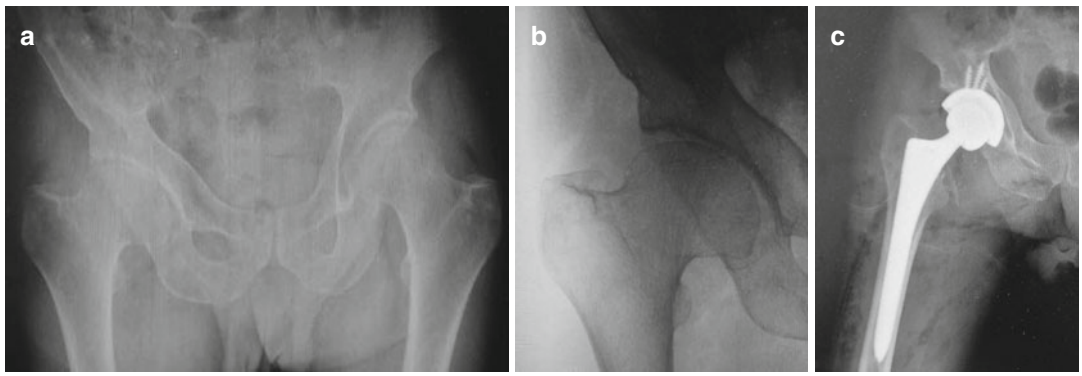

Fig. 31.15 (**a**–**c**) RA affecting the hip joint. The disease caused joint space narrowing and cartilage erosion (**a**, **b**) and necessitates a total hip arthroplasty (**c**)

ruptures are not mendable when occurred [52]. Darrach excision, the resection of distal ulnar joint, is the gold standard for surgery [51, 52]. Many stabilization techniques by using free tendon grafts have been described [51]. Sauve-Kapandji procedure is another alternative that enables other radical procedures as Chamay partial radiocarpal fusion and the wrist prosthesis [51, 52]. Metacarpophalangeal (MKP) joint being the most commonly affected joint of the hand is critical for the function of the fingers [53]. Silicone implants that are used for MKP joint are noted to improve the deformity and function with the same degree of patient satisfaction [53].

The elbow involvement restricts the upper extremity function in many patients of RA within the first 5 years. Conservative approaches are preferred to decrease pain and to protect the wrist function for the synovitis and capsular inflammation at the beginning of the disease [54].

Elbow instability occurs due to the damage of the joint and the ligaments with the increase

of symptoms and the functional deteriorations by time. Arthroscopic and open synovectomy for the patients that have no response to conservative treatment can heal the symptoms by the reservation of the elbow prosthesis for the irreparable cases [54].

Inflammatory process characterized by the synovitis, pannus, and joint destruction in rheumatoid shoulder gives rise to distinct pain and functional limitation that needs conservative treatment preferably. Surgical options are related to the cartilage damage and the condition of soft tissues in the vicinity of the joints (Fig. 31.16) [55].

The typical deformity of the forefoot in RA foot is the hallux valgus that is concurrently with the subluxation and dislocation of the MTF joint. Although many options are evolved to achieve painless, functional, plantigrade foot, first MTF joint fusion together with the excision arthroplasty of the index finger's MTF joint is the gold standard [56]. Cochrane search shows the equivalent pain management by arthroscopic and open synovectomy, although arthroscopic surgery has more risk due to recurrence and radiographic deterioration of RA. New concept sustains that advanced joint destruction preoperatively is not a contraindication for synovectomy [56].

RA may lead to the spinal instability, and although there are surgical techniques for the improvement of the abnormal movement of servical joints, new medical treatments are very effective for the protection of the joint damage [57].

The surgical sequence for the arthroplasty is lower extremity and upper extremity consequently. This order for the lower extremity is the following: the forefoot, hip, knee, barefoot, and then the ankle [48]. The survival time is superior

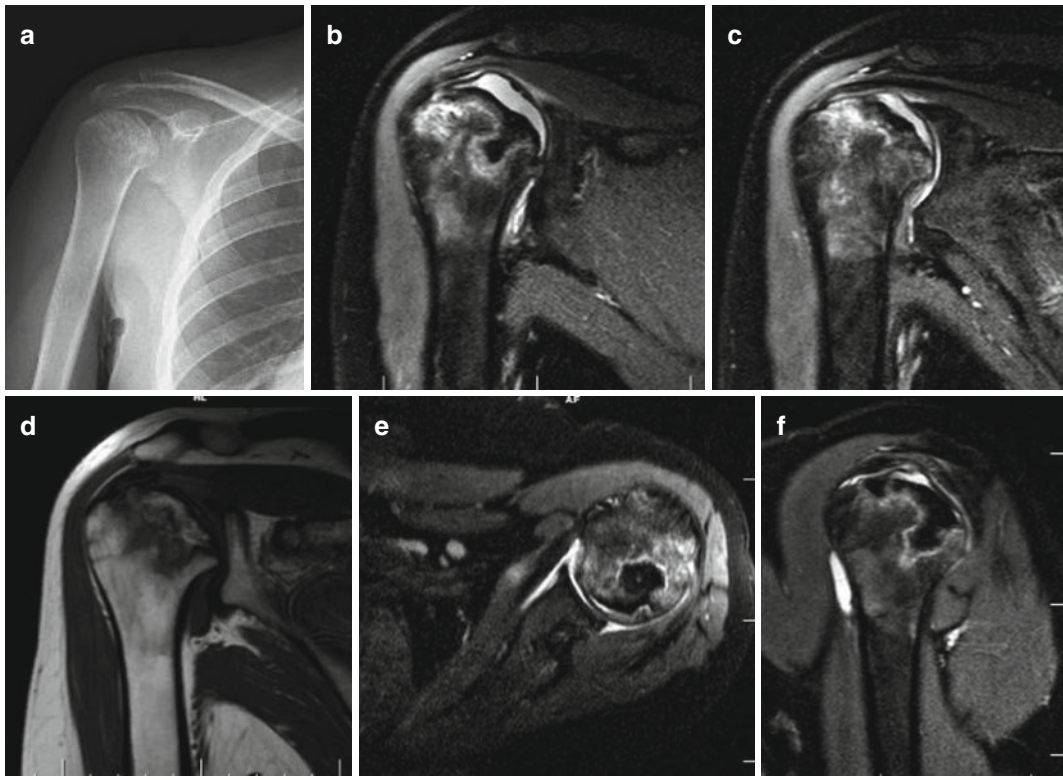

Fig. 31.16 (**a**–**f**) Rheumatoid arthritis shoulder that is complicated by avascular necrosis due to long-term usage of steroids. AP shoulder radiography shows the cartilage destruction (**a**); MRI shows the necrosis, destruction of the humeral head, and joint effusion on coronal T2-weighted images (**b**, **c**) and coronal T1-weighted (**d**), axle T2-weighted (**e**), and sagittal T2-weighted images

for the cemented hip and knee prosthesis than the cementless [48]. But there are increased fracture risk, component migration, and mechanical stem complications during the surgery in cementless fixations. But although systematic meta-analysis of Cochrane-MEDLINE-EMBASE database shows that the cementless hip stems increase the fracture risk during and after the surgery, it cannot be concluded that it will be a cause of early loosening [58]. And also there is no clear knowledge supporting the superiority of one to another [58]. Despite the proofs about the ACL retaining and sacrificing knee prosthesis that are poor, ligament-sacrificing types are thought to limit the early instability and revision risk [48]. Patellar resurfacing has the additional contribution [48]. The results of the ankle arthroplasties are not as satisfactory as the hip and knee replacements [48, 59]. Pain continues in 27–60 % of the ankle replacement patients and there is 10 % failure in 5 years [60]. One cannot claim the superiority of any ankle prosthesis design with the current data [60]. When RA and osteoarthritis patients are compared, pain decreases by the same ratio after the arthroplasty, but the functional results of RA patients are not as good as OA patients besides having a slower rehabilitation [58]. Orthopedists should know that the NSAIDs, glucocorticoids, DMARDs, and biologic drugs that those patients often use may have some effects on the surgical results. So it is very important to provide a safety use of these drugs to lessen the potential surgical complications besides a good collaboration with the rheumatologist to control the illness [61]. The risk of infection is not increased by continued usage of methotrexate with a positive impact on recovery. But the biologic agents (TNF antagonists) should be stopped preoperatively because of the increased risk of infection [48]. As RA patients have 2.6 times increased risk of infection, those patients need to be informed about the increased risk of infection and periprosthetic fracture preoperatively [48]. The perioperative procedures of the lower extremity arthroplasties planned for the RA patients necessitate multidisciplinary approach [58]. If the RA patient consults a rheumatologist later in the disease course, orthopedic surgery requirement will increase [59].

References

1. Burmester GR, Pratt AG, Scherer HU, van Laar JM (2012) Rheumatoid arthritis pathogenesis and clinical features. In: Bijlsma JWJ (ed) EULAR textbook of rheumatic diseases, 1st edn. BMJ Group, London, pp 206–231
2. Brasington RD (2011) Clinical features of rheumatoid arthritis. In: Hochberg MC, Silman AJ, Smolen JS, Weinblatt ME, Weisman HM (eds) Rheumatology, 5th edn. Mosby-Elsevier, Philadelphia, pp 823–838
3. Scheinecker C (2011) Pathogenesis of rheumatoid arthritis. In: Hochber MC, Silman AJ, Smolen JS, Weinblatt ME, Weisman HM (eds) Rheumatology, 5th edn. Mosby Elsevier, Philadelphia, pp 436–472
4. Pile K, Kennedy L (2008) Rheumatoid arthritis. In: Pile K, Kennedy L (eds) Problem solving in rheumatology. Clinical Publishing, Oxford, pp 71–103
5. Symmons DP (2002) Epidemiology of rheumatoid arthritis: determinants of onset, persistence and outcome. Best Pract Res Clin Rheumatol 16:707–722
6. van Vollenhoven RF (2009) Sex differences in rheumatoid arthritis: more than meets the eye. BMC Med 7:12
7. Firestein GS (2006) Etiology and pathogenesis of rheumatoid arthritis. In: Ruddy S, Harris ED, Sledge CB (eds) Kelley's textbook of rheumatology. WB Saunders Company, Philadelphia, pp 996–1042
8. Arias MV, Domingues EV, Lozano RB, Flores CV, Peralta MM, Salinas CZ (2010) Study of class I and II HLA alleles in 30 ecuadorian patients with rheumatoid arthritis compared with alleles from healthy and affected subjects with other rheumatic diseases. Rev Bras Rheumatol 50:423–33
9. Fugger L, Svejgaard A (2002) Association of MHC and rheumatoid arthritis HLA-DR4 and rheumatoid arthritis: studies in mice and men. Arthritis Res 2(3):208–211
10. Costenbader KH, Chang SC, De Vivo I, Plenge R, Elizabeth W, Karlson EW (2008) Genetic polymorphisms in PTPN22, PADI-4, and CTLA-4 and risk for rheumatoid arthritis in two longitudinal cohort studies: evidence of gene-environment interactions with heavy cigarette smoking. Arthritis Res Ther 10(3):R52
11. Bas S, Perneger TV, Seitz M et al (2002) Diagnostic tests for rheumatoid arthritis: comparison of anti-cyclic citrullinated peptide antibodies, anti-keratin antibodies and IgM rheumatoid factors. Rheumatology 41:809–814
12. Vencovsky J, Machacek S, Sedova L et al (2003) Autoantibodies can be prognostic markers of an erosive disease in early rheumatoid arthritis. Ann Rheum Dis 62:427–430
13. Symmons DP (2003) Environmental factors and the outcome of rheumatoid arthritis. Best Pract Res Clin Rheumatol 17:717–727
14. DeLisa F, Sylvia Frisancho-Kiss S, Rose NR (2008) Sex differences in autoimmune disease from a pathological perspective. Am J Pathol 173:600–609

15. Papadopoulos NG, Alamanos Y, Voulgari PV, Epagelis EK, Tsifetaki N, Drosos AA (2005) Does cigarette smoking influence disease expression, activity and severity in early rheumatoid arthritis patients? Clin Exp Rheumatol 23:861–866
16. Choy E (2012) Understanding the dynamics: pathways involved in the pathogenesis of rheumatoid arthritis. Rheumatology 51(suppl 5):3–11
17. Sacre SM, Drexler SK, Foxwell BM (2004) Toll-like receptors and rheumatoid arthritis synovial fibroblasts. Stimulated by toll-like receptors 2 ligand. J Immunol 172:1256–1265
18. Kinne RW, Brauer R, Stuhlmüller B, Kinne EP, Burmester GR (2000) Macrophages in rheumatoid arthritis. Arthritis Res 2:189–202
19. Lefevre S, Knedla A, Tennic C et al (2009) Synovial fibroblasts spread rheumatoid arthritis affected joints. Nat Med 15:1414–1420
20. Huizinga TW, Pincus T (2010) Rheumatoid arthritis. Ann Intern Med 153:1–16
21. Turesson C, Matteson EL (2011) Extraarticular features of rheumatoid arthritis and systemic involvement. In: Hochberg MC, Silman AJ, Smolen JS, Weinblatt ME, Weisman HM (eds) Rheumatology, 5th edn. Mosby-Elsevier, Philadelphia, pp 839–847Ç
22. Colglazier CR, Sutej PG (2005) Laboratory testing in the rheumatic diseases. South Med J 98:185–191
23. Van Boekel MA, Vassenaar ER, van dem Hoogen FH, van Venrooij WJ (2002) Autoantibody system in rheumatoid arthritis: specificity, sensitivity and diagnostic value. Arthritis Res 4:87–93
24. Mallya RK, de Beer FC, Berry H, Hamilton ED, Mace BE, Pepys MB (1982) Correlation of clinical parameters of disease activity in rheumatoid arthritis with serum concentration of C-reactive protein and erythrocyte sedimentation rate. J Rheumatol 9(2):224–228
25. Ostergaard M, Ejbjerg B, Szkudlarek M (2005) Imaging in early rheumatoid arthritis: roles of magnetic resonance imaging, ultrasonography, conventional radiography and computed tomography. Best Pract Res Clin Rheumatol 9:91–116
26. Heijde VD (1999) How to read radiographs according to the Sharp/van der Heijde method. J Rheumatol 26:743–745
27. Szkudlarek M (2010) Rheumatoid arthritis. In: Wakefield RJ, Dagostina MA (eds) Essential applications of musculoskeletal ultrasound in rheumatology. Saunders-Elsevier, Philadelphia, pp 155–163
28. Aletaha D, Neogi T, Silman AJ et al (2010) Rheumatoid arthritis classification criteria: an American College of Rheumatology/European League Against Rheumatism collaborative initiative. Ann Rheum Dis 69:1580–1588
29. Prevoo ML, van't Hof MA, Kuper HH, van Leeuwen MA, van de Putte LB, van Riel PL (1995) Modified disease activity scores that include twenty-eight-joint counts. Development and validation in a prospective longitudinal study of patients with rheumatoid arthritis. Arthritis Rheum 38:44–48
30. van Gestel AM, Prevoo ML, van't Hof MA, van Rijswijk MH, van de Putte LB, van Riel PL (1996) Development and validation of the European League Against Rheumatism response criteria for rheumatoid arthritis. Comparison with the preliminary American College of Rheumatology and the World Health Organization/International League Against Rheumatism Criteria. Arthritis Rheum 39:34–40
31. Aletaha D, Smolen J (2005) The Simplified Disease Activity Index (SDAI) and the Clinical Disease Activity Index (CDAI): a review of their usefulness and validity in rheumatoid arthritis. Clin Exp Rheumatol 23:100–108
32. Kuçukdeveci AA, Sahin H, Ataman S, Griffiths B, Tennant A (2004) Issues in cross-cultural validity: example from the adaptation, reliability, and validity testing of a Turkish version of the Stanford Health Assessment Questionnaire. Arthritis Rheum 5:14–19
33. Fries JF, Spitz P, Kraines RG, Holman HR (1980) Measurement of patient outcome in arthritis. Arthritis Rheum 23:137–145
34. Ware JE Jr, Sherbourne CD (1992) The MOS 36-item short-form health survey (SF-36). I. Conceptual framework and item selection. Med Care 30:473–483
35. Wolfe F, Mitchell DM, Sibley JT et al (1994) The mortality of rheumatoid arthritis. Arthritis Rheum 37(4):481–494
36. Singh JA, Furst DE, Bharat A, Curtis JR, Kavanaugh AF et al (2012) Update of the 2008 American College of Rheumatology recommendations for the use of disease-modifying antirheumatic drugs and biologic agents in the treatment of rheumatoid arthritis. Arthritis Care Res 2012(64):625–639
37. Ataman S, Borman P, Evcik D, Aydog E, Ayhan F et al (2011) Management of rheumatoid arthritis: consensus recommendations from the Turkish league against rheumatism. Turkish J Rheumatol 26:273–294
38. Stenström CH (1994) Therapeutic exercise in rheumatoid arthritis. Arthritis Care Res 44:515
39. Belza B, Minor M (2011) Interdisciplinary care in the management of rheumatoid arthritis. In: Hochberg MC, Silman AJ, Smolen JS, Weinblatt ME, Weisman HM (eds) Rheumatology, 5th edn. Mosby-Elsevier, Philadelphia, pp 915–921
40. Gotzsche PC, Johansen HK Short-term low-dose corticosteroids vs placebo and nonsteroidal antiinflammatory drugs in rheumatoid arthritis. Cochrane Database Syst Rev 004;(3):CD000189
41. Smolen JS, Landewé R, Breedveld FC, Dougados M et al (2010) EULAR recommendations for the management of rheumatoid arthritis with synthetic and biological disease-modifying antirheumatic drugs. Ann Rheum Dis 69:964–975
42. Cutolo M, Sulli A, Pizzorni C, Seriolo B (2001) Anti-inflammatory mechanisms of methotrexate in rheumatoid arthritis. Ann Rheum Dis 60:729–735
43. Mclnnes IB, Vieria-Sousa E, Fonseca JE (2012) Rheumatoid arthritis treatment. In: Bijlsma JWJ (ed) EULAR textbook of rheumatic diseases, 1st edn. BMJ Group, London, pp 232–254
44. Wiens A, Venson R, Correr CJ, Otuki MF, Pontarolo R (2010) Meta-analysis of the efficacy and safety of adalimumab, etanercept and infliximab for the

treatment of rheumatoid arthritis. Pharmacotherapy 30:339–353
45. Cohen S, Hurd E, Cush J, Schiff M, Weinblatt ME, Moreland LW et al (2002) Treatment of rheumatoid arthritis with anakinra, a recombinant human interleukin-1 receptor antagonist, in combination with methotrexate: results of a twenty-four-week, multicenter, randomized, double-blind, placebo-controlled trial. Arthritis Rheum 46:614–624
46. Martín Mola E, Balsa A, Martínez Taboada V, Sanmartí R, Marenco JL et al (2013) Abatacept use in rheumatoid arthritis: evidence review and recommendations. Reumatol Clin 9:5–17
47. Cutolo M (2013) The kinase inhibitor tofacitinib in patients with rheumatoid arthritis: latest findings and clinical potential. Ther Adv Musculoskelet Dis 5:3–11
48. Clement ND, Breusch SJ, Biant LC (2012) Lower limb joint replacement in rheumatoid arthritis. J Orthop Surg Res 7:27
49. Leon L, Abasolo L, Carmona L et al (2013) Orthopedic surgery in rheumatoid arthritis in the era of biologic therapy. J Rheumatol 40(11):1850–1855
50. Aaltonen KJ, Virkki LM, Jämsen E et al (2013) Do biologic drugs affect the need for and outcome of joint replacements in patients with rheumatoid arthritis? A register-based study. Semin Arthritis Rheum 43(1):55–62
51. De Smet L (2006) The distal radioulnar joint in rheumatoid arthritis. Acta Orthop Belg 72(4):381–386
52. Papp SR, Athwal GS, Pichora DR (2006) The rheumatoid wrist. J Am Acad Orthop Surg 14(2):65–77
53. Abboud JA, Beredjiklian PK, Bozentka DJ (2003) Metacarpophalangeal joint arthroplasty in rheumatoid arthritis. J Am Acad Orthop Surg 11(3):184–191
54. Kauffman JI, Chen AL, Stuchin S, Di Cesare PE (2003) Surgical management of the rheumatoid elbow. J Am Acad Orthop Surg 11(2):100–108
55. Chen AL, Joseph TN, Zuckerman JD (2003) Rheumatoid arthritis of the shoulder. J Am Acad Orthop Surg 11(1):12–24
56. Amin A, Cullen N, Singh D (2010) Rheumatoid forefoot reconstruction. Acta Orthop Belg 76(3): 289–297
57. Borenstein D (2006) Inflammatory arthritides of the spine: surgical versus nonsurgical treatment. Clin Orthop Relat Res 443:208–221
58. Zwartelé RE, Witjes S, Doets HC, Stijnen T, Pöll RG (2012) Cementless total hip arthroplasty in rheumatoid arthritis: a systematic review of the literature. Arch Orthop Trauma Surg 132(4):535–546
59. Feldman DE, Bernatsky S, Houde M et al (2013) Early consultation with a rheumatologist for RA: does it reduce subsequent use of orthopaedic surgery? Rheumatology (Oxford) 52(3):452–459
60. Gougoulias N, Khanna A, Maffulli N (2010) How successful are current ankle replacements? A systematic review of the literature. Clin Orthop Relat Res 468(1):199–208
61. Howe CR, Gardner GC, Kadel NJ (2006) Perioperative medication management for the patient with rheumatoid arthritis. J Am Acad Orthop Surg 14(9):544–551

Osteonecrosis and Metabolic Bone Disorders

32

Ahmet Turan Aydın

Abstract

Osteonecrosis has been defined as death of bone and bone marrow cell as a result of ischemia. Bone matrices (organic and inorganic) are not affected. Possible mechanism is vascular compromise of the bone and non-traumatic etiology and it is not well understood. Studies suggested that osteocyte necrosis occurs after 2–3 h of anoxia. However, 24–72 h are necessary before histological signs are apparent. The magnitude of clinical symptoms and extended disability caused by osteonecrosis is related to size and anatomic location of the lesion. The histological changes that occur during bone necrosis and bone remodeling are associated with characteristic finding on plain radiographs and MR imaging.

Metabolic bone diseases result due to imbalances between bone formation and resorption and from impairments in mineralization of the bone. These disorders may be caused by cellular dysfunctions, genetic and nutritional defects, menopause, aging, drugs, renal and hepatic diseases, and endocrinopathies. These disorders manifest themselves as general musculoskeletal pain, deformities, stress fractures, and osteoporotic fractures caused by minor traumas. Clinical and radiological findings are efficient diagnostic tools for differential diagnosis. Histopathologic studies are made for diagnosis and differential diagnosis of various metabolic bone disorders and especially for academic purposes.

Clinical Relevance

The use of bisphosphonate in the treatment of avascular necrosis of the femoral head (Fig. 32.1).

A 29-year-old man admitted to our outpatient clinic with bilateral hip pain and limp which was prominent left side. One

A.T. Aydın, MD
Department of Orthopaedic Surgery and Traumatology, Memorial Antalya Hospital, Zafer Mah. Yildirim Beyazit Cad. No: 69, Kepez-Antalya 07025, Turkey
e-mail: ataydin07@gmail.com

F. Korkusuz (ed.), *Musculoskeletal Research and Basic Science*,
DOI 10.1007/978-3-319-20777-3_32

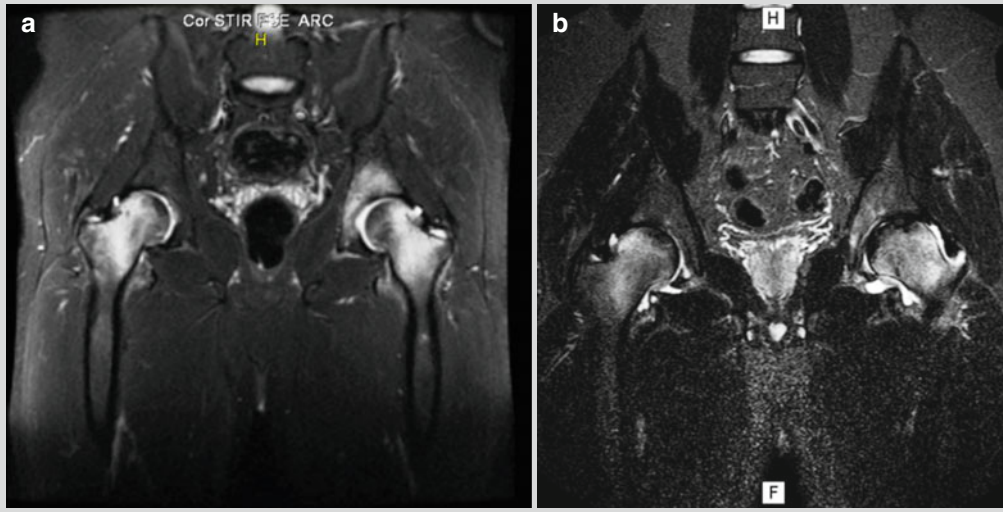

Fig. 32.1 (**a**) Notice the left-sided acetabulum and proximal femur regions' bone marrow edema (fat-suppressed T2-weighted coronal image). This scan was obtained at the beginning of bisphosphonate treatment. (**b**) Three months after the bisphosphonate treatment of the patient, left-sided acetabulum and bilateral proximal femoral regions' bone marrow edema was apparently subsided (resolved)

year before he underwent cortisol treatment after the intracranial surgery due to situation of intracerebral hemorrhage which caused by intracerebral vascular malformation. The patients' complaints have started 1 month before the admission to our outpatient clinic. The physical examination revealed limited range of motion at flexion and rotations of the hips. The Trendelenburg test was also positive. MRI fat-suppressed T2-weighted coronal images were consistent with bone marrow edema at left acetabulum and bilateral proximal femoral region.The patient was diagnosed as cortisol-induced osteonecrosis under the lights of MRI imagining findings and well-documented anamnesis. The weekly 70 mg alendronate/oral and vitamin D3-calcium (oral way) treatment were initiated. The nonweight bearing with the crutches (only finger touch was allowed) was recommended. The patient uneventfully healed with the evidence of non-painful hips and resolution of limited range of motion. After the 3-month treatment with bisphosphonates, the control MRI revealed that even if the total resolution of the bone marrow edema does not exist, a significant amount of edema was subsided especially at the acetabulum and at both hips and after the treatment. The regions of avascular necrosis were also precipitated. After this clinical and radiological advancement of the patient, 1-year bisphosphonate treatment was considered.

Avascular necrosis of the femoral head (ANFH) can cause structural failure of bone with collapse and dysfunction of the hip. Collapse of the femoral head was observed in 75 % of cases of avascular necrosis of the femoral head within 3 years [16]. According to Aaron et al., more than 50 % of patients with avascular necrosis of the femoral head require THR within 3 years of diagnosis [17].

Statins [18], anticoagulants [19], prostacyclin [20], and bisphosphonates (Bps) [21] have been used to treat osteonecrosis of the hip. The theoretical benefit of statins is based on the association of increased fat cell size with an increased risk of the development of osteonecrosis of the hip. Anticoagulants inhibit the aggregation of platelets and enhance blood flow to ischemic areas of bone. Prostacyclin promotes bone regeneration on a cellular or systemic level but fail to show efficacy in the advanced stages of ANFH. Bps are potent antireabsorptive agents that act by

inhibiting the action of mature osteoclasts in the bone, which theoretically normalized the uncoupled bone remodeling contributing to femoral head collapse.

Agarwala et al. first reported the efficacy of alendronate, a bisphosphonate, in the treatment of avascular necrosis of the femoral head and showed that it not only improved the symptoms but also retarded progression of the disease and reduced the rate of collapse of the femoral head [22]. Other studies have shown similar results and bisphosphonates are now considered to be one of the standard options of treatment for avascular necrosis of the femoral head [23]. Favorable long-term results were also presented by Agarwala's 10-year study in treated patients even after alendronate discontinuation [24]. In addition, there were no severe adverse effects associated with alendronate treatment observed during short- or long-term follow-up. Another finding of the current review is that although patients in all stages appeared to have potential benefit from alendronate treatment, the application in early AVN with small-size lesion was suggested by most of the included studies. Specially, as shown in Chen's study, when extensive osteonecrosis (stages II C and III C) was radiographically presented, alendronate did not have any benefits. Thus, the efficacy of alendronate for AVN with large necrotic legions should be considered more carefully [25].

Osteonecrosis

Osteonecrosis (ON) is the ischemic necrosis of the bone and bone marrow. Ischemia only affects the cells and not the organic or inorganic matrix. It might develop in every bone and every part of the bone. Clinical status is determined by the ischemic location on the bone. While an ischemic island on a spongious bone is symptom-free, a necrosis toward subchondral bone (such as femur head avascular necrosis) shows quite dramatic clinical features.

Etiopathogenesis

ON is usually caused by the disturbed blood flow in the bone due to vascular trauma or vascular embolism. The main causes can be summarized by the mnemonic "VINDICATE" (Table. 32.1).

Most frequent is the association with prolonged corticosteroid therapy or excessive alcohol intake. Other risk factors include hyperlipidemias, coagulopathies (thrombophilia, hypofibrinolysis), abnormal red blood cells (sickle cell), dysbarism, HIV infection, smoking, and genetic factors [1, 2]. Many etiological factors are responsible for vascular damage. These mechanisms are mechanical interruption, thrombotic occlusion, or extravascular compression (Fig. 32.2).

Table 32.1 Causes of avascular necrosis

	Causes
V	**V**ascular
IN	**In**fection
D	**D**rugs
I	**I**nflammation
C	**C**ongenital
A	**A**utoimmune
T	**T**rauma
E	**E**ndocrine

Factors for Pathogenesis

1. Idiopathic (bilateral in 40–50 %): Most of the time, there is no clear reason for pathogenesis. Coagulation anomalies might be the cause in this group.
2. Arterial tears: In dislocations and fractured bones
3. Arteriolar embolism: Embolism, sickle-cell crisis, and decompression sickness (caisson disease)

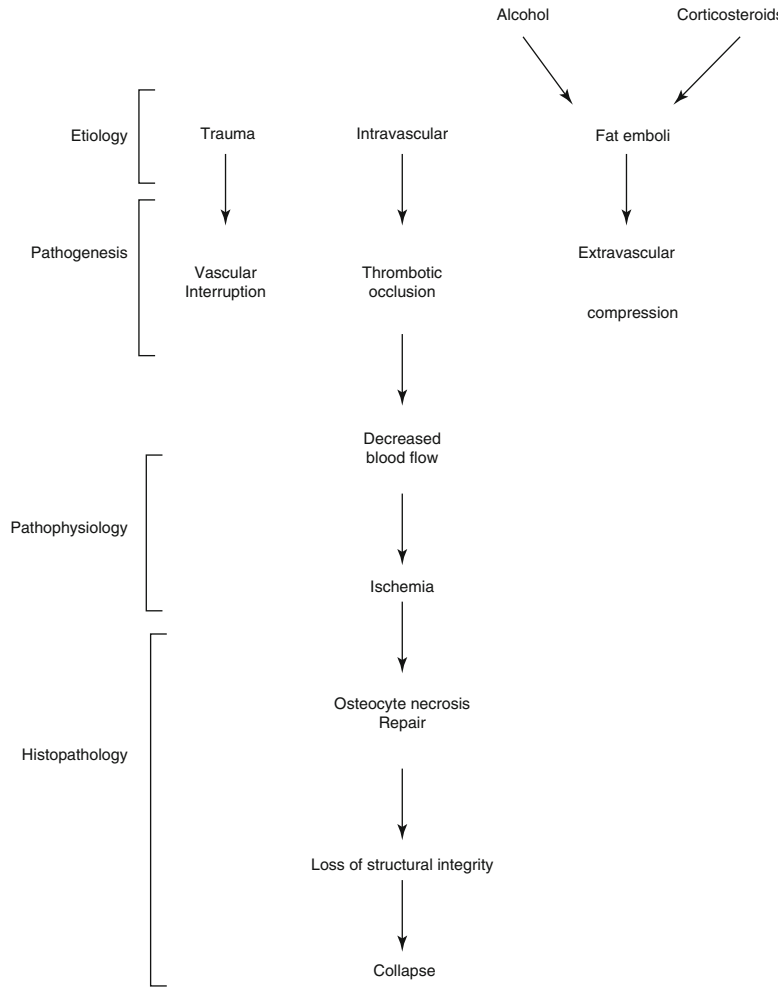

Fig. 32.2 Many etiological factors are responsible for vascular damage. These mechanisms are mechanical interruption, thrombotic occlusion, or extravascular compression [3]

4. Vascular wall damage: Vasculitis (SLE) and radiation
5. Capillary embolism due to fat tissue infiltration of bone marrow:
   (a) Steroid treatment (>30 mg prednisolone, >30 days, 37 % risk, 80 % bilateral)
   (b) Heavy alcohol abuse (20 %)
   (c) Gaucher's disease (Gaucher's macrophages filling the bone marrow space)
   (d) Pancreatitis
   (e) Hyperlipidemia
   (f) Others: Renal transplant, diabetes, sepsis, inflammatory bowel disease, and hematological diseases

To sum up, in 40 % of the cases, the pathogenesis is unknown, 30 % are caused by cortisone usage, and 20 % by alcohol abuse and 10 % have other reasons.

Pathology

Necrosis happens when the bone tissue is not properly nourished. This does not affect the organic-inorganic matrix. The hematopoietic cells are most sensitive to anoxia. Bone marrow and osteocyte necrosis develops after 2–3 h of ischemia and is permanent [3]. Histological differences can be seen only after 24–72 h (Fig. 32.3).

Repair of the Dead Bone

An inflammatory response develops against dead bone marrow. This is followed by chemotaxis and arrival of the mesenchymal cells with vascular generation to repair zone. In the literature, resorption of the dead bone tissue and new bone formation is named as "creeping substitution."

The repair period is determined by the necrotic area size and whether the necrotic bone is spongious or cortical type. In spongious bones, this situation can be fixed by the new bone tissue covering the dead bone tissue directly. However, in cortical bones, this happens with a mechanism named "*osteoclast cutting cone*" (Fig. 32.4). In this mechanism, osteoclasts get into the dead bone with vascular extensions, removing the dead bone tissue, meanwhile mesenchymal cell-developed osteoblasts fill the area with new bone tissue. In direct radiological viewing studies, early ON can be seen as a local density decrease in the necrotic areas. The previous density levels are achieved after the bone healing in 12–18 months. MRI studies however show the bone marrow edema as hypointense in T1 and hyperintense signals in T2 sequence.

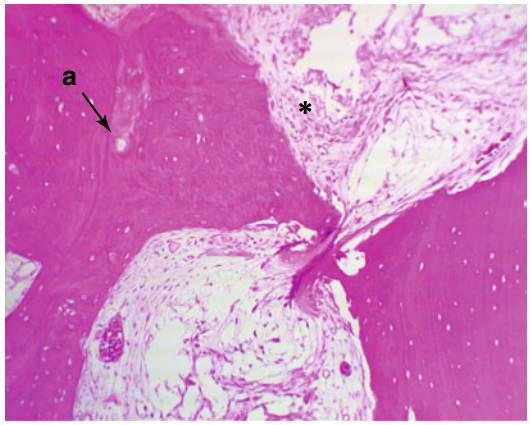

Fig. 32.3 Early stage of osteonecrosis, a. empty lacunas due to osteocyte death, *necrotic bone marrow (Courtesy of Gürer İ MD)

Dead bone tissue has lost its living cells and vitality. Since there are no living cells present, bone turnover cycle does not happen in necrotic area. For this reason, stress fractures or necrotic bone collapse can be seen with physiological stress in the necrotic area. Those changes are especially important in subchondral bones. The collapse and destruction of subchondral bone (*crescent sign*) (Fig. 32.5) disturb the integrity of the joint such as hip joint and causes early arthrosis. If the subchondral bone is protected from the stress, microfractures, and collapses, the joint can be saved by the repair of dead bone

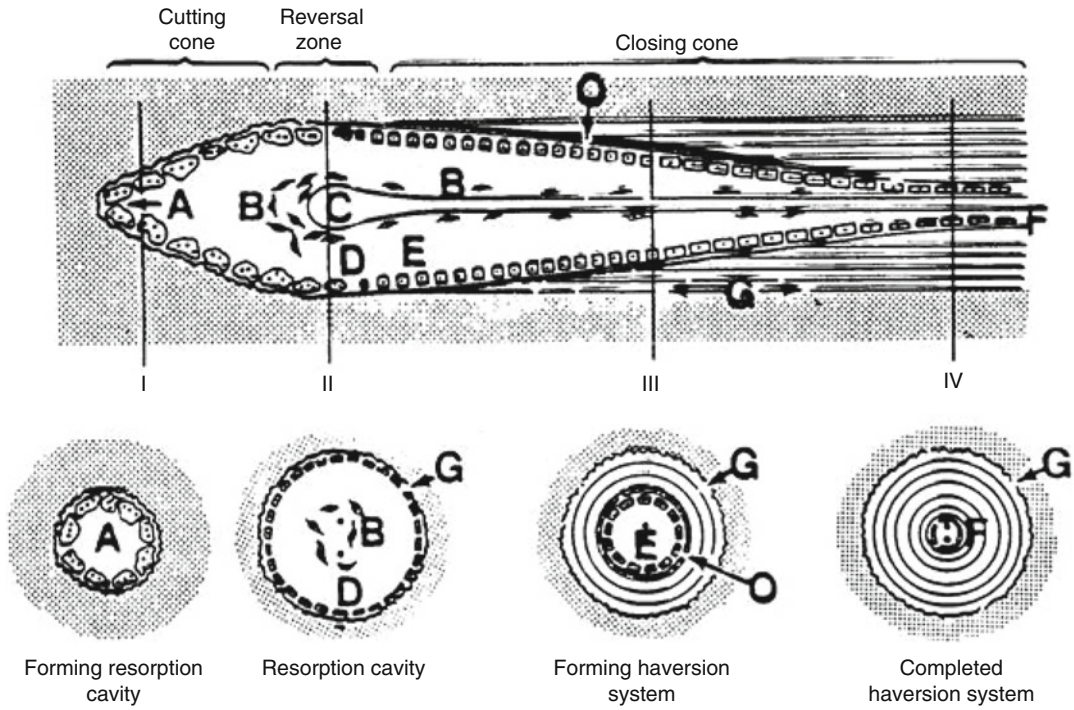

Fig. 32.4 Osteoclast cutting cone in repairing and reshaping the dead bone. Osteoclasts bore the dead matrix like a tunnel-boring device in front of a vascular extension and osteoblasts cover the surface with bone tissue. This is called "creeping substitution" (http://www.mobile-appscentre.co.uk/healthapp/author/admin/)

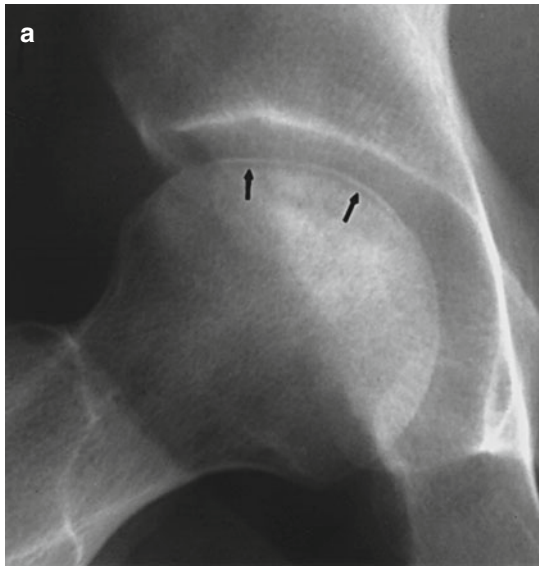

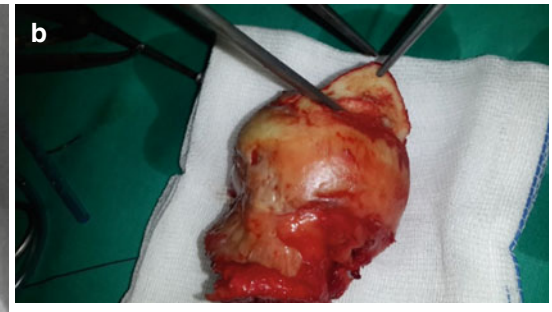

Fig. 32.5 Separation of subchondral bone (*crescent sign*). (**a**) X-ray (*arrows*) and pens show the separation of subchondral bone. (**b**) Intraoperative photo

tissue. The repair tissue that covers the subchondral bone (Fig. 32.6) can sometimes inhibit the vascular entry to the bone [4]. In osteonecrosis of femoral head (ONFH), multiple drilling and vascular-avascular fibular grafts are used to facilitate the vascular entry to dead zone and prevent collapses.

Clinical Features and Imaging

Clinical symptoms and features show the location and area width of the necrosis. Small, metaphyseal area and spongious bone-located necrosis shows no symptoms, yet necrosis that extends toward subchondral bone shows clear features. If the area of involvement is small (<25 % of the femoral head) and if it is not close to the articular surface, the repair process may be sufficient to maintain the structural integrity of bone. Small medial lesion of femoral head has an especially good prognosis [1].

Imaging studies can show the different stages of osteonecrosis (early stage, fragmentation, repair, and late) by changes in density, subchondral separation and fragmentation, repair, and arthrosis development. Radiographic studies of avascular necrosis in the early stages usually appear normal. The earliest radiographic sign of osteonecrosis is the presence of radiolucent

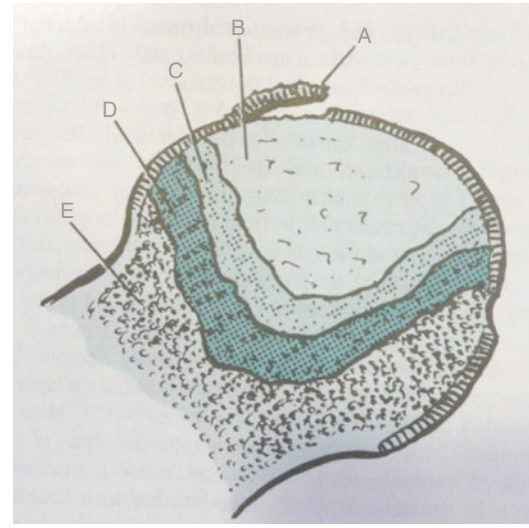

Fig. 32.6 Avascular necrosis pathology. *A* Joint cartilage and subchondral separation. *B* Necrotic bone. *C* Reactive connective tissue surrounding dead tissue (keeps vascular tissue out of dead bone zone). *D* Reactive bone tissue that limits the dead bone. *E* Normal bone tissue (Miller [4])

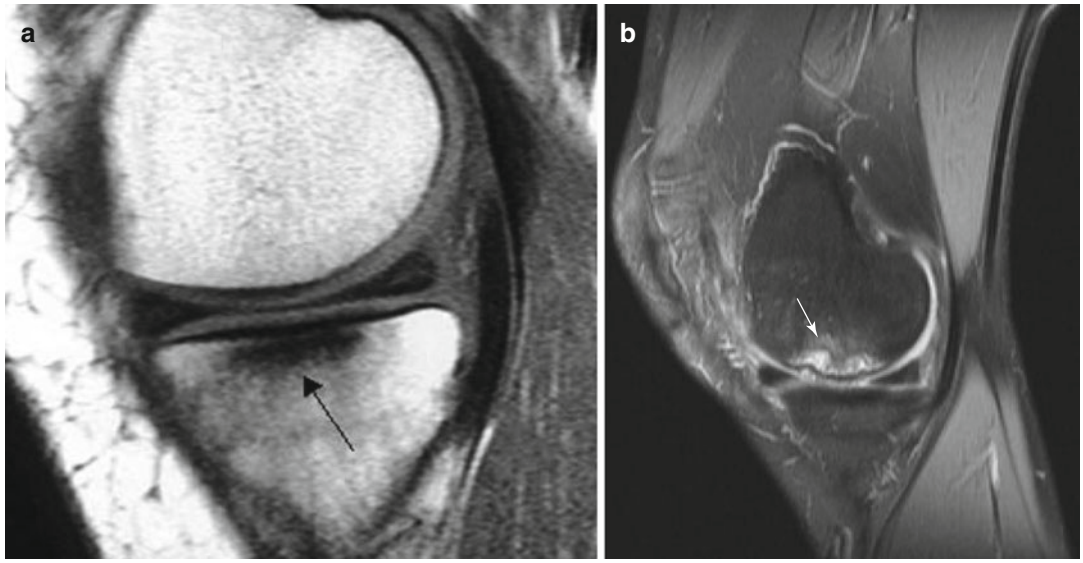

Fig. 32.7 (**a**) T1 sequence shows osteonecrosis area as hypointense (*arrow*). (**b**) T2 sequence shows osteonecrosis area as hyperintense (*white arrow*)

crescent (the so-called crescent sign) (Fig. 32.5a). In the later stages, it appears relatively sclerotic due to nearby living bone becoming low density secondary to reactive hyperemia. Ficat and Arlet [5] described the first staging system. They described four stages based on plain radiographs of the affected hip. Stage I indicated a clinical suspicion of ONFH with no changes noted on X-ray films. In stage II there are changes, including osteosclerosis and/or cysts with conservation of the normal contour of the femoral head. The crescent sign characterizes stage III, which is seen as subchondral collapse or flattening of the femoral head on plain radiographs. Stage IV consists of narrowing of the joint space and secondary degenerative changes within the acetabulum.

MRI of osteonecrosis can show changes earlier than radiography or CT. The sensitivity and specificity of MRI are also very high. MRI can show the ischemic bone marrow changes faster than scintigraphy. Ischemic area shows itself as hypointense signals in T1-weighted images (Fig. 32.7a) and hyperintense in T2-weighted images (Fig. 32.7b) due to bone marrow edema. When present, the double-line sign on the T2-weighted image is essentially pathognomonic for osteonecrosis [1].

Metabolic Bone Disorders

Metabolic bone diseases are systemic diseases that affect the bone development, mineralization, and remodeling. They make the bone easily breakable and deformable by causing disruptions in bone mass, composition, and remodeling.

Bone mass is the weight of the bone unit volume. It is not possible to weigh the bone in vivo. Bone mass is determined by bone mineral density measurements and changes in the radiological density of the bone (osteopenia, osteosclerosis). Bone mass is mainly affected by osteoblastic activity and the changes in bone turnover cycle. The most important metabolic disease that affects bone mass is osteoporosis. In osteoporosis, bone mass is reduced and bones are easily breakable.

Bone composition is the rate of mineralized and demineralized matrix (Fig. 32.8). This is directly connected to the matrix mineralization. Metabolic bone diseases affect the mineral metabolism, therefore changing bone composition. In rickets-osteomalacia syndromes, demineralized bone matrix rate is increased and bone composition is changed. In this disease group, the bones become softer since the bone matrix is not properly mineralized and could be easily deformed without breaking.

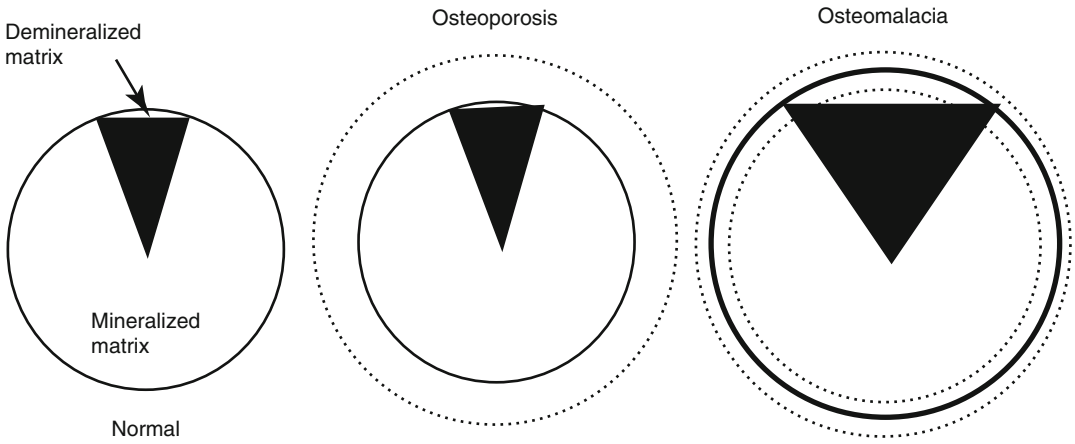

Fig. 32.8 Composition of the bone. In osteoporosis, there is a loss of mass without the composition change. On osteomalacia, the mass can either increase or decrease. The main change is the increased demineralized matrix amount (From Netter [6])

Fig. 32.9 Bone remodeling cycle (http://ns.umich.edu/Releases/2005/Feb05/bone.html)

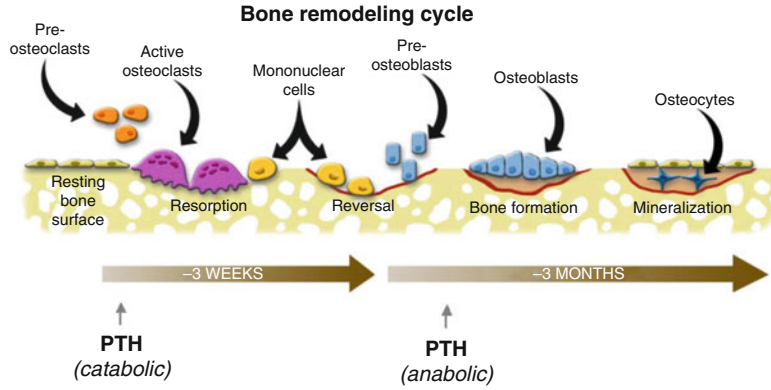

Bone remodeling is controlled by the bone remodeling cycle (Fig. 32.9). Bone remodeling cycle is one of the most important homeostasis mechanisms of the body. Development and persistency of the bone are regulated by this mechanism in addition to fracture healing, repair of the dead bone areas and grafts. The most typical diseases which cause a disruption in the local and wide bone remodeling mechanism are Paget's disease and osteopetrosis. In both diseases, bone mechanic properties were changed and bone can be easily fractured and deformed.

Cellular Biology [7]

The development and change of bone mass are by this mechanism. In bone remodeling cycle, osteoblasts, osteoclasts, and osteocytes play an active role.

Osteoblasts synthesize the osteoid (type I collagen) tissue which is bone matrix. They are the primary bone-building cells and develop from mesenchymal stem cell. They synthesize the osteoid matrix and control the mineralization of bone matrix in addition to calcium-phosphate balance of the body. They also secrete osteocalcin and alkaline phosphatase. By activation of osteoclasts, they are also responsible for the bone resorption and regulation. They contain parathyroid, thyroid, and growth hormone receptors in addition to estrogen, androgen, and vitamin D. They can produce local cytokines, growth hormones (IGF, PDGF, bFGF, TGF-b), and bone morphogenetic factor (BMP).

Osteoclasts are responsible for bone resorption. They differentiate from hematopoietic stem cells and develop from monocytes. Osteoblasts play an active role in osteoclast activation. They have receptors for calcitonin, colchicine, and gamma-interferon receptors and answer directly.

Osteocytes are differentiated from osteoblasts and found in lacunas within the matrix. They cannot move and they connect either to each other or toward bone surface by cytoplasm extensions. They have a high nucleus/cytoplasm rate. Their function is not yet fully understood. They are thought to play a role in the transfer of mechanical signals to the bone.

Bone Remodeling Cycle

Bone remodeling cycle starts with osteoclastic activity and bone resorption (Fig. 32.9). Osteoclasts are found in Howship's lacunas on bone resorption areas. Osteoclasts are synthesized from hematopoietic stem cells and differentiated from monocytes by the secretion of RANKL (receptor activator NF-κβ ligand) protein from osteoblastic stromal cells due to environmental triggers (BMP, 1,25-dihydroxyvitamin D, and PTH). This protein attaches to the RANK protein on osteoclast progenitor cell to differentiate the cell to osteoclasts (Fig. 32.10). Osteoprotegerin (OPG) secreted from stromal cells inhibits this pathway by connecting to RANKL. PTH, PG-E_2, and 1,25-dihydroxyvitamin D stimulate the osteoclast formation. Macrophage colony-stimulating factor (M-CSF), which is a cytokine secreted from stromal cells and osteoblasts, connects with c- fms on osteoclast progenitor cell membrane to stimulate the reproduction and fusion of those cells.

The structural integrity and mass are controlled by bone turnover cycle. Systemic and local control mechanisms are responsible for this cycle's continuity.

Systemic factors: Parathyroid hormone (PTH) is the most important hormone in turnover cycles in many of the target organs. It also plays an important role in calcium metabolism by stimulating osteoclastic resorption, increasing calcium resorption from renal tubules, and stimulating calcitriol synthesis in renal parenchyma. If

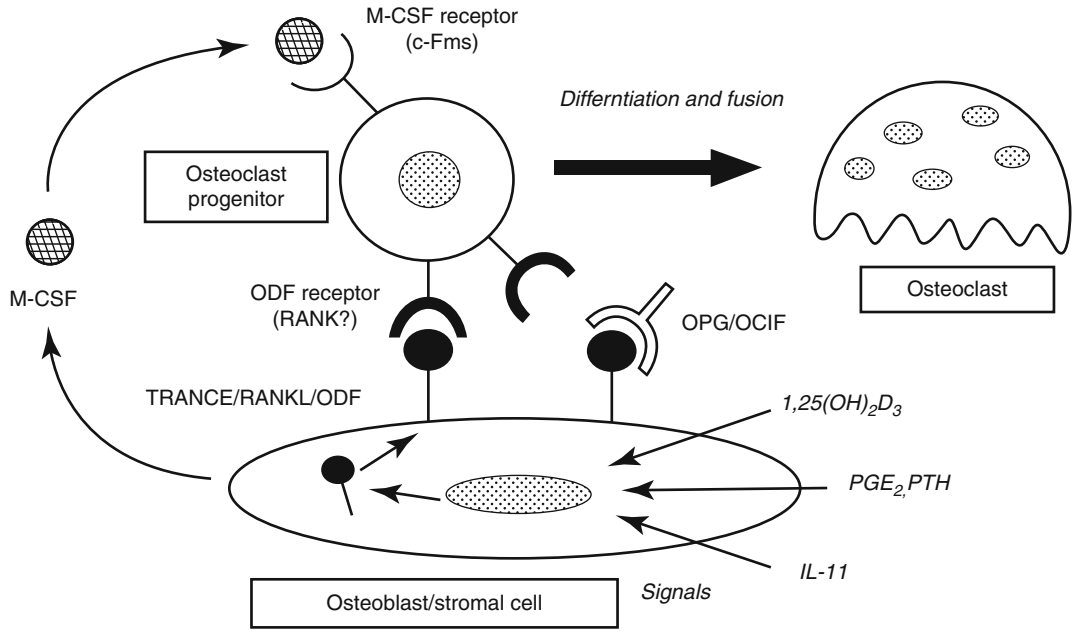

Fig. 32.10 Osteoclastogenesis. Stromal cells differentiate to osteoclast precursors to osteoclast by RANK/RANKL system. Osteoprotegerin (OPG) inhibits osteoclastogenesis by blocking this mechanism. *RANK/RANKL* reseptor activator of nuclear factor-kappa B ligand, *ODF* osteoclast differentiation factor, *OCIF* osteoclastogenesis inhibitory factor, *M-CSF* macrophage colony-stimulating factor

PTH is given constantly, the bone resorption, if it is given intermittent bone development, is stimulated. Calcitriol (Vitamin D_3) has an anabolic effect. Calcitonin inhibits the osteoclasts according to dosage to decrease bone resorption. During growth phase, growth hormones (GH, IGF-I and II) enable the growth (increase in bone mass) by their effect on endochondral ossification, growth plates, and bone turnover cycle. Thyroid hormones and glucocorticoids have both stimulating and inhibiting effects on bone cells. The most important hormones that show anabolic effect on the bones are the sex hormones. Estrogen stimulates osteoblast replication while desensitizing osteoclast progenitor cells toward RANKL, therefore limiting osteoclast production. This saves the bone mass. With menopause, this system ends and postmenopausal osteoporosis develops.

Local factors: Local factors affecting the bone turnover cycle in bone cells are the interactions between OPG and RANKL and RANK systems. RANKL/RANK system controls the change from osteoclast primary cells to osteoclasts while OPG totally inhibits this system. Systemic (hormones) and local (cytokines) factors both affect this cycle by "intersection hypothesis." TNF-alpha and IL-10 cytokine groups increase the osteoclastic function by stimulating m-CSF and RANKL production. This mechanism is effective on bone resorption against prostheses.

Mineral Metabolism and Hormonal Effects [8]

When talked about the metabolic function of the bones, one must understand the balanced storage of calcium, phosphorus, and magnesium minerals within the bones. This regulates the intracellular and serum mineral levels. This function is controlled by two hormones (PTH, vitamin D), and their target organs are the intestines, kidneys, and bones.

Calcium plays an important role on muscle and nerve function, coagulation mechanism, and many other important biological functions. The matter that gives the bone its hardness and makes up about 65 % of the total body weight is a bioceramic named calcium hydroxyapatite ($Ca_{10}(PO_4)_6(OH)_2$) made of calcium and phosphorus. Ninety-nine percent of the total calcium is deposited in the bones. Other 1 % is found on serum and cell membranes as free calcium. Serum calcium levels are between 8.5 and 10.5 mg/dl (2.1–2.6 mmol/L). Approximately 45 % of the serum calcium (1.1–1.4 mmol/L) is in ions as free calcium, which is biologically active. Keeping blood calcium levels steady is an important biological activity. The small intestines, kidneys, and bones play an important role on this function. PTH, calcitonin, and vitamin-D_3 balance calcium levels. If there is a decrease on blood calcium levels, PTH secretion allows the free calcium to be extracted from the bones and vitamin-D_3 synthesis stimulates the reabsorption of calcium from the intestines and renal tubules. Daily recommended value for calcium changes with age, sex, and gestation. Adults are typically recommended as 1,000 mg/day. This amount increases in adolescent period, pregnancy, and lactation and during advanced age period. The most important sources for daily calcium are milk and dairy products. The calcium within those products can be absorbed relatively easily and vitamin D found in small amounts makes it easier to absorb. Only 30–40 % of the calcium taken from foods can be absorbed and the rest is filtered through the kidneys. Bioavailability (absorption potential) of calcium in food is dependent on many factors. Environmental pH levels; existence of inhibiting factors such as citrates, phytates, and antacids; malabsorption syndromes; and vitamin D deficiency can be summed up as those factors. Growth and sex hormones increase the absorption levels, while corticosteroids and thyroid hormones decrease those levels. Fifty percent of the calcium filtered through the kidneys from blood is reabsorbed. Sixty to 70 % of this reabsorption happens in proximal tubes. Daily calcium levels excreted in urine are about 5–200 mg/day. High usage of salt also decreases the reabsorption of calcium in the kidneys. In addition, 15 mg/day calcium is lost from the sweat.

Phosphorus is the second most abundant mineral found in the body after calcium. It

makes up about 1 % of the total body weight (600–700 g) and 85 % of the phosphorus is found in the bone as calcium hydroxyapatite (Ca_{10} $(PO_4)_6(OH)_2$). The remaining phosphorus is found in phospholipids (70 %) as organic phosphorus and 30 % of it is found in inorganic form in soft tissues and intracellular-extracellular fluids. Inorganic phosphorus levels in the blood play an important role in many biological functions (cellular membrane activity, mitochondrial functions, thrombocyte aggregation, and such). Blood serum phosphorus levels are between 2.5 and 4.5 mg/dl (0.81–1.45 mmol/L). Regulation of phosphorus mechanism is similar to calcium. Daily recommended value also changes with the age like in calcium. The necessity for phosphorus peaks during adolescence. Daily recommended value for adults is 700–800 mg/day. Phosphorus is usually found in milk and dairy products, in addition with meat and eggs. Sixty to 70 % of the phosphorus from food is absorbed through the intestines. Environmental pH and phosphorus compounds play a determining role in absorption. PTH, vitamin D, and phytase enzyme all increase phosphorus absorption. Reabsorption of phosphorus through the kidneys is very similar to calcium mechanisms. However, enzyme groups called "phosphatonins," which are in protein form, affect the reabsorption in kidneys. Those enzymes cause phosphaturia and hypophosphatemia and decrease the absorption in the intestines by inhibiting vitamin D synthesis.

Magnesium is the fourth cation and second most abundant element in the body after potassium. It plays an important role in many biological functions and is a cofactor to over 300 enzymatic reactions. The most important of them all is to stabilize ATP structure in ATP-induced enzymatic reactions. It is also found in nerve and muscle cells to regulate their functions. Calcium contracts the muscles while potassium relaxes the muscles. About 20–28 g of magnesium can be found in an adult's body. Those are stored in bones (67 %), intracellular fluids (31–20 % in muscle cells), and extracellular fluids (1–2 %). They cover the hydroxyapatite crystal surfaces on the bones and 50 % of the magnesium can get into reactions. Nuts, seeds, grains, and green-leafed vegetables that contain chlorophyll are rich in magnesium. Blood serum level of magnesium is between 1.7 and 2.5 mg/dl (0.7–1.0 mmol/L). This is regulated by the nutritional magnesium amount, absorption in the intestines, and excretion through kidneys. PTH is the hormone that regulates the absorption in the intestines and excretion from the kidneys.

Parathyroid Hormone (PTH)

Parathyroid hormone is a polypeptide made of 84 different amino acids (Fig. 32.11) synthesized by the chief cells of parathyroid gland. Normal blood levels are between 10 and 60 pg/ml. PTH secretion is regulated by "calcium-sensitive receptors (CaSR)" that monitor serum inorganic calcium levels. It increases in hypocalcemia, hypophosphatemia, and vitamin-D_3 (calcitriol) deficiency and decreases in serious magnesium deficiencies.

PTH affects the target organs directly in bones and kidneys and indirectly (through vitamin D) in gastrointestinal system. Those can be summed up like this:

Kidney:

- Stimulates vitamin-D_3 synthesis in kidney parenchyma
- Increases reabsorption of calcium and magnesium in renal tubules and excretion of potassium, phosphorus, and bicarbonate

Bones:

- It has both an anabolic and catabolic effect on the bones according to dosage and an important hormone which regulates bone mass.
- Increases calcium and phosphorus levels by reabsorption of the bone. Even though it seems as osteoclastic resorption, this is a very complex mechanism in which PTH decreases collagen synthesis in osteoclasts, stimulating osteocytes, osteoclastogenesis, and osteoblastogenesis and inhibiting the bone capacity of calcium binding.

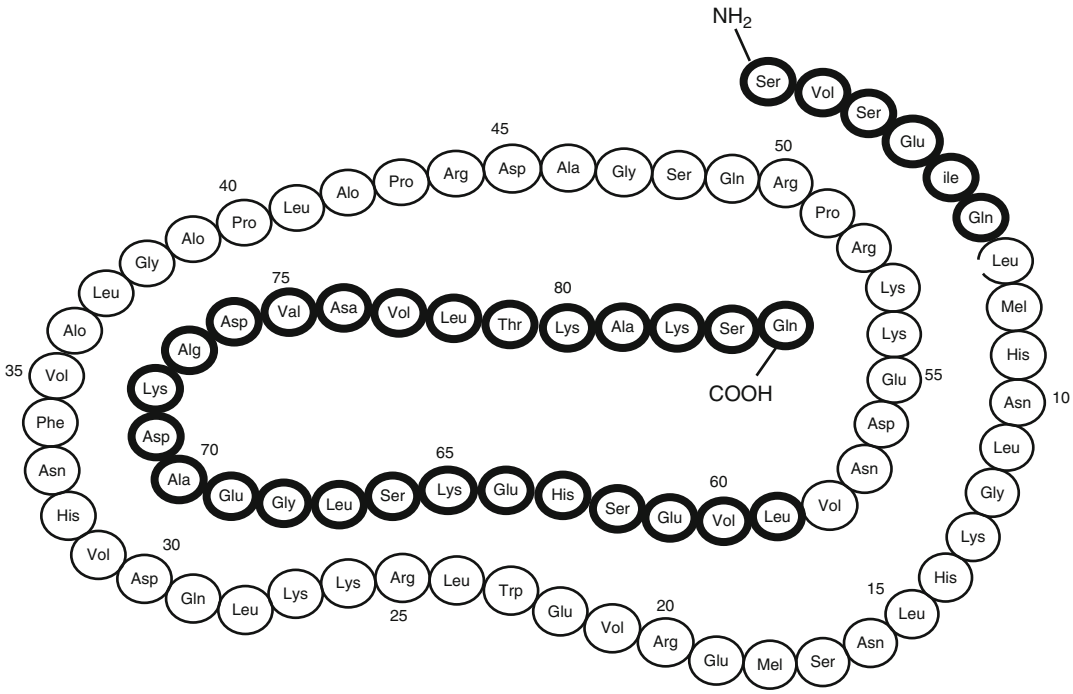

Fig. 32.11 Parathormone is a polypeptide made out of 84 amino acids. It is produced in parathyroid glands and the most important hormone in bone metabolism

Intestines:

- Increases phosphorus and calcium absorption in the kidneys. This happens indirectly by stimulating vitamin-D_3 synthesis.

PTH is one of the most important hormones of the bone metabolism. It regulates blood serum levels of calcium and phosphorus. When used intermittently in small dosages, it stimulates bone growth. By this discovery, it is used on refractory and heavy osteoporosis treatments.

Calcitonin

Calcitonin is a polypeptide made of 32 amino acids (Fig. 32.12) in thyroid gland parafollicular C-cells. It directly inhibits osteoclastic activity (decreased cell motility, shrinkage of cytoplasmic extensions, and bone resorption area). For this reason, its secretion increases with the increase in blood calcium levels. Effect mechanism is the opposite of PTH. It lowers calcium and phosphorus levels in the blood by its effects on bones and kidneys. It has no effect on the intestines.

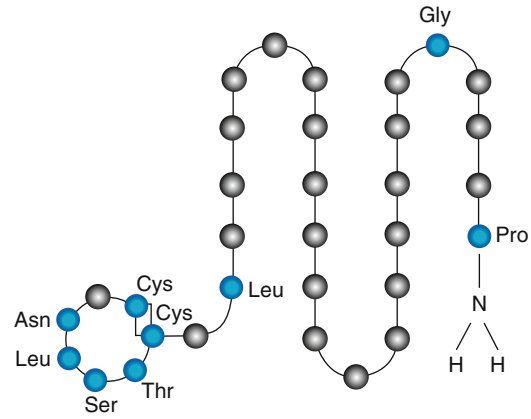

Fig. 32.12 Calcitonin is a polypeptide secreted from thyroid gland parafollicular C-cells made of 32 amino acids

Vitamin D (Active Metabolites)

Vitamin D is a steroid-structured fat-soluble vitamin taken either from the plants (D_2 – ergocalciferol) or from animal sources (D_3 – cholecarciferol). It is also synthesized by UV stimulation on the skin from 7-dehydrocholesterol. The presence of biliary acids and fats is important in its absorption

from the intestines. Active metabolites are synthesized in the liver by hydroxylation (25-hydroxy vitamin D) as "calcidiol" and in kidney parenchyma (1,25-dihydroxyvitamin D_3) as "calcitriol." Blood levels are regulated by feedback mechanisms and especially through its synthesis in the kidneys. 1-α-Hydroxylase enzyme activity is controlled by PTH, calcitonin, estrogen, prolactin, growth hormone, and blood calcium-phosphorus levels. Vitamin D activity is calculated by measuring blood serum levels of 25 or 1,25-hydroxyvitamin D. Optimal serum level is 30–60 ng/ml (75–150 mmol/L) for 25-hydroxyvitamin D. Twenty nanograms lower from this reference values shows deficiency, while over 150 ng shows toxicity.

Vitamin D has two basic physiological functions. First one is to regulate blood calcium and phosphorus levels by keeping them in the serum, and the other one is to facilitate the mineralized matrix development by moving those two ions from blood toward bones.

Other Hormones and Growth Factors

Estrogen has an anabolic effect on the bone. It helps to maintain the bone mass by inhibiting bone resorption. Also it inhibits the overgrowth of the bones by inhibiting bone build within physiological limits.

Corticosteroids inhibit bone matrix development by decreasing the absorption of calcium in the intestines and increasing excretion through the kidneys. It also suppresses osteoblast activity directly. They cause a decrease in bone density and osteoporosis by their catabolic effects.

Thyroid hormones cause bone loss and osteoporosis by speeding up bone turnover cycle in excessive amounts.

Growth hormone stimulates the bone and cartilage production by maintaining positive calcium balance and its direct anabolic effects on osteoblasts and chondroblasts. Osteoporosis develops in its deficiency.

Growth factors cause osteoclastic resorption in IL-1, IL-6, and TNF-α and bone development in IGF and TGF by stimulating osteoblastogenesis.

Osteoporosis [9]

Etiopathogenesis

Osteoporosis develops with a change in bone remodeling cycle (bone building-destruction). In an adult, a decrease in bone-building activity and an increase in bone resorption cause decreased trabeculae within the bones, thinning and breaking, therefore changing the whole architecture of the bone. Osteoporosis can be silent for years, and once it shows clinical symptoms, it manifests itself with easily fractured bones. Studies determined the osteoporosis frequency as 20 % in females and 2–4 % in males in the USA. In Turkey those values are 18.5 % for females and 9.8 % in males. Osteoporotic fractures usually happen on vertebra, femur, humeral head, and radius of the wrist bones. The fractures with highest morbidity and mortality rates are hip fractures. One-third of the cases die within a year and only one-third of them can return to their previous activity levels. The rest one-third stay bedridden and need constant caretaking.

When etiology of the disease is researched, the reasons for osteoporosis can be classified as primary (idiopathic and directly in the bone) and secondary (endocrine, gastrointestinal, collagen tissue diseases, neuromuscular diseases, due to environmental factors and medications). This approach also founds the basement of the etiological-based classification (Table 32.2). In primary osteoporosis, a very small number of the cases have an unknown cause (idiopathic, juvenile, adult). Most of the time, it is due to the changes in the bones caused by menopause (type I) and advanced age (type II). In type I osteoporosis, vertebra fractures and, in type II osteoporosis, hip fractures are more common. In secondary osteoporosis, different diseases accompany osteoporosis. The most typical example for this situation is osteoporosis after cortisone treatment.

Pathophysiology and Pathology

The basic mechanism of osteoporosis is the decreased bone-building activity (osteoblastic

activity, anabolic activity) and therefore loss in bone mass. Decreased formation in addition to increased resorption is also responsible for this. Bone mass changes vary with the age (Fig. 32.13).

However, apart from age, there are other factors such as genetic factors, sex, racial and geographical properties, diet, environmental factors, and activity level. Bone mass maximizes between 20 and 25 years of age (peak bone mass). Especially in women, there are significant losses in bone mass due to menopause around 45–55 and due to senility after 65. There are many risk factors defined for osteoporosis (Table 32.3).

Table 32.2 Etiological classification of osteoporosis

Primary	Idiopathic juvenile osteoporosis
	Postmenopausal (type I)
	Senile (type II)
Secondary	Endocrine, gastrointestinal reasons
	Inactivity
	Immobilization
	Collagen tissue diseases
	Medications (cortisone, heparin, antimetabolites, anticonvulsants)
	Bad nutritional habits (insufficient Ca ingestion, alcohol, tobacco, caffeine abuse)
Congenital	Osteogenesis imperfecta

This decrease in bone mass is more significant in trabecular bones which are affected more from bone turnover cycle in comparison with cortical bones. Those changes show themselves as decreased trabeculae within the bone, thinning and breaking in trabecular bones, and decreased thickness and widening of medullar canal in cortical bones. The changes can be easily viewed in proximal femur (Fig. 32.14), vertebra, and calcaneus in which the trabeculae are spread out for stress distribution and osteoporosis staging can be done with proper imaging studies. Singh et al. [10] developed a classification system that is based on those changes seen in proximal femur (Fig. 32.15).

There are no pathological studies for diagnosis and treatment of osteoporosis. Bone biopsies are only made for scientific studies or for differential diagnosis in patients with suspected metabolic bone diseases.

For this, a 5–8 mm graft is taken from iliac bone using a special trocar device. The sample is then reviewed either using histological (stained with or without decalcification) or histomorphometric (dynamic, tetracycline-stained) methods. In decalcified samples stained with hematoxylin-eosin (HE), osteoblast surface percentage, eroded surface, and silent area can be

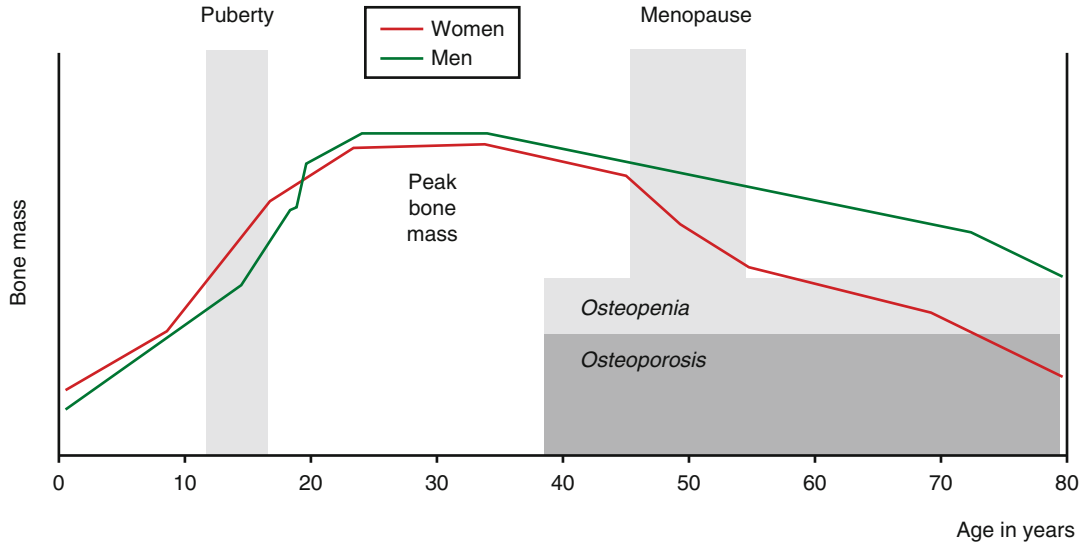

Fig. 32.13 Bone mass changes with age

Table 32.3 Osteoporosis risk factors (from IOF)

Permanent risk factors	Age
	Female sex
	Family history
	Osteoporotic fractures
	Ethnical properties
	Menopause – hysterectomy
	Long-term cortisone treatment
	Rheumatoid arthritis
	Primary or secondary hypogonadism in males
Preventable risk factors	Alcohol and smoking
	Low body mass index (BMI)
	Improper diet
	Vitamin D deficiency
	Anorexia
	Lack of exercise
	Insufficient calcium
	Frequent falling

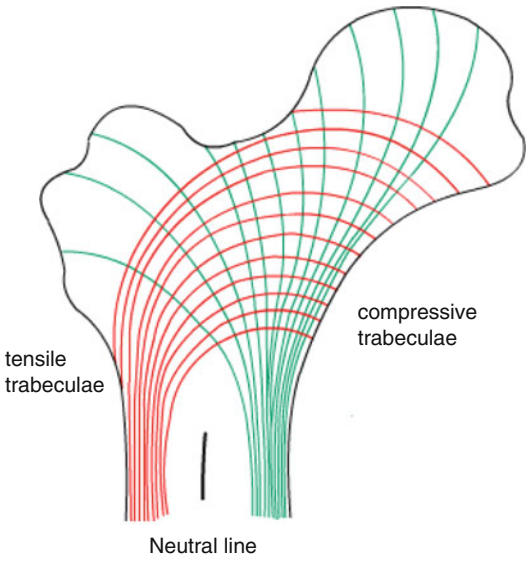

Fig. 32.14 Trabecular organization of proximal femur. Compressive trabeculae start from the head loading area toward medial cortex through the neck. They gather at the neck to produce calcar femorale. Tensile trabeculae start from the medial neck toward trochanter and lateral cortex. Tensile trabeculae are the first ones to go in osteoporosis

calculated using histomorphometric methods. However, special undecalcified bone samples prepared in plastic blocks with microtome cutting and stained with Masson's trichrome stain is very helpful in differentiating osteoporosis and osteomalacia (Fig. 32.16). In osteomalacia, demineralized matrix is stained as red on bone surface. It is also possible to research the bone surface using dynamical histomorphometric methods using autofluorescent properties of tetracycline antibiotics that attach themselves to the bone. In this method, the patient is given 500 mg tetracycline 2×1 PO for 3 days, and after 14 days, the procedure is repeated and then a sample is obtained from the iliac bone after 3–4 days. The sample is reviewed without staining or decalcification under florescent microscope. Tetracycline-stained mineralized bone, normal mineralization, and repeated tetracycline stain make two bands (Fig. 32.17). Mineralization speed is determined by measuring the distance between two tetracycline bands' midpoints, which is divided into the period (days) the tetracycline bands developed. The average value for it is 0.65 μm/day (0.4–0.9 μm/day). Thinning or disappearance of the tetracycline band shows that the bone growth is slow or halted altogether.

Rickets-Osteomalacia Syndromes [11]

Etiopathogenesis

Osteomalacia is a metabolic disease characterized by defective mineralization of osteoid and chondroid matrix. Basic defect is calcium and phosphorus deficiency. During growth phase, both bones and growth are affected (rickets), but in adults, only the bones are affected (osteomalacia). Even though these syndromes vary such as genetic defects; malnutrition; metabolic diseases that affect Ca, P, and vitamin D metabolism; and renal failure, they all have similar clinical outcomes and basic pathology, so it is better to name this group as "*rickets-osteomalacia syndromes.*" Etiological reasons include vitamin D metabolism disorders, kidney diseases, and hereditary diseases that cause hypophosphatemia.

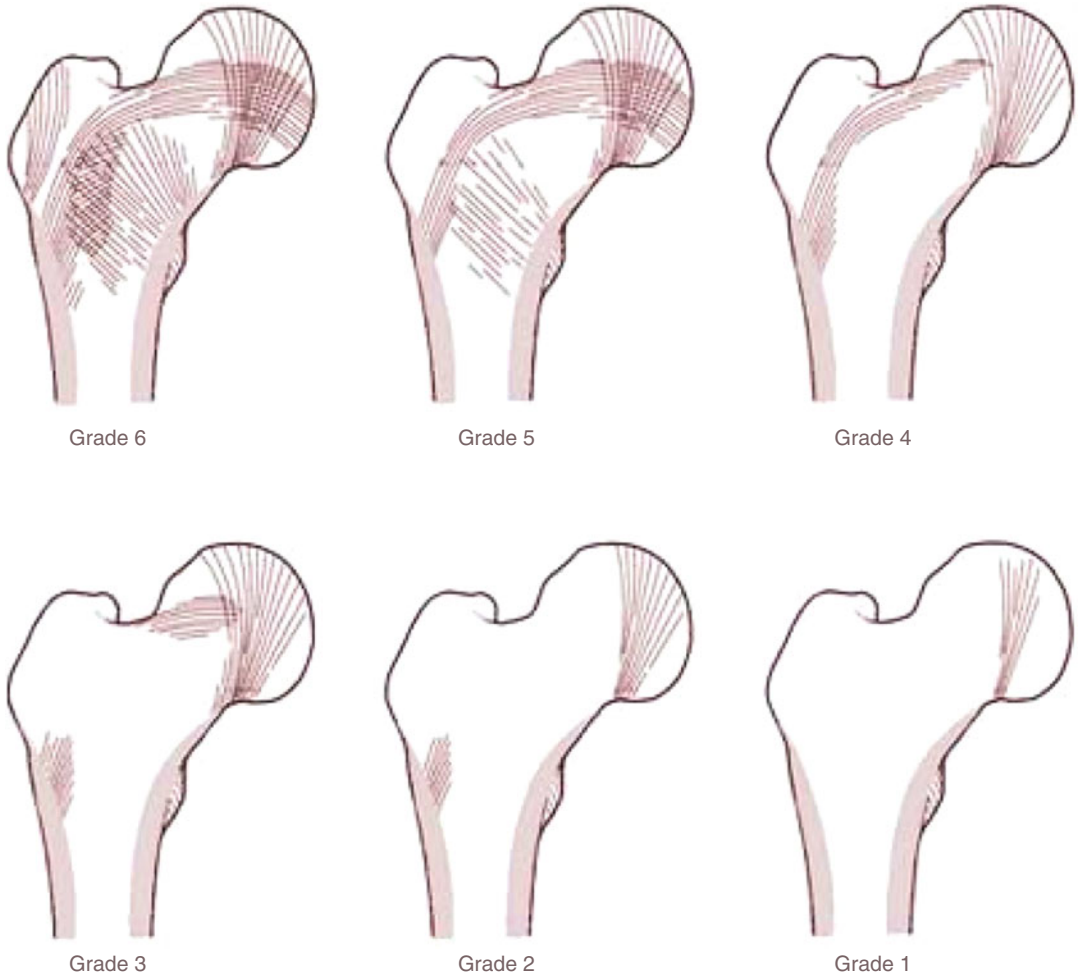

Fig. 32.15 Singh index (proximal femur), Grade I shows advanced osteoporosis; grade 6 shows the normal bone [10]

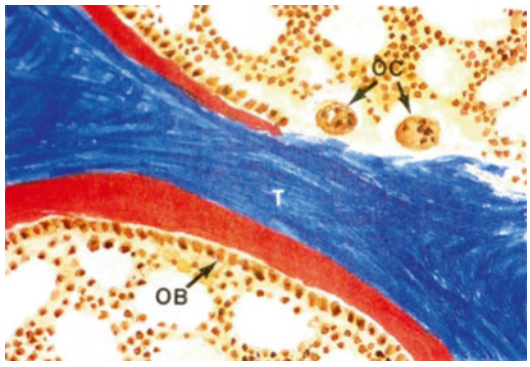

Fig. 32.16 Bone sample gathered from iliac wing and stained with Masson's trichrome stain without decalcification. *T* trabecula, *OC* osteoclast, *OB* osteoblast, *red-stained* areas show demineralized osteoid tissues (From Netter [6])

Vitamin D Metabolism Disorders

(a) *Nutritional causes*: Insufficient consumption of vitamin D, calcium, and phosphate or disorders that cause problems with calcium or phosphate absorption (insufficient biliary acids, over-consumption of phosphate, phytate, oxalate-rich foods, over usage of antacids)

(b) *Endogen synthesis disorders*: Chronic diseases (hereditary or acquired) that cause failures in liver or kidney parenchyma and long-term usage of antiepileptic medications.

(c) *Malabsorption syndromes*: Insufficient absorption of vitamin D, calcium, or phosphate from the intestines due to

Fig. 32.17 Tetracycline-stained mineralized bone, normal mineralization, and repeated tetracycline stain make two yellow bands. Mineralization speed is determined by measuring the distance between two tetracycline bands. The average value for it is 0.65 μm/day (0.4–0.9 μm/day) (From Netter [6])

gastrointestinal disorders (malabsorption syndromes, short intestine syndromes, after gastrectomy)

Kidney Diseases

(a) *Vitamin D-resistant rickets and osteomalacia* are seen in renal tubular (proximal, proximal-distal) insufficiency or renal tubular acidosis. The most common disease in this group is proximal tubular failure, also called phosphate diabetes or hypophosphatemia rickets. Three types of proximal tubular insufficiency were defined. In type I (Albright syndrome, common and sex-linked dominant genetic disorder) phosphate reabsorption, in type II glucose and phosphate, and in type III (Fanconi syndrome), amino acid reabsorptions are all defected. In another example, wide tubular defect (both proximal and distal) is seen on proximal-distal Fanconi syndrome (or Debrè-de Toni-Fanconi syndrome). There are serious defects on reabsorption of calcium, phosphate, glucose, amino acid, water, and bicarbonate. In children, dehydration, serious ricket symptoms, renal acidosis, and renal failure all indicate early kidney transplantation.

(b) *Vitamin D-dependent rickets* is a rare but clinically serious type of rickets. There is a defect on hydroxylation of vitamin-D_3 mechanism. In type I, there is an autosomal recessive defect (chromosome 12q14) in kidney 1α-hydroxylase enzyme, and in type II, there is an insensitivity in the last organ (receptor) toward 1,25-dihydroxyvitamin D.

(c) *Renal tubular acidosis* can also cause rickets and osteomalacia. Systemic acidosis caused by genetic or acquired (pyelonephritis, heavy metal poisoning) tubular insufficiency can cause rickets or osteomalacia due to usage of Ca as base. Renal acidosis mechanism is not yet fully understood and usage of calcium and phosphate can be a trivial reason for that. In those cases, secondary hyperparathyroidism that is caused by renal parenchyma failure also causes calcium and phosphate loss.

Hypophosphatasia

Hypophosphatasia is a rare, hereditary, and autosomal recessive metabolic bone disease. It is diagnosed with decreased blood alkaline phosphatase levels and increased phosphoethanolamine levels in serum and urine. It can be seen in different age groups. Infantile form has a serious prognosis and usually ends up with death. During childhood phase (after 6 months), it has a benign prognosis with sometimes spontaneous healing. Adult form is autosomal dominant. There can be a history of early childhood term tooth loss and rickets. However, they manifest itself as fractures and osteomalacia.

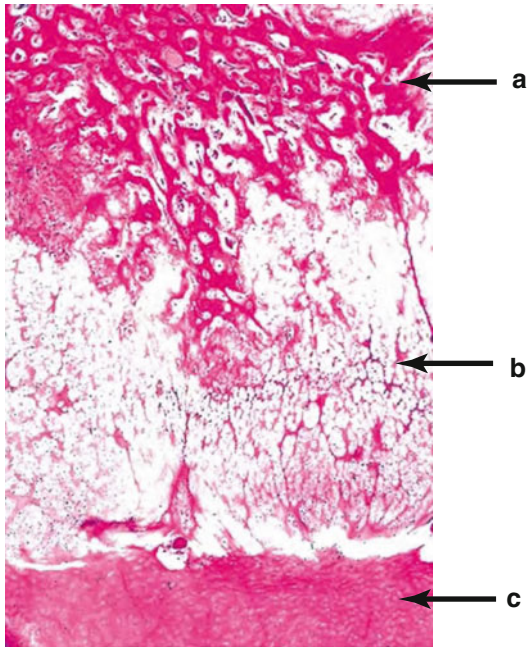

Fig. 32.18 Widening and irregularity of growth plate taken from a rachitic patient's costochondral joint. (**a**) Ossification and calcification irregularities. (**b**) Widening of growth plate. (**c**) Costal cartilage (From Bullough [12])

Pathophysiology and Pathology

In rickets and osteomalacia syndromes, pathological changes are seen on growth plate and mature bone tissue. Histological image of the growth plaque in rickets is pathognomonic (Fig. 32.18).

The height of growth plaque is increased. This is caused by the inability to produce calcified cartilage zone. For this reason, there is a constant cell reproduction in maturation zone and deposit form, thickening the growth plate. This thickening makes the growth plate more sensitive to outside forces. That's why epiphyseal displacement is common in rachitic children with minor traumas. Another effect of this change in growth plates is the slowing of the axial growth of the skeleton. Untreated and serious rickets may cause shortness. In mature bone tissue, mineralization defect of osteoid matrix changes the bone composition. Not properly mineralized bone structure softens and is more susceptible to stress fractures (Looser's zones) (Fig. 32.19a) and deformities on diaphysis of longer bones (Fig. 32.19b).

Renal Osteodystrophy [13]

Renal osteodystrophy is a metabolic bone disease seen in chronic renal failure (CRF) patients. The speed and balance of bone turnover cycle are determined by active vitamin D, PTH, and Ca/P metabolism. Those mechanisms are disrupted in CRF. For example, renal parenchyma is damaged in CRF, and therefore, 1,25-dihydroxyvitamin D_3, the most active metabolite of vitamin D, synthesis is disturbed, causing a decrease in calcium absorption in the intestines and osteoid matrix mineralization. Decreased tubular reabsorption of calcium and the effort to keep Ca-P rate lower the serum ionized calcium levels further due to phosphate retention.

Etiopathogenesis

Phosphate retention caused by creatinine clearance drop due to glomerular insufficiency causes hypocalcemia. It is worsened by the decrease in vitamin D synthesis and renal acidosis. Hypocalcemia increases PTH secretion, therefore causing secondary hyperparathyroidism. This situation also increases bone turnover and frees calcium, phosphate, and magnesium from the bones. Those changes are named as "osteitis fibrosa cystica – brown tumor." In those patients, calcifications in soft tissue such as the bones (osteosclerosis), vascular structures, kidneys, heart, and cornea are also common. Bone changes caused by secondary hyperparathyroidism and osteomalacia (Rugger-Jersey cheese image on vertebra, salt-and-pepper image on cranium and lytic, expansive cystic lesions on the bones) cause fractures, deformities, and pseudotumors.

Pathology

Osteomalacia and pseudotumoral structures cause fractures, deformities, rachitic physical changes, and epiphyseal displacement. Ectopic

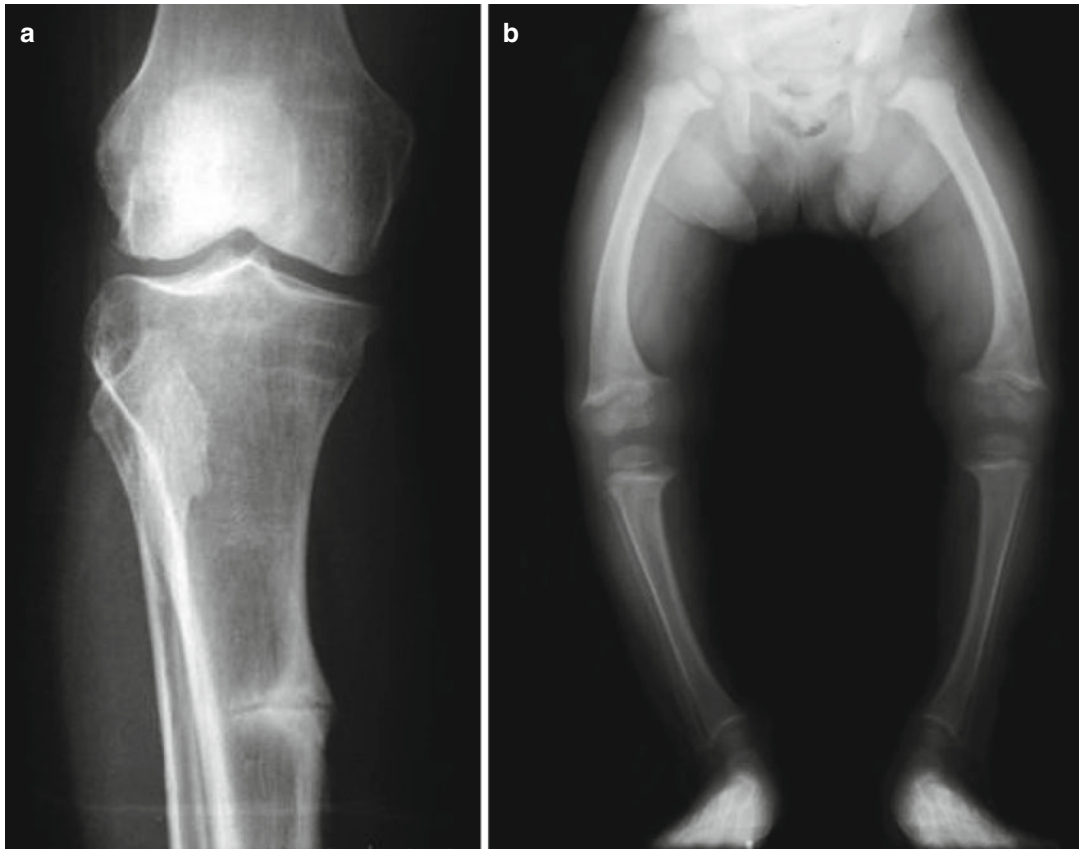

Fig. 32.19 (**a**) Stress fracture (Looser's zone). *Right* Tibia diaphysis. (**b**) Bowing and deformities on both *lower* extremities in the femur and tibia

calcifications are common in many areas (vascular structures, organs, conjunctiva, joints). Histological review shows osteoclastic resorption on the bone and demineralized matrix (osteomalacia) deposits on bone surface (Fig. 32.20).

Primary Hyperparathyrodism [11, 12–15]

von Recklinghausen Disease, Osteitis Fibrosa Cystica

Primary hyperparathyroidism is a metabolic bone disease caused by overproduction of PTH, usually due to benign adenomas on parathyroid gland. Increased PTH levels cause osteoclastic resorption on the bone and increased calcium reabsorption both directly (from the kidneys) and indirectly through vitamin D metabolism (from the intestines), causing hypercalcemia. Serum alkaline phosphatase levels also rise since the osteoblastic activity is increased to maintain osteoclastic resorption on the bone. It is diagnosed in routine blood tests in the clinic after noticing hypercalcemia. Patients that give out clinical symptoms are usually middle-aged women. Clinical symptoms are wide bone pain, nausea, vomiting, fatigue, depression, nocturia, and constipation and all caused by hypercalcemia. Since it is seen around the age when osteoporosis is seen, they are usually diagnosed during osteoporosis examinations. Typical blood results are hypercalcemia (>12 mg/100 ml), increased PTH and alkaline phosphatase, and hypophosphatemia. It can be also seen in Brown tumors and pathological fractures. Brown tumors show typical

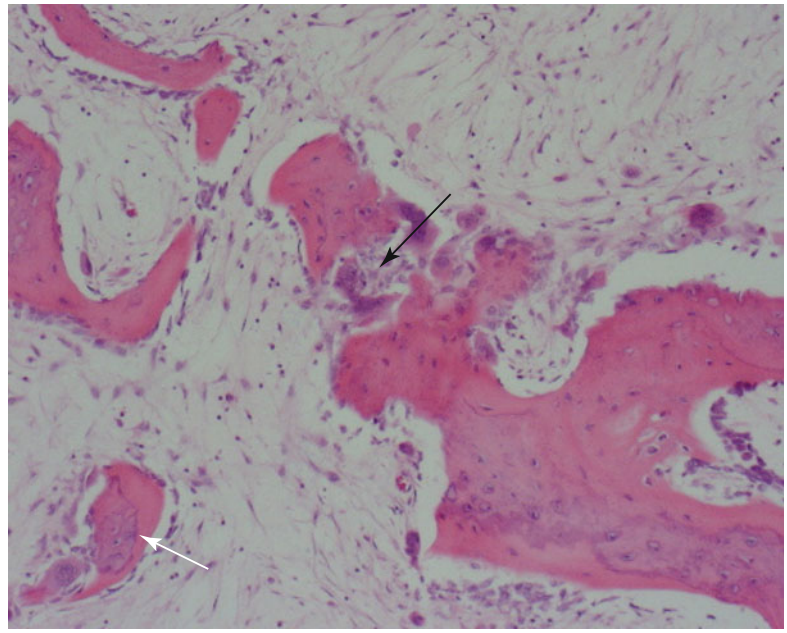

Fig. 32.20 Renal osteodystrophy. Osteoclastic resorption and wide-area demineralized osteoid tissue. Osteoclastic resorption (*black arrow*) and osteoid tissue (*white arrow*) (H&E) (From Bullough [12])

radiological images such as subperiosteal resorption (the phalanx, lamina dura, and distal clavicle), small resorption areas on cranium, osteopenia, and chondrocalcinosis on vertebra.

Etiopathogenesis

The most common reason is solitary parathyroid adenoma (80 %). Other reasons include idiopathic parathyroid hyperplasia (15 %), multiple adenomas (4 %), and parathyroid carcinomas (1 %). Increased PTH secretion causes over-resorption of the bones (Brown tumor formation, subperiosteal resorptions, and osteopenia) and increased reabsorption from the kidneys and intestines. Hypercalcemia causes fatigue, depression, constipation, stomach ulcers, pancreatitis, and calcifications in the kidney and soft tissues. All those symptoms are reversible and a speedy recovery is expected once the adenoma is removed.

Pathology

Microscopic examination of bone biopsies show characteristic tunnel-shaped resorption areas caused by increased osteoclast clusters on bone surfaces (also in subperiosteal areas) (Fig. 32.21). Intraosseous resorption (osteocytic osteolysis), new bone formation, and myelofibrosis in adjacent areas to bone surface are also common microscopic findings (Fig. 32.21). Lytic-cystic lesions (Brown tumor) might be confused with neoplasms in addition to giant cell tumor or

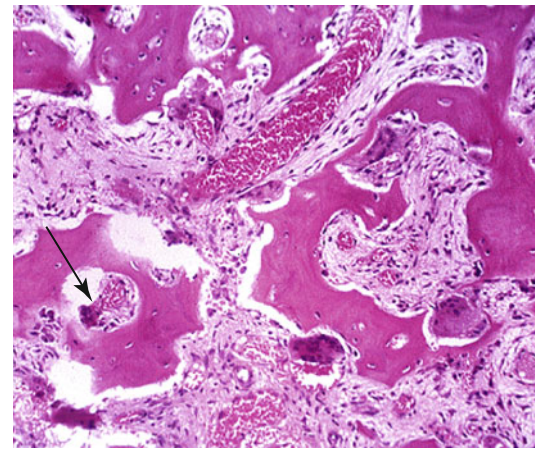

Fig. 32.21 Primary hyperparathyroidism. *Tunnel-shaped* osteoclastic resorption (*black arrow*). It is hard to distinguish this finding from early term Paget's disease (H&E) (From Bullough [12])

aneurysmal bone cyst, but Brown tumor can easily be identified in histological analysis. There are many giant cell clusters within fibrovascular cellular stroma (Fig. 32.21).

Paget's Disease of the Bone [12–15]

Paget's disease is identified in 1876 by Sir James Paget as *osteitis deformans*. This disease is rarely seen before 40. The frequency of the disease is 3–4 % in middle-aged adults and 10 % after 90 years of age. Males are more susceptible to this disease. It can manifest itself on a single (monostotic) or multiple (polistotic) bones. This disease is more frequent among Anglo-Saxons, which shows a preference for geographical and racial preference. There is also a genetic susceptibility around 15–30 %. It is more frequent in people with HLA-DQw1 incompatibility antigen. Ninety-five percent of the case area is asymptomatic and is diagnosed by chance. In symptomatic cases, there are increased bone pain at night, secondary osteoarthritis, deformities and pathological fractures, nerve impingement, heart failure, and rarely secondary malignancy (osteosarcoma after 70 years of age). Pagetic bones have a very typical radiological appearance (Fig. 32.22). In lab results, there are increased alkaline and acidic phosphatase and excretion of collagen destruction by-products.

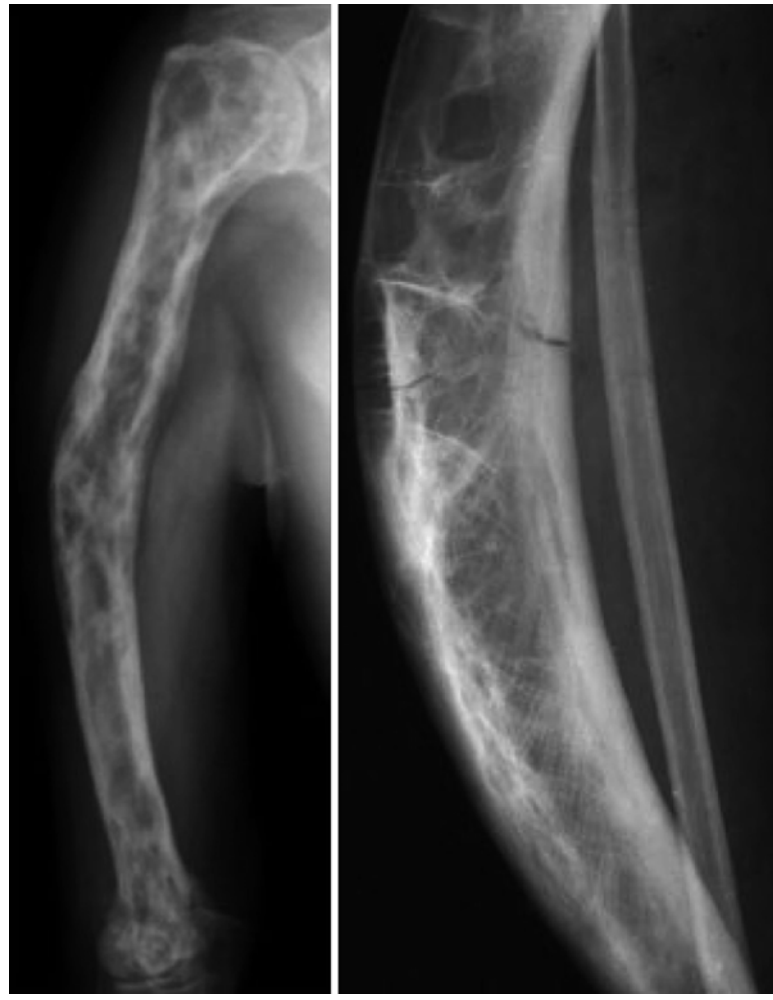

Fig. 32.22 Paget's disease on the right humerus. Lytic and sclerotic areas, bone widening, and deformation make up a very typical appearance. Tibia is thickened, lost its normal form, and deformed and there is a stress fracture

Etiopathogenesis

Etiology of the disease is unclear. The fact that there are viral inclusion particles within osteoclast nuclei might help to consider this disease as a slow virus infection (intranuclear inclusions resemble the nucleocapsids of the paramyxovirus), and in addition, familial and racial tendency show that there are genetic factors as well.

Paget's disease is a syndrome characterized by a local disruption of the bone turnover cycle. Primary pathology is abnormal increase in osteoclastic resorption. This creates a chaotic situation because it also tries to balance the bone mass with increased bone-building activity. For this reason, there is a quite vascular "woven" bone which is not affected by local or systemic factors. Bone structure becomes soft which makes deformities and fractures easier. Intraosseous circulation is also disrupted. This creates an extra load on the heart and increases pumping volume. In advanced cases, this might even lead to heart failure. Pathological changes in bone turnover cycle are divided into active and inactive phases. In early active phase (lytic phase), there is heavy osteoclastic resorption. In late active phase, complimentary new bone tissue growth is seen. In many cases, lytic and sclerotic activities have a typical radiological image (Fig. 32.22). During inactive period, there are no cellular activities. The bone morphology in this phase stays with the patient for life.

Pathology

Microscopic imaging shows differences with disease periods. In early active phase, multinuclear giant cell (osteoclast) resorption is increased, while osteoblasts are building the bone tissue. Bone marrow is loose and is difficult to differentiate from hyperparathyroidism with hypervascularity within a fibrous stroma. Paget's disease is easily differentiated from hyperparathyroidism by osteoclasts being giant cells with more than 1002 nuclei and there are no osteoclastic tunnel resorptions. In active phase, the anarchy between resorption and formation disrupts microarchitecture of the bone. Pagetic bone shows neither spongious nor cortical bone organization. Broken and irregular cement lines that give out a "mosaic" appearance within bone tissues show a very typical sign (Fig. 32.23). During inactive phase, all cellular activity is decreased. There is an appearance of low vascular and trabecular bone with mosaic appearance caused by broken cement lines. Bone marrow seems relatively normal.

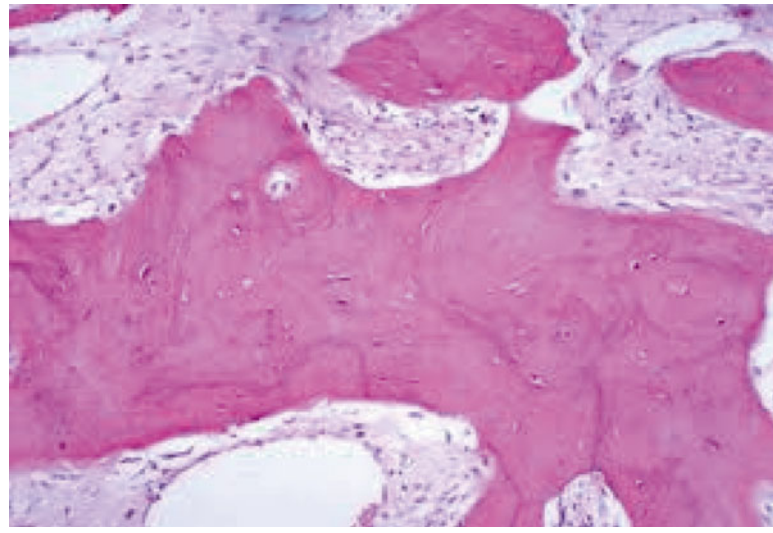

Fig. 32.23 Paget's disease has a very distinct histopathologic appearance. *Broken* and *irregular cement lines* give a mosaic appearance (H&E) (Courtesy of Gürer İ MD)

Osteopetrosis [14, 15]

Marble Bone Disease, Albers-Schönberg Disease

Osteopetrosis is a rare hereditary, heterogeneous disease, characterized by an increase in bone density. Basic pathology is osteoclastic resorption defect. For this reason, skeletal mass increases and wide osteoscleroses are present. There are three clinical types of the disease dependent on age, genetics, and clinical properties (Table 32.4).

Etiopathogenesis, Pathology

Basic pathology in this disease is dysfunction of osteoclasts caused by a defect on their resorption surfaces, even though they look normal. There are three mutations defined that affect osteoclast function and cause osteopetrosis. Those are carbonic anhydrase II deficiency, osteoclast proton pump defect (most common in 50–60 % of the cases), and chloride channel defect. Due to osteoclast function defect, the remodeling will be available of metaphysis cannot be done because calcified cartilage cannot be resorbed in metaphyseal area and there is primary spongious development defect, therefore causing a typical deformity in metaphysis (Erlenmeyer flask deformity). In histological review, even though there are a countless number of osteoclasts present, there is no bone resorption and calcified cartilage areas within bone tissue in adults are typical findings (Fig. 32.24). Bone marrow spaces were obliterated by unresorbed calcified cartilage extensions.

Table 32.4 Clinical classification of osteopetrosis

Type	Genetic properties	Age onset	Pathogenesis	Clinical symptoms	Prognosis
Osteopetrosis tarda	Autosomal dominant	Adult	Osteoclastic resorption defect	50 % asymptomatic, fractures, osteoarthritis, no bone marrow involvement	Good
Osteopetrosis congenita	Autosomal recessive	Infant	Osteoclastic resorption defect	Serious bone marrow involvement, growth defect, blindness, deafness, and hydrocephaly	Bad
Marble bone disease	Autosomal recessive	Childhood	Osteoclastic resorption defect, carbonic anhydrase isoenzyme II deficiency	Renal tubular acidosis, intracerebral calcifications, no bone marrow involvement	Bad

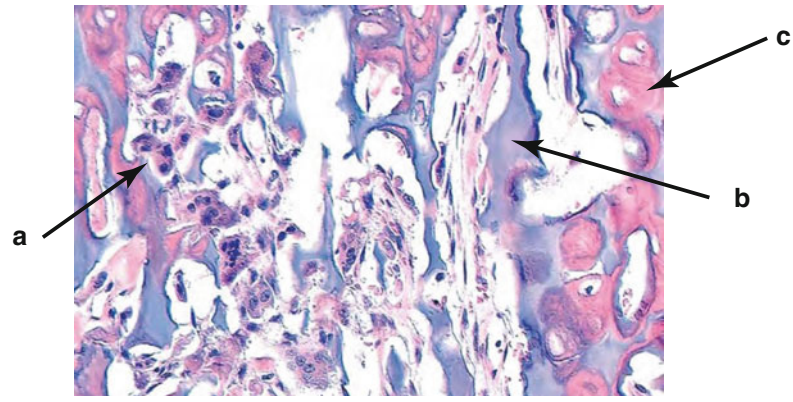

Fig. 32.24 Osteopetrosis. (**a**) Non-active osteoclasts. (**b**) Chondroid matrix. (**c**) Osteoid matrix (H&E) (From Bullough [12])

References

1. Steinberg DR, Steinberg ME (2008) Osteonecrosis: an overview. Tech Orthop 23(1):2–10
2. Lieberman JR, Berry DJ, Mont MA et al (2002) Osteonecrosis of the hip: management in the twenty-first century. J Bone Joint Surg 84-A(5):834–853
3. Aaron RK (1998) Osteonecrosis: etiology, pathophysiology and diagnosis. In: Callaghan JJ, Rosenberg AG, Rubash HE (eds) The adult hip. Lippincott-Raven, Philadelphia, pp 451–466
4. Miller MD (2008) Review of orthopaedics, 5th edn. Elsevier Saunders, Philadelphia, pp 18–36
5. Ficat RP, Arlet J (1980) Necrosis of the femoral head. In: Hungerford DS (ed) Ischemia and necrosis of bone. William & Wilkins, Baltimor, pp 53–74
6. Netter FH (1987) The CIBA collection of medical Illustrations Vol 8. Musculoskeletal system Part I. Anatomy, physiology and metabolic disorders. CIBA-GEIGY Medical Education Division, New Jersey, pp 195–245
7. Eralp L (2010) Cellular morphology of bone and bone remodeling. Türk Klin J Orthop Traumatol Spec Top 3(2):1–6
8. Hasanoğlu A, Okur İ (2010) Bone mineral homeostasis and the effects of endocrine system on bone. Türk Klin J Orthop Traumatol Spec Top 3(2):7–13
9. Tuncer T (2010) Osteoporosis. Türk Klin J Orthop Traumatol Spec Top 3(2):47–55
10. Singh M, Nagrath AR, Maini PS (1970) Changes in trabecular pattern of upper end of femur as an index of osteoporosis. J Bone Joint Surg Am 52(3):457–467
11. Ramachandran M (ed) (2007) Basic orthopaedic sciences, the stanmore guide. Edward Arnold (Publishers) Ltd, London, pp 270–282
12. Bullough PG (2010) Orthopaedic pathology, 5th edn. Mosby Elsevier, Missouri, pp 161–185
13. Ersoy F (2010) Renal osteodystrophy. Türk Klin J Orthop Traumatol Spec Top 3(2):60–67
14. Aydın AT, Yeter B (2010) Osteopetrosis. Türk Klin J Orthop Traumatol Spec Top 3(2):82–86
15. Einhorn TA (2007) In: O'Keefe RJ, Buckwalter JA (eds) Orthopaedic basic science, 3rd edn. American Academy of Orthopaedic Surgeon, Rosemond, pp 415–426
16. Merle d'Aubigné R, Postel M, Mazabraud A, Massias P, Guegen J (1965) Idiopathic necrosis of the femoral head in adults. J Bone Joint Surg [Br] 47-B:612–633
17. Aaron RK, Lennox D, Bunce GE, Ebert T (1989) The conservative treatment of osteonecrosis of the femoral head: a comparison of core decompression and pulsing electromagnetic fields. Clin Orthop 249:209–218
18. Pritchett JW (2001) Statin therapy decreases the risk of osteonecrosis in patients receiving steroids. Clin Orthop Relat Res 386:173–178
19. Wang Y, Yin L, Li Y, Liu P, Cui Q (2008) Preventive effects of puerarin on alcohol-induced osteonecrosis. Clin Orthop Relat Res 466:1059–1067
20. Disch AC, Matziolis G, Perka C (2005) The management of necrosis-associated and idiopathic bone-marrow oedema of the proximal femur by intravenous iloprost. J Bone Joint Surg B 87(4):560–564
21. Agarwala S, Shah S, Joshi VR (2009) The use of alendronate in the treatment of avascular necrosis of the femoral head: followup to eight years. J Bone Joint Surg B 91:1013–1018
22. Agarwala S, Sule A, Pai BU, Joshi VR (2001) Study of alendronate in avascular necrosis of bone. J Assoc Physicians India 49:949–950
23. Mazieres B (2008) Osteonecrosis. In: Hochberg MC, Silman AJ, Smolen JS, Wienblatt ME, Weisman MH (eds) Rheumatology, 4th edn. Mosby Elsevier, Philadelphia, pp 1777–1789
24. Agarwala S, Shah SB (2011) Ten-year follow-up of avascular necrosis of femoral head treated with alendronate for 3 years. J Arthroplast 26(7):1128–1134
25. Chen CH, Chang JK, Lai KA et al (2012) Alendronate in the prevention of collapse of the femoral head in nontraumatic osteonecrosis: a two-year multicenter, prospective, randomized, double-blind, placebo-controlled study. Arthritis Rheum 64(5):1572–1578

Osteoporosis

33

Yuuki Imai

Abstract

Patients with osteoporosis have high risks for vertebral and non-vertebral fractures; therefore, these patients should be adequately diagnosed and treated for prevention of fractures. It is essential to treat patients appropriately and sufficiently that the physicians must understand the mechanisms underlying osteoporosis and physiological bone homeostasis. The large population of osteoporosis is postmenopausal osteoporosis, which is categorized in primary osteoporosis. Postmenopausal osteoporosis is caused by deficiency of estrogen. Estrogen exerts its osteoprotective effects directly and indirectly to bone tissue. Also, secondary osteoporosis can be induced by various pathologic conditions, such as hyperparathyroidism, glucocorticoid treatment, and inflammatory diseases.

Clarification of the molecular basis underlying the pathophysiology of osteoporosis will open the window to develop novel therapeutic strategy for osteoporosis.

Learning Outcome

After you have studied this chapter, you will have an understanding of: (1) definition of osteoporosis, (2) causes of osteoporosis, (3) molecular basis of postmenopausal osteoporosis, (4) phenotypes of the mice lacking ERα, and 5) secondary osteoporosis.

Y. Imai, MD, PhD
Division of Integrative Pathophysiology,
Proteo-Science Center, Ehime University,
Ehime, Japan

Department of Pathophysiology,
Graduate School of Medicine, Ehime University,
Ehime, Japan

Division of Laboratory Animal Research, Advanced Research Support Center, Ehime University,
Ehime, Japan

Division of Osteoscience,
Artificial Joint Integrated Center,
Ehime University Hospital, Ehime University,
Ehime 791-0295, Japan
e-mail: y-imai@m.ehime-u.ac.jp

F. Korkusuz (ed.), *Musculoskeletal Research and Basic Science*,
DOI 10.1007/978-3-319-20777-3_33

Terminology

Osteoblasts Cells forming bone matrix differentiated from mesenchymal stem cells.

Osteocytes Cells buried in extracellular bone matrix differentiated from osteoblasts.

Osteoclasts Cells resorbing bone matrix differentiated from hematopoietic stem cells by stimulation of M-CSF and RANKL.

M-CSF Macrophage colony stimulating factor.

RANKL Receptor activator of Nuclear Factor κB ligand.

FSH Follicle stimulating hormone, secreting from the anterior lobe of the pituitary gland to stimulate the ovary and facilitating estrogen synthesis.

Estrogen receptor A member of nuclear receptor superfamily binding with estradiol and acting as a transcription factor to regulate target gene transcription.

Cre/loxP system One of the site-specific recombinase technologies to carry out deletions, insertions, translocations, and inversions at specific sites in the DNA of cells.

Introduction

Bone tissue is established by biological process, which is called "modeling," during growth and is maintained by the other process, which is called "remodeling" after skeletal maturation [1]. Normal bone remodeling can preserve the quantity and quality of bone tissue in adulthood and can support bone metabolism. Namely, metabolic bone diseases, such as osteoporosis, can be caused by abnormal bone remodeling. Bone tissue plays its own roles as the reservoir of calcium, which can be released into blood flow as occasional demands, and as the center of the locomotive organ. Sufficient calcification of bone by calcium and phosphate enables us to obtain stiffness to support our own bodyweight. In addition, bone tissue can provide the environment for the hematopoiesis for a whole lifetime after birth. Bone cells can develop and support hematopoietic stem cells and hematopoiesis [2], that is, metabolic disorder and aging of bone tissue, such as osteoporosis, are closely related to hematopoietic diseases, such as anemia.

Osteoporosis has been initially defined as a skeletal disorder characterized by low bone mass with normal mineralization ratio, leading to an increase in bone fragility and fracture. The World Health Organization (WHO) defined osteoporosis as decreased bone mineral density (BMD), which is less than 2.5 standard deviations (SDs) of the young adult mean (YAM) value (T-score < −2.5). Patients with BMD between 1 and 2.5 SDs below average (T-score −1 to −2.5) were defined as osteopenia [3]. BMD can be usually determined by DXA, dual X-ray absorptiometry, which is a widely accepted method for BMD measurement. Recently, a National Institutes Consensus Development Conference in the United States refined [4] that (Fig. 33.1):

> Osteoporosis is defined as a skeletal disorder characterized by compromised bone strength predisposing to an increased risk of fracture. Bone strength reflects the integration of two main features: bone density and bone quality. Bone density is expressed as grams of mineral per area or volume and in any given individual is determined by peak bone mass and amount of bone loss. Bone quality refers to architecture, turnover, damage accumulation (e.g., microfractures) and mineralization. A fracture occurs when a failure-inducing force (e.g., trauma) is applied to osteoporotic bone. Thus, osteoporosis is a significant risk factor for fracture, and a distinction between risk factors that affect bone metabolism and risk factors for fracture must be made.

> However, it is still difficult to quantitatively assess bone quality, and the diagnosis is still dependent on BMD and the history of fragile fractures. Based on these definitions, we, orthopedic surgeons, should send the old patients with distal radius fracture, one of the fragile fractures, to DXA measurement to diagnose whether they have osteoporosis and should be monitored or not.

Appropriate diagnosis and treatment for diseases is definitely dependent on the physicians' knowledge and understanding of pathophysiology. In this part, to adequately understand the pathophysiology of osteoporosis, the molecular mechanisms underlying osteoporosis will be dis-

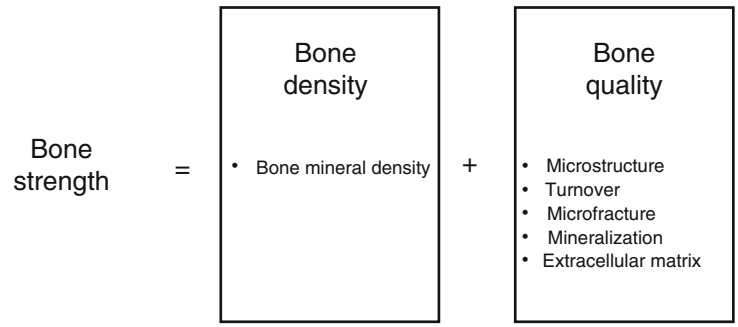

Fig. 33.1 Bone strength consists of bone density and bone quality

cussed, especially focusing on bone density in postmenopausal osteoporosis.

Osteoporosis and Bone Cells

Bone tissue consists of three types of proper bone cells, such as osteoclast, osteoblast, and osteocyte. Osteoclast is a bone-resorbing cell, which is a multi-nucleated giant cell differentiated from hematopoietic stem cells by M-CSF [5] and RANKL [6] stimulation. Osteoblast is a bone-forming cell, which is differentiated from mesenchymal stem cell by function of master regulators, such as Runx2 [7] and Osterix [8]. Osteocyte is differentiated from osteoblast and is embedded in extracellular bone matrix formed by osteoblast itself. Osteocyte has a lot of processes to contact with osteoblasts and osteoclasts as well as other osteocytes. Recently, it has been reported that osteocytes can control bone metabolism by indirectly regulating osteoblastic bone formation and osteoclastic bone resorption. Bone mass is precisely maintained by balances between osteoblastic bone formation and osteoclastic bone resorption. If this balance shifts into either one, which means abnormal remodeling, metabolic bone disorder can be developed. Osteoporosis can be caused by more increased osteoclastic bone resorption than increased osteoblastic bone formation, which called high turnover bone metabolism. This bone turnover can be determined by bone metabolic biomarkers, which are derived from degraded extracellular bone matrix or active osteoclasts or osteoblasts. Bone resorption markers include deoxypyridinoline (DPD), type 1 collagen cross-linked N-telopeptide (NTX), type 1 collagen cross-linked C-telopeptide (CTX), and tartrate-resistant acid phosphatase 5b (TRACP-5b). On the other hand, bone formation markers include osteocalcin, bone alkaline phosphatase (BAP), and type 1 procollagen-N-propeptide (P1NP). These bone metabolic markers are useful for diagnosis and evaluation of effects of therapies for osteoporosis [9].

Assessment of Bone Microstructure and Biomechanical Property Using μCT

Bone microstructure is one of the factors, which consists of bone quality, and can be assessed by high-resolution microcomputed tomography (μCT). μCT measurements can visualize and quantitatively evaluate 2D and 3D bone microstructures. μCT measurements should be performed according to the guideline [10], which determined technical terms and recording methods. Trabecular microstructure analyses were analyzed based on 3D voxel data. These data can provide not only basic parameters, such as bone volume (BV), total tissue volume (TV), relative bone volume (BV/TV), trabecular number (Tb.N), trabecular thickness (Tb.Th), and trabecular separation (Tb.Sp), but also 3D structural parameters, such as connectivity of trabecular per unit volume (Connectivity density) and structure model index (SMI), which is a quantitative parameter of trabecular morphology, rod or plate shape.

The trabecular bone microstructure in osteoporotic bone is characterized by decreased BV/TV, decreased connectivity, increased SMI, increased Tb.Sp, and decreased Tb.N. In addition to trabecular bone, cortical bone in osteoporosis exhibits reduction of cortical thickness and increased cortical porosity. These osteoporotic changes in bone microstructure impair bone quality, followed by increased fragility and fracture risks.

These changes in microstructure are varied among a kind and region of the bone. Distal femur and vertebral bone are usually used for evaluation in an experimental model.

Postmenopausal Osteoporosis

Postmenopausal osteoporosis is caused by deficiency of female sex steroid hormone, estrogen, and is the main reason of primary osteoporosis. Postmenopausal osteoporosis patients and ovariectomized rodents, an experimental model of postmenopausal osteoporosis, exhibit bone loss with high turnover bone metabolism due to increased osteoclastic bone resorption, which is more significant than increased osteoblastic bone formation at same time [11].

Estrogen exerts its function by binding to its own receptor, estrogen receptor (ER), which is a member of nuclear receptor superfamily. ER has subtype ERα and ERβ. Ligand (estrogen) bound ERs can form dimer and translocate into nucleus, and work as a transcription factor to regulate gene expression of target gene [12]. Estrogen/ER signaling is essential for the development, maturation, and maintenance of sex differences and characters in various organs/tissues, especially in reproductive organs. Regarding bone metabolism, the patients harboring loss-of-function mutation at gene locus of ESR1, which encodes ERα, exhibit remarkable osteoporosis that is irresponsible to estrogen treatment [13]. From this point of view, it has been considered that ERα is dominant subtype in regulation of estrogen/ER signaling and estrogen's osteoprotective effects have studied focusing on ERα.

To clarify the effects of estrogen in bone metabolism, the mice lacking ERα (ERαKO) were generated and analyzed. As a result, ERαKO mice exhibited estrogen-deficient phenotypes like postmenopausal women in various tissues/organs [14]. However, bone mass of ERαKO was increased with low bone turnover. This inconsistent bone phenotype can be explained by abnormally high levels of serum estrogen/androgen due to disruption of negative feedback loop of estrogen biosynthesis.

Indirect Effects of Estrogen for Bone Metabolism

Because ERαKO did not exhibit bone loss phenotype like postmenopausal osteoporosis, the studies focusing on estrogen's indirect osteoprotective effects, which mean that secondary effects of estrogen's target tissue can regulate bone metabolism, have been developed.

It has been reported that bone-resorbing osteoclasts can be differentiated by stimulations of inflammatory cytokines as well as RANKL. At this point, Pacifici and colleagues focused estrogen's effects on immune cells and they clarified that estrogen can repress the production of inflammatory cytokines, such as TNFα, IL-1, 6, and 7. In the estrogen-deficient status, immune cells can produce abundant inflammatory cytokines and facilitate osteoclast differentiation and bone resorption followed by bone loss [15].

In addition, Zaidi and colleagues clarified the function of follicle stimulating hormone (FSH), whose concentration is increased postmenopausal status, for bone metabolism. FSH can positively regulate osteoclast differentiation, that is, not only deficiency of estrogen but also increased FSH accelerates osteoclastic bone resorption and progress osteoporosis [16]. In fact, it has been reported that serum levels of FSH negatively correlate with bone mass in a clinical situation [17].

Estrogen exerts its effects in various target tissues/organs. This means that there can be diverse secondary/indirect effects of estrogen for controlling bone mass.

Direct Effects of Estrogen for Bone Metabolism

As mentioned above, estrogen can indirectly regulate bone metabolism via the immune system and brain. However, is there no direct effect of estrogen in bone mass regulation? Indeed, sys-

temic ERαKO did not display osteoporotic phenotype due to abnormal negative feedback loop of estrogen synthesis. To overcome this issue, cell type specific conditional knockout mice have been generated using Cre/loxP system, where mice lack ERα gene only in bone cells and were not affected by endocrine disorders like systemic ERαKO.

Direct Effect for Osteoclasts

Estrogen's direct effects and ERα function in osteoclasts were studied because remarkably increased osteoclastic bone resorption was observed in postmenopausal osteoporosis. To generate osteoclast-specific ERα conditional KO mice ($ER\alpha^{\Delta Oc/\Delta Oc}$), ERα flox mice and Cathepsin K (Ctsk)-Cre knock-in mice, in which Cre recombinase can be driven by endogenous Ctsk promoter activity specifically in mature osteoclasts, were used. $ER\alpha^{\Delta Oc/\Delta Oc}$ showed normal growth and hormonal appearance, however, female $ER\alpha^{\Delta Oc/\Delta Oc}$ exhibited trabecular bone loss with high bone turnover same as postmenopausal osteoporosis. This trabecular bone loss was not attenuated by OVX-induced estrogen deficiency and estrogen replacement therapy. These data indicated that osteoclastic ERα could directly regulate osteoclastic bone resorption. To understand how estrogen/ERα signaling in osteoclast directly affects osteoclastic bone resorption, the differences in gene expression profile between control and $ER\alpha^{\Delta Oc/\Delta Oc}$ was examined. As a result, genes related to regulation of apoptosis, not of osteoclastic differentiation, were enriched. Among them, Fas ligand (FasL) was detected as one of the responsible apoptosis regulation gene [18]. In addition, Brown and colleagues reported estrogen/ERα signaling could directly induce FasL gene expression in osteoblast in vitro [19]. Moreover, Manolagas and colleagues have clarified that another osteoclast-specific ERα conditional knockout mice using LysM-Cre mice also exhibited osteoporotic phenotype with increased osteoclastic bone resorption due to reduced osteoclastic apoptosis [20] (Table 33.1). Taken together, estrogen can directly maintain bone mass via regulation of osteoclastic lifespan through osteoclastic and/or osteoblastic ERα.

Direct Effects for Osteoblasts

The effects of estrogen signaling for osteoblastic bone formation have been reported only in in vitro study and in vivo effects were controversial. Recently, some groups independently reported the phenotypes of mice lacking ERα in various differentiation stages of osteoblasts.

Almeida et al. reported that immature osteoblast-specific ERα knockout mice generated using Prx1-Cre and Osterix-Cre exhibited age-dependent loss of bone mineral density in cortical bone, not in trabecular bone. They claimed that this cortical bone loss was caused by the reduction of Wnt signaling in periosteal osteoblasts [26]. In addition, other groups reported that mature osteoblast-specific ERαKO mice generated by Osteocalcin-Cre mice exhibited reduced bone mass. Bone histomorphometric analyses revealed that this bone loss was caused by low turnover bone metabolism with decrease of both osteoblastic bone formation and osteoclastic bone resorption [27, 28].

These insights suggested that estrogen signaling via ERα in osteoblast could directly influence osteoblastic bone formation in both cortical and trabecular bone homeostasis (Table 33.1).

Direct Effects for Osteocytes

Besides osteoclasts and osteoblasts, osteocytes maintain bone homeostasis. Osteocytes account for more than 90 % of bone cell population. It has been considered that osteocytes can sense mechanical stress and convert it to biological signaling to regulate bone metabolism. In addition, ERα can also be involved in mechanical stress responses. Indeed, systemic ERαKO mice failed to increase bone mass induced by mechanical loading [29]. From this point of view, to clarify whether estrogen signaling directly affects osteocyte or not, osteocyte-specific ERα knockout mice were generated using Dmp1-Cre mice and reported from two independent research groups. Windahl et al. [21] claimed that only male, not female, osteocyte-specific ERα knockout mice displayed decreased trabecular bone mass due to reduced osteoblastic bone formation. On the other hand, Kondoh et al. [22] addressed that only female, not male, mice lacking ERα in osteocytes exhibited decreased tra-

Table 33.1 Summary of bone phenotypes of bone cell type specific ERα knockout mice

Cre promoter	Cell type	Sex	Bone mass		Ref.
Ctsk	Osteoclast	Male	Trabecular	→	[18]
			Cortical	→	
		Female	Trabecular	↓	
			Cortical	→	
LysM	Osteoclast	Male	Trabecular	→	[20]
			Cortical	→	
		Female	Trabecular	↓	
			Cortical	→	
Prx1	Immature osteoblast	Male	Trabecular	→	[26]
			Cortical	↓	
		Female	Trabecular	→	
			Cortical	↓	
Osx	Immature osteoblast	Male	Trabecular	N.D	[26]
			Cortical	N.D	
		Female	Trabecular	→	
			Cortical	↓	
Col1a1	Osteoblast	Male	Trabecular	→	[26]
			Cortical	→	
		Female	Trabecular	→	
			Cortical	→	
OCN	Mature osteoblast	Male	Trabecular	→	[25, 27, 28]
			Cortical	→	
		Female	Trabecular	↓	
			Cortical	↓	
Dmp1	Late osteoblast	Male	Trabecular	↓	[21]
	Early osteocyte		Cortical	→	
		Female	Trabecular	→	
			Cortical	→	
Dmp1	Late osteoblast	Male	Trabecular	→	[22]
	Early osteocyte		Cortical	→	
		Female	Trabecular	↓	
			Cortical	→	

becular bone mass due to reduced osteoblastic bone formation. Gene expression profile of osteocytes derived from conditional ERαKO mice showed increased expression of Wnt signaling antagonists. Although there is a contradiction about phenotypes related on gender between two studies, these reports indicate that osteocytic ERα can regulate osteoblastic bone formation via secretion of humoral factor (Table 33.1).

In summary, estrogen can directly act in all kinds of bone cells though its ERα and regulate bone metabolism as well as indirect effects from other estrogen's target tissues/organs, such as brain and immune cells. The sum total of indirect and direct effects of estrogen can maintain bone homeostasis, and the disruption of these biological protections lead to the establishment of postmenopausal osteoporosis (Fig. 33.2).

Secondary Osteoporosis

Not only primary osteoporosis, such as postmenopausal osteoporosis, we should pay attention to secondary osteoporosis as well, which is caused by primary disease or drug-induced adverse effects.

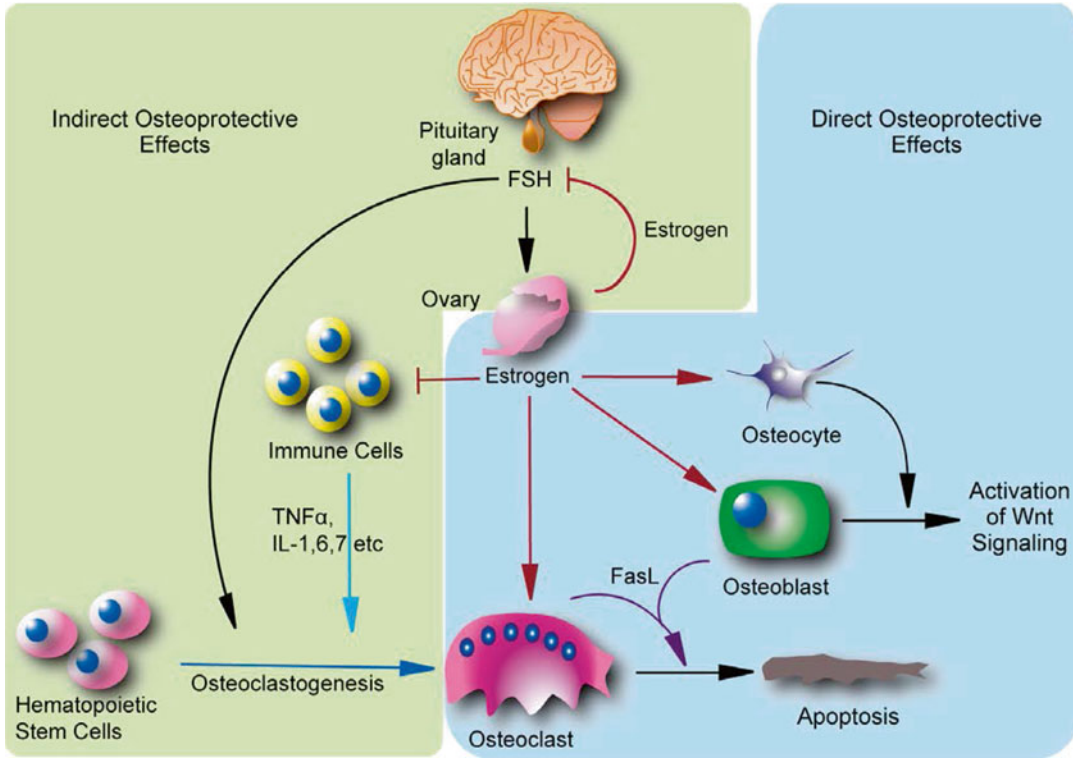

Fig. 33.2 Estrogen's osteoprotective effects. The sum total of indirect (via suppression of FSH secretion and production of inflammatory cytokines from immune cells) and direct (via control of osteoclast life span and Wnt signaling activation in osteoblastic cells) effects of estrogen can maintain bone homeostasis (Modified from Imai et al. [30] and Imai [31])

Hyperparathyroidism

Hyperparathyroidism is caused by chronic abnormal excessive secretion of parathyroid hormone (PTH) and this increased PTH increases bone resorption with high bone turnover, followed by reduction of bone mass. Increased bone resorption result in hypercalcemia and osteoporosis. Hyperparathyroidism-induced osteoporosis is characterized with severer bone loss in cortical bone than that in trabecular bone. Primary hyperparathyroidism-induced osteoporosis can be improved by appropriate treatment for primary disease, such as resection of parathyroid [23]. On the other hand, secondary hyperparathyroidism, which is caused by chronic kidney disease, induced osteoporosis should be treated by a combination therapy with various medications.

Glucocorticoid-Induced Osteoporosis

Glucocorticoid can be biosynthesized and play various roles to maintain homeostasis. However, excess serum levels of glucocorticoid can induce abnormal glucose tolerance, abnormal lipid metabolism, lymphocytopenia, and osteoporosis. High glucocorticoid condition break bone remodeling balances between bone formation and bone resorption due to increased osteoblastic apoptosis and osteoclastic lifespan. This abnormal bone remodeling strongly induces osteoporosis [24]. In addition, a high glucocorticoid level affects absorption of Ca in gut, re-absorption of Ca in kidney, and various hormones' synthesis in the pituitary gland, and facilitates osteoporosis.

Patients with primary high glucocorticoid secretion, Cushing syndrome, exhibit usually bone loss, complicated with vertebral and hip

fractures. This secondary osteoporosis can be recovered by treatment for original disease. In contrast, glucocorticoid-induced osteoporosis can be generally noticed in patients with autoimmune diseases, such as systemic lupus erythematosus and rheumatoid arthritis, to treat their own disorder by glucocorticoids. In the treatment process of these patients, physicians should be careful about their bone loss and must prevent secondary osteoporosis by treatment with appropriate drugs.

Other Secondary Osteoporosis

In addition to the secondary osteoporosis described above, secondary osteoporosis can be induced by various reasons, such as hypogonadism, diabetes mellitus, inflammatory diseases, post-transplantation, immobilization, and so on.

Conclusion

Osteoporosis is a disease, which has an enormous influence on public health, and osteoporotic fractures affect morbidity and mortality as well as medical service and economy. Development of strategies in diagnosis, prevention, and therapy for osteoporosis is desired.

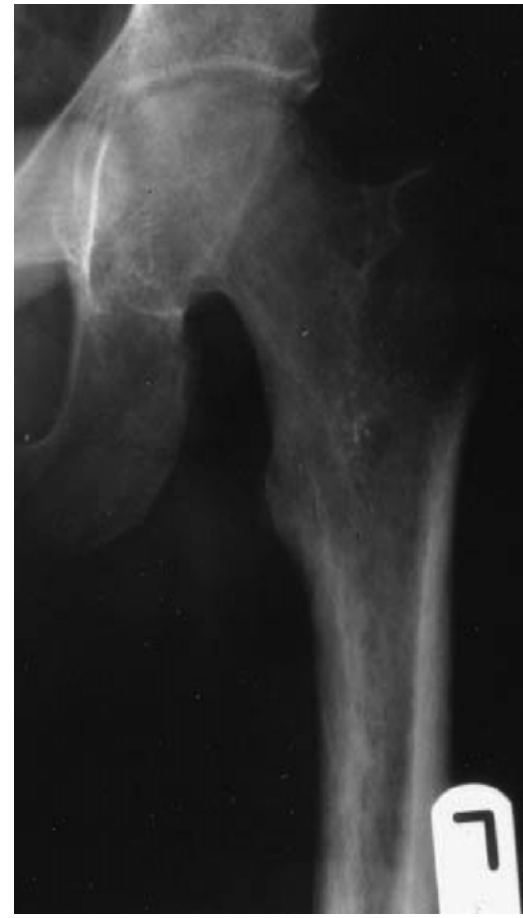

Fig. 33.3 Left hip X-ray of a 56-year-old female patient. Increased radiolucency at greater trochanter and subtrochanteric cortical bone was recognized

Clinical Relevance

#1 Should patients without symptom be treated? (Fig 33.3)

A 56-year-old female patient visited the outpatients without any symptom, but she was anxious about her bone strength because her 79-year-old-mother had an open reduction and internal fixation for osteoporotic hip fracture. The patient has reached menopause at 50 years of age and has no remarkable anamnesis. Dual X-ray absorptiometry (DXA) of vertebrae and hip joint and biochemical analyses including bone metabolic markers were performed. DXA showed −2.0 SD (about 75 %) of YAM (Young adult mean) bone mineral density (BMD) and serum TRAP5b, which is one of bone resorption markers and an index of osteoclast activity, was increased over normal range without any other abnormal data. With these data, the physician prescribed moderate exercise at outside and daily Raloxifene, which is one of SERMs, medication. After 1 year, she spent without any osteoporotic fracture and adverse effects such as deep venous thrombosis, and her TRAP5b was reduced within normal range and BMD was increased.

This patient was diagnosed as postmenopausal osteoporosis, which is caused by

estrogen deficiency. It is not recommended to easily prescribe estrogen and/or estrogen/progestin mixture medication only for the prevention of osteoporotic fracture, because hormone replacement therapy (HRT) with estrogen may increase risks for stroke, thromboembolic events, gallbladder disease, urinary incontinence, and breast cancer [32]. This patient exhibited marginal low BMD with increased bone resorption marker; however, her mother had an osteoporotic fracture. Based on these clinical data and family history, this patient should be treated with anti-osteoporosis agents. Among various kinds of medicine, SERM is one of the first choices for early postmenopausal patients. In addition, on the contrary to HRT, SERM can reduce a risk of invasive breast cancer [33]. SERM can bind to ERα, and therefore it might exert its osteoprotective effects through mechanisms mentioned above in this chapter.

References

1. Karsenty G (2000) How many factors are required to remodel bone? Nat Med 6(9):970–971. PubMed Epub 2000/09/06. eng
2. Yin T, Li L (2006) The stem cell niches in bone. J Clan Invest 116(5):1195–1201. Pubmed Central PM CID: 1451221
3. Kanis JA, Melton LJ 3rd, Christiansen C, Johnston CC, Khaltaev N (1994) The diagnosis of osteoporosis. J Bone Miner Res Off J Am Soc Bone Miner Res 9(8):1137–1141. PubMed
4. Osteoporosis prevention, diagnosis, and therapy (2000) NIH Consens Statement 17(1):1–45. PubMed
5. Yoshida H, Hayashi S, Kunisada T, Ogawa M, Nishikawa S, Okamura H et al (1990) The murine mutation osteopetrosis is in the coding region of the macrophage colony stimulating factor gene. Nature 345(6274):442–444. PubMed Epub 1990/05/31. eng
6. Yasuda H, Shima N, Nakagawa N, Yamaguchi K, Kinosaki M, Mochizuki S et al (1998) Osteoclast differentiation factor is a ligand for osteoprotegerin/osteoclastogenesis-inhibitory factor and is identical to TRANCE/RANKL. Proc Natl Acad Sci U S A 95(7):3597–3602. PubMed Central PM CID: 19881. Epub 1998/05/09. eng
7. Komori T, Yagi H, Nomura S, Yamaguchi A, Sasaki K, Deguchi K et al (1997) Targeted disruption of Cbfa1 results in a complete lack of bone formation owing to maturational arrest of osteoblasts. Cell 89(5):755–764. PubMed Epub 1997/05/30. eng
8. Nakashima K, Zhou X, Kunkel G, Zhang Z, Deng JM, Behringer RR et al (2002) The novel zinc finger-containing transcription factor osterix is required for osteoblast differentiation and bone formation. Cell 108(1):17–29. PubMed eng
9. Nishizawa Y, Ohta H, Miura M, Inaba M, Ichimura S, Shiraki M et al (2013) Guidelines for the use of bone metabolic markers in the diagnosis and treatment of osteoporosis (2012 edition). J Bone Miner Metab 31(1):1–15. PubMed
10. Bouxsein ML, Boyd SK, Christiansen BA, Guldberg RE, Jepsen KJ, Muller R (2010) Guidelines for assessment of bone microstructure in rodents using micro-computed tomography. J Bone Miner Res Off J Am Soc Bone Miner Res 25(7):1468–1486. PubMed
11. Rosen CJ (2005) Clinical practice. Postmenopausal osteoporosis. N Engl J Med 353(6):595–603. PubMed eng
12. Mangelsdorf DJ, Thummel C, Beato M, Herrlich P, Schutz G, Umesono K et al (1995) The nuclear receptor superfamily: the second decade. Cell 83(6):835–839. PubMed eng
13. Smith EP, Boyd J, Frank GR, Takahashi H, Cohen RM, Specker B et al (1994) Estrogen resistance caused by a mutation in the estrogen-receptor gene in a man. N Engl J Med 331(16):1056–1061. PubMed Epub 1994/10/20. eng
14. Windahl SH, Andersson G, Gustafsson JA (2002) Elucidation of estrogen receptor function in bone withvthe use of mouse models. Trends Endocrinol Metab 13(5):195–200. PubMed
15. Pacifici R (2008) Estrogen deficiency, T cells and bone loss. Cell Immunol 252(1-2):68–80. PubMed Epub 2007/09/25. eng
16. Sun L, Peng Y, Sharrow AC, Iqbal J, Zhang Z, Papachristou DJ et al (2006) FSH directly regulates bone mass. Cell 125(2):247–260. PubMed eng
17. Zaidi M, Blair HC, Iqbal J, Davies TF, Zhu LL, Zallone A et al (2009) New insights: elevated follicle-stimulating hormone and bone loss during the menopausal transition. Curr Rheumatol Rep 11(3):191–195. PubMed Epub 2009/07/17. eng
18. Nakamura T, Imai Y, Matsumoto T, Sato S, Takeuchi K, Igarashi K et al (2007) Estrogen prevents bone loss via estrogen receptor alpha and induction of Fas ligand in osteoclasts. Cell 130(5):811–823. PubMed eng
19. Krum SA, Miranda-Carboni GA, Hauschka PV, Carroll JS, Lane TF, Freedman LP et al (2008) Estrogen protects bone by inducing Fas ligand in osteoblasts to regulate osteoclast survival. EMBO J 27(3):535–545. PubMed Pubmed Central PM CID: 2241656. Epub 2008/01/26. eng
20. Martin-Millan M, Almeida M, Ambrogini E, Han L, Zhao H, Weinstein RS et al (2010) The estrogen recep-

tor-alpha in osteoclasts mediates the protective effects of estrogens on cancellous but not cortical bone. Mol Endocrinol 24(2):323–334. PubMed Pubmed Central PM CID: 2817608. Epub 2010/01/08. eng
21. Windahl SH, Borjesson AE, Farman HH, Engdahl C, Moverare-Skrtic S, Sjogren K et al (2013) Estrogen receptor-alpha in osteocytes is important for trabecular bone formation in male mice. Proc Natl Acad Sci U S A 110(6):2294–2299. PubMed Epub 2013/01/25. eng
22. Kondoh S, Inoue K, Igarashi K, Sugizaki H, Shirode-Fukuda Y, Inoue E et al (2014) Estrogen receptor alpha in osteocytes regulates trabecular bone formation in female mice. Bone 60:68–77. PubMed Pubmed Central PMCID: 3944732. Epub 2013/12/18. eng
23. Abe Y, Ejima E, Fujiyama K, Kiriyama T, Ide A, Sera N et al (2000) Parathyroidectomy for primary hyperparathyroidism induces positive uncoupling and increases bone mineral density in cancellous bones. Clin Endocrinol (Oxf) 52(2):203–209. PubMed
24. Okada Y, Tanaka Y (2004) Immune signals in the context of secondary osteoporosis. Histol Histopathol 19(3):863–866. PubMed
25. Maatta JA, Buki KG, Gu G, Alanne MH, Vaaraniemi J, Liljenback H et al (2013) Inactivation of estrogen receptor alpha in bone-forming cells induces bone loss in female mice. FASEB J Off Pub Fed Am Soc Exp Biol 27(2):478–488. PubMed Epub 2012/10/18. eng
26. Almeida M, Iyer S, Martin-Millan M, Bartell SM, Han L, Ambrogini E et al (2013) Estrogen receptor-alpha signaling in osteoblast progenitors stimulates cortical bone accrual. J Clin Invest 123(1):394–404. PubMed Pubmed Central PMCID: 3533305. Epub 2012/12/12. eng
27. Maatta JA, Buki KG, Gu G, Alanne MH, Vaaraniemi J, Liljenback H et al. (2013) Inactivation of estrogen receptor alpha in bone-forming cells induces bone loss in female mice. FASEB J 27(2):478–488. doi: 10.1096/fj.12-213587
28. Melville KM, Kelly NH, Khan SA, Schimenti JC, Ross FP, Main RP, et al. (2014) Female mice lacking estrogen receptor-alpha in osteoblasts have compromised bone mass and strength. J Bone Miner Res 29(2):370–379. doi:10.1002/jbmr.2082
29. Lee K, Jessop H, Suswillo R, Zaman G, Lanyon L (2003) Endocrinology: bone adaptation requires oestrogen receptor-alpha. Nature 424(6947):389. PubMed eng
30. Imai Y, Kondoh S, Kouzmenko A, Kato S (2010) Minireview: osteoprotective action of estrogens is mediated by osteoclastic estrogen receptor-alpha. Mol Endocrinol 24(5):877–885. PubMed Epub 2009/11/17. eng
31. Imai Y (2014) Exp Med 32(7):145–151
32. Nelson HD, Walker M, Zakher B, Mitchell J (2012) Sex steroid hormones and osteoporotic bone diseases. Menopausal hormone therapy for the primary prevention of chronic conditions: a systematic review to update the U.S. Preventive Services Task Force recommendations. Ann Intern Med 157(2):104–113. PubMed Epub 2012/07/13. eng
33. Barrett-Connor E, Cauley JA, Kulkarni PM, Sashegyi A, Cox DA, Geiger MJ (2004) Risk-benefit profile for raloxifene: 4-year data from the Multiple Outcomes of Raloxifene Evaluation (MORE) randomized trial. J Bone Miner Res Off J Am Soc Bone Miner Res 19(8):1270–1275. PubMed

Part V

Oncogenesis and Tumors

Bahtiyar Demiralp

Oncogenesis

34

Metin Manouchehr Eskandari and İrfan Esenkaya

Abstract

Oncogenesis or cancer formation is the expression of impaired cellular events in the favor of uncontrolled cell growth and proliferation. This occurs basically by disruptions in harmonious control effects of the growth-inducing, growth-inhibiting, apoptosis-regulating, and DNA-repairing mechanisms. A simplified understanding of these mechanisms is given in this chapter. In the first part of the chapter, regarding the concepts of susceptibility to and formation of cancers, the basic knowledge of cellular genetic content and events is reviewed. In the second part, molecular basis of oncogenesis is explained regarding the eight hallmarks of cancers. For better understanding, well-described examples of mechanisms responsible in musculoskeletal system tumors are given through the text. Certainly, cellular and molecular aspects of oncogenesis will continue to be the primary field of future investigations to reach better understanding, diagnosis, treatment, and prediction of prognosis of cancers.

Learning Outcomes

After you have studied this chapter, you will have an understanding of (1) factors that take part in susceptibility to and formation of cancers: (a) cellular genetic content including chromosomal DNA, noncoding RNA, epigenetic factors, and mitochondrial DNA and (b) cell events including cell proliferation cycle, cell signaling, and apoptosis; (2) molecular basis of oncogenesis regarding the eight hallmarks of cancers: (a) proliferation capacity without the need of inducing factors from outside of the tumor, (b) unresponsiveness of the tumor cells to growth inhibitory signals, (c) resistance to apoptosis, (d) non-aging state and immortality of tumor cells, (e) the ability of angiogenesis, (f) the ability of invasion and metastasis, (g) the capability of tumor cells to escape from and defend against the host immune mechanisms, and (h) the change of the metabolism of the tumor cells to produce less energy and more carbon side products.

M.M. Eskandari, MD (✉)
Department of Orthopaedics and Traumatology, School of Medicine, University of Mersin, Mersin, Turkey
e-mail: mmeskandari@yahoo.com

İ. Esenkaya, MD
Department of Orthopaedics and Traumatology, School of Medicine, İstanbul Medeniyet University, İstanbul, Turkey

F. Korkusuz (ed.), *Musculoskeletal Research and Basic Science*,
DOI 10.1007/978-3-319-20777-3_34

Terminology

Anti-oncogenes are genes that code tumor suppressive proteins (proteins that take part in inhibition of the cell growth process).

Apoptosis is programmed cell death that in normal tissue is initiated by sensation of irreparable cell abnormalities.

Cadherins are a group of calcium ion dependent transmembrane glycoproteins that provide cell-to-cell adhesions.

Cell cycle is the process of division of a cell into two daughter ones. This process has four phases and three control points.

Chimeric proteins are huge abnormal proteins synthesized by proto-oncogenes.

Chromosomal mutations are permanent alterations of the genome that can spontaneously occur during cell events or under the influence of environmental mutagens.

Chromosomal translocation is a common kind of mutation with exchange of DNA regions between two non-homolog chromosomes.

Chromosomal variations are widely seen hereditary alterations of DNA chains.

Cytoplasmic anaerobic glycolysis is a metabolic process with end products of lactic acid and ATP two each, per single glucose consumption.

Deletion is a common kind of mutation with removal and loss of nucleotides or gene regions.

Gene amplifications are duplications or multiplications of DNA regions.

Genetic polymorphism is the other name of chromosomal variations.

Epigenetic factors are regulating factors of gene expression that are not originated from DNA but mostly concern histones.

Long noncoding RNAs (lncRNAs) enhance and silence gene transcriptions by binding to specific regions of DNA chain.

Major histocompatibility complex (MHC) molecules are molecules that have an important role in cell-mediated immunity by binding the antigens and bringing them to the surface of the cells.

Matrix metalloproteases (MMPs) are enzymes secreted by either tumor cells or responsive inflammatory cells. They have role in tumor metastasis by the function of matrix degradation and mobilization of the loosened cells.

Micro-RNAs (miRNAs) are a kind of noncoding RNAs. Their main functions are regulation of translation of their target mRNAs into the proteins.

Mitochondrial DNA is a small amount of DNA that is found in mitochondria, a cytoplasmic organelle with important roles in cell energy generation, anabolic metabolism, and apoptosis.

Mitochondrial oxidative phosphorylation is a metabolic process that contains the transportation of pyruvate to mitochondria and the production of water, carbon dioxide, and ATPs as the end products.

Neo-angiogenesis is the ability to form new vascular structures.

Noncoding RNAs are transcribed from DNA segments but not translated to proteins. There are two main types of noncoding RNAs, micro-RNAs (miRNAs), and long noncoding RNAs (lncRNAs). Their main functions are modulation of protein synthesis.

p53 protein is a protein with important role in genomic integrity, its ineffectivity lead to increased risk of cancer development (Li-Fraumeni syndrome).

Point mutation is the replacement of a single nucleotide of a codon for another.

Proto-oncogenes are genes that function as inducers of cell growth and proliferation.

Retinoblastoma (Rb) protein is a tumor suppressive protein encoded by Rb anti-oncogene. Mutations of Rb gene that lead to non-functional or total loss of Rb protein functions significantly increase the risk of development of retinoblastoma, osteosarcoma, and soft tissue sarcomas.

Telomerase enzyme takes place in the process of repair of the shortened telomeres. Some cancer cells gain the ability of reactivation of telomerase and thus escape from the apoptosis.

Telomeres are non-transcriptional nucleotide sequences at the ends of the chromosomes. Their function is protection of the chromosomal gene regions. Their loss during repetitive cell divisions leads to apoptosis.

Introduction

Oncogenesis or formation of cancers is driven by genetic mechanisms. These mechanisms are regulated by molecular processes taking part in cellular differentiation, growth, functioning, and death. The main rules of these processes are encoded in cellular genetic content. All of the cellular events, genetic content, and molecular processes are influenced actively by the environmental factors. Eventually, oncogenesis is a cytogenetic event with both hereditary and environmental risk factors. In this chapter a global sight of cellular and molecular sides of oncogenesis is given. It is aimed to explain common basic mechanisms of oncogenesis conceptually, along with well-described examples from musculoskeletal system tumors. It seems that a thorough comprehension of molecular and cellular basis of oncogenesis provides broad fields to design better diagnostic, therapeutic, and prognostic tools.

Oncogenesis occurs as a cytogenetic event when the molecular balance of the cell events disrupt in the favor of uncontrolled cell growth and proliferation. The synonyms of oncogenesis are carcinogenesis and tumorigenesis. This chapter aims to present a conceptual approach to oncogenesis with the emphasis on musculoskeletal tumors and sarcomas that are generally originated from non-hematopoietic mesenchymal cells. This issue also contains the answer of the question "why did we prefer the term oncogenesis rather than the more commonly used carcinogenesis?" We avoid the term carcinogenesis as it might mislead readers to the epithelial cell originated carcinomas.

Genetic Content and Cell Events

Cellular genetic contents are encoded information that control all cellular events and eventually dictate both intercellular and interindividual differences. Cellular events like differentiation, growth, maintenance of function, and division all principally require energy and production of building stones. During these events macromolecules should be synthesized, organelles should be reproduced, products should be placed and organized correctly, and waste materials should be disposed effectively. All of these events are guided and controlled finely by genetic content regarding the needs of the organism and the environmental provisions. Cells of a single living organism, although theoretically have identical genetic content, drive their events in different manners. They differentiate, behave, divide, or even die variously. Individuals of the same species, based on their personally unique cellular genetic content, show both similarities and differences phenotypically. After all, cellular genetic content and its variations or changes prescribe the destiny of both a single cell and the organism. Susceptibility, formation, and response of the cell and the organism to diseases and treatment modalities are placed among the intercellular and interindividual differences [1–4]. In the following paragraphs of this section, individual properties and cell events that have a role in oncogenesis are described.

Chromosomal DNA composes the main part of the cellular genetic content. Consequently, cellular and individual diversities are mainly determined by alterations that involve chromosomal DNA. Other sources of diversities are alterations of noncoding RNAs, epigenetic factors, and mitochondrial DNA. Chromosomal DNA is constituted by a minor part of protein-coding and a major part of non-protein-coding regions. Non-protein-coding regions regulate the expression of the protein-coding regions and host the majority of DNA alterations. Thus, genetic diseases are more likely to be the results of abnormal regulating genes than the protein encoding ones. Alterations of chromosomal DNA are divided into two main types, variations and mutations [2, 4]. Alterations of the cellular genetic content are described in the following paragraphs.

Chromosomal variations, namely, genetic polymorphism, are widely seen hereditary alterations of DNA chains. These alterations that prescribe unique properties of every individual are carried by a very small portion (about 0.5 %) of the human genome. The rest of the genome is identical in all individuals. The most frequent type of polymorphism in human genome is positional variations of single nucleotides. Although the phenotypic importance of a great majority of these single nucleotide variations is not understood, the direct roles of a small number of them in susceptibility to diseases are explored.

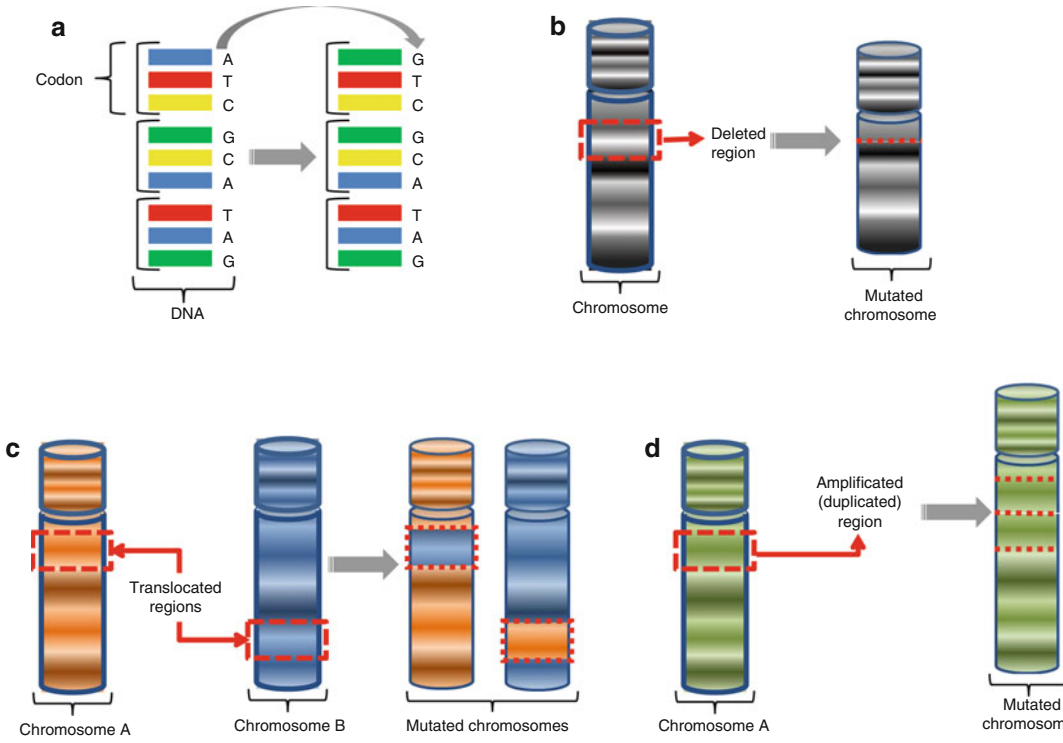

Fig. 34.1 Four forms of mutations commonly responsible in oncogenesis: point mutation (**a**), deletion (**b**), chromosomal translocation (**c**), and gene amplification (**d**)

The other frequent type of polymorphism in human genome is formation of abnormally large genes by multiplication of some regions of the DNA. About half of this type of variations involves the protein encoding regions and determines the majority of the individual differences [2, 4].

Mutations are permanent alterations of the genome that can spontaneously occur during cell events or under the influence of environmental mutagens. Due to their inheritance, mutations are divided into two major groups, germ line and somatic mutations. Germ line mutations can be transmitted to the next generation through the reproductive cells of the organism. Somatic mutations involve the non-reproductive tissue cells and usually do not pass to the descendants. There are many kinds of mutations regarding their effect on the structure of the DNA chain. The most frequent mutations in relation with oncogenesis are point mutations, deletions, chromosomal translocations, and gene amplifications (Fig. 34.1). Point mutations replace a single nucleotide of a codon for another. Actually most of these mutations are corrected or silenced by the cell DNA repair mechanisms. If the mutation remains unrepaired and alters the amino acid sequence of the transcribed protein, it can lead to differences in the cell events. Deletions are removal and loss of nucleotides or gene regions. These mutations can alter the sequence of the amino acids or even lead to the total loss of the proteins. Point mutations and deletions are basic mechanisms of functional deficiency or silencing of the genes (Table 34.1). Chromosomal translocations are exchanges of DNA regions between two non-homolog chromosomes. Translocations lead to oncogenesis by placing a growth-promoting gene beside a proto-oncogene or synthesis of huge chimeric proteins. Gene amplifications are duplications or multiplications of DNA regions [2]. Both chromosomal translocations and gene amplifications are basic genetic mechanisms of gene over-expressions in musculoskeletal tumors (Table 34.2).

Noncoding RNAs are one of two basic mechanisms of gene function regulation in living cell.

Table 34.1 Impairing or silencing mutations of anti-oncogenes in association with musculoskeletal tumors [1, 3, 7, 18–22, 24, 26–28, 34, 35]

Name of gene/s	Type of genetic alteration and associated conditions	Decreased/absent protein and function	Tumor with increased risk and related considerations	
RB	Germline inactivating point mutation or deletion, congenital retinoblastoma	Rb: negative regulator of cell cycle	Osteosarcoma (up to 1,000-fold risk of generation)	
			Soft tissue sarcomas	
P53	Germline inactivating mutation, Li Fraumeni syndrome	p53: genomic integrity receptor, promotion of DNA repair or apoptosis if needed	Osteosarcoma	
			Pleomorphic rhabdomyosarcoma	
			Pleomorphic undifferentiated sarcoma	
INK4a (CDKN2A)	Inactivating small deletions	p16 (a CDK-inhibitor): activation of Rb and regulation of G1/S checkpoint	Osteosarcoma and Ewing sarcoma	
		P14: augmentation of p53 functions		
RECQL4	Mutation, autosomal recessive inherited Rothmund-Thomson syndrome	ATP-dependent DNA helicase Q4 enzyme: occurrence of abnormalities during DNA replication	Osteosarcoma	
PTHR1	Heterozygous function reducing mutations	Reducing the affinity of the receptor for PTH or the receptor expression at the cell surface and subsequent unregulated endochondral ossification	Enchondroma syndromes (Ollier and Maffuci syndromes)	
EXT1 and EXT2	Germline loss-of-function mutation	Glycosaminoglycans: regulation of chondrocyte differentiation by providing normal diffusion of Ihh	Sporadic osteochondroma	Disrupted chondrocyte differentiation and osteochondral mass growth
			Hereditary exostosis	
			Chondrosarcoma (EXT mutations present in chondrosarcomas secondary to hereditary exostosis)	
APC	Sporadic or germline mutations	Abnormal APC protein and subsequent uncontrolled beta-catenin activity and increased cell adhesion and proliferation	Deep fibromatosis (desmoid tumor)	
NF1	Heterogeneous mutations, type I neurofibromatosis	Neurofibromin: negative regulator of the Ras oncogene signal transduction pathway	Neurofibroma	
			Malign peripheral nerve sheath tumor	
IDH1 and IDH2	Heterozygous somatic mosaic mutations	Modified isoforms of isocitrate dehydrogenase (IDH) enzymes leads to epigenetic changes (hypermethylation of DNA and histones leading to activation of oncogenes and inactivation of anti-oncogenes)	Solitary chondroma and enchondroma	Genetically both normal and abnormal cells are present in these masses
			Enchondroma syndromes (Ollier and Maffuci syndromes)	
			Both sporadic and chondromatosis-related chondrosarcomas	

Table 34.2 Over-expression mutations of proto-oncogenes in association with musculoskeletal tumors [3, 17–23, 28, 32, 33]

Gene/s	Type of genetic alteration	Mechanisms of effect	Tumor type and related descriptions	
CTNNB1	Sporadic mutation	Over-expressed beta-catenin and subsequent increased cell adhesion and proliferation	Deep fibromatosis (desmoid tumor)	
MDM2	Amplification	Over-expressed MDM2: inhibition of p53	Osteosarcoma	
CDK4	Amplification	Over-expressed CDK4: inhibition of Rb	Osteosarcoma	
NF1	Heterogeneous mutations at q arm of chromosome 17, type I neurofibromatosis	Neurofibromin: negative regulator of the Ras oncogene signal transduction pathway	Neurofibroma	
			Malign peripheral nerve sheath tumor	
MDR-1	Amplification or translocation	Over-expressed P-glycoprotein (P-gp or ABCB1) and subsequent increased effluxes of structurally diverse compounds from the tumor cell	Various sarcomas (including osteosarcoma), gaining resistance again apoptosis and therapeutic agents	
Fused EWS and FLI1 genes	t(11;22)(q24;q12) (main alteration present in 85 % of Ewing sarcomas)	Abnormal EWS fusion proteins with multiple effects leading to neoplasia formation	Ewing sarcoma (cells of origin is not clear yet)	
Fused EWS and ERG genes	t(21;22)(q22;q12)			
Fused EWS and ER81 genes	t(7;22)(p22;q12)			
Fused EWS and CHN genes	t(9;22)(q22;q12)	Abnormal EWS fusion protein with multiple effects leading to neoplasia formation	Extraskeletal myxoid chondrosarcoma	
Fused EWS and WT1 genes	t(11;22)(q13;q12)		Desmoplastic small round cell tumor	
Fused EWS and ATF1 genes	t(12;22)(q13;q12)		Clear cell sarcoma	
Fused COLA1 and PDGF-beta genes	t(17;22)(q22;q15)	Over-expression of PDGF-beta	Dermatofibrosarcoma protuberans	
Fused USP6 and promoter genes	Rearrangement of chromosome 17p13	USP6 over-expression and subsequent increased activity of NFKB and matrix metalloproteinases	Primary aneurysmal bone cyst	
Fused MYH9 and USP6 genes	t(17;22)	Unknown	Nodular fasciitis (proliferating cells have not all hallmarks of cancer and the condition underwent self-limitation)	
GNAS1	Somatic gain-of-function mutation	A G_s-protein with constant activity leading to interruption of differentiation of osteoblasts from precursor cells	Fibrous cortical defect	Developmental clinical conditions due to mutations after the formation of the skeleton
			Monostotic fibrous dysplasia	

Table 34.2 (continued)

Gene/s	Type of genetic alteration	Mechanisms of effect	Tumor type and related descriptions
Fused M-CSF and promoter genes	t(1;2)(p13;q37)	Over-expressed monocyte colony-stimulating factor and subsequent increased macrophage proliferation	Local type tenosynovial giant cell tumor (giant cell tumor of tendon sheath)
			Diffuse type tenosynovial giant cell tumor (pigmented villonodular synovitis)
Fused PAX3 and FOXO1 genes	t(2;13)(q35;q14)	Synthesis of associated chimeric transcription factors and subsequent disruption of skeletal muscle differentiation and tumor formation	Alveolar rhabdomyosarcoma
Fused PAX7 and FOXO1 genes	t(1;13)(q36;q14)		
Fused SS18 and SSX1 genes	t(x;18)(p11;q11)	Synthesis of associated chimeric transcription factors and interruption in the control mechanisms of cell cycle and tumor formation	Synovial sarcoma
Fused SS18 and SSX2 genes			
Fused SS18 and SSX4 genes			
Fused FUS and DDIT3 genes	Amplification of 12q13-q15	Over-expressed MDM2 and subsequent p53 inhibition and arrest of differentiation of adipose tissue cells	Well-differentiated liposarcoma
	t(12;16)(q13;p11)		Myxoid liposarcoma

The other is driven by epigenetic factors and will be described in the next paragraph. Noncoding RNAs are transcribed from DNA segments but not translated to proteins. The main types of noncoding RNAs are micro-RNAs (miRNAs) and long noncoding RNAs (lncRNAs). The main functions of miRNAs are regulation of translation of their target mRNAs into the proteins. Every miRNA modulates multiple protein-coding processes. Posttranscriptional silencing of a gene comes true by base pairing between associated mRNA's non-translating region and miRNA-multiprotein complex. This pairing process leads to either cleavage or repression of mRNA, ceasing its translation into the protein. It seems that miRNAs have important roles in either non-pathologic or pathologic tissue developments. There are efforts to synthetically produce miRNA-like agents that can bind specific mRNAs. These kinds of agents can be used for diagnostic aims as well as for silencing the oncogenes and treatment of neoplasms. Long noncoding RNAs enhance and silence gene transcriptions by binding to specific regions of DNA chain. To supply these effects, lncRNAs use different mechanisms. Their roles in human diseases including cancers are also under investigation [2, 5, 6].

Epigenetic factors are regulating factors of gene expression that are not originated from DNA. Changes of these factors are also heritable and mostly concern histones. Histones are low molecular weight proteins whose combinations make up a central core for DNA segment envelops. Histones and DNA segment combinations form nucleosomes, the basic structural units of chromosomes. In nucleosomes, the DNA segment is wrapped around histones in changing forms and compactness. These changes occur due to the dynamic and regulating structure of nucleosomes. Proteins and chemical agents can effect on both histones and DNA segments leading to nucleosome structure changes and exposing or obscuring of DNA to gene regulatory factors. These in turn lead to changes in transcription and translation of encoding DNA and protein synthesis (Fig. 34.2). As an example, acetylation of lysine residues of histones opens up the protein-encoding-DNA chain and leads to increase of transcription. Recent studies show that inherited or acquired epigenetic alterations and dysregulations are in close relation to many diseases particularly malignancies. An example of epigenetic changes is the indirect effect of mutant genes of isocitrate dehydrogenase

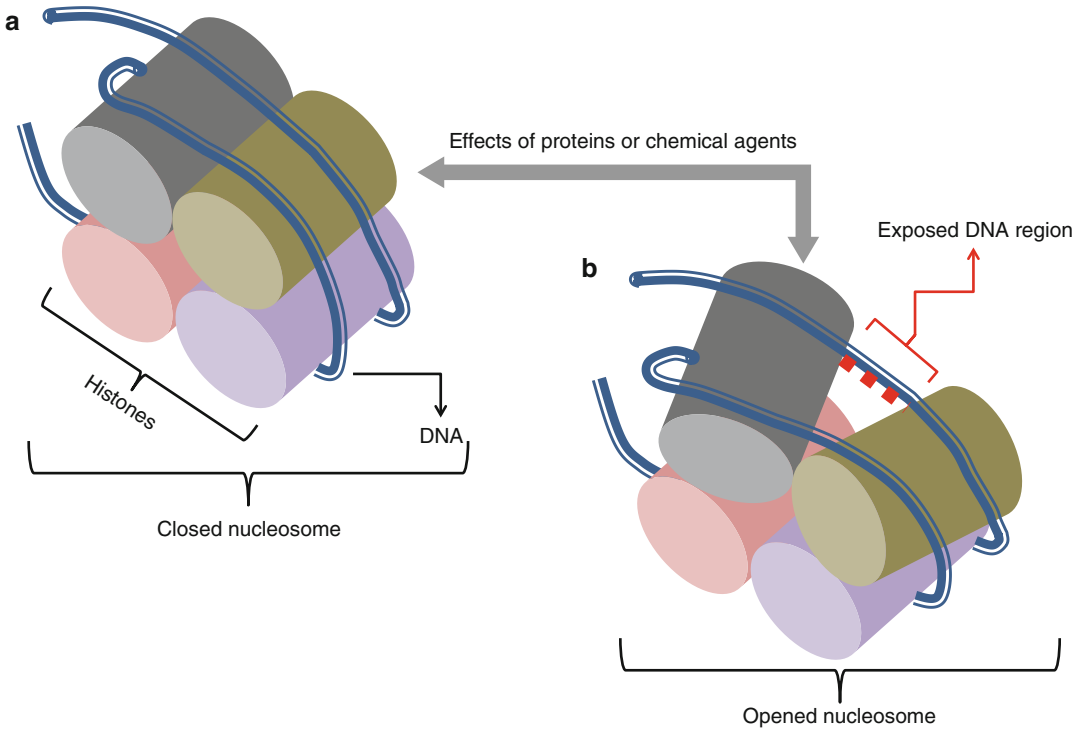

Fig. 34.2 Changes in the form and compactness of nucleosomes as epigenetic factors of gene expression. (**a**) closed (**b**) opened nucleosome under the effects of proteins or chemical agents

(IDH) enzymes and their relation with the formation of chondromas (Table 34.1). Many of the epigenetic alterations and dysregulations are reversible. Thus, diseases that occur on the base of these dysregulations could be treatable [2, 7–9].

Other than nuclear located events another important site of modulation of the cell metabolism and functions is mitochondria. These cytoplasmic organelles have their own DNAs although in small amounts. They can perform their own DNA replication, transcription, and translation. Mitochondria have important roles in cell energy generation, anabolic metabolism, and apoptosis. These functions of mitochondria can be regulated due to the necessities of the cell. Unlike the normal cells, in rapidly growing cells the main function of mitochondria change from energy generation into promotion of synthesis of basic molecules to be used in the structure of cellular components. Mitochondrial DNA, different from nuclear DNA, is inherited maternally. But as mitochondrial proteins can be produced by both nuclear and mitochondrial DNA, genetic diseases in association with mitochondrial dysfunctions can be either maternally inherited, X-linked, or autosomal [2, 10, 11].

Apoptosis or programmed cell death is an important mechanism of both normal and tumor tissue maintenance and growth. In normal tissue, apoptosis is initiated by sensation of irreparable cell abnormalities. These abnormalities might concern any one of cellular events. Genetic alterations responsible for oncogenesis also initiate apoptosis. The mechanism of apoptosis is triggered both by intrinsic and extrinsic pathways. Extrinsic pathway is driven by the cell signaling system and will be explained in the next paragraph. Intrinsic pathway works through mitochondrial functions. Intrinsic signals like DNA damage or inadequate synthesis of vital proteins lead to mitochondrial dysfunction. Consequently, mitochondrial contents leak out into the cytoplasm. Some of these contents form complexes by cytoplasmic proteins, which in turn activate apoptotic enzymes. Failure of apoptosis is one of the basic mechanisms of and requirements for the development of malignancies [1–3].

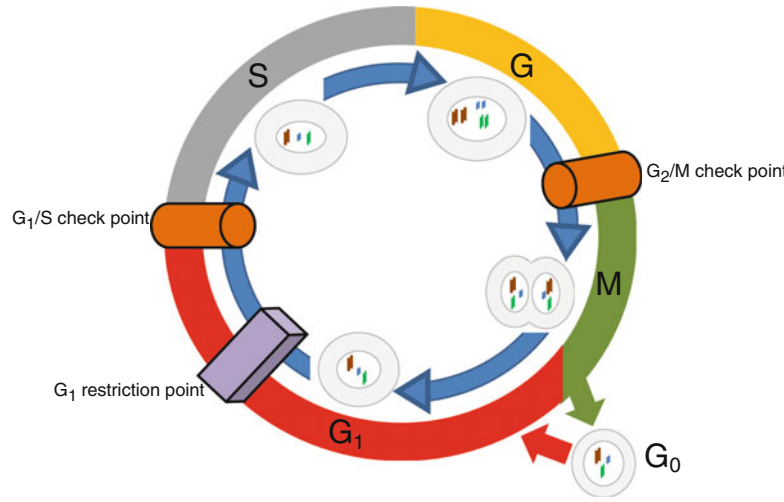

Fig. 34.3 Cell cycle phases and control points

Cell signaling and communications are indispensable features for growth, differentiation, liveliness, proliferation, and apoptosis of the cells and also maintenance of optimal organization of the concerning tissues. These events are controlled by numerous and various signals like ions, growth factors, hormones, and cytokines. Exposure of the cell to the signals is a continuous event. When a cell is exposed to insufficient appropriate signals apoptosis occurs. Signaling molecules or combinations of them ultimately initiate specific cell biological responses. In brief, signals are perceived by the cells through specific receptor proteins that are located over their surfaces. Activated receptor proteins in turn lead to reproduction of active transcription factors through several types of intracellular intermediate pathways. At the end, transcription factors enter nucleus and alter related gene expression. Mutations or alterations of the genes that encode proteins for this pathway might lead to over-inducing or inhibiting of the cell signaling mechanisms. These abnormalities have roles in unregulated cell proliferation and occurrence of cancers. Among the cell signal agents, growth factors and their receptors have the most important roles in oncogenesis. In normal conditions these protein-made factors stimulate cell events like growth, synthesis of cellular components, migration, differentiation, and proliferation. These effects of growth factors are mediated through their specific receptors to enhance or maintain normal tissue balance or to replace injured tissue regions. Dysregulation of the cell signaling pathways due to abnormal growth factors can lead to uncontrolled cell proliferation. Alterations of growth factor genes, leading to over-expression, have roles in several types of cancers. An example is over-expression of platelet-derived growth factor (PDGF)-beta gene and its relation by formation of dermatofibrosarcoma protuberans (Table 34.2) [1–3].

Cells, normal or abnormal, should proliferate to maintain or increase their population. Proliferation of the cells comes true by mitosis of each divisible cell into two daughter ones through the process of cell cycle. Cell cycle has four phases and three control points (Fig. 34.3). Its phases are G1 (initial or presynthetic growth), S (DNA replication and synthesis), G2 (gap or premitotic growth), and M (mitosis). When a cell is not genetically active and has no tendency to be divided, it is in stable or quiescent phase which is shown by G0. Cell cycle can begin both by activation of a G0 quiescent cell or by direct entrance of a just formed daughter cell into a new cycle. This occurs due to the type and necessities of the tissue. Cell cycle is controlled by a network of proteins and enzymes that are appointed one after the other (Fig. 34.4). Regulators of the cell cycle are cyclin-dependent serine/threonine kinase (CDK) named enzymes that are activated by binding to appropriate cyclin named proteins. Cyclin-CDK complexes are phosphorylated and activated by cyclin-activating kinases (CAKs). These activated complexes then, in turn, phosphorylate and activate control point protein

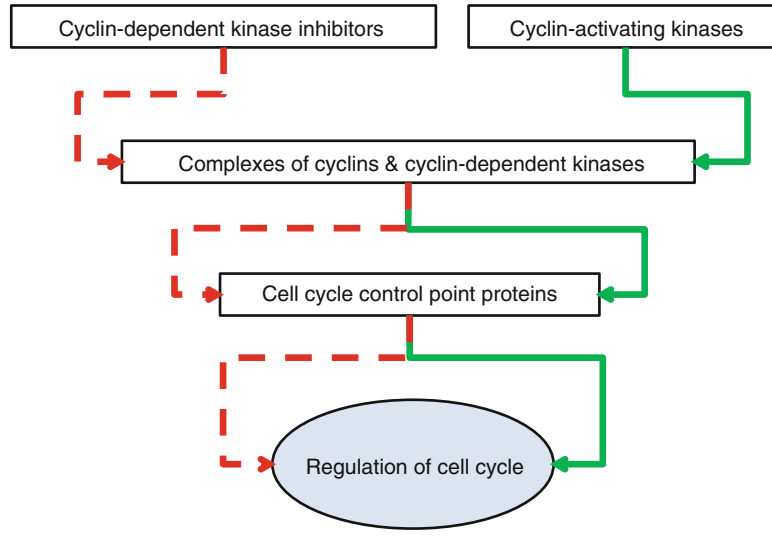

Fig. 34.4 Layers of protein network responsible for the regulation of cell cycle. Inhibitor effect is shown by *red* and activator effect by *green arrows*

components that are necessary for the progression of cell cycle. Two of the most important control point protein components are retinoblastoma (Rb) and p53 proteins. On the other hand, CDK-inhibitors (CDKIs) silence CDKs and halt the cell cycle through the control points. CDK-inhibitors are proteins that are shortly shown by p and a number (i.e., p16). The main aim of the cell cycle control points is fixing probable DNA irregularities. Control points of cell cycle are composed of one restriction point and two checkpoints (Fig. 34.3). The restriction point is located at the G1 phase. After passing this point, the cell would not respond to the removal of the growth factors. Checkpoints are located at the G1/S and G2/M interphases of the cycle (Fig. 34.3). The G1/S checkpoint is the primary location for fixation of the DNA irregularities before the expenditure of the cellular sources for dividing process. When this checkpoint is passed, the cell is forced to complete mitosis. At the G2/M checkpoint, damage or appropriateness of the duplicated DNA is controlled. Mutations of the genes that encode CDKs, cyclins, CDKIs, or control point protein components have roles in the development of cancers when they create a net effect of promoted progression of cell cycle and uncontrolled cell proliferation. Amplifications of CDK and cyclin genes facilitate progression of the cell cycle through checkpoints. The most frequent type of CDK mutation occurs in CDK4 genes. Over-expressed CDK4 binds to D cyclin and facilitates progression of cell cycle through G1 checkpoint by phosphorylation of Rb. Mutation and over-expression of CDK4 is one of the genetic alterations that are in association with osteosarcoma (Table 34.2). Mutations in CDKI, p53, and Rb genes that interrupt the functions of their related proteins lead to the increased tendency of oncogenesis through ineffective cell cycle checkpoints (Table 34.1) [1–3].

Molecular Basis of Oncogenesis

Cancers are expressions of uncontrolled multiplying of the cells due to aberrations in their genetic contents. To be able to lead to cancer, genetic aberrations should not be lethal for the precursor cells and could be passed to their daughters. These aberrations should interest one of the growth-inducing (proto-oncogene), growth-inhibiting (anti-oncogene), apoptosis-regulating, or DNA-repairing genes. In normal conditions, all of the cell events are under the harmonious effects of these genes. Oncogenesis occurs when the balancing effects of these genes is impaired. Actually, any cancer does not occur due to a single gene mutation. New cell generations derived from mutant precursor cells require subsequent accumulating mutations to produce a clinically evident cancer (Fig. 34.5). The number

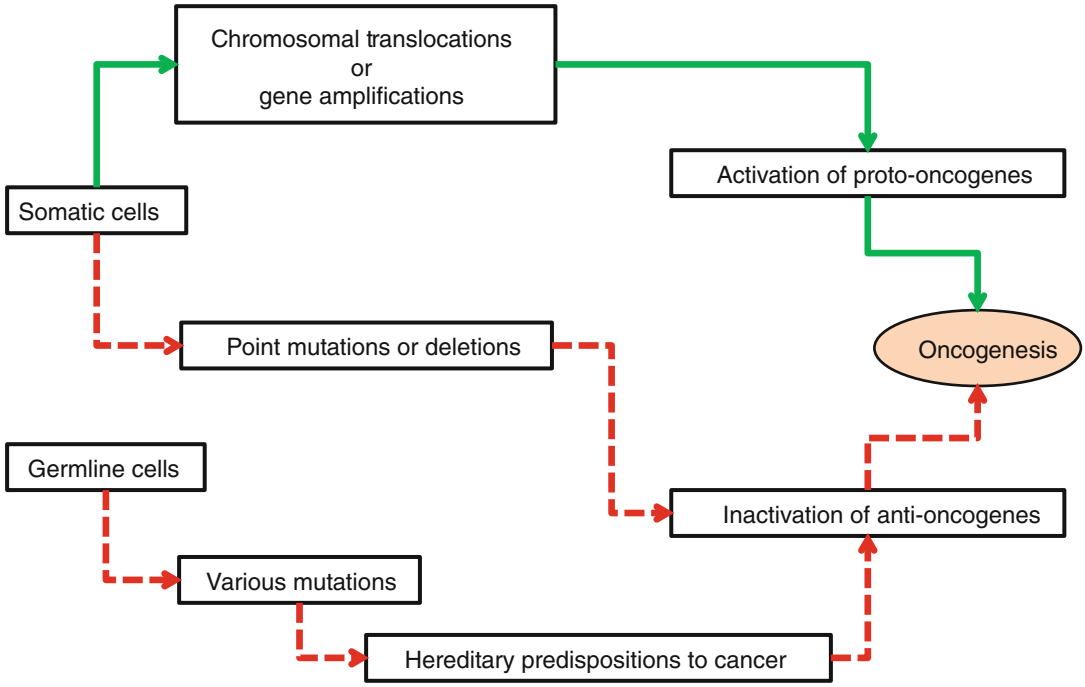

Fig. 34.5 Schematic diagram of subsequent accumulating mutations that are responsible for oncogenesis. *Green arrows* represent the mutation of proto-oncogenes and *red arrows* represent mutations of anti-oncogenes

of these subsequent mutations differs between dozens to even thousands. As DNA-repairing processes are the first step of body mechanisms against the formation of cancers, gene mutations that result in loss of DNA-repairing functions are the main predisposing factors of cancer formation (Table 34.1). These mutations lead to genomic instability without phenotypic change in related cells. With time, these cells acquire several accumulating mutations. Due to myriad numbers of possible genetic and epigenetic alterations, genotypes of tumor cells even in phenotypically similar tumors show significant differences. Despite the genotypic diversity, all the cancer cells are subjected to indispensable common physiological changes. These changes have been described in 2000 and revised in 2011 as *hallmarks of the cancer* by Hanahan and Weinberg. In the following paragraphs, molecular and biochemical bases of oncogenesis are described regarding each one of these standard hallmarks [3, 12–16].

The first hallmark is proliferation capacity without the need of inducing factors from outside of the tumor. This means that tumor cells can produce their own signals for growth. This property is usually gained by proto-oncogene mutations. Proto-oncogenes function as inducers of cell growth and proliferation. Dominant alterations of them produced by mutations are named oncogenes. As mentioned previously, the main mechanisms of over-expression of oncogenes are based on chromosomal translocations and gene amplifications. Over-expressed oncogenes encode oncoproteins that have the ability to induce the cell growth without responding to cell cycle checkpoints. Genetic alterations that lead to over-expression of proto-oncogenes in association with musculoskeletal tumors are summarized in Table 34.2 [3, 14–23].

The second hallmark is unresponsiveness of the tumor cells to growth inhibitory signals. Proteins that take part in inhibition of the cell growth process are called tumor suppressive proteins and are coded by anti-oncogenes. In normal conditions, all of the tumor suppressive proteins work harmoniously as the safe brake system of the cell cycle. In the case of abnormality or insufficiency, inhibitory mechanisms of cell proliferation halt. These create tendency and predisposition to oncogenesis due to failure or decrease in the

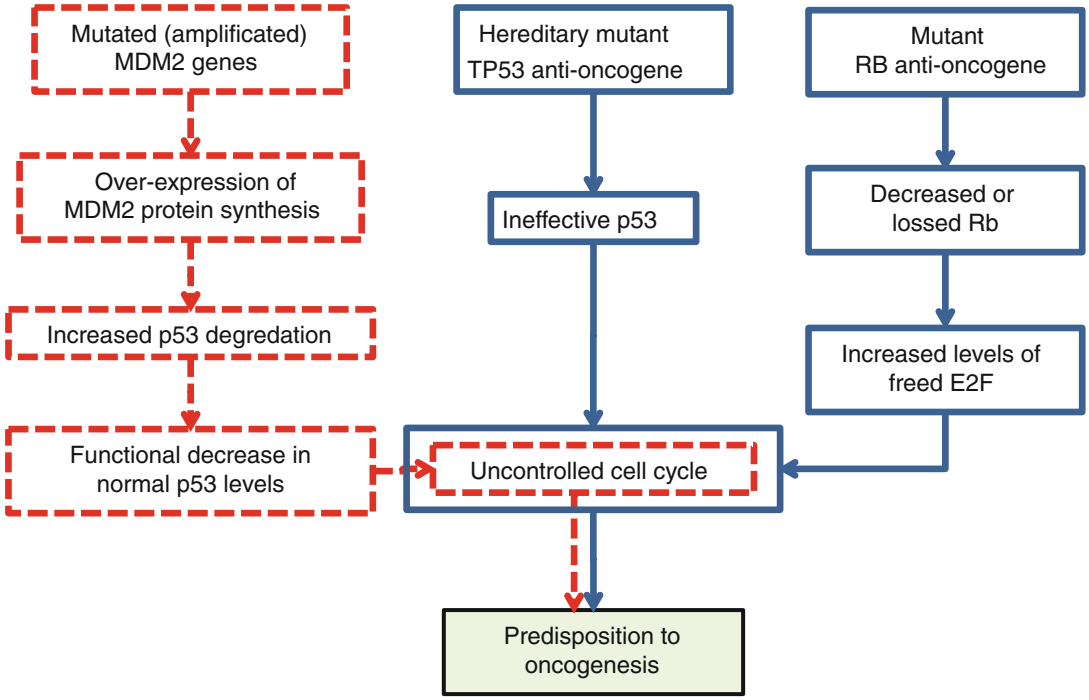

Fig. 34.6 Direct (*blue flowcharts*) and indirect (*red flowchart*) mechanisms of predisposition to oncogenesis

responsiveness of the tumor cells to growth inhibitory signals (Fig. 34.6). This hallmark is a functional loss and usually is gained due to biallelic recessive mutations of anti-oncogenes. As mentioned previously, the most frequent types of anti-oncogene mutations are point mutations and deletions. Alterations of anti-oncogenes that are in relation with increased risk of formation of musculoskeletal tumors are summarized in Table 34.1. In musculoskeletal system tumors, frequent genetic alterations that lead directly to the hallmark of unresponsiveness to the growth inhibitory signals involve TP53 and RB anti-oncogenes (Table 34.1 and Fig. 34.6). Frequently seen indirect mechanism of this hallmark occurs through over-expression of MDM2 gene (Table 34.2 and Fig. 34.6) [3, 14–16, 18–22, 24–26].

Tumor protein53 (TP53) anti-oncogene is located at chromosomal locus 17p13.1. Its encoded protein, p53, is a multifunction factor. Its net biologic function, as the component of both G1/S and G2/M checkpoints, is stopping cell cycle in the case of genetic damage, instability, or abnormality. It also acts as a transcription factor and modulates DNA repair and re-establishment of genetic stability (Fig. 34.7). When both alleles of TP53 gene are mutated, effective p53 cannot be produced and the cell cannot respond appropriately to DNA damage by stopping cell cycle, genetic repair, or apoptosis (Fig. 34.6). Inheritance of a single mutant allele of TP53 to the next generation is clinically represented as increased risk of cancer development. The name of this clinical condition is Li-Fraumeni syndrome with 25-fold increased risk of cancers including sarcomas. In this condition, the reason of high cancer risk is the vulnerability of the other normal TP53 allele to a second mutation and thus functional insufficiency of p53 [1, 3, 14–16, 18–22, 27, 28].

Retinoblastoma (RB) gene locates at chromosome locus 13q14. In normal conditions, the presence of the RB gene encoded protein (Rb) stops cell cycle progression by inhibition of G1/S transition as the final net effect. This effect is regulated by activation of a series of proteins (Fig. 34.8). When the cell completes the G1 phase, cyclin D and CDK4 complex become activated under the influence of the activators. This complex phosphorylates and inactivates Rb protein. Non-phosphorylated and active RB binds

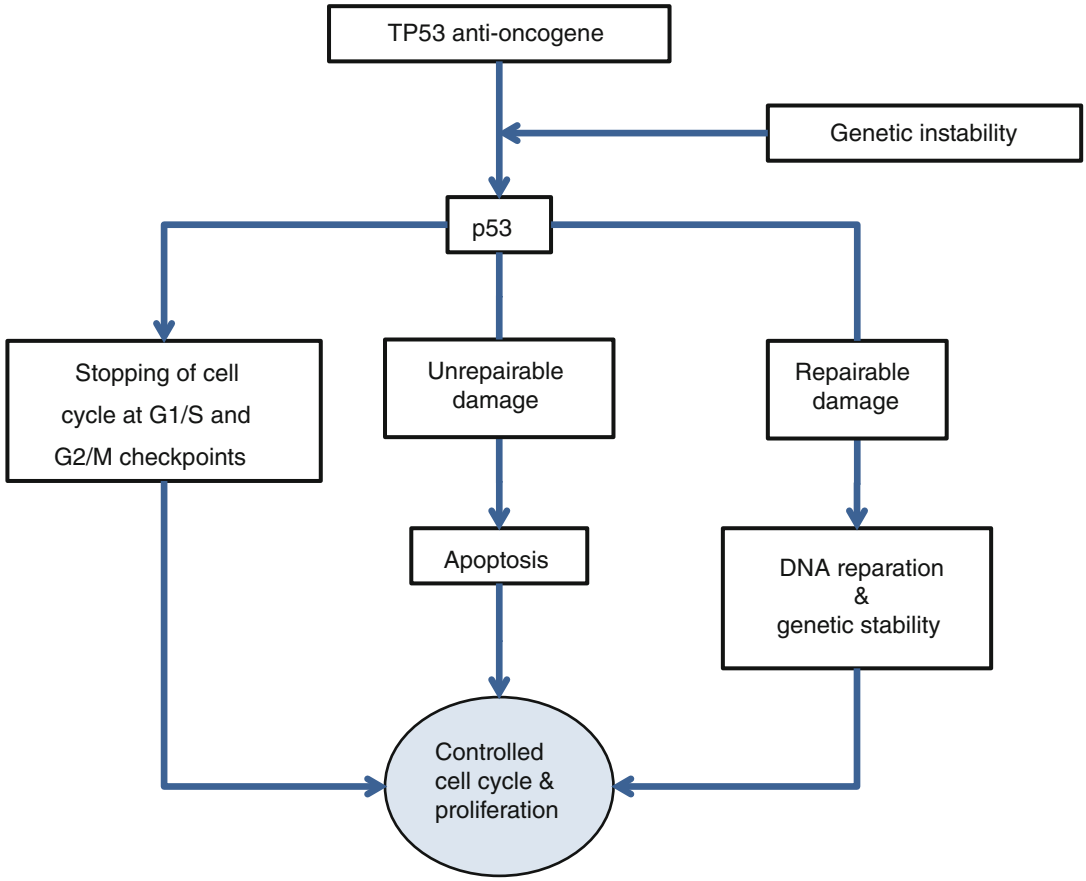

Fig. 34.7 Schematic explanation of the role of p53 in cell cycle control

and suppresses E2F family of transcription factors. Inactivated Rb protein decomposes from E2F. Freed E2F bind DNA and express the genes that their transcriptions are necessary for transition of cell into the phase of synthesis. Mutations that involve both RB alleles and inactivate normal Rb protein functions significantly increase the risk of development of retinoblastoma, osteosarcoma, and soft tissue sarcomas (Table 34.1 and Fig. 34.6). Mutations of RB gene that lead to non-functional or total loss of Rb are frequent deletions or missense point mutations. Single allele RB mutants can also be inherited to the next generations and increase the risk of cancer [1, 3, 14–16, 18–22, 27–29].

The most frequent indirect mechanism of the unresponsiveness to growth factors in musculoskeletal system sarcomas is amplifications of MDM2 genes. In normal conditions, the proteins encoded by MDM2 gene family regulate p53 functions through inducing its degradation (Table 34.2 and Fig. 34.6). Over-expression of MDM2 genes leads to functional decrease of p53 even in the case of normal TP53 alleles. This condition is seen in more than 30 % of sarcomas [1, 3, 14–16, 18–22, 27–31].

The third hallmark is resistance to apoptosis. Apoptosis is a quality control mechanism that should be discarded by tumor cells. Intrinsic mitochondrial pathway of apoptosis is frequently disrupted in cancers. This pathway is regulated by three different groups of proteins. The first group senses the abnormalities that require apoptosis and inhibits the anti-apoptotic effect of the second group. The anti-apoptotic proteins in turn inhibit the functions of the third group, the pro-apoptotic proteins. When the cell death becomes inevitable, the inhibitory effect of the first and second group of proteins diminishes and the pro-apoptotic proteins remain unchained. The unchained

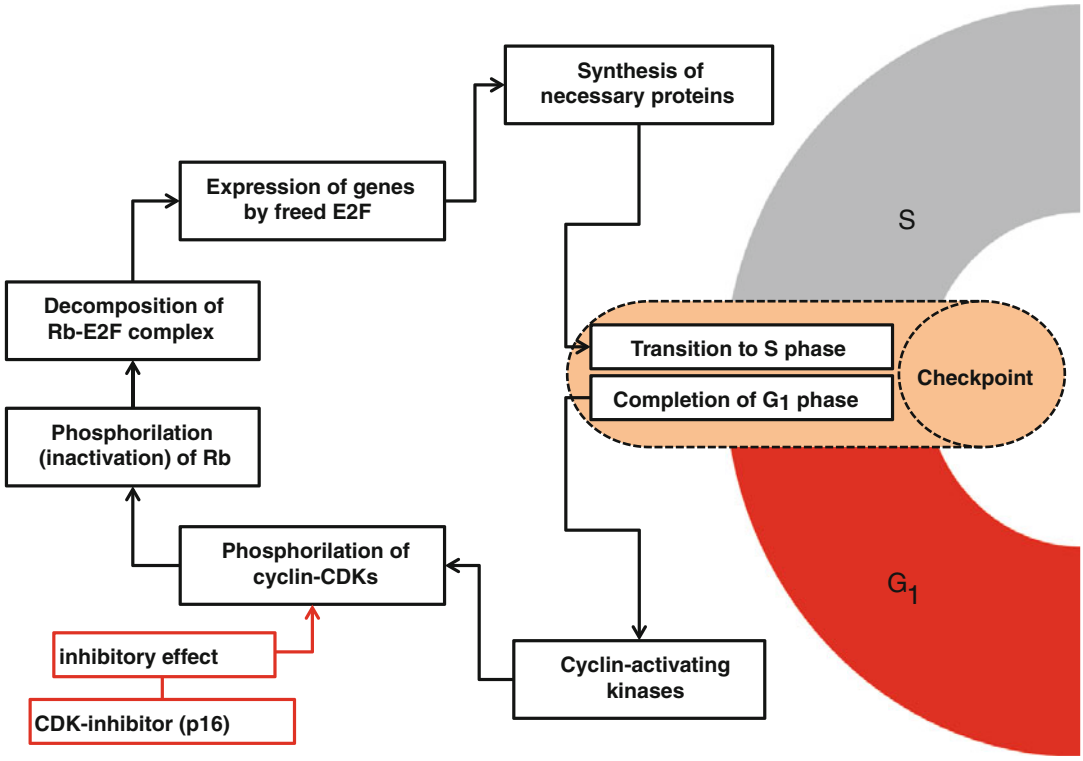

Fig. 34.8 Mechanism of cell cycle transition through G1/S checkpoint and the role of Rb and p16

pro-apoptotic proteins increase the mitochondrial membrane permeability. By leakage of the mitochondrial content to cytoplasm, apoptosis occurs (Fig. 34.9). Protein-53 (p53) is the main sensor protein that gives response to DNA damage. Gene alterations that lead to insufficiency of p53 decrease the probability of apoptosis in genomically unstable cell. A common mechanism of resistance to apoptosis in relation to anti-apoptotic proteins is over-expression of multidrug resistance-1 (MDR-1) gene (Table 34.2). Amplification of MDR-1 by translocation next to an activator gene or by copy number changes leads to over-expressed P-glycoprotein (P-gp or ABCB1) levels. This is a trans-membranous porter protein that can actively throw out harmful compounds from inside of the cell. Tumor cells in several malignancies can gain resistance to apoptosis and therapeutic agents through this mechanism [14–16, 18–21, 27–29, 32, 33].

The fourth hallmark is the non-aging state and immortality of tumor cells. The mechanism responsible for immortality of the tumor cells is described in the next paragraph. Non-aging state means that tumor cells have no limit for proliferation, unlike normal cells that can be divided by a limited number of cell cycle. The main mechanism of this feature is insufficiency of tumor suppressive proteins like p16. Protein16 is the most important CDK-inhibitor protein that might be found inactivated due to the mutation of its encoding gene, INK4a, in osteosarcomas and Ewing's sarcomas. Its functional insufficiency leads to the state of inactivity of Rb. Thus, G1/S checkpoint of cell cycle remains uncontrolled and unlimited cell proliferation enables (Table 34.1 and Fig. 34.8) [12, 14–16, 19–21, 25, 27–29, 34, 35].

The main mechanism of immortality of the cancer cells is the ability of reactivation of the telomerase enzyme by these cells (Fig. 34.10). In normal adult somatic cells there are limited amounts of telomerase. Telomeres are non-transcriptional nucleotide sequences at the ends of the chromosomes. They are synthesized by a reverse transcriptase enzyme. The function of the telomeres is protection of the gene regions next

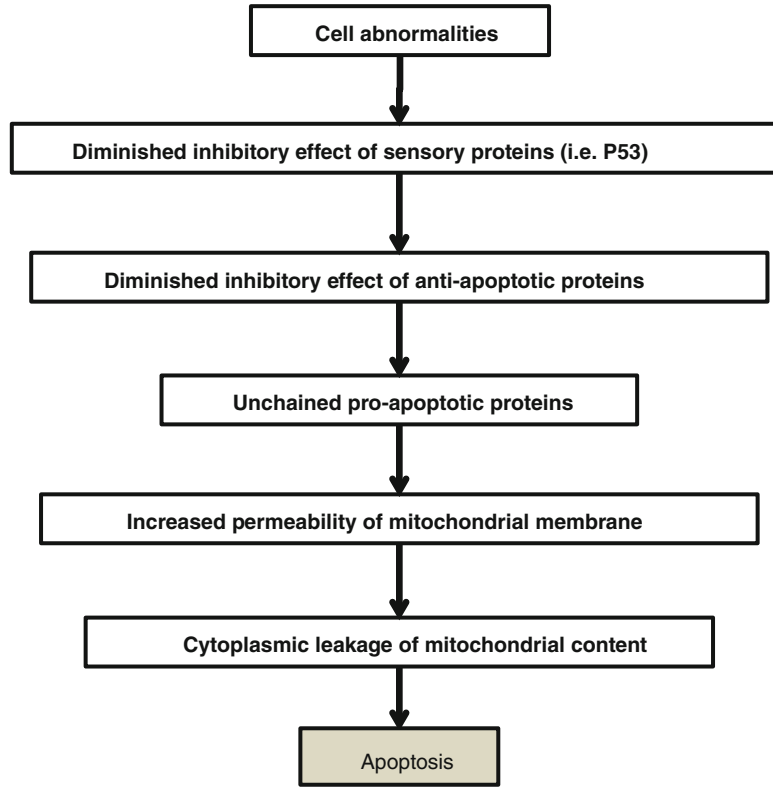

Fig. 34.9 Schematic explanation of intrinsic mitochondrial pathway of apoptosis

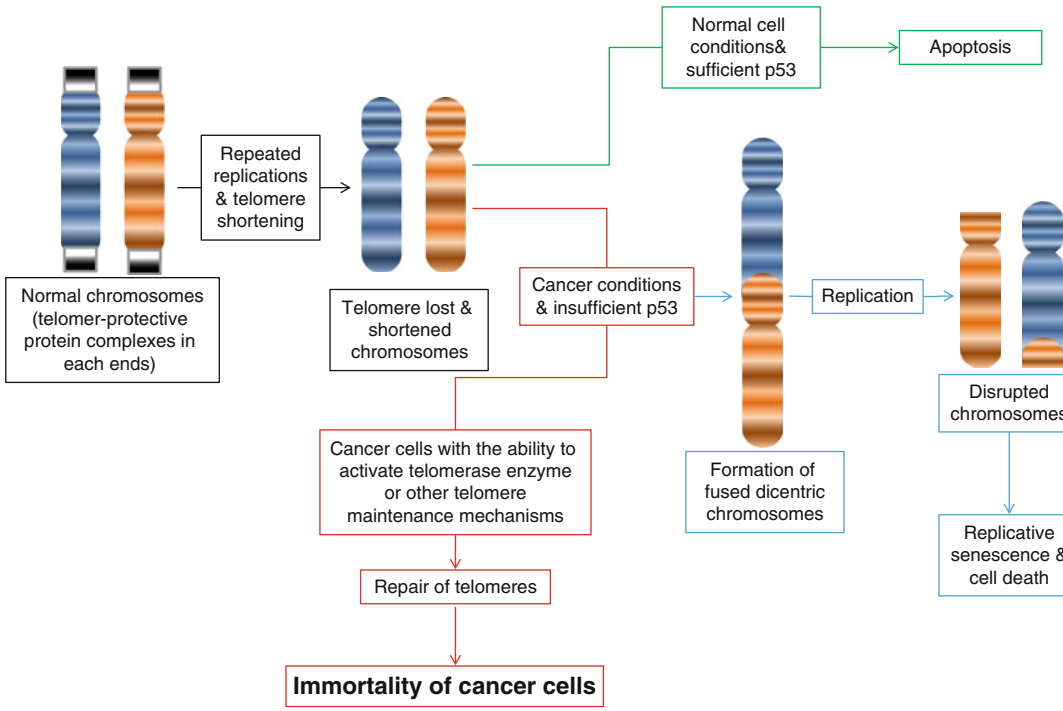

Fig. 34.10 Mechanisms responsible for immortality of cancer cells

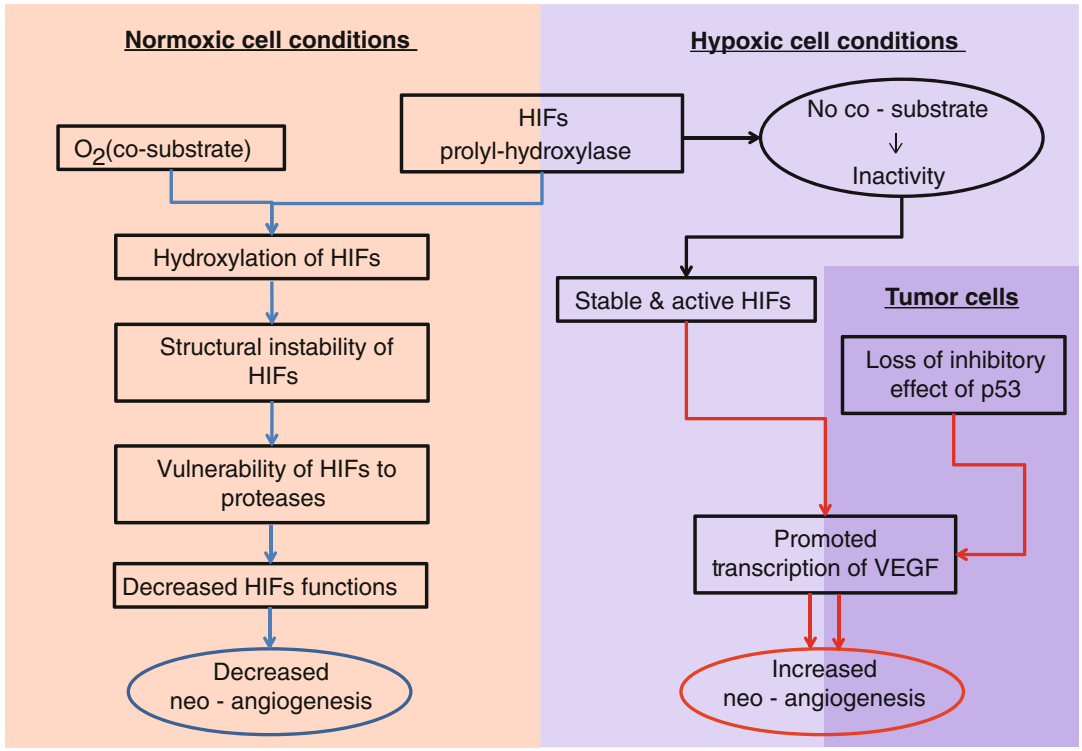

Fig. 34.11 Mechanism of changes in neo-angiogenesis in normoxic, hypoxic, and tumor cell conditions (*HIFs* hypoxy inducible factors and *VEGF* vascular endothelial growth factors)

to them from deterioration or fusion to the other chromosomal ends. This function occurs by binding of the protective proteins by telomeres. During cell cycles, replication of the chromosomes does not occur along the whole length of the chromosome and repetitive cycles result in gradually shortened telomere ends of the chromosomes. In normal cells and in the presence of sufficient p53, chromosomal shortening starts the process of apoptosis. Otherwise, in cancer cells and absence of p53, shortened and unprotected chromosomal ends fuse together and form dicentric long chromosomes. These abnormal chromosomal structures are prone to breaks and disruptions during the subsequent mitotic replication and divisions. This event that even in the case of cancer causes DNA breakage and cell death is named replicative senescence. Some of the cancer cells gain the ability to maintain the length of their telomeres. One mechanism of gaining this ability is reactivation of the telomerase enzyme. These types of cancer cells can repair their telomeres and escape from apoptosis (Fig. 34.10). These are the highest grade malignant cells and are prone to more genetic alterations on their proto-oncogene and anti-oncogene regions. Consequently, they can gain more adaptive changes against many kinds of environmental hazards including therapeutic agents [12, 14–16, 19, 21, 27, 28, 36–38].

The fifth hallmark is the ability of angiogenesis of the tumor to assure uptake of vital requirements, removal of wastes, and growth of the tumor. Actually, without the ability of angiogenesis any solid tumor mass cannot develop and is obligated to remain as very small in situ lesions. Thus, neo-angiogenesis is a basic requirement of neoplastic mass formation. Neo-angiogenesis of the tumors occur by increase of pro-angiogenic and decrease of anti-angiogenic factors' functions under the influence of several mechanisms. One of these mechanisms is driven by hypoxia inducible factors (HIF) family (Fig. 34.11). These are protein macromolecules that are sensitive to cell hypoxia and work as transcriptional factors. Without these factors no vascular system

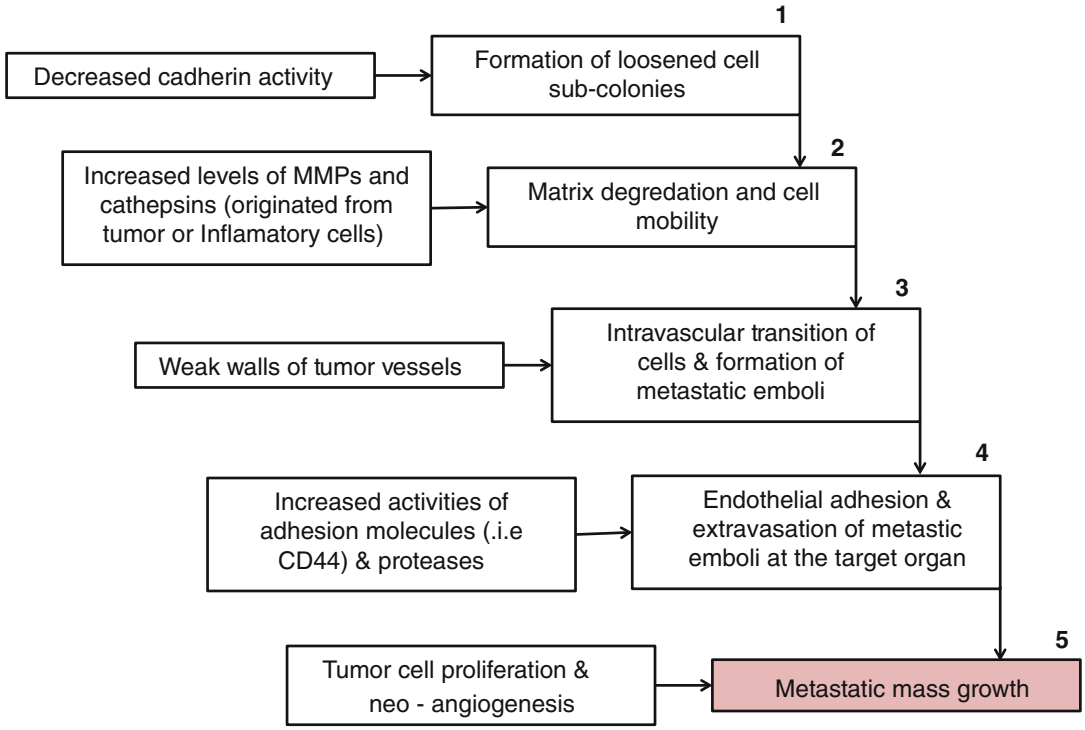

Fig. 34.12 Mechanisms and five steps of invasion and metastasis in tumors

formation and development can occur in both embryo and cancer masses. In normoxic cell conditions HIF prolyl-hydroxylase uses oxygen as co-substrate and becomes activated. This activated enzyme hydroxylates HIFs at their proline residues. By hydroxylation, HIFs become unstable and vulnerable to proteases. In the case of hypoxia, HIF prolyl-hydroxylase becomes inhibited and HIFs remain stabilized. Stabilized HIFs promote the transcription of pro-angiogenic factors like vascular endothelial growth factor (VEGF). This factor stimulates the proliferation of endothelial cells and the formation and branching of vessels. Vascular endothelial growth factor expression is decreased by p53. Thus, in tumor cells both hypoxia and loss of p53 collaborate in the development of neo-angiogenesis (Fig. 34.11). In addition to supplying requirements for tumor cells and enabling growth, neoangiogenesis has other important effects in malignancies. Proliferated endothelial cells secret insulin-like (IGF) and platelet-derived growth factor (PDGF). These growth factors stimulate tumor growth. Malign cancers develop vast vascular structures with abnormally weak walls. Cancer cells can easily pass through these walls and cause metastasis [14–16, 19, 21, 27, 28, 39–41].

The sixth hallmark is the ability of invasion and metastasis. This feature occurs by a chain of consequent events (Fig. 34.12). The first step is loosening of the intercellular links. This occurs due to decline in the functions of cadherin family adhesion macromolecules in tumors. Cadherins are a group of calcium ion dependent transmembrane glycoproteins that provide cell-to-cell adhesions. Loosened cells form metastatic cell sub-colonies. The important event of the second step is matrix degradation. Its reason is increased level of proteases, particularly matrix metalloproteases (MMPs) and cathepsins, in tumors. These enzymes are secreted by either tumor cells or responsive inflammatory cells. Due to overexpression of proteases, extracellular matrix (ECM) and also cell-ECM protein links are degraded. Thus, tumor cells of metastatic subcolony are able to mobilize through degraded matrix gaps. Mobilization and migration of tumor

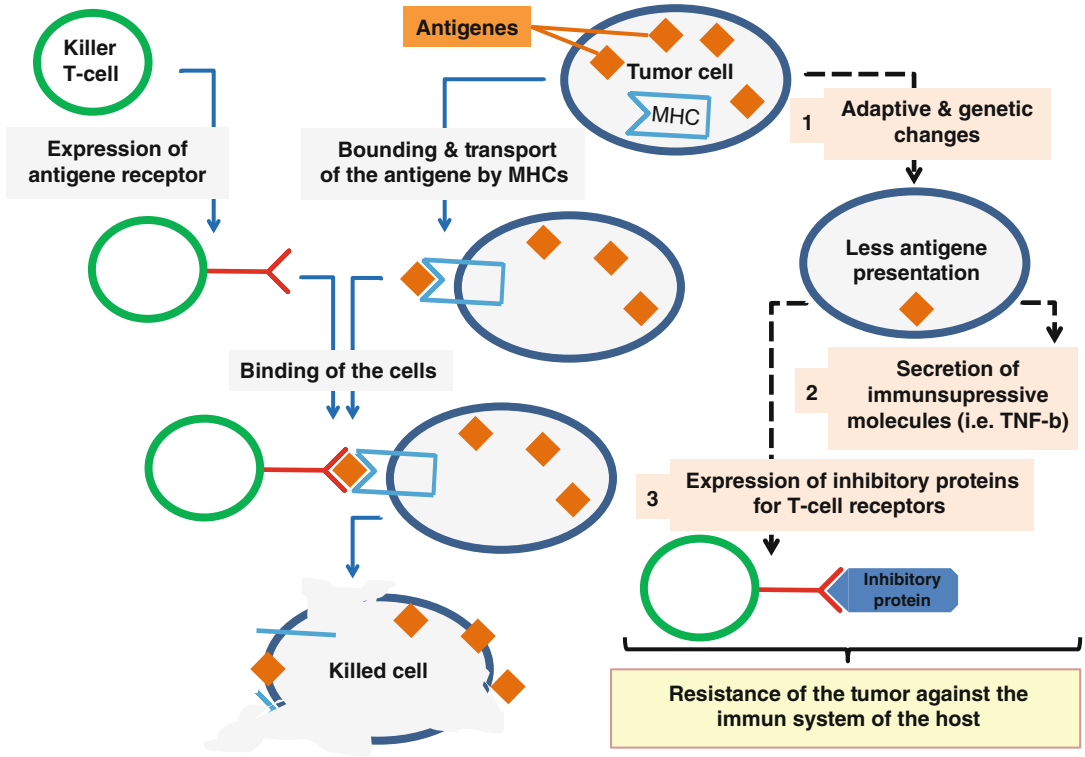

Fig. 34.13 Mechanism of cell-mediated immune response to tumor cells and three ways (*numbered areas*) of resistance of the tumor cells (*MHC* major histocompatibility complex)

cells is modulated by several motility and chemotactic factors. These factors are autocrine (released by tumor cells), paracrine (released by stromal cells), and ECM degradation originated. The third step is transition of the cells into the lumen of the vessels and formation of metastatic emboli. As mentioned earlier, vessels of the tumors have weak walls that can be easily passed by metastatic cells. In blood circulation, tumor cell groups bind platelets and coagulation factors and compose metastatic emboli. The fourth step is extravasation of metastatic emboli at the target organ. Adhesion molecules like CD44 and proteases take part in this process. Expressed CD44 levels are found in many tumors and facilitate adhesion of the metastatic emboli to the hyaluronate component of vascular endothelium of the target organ. Proteases degrade the vascular base membrane and allow cells to pass to the host ECM. The last step consists of cell proliferation, neo-angiogenesis, and mass growth at the metastatic site [1, 14–16, 19, 21, 27–29, 42–46].

The seventh hallmark is the capability of tumor cells to escape from and defend against the host immune mechanisms. For these aims tumor cells adapt their immunogenic properties and suppress the immune system of the host. The main protective immune response of the host to the tumor cells is cell-mediated. Tumor cells have altered genes and produce numerous abnormal proteins. These proteins are recognized as antigens and stimulate host immune response. Antigens are bound and brought to the surface of the tumor cells by major histocompatibility complex (MHC) molecules. Cytotoxic (CD8+) T-lymphocytes express T-cell antigen receptors (TCRs) for each specific antigen. Cytotoxic T and tumor cells are bound together closely by TCR and MHC linkages. Through this intercellular linkage, T cell can destroy tumor cell (Fig. 34.13). Tumor cells try to defuse host immune response by several mechanisms. One of these mechanisms, relying on natural selection rule, is the elimination of cells with high immunogenic properties during tumor growth. By time tumor

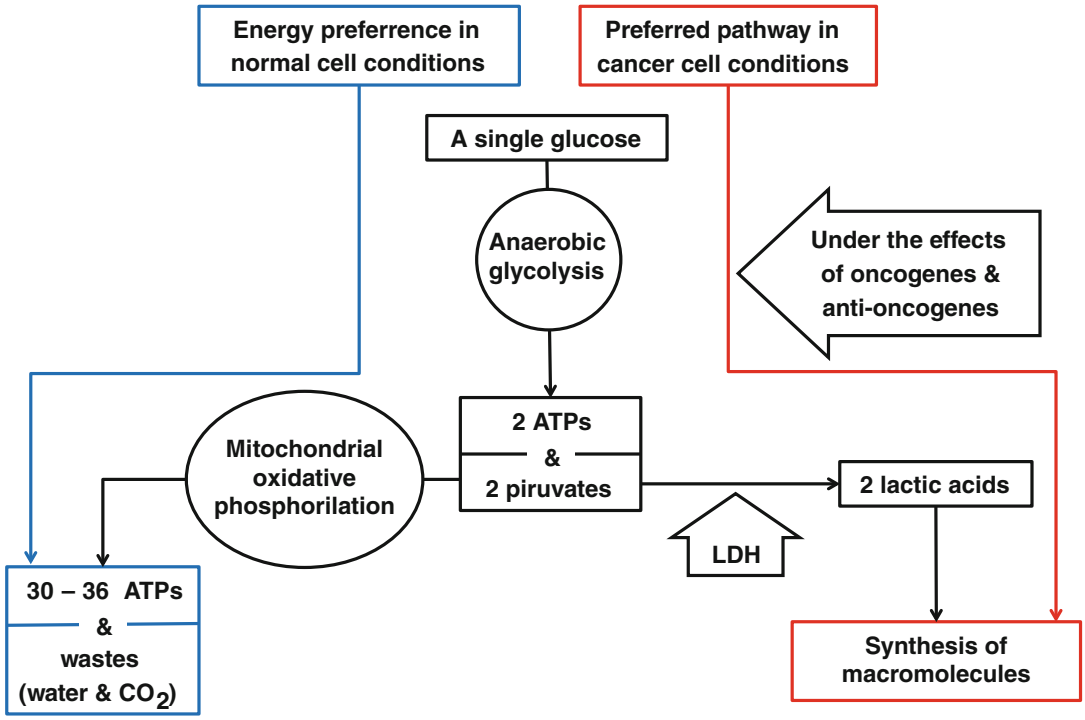

Fig. 34.14 Cell metabolism preference in tumor cell conditions (namely Warburg effect, showed by *red color pathway*) when compared with normal energy preference conditions (*blue color pathway*)

cells gain mutative and adaptive abilities to produce less antigenic proteins. The other main mechanism is expression of proteins that bind to inhibitory surface receptors of T cells. Thus, tumor cells become qualified to actively influence on the regulatory mechanisms of the host immune system. Cancer cells also affect the host immune system by secreting immunosuppressive molecules like TNF-beta (Fig. 34.13). Yet, it is not clear that which one of these mechanisms is the most effective in each tumor type. Treatment approaches based on immune responses to tumors attract increasing interest. Among the musculoskeletal system malignancies, serum TNF-beta levels of Ewing's sarcoma patients are found abnormally elevated. On the other hand, high TNF-beta levels in high-grade osteosarcomas are found correlated with their poor response to chemotherapeutic agents [10, 11, 15, 16, 19, 27, 38, 47–53].

The eighth hallmark is the change of the metabolism of the tumor cells to produce less energy and more carbon side products. The reason of this change is that these cells have more rapid growth and proliferation rates than normal cells and thus need more carbon units to build macromolecules and organelles. This change of cell metabolism is named Warburg effect (Fig. 34.14). By this effect, although in the presence of plenty of oxygen, cytoplasmic anaerobic glycolysis is predominate to mitochondrial oxidative phosphorylation. End products of anaerobic glycolysis are lactic acid and ATP two each, per single glucose consumption. In this process, lactic acid is produced by reduction effect of lactic dehydrogenase (LDH) enzyme on pyruvate. Consumption of pyruvate prevents its transportation to mitochondria and its use in oxidative phosphorylation process which produces water, carbon dioxide, and much more ATPs as end products. Similar to embryonic cells, Warburg effect of cancer cells is produced by the influence of the oncogene and anti-oncogene proteins (i.e., p53), which have a part in cell signalization. Recent studies have shown that various metabolic alterations in different types of osteosarcoma cells have an important role in the tumor's ability of invasion and metastasis [15, 16, 19, 54–59].

Although present in all malignancies the degree of the above mentioned hallmark abilities determines the progressiveness of each cancer. Cells of a tumor do not remain same and genetically stable yet after clinically advanced cancer formation. They change by the rule of natural selection. At the early period of mass formation, all cells might be genetically identical. But by growing the mass, cells should race to reach the nutrients. During this process cell groups with aggressive growth capacity win the race. Thus, the grade of malignancy and genetic diversity of the mass progress by time. This issue is also relevant for the response of the cancers to therapies [2–5, 16].

Clinical Relevance

What can be the practical benefits of the studies in the field of the cellular and molecular aspects of oncogenesis?

Accumulating scientific knowledge on cellular and molecular aspects of oncogenesis opens new doors for better understanding, diagnosis, treatment, and prediction of prognosis of cancers. Common use of modern diagnostic techniques like immunohistochemistry, cytoplasmic staining, and fluorescent in situ hybridization has even revolutionized the classical classifications of tumors. Investigation of new molecular markers enables early diagnosis, determination of predisposition, and prediction of individual responses to oncogenesis. It seems that molecular markers have also the potential of revolutionary changes in grading and delicate prediction of prognosis in each individual cancer case. Molecular markers represent tumor hallmark abilities and thus can be used in the determination of the progressivity of each tumor. Understanding cancer cell growth pathways promises therapeutic alterations in cellular signals to halt oncogenesis in pro-growth phases. Efforts in therapeutic targeting of cellular metabolism, neutralization of the immuno-editing abilities, sensitization to host immune system, immunotherapy, alterations in cellular adhesion-migration abilities, epigenetic changes, and telomere-based therapies are among the promising molecular treatment methods of cancers [5, 8, 24, 26, 30, 36, 37, 44, 45].

References

1. Yuan J, Fuchs B, Scully SP (2007) Molecular basis of cancer. In: OBS-3, Einhorn TA, O'Keefe RJ, Buckwalter JA (eds) Orthopaedic basic science, 3rd edn. American Academy of Orthopaedic Surgeons, Rosemont. ISBN: 139780892039340, Chapter 21, pp 379–393
2. Mitchell RN (2015) The cell as a unit of health and disease. In: Kumar V, Abbas AK, Aster JC (eds) Robbins and Cotran pathologic basis of disease, 9th edn. International edition, Philadelphia. ISBN: 978-0-8089-2450-0, Chapter 1, pp 1–29. 2015, by Saunders, an imprint of Elsevier Inc
3. Jones KB MD (2011) Musculoskeletal oncology. In: Flynn JM MD (ed) Orthopaedic knowledge update, 10th edn. American Academy of Orthopaedic Surgeons, Rosemont, pp 193–212, Chapter 17
4. Hall PA, Watt FM (1989) Stem cells: the generation and maintenance of cellular diversity. Development 106(4):619–633, Review
5. Kafchinski LA, Jones KB (2014) MicroRNAs in osteosarcomagenesis. Adv Exp Med Biol 804:119–127. doi:10.1007/978-3-319-04843-7_6, Review
6. Miao J, Wu S, Peng Z, Tania M, Zhang C (2013) MicroRNAs in osteosarcoma: diagnostic and therapeutic aspects. Tumour Biol 34(4):2093–2098, Review
7. Amary MF, Damato S, Halai D, Eskandarpour M, Berisha F, Bonar F, McCarthy S, Fantin VR, Straley KS, Lobo S, Aston W, Green CL, Gale RE, Tirabosco R, Futreal A, Campbell P, Presneau N, Flanagan AM (2011) Ollier disease and Maffucci syndrome are caused by somatic mosaic mutations of IDH1 and IDH2. Nat Genet 43(12):1262–1265. doi:10.1038/ng.994
8. Lawlor ER, Thiele CJ (2012) Epigenetic changes in pediatric solid tumors: promising new targets. Clin Cancer Res 18(10):2768–2779. doi:10.1158/1078-0432.CCR-11-1921, Review
9. Lee JY, Lee TH (2012) Effects of histone acetylation and CpG methylation on the structure of nucleosomes. Biochim Biophys Acta 1824(8):974–982. doi:10.1016/j.bbapap.2012.05.006, Epub 2012 May 22. Review
10. Galluzzi L, Morselli E, Kepp O, Vitale I, Rigoni A, Vacchelli E, Michaud M, Zischka H, Castedo M, Kroemer G (2010) Mitochondrial gateways to cancer. Mol Aspects Med 31(1):1–20. doi:10.1016/j.mam.2009.08.002, Epub 2009 Aug 19. Review

11. Gogvadze V, Zhivotovsky B, Orrenius S (2010) The Warburg effect and mitochondrial stability in cancer cells. Mol Aspects Med 31(1):60–74. doi:10.1016/j.mam.2009.12.004, Epub 2009 Dec 6. Review
12. Franceschi C (1989) Cell proliferation, cell death and aging. Aging (Milano) 1(1):3–15, Review
13. Tzen CY, Estervig DN, Minoo P, Filipak M, Maercklein PB, Hoerl BJ, Scott RE (1988) Differentiation, cancer, and anticancer activity. Biochem Cell Biol 66(6): 478–489, Review
14. Hanahan D, Weinberg RA (2000) The hallmarks of cancer. Cell 100(1):57–70, Review
15. Hanahan D, Weinberg RA (2011) Hallmarks of cancer: the next generation. Cell 144(5):646–674. doi:10.1016/j.cell.2011.02.013, Review
16. Kumar V, Abbas AK, Aster C (2015) Neoplasia. In: Kumar V, Abbas AK, Aster JC (eds) Robbins and Cotran pathologic basis of disease, 9th edn. International edition, Philadelphia, pp 265–340. ISBN: 978-0-8089-2450-0, Chapter 7. 2015, by Saunders, an imprint of Elsevier Inc
17. Krishnan B MS, Khanna G MD, Clohisy D MD (2008) Gene translocations in musculoskeletal neoplasms. Clin Orthop Relat Res 466(9):2131–2146
18. Flanagan AM, Delaney D, O'Donnell P (2010) The benefits of molecular pathology in the diagnosis of musculoskeletal disease : part I of a two-part review: soft tissue tumors. Skeletal Radiol 39(2):105–115. doi:10.1007/s00256-009-0759-x
19. Flanagan AM, Delaney D, O'Donnell P (2010) Benefits of molecular pathology in the diagnosis of musculoskeletal disease : part II of a two-part review: bone tumors and metabolic disorders. Skeletal Radiol 39(3):213–224. doi:10.1007/s00256-009-0758-y
20. Marina N, Gebhardt M, Teot L, Gorlick R (2004) Biology and therapeutic advances for pediatric osteosarcoma. Oncologist 9(4):422–441, Review. (osteosarcoma oncogenes)
21. Perry JA, Kiezun A, Tonzi P, Van Allen EM, Carter SL, Baca SC, Cowley GS, Bhatt AS, Rheinbay E, Pedamallu CS, Helman E, Taylor-Weiner A, McKenna A, DeLuca DS, Lawrence MS, Ambrogio L, Sougnez C, Sivachenko A, Walensky LD, Wagle N, Mora J, de Torres C, Lavarino C, Dos Santos AS, Yunes JA, Brandalise SR, Mercado-Celis GE, Melendez-Zajgla J, Cárdenas-Cardós R, Velasco-Hidalgo L, Roberts CW, Garraway LA, Rodriguez-Galindo C, Gabriel SB, Lander ES, Golub TR, Orkin SH, Getz G, Janeway KA (2014) Complementary genomic approaches highlight the PI3K/mTOR pathway as a common vulnerability in osteosarcoma. Proc Natl Acad Sci U S A 111(51):E5564–E5573. doi:10.1073/pnas.1419260111, Epub 2014 Dec PubMed PMID: 25512523, PubMed Central PMCID: PMC4280630
22. Puls F, Niblett AJ, Mangham DC (2014) Molecular pathology of bone tumours: diagnostic implications. Histopathology 64(4):461–476. doi:10.1111/his.12275
23. Sorensen PH, Lessnick SL, Lopez-Terrada D, Liu XF, Triche TJ, Denny CT (1994) A second Ewing's sarcoma translocation, t(21;22), fuses the EWS gene to another ETS-family transcription factor. ERG Nat Genet 6(2):146–151
24. Couvineau A, Wouters V, Bertrand G, Rouyer C, Gérard B, Boon LM, Grandchamp B, Vikkula M, Silve C (2008) PTHR1 mutations associated with Ollier disease result in receptor loss of function. Hum Mol Genet 17(18):2766–2775. doi:10.1093/hmg/ddn176
25. Trosko JE, Chang CC, Upham BL, Tai MH (2004) Ignored hallmarks of carcinogenesis: stem cells and cell-cell communication. Ann N Y Acad Sci 1028: 192–201, Review
26. Wang LL, Gannavarapu A, Kozinetz CA et al (2003) Association between osteosarcoma and deleterious mutations in the RECQL4 gene in Rothmund-Thomson syndrome. J Natl Cancer Inst 95(9):669–674. doi:10.1093/jnci/95.9.669
27. Horvai A (2015) Bones, joints, and soft tissue tumors. In: Kumar V, Abbas AK, Aster JC (eds) Robbins and Cotran pathologic basis of disease, 9th edn. International edition, Philadelphia. ISBN: 978-0-8089-2450-0. Chapter 26, pp 1179–1226. 2015, by Saunders, an imprint of Elsevier Inc
28. Morcuende JA, Buckwalter JA (1997) New advances in the molecular biology of musculoskeletal neoplasms. Iowa Orthop J 17:115–120
29. Sandberg AA, Bridge JA (2003) Updates on the cytogenetics and molecular genetics of bone and soft tissue tumors: osteosarcoma and related tumors. Cancer Genet Cytogenet 145(1):1–30, Review. (oncogenes)
30. Duhamel LA, Ye H, Halai D, Idowu BD, Presneau N, Tirabosco R, Flanagan AM (2012) Frequency of mouse double minute 2 (MDM2) and mouse double minute 4 (MDM4) amplification in parosteal and conventional osteosarcoma subtypes. Histopathology 60(2):357–359. doi:10.1111/j.1365-2559.2011.04023.x
31. Momand J, Jung D, Wilczynski S, Niland J (1998) The MDM2 gene amplification database. Nucleic Acids Res 26(15):3453–3459, Review
32. Chufan EE, Sim HM, Ambudkar SV (2015) Molecular basis of the polyspecificity of P-glycoprotein (ABCB1): recent biochemical and structural studies. Adv Cancer Res 125:71–96. doi:10.1016/bs.acr.2014.10.003 (MDR-1)
33. Hattinger CM, Stoico G, Michelacci F, Pasello M, Scionti I, Remondini D, Castellani GC, Fanelli M, Scotlandi K, Picci P, Serra M (2009) Mechanisms of gene amplification and evidence of coamplification in drug-resistant human osteosarcoma cell lines. Genes Chromosomes Cancer 48(4):289–309. doi:10.1002/gcc.20640
34. Brownhill SC, Taylor C, Burchill SA (2007) Chromosome 9p21 gene copy number and prognostic significance of p16 in ESFT. Br J Cancer 96(12):1914–1923, Epub 2007 May 29
35. Mohseny AB, Tieken C, van der Velden PA, Szuhai K, de Andrea C, Hogendoorn PC, Cleton-Jansen AM (2010) Small deletions but not methylations underlie CDKN2A/p16 loss of expression in conventional osteosarcoma. Genes Chromosomes Cancer 49(12): 1095–1103. doi:10.1002/gcc.20817

36. Flynn RL, Cox KE, Jeitany M, Wakimoto H, Bryll AR, Ganem NJ, Bersani F, Pineda JR, Suvà ML, Benes CH, Haber DA, Boussin FD, Zou L (2015) Alternative lengthening of telomeres renders cancer cells hypersensitive to ATR inhibitors. Science 347(6219):273–277. doi:10.1126/science.1257216
37. Gocha AR, Nuovo G, Iwenofu OH, Groden J (2013) Human sarcomas are mosaic for telomerase-dependent and telomerase-independent telomere maintenance mechanisms: implications for telomere-based therapies. Am J Pathol 182(1):41–48. doi:10.1016/j.ajpath.2012.10.001
38. Weng NP (2012) Telomeres and immune competency. Curr Opin Immunol 24(4):470–475. doi:10.1016/j.coi.2012.05.001, Epub 2012 May 22. Review
39. Franovic A, Holterman CE, Payette J, Lee S (2009) Human cancers converge at the HIF-2alpha oncogenic axis. Proc Natl Acad Sci U S A 106(50):21306–21311. doi:10.1073/pnas.0906432106, Epub 2009 Dec 2
40. Marxsen JH, Stengel P, Doege K, Heikkinen P, Jokilehto T, Wagner T, Jelkmann W, Jaakkola P, Metzen E (2004) Hypoxia-inducible factor-1 (HIF-1) promotes its degradation by induction of HIF-alpha-prolyl-4-hydroxylases. Biochem J 381(Pt 3): 761–767
41. Klotzsche-von Ameln A, Prade I, Grosser M, Kettelhake A, Rezaei M, Chavakis T, Flamme I, Wielockx B, Breier G (2013) PHD4 stimulates tumor angiogenesis in osteosarcoma cells via TGF-α. Mol Cancer Res 11(11):1337–1348. doi:10.1158/1541-7786.MCR-13-0201, Epub 2013 Sep 18
42. Kashima T, Kawaguchi J, Takeshita S, Kuroda M, Takanashi M, Horiuchi H, Imamura T, Ishikawa Y, Ishida T, Mori S, Machinami R, Kudo A (1999) Anomalous cadherin expression in osteosarcoma. Possible relationships to metastasis and morphogenesis. Am J Pathol 155(5):1549–1555
43. Kingsley LA, Fournier PG, Chirgwin JM, Guise TA (2007) Molecular biology of bone metastasis. Mol Cancer Ther 6(10):2609–2617
44. Matuschek C, Lehnhardt M, Gerber PA, Poremba C, Hamilton J, Lammering G, Orth K, Budach W, Bojar H, Bölke E, Peiper M (2014) Increased CD44s and decreased CD44v6 RNA expression are associated with better survival in myxofibrosarcoma patients: a pilot study. Eur J Med Res 19:6. doi:10.1186/2047-783X-19-6
45. Sancéau J, Truchet S, Bauvois B (2003) Matrix metalloproteinase-9 silencing by RNA interference triggers the migratory-adhesive switch in Ewing's sarcoma cells. J Biol Chem 278(38):36537–36546, Epub 2003 Jul 7
46. Ramaswamy S, Ross KN, Lander ES, Golub TR (2003) A molecular signature of metastasis in primary solid tumors. Nat Genet 33(1):49–54, Epub 2002
47. Cavallo F, De Giovanni C, Nanni P, Forni G, Lollini PL (2011) The immune hallmarks of cancer. Cancer Immunol Immunother 60(3):319–326. doi:10.1007/s00262-010-0968-0
48. Colotta F, Allavena P, Sica A, Garlanda C, Mantovani A (2009) Cancer-related inflammation, the seventh hallmark of cancer: links to genetic instability. Carcinogenesis 30(7):1073–1081. doi:10.1093/carcin/bgp127, Epub 2009 May 25. Review
49. Holzer G, Pfandlsteiner T, Blahovec H, Trieb K, Kotz R (2003) Serum levels of TNF-beta and sTNF-R in patients with malignant bone tumours. Anticancer Res 23(3C):3057–3059
50. Oliveira ID, Petrilli AS, Tavela MH, Zago MA, de Toledo SR (2007) TNF-alpha, TNF-beta, IL-6, IL-10, PECAM-1 and the MPO inflammatory gene polymorphisms in osteosarcoma. J Pediatr Hematol Oncol 29(5):293–297
51. Susnow N, Zeng L, Margineantu D, Hockenbery DM (2009) Bcl-2 family proteins as regulators of oxidative stress. Semin Cancer Biol 19(1):42–49. doi:10.1016/j.semcancer.2008.12.002, Epub 2008 Dec 24. Review
52. Tennant DA, Durán RV, Boulahbel H, Gottlieb E (2009) Metabolic transformation in cancer. Carcinogenesis 30(8):1269–1280. doi:10.1093/carcin/bgp070, Epub 2009 Mar 25. Review
53. Trieb K, Lechleitner T, Lang S, Windhager R, Kotz R, Dirnhofer S (1998) Evaluation of HLA-DR expression and T-lymphocyte infiltration in osteosarcoma. Pathol Res Pract 194(10):679–684
54. Bonuccelli G, Avnet S, Grisendi G, Salerno M, Granchi D, Dominici M, Kusuzaki K, Baldini N (2014) Role of mesenchymal stem cells in osteosarcoma and metabolic reprogramming of tumor cells. Oncotarget 5(17):7575–7588
55. Dang CV, Hamaker M, Sun P, Le A, Gao P (2011) Therapeutic targeting of cancer cell metabolism. J Mol Med (Berl) 89(3):205–212. doi:10.1007/s00109-011-0730-x, Epub 2011 Feb 8. Review
56. Giang AH, Raymond T, Brookes P, de Mesy Bentley K, Schwarz E, O'Keefe R, Eliseev R (2013) Mitochondrial dysfunction and permeability transition in osteosarcoma cells showing the Warburg effect. J Biol Chem 288(46):33303–33311. doi:10.1074/jbc.M113.507129, Epub 2013 Oct 7
57. Koppenol WH, Bounds PL, Dang CV (2011) Otto Warburg's contributions to current concepts of cancer metabolism. Nat Rev Cancer 11(8):618. doi:10.1038/nrc3038, Epub 2011 Apr 14. Review. Erratum in
58. Ortega AD, Sánchez-Aragó M, Giner-Sánchez D, Sánchez-Cenizo L, Willers I, Cuezva JM (2009) Glucose avidity of carcinomas. Cancer Lett 276(2): 125–135. doi:10.1016/j.canlet.2008.08.007, Epub 2008 Sep 14. Review
59. Sotgia F, Martinez-Outschoorn UE, Lisanti MP (2014) The reverse Warburg effect in osteosarcoma. Oncotarget 5(18):7982–7983

Bone Tumors

35

Bülent Erol, Turgay Er, Osman Emre Aycan, and Osman Mert Topkar

Abstract

Musculoskeletal tumors are uncommon and when they occur usually benign. The diagnosis of these tumors is often delayed. Early detection of a malignant tumor may not only make the difference between life and death, but also may allow for successful limb salvage surgery rather than amputation of the limb. This chapter will cover general principles of musculoskeletal tumor diagnosis and treatment, and the common individual entities.

Primary bone tumors are basically classified according to their originating tissues and each histological variant includes distinctive benign and malignant lesions (Table 35.1). Classification of bone tumors, regarding to their biological and histological behavior is also beneficial (Table 35.2). A detailed history and examination of the patient is of clinical importance for exact diagnosis and treatment. Skeletal tumor patients may present with complaints of pain, bumps, or palpable masses as well as pathological fractures or asymptomatic incidental radiographic findings. Pain, mostly, is the primary symptom; interval, localization, intensity, character and frequency of pain should be well questioned. Besides, duration and

Table 35.1 Classification of bone tumors according to their originating histogenetic tissues

Bone-forming (*osteogenic*) *lesions*
Osteoid osteoma, osteoblastoma, osteosarcoma
Cartilage-forming (*chondrogenic*) *lesions*
Osteochondroma, enchondroma, chondroblastoma, chondromyxoid fibroma, chondrosarcoma
Fibrogenic, *fibro-osseous fibrohistiocytic lesions*
Nonossifying fibroma, fibrous dysplasia, osteofibrous dysplasia, fibrosarcoma, malign fibrous histiocytoma
Round cell lesions
Langerhans cell histiocytosis, Ewing sarcoma-PNET, lymphoma, myeloma
Other/tumor-like lesions
Simple bone cyst, aneurysmal bone cyst, giant cell tumor

B. Erol, MD (✉) • O.M. Topkar, MD
Department of Orthopaedics and Traumatology, Marmara University Hospital, Fevzi Çakmak Mh. Muhsin Yazicioglu Cd. No: 10 34899, Ust Kaynarca, Pendik, Istanbul, Turkey
e-mail: bulerol@hotmail.com

T. Er, MD
Department of Orthopaedics and Traumatology, Istanbul Orthopaedics Center (ISOM), Istanbul, Turkey

O.E. Aycan, MD
Orthopaedics and Traumatology Department, Metin Sabanci Baltalimani Bone Diseases Training and Research Hospital, Istanbul, Turkey

F. Korkusuz (ed.), *Musculoskeletal Research and Basic Science*,
DOI 10.1007/978-3-319-20777-3_35

growth velocity of bumps/masses should be asked and consistency, mobility, and depth should be well examined. Since several tumors are specific to certain age groups, the age of the patient is also important (Table 35.3).

Plain radiographs give the most detailed information about a skeletal lesion. At least two views should be obtained. Radiographic changes may remain undetected until 30–40 % of cortical destruction is reached. Plain radiographs have a limited role in exhibiting soft tissue extension of skeletal tumors. Soft tissue extension and intramedullary involvement are best viewed by magnetic resonance imaging (MRI) [1]. MRI is an essential imaging modality in staging, assessing response to neoadjuvant chemotherapy and evaluation of long-term follow-up of the skeletal malignancies. MRI of the whole affected bone is important to detect skip metastases. Epiphyseal and neurovascular involvement should also be carefully observed. Post-neoadjuvant chemotherapy MRI should be well evaluated; change in size and peripheral edema of the tumor should be compared with initial MRI.

Computerized tomography (CT) is beneficial in axial skeleton involvement due to its complex anatomy. CT is also preferred when cortical integrity and intralesional mineralization is questioned. A whole body bone scan indicates primary lesion's biological activity as well as accompanying skeletal lesions.

Table 35.2 Classification of bone tumors based on their biological behavior

Benign lesions
Osteoid osteoma, osteochondroma, enchondroma, nonossifying fibroma, fibrous dysplasia, simple bone cyst, Langerhans cell histiocytosis
(*Benign but*) *locally aggressive lesions*
Osteoblastoma, chondroblastoma, osteofibrous dysplasia, chondromyxoid fibroma, aneurysmal bone cyst, giant cell tumor
Malignant lesions
Osteosarcoma, chondrosarcoma, malign fibrous histiocytoma, Ewing sarcoma-PNET, multiple myeloma-plasmacytoma

Radiographic Properties of Skeletal Lesions

Localization and Origin

- Epiphyseal, metaphyseal, and diaphyseal
- Medullary (central, eccentric), intra-cortical

Patterns of Bone Destruction (Fig. 35.1)

- Geographic destruction; benign, slowly growing lesions
- Permeative, moth-eaten destruction; aggressive, rapidly growing lesions [2].

Table 35.3 Age ranges of frequent bone tumors

	Benign	Malignant
0–5 years	Langerhans cell histiocytosis	Ewing sarcoma
5–10 years	Simple bone cyst	Osteosarcoma
	Aneurysmal bone cyst	Ewing sarcoma
	Nonossifying fibroma	
	Fibrous dysplasia	
	Osteoid osteoma	
	Langerhans cell histiocytosis	
10–20 years	Fibrous dysplasia	Osteosarcoma
	Osteoid osteoma	Ewing sarcoma
	Aneurysmal bone cyst	
	Chondroblastoma	
	Fibrous dysplasia	
Adult	Giant cell tumor	Multiple myeloma
	Enchondroma chondrosarcoma	
	Metastatic carcinoma	

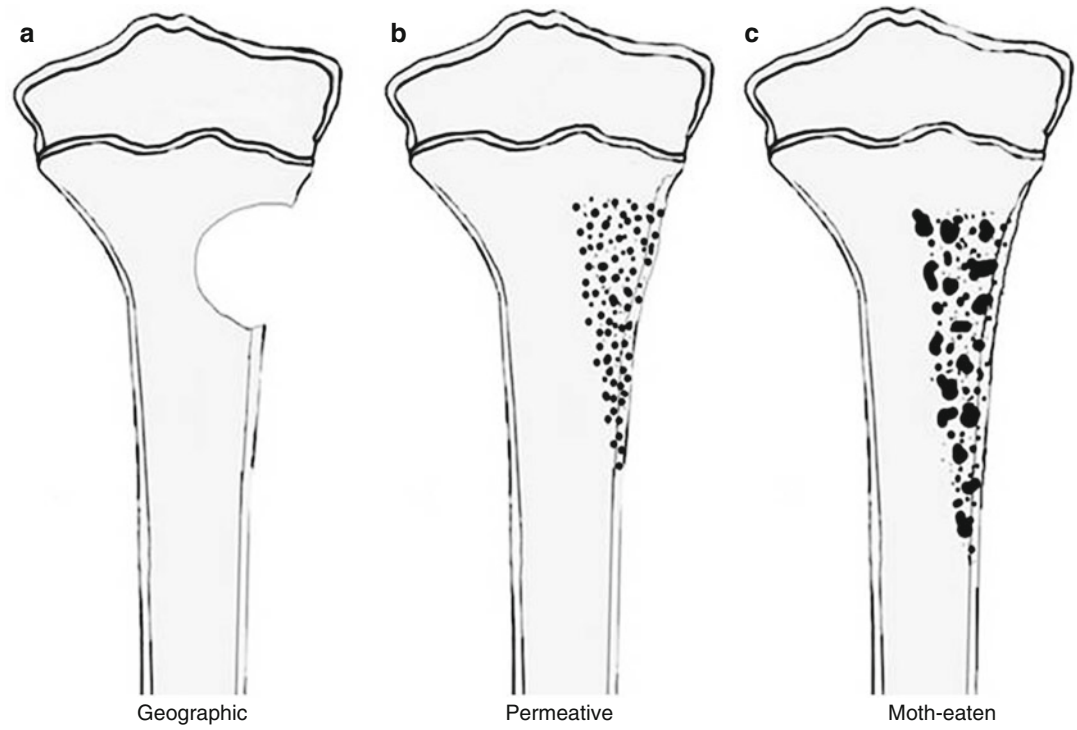

Fig. 35.1 Type of bone destruction. (**a**) geographic, (**b**) permeative, (**c**) moth-eaten destruction

Response of the (Host) Bone

- Limited within intact cortices, static lesions
- Impaired cortical integrity and soft tissue extension, aggressive lesions

Response of the Periosteum (Fig. 35.2)

- May exhibit various patterns (e.g., spiculated, lamellated/onion skin, Codman triangle) [2].

The GTM staging system is commonly used in staging of skeletal tumors in which the capital "G" indicates histological grade, "T" stands for local tumor extension, and "M" represents distant metastasis. The GTM staging system is used for both benign and malignant lesions (Tables 35.4A and 35.4B).

The local extension and metastatic spread of suspected malignant lesions should be evaluated before biopsy; radiological staging includes a chest CT and a whole body bone scan, in addition to MRI of the primary lesion. The entire length of the involved bone should be viewed by MRI to detect satellite lesions. Biopsy is the final diag-

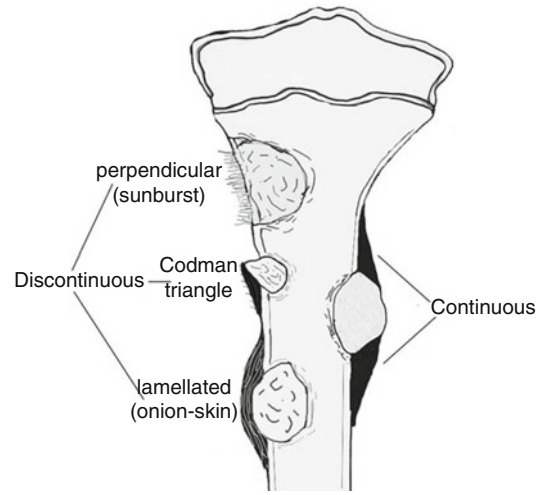

Fig. 35.2 Different types of periost reactions

Table 35.4A Staging of benign bone tumors

Stage 1	Latent	G0	T0	M0
Stage 2	Active	G0	T0	M0
Stage 3	Aggressive	G0	T1–T2	M0–M1

G = Grade; G0: benign, G1:low-grade malignant, G2: high-grade malignant
T = local extent; T0: confined within reactive bone, T1: intracompartmental, T2: extracompartmental
M = metastasis; M0: metastasis (–), M1: metastasis (+)

Table 35.4B Staging of malignant bone tumors

Stage	Grade	Tumor	Metastases	Definition
Low-grade				
IA	G1	T1	M0	A intracompartmental
IB	G1	T2	M0	B extracompartmental
High-grade				
IIA	G2	T1	M0	A intracompartmental
IIB	G2	T2	M0	B extracompartmental
Metastasis				
IIIA–B	G1–2	T1–2	M1	Any grade (A/B) distant metastasis

G = Grade; G0: benign, G1:low-grade malignant, G2: high-grade malignant
T = local extent; T0: confined within reactive bone, T1: intracompartmental, T2: extracompartmental
M = metastasis; M0: metastasis (−), M1: metastasis (+)

nostic step in the evaluation of skeletal malignancies, and should be performed following radiological staging and multidisciplinary assessment (orthopedic oncology, radiology, pathology, medical oncology, radiation oncology). Biopsy material can be obtained by open or closed methods (e.g., fine needle aspiration, tru-cut, trochar). It is mandatory to ascertain the exact histopathological diagnosis of any suspected malignant lesion before deciding its definitive treatment. As a general rule, it is recommended that the biopsy should be performed by the surgeon who will perform the definitive surgery.

Definition and classification of surgical margins is beneficial in planning the treatment. Most skeletal tumors are surrounded by a reactive sclerotic rim. This reactive sclerotic rim is also surrounded by a reactive zone, which includes microscopic tumor invasion. Beyond the reactive zone lies the normal tissue. High-grade sarcomas may not include a reactive sclerotic rim, a feature that indicates the aggressiveness of the lesion. Based on surgical margins, four types of surgical resections are defined: *intralesional*, *marginal*, *wide*, *and radical* (Fig. 35.3). Intralesional (the tumor is removed by disrupting its capsule or pseudocapsule) and marginal resections (the tumor is removed by a margin that may include a contaminated reactive zone) may remain macroscopic and microscopic tumor residues, respectively. Wide resection, which includes reactive zone and non-contaminated surrounding tissues, is the gold standard at local control of malignant bone lesions. Functional loss is a common complication of radical resections, in which the whole compartment including the tumor is resected [4].

Bone-Forming (Osteogenic) Lesions

Osteoid Osteoma

Osteoid osteoma constitutes 10–12 % of all benign skeletal tumors. Osteoid osteoma can be detected in any bone; however, it is most commonly observed in the femur and tibia. The most common presenting symptom is pain. Pain in osteoid osteoma is characteristic for not being relevant with motion, increasing especially during night-time and mostly relieved by aspirin and non-steroid anti-inflammatory drugs (NSAID). Lower extremity lesions may manifest with limping. Vertebral lesions may exhibit a nonstructural scoliosis.

Radiologic Features

The majority of osteoid osteomas are located intracortically and plain radiographs may indicate a dense cortical sclerosis around the lesion. A nidus, which is smaller than 1 cm in diameter, can only be noticed as a hypodense area within the dense cortical thickening (Fig. 35.4a). The best imaging modality to detect a nidus is thin-section CT (1–1.5 mm slice) (Fig. 35.4b). MRI may exhibit an exaggerated image due to the intensive edema around the lesion, resembling a malignant process. Bone scan is active at all three phases.

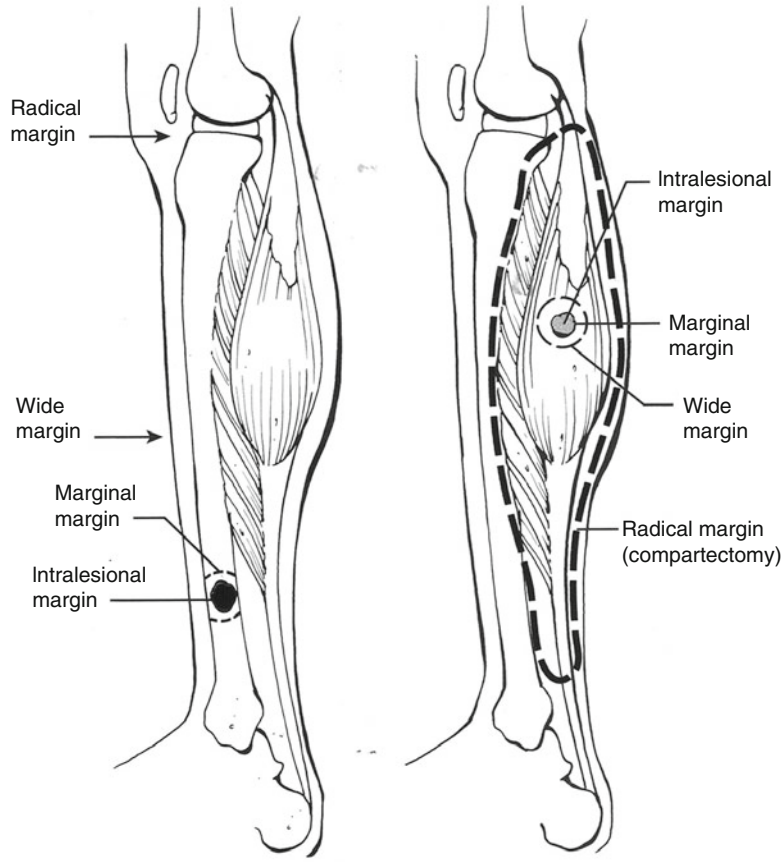

Fig. 35.3 Surgical margins. *Intralesional margin*, passes within the lesion; *marginal*, lies within the reactive zone; *wide margin*, passes intracompartmentally within the normal tissue; *radical margin*, runs extracompartmentally

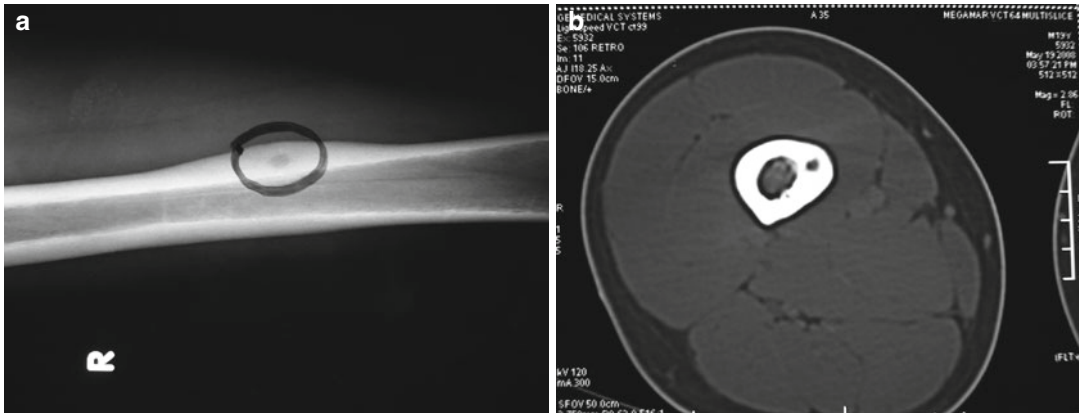

Fig. 35.4 Osteoid osteoma. (**a**) A hypodense nidus surrounded by a dense cortical sclerosis is seen. (**b**) Thin-section (1–1.5 mm) CT scan is the best imaging modality in demonstrating the nidus

Histopathological Features

Macroscopically, nidus is a red colored, hyperemic tissue that is softer than its surrounding sclerotic bone. Microscopic view shows numerous dilated capillaries and irregular woven bone seated within a fibrovascular stroma. The surrounding bone is sclerotic. Soft tissues around the lesion are mostly inflammatory.

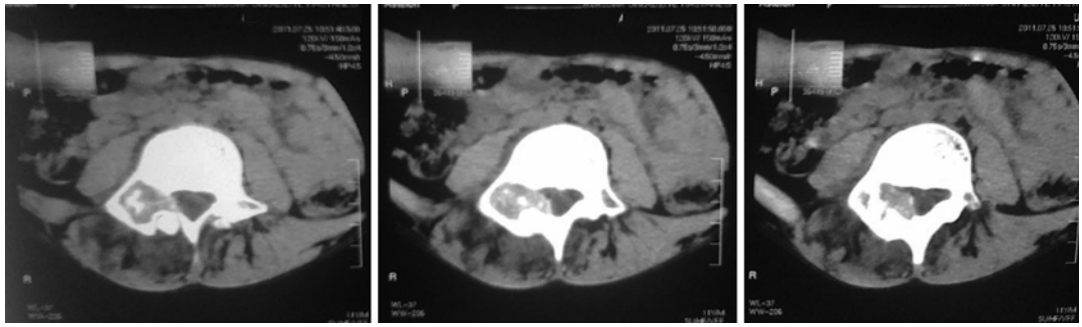

Fig. 35.5 Osteoblastoma. CT scans show a lytic lesion localized in posterior vertebral column, with intralesional punctate calcifications

Treatment

Surgical treatment is commonly the preferred method in the treatment of osteoid osteomas, whereas only selected cases with mild pain or with risk of complicated surgery can be managed by long-term use of NSAID. Complete removal of the nidus is mandatory in the surgical treatment of osteoid osteoma. This can be achieved by surgical resection or thermal radiofrequency ablation (RFA) [5].

Burr down is the recommended surgical method. The sclerotic bone overlying the lesion is removed level by level with a high-speed burr, until a pinhead reddish spot is seen. The nidus is curetted and underlying sclerotic bed is burred for 2–5 mm.

In CT guided thermal RFA method, the heat probe is advanced into the nidus core and heated to burn down the lesion.

Open surgical approaches warrant the removal of nidus; however, they remain disadvantageous in challenging and dangerous localizations (e.g., spinal, intraarticular, intrapelvic). CT-guided RFA, apart from being a minimal invasive procedure, is accepted as a safe method for locating the nidus precisely. Since sampling cannot be performed by CT-guided RFA, the diagnosis and treatment can only be done on the basis of clinical and radiological findings.

Osteoblastoma

Osteoblastoma is a rare bone-forming tumor, whose radiologic and histological properties resemble osteoid osteoma. This lesion is also known as "Giant Osteoid Osteoma." The posterior vertebral arch is the predilection site for osteoblastomas, where more than 40 % of the cases arise. A progressively increasing pain not related with motion, is the most common finding. Limping may be the initial symptom in lower extremity involvement. Similarly vertebral involvement may primarily manifest as scoliosis. In plain radiographic views, lesions may present as lytic areas 2–10 cm in diameter. CT views may show intralesional calcifications (Fig. 35.5). Extended curettage and grafting is recommended for the treatment of this locally aggressive lesion. Larger lesions, vertebral and pelvic involvements, which are prone to intensive bleeding due to their rich vascularization may require selective arterial embolization prior to surgery. Risk of recurrence even after complete resection varies between 10 and 20 %.

Osteosarcoma

Osteosarcoma is characterized by osteoid producing malignant cells. They constitute 20 % of primary malignant skeletal tumors, being the second most common following multiple myeloma. Ninety-five percent of the cases are at the second decade of life. Ninety-five percent of osteosarcomas diagnosed in children and young adults arise as primary tumors. Secondary osteosarcomas that arise over an existing bone lesion (e.g., fibrous dysplasia), an underlying bone disease (e.g., Paget) or

previous radiotherapy, are rare malignancies that mostly occur during the seventh and eighth decades of life.

High-Grade Intramedullary Osteosarcoma (Conventional Osteosarcoma)

High-grade intramedullary osteosarcomas constitute 85 % of all osteosarcoma causes. They commonly involve metaphyses of long bones where the vascularization and growth potential is exceptional. Distal femoral and proximal tibial lesions, where most of the skeletal growth is processed, constitute 50–60 % of all conventional osteosarcoma cases. Proximal humerus, proximal femur, and pelvis are the other common locations, respectively. The main complaints in admission are progressive pain and localized swelling, which are ignored or remain misdiagnosed for several months. Approximately 15 % of newly diagnosed conventional osteosarcoma patients have accompanying pulmonary metastatic disease. The presence of clinically detectable metastatic disease is a strong predictor of poor prognosis [6].

Radiologic Features

Plain radiographic views of conventional osteosarcomas are characterized by mixed lytic (radiolucent) and blastic (radiodense) activity, and mostly a metaphyseal ill-defined, destructive pattern is visible. Characteristic periosteal reaction patterns like sunburst appearance and Codman triangle and soft tissue extension, which include calcified foci, are commonly seen. Whole body Technetium Tc-99 bone scintigraphy reveals increased uptake at tumor localization. MRI is the best imaging modality that demonstrates intraosseous and extraosseous extension of the tumor and its relation with neighboring neurovascular structures (Fig. 35.6). At least one plane of the whole bone MRI is mandatory for the detection of bone marrow extension and skip lesions.

Histopathologic Features

The osteosarcoma family, which is basically characterized by production of osteoid or new bone by neoplastic cells of mesenchymal origin, has various subtypes of similar prognostic properties. Mesenchymal neoplastic cells may differentiate to osteoblastic, chondroblastic, and fibroblastic cells. The most common subtype is characterized by pleomorphic spindle cells of osteoblastic type.

Treatment

A combination of multiagent chemotherapy and surgery is the optimal treatment of osteosarcoma. The standard approach includes neoadjuvant (induction) multiagent chemotherapy, followed by resection and adjuvant chemotherapy. Since osteosarcomas mostly are radioresistant, radiotherapy should be reserved for selected cases. A ratio of 60–75 % 5-year disease-free survival is achieved with multiagent chemotherapy and relevant surgical resection. Neoadjuvant chemotherapy aims the treatment of micrometastatic disease and reduction of tumor size by necrosis, thus enables any limb-salvage procedure. Adjuvant chemotherapy is used for the elimination of micrometastatic disease that remains after surgical resection. Response to induction chemotherapy is determined by the percentage of tumor necrosis in resected specimen. The percentage of tumor necrosis in resected specimen is evaluated histologically; a ratio over 90 % tumor necrosis indicates a good response and is correlated with higher survival rates when compared to lower tumor necrosis ratios [7].

Local control is mostly managed by surgical resection in osteosarcoma (Fig. 35.6d). Achieving tumor-free margins is the aim of wide surgical resection. Tumor-free margins can be achieved by limb-salvage surgery in most patients. Several reconstruction alternatives including endoprosthetic reconstruction, biological reconstruction, structural allografts, or allograft and prosthesis composites are available for bone defects following resections. Clavicular and fibular involvement mostly does not require reconstruction.

Approximately 50 % of osteosarcoma patients may develop local recurrence and/or late onset lung metastases [6]. The standard approach for local recurrences is mostly the radical amputation and chemotherapy. Late onset lung metastases are managed by chemotherapy with or without metastasectomy.

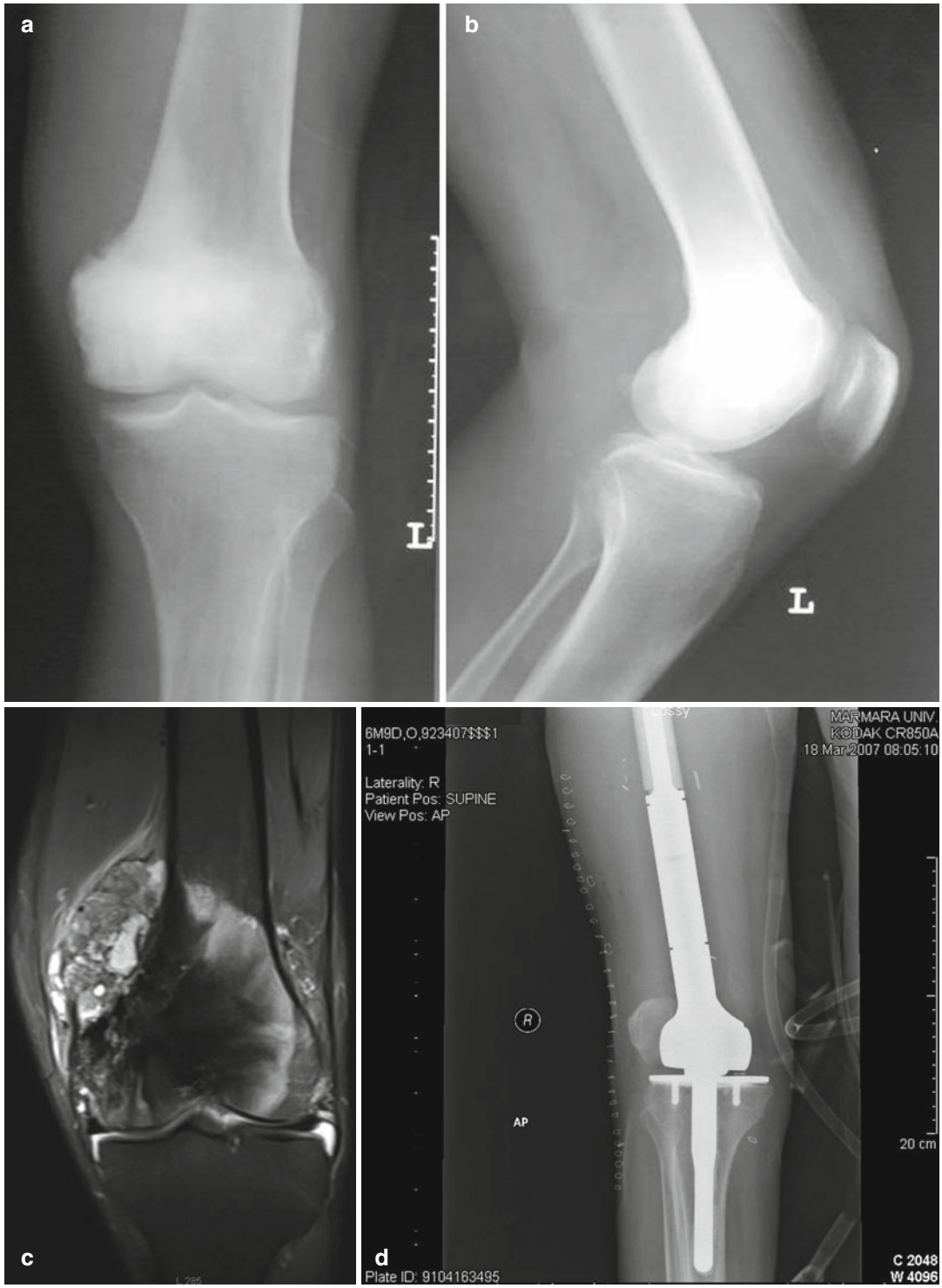

Fig. 35.6 Conventional osteosarcoma. (**a**, **b**) Plain radiographs show permeative destruction and periosteal reaction formed by tumor in distal femur. (**c**) Coronal MRI demonstrates intra- and extraosseous extension of the lesion. (**d**) Wide resection

Surface or Juxtacortical Osteosarcoma

The term "juxtacortical" refers to a group of osteosarcomas, which are originated from the surface of the bone, and composed of parosteal, periosteal, and high-grade surface osteosarcoma variants. They are commonly encountered in the third and fourth decades of life. Parosteal osteosarcomas are low-grade osteosarcomas, which commonly arise from posterior surface of distal femur. Periosteal osteosarcomas are mostly an intermediate-grade chondroblastic type osteosarcoma and, as their name implies, commonly involve more diaphyseal localizations than parosteal osteosarcomas. Parosteal and periosteal osteosarcoma subtypes are managed by wide resection, and since both lesions are low- and intermediate-grade, their metastatic potentials are lower when compared to conventional osteosarcomas. Inadequate surgical resections are related with local recurrence. High-grade surface osteosarcomas are the least common variant of this group, which resemble conventional osteosarcomas histopathologically. Local recurrences may progress to more aggressive and high-grade lesions. High-grade osteosarcomas, like conventional osteosarcomas, require chemotherapy and surgery.

Chondrogenic Lesions

Osteochondroma

Osteochondromas consist of a cartilage cap and a bony stalk in variable sizes. Since a vast majority of osteochondromas develop asymptomatically, their true incidence remains unknown. Osteochondromas consist 45 % of all benign skeletal tumors thus being the most common [5]. They have a great tendency to arise around the knee. Lesions commonly are solid, painless, palpable masses, which are attached to the underlying bone. Rarely, the lesions may compress neighboring muscular, tendinous, and neurovascular structures, and may manifest as muscular strain, numbness, or pseudoaneurysm. Osteochondromas may limit the range of motion when encountered around the joints. The lesions will keep growing until the skeletal maturity is reached. Less than 1 % of osteochondromas may develop malignant degeneration. An osteochondroma in a skeletally mature patient, which gradually increases in size and/or becomes painful, should alert the clinician for possible malignant transformation.

Radiologic Features

Plain radiographic views are characteristic and mostly do not require further investigation (Fig. 35.7a). Pedunculated osteochondromas arise proximal to the physis of bone with a stalk that grow toward diaphysis, whereas sessile osteochondromas are seated on metaphyseal bone with a broad base. The characteristic radiographic feature of osteochondroma is its cortical and medullary continuity with the host bone. MRI is helpful for the evaluation of cartilage cap thickness. Technetium Tc-99 bone scan may exhibit increased uptake, however cannot distinguish osteochondroma from other tumors; instead, it is useful for the detection of multiple lesions.

Histopathological Features

Osteochondromas macroscopically resemble the view of a cauliflower (Fig. 35.7b). The mass is connected to underlying bone with a bony stalk, which is continuous with the medulla of the host bone. Microscopically a 1–3 mm thick hyaline cartilage cap exists on the stalk. A cartilage cap being thicker than 10–15 mm is considered as a sign of malignant transformation [5].

Treatment

Osteochondromas do not require treatment unless they are symptomatic. Surgical resection is indicated for compression symptoms, severe cosmetic disturbance, or any suspected malignant transformation.

Multiple Hereditary Exostosis (MHE)

Multiple hereditary exostosis (MHE), multiple osteochondromatosis (MO), or diaphyseal acla-

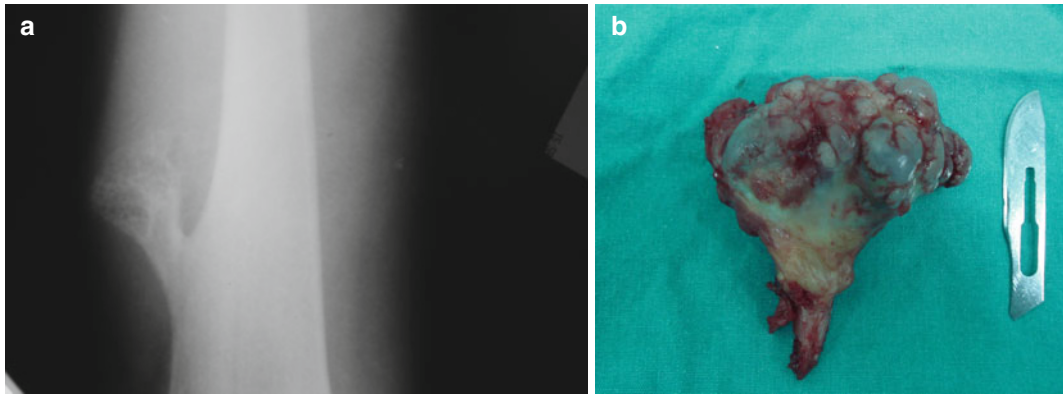

Fig. 35.7 Osteochondroma. (**a**) Continuity of the lesion with cortex and spongiosum of the host bone is seen. (**b**) Macroscopic appearance of the lesion resembles a cauliflower

sis refers to the same, rare autosomal dominant disease. The incidence is 1:50,000. Metaphyses and diaphyses of long bones are most commonly affected. "Metaphyseal flaring", which is defined as enlargement of metaphyses and loss of their remodelling capacity, is the main cause of various deformities. The progressive discrepancy between closely related, parallel bones (tibia-fibula, radius-ulna, metacarpals, and metatarsals) results in various deformities (e.g., Madelung deformity, tibiotalar joint deformity). Deformities can gradually be corrected by external fixators. Malignant transformation before skeletal maturity is exceptional; however, after skeletal maturity, the risk of malignant transformation is reported to be between 5 and 10 %. Consequently, it is highly recommended that MHE patients should closely be followed for malignant transformation, after skeletal maturity is achieved.

Enchondroma

Enchondromas are benign neoplasia of mature hyaline cartilage, and constitute 10 % of all benign tumors. Since enchondromas mostly are asymptomatic, the lesions are encountered incidentally. It most commonly affects individuals between the second and fourth decades. Almost half of the lesions involve short tubular bones of hand, followed by proximal humerus and proximal/distal femur, respectively. If an existing, asymptomatic enchondroma becomes painful, a pathological fracture or malignant transformation (after skeletal maturity) should be considered [8].

Radiologic Features

Plain radiographic view of enchondroma is typical—concentric involvement of the metaphyseal region of long or short tubular bones with intralesional calcified foci. Periosteal thickening or periosteal reactions are almost never encountered. Bones of the hand may exhibit mild expansion and minimal endosteal scalloping (Fig. 35.8). CT and MRI allow a detailed evaluation about tumor extension and cortical changes. Technetium Tc-99 bone scan reveals increased uptake at delayed phase (third phase).

Differential diagnosis between enchondroma and low-grade chondrosarcoma may be difficult clinically and histopathologically. Thus, clinical, radiologic, and histopathologic evaluations should be correlated with each other to proceed to the treatment. Marked endosteal erosion (involving more than two-thirds of the cortices) accompanied by cortical destruction in plain radiographs and CT scans are suggestive of low-grade chondrosarcoma with consistent clinical and histopathologic findings. MRI findings of distinct edema around the lesion and soft tissue extensions are in favor of malignancy [5].

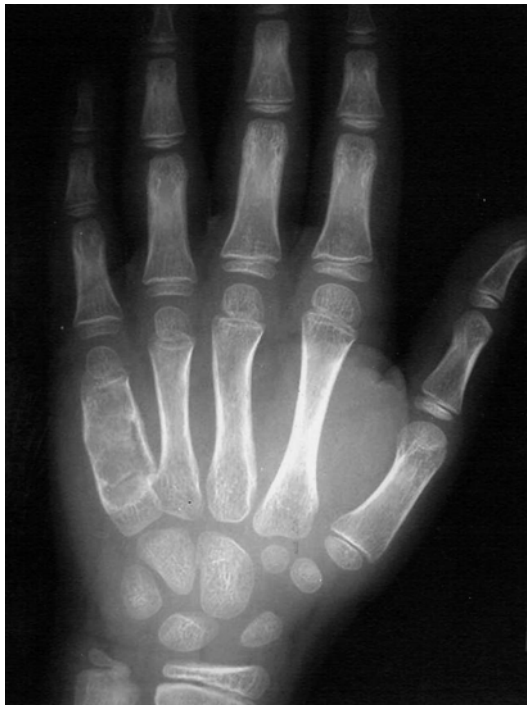

Fig. 35.8 Enchondroma. Short tubular bones of hand are frequently involved. Mild expansion of bone and minimal endosteal erosion formed by intramedullary lesion is seen

Histopathologic Features

Enchondromas macroscopically are a shiny, blue-whitish colored, fragile hyaline cartilage pack of globules that include patchy yellow calcifications. Microscopically they consist of hyaline cartilage lobules with distinct borders.

Treatment

Asymptomatic enchondromas require observation with regular clinical and radiographic evaluation (Fig. 35.9). Patients should be informed that solitary enchondromas have approximately 1 % risk of malignant degeneration after skeletal maturity is achieved. The lesions that are symptomatic and that have tendency to grow may require extended curettage followed by grafting or cementation. Particularly for pathologic fractures involving the hands, the primary step in management should be fracture healing by conservative methods. Extended curettage and grafting should be performed after adequate fracture healing is achieved. In cases that an aggressive enchondroma cannot be distinguished from a low-grade chondrosarcoma, a biopsy should be performed prior to definitive treatment; clinical, radiologic, and histopathologic evaluations should be correlated, only then the definitive treatment can be decided.

Multiple Enchondromatosis

Multiple enchondromatosis are a group of diseases that consist of nonhereditary, sporadic cases mostly; however, recent studies have suggested genetic transmissible cases. A radiologic classification (Spranger) system is defined depending on skeleton involvement and transmission. Ollier's disease (Spranger type I) refers to most commonly encountered, nonhereditary multiple enchondromatosis that affects appendicular skeleton only. Lesions are mostly unilateral and cause deformities that can be managed by corrective osteotomies. Mafucci syndrome (Spranger type II) is like the Ollier's disease accompanied by multiple soft tissue hemangiomas. Ollier's disease and Mafucci syndrome have 15–30 % risk of malignant transformation, and require close monitoring of the lesions. Metachromatosis (Spranger type III) and genochondromatosis also have appendicular involvement but their autosomal dominant inheritance makes them a distinguished type. Metachondromatosis has multiple exostoses, which is differentiated from osteochondromas by the direction of growing. Genochondromatosis is characterized by marked thickening of clavicles and symmetrical lesions. Spondylenchondrodysplasia (Spranger type IV) refers to spinal involvement, with or without spinal cord involvement. Dysspondylenchondromatosis (Spranger type V) defines enchondromatosis with irregular vertebral lesions. Cheirospondyloenchondromatosis (Spranger type VI) shows hand and foot involvement accompanied by mental retardation.

Chondroblastoma

Chondroblastomas are rare benign tumors that occur in long bone epiphyses in the second

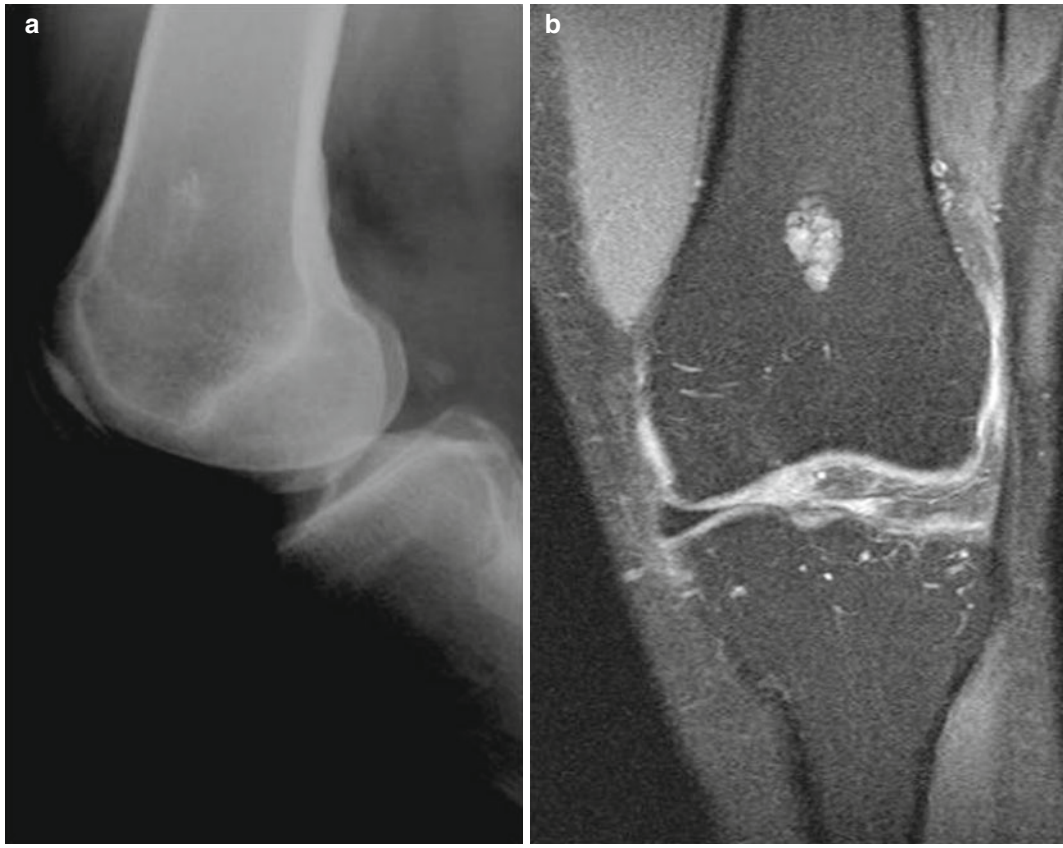

Fig. 35.9 Enchondroma. (**a**, **b**) Clinical and radiologic follow-up of asymptomatic enchondromas, which are generally diagnosed incidentally in adulthood, are sufficient

decade of life mostly. Talus, calcaneus, and short tubular bones of hand can also be involved. The vast majority of chondroblastomas can be detected in patients before skeletal maturity; however, concurrence at older ages is also reported [5]. Long duration of pain is the characteristic presentation of the patients. Joint effusion and associating symptoms at neighboring joint can also be present. Giant cell tumor of bone and clear cell chondrosarcoma are the two other lesions with epiphyseal involvement. Plain radiographs show an intraepiphyseal, sharply demarcated lytic lesion with well sclerotic borders. CT is helpful to visualize cortical integrity and intralesional calcifications, and MRI is useful for the evaluation of soft tissue extension and edema around the lesion. The treatment of chondroblastoma is extended intralesional curettage. Following curettage graft packing should be reserved for patients who have not yet reached skeletal maturity. Cementation can safely be used in cases with skeletal maturity. One should pay great attention to avoid damaging the growth plate and the joint line during surgery. Chondroblastomas are reported to have 10–15 % recurrence rates following surgery.

Chondromyxoid Fibroma

Chondromyxoid fibromas are extremely rare benign skeletal lesions. The lesion frequently involves long bone metaphyses, causing a long duration and ondulant pain. Plain radiographs show an eccentric round or oval lytic lesion in the

metaphysis of bone. lesion commonly are limited by well-defined sclerotic borders. The tumor frequently grows toward cortices and attenuates them gradually, and may moreover completely destruct them [1]. Histopathologic evaluation reveals that the lesions mostly are limited by the periosteum, and even if the cortices may seem completely destructed radiologically. Curettage and grafting is the mainstay of treatment. Because chondromyxoid fibromas have high rates of recurrence, re-curettage, and grafting, marginal or wide resections can be performed when required.

Chondrosarcoma

Chondrosarcomas constitute approximately 9 % of primary skeletal sarcomas, being the third most common primary malignant bone tumor. Chondrosarcoma is a disease of age groups over the third decade. Flat bones of axial skeleton (e.g., pelvis, shoulder girdle) and proximal parts of long bones that are close to axial skeleton are most frequently involved. Chondrosarcomas may be present as primary or may develop secondary to an existing skeletal pathology (e.g., Ollier's disease, MHE, chondroblastoma, synovial chondromatosis, and irradiation); primary chondrosarcomas tend to involve central localizations, whereas secondary chondrosarcomas most frequently are located peripherally. Chondrosarcomas are characterized by gradually increasing pain and palpable mass, which may be present for years. One should keep in mind that chondrosarcoma can most commonly be present as an asymptomatic chondroid lesion for years and can incidentally be detected [6].

Radiologic Features

Plain radiographic views of chondrosarcomas are mostly diagnostic. They originate from medullary cavities and demonstrate irregular calcifications of matrix as enchondromas do; however, the appearance is more aggressive. Marked cortical destruction, endosteal scalloping, periosteal reaction, and less frequently an accompanying soft tissue mass are the characteristic radiographic features of chondrosarcomas (Fig. 35.10) [1].

Histopathologic Features

Microscopic evaluation of conventional chondrosarcoma demonstrates malignant cells within the chondroid matrix. Determination of the grade is of paramount importance to predict lesions with biological aggressiveness and tendency to metastasize. Low-grade chondrosarcomas are locally aggressive; however, they tend to remain within anatomical limits and almost never metastasize. High-grade chondrosarcomas are considerably aggressive and have great potential to metastasize. Histopathologic evaluations alone have limited differential diagnostic value in distinguishing an enchondroma and a low-grade chondrosarcoma. Clinical, radiologic, and histopathologic correlation by a multidisciplinary team is essential to differentiate an enchondroma and a low-grade chondrosarcoma. Chondrosarcomas have three rare variants with distinct histopathologic features, including dedifferentiated, clear-cell, and mesenchymal subtypes.

Treatment

The most significant predilector of prognosis is the grade of tumor; low-grade chondrosarcomas have 90 % 10 year survival rates, whereas high grades are reported to vary between 20 and 40 % [6]. The treatment of low-grade chondrosarcomas remains controversial. Good results have been reported by intralesional curettage and adjuvant use. Reconstruction of the bone defect after curettage by graft packing or cementation is highly suggested. A group of authors, unlikely, favor for wide resection in low-grade chondrosarcoma. Wide or radical resection is highly recommended in the treatment of high-grade chondrosarcoma (Fig. 35.10d). Lung metastases should be surgically resected when possible. Not surprisingly, due to its hypovascular and/or avascular nature, chemotherapy has no role in the management of conventional chondrosarcoma. Radiotherapy has a considerably limited role and can only be beneficial in circumstances where surgery cannot warrant complete resection.

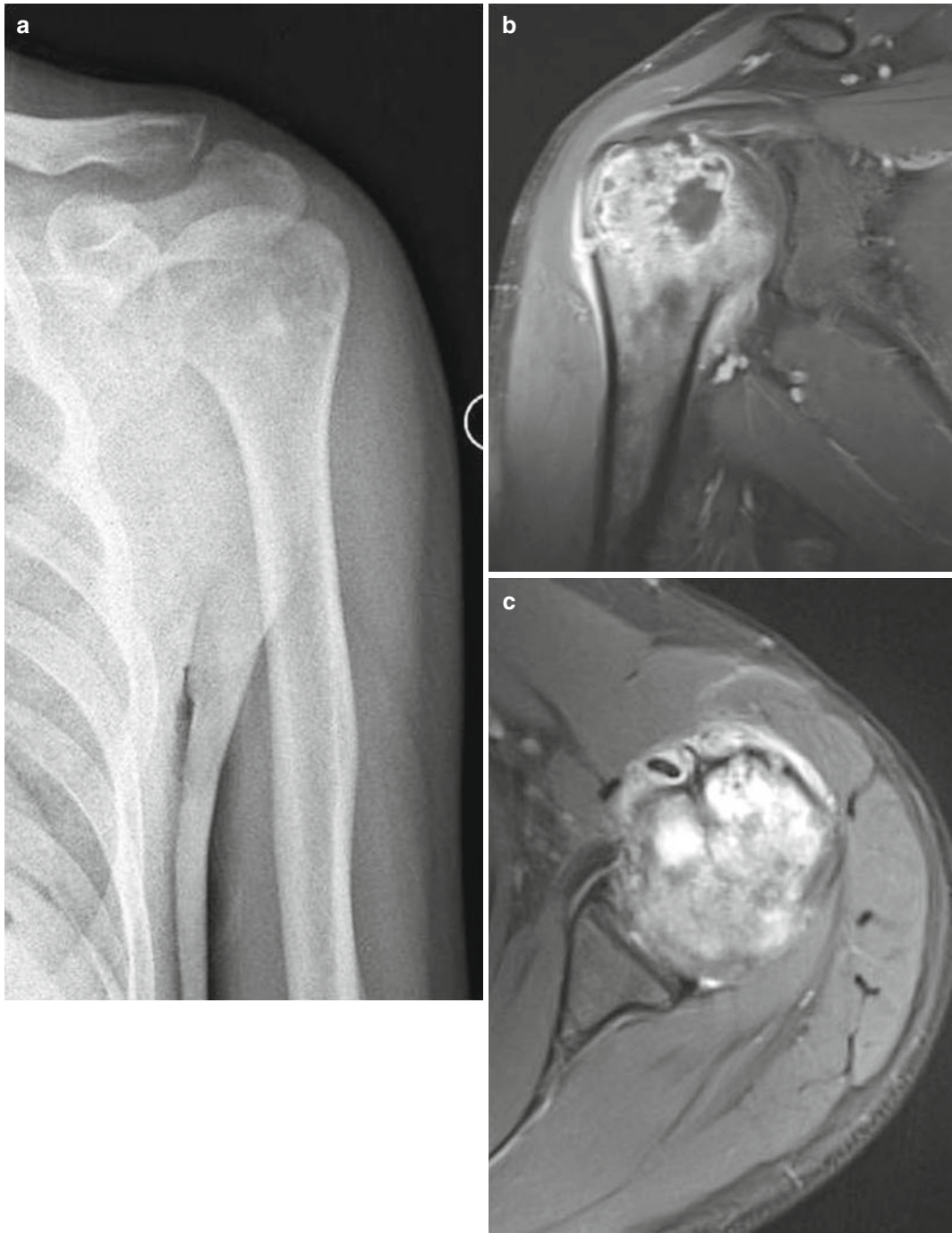

Fig. 35.10 High-grade chondrosarcoma. (**a**) Intralesional calcifications of lytic lesion in proximal humerus can be seen on conventional radiographs. Tumor did not cause a significant cortical erosion. (**b**, **c**) Intramedullary involvement without a soft-tissue component can better be eveluated by MRI. (**d**) Wide resection and endoprosthetic reconstruction was performed

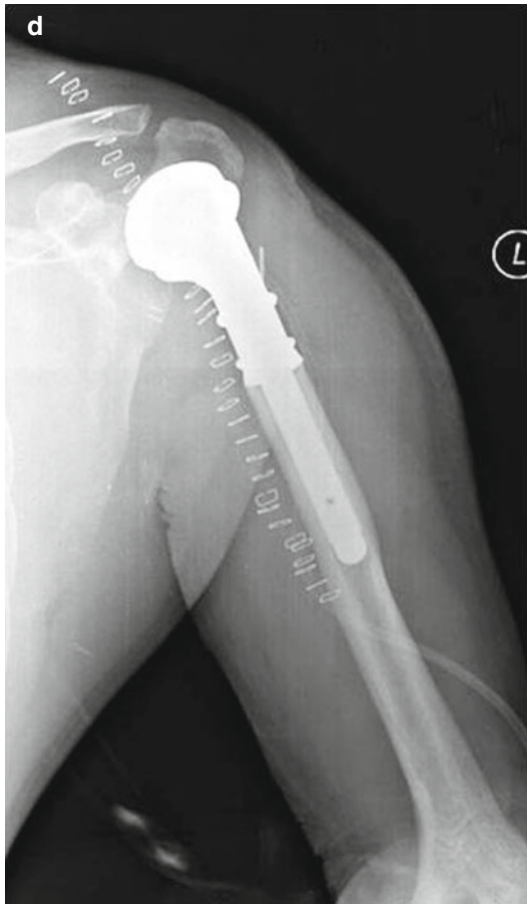

Fig. 35.10 (continued)

Fibrogenic, Fibrosseous, and Fibrohistiocytic Lesions

Nonossifying Fibroma

Rather than being a real neoplasia nonossifying fibromas (NOFs), in a skeletally immature patient, occur as a result of developmental defect of normal subperiosteal membrane ossification. The defect is filled by fibrous tissue. This developmental pathology is estimated to affect 30 % of normal population. Lesions commonly are asymptomatic and found incidentally. Rarely they present with a pathologic fracture.

Radiologic Features

Plain radiographs demonstrate eccentric, metaphyseal lesions, limited by a thin sclerotic rim. Internal septations cause the characteristic view of "bubbly appearance" (Fig. 35.11). Radiographic evaluation is almost diagnostic; however, CT may be useful when the lesions present with a pathologic fracture.

Histopathologic Features

Macroscopically a soft, brownish-yellow tissue is evident. Histologically NOF demonstrate fibroblasts within a dense collagenous matrix, areas of hemorrhagia, and deposits of hemosiderin. Ossification may also accompany.

Treatment

NOF commonly does not require surgical treatment; biannual or annual periodic monitoring with plain radiographs is recommended until skeletal maturity is reached [9]. Lesions tend to regress at the second half of the second decade. Actual or pathological fractures can be managed by curettage, grafting and internal fixation when required [8–10]. Recurrence is extremely rare.

Fibrous Dysplasia

Fibrous dysplasia is accepted as the developmental defect of normal cancellous bone, which is replaced by abnormal fibrooseous tissue. Vast majority of fibrous dysplasias are monostotic (solitary), whereas polyostotic (diffuse) involvement can also be seen. Fibrous dysplasia most frequently affects diaphyses and metaphyses of long bones. Monostotic fibrous dysplasias are mostly asymptomatic and found incidentally; however, lesions that tend to grow progressively may cause pain. Polyostotic fibrous dysplasia is associated with bowing and/or deformity of long bones even in younger ages. Pathological fracture is not an uncommon finding; repetitive pathological microfractures and remodeling may lead deformity.

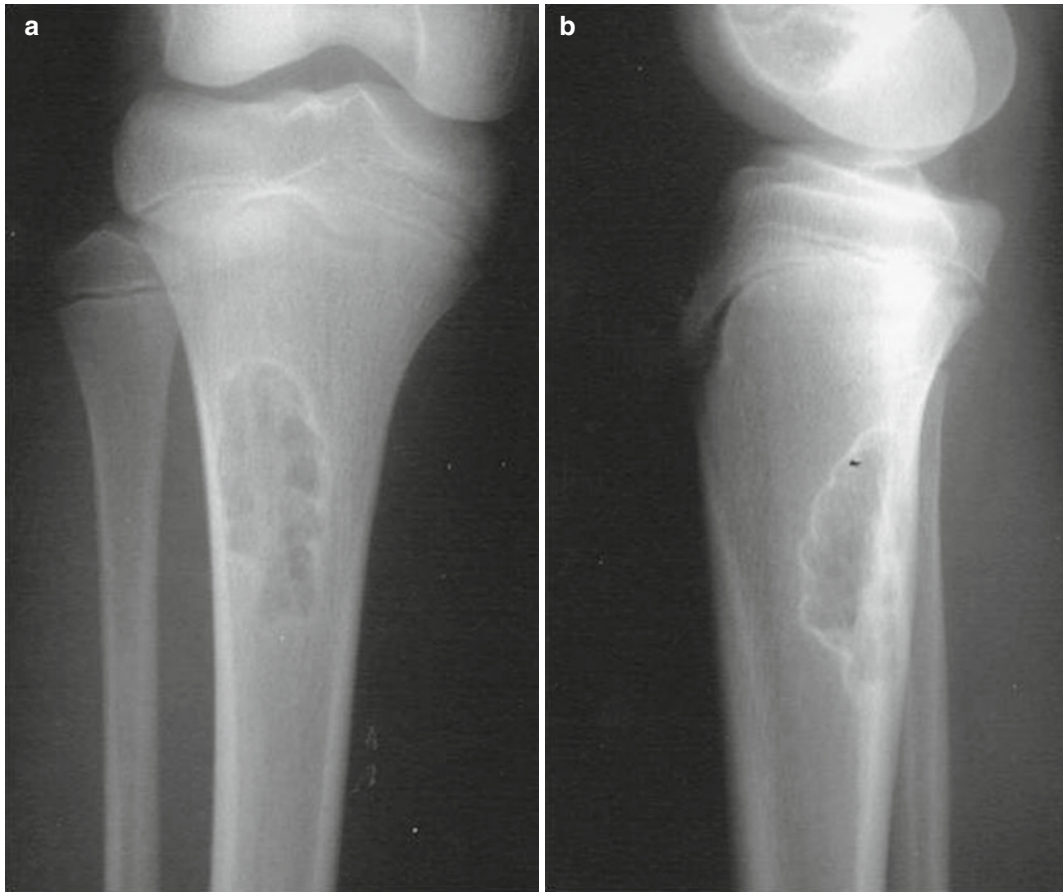

Fig. 35.11 Nonossifying fibroma. (**a**, **b**) A lobulated radiolucent lesion, surrounded by a thin sclerotic border is localized eccentrically at the metaphysis of proximal tibia

Radiologic Features

On plain radiographs fibrous dysplasias have characteristic, "ground-glass appearance" that develops as a result of replacement of normal trabecular bone to woven bone (Fig. 35.12a) [1]. Proximal femoral involvement also have a characteristic plain radiographic view of "Shepherd's crook" deformity, which develops as a result of repetitive microfractures and remodeling. Angular deformities or bowing of long bones are also evident in poliostotic fibrous dysplasia. CT may be helpful to visualize cortical integrity and intralesional mineralization. MRI demonstrates the extent of lesion as hypointense in T1-weighted sequences and hyperintense in T2-weighted sequences. Technetium T-99 bone scan exhibits skeletal distribution of the lesions with mild to moderate uptake.

Histopathologic Features

Macroscopically fibrous dysplasia fills the medullary canal with a yellow-white, firm, rubber-like tissue instead of a normal medullary bone. The microscopic view demonstrates metaplasic bone spicules that are scattered through a fibrous stroma, forming the characteristic view of "Chinese letters."

Treatment

Asymptomatic monostatic fibrous dysplasia can be followed by periodic monitorization.

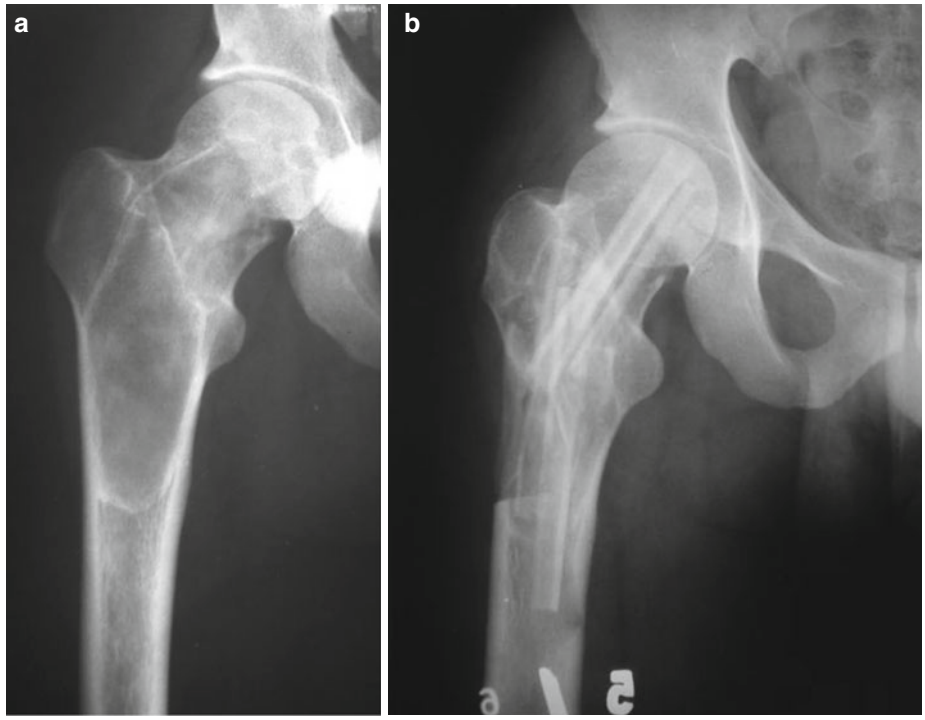

Fig. 35.12 Fibrous dysplasia. (**a**) *Ground-glass appearance* of a proximal femoral lesion is seen. (**b**) Curettage and strut allografting was performed

Progressively growing, painful lesions particularly when present at higher stress yielding locations (e.g., proximal femur) may require surgical intervention [8, 10]. Lesions cannot completely be eradicated because newly developed bone of the healing process is resulted in weak, abnormal fibrous and fibrooseous tissue. Bone stabilization, pain relief, and prevention and/or correction of deformity are the main goals of treatment. Following curettage, the use of structural allograft is recommended, due to their delayed incorporation capacity with the host bone (Fig. 35.12b). Several authors advocate the use of internal fixation combined with graft packing, while others consider that internal fixation alone can be adequate. Correctional osteotomies combined with intramedullary fixation are highly recommended in surgical management of long bone deformities. Common use of Pamidronate has been reported to have regressive effect on lesions [5]. Denosumab similarly has also been reported to have a positive effect in local control of fibrous dysplasia [11].

Round Cell Lesions

Langerhans Cell Histiocytosis

Langerhans cell histiocytosis defines a spectrum of diseases characterized by uncontrolled proliferation and deposition of histiocytes. Four subtypes of Langerhans cell histiocytosis have been reported; eosinophilic granuloma is characterized by solitary/multiple skeletal involvement; Hans-Schueller-Christian syndrome has characteristic triad of diabetes insipidus, exophthalmos, and lytic bone lesions; Letterer-Siwe disease is a fatal, fulminant disease of infants with multiorgan involvement; and Hashimoto-Pritzker disease is a recently defined congenital self-healing reticulohistiocytosis with temporary skin eruptions.

An immune system regulation disorder is responsible for the etiology of disease. The skull is the most frequently involved but least commonly distinguished localization. Long bones, pelvis, ribs, and vertebral bodies are the other common sites, respectively. Localized pain that is worsened by motion, swelling, and tenderness are the common presenting symptoms. Some patients may experience systemic symptoms (e.g., pain, weight loss, increased erythrocyte sedimentation rates) [8, 9]. Vertebral involvement may result with kyphosis and painful scoliosis.

Radiologic Features

The plain radiographic view of Langerhans cell histiocytosis is highly variable; thus it is also called as "the great mimicker." The lesions are typically lytic with well-defined margins. Occasionally they may demonstrate an aggressive appearance characterized by permeative destruction, expansion or periosteal reaction [9]. A characteristic view of eosinophilic granuloma, "vertebra plana" defines vertebral body collapse (Fig. 35.13a).

Histopathologic Features

Macroscopically a soft brown-reddish tissue is present. Microscopically increased proliferation of Langerhans cells (lipid laden histiocytes) on inflammatory matrix is evident. Detection of cytoplasmic "Birbeck granules" in electron microscopy is pathognomonic.

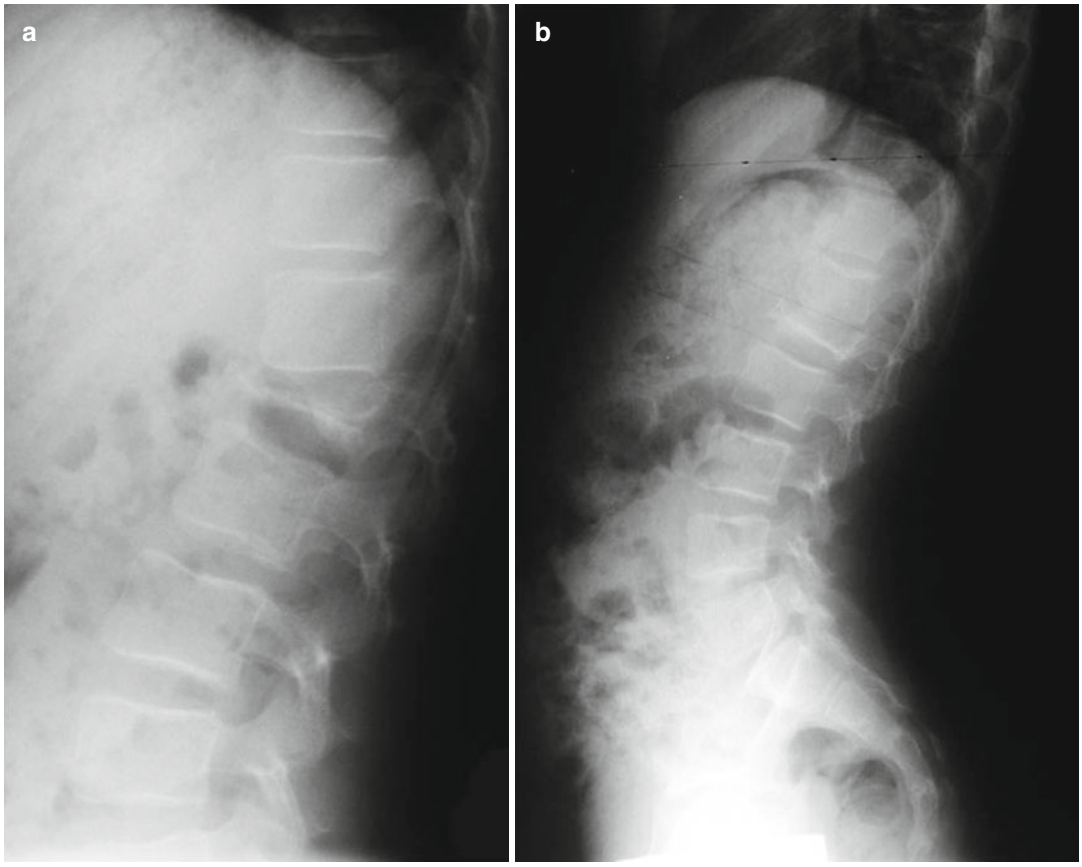

Fig. 35.13 Langerhans cell histiocytosis. (**a**) *Vertebra plana* appearance is seen in L1 vertebrae corpus. Spontaneous restoration of corpus height can be seen in the (**b**) second and (**c**) fifth year follow-up radiographs. This lesion was managed only with a biopsy to confirm the diagnosis

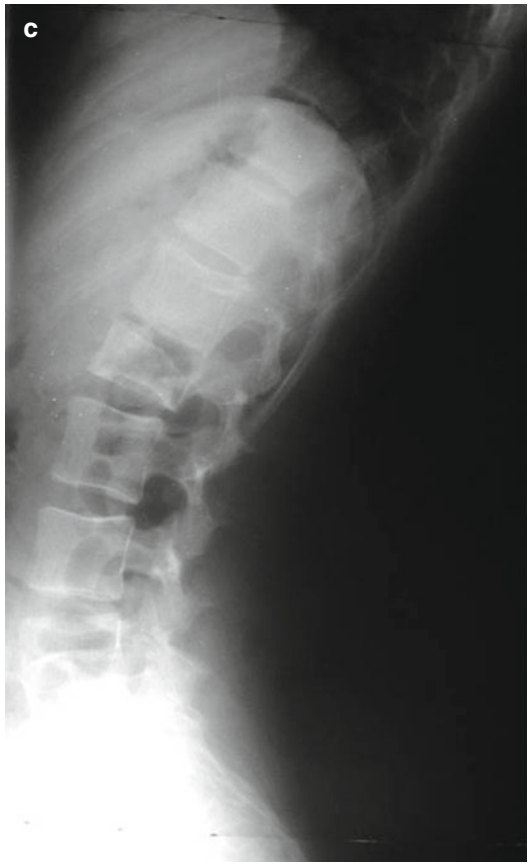

Fig. 35.13 (continued)

Treatment

Because the solitary lesions usually are self-limiting and have spontaneous regression potential, revealing the diagnosis by biopsy is adequate in most cases. Vertebral lesions require periodic screening, unless they cause deformity and/or neurologic deficiency. Collapsed vertebral bodies may gradually restore (Fig. 35.13b, c). Impending fractures and painful lesions can be managed by curettage and local steroid injection [5]. Multiple lesions should always be consulted to medical oncology, because disseminated disease may require chemotherapy.

Ewing Sarcoma

Ewing sarcoma is the second most common primary malignant skeletal tumor of the first and second decades. Approximately 90 % of the patients are between 5 and 25 years. Ewing sarcomas are in close relation with primitive neuroectodermal tumors (PNETs), both tumors are considered to originate from neural crest and at least 90 % of the cases have a characteristic chromosomal translocation. Ewing sarcoma most commonly involves the femur, followed by humerus, ribs, and flat bones (pelvis and scapula). Ewing sarcoma may have a subtle presentation; the average time from the onset of symptoms to diagnosis is about 34 weeks [6]. The presence of pain, localized swelling, erythema, and accompanying constitutional symptoms (e.g., fewer, increased erythrocyte sedimentation rate) may suggest osteomyelitis as a differential diagnosis [8, 9]. Twenty five percent of Ewing sarcoma patients have detectable lung metastasis at the time of diagnosis.

Radiologic Features

On plain radiographs Ewing sarcoma typically involves diaphyseal or metaphysodiaphyseal regions of a long bone. The tumor usually demonstrates diffuse permeative, destructive lesion with poorly defined margins. The lesion frequently is associated with a lamellated periosteal new bone formation that has an onion-skin appearance, and a large soft-tissue mass. MRI is the best imaging modality to demonstrate and determine the tumor size, intraosseous/extraosseous extension, and the relation of the tumor with neighboring anatomical structures.

Histopathologic Features

The macroscopic appearance of Ewing sarcoma may resemble the pus of osteomyelitis and, not infrequently, the whole specimen may be sent for microbiological evaluation.

Ewing sarcoma is a high-grade malignancy, consisting of monotone small round blue cells, which basically demonstrate the characteristic features (increased mitosis, anaplasia, pleomorphism, hyperchromatic nuclei) of malignant cells. Cytogenetic and immunohistochemistry studies exhibit t(11,22) translocation and MIC2 positivity in majority of the patients.

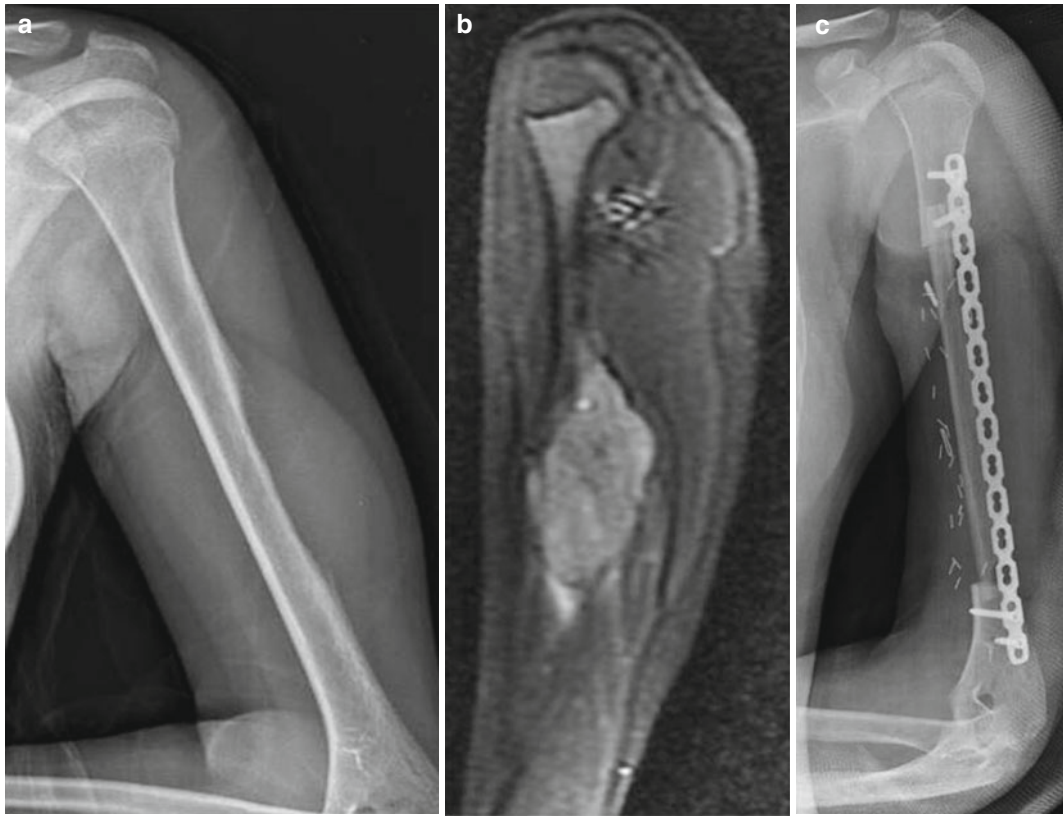

Fig. 35.14 Ewing sarcoma. (**a**) Permeative destruction and periosteal reaction formed by a humeral diaphyseal lesion can be seen on conventional radiograph. (**b**) MRI is shows the intra/extraosseous involvement of the tumor. (**c**) Local control of the tumor is achieved by wide resection after neoadjuvant chemotherapy. Subsequent bone defect is reconstructed by biological reconstruction with vascularized fibular graft

Treatment

Neoadjuvant multiagent chemotherapy, wide surgical resection, and adjuvant chemotherapy constitute the standard management protocol of Ewing sarcoma (Fig. 35.14c). Ewing sarcoma is a highly radiosensitive tumor. Local control may either be maintained by surgical resection or radiotherapy. Local control should be maintained by surgical resection whenever possible to obtain wide margins with acceptable functional outcomes. When wide surgical margins are difficult to obtain or a considerable post-surgical functional loss is estimated, then local control can be obtained by definitive radiotherapy. Radiotherapy can also be applied to maintain local control of the lesion in addition to surgical resection either pre- or post-operatively. Metastatic disease at the time of diagnosis, poor response to neoadjuvant chemotherapy, and relapse of disease indicate poor prognosis.

Myeloma

Multiple myeloma is a malignant skeletal tumor that originates from active bone marrow. The definitive diagnosis of multiple myeloma most frequently is done by detecting local microenvironmental changes in bone marrow biopsy. Detection of abnormal proteins in blood and urine samples is also helpful. Multiple myeloma is the most common primary malignancy of the

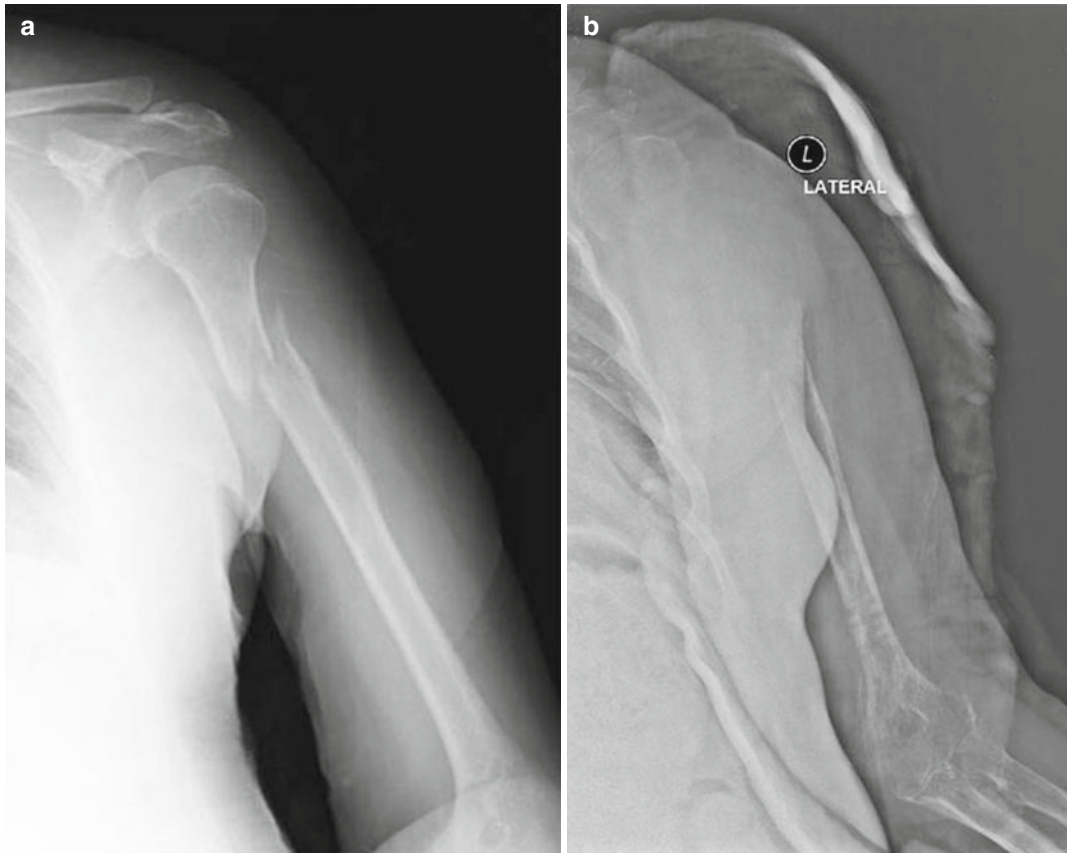

Fig. 35.15 Multiple myeloma. (**a**, **b**) The aggressive course of a lesion can be seen, which caused a pathological fracture at proximal humerus

bone and constitutes over 40 % of primary skeletal malignancies [6]. It is most frequently detected between the fifth and seventh decades and least prevalent at younger age groups. The differential diagnosis of a patient over 40 years with a skeletal tumor should include multiple myeloma and metastatic disease. Plasmacytoma (solitary myeloma) represents an earlier stage of myeloma and frequently transforms into a disseminated form within 5–20 years. Multiple myelomas commonly involve bones of axial skeleton (vertebrae, ribs, and pelvis) that include bone marrow, and mild or moderate transient pain is the first and most frequent symptom. Systemic findings (anemia, fewer, decreased resistance to infection, hypercalcemia, and renal dysfunction) are evident distinctively from other skeletal tumors. Usually an aggressive mode of progression is observed and pathologic fractures may frequently accompany (Fig. 35.15).

Radiologic Features

Multiple myeloma may represent in various radiologic patterns. Lytic lesions without a sclerotic rim may develop endosteal scalloping, cortical destruction, or even a pathological fracture. Punch-out lesions can be seen in the skull. Technetium T-99 bone scan is mostly negative because it demonstrates osteoblastic activity only, which means it may only visualize the lesions that produce bone. Instead a skeletal survey will be more helpful. MRI is the most sensitive imaging modality, particularly in evaluation of spinal lesions. Metastatic disease, brown

tumor of the bone (hyperparathyroidism), and poliostotic fibrous dysplasia should be considered in radiologic differential diagnosis of multiple myeloma.

Histopathologic Features

The histologic appearance exhibits atypical nodules or sheets of plasma cells that replace normal bone marrow. Serum protein electrophoresis (to detect monoclonal gammopathy), bone survey, and bone marrow biopsy are adequate for accurate diagnosis. Biopsy of skeletal lesions is rarely required.

Treatment

Chemotherapy is the mainstay of treatment. Symptomatic bone lesions are commonly radiosensitive and demonstrate a rapid response to radiotherapy. Local control for solitary plasmacytoma can also provided by radiotherapy. The symptomatic treatment of pathologic fractures and impending fractures or chemo/radio resistant lesions requires surgical intervention. The goals of surgical treatment are pain relief and increased functional ability. Internal fixation with or without cementation, cemented partial or total joint replacement, and less commonly resection and endoprosthetic reconstruction are the available options for surgical management. Adjuvant radiotherapy to the involved bone is recommended following surgical stabilization. Long-term survival is rare in multiple myeloma, and the vast majority of the patients died within 3 years of diagnosis [6]. Solitary plasmacytoma has a better prognosis.

Miscellaneous/Tumor-Like Lesions

Unicameral Bone Cysts (UBC)

Unicameral bone cyst (UBC) is a tumor-like, cystic lesion of the bone with an unknown etiology. It is postulated that hemodynamic changes may play a role in pathogenesis. The metaphysis of long bones are most frequently involved, and by ingrowth of the affected bone the lesion migrates toward diaphysis. Proximal portions of humerus and femur are involved in 90 % of the cases. Calcaneus is the third most common location. UBCs are commonly asymptomatic and remain undetected, unless complicated by a pathologic fracture.

Radiologic Features and Histopathologic Features

Table 35.5, Fig. 35.16a.

Prognosis and Treatment

Active cysts with high growth potential progressively enters to latent phase after skeletal maturity. Latent lesions without a growth potential are reabsorbed and replaced by normal bone. Some lesions may persist in adulthood as a latent small cyst. Periodic monitoring and activity restriction is usually adequate for the management of these residual cysts. The main goals of treatment for active cysts are the prevention of pathological fracture and subsequent deformity. Small cysts may be monitored periodically. Larger cysts may lead to an actual or impending fracture, thus these lesions should be treated by conventional methods (open curettage and grafting, intralesional

Table 35.5 Radiologic and histopathologic features of simple bone cyst and aneurysmal bone cyst

Feature	Simple bone cyst	Aneurysmal bone cyst
Histopathologic		
Macro	Cystic cavity filled with yellowish fluid	Dark red spongy tissue
Micro	Single layer endothelial cell lining	Blood-filled cavernous spaces
		Hemosiderin laden macrophages
X-ray	Metaphysis of long bones	Metaphysis of long bones
	Centrally localized	Eccentric or whole bone involvement
	Well-defined lytic lesion with sclerotic edges	Expansile lytic lesion surrounded by a thin but (mostly) intact cortex
		Internal septations
MRI	Fluid-fluid levels (only in the presence of hemorrhage)	Fluid-fluid levels
	Mild expansion	Prominent expansion

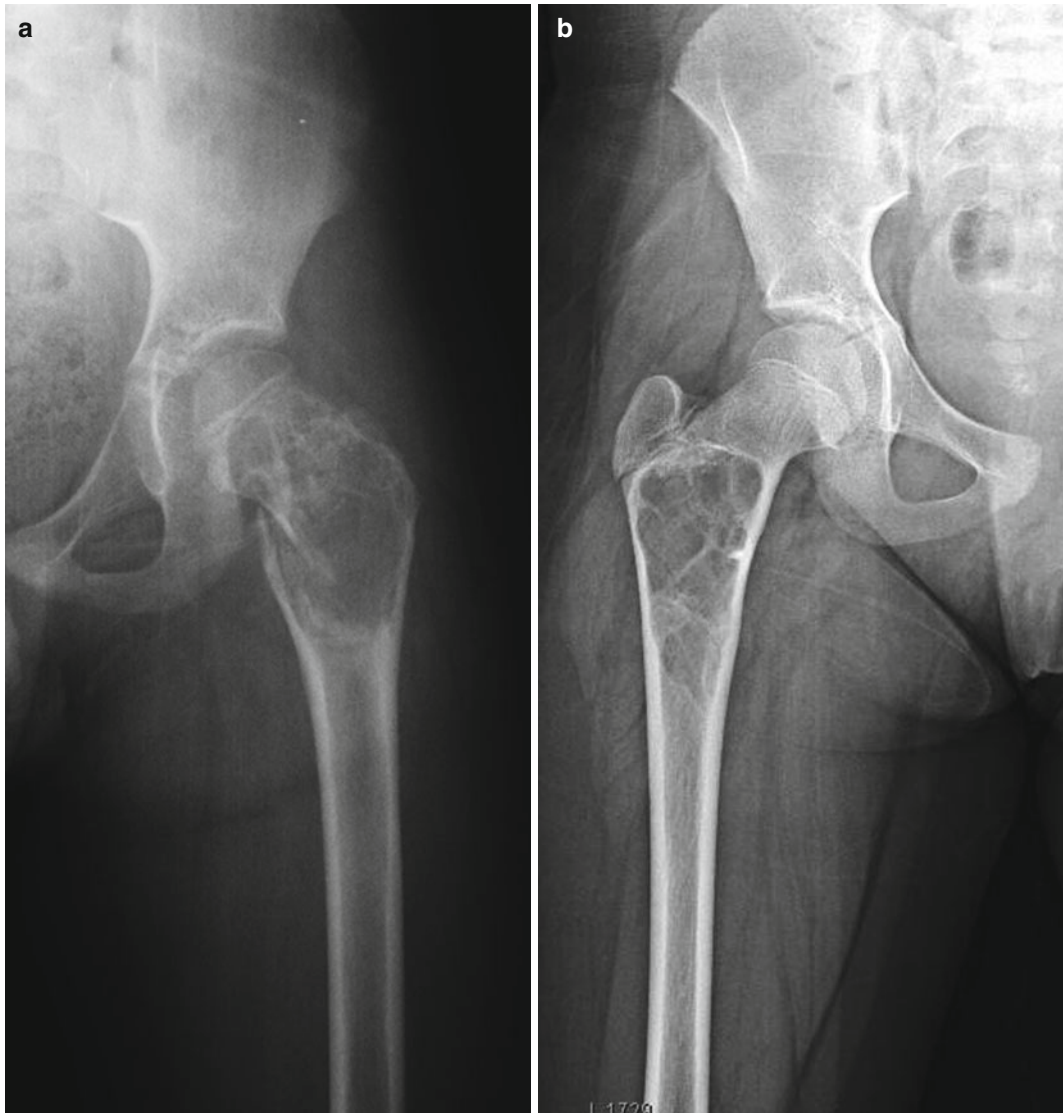

Fig. 35.16 Simple and aneurysmal bone cysts. (**a**) A simple bone cyst located in proximal femur, which is complicated with pathological fracture. (**b**) Cortical thinning and typical internal septations can be seen on radiographic imaging of an aneurysmal bone cyst in the same localization

steroid injection) or recent techniques (autologous bone marrow/ demineralized bone matrix injection, intramedullary decompression) [8–10].

Aneurysmal Bone Cysts (ABC)

ABCs are characterized by dilated vascular channels without endothelial lining. The etiology of ABC remains unclear. It constitutes 1–2 % of all benign bone tumors [5]. Secondary ABCs, which constitute 30 % of all ABCs, usually accompany both benign (e.g., giant cell tumor, chondroblastoma, osteoblastoma) and malignant (e.g., telangiectatic osteosarcoma) lesions. The lesions are most commonly localized in long bone metaphyses. Proximal and distal femur and proximal humerus are the frequently involved sites. ABCs may present with mild to moderate pain and pathological fracture [8].

Radiologic Features Histopathologic Features

Table 35.5, Fig. 35.16b.

Prognosis and Treatment

Although they have a well-differentiated benign histology, ABCs can show aggressive local behavior. They usually require surgical treatment. Recommended treatment is extended curettage and grafting [8, 9]. Local adjuvants (e.g., phenol, hydrogen peroxide) can be applied when required. Lesions involving expandable bones like clavicle, fibula, and distal ulna may be treated by en bloc resection. Recurrence rate is approximately 10 % and when encountered, the lesion requires re-curettage and grafting or resection. Selective arterial embolization should be reserved for vertebral and pelvic lesions either alone or combined with the surgery.

Giant Cell Tumor of Bone

Giant cell tumor of bone (GCTB) is characterized by giant cell rich vascularized tissue and constitutes 20 % of all benign bone tumors [5]. GCTB most frequently affects individual in the third and fourth decades of life. The most common locations of GCTB are distal femur, proximal tibia, distal radius, proximal humerus, and sacrum, respectively. Major complaints are progressive pain, localized swelling, and tenderness. Occasionally, an intraarticular pathological fracture may be the presenting symptom. GCTB has variable clinical courses. The lesion may remain subtle for a long time or it may progress rapidly as in malignant tumors. Malignant transformation is extremely rare. Although being a benign lesion, 1–3 % of GCTB may metastasize to the lungs.

Radiologic Features

Plain radiographs frequently show an eccentric, lytic lesion that involves the epiphyseal and subchondral regions of a long bone (Fig. 35.17a). The transition zone of the lytic lesion is mostly faded. CT is extremely helpful in demonstrating cortical integrity and the presence of pathologic fracture (Fig. 35.17b). MRI is useful to evaluate extension of the lesion; T1-weighted sequences are helpful in demonstrating intraosseous extension, while T2-weighted sequences show extraosseous component better. Intensive edema around the lesion is not a usual finding unless accompanied by a pathologic fracture.

Histologic Features

GCTB macroscopically is a soft and fragile tissue. The color of the lesion may vary from brown-reddish to yellow-gray, depending on bleeding, necrosis, fat, and cystic cavity ratios. Microscopic evaluation demonstrates multinucleated giant cells between the mononuclear stromal cells.

Treatment

The goal of the treatment is complete eradication of the lesion by preserving neighboring joint function. Most of the cases can be managed by extended curettage followed by grafting or cementation (Fig. 35.17c). Performing an intralesional excision through a wide cortical window and extending the margins with a high-speed burr is of paramount importance. The use of phenol as a chemical adjuvant, cryotherapy, argon beam, and cement (generates heat during polymerization of polymethyl methacrylate [PMMA]) as thermal adjuvants are reported to decrease higher recurrence rates. Wide resection and endoprosthetic reconstruction is indicated in cases where an extensive cortical destruction is present and/or the joint line cannot be restored. Recent studies have demonstrated that Denosumab, a nuclear factor kappa-B ligand (RANKL), is successful as an osteoclast inhibitor in the treatment of recurrent, unresectable, or metastatic GCTB. Periodical monitoring or metastasectomy is recommended for rare lung metastases.

Metastatic Disease

Metastatic disease is the most commonly operated bone tumor by orthopedic surgeons. When a new bone lesion is detected in a patient with history of carcinoma, it deserves special consideration about possible metastatic disease. As

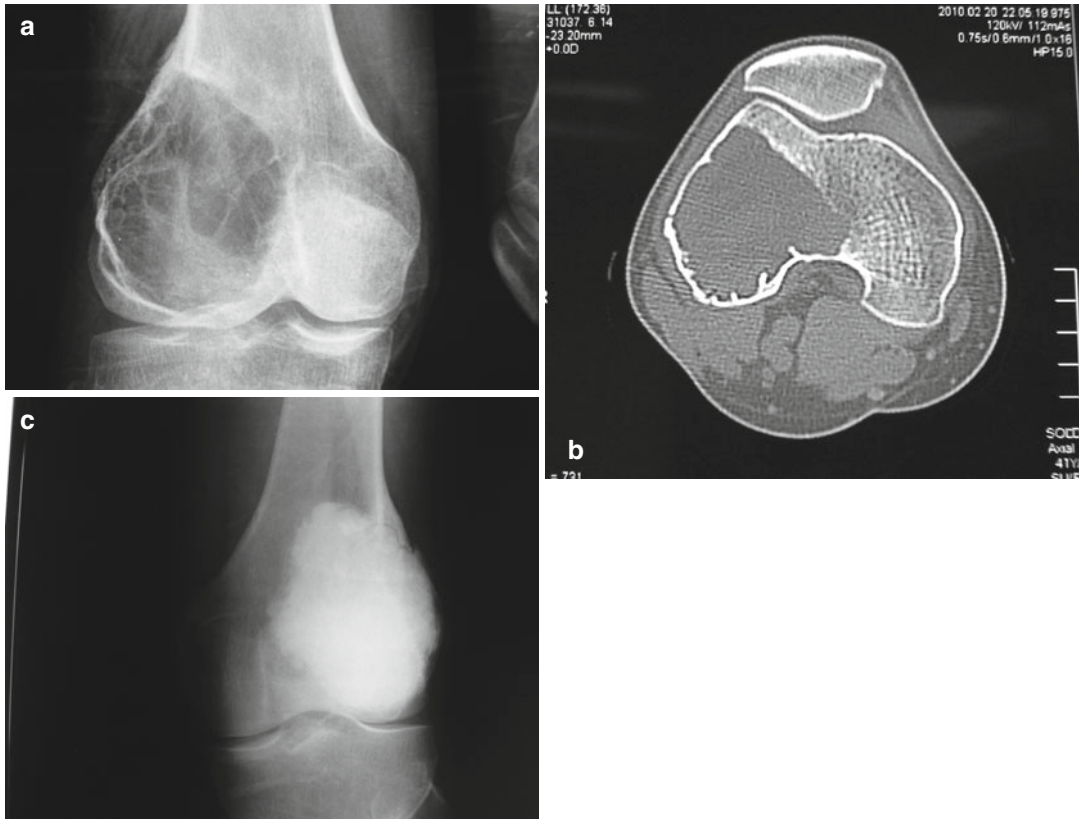

Fig. 35.17 Giant cell tumor. (**a**) Lytic lesion is located eccentrically at the epiphysometaphyseal region of distal femur. (**b**) Cortex remained intact as seen on CT imaging. (**c**) Extended curettage and cementation was performed

previously mentioned in this chapter, the differential diagnosis of a skeletal tumor patient over 40 years should include multiple myeloma and metastatic disease [6]. Metastasis to bone most frequently originates from the breasts, lung, and prostate, respectively, followed by the kidneys, thyroid, and gastrointestinal system. A detailed history, physical examination, blood tests, and imaging studies of the affected bone and the lungs, abdomen and pelvis, demonstrate the primary tumor in 85% of the cases. A subsequent biopsy usually is mandatory to reveal the origin of the metastatic disease.

Plain radiographic findings may be variable in metastatic disease; the lesions may be lytic, blastic or mixed (Fig. 35.18). Metastatic bone lesions of lung cancer are usually detected in distal regions of the appendicular skeleton [6]. Microscopic view of a metastatic bone lesion commonly demonstrates the histopathologic characteristics of the primary lesion.

A multidisciplinary approach is essential in the evaluation of bone metastasis. The vast majority of patients with metastatic disease require systemic chemotherapy. Bisphosphonates, which inhibit the activity of osteoclasts, have been shown to prevent the occurrence of new bone lesions and decelerate the growth rate of preexisting lesions. Metastatic disease of bone most frequently is radiosensitive.

Surgical intervention is indicated especially in the presence of impending or pathological fractures. Mirels' scoring system for risk of pathologic fracture (Table 35.6) is a reliable method for screening impending fractures in metastatic bone lesions [12]. Mirels' scoring system basically has four criteria—site of lesion; size of lesion; lytic, blastic, or mixed nature of lesion;

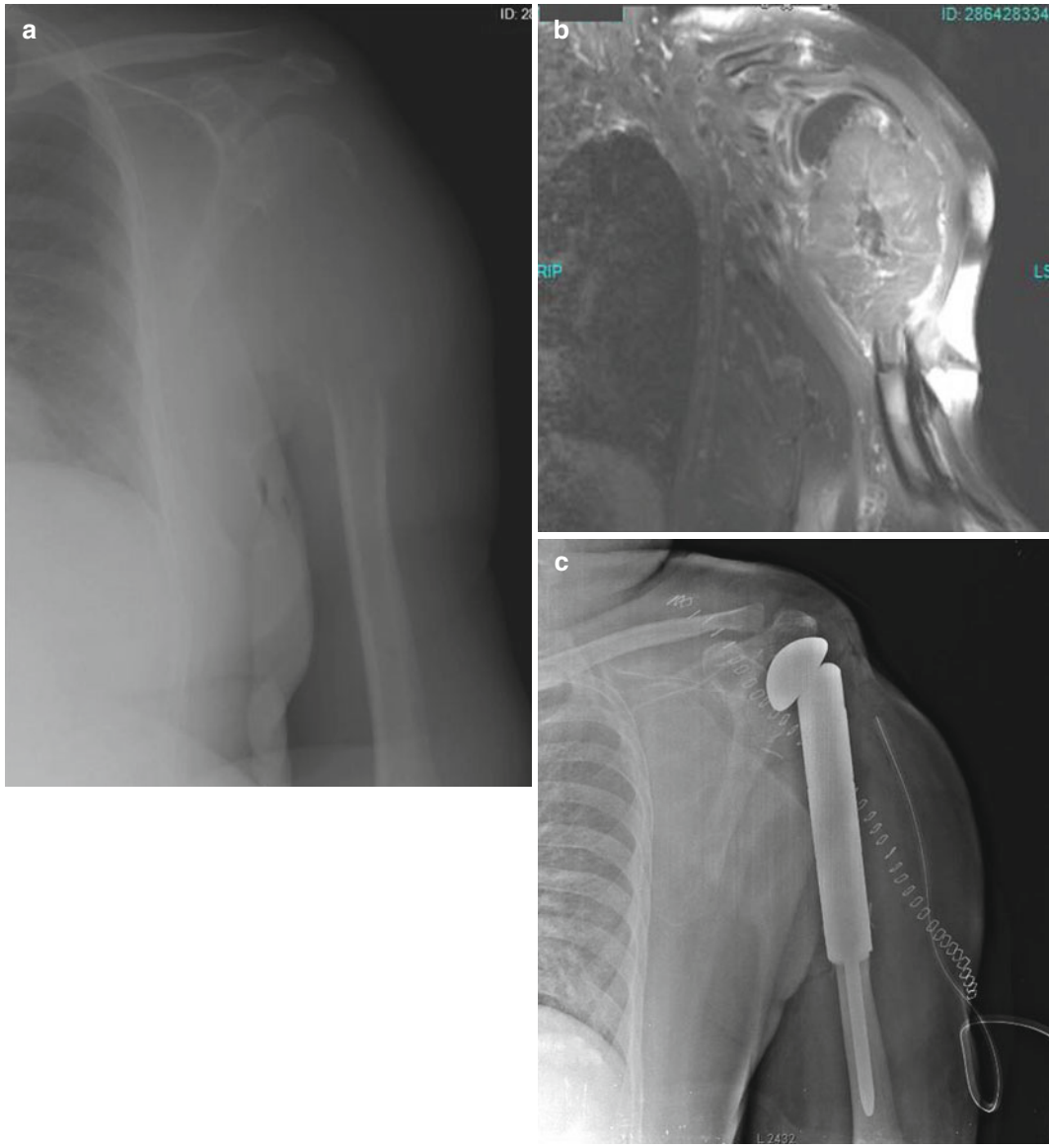

Fig. 35.18 Bone metastasis of lung adenocarcinoma. (**a**) Radiograph, (**b**) MR imaging of the lesion that destructs proximal humerus and extends soft tissues. (**c**) Radiotherapy to the whole humerus is performed after resection and endoprosthetic reconstruction procedure

Table 35.6 Mirels scoring system to predict pathological fracture risk

Score			
Variable	1	2	3
Site	Upper	Limb lower	Limb peritrochanter
Pain	Mild	Moderate	Functional
Size	<1/3	1/3–2/3	>2/3
Lesion	Blastic	Mixed	Lytic

and intensity of pain—and each criteria is scored by three points. A total score of 7 or less is considered as low risk for fracture and conservative methods are recommended; however, an overall score of 9 or more is accepted as high risk for fracture and a prophylactic fixation should be considered. Score of 8 depends mostly on multidisciplinary teams' experience. The two basic principles should be remembered in the surgical

management of metastatic bone disease, especially for lesions with Mirels score of 8:

1. Internal fixation of a lesion with impending fracture is much easier than fixation of a lesion complicated with pathologic fracture.
2. Morbidity of prophylactic fixation of an impending fracture is much lower than the morbidity of fixation of an actual pathological fracture.

Prediction of survey in metastatic bone disease is not always possible. Breast, prostate, and renal cancer patients have longer survival rates following the diagnosis of metastatic bone disease. Unpredictable survival rates of these lesions create contradiction in choosing the most appropriate surgical option. The selected fixation method should allow immediate weight bearing and long-term immobilization should be avoided. The duration of fixation/reconstruction should last longer than the expected life of the patient. The internal fixation method (e.g. plate-screws) frequently require cement augmentation. The fixation of the whole bone (e.g. intramedullary nails) should be secured with internal fixation in most cases. Resection and endoprosthetic reconstruction can be considered if internal fixation cannot warrant stabilization for immediate weight bearing.

References

1. Greenspan A, Jundt G, Remagen W. (2007) Differential diagnosis in orthopaedic oncology. Lippincott Williams & Wilkins, Philadelphia, PA
2. Madewell JE, Ragsdale BD, Sweet DE (1981) Radiologic and pathologic analysis of solitary bone lesions. Part I: internal margins. Radiol Clin North Am 19(4):715–748
3. Ragsdale BD, Madewell JE, Sweet DE (1981) Radiologic and pathologic analysis of solitary bone lesions. Part II: periosteal reactions. Radiol Clin North Am 19(4):749–783
4. Heck R (2008) General principles of tumors. In: Campbell's operative orthopedics. Mosby, New York, pp 775–854
5. Schwartz HS (2007) Orthopaedic Knowledge Update (OKU) Musculoskeletal tumors. American Academy of Orthopaedic Surgeons Publication, Rosemont, IL
6. Heck Jr R (2008) Malignant tumors of bone. In: Campbell's operative orthopaedics, 11th edn, vol 1. Mosby, St. Louis, pp 901–938
7. Picci P et al. (1994) Relationship of chemotherapy-induced necrosis and surgical margins to local recurrence in osteosarcoma. J Clin Oncol 12(12):2699–2705
8. Erol B, Dormans J, States L, Pawel B (2004) Tumors. In: Orthopaedic surgery essentials-pediatrics. Lippincott Williams & Wilkins, Philadelphia, pp 250–270
9. Erol B, Er T, Rodop O, Olgaç V (2012) Çocuklarda kas-iskelet sistemi tüm.rleri. Çocuk Ortopedisi. Bayçınar Tıbbi Yayıncılık, İstanbul, pp 243–280
10. Dormans JP et al. (2001) Pathologic fractures associated with tumors and unique conditions of the musculoskeletal system. In: Beatty JH, Kasser JR (eds) Rockwood and Wilkins' fractures in children, 5th edn. Lippincott Williams and Wilkins, Philadelphia, pp 139–240
11. Boyce AM, Chong WH, Yao J, Gafni RI, Kelly MH, Chamberlain CE et al. (2012) Denosumab treatment for fibrous dysplasia. J Bone Miner Res 27(7):1462–1470
12. Mirels H (1989) Metastatic disease in long bones: a proposed scoring system for diagnosingimpending pathologic fractures. Clin Orthop Relat Res 249:258

Soft Tissue Tumors

36

Nevzat Dabak, Yusuf Yıldız, Bahtiyar Demiralp, and Mert Keskinbora

Abstract

Soft tissue tumors constitute a large group of tumors with diverse histopathological types. Mesenchymal tissues such as fibrous, lipomatous, vascular, synovial, and muscular tissues are described within this group. Neural sarcomas of neuroectodermal origin are also considered in this group due to their similar clinical and pathological characteristics (Enzinger FM, Weis SW (1995) Soft tissue tumors, 3rd edn. Mosby, St Louis).

Soft tissue tumors may present with different histological, clinical, radiological, and pathological features within a wide range of anatomical locations, and thus diagnosis and treatment of these tumors require a multidisciplinary approach. Diagnostic evaluation of soft tissue tumors is critical as many benign soft tissue lesions may be confused with rare sarcomas.

The main goal of this chapter is to throw light on the diagnostic approach to a musculoskeletal tumor patient that every orthopedic resident may encounter in their daily practice and to emphasize the fundamental management algorithm to be followed.

N. Dabak, MD (✉)
Samsun Medical Park Hospital Hospital Orthopaedics ve Traumatology Department,
Atakum, Samsun 55200, Turkey
e-mail: ndabak@gmail.com

Y. Yıldız, MD
Ankara University İbn-i Sina Hospital Orthopaedics ve Traumatology Department, Ankara 06230, Turkey
e-mail: yhyildiz@yahoo.com

B. Demiralp, MD • M. Keskinbora, MD
İstanbul Medipol University Hospital Orthopaedics ve Traumatology Department Unkapanı,
Atatürk Bulvarı No:27, Fatih-İstanbul 34083, Turkey
e-mail: bahtidemiralp@gmail.com; mertkeskinbora@yahoo.com

Epidemiology and Etiology

Benign soft tissue tumors are more frequent than malignant tumors. Suit and Mankin reported this ratio as 100/1 and incidence as 300/100,000. Additionally, benign lesions like lipomas and hemangiomas were excluded in this ratio, due to their occasional excision without a previous biopsy procedure.

In terms of gender, there is no significant difference between men and women. Instead of the wide range of age distribution (10–80 years), they were less frequently seen under 40 years. The incidence was 6.5 % under 15 years of age.

Although, there is no definite reason that has been put forward in the formation of soft tissue sarcomas, several factors like infectious agents,

F. Korkusuz (ed.), *Musculoskeletal Research and Basic Science*,
DOI 10.1007/978-3-319-20777-3_36

chemicals, and radiation were blamed for many years. There is clinical evidence of Epstein Barr Virus (EBV), as playing a critical role in the etiology of pediatric muscle tumors, especially that associated with HIV and immunosuppression [2]. Soft tissue sarcomas (STS) have been reported in HIV-infected adults [3]. Radiation exposure increases the likelihood of STS. In some of the patients who underwent radiotherapy after surgery for breast carcinoma, fibrosarcoma was observed on the chest wall in the following years [4, 5]. STS are seen more often in the fields of trauma, burn scars, and fistula sites due to osteomyelitis.

In some types of STS, chromosome abnormalities have been shown with genetic researches. Translocation of the 18th chromosome in synovial sarcoma [6], translocation between short arms of the 2nd and 13th chromosomes in alveolar type rhabdomyosarcoma [7], and translocation between the 12th and 16th chromosomes in myxoid liposarcoma [8] are some of the examples. In hereditary Li-Fraumeni syndrome, breast cancer is accompanied by STS [9].

Pathology

Malignant fibrous histiocytoma (MFH, also known as pleomorphic sarcoma or fibrosarcoma) is regarded as the most common type of STS. This is followed by liposarcoma, leiomyosarcoma, rhabdomyosarcoma, neuroblastoma, synovial sarcoma, angiosarcoma, and Kaposi sarcoma, respectively.

The pathological classification, according to the predominant cell type inside the tumor, which is presented by Enzinger and Weiss, is the accepted system for STS. This histological classification system was rearranged for STS by the World Health Organization (WHO) [1].

Diagnostic Approach for Soft Tissue Tumors

Symptoms

The major clinical finding is usually a painless mass (Fig. 36.1). Even though benign lesions are more common, the differentiation between benign and malignant lesions is almost always not possible, by means of physical examination. Most STS do not provide clinical evidence without fascial invasion or before reaching 5 cm in size [10]. In the small sized initial phase, lesions can be considered benign in nature. Follow-up of these lesions with short time intervals will prevent unintended mistakes.

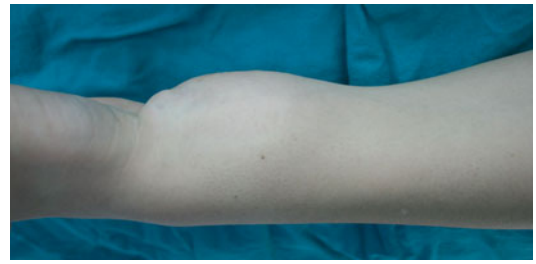

Fig. 36.1 The soft tissue mass appearances at the distal part of the forearm

Before the diagnosis of primary lesion, a portion of the patients may refer with signs of metastatic disease, due to silent or vague symptoms. In such cases, evaluation of the patients by algorithms for musculoskeletal tumors will be appropriate, while unnecessary tests and time loss can be avoided.

Physical Examination

Physical examination should be carried out following general systemic examination to assess the mass and its mechanical effects on the surrounding tissues. Skin alterations over the mass, peripheral edema, muscle atrophies, relation with contiguous anatomical structures, sensorial and motor deficiencies should be evaluated. In particular, the pulse abnormalities proximal or distal to the lesion, in comparison with the unaffected side, should be investigated by advanced tests.

The detection of distant metastases by physical examination may even be possible. While lungs are the most involved side of distant metastasis, meticulous evaluation of the respiratory system must be performed for the soft tissue sarcoma patients.

Laboratory Tests

Although there are no current specific biochemical markers for soft tissue sarcomas, indicators of muscle destruction like LDH and creatine kinase can be used. However, due to high levels of these markers after a trauma, alterations are not always that meaningful.

Metastases of STS may cause an increase in the biochemical parameters by dysfunction of the involved organ.

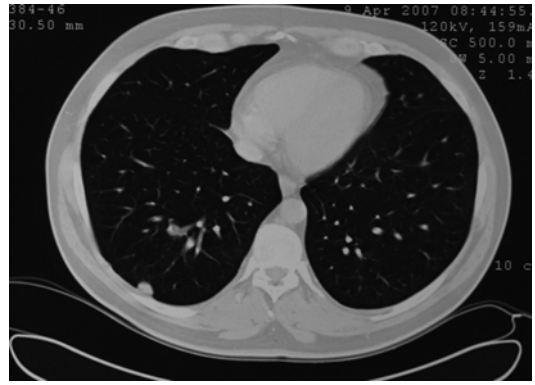

Fig. 36.2 Thoracic CT showing lung metastasis

Imaging Methods

The role of imaging modalities in the evaluation of STS is unquestionable. Plain radiography, ultrasonography, computerized tomography (CT), magnetic resonance imaging(MRI), positron emission tomography(PET), angiography, and scintigraphy hold an important place in the radiological assessment of these lesions.

With the recent advances on imaging techniques, perfusion-diffusion imaging of lesions, three-dimensional anatomy and determination of relationship with the surrounding structures is possible.

As an inexpensive and noninvasive method, ultrasonography is used in the initial assessment of a soft tissue mass, by evaluation of liquid and solid structure and content of the vascularity.

Computerized tomography can be used for the determination of mediastinal and retroperitoneal placement in relation to lung and other organ systems and also useful in the evaluation of detecting metastases in these regions (Fig. 36.2).

Magnetic resonance imaging is used as a screening tool, for diagnostic and staging purposes and also for monitoring the treatment. MRI gives indirect information about the content and nature of the tissue by using various sequences, as well as the overall appearance of the lesion. Heterogeneity and the capsular structure of the tumoral tissue can be demonstrated with MRI. Intra-lesional heterogeneity can be observed in 95 % of T2-weighted images of the malignant tumors, while it was only 20 % in benign tumors. The presence of septations is another finding that gives a malignant impression [11]. While necrosis in the tumor can be demonstrated by contrast-enhanced images, the absence of necrosis does not rule out malignancy (Figs. 36.3, 36.4, and 36.5).

In recent years, information about tumor physiology can be obtained through the evaluation of perfusion and diffusion of contrast agents by dynamic MRI. Rapid contrast enhancement in dynamic MRI is meaningful in terms of malignancy. MRI and CT also play an important role in monitoring and follow-up of the treatment and detection of metastases. Scintigraphy is used both for determination of local invasion and distant metastases of the tumor. Gallium citrate can be used for the detection of non-pulmonary metastases and lymphatic involvement in pediatric rhabdomyosarcomas [12].

Biopsy

Biopsy is considered as the gold standard for the diagnosis of musculoskeletal lesions. However, using this precious diagnostic tool as a first-line method is not the right approach. Biopsy procedures must be applied after all diagnostic methods have been performed to confirm the presumptive diagnosis. An improper biopsy may affect the patient's prognosis and treatment, as well as blurring the definitive diagnosis [13, 14]. Biopsy should be carried out in a tertiary center by the same team who will perform

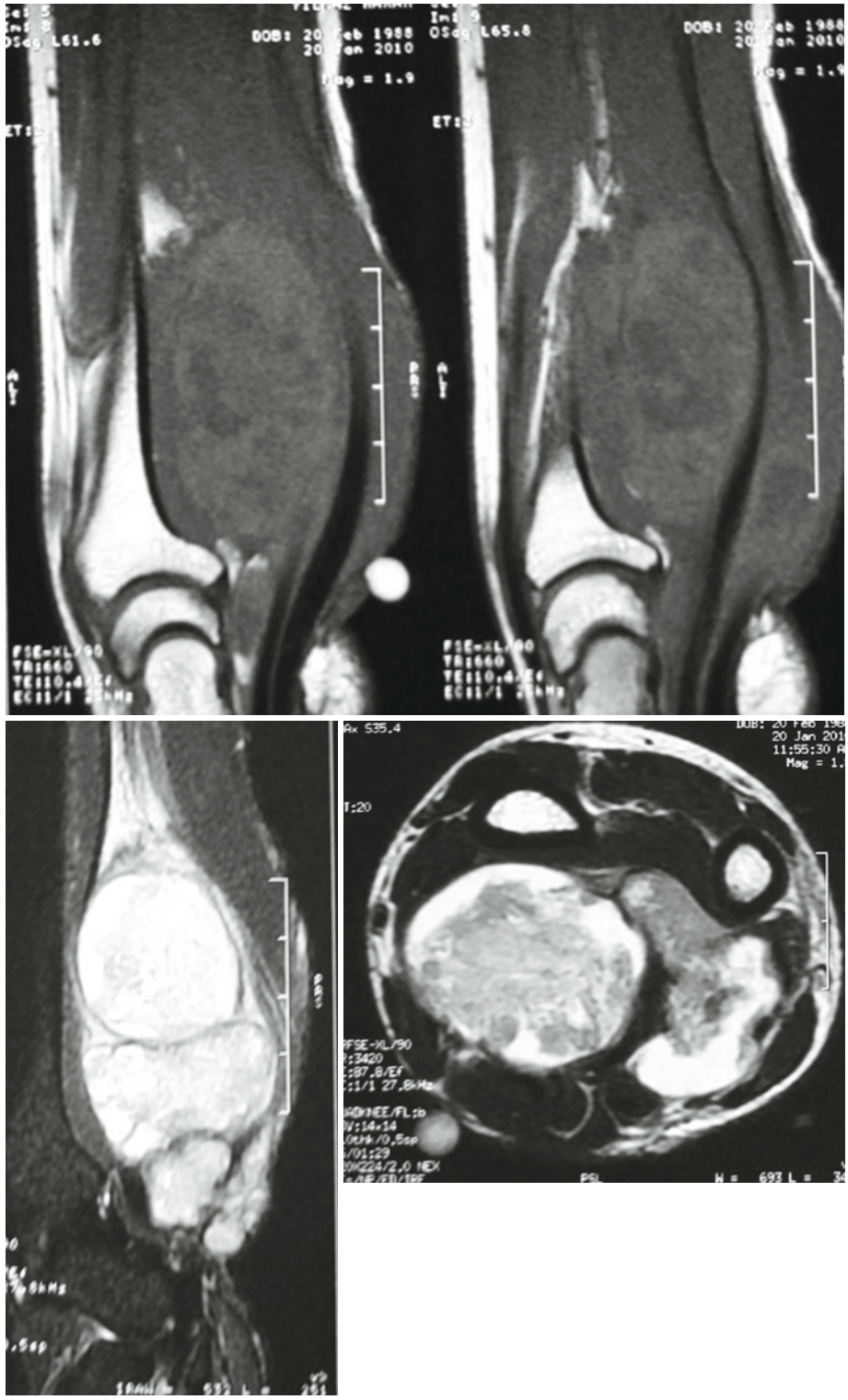

Figs. 36.3, 36.4, and 36.5 Malignant soft tissue tumor as hypointense in sagittal T1-, hyperintense in T2-weighted images, and heterogeneity in contrast-enhanced T1-weighted image

further treatment. Biopsy is an invasive approach that has to be applied through the shortest way to reach the tumor and that can be removed during the definitive surgery. To avoid bleeding that can cause dissemination of tumoral cells, cold application and short-term restriction of movements in the joints near by the biopsy site would be appropriate.

Biopsy Types
Fine needle aspiration biopsy (FNAB)
Core needle biopsy
Incisional biopsy
Excisional biopsy

Biopsy type is selected according to lesion size, location, and pathologist's experience.

FNAB Performed with 21–23 Gauge needles, it requires an experienced cytopathologist. Detection of sarcoma type and grade may fail with this method. Atraumatic and inexpensive application are the advantages [15]. In deep lesions, FNAB can be performed by guidance of CT. The risk of contamination is very low. It is a simple and useful method, particularly in retroperitoneal and intra-abdominal lesions. Very successful in the detection of distant metastases and recurrence of prediagnosed sarcomas.

Core Biopsy Provides tissue 1–10 mm in thickness. It is usually performed by Tru-cut needles. The harvested tissue may be insufficient for diagnosis and grading. Enough material may not be achieved for special staining and electron microscopy [16]. It is still a commonly used method (Fig. 36.6).

Incisional Biopsy Applied in most soft tissue tumors. Longitudinal incisions should be used, especially in the extremities. Incisions must be carried out directly from the closest place to tumor. Appropriate hemostasis should be provided, drains should be avoided, if used it should be in or just near the incision side. If the lesion was diagnosed as malignant, drain pathway should also be excised during the definitive surgery.

Excisional Biopsy Should be performed for lesions smaller than 3 cm, with lower risk of malignancy and for cases that would not risk the subsequent treatment even diagnosed as sarcoma. If it is done in deep lesions, the probability of contamination is very high and may adversely affect the subsequent treatment.

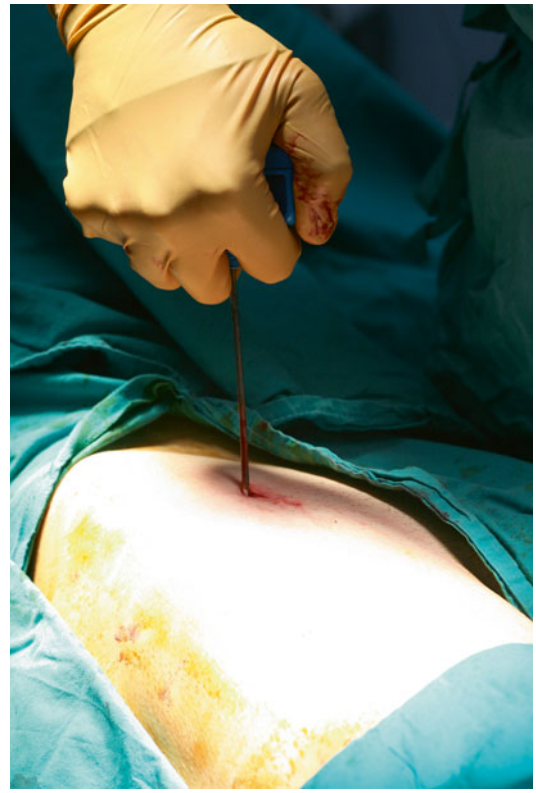

Fig. 36.6 Core biopsy

Staging of Soft Tissue Sarcomas

Staging of soft tissue sarcomas is very important in determining the treatment and prognosis. Therefore, various staging systems have been developed (Table 36.1). These are as follows:

1. *The American Joint Committee on Cancer (AJCC) Staging System*: Tumor, node, and metastasis (TNM) is the basis of this staging system. *In addition, according to the anatomical localization as being deep or superficial to the fascia and the number of grading (high/low grade) was reduced from three to two* [17].

Table 36.1 AJCC and Enneking staging systems for soft tissue sarcomas

American Joint Committee on Cancer (AJCC) staging system				
Stage	Grade	Tumor size and localization	Lymph nodes	Metastases
IA	Low	≤5 cm	–	–
IB	Low	>5 cm, superficial	–	–
IIA	Low	>5 cm, deep	–	–
IIB	High	≤5 cm	–	–
IIC	High	>5 cm, superficial	–	–
III	High	>5 cm, deep	–	–
IVA	L/H	>5 cm/≤5 cm	+	–
		Superficial/deep		
IVB	L/H	>5 cm/≤5 cm	–	+
		Superficial/deep		

Enneking staging system for STS			
Stage	Grade	Site	Metastases
IA	G1	T1	M0
IB	G1	T2	M0
IIA	G2	TI	M0
IIB	G2	T2	M0
III	G1-2	T1-2	M1

Tumor characteristics
Grade 1: Low
Grade 2: High
Site (T)
T1: Intra-compartmental
T2: Extra-compartmental
Metastasis
M0: No metastasis
M1: Regional or distant metastasis

2. *Hajdu System*: In this classification system, the grade, size, and localization of the tumor according to the fascia is taken into account.
3. *Enneking Staging System*: In this system, tumor stage is determined by local invasion (T), nodular (N) or distant metastases (M), and tumor's grade (G) [18].

Treatment

Although the treatment may differ in some types (i.e., fibromatosis), marginal excision will be adequate for benign soft tissue tumors. In STS, treatment should be started immediately after confirming the diagnosis. The goal of the treatment is to remove the existing mass from the body and to control the risks of metastasis and recurrence. The main objective of the treatment is to protect the patient's life. A multidisciplinary approach (orthopedic oncologist, medical oncologist, radiation oncologist, radiologist, and pathologist) is essential in the treatment and prognosis of soft tissue sarcomas. Treatment approaches can be as follows:

- Surgical excision
- Radiotherapy
- Chemotherapy

Surgical Treatment

The development of imaging techniques in recent years, especially revealing the three-dimensional anatomy and new reconstruction methods, provides limb-sparing surgery applicable in 90 % of patients. If adequate surgical margins cannot be achieved by limb salvage surgery, amputation should be considered. As exceptions, a sciatic nerve or a single nerve in the extremity can be excised because of invasion and a resected vascular structure can be bypassed with synthetic or autogenous grafts. Skin grafts and fleps are available, if problems with surgical closure are experienced following a limb salvage procedure. Amputation should be considered at the forefront for treatment of sarcomas that arises from popliteal or antecubital fossa. Invasion of neurovascular structures is considered as a strong indicator for amputation. The removal of previous incision scars, biopsy, and drain pathways is essential. Such contaminated areas have to be removed in an elliptical fashion with 2 cm clear surgical margins (Fig. 36.7).

Chemotherapy

Chemotherapy can be used as a neoadjuvant and/or adjuvant agent in the treatment of STS. The increase in the 5-year survival rates of pediatric soft tissue sarcomas such as rhabdomyosarcoma and neuroblastoma has aroused interest in the use of chemotherapy for other soft tissue sarcomas. Chemotherapy is contraindicated in tumors like

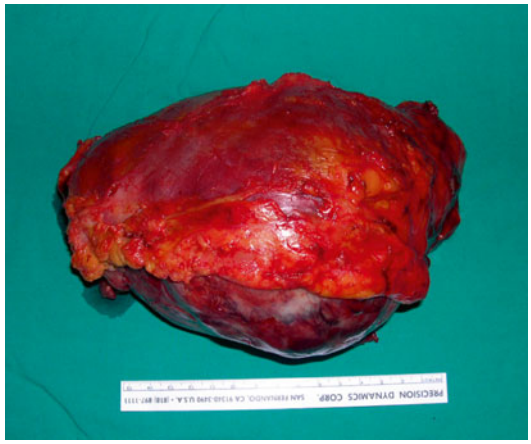

Fig. 36.7 Excision of the previous incision and removal of the soft tissue mass with wide margins

liposarcoma and leiomyosarcoma, which have poor response to conventional chemotherapeutic agents, in non-metastatic skin tumors other than Kaposi sarcoma, for sarcomas less than 5 cm in size that can easily be controlled by local surgical excisions and in patients with severely low overall condition.

After preoperative radiotherapy and/or chemotherapy, obtaining wide margins will minimize local recurrence rates. At least 2 cm of healthy tissue in the tumor area, and in the deep tissues, fascia and even some muscle tissue has to be taken into the surgical margins. Receipt of an intraoperative pathology consultation on via frozen section examination is essential in cases within determinate surgical margins.

Surgical margins after the surgery is very important in the local recurrence, metastasis and survival of STS. The average margin of 2 cm and above are considered as reliable. In a Mayo Clinic's study in 2010, the local recurrence, metastasis and survival rate of patients with less than 2 mm or positive surgical margins, are reported to be significantly below when compared with the 2 mm or above patients [19].

Radiotherapy

In the last quarter of this century, radiotherapy has been an important step in the local control of STS. Feasibility of limb-sparing surgery has increased with the application of preoperative radiotherapy [20, 21]. Although it is associated with acute wound complications, preoperative radiotherapy has increased the local control rates in retroperitoneal sarcomas that are supposed to be unresectable. The best indications for preoperative radiation administration are myxoid liposarcoma, locally advanced proximal sarcomas, elderly patients, and failure after neoadjuvant chemotherapy [22]. Even though there are centers that carry out intraoperative radiotherapy, this procedure brings the risks of elongation in surgical time and infection besides. A variety of skin complications may be encountered during and after the application of radiotherapy. The risks, benefits, and time of radiotherapy must be adjudged by the multidisciplinary oncology team.

Follow-Up

Local recurrences in STS are mostly seen in the 5 years after treatment. Approximately 80 % of all distant organ metastases involve the lungs. Prolonged patient survival rates can be achieved by early detection of local recurrences and metastases. Follow-up of the patients should be performed at appropriate intervals and in a rigorous manner. In the first 3 years, patients must be followed in every 3 months [23]. Evaluation must include a careful analysis of patient symptoms and a precise physical examination. If there are no symptoms or any signs of recurrence, a conventional chest X-ray will be enough, in terms of imaging. Contrast-enhanced CT scans can be used in the follow-up retroperitoneal or pelvic STS.

New Directions

Genomic profiling has displayed unique translocations, mutations, or amplifications that are specific for some types of STS. Recent studies offer a detailed discrimination of histological subtypes. Hereby, significant progress in terms of diagnosis, treatment, and survival rates will be able with histology-driven therapies. Improvements in molecular pathogenesis and targeted therapies

may facilitate individual sarcoma treatment [24]. Further understanding of sarcomagenesis and disease-associated genes will open new prospects in the management of STS.

References

1. Enzinger FM, Weis SW (1995) Soft tissue tumors, 3rd edn. Mosby, St Louis
2. McClain KL, Leach CT, Jenson HB, Joshi VV, Ploock BH, Parmley RT, DiCarlo FJ, Chadwick EG, Murphy SB (1995) Association of Epstein-Barr virus with leiomyosarcomas in young people with AIDS. N Engl J Med 332:12–18
3. Fizazi K, Feuillard J, Le Cesne A, Terrier P, Raphael M, Pouillart P, Tursz T (1996) Soft tissue sarcomas in HIV-infected adult patients. Eur J Cancer 32A:1812–1814
4. Iwasaki K, Nagamitsu S, Tsuneyoshi M (1978) Postirradiation fibrosarcoma following radical mastectomy. Jpn J Surg 8(1):73–77
5. Mark RJ, Poen J, Tran LM, Fu YS, Selch MT, Parker RG (1994) Postirradiation sarcomas. A single-institution study and review of the literature. Cancer 73(10):2653–2662
6. Santos NR et al (2001) Molecular mechanisms underlying human synovial sarcoma development. Gene Chromosome Cancer 30(1):1
7. McManus AP, O'Reilly MA, Jones KP, Gusterson BA, Mitchell CD, Pinkerton CR, Shipley JM (1996) Interphase fluorescence in situ hybridization detection of t(2;13)(q35;q14) in alveolar rhabdomyosarcoma: a diagnostic tool in minimally invasive biopsies. J Pathol 178(4):410–414
8. Knight JC, Renwick PJ, Cin PD, Van den Berghe H, Fletcher CD (1995) Translocation t(12;16)(q13;p11) in myxoid liposarcoma and round cell liposarcoma: molecular and cytogenetic analysis. Cancer Res 55(1):24–27
9. Li FP, Fraumeni JF Jr (1969) Soft-tissue sarcomas, breast cancer, and other neoplasms: a familial syndrome? Ann Intern Med 71:747
10. Peabody TD, Monson D, Montag A et al (1994) A comparison of the prognosis for deep and subcutaneous sarcomas of the extremities. J Bone Joint Surg 76A:1167
11. Hermann G, Abdelwahap I, Miller T, Klein M, Lewis M (1992) Tumour and tumour like conditions of the soft tissue: magnetic resonance imaging features differantiating benign from malignant masses. Br J Radiol 65:14–20
12. Armstrong SJ, Wakeley CJ, Goddard PR, Watt I (1992) Review of the use of MRI in soft tissue lesions. Clin Radiol 46:311–317
13. Mankin HJ, Mankin CJ, Simon MA (1996) The Hazards of the Biopsy Revisited. For the members of the Musculoskeletal Tumor Society. J Bone Joint Surg 78A:656
14. Başbozkurt M (1997) Biopsi özellikleri ve plansız cerrahi girişimlerin prognoza etkisi. In: Ege R (ed). XV. Türk Milli Ortopedi ve Travmatoloji Kongre Kitabı; Mayıs 28–30; İstanbul. pp 43–47
15. Akerman M, Rydholm A, Persson BM (1985) Aspiration cytology and soft-tissue tumors. The 10-year experience at an orthopaedic oncology center. Acta Orthop Scand 56:407
16. Skrzynski MC, Biermann JS, Montag A, Simon MA (1996) Diagnostic accuracy and charge-savings of outpatient core needle biopsy compared with open biopsy of musculoskeletal tumors. J Bone Joint Surg 78A:644
17. American Joint Committee on Cancer (1997) Soft-tissues. In: Fleming ID, Cooper JS, Hensen DE et al (eds) American Joint Committee on Cancer (AJCC) cancer staging manual, 5th edn. Lippincott-Raven, Philadelphia, p 149
18. Enneking WF, Spanier SS, Goodman MA (1980) A system for the surgical staging of musculoskeletal sarcoma. Clin Orthop 153:106–120
19. Novais E, Demiralp B, Alderete J, Larson MC, Rose PS, Sim FH (2010) Do surgical margin and local recurrence influence survival in soft tissue sarcomas? Clin Orthop Relat Res 468(11):3003–3011
20. Suit H, Mankin H, Wood WC et al (1985) Preoperative, intraoperative, postoperative radiation in the treatment of primary soft tissue sarcoma. Cancer 55:2659
21. Tanabe KK, Pollock RE, Ellis LM, Murphy A, Sherman N, Romsdahl MM (1994) Influence of surgical margins on outcome in patients with preoperatively irradiated extremity soft tissue sarcomas. Cancer 73:1652–1659
22. Levy A, Bonvalot S, Bellefqih S, Vilcot L, Rimareix F, Terrier P, Belemsagha D, Cascales A, Domont J, Mir O, Honoré C, Le Cesne A, Le Péchoux C (2014) Is preoperative radiotherapy suitable for all patients with primary soft tissue sarcoma of the limbs? Eur J Surg Oncol 40(12):1648–1654
23. Rutkowski P, Lugowska I (2014) Follow-up in soft tissue sarcomas. Memory 7(2):92–96
24. Takahashi A, Nakayama R, Ishibashi N, Doi A, Ichinohe R, Ikuyo Y, Takahashi T, Marui S, Yasuhara K, Nakamura T, Sugita S, Sakamoto H, Yoshida T, Hasegawa T, Takahashi H (2014) Analysis of gene expression profiles of soft tissue sarcoma using a combination of knowledge-based filtering with integration of multiple statistics. PLoS One 9(9)

Part VI

Basic Pharmacology

Vasfi Karatosun

Pain Pathways and Analgesics

37

Hakan Boya

Abstract

Pain is an unpleasant sensory and emotional experience associated with actual or potential tissue damage. Pain is both a physical phenomenon and a psychological or emotional experience. Surgical tissue damage causes measurable systemic endocrine, metabolic, and immunological changes referred to as the surgical stress response. Noxious stimulus stimulates peripheral nociceptors, which transduce the stimuli into electrochemical impulses, and then it is carried to dorsal root ganglions of the spinal cord by peripheral sensory nerves. Stimuli are transmitted to supraspinal levels via dorsal horn neurons whose axons ascend within the spinal cord to areas in the midbrain, thalamus, and frontal cortex. Autonomic and motor response, affective-motivational response, identification of the intensity-type-location of the pain sensation, associations with memory and cognitive activities, and emotional and behavioral responses are elicited when the painful stimuli are transmitted to the brain stem. Supraspinal centers control transmission of painful stimuli by producing responses that can lead to either an increase in the transmission of pain impulses or a decrease in transmission. Chronic pain caused by rapid and long-term changes occurs in parts of the central nervous system that are involved in the transmission and modulation of pain. This abnormal processing of pain within the peripheral and central nervous system may become independent of the original painful event. Neuropathic pain is initiated or caused by a primary lesion or dysfunction in the nervous system. Relieving pain and preventing acute pain from becoming chronic pain with management options that affect all levels of the pain process are the basic principles of treatment. Opioids, nonsteroidal anti-inflammatories, local anesthetics, and centrally acting nonopioids can be used for this

H. Boya
Zübeyde Hanım Research and Application Center,
Baskent University,
Bostanlı-Karsıyaka, 35350 Izmir, Turkey
e-mail: hakanboya@yahoo.com

F. Korkusuz (ed.), *Musculoskeletal Research and Basic Science*,
DOI 10.1007/978-3-319-20777-3_37

purpose. In acute pain treatment, multimodal analgesia can address multiple mechanisms of pain with the added benefit of reducing side effects through the use of lower doses of individual modalities. Antidepressants, antiepileptics, calcium channel blockers, alpha-adrenergic blockers, and corticosteroids can be used for chronic pain treatment. Effects of preoperative analgesia on surgical stress response, postoperative complications, and rehabilitation are irrefutable. Nonpharmacologic management like behavioral interventions and physical agents are used in multimodal approaches to analgesia.

Learning Outcomes

After studying this chapter, we will have an understanding of: (1) description of pain and pain types, (2) pain pathways and surgical stress response, (3) aim of pain treatments in orthopedics and the universal approach to pain treatment, (4) medication groups used in pain treatment, (5) combined analgesia in acute pain, (6) preemptive analgesia in surgical procedures, and (7) nonpharmacological procedures in pain treatment.

Terminology

Noxious Harmful, destructive.

Nervous system Your brain and all the nerves in your body.

Periosteum The membrane of the fibrous connective tissue that closely invests all bones except those at the articular surfaces.

Axon It also known as a nerve fiber, is a long, slender projection of a nerve cell, or neuron, which typically conducts electrical impulses away from the neuron's cell body.

Neuron It is an electrically excitable cell that processes and transmits information through electrical and chemical signals.

Limbic system It is a complex set of brain structures located on both sides of the thalamus, right under the cerebrum.

Reticular system It is a set of connected nuclei in the brains of vertebrates that is responsible for regulating arousal and sleep-wake transitions.

Somatosensory cortex It is the main sensory receptive area for the sense of touch in the parietal lobe of the human brain.

Spinal cord It is a long, thin, tubular bundle of nervous tissue and support cells that extends from the medulla oblongata in the brain stem. The brain and spinal cord together make up the central nervous system.

Cerebral cortex It is the cerebrum's (brain) outer layer of neural tissue in humans and other mammals.

Opioid It is any chemical that resembles morphine or other opiates in its pharmacological effects.

Antidepressants Drugs used for the treatment of major depressive disorder and other conditions, including dysthymia, anxiety disorders, obsessive compulsive disorder, eating disorders, chronic pain, neuropathic pain and, in some cases, dysmenorrhea, snoring, migraines, and attention-deficit hyperactivity disorder.

Local anesthetic It is a drug that causes reversible local anesthesia, generally for the aim of having a local analgesic effect, that is, inducing absence of pain sensation, though other local senses are often affected as well.

Clinical Relevance

What is the role of nonsteroidal anti-inflammatory drugs (NSAIDs), corticosteroid, and combined anesthesia at acute pain control? What is preventive analgesia? What is the role of antidepressant and antiepileptic drugs on chronic pain control?

A 70-year-old man with bilateral knee pain, deformity, and activity restriction was seen at an outpatient clinic. Medical history revealed rheumatoid arthritis. At the knee radiographs, there was varus alignment, narrowing at medial joint space, and marginal osteophytes. Physician prescribed corticosteroid, NSAID, and proton-pump inhibitor. At the control visit, pain was relieved in part, but he could walk with difficulty due to severe deformity. Thus, bilateral total knee arthroplasty was performed under neuraxial anesthesia (spinal-epidural). Before operation, anesthesiologist prescribed NSAID intravenously. He used NSAID, acetaminophen, and codeine for pain control postoperatively. At the third month postoperative control visit, there was swelling, edema, increased heat and redness, and limitation of motion on the left knee. Moreover, allodynia, hyperesthesia, and hyperalgesia were determined. The physician prescribed antidepressant and antiepileptic drugs with physical therapy program. At the last control visit, he was pain-free and without symptoms of chronic pain on the left knee.

NSAIDs reduce pain and inflammation in acute injuries and are helpful for rapid functional improvement, and the corticosteroids' analgesic effects are controversial except for in inflammatory arthritis [1]. There is a close link between pain and surgical stress response. As a result, in recent years, the effect of preoperative analgesia on surgical stress response, and correspondingly on postoperative complications and wound healing, has become a basic subject of investigation [2]. Combination of pharmacologic modalities in the treatment of acute pain targets many mechanisms that produce pain, reduces doses of each drug in combination, and thus reduces the frequency of side effects [3]. Acetaminophen has antipyretic and analgesic effects via central pathways. It is believed that acetaminophen raises the pain threshold via inhibition of central PG synthesis. Tramadol is a synthetic codeine analog. It is a centrally effectual analgesic [1]. It is possible to use antidepressants and antiepileptics for the treatment of chronic pain. Despite no apparent differences between both drugs providing effects, patients may have satisfactory response to only one of them individually [1].

Acute Pain

Pain is an unpleasant sensory and emotional experience associated with actual or potential tissue damage [2]. Physical and psychological factors together produce the pain experience. Thus, pain is subjective and multifaceted. Despite pain being a function that is useful for protection from tissue damage, there is no parallel advantage postoperatively and during the chronic pain period [2].

Acute pain indicates current tissue damage [4]. Also, it indicates the existence of a healthy nervous system. It is accompanied by autonomous hyperactivity (hypertension, tachycardia, sweating, and vasoconstriction) [2].

Any tissue damage (trauma or surgery) leads to systemic, endocrine, metabolic, and immunological alterations that are called the surgical stress response [5, 6].

Perception of External Stimulus Peripherally and Transportation to Cerebral Cortex (Fig. 37.1)

External stimuli are received via specialized neurologic structures called sensation receptors. Receptors are intensively located in the skin but are also located in the muscles, periosteum, capsule of internal organs, and vessel walls [7, 8].

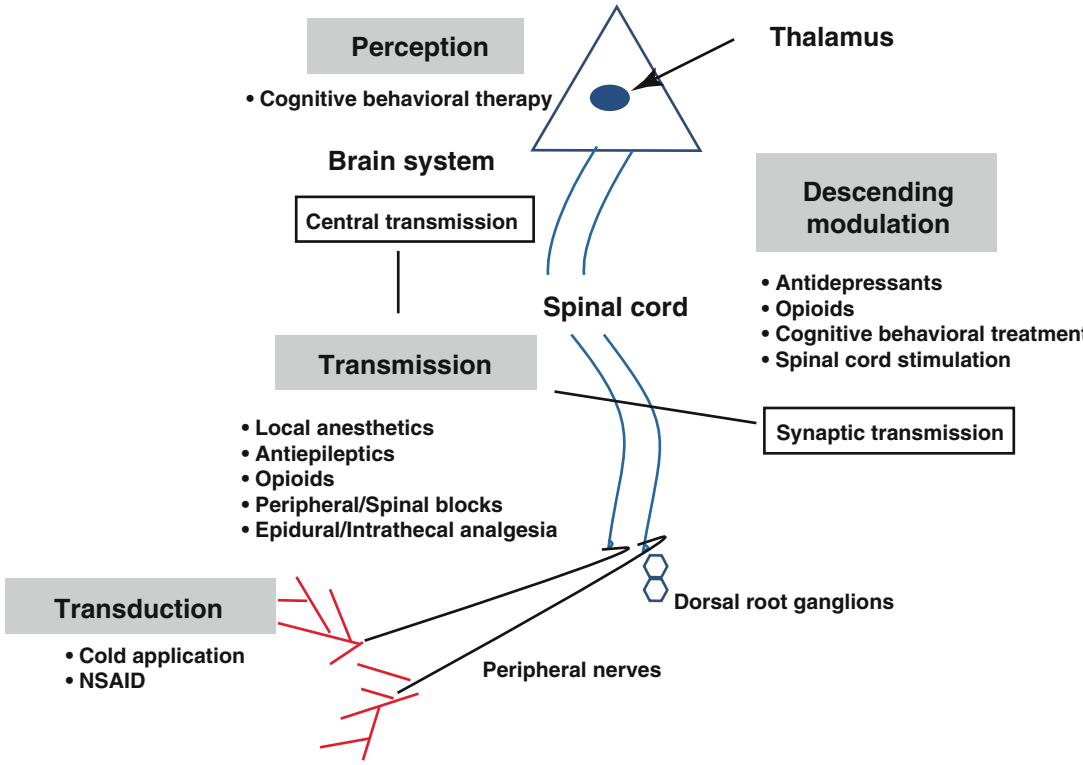

Fig. 37.1 Pain pathways from peripheral to cerebral cortex and treatment targets

Activation of the receptors induces release of algogenic substances like bradykinin, potassium, prostaglandins, hydrogen ions, serotonin, and substance P. These algogenic substances stimulate the sensation receptors aggressively and make them much more sensitive [9–11]. The receptors are sensitive to different forms of physical energy (mechanical, thermal, and chemical). Stimulated sensation receptors transform the external stimulus to "*electrochemical energy*," which is brought to the spinal cord dorsal horn via *A-delta fibers* (fast, surrounded by thin myelin film) and *C-afferent fibers* (slow, unmyelinated) (*transduction* [*membrane potential*], *transformation* [*action potential*]) [2, 12]. This message (action potential) activates the spinal cord dorsal horn neurons that reach the central part of the brain, thalamus, and frontal cortex and produces suprasegmental reflexes and cortical responses via afferent fibers (*transmission*) [2]. Tissue damage activates neurological pathways, and various mechanisms form which control the quantity of transported afferent activation when the stimuli are transported to central areas. Consequently, the stimuli transport is inhibited or facilitated at the spinal cord or supraspinal levels (*modulation*) [2]. There is simultaneous efficiency of afferent fibers and efferent inhibitor fibers for this purpose [2]. Spinal cord dorsal horn cells are the first level that processes the painful stimulus [2, 4]. The stimulus comes from the peripheral sensation nerve fibers terminating at this level. There are three types of neurons in the spinal cord dorsal horn: *projection neurons*, *excitatory neurons*, and *inhibitory neurons* [4]. *Projection neurons* transmit the stimulus to the upper centers via the anterolateral afferent system [13]. *Excitatory neurons* transmit the painful stimulus to the projection neurons and stimulate them [13]. Inhibitory neurons are activated with the signals that come via C-delta and A-delta fibers and transmit the painful stimulus to the projection neurons. When they are activated via large fibers, they inhibit the projection neurons [4]. On the other hand, pain is the patient's experience, not only a physical stimulus. When the stimulus reaches the cerebral cortex, the patient's previous experiences and perception of stimulus are the important factors for specifica-

tion of pain (*Perception*) [2]. Perception of pain is the last stage of neuronal painful stimulus transport. Painful stimulus reaching thalamus and brain system activate various cortical areas, and then responses appear. These are the *reticular system*, *somatosensory cortex*, and *limbic system* [7, 8]. *Reticular system* plays a major role in the formation of autonomic and motor responses (sudden movement of the back of hand after touching a hot object). Also, it has a role in affective motivational response too (looking at the hand and estimating the injury after moving back of the hand from the surface of a hot object) [7, 8]. *Somatosensory cortex* establishes pain severity, localization, and type, and associates it with previous experiences and memory [7, 8]. *Limbic system* produces emotional and behavioral responses in response to pain (attention, emotional state, and motivation) [7, 8].

Formation of Spinal and Supraspinal Reflexes

Stimuli reach the anterior and anterolateral horns of spinal cords, induce sympathetic preganglionic somatomotor neurons, and then produce autonomic spinal reflex response. Spinal and suprasegmental reflexes produce important physiological alterations that affect cardiopulmonary, gastrointestinal, urinary, endocrine, and immunological systems [2].

Perception of Pain Recalls Different Emotional Responses That Are Defined by Anxiety and Fear

Perception and interpretation of pain level increase catecholamine, cortisone, clotting time, fibrinolysis, and platelet aggregation in circulation [2].

Neuronal centers in the cerebral cortex and subcortical areas respond to painful stimuli coming from the periphery and activate inhibitory or exciting efferent pathways, thus modifying painful signals [7, 8]. Centrally located gray matter in the central part of the brain (periaqueductal gray matter, PAG) receives cortical and subcortical responses and starts afferent inhibitory nerve stimulation in the central nervous system (CNS). CNS sends responses to the periphery and can induce the release of neurotransmitters which reduce painful stimulus transport. Inhibitory stimuli reach the dorsal horn of spinal cord, that is, the first place for processing peripheral painful stimuli, and activate the inhibitory neurons therein; as a result, inhibitory transmitters, such as endogenous endorphins, noradrenalin, and serotonin are released [7, 8]. Conversely, supraspinal centers can produce responses that increase afferent painful stimuli transport.

Chronic Pain

Pain persisting for more than 3–6 months is called chronic pain [2]. Inappropriate and insufficient treatment of acute pain makes the CNS sensitive, and thus can produce chronic pain [9, 14]. There is no condition relating to tissue damage in chronic pain. Patients define pain and agony like acute pain. There is no autonomic hyperactivity. Normal activity pathways change, or there is spontaneous activity [2].

Chronic pain is a complicated problem that affects quality of life. Fast and long-term changes take place in different regions of CNS regarding transport and modulation of the painful stimuli [15]. Due to this abnormal mechanism in the peripheral and central nervous system, pain becomes independent of the original injury. The pathologic physiology is not absolutely clear.

There is coordination between input and output of painful stimulus at the spinal cord level (spinal modulation of painful stimulus). The ratio of rise in hyperalgesia and allodynia sometimes reduces and analgesia is formed [4]. If noxious stimuli reach the synapses located in the spinal cord dorsal horn with intense intervals in the long term, progressively increasing painful stimuli occur (windup). Patients feel severe pain even from painless stimulus like touch (Allodynia) [4, 15].

Neuropathic Pain

The primary initiatory cause of pain is nervous system dysfunction or primary lesion. There is no constant painful stimulus [4]. Trauma (complex regional pain syndrome, postsurgical chronic pain), infection (postherpetic neuralgia), ischemia (diabetic neuropathy), and cancer are some etiologic

factors. Some neuropathic pain occurs with peripheral nerve system damage. Repetitive transport of a painful stimulus by nerve fibers and hypersensitive nerve fibers is responsible for pain formation [15].

General Treatment Approach

It is possible to evaluate pain treatment in surgical practice with two modalities: preoperative analgesia and postoperative analgesia (Table 37.1). The purpose of pain treatment in orthopedic practice is reducing pain, simplifying rehabilitation, and returning to normal functions promptly.

Success in reaching these targets, potentially, can be achieved by reducing both pain and inflammation peripherally and centrally [1]. The main principle is utilizing treatment alternatives that affect the pain process at different levels, thus preventing the transformation of acute pain to its chronic form (Fig. 37.1) [1].

Pharmacologic Treatment

- Narcotics
- Nonsteroidal anti-inflammatory drugs
- Local anesthetics
- Centrally effective nonopioids
  - Acetaminophen
  - Codeine
- Others
  - Antidepressants
  - Antiepileptics
  - Membrane-stabilized drugs
  - Adrenergic drugs (alpha-adrenergic blocker)
- Combined analgesia
- Preventive analgesia

Narcotics

Opioids involve both endogenous and exogenous composites like morphine (Table 37.2) [3]. They are used for the treatment of average-severe pain, which has an acute character in orthopedic practice [1, 3]. Opioids produce their effects via opioid receptors in the CNS [16]. They are the most important drugs in the treatment of acute pain.

Table 37.1 Postsurgical pain treatment

Preoperative analgesia	Postoperative analgesia
Regional blocks	Patient controlled analgesia
Parenteral drug administration	Drugs (basic; opioids and NSAIDs)
Oral drug administration	Local/regional anesthetics
	Nonpharmacological applications

Table 37.2 Narcotics (opioids)

Natural opioids	Synthetic opioids
Morphine (oral or parenteral)	Hydromorphone (oral or parenteral)
	Levorphanol (oral)
	Meperidine (parenteral or oral)
	Methadone (oral)
	Oxicam (parenteral)
	Oxymorphone (oral or parenteral)
	Oxycodone (oral)

They have central and peripheral (spinal cord level) actions. Parenteral, oral, transdermal, mucosal, and epidural utilization is possible [1]. Effective dose level is uncertain among individuals; full effects and toxicity levels are associated with the dose level [1]. There are CNS (sedation, confusion) and visceral (ileus, urinary retention, constipation, vomiting, nausea, respiration depression) side effects [16, 17]. Combination with the other drugs is helpful to reduce side effects.

Nonsteroidal Anti-inflammatory Drugs (NSAID)

As they have different action mechanisms, it is possible to combine them with the other drugs. This combination reduces the necessary dose of narcotic drugs, thus reducing the side effects of opioids related to the dose level. They reduce pain and inflammation in acute injuries and are helpful in rapid functional improvement (Table 37.3) [1].

They block prostaglandin (PG) synthesis via inhibition of cyclooxygenase (Cox) enzyme, and hence reduce inflammation [1]. There are two types of isoenzymes: Cox-1 and Cox-2. Arachidonic acid mechanism produces prostanoids that affect gastric mucosa, renal and vas-

Table 37.3 Nonsteroidal anti-inflammatory drugs and the side effect sites

Salicylates	**Propionic acid derivatives**	**Pyrrole acetic acid derivatives**	**Oxicams**
Aspirin, choline magnesium, trisalicylate, salsalate, diflunisal[a,b,c,d]	Fenoprofen calcium, naproxen, ibuprofen, ketoprofen[a,b,c,d]	Indomethacin, sulindac, tolmetin[a,b,c,d]	Piroxicam[a,b,c,d]
Fenamates	**Percarboxylic acid**	**Cox-2 inhibitors**	**Parenteral**
Mefenamic acid, meclofenamate sodium[a,b,c,d]	Etodolac[a,b,c,d]	Vioxx, celebrex, Bextra[e]	Ketoralac[a,b,c,d]

[a]Stomatch
[b]Intestine
[c]Kidney
[d]Platelets
[e]Cardiac

cular endothelial cells. Cox-1 secretes from these fields and various tissues. Also, Cox-2 secretes only from the CNS, kidney, tracheal epithelium, and testicles [1]. Traditional NSAIDs inhibit both Cox-1 and Cox-2 isoenzymes synchronously; their painkiller and anti-inflammatory effects appear via inhibition of Cox-2 isoenzyme (Fig. 37.2) [18]. Side effects of traditional NSAIDs, such as gastrointestinal system (GIS) complications (ulcer), functional disruption of platelets, and elongation of bleeding time, are directly related with the inhibition of Cox-1 isoenzyme synthesis [3]. New generation drugs that have selective Cox-2 isoenzyme inhibitor effect do not disrupt platelet function and renal GIS PG synthesis. As a result, they have an anti-inflammatory effect without renal and GIS side effects [1]. However, there are some reports about raised adverse cardiovascular incidents with the utilization of some selective Cox-2 inhibitor NSAIDs [3].

Centrally Effective Nonopioid Drugs

Acetaminophen

Acetaminophen has antipyretic and analgesic effects via central pathways. It is believed that acetaminophen raises the pain threshold via inhibition of central PG synthesis [1]. The antipyretic effect of the drug is attributed to its impact on hypothalamic heat center [1]. Cox-3, which is a Cox-1 variant, inhibition effect of acetaminophen has been suggested by animal experimental studies [1]. There are some biochemical findings that humans have the Cox-3 isoenzyme and that the isoenzyme leads to central analgesic and antipyretic effects of the drug [3].

Codeine

Tramadol is a synthetic codeine analog. It is a centrally effectual analgesic with two action mechanisms: it has weak affinity to μ, omega, and opioid receptors and has weak inhibitory effect on norepinephrine and serotonin uptake [1].

Local Anesthetics

Using local anesthetics primarily to prevent surgical pain rather than acute injury or nonsurgical pain is usual (Table 37.4). Local anesthesia and regional blocks (neuraxial/peripheral nerve block) are used for anesthesia, or they fall under the multimodal approach to perioperative pain [3]. Sympathetic nerve blocks are effective in reducing pain related with sympathetic dystrophy. It is a treatment method; however, using it as for diagnostic purposes is possible [1].

Local anesthetics can block peripheral nerve functions with a few mechanisms. Their primary effect is on sodium channels, and they prevent axonal transmission. Also, they prevent neurotransmitter release via their effects on presynaptic calcium channels [3]. They are suitable for epidural infusions: 0.1 % diluted solutions with 5–12 ml infusion rate redouble analgesic effect, but also subside hypertensive effects [19]. Analgesic effects of neuraxial blocks depend on

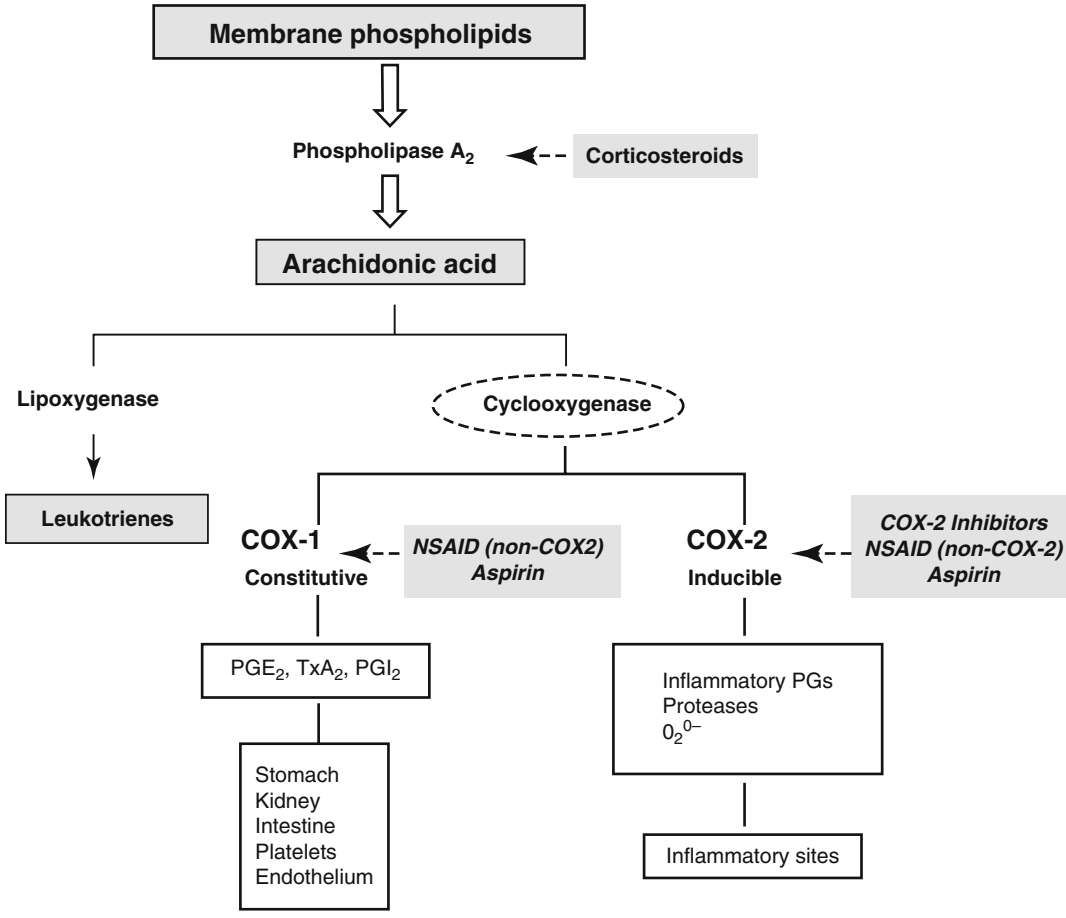

Fig. 37.2 Action mechanism of nonsteroidal anti-inflammatory drugs (*PG* Prostaglandin, *Tx* Thromboxane, O^{0-} Free oxygen radicals)

the partial inhibition of the pain response, and there is no effect on any humoral component like the effect of inflammatory cytokines [3]. If the block stops, analgesic effects disappear promptly [3]. As a result, these drugs should be combined with others at the time of pain control [3]. Keeping patients with neuraxial analgesia under monitoring is desirable, because there are side effects such as respiration depression, pruritus, and nausea [3].

Other Drugs

Orthopedic surgeons do not use these drugs frequently; they have useful effects on chronic pain seen in complex regional pain syndromes (Table 37.5).

It is possible to use them for treatment of chronic pain, for example, antidepressants. Despite no apparent differences between the effects provided by both the drugs, patients may have a satisfactory response to only one of them [1].

Antidepressants

They have useful effects on neuropathic pain produced in neuroma or reflex sympathetic dystrophy [1]. Depending on the circumstances, they may be combined with other painkillers. If desirable effects are not obtained or there is desirable pain subsidence with uncontrollable side effects with traditional painkillers and for the treatment of cancer pain, it is possible to use them with traditional

Table 37.4 Frequently used local anesthetics

Lidocaine	Bupivacaine	Rapivacaine

Table 37.5 Drugs used for chronic pain

Antidepressants	
Tricyclic antidepressants	*Selective serotonin reuptake inhibitors*
Amitriptyline, nortriptyline, desipramine	Sertraline, paroxetine, fluoxetine
Antiepileptics	
Carbamazepine, gabapentin, lamotrigine	
Membrane-Stabilizing Drugs (*calcium channel blockers*)	
Verapamil, diltiazem, Dilacor	
Adrenergic Drugs (*alpha-adrenergic blockers*)	
Phenoxybenzamine, phentolamine, clonidine, propranolol, guanethidine	

painkillers [1]. Simultaneously, they treat sleeping disturbances associated with pain, depression, and anxiety.

Antiepileptics

It is possible to use them for treatment of chronic pain, similar to antidepressants. Despite no apparent differences between the effects provided by both drugs, patients may have satisfactory response to only one of them [1].

Membrane-Stabilized Drugs

These are calcium channel blockers. They block the interaction between actin and myosin that are mandatory for smooth muscle contraction by preventing calcium from entering the endoplasmic reticuli. This effect is responsible for enhancing circulation. They have no effect on the venous system. They have an effective role in the treatment of pain in Raynaud's phenomenon or other sympathetic-mediated pain [1].

Adrenergic Drugs (Alpha-Adrenergic Blocker)

They are effective primarily on the treatment of sympathetic activity-mediated pain [1].

Corticosteroids

Their analgesic effects are controversial except for in inflammatory arthritis [1]. The main problem is with the side effects that appear with high doses. They are useful in the treatment of the early phase of reflex sympathetic dystrophy [1].

Combined Analgesia for Acute Pain Treatment

Combination of pharmacologic and nonpharmacologic modalities in the treatment of acute pain targets many mechanisms that produce pain, reduces doses of each drug in combination, and thus reduces the frequency of side effects [3]. Cox-2-specific inhibitor and opioid combination produces better pain control and reduces the opioid dose required for acute postoperative analgesia [1]. Preoperative use of NSAID (1 h before surgery) reduces the opioid dose which is required postoperatively; however, both the preoperative and postoperative uses of NSAID markedly reduce the opioid dose which is required postoperatively [1].

Preventive Analgesia

There is a close link between pain and surgical stress response. As a result, in recent years, the effect of preoperative analgesia on surgical stress response, and correspondingly on postoperative complications and wound healing, has become a basic subject of investigation [2]. Some anesthesia methods, such as epidural anesthesia, can alter surgical stress response by preventing transmission at specific levels on pain pathways, thus preventing awareness of the brain [1, 2]. Timing of the practice is very important. If surgery starts

when analgesics reach a high level in the peripheral and central nervous systems, the effects on postoperative pain distinctly enhance [3]. Efficiency of preemptive analgesia in patients with marked preoperative pain is insufficient [1].

Nonpharmacologic Treatment Methods

These are *behavioral interventions* and *physical agents*. They do not replace pharmacologic methods and other invasive procedures; however, using them as a part of a combination procedure possibly enhances the effect of pharmacological methods [3].

Cognitive behavioral treatments change the patient's pain perception and modes of behavioral response to pain, thus leading to enhancement of the patient's feelings about positive pain control [3].

Physical agents provide comfort, normalize physical dysfunction, change physiologic response, and reduce anxiety about immobilization or activity restriction. These are hot or cold applications, massages, exercise, and electroanalgesia [3].

References

1. Grana WA (2010) Methods of pain management. – OKO – AAOS Orthoportal – Orthopaedic Knowledge Online Journal – AAOS OrthoPortal. http://orthoportal.aaos.org/oko/article.aspx?article=OKO_PAI004#article. Accessed 25 Oct 2010
2. Grana WA (2006) Physiology of pain, pain mechanisms, and pathways- OKO – AAOS Orthoportal – Orthopaedic Knowledge Online Journal – AAOS OrthoP. http://orthoportal.aaos.org/oko/article.aspx?article=OKO_PAI003#article. Accessed 21 Mar 2006
3. Ekman EF, Koman LA (2004) Acute pain following musculoskeletal injuries and orthopedic surgery. Mechanisms and management. J Bone Joint Surg Am 86:1316–1327
4. Aydın ON (2002) Current inspect to pain and pain mechanism. ADÜ Tıp Fakültesi Dergisi 3:37–48
5. Kehlet H, Wilmore DW (2002) Multimodal strategies to improve surgical outcome. Am J Surg 183:630–641
6. Fine PG, Ashburn MA (1998) Functional neuroanatomy and nociception. In: Ashburn MA, Rice LJ (eds) The management of pain. Churchill Livingston, New York, pp 1–16
7. Calvino B, Grilo RM (2006) Central pain control. Joint Bone Spine 73:10–16
8. Farquhar-Smith P (2007) Anatomy, physiology and pharmacology of pain. Anesth Intensive Care Med 9:3–7
9. Carr DB, Goudas LC (1999) Acute pain. Lancet 353:2051–2058
10. Basbaum AI, Jessell TM (2000) The perception of pain. In: Kandel ER, Schwartz JH, Jessell TM (eds) Principles of neural science, 4th edn. McGraw-Hill, New York, pp 472–491
11. Scholz J, Woolf CJ (2002) Can we conquer pain? Nat Neurosci 5(Suppl):S1062–S1067
12. Bodine SC, Lieber RL (1994) Peripheral nerve physiology, anatomy and pathology. In: Simon SR (ed) Orthopedic basic science. American Academy of Orthopedic Surgeons, Rosemont, pp 335–396
13. Heavner JE, Willis WD (2000) Pain pathways: anatomy and physiology. In: Raj PP (ed) Practical management of pain, 3rd edn. Mosby, St Louis, pp 107–145
14. Woolf CJ, Salter MW (2000) Neuronal plasticity: increasing the gain in pain. Science 288:1765–1769
15. Ko SM, Zhou M (2004) Central plasticity and persistent pain; drug discovery today: disease models. Pain Anesth 1:101–106
16. Reisine T, Pasternak G (1996) Opioid analgesics and antagonists. In: Hardman JG, Limbird LE, Molinoff PB, Ruddon RW, Gilman AG (eds) Goodman & Gilman's the pharmacological basis of therapeutics, 9th edn. McGraw-Hill, New York, pp 521–555
17. Inturrisi CE (2002) Clinical pharmacology of opioids for pain. Clin J Pain 18(4 suppl):S3–S13
18. Vane JR (1971) Inhibition of prostaglandin synthesis as a mechanism of action for aspirin-like drugs. Nat New Biol 231:232–235
19. Sinatra RS, Torres J, Bustos AM (2002) Pain management after major orthopedic surgery: current strategies and new concepts. J Am Acad Orthop Surg 10:117–129

Antibiotics

38

Özal Özcan

Abstract

The use of antibiotics in orthopaedic surgery has become popular since the discovery of penicillin during the second world war. All penicillins are bactericidal, β-lactam class antibiotics and used in the treatment of infections caused by mostly gram-positive and other susceptible bacteria. Especially, methicillin, cephalosporins, vancomycin, teicoplanin, rifampicin, quinolones, aminoglicozides widely used in orthopaedic infection treatment or proflaxy of ortopaedic surgery.

In proflaxy of orthopaedic surgery, first-generation cephalosporins have been used since they are effective against S. Aureus and S. Epidermidis, and are cheaper and non-toxic. The aim of the ostemyelitis treatment whether it is curative or supressive, will define the selection of antibiotics, proper dosage, and duration of treatment.

In the treatment of bone infections should be coise of antibiotics against target pathogens. Usually, vancomycin and teicoplanin are glycopeptid antibiotics that are widely employed in methicillin-resistant infections. Recently, the use of linezolid, daptomycin or tigecycline is popular in the treatment of methicilline-resistant infections. Rifampin and fluoroquinolones combination are frequently used in the treatment of chronic osteomyelitis. Another problem, unfortunately, enterococcus faecalis quickly develop resistance to vancomycin. Linezolid, tigecycline and daptomycine can be used in this cases.

Clinical Relevance

A 28-year-old female patient was admitted to our emergency department with concurrent femoral neck and femoral shaft fracture after a fall-from-height accident. She had closed fractures and no neurovascular

Ö. Özcan, MD, Assoc. Prof.
Department of Orthopaedic and Traumatology Surgery, Afyon Kocatepe Universty, Afyonkarahisar, Turkey
e-mail: ozalozcan@yahoo.com

F. Korkusuz (ed.), *Musculoskeletal Research and Basic Science*,
DOI 10.1007/978-3-319-20777-3_38

injury. For surgical prophylaxis, 1 g IV cefazolin was administered to the patient ½ h prior to the start of surgery and the same dose of IV cefazolin was re-administered every 8 h for the first 24 h postoperatively [1].

Her fractures were reduced and fixed with a proximal femoral nail and a long LISS plate. After postoperative care and routine controls, she was discharged from the hospital without any problems. She was called for routine clinical visits.

At her third-month follow-up visit, she had pain around her fracture site and purulent discharge from the old incision scar. Laboratory results showed elevated levels of erythrocyte sedimentation rate (ESR) and C-reactive protein (CRP). Radiological assessment suggested she also had implant failure. After detailed physical examination, laboratory tests, and X-ray studies she was diagnosed with exogenous osteomyelitis due to implants (see Fig. 38.1a. b) [2].

After removal of all implants and proper debridement, a unilateral external fixator was applied to the femur (see Fig. 38.2). Antibiogram showed methicillin-resistant *Staphylococcus aureus* (MRSA) infection. Patient had teicoplanin plus ciprofloxacin treatment for 6 weeks [3]. Serum levels of ESR and CRP were normalized after regular treatment with antibiotics. After 4 weeks without antibiotic treatment, patient showed no signs of infection. All laboratory findings were normal [4]. Her fracture was fixed with a long plate and the defect in the fracture site was filled with an autolog (tricortical iliac crest) bone graft (see Fig. 38.3). Two months after the procedure, consolidation of the fracture was achieved without any signs of infection. Patient did not have any other complications other than a slightly limited range of motion (ROM) in her knee (0–90), and she was satisfied with the results of definitive treatment.

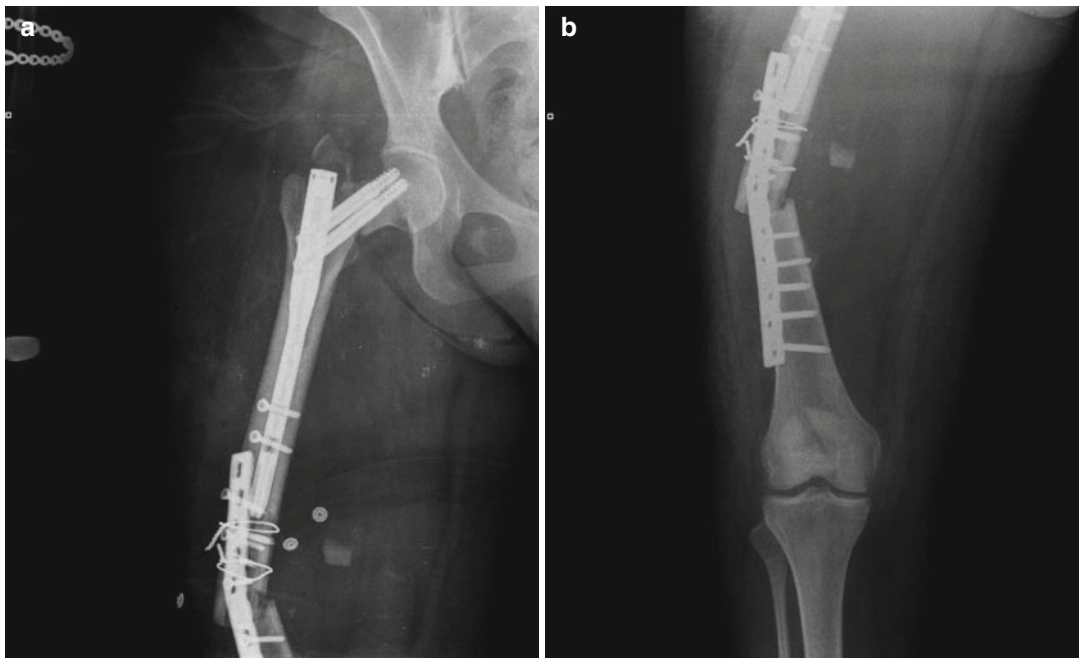

Fig. 38.1 Implant failure due to exogenous osteomyelitis after femur fracture treatment with plate

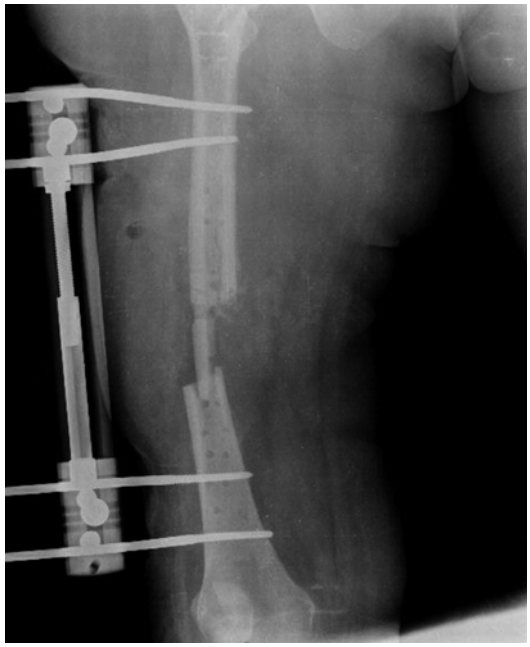

Fig. 38.2 After removal of all implants and proper debridement

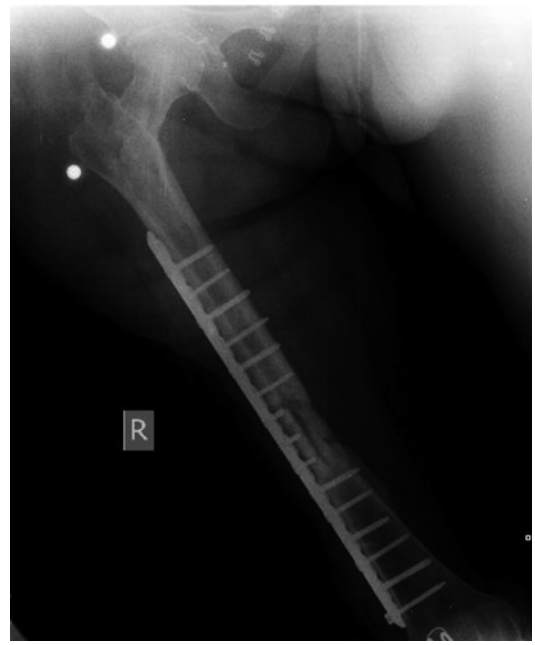

Fig. 38.3 Bone gap was filled an autolog bone graft and fixed with a long plate again

The use of antibiotics in orthopedic surgery has become popular since the discovery of penicillin during the Second World War. Penicillin is a group of antibiotics derived from *Penicillium* fungi. All penicillins are bactericidal, β-lactam class antibiotics and used in the treatment of infections caused by mostly Gram-positive and other susceptible bacteria. They inhibit the formation of peptidoglycan cross-links in the bacterial cell wall. Peptidoglycan, also known as murein, is a polymer that forms a mesh-like layer outside the plasma membrane of all bacteria except the mycoplasma class. The β-lactam ring of penicillin binds and inhibits the trans-peptidase enzyme. Then, the formation of cross-links in the bacterial cell wall is disrupted and an imbalance between cell wall production and degradation develops, causing the bacteria to die. β-lactam antibiotics are structural analogs of D-alanyl-alanine, and the transpeptidase enzyme that binds to them is also called penicillin-binding protein (PBP). In essence, penicillins can show their bactericidal effect on immature and colonizing bacteria that have murein in their cell wall. Penicillin was used frequently from the beginning of the 1940s to the 1970s. However, use of advanced penicillin became popular after increased resistance developed among bacterial pathogens to first-generation penicillin.

Meticillin (or methicillin) is a narrow-spectrum β-lactam antibiotic from the penicillin class. Similar to other β-lactam antibiotics, meticillin disrupts the synthesis of bacterial cell walls by inhibiting cross-linkage between peptidoglycan chains. Meticillin is a penicillinase-resistant antibiotic. Resistant bacteria produce an enzyme called penicillinase, which hydrolyses the β-lactam antibiotic and renders it non-functional. However, this enzyme does not bind to meticillin, meaning it can still function to kill the bacteria. Previously, meticillin was used to treat infections caused by Gram-positive bacteria including *Staphylococcus aureus* (*S. aureus*), *Staphylococcus epidermidis* (*S. epidermidis*), *Streptococcus pyogenes* (*S. pyogenes*), and *Streptococcus pneumoniae* (*S. pneumonia*). But today, due to resistance meticillin is not as

effective against these microorganisms. A newer PBP gene called mec2 confers resistance to meticillin. This gene produces PBP2a, which works in a similar way to other PBPs though it binds β-lactam with a very low affinity. Expression of PBP2a supplies resistance to all β-lactam antibiotics. Recently, meticillin has been used less frequently than before because it is less active compared to other β-lactamase-resistant penicillin, and can be administered only via a parenteral route and has a higher frequency of interstitial nephritis. It has been largely replaced in its role in therapy by other penicillins such as dicloxacillin and flucloxacillin, but the term meticillin-resistant *S. aureus* (MRSA) continues to be used to describe *S. aureus* strains resistant to all penicillin.

The cephalosporins are a class of β-lactam antibiotics and they derive from the fungus *Acremonium*, known as *Cephalosporium*. The first-generation cephalosporins were not used for prophylaxis in orthopedic surgery until 1964. First-generation cephalosporins are active principally against Gram-positive bacteria, though their successors have increased activity against Gram-negative bacteria. Cephalosporins are bactericidal, meaning that they kill the targeted bacteria as opposed to inhibiting reproduction as bacteriostatic antibiotics do. They have the same path of action as other β-lactam antibiotics such as the penicillin class. They disrupt the synthesis process of the peptidoglycan layer, which is essential for bacterial cell wall structural integrity. They are resistant to β-lactamase of *S. aureus*, and this makes them preferable for prophylaxis and treatment. First-generation cephalosporins are narrow-spectrum antibiotics and they are active against Gram-positive (*S. aureus*, *S. pyogenes*, and *S. pneumonia*) and some strains of Gram-negative coccus bacteria. They are also active against a small number of Gram-negative aerobic bacilli such as *E. coli*, *Klebsiella*, *P. mirabilis*, *N. gonore*, and *N. meningitidis*. Cefazolin has the longest half-life among first-generation cephalosporins. It can be administered via intravenous (IV) or intramuscular (IM) routes and is tolerated well by the patient. Since it has a long serum half-life, it is recommended for surgery prophylaxis and doses should be given every 8 h. It is relatively well tolerated by the patient as it causes less pain around the injection site.

Vancomycin is from the glycopeptide antibiotic class and is effective mostly against Gram-positive bacteria. Vancomycin shows its bactericidal effect by inhibiting proper cell wall synthesis in Gram-positive bacteria. Vancomycin forms hydrogen bond interactions with the terminal D-alanyl-D-alanine parts of the N-acetylmuramic acid (NAM) and N-acetylglucosamine (NAG) peptides. This is a five-point interaction. This binding disrupts cell wall synthesis in two ways. It prevents the synthesis of the long polymers of NAM and NAG that are essential for bacterial cell wall structure, and it prevents the formation of cross-links between these polymers. Since Gram-negative bacteria produce their cell walls by different mechanisms and there are various factors related to entering the outer membrane, vancomycin is not active against Gram-negative bacteria (except non-Gonococcal species of *Neisseria*). The activity of vancomycin is considered to be time dependent, which means antimicrobial activity depends on the duration that the serum drug concentration exceeds the minimum inhibitory concentration of the target organism. Vancomycin is a large hydrophilic molecule and must be administered via intravenous route for systemic therapy, since it is not absorbed from the intestine. Due to its short half-life (4–11 h in adults), it is often injected twice daily. Common adverse drug reactions (≥1 % of patients) associated with IV vancomycin include local pain, which may be severe, and thrombophlebitis. IV vancomycin therapy using peripheral lines inherently causes risk of thrombophlebitis. In addition, vancomycin has a potential for nephrotoxicity and ototoxicity, especially in patients with poor renal function and/or immune deficiency to bacterial infections. Hence, therapeutic drug monitoring (measurement of medication concentrations in blood) is warranted in patients with concomitant aminoglycoside therapy, patients on hemodialysis, patients with (potentially) altered pharmacokinetic parameters, patients administered high-dose or prolonged treatment, and patients with impaired renal function. Vancomycin has traditionally been considered a nephrotoxic drug. However, subsequent reviews on vancomycin-related nephrotoxicity suggest that many of the patients had also received other known nephrotoxins, especially aminogly-

cosides, and most of the rest had other confounding factors. In essence, the reputation of vancomycin as a nephrotoxin may be overstated.

Teicoplanin is a semisynthetic glycopeptide antibiotic with a spectrum of activity similar to vancomycin. Recently, it has been used for prophylaxis and treatment of serious infections caused by Gram-positive bacteria including methicillin-resistant *S. aureus* and *Enterococcus faecalis*. It is administered via IM route and has a much longer half-life (70–100 h) than vancomycin.

The quinolones are a family of synthetic broad-spectrum antibiotics. They prevent bacterial DNA from unwinding and duplicating. The majority of quinolones in clinical use belong to the subset fluoroquinolones, which have a fluorine atom attached to the central ring system (Ciprofloxacin, Levofloxacin, and Trovafloxacin). Fluoroquinolones are broad-spectrum antibiotics (effective for both gram-negative and gram-positive bacteria) used against serious bacterial infections, especially hospital-acquired infections and those resistant to other antibiotic classes. First- and second-generation fluoroquinolones selectively inhibit the topoisomerase II ligase domain, whereas third- and fourth-generation fluoroquinolones are more selective for topoisomerase IV ligase domain. Thus, they have enhanced gram-positive coverage. In general, fluoroquinolones are well tolerated, with most side effects being mild to moderate. Common side effects include gastrointestinal effects such as nausea, vomiting, and diarrhea, as well as headache and insomnia. Quinolones are contraindicated for patients with Q-T prolongation, pre-existing CNS (central nervous system) lesions or inflammation, epilepsy, or if the patient has suffered a stroke. Quinolones are also associated with an increased risk of tendinitis and tendon rupture in all age groups. The most severe form of tendinous disorder associated with fluoroquinolones is tendon rupture, which is common in the Achilles tendon. Resistance to quinolones can emerge rapidly, even during a course of treatment. Today, pathogens such as *S. aureus*, *S. enterococci*, and *S. pyogenes* exhibit resistance worldwide.

Aminoglycoside antibiotics are traditional Gram-negative antibacterial therapeutic drugs and contain a portion of the molecule as an amino-modified glycoside. Aminoglycosides exhibit bactericidal activity against gram-negative aerobes and some anaerobic bacilli. Kanamycin A, Tobramycin, Amikacin, Gentamicin, Streptomycin, Netilmicin, and Streptomycin are from this class of antibiotics. Aminoglycosides show concentration-dependent bactericidal activity. Aminoglycoside presence in the cytosol generally disrupts peptide elongation at the 30S ribosomal subunit, resulting in a rise of inaccurate mRNA translation and biosynthesis of proteins. Afterward, aminoglycosides can affect cell membranes and functional integrity of the bacterial cell membrane can be lost.

Clindamycin is recommended for prophylaxis in patients with penicillin allergy. It is from the lincosamide class and has primarily bacteriostatic effect. It inhibits ribosomal translocation and disrupts protein synthesis of the bacteria. It is most effective against infections involving aerobic Gram-positive cocci, including some members of *Staphylococcus* and *Streptococcus* (e.g., pneumococcus) and anaerobic, Gram-negative rod-shaped bacteria, including some *Bacteroides*, *Fusobacterium*, and *Prevotella* (resistance is increasing in *Bacteroides fragilis*). It is primarily used to treat infections caused by susceptible anaerobic bacteria. In addition, it is used to treat bone and joint infections especially those caused by *S. aureus*. Common adverse drug reactions (found in over 1 % of people) associated with systemic clindamycin therapy include diarrhea, vomiting, pseudomembranous colitis, abdominal pain, or cramps and/or rash and nausea.

Rifampicin or rifampin is a bactericidal antibiotic from the rifamycin class. It inhibits bacterial DNA-dependent RNA synthesis by inhibiting bacterial DNA-dependent RNA polymerase. Rifampicin is a more stable, highly efficient, and easy-to-tolerate semisynthetic derivative of the first original molecule, rifamycin. Rifampicin is typically used to treat *Mycobacterium* infections, including tuberculosis and leprosy. Rifampicin in combination with fusidic acid can be used in the treatment of methicillin-resistant *S. aureus* (MRSA) including infections such as osteomyelitis and prosthetic joint infections that are difficult to treat.

Fusidic acid is derived from the fungus *Fusidium coccineum*. Fusidic acid is a bacteriostatic antibiotic and is often used topically but

may also be administered systemically as tablets or injections. Recently, the global emergence of antimicrobial resistance has led to a renewed interest in its use. Fusidic is bacteriostatic, in other words it inhibits bacterial replication and does not kill the bacteria. It inhibits bacterial protein synthesis by preventing the turnover of elongation factor G (EF-G) from the ribosome. It is active mainly against Gram-positive bacteria such as *Staphylococcus* species, *Corynebacterium* species, and *Streptococcus* species.

Prophylaxis

Infection is a major complication in orthopedic surgery since treatment is both difficult and expensive, and it may lead to serious sequelae. Prophylaxis of any bone infection is much more effective and easier than trying to treat it. Many studies suggest that antibiotic prophylaxis has been effective to reduce infection rates in orthopedic surgery. Infection in orthopedic surgery is strongly associated with the number of colonized bacteria in the first 24 h. The patient's immune system reduces the number of colonized bacteria principally in the first 2 h. As the quantity of bacteria continues to increase in the next 4 h, the immune system will be inadequate to gain control. Therefore, the first 6 h is referred to as the "golden period" in prophylaxis. Antibiotics reduce the number of bacteria geometrically while preventing their re-colonization. In this context, prophylactic utilization of antibiotics prolongs the golden period [5, 6]. The antibiotic used for prophylaxis in orthopedic surgery should be effective against common bacteria, safe to use, and bactericidal. Prophylaxis must be effective against *S. epidermidis* and *S. aureus* that are mostly present in skin flora. Today, treatment of *S. epidermidis* infections has become more challenging due to their increased resistance to antibiotics. First-generation cephalosporins have been widely used since they are effective against these bacteria, and are cheaper and non-toxic. Vancomycin is not recommended for the first line of prophylaxis; however, it can be used as an alternative in patients with allergic conditions (Fig. 38.4) [1, 7, 8].

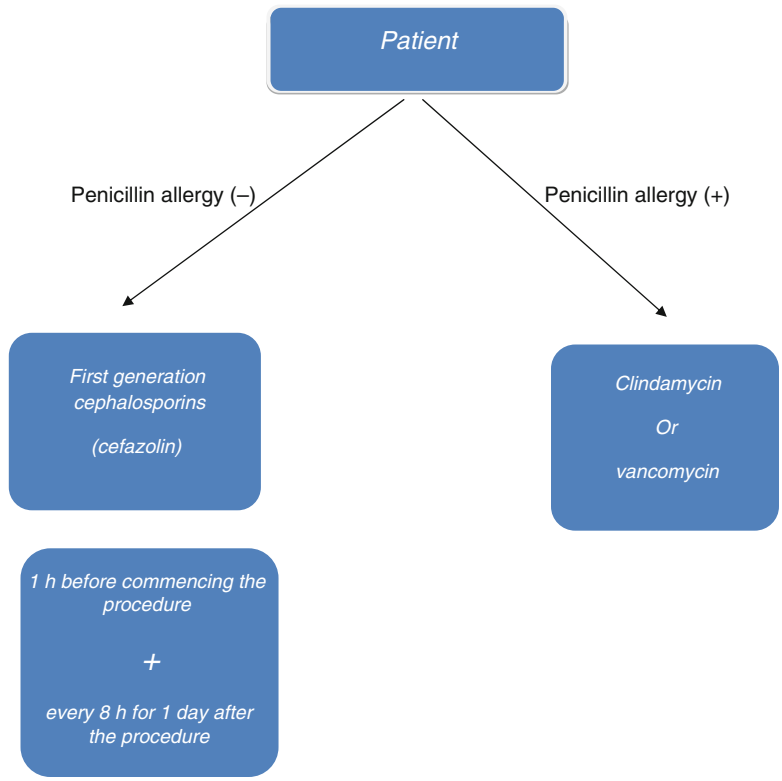

Fig. 38.4 Algorithm for the management of antibiotic prophylaxis in orthopedic surgery

Optimal timing for administration of antibiotics for prophylaxis is 30 min before incision. However, prophylactic antibiotics may be administered within the limit of up to 2 h prior to incision. Maximum dose should be administered and must be re-administered every 4 h of surgery-time or for each 1,000–1,500 cc of hemorrhage. Optimal period for prophylactic utilization of antibiotics is 24 h postoperatively and prolongation is not recommended due to the possible serious side effects of antibiotics [5, 8, 9].

Utilization of antibiotics in open fractures diverges from other "clean" procedures in orthopedic surgery. Since the skin barrier will be impaired after open fracture, bacteria will be in direct contact with bone tissue and be able to colonize much more easily. In 2004, a Cochrane systematic review reported that administration of antibiotics (first-generation cephalosporin) concurrent with proper wound debridement and effective aftercare has been highly effective in open fractures [10]. Antibiotic usage protocol in adults with open fractures is based on the Gustilo classification. First-generation cephalosporins are administered in type I and II open fractures with an initial dosage of 2 g and additional 1 g every 6–8 h for the following 48–72 h. In type III open fractures aminoglycosides with a dose of 3–5 mg/kg/day are administered for 48–72 h in addition to first-generation cephalosporins. If an organic contamination is suspected, an additional administration of 10–12 million units/day of crystallized penicillin is highly recommended [11]. In patients with fecal contamination who also have an allergic condition to penicillin, 500 mg of metronidazole administered every 6 h is recommended. Antibiotics used in open fractures of children are the same, but their dosages vary. In type I and II open fractures, first-generation cephalosporins of 100 mg/kg/day every 8 h are used without exceeding a daily total of 6 g. Aminoglycosides are used in the treatment of type III open fractures with a dosage of 7.5 mg/kg/day, in addition to the treatment protocol explained for type I and II open fractures. If organic contamination is suspected in children, crystallized penicillin (150,000 unit/kg/day) is used every 6 h, without exceeding a total dose of 24 million units. During the use of aminoglycosides, the patient should be checked regularly for ototoxicity [12].

Osteomyelitis

Osteomyelitis can be defined as any form of inflammation involving bone and/or bone marrow. Osteomyelitis is one of the most challenging conditions encountered by orthopedic surgeons. In the early twentieth century, 20 % of patients with osteomyelitis lost their lives, while others had major sequelae. Today, mortality and morbidity rates due to osteomyelitis are much lower due to the help of new antibiotics and aggressive surgical therapy.

Classification of osteomyelitis is according to the mechanism of infection or the patient's response to treatment. Osteomyelitis is classified as acute, subacute, or chronic. However, there are no distinct borders in this classification, which describes the duration of the symptoms. The mechanism of the infection can be either exogenous or hematogenous. Orthopedic surgeons mostly deal with infections of exogenous osteomyelitis, which can be caused by open fractures, surgical intervention (after utilization of implants), or by local infections that can subsequently involve bone. Most cases of hematogenous osteomyelitis are caused by bacterial pathogens. In addition, osteomyelitis is classified as pyogenic or non-pyogenic depending on the patient's response.

Acute osteomyelitis is defined as an infection diagnosed within 2 weeks of the onset of symptoms. Acute hematogenous osteomyelitis typically involves the metaphysis of long tubular bones, with approximately two-thirds of all cases involving the femur, tibia, or humerus, especially in children. The principal cause of osteomyelitis in children is *S. aureus* (70–90 %) and unfortunately, globally emerging meticillin-resistance among *S. aureus* has changed both the epidemiology and treatment options. Other etiological microorganisms include *S. pneumonia*, *S. pyogenes*, coagulase-negative *Staphylococci* (especially in implant-associated infections), Group B *Streptococci* (in infants), *Kingella kingae*, enteric Gram-negative bacilli (especially *Salmonella* spp. in patients with sickle cell disease), and anaerobic bacteria. If the etiologic agent of osteomyelitis is identified, specific antimicrobial treatment based on the susceptibility profile of the organism should be given. The treatment of acute hematogenous osteomyelitis requires

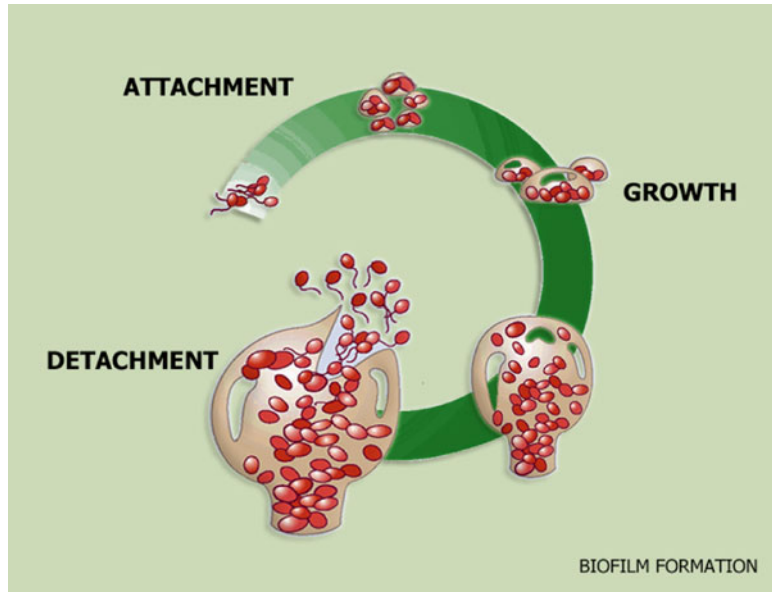

Fig. 38.5 Biofilm formation

appropriate antimicrobial therapy in all cases and may require surgical incision and drainage. Whenever an abscess (intra-osseous, subperiosteal, and/or soft-tissue) exists, incision and drainage should be performed. If MRSA is not a concern, empiric therapy for children (older than 3 months) should be an anti-*Staphylococcal* penicillin (nafcillin and oxacillin) or first-generation cephalosporin (cefazolin). If MRSA is suspected, vancomycin or clindamycin can be used for treatment.

Trauma, orthopedic surgery, prosthetic surgery, and also direct contamination or hematogenous dissemination mechanisms are all implicated in osteomyelitis. These factors in the etiology define the portal of entry of infection into the bone tissue. Infections caused by implants that are used in surgery (plates, joint prosthesis, etc.) should be emphasized particularly as subacute or chronic infections and they are much challenging to treat. In addition, a physician must consider conditions that complicate treatment such as HIV infection, sickle cell anemia, and diabetes, and a thorough investigation should be undertaken for proper selection of antibiotics to be used in treatment. It is common sense that if the implant causes infection, it has to be removed prior to treatment of infection. In particular, *S. aureus* and *S. epidermidis* both form a "biofilm" on the surface of the implant (Fig. 38.5), which can deactivate antibiotics. As long as the implant is present, bacteria will continue to colonize under this barrier. In this context, the purpose of treatment, in fact, directs the selection of the proper antibiotic. The aim of the treatment, whether it is curative or suppressive, will define the selection of antibiotic, proper dosage, and duration of treatment. Poor medical condition of the patient that complicates or limits treatment options, or the presence of drug-resistant bacteria or parasites can lead to failure of therapy. The most important parameter in the treatment of bone infections is the proper choice of antibiotics against target pathogens. Pathogen susceptibility to antibiotics is referred to as "minimal inhibitory concentration" (MIC). However, this definition does not help us to predict the clinical outcomes, since serum or bone-soft tissue concentration of an administered antibiotic differs in clinical terms. Cefazolin concentrations measured in healthy bone tissue samples ranged from 1/10 to 1/5 of the serum concentration. This study reports even lower levels in tissues with poor vascularity [13]. The same parameter (bone tissue concentration/serum concentration) was measured for different antibiotics. Average rates of bone tissue concentration compared to serum concentration were 14.5 % for vancomycin and 12.5 % for both ciprofloxacin and a new generation fluoroquinolone.

Numerous studies have suggested that oral treatment and parenteral treatment are both

Table 38.1 Antibiotics commonly used in the treatment of osteomyelitis

Drug	Class	IV dosage	Oral dosage
Penicillin G	Penicillin	3–4 million units/4–6 h	Substitute for amoxicillin 1 g 1/12 h
Nafcillin	Penicillin	1–2 g/4–6 h	Substitute for diclocacillin 500 mg/12 h
Ampicillin	Penicillin	2 g/4–6 h	500 mg/6 h
Ampicillin/sulbactam	Inhibitor of beta-lactamase	1.5–3 g/6 h	750 mg/12 h
Cefazolin	First-generation cephalosporin	32 g/8 h	Substitute for cephalexin 1 g/12 h

efficient. Fluoroquinolones are suggested as the strongest evidence for efficacy of oral treatment. Some major drawbacks of parenteral therapy are prolonged length of stay in hospital and a much higher cost for treatment. Parenteral treatment protocol involving home therapy with a central venous catheter for these patients may lead to serious complications such as infection or thrombosis [2, 3, 14]. Antibiotics can be used parenterally, orally, solely, or in combination depending on the pathogen's susceptibility, patient's compliance, recommendations of an infectious disease, and the specialist or surgeon's own experience. The most commonly used antibiotics in the treatment of osteomyelitis are listed in Table 38.1 with their dosages.

Meta-analyses report successful results for osteomyelitis treatment with antibiotic therapy for 6–8 weeks commencing after radical debridement and implant removal. Curative treatment involves IV antibiotic therapy for 4–6 weeks and regular measurement of CRP and ESR serum levels for possible recurrent infection [2, 4]. An animal study suggests that an antibiotic therapy period of 4–6 weeks should be enough for osteomyelitis and, moreover, it must be considered that bone revascularization generally occurs almost 4 weeks after debridement [15].

Since the 1970s, to benefit from their local effects antibiotics are added to bone cement. In this method, the bone cement chain with antibiotic treating osteomyelitis, or prosthetic infection treatment using antibiotics in the form of spacer utilizes the local effect of antibiotics. These antibiotics are required to be both heat resistant and hydrophilic. Generally, tobramycin (2.4–3.6 g for 40 g bone cement) or vancomycin (1–4 g for 40 g bone cement) is mixed with bone cement. Furthermore, antibiotics such as gentamycin, meropenem, and cefazolin may be mixed with bone cement solely or in combination. It is possible to benefit from the local efficacy of antibiotics by utilizing synthetic grafts (absorbable reservoir) such as hydroxyapatite blocks, cancellous bone grafts, calcium sulfate, and calcium phosphate. These absorbable reservoirs have gained some popularity since they help to treat osteomyelitis with the lowest rate of re-operation. It has been reported that local concentration of antibiotics sufficient to kill the bacteria under the biofilm barrier must be 10–100 times more than the standard bactericidal concentration [16]. These levels of antibiotic concentrations in bone and soft tissue can only be reached by local antibiotic therapy. It has been suggested that in bone and surrounding soft tissues, it is possible to reach an antibiotic concentration 100 times more than serum levels by utilizing absorbable grafts or bone cement [17].

Recommended Antibiotic Treatment for Specific Pathogens

S. aureus and Methicillin-Resistant *S. aureus* (MRSA)

S. aureus and methicillin-resistant *S. aureus* are quite dominant pathogens that can be seen in all stages and types of osteomyelitis. Recently, hospital-acquired methicillin-resistant *S. aureus* infections have become a common cause of bone and joint infections. Penicillin can be effective for a 5 % portion of *S. aureus* infections. Oxacillin, nafcillin, and floxacillin are widely used in *S. aureus* infections that are penicillin resistant but methicillin sensitive. First-generation

Table 38.2 Antibiotics with both parenteral and oral administration

Drug	Class	IV dosage	Oral dosage
Ciprofloxacin	Fluoroquinolone	400 mg 12 h	750 mg 12 h
Levofloxacin	Fluoroquinolone	500–750 mg 12 h	500–750 mg 12 h
Moxifloxacin	Fluoroquinolone	400 mg 24 h	400 mg 24 h
Clindamycin	Lincomycin	600–900 mg 8 h	300–450 mg 6 h
Linezolid	Oxazolidinne	600 mg 12 h	600 mg 12 h
Metronidazole	Nitroimidazole	500 mg 8 h	500 mg 8 h
Rifampin	Rifamycin	300 mg 12 h	300 mg 12 h

cephalosporins, mainly cefazolin, are used since they have similar effects to the aforementioned group of penicillin. Unnecessary utilization of glycopeptide antibiotics in methicillin-sensitive infections has triggered a rapidly increasing number of methicillin-resistant infections. Clindamycin is used successfully in the treatment of methicillin-sensitive cases in both children and adults who have allergies to penicillin. The recommended treatment is an initial IV therapy for 2 weeks with a dosage of 600 mg every 6–8 h and then oral therapy with a dosage of 300–450 mg four times a day [18].

Vancomycin and teicoplanin are glycopeptide antibiotics that are widely employed in methicillin-resistant infections. Slow bactericidal activity, variable MIC values, toxic effects of long-term therapy, potential resistance by pathogens, and some proportion of unsuccessful outcomes restrict the utilization of vancomycin in methicillin-resistant *S. aureus* infections. In addition to all these adverse factors, vancomycin can only be given by parenteral administration. Hence, indications for vancomycin therapy are limited to cases with vancomycin-susceptible methicillin-resistant *S. aureus* infections only in the short-term and under strict control for adverse effects [19, 20]. Teicoplanin is much preferred for its advantages over vancomycin such as easier administration via intramuscular (IM) route, less toxicity, and higher chance of home therapy. Teicoplanin therapy has a recommended dosage of 400–600 mg/day. However, some cases are reported to develop resistance to teicoplanin treatment as with vancomycin [21].

Fluoroquinolones can be used in both methicillin-susceptible and resistant *S. aureus* infections. Fluoroquinolones have adequate bone and oral absorption. Antibiotics with the same efficacy by oral and IV administration are shown in Table 38.2. Fluoroquinolones have been suggested to inhibit fracture healing in some animal studies but there is a lack of evidence in humans. However, it is known to cause both joint and tendon problems in humans. The third- and fourth-generation fluoroquinolones (levofloxacin and gemifloxacin) are more effective than second-generation fluoroquinolones. It is recommended to combine these with rifampin in order to avoid any development of counter-resistance by pathogens [22].

Recently, the use of linezolid, daptomycin, or tigecycline is popular in the treatment of methicillin-resistant infections. Linezolid, a member of the oxazolidinone family of antibiotics, has a bacteriostatic effect and inhibits protein synthesis. In addition, it can be safely used against methicillin-resistant infections. The oral linezolid absorption rate is almost 100 % and it penetrates to the bone pretty well. However, the patient must be kept under strict observation since therapy longer than 2 weeks has risks such as anemia and thrombocytopenia. Long-term use of linezolid can cause optic neuritis and peripheral neuropathy, so it is not recommended for the chronic suppression of infections [23]. Daptomycin is a new class of cyclic lipopeptide antibiotic with a broad efficacy against gram-positive infections and bactericidal effect. It is effective against methicillin-resistant infections in skin and soft tissue but there is a lack of evidence for bone infections. It is known to have a good penetration to bone [24]. Tigecycline, a new member from the family of glycycline antibiotics, is proven effective in the treatment of osteomyelitis caused by methicillin-resistant *S. aureus* (MRSA) via parenteral administration in animals. However, there is very little experience in humans. Antibiotics that have only parenteral administration are listed in Table 38.3.

Table 38.3 Antibiotics with only parenteral administration

Drug	Class	IV dosage	Oral dosage
Ceftriaxone	Third-generation cephalosporin	1–2 g 24 h	–
Cefepime	Fourth-generation cephalosporin	1–2 g 8–12 h	–
Ceftazidime	Third-generation cephalosporin	2 g 8 h	–
Aztreonam	Monobactam	600–900 mg 8 h	–
Imipenem	Carbapenem	500 mg 6 h	–
Metropenem	Carbapenem	500 mg 8 h	–
Ertapenem	Carbapenem	300 mg 12 h	–
Ampicillin-sulbactam	Inhibitor of β-lactamase	1.5–3 g 6 h	–
Piperacillin-tazobactam	Inhibitor of β-lactamase	4.5 g 6 h	–
Vancomycin	Glycopeptide	1 g 12 h	–
Teicoplanin	Glycopeptide	400 mg 24 h	–
Daptomycin	Lipopeptide	6 mg/kg 24 h	–
Tigecycline	Glycycline	50 mg 12 h	–
Gentamycin	Aminoglycoside	5 mg/kg 24 h	–
Tobramycin	Aminoglycoside	5 mg/kg 24 h	–
Amikacin	Aminoglycoside	15 mg/kg 24 h	–
Polymyxin	Colistin	2.5–5 mg/kg 24 h	–

Rifampin is a well-known antibiotic, has effective oral absorption and tissue penetration against biofilm barrier. Rifampin is effective against MRSA infections when used in combination with fluoroquinolones and is thus frequently used in the treatment of chronic osteomyelitis.

Coagulase-Negative *Staphylococcus*

Coagulase-negative *Staphylococci* infections, which have less virulence than *S. aureus*, are responsible for a significant portion of infections in patients with implants. Since they are usually methicillin-resistant, IV vancomycin treatment is usually used. Daptomycin and linezolid are also used in treatment but clinical outcomes are unclear. Methicillin-sensitive coagulase-negative *Staphylococci* infections are treated in the same way as *S. aureus* infections.

Streptococcus Osteomyelitis

B-hemolytic *Streptococci*, especially *S. agalactiae* (group B) and *S. pyogenes* (group A) are the most common causes. These pathogens are highly susceptible to both penicillin or cephalosporin groups of antibiotics, and 12–24 million units/day IV penicillin therapy is recommended as first-line therapy. Vancomycin treatment is recommended in patients who have allergic reactions to penicillin and cannot tolerate clindamycin [13].

Enterococcus and Vancomycin-Resistant *Enterococcus*

Enterococci osteomyelitis is commonly seen after *Enterococcal bacteremia* or endocarditis. However, it was recently found to cause chronic osteomyelitis accompanied by diabetes and ischemic ulcers. The most common causes are identified as enterococcus faecalis and IV ampicillin treatment is preferred if it is susceptible. Unfortunately, *Enterococcus faecalis* infections are usually resistant to both ampicillin and carbapenem with an increasing tendency to develop resistance against vancomycin as well. Linezolid, tigecycline and daptomycin can be used in these cases; however, a rapid developing resistance to linezolid is also reported [25].

Gram-Negative Osteomyelitis

Parenteral antibiotics used in the treatment of Gram-negative osteomyelitis are the penicillin

group, cephalosporin group, aztreonam, carbapenem, or aminoglycosides. There are relatively small numbers of antibiotics (fluoroquinolones and trimethoprim-sulfamethoxazole) that can be used in oral therapy in Gram-negative infections unlike Gram-positive ones. It is known that the efficacy of oral fluoroquinolone therapy is almost equal to parenteral therapy in acute and chronic osteomyelitis caused by susceptible Gram-negative infections including pseudomonas aeruginosa. Therefore, we have a chance to treat these cases without hospitalization. However, treatment options are reducing for Gram-negative bacterial infections including *E. coli*, *Klebsiella*, and pseudomonas, since an increasing resistance against antibiotics is being determined among these.

Parenteral treatment options against susceptible enterobacterial infections include cephalosporins, carbapenem (imipenem, meropenem, estrapenem), and beta-lactamase inhibitor antibiotics (ampicillin-sulbactam, ticarcillin-clavulanate, and piperacillin-tazobactam). Aztreonam should be preferred in patients with cephalosporin and penicillin allergies. Aminoglycosides are highly effective against Gram-negative bacteria but they are rarely preferred due to their nephrotoxicity in higher doses. If they are used, renal function must be strictly monitored.

Aminoglycoside antibiotics in combination with beta-lactam or ciprofloxacin are recommended to provide effective treatment in pseudomonas aeruginosa osteomyelitis. This can ensure minimizing adverse effects and maximizing the local efficacy. Piperacillin-tazobactam, ceftazidime, cefepime, aztreonam, imipenem, meropenem, and aminoglycosides are parenteral antibiotics that can be used against pseudomonas. Fluoroquinolones are suitable for oral administration. It should be noted that recurrence rate of *S. aureus* osteomyelitis is three times more than pseudomonas osteomyelitis [26].

Colistin and polymyxin-E are used in the treatment of *Acinetobacter* and "carbapenem-resistant" *Klebsiella* infections. In addition, as a new generation antibiotic, tigecycline can be used against these infections, but it is not effective against pseudomonas.

Anaerobic Infections

Second-generation cephalosporins (cefoxitin and cefotetan), beta-lactamase inhibitors, and carbapenem can be used for these infections. Metronidazole is especially effective against Gram-negative anaerobic bacteria and clostridium whereas it is ineffective against anaerobic *Streptococcus* bacteria of the oral flora. Oral absorption of both metronidazole and clindamycin are quite good. A fourth-generation fluoroquinolone, moxifloxacin, is very effective against anaerobic bacteria.

Osteomyelitis Due to Miscellaneous (?) and Atypical Pathogens

Bone and joint tuberculosis frequently involves the spine. Treatment is the same as for lung tuberculosis with initial therapy of isoniazid, rifampin, ethambutol, and pyrazinamide used for at least 6–9 months. Treatment protocol may be revised according to the clinical course. *Mycobacterium marinum*, *M. kansasii*, and *M. avium* infections can rapidly progress and be complicated. Treatment options are linked to the patient's immune condition and type of pathogen.

Solo or combination of doxycycline, aminoglycosides, fluoroquinolone, rifampicin, and trimethoprim-sulfamethoxazole drugs can be used in the treatment of brucellosis spondylitis. The recommended treatment period is at least 3 months [27].

Actinomycosis rarely causes osteomyelitis but it is important if determined. *Actinomyces* is an anaerobic bacterium and sensitive to penicillin, clindamycin, tetracycline, or erythromycin therapy. Treatment may be extended up to 12 months.

References

1. Mini E, Grassi F, Cherubino P et al (2001) Preliminary results of a survey of the use of antimicrobial agents as prophylaxis in orthopaedic surgery. J Chemother 13(1):73–79

2. Lazzani L, Lipsky BA, Mader JT (2005) Antibiotic treatment of osteomyelitis: what have we learned from 30 years of clinical trials? Int J Dis 9(3):127–138
3. Rissing JP (1997) Antimicrobial therapy for chronic osteomyelitis in adults: role of quinolones. Clin Infect Dis 25(6):1327–1333
4. Stengel D, Bauwens K, Sehouli J et al (2001) Systematic review and meta-analysis of antibiotic therapy for bone and joint infections. Lancet Infect Dis 1(3):175–188
5. Bratzler DW, Houck PM, Surgical Infection Prevention Guidelines Writers Workgroup, American Academy of Orthopedic Surgeons, American Association of Critical Care Nurses, American Association of Nurse Anesthetics, American College of Surgeons, American College of Osteopathic Surgeons, American Geriatrics Society, American Society of Anesthesiologists, American Society of Colon and Rectal Surgeons, American Society of Health-System Pharmacists, American Society of PeriAnesthesia Nurses, Ascension Health, Association of PeriOperative Registered Nurses, Association of Professionals in Infection Control and Epidemiology, Infectious Diseases Society of America, Medical Letter, Premier, Society for Healthcare Epidemiology of America, Society of Thoracic Surgeons (2004) Surgical infection society antimicrobial prophylaxis for surgery: an advisory statement from the national surgical infection prevention project. Clin Infect Dis 38(12):1706–1715
6. Cleveland KB (2008) General principles of infection. In: Campbell WC, Canale ST, Beaty JH (eds) Campbell's operative orthopaedics, 11th edn. Mosby/Elsevier, Philadelphia, pp 675–694
7. American Academy of Orthopaedic Surgeons. Information statement: recommendations for the use of intravenous antibiotic prophylaxis in primary total joint arthroplasty. http://www.aaos.org/about/papers/advistmt/1027.asp
8. Dellinger EP, Gross PA, Barrett TL et al (1994) Quality standard for antimicrobial prophylaxis in surgical procedures. Infection Diseases Society of America. Clin Infect Dis 18(3):422–427
9. Nelson CL, Green TG, Porter RA et al (1983) One day versus seven days of preventive antibiotic therapy in orthopedic surgery. Clin Orthop Relat Res 176:258–263
10. Gosselin RA, Roberts I, Gillespie WJ (2004) Antibiotics for preventing infection in open limb fractures. Cochrane Database Syst Rev 1:CD003764
11. Gustilo RB, Merkow RL, Templeman D (1990) The management of open fractures. J Bone Joint Surg Am 72(2):299–304
12. Kay RM, Tolo VT (2006) Management of the multiply injured child. In: Beaty JH, Kasser JR (eds) Fractures in children, 6th edn. Lippincott Williams & Wilkins, Philadelphia, pp 77–98
13. Lew DP, Waldvogel FA (2004) Osteomyelitis. Lancet 364(9431):369–379
14. Mader JT, Cantrell JS, Calhoun J (1990) Oral ciprofloxacin therapy compared with standard parenteral therapy for chronic osteomyelitis in adults. J Bone Joint Surg Am 72(1):104–110
15. Norden CW, Dickens DR (1973) Experimental osteomyelitis. Treatment with cephaloridine. J Infect Dis 127(5):525–528
16. Nelson CL (2004) The current status of material used for depot delivery of drugs. Clin Orthop Relat Res 427:72–78
17. Winiger DA, Fass RJ (1996) Antibiotic-impregnated cement and beads for orthopedic infections. Antimicrob Agents Chemother 40(12):2675–2679
18. Norden CW, Shinners E, Niederriter K (1986) Clindamycin treatment of experimental chronic osteomyelitis due to Staphylococcus aureus. J Infect Dis 153(5):956–959
19. Levine DP (2006) Vancomycin: a history. Clin Infect Dis 42(Suppl 1):S 5–S 12
20. Kollef MH (2007) Limitation of vancomycin in the management of resistant staphylococcal infections. Clin Infect Dis 45(Suppl3):S191–S195
21. Matthews PC, Taylor A, Byren I (2007) Teicoplanin levels in bone and joint infections: are standard dose subtherapeutic? J Infect 55(5):408–413
22. Drancourt M, Stein A, Argenson JN et al (1993) Oral rifampin plus ofloxacin for treatment of Staphylococcus-infected orthopedic implants. Antimicrob Agents Chemother 37(6):1214–1218
23. Senneville E, Legout L, Valette M et al (2006) Effectiveness and tolerability of prolonged linezolid treatment for chronic osteomyelitis: a retrospective study. Clin Ther 28(8):1155–1163
24. Rouse MS, Piper K, Jacobson M et al (2006) Daptomycin treatment of Staphylococcus aureus experimental chronic osteomyelitis. J Antimicrob Chemother 57(2):301–305
25. Rice LB (2006) Antimicrobial resistance in gram-positive bacteria. Am J Infect Control 34(5 Suppl1): S11–S19
26. Tice AD, Hoagland PA, Shoultz DA (2003) Risk factor and treatment outcomes in osteomyelitis. J Antimicrob Chemother 51(5):1261–1268
27. Pappas G, Akritidis N, Bosilkovski M et al (2005) Brucellosis. N Engl J Med 352(22):2325–2536

Chondroprotective Agents

39

Vasfi Karatosun

Abstract

Osteoarthritis is a progressive disorder of the joints, caused by gradual loss of cartilage, and the resulting joint pain and functional limitations. Treatment for osteoarthritis aims to relieve pain and reduce other symptoms. However, there are agents (chondroprotective) suggested to prevent the loss of cartilage. The aim of this chapter is to examine the chondroprotective efficacy of nutritional agents, diacerein, and viscosupplementation, which may change the course of the disease.

Osteoarthritis is a progressive process characterized with pain, deformities, swelling, dysmotility, and loss of functionality in the joints. Loss of the joint cartilage and degeneration are inevitable at the end of the process. The impact of various factors such as age, inherited conditions, obesity, gender, hormonal issues, hypermobility, trauma, joint anomalies, occupation, and sportive activities has been proven to accelerate the onset of osteoarthritis in conjunction with the process. However, the reason underlying such onset is yet unclear.

The pathological process of osteoarthritis does not take place only in the joint cartilage. In addition to the loss of cartilage, other pathological changes also occur. These include baring of the bone surface, deformation of the bone, osteophyte, subchondral cyst formation, synovitis, thickening of the joint capsule, degeneration of the meniscus, and periarticular muscular atrophy. Radiology assists observation of pathologic changes greatly. Numerous classifications have been proposed to grade osteoarthritis radiologically. The Kellgren–Lawrence classification [1] is the most commonly referenced one. According to this classification, 0—No findings; 1—Minimal osteophyte and suspicious clinical findings; 2—Greater osteophyte and intraarticular narrowing; 3—Moderate level of intraarticular narrowing; and 4—Extreme narrowing of the articular surface, sclerosis, and subchondral cyst [1]. Though the pathologic stages can be laid out radiologically, there is no correlation between such staging and scores that determine the articular function [2–5]. This situation may be problematic when it comes to establishing a treatment plan. Treatment of osteoarthritis revolves around

V. Karatosun
Department of Orthopedics and Traumatology, Medical Faculty, Dokuz Eylül University, İzmir, Turkey
e-mail: vasfi.karatosun@gmail.com

F. Korkusuz (ed.), *Musculoskeletal Research and Basic Science*,
DOI 10.1007/978-3-319-20777-3_39

the pain, as cartilage degeneration may not always lead to pain; subchondral pain might occur later; and synovial and capsular tissues are the primary sources of pain [6].

The agents that are used to treat osteoarthritis and claimed to possibly reduce cartilage volume and quality are called chondroprotectives. Agents that modify the connective tissue structure (Connective Tissue Structure-Modifying Agents/CTSMAs) directly influence IL-1 synthesis and activate collagenase, proteoglycanase, and matrix metalloproteinases. They also stimulate nitric oxide synthesis and release, as well as expression of prostaglandins E_2, IL-6, and IL-8. Drugs that modify the progression of osteoarthritis are called disease-modifying OA drugs (DMOADs) [7]. The objective of this chapter is to evaluate the chondroprotective activity of DMODs and viscosupplementation.

Nutritional Agents

Nutritional agents are products that are not presented in the form of drugs, but rather as alternative nutritional supplements. Glucosamine and chondroitin sulfate are the most prominent products of this category. The CTSMA (connective tissue structure-modifying agent) and DMOAD (disease-modifying osteoarthritis drugs) impacts of these agents should be discussed. Glucosamine sulfate could not be obtained through in vitro or in vivo processes. So, glucosamine and sulfate were prepared in two different crystallized forms. Being a building block for the cartilage, glucosamine is synthesized by chondrocytes. Experimentation on rats revealed that glucosamine activates NFκB transcription factor, while reducing IL-1 β [8]. Glucosamine was also found to reduce phospholipase A2 activity [9], COX-2 mRNA and protein levels [10–12], and PGE_2 release [11–14] in the articular cartilage. However, it could not be proven in in vivo studies that externally administered glucosamine provides the same effect [15]. Though there are some studies related to chondroitin that claim that cartilage volume is increased through similar mechanisms, there is also serious uncertainty as to its effectiveness in in vivo studies [16].

During experimental studies, the onset of osteoarthritis could not be prevented in rabbits which were given glucosamine and had their anterior cruciate ligaments severed thereafter [17]. In another experiment with rabbits, a chondroprotective effect could not be observed [18].

It is interesting to see that both glucosamine and chondroitin are utilized in nonmedical products in different dosages and obtained through nonstandardized means. Additionally, it is also interesting that studies that yielded positive results were all sponsored by the relevant product brands. Scientific data regarding dosages, half-life, active ingredients, effectiveness, and reliability of those products is insufficient. Furthermore, almost all points as to the side effects and toxic dosages are unknown [19].

It was observed as a result of the GAIT (Glucosamine/Chondroitin Arthritis Intervention Trial) study that was performed in 16 centers around the United States to prove the effectiveness of glucosamine and chondroitin sulfate on osteoarthritis that the use of those agents was no superior than the placebo drugs [20]. Also, as the result of an evaluation made at Western Ontario and McMaster Universities, within the scope of the Osteoarthritis Index (WOMAC), no clinically significant difference was observed [21]. Radiologically, the use of glucosamine and chondroitin sulfate was not found to have any positive or significant impact on osteoarthritis. According to the American College of Rheumatology (ACR) Guidelines for Hand, Hip, and Knee (2012), the use of glucosamine and chondroitin is not recommended in the case of knee and hip osteoarthritis [22].

Diacetylrhein/Diacerein

DMOAD is a product with proven effectiveness. It offers anti-inflammatory, analgesic, and chondroprotective effect; yet, its analgesic effectiveness is far lower than NSAIDs [15]. While its pharmacodynamic interference is disputed, it inhibits IL-1β and NO synthesis and stimulates PGE2 synthesis [23, 24]. Whereas the number of studies is not adequate, there are publications that provide results indicating recovery in osteoarthritis symptoms and radiological parameters [25,

26]. Its side effects on the gastrointestinal system [25] and genotoxic effects [27] prevent widespread use of the drug. Diacerein is not listed in the treatment guidelines.

Viscosupplementation

Discovery of the Hyaluronan molecule dates back to 1934. It is present within all living beings that share the same chemical structure [28]. The initial clinical trials were run in the early 1970s, and the first-gen hyaluronic acid (HA) was created in the form of a complete product in the 1980s. Initially, it was utilized to halt the process of degeneration in the articular cartilage of race horses.

In its ordinary course, HA manifests its protective effect on the synovia by repressing and barring nociceptors. In the cartilage, it functions in the form of a barrier and proteoglycan aggregate in the bone tissue. During the course of osteoarthritis, viscosity of the synovial fluid and lubrication decrease, leading to reduced shock absorption. The cartilage and synovium are separated from the articular surface covered with HA, causing mechanical and inflammatory damage. This, in turn, starts an inflammatory process in the synovium, and damage occurs on the articular cartilage. The lack of HA in the synovial liquid causes proinflammatory and IL-1 damage on pain mediators. HA ensures viscosity of the synovial liquid, shock absorption, and filtration [28]. When orally administered, the HA acid is completely metabolized. Therefore, it should be exogenously administered. Upon being administered exogenously, the mechanical and barrier functions of HA establish the primary effect, and the pharmacologic activity provides the secondary effect.

Currently, HA treatment is practiced in various areas of medicine in addition to articular atrophies. However, disputes on the number and location of injections (active substances and molecular weight), storage (active substance formulation), indications, effectiveness, reliability, and cost–benefit relation are still going on.

A study by Jackson et al. [29], on the location of injection, makes comparisons among suprapatellar, anterolateral, anteromedial, and central injections, and concludes that the lateral midpatellar area is the most convenient area for injection with 93 % articular reach.

In addition to being used for articular motile difficulty and pain, HA was administered for rheumatoid arthritis, hemophilic arthropathy, and crystal arthropathy. While it is most commonly applied on the knee joint, HA is also applied on the temporomandibular and primary metatarsophalangeal joints, and on the joints of the hip, shoulder, ankle, and elbow [28, 30]. As for the treatment cycle, recommended application frequency is at least three injections in a fortnight. While not superior to placebo drugs, some synthetic products of nonanimal origin are suitable for single injections [31]. The treatment may be reiterated with at least a period of 4 weeks allowed in between each treatment course and no more than two treatment cycles within every 6 months. Administering different products during the same cycle or during consecutive cycles should be a topic of discussion. It is not convenient to apply anesthetic agents on the knee joint or other drugs during treatment, as such products might dilute HA and pose the risk of disrupting its reliability.

HA may be administered throughout all radiological stages [32, 33]. The flexibility of application stems from the facts that there is no correlation between knee degeneration and pain and that the effect of HA on knees with varying degrees of degeneration is not yet known.

Though the exact term of relief is not known, the use of HA was found to offer relief, improved mobility, and better living quality for up to a year as well as good cost–benefit performance [34]. Karatosun et al. [35] were able to find a more prolonged period of activity in their study on comparison of administering HA and physiotherapy for knee osteoarthritis. Published studies concluding that administration of HA reduces intraarticular narrowing are present [36]. On the other hand, there are other published studies indicating that it does not have any impact on the process [37, 38].

The comparative effectiveness of HA in different molecular weight ratios has not been researched yet [39]. Nevertheless, HA products with lower molecular weight require more frequent injections, which are accompanied with

increased risks of occurrence of side effects and infections. [40].

According to the analysis by Bellamy et al. [41], which was based on a comprehensive evaluation, HA was found to be more effective than placebo products and efficient than corticosteroids. While the ACR does not have any recommendations regarding its administration for knee and hip osteoarthritis [7], viscosupplementation is not recommended according to the AAOS knee osteoarthritis treatment guidelines [22].

References

1. Kellgren JH, Lawrence JS (1957) Radiological assessment of osteo-arthrosis. Ann Rheum Dis 16(4):494–502
2. Schiphof D, Boers M, Bierma-Zeinstra SM (2008) Differences in descriptions of Kellgren and Lawrence grades of knee osteoarthritis. Ann Rheum Dis 67(7):1034–1036
3. Chang CB, Han I, Kim SJ, Seong SC, Kim TK (2007) Association between radiological findings and symptoms at the patellofemoral joint in advanced knee osteoarthritis. J Bone Joint Surg Br 89(10):1324–1328
4. Phan CM, Link TM, Blumenkrantz G, Dunn TC, Ries MD, Steinbach LS, Majumdar S (2006) MR imaging findings in the follow-up of patients with different stages of knee osteoarthritis and the correlation with clinical symptoms. Eur Radiol 16(3):608–618
5. Kocak FU, Unver B, Karatosun V, Bakırhan S (2009) Associations between radiographic changes and function, pain, range of motion, muscle strength and knee function score in patients with osteoarthritis of the knee. J Phys Ther Sci 21:93–97
6. Hadler NM (1992) Knee pain is the malady – not osteoarthritis. Ann Intern Med 116(7):598–599
7. Hochberg MC, Altman RD, April KT, Benkhalti M, Guyatt G, McGowan J, Towheed T, Welch V, Wells G, Tugwell P, American College of Rheumatology (2012) American College of Rheumatology 2012 recommendations for the use of nonpharmacologic and pharmacologic therapies in osteoarthritis of the hand, hip, and knee. Arthritis Care Res (Hoboken) 64(4):465–474
8. Gouze JN, Bianchi A, Bécuwe P, Dauça M, Netter P, Magdalou J, Terlain B, Bordji K (2002) Glucosamine modulates IL-1-induced activation of rat chondrocytes at a receptor level, and by inhibiting the NF-kappa B pathway. FEBS Lett 510(3):166–170
9. Piperno M, Reboul P, Hellio Le Graverand MP, Peschard MJ, Annefeld M, Richard M, Vignon E (2000) Glucosamine sulfate modulates dysregulated activities of human osteoarthritic chondrocytes in vitro. Osteoarthritis Cartilage 8(3):207–212
10. Shikhman AR, Kuhn K, Alaaeddine N, Lotz M (2001) N-acetylglucosamine prevents IL-1 beta-mediated activation of human chondrocytes. J Immunol 166(8):5155–5160
11. Largo R, Alvarez-Soria MA, Díez-Ortego I, Calvo E, Sánchez-Pernaute O, Egido J, Herrero-Beaumont G (2003) Glucosamine inhibits IL-1beta-induced NFkappaB activation in human osteoarthritic chondrocytes. Osteoarthritis Cartilage 11(4):290–298
12. Nakamura H, Shibakawa A, Tanaka M, Kato T, Nishioka K (2004) Effects of glucosamine hydrochloride on the production of prostaglandin E2, nitric oxide and metalloproteases by chondrocytes and synoviocytes in osteoarthritis. Clin Exp Rheumatol 22(3):293–299
13. Gouze JN, Bordji K, Gulberti S, Terlain B, Netter P, Magdalou J, Fournel-Gigleux S, Ouzzine M (2001) Interleukin-1beta down-regulates the expression of glucuronosyltransferase I, a key enzyme priming glycosaminoglycan biosynthesis: influence of glucosamine on interleukin-1beta-mediated effects in rat chondrocytes. Arthritis Rheum 44(2):351–360
14. Tung JT, Venta PJ, Eberhart SW, Yuzbasiyan-Gurkan V, Alexander L, Caron JP (2002) Effects of antiarthritis preparations on gene expression and enzyme activity of cyclooxygenase-2 in cultured equine chondrocytes. Am J Vet Res 63(8):1134–1139
15. Verbruggen G (2006) Chondroprotective drugs in degenerative joint diseases. Rheumatology (Oxford) 45(2):129–138
16. Black C, Clar C, Henderson R, MacEachern C, McNamee P, Quayyum Z, Royle P, Thomas S (2009) The clinical effectiveness of glucosamine and chondroitin supplements in slowing or arresting progression of osteoarthritis of the knee: a systematic review and economic evaluation. Health Technol Assess 13(52):1–148
17. Tiraloche G, Girard C, Chouinard L, Sampalis J, Moquin L, Ionescu M, Reiner A, Poole AR, Laverty S (2005) Effect of oral glucosamine on cartilage degradation in a rabbit model of osteoarthritis. Arthritis Rheum 52(4):1118–1128
18. Shikhman AR, Amiel D, D'Lima D, Hwang SB, Hu C, Xu A, Hashimoto S, Kobayashi K, Sasho T, Lotz MK (2005) Chondroprotective activity of N-acetylglucosamine in rabbits with experimental osteoarthritis. Ann Rheum Dis 64(1):89–94
19. Hathcock JN, Shao A (2007) Risk assessment for glucosamine and chondroitin sulfate. Regul Toxicol Pharmacol 47(1):78–83
20. Clegg DO, Reda DJ, Harris CL, Klein MA, O'Dell JR, Hooper MM, Bradley JD, Bingham CO 3rd, Weisman MH, Jackson CG, Lane NE, Cush JJ, Moreland LW, Schumacher HR Jr, Oddis CV, Wolfe F, Molitor JA, Yocum DE, Schnitzer TJ, Furst DE, Sawitzke AD, Shi H, Brandt KD, Moskowitz RW, Williams HJ (2006) Glucosamine, chondroitin sulfate, and the two in combination for painful knee osteoarthritis. N Engl J Med 354(8):795–808
21. Sawitzke AD, Shi H, Finco MF, Dunlop DD, Harris CL, Singer NG, Bradley JD, Silver D, Jackson CG, Lane NE, Oddis CV, Wolfe F, Lisse J, Furst DE, Bingham CO, Reda DJ, Moskowitz RW, Williams HJ, Clegg DO (2010) Clinical efficacy and safety of

glucosamine, chondroitin sulphate, their combination, celecoxib or placebo taken to treat osteoarthritis of the knee: 2-year results from GAIT. Ann Rheum Dis 69(8):1459–1464
22. AAOS. American Academy of Orthopaedic Surgeons (2013) Treatment of osteoarthritis of the knee. Evidence-based guideline, 2nd edn. Adopted by the American Academy of Orthopaedic Surgeons
23. Pelletier JP, Mineau F, Fernandes JC, Duval N, Martel-Pelletier J (1998) Diacerhein and rhein reduce the interleukin 1beta stimulated inducible nitric oxide synthesis level and activity while stimulating cyclooxygenase-2 synthesis in human osteoarthritic chondrocytes. J Rheumatol 25(12):2417–2424
24. Yaron M, Shirazi I, Yaron I (1999) Anti-interleukin-1 effects of diacerein and rhein in human osteoarthritic synovial tissue and cartilage cultures. Osteoarthritis Cartilage 7(3):272–280
25. Fidelix TS, Soares BG, Trevisani VF (2006) Diacerein for osteoarthritis. Cochrane Database Syst Rev 1:CD005117
26. Dougados M, Nguyen M, Berdah L, Maziéres B, Vignon E, Lequesne M, ECHODIAH Investigators Study Group (2001) Evaluation of the structure-modifying effects of diacerein in hip osteoarthritis: ECHODIAH, a three-year, placebo-controlled trial. Evaluation of the chondromodulating effect of diacerein in OA of the hip. Arthritis Rheum 44(11): 2539–2547
27. Mukhopadhyay MJ, Saha A, Dutta A, De B, Mukherjee A (1998) Genotoxicity of sennosides on the bone marrow cells of mice. Food Chem Toxicol 36(11):937–940
28. Iannitti T, Lodi D, Palmieri B (2011) Intra-articular injections for the treatment of osteoarthritis: focus on the clinical use of hyaluronic acid. Drugs R D 11(1): 13–27
29. Jackson DW, Evans NA, Thomas BM (2002) Accuracy of needle placement into the intra-articular space of the knee. J Bone Joint Surg Am 84(9):1522–1527
30. Karatosun V, Unver B, Ozden A, Ozay Z, Gunal I (2008) Intra-articular hyaluronic acid compared to exercise therapy in osteoarthritis of the ankle. A prospective randomized trial with long-term follow-up. Clin Exp Rheumatol 26(2):288–294
31. Altman RD, Akermark C, Beaulieu AD, Schnitzer T, Durolane International Study Group (2004) Efficacy and safety of a single intra-articular injection of non-animal stabilized hyaluronic acid (NASHA) in patients with osteoarthritis of the knee. Osteoarthritis Cartilage 12(8):642–649
32. Lussier A, Cividino AA, McFarlane CA, Olszynski WP, Potashner WJ, De Médicis R (1996) Viscosupplementation with hylan for the treatment of osteoarthritis: findings from clinical practice in Canada. J Rheumatol 23(9):1579–1585
33. Wang CT, Lin J, Chang CJ, Lin YT, Hou SM (2004) Therapeutic effects of hyaluronic acid on osteoarthritis of the knee. A meta-analysis of randomized controlled trials. J Bone Joint Surg Am 86-A(3):538–545
34. Raynauld JP, Torrance GW, Band PA, Goldsmith CH, Tugwell P, Walker V, Schultz M, Bellamy N, Canadian Knee OA Study Group (2002) A prospective, randomized, pragmatic, health outcomes trial evaluating the incorporation of hylan G-F 20 into the treatment paradigm for patients with knee osteoarthritis (Part 1 of 2): clinical results. Osteoarthritis Cartilage 10(7): 506–517
35. Karatosun V, Unver B, Gocen Z, Sen A, Gunal I (2006) Intra-articular hyaluranic acid compared with progressive knee exercises in osteoarthritis of the knee: a prospective randomized trial with long-term follow-up. Rheumatol Int 26(4):277–284
36. Jubb RW, Piva S, Beinat L, Dacre J, Gishen P (2003) A one-year, randomised, placebo (saline) controlled clinical trial of 500–730 kDa sodium hyaluronate (Hyalgan) on the radiological change in osteoarthritis of the knee. Int J Clin Pract 57(6):467–474
37. Sun SF, Hsu CW, Hwang CW, Hsu PT, Wang JL, Tsai SL, Chou YJ, Hsu YW, Huang CM, Wang YL (2006) Hyaluronate improves pain, physical function and balance in the geriatric osteoarthritic knee: a 6-month follow-up study using clinical tests. Osteoarthritis Cartilage 14(7):696–701
38. Criscione LG, Elliott AL, Stabler T, Jordan JM, Pieper CF, Kraus VB (2005) Variation of serum hyaluronan with activity in individuals with knee osteoarthritis. Osteoarthritis Cartilage 13(9):837–840
39. Karatosun V, Unver B, Gocen Z, Sen A (2005) Comparison of two hyaluronan drugs in patients with advanced osteoarthritis of the knee. A prospective, randomized, double-blind study with long term follow-up. Clin Exp Rheumatol 23(2):213–218
40. Adams ME, Lussier AJ, Peyron JG (2000) A risk-benefit assessment of injections of hyaluronan and its derivatives in the treatment of osteoarthritis of the knee. Drug Saf 23(2):115–130
41. Bellamy N, Campbell J, Welch V, Gee TL, Bourne R, Wells GA (2006) Viscosupplementation for the treatment of osteoarthritis of the knee. Cochrane Database Syst Rev: CD005321.pub2

Venous Thromboembolism

40

Osman Tuğrul Eren, Raffi Armağan,
and Mehmet Ali Talmaç

Abstract

Venous thromboembolism is a preventable disease that occurs frequently throughout the world. Diagnosis, prophylaxis, and management of venous thromboembolism have not yet been totally elucidated. An increase in orthopedic surgeons' awareness of venous thromboembolism and related diseases such as deep vein thrombosis, chronic venous diseases, and pulmonary embolism is needed. This chapter discusses diagnosis of venous thromboembolism, anticoagulant drug-effect mechanisms and complications during treatment, and novel findings in the American Academy of Orthopaedic Surgeons and American College of Chest Physicians guidelines.

Learning Outcomes

Venous thromboembolism (VTE) is a group of diseases that require detailed understanding in Orthopedics and Traumatology. VTE is a cause of morbidity and mortality, and the drugs that are used in therapy may lead to serious bleeding. Topics to be learned include etiopathogenesis of VTE, diagnosis and treatment, complications of treatment, and innovations in the American Academy of Orthopaedic Surgeons (AAOS) and American College of Chest Physicians (ACCP) guidelines.

Clinical Relevance

Is venous thromboembolism prophylaxis with low-molecular-weight heparin safe?

A 70-old-male patient was admitted to the emergency room with a history of falling at home and inability to walk. An intertrochanteric fracture of the right femur was confirmed by X ray studies and examination. Intramedullary nailing for unstable fracture was planned. Prompt prophylaxis for thromboembolism was initiated with 0.4 IU of enoxoparine while anesthesiologic stabilization of internal diseases of the patient continued. A closed nailing of the fracture was performed with epidural anesthesia the following day. On the postoperative first day, a hemorrhagic discharge and staining of the dressings was revealed. There was an inequality of radius of right thigh and exten-

O.T. Eren (✉) • R. Armağan • M.A. Talmaç
Orthopaedics and Traumatology, Şişli Etfal Training and Research Hospital, İstanbul, Turkey
e-mail: tugruleren@hotmail.com; rafiarmagan@gmail.com; drtalmac2@gmail.com

F. Korkusuz (ed.), *Musculoskeletal Research and Basic Science*,
DOI 10.1007/978-3-319-20777-3_40

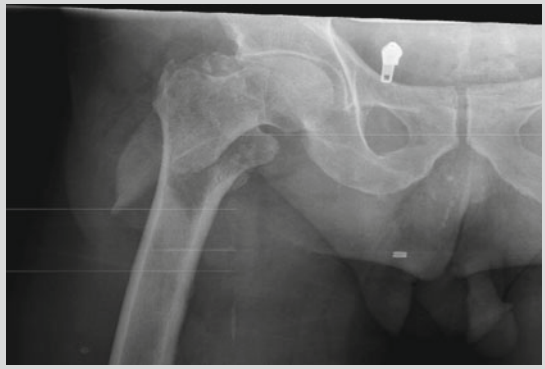

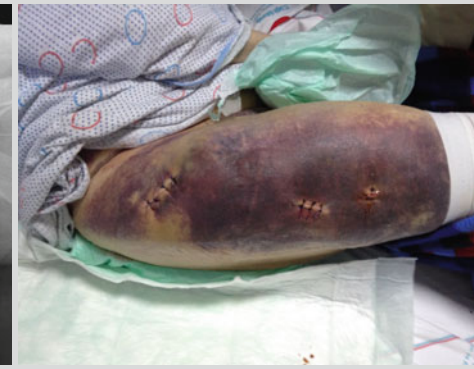

sile subcutaneous hemorrhagic ecchymosis was revealed. Medical prophylaxis was stopped and prophylaxis was continued with mechanical prophylactic measures and encouragement of early mobilization.

The risk analysis for thrombophylaxis was assessed with the Padua Score. The age of the patient, obesity, the planned orthopedic operation, and prolonged immobilization pose a high risk of thromboembolism to the patient [1]. A dose of 0.4 IU of enoxoparine is appropriate for a patient weighing 70 kg. Although prophylaxis lowers the risk of thrombophylaxis, it can cause exaggerated hemorrhagia at the postoperative surgical site [2]. In case of such an event, discontinuation of low-molecular-weight heparins until hemostasis is obtained is advised. Although low-molecular-weight heparins lower the risk for thromboembolic events, they can cause some secondary morbidities with the increase of hemorrhagic events.

Introduction

Venous thromboembolism (VTE) is the general name of all pathological thrombosis in the venous circulation. The three main components of VTE are deep vein thrombosis (DVT), chronic venous disease, and pulmonary embolism. It occurs most often in lower-extremity deep veins and rarely in upper-extremity, pelvic, and other veins. The most important component of VTE that threatens life is pulmonary embolism (PE). Two million DVT cases and 600,000 PE cases are seen in the United States annually. In addition, about 200,000 people die each year in the United States from PE. VTE is a disease with more than one cause. and multiple risk factors may coexist simultaneously in patients. The more risk factors a patient has, the higher the risk of developing VTE (Tables 40.1 and 40.2). Three basic pathogenetic mechanisms that facilitate the development of VTE are described by Virchow. Virchow's triad includes slowing of blood flow (stasis), damage to the blood vessel wall (primarily endothelial

Table 40.1 Fatal DVT and PE ratios determined by venography

Without prevention (prophylaxis)	DVT	Fatal PE
Total hip prosthesis	42–57 % (Proximal DVT: 18–36 %)[a]	1–2 %
Total knee arthroplasty	41–85 % (Proximal DVT: 5–22 %)[a]	0.1–1.7 %
Open menisectomy	20 %	Unknown
Femur fracture	60 %	3.5 %
Spinal trauma + paralysis	100 %	1 %
Multivariate trauma	35–58 %	Unknown
Pelvis fracture	20–60 %	Unknown

Data of USA

[a]Proximal DVT: Rate of incidence VTE above the knee level

damage and dysfunction), and hypercoagulability [3]. These pathogenetic mechanisms are still accepted and genetic changes (polymorphisms/mutations) were added to these mechanisms with today's technology (Table 40.3).

Coagulation Mechanism

Coagulation is the formation of fibrin by the interaction of more than a dozen proteins. After extrinsic and intrinsic pathways independently start, the coagulation engages in a common way. The damage of the subendothelial area of a vein activates the intrinsic pathway by activation of factor VII, which is measured with partial thromboplastin time (PTT). The extrinsic pathway is activated by thromboplastin, which is released into circulation after the cellular damage and measured with prothrombin time (PT). The common path begins with the activation of Factor X. Activated Factor X generates thrombin from prothrombin. Thrombin works agonist with thrombocytes. Thrombin converts fibrinogen to fibrin and activates factor XIII, which stabilizes the fibrin [4] (Fig. 40.1).

Table 40.2 PE ratios

With prevention (prophylaxis)	PE (%)	Fatal PE (%)
Total hip prosthesis	0.9–28	1–2
Total knee arthroplasty	1.5–10	0.1–1.7
Total hip prosthesis + warfarin prophylaxis		<0.1

Fibrinolytic System

The fibrinolytic system prevents clotting and maintains vessel patency. There are natural mechanisms functioning opposite of coagulation. There are three systems; antithrombin, proteins C and S, and plasminogen-plasmin. Antithrombin binds thrombin, proteins C and S inhibit factors Va and VIIIa, and plasmin destroys fibrin [5]. If the coagulation and fibrinolytic systems becomes unbalanced, venous thrombosis occurs because of stasis, endothelial damage, and hypercoagulability, known as Virchow's triad.

Venous Thromboembolic Disease

Epidemiology and Risk Factors

After major orthopedic surgeries, the prevalence of DVT is between 30 % and 50 %. When VTE prophylaxis is not provided after hip fracture, the prevalence of fatal pulmonary embolism is 7 %. Most sources of PE are proximal veins.

Table 40.3 The influential factors in the formation of Virchow's triad

Venous stasis	Injury on blood vessel wall	Hypercoagulability
Long-term bed rest, long travel, inactivity that depends on the surgery operation Tumors, obesity, pregnancy-related venous obstruction Cardiomyopathy, congestive heart failure, and myocardial infarction dependent left ventricular failure Atrial fibrillation	Vein injury/traumata Catheter insertion Deep vein thrombosis formation (varicose vein formation + valve damage) Artificial heart valve Acute myocardial infarction Surgical intervention Bone fractures Cardiovascular disease Tumor invasion Ambustion	Acquired thrombophilias History of deep vein thrombosis Surgical procedures Antiphospholipid antibody syndrome Others Hereditary thrombophilias *Frequently seen* Activated protein C Resistance Factor V Leiden mutation Prothrombin gene (G20210A) mutation Protein C/S deficiencies Lack of antithrombin *Rarely seen* Family history

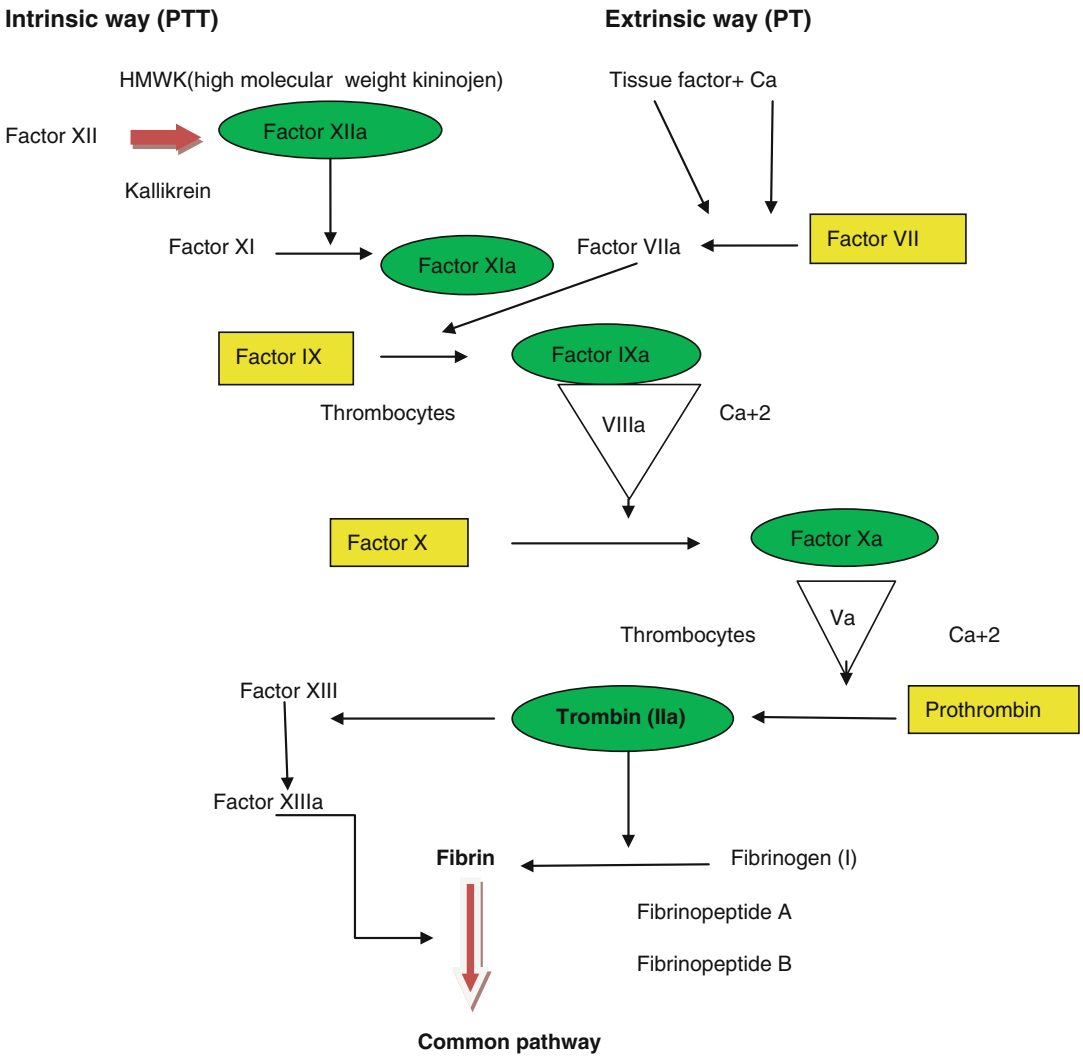

Fig. 40.1 Intrinsic and extrinsic coagulation pathways. *Rectangular shapes* **vitamin K-dependent factors – sensitive to warfarin**, *Oval shapes* **inhibited factors in heparin side – antithrombin III**

Symptomatic PE ratios after electively applied total hip arthoplasty (THA) and total knee arthoplasty (TKA) without prophylaxis are 20 % and 8 %, respectively. DVT was seen more frequently in venographs taken after TKP, but symptomatic PE is seen less than with THA than TKP. Risk factors include age, gender, race, history of DVT, varicose veins, cancer, oral contraceptives, heart failure, obesity, smoking, stroke, immobility, tissue injury, trauma, pregnancy, nephrotic syndrome, and surgical intervention. For example, antithrombin III level drops due to blood loss during THA. The incidence of VTE risk is higher when the femur is cavitated in THA and the femoral side of the prosthesis (especially in cemented prosthesis) is applied.

Age

Advancing age increases the risk of VTE, and age is a strong risk factor for VTE. VTE risk is 0.01 % per year for people under age 40; for older people, the risk increases by 1 % each year. Although

the exact cause is unknown, an increase in VTE is seen because of a combination of factors, including decreased mobility, the development of additional diseases, thrombosis, and an increase in coagulability with age [6].

Gender

Although men and women are equally at risk for VTE, it is seen more among young women because of their use of oral contraceptives (OC). VTE is two to four times higher among patients who use OC compared with those who do not.

Race

VTE is seen 25 % more often among Caucasians and African Americans. It is 70 % less common among American Indians, Pacific Islanders, and Hispanics.

Season

According to some meta-analyses, fatal PE and VTE are 43 % more likely during the winter. A decrease in physical activity may be the cause for this.

Obesity

Although the reason remains uncertain, coagulation and inflammation are increased in obese people [7]. The risk of VTE is increased 2 to 3 times if BMI is over 30 kg/m^2.

Hormone Therapy

OC users are at a higher risk of VTE, with VTE seen in approximately 85 of 100,000 persons.

Inpatients

In hospitalized patients, venous thrombosis is higher due to immobilization, cancer, and surgery. VTE occurs 100 times more often than in the general population. Fifty percent of hospitalized patients are at risk of VTE, and VTE can occur even 3 months after discharge.

Surgery

Immobility due to surgery and general anesthesia creates the Virchow triad and increases the risk of VTE. Long immobilization in the perioperative period reduces the effects of massage in the calf muscles and causes venous stasis. General anesthesia causes endothelial damage by reducing venous tone. Orthopedic surgery and trauma cause multiple prothrombotic events. After THA, TKA, and hip fracture surgery, asymptomatic DVT is commonly seen [8].

Cancer

VTE is seen among approximately 1 in 200 of cancer patients and if 4.1 times more frequent than in the general population. Cancer cells increase the risk of VTE by activating thrombocytes and coagulation pathways [9].

Thrombophilia

Severe thrombophilia occurs due to antithrombin and protein C and S deficiency. It is not common, but it causes strong thrombosis. Light thrombophilia causes thrombosis by increasing procoagulant factors if there is a deficiency of factor V Leiden and PG20210A [10].

Travel

After traveling by plane, car, train, or bus for more than 4 h, the risk of VTE is increased by nearly 3 times for a few weeks.

VTE Diagnosis

Clinically, VTE and PE have no specific diagnostic symptoms. Pain, swelling, and pain in the calf

of the leg by forcing the foot to dorsiflexion (Homans sign) are the symptoms. The examinations used in diagnosis are chest radiography, electrocardiography, arterial blood gases (evaluation of oxygen), ventilation-perfusion scintigraphy, high-resolution spiral chest computed tomography, pulmonary angiography, and Doppler ultrasonography [11]. D-dimer is an additional examination. High D-dimer is an indication of fibrin degradation. Low D-dimer values indicate a low risk of VTE (high negative predictive value) [12]. Venography is the gold standard, but there are undesirable effects, such as its being expensive and invasive and the need for radiation exposure.

Prophylaxis

High risk of thromboembolic events causing morbidity and mortality after major orthopedic surgery and the difficulty of diagnosis usually warrants prophylaxis. There are mechanical and pharmacologic prophylaxis modalities available. The duration of prophylaxis is controversial. There is no consensus, but most of the literature includes the guidelines for prevention of VTE after surgery. In prophylaxis, some studies that are intended to prevent PE are needed, which would be possible with a single-center prospective study involving 50,000 patients.

Mechanical Approaches

A sequential pneumatic pressure-applying apparatus (IPC) prevents the development of stasis by increasing venous current and stimulates the fibrinolytic system so there is no risk of bleeding. Poor patient compliance and misuse are common. Good results have been reported after THA.

Plantar pressure applying devices provide deep vein pulsatile flow by applying pressure to the deep vein plexus in the foot (an effect like walking). The patient should not use this while alone.

Graduated pressurized stockings prevent venous stasis by applying different pressures to the lower and upper levels of the lower extremity. These socks are recommended in addition to medical prophylaxis [13].

Inferior Vena Cava Filters (IVCF)

Indications

1. If the use of anticoagulants is contraindicated (head and spinal cord injury)
2. If hemorrhage develops secondary to anticoagulants
3. If VTE develops despite anticoagulant therapy
4. If clot continues to grow and duplicate
5. If the patient has a low cardiopulmonary reserve, prophylactic IVCF is implemented for the patient due to of the high risk of morbidity and mortality. This is expensive and morbidity is high [14].

Pharmacological Prophylaxis

Heparin

Heparin is an indirect thrombin inhibitor. There are different molecular weights (approximately 15,000 Da). The pentasaccharide unit is extended so that, by binding to antithrombin, it also binds factors VII, IX, X, and XL and thrombin. Heparin does not pass the placenta and is the only anticoagulant that can be used safely during pregnancy. Contraindications include hemorrhagic diathesis, malignant hypertension, cerebral hemorrhage, and peptic ulcers. Although dose-adjusted heparin is effective, the possibility of bleeding complications and need for close monitoring are disadvantages. Heparin can cause osteopenia or osteoporosis. Thrombocytopenia and thrombosis, which are formed by development of antibodies against platelets, are seen at the same time. If thrombocytes are reduced by 50 %, it is considered heparin-induced thrombocytopenia (HIT). Hypersensitivity, skin necrosis, alopecia, mild transaminase elevation, and hypoaldosteronism are seen. In cases of HIT, heparin is interrupted and the thrombin inhibitors argatroban and lepirudin are given. Protamine sulfate is heparin's antidote [15, 16].

Low-Molecular-Weight Heparin (LMWH)

In the authors' country (Turkey), only enoxaparin is available. Heparin is degraded by the chemical and enzymatic pathway and its weight is reduced to 5000 Da. It acts like heparin, in that the pentasaccharide chain binds antithrombin.

But is does not have a binding effect like enoxaparin, so side effects such as bleeding and thrombocytopenia are fewer with enoxaparin. Dose adjustment must be implemented for patients with chronic kidney failure because it is mostly excreted via the kidneys. When compared with warfarin, DVT is less commonly seen via venography, but bleeding complications are increased. LMWHs do not prolong PTT, so it is not necessary to follow. The half-life if LMWH is 4.5 h. It is not used to patients who have epidural catheters [17].

Fondaparinux

Fondaparinux is a synthetic pentasaccharide and an indirect selective factor Xa inhibitor. It comprises five saccharide units, with a weight of 500 Da. It not only stops thrombus production but also stops thrombus growth. This also increases the effect of antithrombin. Its half-life is 17 h. After hip fracture and TKA, it was found to decrease the incidence of DVT venographically. It increases bleeding tendency. For patients weighing less than 50 kg and with renal failure, implementation is not recommended with permanent epidural catheter [18].

Idraparinux

The sulfated derivative of fondaparinux is idraparinux. Its half-life is 130 h.

Warfarin

Warfarin in an antagonist of vitamin K. It inhibits the formation of vitamin K-dependent coagulation factors II, VII, IX, and X. Formation of proteins C and S is also inhibited. This is followed with tests of international normalized ratio (INR) (INR range 2–2.5). Warfarin reduces symptomatic thromboembolic events. Bleeding is an undesired effect (vitamin K is given as treatment). The anticoagulant effect begins later (24–36 h) and the target INR value is reached on third day. as Although the anticoagulant level is a controversial topic, an INR value of 2 is sufficient for orthopedic surgery. Warfarin's advantages are that it is inexpensive and may be taken orally. Its disadvantages are the need for dose adjustment and blood monitorization. Patients with liver disease require careful dose adjustment and monitoring of blood. Drug interactions are possible. Use with nonsteroidal anti-inflammatory drugs increases the probability of bleeding. Patients fed with high nutritional values of vitamin K may need an increased dose to achieve the target INR. The effect of vitamin K is reversible within a few days, but its effect can be removed immediately by fresh frozen plasma [19].

Aspirin

Aspirin causes cyclooxygenase (COX) enzyme inhibition in platelets. As a result, thromboxane A2 cannot be formed and platelet aggregation does not occur. When used with mechanical prophylaxis, it may be as effective as LMWH. Its advantages are ease of use, low cost, and lower risk of bleeding. In TKA, THA, and hip fracture surgery there is evidence (Grade 1) for their use in prophylaxis of VTE for 10–15 days [20].

Dabigatran

Dabigatran is an oral direct thrombin (factor IIa) inhibitor. It is used 1–4 h after an operation. Patient compliance is good [21].

Melagatran

Melagatran is the active form of ximelagatran and is a thrombin inhibitor [22].

Hirudin and Argatroban

Hirudin and argatroban are direct thrombin inhibitors and are used in HIT.

Rivaroxaban

Rivaroxaban is an oral factor Xa inhibitor [23].

Guidelines

ACCP Guidelines

Many guidelines are referenced in the treatment of VTE. The most commonly used guideline is that of the ACCP. A new guideline is published every 4 years, and the latest was published in 2012. The recommendations are generated by taking into consideration 5 to 10 phase I studies performed by observers from outside of the committee. Recommendations are based on rates of profit and risk. According to this, strong advice is

Table 40.4 Padua score

Disease	Score
Active cancer	+3
Previous VTE (excluding superficial vein thrombosis)	+3
Reduced mobility	+3
Already known thrombophilic condition	+3
Recent (≤1 month) trauma and/or surgery	+2
Elderly Age (≥70 years)	+1
Heart and/or respiratory failure	+1
Acute MI and/or Ischemic Stroke	+1
Acute infection and/or rheumatologic disorder	+1
Obesity (BMI ≥30)	+1
Ongoing hormonal treatment	+1

Grade 1, weak advice is Grade 2. These are further divided to three parts, A, B, and C, according to the quality of the articles that support the recommendations.

Grade 1A: Strong recommendation, high-quality evidence level, the desired effects significantly surpass adverse effects, supported by randomized clinical studies (RCTs); it is recommended to use for many cases; it is difficult to change the decision.

Grade 1B: Strong recommendation, moderate evidence, supporting RCT has some mistakes, their significant level of desired effects surpass the undesirable effects; decisions may vary with very strong studies.

Grade 1C: Strong recommendation, low grade of evidence, supported by RCTs with serious errors, the desired effects significantly surpass unwanted effects, decision supported by good studies.

Grade 2A: Weak recommendation, undesired effects balanced with desired effects, supported by RCTs; further studies may change the decision.

2B Grade: Weak recommendation, any undesired effects counterbalance the desired effects; methodical mistakes in supporting RCTs; may change the decision.

Grade 2C: Weak recommendation, any undesired effects counterbalance desired effects, supported by RCTs with serious errors; decision can be changed.

Padua Score (VTE Risk Assessment Score)

In Padua Scores (Table 40.4), a total score of 4 or higher is considered a high risk of developing VTE. The risk in hospitalized patients is low in 60 %, 39.7 % score 3 and higher. In 11 % of high-risk patients and 0.3 % of low-risk patients, VTE developed. In patients who have high risk, 6.7 % develop DVT, 3.9 % develop nonfatal PE, and 0.4 % develop fatal PE [1]. According to the 2012 ACCP guidelines, instead of investigating DVT in all patients, patients were classified for pretest as low risk (DVT probability 5 %), moderate risk (DVT probability 17 %), and high risk (DVT probability 53 %) according to Wells Score (Grade 2B). Accordingly, pretests (D-dimer, Doppler ultrasonography, and venography) are planned [24].

Wells Score

For the patient:

- Is there any active cancer?
- Did he/she remained bedridden for more than 3 days or have major surgery within the past 4 weeks?
- Is there any swelling of calf of the leg more than 3 cm compared with the other leg?
- Is there swelling of the entire leg?
- Is there any evident superficial venous collaterals that are not varicose.
- Have had DVT before?
- Is there a localized tenderness in the deep venous system?

Table 40.5 VTE, PE, and DVT rates based on performing prophylaxis

	Beginning prophylaxis (0–14 days)	Extended prophylaxis (15–35 days)	Cumulative postop (0–35 days)
No prophylaxis	VTE % 2.80 PE % 1 DVT % 1.80	VTE % 1.5 PE % 0.5 DVT % 1	VTE % 4.3 PE % 1.5 DVT % 2.80
Prophylaxis with LMWH	VTE % 1.15 PE % 0.35 DVT % 0.80	VTE % 0.65 PE % 0.2 DVT % 0.45	VTE % 1.8 PE % 0.55 DVT % 1.25

- Is there any pitting symptomatic edema in the leg?
- Is there paralysis paresthesia? Or a recently implemented plaster cast on the leg? By such questions, classification can been done and preliminary tests planned [25].

According to the ACCP Guideline (February 2012)

- If DVT is detected in the thigh in humans, warfarin is initiated until an INR value of 2 is achieved. Simultaneously, heparin (standard or low molecular weight; subcutaneous or intravenous) or fondaparinux is started for 5 days (Grade 1B). If before the end of 5 days INR value rises to 3, heparin/fondaparinux is interrupted.
- If patients have high clinical suspicion of DVT, treatment is started without waiting for test results. If there is an intermediate level of suspected DVT, treatment can be delayed for up to 4 h while waiting for test results. If there is a low risk of DVT, treatment can be delayed for up to 24 h (Grade 2C).
- If isolated DVT is detected in the calf, most are asymptomatic and do not extend to the proximal and, therefore, do not require anticoagulant. But in 15 % of untreated patients, the distal DVT expands to proximal within 2 weeks and may cause PE. In patients with detected distal DVT, following is recommended with Doppler ultrasonography at 1–2 week intervals (Grade 2C).
- Treatment of acute DVT with low-molecular-weight heparin (enoxaparin, tinzaparin) or fondaparinux is preferred to standard heparin (Grade 2B/2C).
- If the patient's home environment is favorable (there is good social support, he or she has a phone, the patient can come to the hospital immediately) initial treatment of acute DVT is recommended to done at home (Grade 1B).
- Walking instead of bed rest is recommended for reducing post-thrombotic syndrome in patients who have acute DVT (Grade 2C) [20].

2012 ACCP Guidelines for Prevention of VTE in Patients Undergoing Orthopedic Surgery

- Although VTE is serious problem, complications after major orthopedic surgeries (THA, TKA, and hip fracture) started to decrease. When prophylaxis is planned according to the guidelines, the negative results of PE and DVT are reduced (Table 40.5).
- The authors prefer to do prophylaxis within 10–14 days after major orthopedic surgery rather than not do any. Prophylaxis with LMWH, fondaparinux, apixaban, dabigatran, rivaroxaban, low-dose unfractionated heparin (DDAH), adjusted-dose vitamin K antagonists, aspirin (all Grade 1B), or intermittent pneumatic compression devices (IPCDs) can be used (Grade 1C).
- In patients who will be undergoing major orthopedic surgery, initiating LMWH within 12 h preoperatively and postoperatively is preferred to initiating 4 or more hours earlier (Grade 1B).
- In patients undergoing TKA and THA surgery, regardless the duration of treatment and the simultaneous use of IPCD, we prefer LMWHs over fondaparinux, apixaban, dabigatran, rivaroxaban, and DDAH (all Grade 2B),

adjusted-dose vitamin K antagonists, or aspirin (all Grade 2C).
- We prefer to use thromboprophylaxis within 35 days or more instead of 10–14 days in patients undergoing major orthopedic surgery (Grade 2B).
- In patients undergoing major orthopedic surgery, IPCD use is recommended along with antithrombotic agents for long as they are in the hospital (Grade 2C).
- Patients undergoing major orthopedic surgery, apixaban or dabigatran is recommended if they refuse injection or if they cannot being injected regularly and cannot use an IPCD. As an alternative, rivaroxaban or adjusted-dose vitamin K antagonist is recommended (if not appropriate, apixaban and dabigatran) (Grade 1B).
- If there is a risk of bleeding in patients who will be undergoing major orthopedic surgery, antiplatelet agents should be interrupted and IPCD implementation is recommended (Grade 2C).
- After major orthopedic surgery, Doppler ultrasonography is not recommended in asymptomatic patients (Grade 1B).
- Prophylaxis is not recommended in patients with isolated injuries of the lower extremity (Grade 2C).
- Routine prophylaxis is not recommended in patients without a history of VTE (Grade 2B).
- If there is bleeding risk in patients undergoing major orthopedic surgery or pharmacological and mechanical prophylaxis are contraindicated, primary use of VCI filters is not recommended (Grade 2C) [20, 26].

AAOS Guidelines

These clinical guidelines have been developed by a group of volunteer doctors working in the AAOS and systematic review experts. This clinical practice-based guideline has made recommendations for prevention of venous thromboembolic diseases in patients undergoing elective hip and knee replacement surgery based on systematic examination of related articles. Suggestions are classified as strong, moderate, limited, ineffective, and consensus levels.

Strong level of advice: There is need for at least two or more high-quality scientific studies. Moderate suggestions: At least two or more moderate-quality scientific studies are needed. Limited suggestions: determined by at least two or more low-quality scientific works. Ineffective level advice: a single low-quality scientific study with contradictory evidence, does not allow making of recommendations. Consensus: lack of supporting evidence or a suggestion is made associated with treatment based on the expert opinion of the working group by considering the potential harm and benefits.

AAOS 2011 Guideline: Innovations

1. After total hip and knee replacement surgery, routine Doppler ultrasound is not recommended (Grade of recommendation: Strong).
2. Patients after total hip and knee replacement surgery are at risk for VTE, so it should be evaluated to see whether patient has a history of DVT (Grade of recommendation: Limited).
3. In patients with a history of DVT for whom THA or TKA are planned, routine investigation of DVT is not recommended (Grade of recommendation: Ineffective).
4. In patients who are scheduled for THA and TKA with a tendency to bleeding and bleeding complications, even though there is no reliable evidence, the working group thinks that hemorrhagic disease (hemophilia) and liver diseases should be taken into consideration due to increases in bleeding and bleeding-related complications (Grade of recommendation: there is consensus).
5. In patients will be undergoing elective THA and TKA, antiplatelet drugs (aspirin, clopidogrel) should be discontinued (Grade of recommendation: medium).
6. Pharmacological drugs and/or mechanical compressive devices are protected from VTE in patients undergoing THA and TKA (Grade of recommendation: medium).
7. The recommendation of the working group is that decision making regarding the duration of prophylaxis is determined by discussion between the doctor and patient (Grade of recommendation: there is consensus).

8. Although there is no reliable evidence in patients undergoing THA and TKA, the working group recommends prophylaxis of VTE with pharmacological measures and mechanical pressure devices (Grade of recommendation: there is consensus).
9. Although there is no reliable evidence, the study group thinks that for patients who undergoing elective THA and TKA, early movement is an inexpensive modality with minimal risk and is convenient for current practice (Grade of recommendation: there is consensus).
10. In patients pending for TKA or THA, if a bleeding tendency (hemophilia) or liver disease is present, even though there is no reliable evidence, the study group recommends the use of pneumatic devices for VTE prophylaxis.
11. Although neuraxial (intrathecal, epidural, spinal) anesthesia has the effect of reducing blood loss in patients with the hip and knee replacement, there is no protective effect against VTE based on evidence-based recommendation (Grade of recommendation: medium).
12. According to current evidence, when chemoprophylaxis is contraindicated and in patients with known residual VTE, use of inferior vena cava filters is controversial (Grade of recommendation: Ineffective) [27].

References

1. Barbar S, Noventa F, Rossetto V, Ferrari A, Brandolin B, Perlati M, De Bon E, Tormene D, Pagnan A, Prandoni P (2010) A risk assessment model for the identification of hospitalized medical patients at risk for venous thromboembolism: the Padua Prediction Score. J Thromb Haemost 8:2450–2457
2. Yeung V, Formal C (2015) Lower extremity hemorrhage in patients with spinal cord injury receiving enoxaparin therapy. J Spinal Cord Med 38:236–8
3. Virchow R (1856) "Thrombose und Embolie. Gefässentzündung und septische Infektion". Gesammelte Abhandlungen zur wissenschaftlichen Medicin (in German). Von Meidinger & Sohn, Frankfurt am Main, pp 219–732, Matzdorff AC, Bell WR (1998) Thrombosis and embolie (1846–1856). Science History Publications, Canton
4. Pallister CJ, Watson MS (2010) Haematology. Scion Publishing, United Kingdom, pp 336–347
5. Gebbink MF (2011) Tissue-type plasminogen activator-mediated plasminogen activation and contact activation, implications in and beyond haemostasis. J Thromb Haemost 9 Suppl 1:174–178
6. Anderson FA Jr, Wheeler HB, Goldberg RJ, Hosmer DW, Patwardhan NA, Jovanovic B, Forcier A, Dalen JEA (1991) Population-based perspective of the hospital incidence and case-fatality rates of deep vein thrombosis and pulmonary embolism. The Worcester DVT Study. Arch Intern Med 151(5):933–938
7. Heit JA, Silverstein MD, Mohr DN et al (2000) Risk factors for deep vein thrombosis and pulmonary embolism: a population-based case-control study. Arch Intern Med 160:809–815
8. Beksac B, Gonzalez DV, Salvati EA (2006) Thromboembolic disease after total hip arthroplasty: who is at risk? Clin Orthop Relat Res 453:211–224
9. Kennedy M, Andreescu ACM, Greenblatt MS, Jiang H, Thomas CA, Chassereau L, Wong C, Durda P, Cushman M (2005) Factor V Leiden, prothrombin 20210A and the risk of venous thrombosis among cancer patients. Br J Haematol 128(3):386–388
10. Egeberg O (1965) Inherited antithrombin deficiency causing thrombophilia. Thromb Diath Haemorrh 13:516–530
11. Wells PS, Lensing AW, Davidson BL et al (1995) Accuracy of ultrasound for the diagnosis of deep vein thrombosis in asymptomatic patients after orthopedic surgery. A meta-analysis. Ann Intern Med 122:47–53
12. Wells PS, Anderson DR, Rodger M, Forgie M, Kearon C, Dreyer J, Kovacs G, Mitchell M, Lewandowski B, Kovacs MJ (2003) Evaluation of D-dimer in the diagnosis of suspected deep-vein thrombosis. N Engl J Med 349(13):1227–1235
13. Morris RJ, Woodcock JP (2004) Evidence-based compression prevention of stasis and deep vein thrombosis. Ann Surg 239:162–171
14. Patel SH, Patel R (2007) Inferior vena cava filters for recurrent thrombosis current evidence. Tex Heart Inst J 34:187–194
15. Baughman RA, Kapoor SC, Agarval RK et al (1998) Oral delivery of anticoagulant doses of heparin; a randomized, double-blind, controlled study in humans. Circulation 98:1610–1615
16. Levine MN, Hirsh J, Gent M et al (1994) A randomized trial comparing activated thromboplastin time with heparin assay in patients with acute venous thromboembolism requiring large daily doses of heparin. Arch Intern Med 154:49–56
17. Whang PG, Lieberman JR (2002) Low-molecular-weight heparin. J Am Acad Orthop Surg 10(5):299–302
18. Cohen AT, Davidson BL, Gallus AS et al (2006) Efficacy and safety of fondaparinux for the prevention of VTE in older acute medical patients. BMJ 332:325–329
19. Ansell J, Hirsh J, Dalen J et al (2000) Managing oral anticoagulant therapy. Chest 119(Suppl):22–38
20. Kearon C et al (2012) Antithrombotic therapy for VTE disease: antithrombotic therapy and prevention of thrombosis, 9th ed: American College of Chest

Physicians evidence-based clinical practice guideline. Chest 141(2_suppl):e419–e494S
21. Guyatt GH, Akl EA, Crowther M, Gutterman DD, Schuünemann HJ (2012) FCCP and for the American College of Chest Physicians antithrombotic therapy and prevention of thrombosis panel. Chest 141(2-suppl):7–47
22. Colwell C, Mouret P (2005) Ximelagatran for the prevention of venous thromboembolism following elective hip or knee replacement surgery. Semin Vasc Med 5(3):266–275
23. Cao YB, Zhang JD, Shen H, Jiang YY (2010) Rivaroxaban versus enoxaparin for thromboprophylaxis after total hip or knee arthroplasty: a meta-analysis of randomized controlled trials. Eur J Clin Pharmacol 66(11):1099–1108
24. Wells PS, Owen C, Doucette S, Ferguson D, Tran H (2006) Does this patient have deep vein thrombosis? JAMA 295(2):199–207
25. Scarvelis, Wells PS (2006) Diagnosis and treatment of deep-vein thrombosis. CMAJ 17(9):1087–1092
26. Bates SM et al (2012) Diagnosis of DVT. Antithrombotic therapy and prevention of thrombosis, 9th ed: American College of Chest Physicians evidence-based clinical practice guidelines. Chest 141:e351S–e418S
27. Johanson NA, Lachiewicz PF, Lieberman JR, Lotke PA, Parvizi J, Pellegrini V, Stringer TA, Tornetta P III, Haralson RH III, Watters WC III (2009) Prevention of symptomatic pulmonary embolism in patients undergoing total hip or knee arthroplasty. J Am Acad Orthop Surg 17:183–196

Nonsteroidal Anti-inflammatory Drugs (NSAIDs) and Corticosteroids

41

Osman Tuğrul Eren, Raffi Armağan, and Mehmet Ali Talmaç

Abstract

All nonsteroidal anti-inflammatory drugs (NSAIDs), including selective COX-2 inhibitors, have anti-inflammatory analgesic and antipyretic effects, and some of them also have antithrombotic effects. Although NSAIDs are structurally organic acids, chemically they constitute a heterogeneous group. Long-term use of NSAIDs may cause many side effects, especially in older patients, so they should be used cautiously. Corticosteroids effectively suppress inflammation, and they are used in the treatment of both systemic and local inflammation. This chapter mainly discusses local intra-articular injections of steroids, to the tendon sheath, in bursitis and simple bone cysts.

Learning Outcomes

The aim of this chapter is to explain the structure, mechanism of action, contraindications, and side effects of nonsteroidal anti-inflammatory drugs (NSAIDs) and corticosteroids, medicines that are frequently used in clinical orthopedic therapy.

Clinical Relevance

Is there a clinical risk of prescribing NSAIDs?

A 54-year-old female patient was admitted to our outpatient clinic with the complaint of bilateral knee pain, morning stiffness, and decreased walking distance. The diagnosis was bilateral grade 2 osteoarthritis. Activity modification, weight loss, and an NSAID were prescribed. After 3 weeks, the patient returned for a control visit. She was happy with the pain control in her knees with the increase in walking distance, but she had been admitted to the emergency department with stomach pain on the 10th day of treatment. Gastroscopy (endoscopy) revealed hemorrhagic ulcers of the gut. Treatment was initiated with pro-

O.T. Eren (✉) • R. Armağan • M.A. Talmaç
Orthopaedics and Traumatology,
Şişli Etfal Training and Research Hospital,
Istanbul, Turkey
e-mail: tugruleren@hotmail.com;
rafiarmagan@gmail.com; drtalmac2@gmail.com

F. Korkusuz (ed.), *Musculoskeletal Research and Basic Science*,
DOI 10.1007/978-3-319-20777-3_41

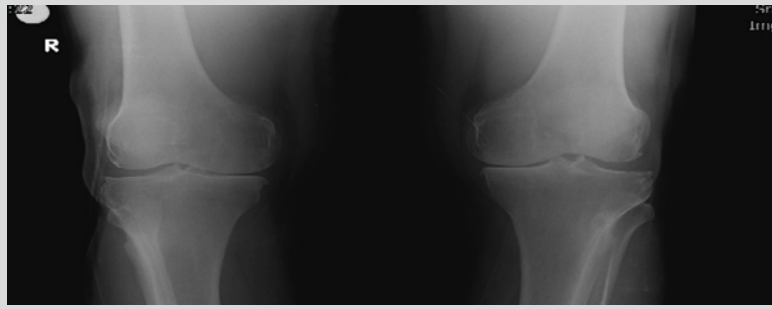

ton pump inhibitors (PPIs). We changed our treatment to viscosupplementation therapy.

Nonsteroidal drugs have a wide spectrum of effects on metabolism that can have some relevant consequences on respiratory, gastrointestinal (GI), renal, hematological, and bone metabolism [1]. Use of these drugs as pain killers is accompanied by the risk of side effects in these systems. The most frequent complication is GI intolerance, which can have dangerous consequences such as fatal gastrointestinal bleeding. Countermeasures should be taken by prophylaxis with PPI drugs.

Introduction

NSAIDs show their effect through inhibition of the cyclooxygenase (COX) enzyme [2]. The COX enzyme provides arachidonic enzyme metabolism and therefore prostaglandin (Fig. 41.1) and thromboxane synthesis. The analgesic and anti-inflammatory effects of NSAIDs occur by inhibition of prostaglandin synthesis [3]. Prostaglandins have little effect on pain; other mediators of inflammation can cause pain. Although NSAIDs do not affect other mediators of the inflammatory response, they cause a decrease in inflammation. All NSAIDs have different COX inhibition mechanisms, and their analgesic, antipyretic, and anti-inflammatory effects in high doses are different from one another [4].

Anti-inflammatory Effect

NSAIDs inhibit the activation of neutrophil leucocytes by the effects that cause inflammation and accompanying events (such as selectin and integrin up-regulation, adhesion to the microvascular wall, and extravasation). They reduce the synthesis of prostaglandins (PGE2, PGI2), which cause vasodilation and edema. They inhibit the activation of polymorphonuclear leukocytes by various stimuli. NSAIDs bind to and inactivate active oxygen radicals and reduce inflammation. They stabilize the lysosome membrane. Because NSAIDs are acidic drugs, they can easily enter into the cells in inflammation and gather there [5, 6].

Analgesic Effect

NSAIDs act by inhibiting the synthesis of prostacyclin and prostaglandin (especially PGE2), which do not create pain alone but increase the awareness of nerve endings to algesic factors (bradykinin, histamine, serotonin, substance P, and angiotensin) and strengthen the pain constructive effects. In addition to inhibiting cyclooxygenase peripherally in their analgesic effects, some NSAIDs (such as dipyrone) play a role in inhibiting in the central nervous system [7] (Table 41.1).

Antipyretic Effect

Pyrogenic cytokines, released by inflammatory cells that are stimulated by bacterial toxins (interleukin (IL)-1 and tumor necrosis factor (TNF)-alpha), depend on the blocking effect in the thermoregulatory center via prostaglandins in the hypothalamus. They thereby reduce fever by

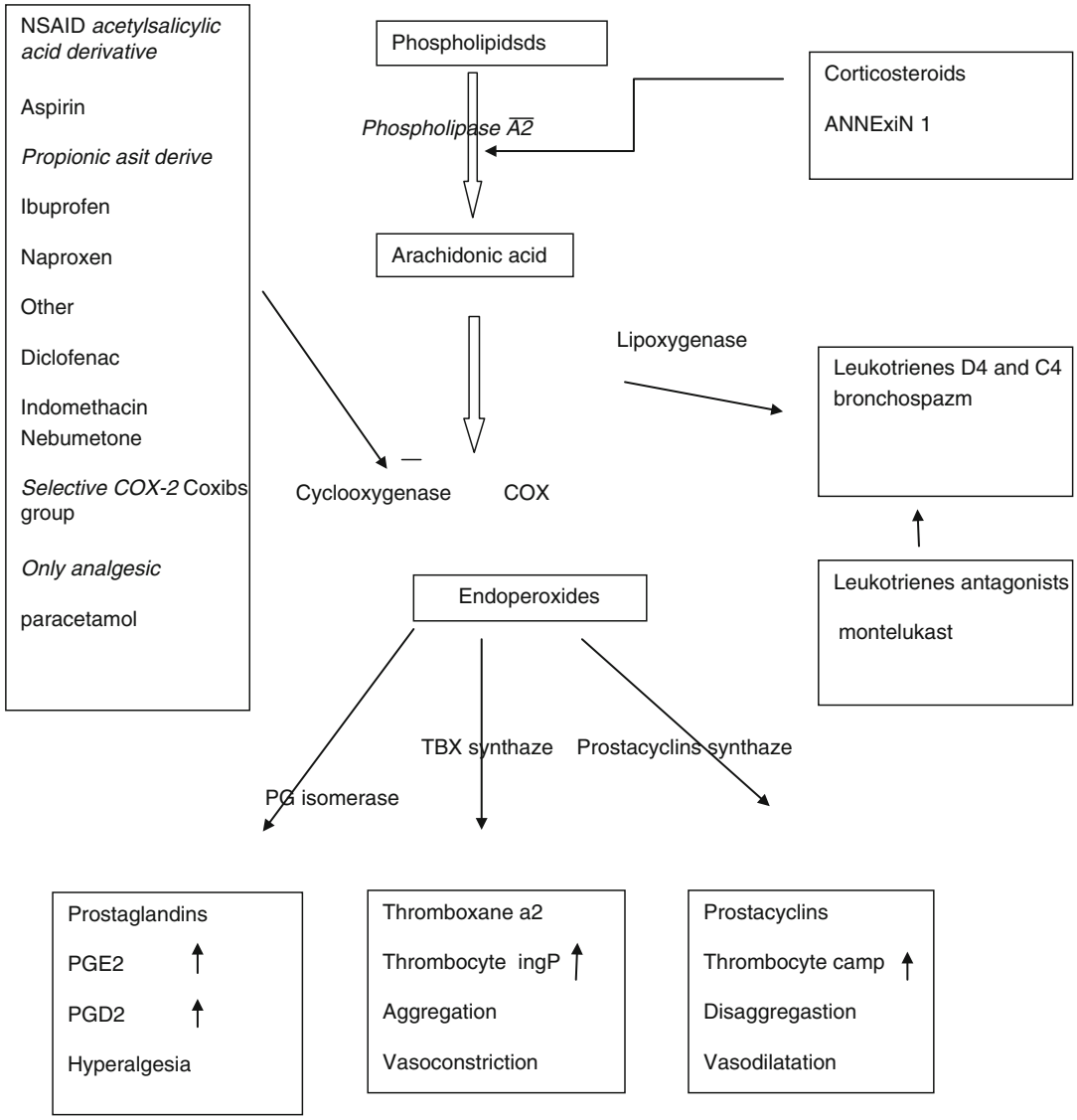

Fig. 41.1 Mechanism of action of NSAIDs and corticosteroids in phospholipid and prostaglandin metabolism

Table 41.1 Physiological and pathological effects of prostaglandins

Functions of prostaglandins	
Pathological effects	Physiological effects
Fever	Fever control
Myocardium	Bronchial tonus
Asthma	Blood pressure
Thrombosis	Gastric mucosa
Ulcers	Renal function
Diarrhea	Bowel movement
Dysmenorrhea	Semen viability
Pain	Cell protector
Inflammation	
Bone degeneration	

increasing heat loss. They do not affect normal temperature and hypothermia. It has been found that PGE-2 plays a role in the endogenous fever formation mechanism. Pyojenic cytokines are produced by the enzyme COX-2 and cause fever with the enzyme IL-1. It is suggested that inhibition of the COX-2 enzyme would have a greater antipyretic effect [8, 9].

NSAIDs and COX Inhibition

In the amino acid sequence of the COX-2 enzyme there is valine, which is a smaller amino acid, instead of isoleucine (COX-1) at the 120th position. The COX-2 enzyme has a small gap in the inner

surface of the enzyme. The ability to connect to this gap determines a drug's COX-2 specificity. The two isoenzymes of COX (COX-1 and COX-2) are responsible for the side effects in the gastrointestinal system (GIS) and NSAIDs' anti-inflammatory effects. The COX-1 isoenzyme is present in many tissues. It allows the formation of homeostatic and cytoprotective prostanoids, which are responsible for physiological functions in organs such as the kidneys and platelets [2, 10]. Well-known side effects of NSAIDs appear with the inhibition of this enzyme. The COX-2 enzyme is induced only by simulation. Synthesis of proinflammatory PG in leukocytes, vascular smooth muscle cells, human rheumatoid synoviocytes, and brain neurons is stimulated with cytokines, mitogens, and endotoxins. The analgesic anti-inflammatory activity of COX-2 is the same as with the classic NSAID, but there are no gastrointestinal, platelet, or renal side effects. However, the effect of the COX-2 inhibitor on fracture healing is different.

NSAIDs have COX-1/COX-2 inhibition rates that have been determined by many different laboratories. Many NSAIDs (nonselective NSAIDs) such as aspirin, naproxen, indomethacin, tolmetin, piroxicam, and ibuprofen cause inhibition in different ratios in the two isoenzymes. It is accepted that COX-1 inhibition of NSAIDs such as etodolac and meloxicam (COX-2 selective) is less than with COX-2 and it is also accepted that COX-2-specific NSAIDs do not effectively inhibit COX-1 [11]. COX-2 is inhibited most powerfully by meloxicam. The GIS side effects are significantly lower compared with classic NSAIDs. Thus, the use of COX-2-specific NSAIDs, which came into use because it was thought that they had no side effects on the stomach, are today discussed and restricted because of the uncertainties of cardiac side effects [4]. Studies show that the COX-2 enzyme inhibits 100.054 more than COX-1 enzyme. NSAIDs that inhibit COX-1 also show an antiaggregant, or antiplatelet, effect with the inhibition of COX-1, which is the only isoform in the platelets. Aspirin acetylates platelet COX-1 irreversibly and, thus, the antiaggregant effect lasts up to 4–6 days until new platelets are made by bone marrow. With other NSAIDs, the inhibition of platelet aggregation is reversible and dependent on the concentration of a drug in the platelets [12]. The antiaggregant effect of aspirin is the reason for its popular use in cardiovascular prophylaxis. But it is also shown that if aspirin is taken with other NSAIDs, there may be an interaction in terms of the antiaggregant effect. The effects of NSAIDs on cartilage have been under discussion for years. Although some animal experiments have shown that NSAIDs may have negative effects on cartilage, there is no clear information about the effects on humans [13].

NSAID Clinical Uses

NSAIDs implement analgesia with both regional and central effects in clinical and soft tissue injuries. NSAIDs are commonly used in the treatment of such diseases as rheumatoid arthritis, gouty arthritis, ankylosing spondylitis, systemic lupus erythematosus and other connective tissue disease, juvenile chronic arthritis, and osteoarthritis because of their anti-inflammatory and analgesic effects. It is also chosen for treatment of soft tissue lesions such as tendinitis, bursitis, tenosynovitis, and periarteritis; back, neck, and cancer pain; dysmenorrhea; and oral and maxillofacial surgery [14]. It is thought that, in the future, after the side effect profile gains clarity, particularly COX-2-specific (coxibs group) drugs will be used in the prophylaxis of malignancies such as colorectal and prostate cancers and Alzheimer's disease. The most commonly used NSAIDs and their characteristics are listed in Table 41.2.

NSAIDs affect healing negatively by inhibiting prostaglandin synthesis in fracture healing (Table 41.3).

Table 41.2 Comparison of the therapeutic effects of NSAIDs and steroids with narcotics

	Analgesic	Anti-inflammatory	Antipyretic	Local
Narcotics	+++	–	–	–
Glucocorticoids	+	+++	–	+
NSAID	++	++	+/–	+

Table 41.3 NSAIDs and their effects

1. Those with analgesic effects and low grades of anti-inflammatory effects
(a) Aniline derivatives: paracetamol (acetaminophen)
Analgesic antipyretic – but there are no antithrombotic and anti-inflammatory effects
2. Those with analgesic effects and low-to-moderate intensity of anti-inflammatory effects
(a) Propionic acid derivatives: ibuprofen, fenoprofen, ketoprofen, naproxen
Analgesic anti-inflammatory effect
(b) Fenamic acid derivatives: mefenamic acid
3. Those with analgesic effects and high anti-inflammatory effects
(a) Salicylic acid derivatives: aspirin, sodium salicylate
(b) Pyrazolone derivatives: propyphenazone, aminopyrine, metamizol, phenylbutazone
Analgesic, antipyretic, antispasmodic effect, no anti-inflammatory effect
(c) Phenylacetic acid derivatives: diclofenac, etodolac, fenclofenac
Strong anti-inflammatory analgesic
(d) Indole derivatives: indomethacin, sulindac, tolmetin
More anti-inflammatory and antipyretic than aspirin
(e) Oxicam derivatives: piroxicam, meloxicam, tenoxicam
Long-acting analgesic
4. COX-2 Inhibitors: celecoxib, rofecoxib and parecoxib
Usage is controversial

Salicylates

Although many drugs are in use, aspirin is still the most widely used analgesic, antipyretic, and anti-inflammatory drug. Salicylates often act through the salicylic acid content in them. Aspirin is used for low-intensity pains such as myalgia headache and arthralgia, and it effectively reduces increased body temperature. Low doses of aspirin (<100 mg) are widely used for cardioprotective effects. If healthy people use aspirin, it prolongs their bleeding time. A single 325-mg dose of aspirin extends a normal individual's bleeding time by 2 times, for a period of 4–7 days. Thrombocytes reduce COX's irreversible acetylation and consequently the formation of thromboxane A2 until a sufficient number of unmodified thrombocytes is formed from the megakaryocytes' precursors [15]. If possible, aspirin therapy should be discontinued 7 days before surgery. Aspirin use should be avoided in patients with severe liver disease, hypoprothrombinemia, vitamin K deficiency, and hemophilia [16]. There is no specific antidote to salicylate poisoning. Treatment should start with rapid assessment and medical emergency intervention.

Table 41.4 Studies on the effects of NSAIDs on fracture healing

Negative effects on fracture healing	No retarding effect on fracture healing
Altaian RD, *J Orthop Trauma* 1995	Adolphson P, *Arch Orthop Trauma Surg* 1993
Beck A, *Arch Orthop Trauma Surg* 2003	Bichara J, *J Perodontol* 1993
Giordano V, *Injury* 2003	Bragger IL, *J Perodontal Res* 1997
Glassman S, *Spine* 1998	Moore KD, *J Bone Joint Surg Br* 1998
Ho M, *Pharmacology* 1998	

Para-aminophenol Types (Paracetamol)

Paracetamol is an effective alternative to aspirin as an antipyretic, analgesic agent; however, its anti-inflammatory effect is very low [17]. It is effective as a painkiller in noninflammatory osteoarthritis but cannot be used in place of aspirin or other NSAIDs in chronic inflammatory diseases such as rheumatoid arthritis. Paracetamol is well tolerated and the incidence of GI side effects is low. Acute overdose can cause serious liver damage. Chronic use of less than 2 g per day does not cause liver dysfunction [18] (Table 41.4).

Acetic Acid Derivatives (Indomethacin, Sulindac, and Etodolac)

High rates of intolerance restrict the long-term use of indomethacin as an analgesic. Indomethacin successfully removes joint pain, swelling, and tenderness; improves grip strength; and reduces the duration of morning stiffness [14]. Typical usage is 25 mg, two to three times a day. It is

more effective than aspirin in the treatment of osteoarthritis and ankylosing spondylitis, if well tolerated. It is approved by the US Food and Drug Administration (FDA) in the closure of patent ductus arteriosus [19].

Sulindac is less potent by half than indomethacin. It is used in the treatment of ankylosing spondylitis, rheumatoid arthritis, osteoarthritis, and acute gout. Its analgesic and anti-inflammatory effect is similar to aspirin. It is used to prevent colon cancer in familial adenomatous polyposis [20].

Etodolac is an acetic acid derivative with some COX-2 selectivity, and its GI side effects are less than other NSAIDs. A single dose (200–400 mg) is effective for 6–8 h after oral intake for pain after surgery [21].

Fenamate

This family consists of meclofenamic acids, mefenamic acids, and flufenamic acids. There are no definitive therapeutic advantages when compared with other common NSAIDS. Fenamates frequently cause GI side effects. They are not recommended for use in children and pregnant women. In general, they are used for treatment of soft tissue injuries, dysmenorrhea, and short-term pain relief in rheumatoid arthritis and osteoarthritis.

Tolmetin, Ketorolac, and Diclofenac

Tolmetin and ketorolac are derivates of heteroaryl acetic acid and are similar to each other structurally, despite their different pharmacological properties. Diclofenac, which was developed as an anti-inflammatory agent, is a derivate of phenyl acetic acid. Tolmetin is used in the treatment of osteoarthritis, rheumatoid arthritis, and juvenile rheumatoid arthritis, and it has similar therapeutic efficacy to aspirin. The recommended maximum daily dose is 2 g. Ketorolac is an effective analgesic but it is only a moderately effective anti-inflammatory drug. Ketorolac is used via oral, intravenous, and intramuscular routes for medium and intense pain as a short-term alternative to opioids [22].

Diclofenac is the most widely used NSAID in Europe. Lumiracoxib, which is a selective COX-2 inhibitor, is a diclofenac analogue. It is used for long-term treatment of ankylosing spondylitis, rheumatoid arthritis, and osteoarthritis [23].

Propionic Acid Derivatives

Propionic acid derivatives are used for rheumatoid arthritis, osteoarthritis, and ankylosing spondylitis and in the symptomatic treatment of acute gouty arthritis or acute tendinitis, bursitis, and primary dysmenorrhea. The ibuprofen propionic acid class is one of the widely used NSAIDs in the United States.

Ibuprofen tablets are available in dose ranges of 200–800 mg. For the treatment of rheumatoid arthritis and osteoarthritis, doses can be increased up to 800 mg, four times a day. It is better tolerated than aspirin and indomethacin. Its half-life is approximately 2 h. Slow balancing in the synovial space continues after a decrease of plasma values for an antiarthritic effect [24].

Other propionic acid derivatives include the following:

Naproxen is completely absorbed after oral intake. Naproxen metabolites are completely excreted in the urine. GIS effects occur with the same frequency as with indomethacin [25].

Oral doses of fenoprofen are easily absorbed, but only 85 % is absorbed. Its half life is 3 h. Side effects are similar to those with ibuprofen.

Ketoprofen, in addition to COX inhibition, stabilizes lysosomal membranes and may antagonize the effects of bradykinin.

Flurbiprofen's pharmacological properties, therapeutic indications, and side effects are similar to other propionic acid derivatives.

Oxaprozin may be used once a day because its half life is 40–60 h.

Enolic Acid Derivates (Oxicams)

Oxicam derivatives, which inhibit COX-1 and COX-2, and have anti-inflammatory, analgesic,

and antipyretic activity, are enolic acids. In general, they are nonselective COX inhibitors, but meloxicam has in vitro COX-2 selectivity. Their effects are similar to aspirin, indomethacin, or naproxen in long-term treatment of osteoarthritis or rheumatoid arthritis.

Piroxicam is used as an anti-inflammatory agent. Piroxicam can inhibit neutrophil functions, and it is believed that this effect is independent of COX inhibition. Thus, it is thought that there is an additional anti-inflammatory mechanism of action like the inhibition of collagenase and proteoglycanase in cartilage. It is used for treatment of osteoarthritis or rheumatoid arthritis.

Meloxicam has received FDA approval for use in osteoarthritis. For rheumatoid arthritis and osteoarthritis, the recommended dose is 7.5–15 mg/day; it has shown important clinical efficacy and has a low incidence of side effects [26].

Nabumetone is used for its anti-inflammatory effect. It has been shown to have important clinical efficacy in the treatment of rheumatoid arthritis and osteoarthritis and to have a low incidence of side effects.

Pyrazolone Derivatives

Phenylbutazone, oxyphenbutazone, antipyrine, dipyrone, and aminopyrine are pyrazolone derivatives. Antipyrine ear drops are now available in the United States. They have been used clinically for many years, but they have been withdrawn from use because they cause irreversible agranulocytosis [27].

Coxibs (Selective COX-2 Inhibitors)

Three members of the coxib class are approved for use in the United States and Europe. Rofecoxib and valdecoxib have been withdrawn from the market because of their undesirable side effect profile. Parecoxib and etoricoxib has been approved in Europe and are presently undergoing evaluation in the United States. The drug lumiracoxib is under investigation in Europe and the United States. Current evidence does not support the use of coxibs as the first choice of NSAIDs. Celecoxib has been approved in the chemoprophylaxis of polyposis coli. The use of celecoxib is limited because of adverse effects such as hypertension, edema, myocardial infarction, stroke, abd liver failure [28].

Apazone (Azapropazone)

Apazone (azapropazone) is one of the most widely used NSAIDs and has anti-inflammatory, uricosuric, analgesic, and antipyretic activity. Although it is not available in the United States, it is available in Europe. Its functions include neutrophil migration, degranulation, and inhibition of superoxide production [28].

Nimesulide

Nimesulide is a sulfanilamide compound that is used in Europe. It is a compound similar to celecoxib that exhibits COX-2 selectivity in a whole blood test. It is anti-inflammatory, analgesic, and antipyretic and has a low incidence of adverse GIS effects [29].

Common Traits of NSAIDs

Generally, most NSAIDs are absorbed rapidly and nearly complete after oral intake. Many are converted to inactive metabolites in the liver and excreted in the urine. Some NSAIDs and their metabolites are excreted in the bile. All NSAIDs are structures of organic acids, and they attach to plasma proteins at high rates (98–95 %) [30]. In inflamed tissue, pH drops and plasma proteins become more permeable. Some factors may facilitate the collection NSAIDs in these tissues because the pH of the medium decreases, the drug solubility in oil increases, and, hence, the non-ionizing portion is increased. Thus, the association of the increase in the drug with the lipid structure of cell membranes is visible. However, acid has a tendency to accumulate in these areas, increasing the risk of side effects in the stomach and renal medulla caused by the acidic environment.

Toxicity is the most important side effects of NSAIDs. Toxic symptoms occur in % 20 of people who use NSAIDs. Long-term use of high doses of these drugs, especially for older patients (+65), is associated with more frequently with side effects. Gastrointestinal side effects are the most important. Loss of the gastric mucosa is a consequence of the inhibition of prostaglandin synthesis. Prostaglandins reduce gastric acid secretion and increase the blood flow of the gastric mucosa, thus protecting the stomach cells. As a result of the inhibition of prostaglandin synthesis, mucosal ischemia occurs and the protective layer of the gastric mucosa is lost [1]. NSAIDs also impair the function of thromboxaneA2, which is responsible for vasoconstriction and platelet aggregation. Therefore, NSAIDs should be used carefully as they can cause gastrointestinal bleeding in patients with gastrointestinal disorders. Thirty percent of NSAID-induced stomach ulcers require inpatient treatment.

Another important side effect is renal toxicity. Prostaglandins are produced in the glomeruli and medulla of the kidney and show strong a vasodilator effect in undulant arterioles. Prostaglandins are an important regulator of renal blood flow and the glomerular filtration process. NSAIDs may lead to acute renal failure in patients with liver, heart, or kidney disease.

Other side effects include bronchospasm, rash, a decrease in platelet function, tinnitus, headache, and hepatitis. Valdecoxib and rofecoxib have been removed from market because they caused an increase in the risk of myocardial infarction and stroke. In addition, some NSAIDs in selected in vitro experiments have been found to cause damage in the articular cartilage [13].

Corticosteroids

Corticosteroids are 21-carbon steroid hormones produced in the adrenal glands. These hormones interact with DNA and RNA in the nucleus and thus act on many tissues in the body [31]. Corticosteroids are used in treating many different diseases of the musculoskeletal system because of their anti-inflammatory effects. These anti-inflammatory effects inhibit the synthesis of several molecules, called leukotrienes, prostaglandins, and thromboxanes. This effect, along with secondary inhibition of phospholipase A2, occurs both as a result of arachidonic acid metabolism and lipoxygenase inhibition of COX. Corticosteroid injections are give, intra-articularly and in the tendon sheath and bursa. Injectable corticosteroids have different solubility and half-life properties. Generally, short- and medium-acting (many of them water-soluble) corticosteroids are preferred for acute cases, and long-acting (insoluble in water) are selected for chronic conditions. A mix of short- and long-acting corticosteroids are used in more serious inflammation. The steroid dose varies depending on where the injection will be given. When using prednisolone tebutate in small joints (hands and feet), the dose is 2.5–10 mg; for medium-sized joints (wrist, elbow), 10–25 mg; for knee, shoulder, and ankle, 20–50 mg; and for the sciatic nerve, 20–40 mg. A protracted time between doses is recommended, with shortest repetition period being 4 weeks [32].

Intra-articular Injections

Corticosteroids provide an additional treatment option in osteoarthritis and rheumatoid arthritis due to the maximum local impact of intra-articular steroid injection and the minimal systemic effects. The implementation of intra-articular steroids suppresses angiogenesis. Adding neutrophils to the joint limits production of inflammatory mediators. A few controlled studies have been identified that do not show long-term efficacy of intra-articular corticosteroid injection in hip and knee arthrosis [33, 34]. Intra-articular corticosteroid injection compared with placebo in knee arthrosis showed a significant reduction in pain in the first week. However, similar results were obtained in both groups after 4 weeks. Corticosteroid injection is used to reduce pain and swelling in some patients awaiting joint replacement surgery because of the short-term benefits. Small joints, like the metacarpophalangeal, carpometacarpal, and acromio-

clavicular joints, were found to be responsive corticosteroid injections. These results are probably due to the dose not imposing a burden on these small joints.

Side Effects of Corticosteroids

There are some side effects of intra-articular steroid injection, including arthropathy, systemic absorption effects, intra-articular ligament weakness, flushing, iatrogenic infections, skin changes, and hyperglycemia for diabetics. Corticosteroid-induced arthropathy is controversial because, after injection, both protective and detrimental effects are seen. Therefore, it is difficult to determine whether the arthropathy is caused by the injection or process of disease progression. Intra-articular injections should especially be avoided in large joints that carry load, and load should not be carried in the first 24 h after injection. Injection of steroids into the synovium may cause suppression of the hypothalamic-pituitary-adrenal gland pathway, but it is not clinically observed. To avoid suppression of the adrenal gland should be done just a great addition injection. Infection is rarely seen if attention is paid to ensuring sterile conditions. Synovial fluid should be aspirated using sterile gloves, and the skin should be cleaned with an antiseptic solution. Skin atrophy and hypopigmentation have been reported after frequent steroid injections. The cause is inappropriate positioning of the injection needle and administration of the injection at very high pressure [32].

Contraindications of Intra-articular Corticosteroid Injections

Intra-articular corticosteroid injections are not recommended in the following situations: a known infection is present, hypersensitivity, osteochondral fractures, in patients who will be undergoing joint replacement surgery a few weeks before surgery, patients with bleeding disorders [32, 35].

Extra-articular Injection

Inflammation in the tendons, ligaments, and bursa is usually idiopathic and self-limiting. Local corticosteroids are often used clinically in the treatment of these pathologies. Extra-articular injections are widely used in traumatic lesions of the medial collateral at the elbow, ankle bond, and extra-articular joints of knee. The ideal intervention is injection into the peritendinous tissue rather than the tendon itself. The most important complication of this injection is tendon rupture. Inflammation is inhibited by steroid injection during the beginning period of healing process. Corticosteroid impair tendon structure by affecting collagen synthesis negatively because of the formation of collagen with a large proportion of the dry weight of the tendon. According to biomechanical studies [34], bonds that are newly injured and are treated with steroids and bonds that are not treated with steroids have same tension, but bonds that are treated with steroid are ruptured by clear effect. The same effect was seen with steroid injections given after the inflammatory phase (after 1 week). This indicates that steroids affect another mechanism besides inflammation. The use of corticosteroid injections is a clinically controversial topic in acute ligament injuries.

Tendinitis and Bursitis

Tendinitis, tenosynovitis, and bursitis react differently to corticosteroid injections. As in joints, corticosteroids should be injected into the peritendinous region instead of tendon itself. Tenosynovitis of the thumb flexors is the most common pathology. Successful results have been reported in 95 % of patients. The most successful results have been observed in single-finger involvement and those who have not clarify for more than 4 months. The success rate is 60 % in De Quervain's tenosynovitis. The success rate in external epicondylitis is highly variable and relapse often occurs. Good response is received to treatment after a bit of implementation. The use of corticosteroids in Achilles tendinitis is not

conclusive, and tendon ruptures are seen. In some studies [34], good results were observed in rotator cuff tendinitis, but in others there was no difference with placebo. Effective responses have been seen in the trochanteric and olecranon bursae but corticosteroid implementation was found to be less effective in of the calcaneal and prepatellar bursa [32].

Use in Unicameral Bone Cysts

A unicameral bone cyst (UBC) is an atrophic osteolytic condition, generally seen in the metaphyses of the long bones during the first two decades of life. UBCs can cause pain and pathological fractures without symptoms. Although the pathogenesis of the UBC is not known, bone resorptive factors, including prostaglandins, have been found in the cyst fluid. Methylprednisolone injection is a treatment for UBCs. The success rate is 96 %. Several injections can be given at 2-month intervals. In UBCs, corticosteroid injections have been shown to be effective as curettage and bone grafting [32, 36].

Use in Injury of the Spinal Cord

Spinal cord injuries are a special case for corticosteroid use. It is believed that corticosteroids help in healing process of spinal cord injury because of reduction of edema. Methylprednisolone, with the initial recommended dose of 30 mg/kg given within the first 8 h after injury and 5.4 mg/kg given hourly until 23 h after injury, provided significant improvement in neurological function in patients with spinal cord injury in a prospective, randomized, double-blind, and multicenter study [30, 37].

References

1. Lanas A, Soena F (2009) Nonsteroidal anti-inflammatory drugs and lower gastrointestinal complications. Gastroenterol Clin N Am 38:333–335
2. Vane JR, Botting RM (1998) Mechanism of action of non-steroidal anti-inflammatory drugs. Am J Med 104:2S–8S
3. Page CP, Curtis MJ, Sutter M, Walker M, Hoffman B (1998) Farmacología integrada (in Spanish). Elsevier España, Harcourt brace
4. Green GA (2002) Understanding NSAIDS: from aspirin to COX-2. Clin Cornerstone 3:50–59
5. Buttar NS, Wang KK (2000) The "aspirin" of the new millennium: cyclooxygenase-2 inhibitors. Mayo Clin Proc 75:1027–1038
6. Fitzgerald GA, Patrono C (2001) Drug therapy: the coxibs, selective inhibitors of cyclooxygenase-2. N Engl J Med 345:433–442
7. Bertolini G, Minelli C, Latronico N et al (2002) The use of analgesic drugs in postoperative patients: the neglected problem of pain control in intensive care units. An observational, prospective, multicenter study in 128 Italian intensive care units. Eur J Clin Pharmacol 58:73–77
8. Simmons DL, Wagner D, Westover K (2000) Nonsteroidal anti-inflammatory drugs, acetaminophen, cyclooxygenase 2, and fever. Clin Infect Dis 31:S211–S218
9. Plaisance KI, Mackowiak PA (2000) Antipyretic therapy: physiologic rationale, diagnostic implications, and clinical consequences. Arch Intern Med 160:449–456
10. Verburg KM, Maziasz TJ, Weiner E et al (2001) COX-2 specific inhibitors: definition of a new therapeutic concept. Am J Ther 8:49–64
11. Vane JR, Botting RM (1998) Anti-inflammatory drugs and their mechanism of action. Inflamm Res 47:S78–S87
12. Schafer A (1995) Effects of nonsteroidal anti-inflammatory drugs on platelet function and systemic hemostasis. J Clin Pharmacol 35:209–219
13. Sadowski T, Steinmeyer J (2002) Differential effects of nonsteroidal antiinflammatory drugs on the IL-1 altered expression of plasminogen activators and plasminogen activator inhibitor-1 by articular chondrocytes. Inflamm Res 51:427–433
14. Paulus HE, Bulpitt KJ (1997) Nonsteroidal anti-inflammatory drugs. In: Klippel JH (ed) Primer on the rheumatic disease. Arthritis Foundation, Atlanta, pp 422–426
15. Levy G (1978) Clinical pharmacokinetics of aspirin. Pediatrics 62:867–872
16. Brooks PM (2000) NSAIDs. In: Klippel JH, Dieppe PA (eds) Textbook of rheumatology, 2nd edn. Harcourt Publisher, London, 3.5.1-6
17. Stewart DM, Dillman RO, Kim HS et al (1979) Acetaminophen overdose: a growing health care hazard. Clin Toxicol 14:507–513
18. Pickering G, Loriot MA, Libert F et al (2006) Analgesic effect of acetaminophen in humans: first evidence of central serotonergic mechanism. Clin Pharmacol Ther 79:371–378
19. Chhina AS, Sharma BK, Raja M, Singhal M, Shenoi A (2015) Indomethacin-responsive patent ductus arteriosus in an extremely preterm infant at 8 weeks postnatal age. Indian J Pediatr 82:655–6

20. Huskisson EC, Scott J (1978) Sulindac: trials of a new anti-inflammatory drug. Ann Rheum Dis 37:89–92
21. Pena M (1990) Etodolac analgesic effects in musculoskeletal and postoperative pain. Rheumatol Int 10:9–16
22. Cepeda MS, Carr DB, Miranda N et al (2005) Comparison of morphine, ketorolac and their combination for postoperative pain: results from a large, randomized, double-blind trial. Anesthesiology 103:1225–1232
23. Barden J, Edwards J, Moore RA et al (2004) Single dose oral diclofenac for postoperative pain. Cochrane Database Syst Rev (2):CD004768
24. Brooks CD, Schlagel CA, Sekhar NC et al (1973) Tolerance and pharmacology of ibuprofen. Curr Ther Res 15:180–181
25. Sevelius H, Segre E, Bursick K (1980) Comparative analgesic effects of naproxen sodium, aspirin, and placebo. J Clin Pharmacol 20:480–485
26. Engelhardt G, Bögel R, Schnitzer C, Utzmann R (1996) Meloxicam: influence on arachidonic acid metabolism. Part 1. In vitro findings. Biochem Pharmacol 51(1):21–28
27. Bottiger LE (1977) Phenylbutazone, oxyphenbutazone and aplastic anaemia. Br Med J 23:265
28. Bresalier RS, Sandler RS, Quan H et al (2005) Cardiovascular events associated with rofecoxib in a colorectal adenoma chemoprevention trial. N Engl J Med 352:1092–1102
29. Gupta P, Sachdev HP (2003) Safety of oral use of nimesulide in children: systematic review of randomized controlled trials. Indian Pediatr 40(6): 518–531
30. Davies NM, Skjodt NM (2000) Choosing the right nonsteroidal anti-inflammatory drug for the right patient: a pharmacokinetic approach. Clin Pharmacokinet 38:377–392
31. Hanson JR (2010) Steroids: partial synthesis in medicinal chemistry. Nat Prod Rep 7(6):887–899
32. Buckwalter JA, Einhorn TA, Simon SR (eds) (2000) Orthopaedic basic science: the biology and biomechanics of the musculoskeletal system, 2nd edn. American Academy of Orthopaedic Surgeons, Rosemont
33. Gray RG, Gottlieb NL (1983) Intra-articular corticosteroids. An updated assessment. Clin Orthop 177: 235–263
34. Stefanich RJ (1986) Intra-articular corticosteroids in the treatment of osteoarthritis. Orthop Rev 15:65–71
35. Weisman MH (1995) Corticosteroids in the treatment of rheumatologic diseases. Curr Opin Rheumatol 7:183–190
36. Canavese F, Wright JG, Cole WG, Hopyan S (2011) Unicameral bone cysts: comparison of percutaneous curettage, steroid, and autologous bone marrow injections. J Pediatr Orthop 31(1):50–55
37. Bracken MB, Shepard MJ, Collins WF, Holford TR, Young W, Baskin DS, Eisenberg HM, Flamm E, Leo-Summers L, Maroon J et al (1990) A randomized, controlled trial of methylprednisolone or naloxone in the treatment of acute spinal-cord injury. Results of the Second National Acute Spinal Cord Injury Study. N Engl J Med 322(20):1405–1411

Antiresorptives

42

Akinori Sakai

Abstract

Antiresorptives are frequently used for the treatment of osteoporosis. They include bisphosphonates, selective estrogen receptor modulators (SERMs), denosumab [antireceptor activator nuclear kappa-B ligand (RANKL) antibody], and calcitonin. They suppress excessive bone resorption, increase bone mineral density, and prevent fragility fractures. Side effects of long-term treatment with bisphosphonates or denosumab are osteonecrosis of the jaw and atypical femoral fractures. There are currently no clear conclusions to suggest how long antiresorptives remain beneficial and safe.

Learning Outcomes

After studying this chapter, we will have an understanding of: (1) the kinds of antiresorptives, (2) the action of antiresorptives, (3) the effect of antiresorptives on BMD, (4) the effect of antiresorptives on fracture risk reduction, and (5) the side effects of antiresorptives.

Terminology

Anabolic agents Compounds that stimulate anabolism and inhibit catabolism. They increase bone mineral density and also stimulate the development of muscle mass, strength, and power.

Apoptosis If cells are no longer needed, they commit suicide by activating an intracellular death program. This process is called programmed cell death or apoptosis (from a Greek word, meaning "falling off," as leaves from a tree).

Farnesyl pyrophosphate An intermediate in the HMG-CoA reductase pathway. Nitrogen-containing bisphosphonates (the second and third generations) target osteoclast farnesyl pyrophosphate synthase and inhibit protein prenylation.

A. Sakai, MD, PhD
Department of Orthopaedic Surgery, University of Occupational and Environmental Health,
1-1 Iseigaoka, Yahatanishi-ku,
Kitakyushu 807-8555, Japan
e-mail: a-sakai@med.uoeh-u.ac.jp

F. Korkusuz (ed.), *Musculoskeletal Research and Basic Science*,
DOI 10.1007/978-3-319-20777-3_42

Meta-analysis A statistical procedure that integrates the results of several independent studies considered "combinable."

Mineralization A process where an organism produces an inorganic substance. Mineralization in bone indicates deposition of calcium hydroxyl apatite salts converting osteoid to rigid bone.

Number needed to treat The number of patients you need to treat to prevent one additional bad outcome (fracture, etc.).

Osteoblast A cell with single nucleus that synthesizes bone and is responsible for bone formation.

Osteoclast A large multinucleate cell (a cell with more than one nucleus) that destroys bone and is responsible for bone resorption.

Osteocyte A cell that lies within the substance of a fully formed bone. It occupies a small chamber called a lacuna, which is contained in the calcified matrix of bone. Osteocytes derive from osteoblasts.

Osteonecrosis A disease caused by reduced blood flow to bones in the joints. Bone breaks down faster than the body can make new strong bone.

Post hoc analysis Post-hoc analysis consists of looking at the data, after the experiment has concluded, for patterns that were not specified a priori.

Remodeling A lifelong process where mature bone tissue is removed from the skeleton by bone resorption and new bone tissue is formed by ossification.

Relative risk reduction A measure calculated by dividing the absolute risk reduction by the control event rate.

Ruffled border A specialized cell membrane that the osteoclast forms at a site of active bone resorption.

Serotonin A monoamine neurotransmitter found in the gastrointestinal tract, platelets, and the central nervous system of humans.

Turnover The rate of bone resorption and bone formation. Assessing bone turnover may add valuable information for the management of patients with low bone mass.

Clinical Relevance

Do Bisphosphonates, SERMs, Denosumab or Calcitonin Prevent the Next Hip Fractures?

A 75-year-old female patient came to the hospital by an ambulance with symptoms of the right inguinal and thigh pain after falling down from the standing position. After physical examination and X-ray studies, right trochanteric fracture was recognized (Fig. 42.1). She received surgical treatment with intramedullary nail, the next day after she was admitted to the hospital. T-score of the left femoral neck BMD of the patient was −2.9. At her control visit, after she was discharged from hospital, when she could walk independently, oral tablet of bisphosphonate was prescribed. Under treatment with bisphosphonate, the patient was followed for 2 years.

When the patients have fragility fracture or T-score of BMD below −2.5, medical treatment with antiresorptives or anabolic agents is strongly recommended to prevent the next fragility fractures. In this case, she had low-energy hip fracture from the standing position and T-score was −2.9. The medical treatment for osteoporosis should be started for this case.

Patients with a previous low-energy hip fracture have a relative risk of 9.79 (95 % CI 9.07–10.55) of a subsequent low-energy hip fracture [1]. A relative risk of all low-energy fractures significantly increases for both sexes: 5.55 for men and 2.94 for women.

Bisphosphonates and denosumab have evidence of preventing hip fractures in postmenopausal osteoporotic women on the basis of RCT. RRR of hip fractures is 55 % in alendronate from the results of meta-analysis of six RCTs [2], 40 % in risedronate from one RCT [3], and 40 % in denosumab from

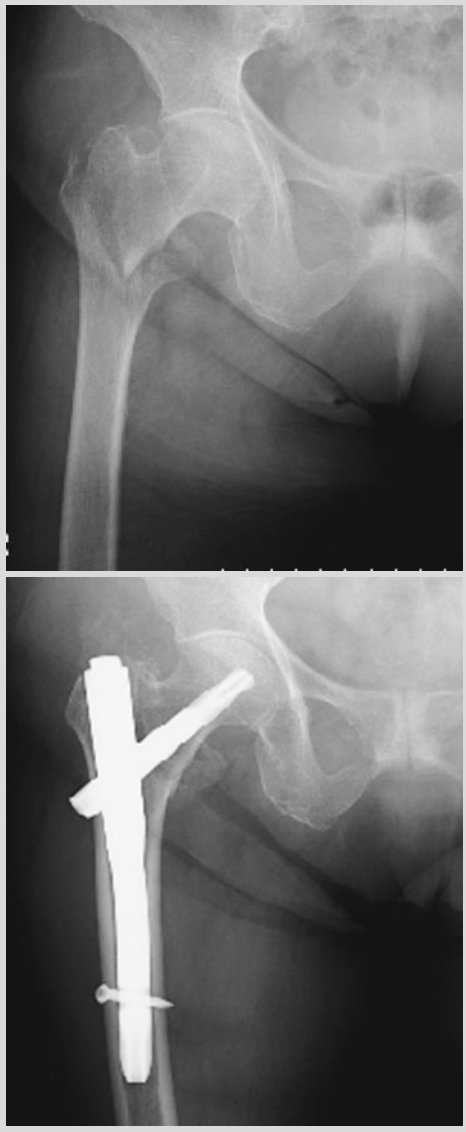

Fig. 42.1 (*Upper*) Anteroposterior X-ray of a 75-year-old female patient. Right trochanteric fracture was recognized on radiological findings. (*Lower*) Surgical treatment with intramedullary nail was undertaken successfully

one RCT [4]. However, there has been no RCT data showing that SERMs or calcitonin reduce the risk of hip fractures. When the target of treatment is to prevent the subsequent hip fractures, we should choose bisphosphonates or denosumab as the appropriate antiresorptives.

Beneficial effect of risedronate for preventing recurrent hip fracture is reported in the elderly Japanese women [5]. The hazard ratios (95 % CI) obtained by univariate and multivariate analysis were 0.31 (0.12–0.80) and 0.22 (0.07–0.64), respectively, indicating a significantly lower incidence of unaffected side hip fracture in the risedronate group.

The aim of the therapy with antiresorptive medicines (bisphosphonates, SERMs, denosumab, and calcitonin) is to restore BMD by decreasing bone remodeling and to reduce the risk of fractures. After the treatment, we should monitor the effectiveness of the treatment by measuring BTMs and BMD, and by checking that there is no subsequent fragility fractures.

AFFs have been reported in the cases of long-term treatment with bisphosphonates. There are currently no clear conclusions to suggest how long an osteoporosis drug remains safe and effective. Evidence is limited regarding the risk of fractures after discontinuation of long-term treatment with bisphosphonates. The benefits may continue for several years, or the beneficial effect begins to lessen with increased bone remodeling rates. Black et al. [6] describes the one possible recommendation. Patients with low BMD at the femoral neck (T-score below −2.5) after 3–5 years of treatment are at the highest risk for vertebral fractures and therefore appear to benefit most from the continuation of bisphosphonates. Patients with an existing vertebral fracture who have a somewhat higher (though not higher than −2.0) T-score for BMD may also benefit from continued therapy. Patients with a femoral neck T-score above −2.0 have a low risk of vertebral fracture and are unlikely to benefit from continued treatment. After 3–5 years of taking bisphosphonates, individuals should discuss whether they should continue taking the medicine, stop taking the medicine, or consider switching to a different medicine. When a patient has a good response to treatment with bisphosphonates, we can consider a drug holiday.

Introduction

Osteoblasts continuously form new bone while osteoclasts resorb old bone through the remodeling process. A balance of bone formation and bone resorption is usually maintained. An imbalance of bone resorption over bone formation occurs with menopause, aging, and other conditions. An imbalance can result in bone loss that eventually leads to osteoporosis and fragility fractures. Most cases of osteoporosis in postmenopausal women have high turnover of bone metabolism, with enhanced bone resorption over bone formation.

Antiresorptive medicines suppress excessive bone resorption during the remodeling cycle. In general, loss of bone mineral density (BMD) is decelerated, and then BMD is gradually increased at 6 months to 1 year, after the patients with osteoporosis take antiresorptives. The goal of the treatment with antiresorptives is to increase BMD and to prevent the incidence of fragility fractures.

Today, there are three types of osteoporosis medicines. The first is antiresorptive medications, such as bisphosphonates, selective estrogen receptor modulators (SERMs), denosumab [anti-receptor activator nuclear kappa-B ligand (RANKL) antibody], and calcitonin, which suppress bone resorption. The second is anabolic agents that enhance bone formation, such as teriparatide. The third is strontium ranelate, which inhibits bone resorption and enhances bone formation.

Antiresorptive agents for treatment of osteoporosis should be appropriately selected according to the effectiveness and safety, on the basis of meta-analyses, randomized controlled trials (RCTs), authorities' opinions, and personal experiences.

Antiresorptive Agents

Bisphosphonates

Action

Bisphosphonates are compounds characterized with two C–P binding sites. Bisphosphonates are not dissolved by any enzymes and are difficult to be metabolized. Bisphosphonates at the first generation (e.g. etidronate) do not contain nitrogen at the side chain. Those at the second generation (e.g. alendronate, ibandronate) contain nitrogen at the side chain without cyclic structure. Those at the third generation (e.g. risedronate, minodronate) contain nitrogen at the side chain with cyclic structure.

Bisphosphonates decrease bone-remodeling rate by decreasing osteoclast activity. They diminish ruffled border and induce apoptosis in osteoclasts (Fig. 42.2). This allows more time for secondary mineralization, increases the degree of trabecular mineralization, and mechanically strengthens the bone.

All kinds of bisphosphonates are approved for the treatment of osteoporosis as well as for the treatment of glucocorticoid-induced osteoporosis. Bisphosphonates can be dosed orally—daily, weekly, or monthly, or intravenously—every month, every 3 months, or annually. Because of the difficulty of gastrointestinal absorption, the oral tablets of bisphosphonates need to be taken

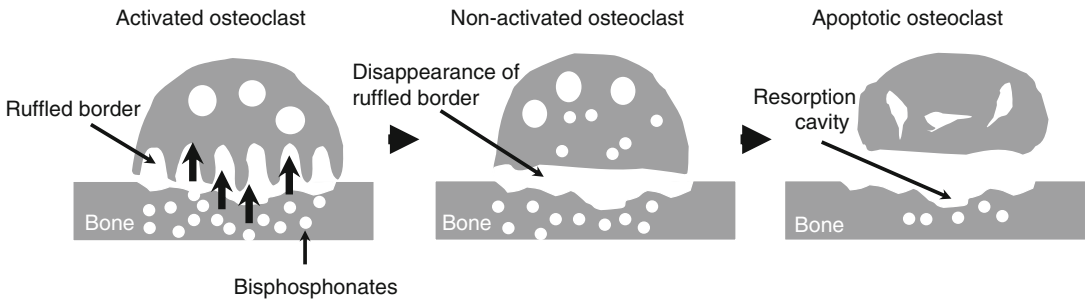

Fig. 42.2 Bisphosphonates have robust affinity to bone matrix and adhere to bone surface. Through the process of bone resorption, bisphosphonates are up-taken into the osteoclasts (*left*). After ruffled border disappears (*middle*), apoptosis of osteoclasts is induced (*right*). In results, bone resorption is suppressed

early in the morning and on an empty stomach, at least 30 min before having anything to eat or drink except water. The tablet is swallowed with at least one cup of water. Patients must not be lying down during the 30 min, after taking the medicine.

Alendronate

Alendronate increases BMD by 13.7 % at the lumbar spine and by 5.4 % at the femoral neck in 10 years [7]. Alendronate reduces the fracture risks of the vertebral, hip and other bones by about 50 % over 2–4 years. The drug is well-tolerated over a 10-year period. Relative risk reduction (RRR) for a 10-mg dose of alendronate in meta-analysis with 11 trials representing 12,068 women is as follows [8]. For vertebral fractures, significant 45 % RRR is found [95 % confidence intervals (CI) 0.45–0.67]. This is significant for both primary prevention with 45 % RRR (95 % CI 0.38–0.80) and secondary prevention with 45 % RRR (95 % CI 0.43–0.69). For nonvertebral fractures, significant 16 % RRR is found (95 % CI 0.74–0.94). This is significant for secondary prevention with 23 % RRR (95 % CI 0.64–0.92), but not for primary prevention (RR 0.89, 95 % CI 0.76–1.04). There is significant 40 % RRR in hip fractures (95 % CI 0.40–0.92), but only secondary prevention is significant with 53 % RRR (95 % CI 0.26–0.85). The only significance found for wrist is in secondary prevention with 50 % RRR (95 % CI 0.34–0.73). According to the results of Fracture Intervention Trial (FIT), the number needed to treat (NNT) of alendronate against vertebral fractures in postmenopausal osteoporotic women is 14.3 [9].

Risedronate

Meta-analysis reveals that risedronate increases BMD by 4.54 % at the lumbar spine and by 2.75 % at the femoral neck in 1.5–3 years [10, 11]. RRR in meta-analysis with seven trials representing 14,049 women for risedronate 5 mg dose is as follows [12]. Risk estimates for primary prevention are available only for vertebral and nonvertebral fractures and show no statistically significant effect of risedronate on fractures. For secondary prevention, significant 39 % RRR in vertebral fractures (95 % CI 0.50–0.76) is found. For non-vertebral fractures, significant 20 % RRR (95 % CI 0.72–0.90), and for hip fractures, there is significant 26 % RRR (95 % CI 0.59–0.94). When primary and secondary prevention studies are combined, the reduction in fractures remains statistically significant for both vertebral (RR 0.63, 0.51–0.77) and nonvertebral fractures (RR 0.80, 0.72–0.90). According to the results of Vertebral Efficacy with Risedronate Therapy—North America (VERT-NA), NNT of risedronate against vertebral fractures in postmenopausal osteoporotic women is 20.0 [9].

Other Bisphosphonates

Ibandronate, minodronate, and zoledronate are promising osteoporosis treatment modalities. Their molecular and cellular action mechanisms are substantially the same as those of alendronate and risedronate, which are described in section "Action". The bone mineral affinity is different among bisphosphonates. The percentages of the fraction bound to bone in vivo after dosing are 40–50 % in ibandronate, 50–62 % in zoledronate, 60 % in risedronate, and 64 % in alendronate [13].

Ibandronate reduces the incidence of vertebral fractures by about 50 % over 3 years. In the USA, ibandronate is taken once monthly as a 150 mg tablet, and it is also available as an intravenous (IV) injection of 3 mg given every 3 months. In Japan, it is available as an IV injection of 1 mg given every month. Medical doctors or nurses have to administer the IV dose in a clinic or a hospital. It takes less than a minute to inject.

Minodronate is developed in Japan. It is the most robust inhibitor of farnesyl pyrophosphate synthase among the bisphosphonates in vitro [14]. Minodronate increases BMD and shows 59 % RRR at vertebral fractures in 2 years [15]. According to the results of the phase III study in Japan, NNT of minodronate against vertebral fractures in postmenopausal osteoporotic women is 7.4 [9]. Minodronate is indicating good efficiency of treatment.

Zoledronate is available in the USA. It is given once a year as an IV infusion to treat osteoporosis. Before approval for use in osteoporosis, zoledronate was already available for use in cancer patients with certain bone conditions. It increases

BMD by 6.71 % at the lumbar spine, 6.02 % at the total hip, and 5.06 % at the femoral neck over the respective values of the placebo group [16]. It also shows 70 % RRR at vertebral fractures and 41 % at hip fractures in 3 years. Zoledronate shows significant 35 % RRR for any new clinical fractures and significant 28 % RRR for death from any causes [17]. Less frequent administration may lead to better adherence and efficacy.

Etidronate is the first generation bisphosphonate and does not contain nitrogen at the side chain. Recently, etidronate is not very often used clinically. RRR in meta-analysis with 11 studies representing a total of 1248 patients is as follows [18]. Significant 41 % RRR in vertebral fractures across eight studies (95 % CI 0.36–0.96) is found. For vertebral fractures, the six secondary prevention trials demonstrate significant RRR of 47 % (95 % CI 0.32–0.87), but the pooled result for the two primary prevention trials (RR 3.03, 95 % CI 0.32–28.44) is not significant. There are no statistically significant risk reductions for nonvertebral (RR 0.98, 95 % CI 0.68–1.42), hip (RR 1.20, 95 % CI 0.37–3.88), or wrist fractures (RR 0.87, 95 % CI 0.32–2.36).

Side Effects

Side effects of the oral tablets for all bisphosphonates may include gastrointestinal disorders such as irritation of the esophagus and gastric ulcer. When the patients receive monthly oral tablets or IV bisphosphonates, flu-like symptoms such as fever, headache, and pain in muscles or joints may occur. These generally disappear within a few days without any treatments and usually do not appear on further administrations.

There have been rare reports of osteonecrosis of the jaw (ONJ) after invasive oral treatment in the patients treated with bisphosphonates. The prevalence of ONJ in osteoporosis patients is 0.028–4.3 % (about 1/100,000 person-year) [19], though cancer patients receiving intravenous bisphosphonates at much larger doses than given for osteoporosis have higher risk at odds ratio of 4.27 (95 % CI 3.38–5.40) than oral bisphosphonates [20].

Atypical femoral fractures (AFFs) in the patients taking bisphosphonates for a long term have been reported. Most patients have thigh or inguinal pain for several weeks before fractures. The findings of fractures on radiographs are characteristic. They are described in detail by a task force of the American Society for Bone and Mineral Research [21]. The prevalence of AFFs in osteoporosis patients is 32–59/1,000,000 person-year.

SERMs

Action

SERMs are neither estrogens nor hormonal agents. SERMs suppress bone remodeling into the premenopausal range, while keeping the function of osteoblasts and osteocytes. SERMs suppress bone resorption within the physiological levels by enhancing the production of osteoprotegerin, decoy receptor of RANKL [22].

SERMs exhibit tissue-specific activity. They are estrogen agonists/antagonists that provide the beneficial effects of estrogens without their potential disadvantages. The selective actions of SERMs in different tissues result from a combinatorial collaboration among several factors [23]. Estrogen and SERMs, all bind to estrogen receptors, inducing distinctly different receptor conformations. These different receptor conformations then interact with the regulatory sequences of target genes in different ways. The type of interaction and the cellular levels of co-regulator proteins (co-activators or co-repressors) determine the distinct patterns of co-regulator recruitment to the ligand–receptor–gene assembly. In this way, either stimulation or inhibition of specific biological effects is elicited.

SERMs act as estrogen agonist in bone and lipid metabolism, while they act as antagonist in female sexual organs such as breast, uterus, and ovary. Substantially, raloxifene therapy shows a favorable or neutral effect in the cardiovascular system and reduces the incidence of estrogen receptor-positive breast cancer [24]. Raloxifene and bazedoxifene are available in Japan. They are approved for the treatment of postmenopausal osteoporosis.

Raloxifene and Bazedoxifene

The evidence supports the efficacy of raloxifene or bazedoxifene for the prevention of osteoporotic fractures. The published systematic reviews

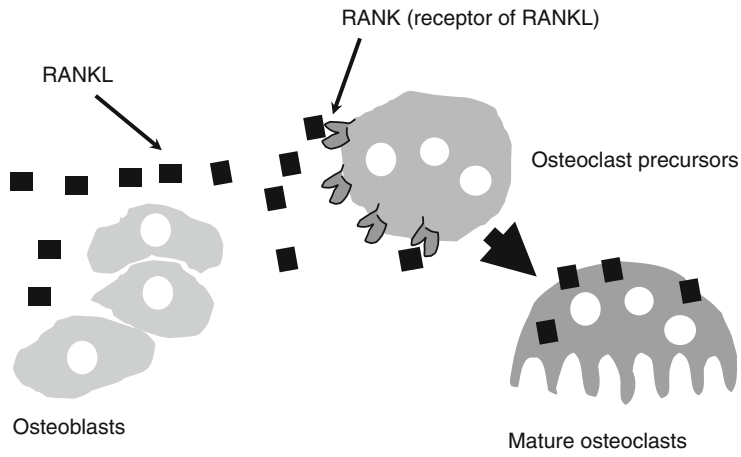

Fig. 42.3 RANKL promotes the process of differentiation from osteoclast precursors to mature osteoclasts. Denosumab (anti-RANKL antibody) suppresses this differentiation process and leads to the reduction of osteoclastic bone resorption. RANKL: receptor activator of nuclear factor kappa-B ligand

did not include other SERMs such as lasofoxifene, ormeloxifene, and femarelle.

Raloxifene and bazedoxifene increase BMD and reduce the risk of vertebral fractures. There are no data showing that raloxifene and bazedoxifene reduce the risk of hip and the other nonvertebral fractures, excluding the post hoc analyses. Raloxifene is taken daily as a 60 mg tablet and bazedoxifene is taken daily as a 20 mg tablet with or without meals. Side effects include hot flashes, leg cramps, and deep vein thrombosis.

Denosumab

Action

Denosumab is a RANKL inhibitor and human monoclonal antibody. RANKL, a key molecule of osteoclast differentiation, is produced by osteoblasts and osteocytes (Fig. 42.3). RANKL production is increased in postmenopausal osteoporotic women and stimulates osteoclast differentiation to destroy bone.

A medical doctor or a nurse gives denosumab by subcutaneous injection every 6 months. Patients need to have a blood test before and 1 week after each injection to confirm serum calcium concentration. All patients administered with denosumab must get sufficient calcium and vitamin D every day, because denosumab may lower the calcium levels in the blood.

Efficacy

Denosumab is approved for the treatment of osteoporosis. Denosumab increases BMD by 15.2 % at the lumbar spine and by 7.5 % at the total hip from baseline in 6 years, according to the Fracture Reduction Evaluation of Denosumab in Osteoporosis Every 6 Months (FREEDOM) extension study [25]. Denosumab reduces the risk of fractures in the spine, hip, and others. In clinical trials, denosumab significantly reduces the incidence of new vertebral fractures by 74 % in 2 years [26] and the incidence of hip fractures by 40 % in 3 years [4].

Side Effects

We should pay attention to low blood calcium levels after administering denosumab. However, most patients with low calcium do not show any clinical signs. Denosumab has caused ONJ when used to treat patients with cancer, while these have been rarely seen in patients with osteoporosis. Patients should practice good dental care and should have an oral examination by a dentist, if necessary, during the treatment.

Calcitonin

Action

Calcitonin is a synthetic hormone involved in calcium regulation. Osteoclasts and osteoclast precursor cells have calcitonin receptors [27]. Calcitonin inhibits osteoclast activity without

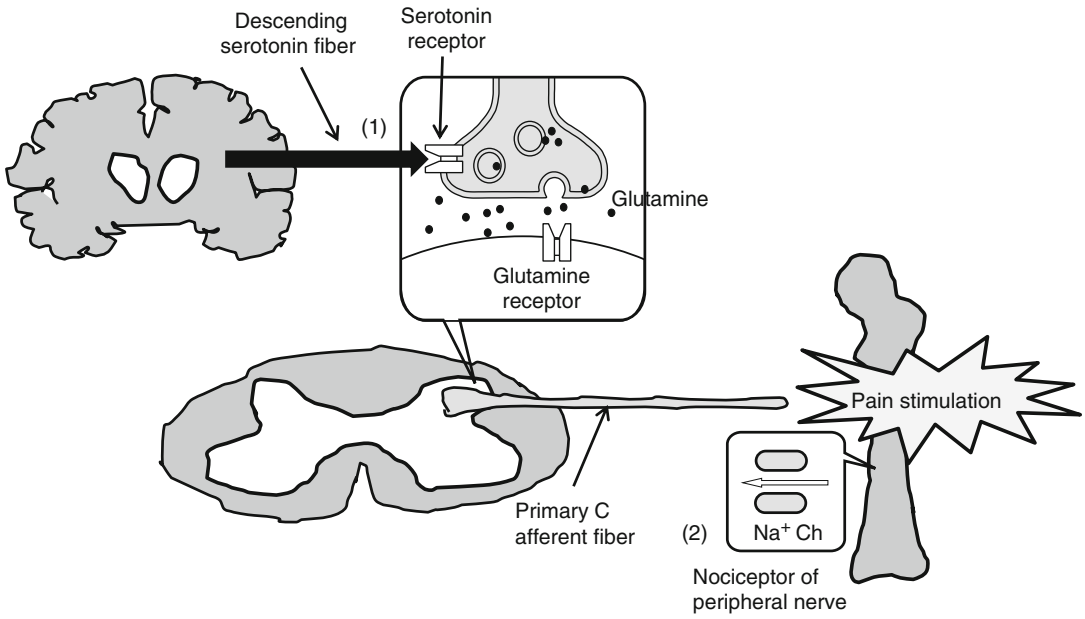

Fig. 42.4 Calcitonin reduces pain signals enhanced by estrogen deficiency. Calcitonin suppresses the expression of serotonin receptors at the central terminals of primary C afferent fiber (*1*) and normalizes the threshold of pain at nociceptors of the peripheral nerve tissues (*2*)

decreasing osteoblast function [28]. Several mechanisms of pain relief have been suggested for the antinociceptive effect of calcitonin. Calcitonin centrally exerts actions on serotonin. Calcitonin receptor mRNA has been elucidated on serotonergic neurons associated with pain processing [29]. The descending serotonergic system is involved in antihyperalgesia. It is proposed that calcitonin modifies the expression of serotonin receptors at the central terminals of primary C afferents in estrogen deficiency-induced hyperalgesia and that calcitonin normalizes the reduced threshold of pain due to estrogen deficiency at the nociceptors of the peripheral nerve tissues (Fig. 42.4) [30–32].

Efficacy

Calcitonin increases lumbar BMD. In the Prevent Recurrence of Osteoporotic Fractures study (PROOF), it reduces the risk of vertebral fractures, but it has not been shown to decrease the risk of hip fractures [33]. Calcitonin relieves pain due to osteoporosis. Calcitonin is approved for the treatment of painful osteoporosis and is available as a subcutaneous injection in Japan.

Other Agents Except Antiresorptives

Strontium

Strontium ranelate inhibits bone resorption and enhances bone formation. The meta-analysis reveals that 37 % reduction in vertebral fractures (95 % CI 0.56–0.71) and 14 % reduction in non-vertebral fractures (95 % CI 0.75–0.98) are demonstrated over 3 years with 2 g of strontium ranelate daily in postmenopausal osteoporotic women [34]. BMD increases at all sites after 2–3 years in both the treatment and prevention populations. An increased risk of diarrhea is found. However, adverse events do not affect the risk of discontinuing treatment.

Teriparatide

Teriparatide is a recombinant form of parathyroid hormone. It is an anabolic agent that enhances bone formation. RCT reveals that the respective relative risks of new vertebral fractures in the 20- and 40-μg teriparatide groups, as compared with the placebo group, are 0.35

and 0.31 (95 % CI 0.22–0.55 and 0.19–0.50) [35]. The respective relative risks of new non-vertebral fragility fractures in each teriparatide group are 0.47 and 0.46 (95 % CI 0.25–0.88 and 0.25–0.86). The 20- and 40-μg doses of teriparatide increase BMD by 9 % and 13 % at the lumbar spine and by 3 % and 6 % at the femoral neck in 2 years.

Osteoporosis in Men

There have been fewer research studies on osteoporosis in men than in women. Treatment of osteoporosis is targeted at increasing BMD and reducing the incidence of fragility fractures as well in men. When osteoporosis is caused by some conditions such as testosterone deficiency and exposure to specific medications, treatment plan should be designed to address the underlying causes. Nonpharmacological interventions include physical exercise, tobacco cessation, the avoidance of excessive alcohol intake, and the supplementation of calcium and vitamin D.

Bisphosphonates are the first-line treatments for the prevention and treatment of osteoporosis in men. Other potential treatments in men include: denosumab, which has been shown to be effective in the prevention of bone loss in the setting of androgen deprivation therapy for nonmetastatic prostate cancer [36], and strontium ranelate [37] and teriparatide for severe osteoporosis [38, 39].

Adherence of Patients to the Medicine

Adherence and Persistence

The treatment options for osteoporosis continue to increase in number, and we have greater choice. The most commonly used medicines are bisphosphonates. In addition to bisphosphonates, treatment options include SERMs, denosumab, calcitonin, strontium, and teriparatide. Despite the numerous options, adherence with all osteoporosis therapies is substantially poor. Back pain is sometimes relieved, but in frequent cases, clinical symptoms do not change at all even after the administration of osteoporosis medicines. There is a lack of self-reinforcing benefit after medication.

Our extended observational study after the BP-MUSASHI study [40] reveals that the proportion of persistent patients with daily or weekly bisphosphonates is 80.5 % at 6 months and 49.6 % at 1 year, but that with monthly minodronate that switched from daily or weekly bisphosphonates is 91.3 % at 6 months and 76.5 % at 1 year (Fig. 42.5). Treatment persistence is significantly higher in the monthly

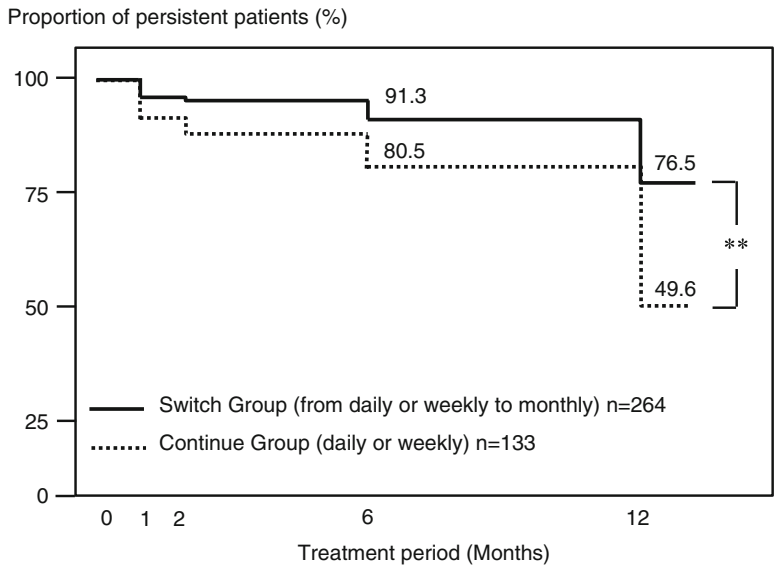

Fig. 42.5 Treatment persistence of oral bisphosphonates in monthy versus daily or weekly. Proportion of persistent patients for monthly minodronate swithced from daily or weekly bisphosphonates (*solid line*) is significantly higher that that for continued daily or weekly bisphosphonates (*dot line*). **p<0.01, significantly different between these two groups as analyzed by log-rank test

"switch" group than the daily or weekly "continue" group. Almost all patients with abnormal bone turnover markers (BTMs) demonstrate normalization after switchover. Monitoring BTM seems to improve treatment persistence. Positive information of BTMs and less frequent administration could lead to better persistence of oral bisphosphonate therapy.

Based on the final results of the DAPS (Denosumab Adherence Preference Satisfaction) study, after women have received each treatment for up to 1 year, postmenopausal women with osteoporosis are more adherent, compliant, and persistent with subcutaneous denosumab injections every 6 months than with weekly alendronate tablets, and report increased the treatment preference and satisfaction with denosumab over alendronate [41].

After Ceasing the Antiresorptives

During antiresorptive therapy, the magnitude of BTM suppression achieved differs depending on the kinds of markers and medicines administered. BTM levels generally increase after the treatment is discontinued, though the magnitude and speed of this offset differ among agents. After discontinuation, BTM levels, more slowly (e.g. bisphosphonates) or more rapidly (e.g. denosumab), increase toward pretreatment levels. These alterations pertain to the posttreatment changes in BMD. Because of the higher bone remodeling rate and lower bone mineral, bone strength may be weakened, and clinical fracture risks may be increased.

The prolonged effects of bisphosphonates on BTMs and BMD after discontinuation may contribute to residual benefit on fracture risk reduction, while it may raise safety concerns. Adequately powered postdiscontinuation studies are lacking for bisphosphonates [42]. Similarly, the effects after discontinuation of denosumab on fracture risk remain unknown. In the absence of the treatment discontinuation data, a doctor should periodically assess the benefits/risks of continuation versus discontinuation versus alternative management strategies.

References

1. Robinson CM, Royds M, Abraham A et al (2002) Refractures in patients at least forty-five years old. A prospective analysis of twenty-two thousand and sixty patients. J Bone Joint Surg Am 84:1528–1533
2. Papapoulos SE, Quandt SA, Liberman UA et al (2005) Meta-analysis of the efficacy of alendronate for the prevention of hip fractures in postmenopausal women. Osteoporos Int 16:468–474
3. McClung MR, Geusens P, Miller PD et al (2001) Effect of risedronate on the risk of hip fracture in elderly women. Hip Intervention Program Study Group. N Engl J Med 344:333–340
4. Cummings SR, San Martin J, McClung MR et al (2009) Denosumab for prevention of fractures in postmenopausal women with osteoporosis. N Engl J Med 361:756–765
5. Osaki M, Tatsuki K, Hashikawa T et al (2012) Beneficial effect of risedronate for preventing recurrent hip fracture in the elderly Japanese women. Osteoporos Int 23:695–703
6. Black DM, Bauer DC, Schwartz AV et al (2012) Continuing bisphosphonate treatment for osteoporosis–for whom and for how long? N Engl J Med 366:2051–2053
7. Bone HG, Hosking D, Devogelaer JP et al (2004) Ten years' experience with alendronate for osteoporosis in postmenopausal women. N Engl J Med 350:1189–1199
8. Wells GA, Cranney A, Peterson J et al (2008) Alendronate for the primary and secondary prevention of osteoporotic fractures in postmenopausal women. Cochrane Database Syst Rev 1, CD001155
9. Hagino H (2009) New development in bisphosphonate treatment. Review of the preventive effect of minodronic acid on fracture in Japanese patients with osteoporosis. Clin Calcium 19:75–84
10. Cranney A, Guyatt G, Griffith L et al (2002) Meta-analyses of therapies for postmenopausal osteoporosis. IX: summary of meta-analyses of therapies for postmenopausal osteoporosis. Endocr Rev 23:570–578
11. Cranney A, Tugwell P, Adachi J et al (2002) Meta-analyses of therapies for postmenopausal osteoporosis. III. Meta-analysis of risedronate for the treatment of postmenopausal osteoporosis. Endocr Rev 23:517–523
12. Wells GA, Cranney A, Peterson J et al (2008) Risedronate for the primary and secondary prevention of osteoporotic fractures in postmenopausal women. Cochrane Database Syst Rev 1, CD004523
13. Bauss F, Russell RG (2004) Ibandronate in osteoporosis: preclinical data and rationale for intermittent dosing. Osteoporos Int 15:423–433
14. Fleish H (2000) Actions. Bisphosphonates in bone disease, 4th edn. Academic, New York, pp 34–55
15. Matsumoto T, Hagino H, Shiraki M et al (2009) Effect of daily oral minodronate on vertebral fractures in Japanese postmenopausal women with established osteoporosis: a randomized placebo-controlled double-blind study. Osteoporos Int 20:1429–1437

16. Black DM, Delmas PD, Eastell R et al (2007) Once-yearly zoledronic acid for treatment of postmenopausal osteoporosis. N Engl J Med 356:1809–1822
17. Lyles KW, Colón-Emeric CS, Magaziner JS et al (2007) Zoledronic acid in reducing clinical fracture and mortality after hip fracture. N Engl J Med 357:nihpa40967
18. Wells GA, Cranney A, Peterson J et al (2008) Etidronate for the primary and secondary prevention of osteoporotic fractures in postmenopausal women. Cochrane Database Syst Rev 1, CD003376
19. Solomon DH, Mercer E, Woo SB et al (2013) Defining the epidemiology of bisphosphonate-associated osteonecrosis of the jaw: prior work and current challenges. Osteoporos Int 24:237–244
20. Lee SH, Chan RC, Chang SS et al (2014) Use of bisphosphonates and the risk of osteonecrosis among cancer patients: a systemic review and meta-analysis of the observational studies. Support Care Cancer 22:553–560
21. Shane E, Burr D, Abrahamsen B et al (2014) Atypical subtrochanteric and diaphyseal femoral fractures: second report of a task force of the American Society for Bone and Mineral Research. J Bone Miner Res 29:1–23
22. Canalis E, Giustina A, Bilezikian JP (2007) Mechanisms of anabolic therapies for osteoporosis. N Engl J Med 357:905–916
23. Katzenellenbogen BS, Katzenellenbogen JA (2002) Biomedicine. Defining the "S" in SERMs. Science 295:2380–2381
24. Lippman ME, Cummings SR, Disch DP et al (2006) Effect of raloxifene on the incidence of invasive breast cancer in postmenopausal women with osteoporosis categorized by breast cancer risk. Clin Cancer Res 12:5242–5247
25. Bone HG, Chapurlat R, Brandi ML et al (2013) The effect of three or six years of denosumab exposure in women with postmenopausal osteoporosis: results from the FREEDOM extension. J Clin Endocrinol Metab 98:4483–4492
26. Nakamura T, Matsumoto T, Sugimoto T et al (2014) Clinical Trials Express: fracture risk reduction with denosumab in Japanese postmenopausal women and men with osteoporosis: denosumab fracture intervention randomized placebo controlled trial (DIRECT). J Clin Endocrinol Metab 99:2599–2607
27. Ikegame M, Ejiri S, Ozawa H (1994) Histochemical and autoradiographic studies on elcatonin internalization and intracellular movement in osteoclasts. J Bone Miner Res 9:25–37
28. Katae Y, Tanaka S, Sakai A et al (2009) Elcatonin injections suppress systemic bone resorption without affecting cortical bone regeneration after drill-hole injuries in mice. J Orthop Res 27:1652–1658
29. Braga PC (1994) Calcitonin and its antinociceptive activity: animal and human investigations 1975–1992. Agents Actions 41:121–131
30. Ito A, Kumamoto E, Takeda M et al (2000) Mechanisms for ovariectomy-induced hyperalgesia and its relief by calcitonin: participation of 5-HT1A-like receptor on C-afferent terminals in substantia gelatinosa of the rat spinal cord. J Neurosci 20:6302–6308
31. Shibata K, Takeda M, Ito A et al (1998) Ovariectomy-induced hyperalgesia and antinociceptive effect of elcatonin, a synthetic eel calcitonin. Pharmacol Biochem Behav 60:371–376
32. Takayama B, Kikuchi S, Konno S et al (2008) An immunohistochemical study of the antinociceptive effect of calcitonin in ovariectomized rats. BMC Musculoskelet Disord 15:164
33. Chesnut CH 3rd, Silverman S, Andriano K et al (2000) A randomized trial of nasal spray salmon calcitonin in postmenopausal women with established osteoporosis: the prevent recurrence of osteoporotic fractures study. PROOF Study Group. Am J Med 109:267–276
34. O'Donnell S, Cranney A, Wells GA et al (2006) Strontium ranelate for preventing and treating postmenopausal osteoporosis. Cochrane Database Syst Rev 3, CD005326
35. Neer RM, Arnaud CD, Zanchetta JR et al (2001) Effect of parathyroid hormone (1–34) on fractures and bone mineral density in postmenopausal women with osteoporosis. N Engl J Med 344:1434–1441
36. Smith MR, Egerdie B, Hernández Toriz N et al (2009) Denosumab in men receiving androgen-deprivation therapy for prostate cancer. N Engl J Med 361: 745–755
37. Kaufman JM, Audran M, Bianchi G et al (2013) Efficacy and safety of strontium ranelate in the treatment of osteoporosis in men. J Clin Endocrinol Metab 98:592–601
38. Orwoll ES, Scheele WH, Paul S et al (2003) The effect of teriparatide [human parathyroid hormone (1–34)] therapy on bone density in men with osteoporosis. J Bone Miner Res 18:9–17
39. Kaufman JM, Orwoll E, Goemaere S et al (2005) Teriparatide effects on vertebral fractures and bone mineral density in men with osteoporosis: treatment and discontinuation of therapy. Osteoporos Int 16:510–516
40. Sakai A, Ikeda S, Okimoto N et al (2014) Clinical efficacy and treatment persistence of monthly minodronate for osteoporotic patients unsatisfied with, and shifted from, daily or weekly bisphosphonates: the BP-MUSASHI study. Osteoporos Int 25: 2245–2253
41. Freemantle N, Satram-Hoang S, Tang ET et al (2012) Final results of the DAPS (Denosumab Adherence Preference Satisfaction) study: a 24-month, randomized, crossover comparison with alendronate in postmenopausal women. Osteoporos Int 23:317–326
42. Boonen S, Ferrari S, Miller PD et al (2012) Postmenopausal osteoporosis treatment with antiresorptives: effects of discontinuation or long-term continuation on bone turnover and fracture risk—a perspective. J Bone Miner Res 27:963–974

Part VII

Surgical and Functional Anatomy

Murat Bozkurt

Upper Extremities

43

İbrahim Tekdemir and Mehmet Ali Güner

Abstract

The importance of knowing the local anatomy during surgical intervention applied to the arm and forearm has been an issue of discussion for years. For this reason, a review and detailed exposition of local anatomy in relation with surgical exposure is presented. This chapter presents the anatomic structures that must be avoided during the surgical procedures to the arm and forearm, according to the surgical dissections.

Anatomy

Operations generally involve open reduction and internal fixations of fractures. The major problem to all these approaches is due to the radial, ulnar, and axillary nerves running very close to the humerus. Especially, on surgical procedures to the body of humerus, radial nerve is at the highest risk [1–3].

Four approaches are described; anterior approach, anterolateral approach, posterior approach, and lateral approach. The anterior and posterior approaches are the most suitable surgical approaches for multipurpose procedures, as they provide access to a larger area of the bone. The anterolateral approach is mostly used in distal humerus surgeries, and the lateral approach is mostly used in procedures toward the local structures and extensor muscles.

İ. Tekdemir, MD, PhD (✉) • M.A. Güner, MD
Department of Anatomy, School of Medicine,
Ankara University, Ankara, Turkey
e-mail: itekdemir@yahoo.com

The radial nerve is the main surgical issue in these approaches because of its posterior, lateral, and anterior course [4–6].

Anterior Approach

- Internal fixation of fractures of the humerus.
- Osteotomy.
- Biopsy and resection of bone tumors.
- Treatment of osteomyelitis. In this procedure, the incision starts from the coracoid process, continues in line with the deltopectoral groove, and can be extended 5 cm till the elbow joint [7].
- During this incision, the deltoid should be medially and pectoralis major should be laterally retracted. Special care should be given to avoid axillary nerve paralysis (Fig. 43.1).
- Moreover, cephalic vein, anterior, and posterior circumflex humeral vessels are the other structures that require special caution (Fig. 43.2) [8, 9].

F. Korkusuz (ed.), *Musculoskeletal Research and Basic Science*,
DOI 10.1007/978-3-319-20777-3_43

Anterolateral Approach

- This is used in operations entering one-fourth distal part of the humerus.
- This approach is used in operations of one-fourth distal part of the humerus. It is used to access the distal part of the radial nerve precisely in open reduction and internal fixation procedures [10, 11]
- A longitudinal incision is used, and this incision is done on the lateral side of the biceps brachii (Fig. 43.2). It can be extended to 10 cm till the elbow joint. During this incision, brachioradialis is excluded laterally, while brachialis and biceps brachii are excluded medially [12]

Posterior Approach

- This approach provides good access to the lower three-fourths of the humerus. The main issue with this approach is that the radial nerve can be damaged easily.
- Open reduction and internal fixation of fractures of the humerus.
- Treatment of nonunion of fractures.
- Biopsy and excision of tumors.
- A longitudinal incision starts from 8 cm below the acromion to the olecranon fossa. The lateral and long heads of the triceps brachii must be separated to explore and protect the radial nerve, because it enters the posterior compartment of arm from close to the muscle heads' origins and the nerve braches pass between this two head (Fig. 43.3) [13, 14].
- A deep dissection should be avoided due to the danger of damaging the radial nerve and profunda brachii artery (Fig. 43.3).

Lateral Approach

- This approach uncovers the lateral epicondyle and the muscles that originated from that area.
- Open reduction and internal fixation of fractures of the lateral condyle.
- Surgical treatment of tennis elbow.
- A curved or straight incision is done on the lateral aspect of the elbow over the lateral supracondylar ridge.

Here, the radial nerve pierces through the lateral intermuscular septum of the arm. This has to be cautiously handled. While approaching the arm, neurovascular structures do not run down a definite path; therefore, they are considered separately. Thus, muscles have to be considered into two important compartments as flexor and extensor muscles.

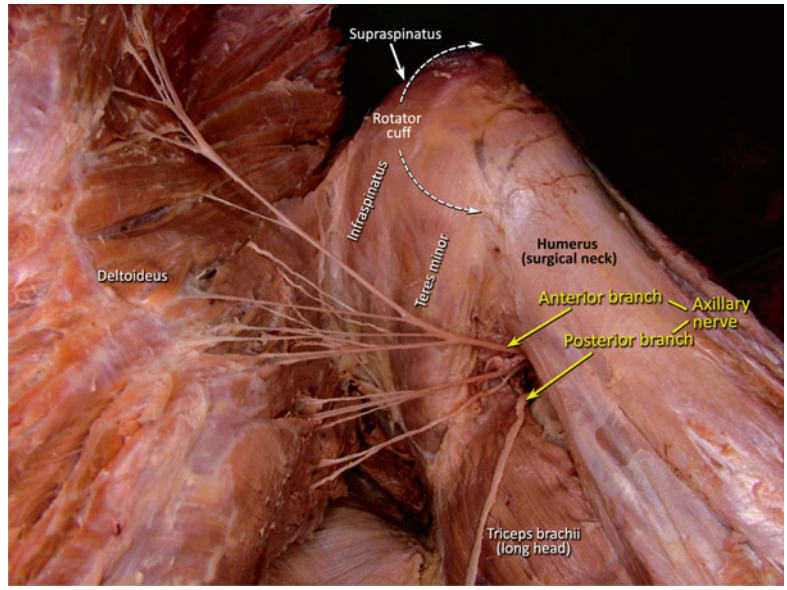

Fig. 43.1 Posterior view of shoulder. The anterior and posterior branches of axillary nerve are seen

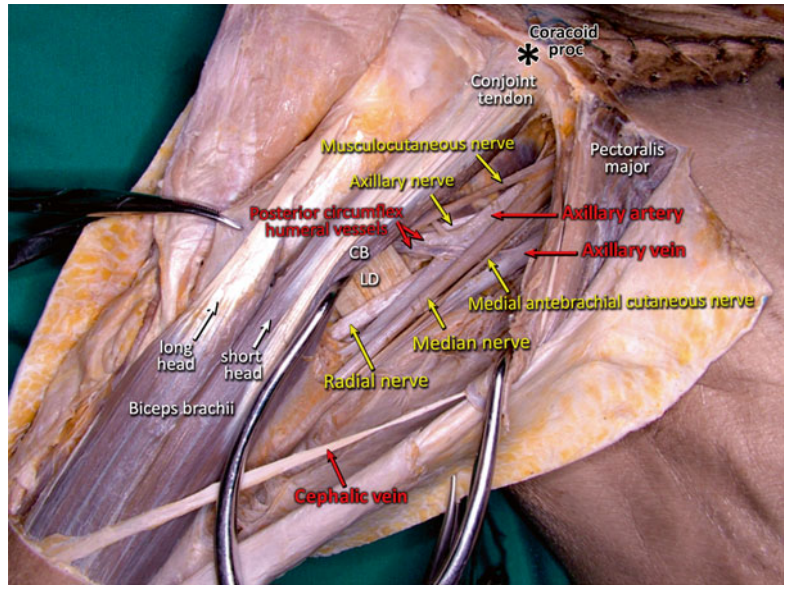

Fig. 43.2 Anterior view of upper arm. The branches of the brachial plexus are seen. *CB* coracobrachialis, *LD* latissimus dorsi

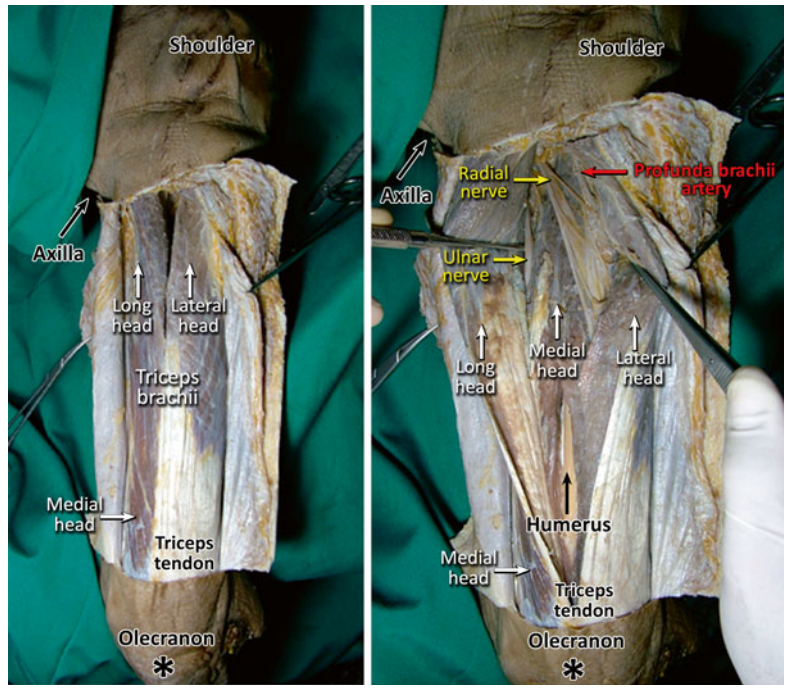

Fig. 43.3 Posterior view of arm. The radial nerve is visualized entering between the long and the lateral heads of triceps

Anterior compartment consists of the coracobrachialis, biceps brachii, and brachialis muscles, and innervation is done by the musculocutaneous nerve. Posterior compartment consists of triceps brachii. These two compartments are separated by lateral and medial intermuscular septums.

Innervation of brachial muscle varies. The lateral part is innervated by radial nerve, whereas the medial part is innervated by musculocutaneous. Therefore, while separating the muscle, some parts may be denervated.

Similarly, the long head of triceps brachii is innervated by the superior branches of the radial nerve, whereas the lateral head is innervated by the inferior branches. The medial head is innervated both by the radial nerve and the ulnar nerve.

Coracobrachialis may sometimes have an extra head that may be attached to ligaments and other structures. These ligaments may attach themselves to the medial supracondylar ridge and medial epicondyle. As a result, entrapment neuropathy can be observed in the median nerve, which is similar to the symptoms seen in carpal tunnel syndrome.

Forearm Approaches

Anterior Approach

- Radius is clearly visible in this approach. The most important aspect is the posterior interosseous nerve (PIN). Damage is possible to this nerve as it is located under the supinator (Fig. 43.4) [15–18].
- Open reduction and internal fixation.
- Bone graft and nonunion fracture treatment.
- Radial osteotomy.
- Bone tumor treatment and biopsy.
- Osteomyelitis excision.
- This approach is used for exposing radial tuberosity. Keeping biceps brachii on the lateral side, the incision can be extended until the radial styloid process. During this

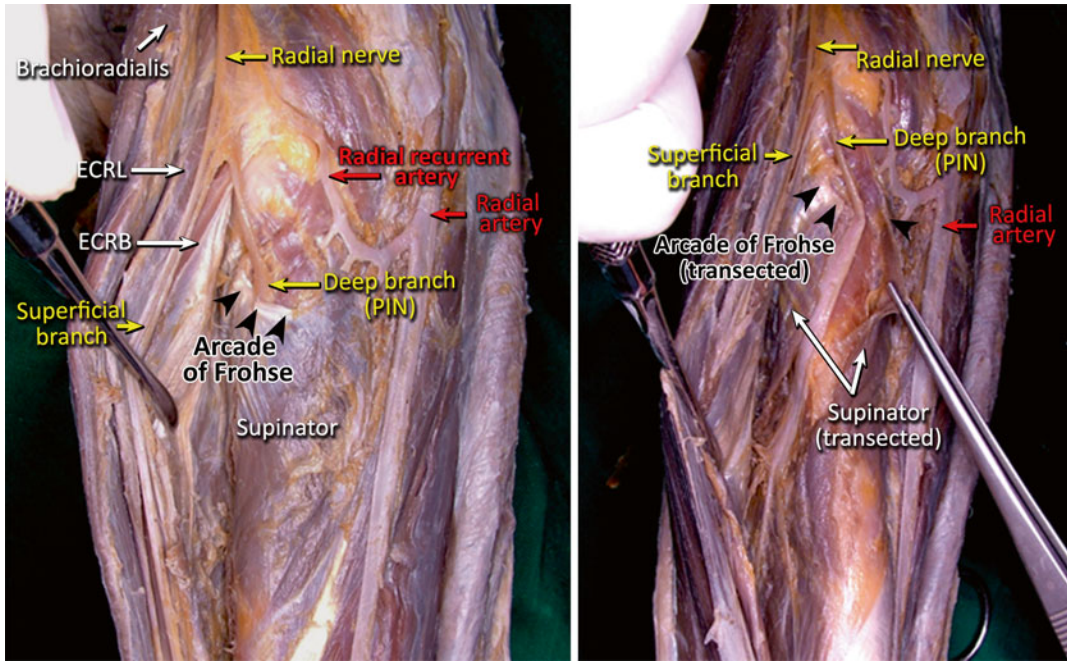

Fig. 43.4 Anterolateral view of forearm. Brachioradialis, extensor carpi radialis longus (*ECRL*), and extensor carpi radialis brevis (*ECRB*) were retracted laterally. The branches of the radial nerve are seen. *PIN* posterior interosseous nerve

incision, the superficial branch of radial nerve and PIN is important (Fig. 43.4). Additionally, radial artery is located below the brachioradialis.

Posterior Approach

- The main reason for preferring this approach is the ease by which PIN can be retracted.
- Open reduction and internal fixation.
- Nonunion fracture treatment.
- PIN decompression.
- Radial osteotomy.
- Osteomyelitis treatment.
- This approach can be used in bone tumor treatment and biopsy. Ulnar styloid process can be reached by the lateral epicondyle on the ulnar side.

Case Questions

Question 1: Following an assault with a knife, the person who was attacked with the knife tried to defend himself by putting his arm forward. This resulted in a knife injury to the victim's forearm. The medical evaluation of the victim's arm at the local hospital revealed partial damage to some extensor muscles on the forearm. What is the most likely nerve injury in this case?

Answer: Posterior interosseal nerve (PIN)

Question 2: A passenger sustained a crush injury to his arm during a traffic accident while traveling in a car. Physical examination at the hospital revealed a midshaft fracture of humerus. The extensor muscles of the must be exculeded forearm are not functioning properly. What is the most likely nerve injury in this case?

Answer: Radial nerve

Question 3: Following a shoulder operation, a patient is unable to elevate his arm. Physical examination reveals that the deltoid is not working properly. Which nerve has most likely been injured during the operation?

Answer: Axillary nerve

Question 4: A person slipped on ice and fell onto his elbow. Physical examination showed a fracture, and the patient has been taken into the theater for an operation to fix the fracture. Following the operation, the patient lost sensation of must be excluded the little finger of the hand. Which nerve is most likely to have been injured?

Answer: Ulnar nerve

References

1. Bandalović A, Cukelj F, Knežević J, Ostojić M, Pavić A, Parać Z, Rošin M (2014) The results of internal fixation of proximal humeral osteoporotic fractures with PHILOS locking plate. Psychiatr Danub 26(Suppl 2):376–381
2. Buturovic S, Krupic F (2014) Comparison of treatment results for fractures of the distal humerus in children according to the indication for conservative or surgical solution. Mater Sociomed 26(4):242–245
3. Reising K, Konstantinidis L, Helwig P, Wagner FC, Südkamp NP, Strohm PC (2014) Minimally invasive stabilization of distal humerus fractures: a pilot study with biomechanical evaluation. Technol Health Care 22(6):909–913
4. Hultgren T, Jönsson K, Roos F, Järnbert-Pettersson H, Hammarberg H (2014) Surgical correction of shoulder rotation deformity in brachial plexus birth palsy: long-term results in 118 patients. Bone Joint J 96-B(10):1411–1418
5. Wu W, Li X, Shi Q, Dai S, Tan W, Hu C (2014) Minimally invasive treatment of Gartland type III humerus supracondylar fracture in children. Nan Fang Yi Ke Da Xue Xue Bao 34(9):1351–1354
6. Laver L, Garrigues GE (2014) Avoiding superior tilt in reverse shoulder arthroplasty: a review of the literature and technical recommendations. J Shoulder Elbow Surg 23(10):1582–1590
7. Saglam Y, Tunali O, Akgul T, Dikmen G, Aksoy M, Dikici F (2014) Mid-term results of pediatric vascular injured supracondylar humerus fractures and surgical approach. J Pediatr Orthop B 23(6):572–578
8. Habib M, Tanwar YS, Jaiswal A, Singh SP, Sinha S, Lal H (2014) Anconeus pedicle olecranon flip osteotomy: an approach for the fixation of complex intra-articular distal humeral fractures. Bone Joint J 96-B(9):1252–1257
9. Lin T, Xiao B, Ma X, Fu D, Yang S (2014) Minimally invasive plate osteosynthesis with a locking compression plate is superior to open reduction and internal fixation in the management of the proximal humerus fractures. BMC Musculoskelet Disord 15:206
10. Al-Hadithy N, Domos P, Sewell MD, Pandit R (2014) Reverse shoulder arthroplasty in 41 patients with cuff

tear arthropathy with a mean follow-up period of 5 years. J Shoulder Elbow Surg 23(11):1662–1668
11. Zhang C, Zhang ZJ, Wang L, Niu SL, Wen YF, Guo YX (2014) Treatment of type C3 distal radius fractures with AO 2.4 mm locking plate system after manipulative reduction. Zhongguo Gu Shang 27(11): 965–969
12. Löw S, Herold A, Eingartner C (2014) Standard wrist arthroscopy: technique and documentation. Oper Orthop Traumatol 26(6):539–546
13. Broyles JM, Abt NB, Shridharani SM, Bojovic B, Rodriguez ED, Dorafshar AH (2014) The fusion of craniofacial reconstruction and microsurgery: a functional and aesthetic approach. Plast Reconstr Surg 134(4):760–769
14. Lew SQ, Nguyen BN, Ing TS (2014). Hemodialysis vascular access construction in the upper extremity: a review. J Vasc Access 0(0):0. doi:10.5301/jva.5000299. [Epub ahead of print]
15. Zimmerman RM, Kalish LA, Hresko MT, Waters PM, Bae DS (2013) Surgical management of pediatric radial neck fractures. J Bone Joint Surg Am 95(20):1825–1832
16. Sen S, Sari S, Kurt I, Cobanoglu M (2014) The use of train of four monitoring for clinical evaluation of the axillary brachial plexus block. J Clin Monit Comput 28(3):243–249
17. Jones JA, Jones CM, Grossman MG (2013) Effect of elbow flexion on the proximity of the PIN during 2-incision distal biceps repair. Orthopedics 36(7):e931–e935
18. Unglaub F, Manz S, Bruckner T, Leclère FM, Hahn P, Wolf MB (2013) Dorsal capsular imbrication for dorsal instability of the distal radioulnar joint. Oper Orthop Traumatol 25:609–614

Lower Extremity

44

Murat Bozkurt, Çetin Işık, Mustafa Akkaya, and Safa Gürsoy

Abstract

Relation between hip, knee, and ankle is mandatory in order to provide adequate lower extremity functions. Besides these joint functions, muscle, tendon, and ligament contribution is essential. In this chapter, the place of knee and ankle in lower extremity functions and surgical approaches will be discussed.

Learning Outcomes

Learning outcomes in this section are identified as follows:

- Evaluation of intra-articular and extra-articular structures of the hip
- Evaluation of anatomical structures of ankle
- Conducting alignment analysis of lower extremity
- Evaluation of normal knee kinematics
- Learning orthopedic surgical approaches to knee and ankle joint

Terminology

ACL Anterior cruciate ligament
MCL Medial collateral ligament
LCL Lateral collateral ligament
PCL Posterior collateral ligament
PLC Posterolateral corner
SIAS Spina iliaca anterior superior
Femoral anteversion angle Forward angling between the surface running through femoral shaft condyles and femoral neck
Recurvatum Is a deformity in the knee joint, in which the knee bends backward
TKR Total knee replacement
PEV Pes eqinovarus
FHL Flexor hallucis longus

M. Bozkurt (✉) • C. Işık • M. Akkaya
S. Gürsoy
Department of Orthopaedics, Ankara Ataturk Training and Research Hospital, Ankara, Turkey
e-mail: nmbozkurt@yahoo.com; ortdrcetin@gmail.com; makkaya@outlook.com; safagursoy@yahoo.com

F. Korkusuz (ed.), *Musculoskeletal Research and Basic Science*,
DOI 10.1007/978-3-319-20777-3_44

Clinical Relevance
Basic anatomical structures must always be taken into consideration and known during clinical implementations. Having a proper knowledge of clinical and functional anatomy of lower extremity facilitates orthopedic surgical interventions.

Several approaches can be adopted while getting access to the knee and ankle joint. This makes it necessary to have proper knowledge of intra-articular and extra-articular structures of both knee and ankle joint. Consequently, surgical approaches would be safer with minimum damage to the surrounding soft tissue.

Knowing the orthopedic surgical pathologies in lower extremity and the degree of anatomical and functional success of treatment procedures to be implemented is quite crucial for the patient's clinic. Knowledge of normal joint functions is necessary for assessment of this matter. This section discusses clinical and functional anatomy of lower extremity with regards to knee and ankle joint.

Knee: Functional and Clinical Anatomy

Knee joint is the largest one in the body. It is a hinge-like joint, according to its surface, shape, and these types of joints have single-axis motion. Bone structure, meniscuses, and ligaments provide a static stability, while the surrounding muscles provide a dynamic stability [1].

Half of the body weight while walking, 3.3 times of it while climbing up stairs, and 6.5 times of it while crouching affect knee joint.

Knee anatomy can be grouped under three main headings:

- Bone structures
- Intra-articular structures
- Extra-articular structures

Bone Structures

There are three main bone structures. These are femoral condyle, tibial plateau, and patella (Fig. 44.1). Frontal face of femoral condyle is oval and rear face is circular. Thanks to this structure, extension stability and a large range of motion are provided. Lateral femoral condyle is larger than medial condyle. Depending on this, tibia engages in internal rotation during flexion and in external rotation during extension [2].

Tibial plateau: it consists of two parts, medial and lateral, and they have different size. The main load-bearing part is medial plateau.

Patella: It is the largest sesamoid bone of the body functioning in the extensor mechanism. Largest contact surface of patella appears when the knee is flexed 45° [2].

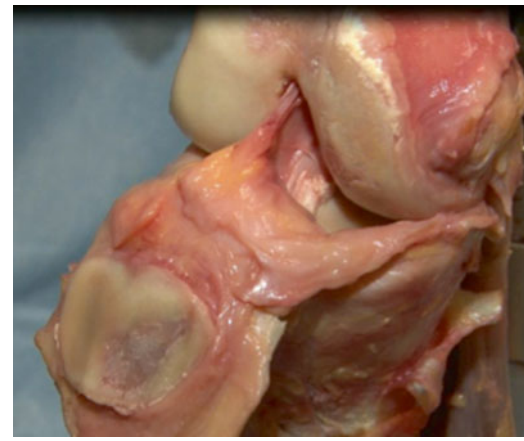

Fig. 44.1 Bone structures of knee joint

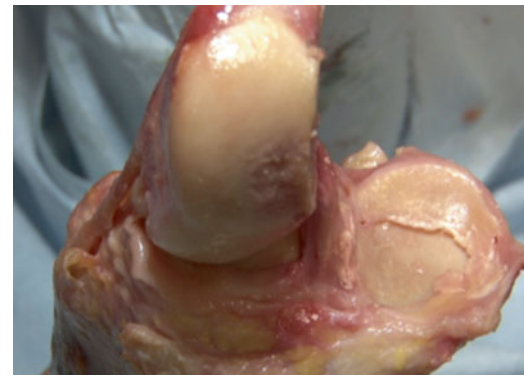

Fig. 44.2 Intra-articular structures of knee joint

Intra-articular Structures

There are three main intra-articular structures. These are synovia, meniscuses, and ligaments.

Synovia provides lubrication to the knee joint. In some cases, its hypersecretion might cause effusion and pain (pigmented villonodular synovitis).

Meniscuses provide equal load distribution on the knee joint and provide shock absorption. It is divided into medial and lateral meniscus.

Medial meniscus: It has a semicircular shape, and its rear part is larger. Its middle one-third portion tightly holds MCL. Most of the injuries occur in the external rotation of tibia (Fig. 44.2).

Lateral meniscus: It has a circular shape compared to medial meniscus and covers a larger portion of the articular surface. It does not have connection to LCL, and therefore is more mobile. There are two ligaments which run to the medial femoral condyle through posterior horn of the lateral meniscus, and named in reference to their relations with PCL. The ligament located anterior to the PCL is called anterior meniscofemoral ligament (Humphrey ligament), while the one located posterior to PCL is called post meniscofemoral ligament (Wrisberg ligament). The injuries usually occur during knee flexion [3]. During medial and lateral meniscus examination, it is assessed through McMurray and Apley tests.

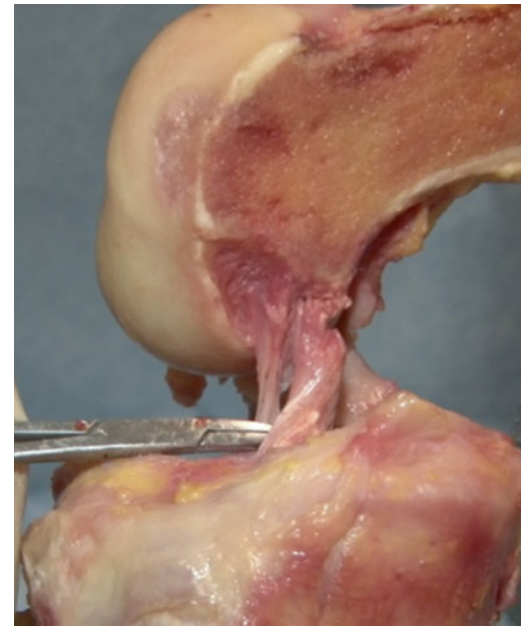

Fig. 44.3 Anterior and posterior cruciate ligaments

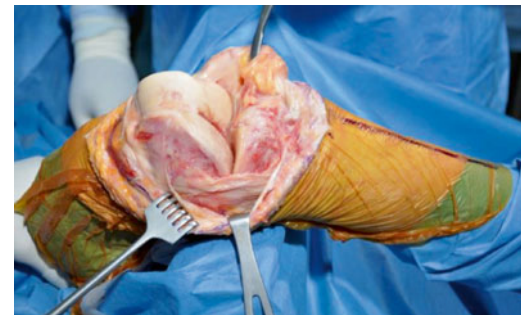

Fig. 44.4 Lateral collateral ligament

Anterior, Posterior Cruciate and Collateral Ligaments

Anterior cruciate ligament resists tibia's displacement to the front. It is assessed by anterior drawer, Lachman, and pivot shift tests. It is composed of two bands named in reference to the place of their tibial attachment: AM (anteromedial) and PL (posterolateral). The positions of the bands are different during flexion and extension, and they cross one another during flexion [3]. AM flexion stability ensures PL extension stability. The injury there usually occurs when the tibia in internal rotation is forced to extension and when it is in hyperextension (Fig. 44.3).

Posterior cruciate ligament resists tibia's displacement to the back. It is assessed by posterior drawer test, and the symptom of posterior sag is checked. The injury there occurs following anterior tibial traumas and when the tibia in internal rotation is forced to hyperflexion.

Medial collateral ligament (MCL) has superficial and deep fibers. It resists against valgus straining and may rupture after valgus traumas. In gonarthrosis with severe varus alignment deformity, it typically loosens superficial fibers during TKR.

Lateral collateral ligament (LCL) resists against varus straining (Fig. 44.4).

Medial collateral ligament is tighter compared to the lateral ligament; therefore, motion is less in the medial compartment.

Posteromedial and lateral capsule structures resist against rotation.

Extra-articular Structures

It consists of extra-articular muscles. Quadriceps is the strongest extensor of the knee. It is composed of four muscle groups. Extensor muscles are three times stronger than flexors.

Hamstring muscles are composed of biceps, sartorius, gracilis, and semitendinosus. Moreover, pes anserinus is composed of sartorius, gracilis, and semitendinosus.

Q Angle

It is the angle between the ASIS and the midpoint of the patella. It is approximately 12° in females while being 15° in males. Growing angles lead to anterior knee pain and patellar chondromalacia. Increased angle may develop patellar subluxation. If femoral anteversion is increased and tibial external rotation is available, then Q angle increases [4].

There are five main structures supporting the knee joint. These are as follows:

Anterior Support Complex: It is composed of quadriceps tendon, patellar tendon, medial and lateral retinacula, and infrapatellar fat pad.

Medial Support Complex: It is composed of medial head of gastrocnemius, hamstring muscles, and MCL. This resists against valgus traumas. If medial (valgus) instability exists, then

- Abduction stress test is positive in flexion, and it becomes positive in PCL rupture in extension as well
- ACL is typically ruptured
- PCL is typically ruptured
- Medial capsular ligament ruptured
- MCL ligament may have ruptured

Lateral Support Complex: It is composed of lateral head of gastrocnemius, popliteus, tendon and LCL (Fig. 44.5). This structure protects against varus traumas. If it has lateral (valgus) instability, then

- Abduction stress test is positive in flexion, and it becomes positive in PCL rupture in extension as well
- ACL is typically ruptured
- PCL is typically ruptured
- Lateral capsular ligament ruptured
- LCL ligament may have ruptured

Posteromedial Corner is supported by posteromedial capsule, semimembranosus tendon, and sheath. It is a significant structure in providing static stability (Fig. 44.6).

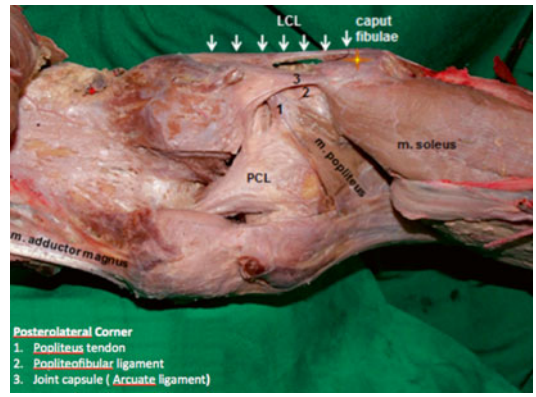

Fig. 44.5 Posterolateral corner of knee joint. Posterolateral corner: *1* popliteus tendon, *2* popliteofibular ligament, *3* joint capsule (arcuate ligament)

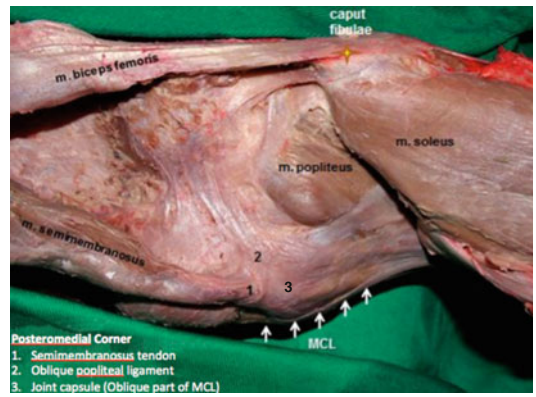

Fig. 44.6 Posteromedial corner of knee joint. Posteromedial corner: *1* semimembranosus tendon, *2* oblique popliteal ligament, *3* joint capsule (oblique part of MCL)

Posterior Support Complex is composed of oblique popliteal ligament, arcuate ligament, popliteus tendon, and gastrocnemius muscle.

Oblique ligament is the continuation of semimembranosus and provides significant stability in extension. Popliteus tendon on the other hand prevents compaction of lateral meniscus and plays a significant role in the stability of the posterolateral corner. Gastrocnemius muscle provides a dynamic contribution to the stability of the posterolateral corner.

Alignment Deformity

- Genu varum → occurs when mechanical axis of lower extremity runs more than 15 mm medial to the alignment center in frontal plane
- Genu valgum→ occurs when mechanical axis of lower extremity runs lateral to the alignment center in frontal plane
- Genu recurvatum → occurs if the knee can be passively extended more than 5° in sagittal plane

Normal Knee Kinematics

Range of Joint Motion The range of motion in knee joint ranges from −10° (recurvatum) to 130°. Functionally acceptable range of motion is between 0 and 90°. The rotation in knee joint varies depending on the flexion. When in full extension, there is little rotation, while in 90° flexion, 45° of external rotation and 30° of internal rotation are possible. During the motion of knee joint, displacement occurs in the medial and lateral meniscus [5].

Joint Motion

Femoral Rollback It is the displacement/rollback to the posterior as the knee flexion increases. Between 0 and 90° of flexion motion, femorotibial contact point displaces 14 mm to the posterior.

Flexion and extension motion → It occurs between the femoral lower point and meniscus upper point.

Twisting motion → It occurs between the meniscus base and tibia [6].

- *Kinetics*
- Extension is performed by quadriceps mechanism with extension patellar system, and flexion is performed by hamstring muscles.
- *Knee Stabilizers*
- The actual stabilizers of the joint are muscles and ligaments around the knee. Anterior cruciate ligament is subjected to 170N and 500N load during normal walking and running, respectively. In a young person, it can bear maximum 1750N. Anterior cruciate can extend as far as 10–15 % at the most, beyond which tear begins to occur [4].

Joint Forces

- *Tibiofemoral joint*
- Surface forces on knee joints increases by three times of normal body weight while walking on a flat plane, and by four times when climbing up stairs. Meniscuses serve as transferring agents in load transfer. Their complete removal increases joint stress.
- *Patellofemoral joint*
- Patella helps in extension by extending support arm and providing stress distribution. It is the thickest cartilage in the body for it is the joint that bears the biggest load. While climbing down the stairs, compressive forces between patella and trochlea increase as far as two to three times of body weight. Following patellectomy, the length of the moment arm decreases as much as the thickness of the patella.

Following are the factors that improve patellar motion in TKR: external rotation of femoral component, placement of tibial and femoral component to lateral, placement of patellar component to medial, and avoiding placement of tibial component to internal rotation.

Axis of Lower Extremity

- *Mechanical axis*: It runs from the femoral head center to the center of ankle.
- *Vertical axis*: It runs to the ground from the center of gravity.
- *Anatomical axis*: It runs to the tibia and femoral shafts. When both of these axes join on the knee, the valgus angle appears.
- *Femoral mechanical axis*: It runs from the femoral head center to the knee center.
- *Tibial mechanical axis*: It runs from the tibia plateau center to the center of ankle.
- Mechanical axis of lower extremity is located 3° to the valgus compared to vertical axis. Anatomical axis of femur is located 6° to the valgus compared to mechanical axis. Anatomical axis of tibia is located 2–3° to the valgus compared to mechanical axis [4].
- Ideal position for knee arthrodesis is 0–7° valgus and 10–15° flexion [4].

Knee: Orthopedic Surgical Approaches

Anterior Approach

This is the most frequently used approach. It perfectly complies with many structures. The patient lies in supine position. This approach does not involve interneural plane, and it is safe. Infrapatellar branch of saphenous nerve may get damaged [7] (Fig. 44.7). The cases where it is often used are as follows:

- Arthroplasty
- Synovectomy
- Open meniscectomy
- Open ligament reconstruction
- Arthrodesis
- *Guide points*
  - Patella–tuberositas tibiae
- *Incision*
  - Start incising from 5 cm above the patella upper pole, following a midline to the tuberositas tibiae [7].

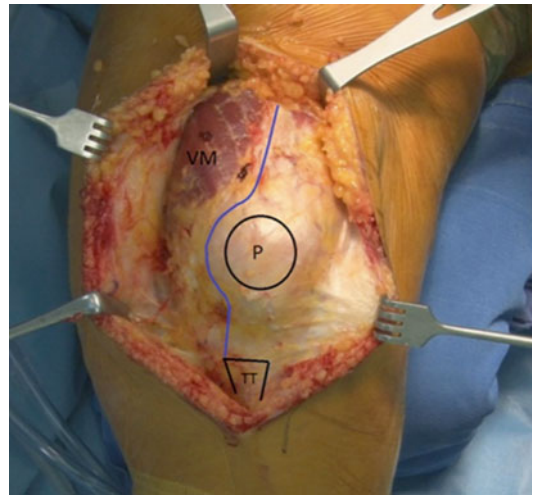

Fig. 44.7 Anterior approach of knee joint

- *Superficial and Deep surgical dissection*
  - To identify the medial margins of quadriceps and patellar tendon, form a medial skin flap.
  - Enter the joint by cutting the joint capsule in a prepatellar way.
  - Exclude or dislocate patella to lateral. Be careful about the patellar tendon rupture, which might occur during this procedure.
  - Clear fat pads behind the patellar tendon for a better vision.
  - Midvastus or subvastus incision is among the alternatives to prepatellar incision.
- *Structures under risk*
  - Infrapatellar branch of saphenous nerve is often cut. The numbness that occurs does not often cause problems.

Medial Approach

It provides access to the medial of the knee. The patient lies in supine position. This approach does not involve the interneural plane. Cutaneous branch of saphenous nerve might be damaged [7]. The cases where it is often used are as follows:

- Medial hemiarthroplasty (unicondylar)
- Ligament repair
- Intra-articular fractures

- *Guide points*
  - Adductor tubercle–tuberositas tibiae
- *Incision*
  - Incise unevenly starting from 2 cm proximal to the adductor tubercle, proceeding to the tibial anteromedial face. Stop at 3 cm medial to the medial edge of patella.
- *Superficial surgical dissection*
  - After removing the skin flap, infrapatellar branch of saphenous nerve is cut as it crosses the surgical area.
  - Saphenous nerve which arises between gracilis and sartorius must be preserved.
  - Following the dissection of sartorial fascia, it is cut along its fibers.
- *Deep surgical dissection*
  - After removing the medial collateral ligaments, conduct the capsular incision following deep fibers.
- *Structures under risk*
  - Infrapatellar branch of saphenous nerve
  - Saphenous vein
  - Inferior medial genicular artery
  - Popliteal artery

Lateral Approach

It provides access to all structures at the lateral side of the knee. The patient lies in supine position. Putting something under the patient's hip to raise it will provide a better operating site [7]. The cases where it is often used are as follows:

- Lateral and posterolateral repair and reconstruction
- Repair of lateral meniscus
- *Guide points*
  - Patella lateral edge and lateral joint space–Gerdy's tubercle
- *Incision*
  - It must be an incision of 10 cm long, which centers the joint line at the posterolateral.
  - The incision must run from the lateral collateral ligament to the anterior of biceps tendon.
- *Superficial surgical dissection*
  - After penetrating the skin and subcutaneous tissue, iliotibial band and biceps tendon appear.
- *Deep surgical dissection*
  - Peroneal nerve must be dissected and preserved (posterior to the biceps muscle).
  - Posterior one-third of iliotibial band and biceps spacing → lateral collateral ligament and popliteus tendon
  - Upper one-third of iliotibial band → lateral femoral epicondyle
- *Structures under risk*
  - Peroneal nerve
  - Lateral superior genicular artery

Posterior Approach

This approach is usually used to make a neurovascular intervention. The patient lies in lateral decubitus or in prone position [7]. The cases where it is often used are as follows:

- Operations on neurovascular structures located posterior to the knee
- Lengthening hamstring tendons
- Removal of Baker's and popliteal cyst
- Avulsion fracture of the tibial attachment of the posterior cruciate ligament
- *Guide points*
  - Gastrocnemius (medial, lateral head) – semimembranosus, biceps
- *Incision*
  - Conduct an incision starting from femur lateral at the proximal and having an "S" shape in the popliteal fossa while extending to the distal.
- *Superficial surgical dissection*
  - After penetrating the skin and subcutaneous tissue, small saphenous vein and medial sural cutaneous nerve appear.
  - These structures are regarded as a guide, and popliteal fascia is cut lateral to the vein.
  - There is a common peroneal nerve in the peak of popliteal cavity, and this is dissected and preserved.
  - Immediately medial to it, tibial nerve and popliteal artery–vein run, and care must be exercised.

- *Deep surgical dissection*
  - Muscles forming the margins of popliteal cavity are excluded, and various parts of the joint capsule may be accessed.
  - To access the medial of joint capsule, gastrocnemius medial head can be removed from the femoral attachment place; similarly, lateral head can be removed from the femoral attachment place to have access to the lateral of the joint.
- *Structures under risk*
  - Small saphenous vein
  - Medial sural cutaneous nerve
  - Tibial nerve
  - Common peroneal nerve

Ankle: Functional and Clinical Anatomy

Ankle is the region of the body which is most frequently exposed to trauma. Trauma mostly occurs when the ankle is in flexion and inversion. There are a total of 28 bones and 25 joints in the foot and ankle complex. Ankle or "talocrural joint" consists of three bones: tibia, fibula, and talus [8]. Articular surface lies between talus–tibia and talus–fibula. It is a strong and stable hinge-like joint. The concave surface created by the articulation of tibia and fibula is called "Mortis." This region is controlled by the proximal and distal tibiofibular joint. Capsule and ligaments contribute to the stability of the ankle (Fig. 44.8).

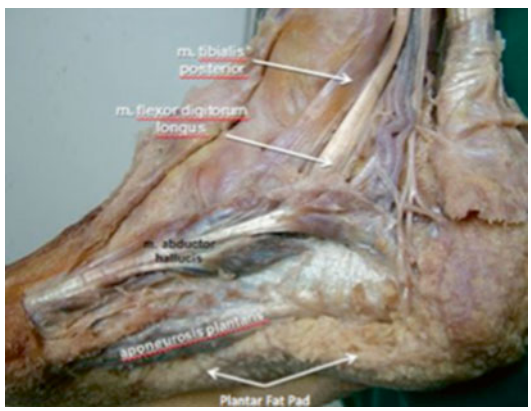

Fig. 44.8 Anatomic dissection of ankle joint

- *Ligaments*
  - Medial/deltoid ligament → resists against valgus stress
  - Lateral ligament→ resists against varus stress
  - Anterior talofibular ligament
  - Calcaneofibular ligament
  - Posterior talofibular ligament
- *Innervation*: it is performed by peroneal and tibial nerves.
- *Motion*: it is performed in ankle on three planes, as dorsiflexion (20°), plantar flexion (30–50°), and rotation (5°).
- *Biomechanics*
  - *Kinematics*: the center of instant rotation is in the talus. During ankle dorsiflexion, talus and fibula are slightly rotated externally. Therefore, ankle dorsiflexion and abduction are done together.
  - *Kinetics*: load-bearing main structure is the tibiotalar articular surface. It is exposed to compressive five times of body weight during walking and shear force equal to body weight. With its large bearing surface, it tries to decrease the stress on the joint. Tibiotalar articular surface bears one-sixth of the load [9].
  - The joint is structurally quite stable. This is provided by its form and ligament support. The state where it has maximum stability is dorsiflexion.
  - Ideal ankle arthrodesis is 5–10° external rotation and 5° hindfoot valgus.

Ankle: Orthopedic Surgical Approaches

Anterior Approach

Anterior approach to ankle is typically preferred in arthrodesis surgery. The patient lies in supine position, and putting something to raise the hip on the same side allows a better surgical view. The cases where it is often used are as follows:

- Drainage of infections of ankle joint
- Free object removal
- Pilon fractures
- *Guide points*
  - Medial malleolus–lateral malleolus
- *Incision*
  - An incision is conducted centering the ankle joint with an equal distance to the internal and external malleolus, starting from the proximal and having 10–15 cm of length, and it is ended at the dorsum of foot.
  - Where required, the end of the incision may be done by curving to the medial.
  - Only the skin must be incised. Superficial peroneal nerve is quite close to this region.
- *Superficial surgical dissection*
  - Superficial peroneal nerve is found and preserved.
  - Deep fascia is opened on the same line with the skin incision.
  - Extensor retinaculum is cut by inserting the fixation suture to repair afterward.
- *Deep surgical dissection*
  - Following exclusion of tendons, have access to the capsule.
  - After incising the capsule longitudinally, you have access to the ankle.
- *Structures under risk*
  - Superficial peroneal nerve runs close to the skin incision.
  - Deep peroneal nerve and anterior tibial artery

Medial Approach

The patient lies in supine position, and something might be put under the opposite hip to raise it. The cases where it is necessary to have medial approach to ankle are as follows:

- Ankle arthrodesis
- Identification or excision of osteochondral fragment
- Joint mice in ankle
- *Guide points*
  - Medial malleolus
- *Incision*
  - Have an incision of 10 cm centering the medial malleolus heading toward the middle foot medial
- *Superficial surgical dissection*
  - Superficial surgical dissection is done, and long saphena and saphenous nerve are found. Then these structures are excluded to the anterior.
- *Deep surgical dissection*
  - The margins of medial malleolus appear, and joint capsule is cut anterior to the malleolus
  - After finding the tibialis posterior tendon, flexor retinaculum is cut posterior to the malleolus.
  - Deltoid ligament is preserved.
- *Structures under risk*
  - Saphenous nerve
  - Great saphenous vein
  - Tibialis posterior tendon

Posteromedial Approach

This is preferred to have access to the structures behind medial malleolus. The patient might lie in supine or lateral decubitus position. The cases where it is often preferred are as follows:

- PEV treatment
- Posterior malleolar fractures
- *Guide points*
  - Medial malleolus and Achilles tendon
- *Incision*
  - Have a longitudinal incision of 8–10 cm between medial malleolus and Achilles tendon
- *Superficial surgical dissection*
  - Following superficial surgical dissection, fascia enclosing flexor tendons is found, and cut longitudinally.
- *Deep surgical dissection*
  - Following blunt dissection, Achilles tendon and fat tissue behind that is excluded to the lateral.

  - Deep flexor compartment is reached.
  - Deep fascia is cut at the same length as the skin incision.
  - Flexor retinaculum is carefully placed inside the middle (posterior vein nerve pack), and then it is excluded to medial, allowing access to posterior malleolus and posterior ankle.
- *Structures under risk*
  - Tibial nerve
  - Tibialis posterior artery

Posterolateral Approach

This is used to have access to the structures located distal to the tibia and posterior to the ankle. The patient lies in prone position. Putting a pillow under the ankle or something to raise it might facilitate manipulation of the ankle. The cases where it is often preferred are as follows:

- Removal or debridement of sequestrum
- Posterior malleolar fractures
- Lengthening of Achilles tendon
- Posterior facet arthrodesis of subtalar joint
- *Guide points*
  - Lateral malleolus and Achilles tendon
- *Incision*
  - Have a longitudinal incision of 8–10 cm between lateral malleolus and Achilles tendon
- *Superficial surgical dissection*
  - Following superficial surgical dissection, short saphenous vein and sural nerve are found and preserved.
  - Deep fascia is cut alongside the skin incision.
  - Both peroneal tendons are found, and brevis is short and located anterior to the fibula.
  - Peroneal retinaculum is opened, and tendons are excluded to the lateral.
  - Flexor hallucis longus tendon is found.
- *Deep surgical dissection*
  - Fascia on the FHL is opened and removed from tibula, following sharp dissection, and pulled toward medial.
  - Periosteum is lifted, and the posterior surface of tibia and ankle is reached.
- *Structures under risk*
  - Short saphenous vein
  - Sural nerve

Conclusion

Human mobilization and daily activities can only be achieved with proper cooperation of the knee, ankle, and hip. Successful surgical outcomes can be improved after understanding of lower extremity functions and learning the proper surgical approaches carefully.

References

1. Mikosz RP (1995) Anatomy and the biomechanics of the knee. OKU hip and knee reconstruction, 1st edn. AAOS Publishing, Rosemont, ILs, 227
2. Norkin CC, Levangie PK (2005) Joint structure & function: a comprehensive analysis, 2nd edn. F.A. Davis Co, Philadelphia
3. Fu FH (1994) Biomechanics of knee ligaments. Basic concepts and clinical application. AAOS Instr Course Lect 43:p137
4. Miller MD (2006) Review of orthopaedics. 5th edition, Biomater Biomech 126–134
5. Malone TR, McPoil T, Nitz AJ (1997) Orthopedic and sports physical therapy, 3rd edn. Mosby-Year Book, St. Louis
6. Ann SS, Fitch GK (1993) Understanding human anatomy and physiology. West Publishing Co, St. Paul
7. Hoppenfeld S (2012) Surgical exposures in orthopaedics: the anatomic approach. Philadelphia, Lippincott Williams & Wilkins, pp 509–577, 623–691
8. Andrews J, Harrelson GL, Wilk KE (2003) Physical Rehabilitation of the Injured Athlete, 3rd edn. Saunders, Philadelphia, pp 365–371
9. Ellis H (2006) Clinical anatomy, 11th edn. Blackwell Publishing, Carlton

The Surgical Anatomy of the Lower Limb

45

Halil Ibrahim Acar

Abstract

The close relationships between pelvic organs, iliac vessels and their braches, spinal nerves which form lumbosacral plexus and fibres originate from this plexus with acetabulum, pubic symphysis and sacroiliac joint could be associated with major complications including death in the course of surgical procedures on these regions. It must be remembered during all anterior, posterior and lateral approaches that; the femoral nerve and vessels lie anteromedial to the sciatic nerve passing just behind of hip joint. Distally, the knee, the largest joint of the body, has a complicated stability. The importance of the structures on posteromedial and posterolateral corners regarding stability of the knee joint frequently takes place in the current reports. The compartments of leg divided by strong fascial layers and the structures they contain must be kept in mind particularly for surgical treatments of compartment syndrome. The placements of tendons and neurovascular structure around the ankle and in tarsal tunnel guide the surgical approaches to these regions.

In this chapter, the surgical anatomy of the lower limb joints and the neighboring neurovascular structures is discussed. The structures of the lower limb and significant units encountered in dissections are evaluated with surgical approaches, maintaining anatomical morphology.

Pelvis

The relationship of the hip joint with the pelvic structures is essential. Obturator blood vessels and nerves are found in the neighborhood of the

H.I. Acar, MD, PhD
Faculty of Medicine, Department of Anatomy,
Ankara University, Ankara, Turkey
e-mail: drhalilacar@gmail.com

F. Korkusuz (ed.), *Musculoskeletal Research and Basic Science*,
DOI 10.1007/978-3-319-20777-3_45

quadrilateral surface on the medial side of the acetabulum [1]. Acetabulum can be separated into four quadrants, with two lines passing from the tips of the anterior superior and posterior inferior iliac spines to its center point. Posterior superior section is the thickest part of the bone. Surgical screws can be placed in this section to protect the obturator blood vessels and nerves that are located medially [2]. Though the anterior inferior section seems like the safest section, the thickness of the bone is about 1 cm. Yet, this thickness is about 3 cm in the posterior superior section.

Urethra and bladder are found right behind the pubic symphysis [3]. Along with these two structures, prostate gland, prostatic and vesical venous plexuses, where the deep dorsal vein of the penis/clitoris drains may be damaged [4]. During surgical approaches to the symphysis pubis, these relationships should be carefully considered.

Vascular structures located on the superior pubic ramus may cause severe bleeding in surgical procedures of this region. Anastomosis can be observed between the pubic branches of the obturator and inferior epigastric arteries. This anastomosis, known as corona mortis, is defined as a connection between the internal and external iliac arterial system, but venous connections were more commonly encountered [5, 6]. By decreasing the diameter of the obturator artery, the diameter of this anastomosis becomes larger, and more blood can be carried to the obturator system. Furthermore, the accessory obturator artery arising from the inferior epigastric artery and extending to the obturator canal can be observed without the existence of the obturator artery originating from the internal iliac artery [7].

The retroperitoneal neurovascular structures passing beneath the inguinal ligament form the majority of vessels and nerves of the thigh. These structures extend within the femoral triangle of the thigh on the front. Under the inguinal ligament, there are two important channels called muscular and vascular spaces (muscular and vascular lacuna). The muscular space where the iliopsoas muscle, femoral, and lateral femoral cutaneous nerves passed through is located laterally. The vascular space where femoral artery and vein run is placed medially [8].

Anatomy of the Hip Joint and Thigh

The cutaneous and subcutaneous structures are passed by incisions parallel to the lateral edge of gluteus maximus during the posterior approach to the hip joint. Gluteus maximus and a small part of gluteus medius are visible underneath the gluteal fascia. The superior cluneal nerves, which are the important sensory nerves of the gluteal region, are located 8 cm anterolateral to the posterior superior iliac spine [9]. Gluteus maximus has a thick fascia which forms compartments that surround the muscular bundles. A large segment of gluteus medius and the superficial branches of superior gluteal vessels can be seen when gluteus maximus is retracted medially (Fig. 45.1). The external rotator muscles consisting of piriformis, superior gemellus, obturator internus, inferior gemellus, and quadratus femoris, respectively, covered with connective tissue are found inferior to this segment [10]. The sciatic nerve is the most significant and obvious structure in this region. Additionally, inferior gluteal vessels, inferior gluteal nerve, posterior femoral cutaneous nerve, and medially, internal pudendal vessels and pudendal nerve can be observed. Sciatic nerve leaves the pelvic cavity through the greater sciatic foramen, inferior to piriformis at the gluteal region (Fig. 45.1). It overlies the small rotator muscles beneath gluteus maximus and passes into the posterior thigh compartment. The tendons of rotator muscles extending to the greater trochanter have to

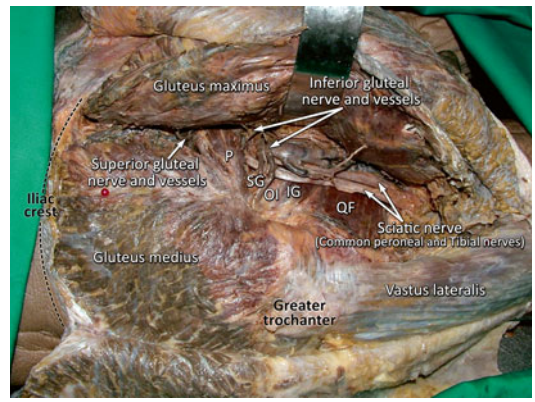

Fig. 45.1 The adjacent structures of the backside of the left hip joint after lifting up the gluteus maximus are seen. *P* piriformis, *SG* superior gemellus, *OI* obturator internus, *IG* inferior gemellus, *QF* quadratus femoris

be detached and elevated in order to reach the hip joint capsule. The head of the femur and the sciatic nerve are observed to be in close proximity, once the hip joint is exposed. The distance between these structures is approximately 1–1.5 cm due to the weakness of the posterior part of the capsule. Sciatic nerve extends slightly medial to the center of the line between ischial tuberosity and greater trochanter.

A vertical incision is made above greater trochanter to approach the hip joint laterally. Thigh fascia (fascia lata) is observed, and then the skin and the superficial fascia are passed. In this region, the fascia thickens to form the iliotibial tract, which lies toward the leg. Gluteus medius, which holds on to the greater trochanter superiorly, and the tendinous attachment of vastus lateralis, which lies in the lateral part of the thigh, can be exposed when the fascia is incised. It is important to recognize the formation of muscles in this area. The tendons of these muscles can be detached from greater trochanter with a "V" shaped incision, with the opening of "V" facing the anterior side in order to protect the muscle fibers [10]. The profound branches of the superior gluteal vessels and nerves passing through the upper part of the greater sciatic foramen (suprapiriform foramen) and lying between gluteus medius and gluteus minimus have to be preserved. These neurovascular structures are found approximately 3–5 cm above the greater trochanter. It should be noted that the distance decreases as we progress toward the front [11]. The terminal branch of the superior gluteal nerve goes to the tensor fascia latae. This muscle is significant, as it is the only muscle innervated posteriorly and flexes the thigh.

For the anterior or anterolateral approaches of the hip joint, skin incision is started from the anterior superior iliac spine to between the tensor fascia latae and sartorius. Lateral femoral cutaneous nerve is the most important structure which must be protected during this incision. This nerve passes under the inguinal ligament and usually over the proximal attachment of the sartorius and enters the fascia of thigh, approximately 2.5 cm below the anterior superior iliac spine [12]. Incisions are performed on the thigh fascia, and deeper levels are reached. The nerve and sartorius must be protected by retracting medially. The incision is deepened in the internervous plane between the sartorius innervated by the femoral nerve and the tensor fascia latae innervated by the superior gluteal nerve. In order to reach the hip joint, we pass between gluteus medius and biceps femoris on the same intravenous plane. Meanwhile, the ascending branch of the lateral femoral circumflex artery lying along the anterior side of the hip joint can cause bleedings [10] (Fig. 45.2). Anterior part of the hip joint capsule can be reached with the removal of the blood vessels and connective tissue.

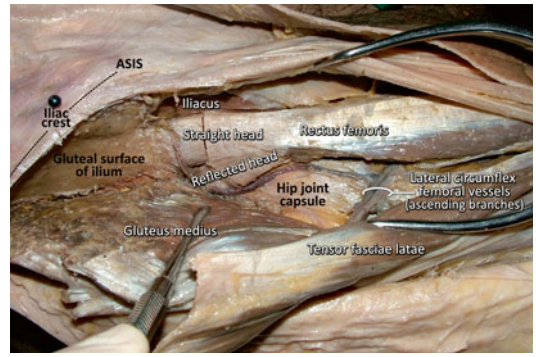

Fig. 45.2 The anterior side of the right hip joint was approached passing between first sartorius and tensor fascia latae, and second gluteus medius and rectus femoris. During this approach, attention must be paid to bleeding from the ascending branch of the lateral femoral circumflex artery. *ASIS* anterior superior iliac spine

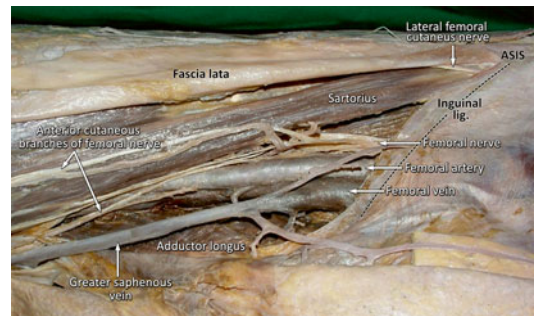

Fig. 45.3 Fascia lata covering the right femoral triangle was removed, and the main neurovascular structures located in this region were made visible. Attention must be paid to the structures located from the medial to lateral, under the inguinal ligament. *ASIS* anterior superior iliac spine

Femoral vessels and nerves in the femoral triangle can be injured during retraction if these are not closely noticed. Femoral triangle is the most important part which is found in the anterior superior part of the thigh (Fig. 45.3). The base of

the femoral triangle is upward; its apex is downward and constituted superiorly by inguinal ligament, medially by adductor longus, and laterally by sartorius. Fascia lata which covers the muscles is observed in this area when the skin and subcutaneous tissue are removed. Saphenous opening where the great saphenous vein enters deeper plane is located on the fascia lata covering femoral triangle. Hence, femoral hernias protrude from this area to underneath the skin. After passing beneath the inguinal ligament, external iliac artery goes into the femoral triangle, and it is named as femoral artery. Deep artery of the thigh (profunda femoris artery), which is supplying the posterior side of the thigh is found 2–5 cm beneath the inguinal ligament, and it originates from the external posterior part of the femoral artery. Femoral artery travels through adductor hiatus, and it is named as popliteal artery in popliteal fossa; it ends at the lower border of the popliteus, where it is separated into the two terminal branches: anterior and posterior tibial arteries [8, 10].

Femoral vein, artery, and nerve (VAN) can be observed from medial to lateral in the femoral triangle, just beneath the inguinal ligament, when the deep fascia is passed [9] (Fig. 45.3). Profunda femoris artery can also be observed coming out from the external posterior part of the femoral artery. Lateral circumflex femoral artery, a branch of profunda femoris artery, is divided into branches slightly below the neck of the femur, and its ascending branch arises through the front of the hip joint [10]. Medial circumflex femoral artery, which is the other branch of profunda femoris artery, passes between the first pectineus and iliopsoas, and then the obturator externus and the adductor brevis muscles. It is separated into branches beneath the quadratus femoris. The branches given to the joint constitute the most important blood supply of femoral head in the adults. Head of femur is supplied by the branches of lateral and medial circumflex femoral artery and acetabular branch of obturator artery during growth. Acetabular branch of obturator artery passes through the ligament of head of femur (ligamentum teres) and reaches the head of femur [8]. This artery loses its significance after 4 years of age.

The adductor canal (canalis adductorius or Hunter's canal) is a tunnel in the middle third of the femur and is found between vastus medialis, adductor longus, adductor magnus, and anteromedial intermuscular septum (subsartorial fascia, vastoadductor intermuscular septum). The starting point is the apex of the femoral triangle, and the exit is the adductor hiatus in the tendon of adductor magnus. Adductor canal is also known as subsartorial canal since it is found beneath the sartorius muscle. Femoral vessels pass through the adductor canal and go into the fossa poplitea and travel in here as popliteal vessels. Saphenus nerve is found in the adductor canal with femoral vessels and does not come out of the lower opening of this canal. Slightly above, it pierces the subsartorial fascia to exit the canal and reaches beneath sartorius. It becomes superficial between the sartorius and gracilis muscles and travels along with the great saphenous vein later [13, 14].

There are many sensory fibers found in the nerve of vastus medialis. Therefore, it is the thickest branch of femoral nerve that travels to the muscles. During the flexion of knee, lateral movement is prevented by the fibers of vastus medialis attached to the patella, which pull the patella to the medial origin to sustain the stability [15, 16]. Hence, any damage to this nerve will affect the stability of the knee.

Aponeurosis of tensor fasciae latae joins with the fascia lata, and a thick band-shaped aponeurotic structure, which is gaining strength is formed from the ilium to tibia on the lateral side of the thigh. This band-shaped structure is called iliotibial tract [8, 9].

Knee and Leg Anatomy

Popliteal fossa is a rhomboid-shaped area limited by ischiocrural muscles [hamstring muscles; lateral hamstring = biceps femoris; medial hamstring = semitendinosus + semimembranosus) superiorly and gastrocnemius muscle with its lat-

eral and medial heads inferiorly. Plantaris joins these limits in the inferior lateral area. Small saphenous vein and sural nerve, which are lying between the heads of the gastrocnemius muscle can be observed when the superficial fascia of the lower half of the popliteal fossa is dissected gently. Separation of the branches of sciatic nerve (tibial and common fibular nerves) can be seen when the hamstring muscles in the upper half of popliteal fossa are parted away. This separation can also occur rather above in the gluteal area. Tibial nerve stays at the posterolateral surface of the popliteal vessels at the back of the knee joint in the inferior section; however, fibular nerve travels parallel with the medial side of the tendon of biceps femoris muscle. Popliteal vessels (popliteal artery and vein) are covered with a sheath and pass through a deeper plane, compared to the tibial nerve. Popliteal artery is found in the closest plane to the knee joint capsule. This vicinity must be noticed for both arthroscopic and open surgical procedures of the knee joint [17].

Fibular nerve which follows the medial edge of biceps femoris winds around the head of fibula and goes between soleus and peroneus longus muscles [18]. Herein, the fibular nerve travels superficially right behind the skin. Therefore, fibular neck fractures and the surgical procedures to this area must be performed carefully [19, 20].

The skin branches separating from the tibial and fibular nerves (medial and lateral sural cutaneous nerves, respectively) generally merge inside the superficial fascia at the posterior face of the gastrocnemius muscle to form the sural nerve. Sural nerve goes along with the small saphenous vein and travels back to the lateral malleolus. At the lateral face of the calcaneus, it spreads to the most lateral part of the dorsal face of the foot [21].

Knee is defined as the structures and layers found in the medial and lateral area. There are differences between sources; however, these structures can be defined as below.

There are three layers found in the medial part of the knee [22–26] (Fig. 45.4):

I. Structures found in the first layer: (1) sartorius muscle and its fascia; (2) medial patellar retinaculum; (3) saphenous nerve (courses between the first and second layer)
II. Structures found in the second layer: (1) gracilis; (2) semitendinosus; (3) superficial layer of the medial collateral ligament; (4) medial patellofemoral ligament; (5) semimembranosus
III. Structures found in the third layer: (1) deeper layer of the medial collateral ligament; (2) joint capsule (coronary ligament)

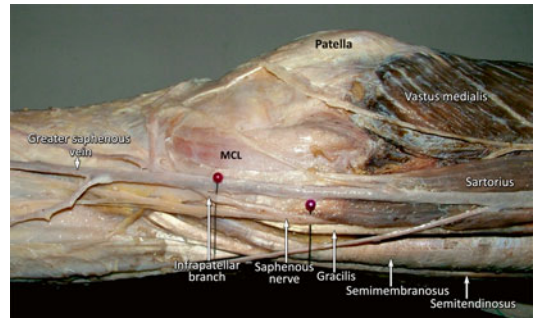

Fig. 45.4 The structures on the medial side of right knee. Attention must be paid to the saphenous nerve arising between the sartorius and gracilis tendons and the infrapatellar branch of this nerve

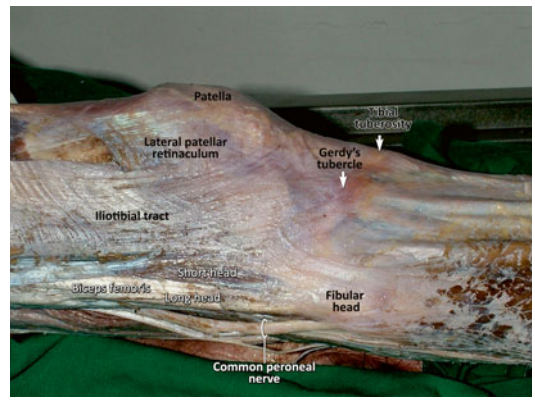

Fig. 45.5 The superficial structures on the lateral side of the right knee. Common fibular (peroneal) nerve was located just behind biceps femoris tendon, and quite superficially

There are three layers found in the lateral part of the knee [23, 27–30] (Fig. 45.5):

I. Structures found in the first layer: (1) iliotibial tract; (2) tendon of biceps femoris muscle; (3) common fibular (peroneal) nerve

II. Structures found in the second layer: (1) lateral patellar retinaculum; (2) lateral patellofemoral ligament
III. Structures found in the third layer: superficial: (1) lateral collateral ligament; (2) fabellofibular ligament; (3) lateral geniculate artery (runs between deep and superficial layer)

Deep: (1) arcuate ligament; (2) popliteus tendon; (3) popliteofibular ligament; (4) joint capsule (coronary ligament)

There are two arterial networks around the knee joint, deep, and superficial. The one which is superficial (patellar network – rete patellare) forms between the skin and deep fascia. On the other hand, deep plexus (genicular anastomosis – rete articulare genus) is found close to the joint surfaces of tibia and femur. The branches separating from this plexus supply the fibrous and synovial membranes of the knee joint. The arteries constituting this network are as follows: descending genicular artery which is the branch of femoral artery, descending branch of the lateral circumflex femoral artery, recurrent branch of the anterior tibial artery, superior lateral and medial genicular arteries with inferior lateral and medial genicular arteries, which are the branches of the popliteal artery, and circumflex fibular artery, which is the branch of the posterior tibial artery [8].

There are four compartments in the leg. Muscles, blood vessels, and nerves found in these compartments are given below: [8–10]

I. *Anterior Compartment*
   1. Anterior tibial artery and vein
   2. Deep fibular nerve
   3. Tibialis anterior
   4. Extensor digitorum longus
   5. Extensor hallucis longus
   6. Fibularis tertius
II. *Lateral Compartment*
   1. Superficial fibular nerve
   2. Peroneus longus
   3. Peroneus brevis
III. *Deep Posterior Compartment*
   1. Posterior tibial artery and vein
   2. Fibular artery and vein
   3. Tibial nerve
   4 Tibialis posterior
   5. Flexor digitorum longus
   6. Flexor hallucis longus
IV. *Superficial Posterior Compartment*
   1. Gastrocnemius
   2. Soleus
   3. Plantaris

Sural nerve and the small saphenous vein lie within the superficial fascia.

Popliteal artery is divided into two branches called anterior and posterior tibial arteries at the lower edge of the popliteus muscle. Posterior tibial artery looks like a continuation of the popliteal artery. It passes underneath the curve at the starting point of the soleus muscle (tendinous arch of the soleus muscle) and travels with tibial nerve in the deep compartment. Fibular artery, the thickest branch of the posterior tibial artery, is found 2.5 cm below the popliteus muscle.

Foot and Ankle Anatomy

There are four channels found in the posterior part of the medial malleolus. From anterior to posterior, the structures that pass from these channels are as follows: tendons of tibialis posterior, tendon of flexor digitorum longus, posterior tibial vessels and tibial nerve, and finally the tendon of flexor hallucis longus (respectively). Flexor retinaculum covers the channels and forms tarsal tunnel. Medial calcaneal branches of the tibial nerve become more superficial by piercing the flexor retinaculum and spread around at the medial heel region. Vessels passing by the third channel are found in front of the nerve and branch out into the foot sole while they are still in this channel [10, 31, 32] (Fig. 45.6).

Superficial fibular nerve passes from the superficial face of the extensor retinaculum, and the tendons of the extensor digitorum longus and fibularis tertius pass deeply at the dorsal surface of the ankle.

Behind the lateral malleolus, small saphenous vein and sural nerve, which accompany each

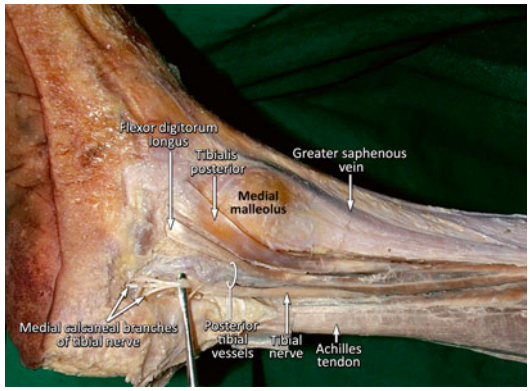

Fig. 45.6 The medial view of the right ankle. Flexor retinaculum was removed, and structures in the first three channels of the tarsal tunnel were made visible

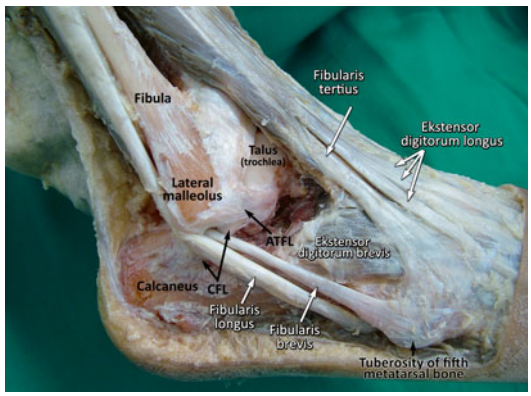

Fig. 45.7 Fibular tendons located on the lateral of right ankle. *ATFL* anterior talofibular ligament, *CFL* calcaneofibular ligament

other, travel through the surface of the peroneal retinaculum inside the superficial fascia. In this area, lateral calcaneal branches spread to the most lateral part of the dorsal face. This branch leading to the foot is called the lateral dorsal cutaneous nerve [21]. Tendons of the peroneus longus and brevis travel underneath the superior and inferior peroneal retinaculum at the back of the lateral malleolus and reach the foot (Fig. 45.7). Peroneus brevis ends up at the base of the fifth metatarsal bone (tuberositas ossis metatarsalis quinti). On the other hand, the peroneus longus tendon runs obliquely forward on the lateral side of the calcaneus, below the fibular trochlea and the tendon of fibularis brevis. It travels on the lateral side of the cuboid and runs under the cuboid in a groove that is converted into a canal by the long plantar ligament. This tendon crosses the sole of the foot obliquely and attaches on the first metatarsal and cuneiform bone [8, 9].

Calcaneofibular ligament can be observed underneath, when the retinaculum and peroneal tendons are removed [33] (Fig. 45.7). This wire-shaped ligament is the longest and the strongest ligament in the lateral side of the ankle. Calcaneofibular ligament is attached to the external surface of the calcaneus by traveling from the lower tip to the posterior inferior of the fibula.

Distal ends of tibia and fibula are connected tightly to each other by a fibrous joint called inferior tibiofibular joint (tibiofibular syndesmosis) (Fig. 45.7). With the help of this joint, the tibia and fibula forming the top of the ankle joint stay attached.

When the skin on the foot sole, plantar fascia, and flexor digitorum brevis muscle are removed, branches of the lateral and medial plantar nerves which are the branches of the tibial nerve can be observed. Plantar calcaneonavicular ligament (spring ligament) and long plantar ligament, which support the foot dome can be observed in deeper investigation [34, 35]. The dome of the foot is supported like a hammock by tibialis posterior from inside and tendons of peroneus longus from outside.

Feet and ankles are supplied by the branches of the anterior tibial, posterior tibial, and fibular arteries [8]. In the malleolar region, lateral and medial malleolar networks are located, which are constituted by the anterior lateral and medial malleolar arteries and posterior medial malleolar artery. Furthermore, networks of vessels are formed by calcaneal branches at the lateral and medial parts of the calcaneus. Entrance points to the ankle with arthroscope are found slightly above the anterior lateral and medial malleolar arteries and at the two sides of the deep fibular nerve with the anterior tibial artery.

References

1. McConaghie FA, Payne AP, Kinninmonth AW (2014) The role of retraction in direct nerve injury in total hip replacement: an anatomical study. Bone Joint Res 3:212–216

2. Wasielewski RC, Cooperstein LA, Kruger MP, Rubash HE (1990) Acetabular anatomy and the transacetabular fixation of screws in total hip arthroplasty. J Bone Joint Surg Am 72:501–508
3. Botanlioglu H, Bilsel N, Kaynak G, Unlu MC (2012) Open reduction technique for overlapping and locked pubic symphysis. Acta Orthop Traumatol Turc 46:77–81
4. Pushkar DY, Godunov BN, Gvozdev M, Kasyan GR (2011) Complications of mid-urethral slings for treatment of stress urinary incontinence. Int J Gynaecol Obstet 113:54–57
5. Berberoglu M, Uz A, Ozmen MM et al (2001) Corona mortis: an anatomic study in seven cadavers and an endoscopic study in 28 patients. Surg Endosc 15:72–75
6. Okcu G, Erkan S, Yercan HS, Ozic U (2004) The incidence and location of corona mortis: a study on 75 cadavers. Acta Orthop Scand 75:53–55
7. Darmanis S, Lewis A, Mansoor A, Bircher M (2007) Corona mortis: an anatomical study with clinical implications in approaches to the pelvis and acetabulum. Clin Anat 20:433–439
8. Standring S (2008) Gray's anatomy: the anatomical basis of clinical practice, 40th edn. Churchill Livingstone Elsevier, Spain
9. Moore KL, Dalley AF, Agur AMR (2014) Moore clinically oriented anatomy, 7th edn. Lippincott Williams & Wilkins, Baltimore
10. Morrey BF, Morrey MC (2008) Master techniques in orthopaedic surgery: relevant surgical exposures, 1st edn. Lippincott Williams & Wilkins
11. Stecco C, Macchi V, Baggio L et al (2013) Anatomical and CT angiographic study of superior gluteal neurovascular pedicle: implications for hip surgery. Surg Radiol Anat SRA 35:107–113
12. Ropars M, Morandi X, Huten D, Thomazeau H, Berton E, Darnault P (2009) Anatomical study of the lateral femoral cutaneous nerve with special reference to minimally invasive anterior approach for total hip replacement. Surg Radiol Anat SRA 31:199–204
13. Wijdicks CA, Westerhaus BD, Brand EJ, Johansen S, Engebretsen L, LaPrade RF (2010) Sartorial branch of the saphenous nerve in relation to a medial knee ligament repair or reconstruction. Knee Surg Sports Traumatol Arthrosc 18:1105–1109
14. Dunaway DJ, Steensen RN, Wiand W, Dopirak RM (2005) The sartorial branch of the saphenous nerve: its anatomy at the joint line of the knee. Arthroscopy: J Arthrosc Relat Surg 21:547–551
15. Lin YF, Lin JJ, Jan MH, Wei TC, Shih HY, Cheng CK (2008) Role of the vastus medialis obliquus in repositioning the patella: a dynamic computed tomography study. Am J Sports Med 36:741–746
16. Herrington L, Malloy S, Richards J (2005) The effect of patella taping on vastus medialis oblique and vastus laterialis EMG activity and knee kinematic variables during stair descent. J Electromyogr Kinesiol 15: 604–607
17. Cosgarea AJ, Kramer DE, Bahk MS, Totty WG, Matava MJ (2006) Proximity of the popliteal artery to the PCL during simulated knee arthroscopy: implications for establishing the posterior trans-septal portal. J Knee Surg 19:181–185
18. Ryan W, Mahony N, Delaney M, O'Brien M, Murray P (2003) Relationship of the common peroneal nerve and its branches to the head and neck of the fibula. Clin Anat 16:501–505
19. Cho D, Saetia K, Lee S, Kline DG, Kim DH (2011) Peroneal nerve injury associated with sports-related knee injury. Neurosurg Focus 31:E11
20. Halm JA, Schepers T (2012) Damage to the superficial peroneal nerve in operative treatment of fibula fractures: straight to the bone? Case report and review of the literature. J Foot Ankle Surg 51:684–686
21. Apaydin N, Bozkurt M, Loukas M, Vefali H, Tubbs RS, Esmer AF (2009) Relationships of the sural nerve with the calcaneal tendon: an anatomical study with surgical and clinical implications. Surg Radiol Anat SRA 31:775–780
22. Cohen M, Astur DC, Branco RC et al (2011) An anatomical three-dimensional study of the posteromedial corner of the knee. Knee Surg Sports Traumatol Arthrosc Off J ESSKA 19:1614–1619
23. Geiger D, Chang EY, Pathria MN, Chung CB (2014) Posterolateral and posteromedial corner injuries of the knee. Magn Reson Imaging Clin N Am 22: 581–599
24. House CV, Connell DA, Saifuddin A (2007) Posteromedial corner injuries of the knee. Clin Radiol 62:539–546
25. Stannard JP, Black BS, Azbell C, Volgas DA (2012) Posteromedial corner injury in knee dislocations. J Knee Surg 25:429–434
26. Tang H (2009) Bai L [Anatomy and biomechanical research progress of knee posteromedial corner]. Chin J Rep Reconstr Surg 23:1058–1061
27. Devitt BM, Whelan DB (2015) Physical examination and imaging of the lateral collateral ligament and posterolateral corner of the knee. Sports Med Arthrosc Rev 23:10–16
28. Lee YH, Song HT, Kim S, Kim SJ, Suh JS (2012) Magnetic resonance arthrographic dissection of posterolateral corner of the knee: revealing the meniscofibular ligament. Yonsei Med J 53:820–824
29. Osti M, Tschann P, Kunzel KH, Benedetto KP (2013) Posterolateral corner of the knee: microsurgical analysis of anatomy and morphometry. Orthopedics 36:e1114–e1120
30. van der Wal WA, Heesterbeek PJ, van Tienen TG, Busch VJ, van Ochten JH, Wymenga AB (2014) Anatomical reconstruction of posterolateral corner and combined injuries of the knee. Knee Surg Sports Traumatol Arthrosc. Epub ahead of print. DOI 10.1007/s00167-014-3369-7

31. Arnold G, Vohra S, Marcantonio D, Doshi S (2011) Normal magnetic resonance imaging anatomy of the ankle & foot. Magn Reson Imaging Clin N Am 19:655–679
32. Kotnis N, Harish S, Popowich T (2011) Medial ankle and heel: ultrasound evaluation and sonographic appearances of conditions causing symptoms. Semin Ultrasound CT MR 32:125–141
33. Dowling A, Downey B, Green R, Reddy P, Wickham J (2003) Anatomical and possible clinical relationships between the calcaneofibular ligament and peroneus brevis-a pilot study. Man Ther 8:170–175
34. Tryfonidis M, Jackson W, Mansour R et al (2008) Acquired adult flat foot due to isolated plantar calcaneonavicular (spring) ligament insufficiency with a normal tibialis posterior tendon. Foot Ankle Surg 14:89–95
35. Shuen V, Prem H (2009) Acquired unilateral pes planus in a child caused by a ruptured plantar calcaneonavicular (spring) ligament. J Pediatr Orthop B 18:129–130

Functional Anatomy of the Hip Joint

46

Murat Bozkurt, Çetin Işık, Mustafa Akkaya, and Safa Gürsoy

Abstract

Human hip joint is built to stand and walk. It has the largest range of motion after shoulder joint. However, it is quite a static joint due to surrounding muscles, bones, and ligaments. A large part of hip joint stability is provided by joint capsule rather than by surrounding muscular structures. In this chapter the functional and anatomical characteristics of the hip joint will be discussed.

Terminology

Inclination or collodiaphyser angle An angle between head and femoral shaft

Coxa vara The decrease of inclination angle

Coxa valga The increase of inclination angle

Anteversion angle Forward angling between the surface running through femoral shaft condyles and femoral neck

Wiberg angle An angle for the assessment of acetabular coverage

Learning Aims

This chapter is designed so that you can:

- Describe the content and structure of the hip joint
- Explain the relations between the anatomical structures and its functions
- Discuss the biomechanics of the hip joint

Clinical Relevance

Proper knowledge of the structures in the hip joint is quite crucial for a better clinical understanding of basic daily functions such as walking and keeping balance. The hip joint is also one of the most dynamic joints in the body.

It is necessary to know properly the clinical and functional anatomy of intra-

M. Bozkurt (✉) • C. Işık • M. Akkaya • S. Gürsoy
Department of Orthopaedics, Ankara Ataturk Training and Research Hospital, Ankara, Turkey
e-mail: nmbozkurt@yahoo.com; ortdrcetin@gmail.com; safagursoy@yahoo.com; makkaya@outlook.com

F. Korkusuz (ed.), *Musculoskeletal Research and Basic Science*,
DOI 10.1007/978-3-319-20777-3_46

articular and extra-articular structures of the hip in order to have a better assessment of how orthopedic surgical interventions to the hip joint might change joint motion, walking, and balance functions.

In this section, clinical and functional anatomy of hip joint is discussed. This will allow a better understanding of normal values, which would serve as basis for orthopedic surgical operations to be conducted.

General Characteristics

The human hip joint is built to stand and walk. Hip joint consists of head and socket. Concave (acetabulum) and convex (femoral head) are symmetrical, and joint spacing is equal almost at any point. It has the largest range of motion after shoulder joint. However, it is quite a static joint due to surrounding muscles, bones, and ligaments. A large part of hip joint stability is provided by joint capsule rather than by surrounding muscular structures. The center of gravity in standing position runs posterior to the hip rotation center. The pelvis is bent to allow the femoral head to directly fit into acetabulum. The frontal part of the capsule (iliofemoral ligament) thickens where static standing is achieved based on ligament support rather than muscle contraction. In sitting position, the weight is placed on both ischial tuberosities.

The surface of the joint formed between the femoral head and acetabulum is peripherally covered with cartilage. The center however has no cartilage. Likening acetabulum to a ring, its bottom part is not completed and is completed by transverse acetabular ligament. Its surrounding is enclosed by labrum that is composed of fibrous cartilage.

Bone Structure

The hip joint consists of the head, which forms proximal femur, neck, greater and lesser trochanter and proximal femoral shaft along with acetabulum composed of the fusion of ilium, ischium, and pubis. Both hip joints form a large majority of the bone pelvis by joining with symphysis pubis at the anterior and sacrum at the posterior.

There are angles in the hip joint created by the head and neck that should be anatomically known, and are functionally significant in preoperative planning in hip joint surgery. These are inclination angles viewed anteriorly, and anteversion angles viewed from the top.

An angle of 125–130° is available between the head and femoral shaft (inclination or collodiaphyser angle). The decrease of this angle is called coxa vara while its increase is called coxa valga. There is a 15° forward angling between the surface running through femoral shaft condyles or plane and the femoral neck anteversion angle [10]. Anteversion is not related with the alignment of other parts of femur but directly associated with hip joint [1, 2]. Any change in anteversion will affect the alignment of the lower extremity on the frontal plane on the transcondylar angle leading to walking disorders [3].

In acetabulum, the assessment of acetabular coverage, which is significant for proper hip joint biomechanics, is conducted through Wiberg angle. The normal value of this angle is $26 \pm 6°$. Insufficient coverage of femoral head by acetabulum results in abnormal orientation and insufficient weight bearing of the acetabulum.

Joint Capsule

Joint capsule clings on the bone edge of acetabulum on the top leaving acetabular labrum and ligamentum transversum within the joint as a result. At the bottom, it clings on femoral neck at the anterior.

Joint Ligaments

The hip joint has three large ligaments, which at the same time are static stabilizers of the hip along with Labrum.

Iliofemoral ligament: It is a very strong ligament with Y shape also known as Bertin ligament. It holds on to the spina iliaca anterior inferior on the top and on the linea intertrochanterica at the

bottom. It crosses the frontal face of the joint. It is the thickest and strongest ligament. It prevents excessive extension while standing.

Ischiofemoral ligament: It is the thinnest of three ligaments. It arises in the farthest posterior point of acetabulum and in corpus ischii at the inferior. Its upper fibers extend horizontally while its lower fibers extend upward and outward. It clings on to the posterior-upper part of the collum femoris. In ligament extensions, it loses its spirality and pulls the femoral head further into the acetabulum. It loosens during ligament flexion and facilitates motion by diminishing contact surface between the femoral head and acetabulum.

Pubofemoral ligament: It is triangular in shape, and its bottom clings on to the upper ramus of the pubis while its top clings on to the lower part of the intertrochanteric line. It restricts extension and abduction, and facilitates adduction.

Internal ligament of hip joint

Ligament of Head of Femur (*Lig. Teres*): It runs to the acetabular fossa from fovea capitis femoris. It is a squamous band. Medial epiphyseal veins run through it.

Hip Joint Motions

The hip joint moves in a horizontal, sagittal, and vertical axis. Sagittal axis: in this axis, flexion and extension motions are done. As hip flexion is restricted by the hamstrings when the knee is extended, this extension is only as much as 80°. When the knee is in full flexion, it can reach up to 120°. Hip extension, on the other hand, is 13°.

Frontal axis: Abduction and adduction motions are possible in this axis. Hip abduction is 30° when the femur is extended, and it is 90° when the hip is flexed. Hip adduction is 10° when standing upright, and it is 40° when the hip is flexed.

Vertical axis: In this axis, internal and external rotation motions are done. Hip internal rotation is 35° when standing, and it is 60° when the femur is slightly flexed. Hip external rotation is 15° when standing, and it is 40° when the femur is slightly flexed.

Apart from these motions, circumduction is done through a combination of these three motions.

Hip Joint Biomechanics

The hip joint serves as an efficient leverage between body weight and hip abductors providing a balance between these two forces. Thanks to this interaction, the pelvis is stabilized during walking cycles.

Primary forces affecting the hip are body weight (W) and abductor muscle strength (M), which play a role in balancing the moment effect of body weight. A combination of these two forces is the effective real vectorial (R) force. As the femoral head will be the center of rotation, the magnitude of (R) will be the vectorial sum of (M) and (W) forces. The studies have revealed that the distance of body weight line to femoral head rotation center is about three folds of the distance of the femoral head to the abductor muscles. Therefore, abductor muscles have to apply a force three times bigger than the body weight in order to keep the pelvis straight in a person standing on single foot [13].

According to the leverage lever principle, in order to keep the pelvis in balance, it must be as follows:

Force X Force lever = Load × Loadlever. Taking this as a standpoint, we find:

$$M \times A = W \times B$$

$$M = W \times B / A$$

$$\text{Since } B = 3 \times A,$$

$$\text{We find 13 } M = W \times 3 \times A / A = 3W$$

$$\text{Since } R = M + W, \text{ then } M = 3W \text{ and } R = 4W$$

where $R = 4 \times 5/6$ body weight =20/6 body weight. As noted above, the sum of weight affecting a single hip is more than three folds the body weight. Besides, motions such as climbing, running, and jumping might apply on the hip a load that is approximately as much as ten folds the body weight [6–9, 12].

Center of gravity of the body runs posterior to the joint axis and causes sagittal inflexion posterior to the stem in a hip with prosthesis. Forces having such effects will increase in a hip with prosthesis especially when the hip is flexed, when climbing up and down the stairs, or sitting on chair. Forces affecting the stem in coronal and

sagittal planes will cause torsional effect. During a walk cycle, forces running toward the femoral head in a hip with prosthesis will arrive creating a 15–25° angle to anterior on sagittal plane. In cases of motions such as climbing up a stairs and straight leg raise, the forces will further come forward. The load to apply on prosthesis during straight leg raise will be more than the body weight. This is quite significant in patient management [4, 5, 12]. These forces will cause retroversion of femoral component or forcing it to posterior. Due to that, stem fractures usually start on the anterolateral surface of the stem. Increasing the width of the proximal part of the stem will better fill the femoral metaphysis and increase the torsional stability of the femoral component [12].

Hip Joint Muscles

We can group the muscles affecting the hip joint as follows according to their functions:

Hip Joint Extensors

These are M. Gluteus Maximus, long head of M. Biceps Femoris, M. semitendinosus, M. semimembranosus, back fibers of M. Adductor Magnus and M. piriformis.

M. Gluteus Maximus is the strongest extensor of the hip. Its deep layer plays a role in the extension of the pelvis when flexed on two sides while the femur is static, and in extension, internal rotation and medial flexion of pelvis when flexed on one side. The surface layer of the gluteus maximus plays a role in extension, external rotation, and abduction of the femur [11].

Hip Joint Flexors

Psoas, iliacus, rectus femoris, sartorius, pectineus, adductor longus, adductor brevis, and gracilis muscles affect the iliacus and pelvis when the femur is static, and affect psoas major and lumbar spine. As they have the same tendon and cause the femur to do the same motion, iliacus and psoas are named as a single muscle, iliopsoas [11].

Hip Joint External Rotators

These are gluteus maximus, obturator internus, obturator externus, quadratus femoris, piriformis, gemellus superior and inferior, posterior of sartorius, and gluteus medius.

Obturator and gemellus muscles tend to "pull and separate" the hip joint though on a small scale. In some painful cases (e.g., like cartilage erosion), this is quite a helpful decompressive effect [11].

Hip Joint Internal Rotators

These are adductor longus, adductor brevis, adductor magnus, anterior of gluteus medius, anterior of gluteus minimus, tensor fasciae latae, pectineus, and gracilis (Fig. 46.1).

Hip Joint Abductors

These are tensor fasciae latae, gluteus minimus, gluteus maximus, gluteus medius, and sartorius muscles. The fundamental task of gluteus medius that is often affected by surgical operations on the hip joint is observed when the individual stands on a single foot that constitutes lateral flexion of the pelvis. When flexed on one side, it provides lateral flexion of the pelvis and stabilizes the pelvis during walks or stepping on one foot [11] (Fig. 46.2).

Hip Joint Adductors

These are adductor longus, adductor brevis, ischiofemoral part of adductor magnus, gracilis, and pectineus muscles.

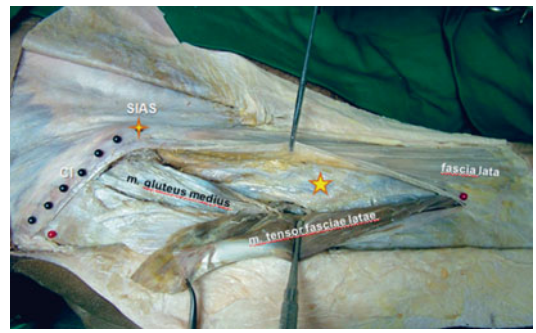

Fig. 46.1 Demonstration of cadaveric dissection of hip joint muscles (SIAS: Spina iliaca anterior superior)

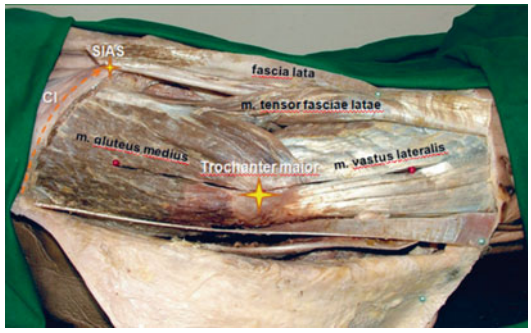

Fig. 46.2 Demonstration of cadaveric dissection of hip joint adductors (CI: Crista iliaca, SIAS: Spina iliaca anterior superior)

Conclusion

The hip is not a simple joint but rather a complex type of joint that is a combination of bones, tendons, ligaments, and muscles. Understanding the functional anatomy of the hip joint is very important since conditions that disturb the normal anatomy can make walking difficult without pain or problems.

Cross-References

Biomechanical Measurement Methods to Analyze the Mechanism of Sport Injuries
Groin Anatomy and Biomechanics

References

1. Jordon RP, Cusack Rosseque B (1983). Foot function and its relationship 10 posture in the pediatric patient with cerebral palsy and other neuro muscular disorders. Lecture notes and instructional material from Neuro developmental Treatment Association meeting, New York
2. McCrea JD (1985) Pediatric orthopeadics of the lower extremity: an instructional handbook. Futura, Mount Kisco
3. Cusick BD (1990) Progressive C; sling and splinting for lower-extremity deformities in children with neuromuscular dysfunctional. Therapy Skill Builders, Tucson
4. Jensen K, Di Fabio RP (1989) Evaluation of eccentric exercise in the treatment of patellartendinitis. Phys Ther 69:211–216
5. Mennell JB (1947) Physical treatment, movement, manipulation, and massage. Blakiston Co, Philadelphia
6. Inman VT (1947) Functional aspects of abductor muscles of the hip. J Bone Joint Surg 29A: 607–619
7. LeVeau B (1977) Application of statics. In: Lissner HR, Williams M (eds) Biomechanics of human motion, 2nd edn. WB Saunders, Philadelphia, pp 100–102
8. Beattie P, Isaacson K, Riddle DL et al (1990) Validity of derived measurement of leg-length differences obtained by use of tape measure. Phys Ther 70:150–157
9. Rydell N (1966) Force acting on the femoral head prosthesis: a study on strain-gauge supplied prosthesis in living persons. Acta Orthop Scand 88(suppl):1–132
10. Slawski DP, Howard RF (1997) Surgical management of refractory trochanteric bursitis. Am J Sports Med 25:86–89
11. Calais-Germain B (2007) Anatomy of movement. Revised edition. Originally published as Anatomie pour le mouvement. Seattle, Eastland Press, pp. 190–255
12. Harkess JW (2003) Arthroplasty of hip. Campbell's operative orthopaedics. Chapter 7
13. Warwick D, Williams MH, Bannister GC (1990) Death and thromboembolic disease after total hip replacement. A series of 1162 case with no routine chemical lprophylaxis. JBJS 77B(1): 983–987

Posterior Approach to the Spine and Intervertebral Foramen: Anatomical Basis

47

Halil İbrahim Açar, Ayhan Cömert, and Berfu Çerçi Öngün

Abstract

In this chapter clinical and surgical anatomy of the spine and its relation with neurovascular anatomical structures was discussed. Applied knowledge of anatomical relations regarding surgical procedures and approaches was discussed and their relations were demonstrated via cadaveric dissections. Anatomy of the intervertebral foramen or osseous canal and neighbouring neurovascular structures was evaluated in details and thorough review of literature was performed. Body movement-associated changes in intervertebral foramen, pedicle and spinal nerve relation and anatomy of ligaments were discussed in details. Their clinical relevance and significance was emphasized by discussion of recent literature.

Learning Outcomes

After studying this chapter, we will have an understanding of the spine anatomy and relative anatomical structures during posterior approaches, the anatomical dissection layers, the structure of the intervertebral foramen, ligaments in this region, body movement associations with the intervertebral canal, anatomy of the spinal nerve canal, and the anatomical relation between the spinal nerve and the pedicle.

Terminology

Spine Vertebral column is a curved linkage of 7 cervical, 12 thoracic, 5 lumbar, 5 sacral, and 4 coccygeal vertebrae.

Facet (zygapophysial) joints Synovial joints between the vertebral articular processes (zygapophyses).

Thoracolumbar fascia It is a deep investing membrane or three-layered (posterior, middle, anterior) fascia in the lumbar region, which covers the deep muscles of the back of the trunk.

Yellow ligament (ligamentum flavum) Ligamenta flava connect laminae of adjacent vertebrae in the vertebral canal.

H.İ. Açar, MD (✉) • A. Cömert, MD • B.Ç. Öngün, MD
Department of Anatomy, Ankara University Faculty of Medicine, Ankara, Turkey
e-mail: drhalilacar@yahoo.com

F. Korkusuz (ed.), *Musculoskeletal Research and Basic Science*,
DOI 10.1007/978-3-319-20777-3_47

Intervertebral foramen (neural foramen) An opening between vertebrae through which nerves leave the spine and extend to other parts of the body. Moreover, it should be described together with its inner part called spinal nerve canal.

Spinal nerve United ventral and dorsal spinal roots, attached in series to the sides of the spinal cord.

Spinal ganglia (dorsal root ganglia, DRG) Large groups of neurons on the dorsal spinal roots, usually located in the intervertebral foramina.

Segmental arteries These vessels derived from the spinal branches of the vertebral, deep cervical, intercostal, and lumbar arteries, and enter the vertebral canal through the intervertebral foramina.

Anatomy of the Spine

The vertebral column anatomy differs within its regions [1]. In the cervical region, cervical vertebrae are small and mobile bones; so, in the thoracic region are larger and less mobile bones and in the lumbar region are large but mobile (less than cervical mobility) bones.

The lumbar spine meets the sacrum at the lumbosacral joint (L5–S1). Some of the distinguishing characteristics of the lumbar spine are more important. The five vertebrae of the lumbar spine are the biggest unfused vertebrae in the spinal column, enabling them to support the weight of the body. Therefore, the lower the vertebra is in the spinal column, the more weight it must bear. The lumbar spine anatomy, and the lumbar plexus branches and medial branch of the posterior ramus innervating the facet joint are depicted in Fig. 47.1. The lumbar spine's lowest two spinal segments are therefore the most prone to degradation and injury.

Pathologies related with lumbar and cervical regions occur more frequently, and therefore, the required surgical interventions are more frequent. During flexion or extension, changes in size and shape of the vertebral canal occur, and particularly those caused by the ligamenta flava essentially involve the central area of the spinal canal, and thus the dural sac undergoes constrictions at the intervertebral level [2].

It is possible to reach all these structures with anterior or posterior approaches. Although anterior approaches are preferred in procedures regarding infections, fractures, and tumors, posterior approaches are used in pathologies related to the spinal cord and intervertebral discs.

Clinical Relevance

Anatomical relations of the intervertebral disc are important in the planning of interventional investigative and therapeutic procedures ranging from diskography to open disc surgery.

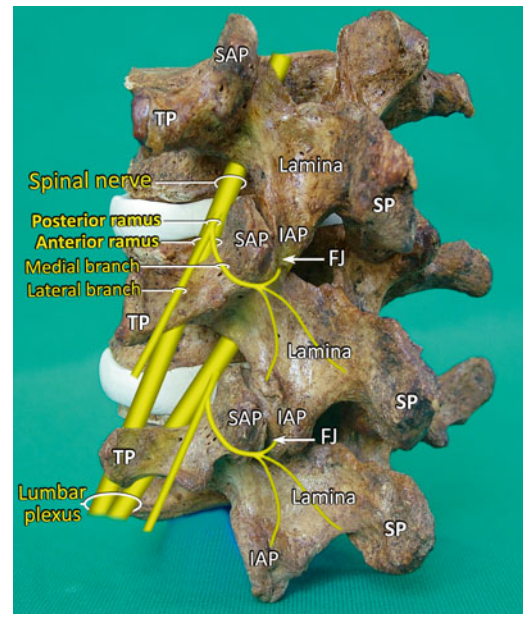

Fig. 47.1 Lumbar spine anatomy and lumbar plexus branches related to the bony anatomy. Spinal nerve and its anterior and posterior branches are demonstrated. Medial branch of the posterior ramus innervating the facet joint. *FJ* facet joint, *SP* spinous process, *TP* transverse process, *SAP* superior articular process, *IAP* inferior articular process

Posterior Approaches to the Spine

Posterior approaches allow us to reach facet joint, lamina, pedicle, spinous process, cauda equina, and spinal cord. Posterior approaches were frequently used in procedures like spinal disc herniations, spinal nerve exploration, and tumor resections.

Additionally, spinous processes were used in deciding the localization of incision line. The line connects the iliac crests, which can be easily palpated, and passes between L4 and L5. Besides this rough method, the precise level can be determined by using needle-guided radiographic evaluation. Planned incision was made longitudinally over the spinous processes after the identification of the line. The length of the incision varies according to the severity of that particular pathology.

Related Anatomical Structures During Dissection via Posterior Approach

In this stage, the skin and the subcutaneous tissue were removed. Then, paraspinal muscles were reached using a dissector, and en block removal of these muscles was performed to the sides. If necessary, the incision can be extended laterally. This maneuver makes the facet joint, spinous, transverse, and the mammillary processes visible.

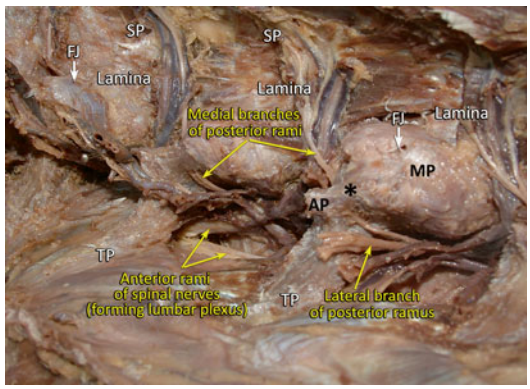

Fig. 47.2 Posterolateral view to the left side of the lumbar spine. Facet joints, laminae spinous processes are demonstrated. Anterior and posterior rami of the spinal nerve and medial and lateral branches of posterior rami are seen. *TP* transverse process, *MP* mamillary process, *TP* transverse process, *AP* accessory process, *FJ* facet joint, * mamilloaccessory ligament

It should be taken into consideration that the nerves and vessels supplying the paraspinal muscles are between the transverse processes and the facet joints (Fig. 47.2). The blood vessels supplying this area aroused directly from the aorta. Therefore, it is essential to protect these branches of the lumbar vessels which may cause severe bleeding. Additionally, the posterior branches of these nerves [3] are located in this area to innervate the local muscles (Fig. 47.2). Damage to these nerves causes denervation and atrophy of paraspinal muscles.

All parts of the yellow ligament (ligamentum flavum) were elevated in the profound dissection in order to reach the epidural space and the dura mater. Meanwhile, blunt dissection must be performed and extra caution should be taken.

Each nerve root must be identified individually and should be protected. In general, spinal nerves can be identified and retracted easily from its distal approach. The venous structures surrounding the peripheral nerves may cause gross bleeding throughout the dissection; therefore, they should be handled with great care. The dissections should be done gently in the inferior lumbar region due to the fact that the iliac vessels located and lying on the anterior aspect of the vertebral bodies and nerve roots may be injured.

To gain better exposure, laminas and facet joints need to be removed. Enlarging the approach provides better access for the fusion of the facet joint and the transverse process.

All these approaches can be applied for all levels from C1 to the sacrum.

Surgical Anatomical Relations

The superficial layer consists of the latissimus dorsi, which contributes a part of the posterior wall of the axilla and extends until the humerus.

Deep layers contain paraspinal muscles. During this approach, these muscles are divided into two layers in which erector spinae muscles are located superficially, and rotatores and multifidus muscles are located deeply. Although this arrangement is not obvious in surgical procedures as the approach involves detaching all these muscles together, it should be kept in mind.

Posterior superior iliac spine (PSIS) and iliac crest make a 45° angle toward the midline. This area can be easily palpated as it is the bonding surface of the muscles to the iliac crest. PSIS passes through the second segment of the sacrum. Additionally, the top of the iliac crests marks the level of disc found between L4 and L5.

Superficial Anatomical Structures: Related with Surgical Dissection

Thoracolumbar fascia and supraspinous ligament were found immediately underneath the skin. This fascia is a broad, relatively thick, wide sheath of tissue and attaches to the spinous processes. Supraspinous ligament extends to the cervical region and continues as a nuchal ligament toward the neck. Thoracolumbar fascia, medially, was attached to the iliac crest. Laterally, it continues on the latissimus dorsi and erector spinae muscles. Supraspinous ligament merges and continues with the thoracolumbar fascia. It was anatomically reported that paraspinal muscle contraction leads to posterior displacement of the posterior layer of the thoracolumbar fascia and that dysfunctional paraspinal muscles would reduce posterior displacement [4].

Arterial supply of the muscles found in this area is also crucial. These segmental lumbar arteries arise directly from the aorta and ascend close to the pedicle, where they divide into two branches. The first branch supplies the spinal cord and the other supplies the muscles around. These arteries pass between the transverse processes and are visible around facet joints. Therefore, dissections close to the midline can be performed without the risk of cutting the arteries. Injury to the lumbar arteries during anterior spinal approaches is often encountered mostly during anterior approaches, and an anatomic relationship of the lumbar segmental arteries is important [5].

Profound Anatomical Structures Related with Surgical Dissection

Yellow ligament (ligamentum flavum in all levels) is the most important structure in the profound layer. These ligaments, consisting of yellow elastic tissue, posteriorly covers the spinal canal between the laminas. This arrangement allows yellow ligament to be attached to the anterior surface of the superior lamina and the posterior surface of the inferior lamina [6]. The two yellow ligaments from each side meet in the midline but do not fuse.

It is important to remove yellow ligament with caution due to its proximity to the dura mater. The endangered major structure in the profound dissections involves dura mater. Hence, in this stage, to protect the dura mater, a thin spatula should be placed beneath the yellow ligament. Additionally, perforations of dura mater can occur easily. Finally, it could be so difficult to distinguish spinal nerves when epidural veins start bleeding.

Anatomy of the Intervertebral Foramen and Its Clinical Relevance

Intervertebral foramen (IF) is a pass between the spinal canal and the periphery and serves as a doorway [7]. The spinal roots, nerves, and ganglia may be damaged here. This large osseous hole or canal is a unique pass in comparison to other foramens of the body due to the presence of two movable joints that attach to its boundaries, where anteriorly lies the ventral intervertebral joint and dorsally lies the zygapophysial joint. There is a small notch in the upper edge of the pedicle and a larger notch in the lower edge. Close distance of these joints increased the susceptibility of narrowing from arthritic pathological and structural alterations [8]. Additionally, IF gains a dynamic structure due to the joints and attached ligaments, and it is not limited by bony structures. Its mobility in the main part changes its diameter and structure. Narrowing of the foramen and all these dynamic changes in morphology can be tolerated easily by passing the neurovascular structures through this canal [7]. One of the functions of the ligaments is to serve as protection elements in preventing injury to the passing neurovascular structures.

Despite numerous studies about IF, there is not a consensus on its anatomical description, and still, agreement has not been made on which classification best describes this area. Some studies describe IF as the exit or the lateral side of the spinal canal, whereas others describe it differ-

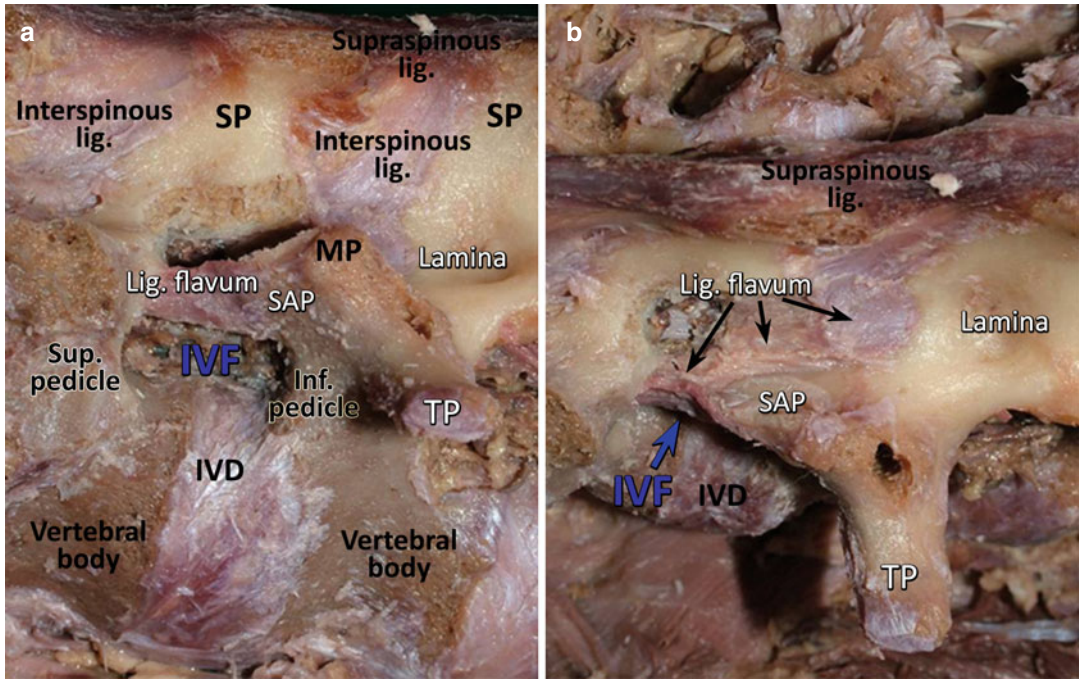

Fig. 47.3 The anterior and posterior boundaries of intervertebral foramen. (**a**) The floor (namely anterior border) of the intervertebral foramen is formed by the posteroinferior margin of the superior vertebral body, the intervertebral disc, and the posterosuperior margin of the inferior vertebral body. The roof of the intervertebral foramen is bounded by the inferior and superior articular processes of the adjacent vertebrae and the lateral prolongation of the ligamentum flavum. (**b**) The inferior articular process was removed from this area in this specimen. *Lig. flavum* ligamentum flavum, *IVF* intervertebral foramen, *Inf. pedicle* inferior pedicle, *Sup. pedicle* superior pedicle, *SAP* superior articular process, *IVD* intervertebral disc, *Corpus* body of vertebra, *SP* spinous process, *Lig. flavum* yellow ligament, *Lamina* lamina arcus vertebra, *Supraspinous lig*. supraspinous ligament, *Interspinous lig*. interspinous ligament, *MP* mamillary process, *TP* transverse process

ently as a complete anatomical canal with real borders. Lee et al. examined IF or intervertebral canal in 1988 by dividing this canal into three sections, as lateral recess zone, midzone, and exit zone [9]. Previously, Crock et al. described IF in 1981 differently, as the narrowest part of the spinal canal [10].

In vitro IF was observed oval and round, and was described to have an inverted teardrop-shaped window when examined medially through the spinal canal and looking outward through the intervertebral foramen [11]. The superior limit of the IF is the inferior aspect of the upper pedicle and the inferior limit of that is the superior aspect of the lower pedicle. As shown in Fig. 47.3, the floor of IF (namely, the anterior border) from above downward is formed by the posteroinferior margin of the superior vertebral body [10], the intervertebral disc, and the posterosuperior margin of the inferior vertebral body. The roof of the intervertebral foramen is bounded by the inferior, removed from this area, and superior articular processes of the adjacent vertebrae [7] at the same level as the foramen, and the lateral prolongation of the ligamentum flavum [10]. Multiple structures bound the anterior aspect of the foramen. These are posterior aspect of the adjacent vertebral bodies, the intervertebral disc, and lateral expansion of the posterior longitudinal ligament; here, additionally located structure is the anterior longitudinal venous sinus. The superior base (posterior border) is formed by the superior and inferior articular processes of the facet joint (zygapophysial joint) at the same level as the foramen, and by the free lateral side prolongation of the ligamentum flavum. The medial canal border contains the dural sleeve. Fascial layer and the neighboring structure is psoas muscle, and it forms its lateral boundary [7]. In addition to these struc-

tures, the superior and the inferior borders are defined by the pedicles of the superior and the inferior vertebrae, respectively. The medial border is defined by the dural sac, and the lateral border is defined by the psoas muscle and the medial fascial sheath of this muscle [7, 13].

The most popular and accepted opinion about true anatomic nerve root canal is that it initially arises from the lateral aspect of the dural sac and travels through the intervertebral canal or neural foramen. At each level, two to six small anterior and posterior nerve rootlets (fila radicularia) converge in the thecal sac to form anterior and posterior roots [12]. Clinically, it is important to know that the nerve roots regularly exit the thecal sac approximately one segmental level above their respective foraminal canals in the lumbar spine region [25]. The anatomic relation between the nerve roots and their corresponding discs in the inervertebral foramina depends on the spinal level. Therefore, for the cervical region of the spine, IF's relative structures are different from other regions. Tanaka et al. found that the shape of the intervertebral foramen is like a funnel. The entrance zone is a narrow part, and the shape of the radicular sheath is conical, with its takeoff points from the central dural sac being the largest part [15]. Consequently, nerve root compression occurs mostly in the entrance zone of the intervertebral foramina. One reason is the equal depth of its superior and inferior vertebral notches. Also, these notches face anterolaterally, which is the same as the pedicles. Finally, the transverse foramen makes up its unique structure [14]. The cervical dorsal root ganglions almost fill the cervical intervertebral foramens. For these anatomic reasons, it seems reasonable to suggest that cervical radiculopathy is strongly correlated with both the cross-sectional area and shape of the intervertebral foramen. Additionally, the general trend of the foraminal height and width increased from the cephalad to caudal except at C2–C3. In addition, in the cervical region, the anterior border of the IF is also defined by the uncovertebral joint [15]. During the procedure just lateral to the uncinate process, the vertebral artery is defined. The vertebral artery pulsation is often visible lateral to the uncinate process. Anteriorly, compression of the nerve roots is caused by protruding discs and osteophytes of the uncovertebral region, whereas the superior articular process, the ligamentum flavum, and the periradicular fibrous tissues affect the nerve posteriorly. IF usually faces the lateral side, and the transverse processes are positioned more posteriorly in the thoracic and lumbar regions. In the thoracic region (T1–T10), the anteroinferior border of IF is surrounded by the synovial space and with intraarticular ligament (intraarticular ligament of the head of rib), which connects the crest of the head of rib and the intervertebral disc. Approaches as endoscopic posterolateral thoracic microdiscectomy under fluoroscopic guidance is between the pedicle and rib head line to be into the safety zone for discectomy. After the removal of the intercostal muscles in this area, we can find the intercostal vein, artery, and nerve. Parietal pleura is located under these structures, and the route passes through this area. Surgeon must avoid causing trauma to the lung, the rib heads, the pedicles, the intercostal nerves and arteries, and the spinal cord. Throughout this route, a probe placed too close to the midline may cause neurologic injury. If a probe is placed too laterally, pneumothorax may occur.

Many studies about spinal ligaments indicated an increased presence of ligaments in the fifth lumbar foramen. The outer opening of intervertebral foramens usually is covered with ligaments, which are formed by the contribution of the medial fascia of psoas major muscle in the lumbar region. The passages found between these ligaments allow the passage of spinal nerve branches and segmental vascular structures [13].

In a study conducted on bones, the foraminal height was determined to be between 19.14 mm (L5–S2 foramen) and 21.06 mm (L3–L4 foramen) [11]. In this study, the sagittal diameter was determined to be changing between 8.02 mm (L3–L4 foramen) and 8.41 mm (L1–L2 foramen) along the sagittal line (the area which meets the spinal nerve or the spinal ganglion), which passes through the inferior border of the superior pedicle and which limits the IF. The narrowest sagittal diameter of IF's minimum distance is between 5.13 mm (L4–L5 foramen) and 6.58 mm (L1–L2 foramen), and it has been shown that this diameter is narrower at the lower lumbar levels compared

to the upper lumbar levels. Experimentally, it has been shown that the removal of the intervertebral disc or the reduction of intervertebral disc space decreases the vertical diameter of IF significantly and does not change the sagittal diameter [16]. There is a direct relationship between the height of the intervertebral foramen (vertical diameter) and the height of the intervertebral disc. Age-related disc degeneration and reduction in disc height cause reduction in the height of this pass, thus narrowing this area [15, 16]. Disc space is the major and the determining factor in vertical diameter and has no effect on the sagittal diameter. The sagittal diameter of IF is directly related to the width of the spinal canal and the length of the pedicle [17]. In cadaver studies, it has been shown that the height of IF, which has an inverted drop shape, in a lumbar region was between 11 and 12 mm, and a cross-sectional area was measured between 40 and 160 mm^2 [18]. In healthy subjects with MR imaging, this distance was determined to be 17.1 ± 2 mm in L1–L2, 18. 4 ± 1.7 mm in L2–L3 level, 18.1 ± 1.5 mm in L3–L4 level, and 17.1 ± 3.6 mm in L4–L5 level [17]. The shortest distance between the disc and nerve root was L1–L2 (by mean, 8.2 mm), and the greatest distance was L3–L4 (mean, 10.5 mm). In the midline, the disc–root distance decreased from L1–2 to L5–S1 [19]. It was found that the distance consistently increased from L1–L2 to L5–S1 for distances between an intersection point between the medial edge of the nerve root and the superior edge of the disc and lateral line of the foramen. At point at which the nerve root crosses the shortest distance from nerve root to the lateral border of the foramen, where disc was at level L1–L2 (mean, 2.6 mm) and the biggest distance, L5-S1 (mean, 8.8 mm). The width of the foramina progressively increased in a craniocaudal direction as in L1–2 was 8.3 to L5-S1 was reported 17.8 mm [19]. Again, the mean height of the foramina was about 19.3–21.5 mm for all disc levels [19].

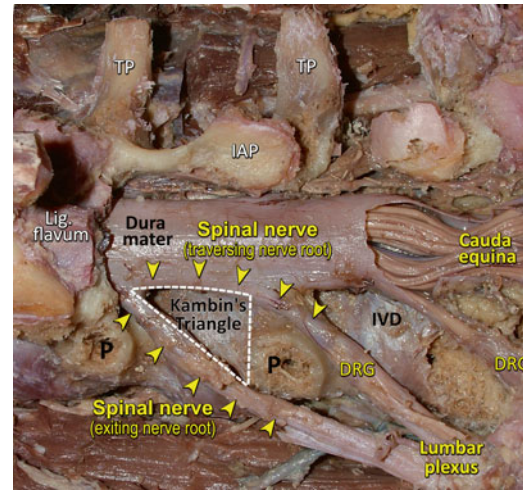

Fig. 47.4 In this picture, we can see the true anatomic nerve root canal initially arising from the lateral aspect of the dural sac and traveling through the neural foramen. The triangular working zone, described as Kambin's triangle, is the safe zone for safe lodging of endoscopic instruments during posterolateral access to the intervertebral disc and the spinal canal. The annular surface in the triangular working zone is bordered anteriorly by the exiting nerve root, inferiorly by the proximal plate of the inferior lumbar vertebra, medially by the dural sac and the traversing nerve root, and posteriorly by the articular processes of the adjacent segment. *P* pedicles, *Lig. flavum* yellow ligament, *TP* transverse process, *IAP* inferior articular process, *IVD* intervertebral disc, *DRG* dorsal root ganglion

Spinal Nerve Canal

The true anatomic nerve root canal initially begins from the lateral aspect of the dural sac and continues toward IF (Fig. 47.4). The actual anatomical spinal never canal is a tube that starts from the lateral surface of the dural sac. At each level, anywhere from two to six anterior and posterior rootlets converge in the dural sac to form anterior and posterior roots. These roots merge to form the spinal nerves [12]. Damage of neural structures occurs in the vertebral and "root" canals and at the intervertebral foramina. The spinal nerve is wrapped with a sheath made out of dura mater when it exits the dural sac. For lumbar segments level, the spinal nerve is wrapped with a sheath. Then, it passes through the IF and extends downward and then outward on an oblique route. This route changes angle slightly depending on the lumbar level. This angle becomes more right-angled in the upper lumbar segments and becomes narrower and oblique in the lower segments of the lumbar spine. The intraspinal section of the spinal nerve is slightly shorter as it exits the dural sac with a more perpendicular angle at the upper seg-

ments. In fact, the spinal nerve root directly enters IF as it immediately exits the dural sac in the upper lumbar segments due to the medial position of the thecal sac to the pedicle [9]. The diameter of the dural sac narrows as it goes distally from L3, and the spinal nerve exiting the sac gains a more oblique angle as it reaches IF. In MR studies, spinal nerve root at L1 level was shown to have a larger angle while exiting the thecal sac and a smaller angle while exiting the thecal sac at S1 level [20].

There is a cushioning structure formed by epidural fat tissue around the nerve roots at IF [9]. The lumbar spinal nerve roots follow the groove found medially to the pedicle just right before entering IF. This groove is prominent in the fifth lumbar IF. The spinal canal extends laterally due to this groove which is formed on the medial side of the pedicle. This extension which gives the spinal canal a three-leafed clover shape or trefoil shape is called the lateral recess. Pathology which causes the narrowing of this area was first identified by Verbiest in 1954 (lateral recess stenosis) and was shown to be presented as radicular leg pain in patients [20]. The spinal nerve goes toward IF when it goes from the medial side to the bottom side of the pedicle. The spinal nerves form an oblique angle between the inferomedial side of the upper pedicle and the superolateral side of the lower pedicle when it passes IF [21, 22]. Epidural venous plexus sinus is clearly observed just closely to the triangular working zone, described as Kambin's triangle (Fig. 47.5).

Posterior root enlarges just before the formation of spinal nerve. This enlargement contains the roots of the sensory nerves and is named dorsal root ganglion. Spinal ganglion is usually found in IF, and it is located on the lateral side of the point where the nerve root penetrates the dura (Fig. 47.5). This ganglion is usually found within the borders of IF in the lumbar section, and it is positioned on the inner side of the opening. Sacral ganglions are located inside the canal. In various studies, it has been shown that the S1 (first sacral) ganglion is found inside the spinal canal; in 80 % of the cases, this leads to injury in case of intraspinal damage [23, 24]. In the cervical region, spinal ganglion turns into spinal nerve and continues outside of IF and just on the posteromedial side of the vertebral artery [15]. Coccygeal ganglion is located inside the spinal canal, and furthermore, it is usually located inside the dural sac [13].

Spinal nerve root takes up 30 % of the cross section of IF. Other studies have shown that this ratio can be as high as 50 % [22, 23]. Tanaka et al. have shown that this ratio can be between one-fourth and one-third in the cervical region [15].

Tanaka et al. take a closer look at the relationship of IF with the spinal nerve and intervertebral disc in the cervical region, on cadaver studies [15]. In this study, IF has shown to have a conical shape, and its inner pass is the narrowest area. Cervical spinal nerve also has a conical shape in this area, and its exiting area from the dural sac is the thickest part. Therefore, spinal nerve compression occurs more frequently at the inner part of IF. The anterior branch of the cervical spinal nerve exits from the dura more caudally. Therefore, the anterior root is found on the immediate caudal side of the posterior root at IF. The anterior root makes up approximately two-thirds of spinal nerve [15].

Spinal nerve continues anterolaterally on the base of the inferior pedicle and transverse process once it exits IF [26]. Spinal nerve branches into two primer branches, namely, ramus anterior and ramus posterior at the exit zone of IF. The poste-

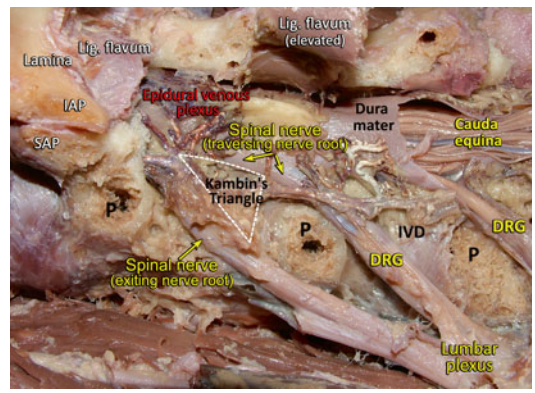

Fig. 47.5 Spinal nerve and the nerve root canal. Epidural venous plexus in the triangular working zone, described as Kambin's triangle. Epidural venous plexus sinus is clearly observed just closely to the Kambin's triangle; *P* pedicles, *Lig. flavum* yellow ligament, *TP* transverse process, *IAP* inferior articular process, *IVD* intervertebral disc, *DRG* dorsal root ganglion, *SAP* superior articular process

rior branch continues posteriorly toward the facet joint. The anterior branch goes toward the deep levels of the psoas muscle and is starting from the outer side of IF. The anterior branches merge inside the psoas muscle to form the lumbar plexus, which continues downward, passing in front of the vertebral bodies and the fusion area of pedicles.

Ligaments of the Intervertebral Foramen

In 1969, Golup and Silverman published a study on the five types of transforaminal ligaments (that include corporotransverse, inferior corporotransverse, superior transforaminal, midtransforaminal, and inferior transforaminal) and suggested that the variations associated with these ligaments may give rise to nerve compression syndromes [27].

However, even though foraminal ligaments were further investigated by many studies that followed, it was not clear whether the observed band-like structures are the ligaments or thickened muscle fascias covering the foramen [3, 28]. In a study by Koufi et al. (1988), ligaments in IF were reported along all the lumbar regions and were shown not to have any muscle attached [13].

Furthermore, ligaments in the upper lumbar foramen were easier to identify and were shown to be thicker and more rounded than those in the fifth lumbar foramen, where they are densely found, as suggested by previous studies [13]. Ligaments in IF are divided into three groups: internal ligaments, intraforaminal ligaments, and external ligaments. Internal ligaments are dense at the lower part of foramen medial surface, and are extended from the posterolateral side of the intervertebral disc to the anterior surface of the superior articular protrusion. These ligaments, which also obliquely extend inferoposteriorly, were divided to the lower sections of foramen formed by superior vertebral notch into its subcompartments by crossing the free lateral edges of ligamentum flavum. In addition, veins also pass through these small compartments [13]. There are three types of intraforaminal ligaments. Among these, deep anterior intraforaminal ligament extends from the pedicle base to the lower edge of the same vertebra. Recurrent meningeal nerve and a branch of spinal artery pass through the compartment formed by these ligaments. The second type, which is called superior oblique transforaminal ligament, extends from the angle between the pedicle posterior edge and root transverse protrusion to the posterolateral surface of the same vertebra. These ligaments also formed the anterosuperior compartment through which the large branch of segmental artery passes. The third, horizontal midtransforaminal ligament provides a strong connection between the upper half front section of the articular protrusion and the posterolateral surface of the upper vertebra. These ligaments also acts as a suitable surface over which spinal nerves can be extended, and their lateral surfaces are usually attached to the inferior corporotransverse ligaments [13].

On the other hand, external ligaments were extended upward, downward, and transversely and forward from the common pedicle at the transverse process. They also extend onto the vertebra corpus on the anterior surface, and therefore, they are also named as corporotransverse ligaments (superior, middle, interior corporotransverse ligaments). Superior ligaments extend upward from the transverse protrusion stem toward the posterolateral face of the vertebra and adjacent intervertebral disc. Transverse ligaments terminate at the adjacent vertebral body while inferior ligaments extend toward the posterolateral surface of the following lower vertebra and the front face of the meeting point between the pedicle and corpus. Fibers of superior corporotransverse ligament cross the lower section of the top IF, whereas those of inferior corporotransverse ligaments cross the IF at the same level. While crossing the IF, inferior corporotransverse ligament fibers pass over the superior ligaments from the lower level [12].

Corporotransverse ligaments together with the associated intraforaminal and internal ligaments divide IF into compartments. The largest one at the center homes and is almost entirely occupied by the front branch of the spinal nerve. It is surrounded by smaller compartments through which other neurovascular structures pass. Recurrent meningeal nerve and a small branch of segmental artery pass through the compartment located deeper anterosuperiorly. This compartment is

divided into two smaller compartments by the ligaments. Therefore, internal ligament bridges across the top of the superior vertebral notch, therefore converting it into a subcompartment in the lower part of the intervertebral canal. Posterior to this compartment, there are two neurovascular passages at the intertransverse gap just near the IF exit point. These passages can reach the deep sections of inferior and superior corporotransverse ligaments. The top channel resides at the bottom part of the top transverse protrusion and homes lumbar artery, venules, and medial branch of the posterior branch of the spinal nerve. In contrast, the bottom channel is located at the angle between the transverse protrusion stem and the lateral face of the superior joint protrusion (the lower half of the intertransverse gap). The lateral branch of the posterior branch and the branches of the segmental arteries and accompanying veins pass through this channel [14].

In a 2004 study by Caglar et al., a reverse "Y"-shaped ligament dividing IF's outer part into compartments was reported in 8 out of 15 cadavers. This ligament that we can observe clearly in the lumbar region, especially at the position of fifth IF, divides IF into three compartments. The smallest compartment is found posterolaterally and is positioned between the anterolateral side of the superior joint protrusion and "Y" ligament's upper arm [29]. Two arteries and two veins of the lumbar artery and vein branches pass through this compartment. In the middle compartment, between the short arms of the "Y" ligament, is located an artery, a vein, and two nerve structures from the posterior branch of the spinal nerve.. On the other hand, the anteromedial compartment has the anterior branch of spinal nerve, an artery, and a vein. The spaces between these structures are occupied by fat and fibrous tissues. In the aspects of neural structures and in comparison to the others, this described posterolateral compartment seems to be safer for the surgeries [29].

On contrary to the previous report by Koufi et al., which reported that these ligaments that divide IF into smaller compartments would not cause radicular pain symptoms by pressurizing spinal nerve and would even prevent spinal nerves from pressures that may have developed as a result of movement-associated changes in IF [14]. In addition, the fact that these compartments through which vascular structures pass are restricted by the ligaments further supports their protective roles [13]. According to a recently published cadaveric study [30] about foraminal ligaments, *five types of transforaminal ligament* were described:

1. *The superior corporopedicular ligament*: runs from the superior pedicle and vertebral notch to the posterolateral aspect of the vertebral body and adjacent annulus fibrosus.
2. *The inferior corporopedicular ligament*: runs from the inferior pedicle and vertebral notch obliquely to the posterolateral aspect of the vertebral body and adjacent annulus.
3. *The superior transforaminal ligament*: runs from the articular capsule and posterior vertebral notch to the superior pedicle.
4. *The midtransforaminal ligament*: extends from the articular capsule across the midforamen to the annulus and superior corporopedicular and inferior corporopedicular ligaments.
5. *The inferior transforaminal ligament*: extends from the superior facet joint across the superior vertebral notch to the junction of the annulus and vertebral body.

In addition, they reported ligaments formed for the intervertebral foramen, the periosteum, and into the tunnel or intervertebral canal. The root and the fatty tissues just surrounding it, intraforaminal vessels, and the abundant intraforaminal ligaments are present inside this canal or tunnel with thin composition. When the straight leg raise test is performed, the intraforaminal root and the nearby ligaments extend from the inside to the outside at the foramina, and can be damaged. Surgeons should be careful about these fragile intraforaminal ligaments around the nerve root besides the better-known transforaminal ligaments. Damage to these ligaments could cause friction during root movements in situations such as stenosis. Additionally, the removal of intraforaminal ligaments can lead to an increase in friction during root movements.

Body Movement-Associated Changes in Intervertebral Foramen

Hasegawa et al. suggested that the cases with posterior disc height less than 4 mm and cases with foraminal height less than 15 mm are associated with foraminal stenosis [31]. IFs are included in two joint structures, and the diameters of IFs were changed during everyday practice because of their dynamic structures. Therefore, the intensities of spinal stenosis symptoms vary depending on the posture [31]. Mayoux-Benhamous et al. suggested that IF diameter decreases with spine movement from flexion to extension [32]. According to the computer-based tomography results and frozen sections, Inufusa et al. reported changes in cadaveric IF diameters during flexion and extension [33]. In the cryomicrotome sections, the cross-sectional area of IF was reported to be 12 % wider in flexion group and 15 % narrower in extension group than that from the vertical position group [35]. In addition to flexion and extension, lateral flexion and axial rotation also seem to influence IF cross-sectional area, as suggested by Fujiwara et al. [17]. According to this study, while flexion widens IF by 11.3 % and extension narrows it by 12 %, lateral flexion causes IF diameter to become 8.4 % smaller and 8 % larger in the bending site and the opposite sites, respectively. In case of axial rotation, IF diameter was reported to be 5.7 % larger in the rotated side and 6.5 % smaller in the opposite side [17]. In an in vivo study by Schmid et al., site-associated changes in FI were reported by using open MR imaging technique, and it was found that IF cross-sectional area gets 19.2 % wider when switched from the vertical position to 90° flexion position, and it gets 23.2 % narrower when movement was practiced in the opposite direction [36]. Besides further supporting these findings, Panjabi and Nowicki et al. also suggested that movement-associated changes were more visible and easier to detect in sections with disc degeneration [37, 38]. For disc degeneration, hypermobility of the associated segment can also be observed. In cases of spinal segments with higher mobility, movement-dependent changes in the IF diameter are more evident [17].

Anatomical Relation Between Spinal Nerve and the Pedicle

The anatomic relation between pedicles that limit IF both superiorly and inferiorly and the spinal nerve has great surgical importance (Fig. 47.4). Broadening our knowledge in this area will help restrict the complications associated with transpedicular approaches. The neighborhood of pedicle and the spinal nerve varies according to the width of the spinal nerve, exit point from the dural sac, and the properties of dural sac at its relevant position. Additionally, accurate anatomical knowledge of the relationships of intervertebral discs to nerve roots is needed for spine surgeons.

In a cadaveric study performed by Ugur et al. in 2000, it was reported that pedicles at the cervical region are mostly in contact with spinal nerve superiorly and with dura at the medial position, and are 1.0–2.5 mm away from spinal nerve inferiorly [39]. Therefore, using inappropriate instruments (i.e. those not suitable for the medial and superior parts of the cervical region) can damage both spinal nerve and dura of the spinal cord. The average pedicle height and width at C3–C7 levels were reported to be between 5.2–8.5 and 3.7–6.5 mm, respectively. The angle between pedicles and sagittal plane was observed to vary from 38° to 48°. Spinal nerve was shown to exit the dural sac with an angle of 69–104°. This angle was the largest at the C3 level while the smallest at the C6 level. The same study also showed that the superoinferior diameter of spinal nerve increases from C3 (2.7 mm) to C6 (3.8 mm) and that it starts to decrease again at the C7 level (3.7 mm) [40].

Pedicle becomes smaller and lean toward the pedicles in the thoracic regions. As in the cervical region, 40 % of dural sac is in contact with the pedicles. The interpedicular distance decreases from T1 to T5 (13.8 mm at T1), and reaches its smallest value at T4 and T5 positions. Then, it starts to increase and becomes 16.6 mm at the T12 level. Therefore, approaches are not suitable for the medial side and can damage the spinal cord at the midthoracic segment at which the interpedicular distances are so small.

According to this study, pedicles are 1.5 and 6.7 mm away from the nerve root above, and 0.8 and 6 mm away from the nerve root below. Therefore, it was concluded that, for surgical attempts, sagittal planes are more suitable and safer than transverse planes [38].

According to another study [40], the superoinferior diameter of spinal nerve ranges between 2.9 mm (T1) and 4.6 mm (T11). Spinal nerve root exits dural sac with an angle close to 90° and then extends laterally. In the lower segments, this angle gets smaller, and the spinal nerve root extends obliquely, as in the case of lumbar nerve roots (average angle at T1 is 104° and at T12 it is 60°). The transverse and vertical diameters of pedicle are between 6.2–21.3 and 2.9–11.4 mm, respectively [35]. According to the results of this study, when compared to other regions, spinal nerves in lumbar region leave the dural sac with a more oblique angle, that is, 35–39°. Because of this oblique extension, spinal nerve runs from the inferomedial side of the upper pedicle to the superolateral side of the lower pedicle. The average distances between pedicles and dural sac, upper nerve roots, and lower nerve roots are 1.5 mm (0.9–2.1 mm), 5.3 mm (2.9–6.2 mm), and 1.5 mm (0.8–2.8 mm), respectively. Therefore, during transpedicular approaches, improper direction with inferomedial deviations can cause both spinal nerve and spinal cord complications. In the lumbar region, interpedicular distances were reported to vary between 22.2 and 27.5 mm. Diameter of the spinal nerve was found to be 3.3–3.9 mm. Mean pedicular width increases from L1 to L5 (5.9–23.8 mm), while pedicular height decreases (10.4–18.2 mm) [34]. Another cadaveric study mentioned that, for both sides, the mean distance from the inferior pedicle to the disc gradually increased from L1–2 to L4–5 and slightly decreased at the L5–S1 levels [41]. Distance from the superior pedicle to the disc was about 1 cm, the same for all disc spaces (range 9.3–11.6 mm and 8.2–10.5 mm for right and left, respectively). Therefore, it can be concluded that to avoid neighboring neurovascular structures, instrumentation should not be inserted into the lumbar disc spaces more than 3 cm from their posterior edge [41].

References

1. Standring S (2008) Gray's anatomy: the anatomical basis of clinical practice, 40th edn. Churchill Livingstone
2. Rauschning W (1993) Pathoanatomy of lumbar disc degeneration and stenosis. Acta Orthop Scand Suppl 251:3–12, Review
3. Bogduk N (1983) The innervation of the lumbar spine. Spine 8:286–293
4. Vleeming A, Schuenke MD, Danneels L, Willard FH (2014) The functional coupling of the deep abdominal and paraspinal muscles: the effects of simulated paraspinal muscle contraction on force transfer to the middle and posterior layer of the thoracolumbar fascia. J Anat 225(4):447–462
5. Arslan M, Comert A, Acar HI, Ozdemir M, Elhan A, Tekdemir I, Tubbs RS, Ugur HC (2011) Surgical view of the lumbar arteries and their branches: an anatomical study. Neurosurgery 68(1 Suppl Operative):16–22; discussion 22
6. Chau AM, Pelzer NR, Hampton J, Smith A, Seex KA, Stewart F, Gragnaniello C (2014) Lateral extent and ventral laminar attachments of the lumbar ligamentum flavum: cadaveric study. Spine J 14(10): 2467–2471
7. Gilchrist RV, Slipman CW, Bhagia SM (2002) Anatomy of the intervertebral foramen. Pain Physician 5:372–378
8. Hadley LA (1949) Constriction of the intervertebral foramen. JAMA 140:473–476
9. Lee CK, Rauschning W, Glenn W (1988) Lateral lumbar spinal canal stenosis: classification, pathologic anatomy and surgical decompression. Spine 13:313–320
10. Crock HV (1981) Normal and pathological anatomy of the lumbar spinal nerve root canals. J Bone Joint Surg (Br) 63:487–490
11. Stephens M, Evans J, O'Brien J (1991) Lumbar intervertebral foramens: an in vitro study of their shape in relation to intervertebral disc pathology. Spine 16:525–529
12. Rauschning W (1987) Normal and pathologic anatomy of the lumbar root canals. Spine 12:1008–1019
13. Amonoo-Kuofi HS, el-Badawi MG, Fatani JA (1988) Ligaments associated with lumbar intervertebral foramina. 1. L1 to L4. J Anat 156:177–183
14. Williams PL, Bannister LH, Berry MM, Collins P, Dyson M, Dussek JE, Ferguson MWJ (1995) Gray's anatomy, 38th edn. ELBS, Edinburgh
15. Tanaka N, Fujimoto Y, An HS, Ikuta Y, Yasuda M (2000) The anatomic relation am nerve roots, intervertebral foramina, and intervertebral discs of the cervical spine. Spine (Phila Pa 1976) 25(3):286–291
16. Cinotti G, De Santis P, Nofroni I, Postacchini F (2002) Stenosis of lumbar intervertebral foramen anatomic study on predisposing factors. Spine 27:223–229
17. Fujiwara A, An HS, Lim T-H, Haughton VM (2001) Morphologic changes in the lumbar intervertebral foramen due to flexionextension, lateral bending, and axial rotation an in vitro anatomic and biomechanical study. Spine 26:876–882

18. Crock HV (1981) Normal and pathological anatomy of the lumbar spinal nerve root canals. J Bone Joint Surg (Br) 63-B:487–490
19. Arslan M, Cömert A, Açar Hİ, Ozdemir M, Elhan A, Tekdemir I, Tubbs RS, Uğur HÇ (2012) Nerve root to lumbar disc relationships at the intervertebral foramen from a surgical viewpoint: an anatomical study. Clin Anat 25(2):218–223
20. Bose K, Balasubramaniam P (1984) Nerve root canals of the lumbar spine. Spine 9:16–18
21. Epstein BS, Epstein JA, Lavine L (1964) The effect of anatomic variations in the lumbar vertebrae and spinal canal on cauda equina and nerve root syndromes. Am J Roentgenol 42:91–99
22. Magnusson PB (1944) Differential diagnosis of causes of pain in the lower back accompanied by sciatic pain. Ann Surg 119:878–901
23. Lee C, Rauschning W, Glenn W (1988) Lateral lumbar spinal stenosis. Spine 13:313–320
24. Smith GA, Aspden RM, Porter RW (1993) Measurement of Vertebral foraminal dimensions using three dimensional computerized tomography. Spine 18:629–636
25. Hasue M, Kunogi J, Konno S et al (1989) Classification by position of dorsal root ganglia in the lumbosacral region. Spine 14:1261–1264
26. Rauschning W (1983) Correlative Multiplanar Computed Tomographic Anatomy of the Normal Spine. In: Judith D, Post M (ed) Computed tomography of the spine. Williams and Wilkins, Baltimore, pp 1–57
27. Golub BS, Silverman B (1969) Transforaminal ligaments of the lumbar spine. J Bone Joint Surg Am 51A:947–956
28. Bachop W, Janse J (1983) The corporotransverse ligament at the L5 intervertebral foramen. Anat Rec 205:13A–14A
29. Caglar YS, Dolgun H, Ugur HC, Kahilogullari G, Tekdemir I, Elhan A (2004) A ligament in the lumbar foramina: inverted Y ligament. An anatomic report. Spine 29:1504–1507
30. Akdemir G (2010) Thoracic and lumbar intraforaminal ligaments. J Neurosurg Spine 13(3):351–355
31. Hasegawa T, An HS, Haughton VM et al (1995) Lumbar foraminal stenosis: critical heights of the intervertebral discs and foramina. A cryomicrotome study in cadavera. J Bone Joint Surg Am 77:32–38
32. Mayoux-Benhamou MA, Revel M, Aaron C et al (1989) A morphometric study of the lumbar foramen: influence of flexion-extension movements and of isolated disc collapse. Surg Radiol Anat 11:97–102
33. Infusa A, An HS, Glover JM, McGrady L, Lim TH, Riley LH 3rd (1996) The ideal amount of lumbar foraminal distraction for pedicle screw instrumentation. Spine (Phila Pa 1976) 21(19):2218–2223
34. Hasue M, Kunogi J, Konno S, Kikuchi S (1989) Classification by position dorsal root ganglia in the lumbosacral region. Spine 14:1261–1265
35. Inufusa A, An HS, Lim T-H, Hasegawa T, Haughton VM, Nowicki BH (1996) Anatomic changes of the spinal canal and intervertebral foramen associated with flexion-extension movement. Spine 21:2412–2420
36. Schmid MR, Stucki G, Duewell S et al (1999) Changes in cross-sectional measurements of the spinal canal and intervertebral foramen as a function of body position: in vivo studies on an open configuration MR system. AJR 172:1095–1102
37. Panjabi MM, Takata K, Goel VK (1983) Kinematics of lumbar intervertebral foramen. Spine 8:348–357. 27
38. Nowicki BH, Haughton VM, Schmidt TA et al (1996) Occult lumbar lateral spinal stenosis in neural foramina subjected to physiologic loading. AJNR Am J Neuroradiol 17:1605–1614
39. Ugur HC, Attar A, Uz A, Tekdemir I, Egemen N, Caglar S, Genc Y (2000) Surgical anatomic evaluation of the cervical pedicle and adjacent neural structures. Neurosurgery 47:1162–1169
40. Ugur HC, Attar A, Uz A, Tekdemir I, Egemen N, Genc Y (2001) Thoracic pedicle: surgical anatomic evaluation and relations. J Spinal Disord 14:39–45
41. Arslan M, Cömert A, Açar Hİ, Özdemir M, Elhan A, Tekdemir İ, Tubbs RS, Attar A, Uğur HÇ (2011) Neurovascular structures adjacent to the lumbar intervertebral discs: an anatomical study of their morphometry and relationships. J Neurosurg Spine 14(5):630–638

The Spine

48

Alpaslan Şenköylü

Abstract

Evolution of human has led to morphological mutations in the spinal column because of its crucial role for maintaining erect posture. The principal functions of the spinal column are weight-bearing, movement, and protection. Spinal column consists of a total of 24 vertebrae (7 cervical, 12 thoracic, and 5 lumbar), 4 fused sacral, and 3 or 4 fused coccygeal segments. All the vertebrae are separated by intervertebral disc.

Atlas and axis have different morphology from the subaxial cervical spine due to their special function in the craniocervical junction. Lateral masses of cervical vertebrae are thick bony structures that can be used during posterior instrumentation procedures as fixation points. Major morphologic differences of thoracic spine rise from the components of the thoracic cage. Pedicle morphologies and orientations change level to level in this region. Lumbar segments are quite larger than the cervical and thoracic segments.

Ligamentous structures are crucial for proper stability of the spinal column. The main ligamentous structures of the spinal column are ligamentum nuchae, anterior longitudinal ligament, posterior longitudinal ligament, ligamentum flavum, facet capsule, interspinous ligament, and supraspinous ligament. The spinal column is surrounded by muscles, which mainly control movements and maintain the posture of the head and trunk. Some of them also support respiratory function.

The spinal column is totally straight in the coronal plane and has physiological curvatures in the sagittal plane. The stability of the spinal column is primarily dependent upon the integrity of ligaments, discs, and bony structures. This concept is involved in the pathophysiology of many spinal disorders.

"Our true mentor in life is science" M. K. Atatürk

A. Şenköylü, MD
Department of Orthopaedics and Traumatology,
Gazi University, Besevler, Ankara 06510, Turkey
e-mail: drsenkoylu@gmail.com;
senkoylu@gazi.edu.tr

F. Korkusuz (ed.), *Musculoskeletal Research and Basic Science*,
DOI 10.1007/978-3-319-20777-3_48

Learning Outcomes
After reading this chapter, the reader will be able to

1. Define basic anatomy of cervical, thoracic, and lumbosacral spine
2. Describe the ligaments of spine and paraspinal muscles
3. List the functions of the spinal column
4. Recognize pedicle morphologies in different regions
5. Identify normal alignment and malalignment of the spinal column
6. Explain the stability concept for spinal column and identify its importance for different spinal disorders

Introduction

Humans consume less energy while walking when compared with other living beings. This is due to their bipedalism as a result of evolution which occurred within approximately 4 million years. Evolution of human has led to morphological mutations in different body parts, including spinal column, upper, and lower extremities. Of these anatomical parts, spine is one of the most prominent structures as it has a crucial role for maintaining erect posture.

The principal functions of spinal column are weight-bearing, movement, and protection. Spine connects the head to the trunk and also the trunk to the pelvis. As a strong link, the spinal column provides weight-bearing and movements of different body parts. This complex structure becomes a giant string, especially when an individual jumps and runs. Moreover, it protects not only the spinal cord located within the medullary canal but also the important intrathoracic and intraabdominal structures.

The spinal column consists of a total of 24 vertebrae (7 cervical, 12 thoracic, and 5 lumbar), 4 fused sacral, and 3 or 4 fused coccygeal segments. Atlas connects the spinal column to the cranium via the articulation of its facets to the occipital condyles. The spinal column is also connected to the pelvis by sacroiliac joints, caudally (Fig. 48.1).

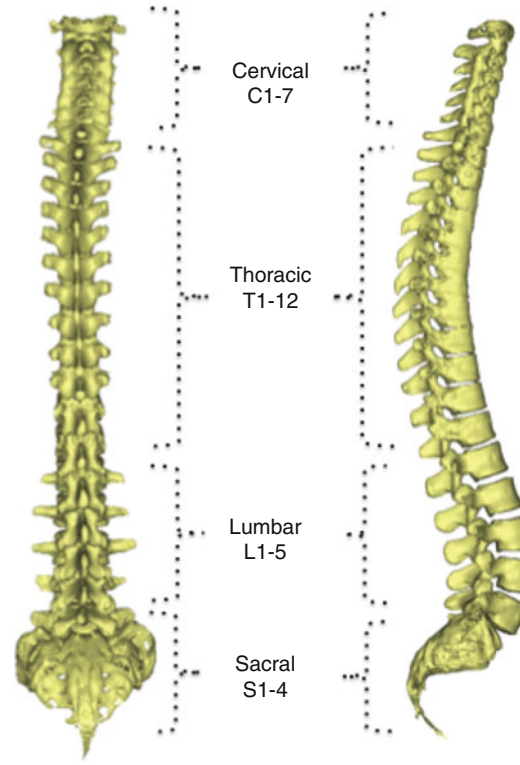

Fig. 48.1 Spinal column consists of cervical, thoracic, lumbar, and sacrococcygeal regions. It has curvatures in the sagittal plane, while it is totally straight in the coronal plane

Every anatomic region demonstrates unique vertebral morphology and all vertebrae are separated by intervertebral discs (Fig. 48.2). The unit including two adjacent vertebrae and one disc in between is called as a "functional spine unit." Summation of all movements raised from these functional units gives spinal column a whole remarkable degree of movement. The following movements are possible in the spinal column: flexion, extension, lateral flexion, rotation, and circumduction. The type and range of movements differ in every region, depending on the thickness of the disc, orientation of facet joints, and tethering of paraspinal structures such as ribs.

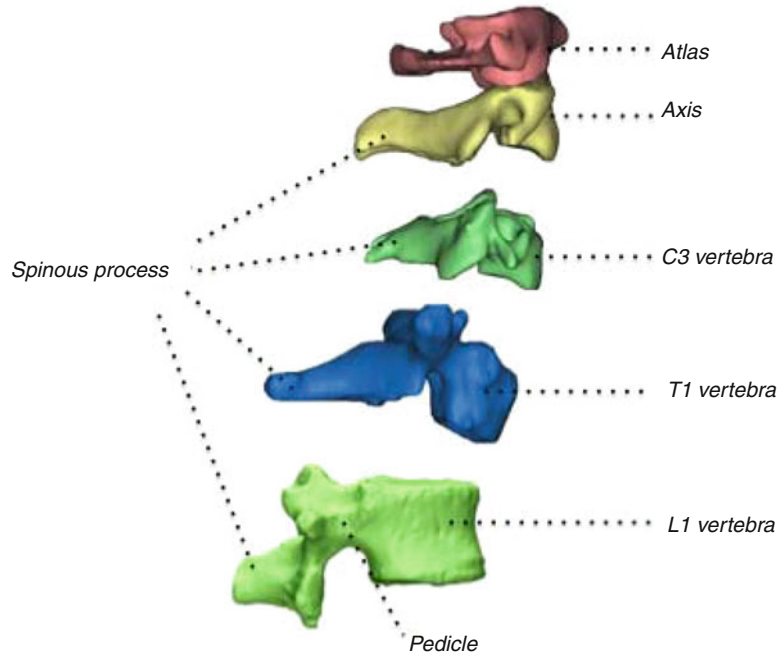

Fig. 48.2 Different vertebral morphologies of all regions. Cervical region has three unique types of vertebra

Basic Anatomy

Cervical Region

All cervical vertebrae are similar, other than the *atlas* (C1) and *axis* (C2), which are unique in shape. Atlas differs from the others in that it does not have a body. However, it consists of two lateral masses, which are connected together with an anterior and a posterior arch (Fig. 48.3). It also does not have a spinous process that is represented by a tubercle located at the apex of the posterior arch. On the superior surface of each lateral mass is a concave facet which articulates with the corresponding occipital condyle. There is also a groove at the posterior side of each lateral mass. This groove contains a vertebral artery and first spinal nerve. Vertebral artery injuries may occur in this location during the C1–2 transarticular screw fixation procedure. Especially in the presence of high-riding vertebral artery, this potential risk becomes higher. It is suggested to take three-dimensional angiographic tomography preoperatively for visualization of possible variations of vertebral artery before the C1–2 transarticular fixation procedure [25].

Axis is another unique vertebra within the spinal column. It has a vertical bony protuberance which projects upward from the corpus called *dens axis* or *odontoid process*. Odontoid process acts as a pivot around where the atlas and head rotate (Fig. 48.3). It has many ligamentous attachments that are very important for atlantoaxial stability. Fractures of the odontoid process may result in nonunion, if, especially, it is broken from its base (Type-II). Histomorphometric analysis showed that the base of the odontoid process has reduced trabecular bone volume, poorer trabecular interconnection, and thinner cortex (cortical thickness is one-third of the other parts) [1]. Another important morphologic feature of axis is its bifid spinous process. This large bony structure provides a prominent landmark for palpation and powerful leverage for the attachment of suboccipital muscles. Due to this important function, surgeons should protect the spinous process of C2 vertebra in order to prevent possible instability.

Subaxial (third to seventh) cervical vertebrae are similar in structure. These have smallest vertebral corpus but largest vertebral foramina of the

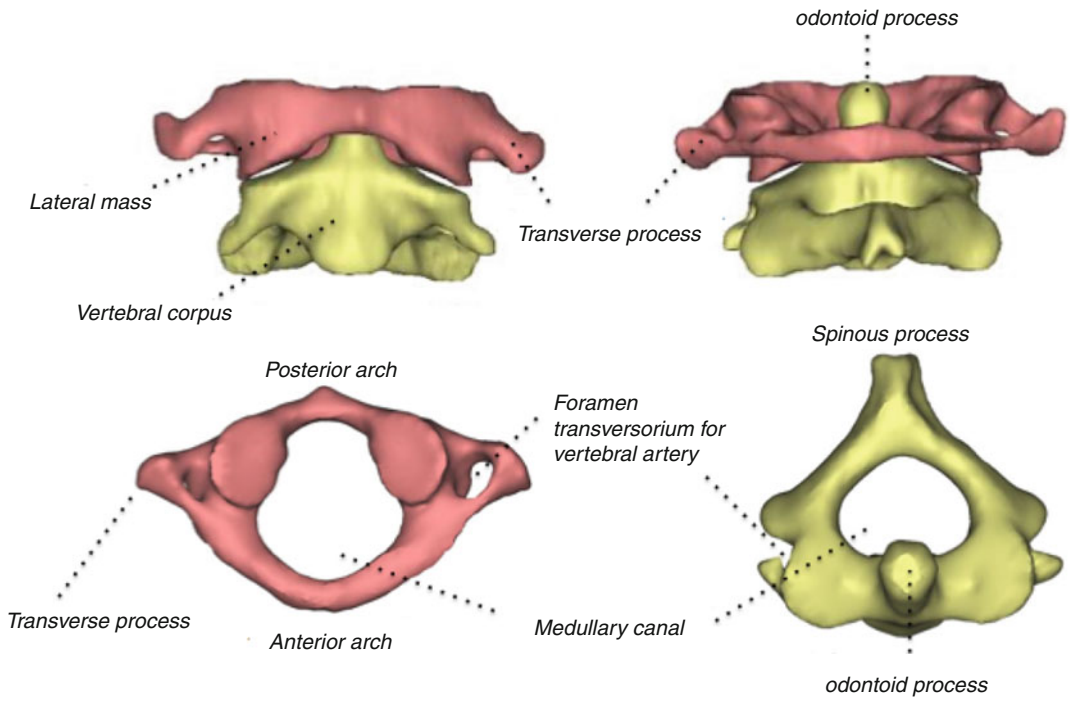

Fig. 48.3 Atlantoaxial complex is seen in first row. Axial views of atlas and axis are shown in second row

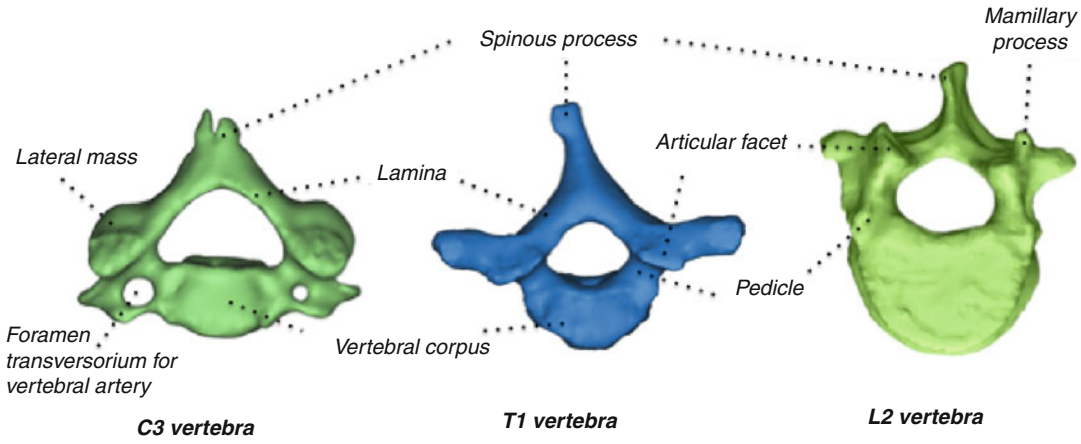

Fig. 48.4 Subaxial cervical, thoracic, and lumbar vertebra samples are shown in the axial plane. It is to be noted that they are all similar but have slight differences

vertebral column. The superior surface of the vertebral corpus is concave at the transverse plane and convex at the sagittal plane. There are bony elevations called *uncinate process* in each side. This process has a separate articulation with the uncinate process of the adjacent vertebra known as *uncovertebral joint* or *joint of Luschka.* Transverse processes arise from two parts that are from the vertebral corpus anteriorly and from the articular process posteriorly. Transverse processes contain foramen transversariums wherein lie the vertebral artery, vein, and sympathetic plexus bilaterally (Fig. 48.4). Only C7 does not contain vertebral artery.

There are lateral masses adjacent to the facet joints bilaterally. These thick bony structures can be used as fixation points during posterior instrumentation procedures. Screw placement to these structures is relatively safe when compared with the cervical pedicle screw placement. Average depth of lateral mass on the sagittal plane is 12.83 ± 1.28 mm, while the average width on the coronal plane is 11.92 ± 0.96 mm. Screw trajectory must be divergent around 20° on the transverse plane and directed caudally 30° on the sagittal plane to prevent vertebral artery and root injuries [17].

Thoracic Region

There are 12 thoracic vertebrae in this region. Major morphologic differences rise from the components of the thoracic cage. Ribs connect to the spine by costotransversal and costovertebral joints and limit the movements of the spinal column. Other reasons for limited motion in thoracic region are orientation of facet joints, sternum, strong intercostal fascia, and the radiate ligament that attaches the head of rib and adjacent vertebra.

Thoracic vertebral body has a cylindrical shape with almost equal anteroposterior and mediolateral dimensions. Vertebral bodies decrease in size from T1 to T3 and then increase to T12, gradually. The primary function of thoracic vertebrae is to bear the weight of the trunk, since the sagittal vertical axis crosses just anterior to the vertebral bodies in the midthoracic region [11] (Fig. 48.5). There are bilateral demifacets on the lateral surfaces of the body, which articulate with the rib heads.

Vertebral foramen is near round shape and small. Medullary canal is narrowest at T6. However, this narrowness extends between T4 and T9. Thus, the spinal cord becomes vulnerable in this part of the medullary canal due to any kind of space occupying lesion or foreign body such as pedicle screw. Pedicles are short bony connections between the body and laminae. Pedicle morphology is especially important for inserting pedicle screws during any posterior instrumentation procedure. Pedicle diameter in transverse plane is the most critical variable for thoracic pedicle screw insertion. Usually, the smallest pedicles are T4 and T6, with the transverse diameter ranging between 4.7 and 6.1 mm. On the other hand, the largest pedicle is T12, with the diameter varying from 6.3 to 7.8 mm. Pedicles progressively become larger between T4 and T1 in the cephalad direction [9].

If the screw diameter exceeds 80 % of outer pedicular diameter there will be three possibility: Pedicle will adapt by expansion, pedicle will be cut out by screw threats or pedicle will break. Pedicle fracture is seen mostly in the lateral wall, because the medial cortex of the pedicle is two to three times thicker than the lateral cortex [10, 16].

Angle of the pedicles on transverse plane also differs from level to level. It decreases gradually from 30° convergent at T1 to neutral at T12. The transverse pedicle angle decreases caudally down to around 14° in the fourth thoracic vertebra. It remains around 14° between T4 and T9 and decreases sequentially to neutral in the lower thoracic spine [22, 26].

Thoracic facets are oriented in the coronal plane. Thus, they allow primarily lateral bending and axial rotation. The superior articular facet of the caudal vertebrae forms the roof of the neural foramen. Transverse processes of thoracic vertebra join the pedicles and the laminae at their bases. They extend laterally and posteriorly to make room for the ribs to pass anterior to them. Thoracic vertebrae typically have long and slender spinous processes that point downward and overlap the vertebral arches of the vertebra below. Thus, thoracic laminectomy requires removal of the inferior portion of the cephalad–spinous process (Fig. 48.4).

Lumbar Region and Sacrum

Lumbar segments are quite larger than the cervical and thoracic segments. There are five lumbar vertebrae, and the bodies of these are oval-shaped on the axial plane. Mediolateral diameter is larger than the anteroposterior diameter. Sagittal vertical axis bisects most of the lumbar vertebrae.

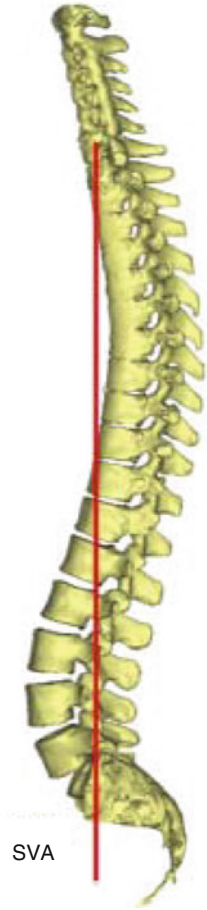

Fig. 48.5 Sagittal vertical axis (*SVA*) is a relative line that is drawn from C7, perpendicular to the ground. It should be passed ±2 cm around sacral promontorium in normal subjects

Thus, lumbar spine bears the whole weight of the trunk, together with the head and upper extremities. Body of the lumbar vertebrae consists of very well designed trabecular system for this function.

Pedicles of lumbar vertebrae are quite large. Pedicle screw, even as large as 8 mm in diameter, can be placed within the pedicles of the lumbar spine. In fact, first pedicle screw was inserted within the lumbar pedicle by Boucher [2].

Laminae are the bony plates projecting each of the pedicles toward the midline. The shape of the lamina in the lumbar region is similar with the thoracic and cervical spine. However, part of the lamina between the superior and inferior articular processes of the lumbar vertebra, called as *pars interarticularis* or *isthmus,* has clinical importance. The biomechanical significance of isthmus comes from its location in a transitional zone of forces. It lies at the junction of vertically oriented lamina and horizontally projecting pedicle. Because of this morphological feature, isthmus exposes serious shear forces. Developmental fusion defect of growth centers or fatigue fracture of isthmus is described as spondylolysis. Spondylolysis is usually seen at the L5 level. Moreover, L5 may slip anteriorly over the lower S1 segment due to spondylolysis, if these vertebrae have dysplastic background. This pathology is defined as spondylolisthesis.

Spinous process, which is formed by the connection of laminae in the midline, can be easily palpated under the skin. Most surgeons use this examination while determining the surgical levels. The spinous process intersected by the line that is drawn between the contralateral iliac crests is generally L4.

Extending laterally from the junction of the pedicle and the lamina on each side, there are transversely oriented flat bony bars. These are called as *transverse processes*. Transverse processes are excellent graft beds beneath well-vascularized paraspinal muscles for posterolateral fusion. Surgeons use this graft bed by decortication of tranverse processes on each side within fusion levels and placement of grafts between them. Another excellent structure for fusion procedure is the facet joint. Articular facets that are covered by hyaline cartilage and facet capsule support the movement function of the spinal column. They also contribute to the stability of the functional anatomic unit with their special orientation.

At the base of the transverse process and lateral to the superior articular facet, there is a bony prominence called *mammillary process*, which is a very good reference point for inserting the lumbar pedicle screw (Fig. 48.4). But, every lumbar vertebrae may not have a mammillary process. Another point to place the lumbar pedicle screw is the transection of two perpendicular lines: (1) Vertical line drawn from the lateral facet. (2) Horizontal line bisects the transverse process.

The sacrum is a large, irregular, and triangular bone at the base of the spinal column. Its broad upper part joins the lumbar spine by S1 vertebra, while the lower part joins the coccyx. It also connects both *os coxae* laterally, and they form a pelvic ring together. S1 pedicles are broad but short structures. Inserting a pedicle screw to the S1 pedicle is technically different from that to the lumbar spine. In order to place a longer pedicle screw, its trajectory should be more divergent, and it should penetrate the anterior cortex with a couple of threads for better purchase. Biomechanically strong screw purchase will be accomplished by this technique [14]. There are bony wings on each side at the top of the sacrum called *sacral ala.* Basically, these structures are identical to the transverse process and also appropriate for screw insertion. But, the last is technically different than the standard pedicle screw fixation and needs convergent trajectory.

Ligaments of Spine

Ligamentous structures are crucial for proper stability of the spinal column. The main ligamentous structures of the spinal column are as follows: ligamentum nuchae (LN), anterior longitudinal ligament (ALL), posterior longitudinal ligament (PLL), ligamentum flavum (LF), facet capsule, interspinous ligament (IL), and supraspinous ligament (SL).

The LN extends from the external occipital protuberance on the skull and median nuchal line to the spinous processes of all cervical vertebrae. It is a fibroelastic membrane and homologous with the supraspinous and interspinous ligaments of the lower regions. LN forms a septum for the attachment of the trapezius and splenius capitis muscles and contributes to the stability of head and neck. Besides this function, it serves as a guide during the posterior exposure of the cervical spine. After the skin incision, the surgeon should stay within LN for preventing excessive bleeding from the muscles and easily reach the spinous processes of the cervical vertebrae.

ALL is a strong band that lies anterior to the vertebral column between the basilar part of the occiput and sacrum. The ligament is thick and slightly more narrow over the vertebral bodies, and thinner but slightly wider over the intervertebral discs. It has three layers: superficial, intermediate, and deep. The deep layer is attached to the underlying periosteum. It functions to limit hyperextension of the vertebral column in the sagittal plane.

PLL extends from the body of axis to the posterior wall of S1 vertebra within the medullary canal. It is broader above than below, and thicker in the thoracic than in the cervical and the lumbar regions. The ligament is more narrow at the vertebral bodies and wider at the intervertebral discs. Some of the intervertebral disc herniations located under the PLL are called as *contained* disc herniation [5]. PLL functions to limit hyperflexion of the vertebral column in the sagittal plane.

LF is a yellowish structure, which connects both the laminae of adjacent vertebrae from their dural surfaces. Its color comes from the intensive elastin content. Proximal origin of LF attaches the middle point of upper lamina and extends down to lower lamina. Distal insertion is located on the superior edge of lower vertebra. LF has much clinical significance during the laminectomy or hemilaminectomy procedure:

1. Buckling of this structure by aging causes spinal stenosis because of its contiguity to the dura.
2. Removing of LF is a crucial part of decompression procedure in the surgical treatment of spinal stenosis.
3. During the surgical procedure, lamina should be removed upward till the proximal origin of LF is found. With this simple manipulation, dura can be protected. After finding the proximal origin, LF should be dissected from dura with a MacDonald dissector by using a cotonete. Because there can be adhesions between dura and LF due to spinal stenosis and incidental dural tear can happen during removal of LF. This complication is easily prevented with the above-mentioned simple maneuver [12].

Facet capsule surrounds the facet joints and contributes to the stability of the spine. This

structure is an integral part of the posterior ligamentous complex, together with IS and SS ligaments.

IL is a thin and membranous ligament, which connects adjacent spinous processes. It extends from the base to the tip of the spinous process in the sagittal plane. IL meets LF ventrally and mixes with SL dorsally.

SL is a cord-like ligament, which connects the spinous processes of the vertebrae from C7 to sacrum. It blends ventrally with IL and dorsally surrounding thoracolumbar fascia. SL is thicker than IL, and they resist hyperflexion of the spinal column together with LF.

Distractive forces or hyperflexion injuries of spinal column during a high-energy trauma can cause rupture of the posterior ligamentous complex. This is one of the principal parameters of many classifications about spinal trauma [4, 15, 23].

Paraspinal Muscles

Spinal column is surrounded by muscles, which mainly control movements and maintain the posture of head and trunk. Muscles that encircle the thoracic spinal column also support respiratory function. Paraspinal muscular structures can be divided into two groups:

1. Muscles anterior to the spinal column: These are located in the cervical and lumbar regions. There is no muscle anterior to thoracic spine within the thoracic cavity. From the lateral to medial, *scalenus anterior*, *longus capitis*, and *longus colli* muscles are situated on the anterior surface of the cervical vertebrae. Longus colli lies between the atlas and third thoracic vertebra. It is a clinically important structure since its medial edge should be elevated and dissected from the anterior surface of the vertebral column during the anterior spinal fusion procedure.

   Psoas major muscle is a long fusiform muscle located on both the anteromedial sides of the lumbar region and joins the iliacus muscle distally to form the iliopsoas. It also has similar clinical importance as it also needs elevation and dissection medially during the anterior exposure of the lumbar spine.
2. Muscles posterior to the spinal column: These structures can be divided into three subgroups.
   (a) Superficial group. These are trapezius, latissimus dorsi, levator scapulae, and rhomboids that function primarily for shoulder movements.
   (b) Intermediate group. These are serratus posterior superior, serratus posterior inferior, and levatores costarum, which contribute to respiratory function.
   (c) Deep group. The deep muscles of the back are in a broad and thick structure that fills the cavity at each side of the spinous processes. As a whole, they extend from the occiput to the sacrum. Origins and insertions of the different muscle groups overlap with each other. They originate from and insert to the spinous processes, transverse processes, sacrum, ilium, ribs, and skull. The main muscle groups are erector spinae (iliocostalis, longissimus, spinalis), transversospinalis (semispinalis, multifidus, rotatores), splenius (capitis and cervicis). There are also smaller muscles such as interspinales and intertransversarii, which help in trunk rotations.

The thoracolumbar fascia envelops all of the back muscles with its three layers. At the base of the lumbar spine, all of the layers of the thoracolumbar fascia fuse together into a thick composite that attaches firmly to the posterior superior iliac spine and the sacrotuberous ligament. It has a biomechanical role in the stability of lumbar spine, especially in flexed posture and in lifting [24].

Clinical Relevance

Alignment of Spinal Column

Spinal column is totally straight in coronal plane, and any lateral deviation of the spinal column is accepted as a pathologic curvature. This pathologic curvature in coronal plane is called as

scoliosis. However, the sagittal alignment is not totally straight in normal subjects. It is kyphotic, like the letter "C," at birth and early childhood. Thus, thoracic and sacral kyphosis is accepted as the primary or structural curve of normal spine (Fig. 48.1).

Cervical lordosis begins to develop at the third month of life as the infant starts to hold its head in an upright position. Then lumbar lordosis appears as the child learns standing up and walking in around 1 year of age. Lordotic curvatures are defined as secondary or compensatory curves of normal spine. Secondary curves have important biomechanical function in helping to weaken vertical compressive forces. Thus, spinal column behaves like a string under vertical loads, and this provides shock-absorbing capacity to the spinal column.

Thoracic vertebrae are wedge-shaped due to the shorter vertical height of the anterior vertebral body. Cumulative effect of this wedge shape gives thoracic kyphosis to the vertebral column. Thoracic discs also contribute to kyphosis, but secondarily [6, 20]. Normal thoracic Cobb's angle measurement is accepted between 20° and 45° by the Scoliosis Research Society. Nevertheless, it is still controversial in the literature [3].

Some disorders like osteoporosis and Scheuermann's kyphosis resulted with changes in the vertebral morphology. This shifts the sagittal alignment from normal to abnormal. A normal subject can compensate this pathological change with its cervical and/or lumbar lordosis. However, pathologies like ankylosing spondylitis cause a stiff spine, and this compensation mechanism will be a failure in these disorders [21].

The lumbar lordosis includes vertebrae between T12 and L5. Greatest portion of lordosis occurs between L3 and L5. Discs contribute lordosis more than the vertebral bodies. L4/5 disc is the highest disc of the lumbar region [27].

Stability of the Spinal Column

Panjabi and White define spinal stability as maintaining alignment of the spine without pain and neurologic deficit under physiological loads. Stability of the spinal column is primarily dependent upon the integrity of ligaments, discs, and bony structures. On the other hand, the strength of paravertebral muscles also have secondary impact on the stability of the spinal column [19].

Stability concept is involved in the pathophysiology of many spinal disorders, including destructive (trauma, tumor, infection) problems and degenerative conditions.

1. Stability in spinal trauma. If the spine surgeon thinks that the spinal column has become instable due to the trauma, there is a necessity of surgical stabilization of the spine. There have been many classifications defined for predicting the stability of spine after trauma since mid 1900s [18]. Holdsworth defined two-column concept, and later Denis refined this idea with the three-column concept [4, 7]. AO group described a more sophisticated classification system based on the injury mechanism [15]. Recently, Spine Trauma Study Group came up with the absence of clinical stability and the importance of posterior ligamentous complex (Fig. 48.6). Then, they developed TLICS (thoracolumbar injury classification system) [23]. All of these classification systems mainly considered the stability of the spinal column.
2. Stability in degenerative spine. The loss of intervertebral disc height because of a decrease in proteoglycan content of the nucleus pulposus is one of the significant components in the pathophysiology of degenerative disc disease. It results with the relative ligamentous laxity and segmental instability due to the "flag post effect" (Fig. 48.7). Again, the major ligaments of spine (especially, ALL, PLL, LF) play a crucial role in this pathophysiologic process. An important clinical symptom of segmental instability is low back pain. However, it is still difficult to determine the source of pain in degenerative disorders [8, 13].

Acknowledgments The author extends his special appreciation to Mr. Murat Eğri for his excellent contribution in figures by 3D modeling of the vertebral column.

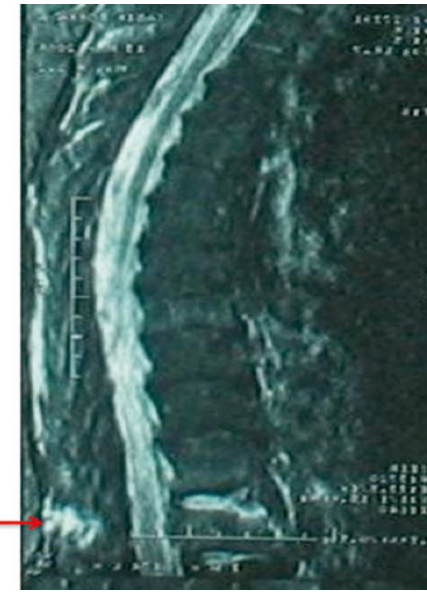

Fig. 48.6 Sagittal T2-weighted magnetic resonance image of thoracolumbar spinal trauma patient shows a hyperintense signal around the posterior ligamentous complex. This suggests rupture of the posterior ligamentous complex

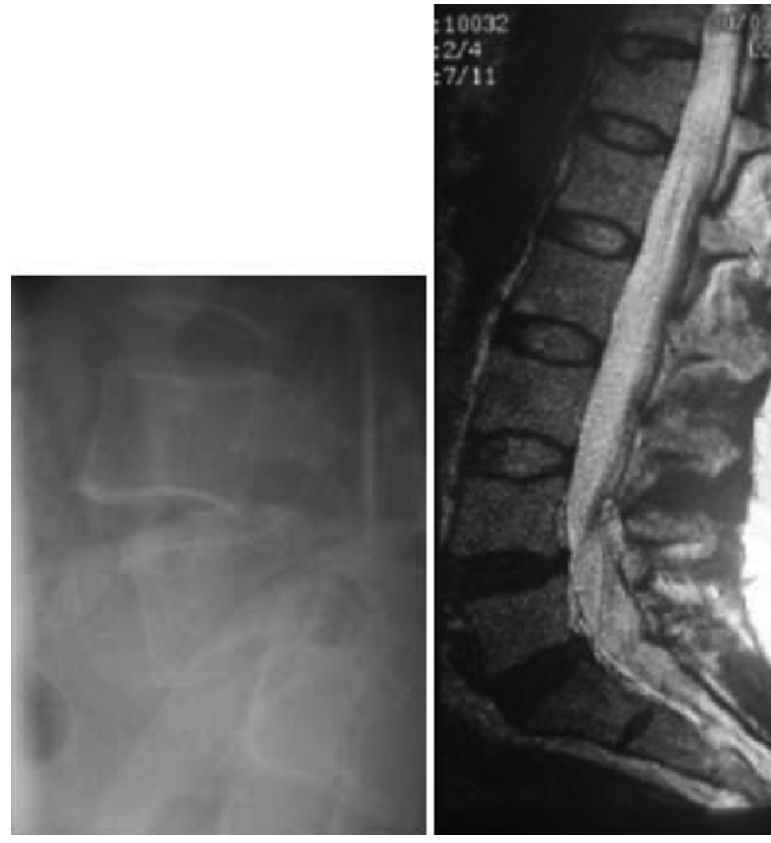

Fig. 48.7 A 46-year-old lady suffered from low back pain, and was not relieved with conservative treatment. Standing lateral lumbosacral X-ray shows a grade-1 spondylolisthesis at L4–5 level. This spondylolisthesis disappeared when MRI was taken in the supine position. This is a typical example of segmental instability due to degenerative disc disease

References

1. Amling M, Wening VJ, Pösl M, Grote HJ, Hahn M, Delling G (1994) Structure of the axis: key to the etiology of the dens fracture. Chirurg 65(11): 964–969
2. Boucher HH (1959) A method of spinal fusion. J Bone Joint Surg Br 41-B(2):248–259
3. Cil A, Yazici M, Uzumcugil A, Kandemir U, Alanay A, Alanay Y, Acaroglu RE, Surat A (2005) The evolution of sagittal segmental alignment of the spine during childhood. Spine 30(1):93–100
4. Denis F (1984) Spinal instability as defined by the three-column spine concept in acute spinal trauma. Clin Orthop Relat Res 189:65–76
5. Jönsson B, Strömqvist B (1996) Clinical appearance of contained and noncontained lumbar disc herniation. J Spinal Disord 9(1):32–38
6. Goh S, Price RI, Leedman PJ, Singer KP (1999) The relative influence of vertebral body and intervertebral disc shape on thoracic kyphosis. Clin Biomech 14(7):439–448
7. Holdsworth F (1970) Fractures, dislocations, and fracture-dislocations of the spine. J Bone Joint Surg Am 52(8):1534–1551
8. Inoue N, Espinoza Orías AA (2011) Biomechanics of intervertebral disk degeneration. Orthop Clin North Am 42(4):487–499
9. Kim YJ, Lenke LG (2005) Thoracic pedicle screw placement: free-hand technique. Neurol India 4:512–519
10. Kothe R, O'Holleran JD, Liu W, Panjabi MM (1996) Internal architecture of the thoracic pedicle. An anatomic study. Spine 21:264–270
11. Lafage V, Schwab F, Skalli W, Hawkinson N, Gagey PM, Ondra S, Farcy JP (2008) Standing balance and sagittal plane spinal deformity. Analysis of spinopelvic and gravity line parameters. Spine 33(14): 1572–1578
12. Lu WW, Luk KD, Ruan DK, Fei ZQ, Leong JC (1999) Stability of the whole lumbar spine after multilevel fenestration and discectomy. Spine 24(13):1277–1282
13. Luk KD, Chow DH, Holmes A (2003) Vertical instability in spondylolisthesis: a traction radiographic assessment technique and the principle of management. Spine 28(8):819–827
14. Luk KD, Chen L, Lu WW (2005) A stronger bicortical sacral pedicle screw fixation through the S1 endplate: an in vitro cyclic loading and pull-out force evaluation. Spine 30(5):525–529
15. Magerl F, Aebi M, Gertzbein SD, Harms J, Nazarian S (1994) A comprehensive classification of thoracic and lumbar injuries. Eur Spine J 3(4):184–201
16. Misenhimer GR, Peek RD, Wiltse LL, Rothman SL, Widell EH Jr (1989) Anatomic analysis of pedicle cortical and cancellous diameter as related to screw size. Spine 14:367–372
17. Mohamed E, Ihab Z, Moaz A, Ayman N, Haitham AE (2012) Lateral mass fixation in subaxial cervical spine: anatomic review. Glob Spine J 2(1):39–46
18. Nicoll EA (1949) Fractures of the dorso-lumbar spine. J Bone Joint Surg Br 31B(3):376–394
19. Panjabi MM, White AA (1980) Basic biomechanics of the spine. Neurosurgery 7(1):76–93
20. Singer KP, Edmondston SJ, Day RE, Breidahl WH (1994) Computer-assisted curvature assessment and Cobb angle determination of the thoracic kyphosis. An in vivo and in vitro comparison. Spine 19(12):1381–1384
21. Sansur CA, Fu KM, Oskouian RJ Jr, Jagannathan J, Kuntz C 4th, Shaffrey CI (2008) Surgical management of global sagittal deformity in ankylosing spondylitis. Neurosurg Focus 24(1):E8. doi:10.3171/FOC/2008/24/1/E8
22. Vaccaro AR, Rizzolo SJ, Allardyce TJ, Ramsey M, Salvo J, Balderston RA (1995) Placement of pedicle screws in the thoracic spine. Part I: morphometric analysis of the thoracic vertebrae. J Bone Joint Surg Am 77:1193–1199
23. Vaccaro AR, Lehman RA Jr, Hurlbert RJ, Anderson PA, Harris M, Hedlund R, Harrop J, Dvorak M, Wood K, Fehlings MG, Fisher C, Zeiller SC, Anderson DG, Bono CM, Stock GH, Brown AK, Kuklo T, Oner FC (2005) A new classification of thoracolumbar injuries: the importance of injury morphology, the integrity of the posterior ligamentous complex, and neurologic status. Spine 30(20):2325–2333
24. Willard FH, Vleeming A, Schuenke MD, Danneels L, Schleip R (2012) The thoracolumbar fascia: anatomy, function and clinical considerations. J Anat 221(6):507–536
25. Yamazaki M, Okawa A, Furuya T, Sakuma T, Takahashi H, Kato K, Fujiyoshi T, Mannoji C, Takahashi K, Koda M (2012) Anomalous vertebral arteries in the extra- and intraosseous regions of the craniovertebral junction visualized by 3-dimensional computed tomographic angiography: analysis of 100 consecutive surgical cases and review of the literature. Spine 37(22):E1389–E1397
26. Zindrick MR, Knight GW, Sartori MJ, Carnevale TJ, Patwardhan AG, Lorenz MA (2000) Pedicle morphology of the immature thoracolumbar spine. Spine 25:2726–2735
27. Zhong W, Driscoll SJ, Wu M, Wang S, Liu Z, Cha TD, Wood KB, Li G (2014) In vivo morphological features of human lumbar discs. Medicine 93(28): e333

Index

F. Korkusuz (ed.), *Musculoskeletal Research and Basic Science*,
DOI 10.1007/978-3-319-20777-3

G